TRACING HYDROTHERMAL FLUID FLOW IN THE ROCK RECORD: GEOCHEMICAL AND ISOTOPIC CONSTRAINTS ON FLUID FLOW IN CARLIN-TYPE GOLD SYSTEMS

by

Jeremy Reid Vaughan

M.S., Clemson University, 2002

A DISSERTATION SUBMITTED IN PARTIAL FULFILLMENT OF
THE REQUIREMENTS FOR THE DEGREE OF

DOCTOR OF PHILOSOPHY

in

THE FACULTY OF GRADUATE AND POSTDOCTORAL STUDIES

(Geological Sciences)

THE UNIVERSITY OF BRITISH COLUMBIA

(Vancouver)

August 2013

Abstract

Mapping relative patterns of mineral alteration and metasomatism reveal the visible manifestation of a hydrothermal system, but the visible expression of the hydrothermal system at the distal margins of fluid circulation may be limited owing to significant kinetic barriers to mineralogical and chemical alteration. Light stable isotopes of oxygen and carbon in carbonate minerals can be sensitive indicators of the interaction between hydrothermal fluids and wall rocks that can be used to delineate fluid flow pathways, evaluate the permeability network and source of fluids, estimate integrated fluid fluxes, and define the distal extent of alteration in carbonate-bearing lithologies.

Carlin-type Au deposits in northeastern Nevada, USA are predominately sediment-hosted Au deposits formed by large hydrothermal systems. Typically, hydrothermal alteration including silicification, carbonate dissolution, clay alteration, and sulfidation are spatially restricted. The Blue Star-Goldstrike district on the Northern Carlin trend is the largest known occurrence of Carlin-type Au with a reported Au endowment of ~1,960 t. At the northern end of the Goldstrike district, the Banshee Au deposit represents a relatively small Carlin-type deposit primarily hosted within Jurassic lamprophyre dike (west Banshee) and polymict breccia units (east Banshee). Proximal alteration at west Banshee consists of silicification, illitization, and sulfidation with the addition of Au, Cs, Hg, K, Rb, Sb, Tl, and W and depletion in Ba, Ca, Mg, Mn, Na, and Sr. The breccia unit and limestone adjacent to the west Banshee lamprophyre exhibit carbonate dissolution and silicification. Outside of visible alteration, $\delta^{18}O$ depletion in wall rock and vein calcite defines a more distal expression of alteration. Analysis of down hole $\delta^{18}O$ in limestone from two transects across the Goldstrike district show that the isotopic alteration footprint surrounding Au mineralization may extend 2 km or more out from the main ore bodies. Reactive transport modeling of $\delta^{18}O$ alteration at Banshee provides a tool for evaluating time integrated fluid flux associated with observed isotopic alteration.

The combined datasets form the basis of an alteration model for Carlin-type Au deposits where alteration zones outward from proximal clay alteration, silicification, sulfidation, and carbonate dissolution to distal trace element metasomatism and $\delta^{18}O$ alteration.

Preface

Samples collected as part of this thesis from the west Banshee lamprophyre were used for a published study on Au and trace element distribution in ore-stage pyrite grains in Carlin-type Au deposits.

Barker, S. L. L., Hickey, K. A., Cline, J. S., Dipple, G. M., Kilburn, M. R., Vaughan, J. R. and Longo, A. A., 2009, Uncloaking Invisible Gold: Use of Nanosims to Evaluate Gold, Trace Elements, and Sulfur Isotopes in Pyrite from Carlin-Type Gold Deposits: Economic Geology, v. 104, no. 7, p. 897-904. I provided samples and thin sections for the study, and provided edits for the final submission draft.

Data from chapter 5 of this thesis was included in a publication reviewing the use of oxygen isotopes in exploration. All data and interpretations presented in Chapter 5 are original work to this thesis and are independent of the Barker et al. (2013) publication.

Barker, S. L. L., Dipple, G. M., Hickey, K. A., Lepore, W. A., and Vaughan, J. R., 2013, Applying Stable Isotopes to Mineral Exploration: Teaching an Old Dog New Tricks: Economic Geology, v. 108, no. 1, p. 1-9. I provided analytical data, interpretations, and drafted original figures for the publication.

Table of Contents

List of Tables

List of Figures

Acknowledgements

Funding for this project was provided by NSERC-CRD grant, CRDP J 355066-07, supported by Teck, Barrick Gold Exploration, Inc., and Newmont Mining Corporation. I thank Barrick Gold Exploration, Inc., Teck, and Newmont Mining for their financial and logistical support. I'd also like to thank Paul Dobak, Charles Weakly, Richard Hipsley, and the exploration staff at Barrick Goldstrike. Special thanks goes to Paul Dobak, Francois Robert, Ed Cope, and Rob Krcmarov for providing financial support and time away from my day job with Barrick Gold Exploration.

I acknowledge the analytical support of the Pacific Centre for Isotopic and Geochemical Research (PCIGR), at the University of British Columbia, namely Janet Gabites for performing oxygen and carbon isotope analyses on the IRMS. I also thank Krystal Li for assisting with the analysis of hundreds of isotope analyses on the laser spectroscopy isotope analyzer, Mati Raudsepp from the University of British Columbia for quantitative XRD analysis with Rietveld refinement, Zach Sharp and Nicu-Viorel Atudorei from the University of New Mexico Stable Isotope Lab for oxygen and carbon stable isotope analyses on their IRMS, Andy Phillips from GNS Science's Stable Isotope Laboratory for oxygen and hydrogen stable isotope analyses of clay separates, and Abe Torchinsky for preparing clay separates of west Banshee dike samples.

Special thanks go to Ken Hickey for supervising this PhD project and providing support and guidance on all aspects of this PhD project, Shaun Barker for his knowledge of isotope analysis and general guidance, Greg Dipple for serving on my committee and teaching me about reactive transport modeling, and Craig Hart for serving on my committee.

Thanks to the many friends I made in Vancouver and their valuable support through the PhD journey. I especially thank Steve Moss and Lizzie Stock for encouraging my journey. I'd also like to thank my parents and family for helping instill a sense of wonder and curiosity in me and for always providing love and support. I thank my two kids, Piper and Finn, for patience and not getting in Daddy's way too much when he's working.

Finally, I wish to thank my wife, Julie, for her incredible support during this process. This document would not have been possible without her. Thank you for putting up with the long hours, the time away from home, and the ever-present stress associated with this thesis.

Dedication

I dedicate this thesis to my wife, Julia Blanchard Vaughan, for all of her love and patience during this journey. Julie, this is as much your thesis as it is mine. Thank you.

Chapter 1 : Introduction

The significance of fluid flow in the earth's crust is documented throughout the geologic literature (Cathles, 1990; Ingebritsen et al., 2006; Manning and Ingebritsen, 1999). Fluids are an important component in several geologic processes, including: the transport of solutes and heat (Bickle and McKenzie, 1987; Manning and Ingebritsen, 1999), the influence of pore fluids on brittle failure in the crust (e.g. earthquakes) (Hickman et al., 1995; Rojstaczer and Bredehoeft, 1988), formation and migration of hydrocarbons (Toth, 1988), compaction and diagenesis of sediments (Schwartz and Longstaffe, 1988), metamorphism (Bickle and Baker, 1990; Bickle and McKenzie, 1987; Ferry and Dipple, 1991), and the formation of ore deposits (Cathles, 1981; Giggenbach, 1992; Kesler, 2005; Robert et al., 1995; Simmons and Brown, 2006; Taylor, 1974; Williams-Jones et al., 2005). Within the broad subject of fluid flow in the crust, the advection of fluid and solutes in hydrothermal solutions is the focus of this thesis.

Fluid flow in active hydrothermal systems has been the focus of many studies (Browne, 1978; Cavarretta et al., 1985; Dobson et al., 2003; Giggenbach, 1992; Simmons and Brown, 2006). Active continental geothermal systems are an important source of energy and have provided extensive knowledge on the scales and duration of hydrothermal fluid systems in the crust (Goff and Gardner, 1994; Hedenquist et al., 1992; Norton, 1984; Simmons and Brown, 2006). Because of the active nature of these systems, direct study of the fluids and alteration features is possible. Observations and analyses may be conducted from surface intersections (i.e. hot springs) or through groundwater and geothermal exploration wells. Much of our understanding of hydrothermal systems both past and present rely on studies of active geothermal areas and the assumption that active systems are correlative with some fossil fluid systems. A significant limitation in the study of active hydrothermal fluids is the lack of access to the deeper parts of the system (Henley and Ellis, 1983). While a number of deep drill holes have been drilled at depths of 3 km or greater in active geothermal areas (Kennedy and van Soest, 2006), a majority of geothermal exploration concentrates on shallow targets in the upper 3 km of the crust (Huttrer, 2001), significantly shallower than the 5-10 km maximum of fluid circulation (Kennedy and van Soest, 2006; Kühn, 2001). In addition, geothermal exploration drilling concentrates on the core of thermal circulation rather than the distal margins of the fluid system. In order to characterize fluid in the deeper parts of hydrothermal systems, it is necessary to study fossil hydrothermal fluid environments that have been exposed near the surface through exhumation and erosion (Henley and Ellis, 1983).

Where fossil hydrothermal systems are exposed in the near surface environment, direct and indirect study of the hydrothermal fluids is possible (Kesler et al., 2005). Surface exposure and exploration drilling (in hydrothermal ore deposits) give access to the deep and distal parts of the fossil system. Fluids may be studied directly using inclusions of the fossil fluid encapsulated within minerals that grew with the fluid (Roedder, 1983; Roedder and Bodnar, 1997; Wilkinson, 2001), or indirectly through the observation/measurement of physiochemical manifestations of the fluid in the rock record, including: mineral alteration, geochemical metasomatism (Meyer and Hemley, 1967; Reed, 1997), and stable isotope systematics (Ohmoto, 1986; Stenger et al., 1998b; Taylor, 1974). There is a broad spectrum of fossil systems hosted in a variety of lithologies under differing fluid regimes from the near surface to >10 km depth (Cathles, 1981, 1997; Kesler, 2005).

1.1 Tracing Fluid Flow in the Crust

1.1.1 Fluid Inclusions

Fluid inclusion analysis allows for the direct characterization of paleo-fluids entrapped within mineral hosts (Roedder, 1983; Roedder and Bodnar, 1997). Fluid inclusions can provide detailed information on the physical and chemical characteristics of the ore fluid and the evolution of these characteristics with respect to time and space (Roedder, 1983; Wilkinson, 2001). While fluid inclusion studies have furthered the study of fossil hydrothermal systems, their use can be limited by a number of factors, including: (i) difficulties in establishing the paragenesis of minerals hosting fluid inclusions, (ii) difficulties in establishing the paragenetic relationships between fluid inclusion assemblages in the same mineral host, (iii) the limited spatial extent of preserved fluid inclusions related to a particular system, and (iv) fluid inclusions are not always formed or preserved (Wilkinson, 2001). Detailed paragenetic studies may compensate for limitations related to the first 2 points. When investigating the cores of hydrothermal fluid upwelling, the spatial extent of entrapped fluid inclusions is not an important factor; however, at the distal extents of fossil systems, the distribution of minerals bearing fluid inclusions from the hydrothermal fluid may be limited.

1.1.2 Rock Record

In areas where fluid inclusions are unavailable or cannot be reliably identified, the fluid must be characterized by identifying the physiochemical manifestations of the fluid in the rock record. At the distal extents of a system this may be the only information available on the nature and evolution of the hydrothermal fluid. Many of the known physiochemical manifestations preserved in the rock record can be identified visibly in the field and mapped (Meyer and Hemley, 1967). Mineral alteration and geochemical metasomatism can be used to describe the evolution of a fluid over time and space with respect to pH, redox conditions, temperature, pressure, and chemistry (Reed, 1997). The mapping of visible mineral alteration patterns has been employed for over a century in the investigation of ore deposits, and is still used today as an effective tool for the identification of potential ore forming fluid migration; however, the expression of alteration features may be subtle at the distal extents of the system (Kelley et al., 2006). High temperature hydrothermal fluid systems typically form large distinct alteration patterns, which may be documented through detailed field mapping (Meyer and Hemley, 1967; Reed, 1997). In some low temperature sediment hosted systems (250°C), alteration haloes are smaller and more subtle (Cline et al., 2005; Leach et al., 2005) owing to less pervasive fluid flow and/or a fluid that is at a lower temperature and chemical disequilibrium with the wall rock (Cline et al., 2005). Many ore deposits form in the low temperature environment, including: sedimentary rock-hosted Au, sedex Pb-Zn, sedimentary Cu, and IOCG-Uranium (Hedenquist et al., 2005). In order to detect the expression of low temperature hydrothermal systems in the rock record, proximal and distal indicators of fluid flow in these systems must be defined.

Chemical disequilibrium between a fluid and wall rock will result in chemical reactions and the preferential partitioning of chemical components into the fluid or the rock (Heinrich et al., 1996; Reed, 1997). The rate at which chemical components equilibrate is variable related to the buffering capacity of the rock or fluid (Reed, 1997). As the fluid progresses through the rock it constantly re-equilibrates, which gives the potential for developing reaction fronts preserved in the rock record. Reaction fronts represent progressive stages of equilibration of the fluid with the rock. The development of reaction fronts is governed by: (i) the chemical composition of the fluid; (ii) the chemical composition of the rock; (iii) the intrinsic permeability of the rock; (iv) the water/rock ratio, and (v) temperature of the fluid (Bickle and Baker, 1990; Bickle and McKenzie, 1987; Heinrich et al., 1996; Reed, 1997). The water/rock ratio, physicochemical conditions, and permeability structure are the key characteristics governing the geometry of reaction fronts (Heinrich et al., 1996).

The distance traveled by a particular chemical component or heat is relative to its fluid/rock partition coefficient (Bickle and McKenzie, 1987). Components which partition largely in the fluid phase such as He and H will be transported greater distances than those with lower fluid/rock partition coefficients. Heat and $\delta^{18}O$ isotopes will travel shorter distances than H and He, but much greater distances than other compatible solutes (Bickle and McKenzie, 1987). Figure 1.1a illustrates the effect of increasing fluid flux over a set time interval of 1 Ma with higher fluxes corresponding to greater transport distances (Bickle and McKenzie, 1987). Where the expression of visible alteration is limited, the use of $\delta^{18}O$ as a tracer may be a better indicator of the extent of hydrothermal fluid circulation. Figure 1.1b illustrates conceptual spacing of reaction fronts in a hydrothermal flow system where $\delta^{18}O$ would travel further along the fluid infiltration path length than trace elements and mineralogical alteration.

1.2 Thesis Goals

Understanding more about the process of hydrothermal fluid flow in the crust relies on deciphering the chemical and hydrological evolution of such hydrothermal systems over as great a spatial range as possible. Establishing such an evolution places constraints on the source(s) of the fluid and the likely extent to which such a fluid will be capable of buffering rocks. In addition, there is direct application to the exploration for undiscovered ore deposits by establishing thermal-chemical vectors to mineralization.

Sedimentary rock hosted Carlin-type Au-deposits in Nevada are the focus of this thesis. Carlin-type Au deposits are the product of large low-temperature hydrothermal systems, and represent one of the highest concentrations of Au in the world. Nevada Carlin-type Au deposits account for ~8% of the world's annual Au-production (Teal, 2002). Carlin-type gold deposits of the northern Carlin trend in north-central Nevada are the field sites for the thesis research.

Defining the evolution of hydrothermal fluid flow is difficult in relatively low temperature sedimentary hosted Carlin systems owing to: (i) visually subtle alteration patterns (Cline et al., 2005); (ii) irregular ore and alteration zoning (Hofstra et al., 1991); (iii) trace metal haloes are generally small (Cline et al., 2005); and (iv) a lack of datable coeval alteration minerals (Arehart et al., 2003; Folger et al., 1998). In addition, chemical and thermal disequilibrium between the hydrothermal fluid and the host rocks is significantly less than for systems where the fluid is largely derived from a high temperature magmatic source (e.g., Cu-Mo-Au porphyry systems). Owing to these problems, the traditional approach of mapping mineral alteration (Meyer and Hemley, 1967; Reed, 1997), so successful for higher temperature (commonly magmatic) hydrothermal systems may be of lesser use in Carlin-type low-temperature systems outside of any central upwelling core. Understanding the physiochemical evolution of such systems and their likely distal expression requires new means for deciphering the history of fluid-rock interaction.

The two main goals of this thesis are to: (i) develop a combination of new and more established analytical techniques better able to characterize the chemical and hydrological evolution of low temperature Carlin-type hydrothermal systems; and (ii) better constrain the distal manifestations of hydrothermal fluid flow and identify physiochemical gradients that could provide exploration vectors toward ore in sedimentary rock hosted Carlin-type hydrothermal systems. The outcomes of this thesis are the development of distal vectoring tools for low temperature sediment hosted hydrothermal systems, and the development of a revised fluid flow and alteration model for the formation of Carlin-type sediment-hosted Au deposits.

1.3 Background of Carlin-type Au Systems

Carlin-type Au deposits were identified as a new deposit type in 1961 after the discovery of 'fine gold' at the Carlin mine in northeast Nevada, USA (Hausen and Kerr, 1968). Hofstra and Cline (2000) defined Carlin-type Au deposits as epigenetic, disseminated auriferous pyrite deposits in typically calcareous sedimentary rocks. Gold is generally found as a trace component of As-rich pyrite/marcasite and as submicron particles disseminated in

As-rich pyrite or marcasite (Bakken and Einaudi, 1986; Wells and Mullens, 1973). Typical alteration associated with Carlin-type deposits is carbonate dissolution (Bakken and Einaudi, 1986; Hofstra et al., 1991), clay alteration (Cail and Cline, 2001; DrewsArmitage et al., 1996; Kuehn and Rose, 1992) and silicification (Hofstra et al., 1988; Lubben, 2004; Yigit et al., 2006). Sulfidation is the primary proposed mechanism for Au deposition (Emsbo et al., 2003; Fortuna et al., 2003; Hofstra et al., 1991; Stenger et al., 1998a). However, a study at the Screamer deposit (Kesler et al., 2003) in the northern Carlin trend questions the viability of sulfidation as the only mechanism for deposition owing to the addition of Fe in host rocks and the lack of correlation between degree of sulfidation and Au content. Most Carlin-type deposits are found along three major mineral trends in northern Nevada, including the Battle Mountain-Eureka trend, the Getchell trend, and the Carlin trend (Figure 1.2). In addition to the three main mineral trends, several Carlin-type deposits are found in the Jerritt Canyon and Alligator Ridge districts. This thesis focuses on the northern portion of the Carlin trend (Figure 1.3).

1.3.1 Geologic Setting of the Northern Carlin Trend

The Carlin trend is a 60 km northwest oriented lineament in northeastern Nevada, USA that hosts the largest known occurrences of sedimentary-hosted Carlin-type Au deposits in the world (Hofstra and Cline, 2000). The northern Carlin trend consists of multiple disseminated Au deposits hosted primarily in Paleozoic silty carbonates (Arehart, 1996). The host lithologies are found within a westward thickening miogeoclinal sequence of Late Proterozoic and Cambrian clastic sediments derived from the craton, and Upper Cambrian to Late Devonian carbonates and minor clastic sediments (Stewart, 1980). The silty carbonate rocks hosting the Au were deposited along the continental shelf margin during the Silurian through the Devonian and are collectively known as the `lower-plate' sequence owing to the fact that they are footwall to the Roberts Mountain Thrust (RMT (Hofstra and Cline, 2000). During the late Devonian through the Mississippian, the Antler orogeny resulted in a western eugeoclinal assemblage of primarily siliceous sediments thrusting over top of the lower-plate assemblage along the RMT (Roberts et al., 1958; Stewart, 1980). This ‘upper plate’ sequence forms the Roberts Mountains allochthon (Hofstra and Cline, 2000). Most of the known Carlin-type Au deposits reside in the lower-plate sequence of rocks.

Mesozoic intrusions ranging in age from Late Jurassic to Late Cretaceous ages are common in northern Nevada and both ages of plutonism are found along the northern Carlin trend. Late Jurassic backarc magmatism is attributed to slab breakoff that triggered continental magmatism that continued until subduction of the Farallon plate occurred (Dickinson, 2006). Nd and Sr isotopic systematics indicate Late Jurassic and Early Cretaceous intrusives were dominated by subcontinental lithospheric mantle (Wright and Wooden, 1991). Jurassic intrusives along the Carlin trend consist of the Goldstrike quartz diorite stock and associate sills and dikes, rhyolite dikes, and lamprophyre dikes (Ressel and Henry, 2006). Jurassic-aged dikes follow the same NW structural trend that characterizes the orientation of the Carlin trend and were all emplaced at ~158 Ma (Ressel and Henry, 2006). The only known Cretaceous intrusion on the Carlin trend is the 112 Ma (Mortensen et al., 2000) Richmond Mountain granite. Although elsewhere in Nevada, Cretaceous magmatism occurred between ~86 to 112 Ma, there is no evidence of Cretaceous intrusives in the Carlin trend younger than Richmond Stock (Ressel and Henry, 2006).

A series of broad amplitude N25-35°W trending, northerly plunging anticlines within the lower plate assemblage are preserved in uplifted tectonic windows along the Carlin trend (Teal, 2002). Tectonic windows along the northern Carlin trend include the Bootstrap, Lynn, and Carlin windows. Most of the known Au deposits are located within these windows (Teal, 2002). Mineralization is thought to be largely coeval with extensional tectonics during the late Eocene (40-37 Ma) (Christiansen and Yeats, 1992; Cline et al., 2005). Eocene magmatism is evidenced by an abundance of dikes along faults of the northern Carlin trend (Henry and Boden, 1998; Ressel and Henry, 2006; Ressel et al., 2000b). Dates for pre- and post-mineralization dikes and alteration minerals along the northern Carlin trend place a minimum age for the onset of hydrothermal activity and gold deposition at ~40 Ma, and maximum age for the end of hydrothermal activity at 37.6 Ma (Emsbo et al., 1996; Ressel et al., 2000b).

The northwest orientation of the Carlin trend is the manifestation of a combination of structures (Hofstra and Cline, 2000; Teal, 2002). These structures include: high-angle, northwest striking faults that served locally as fluid conduits within several deposits (Leonardson and Rahn, 1996; Volk et al., 1995; Williams et al., 2000); high-angle northeast striking faults that served as secondary conduits and flow barriers (Teal, 2002); the broad amplitude northwest trending anticlines in the lower-plate sequence (Leonardson and Rahn, 1996; Volk et al., 1995); and high-angle stratabound, pre-ore collapse breccia (Bakken, 1990; Kuehn, 1989; Radtke, 1985). On the Carlin trend, gold mineralization is commonly associated with intersections of the northwest and northeast trending faults (Teal, 2002), along the crests of anticlines (Hofstra and Cline, 2000), within pre-ore collapse breccia (Emsbo et al., 2003; Williams et al., 2000), within or adjacent to Jurassic lamprophyre dikes (Emsbo et al., 2003), and within coarse-grained sedimentary debris flows (Armstrong et al., 1997; Ye et al., 2003).

1.3.2 Carlin-type Hydrothermal Systems

The fluids that form Carlin-type deposits have been defined primarily on alteration mineral association, lithogeochemistry, and fluid inclusion analysis. Carlin fluids were dominantly meteoric (based on δD and $\delta^{18}O$ stable isotope data) and had a temperature range of 180- 240°C based on fluid inclusion microthermometry in ore stage quartz in several deposits (Cline et al., 2005; Lubben et al., 2012). Alteration and lithogeochemistry studies suggest that the Carlin-type ore bearing fluids were mildly acidic and under saturated with respect to Au (Hofstra and Cline, 2000; Cline et al., 2005).

Many of the highest-grade deposits are associated with northwest trending faults assumed to be potential up-flow zones (Teal, 2002). These structures may be responsible for transient flow of deeply circulating meteoric fluid. The predominant theories for Carlin-type deposits call on the transportation of deeply sourced mineral constituents through thermally driven convection of dominantly meteoric fluids (Cline et al., 2005). Emsbo et al. (2003) suggests that locally some deposits may have formed from the leaching of sedex gold-rich units by topographic driven flow.

A lack of consistency within and between deposits has limited the use of visible alteration features as vectoring tools (Cline et al., 2005). However alteration studies are important for characterizing the character of the mineralizing fluids. Figure 1.4 shows a schematic of the spatial relationship of major alteration types for Carlin deposit on the northern Carlin trend (Kuehn and Rose, 1992).

Carbonate dissolution is a nearly ubiquitous alteration feature of Carlin-type deposits (Cline et al., 2005). In some deposits, the intensity of carbonate dissolution was great enough to produce extensive collapse breccia that significantly enhanced permeability and fluid rock reaction (Bakken, 1990). At Meikle this was likely a primary mechanism for the focusing of high-grade ore deposition (Emsbo et al., 2003). The extent of carbonate dissolution in and around other deposits such as Gold Bug and Screamer is minimal (Ye et al, 2003). Carbonate zoning is common outside areas of complete carbonate dissolution with dolomite stable zones proximal to areas of carbonate dissolution. Calcite-stable zones are found outside of the dolomite zone, and abundant calcite veining is common outside and within the calcite stable zone (Cline et al., 2005). Calcite veining is presumed to be late ore stage or post-ore (Cline et al., 2005).

Silicification is a common alteration feature at many but not all Carlin-type deposits. Jasperoid and late ore-stage fine-grained drusy quartz lining vugs are both common manifestations, although ore-stage quartz veins are rare (Cline et al., 2005; Lubben et al., 2012). Jasperoids occur where calcite and dolomite have been replaced by cryptocrystalline quartz. As defined by Holland et al. (1988), jasperoids should have greater than 70% SiO_2 and less than 10% Al_2O_3. On a district scale, jasperoids have aided the discovery of several deposits, including Betze-Post and Meikle; although, many jasperoids found along the Carlin trend are barren and not considered coeval with Au mineralization (Cline et al., 2005). As many as six later stage silicification events are noted by Yigit et al. (2006) in jasperoids at the Gold Bar deposit. Lubben (2004) proposed that variations in fluid temperatures across the Betze-Post deposit were likely responsible for the variable precipitation of silica.

1.3.3 Relation Between Au and Alteration

1.3.3.1 Clay Alteration

Because of the ubiquitous nature of clay alteration along the Carlin trend it is difficult to differentiate between clays formed from pre-ore hydrothermal events, ore stage fluids, and the post-ore supergene environment in Carlin-type deposits (Hofstra et al., 1999). Within some deposits, 1Md kaolinite and 2M1 dickite were determined to be coeval with ore formation, including: Alligator Ridge (Ilchik, 1990); the Vista ore-body at Twin Creeks (Osterberg and Guilbert, 1991); and Deep Star (Heitt et al., 2003). Increased crystallinity of illite in association with Au ore has been noted at several deposits (Ahmed, 2010; Cail and

Cline, 2001; Folger et al., 1998; Osterberg and Guilbert, 1991). However, fine grained muscovite and illite clays yield pre-Eocene $^{40}Ar/^{39}Ar$ ages, which indicates that these minerals formed prior to an Eocene mineralizing system and remained stable through the Carlin hydrothermal system (Arehart et al., 2003; Folger et al., 1998).

Clay alteration is particularly well developed in silty limestones, calc-silicate hornfels, and igneous stocks and dikes (Hofstra and Cline, 2000). Pure limestones exhibit minimal clay alteration. Detrital clays and potassium feldspar are present in small amounts (3-5%) of silty limestone protolith, and typically formed assemblages of kaolinite ± dickite ± illite (Folger et al., 1998; Hofstra and Cline, 2000). The two clay species most commonly associated with Carlin-type fluids are kaolinite and illite (Hofstra and Cline, 2000).

Important insights into the chemistry, temperature, and duration of hydrothermal fluid systems can be made based on patterns in clay alteration species. The formation of hydrothermal illite is dependent on both the duration and temperature of fluids (Pytte and Reynolds, 1989). For a peak fluid temperature of approximately 150ºC, a period of 10,000 years is necessary to form argillaceous rock containing illite/smectite (I/S) with 80% illite (Jennings and Thompson, 1986). In addition to the time/temperature constraints, the fluid must contain sufficient K^+ ions to form illite (Meunier, 2005). Significant addition of K^+ has not been previously noted in most Carlin-type deposits, and it is likely that the K^+ is locally sourced from K-bearing feldspars (Cail and Cline, 2001). However, K^+-metasomatism might also play a role during alteration. Another important constraint on the fluid chemistry elucidated from the prevalence of differing clay species is the pH of the fluid. Kaolinite can form at both lower temperatures and lower pH than illite. The presence of predominately kaolinite alteration coupled with the absence of illite likely means that the ore fluid was more acidic (Henley, 1984). At higher temperatures and low pH, dickite would be likely to form (Meunier, 2005). Dickite, kaolinite, and illite at several deposits have been found together with Au (Cline et al., 2005).

1.3.3.2 Lithogeochemistry

Previous lithogeochemistry studies have concentrated on establishing the primary pathfinder trace elements associated with gold deposition and the source of those trace elements. Numerous lithogeochemistry studies have been conducted on Carlin-type deposits in northern Nevada (de Almeida et al., 2010; Harris and Radtke, 1976; Heitt et al., 2003; Ikramuddin et al., 1986; Kuehn and Rose, 1992; Nelson, 1990; Radtke et al., 1972; Simon et al., 1999; Yigit and Hofstra, 2003). A relatively consistent pattern of elemental fluxes have been found in several Carlin-type deposits (Cail and Cline, 2001; Emsbo et al., 2003; Hofstra, 1994; Stenger et al., 1998a; Yigit and Hofstra, 2003). A characteristic feature of Carlin-type deposits is the high Au/Ag ratios within the deposits. The Au/Ag ratio is typically greater than 10:1 (Cline et al., 2005). Table 1.1 lists the elements typically added to rocks in Carlin-type deposits. Pathfinder elements include As, Au Sb, Hg, and Tl. While these tracer elements are commonly found within deposits, their relative abundances have not been shown to be coincident with gold grade (Hofstra and Cline, 2000). Cu and Te have been shown to be associated with the early high Au bearing fluids. However other pathfinder elements may have been leached from wall rock (Cline et al., 2005; de Almeida et al., 2010). In general, trace metals are found at relatively low concentration and occur primarily as impurities in pyrite and marcasite (Cline et al., 2005). Elements removed from rocks and immobile elements are listed in Table 1.1. In most of the known Carlin-type deposits Fe is relatively immobile, but work by Cail (1999) and Kesler et al. (2003) indicate that Fe was mobile at the Getchell and Screamer deposits.

1.3.3.3 Light Stable Isotopes

In general stable isotope studies in Carlin-type Au systems have concentrated on determining fluid source and isotopic signatures of the ore fluid rather than delineating paleo-fluid footprints. A variety of stable isotope studies have been conducted on Carlin-type deposits (Arehart and Donelick, 2006; Cline and Hofstra, 2000; Cline et al., 2005; Emsbo et al., 2003; Heitt et al., 2003; Radtke et al., 1980; Stenger et al., 1998b; Yigit et al., 2006). Detailed studies of $\delta^{18}O$ and δD in ore stage silicates and fluid inclusions have been conducted in an attempt to fingerprint the mineralizing fluid source (i.e. magmatic, meteoric, or metamorphic). For most deposits, highly exchanged meteoric signatures dominate (Cline et al., 2005; Emsbo et al., 2003; Hofstra et al., 1999; Kuehn, 1989; Lubben et al., 2012; Radtke et al., 1980). Magmatic fluid signatures have been found at the Getchell deposit (Cline and Hofstra, 2000; Cline et al., 2005) and Deep Star (Heitt et al., 2003).

Stable isotope studies have also proven effective in identifying zones of isotopic depletion around hydrothermal ore deposits (Cathles, 1993; Taylor, 1974). Studies conducted on Carlin-type deposits at Twin Creeks (Stenger et al., 1998b) and Pipeline (Arehart and Donelick, 2006) attempted to delineate isotopic haloes around ore bodies with respect to $\delta^{18}O$ and $\delta^{13}C$ in carbonates. Both the Twin Creeks and Pipeline studies identified distinct haloes of isotopic resetting with respect to oxygen. A similar halo for carbon was not seen in either of the studies. It is likely that much of the carbon is locally sourced as the fluid contained <4 % dissolved CO_2 (Cline et al., 2005).

1.4 Thesis Research

1.4.1 Objectives

The broadest objectives of this research project are to develop a refined model for fluid flow in low temperature carbonate rock hosted deposits and define the physiochemical manifestations of hydrothermal fluids responsible for the formation of Carlin-type Au deposits. The thesis is presented as 4 research chapters, and an integration and conclusions chapter. Below is an outline and summary of each Chapter.

Chapter 2 is a study of the geology, geochemistry, and alteration of the Banshee Carlin-type Au deposit in Nevada. The geology is introduced as a framework for understanding the controls on ore in a small Carlin-type ore system. Of particular interest at Banshee is the west Banshee lamprophyre dike that hosts a majority of ore in west Banshee. The ability to sample the west Banshee dike from unaltered zones through alteration and ore provided a unique opportunity for detailed mass transfer analysis using lithogeochemistry data. Additional data presented in this chapter includes light stable isotopes (S, O, and H) from sulfides and clays within the west Banshee dike, and modal mineralogy from quantitative XRD analyses. This chapter quantifies the addition of chemical components to the west Banshee system, relates mass transfer to alteration processes, and uses the mass transfer data to provide estimates on the minimum fluid volumes necessary for forming this small Carlin-type Au deposit.

Chapter 3 describes alteration of carbonate minerals at the Banshee deposit and contributes to the development of a new model for alteration of carbonate in Carlin-type Au deposits. Light stable isotopes in wall rock calcite and veins are used to define fluid flow pathways and the extent of isotopic alteration at Banshee. Further investigation of the different carbonate cement generations associated with $\delta^{18}O$ depletion indicates that they have distinct cathodoluminescence textures and trace element abundances. Paragenetic relationships and detailed micro-analytical work defines syn-alteration veins formed from hot, reduced hydrothermal fluids. The existence of syn-alteration veins outside of other indicators at Banshee suggests that veining is a potentially important alteration vector for Carlin-type systems.

Chapter 4 uses the $\delta^{18}O$ data presented in Chapter 3 to calibrate 1-dimensional reactive transport modeling for the Banshee system. The recognition of syn-alteration calcite veins in disequilibrium with wall rock calcite provides the opportunity to estimate kinetic dispersion effects at Banshee. Additionally, reactive transport modeling of Banshee data indicates that distinct fluid pathways are present and that they are controlled by permeability contrasts. Estimates of time integrated fluid flux (TIFF) are made for each fluid path as a function of the reactive path length. Comparisons of TIFFs calculated for other flow systems suggest that TIFF estimates for Banshee are reasonable and may form a basis for evaluating fluid flow in a variety of settings in addition to Carlin-type hydrothermal systems.

Chapter 5 builds upon the use of $\delta^{18}O$ in carbonates developed in Chapter 3, by examining larger scale isotopic alteration in the Carlin-type Goldstrike district in Nevada. Over 1500 samples were analyzed for $\delta^{18}O$ and $\delta^{13}C$ in carbonate as part of this study. Isotope and trace element sampling along two transects across the Goldstrike property indicate that $\delta^{18}O$ depletion is spatially associated with Au deposition and forms a larger halo of alteration outside of Au (≥2 km). The data from Goldstrike suggests that $\delta^{18}O$ in carbonate bearing host rocks may be useful as an exploration vector at a variety of scales. Trace element enrichment is also found outside Au at Goldstrike, but $\delta^{18}O$ depletion potentially provides a more a robust and consistent signature.

Chapter 6 provides a summary and key conclusions of the dissertation.

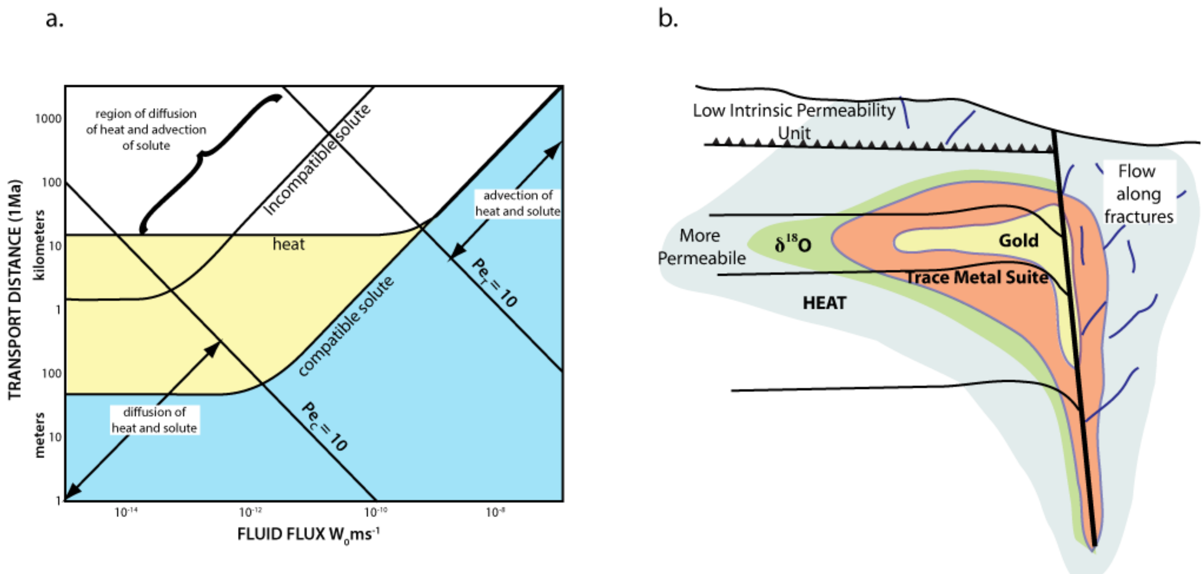

Figure 1.1 a) From Bickle and McKenzie (1987) . Transport distances for heat, an incompatible element, and a compatible element (K_C ρS /ρf=1) as a function of W_0 (fluid velocity) calculated for a porosity of 0.1%. Calculated using the average properties of fluid and rock at ~500 MPa and ~500° C. The blue region denotes the area of compatible solute transport in 1 Ma. The yellow region denotes the area of heat transport in 1 Ma. (K_C = rock-fluid coefficent, ρS = density of the solid, and ρf = density of the fluid) b) Conceptual diagram showing relative extents of reaction fronts based on transport theory and controlled by permeability contrasts for fluid flowing out from a upwelling conduit.

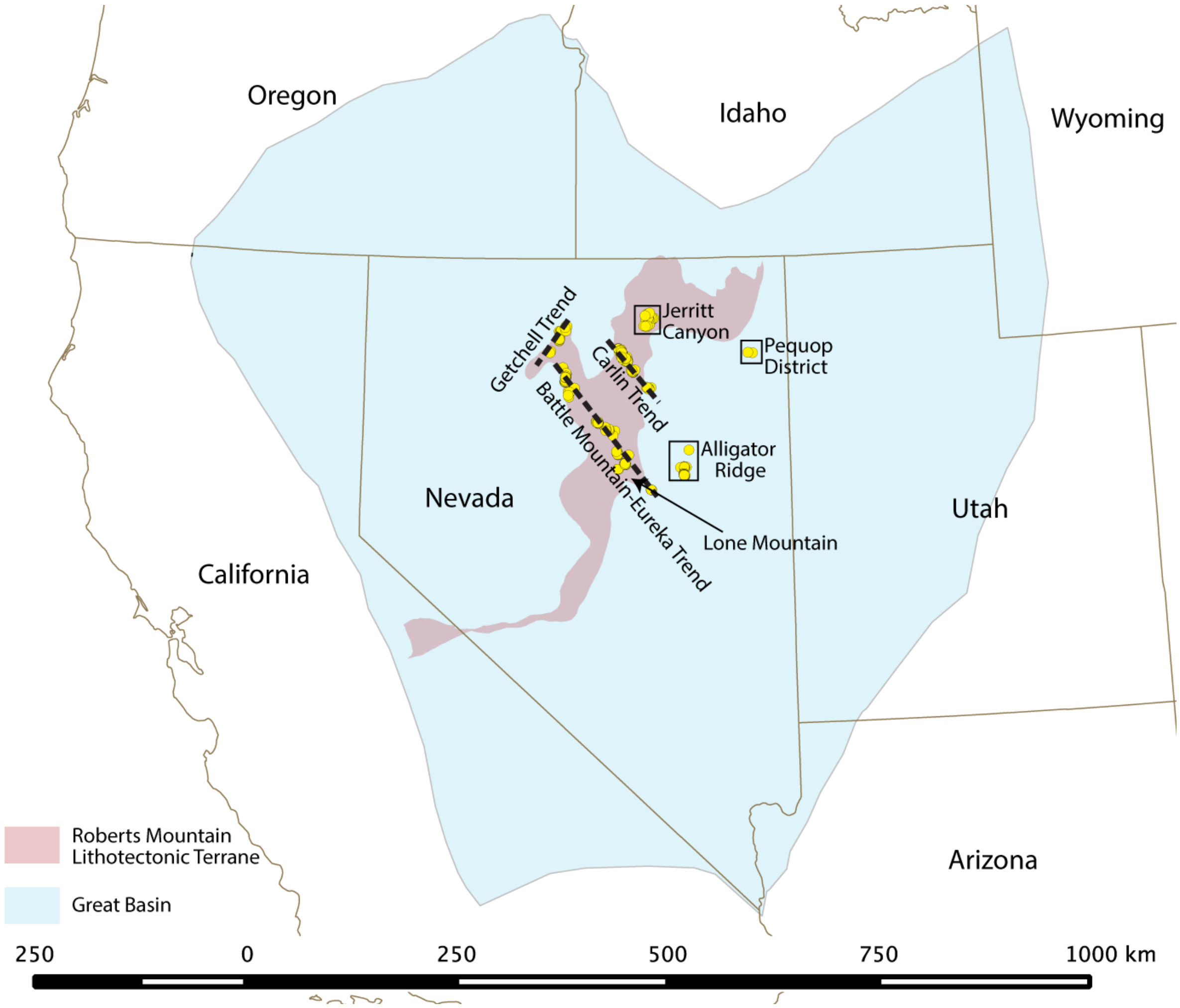

Figure 1.2 Overview map of the Great Basin located in the western United States showing the location of Carlin-type Au deposits in northern Nevada. The Roberts Mountain lithotectonic terrane defines the eastern extent of the Roberts Mountain Thrust (after Silberling, et al., 1987).

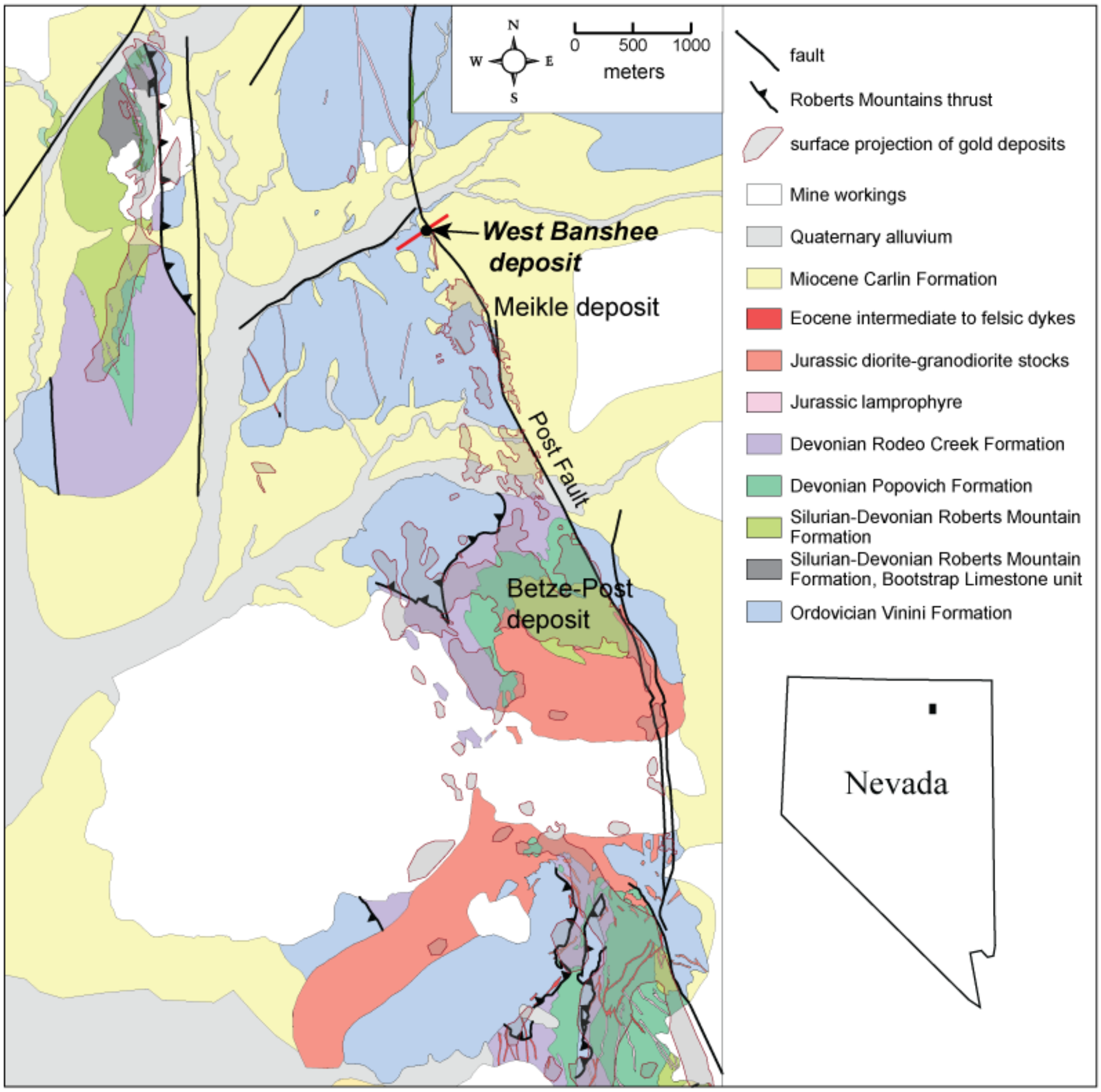

Figure 1.3 Geologic map of the northern Carlin trend with Au deposit locations outlined in red and shaded grey (after Thompson, 2002).

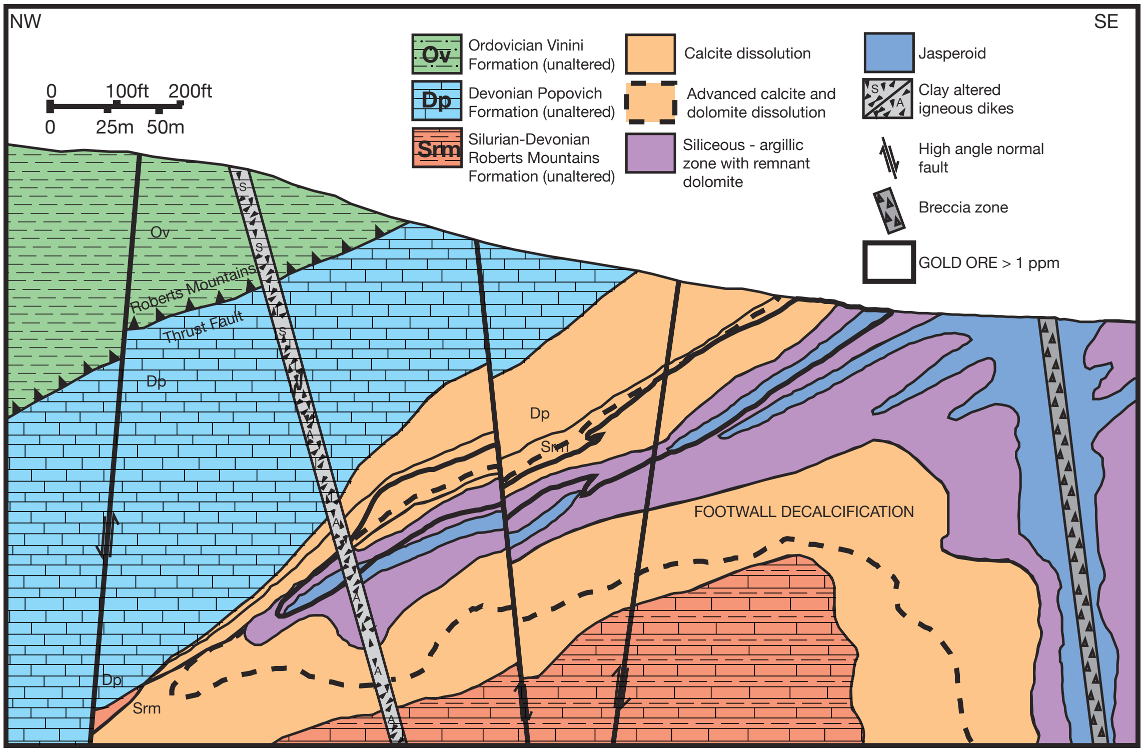

Figure 1.4 Conceptual cross-section illustrating spatial relationships of alteration patterns associated with the Carlin deposit. Modified from Kuehn and Rose (1992).

Table 1.1 Relative elemental abundances and fluxes associated with Carlin-type deposits. Data compiled from Cline et al. (2005).

Immobile Elements	Al, Ti, Th, and Zr
Elements Added	S, As, Au, Sb, Hg, Tl
Variably Added Elements	Te, Cu, W, Mo, Se, Fe, Ag, Pb, Si, Ba, Cs, and Zn
Elements Removed	C, Ca, Mg, Sr, Mn, Na, and Zn

Chapter 2 : Linking Mass Transfer, Alteration, and Fluid flow in the West Banshee Gold Deposit

Defining trace metal metasomatism and linking it to mineral alteration provides important constraints on ore deposit genesis by providing insight into fluid sources, ore fluid components, and the physiochemical conditions during ore precipitation. In Carlin-type Au deposits visible mineral alteration in sedimentary host rocks is limited to carbonate dissolution (Bakken and Einaudi, 1986; Hofstra et al., 1991), clay alteration (Kuehn and Rose, 1992; Drews-Armitage et al., 1996; Cail and Cline, 2001) silicification (Hofstra et al., 1988; Yigit et al., 2006; Lubben, 2004), and Fe-sulfidation (Hofstra et al., 1991; Stenger et al., 1998a; Emsbo et al., 2003; Fortuna et al., 2003). Many studies have shown that several trace elements are linked to Au mineralization including As, Hg, Sb, Te, Tl, and W (Cail and Cline, 2001; de Almeida et al., 2010; Emsbo et al., 2003; Heitt et al., 2003; Hofstra and Cline, 2000; Hofstra et al., 1999; Yigit and Hofstra, 2003), but trace element haloes are generally confined to the deposit area. The occurrence of multiple alteration events within and surrounding some Carlin-type deposits further complicates the interpretation of both trace metal enrichment and alteration (Emsbo et al., 2006; Emsbo et al., 2003; Yigit et al., 2006). Therefore, care has to be taken in linking mineralization with both metasomatic changes and alteration mineralogy. Furthermore, quantifying mass transfer and alteration products relies on the ability to collect samples of consistent protolith and well-defined background in unaltered protolith. Identifying background protolith of identical composition of altered samples is challenging in Carlin-type deposits owing to the chemical heterogeneity of sedimentary host rocks, the lack of continuity in more homogeneous sedimentary host rocks (Cail and Cline, 2001), and the difficulty in tracing a single phase of intrusive host rock from altered to unaltered. A lack of datable coeval alteration minerals and clear paragenetic relationships further complicates the characterization of alteration associated with Au mineralization (Folger et al., 1998; Arehart et al., 2003). Therefore linking and quantifying mineralogical changes to mass transfer requires careful sampling of identical protolith from altered and mineralized to unaltered, and establishing the spatial and statistical correlation between alteration and mass transfer.

Previous authors have characterized the alteration and trace metal metasomatism specifically related to Carlin-type mineralization using mass transfer and alteration paragenesis studies in both sedimentary (Hofstra, 1999; Hofstra and Cline, 2000; Cail and Cline, 2001; Emsbo et al., 2003; Kesler et al., 2003; Yigit, 2003) and igneous hosts (Hofstra, 1999; Emsbo et al., 2005). Cail and Cline (2001) selected a thin continuous marker bed of silty limestone that could be traced over a distance of 1 to 4 meters for their mass transfer study of the Getchell deposit. Cail and Cline (2001) were not able to sample outside of the As enrichment halo surrounding Au mineralization and some of their unmineralized samples exhibited argillic alteration (Cail and Cline, 2001). Lamprophyre dikes also serve as important ore hosts at a number of Carlin-type deposits. Emsbo et al. (2003) looked at mass transfer in lamprophyre dikes with variable protolith chemistry at Goldstrike to define the chemical components directly related to Carlin-type mineralization using samples of variable protolith geochemistry. The lack of consistent protolith can hamper the resolution of mass transfer determinations especially for major element species such as potassium, effectively masking subtle changes (Booden et al., 2011).

Existing studies have defined several key trace element components associated with mineralization, but to gain greater precision on elemental fluxes and more clearly link them to mineralogy, a sample medium should be chosen that has a single consistent protolith and can be traced from where it is unaltered to where it is altered and mineralized. This chapter uses a geologically well-constrained single igneous protolith from the Banshee Carlin-type deposit on the northern Carlin trend in Nevada to conduct studies on chemical mass transfer, stable isotope systematics and mineralogical alteration linked to Carlin-type Au mineralization. The goal of this study is to put constraints on Carlin-type ore deposit genesis by improving the understanding of the fluids, ore components, and the precipitation of ore. Additionally, using a single intrusive dike of consistent protolith allows for linking of mineralogical and chemical changes, and the establishment of minimum mass fluxes associated with the mineralizing event. The dike used for this study is a hornblende lamprophyre that hosts the bulk of mineralization at the west Banshee Carlin-type deposit. The dike varies from relatively unaltered to strongly altered and mineralized. Alteration consists of distinct zones dominated by kaolinite and illite alteration making it possible to more readily characterize the fluid(s) responsible for different types of clay alteration and how they are related to mineralization, providing an advantage over other studies where the paragenetic relationship of clay assemblages is not readily apparent.

In this chapter, a geological framework is provided as a basis to understand mineralization and fluid flow for Carlin-type deposits. Detailed information is provided about the chemistry of variably altered and mineralized lamprophyre dyke material collected from throughout the Banshee deposit. Additional support for the origin of sulfur, and ore-forming fluid is supplied from analysis of sulfur isotopes in Au-bearing lamprophyre, as well as oxygen and hydrogen isotope analysis of clay minerals found within Au-mineralized material. This information is used to place constraints on the likely minimum time-integrated fluid flux that accompanied mineralization; to assess the sources of sulfur, oxygen and hydrogen in the fluid; to infer information about fluid chemistry; to assess K-metasomatism and what it means; and to infer potential fluid flow pathways and why Au is largely localized in the west Banshee dike. The information presented in this chapter provides a framework for exploring for additional Banshee-type Carlin-type deposits where reactive host rocks (such as lamprophyre dikes) crosscut high permeability fluid pathways. This study shows illite alteration, trace metal metasomatism and mineralization are linked and that kaolinite alteration is likely a later stage of alteration not related to the Au mineralizing system at Banshee.

2.1 Previous Mass Transfer and Alteration Studies in Carlin-type Deposits

In order to define mass transfer using lithogeochemical data, the relationship between compositional and volume changes must be established and accounted for. Gresens (1967) derived equations that calculated the relative loss and gains of elements corrected for volume changes that may have occurred during metasomatism. Gresens' equations require the determination of density for altered and unaltered samples of the same protolith. Gresens acknowledged that creating a ratio between an element added or subtracted with an element not affected by hydrothermal alteration would have the same effect as using density, and the use of modified Gresens equations using conserved elements has been employed in numerous studies (Booden et al., 2011; Maclean, 1990; Maclean and Barrett, 1993; Maclean and Kranidiotis, 1987; Mauk and Simpson; Warren et al., 2007). Whether density measurements are used or immobile element species, it is critical that samples of altered and unaltered rock be of identical protolith (Gresens, 1967; Maclean and Barrett, 1993; Mauk and Simpson, 2007).

Hofstra (1994) used the isoconcentration diagram approach of Grant (1986, 2005) to define mass loss/gain in a variety of lithologic units at Jerritt Canyon, and this approach has been used in various studies of mass transfer in Carlin-type deposits. Isoconcentration diagrams are a graphical implementation of Gresens (1967) mass transfer equations where altered samples of like protolith are plotted against their unaltered equivalent. A line is then drawn through immobile elements that define the relative volume change associated with alteration (Grant, 1986, 2005).

Cail and Cline (2001) investigated mass transfer by collecting 50 samples along 13 transects in silty carbonate units at the Getchell deposit and 1 transect through a rhyodacite dike. A total of 3 to 6 samples were collected along each transect at intervals of ~4m. The authors attempted to sample homogenous beds of silty limestone from ore to moderately altered. The authors did not consider the effect of a variable clastic component in the sampled limestone beds, and they were not able to follow sample beds to unaltered material as evidenced by an average As concentration of 1815 ppm in their "least-altered" samples from the 14 transects. Cail and Cline (2001) were able to document enrichment in Au, Hg, Sb, Se, Te, and Tl. Only variable enrichment was noted in As, Cs, Fe, Si, S, W, Cu, and Mo. The variable enrichment in these elements is likely a product of the fact that the authors were not able to sample unaltered protolith. Least-altered samples used for Grant's isoconcentration diagrams contained greater than 2.1% S and 27 ppm W on average (Cail and Cline, 2001). The conclusion that Sc was depleted in ore samples indicates that the samples contained a variable clastic component. Sc is a high field strength element (HFSE) that is unlikely to be mobile in a low temperature hydrothermal system except where Cl^- and F^- are present (Williams-Jones et al., 2012). Cail and Cline (2001) used the results of the mass transfer study to infer the mineralogical controls on observed mass transfer noting that: As, Sb, Hg, Tl, Cu, Te, and S likely precipitated with Au in ore stage pyrite grains; As and S precipitated in realgar and orpiment; and Sb and S precipitated in minor late-stage stibnite. The authors noted that W and Mo are likely found with pyrite and maybe related to Cretaceous metasomatism associated with the Osgood stock. Removal of Ca, Mn, Sc, Sr, and minor Mg was a product of carbonate dissolution (Cail and Cline, 2001).

Emsbo et al.'s (2003) mass transfer study using Jurassic lamprophyre dike, Jurassic Rhyolite dike, Jurassic Goldstrike diorite, and Eocene dacite dike showed variable mass transfer, likely as a function of how protolith influenced alteration. Mineralized material from all rock types showed enrichment in trace elements Au, Ag, Te, W, Hg, Tl, Sb, As, and S as well as depletion in Sr, Mn, Ba, Na, K, Mg, and Ca with variable depletion in Mo, Pb, Cu, V, Zn. Conserved elements including P, Ti, Al, Si, Fe, Co, Ni, V, U, Cr, Mo, Sc, Y, Th, Zr, Hf, Ti, Nb, and Ta were largely immobile for all rock types except Si, which was slightly depleted in Eocene dacite (Emsbo et al., 2003). While each rock type showed a general correlation in elements added and depleted, the relative gain in trace elements associated with the addition of pyrite through sulfidation was much greater in lamprophyre dike. Emsbo et al. (2003) attributed the higher grades in lamprophyre with their greater capacity for sulfidation reactions owing to higher reactive Fe concentrations. While Emsbo et al. (2003) used relatively unaltered hornblende lamprophyre for their study, the dike was not from a singular occurrence of dike and therefore unlikely to have identical protolith. Even unaltered lamprophyres with similar mineralogy can have significant ranges in both major and trace elements (Taylor et al., 1994). The current study aims to use samples collected from a laterally continuous lamprophyre dike of consistent protolith to provide improved constraints on mass transfer in Carlin-type deposits.

2.2 Research Plans and Methods

2.2.1 Study Site Rationale

The Banshee Au deposit lies on the northern Carlin trend in northeastern Nevada. The deposit is positioned along the Post fault corridor on the Goldstrike property just to the north of the Meikle Au deposit and to the south of the Ren Au deposit (Figure 2.1). The Banshee deposit provides the opportunity to study a small well constrained Carlin-type ore system with well-defined alteration and mineralization. Many previous studies of mass transfer and alteration in Carlin-type gold deposits have occurred in large bulk tonnage deposits like Betze-Post, Screamer, and Getchell, in areas with complex geology and heterogeneous distribution of alteration and mineralization. West Banshee in particular provides a unique scenario where all of the economic grade mineralization is contained within a single laterally continuous lamprophyre dike that can be traced from unaltered to altered and mineralized. Even though west Banshee is a small example of a Carlin-type deposits, it occurs within one of the largest Au districts in the world along the northern Carlin trend, and is representative of typical Carlin-type mineralization along the Carlin trend in northern Nevada. While the main focus of the study is to define mass transfer associated with alteration and mineralization of the west Banshee dike, the study also describes alteration of adjacent sedimentary units.

2.2.2 Sampling Plan

The ore-bearing lamprophyre dike was selected from the west Banshee Carlin-type Au deposit to conduct detailed sampling for whole rock geochemistry. Samples were collected from below, above and lateral to mineralization in the dike. The sampling goal was to collect material from a continuous defined dike from unaltered to altered and mineralized material. A total of 33 dike samples were collected for geochemical analysis. Additionally, 10 samples were also collected of Bootstrap limestone, 5 samples of Jurassic rhyolite dike, and 6 samples of Eocene dacite to characterize the lithogeochemistry, alteration and mineralization outside the lamprophyre dike.

2.2.3 Analytical Methods

2.2.3.1 Petrography

Samples were examined petrographically under transmitted and reflected light. Thin section descriptions were generated for a subset of 12 samples of west Banshee lamprophyre representative of unaltered altered/mineralized dike. Further investigation of discrete mineral phases and textures were accomplished using back-scattered scanning electron microscopy (SEM) equipped with an energy dispersive spectroscopy (EDS) detector.

2.2.3.2 X-Ray Diffraction and Quantitative XRD

A subset of samples of unaltered and altered/mineralized dike were analyzed for modal mineralogy by quantitative XRD with Rietveld refinement using the methods of Raudsepp et al. (1999). Samples were initially pulverized using a steel ring mill and then were further reduced to the optimum grain-size range for quantitative X-ray analysis (<10 μm) by grinding under ethanol in a vibratory McCrone Micronising Mill for 7 minutes. Continuous-scan X-ray powder-diffraction data were collected over a range 3-80°2θ with CoKa radiation on a Bruker D8 Focus Bragg-Brentano diffractometer equipped with an Fe monochromator foil, 0.6 mm (0.3°) divergence slit, incident- and diffracted-beam Soller slits and a LynxEye detector. The long fine-focus Co X-ray tube was operated at 35 kV and 40 mA, using a take-off angle of 6°. The X-ray diffractograms were analyzed using the International Centre for Diffraction Database PDF-4 and Search-Match software by Siemens (Bruker). X-ray powder-diffraction data of the samples were refined with Rietveld program Topas 4.2 (Bruker AXS).

2.2.3.3 Lithogeochemistry

A total of 33 samples of west Banshee lamprophyre dike were analyzed geochemically as part of a mass transfer study. Prior to analysis the 33 samples were cut into blocks avoiding vein material, polished, ultrasonically cleaned, and photographed. Additionally, 10 samples of Bootstrap limestone, 5 samples of Jurassic rhyolite, and 6 samples of Eocene dacite were submitted for lithogeochemical characterization. All samples were analyzed for 56 element whole rock geochemistry by ALS Chemex in North Vancouver, Canada (see Appendix A for ALS method details and method detection limits). Au was analyzed by fire assay and ICP-AES, major elements (Si, Al, Fe, Ca, Mg, Na, K, Ti, Mn, P, and LOI) were analyzed using lithium-metaborate fusion and ICP-AES, trace and rare earth elements (Ag, Ba, Ce, Co, Cr, Cs, Cu, Dy, Er, Eu, Ga, Gd, Hf, Ho, La, Lu, Mo, Nb, Nd, Ni, Pb, Pr, Rb, Sm, Sn, Sr, Ta, Tb, Th, Tl, Tm, U, V, W, Y, Yb, Zn, and Zr) by lithium borate fusion and ICP-MS, volatiles (As, Bi, Hg, Sb, Se, and Te) by aqua regia and ICP-MS, and C and S by Leco. Sample preparation was conducted using a low Cr steel mill. Three duplicates and 2 internal standards with known chemical composition were submitted for data quality control. All samples were submitted for fire assay Au analysis with ICP finish as well at ALS Chemex in North Vancouver, Canada. Barrick Gold provided additional Au assay data. ALS quotes analytical precision of 10%, and duplicate samples have analytical precision of ~5% for most elements.

In addition to whole rock geochemical analyses a subset of samples were submitted to the Pacific Centre for Isotopic and Geochemical Research (PCIGR) at the University of

British Columbia (UBC) for Sr and Nd isotope analyses. These isotopic measurements were undertaken to asess the consistency of lamprophyre protolith. Prior to analysis, carbonate was leached from samples to prevent Sr in carbonate from being analyzed. Carbonate leaching was done using the procedure of Deniel and Pin (2001). Samples were firstly treated with ~10mL of HCl 1.5N, and ultra-sonicated for ~10 minutes. The acid was discarded then ~10 mL of 18 MΩ cm^{-1} water was added and the samples were ultra-sonicated for ~10 further minutes. The water was then removed and this step was repeated. The samples were then dried on a hot plate at ~100ºC. Following this, samples were dissolved in PTFE bombs at 190 ºC in a mixture of 48% HF and 14N HNO_3. Samples were then passed through ion exchange columns to separate the elements of interest from interfering elements. A full description of all methods used is given in Weis et al. (2006).

2.2.3.4 Stable Isotopes

A total of 20 samples were analysed for whole rock sulfur isotopes. Samples were weighed into tin capsules with equal or greater amounts of tungstic oxide, and loaded into a VarioEL II elemental analyser (EA) to be flash combusted at 1800°C. Released gases are carried by helium through the EA to be cleaned, then separated and concentrated twice by "trap & purge". SO_2 gas is carried into the DeltaPlus isotope ratio mass spectrometer (ThermoFinnigan, Germany) for analysis. Analytical precision is +/-0.2‰. The GG Hatch Isotope Lab at the University of Ottawa conducted all analyses.

Samples of illite and kaolinite from altered sections of the west Banshee lamprophyre were analyzed for δD and $\delta^{18}O$ to constrain the source of fluids and to compare the isotopic signature of the different clay types. Clay separates of the <2 μm fractions were collected from 2 illite altered and mineralized lamprophyre dike samples and 2 kaolinite altered lamprophyre dike samples from the west Banshee dike. Kaolinite altered dike samples were disaggregated in a Blendtec© blender with 200ml of distilled water for a period of time between 0.5-1 minute. Following disaggregation, the solution was probed with a 500 watt ultrasonic probe for ~5 minutes. The <2 μm fraction was separated using a high speed centrifuge. An additional illite sample previously analyzed by Ahmed (2010) from near the Leeville deposit on the northern Carlin trend was analyzed for QA/QC purposes.

Oxygen was extracted from the clay separates using a CO_2-laser and BrF_5 (Sharp, 1990). Oxygen isotope values are reported relative to Vienna standard mean ocean water (VSMOW). Samples were normalized to the international quartz standard NBS-28 using a value of +9.6 per mil (‰). Values for four NBS-28 analyzed with the samples had values that varied by less than 0.15 ‰. Samples and standards were heated overnight to 150°C prior to loading into the vacuum extraction line. These were then evacuated for approximately 6 hours. Blank BrF_5 runs were done until yield was less than 0.2 mmoles oxygen. Oxygen yields were recorded and CO_2 gas analysed on a Geo20-20 mass spectrometer. Lab data is provided in Appendix B.

For δD isotope analysis, mineral samples were analysed on a HEKAtech high temperature elemental analyser coupled with a GV Instruments IsoPrime mass spectrometer. Samples were pyrolyzed at 1450°C, in silver capsules. All samples were analysed in triplicate. All results are reported with respect to VSMOW, normalized to international standards IAEA-CH-7, NBS30 and NBS22 with reported δD values of -100‰, 66‰ and 118‰ (www.ciaaw.org/Hydrogen.htm). The precision on the standards is 1.5‰. Both δD and $\delta^{18}O$ stable isotopes were analyzed at the GNS Science Stable Isotope Laboratory in New Zealand. Lab data is provided in appendix B.

Modern groundwater pumped from the Paleozoic carbonate aquifer in the area of the Banshee deposit was collected in order to compare the isotopic composition of modern meteoric waters with calculated water values from clay samples. Samples were collected from low flow sample ports on dewatering wells at the Goldstrike property in 40mL vials with zero headspace. Samples were analyzed at the University of British Columbia. $\delta^{18}O$ values of filtered water were measured using a laser spectroscopic Liquid Water Isotope Analyzer from Los Gatos Research, Inc. at the Pacific Centre for Isotopic and Geochemical Research (PCIGR), The University of British Columbia. Three specimens of filtered water, including one replicate specimen, were analyzed for their δ^2H and $\delta^{18}O$ compositions. Reproducibility of known values from three internal UBC water standards was better than 1 ‰ for δ^2H and 0.3‰ for $\delta^{18}O$.

2.3 Banshee Gold Deposit

The Banshee Au deposit sits at the northern end of a series of Carlin-type deposits aligned with the NW striking Post fault system within the Goldstrike district on the northern Carlin trend (Figure 2.1). With > 50 million oz. of Au in past production or reserves, the Goldstrike district is the most endowed Carlin-type deposit currently known (Cline et al., 2005). While the large bulk tonnage deposits of Betze-Post and Screamer are hosted predominantly within slope facies silty limestones and lime mudstones, deposits in the northern portion of the Goldstrike district are hosted within massive platform limestones and dolomites with lower inherent permeability. Platform rocks are generally poor hosts for fluid circulation and mineralization, but the development of extensive brecciation primarily through dissolution and collapse created the necessary permeability network for mineralizing fluids (Emsbo et al., 2003; Evans, 2000). The surface expression of Banshee is minimal as it is covered by both pre- and post-mineral cover. A series of NW trending Jurassic dikes are mapped from trenches and limited surface exposure (Figure 2.2). The Banshee deposit is hosted in Jurassic lamprophyre dike and a series of generally strata-bound breccias of mixed origin. The breccias are located just below the contact between the Devonian Popovich Formation Upper Mud member and the Bootstrap limestone unit of the Silurian-Devonian Roberts Mountain Formation (Figure 2.3).

2.3.1 Lithology

2.3.1.1 Sedimentary Host Rocks

Figure 2.4 summarizes the stratigraphy of Paleozoic sediments at Banshee. The oldest rocks from the autochthonous lower plate at Banshee are from the Silurian-Devonian Bootstrap Limestone subunit of the Roberts Mountain Formation. The Bootstrap is a massively bedded platform carbonate unit up to 600 meters thick (Jory, 2002). The Bootstrap comprises a shoal facies of carbonate ooids and a fossiliferous reef facies (Furley, 2001). The Bootstrap thins to the south and west of the Banshee deposit where it transitions to the slope facies of the Roberts Mountain Formation (Armstrong et al., 1997; Evans and Mullens, 1976). Morgan (2006) conducted an alteration study of the Bootstrap limestone and described 6 different carbonate phases including limestone, diagenetic-planar dolomite, saddle dolomite, ferroan dolomite, zebra dolomite, and spar calcite. Diagenetic dolomite generally increases with depth in the Bootstrap and is not a significant component in upper portion of the Bootstrap found at Banshee (Morgan, 2006). Ferroan and zebra texture dolomite is predominantly found in the area of the Meikle deposit and is thought to result from Late Devonian sedex alteration from hydrothermal fluid flow in sediments below the seawater-sediment interface (Emsbo et al., 1999). Additionally, Morgan (2006) classified a later generation of non-planer, non-ferroan hydrothermal dolomite associate with Jurassic intrusion near the Dee-Rossi and Storm deposits to the northwest of Banshee. Above the Bootstrap limestone, a laterally contiguous 15 to 60 meters thick breccia horizon extends across the Banshee deposit. A more detailed description of the breccia units associated with this horizon is provided in Chapter 3.

Of the four informal units of the Devonian Popovich Formation (Wispy member, Planar member, Soft Sediment Deformed member, and the Upper Mud member), only the Upper Mud member is found at Banshee. The deeper slope facies members of the Popovich Formation are not found on the Bootstrap platform. The Upper Mud Member overlies the breccia horizon and the Bootstrap limestone in the Banshee area. The Upper Mud is a planar laminated muddy lime to limey mudstone deposited in a deeper water anoxic environment (Armstrong et al., 1997). The Upper Mud has a maximum thickness of ~30 meters at Banshee where it occurs in the western portion of Banshee (Figure 2.3). The Devonian Rodeo Creek Formation sits conformably above the Upper Mud. The Rodeo Creek is dominated by mudstone, chert, shale, and calcareous siltstones (Armstrong et al., 1997; Ettner, 1989). The Rodeo Creek is up to 550 meters thick elsewhere on the Carlin trend (Armstrong et al., 1997).

Structurally overlying the Rodeo Creek separated by the RMT, is the allochthonous siliceous rocks of the Ordovician Vinini Formation. The Vinini Formation consists predominantly of chert, carbonaceous mudstone and shale, limey siltstone, and siltstone (Merriam and Anderson, 1942). In the eastern portion of the Banshee deposit, the Vinini formation lies directly above the Bootstrap breccia horizon along a low angle fault presumed to be the Roberts Mountain thrust.

2.3.1.2 Jurassic Lamprophyre

Jurassic lamprophyre dikes are common in the northern Carlin trend and have been classified on the basis that they are porphyritic mafic rocks with no feldspar phenocrysts and contain at least one hydrous mafic mineral (Ressel, 2006). Two primary types of lamprophyre are common along the northern Carlin trend and can be easily differentiated based on mineralogy of mafic phenocrysts, either Mg-rich hornblende or phlogopite. Phlogopite lamprophyres have a ground mass of alkali feldspar, and amphibole bearing lamprophyre have a groundmass of plagioclase (Ressel and Henry, 2006). Recent $^{40}Ar/^{39}Ar$ ages of phlogopite phenocrysts in lamprophyre dikes from the Goldstrike district indicate they formed between 161.3 ± 1.0 and 163.2 ± 1.2 Ma (de Almeida, 2009). At Banshee, Mg-rich hornblende lamprophyres are dominant, and they fit the classification of vogesite defined as a lamprophyre with hornblende phenocrysts in a groundmass of alkali feldspar greater than plagioclase (Le Bas and Streckeisen, 1991; Ressel and Henry, 2006; Rock, 1991).

Hornblende ± phlogopite lamprophyre dike is found in both the east and west Banshee ore zones. At east Banshee the lamprophyre is most commonly found as clasts within breccia units. Intact lamprophyre is found within the Post fault zone that bounds the deposit on its upper side. The west Banshee ore zone is hosted in a northwest trending, east dipping laterally contiguous lamprophyre dike. Although the west Banshee dike is extensively mineralized, mineralization and associated alteration is spatially constrained. Non-mineralized dike exhibiting little alteration is found in close proximity to altered and mineralized dike evidencing steep gradients in alteration. Mineralization is limited to a vertical zone defined at the base by the contact between the permeable breccia horizon and the top of the low permeability Silurian Devonian Bootstrap limestone. The top of mineralization is defined by the intersection of a low angle fault that cuts the top of the ore zone (Figure 2.3).

Least altered lamprophyre dikes at both west and east Banshee are fine grained and contain Mg-rich hornblende phenocrysts with minor chlorite alteration, and dominantly plagioclase groundmass with minor illite, chlorite, calcite, and quartz (defined by XRD and optical petrography). In hand specimen, least altered dike is dark green with visible fine-grained feldspar and euhedral amphibole (Figure 2.5a). In thin section, hornblendes are slightly altered with chlorite and illite, while feldspars are partially illite altered (Figure 2.5b). Least altered samples contain very little visible pyrite (Figure 2.5c).

2.3.2 Jurassic Rhyolite Dikes

Unaltered examples of Jurassic rhyolite dikes are not found at Banshee. Formerly feldspar phenocrysts are completely replaced by illite and quartz and the groundmass contains quartz, illite, pyrite, and marcasite. Jurassic rhyolite dikes at Banshee are equivalent to Jurassic monzonites described by Emsbo et al. (2003) at Meikle to the south. Unaltered Jurassic rhyolite dikes found elsewhere in the Goldstrike district are described as finely porphyritic with plagioclase, biotite, and quartz (Ressel, 2006). Jurassic rhyolite dikes are most common in east Banshee and occur along the shallow to moderate east dipping Ren fault. Rare occurrences of the Jurassic rhyolite dike are also seen at west Banshee but are not traceable between drill holes.

2.3.2.1 Eocene Dacite Dikes

Eocene dacite dikes are found along the Post Fault in east Banshee and are not mineralized. At Banshee, Eocene dikes contain phenocrysts of biotite and hornblende while chlorite is found replacing plagioclase in the groundmass. The Eocene dikes at Banshee are similar to Ressel and Henry's (2006) porphyritic dacite dike that commonly occurs along the Post fault corridor, and are equivalent to the Eocene biotite-feldspar porphyries of Emsbo et al. (2003).

2.3.2.2 Breccia Units

A polyphase polymictic breccia occurs within a laterally continuous stratiform horizon at the upper contact within the Silurian-Devonian Bootstrap limestone. The top of the Bootstrap limestone is commonly brecciated on the northern Carlin trend with characteristic karst-like collapse breccia features and polymict breccias stoping up section along faults (Armstrong et al., 1998; Dobak et al., 2002; Emsbo and Hofstra, 2003; Emsbo et al., 2003; Evans, 2000; Furley, 2001; Williams, 1992). Evidence exists for karsting of the Bootstrap Limestone with subsequent collapse breccia formation before and after the deposition of the overlying Devonian Popovich Upper Mud (Armstrong et al., 1998). Later brecciation is evidenced by the appearance of 'upper-plate' siltstone clasts and Mesozoic and Tertiary dike clasts. The breccia unit at Banshee contains both clast and matrix supported breccias with clasts of Bootstrap Limestone, Upper Mud, lamprophyre, rhyolite, dacite, and less commonly 'upper-plate' siltstone and chert. Chapter 3 of this thesis contains a more detailed description of the breccia unit.

2.3.3 Faults and Structure

The RMT and Post fault are prominent structures along the northern Carlin trend. At Banshee the RMT places upper-plate Vinini siliciclastic rocks above Rodeo Creek mudstone in west Banshee and defines the contact between the breccia horizon and Vinini siliciclastics above east Banshee. The RMT forms a cap to mineralization at East Banshee and is intruded by Jurassic rhyolite. The Post fault is another important control on the geometry of east Banshee and generally defines the eastern margin of mineralization in the entire Goldstrike district (Bettles, 2002). At Banshee the Post fault has approximately 60 meters of normal movement placing upper-plate siliciclastics adjacent to the east of the breccia zone. Additionally, the Post fault hosts multiple generations of Jurassic lamprophyre and Eocene dacite dikes. Normal displacement along the Post fault increases to the south and is estimated to be >800 meters in the area of Betze-Post with some of the movement thought to have occurred prior to the emplacement of the Jursassic Goldstrike Stock (Bettles, 2002).

Like other lamprophyre dikes in the Goldstrike district, the west Banshee lamprophyre has a NW orientation. While the east Banshee lamprophyre dips to the SE along the Post fault system, the west Banshee lamprophyre dips to the SW. The dike was intruded into a fault thought to be a member of the NW striking JB series faults described at Goldstrike (Bettles, 2002). The JB series faults are SW dipping and are commonly intruded by lamprophyre dikes. They are important ore controlling structures in the Betze-Post deposit to the south (Bettles, 2002).

2.4 Alteration and Mineral Paragenesis

2.4.1 West Banshee Lamprophyre

At west Banshee mineralization is contained within the west Banshee lamprophyre dike. There are three alteration events evidenced by mineralogy, texture, and geochemistry.

The first alteration event consists of weak propyllitic alteration evidenced by common chlorite and calcite with trace pyrite in least-altered lamprophyre. All least altered samples exhibit at least minor propyllitic alteration. The second alteration event is spatially associated with Au mineralization and is characterize by silicification, illitization, and sulfidation. Illite-altered samples are grey to dark grey, hornblende is replaced by illite and pyrite, feldspar is replaced by illite, and the groundmass is dominated by illite, quartz, and pyrite (Figure 2.6a-d). Progressive illitization of hornblende is always accompanied with pyrite grains exhibiting arsenian rims. Abundant pyrite is seen in reflected light (Figures 2.6d) including pyrite replacement of hornblende (Figure 2.6e-f). Ore stage pyrite grains from the west Banshee dike samples collected during this study were analyzed by submicron-scale secondary inonizing mass spectrometry (nanoSIMS) and electron probe microanalysis (EPMA) as part of separate study (Barker et al., 2009). NanoSIMS imaging showed the precipitation of Au rich pyrite occurred as discrete narrow rims near the end of pyrite growth while trace element rich pyrite growth occurred both before and after Au precipitation (Barker et al., 2009). Barker et al. (2009) found that in addition to Au, ore-stage rims contained elevated Hg, Ag, Sb, Cu, and As.

The third alteration event affecting the west Banshee lamprophyre is characterized by kaolinite alteration and some brassy pyrite with low levels of Au and little trace element enrichment (Figure 2.7a). Kaolinite alteration occurs adjacent to illite alteration with a sharp contact between the alteration types. In hand specimen, kaolinite altered dike is light grey to white and less dense with a common ‘chalky’ texture with quartz and coarse-grained brassy pyrite. In thin section, kaolinite-altered samples are dominated by quartz and kaolinite (Figure 2.7b) and crosscutting coarse pyrite veining (Figure 2.7c) that cuts quartz. Kaolinite alteration is texturally destructive. Oxidized remnants of pyrite are seen in the kaolinite-altered zone and little to no ore-stage pyrite is found. Albino (1994) noted textural evidence of kaolinite alteration overprinting illite alteration in lamprophyre dikes at the Ren deposit just north of Banshee. At Banshee, textural evidence is lacking, but kaolinite overprinting is consistent with the observation of oxidized relict pyrite grains.

Figure 2.8 shows the distribution of least altered, kaolinite altered, and illite-altered lamprophyre at Banshee and their spatial association with Au mineralization. The illite-altered zone is spatially consistent with the ore zone at Banshee while kaolinite-altered samples generally lie below mineralization. Mixed illite and kaolinite alteration occurs above the ore zone with illite more abundant than kaolinite. Silicification is most intense in the ore zone, but all altered samples contain quartz. Least altered samples are found in relative close proximity to ore, but lack significant illite or kaolinite. A zone of Fe-rich dolomite is found above the ore zone in dominantly illite altered samples. Illite altered dike typically contains Au at concentrations greater than 10 ppm, while the kaolinite dikes are unmineralized to weakly mineralized with Au concentrations less than 500 ppb.

Quantitative XRD data collected from least altered, kaolinite altered, and illite altered samples are summarized in Table 2.1. Modal mineralogy data is in agreement with observations made in hand specimen and thin section. XRD analysis indicates that kaolinite altered dikes contain kaolinite + calcite + illite + quartz + minor pyrite + minor rutile + minor siderite. Mineralized and altered dikes contain illite + minor dolomite + minor rutile + quartz + pyrite + marcasite + minor K-feldspar + minor calcian albite +/- minor jarosite + minor gypsum +/- siderite.

2.4.1.1 Lithogeochemistry

Table 2.2 lists the results from lithogeochemistry analyses. The majority of samples analyzed have at least some alteration. The 2 least altered samples were collected from below mineralization and have very similar chemistry. Mean composition of the west Banshee lamprophyre (from the 2 least altered samples) is 50% SiO_2, 13% Al_2O_3, 8% Fe_2O_3, 7.4% CaO, 9% MgO, 2.2% Na_2O, 1.9% K_2O, 1.1% TiO_2, 0.1% MnO, and 0.3% P_2O_5. These values are in the range of reported values for other lamprophyre dikes in the northern Carlin Trend (Ressel, 2006). Least altered samples report values at detection limit for Au (1 ppb), Tl (0.25 ppm), W (1 ppm), and Hg (0.025 ppm). Other elements typical of Carlin-type alteration have reported values near detection limit including: As (mean<1 ppm), Sb (mean=0.15 ppm), and S (mean=0.1%). Illite altered samples of west Banshee lamprophyre dike have higher concentrations of K_2O, Cs, and Rb and lower concentrations of MgO, Na_2O, MnO, Ba, and Sr relative to least altered samples. Illite altered samples are also uniformly enriched in Au (up to 53.5 ppm) and Carlin-type pathfinder elements including As (up to >10,000 ppm), Tl (up to 77.5 ppm), Hg (up to >25 ppm), W (up to 102 ppm), and Sb (up to >250 ppm. Kaolinite altered samples exhibit marked decreases in MgO, Na_2O, MnO, K_2O, Cs, Rb, Ba, and Sr. Kaolinite altered samples have minimal Au (1-67 ppb) and contain concentrations lower than illite altered samples for typical Carlin-type pathfinder elements including: Tl (0.25-3.7 ppm), As (14.4-306 ppm), Hg (0.9-3.3 ppm), Sb (1.27-36.9 ppm), and W (4-82 ppm).

In addition to lithogeochemistry, bulk samples of lamprophyre dike from west Banshee and east Banshee were analyzed for $^{143}Nd/^{144}Nd$ isotopes (Figure 2.9). $^{43}Nd/^{144}Nd$ isotopes from 4 west Banshee dike samples (3 illite altered and 1 unaltered) have a narrow range of 0.512537-0.512555 that are nearly within analytical error (+/- 0.000008). Two samples from east Banshee lamprophyre dikes (1 unaltered and 1 illite altered) gave slightly lower $^{143}Nd/^{144}Nd$ values of 0.512457±0.000009 and 0.512474±0.000008 indicating the two dikes are isotopically distinct possibly owing to differences in crystallization between the two intrusive phases (DePaolo, 1988).

2.4.2 Other Rock Types

2.4.2.1 Carbonates

Visible mineral alteration of carbonate-bearing rocks consists of carbonate dissolution, Fe-sulfidation, trace clay alteration, and the replacement of carbonate with quartz. Clay alteration is absent from limestone and dolostone units of the Bootstrap Limestone, and only occurs in trace amounts in calcareous mudstones and clasts of Devonian Popovich Upper Mud. Fe-sulfidation is minimal, likely owing to the low reactive Fe content of Bootstrap rocks (see below). Silicification and carbonate dissolution are largely contained within the breccias at Banshee. Calcite veining is common surrounding the deposit. Late coarsely crystalline calcite is seen overprinting silicification within the breccia unit. Brassy pyrite veins also cut silicification.

Lithogeochemistry was conducted on least altered and silicified samples of Bootstrap Limestone and Bootstrap Dolostone. As expected dolostone sample contain higher MgO/CaO. Least altered limestone samples have a mean MgO/CaO ratio of 0.01, and least altered dolostone samples have an MgO/CaO ranging from 0.16 to 0.35. Fe_2O_3 averages below 0.1% for limestone and ~1% for dolostone. Least altered samples contain minimal Au (0.001-0.022 ppm) and low concentrations of typical Carlin pathfinder elements. The highest reported Au value is 0.308 ppm sampled from silicified and decalcified Bootstrap Dolostone proximal to high grade mineralization in the west Banshee lamprophyre dike. The silicified and decalcified sample of Bootstrap Dolostone has decreased concentrations of CaO (3.3%) and MgO (0.28%) and increased concentrations of SiO_2 (84.2%) and S (1.27%).

2.4.2.2 Other Intrusives

Where encountered at Banshee, Jurassic rhyolite is always altered and mineralized. Dikes are altered to illite, quartz, and pyrite±marcasite with the porphyritic texture preserved. While the dikes are generally altered and mineralized, Au contents fall below economic grades for underground mining and thus these dikes are not included in the current resource. Eocene dacite at Banshee is not mineralized, but has undergone propyllitic style alteration with abundant chlorite and smectite after biotite and montmorillonite after feldspar.

Table 2.2 details the lithogeochemistry results for all samples. Jurassic rhyolites are easily distinguishable from Eocene dacite using TiO_2 content. Jurassic rhyolite has TiO_2 values of 0.24-0.28 wt.%, and Eocene dacite has values of 0.42-0.49 wt.%. Jurassic rhyolites are uniformly altered at Banshee and contain 0.2 to 1.6 ppm Au with elevated Carlin-type pathfinder element concentrations including: As (102-903 ppm), Hg (0.9-4.7 ppm), Sb (1.3-42.3 ppm), Tl (1.4-2.2 ppm), and W (3-6 ppm). Jurassic rhyolite has lower Total Fe compared to the west Banshee lamprophyre (mean Fe_2O_3= 1.8 wt.%). Eocene dacite samples have Fe_2O_3 ranging from 0.9 to 3.63% with trace Au (0.001-0.041 ppm) and Carlin-type pathfinders. One sample of Eocene dacite sampled from a dike that cuts mineralized breccia in east Banshee contains elevated As (239 ppm), Sb (30.9 ppm), and W (14 ppm). While the breccia surrounding this sample is silicified, the dacite dike is not silicified.

2.5 Stable Isotope Results

2.5.1 Sulfur Isotopes in Bulk Rock

The only significant source of sulfur in west Banshee lamprophyre samples is from marcasite and pyrite. No sulfate minerals are found in the dike and only minor apatite. Least altered, illite altered mineralized, and kaolinite altered dikes each have distinct $\delta^{34}S$ values (Figure 2.10), and contain low concentrations of S (0.08-0.18 wt.%). Mineralized altered samples contain abundant pyrite. Kaolinite altered samples contain minor finely disseminated pyrite along with overprinting brassy pyrite mostly in veins. Least altered samples have $\delta^{34}S$ values ranging from 9.0-9.9 ‰ (CDT), consistent with $\delta^{34}S$ values determined by ion microprobe in pre-ore pyrite in unaltered Jurassic granodiorite in the Goldstrike stock (Arehart et al., 1993). Mineralized samples have values ranging from 3.5-7.4 ‰ $\delta^{34}S$ (CDT) indicating a sulfur source depleted relative to pre-ore pyrite. Two kaolinite-altered samples with late brassy pyrite have values of -10 and -8.9 $\delta^{34}S$ (CDT), while two kaolinite altered samples without late brassy pyrite have values of 4.7 and 5.2 $\delta^{34}S$ (CDT).

2.5.2 Stable Isotopes in Clay Minerals

Clay separates of kaolinite and illite have significantly different δD_{VSMOW} and $\delta^{18}O_{VSMOW}$ values at Banshee. Illite samples have δD_{VSMOW} values of -120.5‰ and -124.8‰ with $\delta^{18}O_{VSMOW}$ values of 9.2‰ and 11.3‰. The samples have a very similar isotopic composition to illite samples from near the Leeville Carlin-type Au deposit (Ahmed, 2010). Kaolinite samples have δD_{VSMOW} values of -151.8‰ and -157.0‰ and $\delta^{18}O_{VSMOW}$ values of 1.1‰ and 0.7‰.

2.5.3 δD and δ^{18}O in Modern Groundwater

Modern groundwater from the Paleozoic aquifer in the Goldstrike district has δD_{VSMOW} values of -128.1‰ and -132.4‰ and $\delta^{18}O_{VSMOW}$ a value of -15.43‰ for all 3 samples. Temperatures for the collected samples were ~60°C which is typical of temperatures in the Paleozoic aquifer along the northern Carlin trend (Barrick internal data).

2.6 Interpretation

2.6.1 Mass Transfer

In order to determine the degree of mass transfer of specific chemical components during hydrothermal alteration, changes in mass and/or volume must be considered. A number of schemes have been employed for the calculation of mass transfer associated with hydrothermal alteration. The key to calculating the relative change in mass is to account for changes in rock density with alteration. Gresens (1967) derived a set of equations that uses the measured specific gravities of altered and unaltered rocks to account for changes in mass/volume. Alternatively, immobile element concentrations may be used to define relative gain or loss in rock volume (Grant, 1986, 2005; Maclean, 1990; Maclean and Barrett, 1993; Maclean and Kranidiotis, 1987; Warren et al., 2007). Grant (1986, 2005) employed the immobile element approach graphically using isoconcentration diagrams. Using the graphical approach of Grant, elemental concentrations of altered rocks are plotted against unaltered protolith. Immobile elements plot as an isoconcentration line through the origin and chemical gains and losses plot above and below the line respectively. Baumgartner and Olsen (1995) showed one of the problems with the graphical approach of Grant is that scaling will have an effect on the results as immobile elements that plot further from the origin of the graph will have a greater influence over the isoconcentration line than immobile element concentrations nearer the origin. Rather than using the graphical method of Grant, the modified Gresen's equation of Warren et al. (2007) (Equation 2.1), which uses immobile element ratios to define mass/volume loss, was used for all calculations in this study. Immobile elements were defined by degree of correlation between typically immobile elements.

$$\Delta X = \left[\left(X^{Ai} / X^{Bi} \right) \times X^{B} \right] - X^{A}, \qquad \text{Equation 2.1}$$

where ΔX is the mass change for chemical component X, X^{Ai}/X^{Bi} is the ratio of immobile element concentrations between unaltered and altered protolith, X^B is the concentration of the chemical component in the altered rock, and X^A is the concentration of the chemical component in the least altered rock.

In order to evaluate the consistency of protolith chemistry of the west Banshee dike, REE plots and $^{143}Nd/^{144}Nd$ isotope ratios for a subset of 6 samples of mineralized to unmineralized protolith were used. Additionally, REE data from other lamprophyre dikes collected at other deposit areas were used for comparison. The data are consistent with the samples being collected from a single intrusive phase (Figure 2.9). Chondrite normalized rare earth element (REE) plots indicate that West Banshee dike samples have very similar REE patterns (Figure 2.11). The data is consistent with the dike samples representing variably altered material with a nearly identical protolith.

To identify immobile elements to use in mass transfer calculations, correlation coefficients between all analyzed elements were calculated. A total of four immobile elements with R^2 values greater than 0.90 were identified including: Al_2O_3, Hf, Nb, and Zr. Hf and Zr are likely both contained in zircons that were not affected by the hydrothermal fluid system so it's not surprising that they are highly correlated. Other high field strength elements that are unlikely to be mobilized during hydrothermal alteration such as TiO_2 show variable degrees of correlation. Even though the REE and $^{143}Nd/^{144}Nd$ indicate that the west Banshee dike was a single phase of intrusion there appears to be heterogeneity in the concentrations of certain elements in the dike. This heterogeneity is a source of error in mass transfer calculations, but it is difficult to precisely calculate the error owing to the small number of unaltered samples available from the west Banshee lamprophyre. Lamprophyres typically have a high volatile content and this may be a source of some of the heterogeneity (Rock, 1991; Streckeisen, 1980; Woolley et al., 1996). It is likely that larger samples could mitigate some of the error introduced by sampling, but the volume of material available from drill core is limited. The choice of immobile element influences the result of mass transfer calculation, and therefore reduces the precision of the calculated result. Figure 2.12 contains scatter plots showing the correlation between immobile elements. For the purpose of mass transfer calculations using Equation 2.1, Zr was chosen as the immobile element. Table 2.3 contains the calculated mass transfer of each analyzed element for the sample suite using Zr.

Changes in rock density are monitored by the Zr ratio of altered to unaltered samples. The least altered sample used for calculations was U16-H07-34-537. The sample was chosen based on extent of visible alteration in thin section, the low concentrations of volatile elements, and the lack of alkali loss. Where the Zr ratio is greater than 1 the rock has undergone mass loss and where the Zr ratio is less than 1 mass gain has occurred. The majority of altered samples have undergone variable degrees of mass loss (2-34%) with kaolinite samples having more variable results. Samples showing mass gain typically have increases in CaO with associated calcite precipitation in open space likely created by prior mineral dissolution or volume creation evidenced by veins of calcite, quartz, and pyrite. One kaolinite-altered sample (NBC-11C-1569) contains 31.7% calcite as determined by quantitative XRD (Table 2.1). One sample showing mass gain is likely owing to a high concentration of pyrite/marcasite as indicated by a >15.65 wt.% increase in S (sample U16-

H07-24-422). The more typical mass loss is due to the removal of major elements such as CaO, MgO, MnO, and Na_2O.

2.6.1.1 Major Elements

Major elements in mineralized illite altered dike samples from west Banshee show Si was added in all but two samples and K was added in all samples (Table 2.3). Fe was variably added or depleted, and Ca, Mg, Mn, and Na were depleted. Ti and P were conserved, although covariation scatter plots of Ti and P show poor correlations with immobile elements indicating P and Ti were likely mobile at least locally as indicated by the occurrence of elongate hydrothermal apatite and hydrothermal rutile identified in illite altered dike samples under SEM and XRD (as anatase).

In kaolinite altered dike samples from west Banshee Si, Al, Mn, and Ca were variably added or depleted (Table 2.3). Ca addition is likely due to the precipitation of late calcite precipitated in open space (Figure 2.13). Fe, Mg, Mn, Na, and K were all depleted. Ti and P were conserved.

2.6.1.2 Trace Elements

Trace elements in illite altered dike samples from west Banshee show Au, Ag, Cs, Rb, Tl, U, W, Hg, Sb, As, and Te were added. Ce, Cu, and Zn were variably added or removed. Sr and Ba were removed from all samples. In kaolinite-altered dikes from west Banshee U, W, As, Hg, and Sb were added. Ce, Cu and Zn were variably added or removed. Rb, Sr, and Ba were removed from all samples. Table 2.4 shows correlation coefficients for calculated mass transfer values using Spearman rank correlation. Au positively correlates (correlation coefficient >0.6) with the addition of Si, K, S, Cs, Rb, Tl, W, As, Hg, and Sb. Au has a negative correlation (>-0.6) with Ca, Mn, and C. Tl has the strongest positive correlation with Au (0.88) and Mn has the strongest negative correlation with Au. The strong correlation between Au and K/Cs/Rb has not been noted by previous studies possibly owing to the lack of constrained sampling of unaltered to altered material of relatively homogeneous protolith.

2.6.2 Mineralogical Change and Mass Transfer

Mineralogical alteration associated with mineralization in the west Banshee dike consists of silicification, sulfidation and clay alteration. The mass transfer data provides additional detail regarding the chemical changes associated with the formation of alteration minerals. Most of the illite altered samples show that silica was added during silicifiation. However, six illite altered samples show a slight decrease in silica (Figure 2.14) (Table 2.3). These six samples were collected from areas of less intense alteration and mineralization immediately above high-grade regions. The highest-grade samples all have silica addition in excess of 4 wt% indicating silica addition with silicification did accompany mineralization at west Banshee. Kaolinite altered samples also show both silica addition and silica depletion. Silicification in both kaolinite and illite altered dikes likely involved both the addition of Si from hydrothermal fluids and the alteration of pre-existing silicate minerals, with illite altered samples containing slightly higher modal abundances of quartz and greater Si addition on average (Tables 2.1 and 2.3).

The variable addition and removal of Fe indicates that both Fe-sulfidation and pyritization occurred in lamprophyre samples. Evidence of pyrite addition by pyritization is found in 4 out of 23 samples with >1 wt% gains in Fe_2O_3 (Figure 2.15) (Table 2.3). However, two samples with addition of Fe plot above the pyrite line when plotted against S indicating that Fe is found in additional mineral phases. A total of 16 out of 23 dike samples show conservation or removal of Fe indicating that sulfidation controlled pyrite and marcasite growth at Banshee. While pyrite is found in both kaolinite and illite altered dike samples, marcasite is only found in illite altered samples indicating that marcasite was not precipitated in kaolinite altered samples or marcasite was converted or destroyed during overprinting alteration. Lithogeochemical and petrographic analysis of kaolinite-altered samples indicates that most of the pyrite in the kaolinite-altered samples is brassy in colour, Au and trace element free, and commonly constrained to veins. Depleted $\delta^{34}S$ values in late pyrite dominated samples are indicative of a separate source of sulfur compared to ore stage pyrite, or to fractionation associated with oxidation (Figure 2.10).

In illite altered rocks most Fe is found in pyrite/marcasite as indicated by molar plots of mass transfer calculations of Fe versus S (Figure 2.15). However, Fe was removed from many samples, at least locally, leading to an interpretation that either the flux of sulfur added from the fluid was not sufficient to bind all reactive Fe before it entered into aqueous solution, or the sulfidation reactions forming arsenian pyrite were rate limited leading to the loss of Fe to the fluid during sulfidation.

Mass transfer data shows illite alteration was accompanied by K addition (Table 2.3, Figure 2.16). Illite alteration is also accompanied by significant enrichment in Cs and Rb (Table 2.3). Removal of K is indicative of kaolinite alteration, and all kaolinite altered samples show removal of K, Rb, and Cs. Figure 2.16 suggests that kaolinite alteration occurred as an overprint of illite alteration. There are no samples plotting along a kaolinite alteration path from least altered samples where as samples do plot along an alteration path from illite to kaolinite. Quantitative XRD data is supportive of the mass transfer data. Kaolinite altered samples have lost all orthoclase and contain only 2.3-7.7% illite while illite altered samples contain 1.5-2.1% orthoclase and 16.8-33.5% illite (Table 2.1). In least altered samples, K is confined to feldspar.

Kaolinite altered samples show depletion in K, Ca, Mg, Mn, and Ca with variable Si addition or depletion consistent with near complete alteration to kaolinite and quartz. Quantitative XRD data indicates kaolinite altered samples still contain up to 7.7% illite. Many of the kaolinite altered samples and some of the illite altered samples show an increase in Ca and C owing to the precipitation of calcite in open space late in the alteration paragenesis. Late coarse calcite veining is common in deposits of the northern Carlin trend (Emsbo and Hofstra, 2003; Emsbo et al., 2003; Evans, 2000; Williams, 1992). In addition to calcite, quantitative XRD indicates that dolomite, Fe-rich dolomite, and siderite were added to some samples. Figure 2.17 shows the distribution of Ca data versus C and differentiates samples with calcite addition from those with variable dolomite addition. When illite altered samples are ordered by Au concentration, Mg depletion is seen to increase with increasing Au grades with a steep drop off at between ~0.5-2 ppm Au (Figure 2.18). Petrography and quantitative XRD data indicates that hornblende destruction was complete for all illite altered samples. In the most intensely altered parts of the dike, the Mg released from hornblende was removed by the infiltrating fluid. In the less illitized samples less of the Mg was removed from the rock. Rather it was incorporated into newly formed dolomite (Figure 2.19). These samples also contain lower abundances of pyrite indicative of incomplete sulfidation allowing Fe to be precipitated into dolomite. All of the dolomite altered samples sit outside and above the main Au mineralized zone suggesting that there is a dolomite alteration zone peripheral to high grade Au zones where the hydrothermal fluid was presumably buffered to higher pH values by fluid-rock interaction (Figure 2.20). The existence of a dolomite alteration zone could be used as a vector toward fluid buffered zones of increased wall rock alteration and possibly economic grades of Au mineralization.

2.6.3 Fluid Sources Inferred from Stable Isotopes

δD and $\delta^{18}O$ isotopes in various clay minerals from Carlin-type Au deposits have been used to define variable input of magmatic and meteoric fluids. The data has also been used to define clay alteration consistent with precipitation from exchanged hydrothermal fluids (Cline and Hofstra, 2000; Cline et al., 2005; Hofstra and Cline, 2000). Figure 2.20 plots H_2O equivalent values for δD and $\delta^{18}O$ kaolinite and illite clay separates from Banshee against previous data collected from Carlin-type Au deposits. Calculations of fluid equivalent values are conducted at a specific temperature to account for temperature dependent fractionation. Banshee illite separates are assumed to have formed within the range of temperatures (180-240°C) reported from fluid inclusions in ore stage quartz (Cline et al., 2005; Hofstra and Cline, 2000; Lubben, 2004). Kaolinite alteration is interpreted to be an overprint of the hypogene hydrothermal system at Banshee and has different δD and $\delta^{18}O$ values than illite that could not have formed in equilibrium. The temperature for kaolinite is unknown, but if it represents post-mineralization overprinting it likely formed at lower temperatures. Emsbo and Hofstra (2003) estimate a temperature of ~70°C from post-ore calcite and barite fluid inclusions at the Meikle deposit. Figure 2.20 calculates fractionation of δD and $\delta^{18}O$ with Banshee kaolinite at 70°C. At 70°C, fluid equivalent δD and $\delta^{18}O$ values from Banshee kaolinite are indistinguishable from modern groundwater, which is close to the meteoric water line. If kaolinite fractionation is calculated at 200°C, Banshee kaolinite samples plot within a group of kaolinite determined by previous studies (Figure 2.20). This result indicates that the fluids responsible for much of the kaolinite alteration described on the Carlin trend may have been at much lower temperatures and only weakly exchanged with the surrounding carbonate bearing wall rocks. Further work should concentrate on establishing more concrete criteria for evaluating the paragenesis of kaolinite alteration relative to Au mineralization in other Carlin-type deposits. At Banshee, kaolinite is unrelated to Au, post dates illite, and is an alteration product of a separate relatively cool unexchanged meteoric fluid.

$\delta^{34}S$ isotope data is further supportive of two fluids being responsible for the observed illite and kaolinite alteration in wall rocks. Illite altered samples have a narrow range of $\delta^{34}S$ values consistent with the interpretation of a common reservoir of sulfur for Au-bearing arsenian pyrite. The data also shows a decrease in $\delta^{34}S$ relative to least altered lamprophyre samples. The fact that least altered samples contain minimal sulfur (~0.1%) means that early pyrite sulfur does not greatly influence the measured values from bulk samples of dike. $\delta^{34}S$ values from brassy pyrite associated with kaolinite-altered dikes have lower $\delta^{34}S$ values clearly indicating a separate source of sulfur for later stage pyrite alteration. In addition to bulk rock $\delta^{34}S$ data presented in this study, ore-stage pyrite grains from the west Banshee lamprophyre have been analyzed using nanoSIMS (Barker et al., 2009). The nanoSIMS study produced images that show relative changes in $\delta^{34}S$ in pyrite as related to Au-rich zones in pyrite (Figure 2.22). Data from both the nanoSIMS study and this thesis suggest that earlier stages of pyrite in Banshee lamprophyre had heavier $\delta^{34}S$ signatures and that mineralized and sulfidized dike had relatively lighter $\delta^{34}S$ values. The nanoSIMS imagery further supports this conclusion by showing a shift in the relative ratio of $\delta^{34}S$ between the earlier pyrite core and arsenian pyrite overgrowth. This observation provides compelling evidence that bulk sampling in this constrained set of dike samples at Banshee differentiates separate populations of $\delta^{34}S$ data related to different pyrite growth events, and also clearly links ore stage pyrite with $\delta^{34}S$ values within a narrow range of 3.5‰ to 7.4‰. Another benefit of the $\delta^{34}S$ data at Banshee is that it does not include earlier syn-sedimentary and/or diagenetic pyrite providing for a more straightforward interpretation of the results. The combination of a depleted sulfur source for pyrite and the possibility of a lightly to unexchanged cool meteoric fluid being responsible for kaolinite alteration further argues for an interpretation that kaolinite alteration is indeed an overprint on mineralization.

2.7 Discussion

2.7.1 Relationship of Mineralization to Clay Alteration

Illitization accompanying Au mineralization at west Banshee is associated with addition of K, Cs, and Rb. Most previous studies of Carlin systems have not identified the elements clearly tied to illite formation, such as K, Cs, and Rb, with the addition of Au (Cail and Cline, 2001; Emsbo et al., 2003; Hofstra and Cline, 2000; Hofstra et al., 1999; Kesler et al., 2003; Yigit and Hofstra, 2003). Previous mass transfer studies have concluded that Rb, K, and Cs were not uniformly added to the wall rock during alteration (Cail and Cline, 2001; Emsbo et al., 2003; Hofstra and Cline, 2000; Hofstra et al., 1999; Kesler et al., 2003; Yigit and Hofstra, 2003), and in some cases authors have described the removal of K with illite alteration (Cail and Cline, 2001). The lack of correlation between Au and K/Al molar ratios and other chemical indicators of clay alteration may be an artifact of the predominance of pre-mineralization K-phylosilicates within sedimentary packages. At Banshee, the Jurassic lamprophyre removes the potential for pre-Jurassic sedimentary K-silicate alteration. Indeed the addition of K, Rb, and Cs identified in mass transfer calculations correlates well with Au mineralization (Table 2.4). The observation of K, Rb, and Cs addition as well as their spatial and statistical correlation with Au provides a clear link between illite alteration and Au mineralization not previously documented. The constrained nature of this study demonstrates that K-metasomatism, and by inference illite growth, and Carlin-type Au mineralization are linked at Banshee.

Kaolinite alteration is thought to be associated with many Carlin-type Au systems. At Banshee, kaolinite is found in close proximity to illite alteration and Au mineralization, but there is no clear link between mineralizing fluids and kaolinite. On the contrary, evidence presented in this chapter argues that kaolinite alteration occurs as an overprint on mineralization and has no connection to mineralization.

2.7.1.1 Trace Element Metasomatism

The best-constrained relationship between Au mineralization and alteration is auriferous arsenian pyrite. Previous studies have clearly placed Au as occurring within rims on ore-stage pyrite grains (Bakken et al., 1989; Barker et al., 2009; de Almeida et al., 2010;

Large et al., 2011; Large et al., 2009; Wells and Mullens, 1973). The west Banshee dike affords the opportunity to analyze pyrite without the complications of syn-genetic and diagenetic pyrite growth events recognized in the surrounding sediments (Emsbo et al., 1999; Large et al., 2011; Large et al., 2009). Electron probe microanalysis (EMPA) and submicron secondary ionizing microscopy (nanoSIMS) was performed on ore stage pyrite grains from the suite of lamprophyre dike samples presented in this study from Banshee (Barker et al., 2009). The Barker et al. (2009) study provides valuable insight on the distribution of trace elements defined in this mass transfer study as well as additional clarity regarding the depletion in $\delta^{34}S$ seen with mineralized dike samples at Banshee. The authors found that while As and Sb are ubiquitous through the entire pyrite growth stage, Au always occurs later in the growth of arsenian trace element rich pyrite as discrete narrow zones within the As enriched rim. Consequently, whereas all trace elements might be transported as part of the same hydrothermal event, incorporation rates of trace elements and Au into pyrite were not equal. This study shows that several elements added during alteration that were likely incorporated into pyrite were not detected by EPMA due to high detection limits or matrix issues including W, Tl, and Te.

It is believed that the growth of arsenian pyrite through Fe-sulfidation reactions was the dominant control on the addition of Au and associated pathfinder element in Carlin-type Au deposits (Cline et al., 2005; Hofstra and Cline, 2000; Hofstra et al., 1991). However, the addition of Au is not proportional to the incorporation of other trace metals in pyrite. Barker et al. (2009) showed that Au occurs in discrete rims bracketed by Au-poor trace element rich pyrite. Four potential causes for the incorporation of discrete Au rims nearer the edge of ore stage are: 1) Au was sourced from exotic fluid pulses that were injected into an otherwise Au poor hydrothermal system; 2) Au precipitation is the result of repeated changes in the physiochemical condition of the hydrothermal system that drove supersaturation and rapid precipitation of Au; 3) cyclic changes at the pyrite/fluid interface drove the precipitation of Au from Au undersaturated fluids; or 4) cyclic reduction in the concentration of S in the fluid sufficient to destabilize Au bearing S complexes causing rapid precipitation of Au. Future work should seek to resolve the mechanism of incorporation of Au and trace elements into pyrite in Carlin-type Au systems.

2.7.2 Fluid Chemistry

The addition and removal of chemical component during fluid rock interaction provides insight into the physiochemical conditions of the fluid during ore deposition. Hofstra and Cline (2000) note that low temperature fluids (<250°C) with high H_2S concentration (>10^{-2}m) will have low concentrations of base metals due to the suppression of chloride complexes in favor of reduced sulfur complexes. Fluid inclusion data indicates ore fluids had ~2-3 wt% NaCl equivalent and 10^{-1}-10^{-2} m H_2S (Cline et al., 2005). Au can be transported as $Au(HS)^0$ or $Au(HS)_2^{-1}$ in solutions with sufficient H_sS (Seward, 1973). As and Sb have similar properties and can be transported by reduced sulfur complexes, hydroxyl complexes, and oxyanion complexes. At temperatures >150-200°C, oxyanion and hydroxyl complexes are favored (Spycher and Reed, 1989). Hofstra and Cline (2000) note that sulfur complexes are still significant even if they are not the predominant complexes. Another element consistently added to the wall rock at Banshee is W, which is typically associated with oxyanion complexes. The deportment of W is unknown due to the high minimum detection limits of EPMA analyses, but they are assumed to occur in ore stage pyrite as other known tungsten bearing minerals are absent.

The lack of K, Rb, and Cs addition noted in other Carlin-type deposits is likely a function of sampling design and the lack of available materials for testing altered rocks against their unaltered equivalents rather than indicating that the fluid was not capable of K metasomatism. Potassium is not locally abundant within the wall rocks at Banshee except in volumetrically minor igneous dikes; therefore, the source of K is likely deeper along the flow path where the fluid interacted potassium bearing rocks such as felsic intrusive or arkosic siliciclastic rocks. In epithermal and geothermal environments, potassic metasomatism is used as evidence of a cooling fluid path that results in the precipitation of K-silicates. Published work invoking the cooling path concept is predominantly in volcanic terrains where fluids are buffered with feldspar (Giggenbach, 1997). The interpretation at Banshee is that the presence of K-metasomatism is similarly a product of cooling. The key to recognizing K-metasomatism in Carlin-type Au systems is to design sampling programs to collect material that has sufficient Al available to grow common K-silicate minerals such as illite.

Dating of K-silicate alteration products has proved challenging in Carlin-type deposits with illite ages being uniformly older than the mid-Tertiary age ascribed to Carlin-type deposits in Nevada (Arehart et al., 2003). Illite samples dated to present either define an unrecognized earlier stage of alteration broadly coincident with Carlin-type mineralization, or they represent mixtures of younger illites associated with Carlin mineralization and older illites formed from older alteration events such as deep diagenesis or igneous activity. The interpretation of Arehart et al. (2003) and Folger et al. (1998) is that older dates represent mixes of older and younger illites. Modeling by Hall et al. (2000) indicates that Carlin fluids (<250C) were not capable of thermally resetting the Ar^{40}/Ar^{39} thermochronometer of older stages of illite growth on reasonable time scales. Arehart et al. (2003) suggests that the addition of K during alteration is an indication that new mineral growth of illite likely occurred and that material may be a good candidate for either K/Ar or Ar^{40}/Ar^{39} dating. The well constrained addition of K at Banshee provides just such material, and further work should involve the dating of illite separates from the west Banshee ore zone.

2.7.3 Sources of Fluid Components

δD_{VSMOW} and $\delta^{18}O_{VSMOW}$ isotope values from Banshee fit within the range of previous published values, but the constrained nature of sampling where samples were collected from rocks altered by K-metasomatism correlated to Au, and the careful preparation procedures for mineral separation should provide for more representative results. The data here supports meteroric-derived fluids that have undergone exchange with rocks along the flow path. The lack of data trending toward magmatic values does not support a dominantly magmatic fluid although the number of samples collected for this study is not sufficient to evaluate this question conclusively, but the data is permissive of chemical components in the fluid (i.e. Au and S) being source from magmas at depth. An important point to note on the interpretation of this and previous isotope data is the importance of temperature dependent fractionation. Calculating kaolinite values for temperatures of 70°C and 200°C has a significant impact on where the results plot in δD and $\delta^{18}O$ space. It is possible that some of the previous isotope data collected from Carlin-type deposits comes from clays unrelated to the Carlin mineralizing events. Clear paragenetic relationships between Au precipitation and clay formation are typically lacking in Carlin-type Au system and relationships are commonly assumed based on whether or not a sample is mineralized and if the observed alteration is in veins or matrix. Data presented in Figure 2.20 shows 6 samples from previous studies plot in the same field as Banshee kaolinite when fractionation is calculated at 200°C. The 2 samples from the Carlin deposit are described as kaolinite hand picked from pods and pockets from a severely altered dike sample and from veinlets in unoxidized bedded jasperoid (Kuehn, 1989). In this case the δD_{VSMOW} and $\delta^{18}O_{VSMOW}$ isotope values were used as the criteria for defining the samples as hypogene (Kuehn, 1989) owing to the fact that they plotted off the kaolinite line of Taylor (1997). However, this conclusion assumes that waters responsible for kaolinite alteration were cooler than the 70°C used for calculations in this study. Another kaolinite sample collected by Ahmed (2010) is from a clay seam that also contains smectite/montmorillonite. The sample was collected from 'upper-plate' siliciclastic rock and is not clearly linked to mineralization as it was collected well above known mineralization (Ahmed, 2010). Samples of kaolinite collected from the Deep Post/Betze deposits at Goldstrike are interpreted to be hypogene because δD_{VSMOW} values fall within range of δD_{VSMOW} presumed to be correlated to Tertiary meteoric waters (Cline et al., 2005). However, δD_{VSMOW} values from modern groundwaters from Goldstrike fall within the same range of δD_{VSMOW} values purported to be indicative of the Tertiary (Hofstra et al., 1999). Further the lack of mid-Tertiary ages of K-silicate minerals raises questions about the age of clay alteration and its correlation to the Au event. Previous attempts at dating illites using K-Ar or Ar^{40}/Ar^{39} have reported ages much older (commonly Cretaceous (Hall et al., 2000)) than the presumed Eocene mineralization age for Carlin-type Au systems in Nevada (Arehart et al., 2003).

Samples from this study show a significant relationship between addition of K/Al and Rb with Au addition (Table 2.4) strongly arguing for a direct link between mineralization and illite clay alteration. Quantitative XRD data and the K/Al molar ratio plot (Table 2.1, Figure 2.16) show that Au enriched samples have significant illite growth. The link between illite growth and Au mineralization provides further evidence that δD_{VSMOW} and $\delta^{18}O_{VSMOW}$ isotope values measured from illite at Banshee are representative of ore fluids. The fact that the Banshee illite plot within a range of other illite samples collected at various Carlin-type deposits adds further support to the interpretation that these samples are representative of typical Carlin ore fluids.

$\delta^{34}S$ values reported here from illite altered mineralized samples show a consistent source of sulfur with a narrow range of isotopic composition. The data also shows that bulk sampling of Jurassic lamprophyre with limited pre-ore sulfide is an acceptable method for determining $\delta^{34}S$ for Carlin-type deposits. H_2S equivalent values for $\delta^{34}S$ at Banshee are 1.7-5.6‰ using the fractionation calculations of Ohmoto and Rye (1979) at 200°C. At the Screamer deposit in the Goldstrike district, Kesler estimated that ore-fluid had an average $\delta^{34}S$ of ~0‰ using SIMS analysis of ore stage rims on pyrite. Kesler et al. (2005) concluded that the data at Screamer was indicative of a magmatic input of sulfur with $\delta^{34}S$ from -1 to 3‰. Kesler et al. (2005) also noted that Au-poor arsenian pyrite had an average value of 10‰ and that mineral separates were likely a mixture of values. Emsbo et al. (2003) reported a range of 7-13‰ (H_2S equivalent values) for ore stage pyrite separates at Meikle and 8-11‰ for Betze-Post and concluded sedimentary sources could account for the $\delta^{34}S$ values at Meikle in both deposits. The whole rock data from Banshee is more similar to Kesler et al.'s (2005) estimates for the ore fluid. While the data collected from Banshee are not conclusive for a source of sulfur, the data is consistent with the magmatic source inferred by Kesler et al. (2005). Further work should seek to constrain the $\delta^{34}S$ values using microanalysis of the ore-stage rims identified by Barker et al. (2009).

2.7.4 Fluid Volumes

Mass transfer calculations and mineral alteration observations indicate that very little sulfur was present in the west Banshee lamprophyre prior to Carlin-type mineralization. Pre-ore pyrite represents a minimal contribution to the concentration of sulfur in mineralized dike. The total amount of sulfur added to the west Banshee dike during hydrothermal alteration can therefore be estimated using the mean value of sulfur addition from mass transfer calculations and the volume of mineralized dike material. The volume of mineralized west Banshee dike is estimated to be ~168,000 m^3 using a cutoff of 3.4 ppm (C. Weakly, pers. comm.), and the mean sulfur concentration within the dike determined from mass transfer calculations is ~2000 moles/m^3. The cutoff concentration for Au does not remove a significant volume of mineralized material from the calculation as mineralized dike rarely has Au concentrations below cutoff grade (C. Weakly, Pers. Com.). The specific gravity of lamprophyre dike is estimated at ~0.37 m^3/ton, and 22 cm^3 is used as the molar volume of water (same as for reaction path modeling in Chapter 4 of this thesis). Hofstra and Cline (2000) report that ore stage fluid inclusions from Carlin-type Au deposits average 0.036 to 0.071 mol% H_2S. For simplicity a value of 0.05 mol% H_2S is used. Using these parameters, simple mass balance calculations can provide a minimum estimate of fluid necessary to account for the amount of sulfur added to the dike. Certain assumptions must be made for such a calculation including: that the sampling of the west Banshee dike is representative of the distribution of sulfur in the entire dike, the concentration of H_2S in fluid inclusions of other Carlin-type deposits is representative of H_2S in Banshee ore fluids, and the supply of reactive Fe was sufficient to sequester S into pyrite through sulfidation reactions (Equation 2.2).

$$2H_2S + Fe^{+2} = FeS_2 + 2H^+ + H_2 \qquad \text{Equation 2.2}$$

While auriferous pyrite represents a volumetrically minor component of arsenic rich ore pyrite (Barker et al., 2009), calculations assume arsenian (Au-poor) pyrite was precipitated during the same hydrothermal event as Au. Nearly all of the pyrite growth occurred from sulfidation reactions with the ore fluid. Fluid volumes calculated in this manner are minimum estimates of the total fluid flux of the hydrothermal system at Banshee.

Using the above constraints the amount of fluid required to account for the total amount of sulfur added to the west Banshee dike is estimated to be ~1.5×10^7 m^3 of fluid. Taking the calculations further a minimum concentration of Au in the fluid can be estimated using the total contained ounces of Au. The current estimate of contained ounces within the west Banshee dike is ~220,000 ounces or 6.237 million grams. Using the calculated minimum volume of fluid at west Banshee the concentration of Au in the fluid would need to be up to ~500 ppb to account for the total Au endowment. There are few direct measurements of Au concentrations in hydrothermal ore fluids. Studies of active Au bearing hydrothermal fluids have measured <0.1 to 23 ppb Au (Simmons and Brown, 2007) in the Taupo volcanic zone of New Zealand and ~15 ppb (Simmons and Brown, 2006) in deep fluids associated with the Ladolam deposit in Papua New Guinea indicating that the estimate of Au in fluids at Banshee is higher than that measured for modern epithermal-type systems. Ladolam has only ~6×10^{-4} mol/kg (or ~0.002 mol%) H_2S. Much less than the 0.036 to 0.071 mol% H_2S estimated from CO_2/H_2S ratios measured from fluid inclusions in Carlin-type deposits (Hofstra and Cline, 2000). Without measurements from modern analogues of Carlin hydrothermal fluids, it is not possible to validate the estimated concentration of Au in the fluids at Banshee, but the concentration is consistent with estimates of Au solubility in Carlin-type deposits by Hofstra and Cline (2000). Hofstra and Cline (2000) used 0.01 mol% H_2S for their calculation, but using their solubility modeling 0.036 to 0.071 mol% H_2S would increase the solubility of Au. The supply of sulfur likely exceeded the reactive capacity of the dike and the real flux of sulfur and fluid was probably much higher than the estimates calculated here. Simmons and Brown (2007) estimated that the Ladolam epithermal system could have formed over the course of 55,000 years with 50 kg/s fluid flux. Over that time the total volume of fluid would be 8.7×10^{12} m^3. Ladolam is a ~44 million ounce Au deposit compared to the ~220,000 contained ounces at Banshee (200 times larger). At the Jerritt Canyon Carlin-type deposit, Hofstra and Cline (2000) estimated a minimum total fluid volume of 3.1×10^9 m^3 with 0.01 mol% H_2S and 100 ppm Au to account for the 10 million ounce Au endowment of the district. The estimate from west Banshee is a minimum, and it is likely that the actual fluid volumes were much higher than calculated.

2.7.5 Deposit Formation – Comparison to Carlin-type Deposit Models

The data presented here provides means to develop a framework for the formation of the Banshee Au deposit. Prior to mineralization extensive collapse brecciation occurred on the top of the bootstrap limestone. This early stage of brecciation was important for providing high permeability flow path through relatively impermeable massive Bootstrap limestone. During the Mississippian, the RMT placed the low permeability siliciclastic rock above the more permeable breccia zone creating a low permeability cap to focus fluids through the breccia. In the Jurassic, porphyritic rhyolite dikes exploited pre-existing faulting and intruded along the upper contact of the breccia below the RMT. Jurassic lamprophyre dikes intruded along high angle NW trending structures along the Post fault in east Banshee and a JB series fault at west Banshee. The lamprophyre dike cut across the breccia zone creating a lower permeability barrier to fluids flowing across the breccia.

At some stage well after dike emplacement, during the Carlin hydrothermal event(s), reduced, acidic, auriferous, hydrothermal fluids moved up along faults and exploited the permeable breccia horizon resulting in carbonate dissolution and permeability enhancement. The acidity of the fluid is evidenced by dissolution of carbonate minerals within the breccia zone and dissolution of feldspar and hornblende in dikes. The oxidation state of the fluid and its Au carrying capacity is evidenced by abundant sulfidation of Fe in the wall rocks, the precipitation of Au within rims of ore stage pyrite, and the lack of sulfate minerals. Isotope data from illite in west Banshee lamprophyre indicates the fluid is largely exchanged meteoric water. When the ore fluids dissolved sufficient carbonate bearing wall rock, collapse breccia formed containing clasts of multiple lithologies. Sulfidation reactions occurred when reduced sulfide complexed with Au and other trace elements reacted with Fe liberated from reactive Fe bearing minerals to produce pyrite (Hofstra et al., 1991). As sulfur was removed from the fluid, trace metals in the fluid became saturated and precipitated ore-stage pyrite. This process eventually lead to the precipitation of Au-rich rims on arsenian pyrite. Fluids continued to be focused through the permeable breccia horizon as they moved through the west Banshee dike. Reactive Fe-rich hornblende reacted with the fluid leading to pseudomorphic replacement of the hornblendes by arsenian pyrite and the transfer of significant metal from the fluid to the dike. Lithogeochemical and mass transfer data indicate that Fe in the west Banshee lamprophyre, where it intersected the breccia, was completely consumed by sulfidation reactions (Figure 2.15). As the hydrothermal system shut off, the fluid began to cool and as cooler meteoric groundwater infiltrated the system silica was driven out of solution and precipitated as quartz (Hofstra and Cline, 2000). These processes of cooling and quartz precipitation lead to the nearly complete silicification of the ore zone and primary fluid pathway within the breccia.

It is proposed that kaolinite alteration at Banshee is a post-mineral alteration event on the basis of the isotope data and the lack of arsenian pyrite, the observation of overprinting kaolinite alteration in lamprophyres at Ren just to the north (Albino, 1994), and the near complete textural destruction by kaolinite alteration of lamprophyre dike immediately adjacent to silicified high grade illite altered dike. While these observations are not diagnostic of younger groundwater being the source of all kaolinite alteration in Carlin-type Au systems, the data indicates that at least some kaolinite within the Banshee Carlin-type deposit overprints the Au-mineralizing system.

A post-mineralization hydrothermal fluid in the area of Banshee is also consistent with the Emsbo et al. (2003) study of Meikle. In their work they describe a Pleistocene age, low temperature (70°C) fluid that caused extensive carbonate dissolution and formation of late stage brecciation. Emsbo et al.'s (2003) dating of calcite from this later event indicates a Pleistocene age. The fluid at Meikle was also responsible for the precipitation of late brassy pyrite and precipitation of calcite. The fact that late brassy pyrite with a distinctly low $\delta^{34}S$ signature is found as veins within kaolinite altered dike at west Banshee is consistent with the data from Meikle. Elevated trace elements and the presence of relict arsenian pyrite with $\delta^{34}S$ values consistent with ore stage pyrite indicates that some of the kaolinite altered dike might have originally been altered by the ore fluid as well. It is possible that oxidation of preexisting pyrite both in the dike and sediments along the flow path of the post-mineralization alteration fluid was responsible for driving the acidity needed to break down illite into kaolinite. The evidence for extensive oxidation is weak as there is very little Fe-oxide found in the kaolinite-altered dike. Emsbo and Hofstra (2003) propose a model for acid generation in later fluids through the generation of sulfuric acid by oxidation of H_2S rich fluids from interaction with oxidized meteoric fluid. A similar process could be responsible for the generation of acid rich fluids at Banshee. At Meikle later acidic fluids were responsible for extensive dissolution of carbonate and sedimentation of ore stage pyrite grains resistant to acid alteration (Emsbo and Hofstra, 2003).

Following mineralization at Banshee acidic meteoric fluids may have descended along faults altering Lamprophyre dike above and below the ore zone. It is proposed that silicification of the ore zone effectively destroyed permeability and protected the ore deposit from groundwater descending along the fault hosting the west Banshee lamprophyre. A lack of post mineral alteration attests to the fact that the ore zone was not affected by this later event.

2.7.6 Fluid Flow Pathways, the PRB and Implications for Exploration

The genesis of the Banshee Au-deposit is similar to other Carlin-type Au deposits in Nevada. Alteration and ore assemblages are consistent with the general characteristics that define Carlin-type Au systems (Hofstra and Cline, 2000). The 2 primary controls for the Banshee Au system were: 1) the focusing of ore fluids in pre- and syn-mineralization breccias; and 2) the reactivity of lamprophyre dike to sulfidation reactions with precipitation of trace metal and Au-rich pyrite. The lack of visible alteration (i.e. carbonate dissolution and silicification) and Au outside of the breccia unit at Banshee is consistent with an interpretation that the permeability network within the breccia was the primary control on the migration of ore forming fluids within the deposit. The presence of low permeability massive limestones below, and siliciclastic rocks above, the breccia horizon served to further focus fluids through the breccia. Whereas polymict breccias within the breccia unit in east Banshee hosts considerable Au owing to the abundance of lamprophyre clasts, at west Banshee reactive lamprophyre clasts are largely absent within the breccia. Breccia in the area of west Banshee is dominated by Bootstrap limestone and Popovich Upper Mud clasts. The breccia unit at west Banshee is intensely silicified proximal to the dike but contains only low sub-economic Au concentrations (typically <300 ppb). The reason for the lack of significant quantities of Au in the breccia at west Banshee was likely due to the lack of reactive Fe in the protolith. Bootstrap limestone from this study has a median value of 0.07 wt.% Fe and Bootstrap dolostone contains a median value of 0.62 wt% Fe. Previous authors have clearly demonstrated the correlation between reactive Fe content, the degree of wall rock sulfidation, and the potential for high grade Au mineralization (Emsbo et al., 2003; Hofstra and Cline, 2000; Hofstra et al., 1991). Jurassic rhyolite within the flowpath of the mineralizing fluid is also intensely altered and mineralized but contains a maximum value of 1.99 wt.% Fe_2O_3 and 1.615 ppm Au. Jurassic lamprophyre from west Banshee has a median value of 7.52 wt.% Fe_2O_3 and a maximum Au concentration of 53.5 ppm. The greater reactivity of the west Banshee lamprophyre is evident when compared to other rocks within the deposit, but the west Banshee lamprophyre was an even more ideal host owing to the fact that it cut completely across the main flow path in the breccia horizon into lower permeability lithologies above and below the breccia. In this way the west Banshee dike acted as a permeable reactive barrier (PRB) to fluid flow. A PRB is a volume of reactive material that intercepts fluids, provides a flow path for fluids, and reacts with the fluid to precipitate immobile species (Khan et al., 2004). PRB's are typically thought of as engineered barriers for remediation of subsurface contaminant plumes, but the concept of PRB's can be extended to natural systems as well. At west Banshee the lamprophyre dike serves as an efficient PRB by creating a laterally continuous barrier that intersects high permeability zones and forces fluid to flow through the less permeable barrier.

The model of a natural PRB system at west Banshee has implications for exploration for other Banshee-type occurrences of Carlin-type mineralization. As the fluids infiltrated the west Banshee dike progressive alteration occurred along the flow path eventually propagating through the entire thickness of the dike. Once the reactive capacity of the dike was reached, the precipitation of ore ceased. The fact that all of the Fe in the dike was sulfidized by the fluids within the mineralized zone indicates the concentration of reactive components in the fluid (i.e. reduced S species) exceeded the supply of Fe in reactive mineral phases. Assuming the fluid still had a sufficient supply of sulfur complexed to Au and other trace elements the system would pass through the dike and continue along the flow path until another reactive host was intersected or reactive fluid components were attenuated to the point where significant reaction was no longer possible.

Brecciation at the top of the Bootstrap limestone is extensive on the Goldstrike property and to the north where additional Carlin-type deposits are found (pers. com. C. Weakly). Additionally, in areas surrounding Banshee, the breccia is consistently silicified or otherwise altered and contains anomalous levels of Au and other trace elements. The PRB model suggests that the breccia horizon found at the upper contact of the Bootstrap serves as an excellent pathway for focusing fluids across a large area. Furthermore, owing to the lack of significant reactive Fe within the permeable breccia, it is unlikely to strip much Au and other elements out of the fluid except across longer path lengths. Because the fluid is being focused laterally and not depleted of ore forming elements there exists the potential for the mineralizing fluids to intersect another PRB of similar qualities to the west Banshee dike (Figure 2.23). Using the PRB framework, an effective strategy for exploring for Banshee-type deposits would be to project structures intruded with lamprophyre to unexplored areas and target drill holes for the intersection of lamprophyre with the breccia horizon at the top of the Bootstrap limestone.

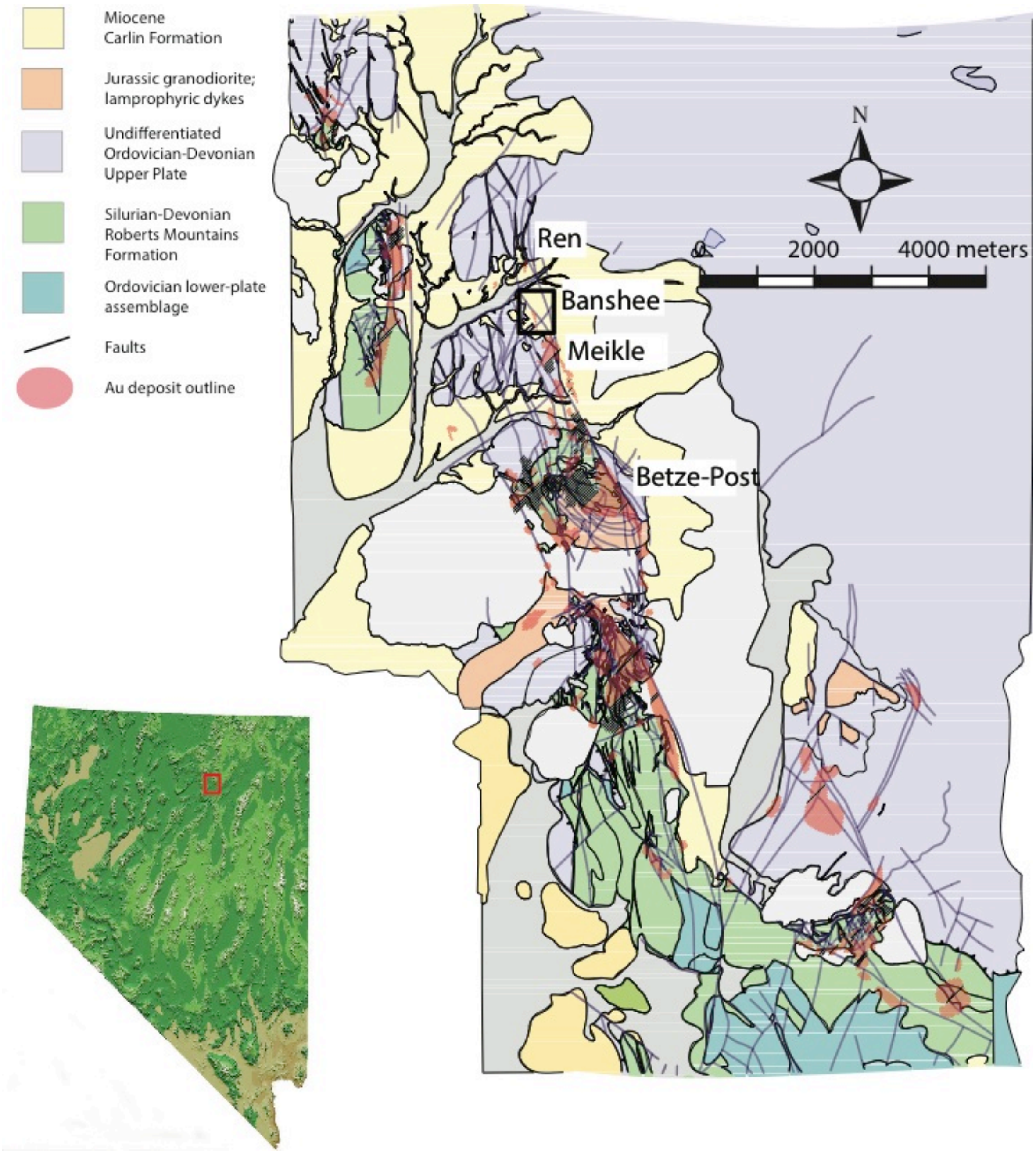

Figure 2.1 Geologic Map of the northern Carlin Trend in northeast Nevada, USA showing the location of Banshee and other key deposits in the Goldstrike district. After Thompson et al. (2002)

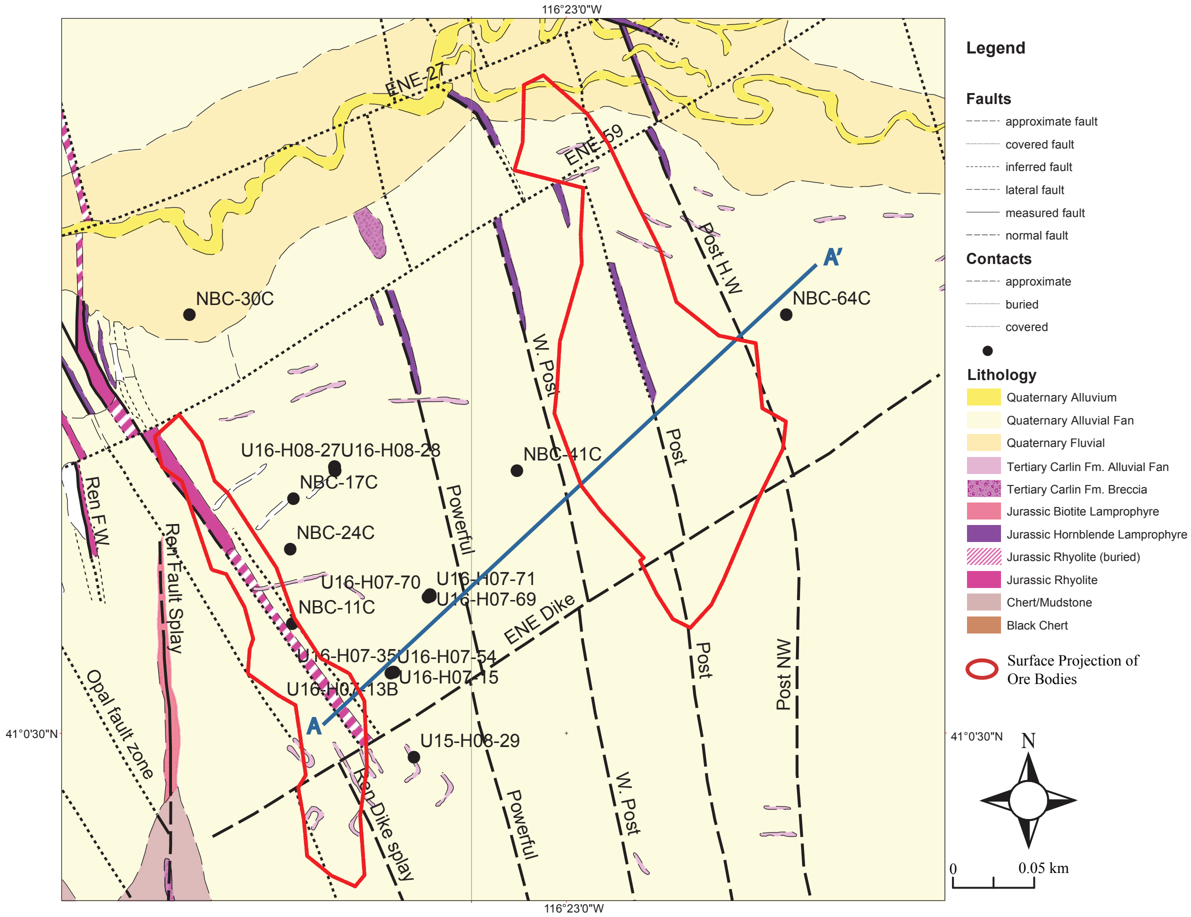

Figure 2.2 Surface geology map of the Banshee area showing collar locations of sampled drill holes and cross-section location. Map generated from internal Barrick data.

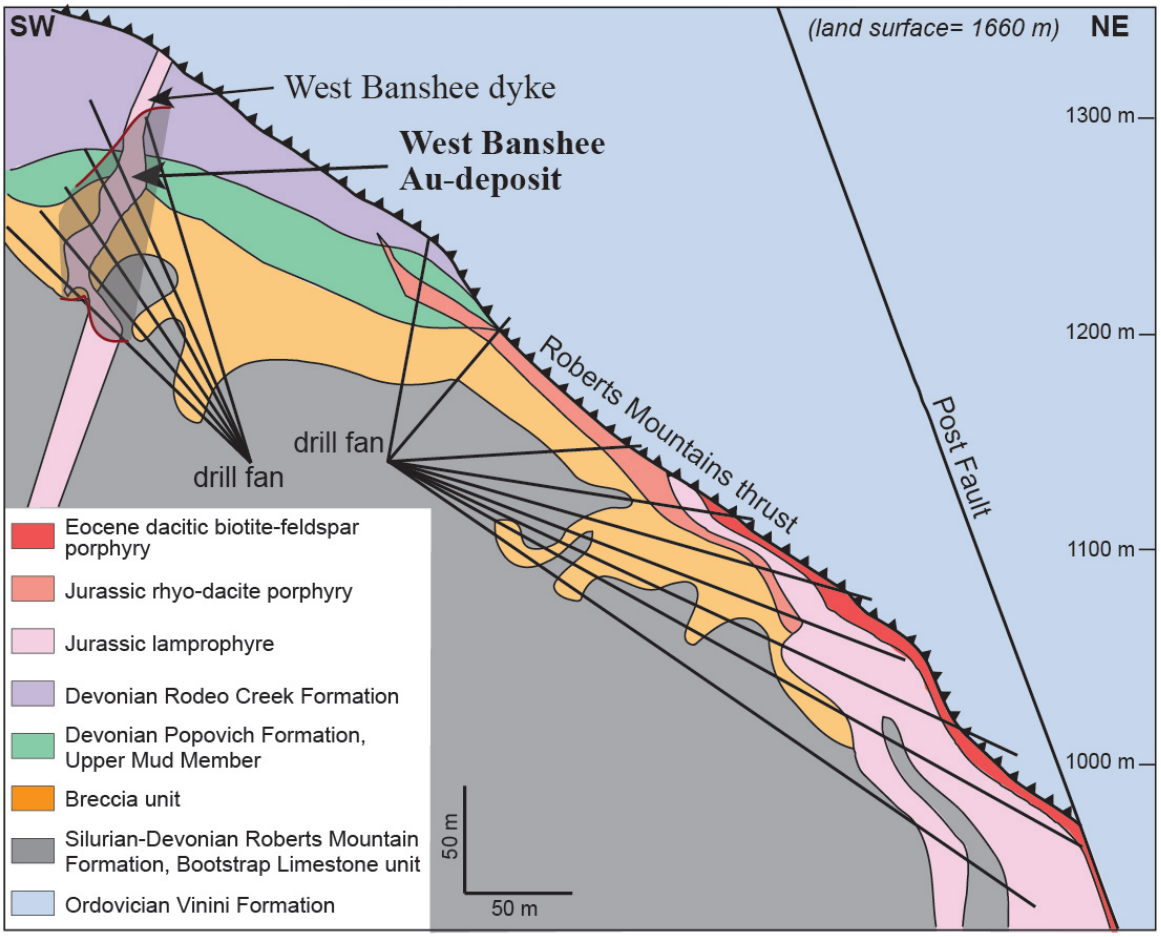

Figure 2.3 Cross-section A-A' through west and East Banshee. The west Banshee gold shell encompasses Au mineralization >0.2 ppm. The Powerful and West Post faults mapped from surface are not projected in this section owing to a lack of evidence in the geology on this section. Drill hole data used to generate the cross-section are from Barrick's internal database.

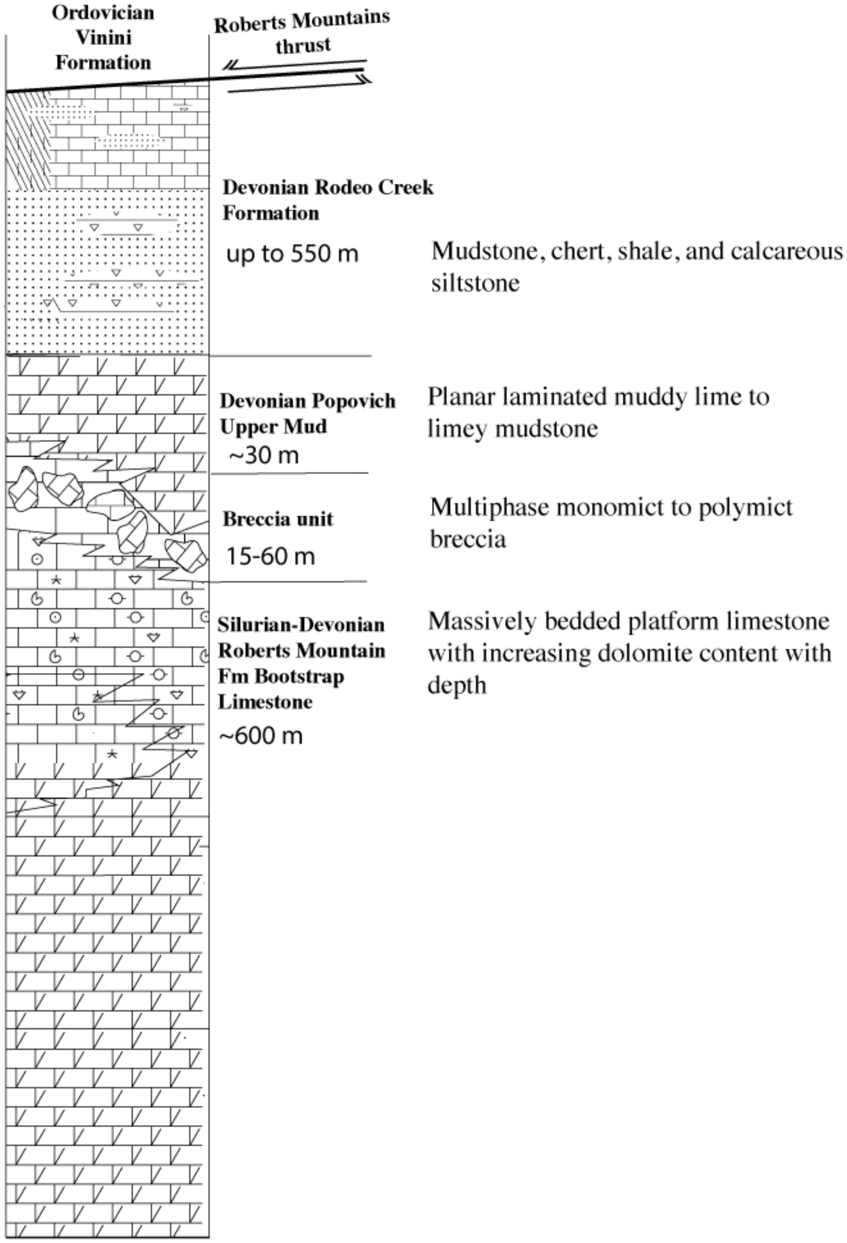

Figure 2.4 Stratigraphic column for the Banshee Paleozoic section modified from Armstrong et al. (1997).

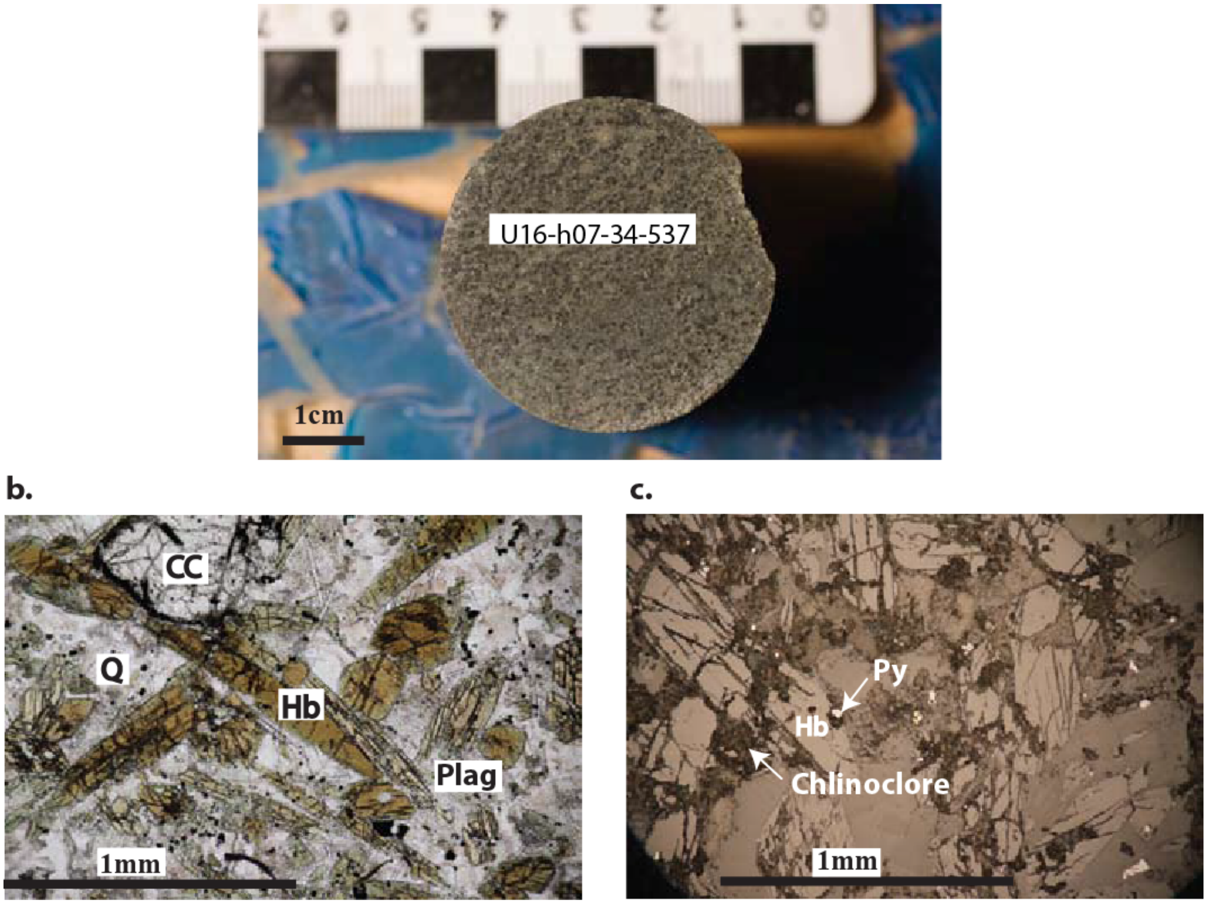

Figure 2.5 (a) Polished block of least altered hornblende lamprophyre sample U16-h07-34-537 showing fine-grained hornblende phenocrysts and characteristic dark green hue. (b) Transmitted light cross-polarized photomicrograph of U16-h07-537 showing elongate hornblende phenocrysts within a dominantly plagioclase groundmass. (c) Reflected light photomicrograph showing volumetrically minor early pyrite in U16-h07-34-537.

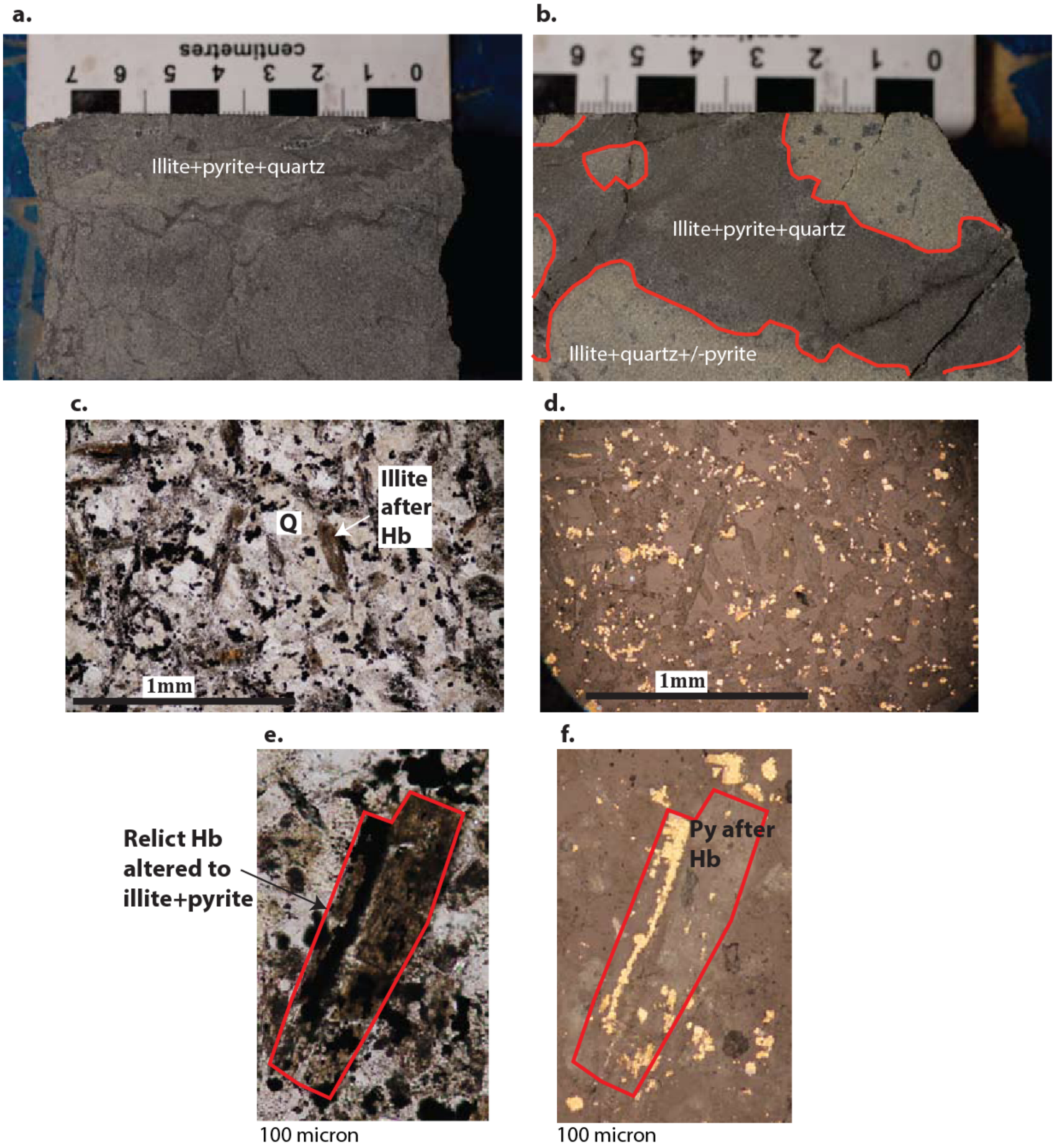

Figure 2.6 (a) Hand specimen of illite altered dike sample U16-h08-03 from drill core. (b) Hand specimen of illite altered dike sample U16-h07-24-422 showing a zone of increased pyrite addition through sulfidation easily noted base on darker color typical of arsensian pyrite grains in Carlin-type deposits. (c) Transmitted light photomicrograph of illite altered sample U16-h07-13b-461 showing illite and pyrite pseudomorphing hornblende. (d) Reflected light photomicrograph showing the addition of arsenian pyrite disseminated through the sample (U16-h07-13b-461). (e-f) Transmitted and refected light photomicrographs showing pyrite pseudomorphing hornblende in sample U16-h07-13b-461-466.

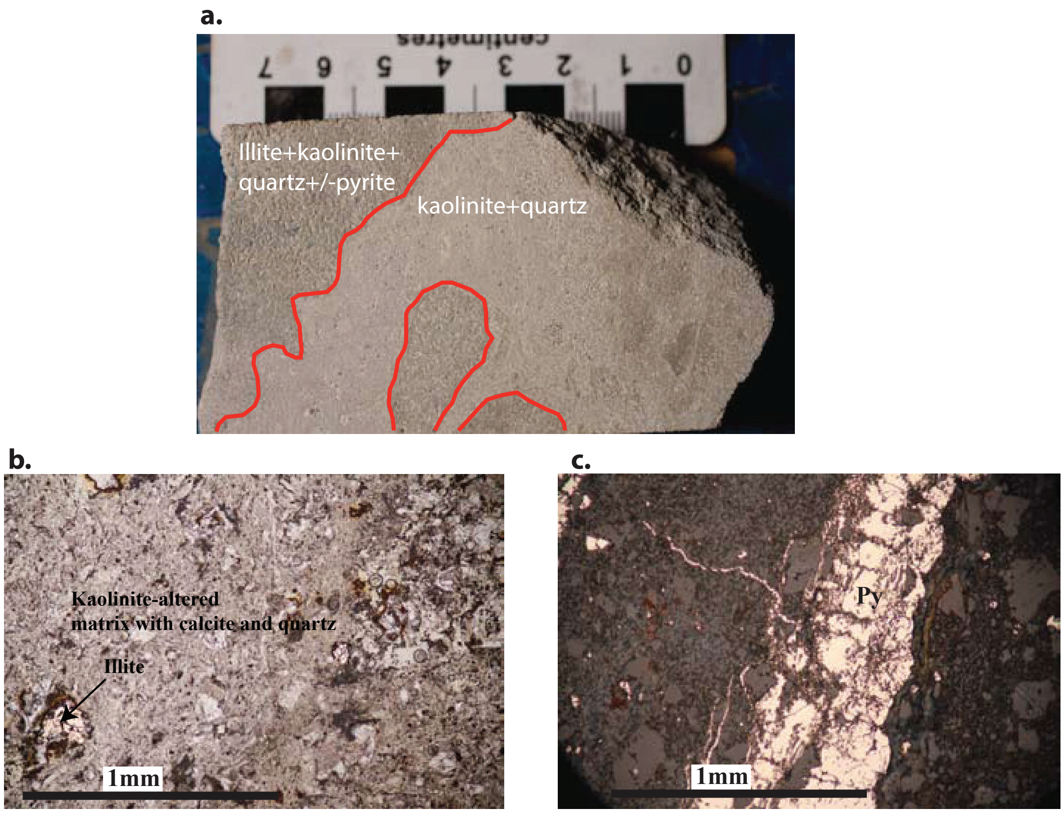

Figure 2.7 (a) Hand specimen of kaolinite alteration of previsouly illite altered dike. (sample U16-h08-27-645) b.) Transmitted light photomicrograph of illite altered dike sample showing textural desctruction of Mg-hornblende lamprophyre (sample U16-h07-54-298-302). c.) Reflected light photo-micrograph showing coarse-grained late 'brassy' pyrite common to kaolinite altered samples (sample U16-h07-54-298-302). Py=Pyrite

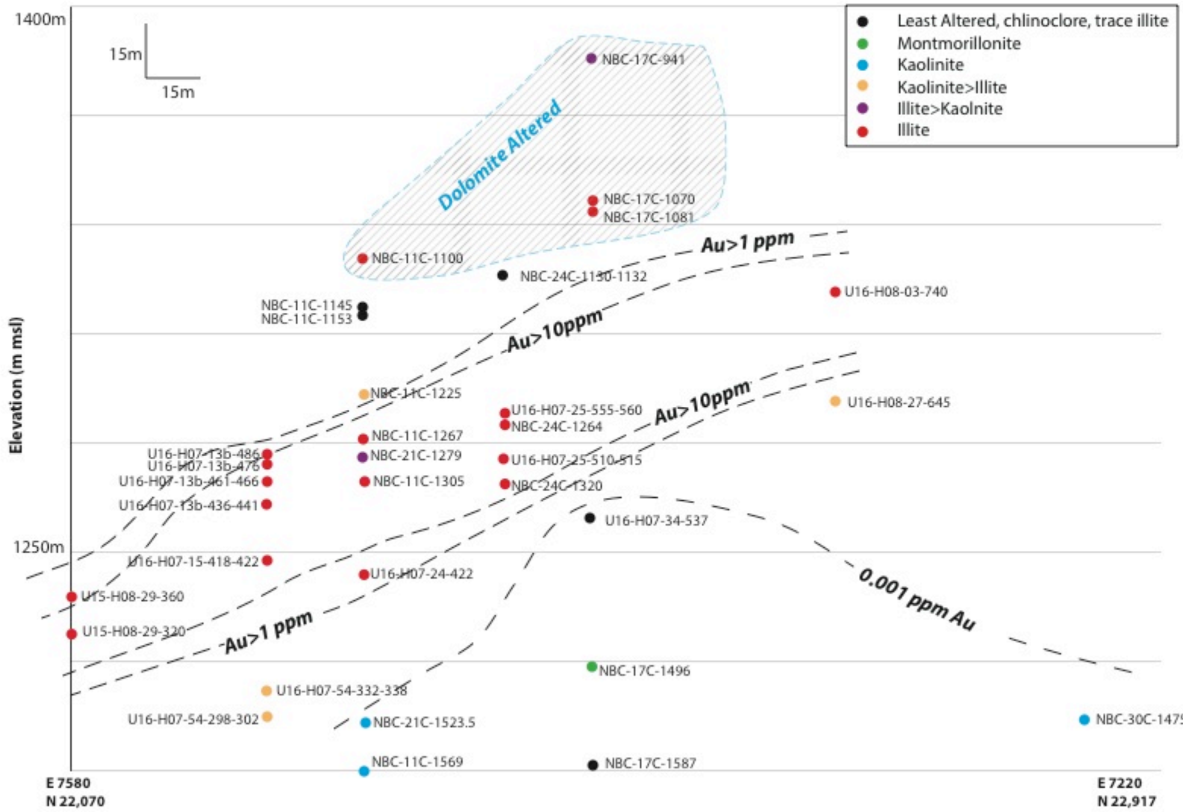

Figure 2.8 Planar view aligned parallel to the west Banshee lamprophyre dike showing the distribution of samples, extent of Au mineralization, clay alteration, and Fe-rich dolomite.

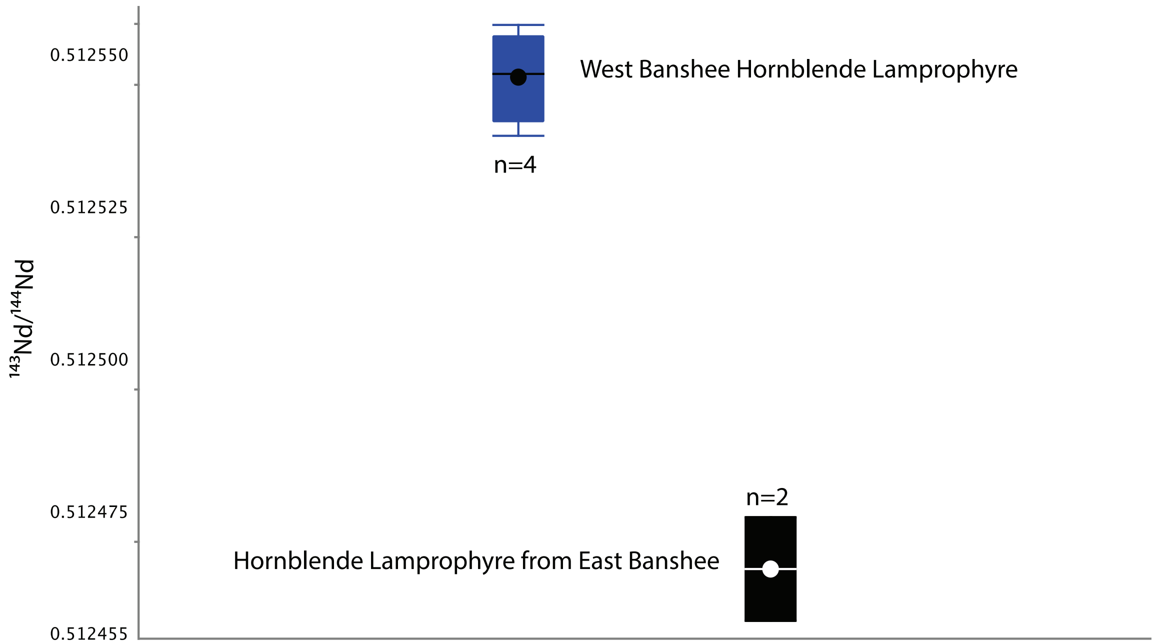

Figure 2.9 Box and whisker plot of $^{143}Nd/^{144}Nd$ from 6 hornblende lamprophyre samples from Banshee. The 4 samples with higher $^{143}Nd/^{144}Nd$ values are all from the west Banshee lamprophyre while the remaining 2 samples come from texturally similar hornblende lamprophyre from the Post Fault zone in east Banshee (see Appendix B for data).

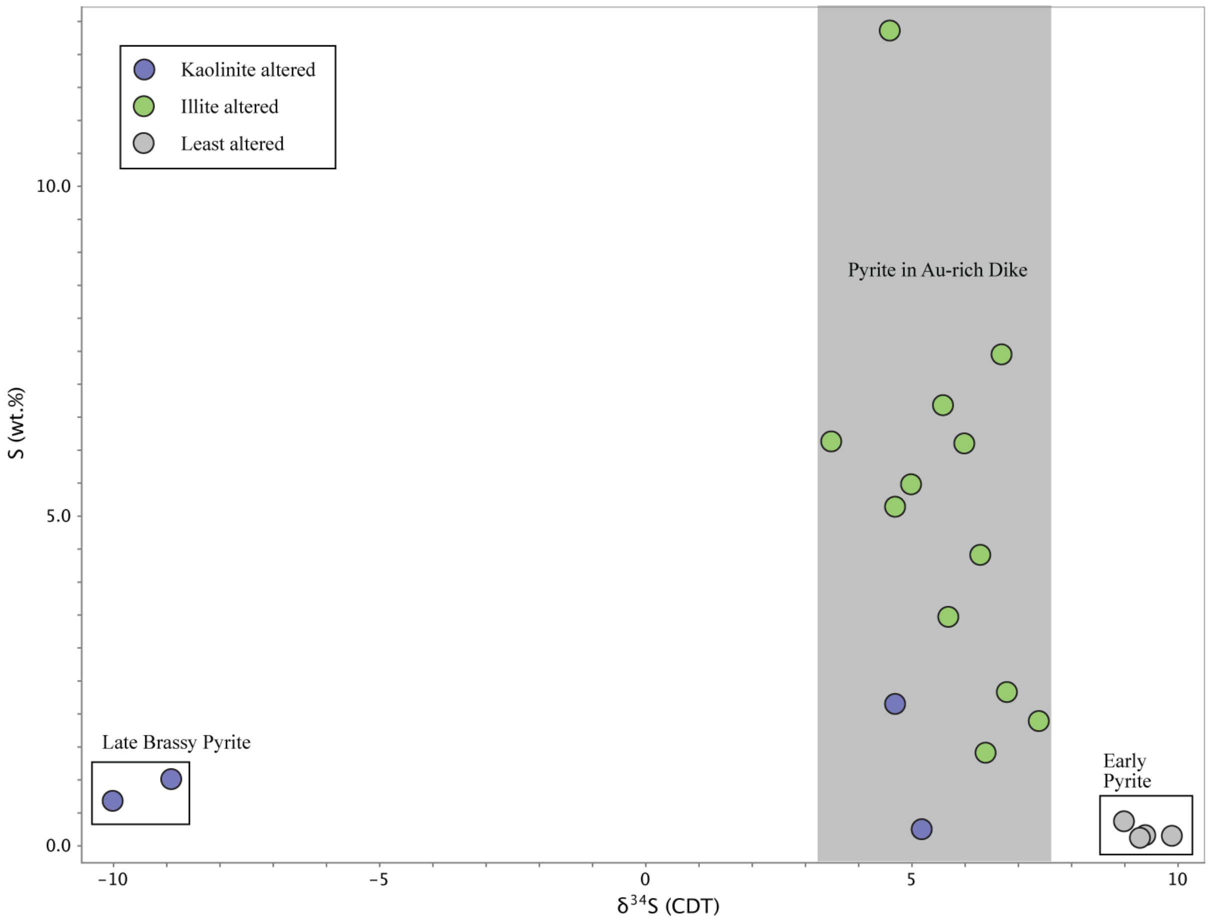

Figure 2.10 Plot of δ^{34}S data versus total S from12 illite altered, 4 kaolinite altered, and 4 least altered lamprophyre dikes at Banshee. Samples with highly negative δ^{34}S values contained abundant late brassy pyrite. The ore-stage pyrite zone is estimated based on the range of δ^{34}S in mineralized samples (see Appendix B for raw data).

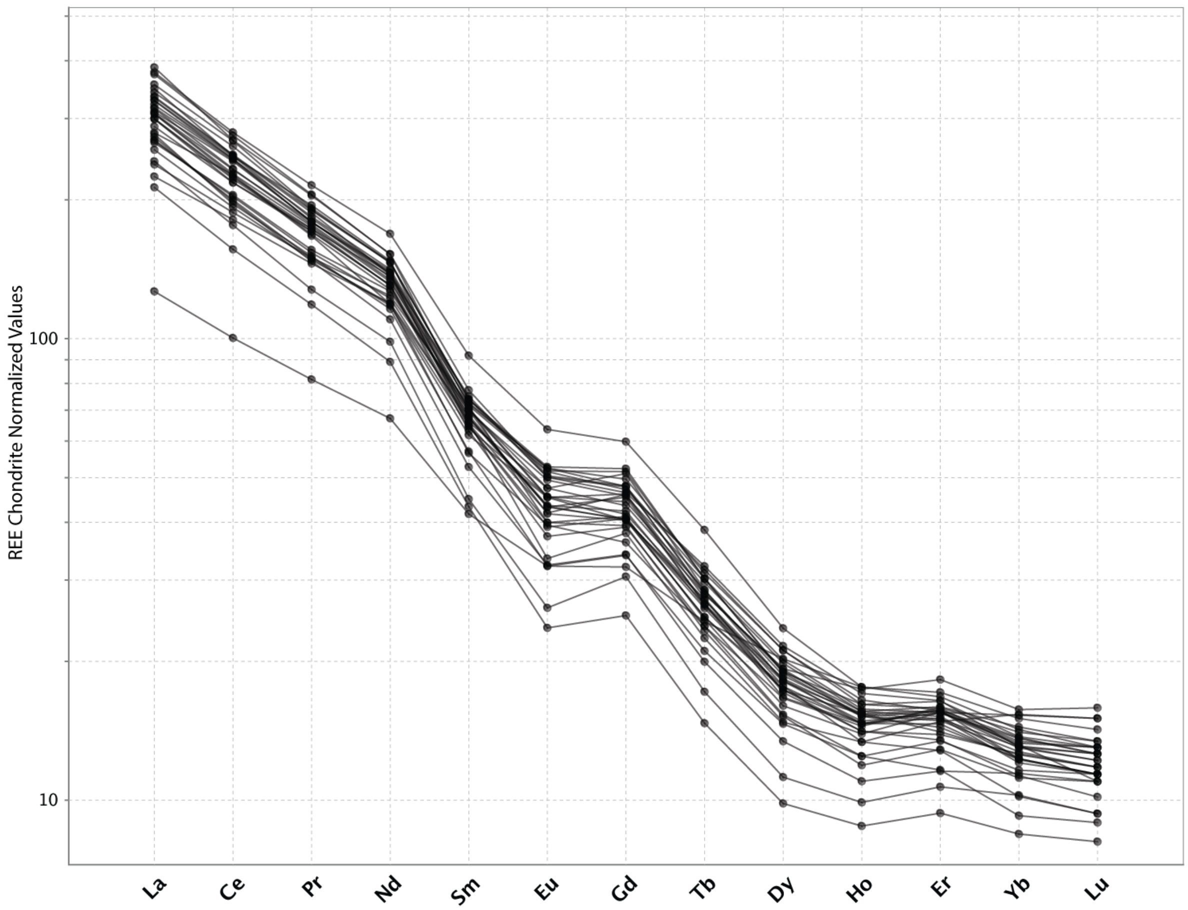

Figure 2.11 Chondrite normalized (Sun and Mcdonough, 1995) rare earth element plot of West Banshee dike samples showing the consistency in REE patterns. Variability between samples can be attributed to mass loss/gain in altered samples and natural variability of samples.

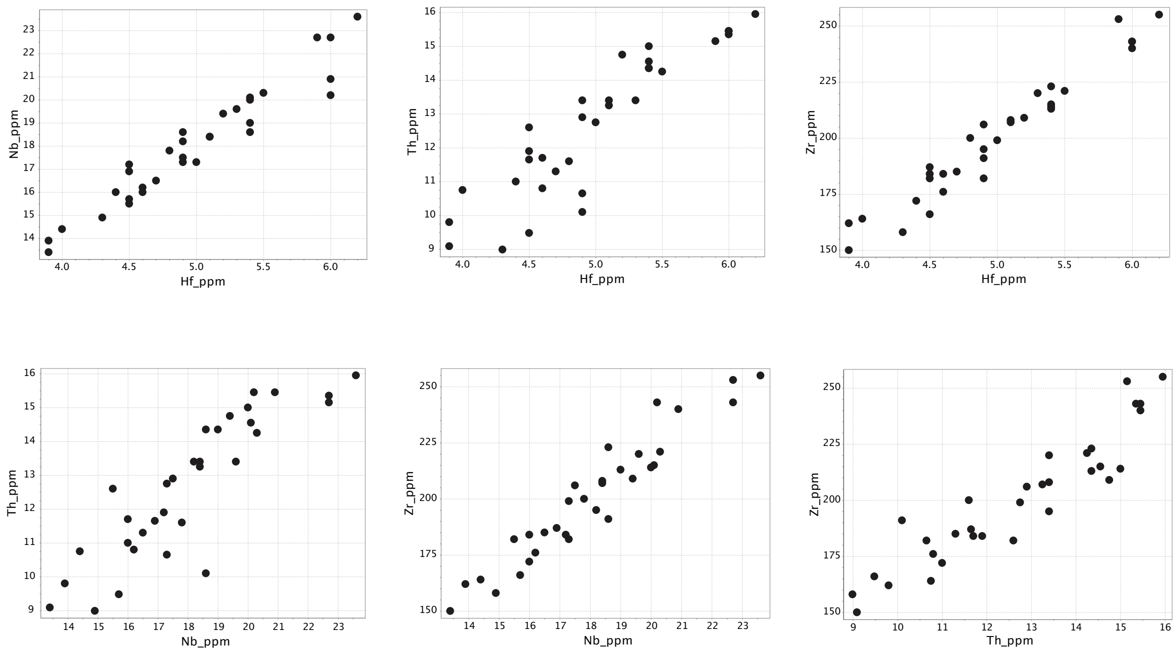

Figure 2.12 Immobile element scatter plots showing the correlation between immobile elements in the West Banshee dike.

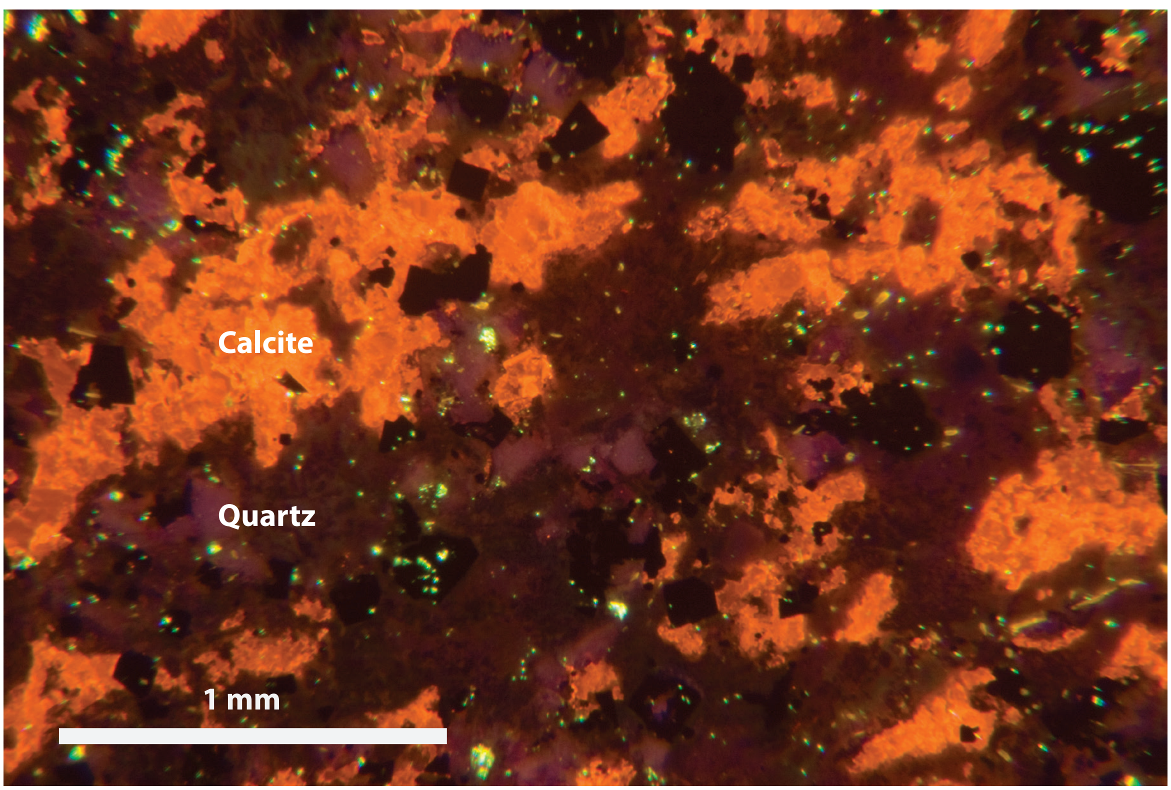

Figure 2.13 Cathodoluminescence (CL) photomicrograph from thin section of sample U16-h07-54-332. Bright orange CL response is calcite filling pore space.

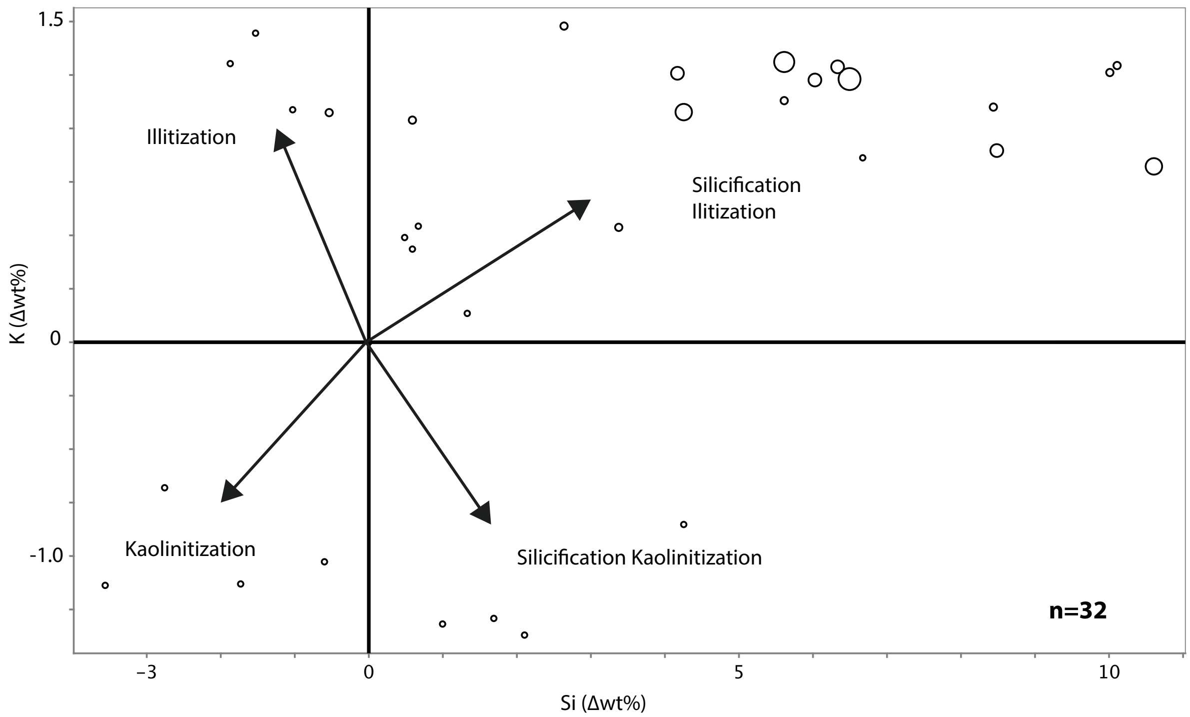

Figure 2.14 Plot of % mass change for Si and K for west Banshee lamprophyre samples. Symbols are sized to Au grade with larger symbols representing higher Au concentrations. All high-grade Au samples plot within the silicified and illitized field indicating that Au mineralization is linked to these alteration products. A small number of samples with illitization without silicification have low Au concentrations, and samples plotting with kaolinite alteration have low Au concentrations.

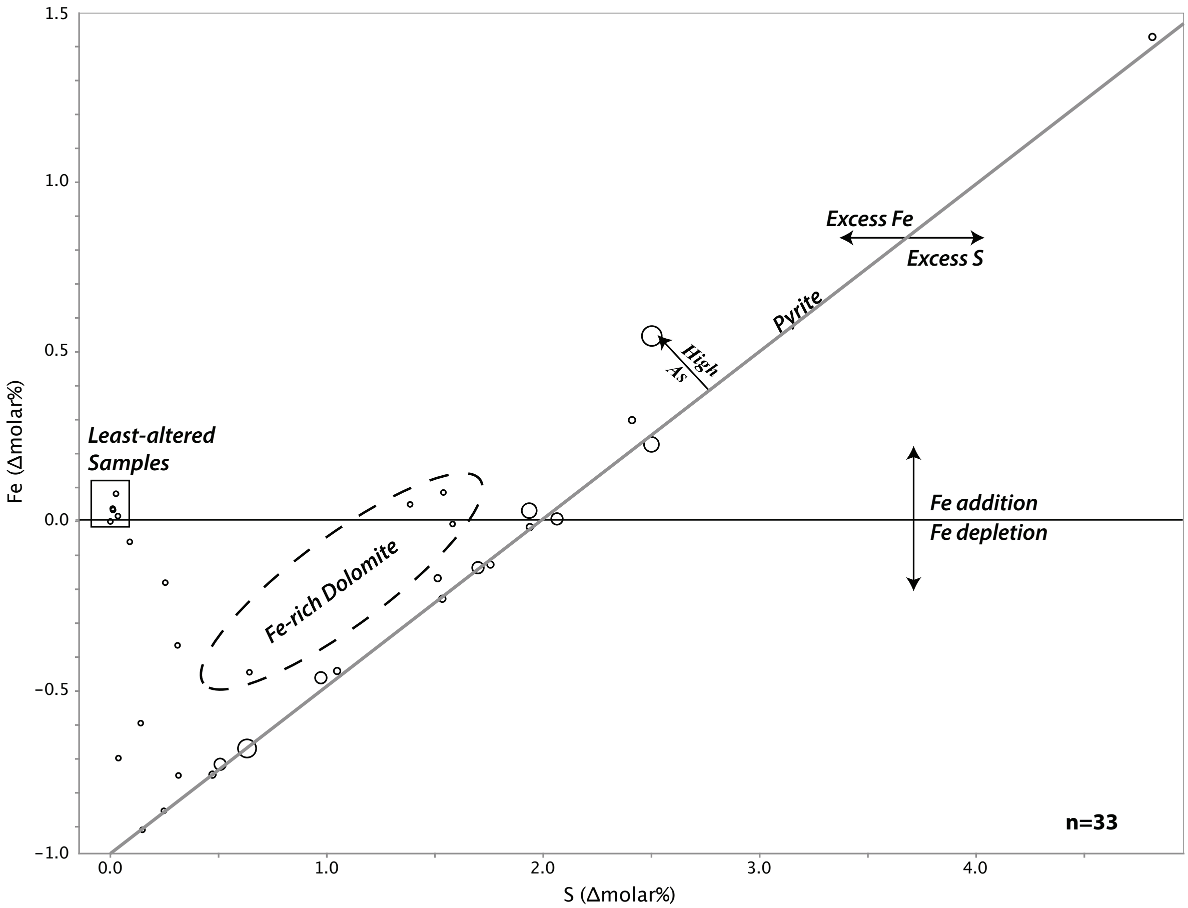

Figure 2.15 Plot of calculated Δmolar% for Fe and S illustrating Fe-sulfidation of the west Banshee dike. Symbols are sized to Au grade with larger symbols representing higher Au concentrations. All but one high grade Au sample plot on or near the pyrite line. One sample plots above the line indicating higher As content in pyrite owing to the substitution of As for S in the pyrite structure. Samples containing significant Fe-rich dolomite are circled for reference.

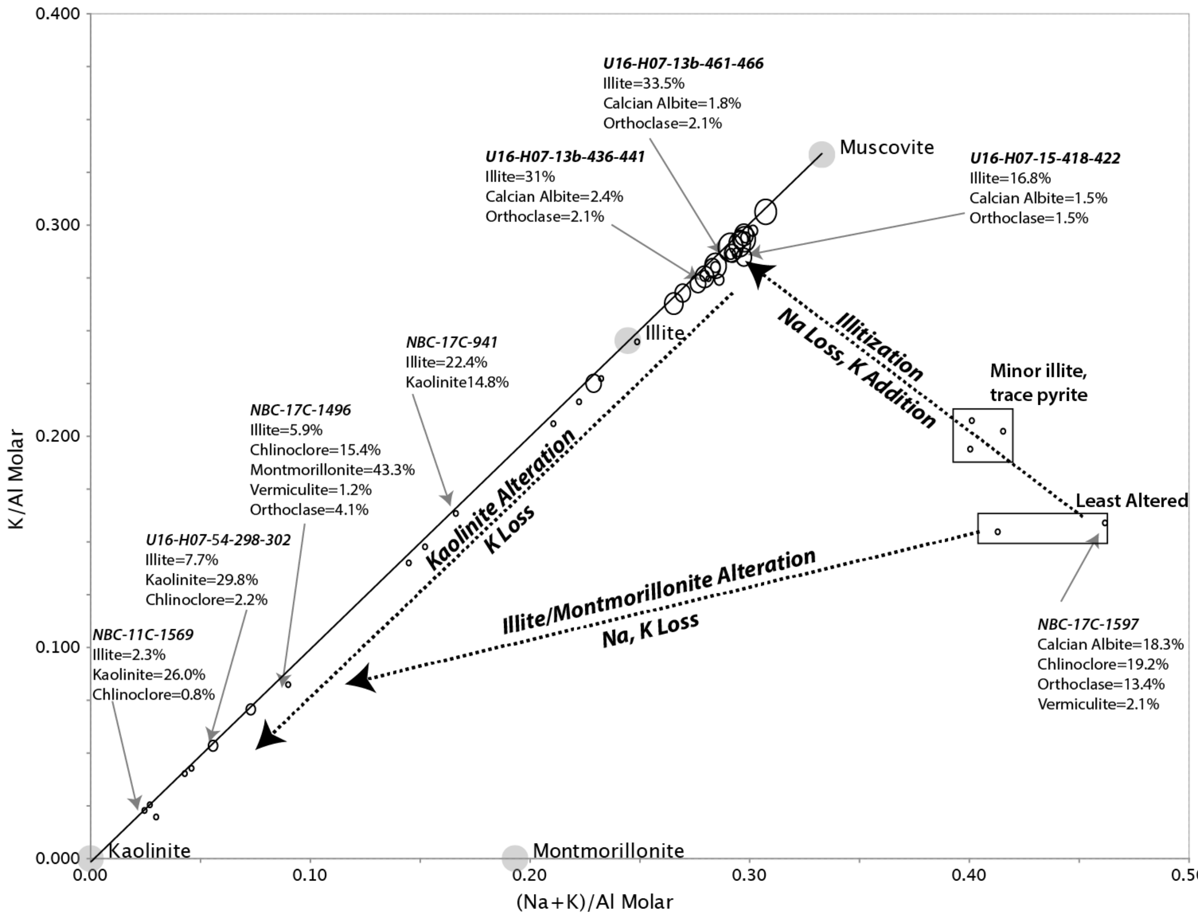

Figure 2.16 Molar ratio plot illustrating mass changes associated with clay alteration in the west Banshee lamprophyre. Symbols are sized to Au grade with larger symbols representing higher Au concentrations. Samples with quantitative XRD data are labeled for comparison of XRD and molar ratio data. High-grade mineralization accompanies illitization with K addition and Na loss. Kaolinite altered samples contain low abundances of illite.

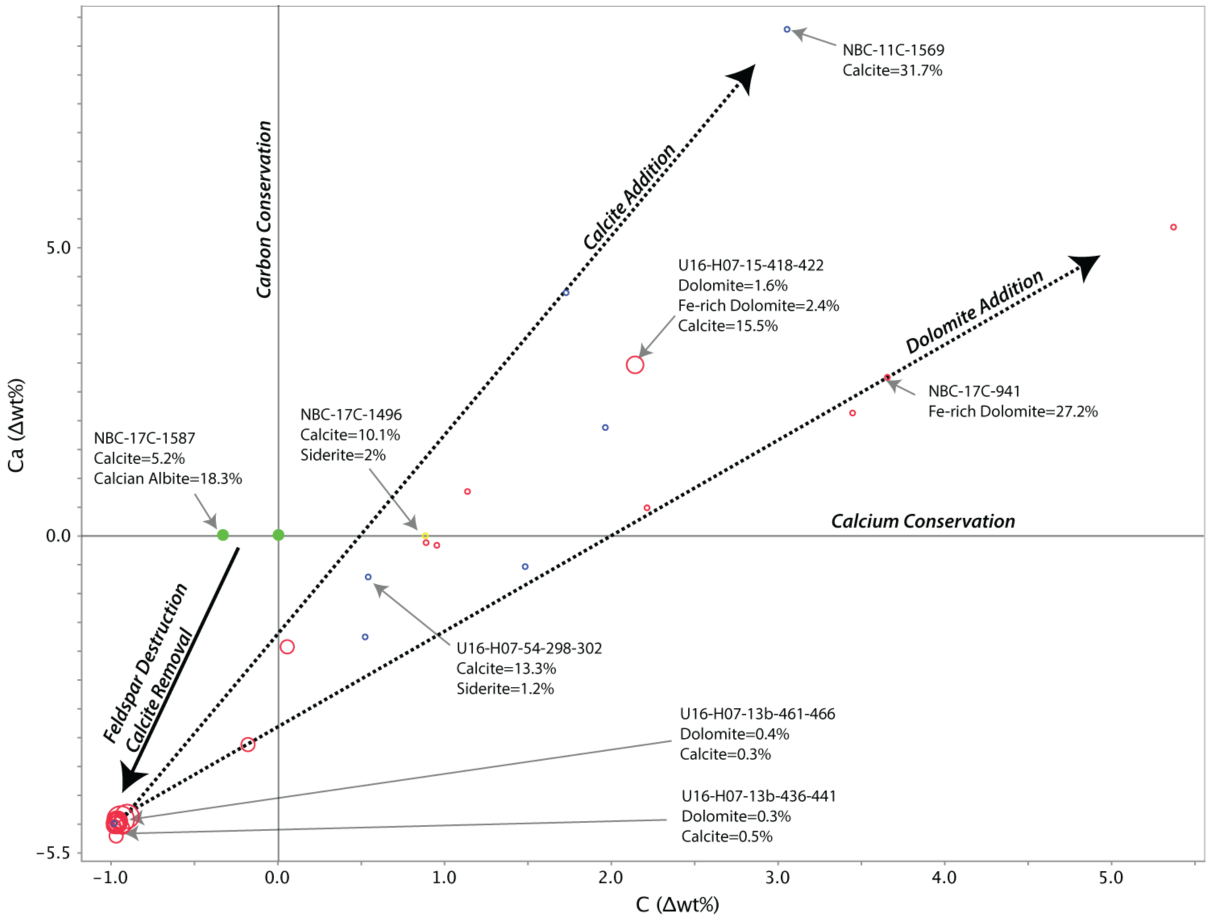

Figure 2.17 Carbonate alteration plot using calculated mass transfer data. Symbols are sized to Au grade with larger symbols representing higher Au concentrations. Illite altered samples are colored red. Kaolinite altered samples are colored blue, and least altered samples are colored green. Annotated mineral abundances are from quantitative XRD and include minerals with Ca and/or C, and tie lines for calcite and dolomite addition are drawn to intersect known samples with dominant calcite or dolomite. A total of 6 samples lie on or near the dolomite line indicating dolomite addition.

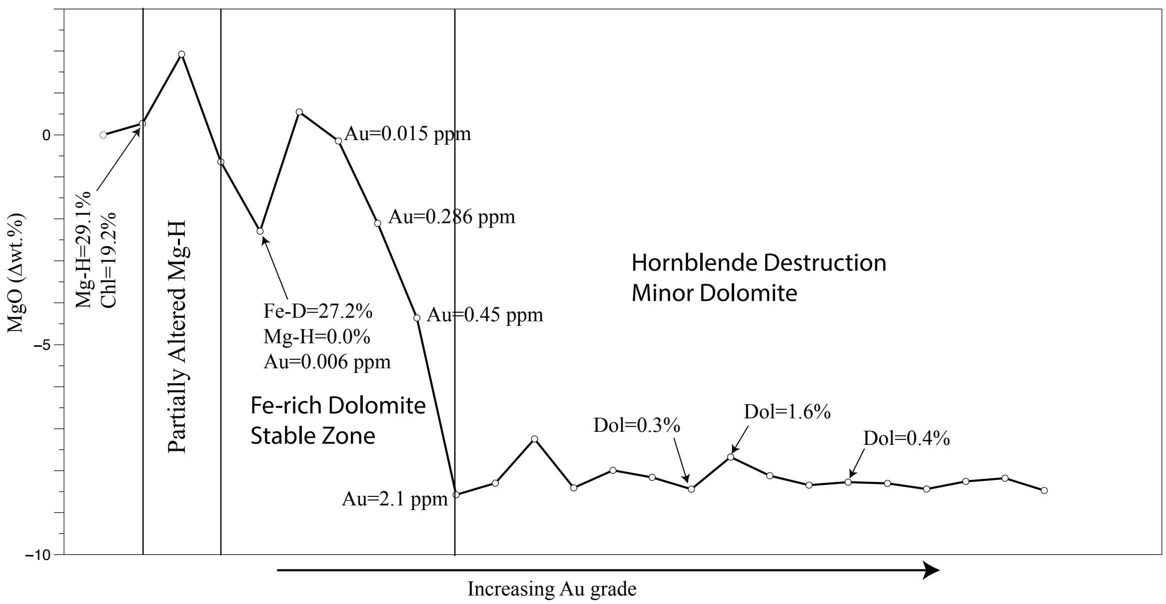

Figure 2.18 Gold ordered diagram where samples are ordered according to increasing Au grade. Kaolinite altered samples are excluded. MgO values are mass change in wt%. Annotated mineral abundances are from quantitative XRD determinations. Fe-rich dolomite zone is estimated based on carbonate alteration molar ratio plots and thin section petrography with CL. Mg-H=Mg-Hornblende, Chl=Chlinoclore, Fe-D=Fe-rich Dolomite, Dol=Dolomite

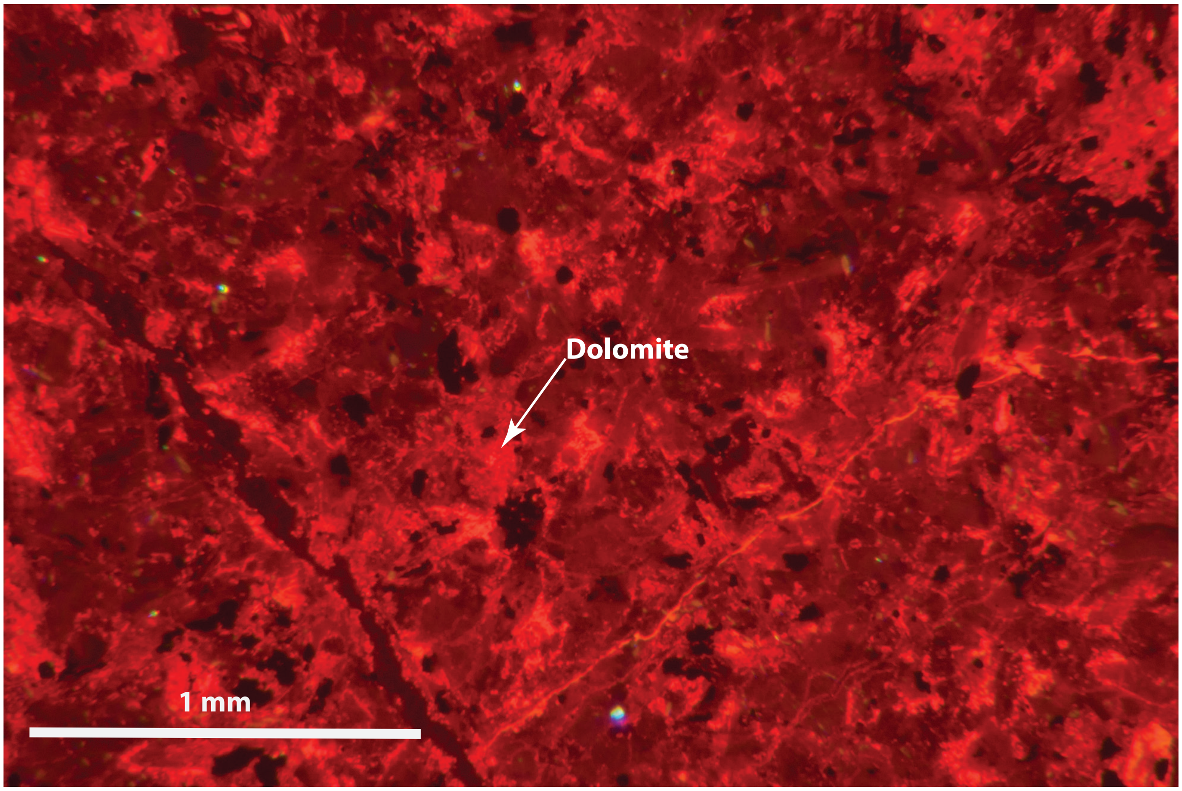

Figure 2.19 Cathodoluminescence (CL) photomicrograph from thin section of sample NBC-17C-1070 shows bright red CL response for dolomite in veins and filling pore space.

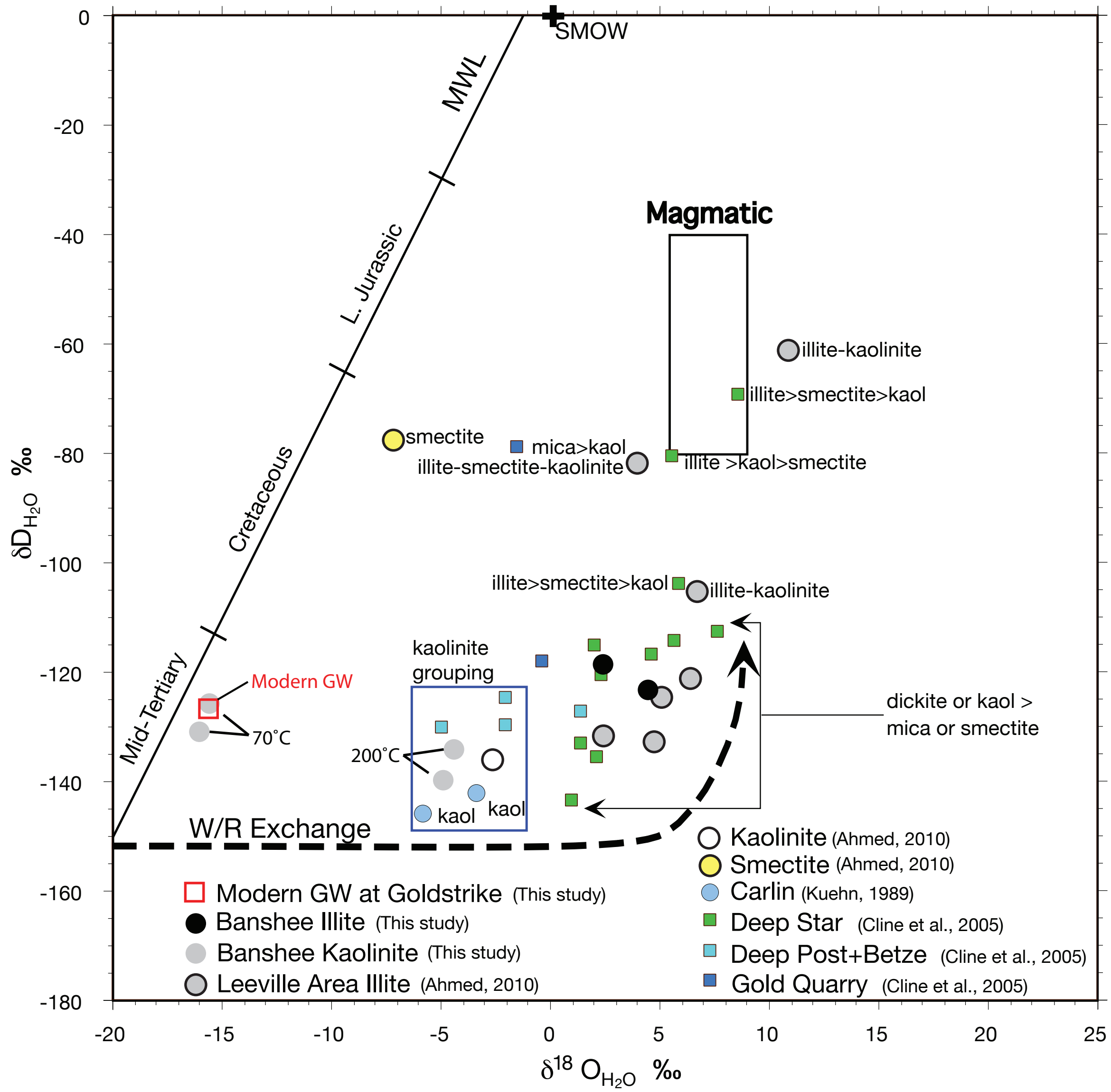

Figure 2.20 Modified from Cline et al. (2005). $\delta^{18}O_{H2O}$ versus δD_{H2O} for clay separates from the west Banshee lamprophyre, modern groundwater from Goldstrike, and clays from other studies of Carlin-type Au deposits relative to the meteoric water line (MWL) and magmatic water. Estimated geologic ages plotted along the MWL are from Hofstra et al. (1999). Banshee kaolinite plots near modern groundwater when calculated at 70°C indicating that it possibly formed from similar cool meteoric waters. Illite samples from west Banshee plot similarly to other illite and clay samples from deposits along the Carlin trend. Fluid equivalent values were calculated at 200°C for illite and 70°C for kaolinite using the fractionation factors of Sheppard and Gilg (1996), Gilg and Sheppard (1996), and Capuano (1992).

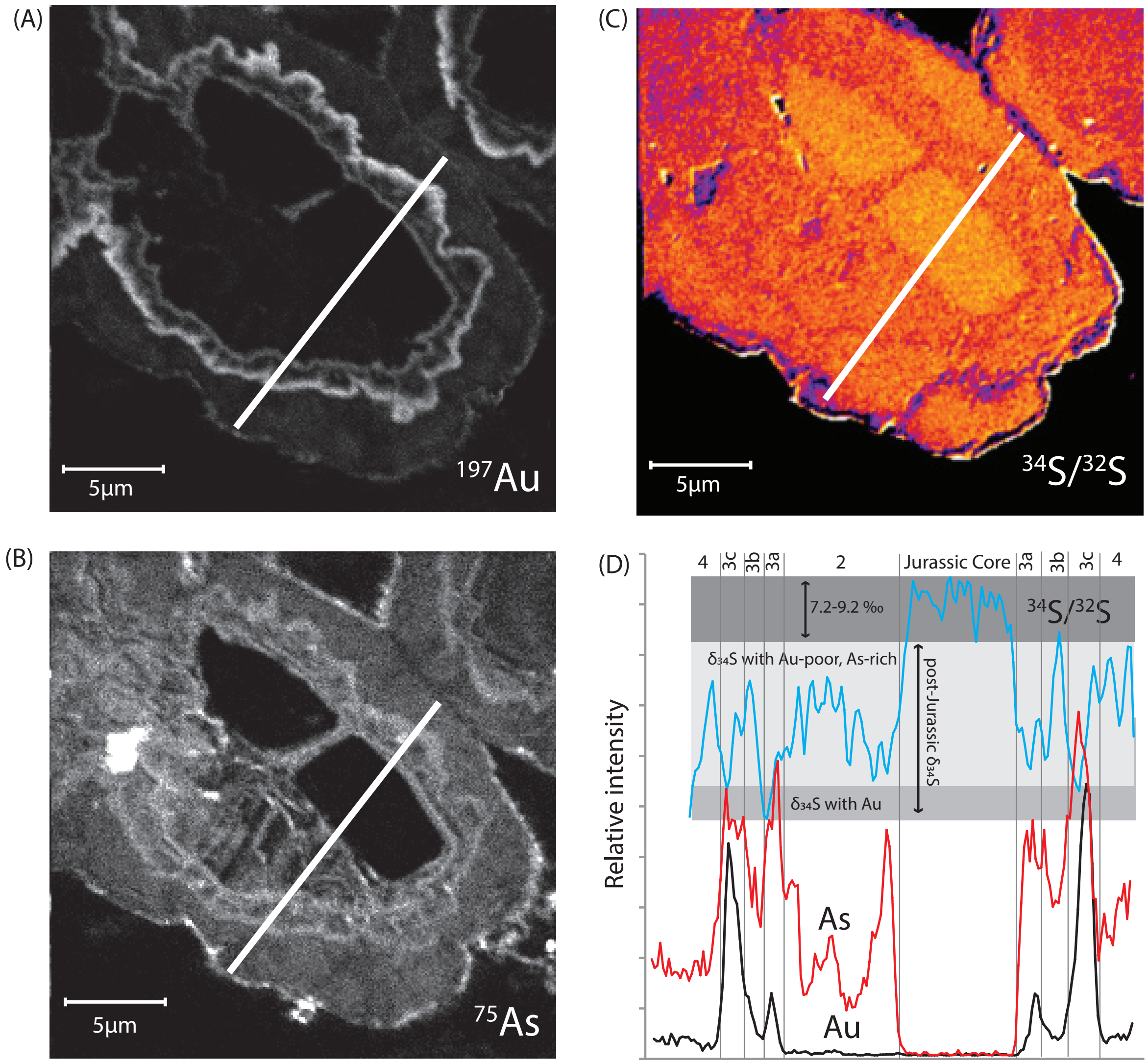

Figure 2.21 nanoSIMS image from Barker et al. (2009) showing the distribution of Au (A), As (B), and $\delta^{34}S$ (C) in ore stage pyrite from west Banshee lamprophyre sample U16-h07-13b-476. Brighter colors indicate increased relative intensity and high concentrations. (D) Line profile across the image as indicated by the cross-section lines in A-C showing the relative response of each parameter in section. Stage 2 pyrite growth is defined by elevated As with no Au and $\delta^{34}S$ depleted relative to the Jurassic core. Stage 3 pyrite growth contains auriferous pyrite growth in 2 rims (3a and 3c) with lower $\delta^{34}S$ values and higher As values. An intervening stage of pyrite growth within stage 3 (3b) contains lower Au and As with higher $\delta^{34}S$ values. Stage 4 represents Au-poor pyrite growth post-dating Au precipitation.

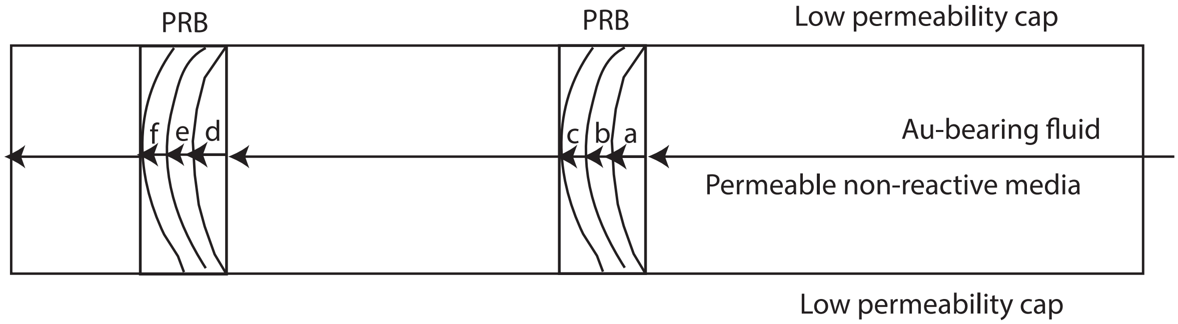

Figure 2.22 Conceptual model of PRB showing a hypothetical ore fluid propagating through a zone of high permeability intersecting a PRB. With progressive reaction (steps a-c) the reactive capacity of the PRB is eventually consumed and the fluid moves further down the flow path until it encounter a 2nd PRB which then leads to progressive reaction again (steps f-d).

Table 2.1 Modal mineral abundances from west Banshee lamprophyre samples from quantitative XRD

Sample	NBC-11C-1569	NBC-17C-1496	NBC-17C-1587	NBC-17C-941	U16-h07-13b-436-441	U16-h07-13b-461-466	U16-h07-15-418-422	U16-h07-54-298-302
Alteration Type	**Kaolinite**	**Smectite**	**Least Altered**	**Illite/ Kaolinite**	**Illite**	**Illite**	**Illite**	**Kaolinite**
Mg-Horblende	0	0	29.1	0	0	0	0	0
Albite low, calcian	0	0	18.3	1.6	2.4	1.8	1.5	0
Anatase	1.1	1.3	0	1	1.1	0.7	0.7	1.3
Fe-rich dolomite	0	0	0	27.2	0	0	2.4	0
Bassanite	0	0.9	0	0	0	0	0.0	0
Calcite	31.7	10.1	5.2	0	0.5	0.3	15.5	13.3
Clinochlore	0.8	15.4	19.2	0	0	0	0	2.2
Dolomite	0	0	0	0	0.3	0.4	1.6	0
Gypsum	0	0	0	1.3	0.8	0.5	1.5	0
Illite-Muscovite	2.3	5.9	0	22.4	31	33.5	16.8	7.7
Jarosite	0	0	0	0	1.3	1.6	0	0
Kaolinite	26	0	0	14.8	0.0	0	0	29.8
Marcasite	0	0	0	0.8	4.1	1.7	5.3	0
Orthoclase	0	4.1	13.4	1.6	2.1	2.1	1.5	0
Pyrite	2.4	0.4	0.3	0.9	8.8	4.5	5.7	0.4
Quartz	35.5	15.4	12.3	28.3	46.2	52.2	47.5	42.5
Siderite, Mg, Ca	0.2	0.0	0	0	1.4	0.7	0	1.2
Siderite	0	2	0	0.1	0	0	0	1.7
Vermiculite 2M	0	1.2	2.1	0	0	0	0	0
Montmorillonite	0	43.3	0	0	0	0	0	0
Total	100	100	100	100	100	100	100	100

Table 2.2 Lithogeochemistry data for samples of west Banshee lamprophyre, Jurassic rhyolite, Eocene Dacite, and Bootstrap Limestone

Sample	NBC-30C-1475	NBC-11C-1569	NBC-21C-1523.5	NBC-11-1225	U16-h07-54-332-338	U16-h07-54-298-302	H16-H08-27-645	NBC-17C-1496	U16-H07-34-537	NBC-17C-1587
Lithology	**WB Lamp**	**WB Lamp**	**WB Lamp**	**WB Lamp**	**WB Lamp**	**WB Lamp**	**WB Lamp**	**WB Lamp**	**WB Lamp**	**WB Lamp**
Alteration	**Kaolinite**	**Kaolinite**	**Kaolinite**	**Kaolinite**	**Kaolinite**	**Kaolinite**	**Kaolinite**	**Montmorill-onite**	**Least Altered**	**Least Altered**
Hf Ratio	**1**	**1.09**	**0.98**	**0.96**	**0.79**	**0.83**	**0.82**	**1.00**	**1.00**	**1.04**
Zr Ratio	**0.98**	**1.02**	**0.96**	**0.92**	**0.75**	**0.75**	**0.80**	**1.05**	**1.00**	**1.03**
Au (ppm)	0.001	0.001	0.001	0.003	0.021	0.048	0.067	0.001	0.001	0.001
SiO2 (wt.%)	54.2	47.6	54.4	43.8	58.2	58.3	72	43.8	49.7	50.4
Al2O3 (wt.%)	11.9	12.2	13.5	13.95	16.2	15.4	15.8	13.8	13.1	13.3
Fe2O3 (wt.%)	4.77	2.15	1.54	7.16	4.52	3.31	1.3	8.59	8.32	8.27
CaO (wt.%)	10.2	18.25	13.75	7.1	6.47	7.91	0.71	7.57	7.59	7.28
MgO (wt.%)	1.74	0.82	0.2	8.93	0.89	1.36	0.27	6.18	8.96	8.94
Na2O (wt.%)	0.08	0.02	0.02	0.03	0.04	0.03	0.03	0.07	2.05	2.44
K2O (wt.%)	0.21	0.25	0.31	0.51	0.63	0.75	1.02	1.04	1.86	1.94
TiO2 (wt.%)	0.99	0.9	1.11	1.09	1.29	1.1	1.02	1.18	1.16	1.08
MnO (wt.%)	0.07	0.06	0.05	0.14	0.05	0.05	0.01	0.1	0.12	0.11
P2O5 (wt.%)	0.35	0.36	0.34	0.35	0.4	0.37	0.46	0.31	0.33	0.31
C (wt.%)	2.95	3.71	2.77	2.57	1.91	1.84	0.005	1.87	0.99	0.63
S (wt.%)	2.14	1	0.89	0.93	0.67	0.24	0.68	0.12	0.08	0.11
Ag (ppm)	0.5	0.5	0.5	0.5	0.5	0.5	0.5	0.5	0.5	0.5
Ba (ppm)	167.5	194	555	150	73.4	524	95.1	480	2380	1450
Ce (ppm)	138	171.5	142.5	150	164.5	148.5	153	118	133.5	124.5
Co (ppm)	36.5	13.2	24.8	43.6	30.4	26.1	27.7	37.3	38.6	37.9
Cr (ppm)	560	410	740	670	740	480	340	880	580	590
Cs (ppm)	0.71	1.31	3.63	6.73	4.27	2.51	3.57	8.21	3.77	1.91
Cu (ppm)	41	67	72	76	59	72	77	66	60	86
Dy (ppm)	3.77	5.8	4.95	5.2	4.64	4.21	4.26	4.35	5.31	4.73
Er (ppm)	1.86	2.68	2.48	2.53	2.49	2.22	2.5	2.05	2.63	2.3
Eu (ppm)	2.22	3.58	2.95	2.95	2.97	2.55	2.2	2.56	2.82	2.67
Ga (ppm)	15.5	16.4	19.1	17.3	21.8	19.8	19	17.9	17.3	16.4
Gd (ppm)	7.2	11.9	9.52	9.87	10.4	9.17	8.11	8.29	9.23	8.65
Hf (ppm)	4.9	4.5	5	5.1	6.2	5.9	6	4.9	4.9	4.7

Sample	NBC-30C-1475	NBC-11C-1569	NBC-21C-1523.5	NBC-11-1225	U16-h07-54-332-338	U16-h07-54-298-302	H16-H08-27-645	NBC-17C-1496	U16-H07-34-537	NBC-17C-1587
Lithology	**WB Lamp**	**WB Lamp**	**WB Lamp**	**WB Lamp**	**WB Lamp**	**WB Lamp**	**WB Lamp**	**WB Lamp**	**WB Lamp**	**WB Lamp**
Alteration	**Kaolinite**	**Kaolinite**	**Kaolinite**	**Kaolinite**	**Kaolinite**	**Kaolinite**	**Kaolinite**	**Montmorill-onite**	**Least Altered**	**Least Altered**
Hf Ratio	**1**	**1.09**	**0.98**	**0.96**	**0.79**	**0.83**	**0.82**	**1.00**	**1.00**	**1.04**
Zr Ratio	**0.98**	**1.02**	**0.96**	**0.92**	**0.75**	**0.75**	**0.80**	**1.05**	**1.00**	**1.03**
Ho (ppm)	0.68	0.96	0.86	0.88	0.83	0.77	0.84	0.73	0.93	0.83
La (ppm)	72.7	89.4	72.9	77.7	84.2	73.5	78.9	60.8	68.3	63.5
Lu (ppm)	0.22	0.32	0.3	0.31	0.27	0.29	0.32	0.23	0.31	0.28
Mo (ppm)	2	3	2	2	2	2	1	2	1	2
Nb (ppm)	18.2	16.9	17.3	18.4	23.6	22.7	20.9	17.3	18.6	16.5
Nd (ppm)	54.3	77.1	63.4	64.6	66.7	62.1	62.9	54.4	62.5	55.9
Ni (ppm)	167	71	96	215	166	142	111	240	176	207
Pb (ppm)	10	5	9	11	10	8	6	8	8	8
Pr (ppm)	15.5	19.95	16.6	17.05	17.8	16.65	17.4	13.75	16.05	14.25
Rb (ppm)	10.4	12.1	14.9	30.2	35.2	42	52.4	36.4	53.4	49.8
Sm (ppm)	8.36	13.6	10.75	10.7	10.9	10.4	9.57	9.48	11.1	9.76
Sn (ppm)	2	1	2	2	2	2	1	2	1	2
Sr (ppm)	106.5	32.1	78.4	191	68.6	41.6	37.4	176	1030	1015
Ta (ppm)	1.2	1.1	1.2	1.2	1.4	1.3	1.4	1.1	1.1	1.1
Tb (ppm)	0.86	1.39	1.09	1.12	1.09	0.99	0.94	0.98	1.16	1.01
Th (ppm)	13.4	11.65	12.75	13.4	15.95	15.15	15.45	10.65	10.1	11.3
Tl (ppm)	0.25	1.3	1.9	1	1.4	0.5	3.7	0.25	0.25	0.25
Tm (ppm)	0.23	0.34	0.32	0.33	0.31	0.29	0.32	0.25	0.35	0.3
U (ppm)	4.04	14	11.25	3.42	15.2	13.45	16	2.5	2.52	2.72
V (ppm)	156	116	178	173	183	136	169	190	172	168
W (ppm)	21	35	37	4	82	45	29	19	1	1
Y (ppm)	16.5	24	22.7	22.6	21.8	18.9	20.1	18.3	24.1	20.7
Yb (ppm)	1.49	2.29	2.09	2.11	2.12	2.03	2.16	1.64	2.1	1.98
Zn (ppm)	153	47	47	80	92	98	67	75	79	80
Zr (ppm)	195	187	199	208	255	253	240	182	191	185
As (ppm)	220	306	245	36	300	14.4	178	0.8	0.3	1.4

Sample	NBC-30C-1475	NBC-11C-1569	NBC-21C-1523.5	NBC-11-1225	U16-h07-54-332-338	U16-h07-54-298-302	H16-H08-27-645	NBC-17C-1496	U16-H07-34-537	NBC-17C-1587
Lithology	**WB Lamp**	**WB Lamp**	**WB Lamp**	**WB Lamp**	**WB Lamp**	**WB Lamp**	**WB Lamp**	**WB Lamp**	**WB Lamp**	**WB Lamp**
Alteration	**Kaolinite**	**Kaolinite**	**Kaolinite**	**Kaolinite**	**Kaolinite**	**Kaolinite**	**Kaolinite**	**Montmorill-onite**	**Least Altered**	**Least Altered**
Hf Ratio	**1**	**1.09**	**0.98**	**0.96**	**0.79**	**0.83**	**0.82**	**1.00**	**1.00**	**1.04**
Zr Ratio	**0.98**	**1.02**	**0.96**	**0.92**	**0.75**	**0.75**	**0.80**	**1.05**	**1.00**	**1.03**
Bi (ppm)	0.02	0.01	0.02	0.05	0.02	0.01	0.04	0.02	0.01	0.005
Hg (ppm)	0.875	3.32	2.83	0.172	0.809	1	3.37	0.046	0.0025	0.0025
Li (ppm)	3.7	N/A	N/A	N/A	N/A	N/A	N/A	19.9	40.9	N/A
Sb (ppm)	19.45	36.9	34.6	1.27	26.9	1.7	62.3	0.15	0.16	0.41
Se (ppm)	0.2	0.7	1.6	3.1	0.6	0.7	2.3	0.3	0.1	0.1
Te (ppm)	0.01	0.01	0.005	0.04	0.005	0.005	0.005	0.01	0.01	0.005
LOI (%)	13.7	16.95	14.65	15.3	9.98	10	6.31	15.85	6.86	5.44
Total (%)	98.3	99.6	100	98.5	98.8	98.7	99	98.7	100.5	99.9

Sample	NBC-17C-941	NBC-11C-1153	NBC-11C-1145	NBC-24C-1130-1132	NBC-21C-1279	U15-29-320	U16-H07-13b-486	U16-h07-25-510-515	NBC-17C-1081	NBC-17C-1070
Lithology	**WB Lamp**	**WB Lamp**	**WB Lamp**	**WB Lamp**	**WB Lamp**	**WB Lamp**	**WB Lamp**	**WB Lamp**	**WB Lamp**	**WB Lamp**
Alteration	**Illite/Kaol-inite**	**Illite**	**Illite**	**Illite**	**Illite**	**Illite**	**Illite**	**Illite**	**Illite**	**Illite**
Hf Ratio	**1.36**	**1.09**	**1.07**	**1.02**	**0.82**	**1.11**	**0.96**	**0.89**	**1.14**	**1.23**
Zr Ratio	**1.37**	**1.15**	**1.09**	**0.96**	**0.79**	**1.11**	**0.92**	**0.86**	**1.21**	**1.16**
Au (ppm)	0.005	0.003	0.008	0.007	11.1	32.6	4.09	10.6	0.252	0.013
SiO2 (wt.%)	47	46.8	48	49.7	69.7	65	57.6	54.5	40.1	37.9
Al2O3 (wt.%)	14.2	12.3	12.7	12.6	14.85	10.6	15.4	14.15	11.95	11.65
Fe2O3 (wt.%)	3.97	8.24	7.93	7.68	2.89	9.1	7.27	8.2	7.9	7.12
CaO (wt.%)	8.39	7.94	6.95	7.19	0.34	0.57	2.6	5.47	9.26	12.3
MgO (wt.%)	4.85	9.46	8.76	8.71	0.7	0.47	1.86	1.12	5.67	7.57
Na2O (wt.%)	0.03	1.54	1.64	1.48	0.04	0.02	0.02	0.04	0.09	0.05
K2O (wt.%)	2.13	2.19	2.36	2.4	3.07	2.56	3.79	3.54	3.01	2.94
TiO2 (wt.%)	0.99	1.28	1.08	0.98	1.2	1.01	1.1	1.09	1.43	0.85
MnO (wt.%)	0.11	0.12	0.11	0.13	0.01	0.01	0.03	0.02	0.13	0.11
P2O5 (wt.%)	0.23	0.28	0.33	0.33	0.19	0.37	0.35	0.34	0.26	0.25
C (wt.%)	3.41	1.95	1.76	1.9	0.02	0.02	0.84	1.17	3.89	5.19
S (wt.%)	0.79	0.15	0.18	0.36	1.95	7.27	5.13	6.41	4.4	3.69
Ag (ppm)	0.5	0.5	0.5	0.5	4	2	1	0.5	0.5	0.5
Ba (ppm)	242	978	1240	1155	223	102.5	232	269	323	517
Ce (ppm)	61.5	115	125.5	139.5	165	120	143	149.5	111	122.5
Co (ppm)	54.2	39.3	37.3	37.2	34	35.6	37.7	39.4	45.4	27.5
Cr (ppm)	1010	650	560	600	510	490	590	610	790	420
Cs (ppm)	12	15.45	7.97	7.25	10.6	18.3	20.6	29.4	19.2	11.75
Cu (ppm)	39	39	62	68	36	61	59	60	40	35
Dy (ppm)	4.98	5.19	4.87	4.58	4.74	3.6	4.45	4.26	4.51	4.27
Er (ppm)	2.74	2.5	2.43	2.25	2.92	2.15	2.4	2.41	2.38	2.16
Eu (ppm)	1.81	2.9	2.78	2.56	2.84	1.81	2.45	2.36	2.43	2.55
Ga (ppm)	14.8	15.9	15.9	16.3	21.7	18.1	17.9	17.7	14.8	13.9
Gd (ppm)	6.37	9.37	9.08	8.82	9.55	6.75	8.42	9.14	8.09	8.05
Hf (ppm)	3.6	4.5	4.6	4.8	6	4.4	5.1	5.5	4.3	4

Sample	NBC-17C-941	NBC-11C-1153	NBC-11C-1145	NBC-24C-1130-1132	NBC-21C-1279	U15-29-320	U16-H07-13b-486	U16-h07-25-510-515	NBC-17C-1081	NBC-17C-1070
Lithology	**WB Lamp**	**WB Lamp**	**WB Lamp**	**WB Lamp**	**WB Lamp**	**WB Lamp**	**WB Lamp**	**WB Lamp**	**WB Lamp**	**WB Lamp**
Alteration	**Illite/Kaol-inite**	**Illite**	**Illite**	**Illite**	**Illite**	**Illite**	**Illite**	**Illite**	**Illite**	**Illite**
Hf Ratio	**1.36**	**1.09**	**1.07**	**1.02**	**0.82**	**1.11**	**0.96**	**0.89**	**1.14**	**1.23**
Zr Ratio	**1.37**	**1.15**	**1.09**	**0.96**	**0.79**	**1.11**	**0.92**	**0.86**	**1.21**	**1.16**
Ho (ppm)	0.96	0.9	0.85	0.84	0.95	0.68	0.84	0.8	0.83	0.77
La (ppm)	30	56.5	63	72.8	91.7	65.7	74.7	75	53.2	63.9
Lu (ppm)	0.35	0.28	0.28	0.29	0.39	0.28	0.3	0.28	0.29	0.25
Mo (ppm)	1	1	2	2	8	6	2	4	2	2
Nb (ppm)	9.9	15.7	16.2	17.8	20.2	16	18.4	20.3	14.9	14.4
Nd (ppm)	30.7	56.6	57.9	60.7	69.7	53	61.3	63.1	54.5	53.9
Ni (ppm)	397	195	186	186	119	185	194	182	224	101
Pb (ppm)	5	8	9	9	25	10	10	9	7	5
Pr (ppm)	7.57	13.9	14.45	16.25	18.95	14	16.4	16.6	13.5	13.85
Rb (ppm)	108	93.8	89.8	92.4	121.5	132	187	200	159	108
Sm (ppm)	6.17	10.6	10.3	10.45	11.45	8.43	10	9.67	9.95	9.14
Sn (ppm)	1	2	2	1	2	2	2	2	2	1
Sr (ppm)	93.1	787	809	1010	39.6	43.7	106.5	60	394	815
Ta (ppm)	0.7	1.1	1.1	1.1	1.4	1.1	1.3	1.3	1	1
Tb (ppm)	0.88	1.14	1.07	1.03	1.01	0.76	0.95	0.96	0.96	0.9
Th (ppm)	6.52	9.48	10.8	11.6	15.45	11	13.25	14.25	8.99	10.75
Tl (ppm)	1.3	1.5	1	0.9	6.8	45.6	30	10.7	9.2	1.6
Tm (ppm)	0.37	0.32	0.32	0.29	0.39	0.26	0.3	0.3	0.3	0.28
U (ppm)	25.6	2.52	2.8	2.83	10.15	8.5	6.93	3.85	18.65	15.8
V (ppm)	166	199	168	148	216	169	173	142	223	133
W (ppm)	7	1	2	1	14	48	47	82	38	9
Y (ppm)	25.9	22.4	21.4	21.6	26.9	18.8	20.5	19.6	21.5	20.4
Yb (ppm)	2.42	1.98	1.98	2.02	2.53	1.87	2.1	1.94	2.05	1.82
Zn (ppm)	102	74	73	74	84	78	92	96	97	54
Zr (ppm)	139	166	176	200	243	172	207	221	158	164
As (ppm)	609	3.2	17	1.1	1795	2270	1010	700	1560	593

Sample	NBC-17C-941	NBC-11C-1153	NBC-11C-1145	NBC-24C-1130-1132	NBC-21C-1279	U15-29-320	U16-H07-13b-486	U16-h07-25-510-515	NBC-17C-1081	NBC-17C-1070
Lithology	**WB Lamp**	**WB Lamp**	**WB Lamp**	**WB Lamp**	**WB Lamp**	**WB Lamp**	**WB Lamp**	**WB Lamp**	**WB Lamp**	**WB Lamp**
Alteration	**Illite/Kaol-inite**	**Illite**	**Illite**	**Illite**	**Illite**	**Illite**	**Illite**	**Illite**	**Illite**	**Illite**
Hf Ratio	**1.36**	**1.09**	**1.07**	**1.02**	**0.82**	**1.11**	**0.96**	**0.89**	**1.14**	**1.23**
Zr Ratio	**1.37**	**1.15**	**1.09**	**0.96**	**0.79**	**1.11**	**0.92**	**0.86**	**1.21**	**1.16**
Bi (ppm)	0.06	0.01	0.01	0.03	0.04	0.02	0.03	0.02	0.05	0.08
Hg (ppm)	1.17	0.025	0.0025	0.013	5.81	25	7.23	8.95	3.54	0.382
Li (ppm)	3.8	N/A	N/A	35.4	N/A	N/A	1.6	N/A	1.7	N/A
Sb (ppm)	14.6	0.41	0.24	0.2	33.3	159.5	27.5	35.6	17.9	1.98
Se (ppm)	0.6	0.1	0.1	0.1	2	1.9	0.7	1.3	1.2	1
Te (ppm)	0.01	0.005	0.005	0.02	1.8	0.92	0.68	0.16	0.04	0.02
LOI (%)	16.25	9.01	9.48	9.06	5.55	8.44	8.26	9.67	12.5	17.05
Total (%)	98.3	99.5	99.7	100.5	98.6	98.2	98.4	98.3	92.5	98

Sample	U16-h07-13b-436-441	NBC-11C-1100	U15-H08-29-360	U16-H07-24-422	U16-H07-13b-476	U16-h07-15-418-422	NBC-11C-1305	NBC-11C-1267	U16-h07-13b-461-466	NBC-24C-1320
Lithology	**WB Lamp**	**WB Lamp**	**WB Lamp**	**WB Lamp**	**WB Lamp**	**WB Lamp**	**WB Lamp**	**WB Lamp**	**WB Lamp**	**WB Lamp**
Alteration	**Illite**	**Illite**	**Illite**	**Illite**	**Illite**	**Illite**	**Illite**	**Illite**	**Illite**	**Illite**
Hf Ratio	**0.82**	**1.00**	**0.91**	**1.26**	**1.09**	**1.26**	**1.07**	**0.91**	**0.92**	**1.09**
Zr Ratio	**0.79**	**0.93**	**0.86**	**1.27**	**1.04**	**1.18**	**1.04**	**0.90**	**0.87**	**1.05**
Au (ppm)	26.4	0.454	2.32	2.11	49.4	18.85	12.3	53.5	35.1	21.6
SiO2 (wt.%)	62.4	47.5	68	56.6	58.4	54	63.6	68	67.7	65.5
Al2O3 (wt.%)	15.05	12.5	13.8	10.45	11.9	8.94	11.35	14.25	13.5	11.65
Fe2O3 (wt.%)	7.96	8.26	5.29	15.7	11.65	6.67	10.05	3.28	5.02	7.52
CaO (wt.%)	0.62	8.25	0.7	0.47	0.62	9.33	0.46	0.83	0.59	0.58
MgO (wt.%)	0.66	4.96	0.45	0.52	0.47	1.09	0.77	0.87	0.79	0.8
Na2O (wt.%)	0.04	0.03	0.03	0.03	0.03	0.07	0.04	0.02	0.04	0.02
K2O (wt.%)	3.81	3.17	3.55	2.69	3.07	2.34	2.99	3.79	3.61	3.14
TiO2 (wt.%)	1.23	0.98	0.89	0.89	1.11	0.77	0.93	1.11	1.09	0.94
MnO (wt.%)	0.005	0.15	0.01	0.01	0.005	0.005	0.01	0.005	0.005	0.005
P2O5 (wt.%)	0.36	0.33	0.4	0.24	0.31	0.39	0.27	0.39	0.36	0.32
C (wt.%)	0.005	3.2	0.03	0.03	0.04	2.49	0.05	0.09	0.01	0.04
S (wt.%)	6.12	5.15	3.79	12.35	7.44	5.33	7.33	2.32	3.46	5.78
Ag (ppm)	5	0.5	0.5	21	2	8	0.5	0.5	1	2
Ba (ppm)	177	217	146.5	650	146.5	347	265	176	709	98.5
Ce (ppm)	160	139	137	95.7	136	108	133.5	153.5	152.5	121.5
Co (ppm)	42.8	40.4	20.7	35.6	47.6	27.4	31.3	41.7	38.1	34.5
Cr (ppm)	670	690	200	560	860	450	480	680	600	580
Cs (ppm)	20	22.6	9.53	12.55	7.52	25.2	15.95	11.25	18.15	22.6
Cu (ppm)	65	26	56	61	58	45	57	69	47	65
Dy (ppm)	4.66	4.49	4.09	2.42	3.74	2.76	4.34	4.68	4.11	3.3
Er (ppm)	2.62	2.34	2.54	1.5	2.06	1.71	2.48	2.55	2.51	1.85
Eu (ppm)	2.91	2.35	2.1	1.33	2.25	1.47	2.44	2.82	2.43	1.82
Ga (ppm)	23.1	16.3	16.1	13.3	16.3	15.9	17.4	18.9	18.9	20.2
Gd (ppm)	10.25	8.04	7.77	5	7.83	6.07	8.06	9.5	9.02	6.78
Hf (ppm)	6	4.9	5.4	3.9	4.5	3.9	4.6	5.4	5.3	4.5

Sample	U16-h07-13b-436-441	NBC-11C-1100	U15-H08-29-360	U16-H07-24-422	U16-H07-13b-476	U16-h07-15-418-422	NBC-11C-1305	NBC-11C-1267	U16-h07-13b-461-466	NBC-24C-1320
Lithology	**WB Lamp**	**WB Lamp**	**WB Lamp**	**WB Lamp**	**WB Lamp**	**WB Lamp**	**WB Lamp**	**WB Lamp**	**WB Lamp**	**WB Lamp**
Alteration	**Illite**	**Illite**	**Illite**	**Illite**	**Illite**	**Illite**	**Illite**	**Illite**	**Illite**	**Illite**
Hf Ratio	**0.82**	**1.00**	**0.91**	**1.26**	**1.09**	**1.26**	**1.07**	**0.91**	**0.92**	**1.09**
Zr Ratio	**0.79**	**0.93**	**0.86**	**1.27**	**1.04**	**1.18**	**1.04**	**0.90**	**0.87**	**1.05**
Ho (ppm)	0.88	0.8	0.79	0.48	0.65	0.54	0.8	0.85	0.8	0.6
La (ppm)	80.9	66.2	71	50.4	70.9	57.4	70.9	79.3	82.5	64.8
Lu (ppm)	0.32	0.28	0.33	0.2	0.27	0.23	0.32	0.33	0.31	0.27
Mo (ppm)	20	3	2	11	4	9	8	5	12	5
Nb (ppm)	22.7	17.5	18.6	13.4	17.2	13.9	16	19	19.6	15.5
Nd (ppm)	67	58.4	59.5	40.7	59.6	45	59.7	66.8	63.5	50.3
Ni (ppm)	190	211	68	221	253	142	148	209	173	181
Pb (ppm)	11	8	8	19	8	9	9	10	13	13
Pr (ppm)	17.65	15.6	16.05	11	15.85	11.85	15.85	17.6	16.9	13.65
Rb (ppm)	193.5	151	164.5	128.5	135.5	128.5	144	189	204	188
Sm (ppm)	10.95	10.35	9.34	6.4	9.57	6.65	9.99	10.95	10.1	7.8
Sn (ppm)	5	1	1	1	3	2	3	3	2	3
Sr (ppm)	50.9	267	49.1	27.1	43.9	60.5	47.6	43.6	49.6	23.1
Ta (ppm)	1.4	1.1	1.2	0.9	1.1	0.8	1	1.3	1.2	1.1
Tb (ppm)	1.09	0.98	0.86	0.53	0.84	0.62	0.9	1.02	0.96	0.72
Th (ppm)	15.35	12.9	14.35	9.09	11.9	9.8	11.7	14.35	13.4	12.6
Tl (ppm)	42.3	12.7	13	19.4	77.5	21.7	40.2	63.8	23.2	18.9
Tm (ppm)	0.33	0.33	0.33	0.18	0.28	0.23	0.32	0.34	0.3	0.26
U (ppm)	9.68	12.95	3.63	8.59	4.64	10.25	9	4.77	12.25	6.21
V (ppm)	185	164	144	162	227	167	174	172	163	208
W (ppm)	85	26	91	54	83	55	36	76	64	63
Y (ppm)	22.6	22.7	21.7	11.4	17.2	15	24.3	22.3	21.4	16.5
Yb (ppm)	2.21	1.97	2.26	1.36	1.8	1.65	2.14	2.32	2.2	1.84
Zn (ppm)	102	72	66	62	91	84	66	94	89	74
Zr (ppm)	243	206	223	150	184	162	184	213	220	182
As (ppm)	2300	581	3870	2730	10000	1000	3740	4280	1900	918

Sample	U16-h07-13b-436-441	NBC-11C-1100	U15-H08-29-360	U16-H07-24-422	U16-H07-13b-476	U16-h07-15-418-422	NBC-11C-1305	NBC-11C-1267	U16-h07-13b-461-466	NBC-24C-1320
Lithology	**WB Lamp**	**WB Lamp**	**WB Lamp**	**WB Lamp**	**WB Lamp**	**WB Lamp**	**WB Lamp**	**WB Lamp**	**WB Lamp**	**WB Lamp**
Alteration	**Illite**	**Illite**	**Illite**	**Illite**	**Illite**	**Illite**	**Illite**	**Illite**	**Illite**	**Illite**
Hf Ratio	**0.82**	**1.00**	**0.91**	**1.26**	**1.09**	**1.26**	**1.07**	**0.91**	**0.92**	**1.09**
Zr Ratio	**0.79**	**0.93**	**0.86**	**1.27**	**1.04**	**1.18**	**1.04**	**0.90**	**0.87**	**1.05**
Bi (ppm)	0.02	0.02	0.01	0.01	0.07	0.02	0.02	0.02	0.02	0.02
Hg (ppm)	25	2.45	20.2	23.6	25	17.15	25	25	20.8	20.3
Li (ppm)	N/A	N/A	N/A	N/A	N/A	N/A	N/A	1.7	N/A	1.8
Sb (ppm)	194.5	10.1	44.6	156.5	250	131	250	118	84.9	72.8
Se (ppm)	2.6	0.5	0.7	5.1	3	3.5	2.6	1.8	2.2	2.2
Te (ppm)	3.16	0.01	0.02	1.49	2.51	4.13	0.76	1.04	1.04	1.22
LOI (%)	8.03	11.8	5.29	10.85	10.8	6.19	7.9	5.41	5.65	7.65
Total (%)	100.5	98.1	98.5	98.6	98.5	89.9	98.5	98.1	98.5	98.2

Sample	U16-H07-25-555-560	NBC-24C-1264	H08-03-740	U16-h07-67-241	U16-h07-68-247	U15-29-30	NBC-41C-1451	U16-h07-15-179-181	U16-H07-69-337	U16-h07-71-400
Lithology	**WB Lamp**	**WB Lamp**	**WB Lamp**	**Jurassic Rhyolite**	**Jurassic Rhyolite**	**Jurassic Rhyolite**	**Jurassic Rhyolite**	**Jurassic Rhyolite**	**Eocene Dacite**	**Eocene Dacite**
Alteration	**Illite**	**Illite**	**Illite**	**Illite**	**Illite**	**Illite**	**Illite**	**Illite**	**Propyllitic**	**Propyllitic**
Hf Ratio	**0.91**	**0.91**	**0.94**	**N/A**	**N/A**	**N/A**	**N/A**	**N/A**	**N/A**	**N/A**
Zr Ratio	**0.89**	**0.89**	**0.91**	**N/A**	**N/A**	**N/A**	**N/A**	**N/A**	**N/A**	**N/A**
Au (ppm)	34.6	30.7	45.1	0.209	0.621	0.041	1.615	1.565	0.034	0.041
SiO2 (wt.%)	64.6	69.7	62.4	77.1	71.5	73.8	71.7	74.5	61.5	73.1
Al2O3 (wt.%)	13.8	13.85	11.9	12.45	15.2	14.5	14.6	15.35	14.95	15.65
Fe2O3 (wt.%)	7.97	2.87	9.1	1.7	1.54	1.99	1.79	1.89	2.41	0.9
CaO (wt.%)	0.61	0.71	0.62	0.19	1.33	0.41	1.62	0.31	6.91	0.5
MgO (wt.%)	0.74	0.69	0.77	0.35	0.78	0.36	0.87	0.49	0.73	0.49
Na2O (wt.%)	0.04	0.02	0.01	0.06	0.05	0.04	0.04	0.04	0.05	0.05
K2O (wt.%)	3.72	3.76	3.35	3.28	4	3.26	3.99	4.15	1.92	2.12
TiO2 (wt.%)	1.08	1.22	1.22	0.24	0.28	0.27	0.27	0.28	0.42	0.43
MnO (wt.%)	0.01	0.005	0.005	0.01	0.03	0.01	0.04	0.01	0.04	0.01
P2O5 (wt.%)	0.37	0.41	0.39	0.06	0.08	0.07	0.07	0.09	0.19	0.2
C (wt.%)	0.02	0.03	0.02	0.02	0.51	0.08	0.6	0.06	1.47	0.07
S (wt.%)	6.09	1.88	6.67	0.99	0.31	1.25	0.64	0.92	1.03	0.41
Ag (ppm)	6	15	38	0.5	<0.5	0.5	0.5	<1	<0.5	0.5
Ba (ppm)	148.5	166.5	2850	437	239	276	405	326	355	354
Ce (ppm)	150.5	169	152	47.1	44.4	43.9	42.9	48.6	70.3	75.8
Co (ppm)	36.8	41.3	38.6	3.1	3.1	2.8	2.9	3.5	4.2	5.2
Cr (ppm)	610	630	570	20	30	10	10	30	<10	<10
Cs (ppm)	26.8	27.2	26.7	4.26	7.52	4.93	4.61	6.26	7.53	7.31
Cu (ppm)	65	48	128	5	14	6	5	5	1	4
Dy (ppm)	4.45	3.94	3.63	1.16	1.67	1.57	1.63	1.8	3.35	3.12
Er (ppm)	2.47	2.48	2.37	0.76	0.97	0.98	0.95	1.07	1.98	1.86
Eu (ppm)	2.67	2.25	1.88	0.51	0.66	0.55	0.64	0.74	1.24	1.1
Ga (ppm)	18.7	19.5	23	15.6	16.9	16.6	16.5	18	17.2	18.8
Gd (ppm)	10.15	8.19	7.54	2.07	2.59	2.31	2.42	3.04	4.97	4.9
Hf (ppm)	5.4	5.4	5.2	3.3	3.7	3.7	4.4	3.9	5.2	5.6

Sample	U16-H07-25-555-560	NBC-24C-1264	H08-03-740	U16-h07-67-241	U16-h07-68-247	U15-29-30	NBC-41C-1451	U16-h07-15-179-181	U16-H07-69-337	U16-h07-71-400
Lithology	**WB Lamp**	**WB Lamp**	**WB Lamp**	**Jurassic Rhyolite**	**Jurassic Rhyolite**	**Jurassic Rhyolite**	**Jurassic Rhyolite**	**Jurassic Rhyolite**	**Eocene Dacite**	**Eocene Dacite**
Alteration	**Illite**	**Illite**	**Illite**	**Illite**	**Illite**	**Illite**	**Illite**	**Illite**	**Propyllitic**	**Propyllitic**
Hf Ratio	**0.91**	**0.91**	**0.94**	**N/A**	**N/A**	**N/A**	**N/A**	**N/A**	**N/A**	**N/A**
Zr Ratio	**0.89**	**0.89**	**0.91**	**N/A**	**N/A**	**N/A**	**N/A**	**N/A**	**N/A**	**N/A**
Ho (ppm)	0.81	0.76	0.73	0.24	0.33	0.32	0.31	0.36	0.67	0.61
La (ppm)	76.1	88.6	77.8	34	26.3	27.6	25.7	27.6	36.7	38.8
Lu (ppm)	0.31	0.37	0.37	0.11	0.14	0.15	0.13	0.14	0.28	0.27
Mo (ppm)	3	3	2	5	4	6	<1	<2	<1	6
Nb (ppm)	20.1	20	19.4	10.2	12.7	11.7	12.2	13.4	15.3	16.2
Nd (ppm)	64.1	69.6	67.4	16.3	15.9	15.3	15.2	16.8	30.4	32.2
Ni (ppm)	173	186	161	4	2	2	1	7	1	4
Pb (ppm)	12	21	37	8	14	8	12	12	23	26
Pr (ppm)	16.6	19.05	18.05	4.93	4.62	4.6	4.5	4.83	8.16	8.77
Rb (ppm)	207	201	205	133.5	177.5	114.5	156	160	67.7	80.1
Sm (ppm)	10.4	10.55	9.75	2.5	2.63	2.46	2.61	2.93	5.31	5.32
Sn (ppm)	4	2	13	2	2	2	2	2	1	2
Sr (ppm)	47.5	47.4	54	18.8	52.2	35.6	57.8	38.5	39	24.1
Ta (ppm)	1.2	1.4	1.3	1.1	1.3	1.2	1.2	1.3	1.2	1.2
Tb (ppm)	1.03	0.89	0.81	0.24	0.33	0.29	0.32	0.35	0.67	0.64
Th (ppm)	14.55	15	14.75	9.89	11.6	10.95	11.15	11.7	9.58	10.15
Tl (ppm)	21.2	18.5	22	1.4	1.9	2.2	1.9	1.7	1.8	1.3
Tm (ppm)	0.32	0.35	0.34	0.1	0.12	0.13	0.13	0.14	0.25	0.24
U (ppm)	4.94	5.74	5.96	5.13	5.78	4.7	4.63	6	4.22	4.66
V (ppm)	190	230	285	70	21	40	20	25	34	36
W (ppm)	102	73	72	6	6	3	4	5	14	2
Y (ppm)	22.1	21.2	19.7	6.9	8.9	9.8	9.1	10.3	20.8	17.2
Yb (ppm)	2.19	2.46	2.47	0.79	0.87	1	0.87	0.97	1.79	1.84
Zn (ppm)	87	103	70	29	46	64	36	67	75	13
Zr (ppm)	215	214	209	122	144	140	144	152	198	213
As (ppm)	1500	1595	1410	102	309	273	903	500	239	51.5

Sample	U16-H07-25-555-560	NBC-24C-1264	H08-03-740	U16-h07-67-241	U16-h07-68-247	U15-29-30	NBC-41C-1451	U16-h07-15-179-181	U16-H07-69-337	U16-h07-71-400
Lithology	**WB Lamp**	**WB Lamp**	**WB Lamp**	**Jurassic Rhyolite**	**Jurassic Rhyolite**	**Jurassic Rhyolite**	**Jurassic Rhyolite**	**Jurassic Rhyolite**	**Eocene Dacite**	**Eocene Dacite**
Alteration	**Illite**	**Illite**	**Illite**	**Illite**	**Illite**	**Illite**	**Illite**	**Illite**	**Propyllitic**	**Propyllitic**
Hf Ratio	**0.91**	**0.91**	**0.94**	**N/A**	**N/A**	**N/A**	**N/A**	**N/A**	**N/A**	**N/A**
Zr Ratio	**0.89**	**0.89**	**0.91**	**N/A**	**N/A**	**N/A**	**N/A**	**N/A**	**N/A**	**N/A**
Bi (ppm)	0.02	0.02	0.03	0.09	0.18	0.09	0.04	0.05	0.02	0.32
Hg (ppm)	17	20.5	22	0.914	1.31	4.74	1.375	0.627	0.583	0.529
Li (ppm)	N/A	1.4	N/A	N/A	N/A	N/A	N/A	N/A	N/A	N/A
Sb (ppm)	60.1	91.2	119	9.08	1.27	42.3	2.73	4.72	30.9	2.92
Se (ppm)	2.6	1.8	4.9	0.3	<0.2	2.2	0.4	0.2	0.2	0.2
Te (ppm)	1.49	5.34	32.8	<0.01	<0.01	0.01	<0.01	0.02	0.01	0.01
LOI (%)	7.56	4.98	7.79	3.06	4.78	4.08	4.55	3.01	8.87	6.35
Total (%)	100.5	98.3	98	98.6	99.6	98.8	99.6	100	98	99.8

Sample	NBC-41C-1165	U16-H07-69-940	U16-H07-70-936	U16-H07-25-25	U16-25-167	U16-H07-34-84	U16-H07-34-138	U16-H07-25-80	U16-807-25-251
Lithology	**Eocene Dacite**	**Eocene Dacite**	**Eocene Dacite**	**Bootstrap Limestone**	**Bootstrap Limestone**	**Bootstrap Limestone**	**Bootstrap Limestone**	**Bootstrap Limestone**	**Bootstrap Dolomite**
Alteration	**Propyllitic**	**Propyllitic**	**Propyllitic**	**Least Altered**	**Least Altered**	**Least Altered**	**Least Altered**	**Least Altered**	**Silicified**
Hf Ratio	**N/A**	**N/A**	**N/A**	**N/A**	**N/A**	**N/A**	**N/A**	**N/A**	**N/A**
Zr Ratio	**N/A**	**N/A**	**N/A**	**N/A**	**N/A**	**N/A**	**N/A**	**N/A**	**N/A**
Au (ppm)	0.003	0.001	0.003	0.004	0.006	0.01	0.001	0.001	0.308
SiO2 (wt.%)	61.3	61.3	64.5	0.73	1.6	2.83	0.65	0.61	84.2
Al2O3 (wt.%)	15.05	14.75	15.65	0.21	0.32	0.29	0.18	0.14	3.34
Fe2O3 (wt.%)	3.96	3.63	3.63	0.08	0.12	0.12	0.07	0.05	1.7
CaO (wt.%)	3.09	3.88	2.33	54.3	54	53.2	55.3	54.7	3.52
MgO (wt.%)	1.86	1.74	1.58	1.06	0.78	0.77	0.7	0.75	0.28
Na2O (wt.%)	0.06	0.05	0.05	0.07	0.06	0.07	0.06	0.06	0.05
K2O (wt.%)	2.99	3.08	2.96	0.05	0.09	0.09	0.07	0.04	0.89
TiO2 (wt.%)	0.45	0.43	0.46	0.01	0.01	0.01	0.01	0.01	0.22
MnO (wt.%)	0.07	0.1	0.13	0.005	0.01	0.01	0.005	0.005	0.01
P2O5 (wt.%)	0.21	0.19	0.23	0.85	0.14	0.09	0.13	0.15	1.25
C (wt.%)	0.95	1.62	0.79	13.4	12.4	12.3	12.6	12.3	1.03
S (wt.%)	0.04	0.05	0.02	0.15	0.09	0.08	0.04	0.08	1.27
Ag (ppm)	<0.5	<0.5	0.5	0.5	0.5	0.5	0.5	0.5	3.1
Ba (ppm)	590	577	485	127.5	94.8	290	159	2010	3130
Ce (ppm)	73.3	70.2	74.4	2.5	2.6	3.5	2	2.8	31.6
Co (ppm)	4	4.3	4.6	2	1	2	2	1	5.3
Cr (ppm)	<10	10	<10	10	5	10	5	5	80
Cs (ppm)	10.15	9.92	10.85	0.14	0.12	0.19	0.06	0.05	5.8
Cu (ppm)	1	3	2	2	2	4	2	2	16
Dy (ppm)	3.08	3.05	3.26	0.31	0.25	0.36	0.2	0.34	2.2
Er (ppm)	1.72	1.69	1.86	0.22	0.17	0.24	0.15	0.22	1.19
Eu (ppm)	1.25	1.29	1.34	0.07	0.05	0.09	0.04	0.09	0.76
Ga (ppm)	18.7	18.1	20.3	0.3	0.4	0.3	0.3	0.2	4
Gd (ppm)	4.61	4.5	4.79	0.32	0.24	0.47	0.21	0.42	3.06
Hf (ppm)	6.3	5.8	6.4	0.2	0.2	0.3	0.1	0.1	2.4

Sample	NBC-41C-1165	U16-H07-69-940	U16-H07-70-936	U16-H07-25-25	U16-25-167	U16-H07-34-84	U16-H07-34-138	U16-H07-25-80	U16-807-25-251
Lithology	**Eocene Dacite**	**Eocene Dacite**	**Eocene Dacite**	**Bootstrap Limestone**	**Bootstrap Limestone**	**Bootstrap Limestone**	**Bootstrap Limestone**	**Bootstrap Limestone**	**Bootstrap Dolomite**
Alteration	**Propyllitic**	**Propyllitic**	**Propyllitic**	**Least Altered**	**Least Altered**	**Least Altered**	**Least Altered**	**Least Altered**	**Silicified**
Hf Ratio	**N/A**	**N/A**	**N/A**	**N/A**	**N/A**	**N/A**	**N/A**	**N/A**	**N/A**
Zr Ratio	**N/A**	**N/A**	**N/A**	**N/A**	**N/A**	**N/A**	**N/A**	**N/A**	**N/A**
Ho (ppm)	0.58	0.56	0.6	0.07	0.05	0.07	0.04	0.07	0.42
La (ppm)	38.1	36.7	38.8	3.4	2.3	2.7	1.7	2.4	19.8
Lu (ppm)	0.25	0.24	0.26	0.03	0.02	0.03	0.02	0.03	0.12
Mo (ppm)	<1	<1	<1	3	5	2	4	6	27
Nb (ppm)	16.5	15.4	16.9	0.2	0.3	0.3	0.2	0.2	4.1
Nd (ppm)	31.1	29.5	32	1.5	1.3	2.1	1	1.9	16.3
Ni (ppm)	<1	<1	<1	8	5	10	2	6	56
Pb (ppm)	20	18	19	4	2	2	3	2	76
Pr (ppm)	8.53	8.07	8.65	0.38	0.34	0.5	0.25	0.43	4.08
Rb (ppm)	96.7	99.2	101	1.3	2.4	2.2	1.4	1	28.3
Sm (ppm)	5.39	5.27	5.5	0.3	0.23	0.36	0.16	0.34	2.82
Sn (ppm)	2	1	1	0.5	0.5	0.5	0.5	0.5	1
Sr (ppm)	238	118.5	65	117.5	186.5	145	191.5	161.5	31.6
Ta (ppm)	1.2	1.1	1.2	0.05	0.05	0.05	0.05	0.05	0.3
Tb (ppm)	0.63	0.61	0.65	0.05	0.04	0.06	0.03	0.06	0.41
Th (ppm)	9.79	9.39	10.2	0.18	0.29	0.32	0.19	0.2	3.89
Tl (ppm)	0.7	1.5	0.8	0.25	0.25	0.25	0.25	0.25	2.3
Tm (ppm)	0.24	0.24	0.26	0.02	0.01	0.02	0.01	0.01	0.13
U (ppm)	3.66	3.76	3.68	12.7	7	3.7	5.33	2.32	30
V (ppm)	35	33	37	39	2.5	13	2.5	2.5	62
W (ppm)	2	4	5	1	1	0.5	0.5	0.5	8
Y (ppm)	16	15.5	17.1	5.2	3.1	4	2.7	4	17.2
Yb (ppm)	1.65	1.65	1.71	0.2	0.15	0.18	0.13	0.16	0.83
Zn (ppm)	76	52	66	2	2	14	3	8	263
Zr (ppm)	214	195	219	8	8	12	5	3	91
As (ppm)	20.9	26.8	9.3	93.4	11.9	61.9	5	4.9	1650

Sample	NBC-41C-1165	U16-H07-69-940	U16-H07-70-936	U16-H07-25-25	U16-25-167	U16-H07-34-84	U16-H07-34-138	U16-H07-25-80	U16-807-25-251
Lithology	**Eocene Dacite**	**Eocene Dacite**	**Eocene Dacite**	**Bootstrap Limestone**	**Bootstrap Limestone**	**Bootstrap Limestone**	**Bootstrap Limestone**	**Bootstrap Limestone**	**Bootstrap Dolomite**
Alteration	**Propyllitic**	**Propyllitic**	**Propyllitic**	**Least Altered**	**Least Altered**	**Least Altered**	**Least Altered**	**Least Altered**	**Silicified**
Hf Ratio	**N/A**	**N/A**	**N/A**	**N/A**	**N/A**	**N/A**	**N/A**	**N/A**	**N/A**
Zr Ratio	**N/A**	**N/A**	**N/A**	**N/A**	**N/A**	**N/A**	**N/A**	**N/A**	**N/A**
Bi (ppm)	0.09	0.04	0.02	0.005	0.02	0.01	0.01	0.01	0.05
Hg (ppm)	0.063	0.076	0.042	0.237	0.1	0.084	0.008	0.072	4.1
Li (ppm)	N/A	N/A	N/A	N/A	N/A	N/A	N/A	N/A	N/A
Sb (ppm)	0.16	0.5	0.53	0.65	2.41	2.64	0.32	0.38	103.5
Se (ppm)	0.2	<0.2	0.2	0.3	0.4	0.3	0.3	0.3	2.5
Te (ppm)	<0.01	<0.01	<0.01	0.01	0.01	0.01	0.01	0.005	0.19
LOI (%)	10.15	9.71	7.6	42.7	42.8	42.3	42.6	43	4.06
Total (%)	99.3	98.9	99.2	100	100	99.8	99.8	99.8	99.9

Sample	U16-h07-34-405	H16-H07-34-497	U16-H07-34-245	U16-h07-34-316
Lithology	**Bootstrap Dolomite**	**Bootstrap Limestone**	**Bootstrap Dolomite**	**Bootstrap Dolomite**
Alteration	**Least Altered**	**Least Altered**	**Least Altered**	**Least Altered**
Hf Ratio	**N/A**	**N/A**	**N/A**	**N/A**
Zr Ratio	**N/A**	**N/A**	**N/A**	**N/A**
Au (ppm)	0.197	0.01	0.006	0.022
SiO2 (wt.%)	11.75	4.49	8.06	14.9
Al2O3 (wt.%)	2.75	1.04	1.62	3.97
Fe2O3 (wt.%)	0.89	0.59	0.42	1.52
CaO (wt.%)	36.7	50.8	41.1	30.3
MgO (wt.%)	7.98	1.01	6.78	10.55
Na2O (wt.%)	0.03	0.01	0.03	0.04
K2O (wt.%)	0.86	0.3	0.66	1.24
TiO2 (wt.%)	0.13	0.05	0.08	0.19
MnO (wt.%)	0.01	0.03	0.01	0.01
P2O5 (wt.%)	0.43	0.23	0.44	0.58
C (wt.%)	12.15	11.5	12.05	12.4
S (wt.%)	0.87	0.3	0.41	1.43
Ag (ppm)	0.5	0.5	0.5	0.5
Ba (ppm)	268	1085	384	296
Ce (ppm)	18.3	10	11.5	20.2
Co (ppm)	3	1.1	1.7	4
Cr (ppm)	30	10	20	50
Cs (ppm)	1.55	0.45	0.57	2.15
Cu (ppm)	17	0.5	5	26
Dy (ppm)	1.74	0.72	1.2	2.01
Er (ppm)	1.05	0.38	0.76	1.24
Eu (ppm)	0.45	0.26	0.29	0.5
Ga (ppm)	4.5	1.3	1.7	6.5
Gd (ppm)	2.13	1	1.44	2.47
Hf (ppm)	1.6	0.4	1.5	2.3

Sample	U16-h07-34-405	H16-H07-34-497	U16-H07-34-245	U16-h07-34-316
Lithology	**Bootstrap Dolomite**	**Bootstrap Limestone**	**Bootstrap Dolomite**	**Bootstrap Dolomite**
Alteration	**Least Altered**	**Least Altered**	**Least Altered**	**Least Altered**
Hf Ratio	**N/A**	**N/A**	**N/A**	**N/A**
Zr Ratio	**N/A**	**N/A**	**N/A**	**N/A**
Ho (ppm)	0.36	0.13	0.25	0.41
La (ppm)	13	5.8	8.7	14.6
Lu (ppm)	0.14	0.04	0.1	0.15
Mo (ppm)	29	12	34	44
Nb (ppm)	2.8	0.8	2.2	4.2
Nd (ppm)	11.1	4.8	7.1	12.6
Ni (ppm)	112	12	85	167
Pb (ppm)	6	3	4	7
Pr (ppm)	2.81	1.25	1.77	3.13
Rb (ppm)	28.2	9.2	14.2	39.2
Sm (ppm)	2.02	0.96	1.28	2.31
Sn (ppm)	1	0.5	0.5	1
Sr (ppm)	127.5	125	138.5	124
Ta (ppm)	0.2	0.1	0.1	0.3
Tb (ppm)	0.3	0.13	0.2	0.34
Th (ppm)	2.24	1.26	1.6	3.46
Tl (ppm)	0.8	0.7	0.5	1.1
Tm (ppm)	0.21	0.05	0.11	0.19
U (ppm)	13.45	7.45	15.75	19.05
V (ppm)	288	14	101	438
W (ppm)	4	1	2	4
Y (ppm)	14.1	5.2	12.3	15.8
Yb (ppm)	0.95	0.32	0.68	1.14
Zn (ppm)	542	3	122	816
Zr (ppm)	63	16	59	87
As (ppm)	41.6	45.1	45.8	59

Sample	U16-h07-34-405	H16-H07-34-497	U16-H07-34-245	U16-h07-34-316
Lithology	**Bootstrap Dolomite**	**Bootstrap Limestone**	**Bootstrap Dolomite**	**Bootstrap Dolomite**
Alteration	**Least Altered**	**Least Altered**	**Least Altered**	**Least Altered**
Hf Ratio	**N/A**	**N/A**	**N/A**	**N/A**
Zr Ratio	**N/A**	**N/A**	**N/A**	**N/A**
Bi (ppm)	0.03	0.01	0.02	0.05
Hg (ppm)	1.94	0.57	0.174	2.88
Li (ppm)	1.5	0.4	1.3	N/A
Sb (ppm)	2.15	14.75	0.71	2.43
Se (ppm)	7	0.4	2.2	18.7
Te (ppm)	0.07	0.02	0.04	0.15
LOI (%)	37.7	40.3	39.4	35.1
Total (%)	99.3	99	98.7	98.5

Table 2.3 Tabulated mass transfer calculations for the west Banshee dike. Zr was used as the immobile element for calculations according to Equation 2.1. Calculation error is the percent difference in mass transfer calculations between using Zr and Hf as the conserved element.

Sample	NBC-30C-1475	NBC-11C-1569	NBC-21C-1523.5	NBC-11-1225	U16-h07-54-332-338	U16-h07-54-298-302	H16-H08-27-645	NBC-17C-1496	U16-H07-34-537	NBC-17C-1587	NBC-17C-941	NBC-11C-1153
Alteration	**Kaolinite**	**Kaolinite**	**Kaolinite**	**Kaolinite**	**Kaolinite**	**Kaolinite**	**Kaolinite**	**Montmorillonite**	**Least Altered**	**Least Altered**	**Illite/Kaolinite**	**Illite**
Hf ratio	**1.00**	**1.09**	**0.98**	**0.96**	**0.79**	**0.83**	**0.82**	**1.00**	**1.00**	**1.04**	**1.36**	**1.09**
Zr Ratio	**0.98**	**1.02**	**0.96**	**0.92**	**0.75**	**0.75**	**0.80**	**1.05**	**1.00**	**1.03**	**1.37**	**1.15**
Au (ppm)	BDL	BDL	BDL	0.002	0.015	0.035	0.052	BDL	0	BDL	0.006	0.002
SiO2 (wt.%)	3.39	-1.08	2.51	-9.48	-6.11	-5.69	7.60	-3.73	0	2.33	14.88	4.15
Al2O3 (wt.%)	-1.44	-0.64	-0.14	-0.29	-0.97	-1.47	-0.53	1.38	0	0.63	6.41	1.05
Fe2O3 (wt.%)	-3.65	-6.12	-6.84	-1.75	-4.93	-5.82	-7.29	0.69	0	0.22	-2.86	1.16
CaO (wt.%)	2.40	11.05	5.61	-1.07	-2.74	-1.62	-7.02	0.35	0	-0.07	3.94	1.55
MgO (wt.%)	-7.26	-8.12	-8.77	-0.76	-8.29	-7.93	-8.75	-2.47	0	0.27	-2.30	1.92
Na2O (wt.%)	-1.97	-2.03	-2.03	-2.02	-2.02	-2.03	-2.03	-1.98	0	0.47	-2.01	-0.28
K2O (wt.%)	-1.65	-1.60	-1.56	-1.39	-1.39	-1.29	-1.05	-0.77	0	0.14	1.07	0.66
TiO2 (wt.%)	-0.19	-0.24	-0.09	-0.16	-0.19	-0.33	-0.35	0.08	0	-0.04	0.20	0.31
MnO (wt.%)	-0.05	-0.06	-0.07	0.01	-0.08	-0.08	-0.11	-0.02	0	-0.01	0.03	0.02
P2O5 (wt.%)	0.01	0.04	0.00	-0.01	-0.03	-0.05	0.04	0.00	0	-0.01	-0.01	-0.01
C (wt.%)	1.90	2.80	1.67	1.37	0.44	0.40	-0.99	0.97	0	-0.34	3.70	1.25
S (wt.%)	2.02	0.94	0.77	0.77	0.42	0.10	0.46	0.05	0	0.03	1.01	0.09
Ag (ppm)	0.0	0.0	0.0	0.0	-0.1	-0.1	-0.1	0.0	0	0.0	0.2	0.1
Ba (ppm)	-2215.9	-2181.9	-1847.3	-2242.3	-2325.0	-1984.4	-2304.3	-1876.3	0	-883.0	-2047.5	-1254.7
Ce (ppm)	1.7	41.7	3.3	4.2	-10.3	-21.4	-11.7	-9.7	0	-5.0	-49.0	-1.2
Co (ppm)	-2.8	-25.1	-14.8	1.4	-15.8	-18.9	-16.6	0.5	0	0.5	35.9	6.6
Cr (ppm)	-31	-161	130	35	-26	-218	-309	344	0	29	808	168
Cs (ppm)	-3.07	-2.43	-0.29	2.41	-0.57	-1.88	-0.93	4.85	0	-1.80	12.72	14.01
Cu (ppm)	-20	8	9	10	-16	-6	1	9	0	29	-6	-15
Dy (ppm)	-1.62	0.61	-0.56	-0.53	-1.83	-2.13	-1.92	-0.74	0	-0.43	1.53	0.66
Er (ppm)	-0.81	0.11	-0.25	-0.31	-0.76	-0.95	-0.64	-0.48	0	-0.26	1.14	0.25
Eu (ppm)	-0.65	0.84	0.01	-0.11	-0.60	-0.89	-1.07	-0.13	0	-0.06	-0.33	0.52
Ga (ppm)	-2.1	-0.5	1.0	-1.4	-1.0	-2.4	-2.2	1.5	0	-0.4	3.0	1.0
Gd (ppm)	-2.2	2.9	-0.1	-0.2	-1.4	-2.3	-2.8	-0.5	0	-0.3	-0.5	1.6
Hf (ppm)	-0.1	-0.3	-0.1	-0.2	-0.3	-0.4	-0.1	0.2	0	0.0	0.0	0.3
Ho (ppm)	-0.26	0.05	-0.10	-0.12	-0.31	-0.35	-0.26	-0.16	0	-0.07	0.39	0.11

Sample	NBC-30C-1475	NBC-11C-1569	NBC-21C-1523.5	NBC-11-1225	U16-h07-54-332-338	U16-h07-54-298-302	H16-H08-27-645	NBC-17C-1496	U16-H07-34-537	NBC-17C-1587	NBC-17C-941	NBC-11C-1153
Alteration	**Kaolinite**	**Kaolinite**	**Kaolinite**	**Kaolinite**	**Kaolinite**	**Kaolinite**	**Kaolinite**	**Montmorillonite**	**Least Altered**	**Least Altered**	**Illite/Kaolinite**	**Illite**
Hf ratio	**1.00**	**1.09**	**0.98**	**0.96**	**0.79**	**0.83**	**0.82**	**1.00**	**1.00**	**1.04**	**1.36**	**1.09**
Zr Ratio	**0.98**	**1.02**	**0.96**	**0.92**	**0.75**	**0.75**	**0.80**	**1.05**	**1.00**	**1.03**	**1.37**	**1.15**
La (ppm)	2.9	23.0	1.7	3.0	-5.2	-12.8	-5.5	-4.5	0	-2.7	-27.1	-3.3
Lu (ppm)	-0.09	0.02	-0.02	-0.03	-0.11	-0.09	-0.06	-0.07	0	-0.02	0.17	0.01
Mo (ppm)	1	2	1	1	0	1	0	1	0	1	0	0
Nb (ppm)	-0.8	-1.3	-2.0	-1.7	-0.9	-1.5	-2.0	-0.4	0	-1.6	-5.0	-0.5
Nd (ppm)	-9.3	16.2	-1.6	-3.2	-12.5	-15.6	-12.4	-5.4	0	-4.8	-20.3	2.6
Ni (ppm)	-12	-103	-84	21	-52	-69	-88	76	0	38	370	48
Pb (ppm)	2	-3	1	2	-1	-2	-3	0	0	0	-1	1
Pr (ppm)	-0.9	4.3	-0.1	-0.4	-2.7	-3.5	-2.2	-1.6	0	-1.3	-5.6	-0.1
Rb (ppm)	-43.2	-41.0	-39.1	-25.7	-27.0	-21.7	-11.7	-15.2	0	-2.0	95.0	54.5
Sm (ppm)	-2.91	2.79	-0.78	-1.27	-2.94	-3.25	-3.48	-1.15	0	-1.02	-2.62	1.10
Sn (ppm)	1	0	1	1	0	1	0	1	0	1	0	1
Sr (ppm)	-925.7	-997.2	-954.8	-854.6	-978.6	-998.6	-1000.2	-845.3	0	17.9	-902.1	-124.5
Ta (ppm)	0.1	0.0	0.1	0.0	-0.1	-0.1	0.0	0.1	0	0.0	-0.1	0.2
Tb (ppm)	-0.32	0.26	-0.11	-0.13	-0.34	-0.41	-0.41	-0.13	0	-0.12	0.05	0.15
Th (ppm)	3.0	1.8	2.1	2.2	1.8	1.3	2.2	1.1	0	1.6	-1.1	0.8
Tl (ppm)	-0.01	1.08	1.57	0.67	0.80	0.13	2.69	0.01	0	0.01	1.54	1.48
Tm (ppm)	-0.12	0.00	-0.04	-0.05	-0.12	-0.13	-0.10	-0.09	0	-0.04	0.16	0.02
U (ppm)	1.44	11.78	8.28	0.62	8.87	7.63	10.21	0.10	0	0.29	32.66	0.38
V (ppm)	-19	-54	-1	-13	-35	-69	-38	27	0	1	56	57
W (ppm)	20	35	35	3	60	33	22	19	0	0	9	0
Y (ppm)	-7.9	0.4	-2.3	-3.3	-7.8	-9.8	-8.1	-4.9	0	-2.7	11.5	1.7
Yb (ppm)	-0.64	0.24	-0.09	-0.16	-0.51	-0.57	-0.38	-0.38	0	-0.06	1.23	0.18
Zn (ppm)	71	-31	-34	-6	-10	-5	-26	0	0	4	61	6
Zr (ppm)	0	0	0	0	0	0	0	0	0	0	0	0
As (ppm)	215	312	235	33	224	11	141	1	0	1	837	3
Bi (ppm)	0.01	0.00	0.01	0.04	0.00	0.00	0.02	0.01	0	0.00	0.07	0.00
Hg (ppm)	0.855	3.389	2.714	0.155	0.603	0.752	2.679	0.046	0	0.000	1.605	0.026

Sample	**NBC-30C-1475**	**NBC-11C-1569**	**NBC-21C-1523.5**	**NBC-11-1225**	**U16-h07-54-332-338**	**U16-h07-54-298-302**	**H16-H08-27-645**	**NBC-17C-1496**	**U16-H07-34-537**	**NBC-17C-1587**	**NBC-17C-941**	**NBC-11C-1153**
Alteration	**Kaolinite**	**Kaolinite**	**Kaolinite**	**Kaolinite**	**Kaolinite**	**Kaolinite**	**Kaolinite**	**Montmorillonite**	**Least Altered**	**Least Altered**	**Illite/Kaolinite**	**Illite**
Hf ratio	**1.00**	**1.09**	**0.98**	**0.96**	**0.79**	**0.83**	**0.82**	**1.00**	**1.00**	**1.04**	**1.36**	**1.09**
Zr Ratio	**0.98**	**1.02**	**0.96**	**0.92**	**0.75**	**0.75**	**0.80**	**1.05**	**1.00**	**1.03**	**1.37**	**1.15**
Li (ppm)	-37.3	N/A	N/A	N/A	N/A	N/A	N/A	-20.0	0	N/A	-35.7	N/A
Sb (ppm)	18.89	37.53	33.05	1.01	19.99	1.12	49.42	0.00	0	0.26	19.90	0.31
Se (ppm)	0.1	0.6	1.4	2.7	0.3	0.4	1.7	0.2	0	0.0	0.7	0.0
Te (ppm)	0.00	0.00	-0.01	0.03	-0.01	-0.01	-0.01	0.00	0	0.00	0.00	0.00
LOI (%)	6.6	10.5	7.2	7.2	0.6	0.7	-1.8	9.8	0	-1.2	15.5	3.5
Calculation Error	-2.09	-6.61	-2.10	-4.63	-5.51	-10.01	-2.62	4.71	0.00	-0.98	0.95	5.36

Sample	NBC-11C-1145	NBC-24C-1130-1132	NBC-21C-1279	U15-29-320	U16-H07-13b-486	U16-h07-25-510-515	NBC-17C-1081	NBC-17C-1070	U16-h07-13b-436-441	NBC-11C-1100	U15-H08-29-360	U16-H07-24-422
Alteration	**Illite**	**Illite**	**Illite**	**Illite**	**Illite**	**Illite**	**Illite**	**Illite**	**Illite**	**Illite**	**Illite**	**Illite**
Hf ratio	**1.07**	**1.02**	**0.82**	**1.11**	**0.96**	**0.89**	**1.14**	**1.23**	**0.82**	**1.00**	**0.91**	**1.26**
Zr Ratio	**1.09**	**0.96**	**0.79**	**1.11**	**0.92**	**0.86**	**1.21**	**1.16**	**0.79**	**0.93**	**0.86**	**1.27**
Au (ppm)	0.008	0.006	8.724	36.200	3.773	9.160	0.304	0.014	20.750	0.420	1.986	2.686
SiO2 (wt.%)	2.39	-2.24	5.08	22.48	3.45	-2.60	-1.22	-5.56	-0.65	-5.66	8.54	22.37
Al2O3 (wt.%)	0.68	-1.07	-1.43	-1.33	1.11	-0.87	1.35	0.47	-1.27	-1.51	-1.28	0.21
Fe2O3 (wt.%)	0.29	-0.99	-6.05	1.79	-1.61	-1.23	1.23	-0.03	-2.06	-0.66	-3.79	11.67
CaO (wt.%)	-0.05	-0.72	-7.32	-6.96	-5.19	-2.86	3.60	6.73	-7.10	0.06	-6.99	-6.99
MgO (wt.%)	0.55	-0.64	-8.41	-8.44	-7.24	-7.99	-2.11	-0.14	-8.44	-4.36	-8.57	-8.30
Na2O (wt.%)	-0.27	-0.64	-2.02	-2.03	-2.03	-2.02	-1.94	-1.99	-2.02	-2.02	-2.02	-2.01
K2O (wt.%)	0.70	0.43	0.55	0.98	1.64	1.20	1.78	1.56	1.13	1.08	1.18	1.57
TiO2 (wt.%)	0.01	-0.22	-0.22	-0.04	-0.15	-0.22	0.57	-0.17	-0.19	-0.25	-0.40	-0.03
MnO (wt.%)	0.00	0.00	-0.11	-0.11	-0.09	-0.10	0.04	0.01	-0.12	0.02	-0.11	-0.11
P2O5 (wt.%)	0.03	-0.01	-0.18	0.08	-0.01	-0.04	-0.02	-0.04	-0.05	-0.02	0.01	-0.02
C (wt.%)	0.92	0.82	-0.97	-0.97	-0.21	0.02	3.71	5.05	-0.99	1.98	-0.96	-0.95
S (wt.%)	0.12	0.26	1.45	7.99	4.65	5.46	5.24	4.22	4.73	4.70	3.17	15.65
Ag (ppm)	0.0	0.0	2.6	1.7	0.4	-0.1	0.1	0.1	3.4	0.0	-0.1	26.2
Ba (ppm)	-1034.3	-1277.0	-2204.7	-2266.2	-2165.9	-2147.5	-1989.5	-1777.9	-2240.9	-2178.8	-2254.5	-1552.3
Ce (ppm)	2.7	-0.3	-3.8	-0.2	-1.6	-4.3	0.7	9.2	-7.7	-4.6	-16.2	-11.6
Co (ppm)	1.9	-3.1	-11.9	0.9	-3.8	-4.5	16.3	-6.6	-5.0	-1.1	-20.9	6.7
Cr (ppm)	28	-7	-179	-36	-36	-53	375	-91	-53	60	-409	133
Cs (ppm)	4.88	3.15	4.56	16.55	15.24	21.64	19.44	9.91	11.95	17.18	4.39	12.21
Cu (ppm)	7	5	-32	8	-6	-8	-12	-19	-9	-36	-12	18
Dy (ppm)	-0.02	-0.94	-1.58	-1.31	-1.20	-1.63	0.14	-0.34	-1.65	-1.15	-1.81	-2.23
Er (ppm)	0.01	-0.48	-0.33	-0.24	-0.42	-0.55	0.25	-0.11	-0.57	-0.46	-0.45	-0.72
Eu (ppm)	0.20	-0.38	-0.59	-0.81	-0.56	-0.78	0.12	0.15	-0.53	-0.64	-1.02	-1.13
Ga (ppm)	0.0	-1.7	-0.2	2.8	-0.8	-2.0	0.6	-1.1	0.9	-2.2	-3.5	-0.4
Gd (ppm)	0.6	-0.8	-1.7	-1.7	-1.5	-1.3	0.5	0.1	-1.2	-1.8	-2.6	-2.9
Hf (ppm)	0.1	-0.3	-0.2	0.0	-0.2	-0.1	0.3	-0.2	-0.2	-0.4	-0.3	0.1
Ho (ppm)	-0.01	-0.13	-0.18	-0.17	-0.15	-0.24	0.07	-0.03	-0.24	-0.19	-0.25	-0.32

Sample	NBC-11C-1145	NBC-24C-1130-1132	NBC-21C-1279	U15-29-320	U16-H07-13b-486	U16-h07-25-510-515	NBC-17C-1081	NBC-17C-1070	U16-h07-13b-436-441	NBC-11C-1100	U15-H08-29-360	U16-H07-24-422
Alteration	**Illite**	**Illite**	**Illite**	**Illite**	**Illite**	**Illite**	**Illite**	**Illite**	**Illite**	**Illite**	**Illite**	**Illite**
Hf ratio	**1.07**	**1.02**	**0.82**	**1.11**	**0.96**	**0.89**	**1.14**	**1.23**	**0.82**	**1.00**	**0.91**	**1.26**
Zr Ratio	**1.09**	**0.96**	**0.79**	**1.11**	**0.92**	**0.86**	**1.21**	**1.16**	**0.79**	**0.93**	**0.86**	**1.27**
La (ppm)	0.1	1.2	3.8	4.7	0.6	-3.5	-4.0	6.1	-4.7	-6.9	-7.5	-4.1
Lu (ppm)	-0.01	-0.03	0.00	0.00	-0.03	-0.07	0.04	-0.02	-0.06	-0.05	-0.03	-0.06
Mo (ppm)	1	1	5	6	1	2	1	1	15	2	1	13
Nb (ppm)	-1.0	-1.6	-2.7	-0.8	-1.6	-1.1	-0.6	-1.8	-0.8	-2.4	-2.7	-1.5
Nd (ppm)	0.3	-4.5	-7.7	-3.6	-5.9	-8.0	3.4	0.3	-9.8	-8.4	-11.5	-10.7
Ni (ppm)	26	2	-82	29	3	-19	95	-58	-27	20	-118	105
Pb (ppm)	2	1	12	3	1	0	0	-2	1	-1	-1	16
Pr (ppm)	-0.4	-0.5	-1.2	-0.5	-0.9	-1.7	0.3	0.1	-2.2	-1.6	-2.3	-2.0
Rb (ppm)	44.1	34.8	42.1	93.2	119.1	119.5	138.8	72.4	98.7	86.6	87.5	110.2
Sm (ppm)	0.08	-1.12	-2.10	-1.74	-1.87	-2.74	0.93	-0.46	-2.49	-1.50	-3.10	-2.95
Sn (ppm)	1	0	1	1	1	1	1	0	3	0	0	0
Sr (ppm)	-152.1	-65.5	-998.9	-981.5	-931.7	-978.1	-553.7	-80.8	-990.0	-782.4	-987.9	-995.5
Ta (ppm)	0.1	0.0	0.0	0.1	0.1	0.0	0.1	0.1	0.0	-0.1	-0.1	0.0
Tb (ppm)	0.00	-0.18	-0.37	-0.32	-0.28	-0.33	0.00	-0.11	-0.30	-0.25	-0.42	-0.49
Th (ppm)	1.6	1.0	2.0	2.1	2.1	2.2	0.8	2.4	2.0	1.9	2.2	1.5
Tl (ppm)	0.84	0.61	5.09	50.39	27.43	9.00	10.87	1.61	33.00	11.53	10.88	24.45
Tm (ppm)	0.00	-0.07	-0.04	-0.06	-0.07	-0.09	0.01	-0.02	-0.09	-0.04	-0.07	-0.12
U (ppm)	0.52	0.18	5.46	6.92	3.87	0.81	20.03	15.88	5.09	9.49	0.59	8.42
V (ppm)	10	-31	-2	16	-12	-49	98	-17	-27	-20	-49	34
W (ppm)	1	0	10	52	42	70	45	9	66	23	77	68
Y (ppm)	-0.9	-3.5	-3.0	-3.2	-5.2	-7.2	1.9	-0.3	-6.3	-3.1	-5.5	-9.6
Yb (ppm)	0.05	-0.17	-0.11	-0.02	-0.16	-0.42	0.38	0.02	-0.36	-0.27	-0.16	-0.37
Zn (ppm)	0	-8	-13	8	6	4	38	-16	1	-12	-22	0
Zr (ppm)	0	0	0	0	0	0	0	0	0	0	0	0
As (ppm)	18	1	1411	2520	932	605	1886	690	1808	538	3314	3476
Bi (ppm)	0.00	0.02	0.02	0.01	0.02	0.01	0.05	0.08	0.01	0.01	0.00	0.00
Hg (ppm)	0.000	0.010	4.564	27.759	6.669	7.733	4.277	0.442	19.648	2.269	17.299	30.048

Sample	NBC-11C-1145	NBC-24C-1130-1132	NBC-21C-1279	U15-29-320	U16-H07-13b-486	U16-h07-25-510-515	NBC-17C-1081	NBC-17C-1070	U16-h07-13b-436-441	NBC-11C-1100	U15-H08-29-360	U16-H07-24-422
Alteration	**Illite**	**Illite**	**Illite**	**Illite**	**Illite**	**Illite**	**Illite**	**Illite**	**Illite**	**Illite**	**Illite**	**Illite**
Hf ratio	**1.07**	**1.02**	**0.82**	**1.11**	**0.96**	**0.89**	**1.14**	**1.23**	**0.82**	**1.00**	**0.91**	**1.26**
Zr Ratio	**1.09**	**0.96**	**0.79**	**1.11**	**0.92**	**0.86**	**1.21**	**1.16**	**0.79**	**0.93**	**0.86**	**1.27**
Li (ppm)	N/A	-7.1	N/A	N/A	-39.4	N/A	-38.8	N/A	N/A	N/A	N/A	N/A
Sb (ppm)	0.10	0.03	26.01	176.96	25.21	30.61	21.48	2.15	152.72	9.20	38.04	199.12
Se (ppm)	0.0	0.0	1.5	2.0	0.5	1.0	1.4	1.1	1.9	0.4	0.5	6.4
Te (ppm)	0.00	0.01	1.40	1.01	0.62	0.13	0.04	0.01	2.47	0.00	0.01	1.89
LOI (%)	3.4	1.8	-2.5	2.5	0.8	1.5	8.3	13.0	-0.5	4.1	-2.3	7.0
Calculation Error	1.84	-6.89	-3.90	-0.29	-4.13	-3.08	5.73	-5.18	-3.90	-7.85	-5.94	1.33

Sample	U16-H07-13b-476	U16-h07-15-418-422	NBC-11C-1305	NBC-11C-1267	U16-h07-13b-461-466	NBC-24C-1320	U16-H07-25-555-560	NBC-24C-1264	H08-03-740
Alteration	**Illite**	**Illite**	**Illite**	**Illite**	**Illite**	**Illite**	**Illite**	**Illite**	**Illite**
Hf ratio	**1.09**	**1.26**	**1.07**	**0.91**	**0.92**	**1.09**	**0.91**	**0.91**	**0.94**
Zr Ratio	**1.04**	**1.18**	**1.04**	**0.90**	**0.87**	**1.05**	**0.89**	**0.89**	**0.91**
Au (ppm)	51.278	22.223	12.767	47.973	30.472	22.667	30.737	27.399	41.215
SiO2 (wt.%)	10.92	13.97	16.32	11.28	9.08	19.04	7.69	12.51	7.33
Al2O3 (wt.%)	-0.75	-2.56	-1.32	-0.32	-1.38	-0.87	-0.84	-0.74	-2.22
Fe2O3 (wt.%)	3.77	-0.46	2.11	-5.38	-3.96	-0.43	-1.24	-5.76	0.00
CaO (wt.%)	-6.95	3.41	-7.11	-6.85	-7.08	-6.98	-7.05	-6.96	-7.02
MgO (wt.%)	-8.47	-7.67	-8.16	-8.18	-8.27	-8.12	-8.30	-8.34	-8.26
Na2O (wt.%)	-2.02	-1.97	-2.01	-2.03	-2.02	-2.03	-2.01	-2.03	-2.04
K2O (wt.%)	1.33	0.90	1.24	1.54	1.27	1.44	1.44	1.50	1.20
TiO2 (wt.%)	-0.01	-0.25	-0.19	-0.16	-0.21	-0.17	-0.20	-0.07	-0.05
MnO (wt.%)	-0.11	-0.11	-0.11	-0.12	-0.12	-0.11	-0.11	-0.12	-0.12
P2O5 (wt.%)	-0.01	0.13	-0.05	0.02	-0.02	0.01	0.00	0.04	0.03
C (wt.%)	-0.95	1.95	-0.94	-0.91	-0.98	-0.95	-0.97	-0.96	-0.97
S (wt.%)	7.64	6.20	7.53	2.00	2.92	5.99	5.33	1.60	6.02
Ag (ppm)	1.6	8.9	0.0	-0.1	0.4	1.6	4.8	12.9	34.2
Ba (ppm)	-2227.9	-1970.9	-2104.9	-2222.2	-1764.5	-2276.6	-2248.1	-2231.4	224.5
Ce (ppm)	7.7	-6.2	5.1	4.1	-1.1	-6.0	0.2	17.3	5.4
Co (ppm)	10.8	-6.3	-6.1	-1.2	-5.5	-2.4	-5.9	-1.7	-3.3
Cr (ppm)	313	-49	-82	30	-59	29	-38	-18	-59
Cs (ppm)	4.04	25.94	12.79	6.32	11.99	19.95	20.04	20.51	20.63
Cu (ppm)	0	-7	-1	2	-19	8	-2	-17	57
Dy (ppm)	-1.43	-2.06	-0.80	-1.11	-1.74	-1.85	-1.36	-1.79	-1.99
Er (ppm)	-0.49	-0.61	-0.06	-0.34	-0.45	-0.69	-0.44	-0.42	-0.46
Eu (ppm)	-0.48	-1.09	-0.29	-0.29	-0.71	-0.91	-0.45	-0.81	-1.10
Ga (ppm)	-0.4	1.4	0.8	-0.4	-0.9	3.9	-0.7	0.1	3.7
Gd (ppm)	-1.1	-2.1	-0.9	-0.7	-1.4	-2.1	-0.2	-1.9	-2.3
Hf (ppm)	-0.2	-0.3	-0.1	-0.1	-0.3	-0.2	-0.1	-0.1	-0.1
Ho (ppm)	-0.26	-0.29	-0.10	-0.17	-0.24	-0.30	-0.21	-0.25	-0.26

Sample	U16-H07-13b-476	U16-h07-15-418-422	NBC-11C-1305	NBC-11C-1267	U16-h07-13b-461-466	NBC-24C-1320	U16-H07-25-555-560	NBC-24C-1264	H08-03-740
Alteration	**Illite**	**Illite**	**Illite**	**Illite**	**Illite**	**Illite**	**Illite**	**Illite**	**Illite**
Hf ratio	**1.09**	**1.26**	**1.07**	**0.91**	**0.92**	**1.09**	**0.91**	**0.91**	**0.94**
Zr Ratio	**1.04**	**1.18**	**1.04**	**0.90**	**0.87**	**1.05**	**0.89**	**0.89**	**0.91**
La (ppm)	5.3	-0.6	5.3	2.8	3.3	-0.3	-0.7	10.8	2.8
Lu (ppm)	-0.03	-0.04	0.02	-0.01	-0.04	-0.03	-0.03	0.02	0.03
Mo (ppm)	3	10	7	3	9	4	2	2	1
Nb (ppm)	-0.7	-2.2	-2.0	-1.6	-1.6	-2.3	-0.7	-0.7	-0.9
Nd (ppm)	-0.6	-9.4	-0.5	-2.6	-7.4	-9.7	-5.6	-0.4	-0.9
Ni (ppm)	87	-9	-22	11	-26	14	-22	-10	-29
Pb (ppm)	0	3	1	1	3	6	3	11	26
Pr (ppm)	0.4	-2.1	0.4	-0.3	-1.4	-1.7	-1.3	1.0	0.4
Rb (ppm)	87.3	98.1	96.1	116.1	123.7	143.9	130.5	126.0	133.9
Sm (ppm)	-1.17	-3.26	-0.73	-1.28	-2.33	-2.91	-1.86	-1.68	-2.19
Sn (ppm)	2	1	2	2	1	2	3	1	11
Sr (ppm)	-984.4	-958.7	-980.6	-990.9	-986.9	-1005.8	-987.8	-987.7	-980.7
Ta (ppm)	0.0	-0.2	-0.1	0.1	-0.1	0.1	0.0	0.1	0.1
Tb (ppm)	-0.29	-0.43	-0.23	-0.25	-0.33	-0.40	-0.24	-0.37	-0.42
Th (ppm)	2.3	1.5	2.0	2.8	1.5	3.1	2.8	3.3	3.4
Tl (ppm)	80.20	25.33	41.48	56.96	19.89	19.58	18.58	16.26	19.86
Tm (ppm)	-0.06	-0.08	-0.02	-0.05	-0.09	-0.08	-0.07	-0.04	-0.04
U (ppm)	2.30	9.56	6.82	1.76	8.12	4.00	1.87	2.60	2.93
V (ppm)	64	25	9	-18	-30	46	-3	33	88
W (ppm)	85	64	36	67	55	65	90	64	65
Y (ppm)	-6.2	-6.4	1.1	-4.1	-5.5	-6.8	-4.5	-5.2	-6.1
Yb (ppm)	-0.23	-0.15	0.12	-0.02	-0.19	-0.17	-0.15	0.10	0.16
Zn (ppm)	15	20	-10	5	-2	-1	-2	13	-15
Zr (ppm)	0	0	0	0	0	0	0	0	0
As (ppm)	10380	1179	3882	3838	1649	963	1332	1423	1288
Bi (ppm)	0.06	0.01	0.01	0.01	0.01	0.01	0.01	0.01	0.02
Hg (ppm)	25.949	20.218	25.949	22.415	18.056	21.301	15.100	18.294	20.103

Sample	U16-H07-13b-476	U16-h07-15-418-422	NBC-11C-1305	NBC-11C-1267	U16-h07-13b-461-466	NBC-24C-1320	U16-H07-25-555-560	NBC-24C-1264	H08-03-740
Alteration	**Illite**	**Illite**	**Illite**	**Illite**	**Illite**	**Illite**	**Illite**	**Illite**	**Illite**
Hf ratio	**1.09**	**1.26**	**1.07**	**0.91**	**0.92**	**1.09**	**0.91**	**0.91**	**0.94**
Zr Ratio	**1.04**	**1.18**	**1.04**	**0.90**	**0.87**	**1.05**	**0.89**	**0.89**	**0.91**
Li (ppm)	N/A	N/A	N/A	-39.4	N/A	-39.0	N/A	-39.7	N/A
Sb (ppm)	259.35	154.29	259.35	105.65	73.55	76.24	53.23	81.24	108.59
Se (ppm)	3.0	4.0	2.6	1.5	1.8	2.2	2.2	1.5	4.4
Te (ppm)	2.60	4.86	0.78	0.92	0.89	1.27	1.31	4.76	29.97
LOI (%)	4.4	0.4	1.3	-2.0	-2.0	1.2	-0.1	-2.4	0.3
Calculation Error	-4.90	-6.56	-2.62	-1.19	-6.49	-3.76	-2.14	-1.67	-3.11

Table 2.4 Spearman rank correlation matrix for mass transfer data.

	Au (ppm)	Si %	Na %	Mg %	Ca %	K %	Mn %	C %	S %	Ag (ppm)	Ba (ppm)	Cs (ppm)
Au (ppm)	1	0.58	-0.4	-0.52	-0.67	0.68	-0.76	-0.61	0.73	0.52	-0.33	0.66
Si %	0.58	1	-0.21	-0.5	-0.44	0.37	-0.61	-0.47	0.54	0.52	-0.19	0.34
Na %	-0.4	-0.21	1	0.58	0.28	-0.12	0.48	0.29	-0.22	0.018	0.54	-0.14
Mg %	-0.52	-0.5	0.58	1	0.6	-0.1	0.73	0.66	-0.44	-0.16	0.57	-0.067
Ca %	-0.67	-0.44	0.28	0.6	1	-0.33	0.73	0.93	-0.38	-0.28	0.36	-0.27
K %	0.68	0.37	-0.12	-0.1	-0.33	1	-0.33	-0.24	0.62	0.49	-0.056	0.69
Mn %	-0.76	-0.61	0.48	0.73	0.73	-0.33	1	0.79	-0.44	-0.37	0.37	-0.3
C %	-0.61	-0.47	0.29	0.66	0.93	-0.24	0.79	1	-0.25	-0.29	0.31	-0.17
S %	0.73	0.54	-0.22	-0.44	-0.38	0.62	-0.44	-0.25	1	0.55	-0.29	0.64
Ag (ppm)	0.52	0.52	0.018	-0.16	-0.28	0.49	-0.37	-0.29	0.55	1	0.12	0.58
Ba (ppm)	-0.33	-0.19	0.54	0.57	0.36	-0.056	0.37	0.31	-0.29	0.12	1	-0.023
Cs (ppm)	0.66	0.34	-0.14	-0.067	-0.27	0.69	-0.3	-0.17	0.64	0.58	-0.023	1
Cu (ppm)	-0.056	0.17	-0.11	-0.057	-0.068	-0.18	-0.079	-0.13	-0.0053	0.039	0.17	-0.21
Rb (ppm)	0.79	0.45	-0.18	-0.18	-0.47	0.87	-0.5	-0.41	0.66	0.59	-0.033	0.87
Sr (ppm)	-0.55	-0.53	0.57	0.77	0.64	-0.17	0.76	0.62	-0.39	-0.2	0.56	-0.1
Tl (ppm)	0.88	0.64	-0.39	-0.55	-0.54	0.71	-0.67	-0.48	0.82	0.53	-0.31	0.63
W (ppm)	0.77	0.44	-0.43	-0.67	-0.47	0.52	-0.73	-0.46	0.73	0.31	-0.48	0.49
Zn (ppm)	0.26	0.22	0.2	0.2	0.095	0.27	-0.077	0.081	0.21	0.26	-0.043	0.29
As (ppm)	0.79	0.62	-0.31	-0.61	-0.53	0.68	-0.62	-0.44	0.8	0.49	-0.37	0.49
Hg (ppm)	0.84	0.74	-0.43	-0.69	-0.57	0.57	-0.75	-0.51	0.86	0.52	-0.37	0.54
Sb (ppm)	0.79	0.75	-0.42	-0.75	-0.56	0.45	-0.79	-0.54	0.8	0.5	-0.4	0.44

	Cu (ppm)	Rb (ppm)	Sr (ppm)	Tl (ppm)	W (ppm)	Zn (ppm)	As (ppm)	Hg (ppm)	Sb (ppm)
Au (ppm)	-0.056	0.79	-0.55	0.88	0.77	0.26	0.79	0.84	0.79
Si %	0.17	0.45	-0.53	0.64	0.44	0.22	0.62	0.74	0.75
Na %	-0.11	-0.18	0.57	-0.39	-0.43	0.2	-0.31	-0.43	-0.42
Mg %	-0.057	-0.18	0.77	-0.55	-0.67	0.2	-0.61	-0.69	-0.75
Ca %	-0.068	-0.47	0.64	-0.54	-0.47	0.095	-0.53	-0.57	-0.56
K %	-0.18	0.87	-0.17	0.71	0.52	0.27	0.68	0.57	0.45
Mn %	-0.079	-0.5	0.76	-0.67	-0.73	-0.077	-0.62	-0.75	-0.79
C %	-0.13	-0.41	0.62	-0.48	-0.46	0.081	-0.44	-0.51	-0.54
S %	-0.0053	0.66	-0.39	0.82	0.73	0.21	0.8	0.86	0.8
Ag (ppm)	0.039	0.59	-0.2	0.53	0.31	0.26	0.49	0.52	0.5
Ba (ppm)	0.17	-0.033	0.56	-0.31	-0.48	-0.043	-0.37	-0.37	-0.4
Cs (ppm)	-0.21	0.87	-0.1	0.63	0.49	0.29	0.49	0.54	0.44
Cu (ppm)	1	-0.11	-0.073	-0.013	-0.017	-0.23	-0.12	0.092	0.12
Rb (ppm)	-0.11	1	-0.27	0.74	0.62	0.32	0.64	0.65	0.55
Sr (ppm)	-0.073	-0.27	1	-0.49	-0.63	0.11	-0.54	-0.68	-0.69
Tl (ppm)	-0.013	0.74	-0.49	1	0.74	0.21	0.89	0.91	0.88
W (ppm)	-0.017	0.62	-0.63	0.74	1	0.19	0.74	0.82	0.79
Zn (ppm)	-0.23	0.32	0.11	0.21	0.19	1	0.19	0.19	0.11
As (ppm)	-0.12	0.64	-0.54	0.89	0.74	0.19	1	0.9	0.86
Hg (ppm)	0.092	0.65	-0.68	0.91	0.82	0.19	0.9	1	0.96
Sb (ppm)	0.12	0.55	-0.69	0.88	0.79	0.11	0.86	0.96	1

Chapter 3 : Recognition of Alteration in Low Temperature Carbonate Hosted Gold Deposits

Carbonate-bearing sedimentary rocks host significant base and precious metal ore deposits (e.g. skarns, carbonate replacement manto-style deposits, Mississippi Valley-type deposits, epithermal deposits, and Carlin-type deposits) (Hedenquist et al., 2005). The expression of hydrothermal alteration in carbonate wall rocks is variable depending on the temperature of the fluid, the chemical composition of the fluid, and the composition of the wall rock. In high temperature magmatic systems (i.e. skarns) alteration of carbonate rocks typically includes proximal silicification, CO_2 loss, and cation metasomatism (Meinert, 1992; Meinert et al., 2005). Outside the proximal alteration zone, where the fluid has become progressively rock buffered, other indicators of alteration may include textural re-equilibration and/or isotopic shifts in $\delta^{18}O$ and $\delta^{13}C$ in carbonate minerals (Dipple and Ferry, 1992a; Meinert et al., 2005). In lower temperature carbonate hosted hydrothermal systems like the world-class Carlin-type gold deposits of Nevada, proximal alteration is limited to carbonate dissolution and silicification. Similar to high temperature systems, zones of $\delta^{18}O$ depletion of calcite in Paleozoic limestone wall rocks may form distal alteration halos in Carlin-type deposits where the wall rock has been buffered by the infiltration of hydrothermal fluids (Arehart and Donelick, 2006; Stenger et al., 1998b; Vaughan et al., 2010).

Isotope depletion zones have great potential as metrics of hydrothermal fluid flow that extend beyond more visual manifestations of fluid:rock interaction (e.g. carbonate dissolution) (Criss and Campion, 1991; Criss et al., 1991; Criss and Taylor, 1983; Engel et al., 1958; Kelley et al., 2006; Kesler et al., 1995; Taylor, 1974; Vazquez et al., 1998). Reviews of the application of light stable isotopes in mineral exploration include Ohmoto (1986), Nesbitt (1996), and more recently Barker et al. (2013). Nesbitt's (1996) review suggests isotopic alteration haloes can extend >1 km around hydrothermal mineral deposits with stable isotope ratios varying by >10‰. For low temperature carbonate hosted Carlin-type deposits broad spaced sampling of limestones at the Carlin (Radtke et al., 1980), Twin Creeks (Stenger et al., 1998b), Meikle (Emsbo et al., 2003), and Pipeline (Arehart and Donelick, 2006) Carlin-type deposits showed that isotopic depletion in calcite is a common alteration product. Additionally, Twin Creeks (Stenger et al., 1998) and Pipeline (Arehart and Donelick, 2006) exhibit a spatial association with Au mineralization and other alteration products.

At high temperatures, isotopic exchange can occur through diffusion into carbonate minerals on spatial scales of ~100 μm with virtually no kinetic inhibition to equilibrium exchange, or through dissolution-precipitation reactions (Dipple and Ferry, 1992a; Labotka et al., 2011). At low temperatures, such as the temperatures defined for Carlin systems (<250°C) (Hofstra and Cline, 2000), isotopic exchange proceeds primarily through dissolution/precipitation reactions resulting either in recrystallization or mineral replacement with relatively homogenous $\delta^{18}O$ values (Cole and Chakraborty, 2001). Bowman et al. (2009) presented evidence regarding dissolution/precipitation of calcite and its relationship with calcite textures and isotopic alteration with high temperature fluids (>500 °C), but similar studies of low-temperature hydrothermal fluid systems are lacking.

The goal of this study is to (1) document the spatial pattern of isotopic depletion associated with low temperature (<250°C) auriferous hydrothermal fluid flow in carbonate rocks; (2) use integrated textural, micro-chemical, and isotopic analysis of carbonate alteration to better understand the process by which carbonate minerals undergo alteration/isotopic exchange in low temperature systems; and (3) assess the genetic relationship of carbonate veins to carbonate alteration/isotopic exchange in low temperature systems. This study uses the Banshee Carlin-type deposit on the northern Carlin trend, a relatively small carbonate-hosted paleo-hydrothermal system that resulted in the precipitation of economic quantities of Au (see Chapter 2 for description of the Banshee Carlin-type deposit). At Banshee, visible alteration is confined to limestone breccia unit and intrusive dikes. Lower permeability limestone and siliciclastic rocks bound the breccia unit and likely served to focus fluid flow along a well-defined flow path. Owing to the constrained nature of hydrothermal fluid flow at Banshee, it serves as ideal study site for evaluating the alteration effects of hydrothermal fluid flow through highly permeable wall rocks and less permeable limestone. Additionally, the availability of dense drilling across the Banshee deposit allows for close spaced sampling across potential fluid flow pathways allowing for an evaluation of alteration in three dimensions within the deposit area.

This chapter illustrates how $\delta^{18}O$ stable isotopes in wall rock carbonate and calcite veins can be used to infer the geometry of fluid flow pathways and the extent of hydrothermal alteration in a low temperature carbonate hosted hydrothermal system. Secondly, textural evidence is presented showing complete replacement of wall rock calcite resulting from low temperature hydrothermal alteration. Finally, mineral chemistry of altered calcite grains is used to clearly demonstrate chemical changes occurring with alteration and to identify the physiochemical characteristics of the altering fluids. In combination the data is used to define the character and extent of alteration in visibly unaltered carbonate rocks.

3.1 Isotope Exchange

3.1.1 Mechanisms and Process

Isotopic exchange of both $\delta^{18}O$ and $\delta^{13}C$ proceed either through diffusion of O and C from chemical components in the fluid (e.g. CO_2 and H_2O) into calcite grains, or through dissolution and precipitation of calcite grains that then inherit the $\delta^{18}O$ and $\delta^{13}C$ values of the fluid (Cole and Chakraborty, 2001). Temperature is a primary control on the scale at which diffusion operates as a mechanism for isotopic exchange. Low temperature systems are limited in there ability to diffuse C and O across significant length scales (Labotka et al., 2011). Labotka et al. (2011) published modeled diffusion length scales at high temperatures (>400°C) in calcite based on closure temperature, pressure, and cooling rate. Closure temperature is the temperature at which diffusive exchange between a mineral and its environment ceases to occur (Dodson, 1973). The closure temperature is proportional to the diffusivity (D) and can be estimate using (Labotka et al., 2011; Lasaga et al., 2001):

$$T_C = \frac{E_A/R}{\ln\left[2D_O T_C^2/(a^2 S E_A/R)\right]} \quad \text{Equation 3.1}$$

where E_A/R is the activation energy divided by the gas constant, D_O is the frequency factor, a is the grain radius, and S is the cooling factor. The frequency factor can be calculated using:

$$D_O = \frac{D}{e^{-E_a/RT_c}} \quad \text{Equation 3.2}$$

and then the grain radius, a, can then be solved using:

$$a = \sqrt{\frac{1}{(e^{E_A/RD_0}E_A S)/(2SRT_C^2)}} \qquad \text{Equation 3.3}$$

Cooling rates of 10 °K/my is characteristic in orogenic settings (Reiners and Brandon, 2006), but hydrothermal systems involve significant advective and conductive heat transport with associated cooling rates orders of magnitude greater than those associated with normal continental processes (Hickey et al., 2013). For low temperature Carlin-type deposits with a closure temperature of 200°C (474.15°K) and a cooling rate of 10,000°K/my the value of D is estimated to be 2.34×10^{-24} cm^2/s based on linear extrapolation of modeling by Labotka et al. (2011). Using these inputs with an E_A of 242,340 J/mol the grain radius at which diffusion would be significant is ~0.003 μm. For a cooling rate of 100 °K/my the diffusion length scale is 0.011 μm. Effectively, mineral grains with a radius of 0.011 to 0.003 μm would undergo limited diffusive exchange at or below 200°C making diffusion an unlikely mechanism for exchange in low temperature hydrothermal systems such as Carlin-type Au deposits where typical calcite grain size is >4 μm in limestone.

In the absence of diffusion, isotopic and chemical exchange can occur via surface reactions resulting in the dissolution and precipitation of a mineral phase (Cole and Chakraborty, 2001). Isotopic exchange controlled by chemical reactions are dependent on temperature, pressure, solution-to-solid ratio, surface area, solution composition, mineral composition and structure, and defects (Cole and Chakraborty, 2001). Putnis (2009) describes a process where progressive dissolution/precipitation of minerals takes place in response to changes in physiochemical conditions where nearly simultaneous dissolution then precipitation occur with preservation of the original texture. The resulting mineral precipitant will be representative of the chemical and isotopic composition of the fluid. The process is driven by chemical disequilibrium between a fluid and mineral and results in progressive reaction until equilibrium is attained (Cole and Chakraborty, 2001; Cole et al., 1983; Putnis, 2009).

3.1.2 Equilibrium Versus Kinetic Exchange

If equilibrium exchange occurs, the $\delta^{18}O$ and $\delta^{13}C$ value of the wall rock calcite will be equal to that of the altering fluid corrected for temperature dependent fractionation. Mass dependent fractionation occurs during fluid-mineral, fluid-fluid, and mineral-mineral isotopic exchange. The amount of fractionation that occurs between two species is primarily controlled by temperature changes, although other factors such as chemical composition, crystal structure of minerals, and pressure also can affect the degree of fractionation (O'Neil, 1986; O'Neil et al., 1969). Molecules with heavy isotopes have greater binding energies due to increased mass; however, at elevated temperatures the differences in energy between light and heavy isotope species diminish resulting in less fractionation between fluid an mineral phases (O'Neil, 1986). In the case of hydrothermal alteration of calcite, equilibrium exchange of O and C between fluid and mineral phases occurs according to the equations:

$$H_2^{18}O + \tfrac{1}{3}CaC^{16}O_3 = H_2^{16}O + \tfrac{1}{3}CaC^{18}O_3 \qquad \text{Equation 3.4}$$

$$Ca^{13}CO_3 + ^{12}CO_2 = Ca^{12}CO_3 + ^{13}CO_2 \qquad \text{Equation 3.5}$$

Previous authors have suggested that equilibrium exchange occurs at hydrothermal temperatures even when dissolution/precipitation reactions are the dominant mode of exchange (O'Neil et al., 1969; Zheng and Hoefs, 1993). Other workers suggest that there is some kinetic control on the exchange of $\delta^{18}O$ between hydrothermal fluids and minerals in the wall rock at the relatively low temperature considered in this study (<250°C) (Cole, 1994; Cole and Chakraborty, 2001). The relative significance of kinetically controlled exchange is assumed to be largely dependent on temperature per the Arrhenius equation with lower rate constants corresponding to lower temperatures (Cole and Chakraborty, 2001). The rate of exchange is also influenced by pressure, grain size, surface area, solution composition, mineral composition and structure, and crystal defects (Cole and Chakraborty, 2001). The relative importance of non-equilibrium (i.e. kinetic) exchange through fluid-rock reaction during advective mass transport can be defined by the Damkohler number (Bowman et al., 1994; Lassey and Blattner, 1988), N_D, which can be expressed as:

$$N_D = \frac{t_{tr}}{t_r} \qquad \text{Equation 3.6}$$

where t_{tr} is the time of transport and t_r is the time of reaction. High Damkohler numbers indicate that the rate of reaction is greater than the rate of transport and thus indicates equilibrium conditions. At lower Damkohler numbers, the rate of transport exceeds the rate of reaction indicating that non-equilibrium exchange will occur. Experimental data indicates that the rate of isotopic exchange reactions increases exponentially with temperature (Bowman et al., 1994; Cole and Chakraborty, 2001; Cole and Ohmoto, 1986). At lower temperature the non-equilibrium conditions will result in lower rates of isotopic exchange between the fluid and mineral, reducing N_D, resulting in the isotopic composition of the mineral being out of equilibrium with the fluid. In the case of mineral surface reaction (e.g. dissolution-precipitation of calcite) the rate of isotopic exchange is likely controlled by the rate of the dissolution-precipitation reactions (Bowman et al., 1994).

3.2 Research Plan and Methods

In order to evaluate the nature and extent of carbonate alteration and fluid flow across the Banshee Au deposit and characterize the manifestation of dissolution/precipitation reactions of carbonate minerals, 12 drill holes were sampled along the ~600 meter long semi-continuous cross-section through west and east Banshee (Figure 3.1, section A-A'). Seven (7) drill holes were also sampled to the north of the east-west section along strike of the west Banshee ore zone (Figure 3.1, sections B-B' and C-C'). These additional holes were selected to define the extent of alteration and associated fluid flow along strike of the west Banshee deposit. Thus, this study defines the extent of chemical and textural alteration of carbonate minerals associated with hydrothermal fluid flow in west Banshee. Sampling concentrated on defining the alteration patterns associated with Au deposition above, below, and peripheral to mineralization. Samples were collected from all carbonate-bearing lithologies above and below the Roberts Mountain thrust (RMT). Care was taken to sample different breccia types. Drill holes were sampled at 5-20 meter intervals depending on the presence of matrix carbonate. A total of 434 samples were analyzed for stable isotopes in carbonate minerals.

Samples collected for stable isotope analysis were micro-drilled using a Dremel® tool with diamond tipped drill bits in order to target individual carbonate cement generations on a scale of <5-mm. Stable isotope analyses were performed by the Pacific Centre for Isotopic and Geochemical Research (PCIGR) at the University of British Columbia (UBC) in Vancouver, Canada. Sample powders were weighed then reacted with 99% phosphoric acid in a sealed glass Exetainer® that had been flushed with inert helium gas. The reaction forms CO_2 gas that is introduced into a Delta Plus stable isotope ratio mass spectrometer (IRMS) using He_2 as a carrier gas. The CO_2 gas created from the sample is analyzed along with reference samples with a known isotopic composition. Isotopic fractionation is calculated by conducting multiple analyses of internal lab standards previously calibrated against the internationally accepted standards NBS-18 and NBS-19. Calculated values for $\delta^{13}C$ and $\delta^{18}O$ are reported as permil (‰) values for ratios of $^{13}C/^{12}C$ and $^{18}O/^{16}O$. Reported values are standardized to Vienna Standard Mean Ocean Water (VSMOW) for $\delta^{18}O$ and Vienna Pee Dee Belemnite (VPDB) for $\delta^{13}C$ (Coplen et al., 1982; Coplen et al., 1983).

A total of 9 samples were chosen for detailed study of carbonate texture and chemistry including: U16-H07-13b-11, U16-H07-13b-31, U16-H07-13b-81, U16-H07-24-145, U16-H07-25-167, U16-H07-34-405, U16-H07-54-5, U16-H07-54-338, and U16-H07-67-129. All 9 samples were collected from either the Banshee breccia horizon or the Silurian-Devonian Bootstrap limestone at the Banshee deposit. Samples were chosen to represent the range of carbonate textures and paragenetic relationships found within the Banshee deposit, and were prepared as 1 inch round polished pucks at the Sample Preparation and Thin Section Lab at the University of Utah in Salt Lake City, USA. CL characterization of samples was conducted using a Cambridge Image Technology Ltd. MK4 optical CL unit at UBC operating at 15.5 kV potential and 200 μA beam current. Imaging was standardized for exposure to facilitate comparisons between images.

After CL characterization, laser ablation ICP-MS (LA-ICP-MS) sample points were chosen to measure the range of trace element chemistry associated with the different CL textures and $\delta^{13}C$ and $\delta^{18}O$ isotope data. A total of 391 spot analyses were performed on the 9 samples. Laser ablation ICP-MS measurements of the concentrations of a range of trace elements was carried out using a Resonetics Resolution M-50-LR laser ablation system housed at PCIGR, based on a 193 nm ArF excimer laser (LPX220, Lambda Physik) attached to a N_2 purged beam delivery unit. A spot size of 60 μm and laser fluence of ~ 8 J cm^{-2} was used. Ablation took place in a two-volume cell, developed by Laurin Technic (Australia; Mueller et al, 2009). Before analysis, the cell was purged by a vacuum pump and then filled with He, which washed the ablated aerosol out of the cell. The carrier gas was mixed downstream with a small amount of N_2 (2.8 mL per minute) to increase plasma temperature (Hu et al. 2008) and with Ar. The ablation aerosol was transported through a nylon manifold signal smoothing device ("squid") before reaching the torch of an Agilent 7700x quadrupole ICPMS. The ICPMS was tuned using NIST 612 glass for high sensitivity and low oxide production rates (ThO/Th < 0.25%). The quadrupole mass analyzer sequentially peak hops between masses of interest (Mg^{24}, Si^{29}, Sc^{45}, Ti^{47}, V^{51}, Mn^{55}, Fe^{57}, Rb^{85}, Sr^{88}, Y^{89}, Ba^{137},

La^{139}, Ce^{140}, Pr^{141}, Nd^{146}, Sm^{147}, Eu^{153}, Gd^{157}, Tb^{159}, Dy^{163}, Ho^{165}, Er^{166}, Tm^{169}, Yb^{172}, Lu^{175}, Pb^{208}, Th^{232}, U^{238}, and Ca^{43}) during the laser ablation process, with a sweep time over the entire mass range of less than 1 second. 40 seconds of laser ablation data was collected for each analysis point, and at least 20 seconds of gas blank were collected for each sample. The ICPMS collected data continuously in time-resolved analysis mode, with gas blank collected before and after each laser ablation point to facilitate blank subtraction. NIST 612 was used as a calibration standard, and BCR-2g was analyzed as a quality control monitor. Data reduction followed established protocols for time-resolved analysis (Longerich et al, 1996). Iolite software (Hellstrom et al, 2008) was used for data reduction, with ^{43}Ca used as an internal standard. Carbonate minerals were assumed to be pure calcite, with Ca = 40.04 $\%_{wt}$ for the internal standard concentration. Appendix D includes RSD (2s) and detection limits for each element and analysis.

3.3 Calcite Veining in Carlin-type Au Deposits

While calcite veins are a commonly recognized feature in Carlin-type Au deposits (Cline et al., 2005; Hofstra and Cline, 2000), the timing of veining relative to mineralization has not been well studied owing to near complete calcite dissolution in ore zones. Cline et al. (2005) noted that a zoning pattern exists where calcite veins peripheral to ore zones may represent precipitation from rock buffered ore fluids that have become saturated in CO_2 as a result of massive carbonate dissolution. Hofstra and Cline (2000) showed evidence of co-precipitation of realgar and calcite in veins directly adjacent to carbonate dissolution at the Meikle deposit. Kuehn and Rose (1992) described calcite veinlets associated with late ore stage minerals of realgar and stibnite at the Carlin mine, and Ilchik (1990) described calcite veins with realgar at the Alligator Ridge deposit that occurs immediately adjacent to carbonate dissolution zones and extends at least 150m laterally. Ilchik (1990) also noted that the intensity of veining increased nearer proximal carbonate dissolution alteration, but no distinct textures were noted. Oxygen and carbon isotopes of vein-rock calcite pairs from altered rock at Alligator ridge show greater depletion in $\delta^{18}O$ and enrichment in $\delta^{13}C$ in calcite veins relative to wall rock calcite (Ilchik, 1990). The ubiquity of calcite veining around Carlin-type deposits is likely a function of calcite precipitating into fractures and voids generated by calcite dissolution processes. Precipitation of calcite veins may be a function of progressive rock buffering of the fluid leading to calcite saturation in the fluid.

Pre- and post-ore veining are also common and can be difficult to distinguish where cross cutting relationships are absent. Post-ore calcite veining (Emsbo and Hofstra, 2003; Emsbo et al., 2003; Evans, 2000) is typically coarsely crystalline, cross cuts mineralization, and has $\delta^{18}O$ values consistent with precipitation from low temperature isotopically unexchanged meteoric fluids. Late stage calcite veining at Alligator Ridge also has distinct isotopic values relative to alteration related calcite veins (Ilchik, 1990). Radtke et al. (1980) indicated that $\delta^{18}O$ values could be an effective tool for discriminating between generations of calcite veining, and Kuen and Rose (1995) used $\delta^{18}O$ in calcite veins to discriminate between late ore stage calcite veining and more $\delta^{18}O$ depleted post ore calcite veining at the Carlin deposit.

3.4 Banshee Geology

Chapter 2 contains a complete description of the geology of the Banshee Carlin-type deposit. The main carbonate bearing units at Banshee are the laterally contiguous multiphase breccia unit, Silurian Devonian Roberts Mountain Formation Bootstrap Limestone unit, and Devonian Popovich Formation Upper Mud unit (Figure 2.4). The Bootstrap Limestone has previously been described by Armstrong et al. (1998), Furley (2001) and Morgan (2006). Calcite is the dominant carbonate mineral found in limestones and breccias at the Banshee deposit. Diagenetic and hydrothermal dolomites described in other areas of the Bootstrap limestone (Diehl et al., 2010; Emsbo et al., 2003; Morgan, 2006) are largely absent from Banshee. Bootstrap dolostone is primarily found in the northern most drill fan in this study but is spatially discontinuous.

3.4.1 Breccia Units

The Banshee Au deposit hosts at least four temporally and/or texturally distinct breccia types contained within a laterally continuous stratiform breccia horizon at the upper contact within the Silurian-Devonian Bootstrap limestone (see Figure 2.3 for geologic cross-section). Breccias at Banshee have been classified based on their textural characteristics and paragenetic relationships following the approach of Davies et al. (2008). Table 3.1 summarizes the key characteristics of the four breccias at Banshee.

3.4.1.1 Stage 1 Breccia Unit

Paragenetically early breccia units are both clast- and matrix-supported with monomict clast composition (Figure 3.2a). The breccia clasts are almost exclusively derived from the Bootstrap Limestone. Matrix material may be finely laminated or chaotic and consists of silt-sized quartz with dark carbonaceous carbonate muds and pyrite. Bootstrap clasts in clast-supported breccia units are commonly but not always stylolitized. Clasts are angular and rotated relative to one another forming a mosaic texture. Clasts range in diameter from 1 to 10 cm. Calcite veins in clasts are cut by breccia matrix and stylolitization, indicating they formed prior to brecciation. Minor dolomitization of clasts is evident under cathode luminescence. Early monomict breccia units extend beyond the ore zone where they are not visibly altered by hydrothermal fluids (except where overprinted by later brecciation). Breccia textures such as sedimentary cave fill textures and graded clast size distributions are consistent with paleokarsting during subaerial exposure and subsequent collapse with burial (Armstrong et al., 1998; Loucks, 1999).

3.4.1.2 Stage 2 Matrix Supported Polymict Breccia Units

Matrix-supported polymict breccias (Figure 3.2b) post-date the earlier clast and matrix-supported Stage-1 breccias. Polymict breccias contain clasts of earlier breccias, Jurassic lamprophyre and Jurrasic rhyolite, Silurian-Devonian Bootstrap Limestone, Devonian Popovich Upper Mud, and less commonly Devonian Rodeo Creek. Clasts typically range in size from 5mm to 5 cm. Clasts are commonly altered by carbonate dissolution, clay alteration, silicification, and pyritization. Stage-2 breccias are commonly overprinted by pervasive silicification, and are considered to have formed prior to and possibly during Au mineralization.

3.4.1.3 Stage 3 Calcite Cemented Breccia Unit

Calcite cemented breccia units (Figure 3.2c) are polymict and contain clasts of earlier breccia units (including Stage 2 breccia), Bootstrap limestone, Devonian Popovich Upper Mud, Devonian Rodeo Creek, Jurassic lamprophyre, and Jurassic rhyolite. Silicified clasts are commonly mineralized and contain Stage-1 and -2 breccia as clasts. Stage 3 calcite cemented breccia occurs post mineralization as they cut ore stage silicification. (Figure 3.2c). The characteristic coarse-grained sparry calcite cements likely precipitated fluids during brittle fracturing of earlier silicified breccia (Figure 3.2c).

3.4.1.4 Stage 4 Late Matrix Supported Polymict Breccia

The fourth breccia facies at the Banshee deposit is matrix supported polymict breccia (Figure 3.2d) characterized by soft, poorly consolidated, matrix composed of abundant pyrite, carbonaceous material, clay, and silt. Breccia clasts are derived from a range of lithologies and may include Jurassic lamprophyre and rhyolite, Upper Mud, Bootstrap, Rodeo Creek, Eocene dacite and/or Vinini chert/mudstone. Stage-4 breccia units fill cavities that are commonly lined with coarse calcite cement. In some cases precipitated calcite is interlayered with silty laminations of dissolution residuum. Stage-4 breccia units are not overprinted by silicification, but clasts are commonly silicified and decalcified. Stage-4 matrix supported polymict breccias were likely formed via carbonate dissolution forming caves and voids that subsequently were in-filled by cave sedimentation and collapse brecciation. The timing relationship between Stage-3 and -4 breccias is difficult to resolve owing to the lack of cross cutting relationships.

3.4.2 Calcite Veins

Calcite veining is a common feature within brecciated and unbrecciated wall rocks at Banshee. The veins are of multiple generations exhibiting variable textures and cross cutting relationships. Based on logging of drill core from the West Banshee ore zone, calcite veining ranges between 5-20% of the core immediately adjacent to the ore zone (Barrick Gold logging data). Wall rock limestone distal to alteration typically contain <2% calcite veins based on geologist logs of exploration drill holes (Barrick Gold logging data).

The relationship between calcite veining and mineralization at Banshee is unclear based on cross cutting relationships, but it is possible to infer timing of vein sets relative to each other and silicification. For this study, calcite veins are divided into three groups based on their timing relative to one another: early veins, intermediate veins, and late veins. Early and late veins contain a number of textural variants with complex timing relationships and are grouped according to their relationship to alteration.

Early veins are common in visibly unaltered rocks outside of defined visible alteration at Banshee and within breccia clasts of Bootstrap limestone. Early veins commonly contain equant grains of calcite and are texturally consistent with precipitation along fractures (Bons et al., 2012) (Figure 3.3a). Early veins are cut by extensive stylolitization of the Bootstrap limestone (Figure 3.3b). Stylolitization in the Bootstrap limestone is attributed to early diagenesis during the late Devonian through deep-burial diagenesis of the early Mississippian (Emsbo et al., 2003). Intermediate veins are observed cutting stylolites clearly placing them as younger than the early veins (Figure 3.3c). Intermediate veins are found proximal to silicified and carbonate dissolved rocks, but are absent from the ore zone at Banshee where carbonate has been completely removed or replaced by quartz. Texturally, intermediate veins are blocky and generally lack growth zoning indicating that they precipitated in open space fractures possibly as a single precipitation event (Bons et al., 2012) (Figure 3.3C). Late veins are common inside and outside the ore zone at Banshee. Late calcite veins are coarsely crystalline and commonly exhibit zoned growth. The most common occurrence of late calcite veins is as coarse calcite cement in Stage 3 breccia. Within the ore zone, late veining cuts silicification verifying that the veins post-date alteration and are likely post-mineral as massive silicification is generally considered a late ore stage event (Hofstra and Cline, 2000).

3.4.3 Geologic Setting of Detailed Sampling

Of the nine samples selected for detailed analysis, three were chosen from visibly unaltered Bootstrap limestone with variable $\delta^{18}O$ alteration: U16-H07-24-145, U16-H07-25-167, and U16-H07-34-405. Five samples were selected from visibly unaltered Stage 1 breccia variably $\delta^{18}O$ altered: U16-H07-13b-11, U16-H07-13b-31, U16-H07-13b-81, U16-H07-54-5, and U16-H07-67-129. One sample was selected from a calcite-replaced Bootstrap limestone clast from non-silicified Stage 2 breccia directly adjacent to the west Banshee lamprophyre: U16-H07-54-338. Two of the samples selected were from strongly $\delta^{18}O$-depleted wall rock: U16-h07-13b-31 and -81. Three of the samples selected were from moderately $\delta^{18}O$-depleted wall rock: U16-H07-24-145, U16-H07-25-167, and U16-H07-54-

5. Three of the samples selected were from weakly $\delta^{18}O$-depleted wall rock: U16-H07-13b-11, U16-H07-34-405, and U16-H07-129. All samples were collected outside of mineralization and visible alteration owing to the lack of calcite in altered and mineralized wall rock. The goal of the sampling was to test for textural and chemical evidence of dissolution/precipitation of calcite associated with $\delta^{18}O$ alteration in wall rock calcite, and to evaluate chemical and textural variations in calcite veins.

3.5 Results

3.5.1 CL and Transmitted Light Petrography

Cathodoluminescence (CL) was used for textural characterization of carbonate cements in combination with transmitted light microscopy. Conditions were standardized for all CL images to facilitate direct comparison of results. CL responses vary from non-luminescent to dully luminescent to bright orange and yellow luminescent calcite. In samples distal to mineralization and alteration, calcite is non-luminescent to dully luminescent for both carbonate grains and cements (Figure 3.4a-b). Occasional dolomite is found in the distal samples as bright red rhombs typically surrounding ooids of calcite and as a small proportion of intergranular cement. Samples collected proximal to mineralization are typically silicified and contain little relict carbonate minerals indicating near complete replacement of calcite with silica. Calcite cemented Stage 3 breccia exhibit a zoned bright yellow CL response. Samples collected just outside the visibly altered zone contain abundant calcite with dull to bright orange luminescence (Figure 3.4c-f). In oolitic limestone samples collected proximal to alteration, ooids exhibit a bright orange CL response while interstitial calcite cement is variably replaced by bright CL calcite (Figure 3.4f). Although CL response varies in oolitic limestone, sedimentary textures are preserved indicating that processes responsible for the variability in CL response did not modify primary textures.

Calcite veins exhibited 3 distinct CL responses: dully luminescent, moderate to bright orange luminescent, and bright yellow luminescent (Figure 3.5b-d). Early veins at Banshee are dully luminescent and are common in unaltered rocks and less common proximal to mineralization. Orange luminescent veins with blocky crystal texture were observed cross cutting early dully-luminescent veins (Figure 3.5c). Late veins at Banshee are bright yellow luminescent (Figure 3.5d), zoned, and overprint silicification within intensely altered areas (Figure 3.5d).

3.5.2 Isotope Results

3.5.2.1 Wall Rock Carbonates

Data from all samples analyzed for oxygen and carbon isotopes are located in Appendix C. Background $\delta^{18}O$ and $\delta^{13}C$ values for Ordovician through Devonian marine carbonates in northern Nevada were established by analyzing samples from the Lone Mountain area NW of Eureka Nevada, USA (see Figure 1.2). All isotope values were determined assuming calcite. Three samples of Devonian Nevada Group Limestone varied between +19.6 to +26.2‰ $\delta^{18}O$ and -1.2 to +3.5‰ $\delta^{13}C$. The Nevada Group Limestone is correlative with the Popovich Formation at Goldstrike. Two samples of Devonian Lone Mountain Dolomite (containing calcite>dolomite) varied between +24 to +25.5 $\delta^{18}O$ and -0.7 to 0.9‰ $\delta^{13}C$. The Lone Mountain Dolomite is correlative with Bootstrap Limestone. Silurian-Devonian Roberts Mountain Limestone varied between +24.3 to +26.7‰ $\delta^{18}O$ and -0.1 to 0.2‰ $\delta^{13}C$. Lower in the stratigraphic section, one sample of Ordovician Hanson Creek Limestone had values of +24.1‰ $\delta^{18}O$ and +1.5‰ $\delta^{13}C$, and one sample of Ordovician Pogonip Limestone had values of +19.1‰ $\delta^{18}O$ and +0.3‰ $\delta^{13}C$. These background values are consistent with the global background data compiled by Veizer (1999) et al. for Ordovician through Devonian marine carbonates. Results from Banshee show $\delta^{18}O$ and $\delta^{13}C$ values range between background Silurian-Devonian marine calcite to values significantly depleted relative to background with matrix calcite values varying between +4.7 to +26.1‰ $\delta^{18}O$ and -4.0 to +4.3‰ $\delta^{13}C$ (Figure 3.6, Appendix C). The majority of samples were collected from Stage 1 breccias and Bootstrap Limestone as these units contain most of the carbonate bearing wall rock in the area (Figure 3.6a). The majority of Stage 2 and 3 breccias contain little to no carbonate due to extensive carbonate dissolution; however, a number of samples collected from Stage 2 and 3 breccias contained sufficient carbonate for analysis (Figure 3.6b). Stage 2 and 3 breccias are consistently depleted in comparison to unaltered protolith with matrix calcite ranging +4.7 to +20.4‰ $\delta^{18}O$ and -1.7 to +3.0‰ $\delta^{13}C$ (Figure 3.6b).

Figure 3.1 shows the distribution of sampled drill hole collars at Banshee in plan view. Figure 3.7 shows the spatial variation in $\delta^{18}O$ isotope values across the main Banshee section (section A-A'). The majority of the section is depleted relative to background values. Samples collected from the west Banshee drill fan are uniformly depleted in $\delta^{18}O$ with depletion generally increasing nearer mineralization. In east and west Banshee isotopic depletion has a strong correlation with brecciation and is bounded to the east by the Post fault and above by the RMT (Figure 3.7). In addition to the main Banshee cross-section, samples were collected from two West Banshee drill fans stepping to the north. $\delta^{18}O$ depletion is less pervasive in the northern drill fans (Figure 3.8a-b). In the northern most drill fan, the wall rock is largely unaltered except proximal to the west Banshee lamprophyre (Figure 3.8b). The magnitude of $\delta^{18}O$ depletion is variable in space, but the extent of $\delta^{18}O$ depletion envelopes known mineralization and brecciation (Figure 3.8b). Samples collected from the breccia unit at Banshee have more depleted $\delta^{18}O$ values in general as can be seen by the distribution of $\delta^{18}O$ values of <15‰ (VSMOW) in Figure 3.7.

$\delta^{18}O$ and $\delta^{13}C$ stable isotopes for rock carbonate samples show a poor correlation (Figure 3.6) indicating that the fluid responsible for $\delta^{18}O$ depletion was largely rock buffered with respect to $\delta^{13}C$. Samples depleted in $\delta^{13}C$ are generally depleted in $\delta^{18}O$ as well, indicating that depleted $\delta^{13}C$ values may correspond with $\delta^{18}O$ depletion for many samples. Additionally, $\delta^{13}C$ values trend lower on average with decreasing $\delta^{18}O$ values. $\delta^{13}C$ values corresponding to the lowest $\delta^{18}O$ values (<9‰) plot below 1.5 ‰ $\delta^{13}C$. The spread of data is consistent with studies of other Carlin-type Au deposits at Twin Creeks (Stenger et al., 1998b), Carlin (Radtke, 1985; Radtke et al., 1980), Jerritt Canyon (Hofstra, 1994), and Pipeline (Arehart and Donelick, 2006). Alligator Ridge (Ilchik, 1990) and Meikle (Emsbo et al., 2003) are two deposits that show a trend of increasing $\delta^{13}C$ towards mineralization with both authors attributing the trend to sourcing of CO_2 from isotopically heavier carbonate sequences below the host rocks. The measured values of $\delta^{13}C$ are likely controlled by interaction with wall rock carbonate rather than exotic source of depleted $\delta^{13}C$.

A number of hand specimens were sampled to test for isotopic variability. Samples were analyzed from the different lithologies and breccia facies to establish the isotopic variability of carbonate minerals in carbonate bearing matrix, clasts, and veins. Samples of

Bootstrap limestone and Stage 1 breccia consistent with regional background $\delta^{18}O$ have relatively uniform $\delta^{18}O$ values in limestone clasts, carbonate rich matrix, and calcite veins with a mean $\delta^{18}O$ value of 24.2 ±1.0‰ (Figure 3.9). Isotopically altered Bootstrap limestone and Stage 1 breccia have more variable $\delta^{18}O$ values across matrix and clasts with a mean $\delta^{18}O$ value of 15.1 ±1.9‰ (Figure 3.10). Nearly all samples of Stage 2 and 3 breccia are completely silicified with rare relict calcite. Stage 4 breccia could not be sampled owing to near complete carbonate dissolution.

3.5.2.2 Calcite Veins

Calcite veins consist of 4 isotopically distinct clusters (Figure 3.6c). The first cluster contains early veins with values consistent with Silurian-Devonian marine carbonate background values. The second cluster contains intermediate veins with variable alteration from background rock values with a range of +7.3 to +24.6‰ $\delta^{18}O$ and -1.8 to +1.9‰ $\delta^{13}C$. Intermediate veins generally follow a pattern of decreasing $\delta^{13}C$ and $\delta^{18}O$. The third cluster of data consists of late veins with uniformly depleted $\delta^{18}O$ values with a range of +3 to +6‰ $\delta^{18}O$ and 0 to +2‰ $\delta^{13}C$. Cluster 3 early veins are dominantly late coarse-grained calcite veins from Stage 3 calcite-cemented breccia and are indicative of unexchanged to slightly exchanged meteoric fluids. The fourth cluster of isotope data are late veins with similar $\delta^{18}O$ values to cluster three, but have isotopically heavier $\delta^{13}C$ values with a range of +1.8 to +4.5 ‰ $\delta^{13}C$. Early veins associated with the fourth cluster are commonly found lining dissolution cavities associated with Stage 4 breccia. Cluster three veins have similar isotopic signature to Emsbo et al. (2003) post ore calcite, and cluster four veins have a similar isotopic signature to Emsbo et al. (2003) late ore stage calcite. The textural occurrence of clusters three and four is also similar to Emsbo et al.'s (2003) description of late ore stage and post ore stage calcite.

Calcite veins in unaltered wall rock generally have values consistent with Devonian marine carbonates (Figure 3.9a,c,e). Veins in isotopically altered samples are more variable (Figure 3.10). A number of veins have similar values to depleted matrix carbonate (Figures 3.10a,b and 3.11a). Common coarse calcite veining found as cement in Stage 3 breccia and lining cavities in Stage 4 breccia have highly depleted $\delta^{18}O$ values with a mean of 6.8 ±1.6‰

(Figure 3.11b-c). In a few samples veins have $\delta^{18}O$ values higher than the rock matrix or clasts (Figure 3.11a). Multiple generations of carbonate veins may cross cut with varying isotopic signatures. Figure 3.11a shows a calcite vein with a $\delta^{18}O$ value of 17.2‰ cross cutting a darker calcite vein with a value of 25.2‰ $\delta^{18}O$.

3.5.3 LA-ICPMS Results

The goal of the LA-ICPMS study was to document the chemical controls on CL response in calcite. LA-ICPMS analysis was conducted on samples with a range of isotopic values and CL textures on both wall rock carbonate and veins. Dolomite grains were avoided. Analyses were generally conducted where calcite grains were greater than the 60 μm spot size of the laser although some ablation points sampled across grain boundaries within calcite matrix and ooids. Appendix D includes a table of all results. Samples exhibiting bright orange luminescence have uniformly higher Mn concentrations (Figure 3.12). Luminescent samples of rock carbonate and veins also contain elevated Fe concentrations and slightly lower concentrations of Mg (Figures 3.13 and 3.14). The increase observed in Fe with higher Mn samples is not sufficient to quench the CL response (Figure 3.12). Bright yellow luminescent calcite also has higher Mn concentrations in calcite but does not exhibit similar increases in Fe or decreases in Mg. Post Archean Australian shale (PAAS) normalized REE plots (Taylor and McLennan, 1985) show bright orange luminescent calcite with lighter $\delta^{18}O$ values from veins, ooids, and cements exhibit higher REE concentration and positive Eu anomalism (Figure 3.15). Figures 3.16 and 3.17 show the relationship between $\delta^{18}O$ values, CL textures, and Mn concentration for calcite veins and wall rock calcite for two samples analyzed as part of this study.

3.6 Interpretation

3.6.1 Spatial Distribution of Isotopic Alteration, and Links to Lithology, Structure, and Alteration

Figure 3.18 shows the extent of anomalous Au (>0.2 ppm), visible alteration, and $\delta^{18}O$ depletion along the main Banshee cross-section. The extensive breccia unit at Banshee likely focused fluids laterally out from structures hosting upwelling hydrothermal fluids. The extent and range of isotopic depletion within the breccia units indicates that the hydrothermal fluid variably altered breccia. A majority of pre-mineralization (Stage 1) breccia sampled was depleted with respect to $\delta^{18}O$, but the same samples were not visibly altered by silicification and/or carbonate dissolution except in areas immediately adjacent to higher grades of ore. The fluid responsible for $\delta^{18}O$ depletion in relatively unaltered breccia was likely pH buffered, and therefore, was incapable of dissolving large amounts of carbonate. The Silurian-Devonian Bootstrap limestone is visibly unaltered in much of the Banshee deposit. Bootstrap limestone does exhibit $\delta^{18}O$ depletion outside of the more permeable breccia. Alteration patterns indicate that competent Bootstrap limestone served as a low permeability boundary for both east and west Banshee that likely focused fluids through permeable lithologies and structures. The Upper Mud contains anomalous Au values in both east and west Banshee, but is not consistently depleted in $\delta^{18}O$. The Au located in this horizon could be associated with Devonian aged sedimentary-exhalative (sedex) Au mineralization described by Emsbo (1999) to the south, and may not have been associated with the Carlin mineralizing system, and, thus, was not isotopically altered by it. Hofstra et al. (2011) suggested that the absence of $\delta^{18}O$ alteration in Au mineralized Devonian Popovich rocks at Goldstrike could be linked to an earlier stage of mineralization noting that they are not depleted in $\delta^{18}O$ and lack the typical trace element suite associated with Carlin-type mineralization. The data presented here is consistent with the interpretation of a separate Au-bearing event unrelated to Carlin-type hydrothermal mineralization. The other possibility is that hydrothermal fluids interacting with Upper Mud rocks were rock buffered to the extent that they were incapable of causing modification of $\delta^{18}O$ rock calcite.

Isotopic alteration patterns indicate that Post fault and the fringe of the Jurassic monzonite dike below the RMT were exposed to higher integrated fluid fluxes. Wall rocks within the ore zone exhibit a greater degree of $\delta^{18}O$ depletion independent of lithology. It is likely that the primary control on fluid migration into the deposit was structural (i.e. faults), but laterally continuous permeable horizons were the primary control for the bulk of stable isotope alteration. While Jurassic lamprophyre dike is mineralized in the east Banshee ore zone, below the ore zone the same dike is only variably altered with minor occurrences of Au (<0.05 ppm) (See Chapter 2). The lack of isotopic depletion, visible alteration, and Au mineralization in areas immediately adjacent to ore zones indicates that fluids did not pervasively penetrate the massive limestone beneath the breccia horizon.

Variable depletion in $\delta^{13}C$ at Banshee indicates that the altering fluid was largely rock buffered with respect to $\delta^{13}C$. Morgan (2006) noted that $\delta^{13}C$ values down to -3.8‰ (PDB) associated with ferroan dolomites and zebra textured dolomites of the Bootstrap unit within the Meikle deposit. The relatively depleted values reported by Morgan (2006) may be related to the Late Devonian hydrothermal system described by Emsbo et al. (2003). Previous studies at other Carlin-type deposits have noted more depleted $\delta^{13}C$ values consistent with an input of organic sourced carbon (Arehart and Donelick, 2006; Hofstra, 1994; Stenger et al., 1998b) or possibly magmatic carbon. Only a limited number of samples at Banshee exhibit significant $\delta^{13}C$ depletion (Figure 3.6).

3.6.2 Chemical Changes Associated with Isotopic Depletion of Host Rocks

LA-ICPMS analysis of rock calcite with different CL textures and luminescence, and paragenetically defined veins at Banshee provides additional criteria for evaluating the different generations of calcite observed. The main control on CL response in calcite is the Fe-Mn chemistry of calcite cements with Mn^{2+} serving as a CL activator, and Fe^{2+} as a CL quencher. Mn concentrations above ~20 ppm are necessary to activate dull luminescence and concentrations greater than ~225 ppm will activate bright luminescence (Savard et al., 1995). Concentrations of Mn between 20 and 225 ppm can have the full range of CL responses including dull, bright, and non-luminescent (Savard et al., 1995). Non-luminescent calcite at Banshee contains low concentrations of Mn and Fe and fall below the bounds of the theoretical Mn concentrations needed for CL activation (Machel and Burton, 1991) (Figure 3.12). Increases in CL response correspond to increases in Mn concentration (Figure 3.12). For Banshee, bright CL response occurs at Mn concentration above ~100 ppm and Fe contents are sufficiently low as to have no effect on CL response in this sample set. The highest Mn concentrations are associated with samples exhibiting a bright orange CL response. Near the CL activation threshold of 20 ppm Mn samples are variably luminescent as indicated by Figure 3.12. Other studies have shown that the concentration of Mn in calcite necessary for CL activation can be highly variable (Savard et al., 1995), but the samples from Banshee are consistent with the CL activation fields of Machel and Burton (1991).

REE abundances in calcite can be another source of CL activation, but REEs typically only become important as activators at concentrations >10 ppm in calcite (Machel and Burton, 1991). REE concentrations in calcite at Banshee are 1-2 orders of magnitude too low to effect the observed CL activation for samples in this study. Never the less, LA-ICPMS data from Banshee calcite indicates that distinct REE concentrations and patterns occur between early, intermediate, and late veins. Early and late veins uniformly contain lower abundances of REE than intermediate veins (Figure 3.15). Additionally, CL activated rock carbonate plots with similar REE abundances to intermediate veins and are enriched relative to non-luminescent rock carbonate (Figure 3.15). An important feature of the intermediate calcite veins is a positive Eu anomaly for several of the samples. Eu anomalies are commonly expressed as the elemental ratio Eu/Eu* (Eu/Eu*=Eu_{SN}/(0.5SM_{SN}+0.5Gd_{SN}) where the subscript $_{SN}$ indicates that concentrations are normalized to the Post Archean Australian Shale of McLennan (1989) (Bau et al., 2010). A positive Eu/Eu* anomaly is indicated at values >1.0. Intermediate veins at Banshee have Eu/Eu* values ranging from 0.87 to 6.90 with a mean value of 2.48. Early and late veins have Eu/Eu* values close to 1 for all samples.

The redox potential of Eu^{3+}/Eu^{2+} in aqueous solution depends on REE speciation, pH, and pressure (Bau and Moller, 1992). However, experimental studies indicate that temperature is the predominant factor in producing positive Eu anomalies (Bilal, 1992). Low temperature fluids are unlikely to produce positive Eu anomalies owing to the extremely low fO_2 required (Bau and Moller, 1992). Only at temperatures in excess of ~220ºC can oxidized ($SO_4^{2-} > H_2S$) fluids produce a positive Eu anomaly in carbonate minerals (Bau and Moller, 1992). Hofstra and Cline (2000) suggest a log fO_2 of ~-45 is consistent with the mineral assemblage associated with Carlin-type mineralization and fluid inclusion data indicates that the Carlin-type hydrothermal systems were ~220ºC (Cline et al., 2005; Hofstra and Cline, 2000). The pH of Carlin-type fluids is not precisely known and will have an effect on the redox equilibrium calculations for Eu^{3+}/Eu^{2+}. According to Bau and Moller's (1992) model a fluid at 0.5 kbar and pH=3 with log fO_2=-40 would need a minimum temperature of ~200ºC to produce a positive Eu anomaly in precipitated calcite (Figure 3.19). If higher pH conditions are used Eu^{3+}/Eu^{2+} redox equilibrium is shifted towards higher log fO_2. The position of redox equilibrium for SO_4^{2-}/H_2S does not shift at higher pH and since Carlin-type systems are H_2S dominated, pH variations would not change the interpretation that intermediate veins were precipitated from reduced hydrothermal fluids. At lower log fO_2 minimum temperatures for a Eu anomaly decrease so better constraints on log fO_2 and pH of Carlin-type fluids could provide more precise estimates of minimum temperatures necessary for the observed data from Banshee. The presence of the positive Eu anomaly in veins classified as intermediate supports the conclusion that the veins were part of the ore-forming hydrothermal system at Banshee and should be included in the formulation of alteration models for Carlin-type systems.

CL and trace element data indicate chemical and textural modification of calcite coincided with $\delta^{18}O$ alteration and is supportive of an interpretation that recrystallization of calcite was the mechanism that enabled cation exchange between fluid and rock with subsequent isotopic exchange. CL response from $\delta^{18}O$ depleted calcite is consistently brighter than unaltered Silurian-Devonian marine calcite. When $\delta^{18}O$ values are plotted against Mn concentration determined from LA-ICPMS a correlation is evident with increasing Mn occurring with decreasing $\delta^{18}O$ values (Figure 3.20). The inverse correlation of $\delta^{18}O$ and Mn indicates that the recrystallization textures seen in CL correspond with $\delta^{18}O$ alteration of wall rock calcite at Banshee. In addition to Mn enrichment in altered calcite, REE data distinguishes unaltered and altered calcite phases. Unaltered non-luminescent marine calcite is REE poor. Luminescent $\delta^{18}O$ altered wall rock calcite has elevated concentrations of REE relative to unaltered background indicating addition of REE. One potential source of REEs is feldspar from intrusive dikes in the area of Banshee. Alteration of lamprophyre and monzonite dikes in the area during mineralization would have put some REE into solution for later incorporation in recrystallized calcite. The increased acidity of fluids associated with Carlin-type alteration would have facilitated REE solution (Sverjensky, 1984).

3.6.3 Syn-alteration Calcite Veins

Samples collected of early calcite veins exhibit dully-luminescent CL responses that correspond to non-depleted $\delta^{18}O$ values for calcite. These early vein samples also contain lower abundances of Mn and REEs, and are considered to represent unaltered background for

Silurian-Devonian marine carbonates in the area. In areas more proximal to the ore zone at Banshee, intermediate calcite veins exhibit a bright orange CL response with $\delta^{18}O$ values depleted relative to Silurian-Devonian background and contain increased Mn and REEs. Bright orange luminescent calcite with higher Mn values is positively correlated with $\delta^{18}O$ isotopic depletion (Figure 3.20) and spatially consistent with hydrothermally driven alteration of limestone at Banshee. Intermediate veins have $\delta^{18}O$ values that fall on the same depletion trend as altered wall rock and have an isotopic signature distinct from early and late calcite veins. Additionally, intermediate veins have CL responses similar to altered recrystallized wall rock and do not have the zoning characteristic of late veins. Finally, intermediate veins have positive Eu* anomalies that are indicative of calcite precipitation from reduced hydrothermal fluids consistent with published fluid temperatures and fO_2 for Carlin-type Au deposits (Cline and Hofstra, 2000; Cline et al., 2005; Lubben et al., 2012). Based on all these lines of evidence, intermediate calcite veins at Banshee are interpreted to synchronous with hydrothermal alteration.

3.7 Discussion and Implications

3.7.1 Isotopic Exchange Mechanisms in Low Temperature Systems

CL textures of altered wall rock calcite at Banshee indicate that primary textures were preserved during alteration. The implication of preserved textures with trace element and isotopic alteration is that pseudomorphic replacement of calcite has occurred. Dissolution-precipitation reaction is a coupled process that can result in pseudomorphic replacement of calcite. Pseudomorphic replacement of mineral grains requires that dissolution and precipitation occur at the same time and implies that the rate of dissolution is the controlling factor rather than the rate of nucleation (Putnis, 2009). If the rate of nucleation were the controlling factor, dissolution would likely advance faster than nucleation/precipitation and pseudomorphic replacement would not occur. In Carlin-type deposits, intense alteration results in the removal of calcite through carbonate dissolution (Hofstra and Cline, 2000). Where the fluid was rock buffered outside of carbonate dissolution it is possible that coupled dissolution-precipitation could occur.

While pH and temperature are commonly cited controls on calcite solubility, solubility is complex and could be affected by temperature, pH, salinity, and/or the activity of CO_2 (Morse et al., 2007). The composition of ore fluids with respect to CO_2 and NaCl have been determined from ore stage quartz fluid inclusions commonly occurring within zones of intense alteration including carbonate dissolution (Cline and Hofstra, 2000; Hofstra and Cline, 2000). Data measured from fluid inclusions may not be representative of the fluid in areas where dissolution-precipitation of calcite is occurring. It is likely that the acidic fluid involved in complete carbonate removal became progressively rock buffered as it infiltrated carbonate stratigraphy and eventually was capable of coupled dissolution-precipitation reactions. As the fluid was progressively rock buffered dissolution of primary calcite still occurred, but as calcite dissolved the chemical components put into solution drove the saturation of calcite and lead to precipitation of new calcite with textural preservation. In this case it is not the bulk fluid composition controlling the reactions but rather the composition of the fluid at the mineral interface (Putnis, 2009). Pseudomorphic replacement requires that the process be closely coupled and that controlling mechanism be the dissolution rate with a low activation energy barrier for nucleation (Putnis, 2009).

Chemical, isotopic, and CL textural data from Banshee clearly demonstrates near complete replacement of protolith calcite in areas of hydrothermal $\delta^{18}O$ alteration of calcite. The fact that ooids are preferentially replaced over cement likely indicates a difference in porosity where the infiltration of altering fluids was greater in ooids and possibly enhanced through the dissolution-precipitation reaction. Putnis (2002) suggests that mineral replacement in calcite initially results in the replacement of the rims with continuous reaction eventually replacing the entire calcite grain. Putnis (2002) also suggested that dissolution-precipitation reactions significantly increase porosity causing reaction enhanced permeability thereby allowing increased access of the fluid to the replacement front. Bowman et al. (2009) showed that complete replacement will result in relatively homogenous $\delta^{18}O$ and trace element composition in the replaced calcite.

Calcite cements in oolitic limestone at Banshee show an interlocking granular texture with relatively consistent crystal size. Micritization of ooids can result in the creation of intragranular microporosity (Asquith, 1986) leading to an increase in permeability. The increased permeability would make the ooids more susceptible to replacement owing to increased interaction with the altering fluid. $\delta^{18}O$ data indicates relatively consistent alteration of replaced calcite with similar values measured from various drilled locations at a scale of >2cm. The lack of zoning observed using CL further supports a relatively consistent composition of replaced calcite.

3.7.2 Evidence of Kinetically Limited Exchange

In high temperature systems, equilibrium exchange is generally assumed. Data from this study of syn-alteration veins within altered wall rock indicate that equilibrium may not have been achieved in the low temperature Banshee deposit. With equilibrium exchange, $\delta^{18}O$ values of syn-alteration veining and altered wall rock should be equivalent. Owing to the fact that syn-alteration veining is consistently depleted in $\delta^{18}O$ relative to the wall rock indicates that exchange between the fluid and recrystallized wall rock calcite may have been rate (i.e. kinetically) limited (Figure 3.21). Since syn-alteration veins were precipitating directly out of the fluid their $\delta^{18}O$ values are considered to be representative of the fluid. Temperature is thought to exert a strong control on non-equilibrium (i.e. kinetic) exchange, and the relatively low temperature of Carlin-type hydrothermal systems was likely the key factor for non-equilibrium conditions. The rate of exchange is likely dominated by the rate of dissolution-precipitation reactions of wall rock calcite grains. The textural evidence of pseudormorphic replacement of calcite seems to support rapid surface reaction. The lack of agreement between textural observations and vein-rock pair data may be due to the scale at which equilibration is occurring. At the grain scale where dissolution-precipitation reactions are occurring it's possible that the fluid is significantly more rock buffered relative to fluid precipitating calcite veins along fractures with higher fluid:rock ratios. If wall rock values are not representative of the bulk fluid values, the use of simple mass balance box reactor models are not appropriate for estimating W/R ratios and isotopic change in a Carlin-type hydrothermal system (Bowman et al., 1994).

Stenger et al. (1998b) used $\delta^{18}O$ from wall rock carbonate to infer the source of fluids and proposed a 2-fluid mixing model to explain the degree and variability in $\delta^{18}O$ values. These models assume equilibrium conditions with temperature dependent fractionation as the primary cause of $\delta^{18}O$ variability. If equilibrium conditions prevailed, the paired rock and vein data should have near identical $\delta^{18}O$ values. The vein-rock pair data presented here supports a more complex model for isotopic exchange for Carlin-type deposits where non-equilibrium conditions may be important. Accounting for the potential of kinetic inhibition relies on more sophisticated modeling of data than simple zero-dimensional mass balance models can provide. Chapter 4 uses the $\delta^{18}O$ isotopic data from syn-alteration calcite veins and wall rock presented in this chapter and employs 1-dimensional reactive transport modeling in an attempt to provide a better understanding on fluid rock reaction and isotopic exchange. This approach uses data from well-constrained syn-alteration vein-rock pair samples from this chapter to place estimates on time integrated fluid flux and reactive path length for isotopic exchange.

3.7.3 Model for Zoned Alteration of Carbonates

Alteration models for Carlin-type systems typically consider the spatial distribution of silicification, clay alteration, and carbonate dissolution as the primary attributes of hydrothermal alteration; however, this study indicates that $\delta^{18}O$ alteration of wall rock and syn-alteration calcite veining should be considered in the formulation of a fluid flow and alteration model. Cline et al. (2005) describe zoning of carbonate alteration associated with Carlin-type alteration. However, few studies have identified calcite veining that is linked to mineralization. By establishing a link between calcite veining and hydrothermal alteration using textures, CL, isotopes, and trace elements, this study provides an improved understanding of how altering fluids evolved through space out from zones of carbonate dissolution.

Figure 3.22 illustrates a conceptual model for carbonate alteration zoning, as the altering fluid is progressively rock buffered along the fluid flow path. The carbonate dissolution zone and the dolomite stable zone are easily distinguishable manifestations of Carlin-type alteration. The calcite stable zone may not have an obvious expression of fluid rock interaction. This chapter demonstrates that $\delta^{18}O$ isotope data from rock calcite provides a tool for defining fluid flow driven alteration within the calcite stable zone where other indicators may be lacking. The edge of isotopic depletion likely defines one of the more distal indicators of alteration. While the conceptual model shows spaced reaction fronts of alteration along the permeable flow path, sides to reaction fronts are more commonly encountered. The distance separating alteration zones is primarily controlled by permeability contrasts. At Banshee this occurs when permeable breccia is in contact with less permeable wall rocks. As shown in Figure 3.21 calcite veins may be discrete indicators of flow outside of other recognized indicators; however, calcite veins need to be linked to the hydrothermal event of interest. The existence of syn-alteration calcite veins has not been established at most known Carlin-type Au deposits, but isotope and textural data suggest that syn-alteration veins may occur at the Carlin deposit (Kuehn and Rose, 1995), the Pipeline deposit (Ahmed, 2010), and at Alligator Ridge (Ilchik, 1990). Future work should seek to further define the extent of syn-alteration calcite veining associated with Carlin-types systems as a distal indicator of hydrothermal fluid flow.

3.7.4 Implications for Fluid Flow and Exploration in Carbonate Terrains

While isotopic depletion of carbonate rocks by low temperature hydrothermal fluids has been previously recognized, detailed sampling across a defined flow path provides for a better understanding of fluid pathways and progressive fluid-rock reactions than along those pathways. In reality, sampling along a presumed fluid flow path presents a significant challenge owing to the inherent heterogeneity of porous media leading to significant hydrodynamic dispersion. In theory, sampling along the flow path should define a series of fronts defined by the extent of chemical and exchange reactions induced through fluid infiltration. The sharp gradients defined by this study are more likely to represent metasomatic sides defined by permeability contrasts rather than fronts. Yardley and Lloyd (1995) argued that sharp gradients are more likely to be linked to permeability contrasts rather than reactivity between the fluid and wall rock. Visible alteration products such as carbonate dissolution, clay alteration, and silicification may also serve to define fluid flow paths and permeability controls. At the distal extents of low temperature systems hosted in carbonates the visible expression of fluid-rock interaction is commonly lacking. In these settings, other tools can be useful for defining the permeability network and vectoring fluid flow. This study shows that alteration of carbonate host rocks extends some distance from visible alteration and can be defined using $\delta^{18}O$ isotopes in calcite, recrystallization textures in calcite defined by CL, and calcite mineral chemistry. In the case of Banshee, each of these tools is consistent with an interpretation that fluid rock reaction is more extensive than previously defined and may serve as the most distal indicators of hydrothermal alteration in Carlin-type deposits.

Using the tools developed in this chapter for exploring in carbonate terrains extends the targetable footprint of potential ore bearing systems. In cases where mineralization is hosted within small volumes of rock the likelihood of missing an ore bearing system with drilling is increased. In these cases it is appropriate to employ the techniques presented here to determine the potential for proximity to ore bearing zones. While these methods are not diagnostic of ore bearing hydrothermal systems, they could be powerful tools for assessing existence of hydrothermal fluid systems that are potentially related to an ore system. In addition to defining the presence of hydrothermal systems, these tools can be used to better constrain the permeability network of a potential ore system, and provide further constraints on potential stratigraphic and structural hosts for mineralization. While $\delta^{18}O$ values and CL textures may serve to identify the presence and lateral extent of hydrothermal alteration, calcite mineral chemistry can further constrain the hydrothermal system by looking at the REE chemistry. Using the approach defined here the presence of positive Eu anomalies in altered wall rock calcite and syn-mineral veins builds the explorationist's confidence that an alteration system is the result of reduced hydrothermal fluids within the range of temperatures common to Carlin-type ore deposits. Chapter 5 of this thesis applies the use of $\delta^{18}O$ isotopes and trace element geochemistry to look at the distal extent of hydrothermal alteration of carbonates on the Goldstrike property, the largest known Carlin-type Au system.

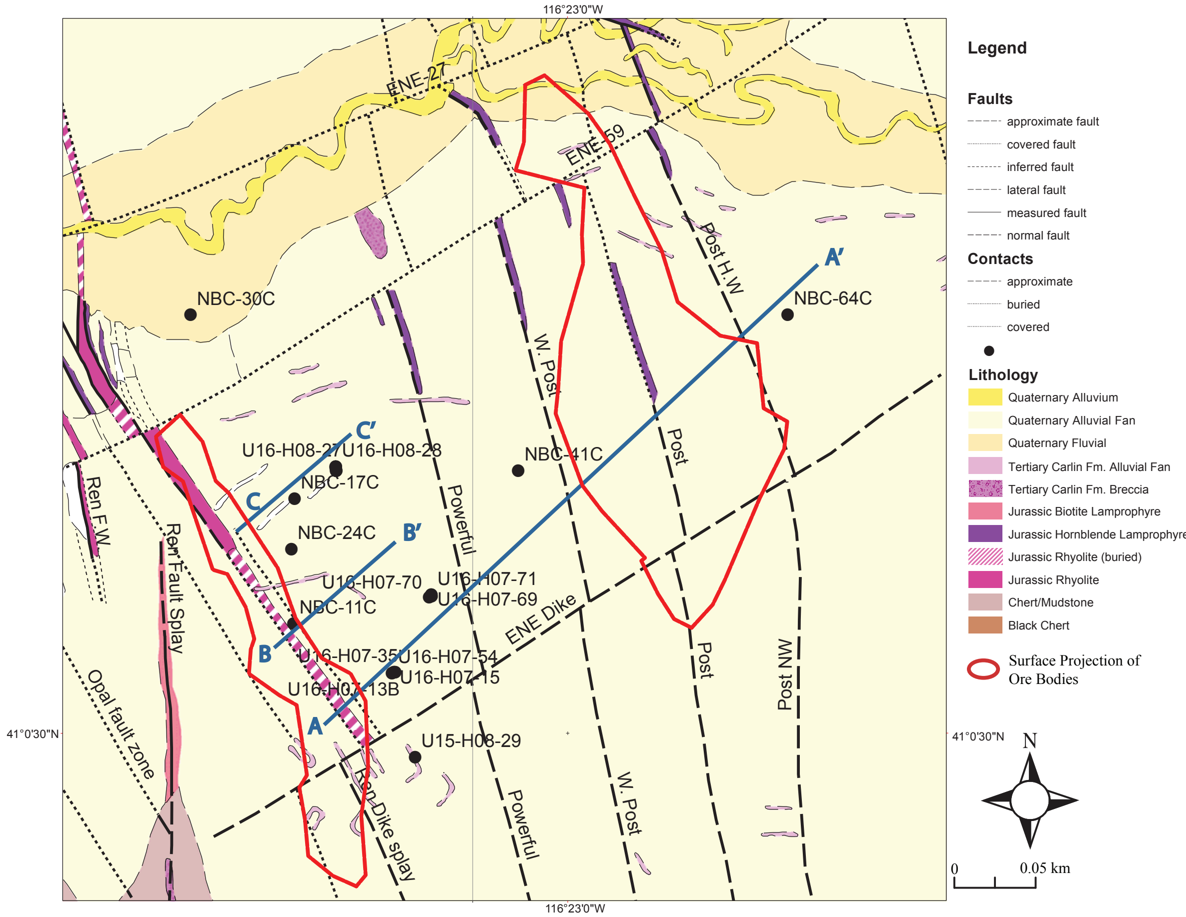

Figure 3.1 Surface geology map of the Banshee area showing the location of the three cross-sections sampled for O and C isotope analysis in this chapter (after Barrick internal data).

Figure 3.2 Photos of (a) Stage 1 breccia with Bootstrap limestone clasts and carbonaceous silty matrix cross cutting calcite vein; (b) silicified Stage 2 polymict breccia with clasts of Ordovician Vinini mudstone (Ov), Silurian-Devonian Bootstrap limestone (SDbs), and Jurassic rhyolite (Jmp); (c) silicified Stage 3 breccia with calcite veining cutting silicification and Stage 2 brecciation; and, d.) weakly consolidated polymict Stage 4 breccia.

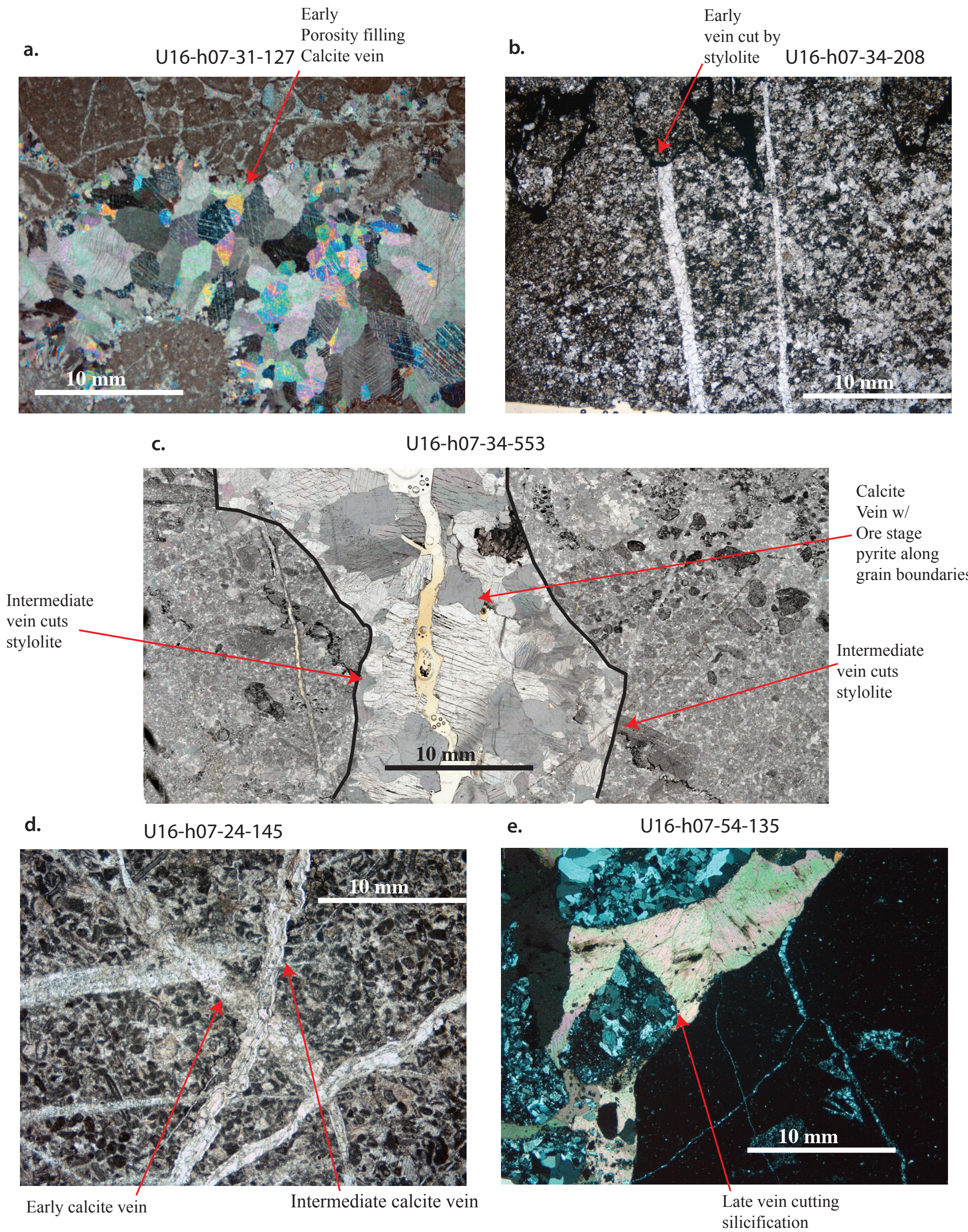

Figure 3.3 a) Cross polarized thin section scan shows early calcite vein filling open space in Bootstrap limestone characterized by fine grained calcite near the edge of vein and coarser calcite near the center of the vein. Early calcite is also seen filling pore space between ooid grains. b) Plane polarized light thin section scan of early calcite vein cut by a stylolite placing the age of the vein prior to stylolitization. c) Cross-polarized thin section scan of intermediate calcite vein cutting stylolitization in a Bootstrap limestone sample. d) Cross-polarized thin section scan of a late coarse-grained calcite vein cutting silicified limestone breccia within the Banshee ore zone.

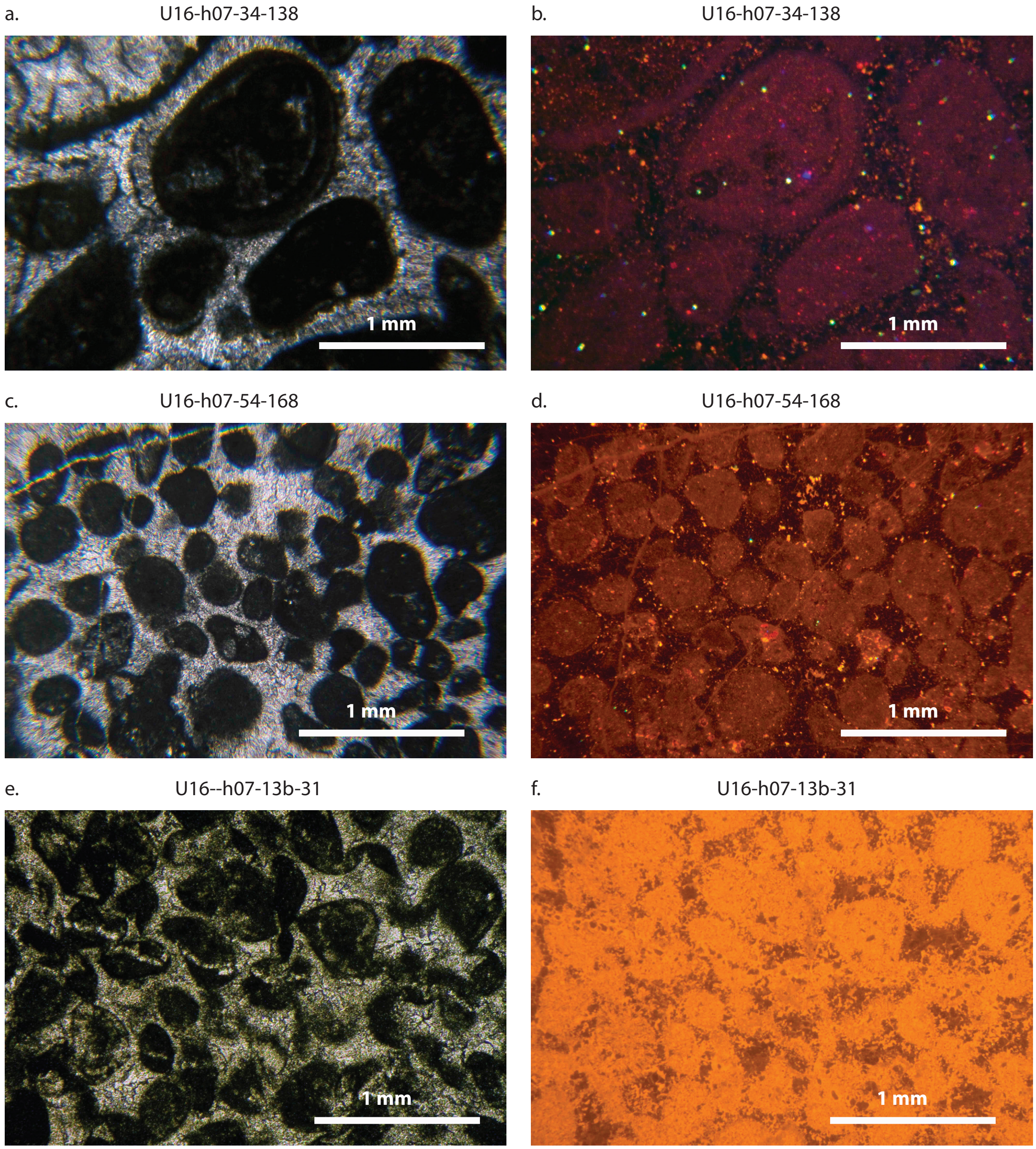

Figure 3.4 Transmitted light photomicrographs and CL images of ooilitic Bootstrap limestone from west Banshee illustrating the changes in CL response with recrystallization of calcite. a-b) Non-luminescent and dully luminescent calcite from isotopically unaltered limestone ($\delta^{18}O$ =25‰). c-d) Dully luminescent calcite with some recrystallization of ooids from lightly $\delta^{18}O$-altered limestone ($\delta^{18}O$=20‰). e-f) Brightly luminescent calcite with near complete recrystallization of ooids and partial recrystallization of matrix calcite from strongly $\delta^{18}O$-altered limestone ($\delta^{18}O$=13‰).

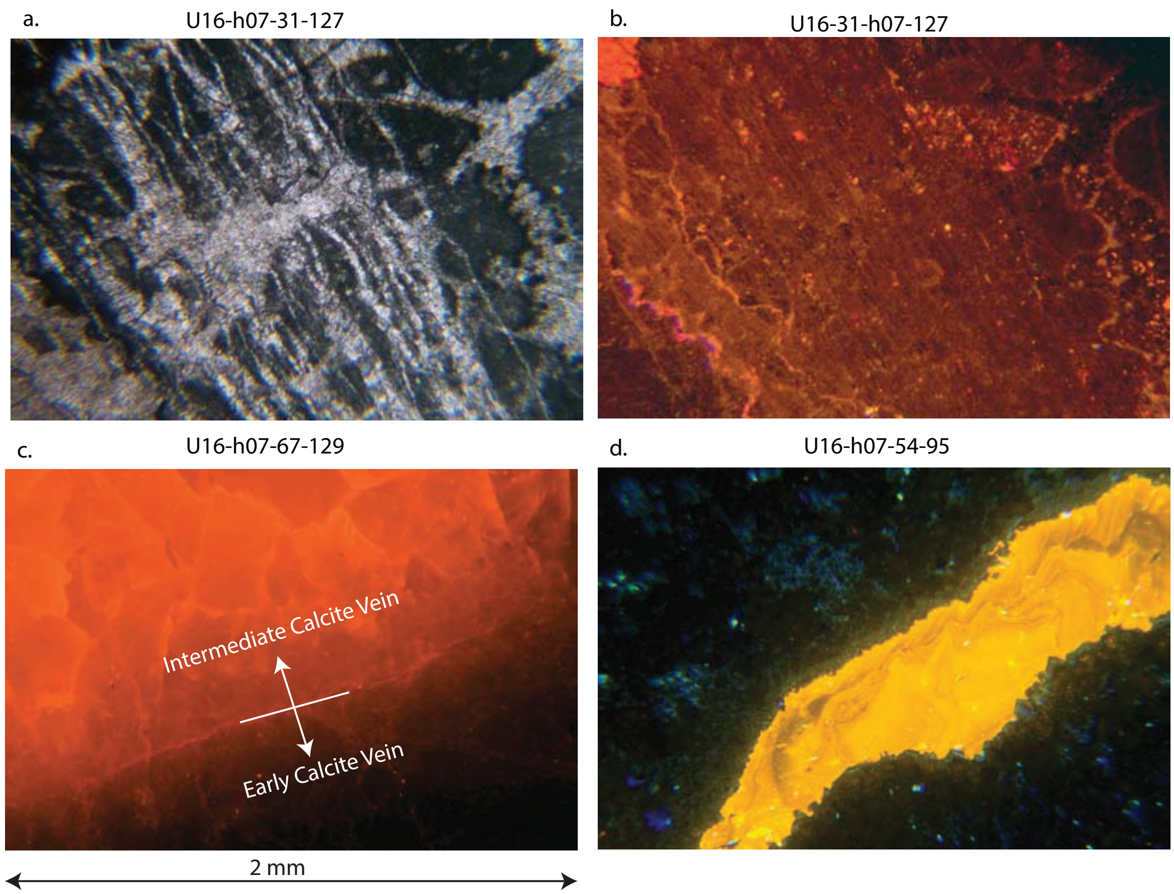

Figure 3.5 a) Plane polarized light photomicrograph of early veining in $\delta^{18}O$ unaltered Bootstrap limestone. b) CL photomicrograph of the same sample as Figure 3.17a with the same field of view shows dully-luminescent calcite of early veining indistinct from rock calcite. c) CL photomicrograph of dull to bright intermediate calcite vein ($\delta^{18}O$= 17‰) cutting non-luminescent early calcite vein ($\delta^{18}O$ = 25‰). d) CL photomicrograph of late calcite vein cutting silicified limestone breccia in the west Banshee ore zone with bright yellow-orange CL response and zoning.

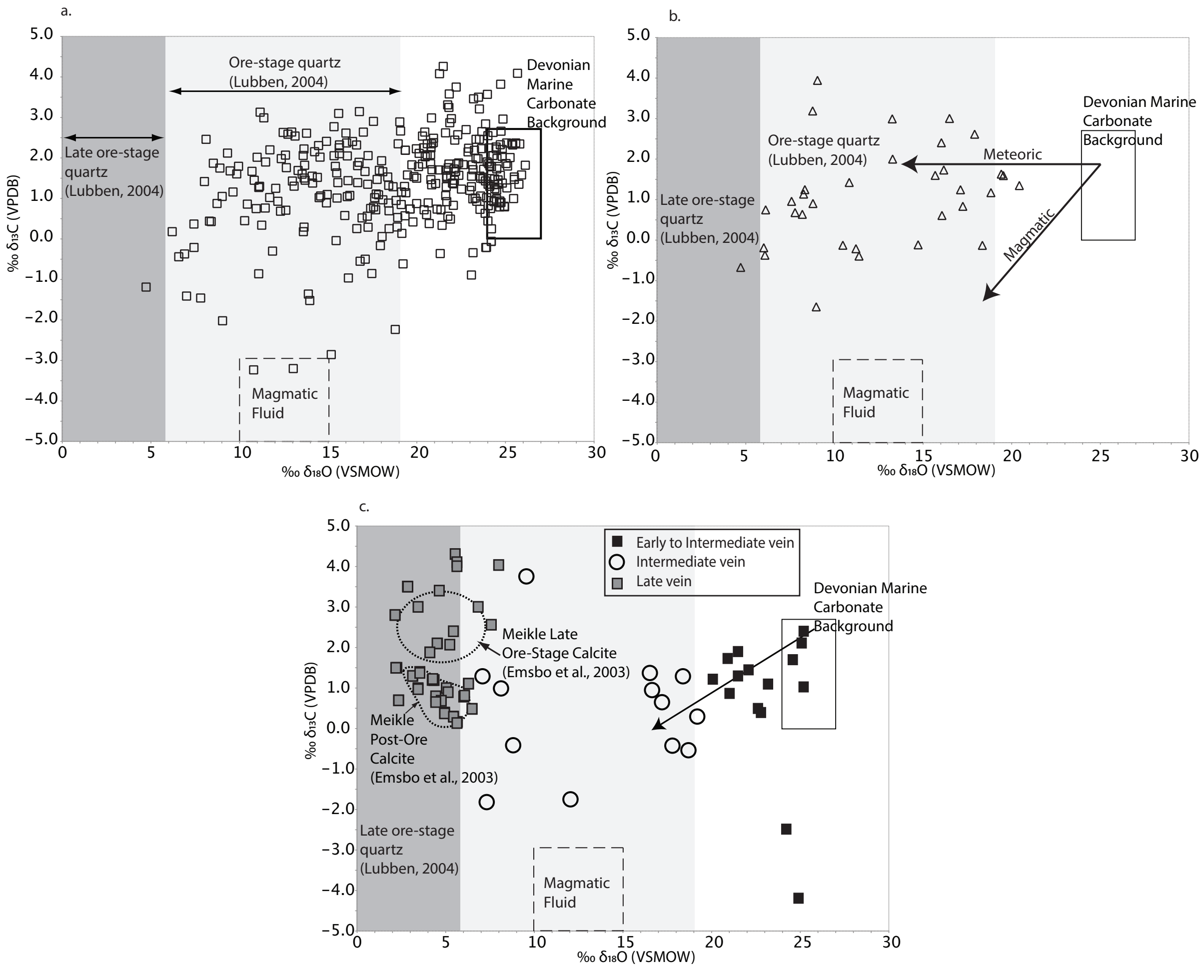

Figure 3.6 a. Covariation plot of rock calcite δ^{18}O (VSMOW) and δ^{13}C (VPDB) values for Silurian-Devonian Bootstrap limestone and Stage 1 breccias. Dark grey field delineates the range of calcite equivalent δ^{18}O values reported by Lubben (2004) for late ore-stage quartz at the Betze-Post Carlin-type Au deposits (calculated at 200°C using the fractionation factor of Kim and O'neil (1997) for δ^{18}O and Ohmoto and Rye (1979) for δ^{13}C). Light grey field delineates the range of calcite equivalent δ^{18}O values reported by Lubben (2004) for ore-stage quartz. Magmatic fluid box is calcite equivalent values from Eiler (2001) calculated at 200°C. Range of Devonian marine carbonate background values from Veizer et al. (1999) and regional background samples from Lone Mountain, NV (Chapter 5 of this thesis). b. Covariation plot of rock calcite δ^{18}O and δ^{13}C for Stage 2 and Stage 3 breccias from Banshee with meteoric and magmatic fluid mixing lines. c. Covariation plot of vein calcite from Banshee. Meikle late ore-stage and post-ore calcite fields are calcite values from Emsbo et al. (2003). Early, intermediate, and late classification of calcite veins determined based on texture, chemistry, isotopes, and cross-cutting relationships.

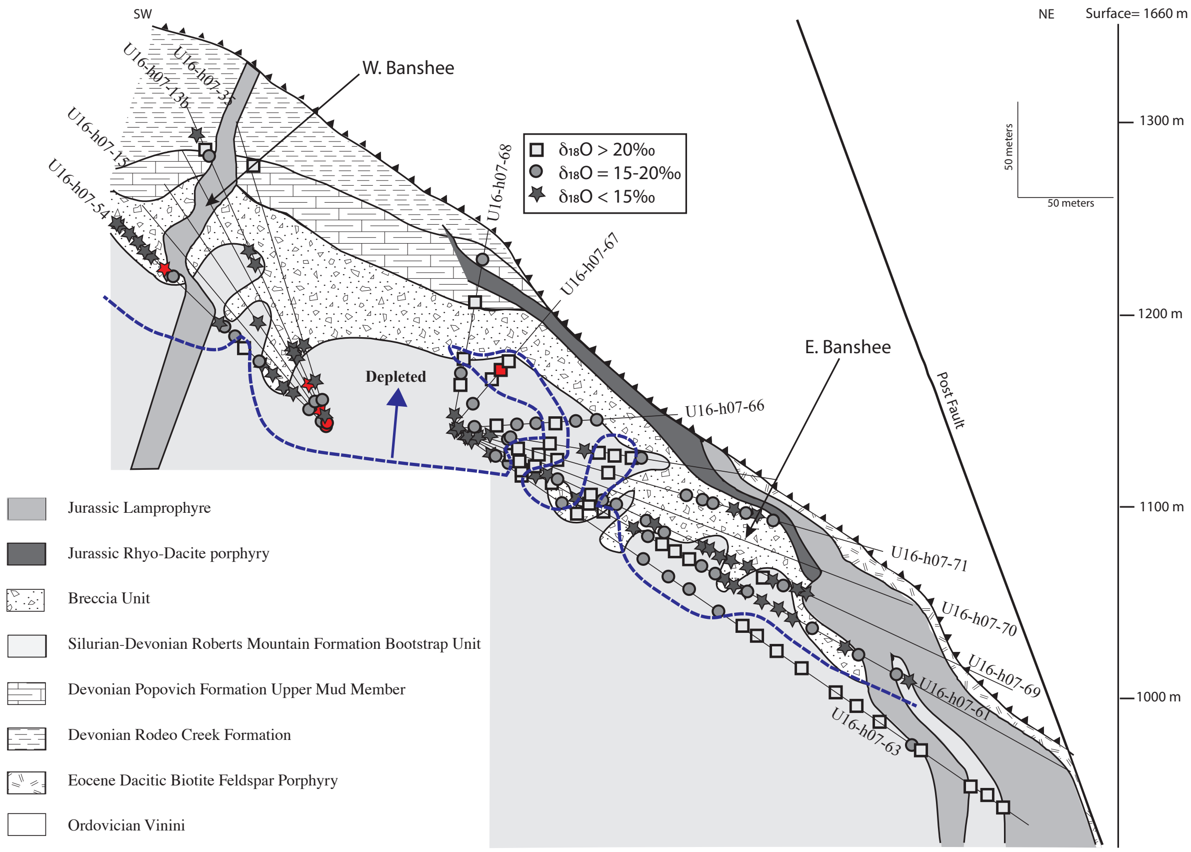

Figure 3.7 Cross-section A-A' of the east and west Banshee zones (See Chapter 2 for detailed description of cross-section and geology of Banshee) showing the distribution of isotope samples and the range of δ^{18}O values. Sample locations in red denote samples used for detailed studies of CL and LA-ICPMS. Note the spatial relationship between degree of δ^{18}O depletion and breccia. Sampling is limited within the breccia unit due to intense carbonate dissolution and silicification. Carbonate dissolution and silicification is diminished outside of the breccia unit. The dashed blue line is the estimated extent of δ^{18}O depletion in wall rock carbonate. In several locations the absolute extent of the depletion halo is not defined by the sampling.

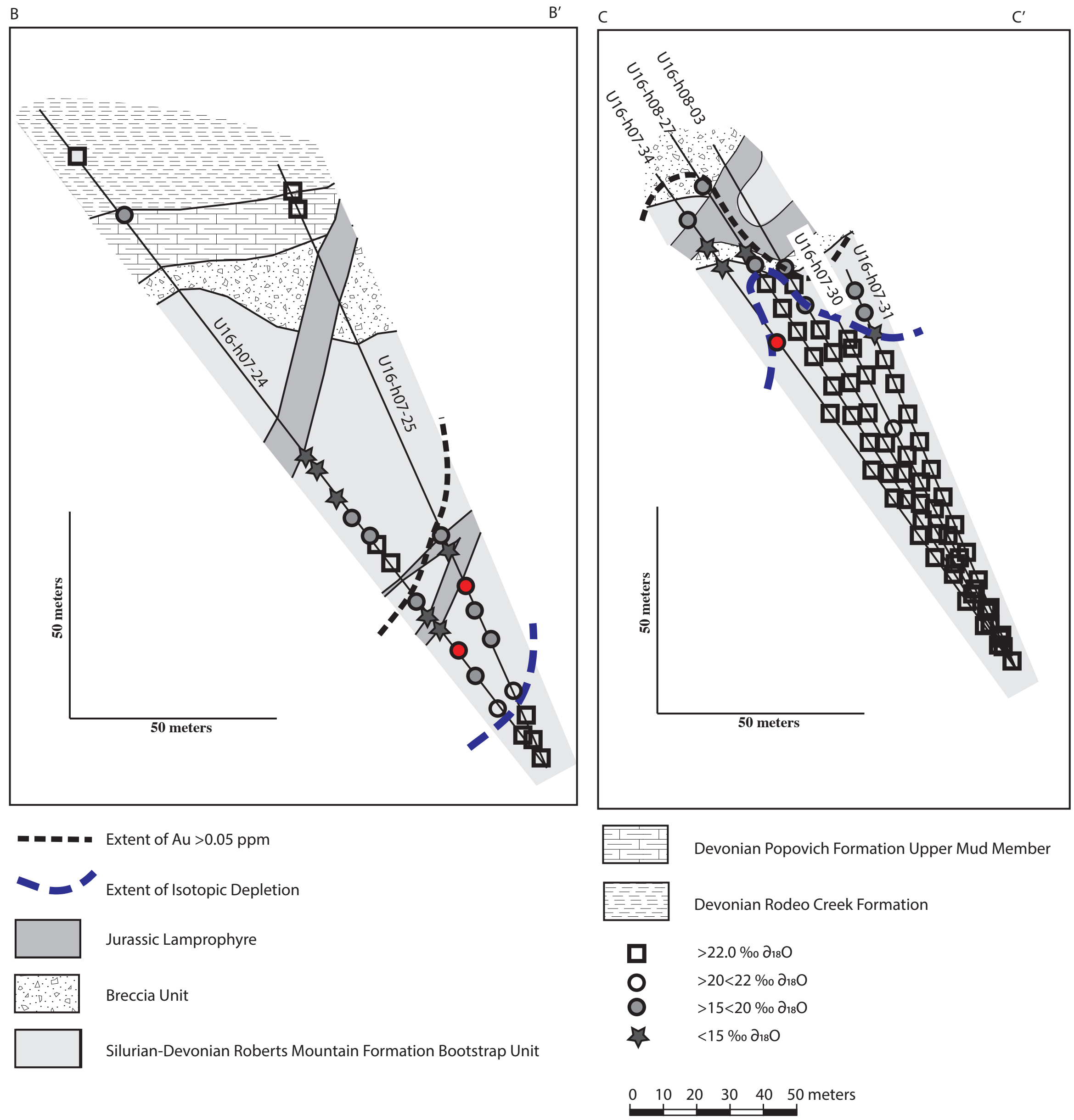

Figure 3.8 Cross-sections B-B' and C-C' in drill fans to the north of the section A-A'. The relative locations of isotopic depletion and anomalous Au are indicated by dashed lines. Sample locations in red denote samples used for detailed studies of CL and LA-ICPMS. Areas of minimal or no sampling represent areas of near complete carbonate dissolution. Stepping to the north the breccia unit thins and $\delta^{18}O$ alteration is less extensive. The northernmost drill fan (C-C') shows that $\delta^{18}O$ alteration and Au enrichment in that part of the deposit is proximal to the mineralized dike. Ore grades in the dike are similar from south to north indicating that fluid flow was channelized and contained to the volume of rock immediately adjacent to the dike. Note the lack of depletion seen in U16-h07-34. The least altered dike sample from Chapter 2 (U16-h07-34-537) came from this drill hole.

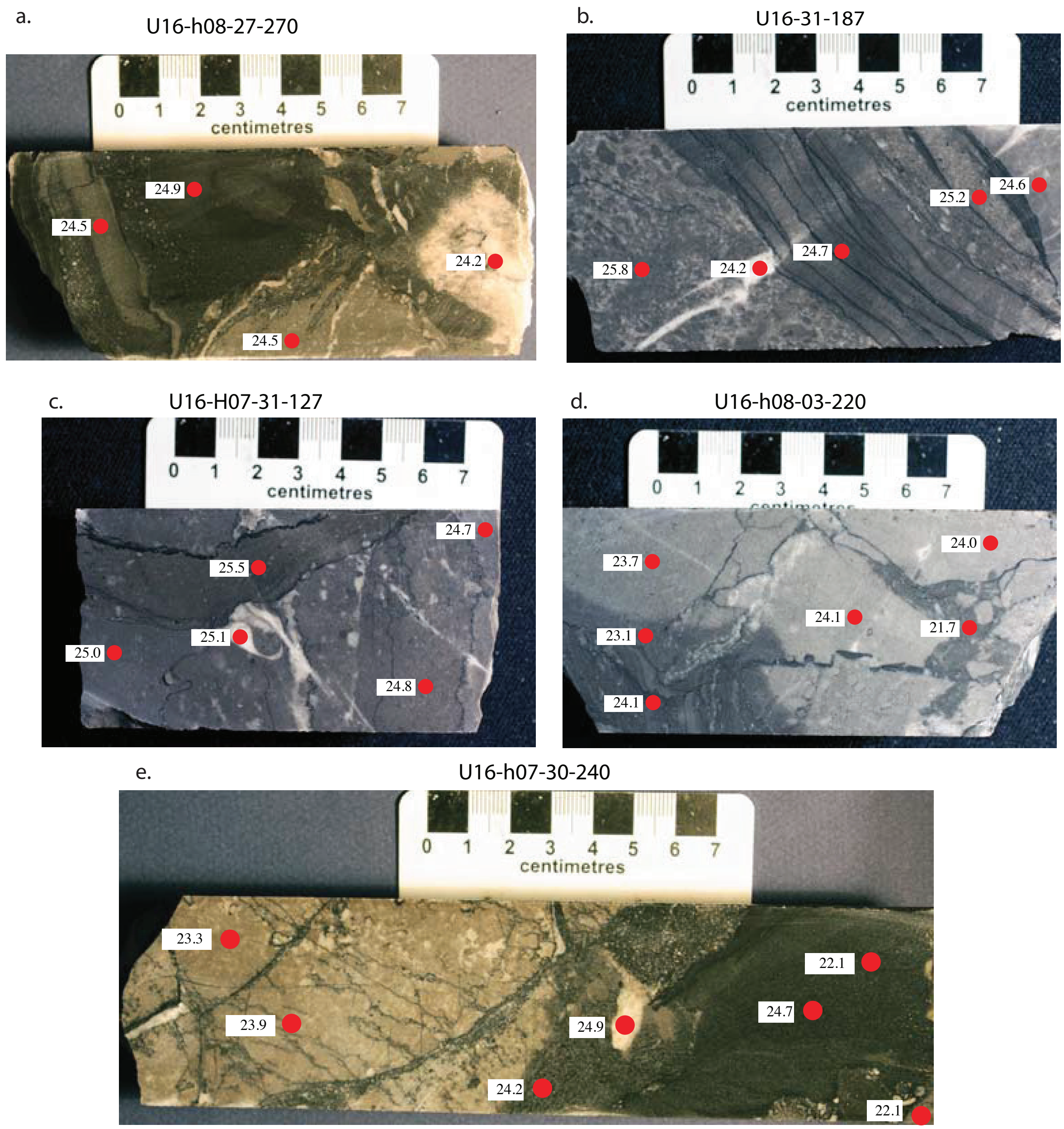

Figure 3.9 a-e. Drilled isotope data ($\delta^{18}O$ ‰) from isotopically unaltered core samples at Banshee from Stage 1 breccias showing $\delta^{18}O$ (VSMOW) values consistent with Silurian-Devonian marine carbonate background values across clasts, matrix, and early calcite veins and coarse calcite.

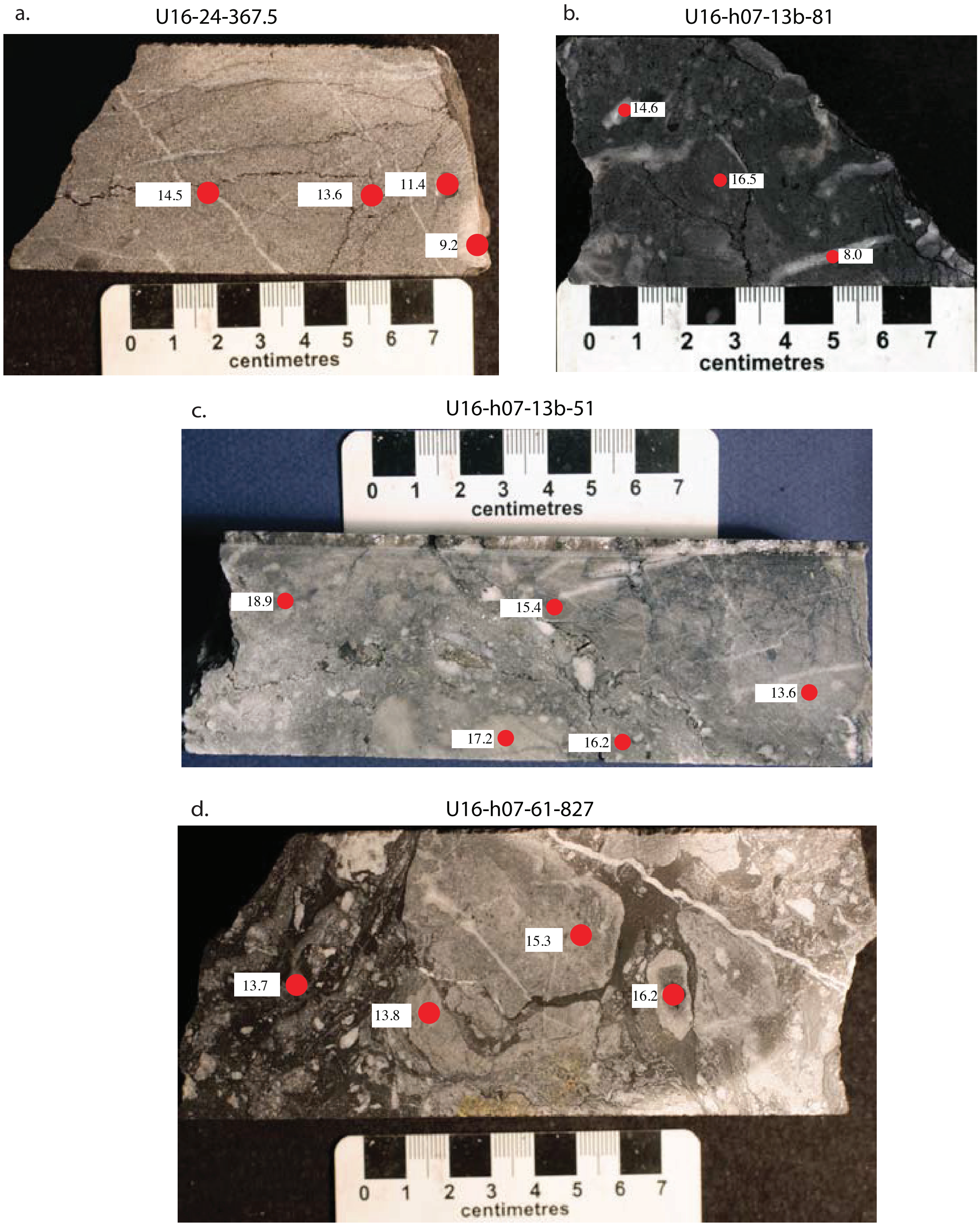

Figure 3.10 a-e. Drilled isotope data ($\delta^{18}O$ ‰) from isotopically altered core samples at Banshee of Stage 1 breccias and Silurian-Devonian Bootstrap limestone showing consistently depleted $\delta^{18}O$ (VSMOW) values in clasts and matrix. The drilled samples also show minimal variation across individual core samples.

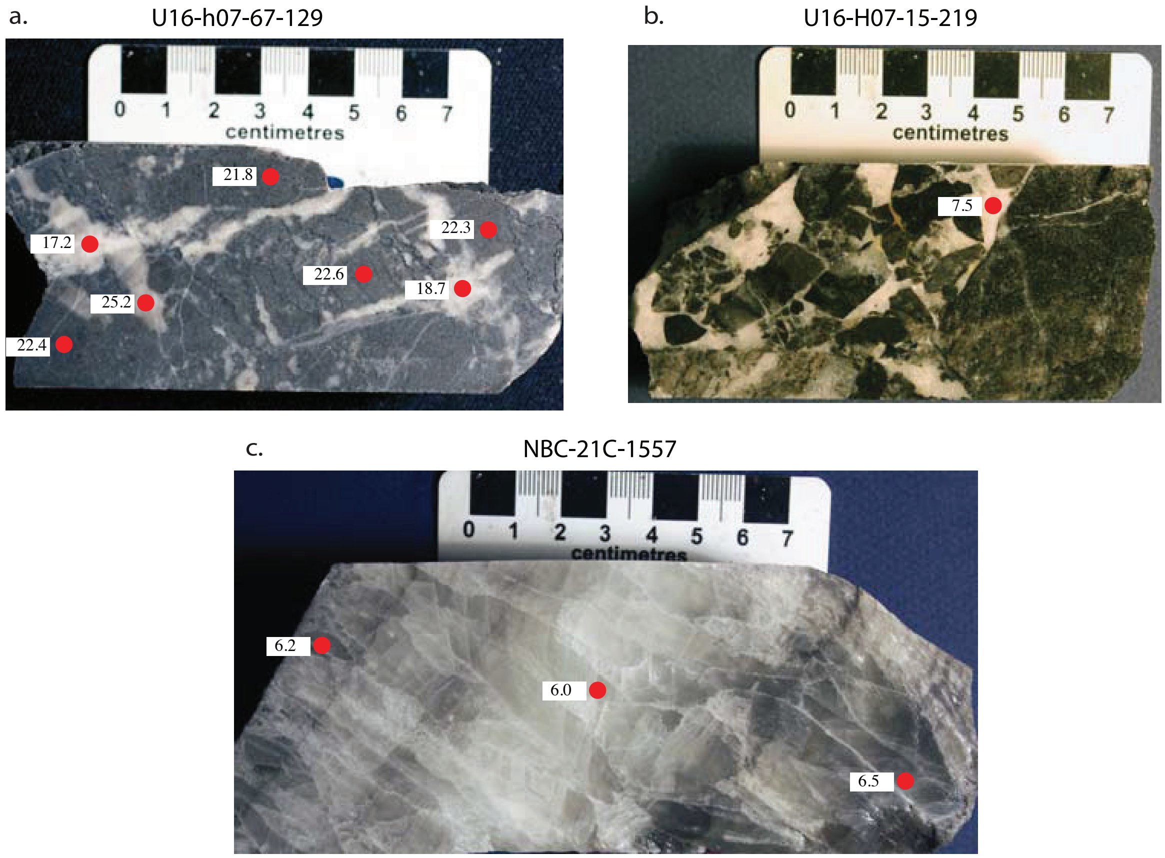

Figure 3.11 a-c. Drilled isotope data ($\delta^{18}O$ ‰) from calcite veins with $\delta^{18}O$ values depleted relative to Silurian-Devonian marine carbonate background values. a.) Core sample shows two distinct generations of calcite veining. The dark vein has $\delta^{18}O$ values consistent with background calcite values while the overprinting lighter calcite vein is depleted relative to background. Rock calcite has values in between the two vein sets indicating disequilibrium between vein and wall rock calcite. b.) Core sample of Stage 3 breccia shows post-mineral coarse calcite cement overprinting silicified breccia with isotopically light $\delta^{18}O$. c.) Sample of coarse calcite lining cavity associated with Stage 4 brecciation with consistent isotopically light $\delta^{18}O$ values.

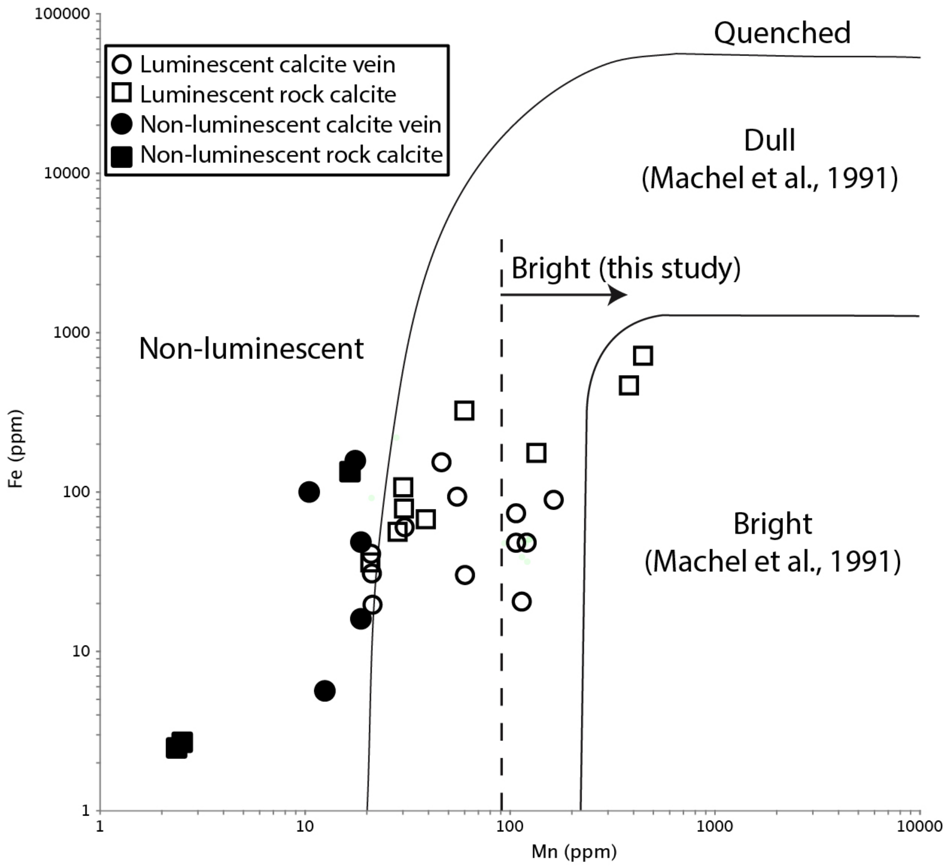

Figure 3.12 Fe versus Mn scatter plot of LA-ICPMS data for rock calcite and vein calcite from Banshee. Square symbols represent rock calcite and circles represent vein calcite. Filled symbols are non-luminescent and open symbols are variably luminescent. Theoretical fields for non-luminescent, dull, and bright CL response are taken from Machel et al. (1991). Dashed line represents the threshold value of Mn associated with bright CL response in this study. Both rock calcite and vein calcite are consistent with theoretical thresholds for CL response. Figure modified from Machel et al. (1991) and Savard et al. (1995).

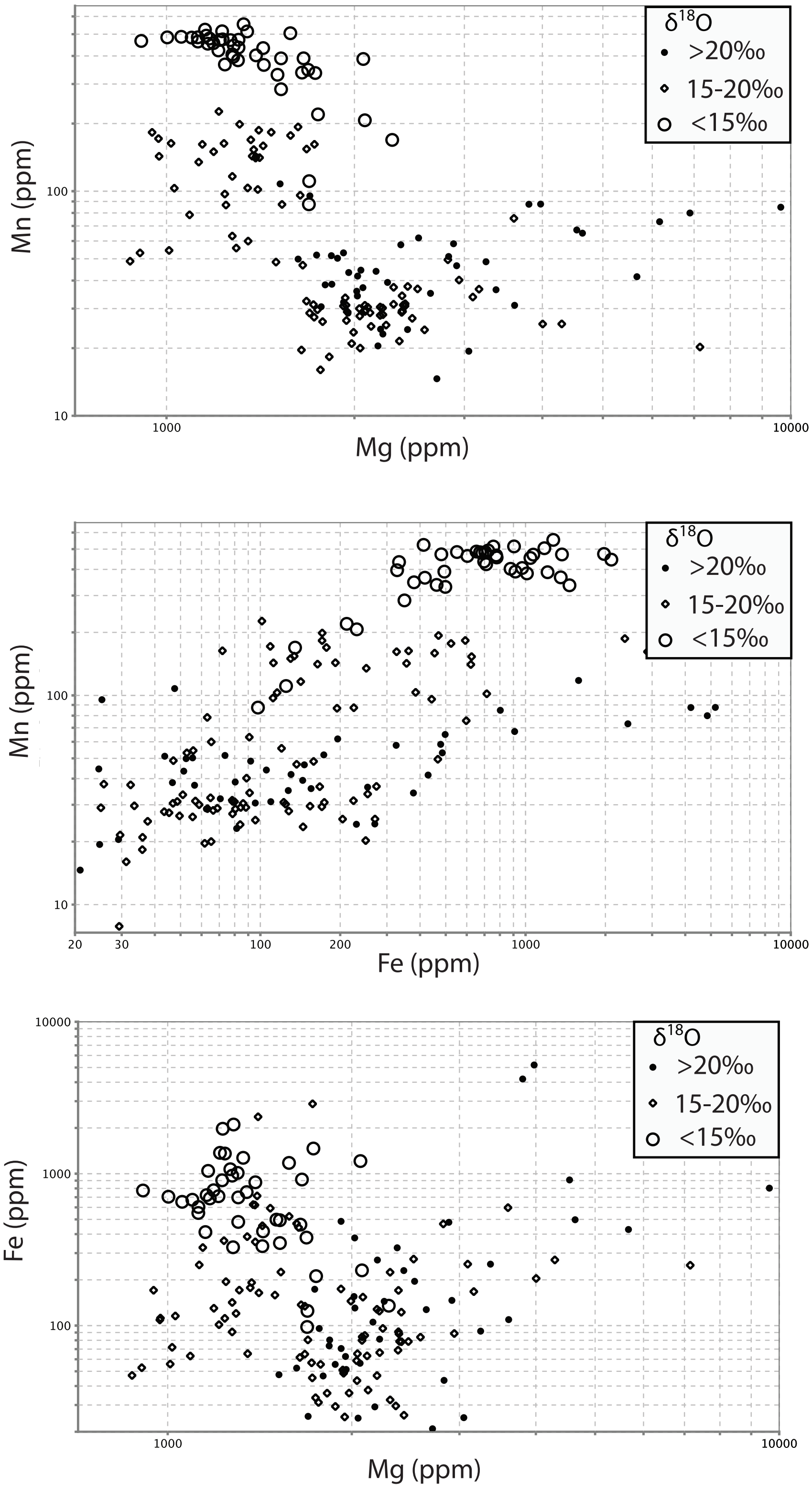

Figure 3.13 Plots of LA-ICPMS data from wall rock calcite showing the relationship between relative changes in Mn, Fe, and Mg at variable $\delta^{18}O$.

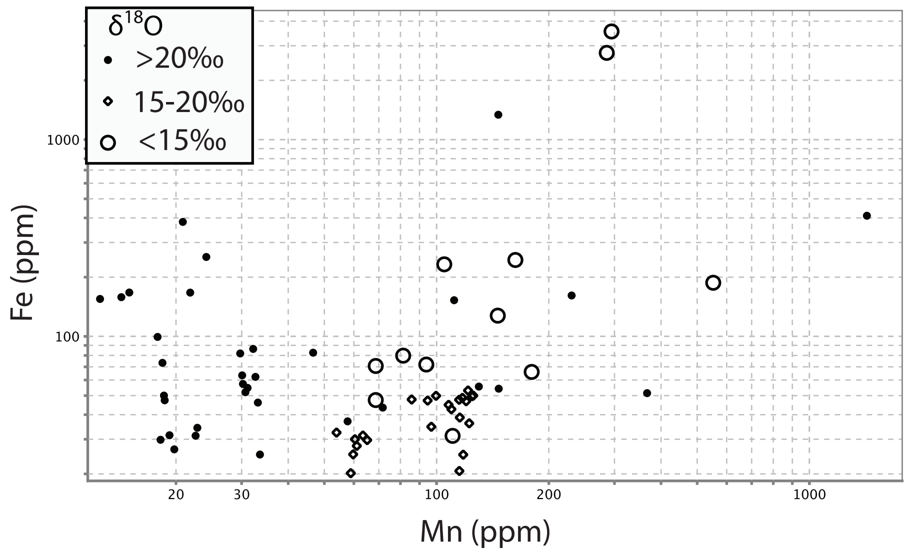

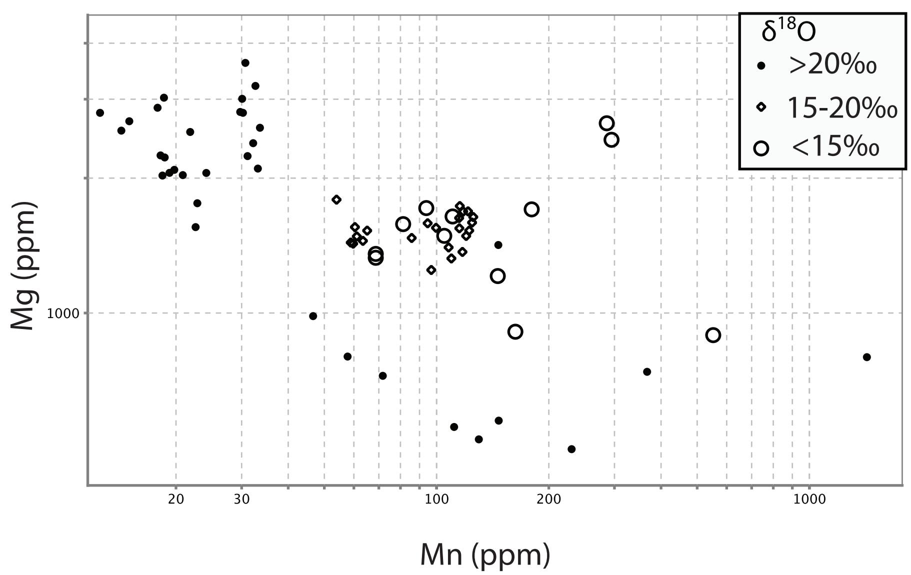

Figure 3.14 Plots of LA-ICPMS data from calcite veins showing the relationship between Fe, Mg, and $\delta^{18}O$.

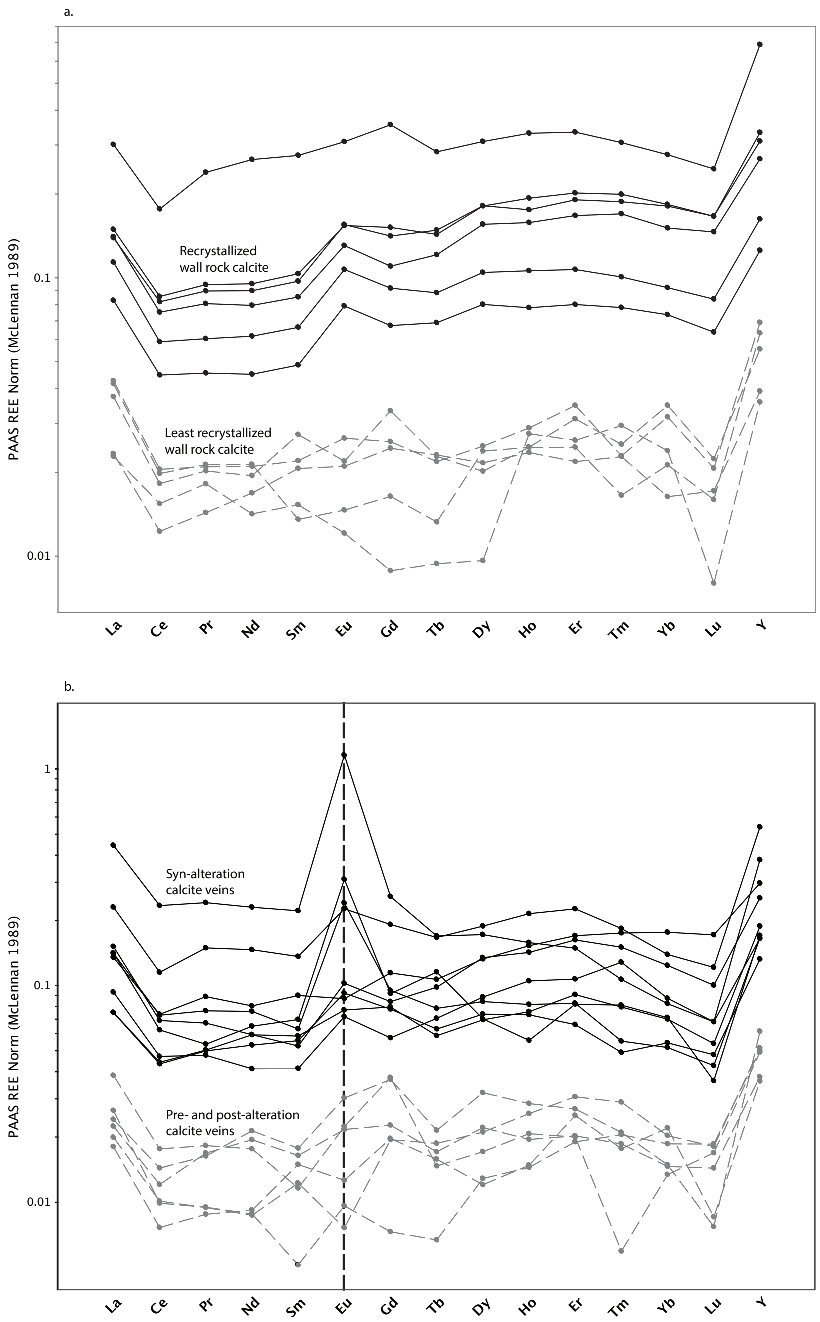

Figure 3.15 REE spider plot of LA-ICPMS data (data points represent median values from multiple analyses of individual veins and cements) normalized to Post Archean Australian Shale (PAAS) (McLennan, 1989). (a) Wall rock calcite analyses from recrystallized wall rock (solid lines) and least recrystallized wall rock (dashed lines). (b) Solid lines represent samples from intermediate calcite veins and dashed lines represent both early and late veins. Note the positive Eu anomaly associated with most of the intermediate veins. REE concentrations are consistently higher in intermediate vein calcite.

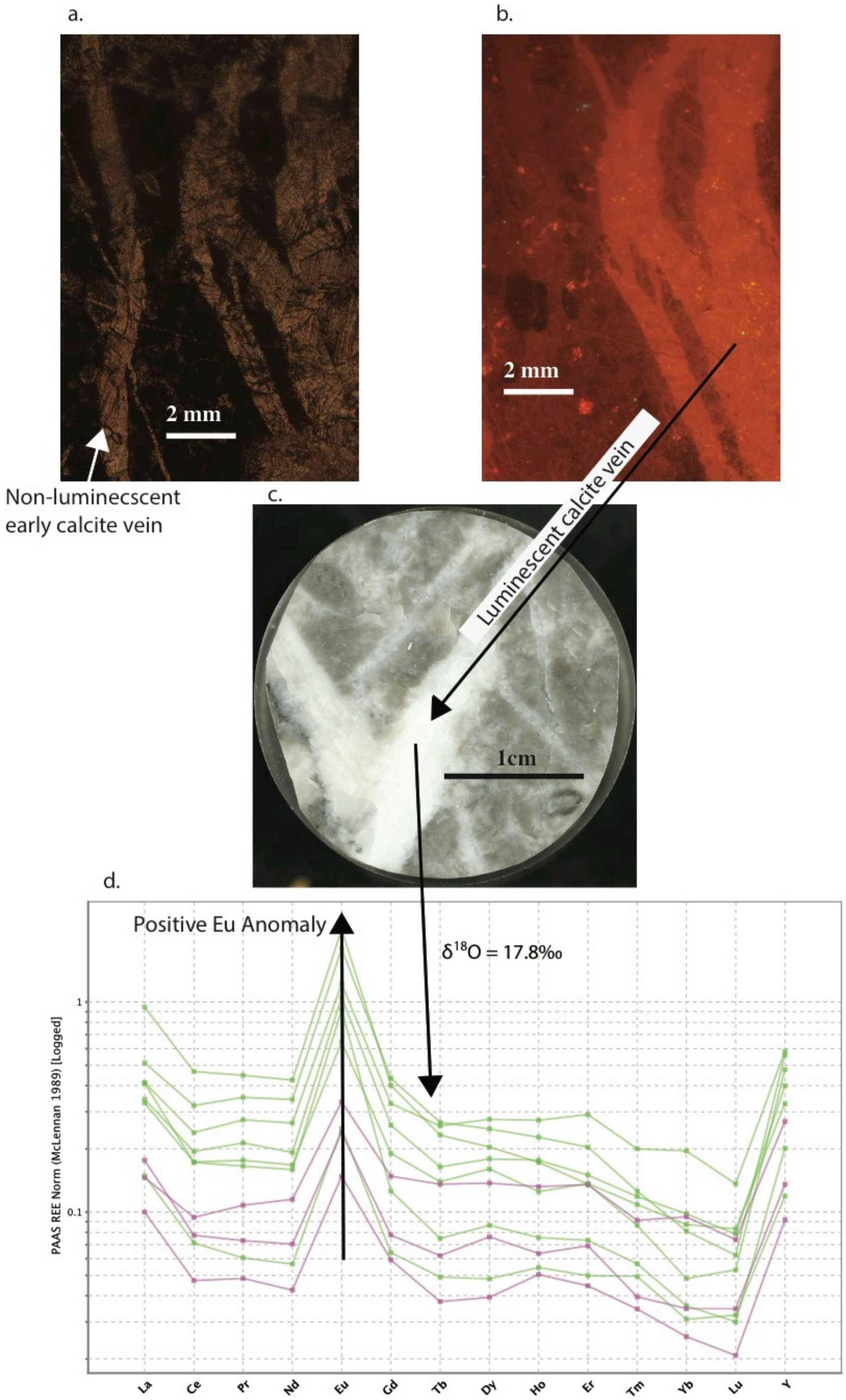

Figure 3.16 Synthesis diagram of (a) transmitted light photomicrograph, (b) CL photomicrograph, (c) polished block, and (d) LA-ICPMS REE data from sample U16-h07-13b-11 illustrates the relationship between the three datasets. The example is an intermediate calcite vein with characteristic orange CL response, depleted $\delta^{18}O$ relative to wall rock, and strong Eu anomaly.

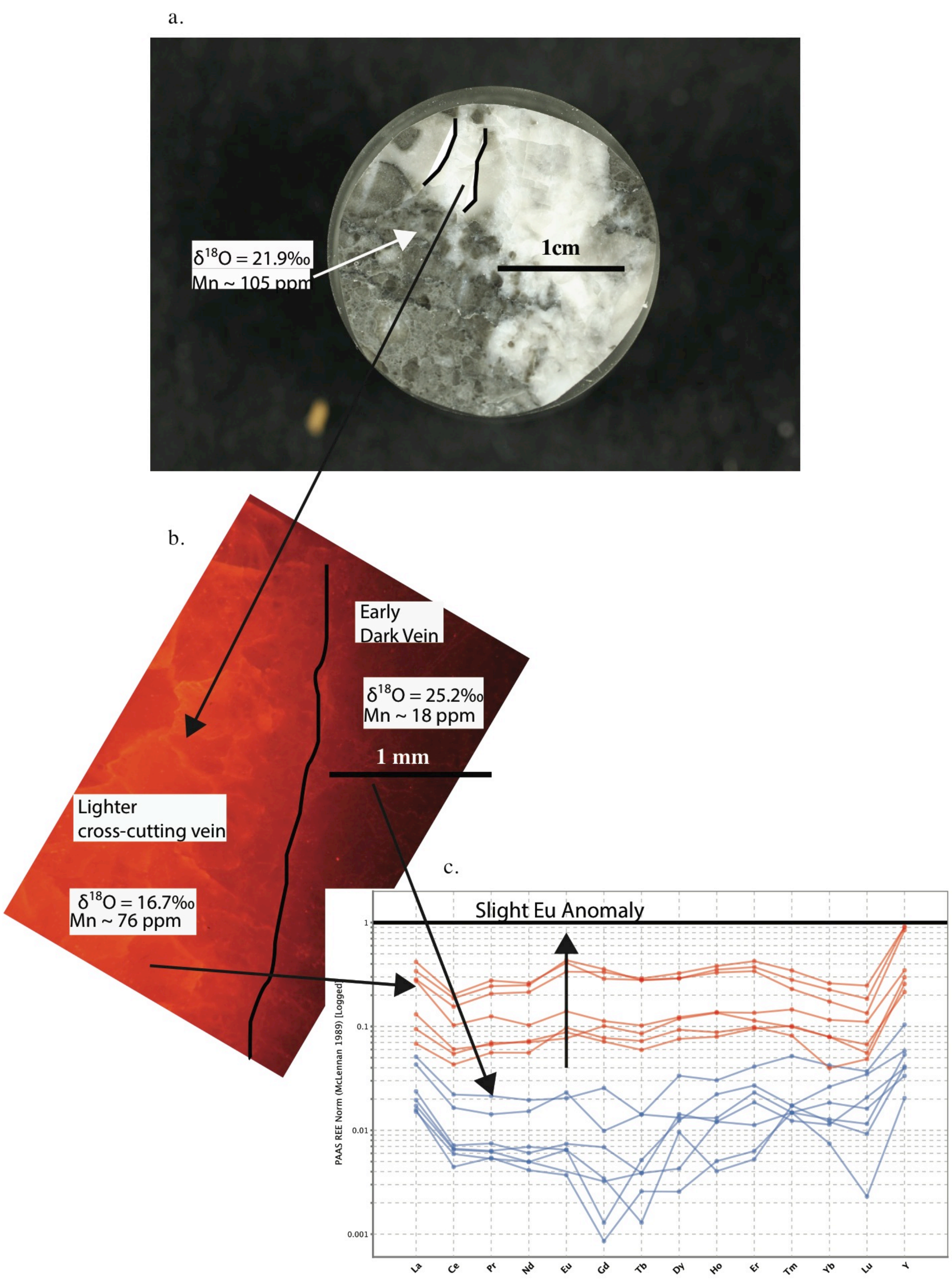

Figure 3.17 Synthesis diagram of (a) polished block, (b) CL, isotope, and (c) LA-ICPMS REE data from sample U16-h07-67-129 illustrates the relationship between the three datasets. This example shows a intermediate calcite vein cutting an early vein. The intermediate vein is depleted in $\delta^{18}O$ relative to the early vein and wall rock, has a characteristic bright orange CL texture and has elevated REEs relative to the early vein. This sample exhibits a weak Eu anomaly.

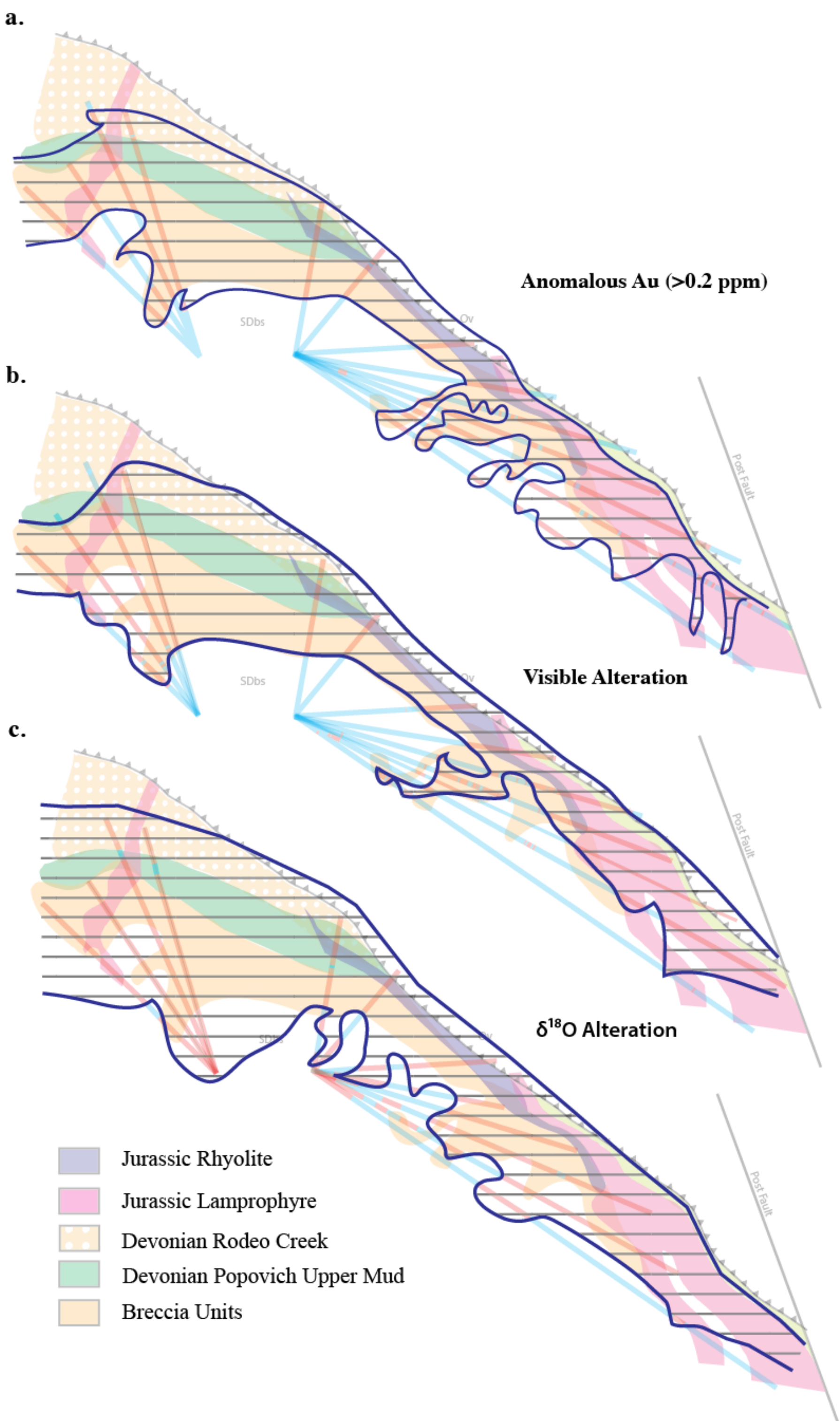

Figure 3.18 Cross-section A-A' (Figure 3.1) with overlays that show the extent of (a)Au >0.2 ppm, (b) visible alteration (including silicification, clay alteration, and carbonate dissolution), and (c)δ^{18}O isotope depletion. The δ^{18}O isotopic depletion halo is a minimum extent as drilling has not defined the extent below the west Banshee drill fan.

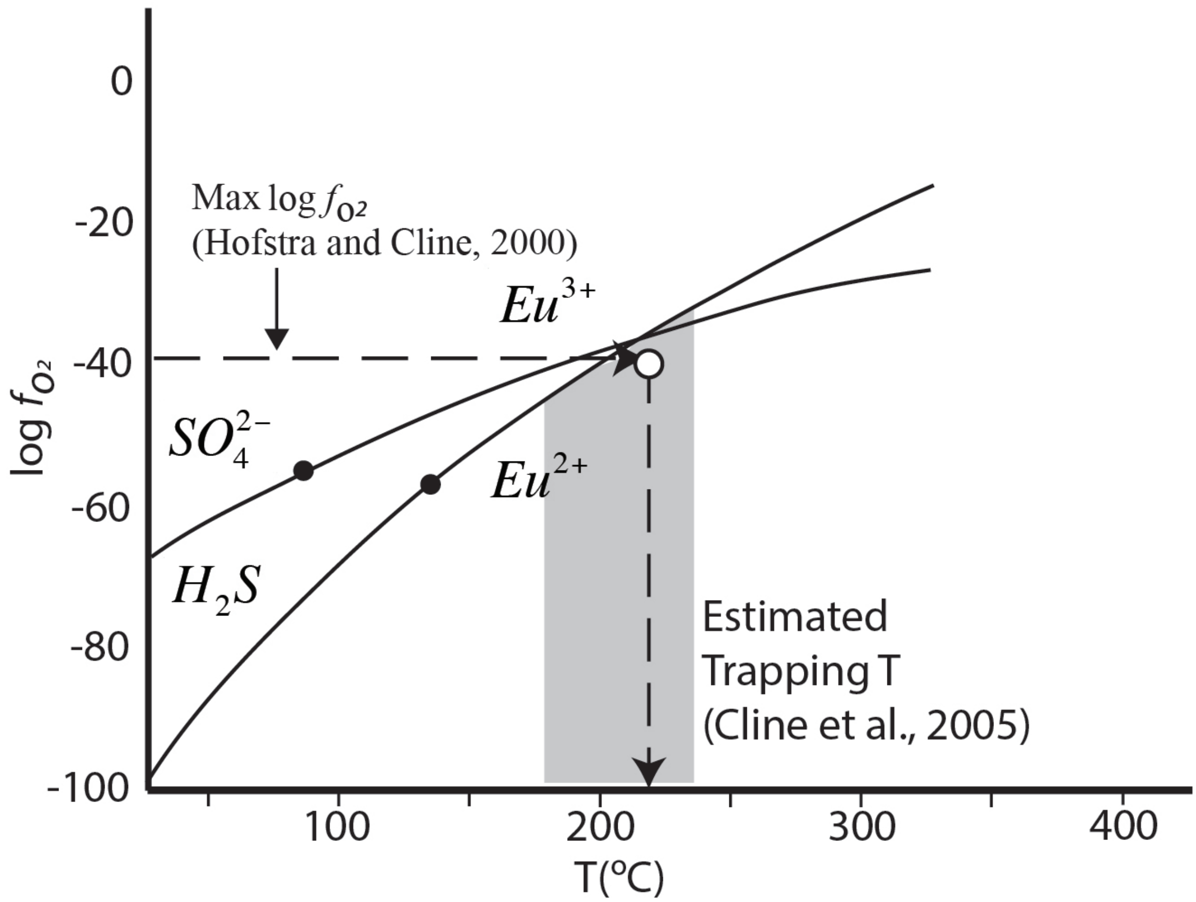

Figure 3.19 Modified from Bau and Moller (1992). Redox equilibria for Eu and Yb as a function of log f_{O2} and temperature at pH=3. Eu^{3+}/Eu^{2+} and SO_4^{2-}/H_2S equilibria calculated at 0.5 kbar. Open circle is the estimated conditions of main ore stage fluids in Carlin-type systems based on mineral assemblages and fluid inclusion data. Dashed lines show the log f_{O2} and temperature conditions of main ore stage fluids.

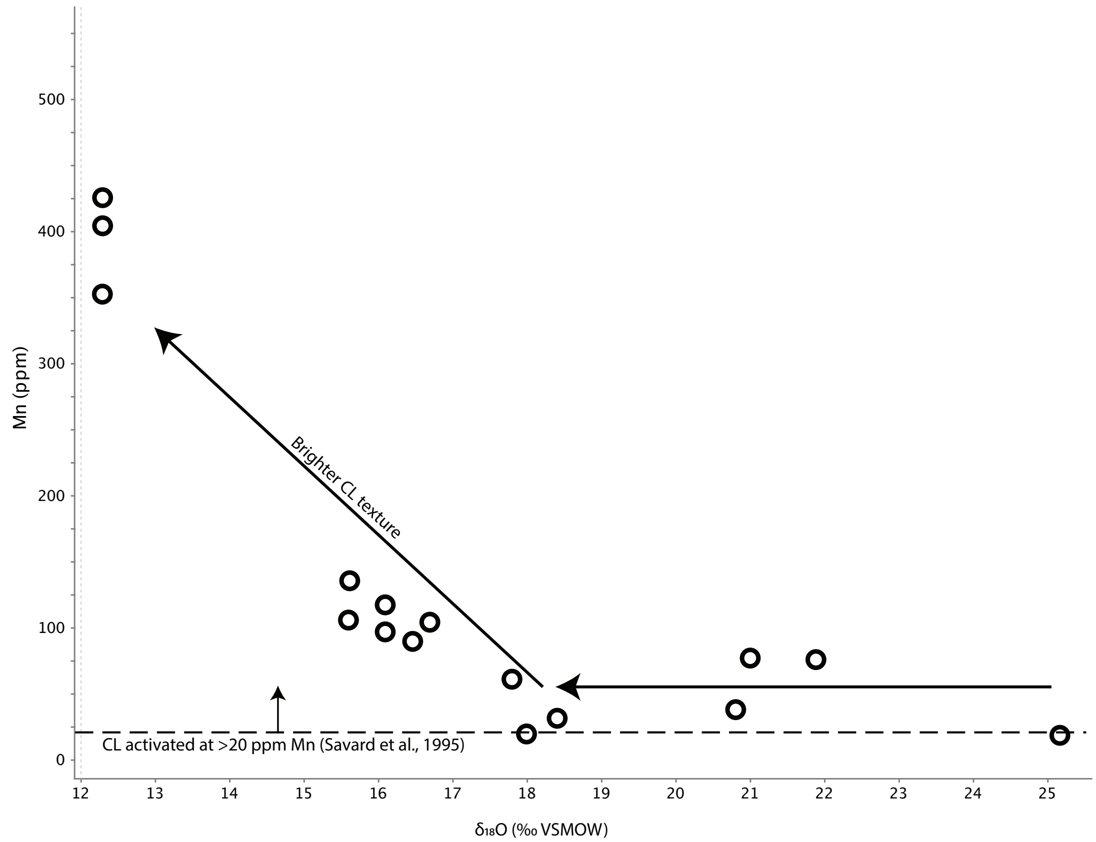

Figure 3.20 Scatter plot of Mn versus $\delta^{18}O$ from rock calcite samples shows a trend of increasing Mn with decreasing $\delta^{18}O$ values less than ~18‰ (VSMOW) indicating brighter CL response is associated with depletion of $\delta^{18}O$. Dashed line indicates the threshold value for CL response as determined by Savard et al. (1995).

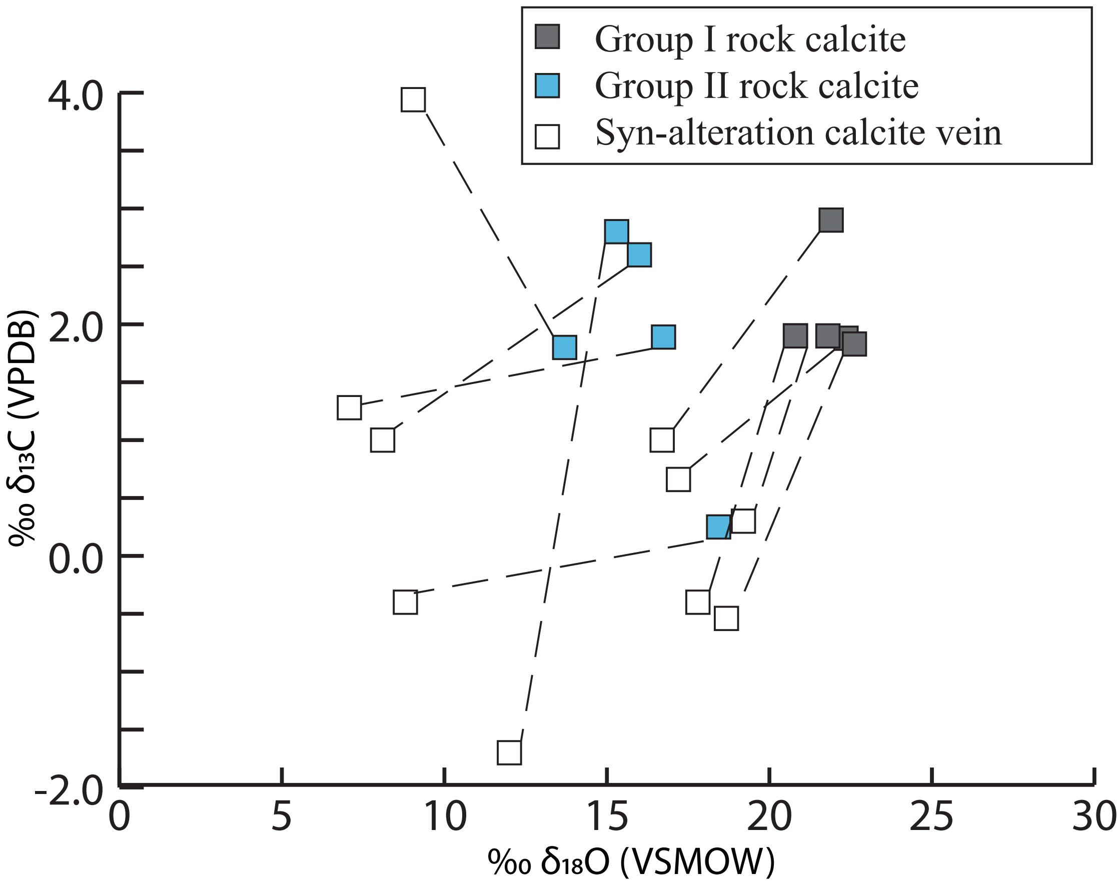

Figure 3.21 Covariation plot of $\delta^{13}C$ versus $\delta^{18}O$ from wall rock calcite and interpreted syn-alteration vein calcite pairs from Banshee illustrating the difference in $\delta^{18}O$ values between the vein-rock pairs. Filled squares are rock calcite samples and open squares are vein calcite samples. Dashed lines connect vein-rock pairs for individual samples.

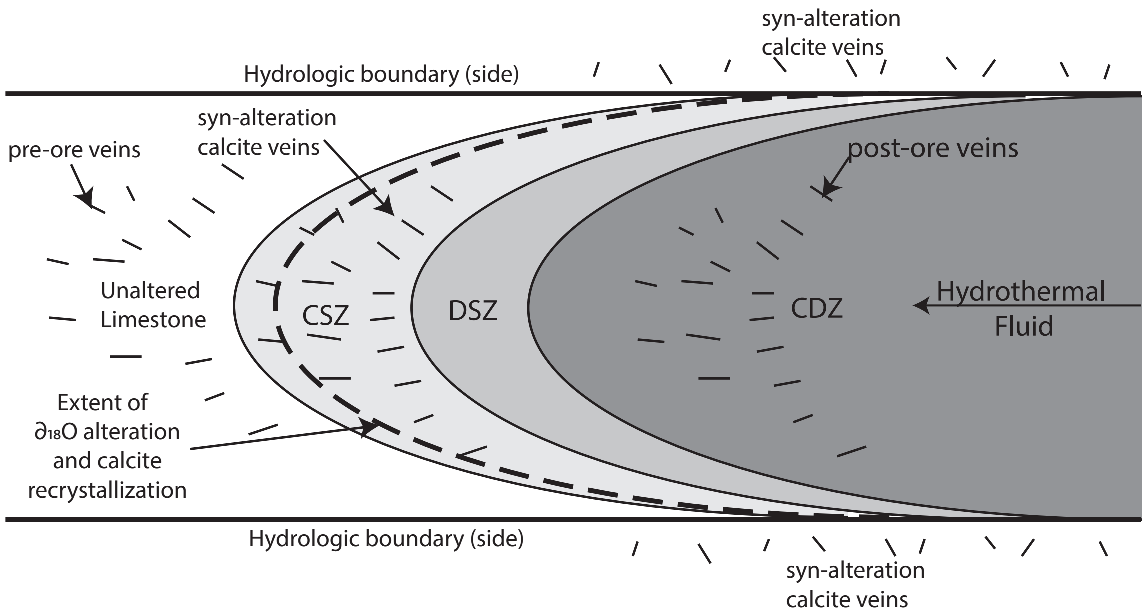

Figure 3.22 Conceptual model of carbonate-hosted hydrothermal alteration associated with Carlin-type Au systems of northeast Nevada. CDZ refers to carbonate dissolution zone where all near complete dissolution of carbonate mineral occurs. DSZ is the dolomite stable zone where calcite is dissolved but dolomite is stable due to pH buffering along the flow path. CSZ refers to the calcite stable zone where dissolution of calcite does not occur although calcite recrystallization does occur as indicated by CL textures, trace elements, and isotope data.

Table 3.1 Summary breccia units found at Banshee breccia.

Breccia Facies	Internal Organization	Clast shape and type	Matrix/Cement	Alteration	Intepreted Origin
Stage 1	Monomict, clast- to matrix-supported breccia; some cave fill sedimentation	Shape: angular Type: SDbs and calcite vein fragments	Clay- to silt-sized carbonaceous residuum	Generally visibly unaltered except when overprinted by later breccias	Paleokarsting and collapse brecciation
Stage 2	Polymict, clast- to matrix-supported breccia	Shape: angular to sub-rounded Type: SDbs, Stage 1 breccia, Jla, Jmp, Dp UM, Ov, and Drc	Dark clay- to silt-sized carbonaceous matrix	Silicified, decalcified, dike clasts clay altered, pyritized	Faulting and hydrothermal dissolution
Stage 3	Polymict, calcite cemented breccia	Shape: angular to sub-rounded Type: SDbs, Stage 1 breccia, Stage 2 breccia	Coarse calcite cement	Silicified, decalcified, pyritized	Faulting
Stage 4	Polymict, carbonaceous matrix-supported breccia	Shape: angular, to sub-angular Type: variable	Unconsolidated to partially consolidated mud- to silt-sized pyrite rich carbonaceous residuum	Partially decalcified, kaolinite altered dike clasts	Post-ore dissolution by low temperature (~65°C) (Emsbo and Hofstra, 2003) fluids

Chapter 4 : Estimating Time Integrated Fluid Flux (TIFF) and Defining Fluid Pathways Using $\delta^{18}O$ Isotopes in Vein-Rock Pairs

An understanding of fluid flux and associated flow pathways is integral to the development of fluid flow models for hydrothermal systems. If the fluid flux of a flow system can be estimated, it can help put constraints on the time and length scale of fluid flow, which in turn may provide insight into the nature of the flow system (e.g. pulsed versus continuous flow), the source of fluids, and potential driving forces (e.g. convection or overpressuring). Metamorphic systems have been the focus of many investigations into the determination of integrated fluid fluxes associated with reactive hydrothermal fluid flow. Early approaches at estimating fluid volumes associated with hydrothermal fluid used water:rock ratios calculated from zero-dimensional closed (Clayton et al., 1968) and open (Nabelek, 1987; Taylor, 1977) box reactor models (Taylor, 1997). A one-dimensional solution of the box model with compartmentalized incremental batch flow was presented by Spooner et al. (1977). Box reactor models of mass conservation seek to estimate minimum water:rock mass ratios for hydrothermal fluid systems (Bowman *et al*., 1994). These zero-dimensional and one-dimensional models are generally used in association with oxygen isotopes to determine the degree and extent of water-rock interaction. However, box reactor models have limitations. Box reactor models assume complete equilibration. If complete equilibration fails to occur, calculated W/R values will be underestimated (Taylor, 1971). Additionally, box reactor models cannot properly account for alteration products at high integrated fluid fluxes where integrated fluid/rock ratios are >1 as the amount of fluid exceeds the relative porosity volume of a rock (Heinrich et al., 1996). Another limitation is that box reactor models will incorrectly estimate the degree of fluid infiltration at specific sites within flow systems because box models do not account for the progressive modification of the fluid along the flow path (Bowman *et al*., 1994). Analytical and numerical transport modeling provides a more robust framework for investigating fluid rock interaction both spatially and temporally (Bowman *et al*., 1994). Using transport theory, analytical and numerical models can be applied to determine the cumulative effects of fluid-rock exchange of chemical components between an infiltrating fluid and the wall rock over a variety of length scales (Bowman *et al*., 1994).

The degree of isotopic resetting derived from fluid-rock interaction observed in the rock record may be a consequence of either equilibrium or non-equilibrium (i.e. kinetic) exchange (Blattner and Lassey, 1990; Bowman and Willett, 1991; Bowman et al., 1994; Lassey and Blattner, 1988). When modeling reactive transport of chemical components through porous media, the relative influence of equilibrium and kinetic effects should be defined when possible. As shown in Chapter 3, oxygen stable isotopes in calcite can be a tool for defining fluid-rock interaction related to a hydrothermal system, but additional steps are required to use oxygen isotope data for evaluating the fluid fluxes associated with observed $\delta^{18}O$ alteration and distinguishing between multiple fluid pathways. Recent studies have used non-equilibrium oxygen isotope exchange between rock-vein calcite pairs with reactive path modeling to investigate kinetically controlled isotope exchange processes, integrated fluid fluxes, and the reactive path length of regional fluid flow systems (Cox, 2007; Knoop et al., 2002). The recognition of syn-alteration calcite veins in disequilibrium with wall rock calcite at the Banshee Carlin-type Au deposit (Chapter 3) provides an opportunity to investigate kinetically controlled oxygen isotope exchange that occurred during the evolution of a Carlin-type hydrothermal system. The goal of this chapter is to investigate the relationship between permeability, integrated fluid flux, and fluid flow path lengths at the Banshee Au deposit using results from reactive transport modeling.

Using paired vein-rock isotope data from Banshee, 1-dimensional reactive transport modeling allows for estimates of integrated fluid fluxes associated with individual fluid pathways at specific reactive path lengths. Reactive transport modeling of these data allows for the estimation of time integrated fluid flux (TIFF) for fluid pathways at specified length scales. Alternatively, the length scales can be estimated for specified TIFFs. The results of this study provide a framework for evaluating integrated fluid fluxes between various hydrothermal and metamorphic systems, and document a method for estimating TIFF in low temperature hydrothermal systems using reactive transport modeling of $\delta^{18}O$ isotope from calcite rock-vein pairs.

4.1 $\delta^{13}C$ and $\delta^{18}O$ Isotopes in Syn-alteration Calcite Veins and Rock Calcite at Banshee

In order to perform reactive transport modeling between rock-vein pairs, the paragenesis of syn-alteration veins must be genetically tied to alteration of wall rock calcite. Chapter 3 details the distinct nature of syn-alteration veining at Banshee. The recognition of syn-alteration veins allows for further investigation of fluid-rock isotopic exchange processes. Chapter 3 presented $\delta^{18}O$ and $\delta^{13}C$ stable isotope data from rock calcite and vein calcite for the Carlin-type Banshee Au deposit. In this chapter, oxygen isotope data from the syn-alteration veins are compared to rock calcite collected from the same sample. A combination of isotopic analysis, CL textures, and LA-ICPMS data defined at least 12 syn-alteration veins at Banshee and 10 of those samples had data from adjacent wall rock calcite (see Chapter 3 for more detail). The 10 vein-rock alteration pairs were selected for use in this chapter to investigate kinetic dispersion and perform 1-dimensional reactive transport modeling. Seven samples are from the main A-A' section though the deposit (Figure 4.1), one sample was collected from the B-B' drill fan and two samples were collected from the C-C' drill fan (Figure 4.2). The samples cluster into two groups based on $\delta^{18}O$ depletion in rock calcite. Samples from Group I are rocks with minimally depleted $\delta^{18}O$ values in rock carbonate. Samples from Group II are rocks with significant $\delta^{18}O$ depletion in rock carbonate. Group I samples are from visibly unaltered limestone of the Silurian Devonian Bootstrap limestone. Group II samples are from Stage 1 breccia and Bootstrap Limestone with minimal visible alteration. Group II samples were collected within the zone of consistently depleted $\delta^{18}O$ from east and west Banshee, and have wall rock $\delta i^{18}O$ values ranging from 13.7 to 18.4‰ (VSMOW) in rock calcite and values of 7.1 to 12 ‰ in vein calcite (Table 4.1). The lack of wall rock calcite and syn-alteration calcite veins within the carbonate dissolution zone precludes sampling nearer to gold mineralization. Group I samples have $\delta^{18}O$ values in rock calcite ranging from 20.8 to 22.6‰ and vein calcite $\delta^{18}O$ values of 16.7 to 19.2‰ (Table 4.1). The syn-alteration veins have consistently lower $\delta^{18}O$ values relative to wall rock indicating non-equilibrium (i.e. kinetic) isotopic exchange between the rock and the fluid (Figure 4.3). The difference between rock and vein $\delta^{18}O$ values ($\Delta_{rock\text{-}vein}$) in Group II samples is 3 to 9 ‰, and the $\Delta_{rock\text{-}vein}$ for Group II samples is 3 to

5 ‰. A majority of the samples show $\delta^{13}C$ depletion between rock calcite and vein calcite as well. Group I samples have vein $\delta^{13}C_{rock\text{-}vein}$ = 1 to 2.5 ‰. Group II samples have a less consistent pattern. Three Group II samples show slight to moderate depletion in $\delta^{13}C$ values between rock and vein of 0.5 to 1.5 ‰, one sample shows more significant depletion of 4.5 ‰, and one sample shows $\delta^{13}C$ enrichment of 2.3 ‰ in vein calcite relative to rock calcite. The variability in $\Delta^{13}C_{rock\text{-}vein}$ values is likely owing to the variability of $\delta^{13}C$ in primary marine carbonate as $\delta^{13}C$ is likely locally derived from surrounding wall rocks.

4.2 Reactive Path Modeling

Reactive transport modeling of heat and mass can be used to investigate the cumulative effects of fluid flow and fluid-rock interaction to the isotopic evolution of a fluid and rock (Bickle and McKenzie, 1987; Cathles, 1983; Blattner and Lassey, 1989; Lassey and Blattner, 1988; Bowman and Willett, 1991; Bowman *et al.*, 1994; Heinrich *et al.*, 1996). In some high temperature regimes, equilibrium exchange may occur between rock and fluid. However, in lower temperature systems like Banshee exchange reactions between fluid and rock are more likely to be rate limited (Cole and Chakraborty, 2001). The variation between rock calcite and vein calcite indicates that isotope exchange may not have been in equilibrium. The change in $\delta^{18}O$ values in wall rock calcite depends on the position in the fluid flow path, the rate of exchange (kinetically controlled) with the fluid, and the time integrated fluid flux (TIFF) (Bowman and Willett, 1991) (see Figure 4.4). The rate of isotopic exchange is controlled by the rate of surface reaction when dissolution-precipitation reactions are the dominant exchange mechanism (Bowman et al., 1994). Vein calcite at Banshee is assumed to have precipitated in equilibrium with the fluid and thus is a proxy for $\delta^{18}O_{fluid}$ at any one point on the fluid flow path within the hydrothermal system. The variance between vein and rock calcite values can be used to constrain reactive transport models to a narrow range of kinetic conditions (Knoop et al., 2002). The rate of surface reaction for calcite was sufficient to preserve calcite textures in wall rocks at Banshee, but may not have been sufficient for equilibrium to be attained between the fluid and the wall rock. At high temperatures (>600°C) equilibrium fractionation for the calcite-water system can be assumed for $\delta^{18}O$ (Clayton et al., 1989), but low temperature experiments have shown that non-equilibrium conditions do occur for $\delta^{18}O$ in the calcite-water system (Kim and Oneil, 1997). The controls on non-equilibrium exchange have not investigated at the temperature range of Carlin-type hydrothermal systems (180-240°C), but experiments at low temperatures (25°C) indicate that temperature, fluid chemistry, and pH can all influence non-equilibrium exchange conditions (Kim and Oneil, 1997; Richard, 1999). In addition to experimental work, Frimmel (1992) provides evidence of rate-limited $\delta^{18}O$ exchange in low-temperature (<300°C) hydrothermal systems where dissolution-precipitation reactions are the dominant exchange mechanism.

Lassey and Blattner (1988) present a 1-dimensional analytical solution to fluid mass transport with non-equilibrium fluid-mineral exchange of oxygen isotopes using two equations for the oxygen isotope content of both rock and fluid in a single mineral system. The first equation is the mass balance

$$\frac{\partial}{\partial_\tau}(\Phi\delta^{18}O_{water} + \Phi'\delta^{18}O_{rock}) + \Phi'\frac{\partial}{\partial Z}\delta^{18}O_{water} = 0 \qquad \text{Equation 4.1}$$

and the second defines kinetic exchange

$$\frac{\partial}{\partial_\tau}\delta^{18}O_{rock} = N_D(\alpha\delta^{18}O_{water} - \delta^{18}O_{rock} + \Delta) \qquad \text{Equation 4.2}$$

where τ is dimensionless time since the start of fluid infiltration, ϕ' is the ratio of oxygen in pore-bound fluid to that in the rock, Z is the dimensionless position in the aquifer, α is the equilibrium fractionation factor between fluid and mineral phases for ^{18}O, Δ is the ‰ oxygen isotope deviation of α from unity ($\Delta=10^3(\alpha-1)$), and Damköhler number $(N_D)=\kappa L/q$. N_D is the ratio between the rate constant for ^{18}O exchange between water and rock, κ, and flow rate, q, multiplied by the total aquifer length infiltrated by the fluid (Lassey and Blattner, 1988).

The Damkohler number (Lassey and Blattner, 1988) describes the degree and relative importance of both equilibrium and kinetic exchange in a system. When N_D is between 0.1 and 100, kinetic-limited exchange dominates. Damkohler numbers less than 0.1 indicate very slow reaction rates relative to transport rates (i.e. typical of non-reactive flow conditions). Damkohler numbers in excess of 100 reflect high reaction rates relative to the rate of transport indicating equilibrium exchange conditions are predominant (Bowman *et al*., 1994). Changes in N_D will result in different exchange profiles over the reactive path length of an infiltrating fluid (Figure 4.5) for both vein and rock $\delta^{18}O$ as the fluid and rock are progressively modified creating distended rather than sharp exchange fronts. The difference between vein and rock $\delta^{18}O_{fluid}$ values can thus be an indicator of both the degree of non-equilibrium exchange, as expressed by N_D, and the position along the reactive flow path. The length of the reactive path will be controlled by the TIFF (Figure 4.4). Higher TIFF's will result in progressively longer reactive path lengths.

4.3 Methods

The Lassey and Blattner (1988) model was implemented using the FORTRAN program of Knoop et al. (2002), which uses an algorithm from Lassey (1982) for evaluating the K function of Lassey and Blattner (1988). The K function is a modified Bessel step function used for modeling dispersive exchange processes and is used to define the advance of the infiltration front by calculating the potential isotopic shift available to the rock and the fluid (Lassey, 1982; Lassey and Blattner, 1988). The K function provides a step input solution to Equations 4.1 and 4.2 using the equations:

$$\delta^{18}O_{rock}(Z,\tau) = \delta^{18}O_{rock-initial} - PK(N_D(\tau - Z), \frac{N_D \alpha Z}{\Phi'}), \qquad \text{Equation 4.3}$$

$$\delta^{18}O_{water}(Z,\tau) = \delta^{18}O_{water-initial} + \left(\frac{P}{\alpha}\right) K(\frac{N_D \alpha Z}{\Phi'}, N_D(\tau - Z)) \qquad \text{Equation 4.4}$$

where $P = \delta^{18}O_{rock-initial} - \alpha\delta^{18}O_{water-initial} - \Delta$

Equations 4.3 and 4.4 calculate the $\delta^{18}O$ rock and fluid values at position Z at time τ. The model assumes isothermal fluid flow at a temperature of 200ºC (estimated from fluid inclusion data from Carlin-type Au systems (Cline et al., 2005; Lubben et al., 2012); initial $\delta^{18}O$ rock and fluid values of 25‰ and 4‰ were chosen based on background for Silurian-Devonian limestone (see Chapters 3 and 5) in Northern Nevada and fluid inclusions in ore-stage quartz (Lubben et al., 2012); permeable porosity of 0.1; and a molar H_2O volume of 22 cm^3. Permeable porosity of 0.1 was chosen as an estimate based on the world average limestone (Anna et al., 2007). Permeable porosity is highly variable in limestone and generally decreases with depth (Ehrenberg et al., 2006). Varying the porosity between 0.05 to 0.1 has a minimal effect on the modeling results. Models were generated for a range of N_D

from 0.5 to 5 and variable TIFF to investigate the range of kinetic dispersion conditions represented by the vein-rock data and the reactive path lengths associated with variable TIFF modeled to the data. The modeling produces values for rock and fluid $\delta^{18}O$ values during progressive fluid infiltration for specific N_D.

4.4 Results

Tables of results for modeling at N_D from 0.5 to 5 calculated for TIFFs of $1x10^2$, $1x10^3$, $1x10^4$, $1x10^5$, and $1x10^6$ moles H_2O/cm^2 are included in Appendix E. Reactive path modeling results are plotted with rock-vein oxygen isotope data from Banshee in Figure 4.6. Figure 4.6 plots $\delta^{18}O$ versus the difference in $\delta^{18}O$ between rock and vein ($\Delta_{rock\text{-}vein}$) and rock and fluid ($\Delta_{rock\text{-}fluid}$) at Banshee where $\Delta_{rock\text{-}vein}$ is assumed to reflect $\Delta_{rock\text{-}fluid}$. Plotting measured rock-vein $\delta^{18}O$ data from Banshee with modeled curves at varying N_D shows the range of N_D that encompasses the spread of the data. The modeled curves are independent of the TIFF used in calculations. However, calculations at higher TIFF do yield longer path lengths (Figure 4.2). The calculations were also evaluated at varying porosity, molar H_2O volume, temperature. Porosity and molar H_2O volumes had minimal effects on the modeling, but temperature will have a more pronounced effect. At lower temperatures fractionation between calcite and H_2O increases (O'Neil et al., 1969), and therefor the input parameter for vein calcite increases. The increase in $\delta^{18}O$ in vein calcite thus reduces the calculated reactive path length for any given TIFF. If a higher temperature is used to calculate fractionation between calcite and H_2O the opposite effect occurs leading to longer reactive path lengths, relative the results presented here, for the infiltrating fluid at any given TIFF.

4.5 Discussion

Figures 4.6a-b compares real data to modeled curves at varying N_D to show the range of N_D that encompasses the spread of the data. Plotting both $\delta^{18}O_{rock}$ and $\delta^{18}O_{vein}$ values with model results yields two significant results: (1) Group I and Group II plot as distinct arrays across the range of N_D values, and (2) the range of N_D that encompasses observed $\delta^{18}O$ is consistent with non-equilibrium exchange within an N_D envelope of N_D= 0.5 to 5. Variable N_D could reflect changes in temperature, pressure, solution-to-solid ratio, surface area, solution composition, mineral composition and structure, and defects (Cole and Chakraborty, 2001). Additionally, fast reaction rates could also lead to the formation of reaction rims inhibiting further exchange with the unreacted crystal (Cole and Chakraborty, 2001).

The only temperature effects considered by the model are temperature dependent fractionation between fluid and mineral phases. The reaction model of Lassey and Blattner (1988) does not account for temperature dependent kinetic exchange. Temperature effects on kinetic exchange are not easily simulated due to competing exchange mechanisms and additional dependence on the environment of reaction (Lassey and Blattner, 1988). Owing to a lack of constraints on the range of temperature variation at Banshee conditions were assumed to be isothermal at 200°C. However fluid inclusion data from Carlin-type Au deposits of Nevada suggest a range of fluid temperatures (~180° to 240°C). This might explain the range of N_D values implied by the $\delta^{18}O$ data. Dashed lines for Groups I and II in Figure 4.6 are iso-distance lines connecting points of equal distance along the reactive path length of the model system at varying N_D. The data from Banshee forms a linear array that matches well with the iso-distance lines on the model. Changes in the input parameters of porosity (varied between 0.05 to 0.2) and TIFF do not significantly impact the position of the N_D curves on the Δ-δ diagrams. The main impact of varying the TIFF for the model is on the reactive path length distance associated with the iso-distance lines on the diagrams and not on the geometry of the modeled curves of Figure 4.6a-b.

4.5.1 Isolated Fluid Pathways or Heterogeneous Permeability

The observation that Groups I and II form two distinct clusters argues that the two sets of data represent different fluid flow pathways. If samples were collected along the reactive flow path of a single fluid, the data would show a gradational pattern rather than distinct clusters as observed at Banshee. However, the fluid pathways were not necessarily isolated from one another. The two groups of data more likely represent different fluid flow velocities due to heterogeneities in porosity/permeability rather than discrete flow paths. Samples from Group I were collected from visibly unaltered limestone with relatively low inherent permeability, while samples from Group II were collected from areas within or proximal to the breccia unit with presumably higher permeability (see Chapter 3). Sample U16-54-17 from Group II sits outside mapped breccia on the main cross-section (Figure 4.1), but it is located within a discrete zone of brecciation not captured on the broader section. It is proposed that permeability contrast between the two groups of samples is the strongest control on the relative degree of alteration and creates the appearance of 2 distinct flow paths. Alteration patterns suggest that the highest fluid flux at Banshee is associated with a core zone of near complete carbonate dissolution and Au mineralization. The lack of carbonate dissolution in the sampled rocks and the sharp contact between carbonate dissolution and visibly unaltered carbonate-bearing wall rocks at Banshee (see Chapter 3) indicates that a distinct permeability contrast is associated with the degree of $\delta^{18}O$ alteration in wall rock calcite. The bimodal distribution of the samples from Banshee argues for distinct alteration clusters controlled by the difference in permeability between breccia and limestone. A potential analogue of the alteration system observed at Banshee is fracture-controlled percolation networks of Cox (2005, 2007) and Cox et al. (2001) where flow is governed by the connectivity of fractures that serve as the permeability network. Cox defines the high permeability main flow zone as the flow backbone where fluids are connected to the upstream and downstream portions of the flow network. Flow paths that connect to flow backbone but terminate in low-permeability rock are called dangling elements and these dangling elements are associated with lower fluid fluxes. At Banshee, limestone forms a low permeability portion of the flow system and the breccia serves as a higher permeability portion. The highest permeability part of the flow, the backbone, is hosted in the most altered breccia at the core of the system. During the infiltration of Carlin-type hydrothermal fluids permeability would be further enhanced through the dissolution of carbonate thus enabling greater fluid flow and more carbonate dissolution. Permeability enhancement would continue as long as the fluid was able to dissolve carbonate. Once massive silicification occurred permeability was destroyed limiting the access of later fluids. This is evidenced by the late calcite precipitation along fractures in silicified breccia (Stage 3 breccia from Chapter 3)

Figure 4.7 is a simplified cross-section of the Banshee deposit illustrating the permeability controls on fluid flow. Under this conceptual framework, the oxygen isotope data from Banshee distinguishes permeability contrasts with lower permeability rocks separated from the highest permeability backbone flow associated with the most intense alteration of wall rocks. The greater permeability of the breccia unit at Banshee served to focus infiltrating fluids along a relatively narrow path. Lower permeability wall rocks adjacent to the breccia unit experienced significantly less fluid:rock interaction limiting the vertical expression of the fluid flow above and below the breccia unit owing to the steep permeability gradients. Dikes that intersect the breccia unit are altered to illite, pyrite, and quartz (see Chapter 2), but dikes that do not intersect the breccia are only weakly altered. Even along the Post fault, unaltered Jurassic lamprophyre is observed where the breccia unit is not intersected.

4.5.2 Estimating TIFF and Distance

Reaction path modeling was performed for a range of TIFF values ($1x10^2$ to $1x10^6$ moles H_2O/cm^2) (see Appendix E for full modeling results). As TIFF increases, the reactive path length (i.e. the isotopic alteration front) of the fluid system propagates further down flow path. The models presented in Figure 4.8 show that if TIFF is considered to be the same for both groups of data, the distance along the reactive path length is greater for the more rock buffered path (Group II). Modeling the Banshee data with increasing TIFFs illustrates the relative change in distance along the reactive path length for both fluid 'paths' (Groups I and II) recognized at Banshee (Figure 4.8). TIFF and distance have a linear relationship with the 1-dimensional model solution presented in this chapter, allowing for the estimation of one parameter if the other parameter is known (Figure 4.8). The graph in Figure 4.8 was created by using reactive path modeling and the vein-rock pair data. The iso-distance lines for Groups 1 and 2 in Figure 4.6 give both vein and rock $\delta^{18}O$ values for specific N_D. The values for $\delta^{18}O$ for each group were then matched against the modeled results to estimate the reactive path length for specific values of $\delta^{18}O$ in the wall rock and vein for each N_D calculated. At Banshee, the two sample groups form 2 separate trend lines on the TIFF-distance graph that correspond to different integrated fluid fluxes at equal distances. The minimum fluid volume calculated in Chapter 2 for west Banshee converted into TIFF is $1.7x10^4$ moles H_2O/cm^2. Using this value for both fluid samples groups, the distance from the initial fluid reservoir would be 1 km for Group I and 2 km for Group II. Conversely, if we assume that the path length of flow from the initial fluid reservoir is constrained to a distance of 5 km flow (the approximate strike length of the mineralization corridor along the

Post fault in the northern Carlin trend), path A would have a TIFF of $2.5x10^4$ (moles H_2O/cm^2) and flow path B would have a TIFF of $5x10^4$ (moles H_2O/cm^2).

At Banshee, the actual reactive path length is unknown. It is believed that fluids in Carlin-type Au systems emanated from depths of >10km along deep crustal faults activated during Eocene extension (Cline et al., 2005; Hofstra and Cline, 2000; Ilchik and Barton, 1997; Muntean et al., 2011). Person et al. (2008) propose a depth of >5km for fluid circulation based on hydrologic modeling of amagmatic geothermal fluid systems in Nevada. However, the sequence of rocks (ratio of carbonate-bearing rocks to siliciclastic rocks) at depth is not well characterized, and fluid reservoir depths are poorly constrained. Studies of other hydrothermal flow systems have been able to constrain flow path length (Cox, 2007; Knoop et al., 2002), and in those cases more precise estimates of TIFF were possible (see Table 4.2). While the path length of fluid flow in Carlin-type systems is poorly constrained, this study provides a framework for understanding the effects of the path length on estimated TIFF. If the estimate of 5km (~strike length of Post fault mineralization corridor and the minimum depth for fluid circulation from Person et al. (2008) is used for the reactive path length at Banshee, the TIFF for the permeable breccia horizon (represented by Group 2 samples) is $5x10^4$ (moles H_2O/cm^2). If path length is defined as the extent of alteration defined along the breccia unit at Banshee (~600 m) the TIFF is ~$2.5x10^3$ (moles H_2O/cm^2).

The TIFF estimated in Chapter 2 from mass transfer in west Banshee is within an order of magnitude of the value calculated here for the Banshee breccia horizon. The TIFF calculated from the mass transfer study in Chapter 2 represents a minimum value and assumes efficient precipitation of sulfur from the fluid, and therefore, it is not surprising that the TIFF estimated from Figure 4.7 is larger. If the TIFF's are treated strictly, the difference between the mass transfer-calculated TIFF for Banshee and the vein-rock estimate TIFF indicates that only 34% of the sulfur in the fluid was precipitated into pyrite at west Banshee. Ridley et al. (1996) estimated that 10-50% of sulfur and Au are stripped from fluids responsible for Archean lode-gold deposits.

Table 4.2 lists TIFF's calculated from other hydrothermal fluid systems. A majority of examples comes from the metamorphic literature, but the estimate for black smoker systems may be a better analogue for Carlin-type hydrothermal systems. The values estimated from Banshee are equivalent to ~5 black smoker systems similar to those investigated by Teagle et al. (2003).

4.5.3 Calculating Fluid Volumes from TIFF

Since TIFF's have units of moles per cross-sectional area, it is possible to estimate fluid volumes. If the cross-sectional area of a fluid conduit is multiplied by the estimated TIFF, the product is equal to the total mass of fluid. The primary zone of fluid flow at Banshee is the breccia horizon. The cross-sectional area of the breccia can be measured using a representative cross-section through the deposit. Using an average thickness of 40 meters and estimated 250 m strike length the cross-sectional area of the breccia horizon is $\sim 1 \times 10^4$ m^2. The TIFF for the entire volume of breccia is unknown due to the lack of available sample material in the most altered portions of the breccia; however, the estimated TIFF from Group I breccia samples provides an estimate of minimum TIFF for the breccia. Using a TIFF of 5×10^4 (moles H_2O/cm^2) and an estimated cross-sectional area of $\sim 10^4$ m^2 for the breccia, the mass of fluid at Banshee would be $\sim 10^{11}$ kg. The volume of fluid would be $\sim 10^8$ m^3 (assuming a molar volume 22 cm^3).

Hickey et al. (2013) estimate a minimum Darcy flux of $\sim 10^{-8}$ $m^3 m^{-2} s^{-1}$ for the giant Betze-Post Carlin-type deposit ~4km south of Banshee, based on heat transfer modeling, over an estimated time scale of 15,000 to 45,000 years. Using Hickey et al.'s (2013) estimates, the range of minimum fluid volumes for Betze-Post would be $\sim 10^{11}$ m^3. The larger estimated volume of fluid for Betze-Post reflects the fact that it is a significantly larger ore body (~100 times the reported Au endowment for west Banshee). Hofstra and Cline (2000) estimated the volume of fluid necessary to produce the 10 Moz Au endowment in the Jerritt Canyon Carlin-type Au district was $\sim 10^9$ m^3. Using Betze-Post and Jerritt Canyon for comparison, the fluid volume estimated for Banshee appears to be a reasonable estimate for a relatively small Carlin-type hydrothermal system.

For a time scale of 15,000 to 45,000 years, TIFF estimates at Banshee yield a Darcy flux range of 2×10^{-8} to 7×10^{-9} $m^3 m^{-2} s^{-1}$. These Darcy flux estimates are similar to the minimum estimates of Hickey et al. (2013) for the Betze-Post system. Person et al. (2008) estimated that the duration of the hydrothermal event of Betze-Post was up to 200,000 years, but Darcy flux calculations for Banshee at 200,000 years are likely too low to be reasonable.

Another possibility is that fluid flow at Banshee was pulsed and the estimate of TIFF integrates flux over multiple episodes of hydrothermal flow. Depending on the time spacing between events, individual pulses might have had variable fluid flux associated with them. If multiple pulses of fluid were responsible for alteration and calcite veining at Banshee, more variability in the isotopic and chemical signature of the calcite veins and wall rock alteration might be expected with evidence for multiple calcite precipitation events. There is also a lack of evidence for over-pressuring being the dominant driving force for fluids owing to the lack of textural evidence in wall rocks and calcite veins sampled in this study. The data argues for a relatively continuous flow system of isotopically exchanged hydrothermal fluid emanating from depths >5km over a relatively short time frame.

4.6 Use of Reaction Path Modeling for Evaluating Fluid Flow in Carlin-type Hydrothermal Systems

Oxygen isotope data collected from vein-rock pairs provides a basis for evaluating kinetically controlled reactive transport in hydrothermal fluid systems. Plotting the data against 1-dimensional reactive transport model simulations has the potential to not only evaluate the role of kinetic dispersion, but also to define permeability contrasts on the basis of relative integrated fluid fluxes. Additionally, if the reactive path length of differentiated flow pathways is known, specific integrated fluid fluxes can be estimated based on the reactive transport model. Once a TIFF is estimated for a hydrothermal system, volumes of fluid can be calculated putting important constraints on the development of mineral deposits. Further work is needed to validate this approach through application on a variety of similar hydrothermal systems, but using vein-rock pairs in combination with reactive transport modeling has the potential to be a powerful tool for establishing fluid flux constraints on hydrothermal flow systems. Using vein-rock pairs with 1-dimensional reactive path modeling may also have application for mineral exploration as a vectoring tool by defining where specific areas sit with in the permeability system.

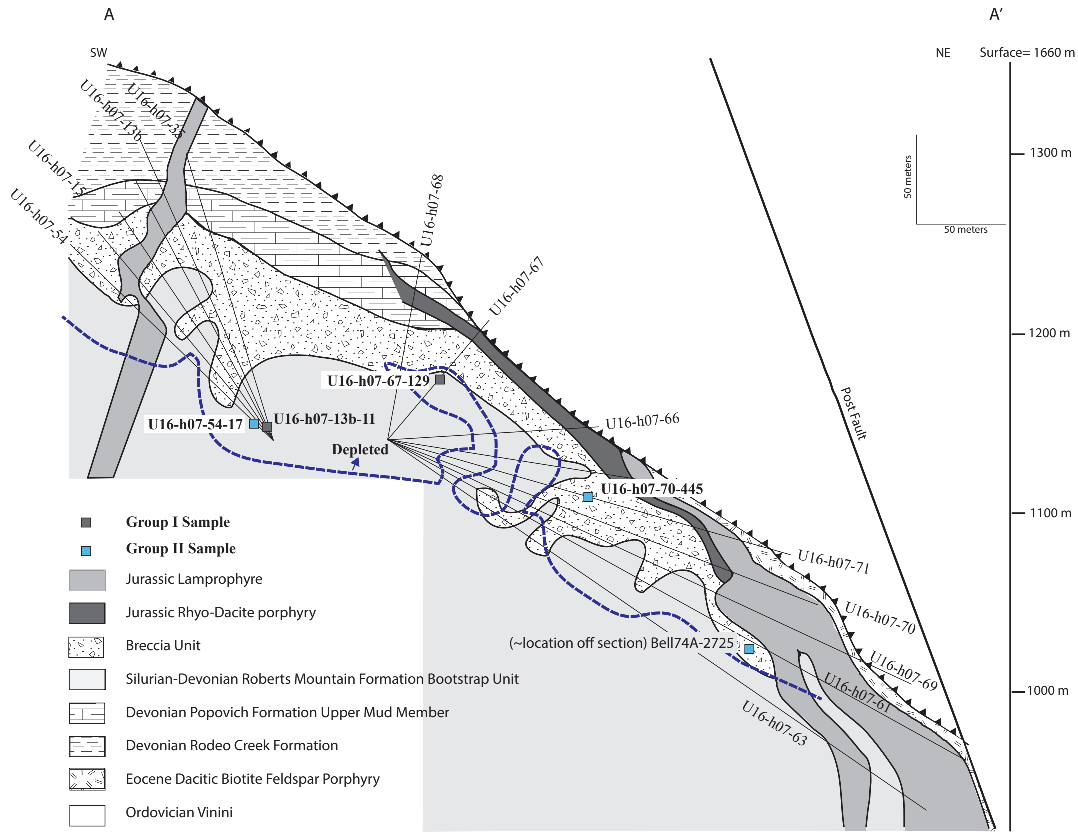

Figure 4.1 Cross section A-A' showing the location of samples used for this study. For the location of the section in plan view see Figure 3.1. Three vein-rock pair sets were used from U16-h07-67-129. All of the other sample locations include one sample each. The blue dashed line is the estimated extent of δ^{18}O depletion from Chapter 3 within wall rock calcite at Banshee. Solid black lines denote drill hole traces.

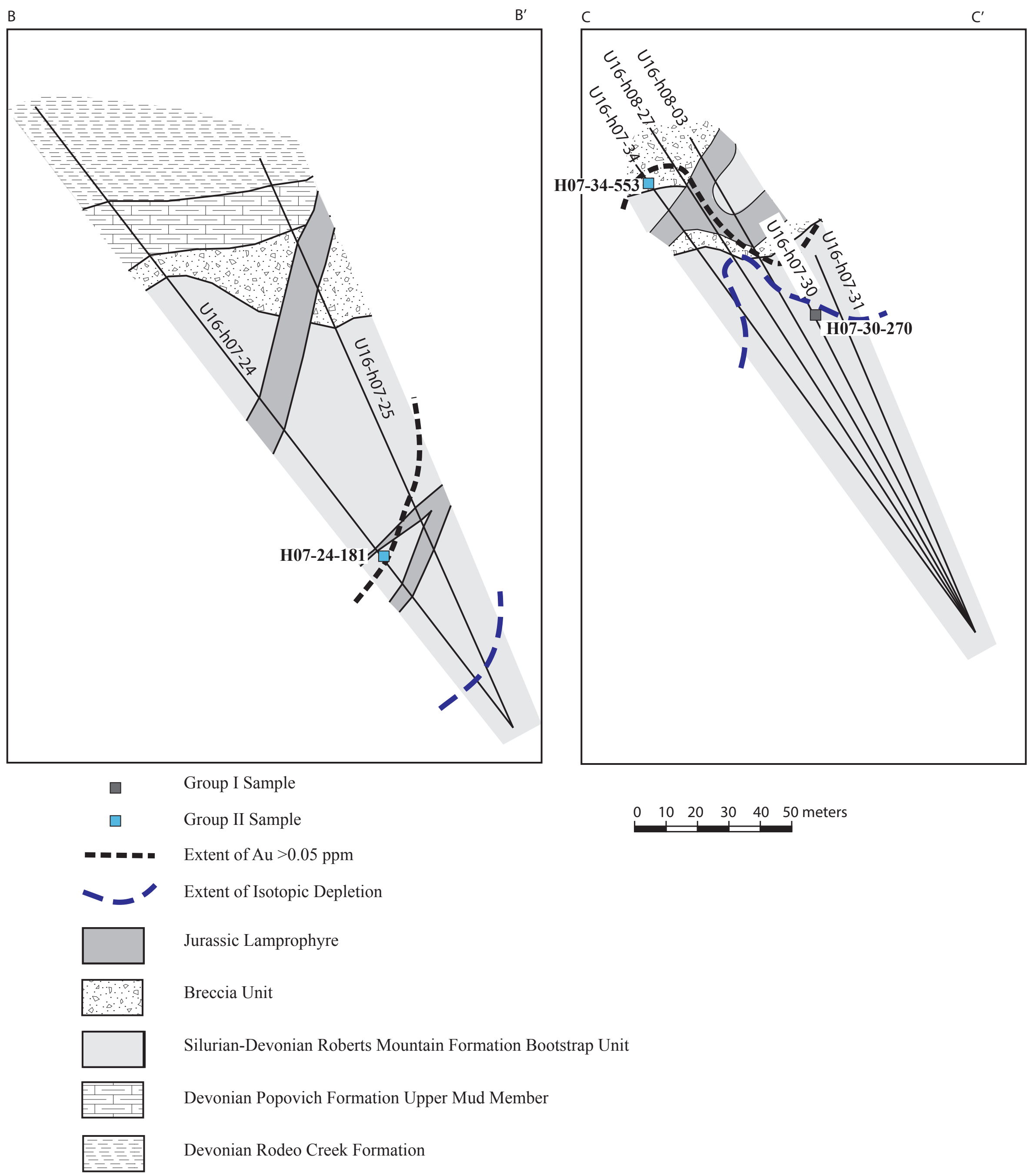

Figure 4.2 Cross-sections B-B' and C-C' showing the distribution of samples used for this study. For the locations of the sections in plan view see Figure 3.1.

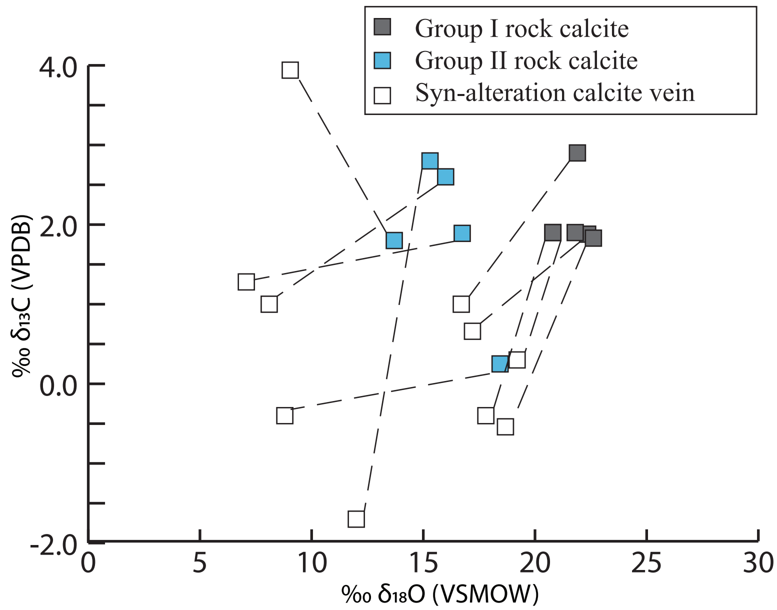

Figure 4.3 Covariation plot of $\delta^{13}C$ versus $\delta^{18}O$ from wall rock calcite and vein calcite pairs from Banshee. Filled squares are rock calcite samples and open squares are vein calcite samples. Dashed lines connect vein-rock pairs for individual samples.

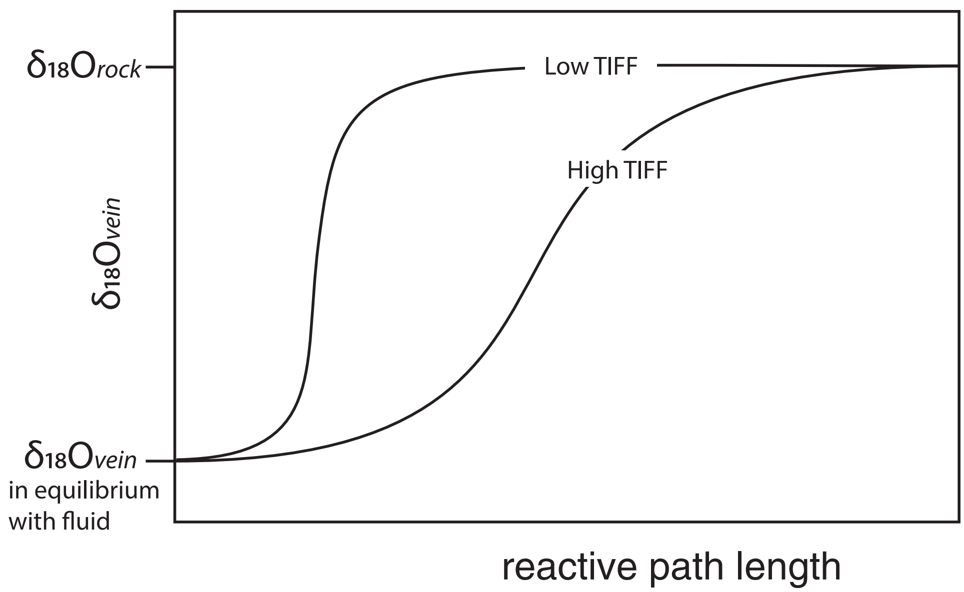

Figure 4.4 Schematic illustration of the relationship between reactive path length and TIFF. Even though the scale of fluid infiltration may be the same, increases in TIFF will result in isotopic exchange occurring further down the flow path. After Cox (2007).

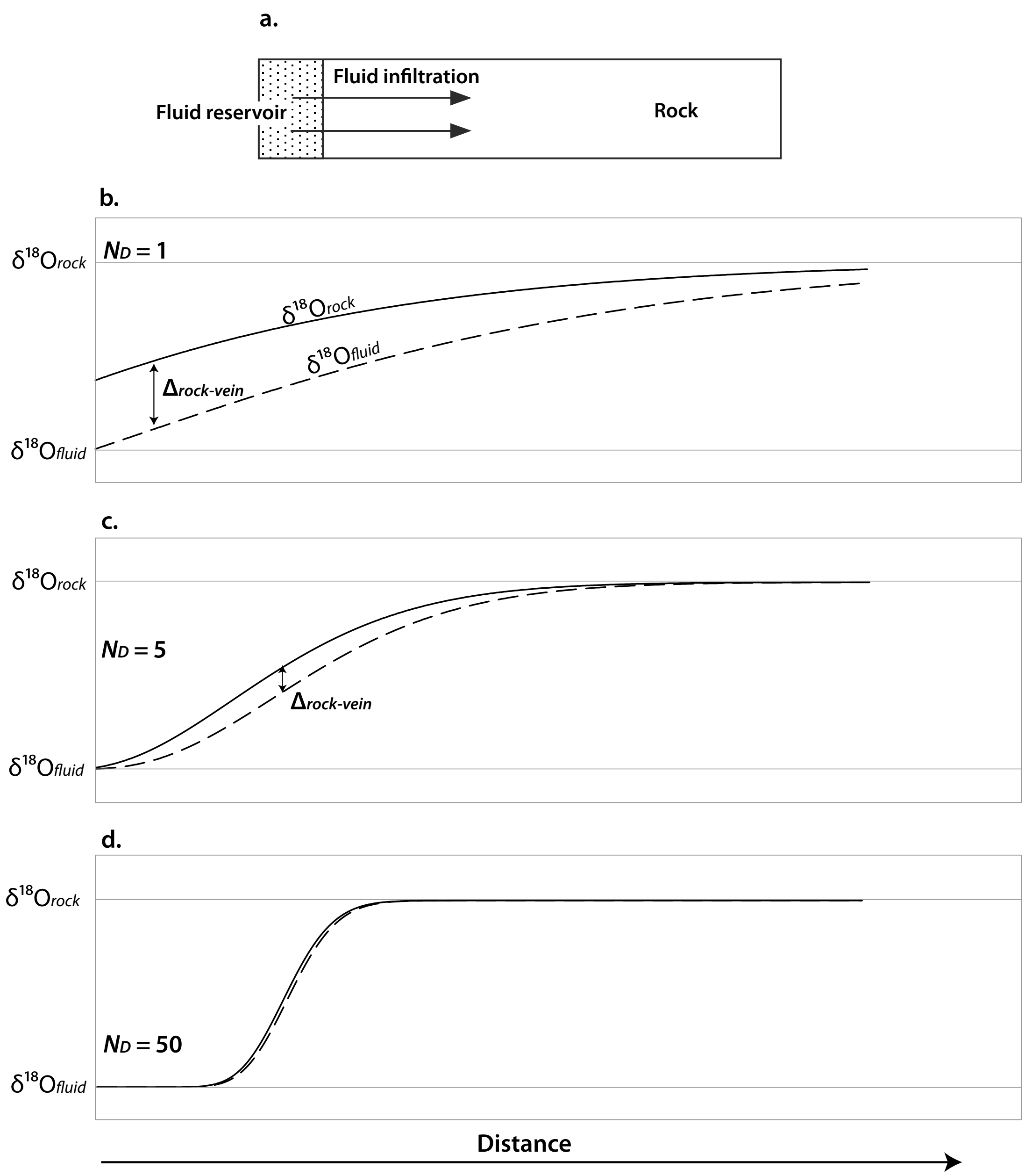

Figure 4.5 Illustration of the effects changes in N_D have on the geometry of exchange fronts and the degree of disequilibrium between rock and fluid $\delta^{18}O$ ($\Delta_{rock\text{-}vein}$). For the purposes of this study, $\delta^{18}O_{vein}$ is assumed to be in equilibrium with $\delta^{18}O_{fluid}$. The diagrams were calculated using the model of Lassey and Blattner (1988) for an infiltrating fluid out of equilibrium with wall rock. The actual reactive path length (distance) will vary with TIFF, but the geometry of the isotopic exchange fronts is governed by N_D. a) Illustration of fluid infiltration along a flow path from the fluid reservoir into the wall rock (after Cox, 2007). b) At N_D=1 the degree of disequilibrium between rock an fluid is greatest nearer the fluid entry point, and the fluid never reaches equilibrium along the reactive path length. c) At N_D=5 disequilibrium between rock and vein is greatest midway down the reactive path length. d) At N_D=50 the degree of disequilibrium between rock and vein is minimal.

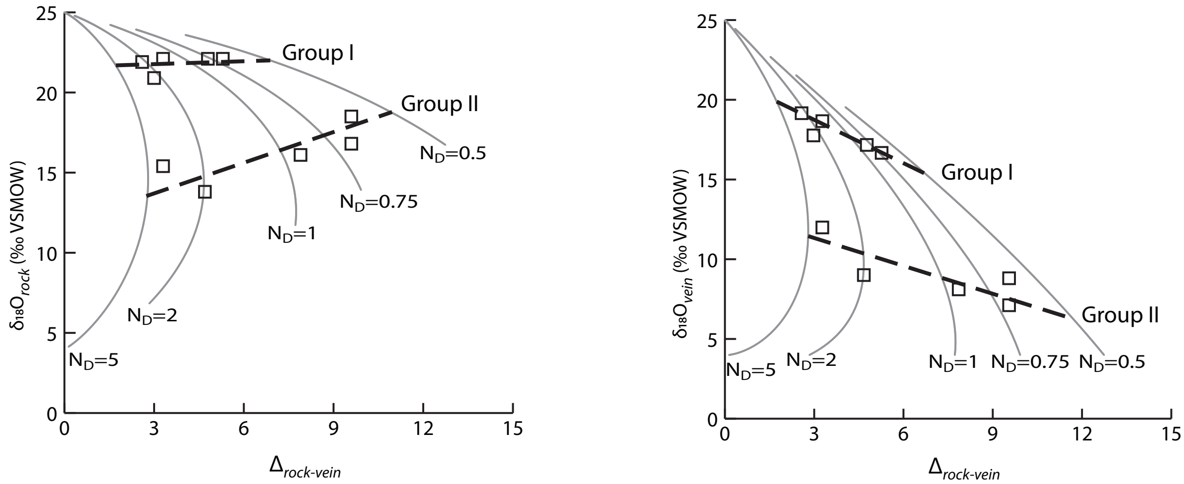

Figure 4.6 δ-Δ plots of calculated non-equilibrium exchange paths with varying N_D for rock calcite and vein calcite. Dashed lines connect points of equal distance across calculated N_D curves. Data plots along two separate equal distance lines (Group I and II). (a) Rock calcite δ^{18}O values plotted against the variance of δ^{18}O between rock calcite and co-precipitated calcite veins ($\Delta_{rock\text{-}vein}$). (b) Vein calcite δ^{18}O values plotted against the variance of δ^{18}O between vein calcite and rock calcite pairs ($\Delta_{rock\text{-}vein}$).

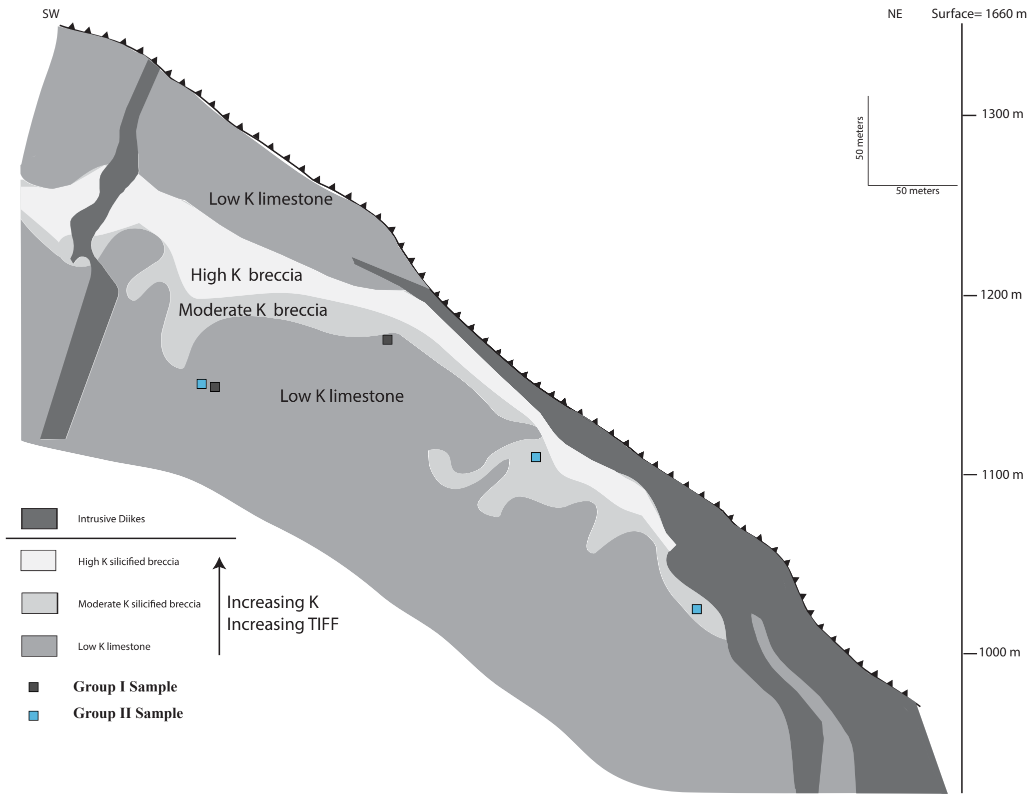

Figure 4.7 Simplified cross-section of the Banshee Au deposit illustrates permeability boundaries within the deposit. The extensively altered zone within the breccia at Banshee represents the high permeability pathway associated with the high flux backbone network. Zoning outward from the backbone pathway is lower permeability breccia with a lack of visible alteration. Visibly unaltered limestone represents the lowest permeability in the flow network. In this model, higher TIFF's are associated with the backbone network. The locations of samples along the section are plotted for reference.

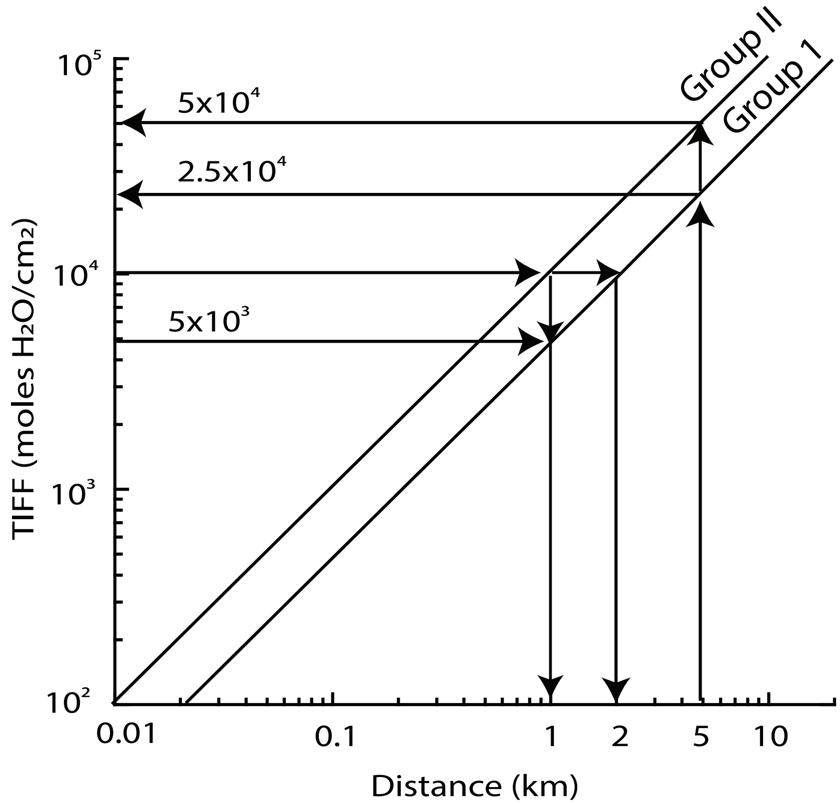

Figure 4.8 Plot of calculated reactive path lengths for different TIFF for the 2 fluid paths (Groups I and II) recognized at Banshee. The path lengths of the 2 data groups were determined by matching the $\delta^{18}O$ values of rock and vein calcite determined from the isodistance lines of Figure 4.5 with the modeled distance at which the same $\delta^{18}O$ values of rock and vein calcite are predicted.

Table 4.1 Isotope data in ‰ (VSMOW) from syn-mineralization vein-rock pairs used with reactive path modeling at Banshee.

	Sample	$\delta^{18}O_{rock}$	$\delta^{18}O_{vein}$	$\Delta^{18}O_{rock-vein}$	$\delta^{13}C_{rock}$	$\delta^{13}C_{vein}$	$\Delta^{13}C_{rock-vein}$
Group I	U16-H07-30-270	21.8	19.2	2.6	1.9	0.3	1.6
	U16-H07-13b-11	20.8	17.8	3.0	1.9	-0.4	2.3
	U16-H07-67-129A	21.9	16.7	4.2	2.9	1.0	1.9
	U16-H07-67-129B	22.4	17.2	5.4	1.9	0.7	1.2
	U16-H07-67-129C	22.6	18.7	3.9	1.8	-0.5	2.3
Group II	U16-H07-24-181	13.7	9.0	4.7	1.8	3.9	-2.1
	Bell-74A-2725	16.7	7.1	9.6	1.9	1.3	0.6
	U16-H07-34-553	16.0	8.1	7.9	2.6	1.0	1.6
	U16-H07-54-17	15.3	12.0	3.3	2.8	-1.7	4.5
	U16-H07-70-445	18.4	8.8	9.6	0.3	-0.4	0.7

Table 4.2 Compilation of estimated TIFF's (modified from Knoop et al. (2002). Estimate from west Banshee calculated by dividing minimum estimated volume of fluid (from Chapter 2) by the cross-sectional area of the west Banshee dike.

Location	TIFF (mol H_2O/cm^2)	Reference
Vermont (metamorphic hydrothermal)	1×10^4 to 7×10^5	(Ferry, 1992)
Ductile shear zones	5×10^4 to 2×10^5	(Dipple and Ferry, 1992b)
Glarus Thrust (mylonite)	$1.2\text{-}2.9 \times 10^4$	(Bowman et al., 1994)
Alice Springs orogeny (shear zone)	2.1×10^6	(Cartwright and Buick, 1999)
Canadian cordillera thrust	1.1×10^5	(Knoop et al., 2002)
Utah (contact metamporphism)	5.6×10^4	(Cui et al., 2001)
Utah (Alta contact aureole)	2.4×10^3	(Bowman et al., 1994)
Ocean ridge black smoker	9.4×10^3	(Teagle et al., 2003)
Northern Italy (hydrothermal dolomite)	$2\text{-}4 \times 10^6$	(Carmichael and Ferry, 2008)
West Banshee Au deposit	$>1.7 \times 10^4$	Chapter 2 of this thesis
Banshee Carlin-type deposit*	5×10^4	This chapter

*(estimated from Figure 4.8 at a reactive path length of 5 km)

Chapter 5 : Isotopic and Geochemical Expression of Fluid Flow in Carlin-type Au Deposits: Implications for Using Oxygen Isotopes as and Exploration Tool in Carbonate-hosted Systems

As shown in Chapters 3 and 4 of this thesis, sampling of oxygen isotope ratios in carbonate minerals can be used to delineate fluid-rock interaction in Carlin-type hydrothermal systems, provide estimates of integrated fluid fluxes, and differentiate fluid pathways. A further implication of the detailed oxygen isotope studies at the Banshee Au deposit is that oxygen isotope depletion may reveal fluid-rock interaction outside of other traditional indicators of hydrothermal alteration, such as trace element metasomatism. This chapter evaluates the use of oxygen isotope ratios in carbonate-hosted Carlin-type hydrothermal systems to define the relative scale of oxygen isotope alteration compared to Au and other trace elements. Additionally, $\delta^{18}O$ is evaluated as a tool for vectoring along hydrothermal fluid flow pathways towards zones of Au deposition.

Banshee is an example of a small Carlin-type Au deposit with a somewhat restricted hydrothermal footprint defined by $\delta^{18}O$ depletion in limestone, proximal silicification, carbonate dissolution and clay alteration. Chapter 3 showed that $\delta^{18}O$ in carbonate was capable of defining a footprint of $\delta^{18}O$ alteration spatially coincident with the Au deposit. Traditionally, oxygen and carbon isotopes in carbonate minerals have been measured using an isotope ratio mass spectrometer (IRMS). Recent advances in the measurement of $\delta^{18}O$ and $\delta^{13}C$ in carbonate minerals using laser spectroscopy has greatly reduced the time and cost of analysis allowing larger datasets to be collected (Barker et al., 2011; Barker et al., 2013). The laser spectroscopy method was utilized for this study to collect $\delta^{18}O$ and $\delta^{13}C$ data from >1500 drill pulp samples allowing $\delta^{18}O$ alteration to be investigated on larger scale than previous studies. Sampling occurred along two cross-sections in the southern and northern portions of the Goldstrike property on the Northern Carlin trend. The southern cross-section attempts to define the scale of $\delta^{18}O$ alteration associated with the giant Betze-Post-Screamer ore system in the southern portion of the property. The northern cross-section attempts to define $\delta^{18}O$ alteration across an area of weak localized alteration in the northwest portion of the property into the high grade Meikle Au deposit located along the Post fault system.

Additionally, data collected over the district is used to help define primary fluid pathways and the permeability network of the hydrothermal flow system across the property. The data provide insight into the scale of fluid driven $\delta^{18}O$ alteration in an area hosting the largest occurrences of Carlin-type mineralization known. Another important question addressed in this chapter is whether or not $\delta^{18}O$ in carbonate could be an effective tool for exploration and vectoring, as the recognition of $\delta^{18}O$ depletion well outside other indicators may provide the most easily identifiable expression of the Au system. This chapter also attempts to answer the question of just how far oxygen and trace element alteration can be identified around gold mineralization.

This study builds on the detailed deposit scale study at the Banshee Au deposit by testing the utility of sampling oxygen isotopes at the same scale as gold concentrations are measured in exploration drill holes. The advantages of micro-drilling carbonate for isotopes are discussed in Chapter 2, but there are also advantages to working with bulk samples from assay pulps. Specifically, bulk sampling over defined intervals mitigates the smaller scale effects of hydrodynamic dispersion by providing an average isotopic composition over the sampled interval. Hydrodynamic dispersion leads to differing degrees of fluid-rock interaction at scales both large and small. Bowman et al. (1994) defines hydrodynamic dispersion as “the process of mixing due to the heterogeneity of fluid velocity on several scales.” Heterogeneous permeability is an inescapable fact of rock properties in most natural systems and permeability may vary both spatially and temporally. Whether samples are collected at a microscopic scale or meter-scale the degree of isotopic resetting will have an inherent variability. Bowman et al. (1994) suggests that the best way to account for dispersion is to collect a large number of samples, and then laterally average the samples to give the most representative understanding of permeability, flow velocity, and fluid conditions associated with the hydrothermal event. Bowman et al. (1994) calls this a representative elemental volume (REV). Assay pulps from subsurface exploration can be used in the same way. Assay pulps are crushed and pulverized samples prepared for Au fire assay analysis. Since assay pulps are derived from a sub sample over a set interval, they can be considered a REV. For drill core, the subsample from split core is typically over 1.5-3 meter intervals. For reverse circulation (RC) drilling, the subsample is a split of the drill cuttings over a ~3 meter interval. An added benefit of sampling assay pulps is that the data is collected over the same interval as Au assay data which allows for a more direct comparison of covariation between Au and isotopic depletion related to the hydrothermal fluid system. A potential disadvantage to analyzing pulps for oxygen isotopes is that the sample contains a mixture of material that may have significant calcite veining or other carbonate cements that are unrelated to hydrothermal alteration associated with mineralization. Also as the results are integrated over a larger sampling interval, discrete zones of alteration may be masked by the predominance of unaltered material. Additionally, pulp samples do not allow for detailed sampling of discrete textural features or the evaluation of different carbonate cements that might be recognized in hand sample or thin section.

Trace element geochemistry is another potential tracer of fluid flow in hydrothermal systems. In Carlin-type Au deposits several pathfinder elements have been identified as being linked with mineralization (see Chapter 2), and while trace element geochemistry is a common exploration tool in Carlin-type deposits, analyses are usually carried out on composites of multiple assay intervals. While data collected over multiple assay intervals may represent a REV for evaluating trace element geochemistry in isolation, it is collected on a different scale from Au assay data. Sampling isotopes and geochemistry on the same scale as Au should mitigate the effects of spatial and temporal variability of the permeability network, and allow for direct comparisons of these different geochemical datasets.

This study uses a REV approach to analyze for $\delta^{13}C$ and $\delta^{18}O$ in rock carbonates and trace element geochemistry allowing for interpretation of the effects of water-rock interaction during the hydrothermal fluid system at equivalent resolutions. While this approach may mask fluid flow occurring over small discrete intervals, it has the potential to better expose larger scale fluid flow and define relative patterns of Au, trace element, and isotopic haloes. Used in this way, $\delta^{18}O$ isotopes in rock carbonates can be used as a tool for vectoring towards Au mineralization in Carlin-type Au deposits. An evaluation of the effectiveness of sampling pulps for oxygen isotope analysis indicates that calcite veining is unlikely to affect data interpretation and pulp samples are capable of elucidating hydrothermal alteration of $\delta^{18}O$. The results of this study define a halo of $\delta^{18}O$ alteration that extends at least 2 km out from major Carlin-type ore deposits. Additionally the isotope data show that depletion in $\delta^{18}O$ becomes more pronounced nearer the ore zone.

5.1 Review of $\delta^{18}O$ Depletion Haloes

As discussed in Chapter 3, $\delta^{18}O$ alteration has been described in many hydrothermal ore systems including Carlin-type Au deposits. Taylor (1974) showed that $\delta^{18}O$ depletion can form a halo that extends 2.5 to 3x the diameter of the intrusive magmatic body in intrusive related Au systems with concentric zoning of progressively fluid buffered values toward causative intrusions. Cathles (1993) defined a 2-4 km area of $\delta^{18}O$ depletion in the Noranda mining district in the Abitibi Greenstone-belt spatially coincident with known mineralizing systems. Nesbitt's (1996) review of the use of stable isotopes in mineral exploration suggested that haloes can extend >1km from mineralization. In addition to the lateral distribution of $\delta^{18}O$ alteration, Kesler et al. (1995) suggested that $\delta^{18}O$ alteration haloes are largest above the ore zones in carbonate hosted chimney-manto Pb-Zn-Cu-Ag ore systems. The principal studies in Carlin-type deposits showed that $\delta^{18}O$ alteration is coincident with Au mineralization at Carlin (Radtke et al., 1980), Twin Creeks (Stenger et al., 1998b) and Pipeline (Arehart and Donelick, 2006). Stenger et al. (1998) suggested that variable alteration of $\delta^{18}O$ might extend several kilometers out from known mineralization at Twin Creeks based on limited sampling of outcrop and drill holes well away from known mineralization. However, the limited sampling inhibits the interpretation of the absolute size of the $\delta^{18}O$ alteration halo.

A recent study by Hofstra et al. (2011) presented oxygen, sulfur, and carbon isotope data along with lithogeochemistry data collected from assay pulps of 5 drill holes along two cross-sections through the Screamer ore zone at Goldstrike. Hofstra et al.'s (2011) sampling was concentrated within the Screamer ore zone and did not attempt to define alteration in distal drill holes at Goldstrike. Rather than defining the scale of $\delta^{18}O$ alteration, Hofstra et al. (2011) focused on defining the relationship between $\delta^{18}O$, $\delta^{34}S$, lithogeochemistry, alteration, and Au mineralization. The study showed that $\delta^{18}O$ alteration is coincident with both Au mineralization and alteration at Screamer.

5.2 Study Areas

Chapter 3 introduced isotope data collected from the Banshee Au deposit, which is a small Au deposit in the northern Carlin trend. Banshee is within Barrick Gold Corporation's

Goldstrike property, which contains a number of both small and large Carlin-type Au deposits the most significant of which are Betze, Post, Screamer, Rodeo, and Meikle (Bettles, 2002). In order to define $\delta^{18}O$ alteration in the larger Goldstrike district two cross-sections of drill holes were chosen that allowed for sampling from volumes distal to mineralization, all the way through a well defined, world class Au deposit. Section A is the Clydesdale to Meikle section on Barrick's Goldstrike property (Figure 5.1). This cross-section has been the focus of previous internal Barrick studies on alteration and geochemistry. The western portion of the section has no known Au deposits and is thought to represent near background conditions with respect to Au mineralization. The eastern portion of the section terminates in the Meikle Au deposit. The cross-section crosses several major faults and the sedimentary facies change between the Lower Laminated silty limestone and the Bootstrap limestone in the Silurian-Devonian Roberts Mountain Formation (Figure 5.2).

Section B is located to the south of Section A (Figure 5.1). Section B (Figure 5.3) has also been the focus of previous studies on pyrite geochemistry and alteration (de Almeida et al., 2010). The cross-section begins at the far west of the Goldstrike property and cuts through the northern Screamer deposit all the way through to the Post fault zone. Much of Section B is mineralized with only the western most drill holes having near background values for Au. Unlike the Clydesdale to Meikle section, Section B does not cross the Silurian-Devonian Roberts Mountain Formation facies change. The data collected provides an understanding of the nature of fluid flow and the extent of isotope alteration and trace element metsomatism in and around a large Carlin-type Au district.

5.3 Local Geology

The geology of the Goldstrike district is described in detail by Leonardson and Rahn (1996), Volk et al. (1995; 2001), and Bettles (2002), and the description here is largely summarized from their work along with internal Barrick reports and geologic models.

5.3.1 Stratigraphy

In the west of section A, drill holes pierce the Roberts Mountain Thrust (RMT) into the lower plate assemblage of Paleozoic carbonates. Drill holes generally terminate in silty limestone of the Lower Laminated unit of the Roberts Mountain Formation with the exception of CD-96-2C that terminates in limestone of the underlying Ordovician Hanson Creek Formation. This portion of the section contains all four units of the Devonian Popovich Formation including the Upper Mud, Soft Sediment Deformed, Wispy, and the Planar Laminated units. Moving eastward in the section, the Roberts Mountain Formation transitions from silty carbonates to platform carbonates of the Bootstrap Unit and the lower units of the overlying Popovich Formation thin against the Bootstrap. Drill hole GA-35C is the furthest west drill hole that intersects the Bootstrap Formation. Zones of dissolution brecciation are common in the upper Bootstrap especially near the contact with the Upper Mud unit. Nearer to the Meikle deposit, these breccias commonly host mineralization and are extensively altered. The breccia zones commonly contain abundant coarse calcite cement that is interpreted to post-date mineralization (Emsbo and Hofstra, 2003; Emsbo et al., 2003).

Figure 5.3 illustrates the geology for section B. The western portion of the section underlies a thick sequence of the Miocene Carlin Formation volcanics and has the typical sequence of Paleozoic sediments similar to Clydesdale area of section A. To the east of drill hole PD-20C, the upper plate assemblage is absent and lower plate carbonates are in direct contact with Carlin Formation. A thin sequence of the upper plate reappears in the middle of the section and then is absent again near the Post fault where it was likely eroded prior to and after deposition of the Carlin Formation. The Bootstrap Limestone Unit is absent on Section B, and the Devonian Popovich does not thin across the section as it does for Section A.

5.3.2 Structure

The structural setting of the Goldstrike area is detailed by Volk et al. (2001) and Bettles (2002). Figure 5.2 shows the salient structural features along the Clydesdale to Meikle section. Faulting is common along the cross-section and is dominated by northwest trending high angle faults that dip both east and west. Several faults are projected from the southern block of the Goldstrike property. In the western portion of the section, the Clydesdale anticline is the dominant feature and is cut by a series of high angle faults. The anticline brings the lower plate assemblage very near the present topographic surface. To the east of the Clydesdale anticline the stratigraphy ramps upwards toward Meikle. In the area of Meikle, extensive faulting drops the sequence down east of the Post fault and Post parallel faults. Ore at Meikle is hosted in fault controlled breccia units and intrusive dikes and is bounded by the Post fault system to the east, which places upper plate siliciclastic rocks in contact with the lower plate hosted deposit (Bettles, 2002).

Section B has a multitude of mapped high angle faults that cut stratigraphy. The north-northwest to west-northwest moderate amplitude Post anticline is believed to be an important control on Au mineralization along the northern Carlin-trend (Teal, 2002). In the eastern portion of Section B the east limb of the Post anticline is cut by the north-northwest trending Post fault zone and the west limb is dropped to the west by a series of north-northwest trending normal faults of moderate displacement (Bettles, 2002). Low angle reverse faults strike 290 to 030° (Bettles, 2002). The east dipping Post fault zone has normal displacement of 800-1,600 meters with pre- and post-Late Jurassic movement constrained by the Late Jurassic Goldstrike granodiorite stock (Bettles, 2002). Shallow dipping (25° to 45°W) north to northeast trending reverse faults are though to be related to the Antler orogeny similar to the RMT (Bettles, 2002). The western portion of the section is unconstrained owing to limited drill control and the lack of surface exposure.

5.3.3 Intrusives

Chapter 2 contains a description of intrusive dikes from the northern Carlin trend and the Banshee deposit. Ressel et al. (2006) further details the igneous geology of the northern Carlin trend. While not visible at the resolution of Figures 5.2 and 5.3, Jurassic lamprophyre dikes are common along both sections and generally follow the northwest structural trend of faulting. The dikes are variably altered in the western portion of the Sections A and B, but are commonly altered and mineralized nearer deposits (Barrick internal data). In the area of Meikle, Jurassic aged rhyodacites and Eocene rhyolites are common in addition to the Jurassic lamprophyres. The Goldstrike stock lies to the south of both cross-sections.

5.3.4 Mineralization

The only significant Au deposit along Section A is the Meikle deposit (7 Moz at ~24 g/t (Bettles, 2002)) at the eastern end of the section, but lower grade Au mineralization (<1.5 ppm from Barrick database) occurs over narrow intervals through much of the eastern portion of the section (Figure 5.4). The Golden April deposit lies off section just to the south of drill hole GA-35C (Figure 5.1). Pervasive alteration in the form of carbonate dissolution, silicification, clay alteration, and sulfidation is concentrated in the eastern part of the section as well (Barrick database). Carbonate dissolution and silicification is common in brecciated intervals of drill core through the lower Popovich and upper Bootstrap limestone, and these alteration zones are typically less than 10-20 meters thick away from Meikle (Barrick drill logs). In the western portion of the section, anomalous Au values are concentrated in narrow intercepts within lamprophyre dikes that were intruded along faults in the area of the Clydesdale anticline (Barrick database). Maximum Au concentrations in the Clydesdale area are <0.5 ppm, and alteration is limited to weak illite alteration of dike (Barrick drill hole logs).

Section B goes through extensively mineralized zones of the north Screamer deposit and north Post deposit (Figure 5.5). All drill holes east of PD-20C have mineralized intervals (Figure 5.5). Mineralization through Screamer has a strong stratigraphic control and is hosted primarily in the Wispy Unit of the Popovich Formation (Ye et al., 2003). Carbonate dissolution and silicification are less pervasive than other mineralized areas and show weak correlation with Au (Ye et al., 2003). The availability of carbonate minerals in mineralized zones within Screamer makes it a good candidate for isotopic alteration studies of carbonate minerals. De Almeida et al. (2010) noted that the Screamer deposit area had generally lower abundances of Carlin-type trace elements. However, Au grades at Screamer are similar to other deposits in the area (e.g. Betze-Post). To the west of Screamer, drill holes PD-20C and WM-01C contain low concentrations of Au (<1.0 ppm) at discrete intervals within the Popovich Formation (Figure 5.5).

5.4 Methods

For each drill hole on the cross sections, splits of assay pulps previously analyzed by Barrick for Au were collected. Samples were collected for all carbonate-bearing intervals within the Devonian Popovich and Silurian-Devonian Roberts Mountain Formations. Sampled intervals with significant calcite veining, >10-20%, were noted in order to account for their influence on the isotopic value of an individual pulp sample. In addition to the cross sections, 2 additional unmineralized drill holes were sampled from the western portion of the Goldstrike property. A total of 1658 samples were collected for analysis from 29 drill holes. This is the largest known dataset of $\delta^{13}C$ and $\delta^{18}O$ in carbonates collected for mineral exploration. In order to determine the average $\delta^{13}C$ and $\delta^{18}O$ values of host limestone well away from hydrothermal alteration, 15 limestone and dolostone 'background' samples were collected from a type section of the Paleozoic carbonate sequence located at Lone Mountain 145 km south of the northern Carlin trend and 27 km west-northwest of Eureka, NV (Figure 5.6). These samples were collected across stratigraphy to define the variability of stable isotope compositions in stratigraphically equivalent carbonates of Silurian-Devonian age. Lone Mountain is an area where 'lower plate' carbonates are exposed as a window through the 'upper plate' (Cook and Corboy, 2004). Carlin-type Au mineralization and alteration have not been identified in the Lone Mountain window, making it an ideal location for background sampling.

5.4.1 $\delta^{13}C$ and $\delta^{18}O$ Analysis

The analytical procedures of Barker et al. (2011) were followed for $\delta^{13}C$ and $\delta^{18}O$ stable isotope analysis of pulps samples. Samples were weighed out into clean gas tight 12 mL borosilicate vials and acidified with 85% H_3PO_4 for 1 hour at 72°C following the procedure of Barker et al. (2011). Repeat analyses of samples and standards were used to monitor the completeness of the carbonate dissolution reaction. The CO_2 created by reaction of the carbonate with the acid was then analyzed for $\delta^{13}C$ and $\delta^{18}O$ stable isotopes in rock carbonate using a Los Gatos Research Carbon Dioxide Isotope Analyzer. The isotope analyzer is based on off-axis integrated cavity output spectroscopy (OA-ICOS) using a tunable laser diode to measure the isotopologues of $^{12}C^{16}O^{16}O$, $^{13}C^{16}O^{16}O$, and $^{12}C^{16}O^{18}O$ simultaneously. Data correction was performed using an experimentally derived CO_2 concentration correction factor and comparison with internal lab standards with known values (Barker et al., 2011). All $\delta^{13}C$ data was standardized to Vienna Pee Dee Belemnite (VPDB) and $\delta^{18}O$ was standardized to Vienna Standard Mean Ocean Water (VSMOW). CO_2 concentrations measured by laser spectroscopy are reported in ppm. Measured CO_2 concentrations generated from dissolution of carbonate were converted to $\%CO_3$ for estimates of the carbonate content of individual samples.

A subset of samples was selected for analysis by conventional methods using the Delta Plus isotope ratio mass spectrometer (IRMS) at the isotope lab at University of New

Mexico under the supervision of Zach Sharpe. Chapter 3 describes conventional $\delta^{13}C$ and $\delta^{18}O$ stable isotope analysis in detail.

Stable isotope studies at the Banshee Au deposit concentrated on analyses of micro-drilled rock calcite and calcite veins. The rationale behind micro drilling was to avoid contamination of different generations of carbonate cements with varying isotope values. One of the findings of the Banshee study is that isotopic alteration is typically pervasive and results in the depletion of $\delta^{18}O$ isotopes on a bulk scale. As part of the pulp study presented in this chapter, pulp samples were analyzed for $\delta^{13}C$ and $\delta^{18}O$ isotopes from the intervals corresponding to micro-drilled data for a subset of samples.

5.4.2 Trace Element Geochemistry

Subsets of 524 samples from eight drill holes along Section A and 243 samples from 3 drill holes along Section B were selected for aqua regia digestible trace element geochemistry. Sampling concentrated on distal drill holes to define the extent of trace element metasomatism at Goldstrike and its relation to $\delta^{18}O$ alteration. Samples underwent an aqua regia digestion and 51-element analysis by ICP-MS and ICP-AES at ALS Chemex in North Vancouver, Canada (see Appendix A for detailed method description, list of analytes, and method detection limits). Duplicate analyses were performed on a subset of 10 samples, and 2 samples with known compositions were analyzed. An additional 48 samples from Section B were analyzed for four-acid digestible trace element geochemistry. Samples underwent four-acid digestion and 49-element analysis by ICP-MS and ICP-AES at ALS Chemex (see Appendix A for full method description, list of analytes, and method detection limits). The purpose of analyzing aqua regia digestible geochemistry and four-acid digestible geochemistry was to evaluate variance between aqua regia data with data produced from a more aggressive digestion.

5.5 Results

5.5.1 $\delta^{18}O$ Background

Both regional and local background samples were collected as part of this thesis. As introduced in Chapter 3, regional samples were collected from Lone Mountain near Eureka, NV (Figure 5.6). A total of 14 samples were analyzed from Ordovician Pogonip, Ordovician Hanson Creek, Silurian-Devonian Roberts Mountain Formation, Devonian Lone Mountain dolomite, and the Devonian Nevada Group (Table 5.1). The sample of Ordovician Pogonip has a $\delta^{18}O$ isotope value of 18.8‰ ±0.3. Ordovician Hanson Creek has an average $\delta^{18}O$ isotope value of 25.4‰ ±0.2. Silurian Devonian Roberts Mountain Formation has an average $\delta^{18}O$ isotope value of 26.4‰ ±0.8. Devonian Lone Mountain dolomite has an average $\delta^{18}O$ isotope value of 24.6‰ ±0.2. Devonian Nevada Group has an average $\delta^{18}O$ isotope value of 26.7‰ ±0.6. These values are within the range of values reported for Paleozoic marine carbonates worldwide (Veizer et al., 1999).

Local background samples from the Goldstrike area were collected from 5 distal drill holes (CD-15C, CD-96-9, DR-1C, GA-12CR, and WM-01C) on Barrick's Goldstrike property. Owing to the pervasive alteration at the Goldstrike property it is difficult to define true background values for isotopes (Figure 5.7). Even distal drill holes have intervals of material depleted in $\delta^{18}O$ compared to regional samples. However, the degree of isotopic depletion in distal drill holes is relatively low. Sampled intervals with little to no depletion have average $\delta^{18}O$ values of 25.5‰ ±1.0 for the Devonian Popovich and 23.9‰ ±1.1 for silty limestone of the Roberts Mountain Formation. Local $\delta^{18}O$ background values for the Bootstrap limestone are 25.2‰ ±1.0 consistent with unaltered drilled $\delta^{18}O$ values from the Banshee deposit (see Chapter 3). The similarity between local and regional background samples indicates that $\delta^{18}O$ background values for Silurian-Devonian marine carbonates in the study area are relatively uniform. The slightly lower values reported for local background likely reflects minor, heterogeneous alteration of rocks by hydrothermal fluids.

5.5.2 Isotopes

The complete isotope dataset is presented in Appendix F. Figure 5.8 is a scatter and data density plot of $\delta^{13}C$ and $\delta^{18}O$ isotope data. The majority of $\delta^{13}C$ data ranges from -3.0 to 3.5‰. The majority of $\delta^{18}O$ data ranges from 10 to 27‰. The lack of correlation between $\delta^{13}C$ and $\delta^{18}O$ (R^2=0.13) is typical for isotope analysis of rock carbonate in Carlin-type Au systems although both Twin Creeks and Pipeline exhibit some $\delta^{13}C$ depletion with $\delta^{18}O$ depletion (Arehart and Donelick, 2006; Stenger et al., 1998b) while Alligator Ridge has enrichment in $\delta^{13}C$ with $\delta^{18}O$ depletion (Ilchik, 1990) (see Chapter 3). Figure 5.8 seems to show moderate depletion in $\delta^{13}C$ with $\delta^{18}O$ depletion; however, the scale of $\delta^{13}C$ depletion is much less. Variable depletion in $\delta^{18}O$ is consistent with $\delta^{18}O$ analyses of micro-drilled carbonate matrix from the Banshee deposit.

Patterns of isotopic depletion for select drill holes on Section A are shown in Figure 5.9. The scale of $\delta^{18}O$ depletion is variable across both sections, but there are significant trends (Figure 5.10). In the western portion of Section A there is a distinct $\delta^{18}O$ depletion trend. The average down hole $\delta^{18}O$ value decreases steadily from west to east in the Clydesdale region. The region of greatest depletion is in drill hole CD-96-2C. East of CD-96-2C, $\delta^{18}O$ values increase slightly in drill hole CD-95-3. This area of depletion is centered along high angle faults that likely focused fluid flow (Figure 5.2). To the east of the CD-95-3, the Roberts Mountain Formation transitions from silty limestone to the more massive Bootstrap limestone. East of the Bootstrap facies change, depletion occurs primarily within discrete intervals of 80-120 feet (24-37 m) and is controlled by stratigraphy (Figure 5.9). Many of the depleted intervals are hosted within intervals of brecciated limestone of the Popovich and Bootstrap limestone. Nearer the Meikle deposit, significant alteration resulting in carbonate contents less than 1 wt% carbonate thus stable isotope analysis was not possible. Many of the depleted zones near Meikle are hosted in the Upper Mud Unit and breccia.

Figure 5.11 shows the patterns of isotopic depletion for select drill holes on Section B. Drill hole WM-01C at the western extent of Section B shows only slight depletion and is closer to background with respect to $\delta^{18}O$ depletion. To the east of WM-01C, all the sampled drill holes have variably depleted $\delta^{18}O$ values. Similar to Section A, average down hole $\delta^{18}O$ values decrease from west to east (Figure 5.12). In Section B, drill hole SJ-390C has the most depleted average $\delta^{18}O$ values. West of SJ-390C, average $\delta^{18}O$ values increase in drill hole SJ-464C; although, $\delta^{18}O$ values in SJ-464C are still depleted relative to background. The west to east trend in $\delta^{18}O$ is consistent with the trend for Au along Section B (see Figure 5.5). Depletion occurs across the sampled stratigraphy throughout the Popovich and into the Roberts Mountain Formation. However, there are discrete zones of less depleted materials within mineralized material indicating that fluid flow and/or fluid/rock interaction was not uniform through stratigraphic units.

In addition to the stable isotope data, drill holes for Section B were evaluated for inorganic carbonate content. Carbonate content was calculated from CO_2 concentrations measured during isotope analyses. Figure 5.11 shows the variation in carbonate content down drill holes. Two potential sources of variability in carbonate content are primary lithological variation and removal or addition of carbonate by a fluid. There are intervals where $\delta^{18}O$ correlates to lower carbonate content indicating that $\delta^{18}O$ depletion in these intervals occurred with carbonate dissolution. However, there is no uniform relationship between $\delta^{18}O$ and carbonate content. Previous authors have shown poor correlation between degree of carbonate dissolution and other alteration indicators at the Screamer deposit (Ye et al., 2003).

5.5.3 Micro-drilling Versus Pulp Sampling

Comparison of results from micro-drilled samples with pulp samples indicates that the scale of depletion is sufficient to be expressed in pulp samples. Figure 5.13 plots drilled isotope data from discrete intervals against pulp isotope data from 1.5 to 6 meter intervals. In background areas, pulp and drilled data show good correlation (Fig 5.12). This indicates that very little alteration occurred on both the micro and bulk scale. In altered zones the correlation between drilled and pulp data shows greater variability. Some of the pulp data may have carbonate vein contamination, but much of the variability is likely owing to the different scales of sampling.

5.5.4 Geochemistry

Similar to $\delta^{18}O$, trace element background values were established using both regional samples from Lone Mountain and local samples from distal drill holes on the Goldstrike property. Table 5.2 lists average and standard deviations for regional and local background samples for the suite of Carlin-type pathfinder elements. Regional background values are from samples collected from Lone Mountain. Local background is difficult to constrain owing to the variable trace element content of distal drill holes. However, trace element concentrations from DR-1C and WM-01C are similar to other reported background values from the northern Carlin trend (Heitt et al., 2003). In general, concentrations of Carlin-type pathfinder elements in local background rocks are an order of magnitude higher than in the regional background samples. The relative enrichment of local background is likely due to the multiple metasomatic events in the northern Carlin trend's history and the broad dispersion of trace elements in the region (Emsbo et al., 2006). Syn-sedimentary pyrite common in the Popovich Formation contains significantly elevated concentrations of trace elements including elements commonly associated with Carlin-type mineralization in Devonian Popovich rocks (Large et al., 2009). Additionally, the Jurassic Goldstrike Stock is associate with significant As enrichment within calc-silicate rocks immediately to the south of the Goldstrike section. Without clear discriminators between pre- and syn-mineralization trace element enrichment is difficult to define the true extent of trace element enrichment associated with Carlin-type mineralization. Therefore, it is likely inappropriate to use the regional background samples from Lone Mountain as a baseline on the Goldstrike property. Rather than using absolute background values, this study uses threshold values defined as the average plus standard deviation from the local background samples. Local threshold values are provided in Table 5.2.

Data from aqua regia geochemistry is presented in Appendix G. Only 7 samples collected from Section A have aqua regia digestible Au concentrations greater than the method detection limit (MDL) of 0.2 ppm, while a total of 35 samples have fire assay concentrations >0.2 ppm Au (Barrick internal data). The lack of Au in aqua regia analyses is likely owing to the carbonaceous (graphite or reduced carbon) nature of the ore in the Goldstrike property. Several of the typical pathfinder elements are commonly above threshold values including Ag, As, Hg, Sb, Tl, and W. Concentrations of Te are near the threshold value for a majority of samples. Correlation between trace elements was determined by calculating correlation coefficients for the sample population (n=524). Using a sample population >500, correlation is statistically significant at r>0.115 at the 99% confidence level (Sachs, 1984). The correlation matrix in Table 5.3 shows the correlation of trace elements with Au fire assay concentrations with Mn having the highest correlation (r=0.39). The highest correlation between Carlin-type pathfinder elements is Hg with Tl (r0.77). The calculated correlation coefficients show that when Au is elevated the typical suite of Carlin-type pathfinders is elevated as well, including As, Hg, Sb, Tl, and W (Figure 5.14). Arsenic is generally the most broadly dispersed element in Carlin-type Au systems and increases in As correspond to increases in the other pathfinder elements at Goldstrike

(Figure 5.14). Additionally, increasing concentrations in Au and pathfinders corresponds to depletion in $\delta^{18}O$ and increases in Mn (Figure 5.14) consistent with the finding in Chapter 3 that Mn enrichment accompanies alteration with new calcite growth. Hofstra et al. (2011) noted a similar increase in Mn in their geochemistry study of the north Screamer deposit.

Like $\delta^{18}O$, pathfinder elements are enriched in the area of the Clydesdale anticline on section A. Figure 5.15 are down hole plots showing the spatial relationships between $\delta^{18}O$, Au, Ag, As, Hg, Sb, and Tl. Concentrations of key pathfinder elements increase with depth in CD-14C, CD-96-2C, and CD-95-3 (Figure 5.15). To the east of the Bootstrap facies change, pathfinder elements also show enrichment patterns similar to $\delta^{18}O$ depletion indicating enrichment is focused along more permeable lithologies. These enriched intervals correspond to zones of brecciation and faulting (from Barrick drill logs) where permeability is increased. For many of the sampled drill holes $\delta^{18}O$ and trace elements show similar patterns, however, they are poorly correlated within some intervals.

Samples analyzed for aqua regia and 4-acid digestible geochemistry show consistent high correlation for concentration measured by both methods for most elements. Both aqua regia and 4-acid digestions are capable of near total digestion of sulfide minerals, and since sulfide minerals host the bulk of Carlin-type trace elements, it is not surprising that strong correlations between the data sets exist. Sb and Tl exhibit lower correlations at high concentration (Figure 5.16). Issues with high concentration of Sb and Tl are likely due to matrix interferences during analysis and/or the inclusion of these trace elements in mineral phases not completely digested by aqua regia. Tl is known to occur in potassium silicate minerals such as illite (Gemmell, 2007), and the presence of Tl in illite would explain the poor correlation between aqua regia and 4-acid digestion. Aqua regia is not effective at dissolving more resistive minerals such as silicates (as indicated by poor correlations in elements such as K and Rb).

5.6 Interpretation

5.6.1 Relationship Between $\delta^{18}O$ Depletion and Au Mineralization

$\delta^{18}O$ isotope data is consistent with variable depletion of rock carbonate by a hydrothermal system as $\delta^{18}O$ values are too low to be caused by primary stratigraphic changes related to changes in oceanic water (Veizer et al., 1999). Furthermore, the range in isotopic depletion is consistent with observed $\delta^{18}O$ depletion in other Carlin-type Au systems (Arehart and Donelick, 2006; Cline and Hofstra, 2000; Emsbo et al., 2003; Hofstra and Cline, 2000; Nutt and Hofstra, 2003; Radtke et al., 1980; Stenger et al., 1998b; Yigit, 2001). Proportional variation between Au and $\delta^{18}O$ is absent. However, the lack of a linear correlation between Au and $\delta^{18}O$ is not surprising. For a strong linear correlation, the degree of isotopic alteration would have to be proportional to the addition of Au. $\delta^{18}O$ is a proxy measurement of fluid-rock interaction, but higher fluid-rock ratios do not necessarily lead to proportionately greater Au deposition. Specific physiochemical conditions for dissolution/precipitation reactions for calcite are required for isotopic exchange to occur (see discussion in Chapter 3), whereas Au is thought to precipitate as a consequence of Fe-sulfidation reactions. If there were insufficient reactive Fe available in the wall rock, Fe-sulfidation reactions would not occur. Additionally Barker et al. (2009) found that Au precipitation only occurred at discrete intervals within the hydrothermal fluid system. Another issue that could affect the strength of linear correlation is the presence of pre-Carlin Au enrichment. Hofstra et al. (2011) propose that areas of Au enrichment without $\delta^{18}O$ depletion and significant Carlin-type trace element alteration are not related to Carlin-type mineralization, but rather, are representative of syn-genetic Au enrichment similar to that described by Emsbo (1999).

Spatially, the correlation between Au enrichment and $\delta^{18}O$ depletion are evident. Figures 5.4 and 5.17 show the spatial extent of both anomalous Au and $\delta^{18}O$ depletion on the Clydesdale-Meikle section, and Figures 5.5 and 5.18 show the spatial extent of Au and $\delta^{18}O$ depletion on section B. On the Clydesdale-Meikle section, the only contiguous ore-grade mineralization is found within the Meikle deposit at the eastern part of the section. The footprint of the Meikle ore body sits within a narrow zone along the Post fault (Figure 5.2).

Anomalous Au enrichment (>0.2 ppm) extends to the west along the Bootstrap-Popovich contact for approximately 2 km, but $\delta^{18}O$ depletion extends a further approximately 1.5 km (a total of ~3.5 km west of Meikle) to the west of Au anomalism. The extended footprint of $\delta^{18}O$ depletion relative to Au enrichment is consistent with the model presented in Figure 3.21.

5.6.2 Trace Element Enrichment

Most trace element studies along the Carlin trend have focused on trace element enrichment within and peripheral to deposits and have found significant correlation (R^2>0.5) between Carlin-type pathfinder elements (Albino, 1994; de Almeida et al., 2010; Emsbo et al., 2003; Fortuna et al., 2003; Heitt et al., 2003; Kesler et al., 2003; Kuehn and Rose, 1992). The samples collected in this study represent the more distal chemical signature of the hydrothermal system. The low correlation coefficients between Au pathfinder trace elements (As, Hg, Sb, Tl, and W) in this study indicate a lack of proportional enrichment in trace elements at the distal extents of fluid flow, although, the suite of Carlin-type pathfinder elements are commonly above threshold values in holes distal to mineralization. These zones of trace element enrichment spatially correspond to $\delta^{18}O$, and are appropriate tracers of Carlin-type hydrothermal fluid flow. De Almeida et al. (2010) found that Tl and Hg were the best tracers for Au in the proximal parts of the hydrothermal system. It is difficult to ascertain which trace element is the best tracer of Au distal to mineralization as the entire suite of pathfinder elements are variably enriched along the Clydesdale to Meikle section (Figure 5.15). Further sampling and trace element analysis are needed to establish the best tracer of Au distal to mineralization.

5.6.3 Relationship Between $\delta^{18}O$ and Trace Element Geochemistry

Table 5.3 shows correlation coefficients between $\delta^{18}O$ and trace elements collected with this study. A total of 760 samples were used for calculating the correlation coefficients. With such a large dataset the level of correlation considered significant at the 99% confidence level is r=0.093 (Sachs, 1984). Depletion in $\delta^{18}O$ and enrichment in pathfinder elements will result in a negative correlation coefficient. Several pathfinder elements including Ag, As, Au, Hg, Mn, Sb, and Tl have negative correlation with $\delta^{18}O$ greater than the critical value (0.093) indicating a statistically significant relationship between $\delta^{18}O$ alteration and trace element alteration.

Spatial plots of Au, pathfinder elements, and $\delta^{18}O$ show that anomalous populations are coincident with one another. Figure 5.15 shows a series of depth profiles for drill holes sampled for both $\delta^{18}O$ and aqua regia geochemistry. The plots show similar relative enrichment and depletion patterns for $\delta^{18}O$ and pathfinder elements. In the western portion of the cross-section the convergence of trace element enrichment and $\delta^{18}O$ depletion indicates that extensive high angle faulting associated with the Clydesdale anticline were strong controls on hydrothermal fluid flow in the area. Spatial patterns of enrichment in trace elements and depletion in $\delta^{18}O$ indicate that fluid flow was pervasive along these high angle faults (likely reflecting enhanced permeability). To the east, both $\delta^{18}O$ and trace element anomalies again show similar patterns spatially. The depth profile of drill hole GA-35C shows consistent patterns of enrichment and depletion between trace elements and $\delta^{18}O$ isotopes (Figure 5.15).

5.6.4 Pervasive Versus Focused Fluid Flow

When plotted in space, the $\delta^{18}O$ isotope data indicates the primary controls on fluid flow are faults and stratigraphy. In the western portion of the section, isotopic depletion is focused along or near faults associated with the Clydesdale anticline (Figure 5.17). The data indicates that fluid flow in this area was pervasive at the scale of sampling and exploited the enhanced permeability surrounding faults and the intrinsic primary permeability of silty carbonates of the Silurian-Devonian Roberts Mountain Formation and overlying Devonian Popovich.

East of the facies change between silty carbonates of the Roberts Mountain Formation and massive carbonates of the Bootstrap limestone, fluid flow is focused along zones of increased permeability (typically the breccia at the top of the Bootstrap Limestone). These zones are commonly altered and associated with varying degrees of Au enrichment (Figure 5.4). The spiky nature of isotopic depletion in drill hole GA-35C (Figure 5.15) is a good example of the depletion patterns on the east side of the facies change. The Bootstrap limestone exhibits low permeability compared to the silty carbonates to the west. However, brecciated zones of increased permeability are common. The isotope data is consistent with fluids exploiting relatively narrow and more permeable zones in the Bootstrap. Trace element enrichment of Ag, As, Hg, Sb, and Tl show similar patterns to the $\delta^{18}O$ depletion in GA-35C (Figure 5.15).

5.7 Discussion

5.7.1 Micro-drilling Versus Pulp Sampling

One of the key concerns expressed in the Banshee isotope study (Chapter 2) was the impact of post mineral carbonate veining, as it can dilute the isotopic signature of hydrothermally altered carbonate in the wall rock. The other reason for micro-drilling is to define the isotopic variation of individual veins and vein sets. While vein data was important for Chapters 3 and 4, in this chapter the focus is on defining larger zones of depletion through the use of bulk sampling. If the amount of carbonate veining can be estimated through normal drill hole logging procedures, the degree of dilution by veining may be accounted for. Simple mass balance calculations can be used to determine the effect of vein dilution if the amount of vein material contained in a sample is known and the isotopic values of the carbonate veins are known.

The example presented in Figure 5.19a shows that a 30 cm zone of $\delta^{18}O$ alteration and 15 cm zone of trace element enrichment will have a minimal effect on the bulk value over a 2-meter sample interval. Figures 5.19b-c are calculated curves that define the fraction of altered rock within a bulk-sampled interval necessary for the bulk $\delta^{18}O$ and trace element values to exhibit alteration. The main controls on the expression of alteration on a bulk scale are the fraction of altered material and the $\delta^{18}O$ and/or trace element values associated with the altered material. If the altered material has highly depleted $\delta^{18}O$ values it will show alteration on the bulk scale at lower fractions of altered rock than altered material with less depleted $\delta^{18}O$ values. Using the conceptual model presented in Figure 5.19a, micro-drilled samples collected from altered zones would be more effective at defining discrete alteration. However, if samples were micro-drilled outside the relatively narrow alteration zone they would yield background values. In cases where the fraction of altered material is high it is more appropriate to sample larger intervals, as they will represent a more statistically accurate REV.

The effects of vein contamination are a concern when analyzing isotopes in assay pulps. Micro-drilled calcite veins at Banshee gave low $\delta^{18}O$ values consistent with precipitation from cool unexchanged meteoric waters (see Chapter 3). Figure 5.20 shows the effects of vein contamination on bulk isotope values when carbonate veins at 5 ‰ (approximate value for late stage calcite veins from Chapter 3) are mixed with unaltered rock carbonates of 24 ‰ at different proportions. When vein material with a value of 5 ‰ exceeds 20% of the sampled carbonate in a sample, the bulk $\delta^{18}O$ value will fall below 20 ‰ and $\delta^{18}O$ alteration will be apparent. It is important to document the amount of veining collected from a bulk sample so that false results can be identified. Sampling intervals where veins represent greater than 20 % of the carbonate has the potential to produce misleading results and should be avoided when possible. Veining is typically noted during drill hole logging and should serve as a guide for sampling and data interpretation.

5.7.2 Vectoring and Haloes

Data collected from assay pulp samples as part of the Goldstrike district study show that the spatial correlation between Au enrichment, $\delta^{18}O$ isotopes, and trace elements is more robust than linear numerical correlation. Depth profiles of Ag, Hg, Sb, and Tl show enrichment patterns similar to Au and $\delta^{18}O$ isotopes (Figure 5.15). Plotted in space, the data indicates that the flow path for fluids responsible for Au enrichment, $\delta^{18}O$ depletion, and trace element enrichment was co-spatial. The data cannot resolve whether or not the same fluid was responsible for the observed data. However, the coincidence of the spatial patterns argues for a common genesis. Even if the multiple fluids were involved for the observed patterns, the fact that the same fluid pathways were exploited indicates that $\delta^{18}O$ and trace elements are effective tools for vectoring fluid flow on the sampled scale. The depletion patterns down drill holes reveal additional information regarding fluid flow. Figures 5.21 and 5.22 are schematic diagrams illustrating pervasive versus channelized fluid flow and the effect on down hole isotopic depletion profiles. These profiles are representative of flow regimes common in Carlin-type deposits. Using this conceptual framework the paleo-permeability structure of hydrothermal fluid flow can reveal the relative position of a drill hole along a fluid flow path. Down hole alteration patterns in individual drill holes may be characteristic of distal, proximal, or mineralized portions of the ore system. Additionally, the presence of background $\delta^{18}O$ values in distal drill holes puts a boundary on isotopic depletion and allows for the determination of the sides of isotopic haloes on a deposit scale. With sufficient sample density, the data can provide 3D imaging of isotopic haloes that could help the evaluation of fluid flow pathways along faults, dikes, and stratigraphy. A potential complication to the simplified schematic diagrams is the effect of overlapping alteration caused by multiple upflow zones along the fluid flow path. Overlapping $\delta^{18}O$ alteration could complicate the interpretation of $\delta^{18}O$ depletion patterns by creating multiple zones of highly depleted calcite along the flow path making it difficult to vector down the length of the flow path. In order to interpret complex alteration patterns it is important to understand the structural framework of a deposit area and the controls on the permeability network.

Vectoring down fluid flow paths could be an effective exploration tool. Figure 5.23 shows the down hole alteration patterns in sampled drill holes along section B and has broad consistencies with the conceptual diagram presented in Figure 5.21. Distal drill holes show moderate to low $\delta^{18}O$ alteration while the frequency and degree of $\delta^{18}O$ alteration increases in drill holes proximal and within mineralization. Nearer mineralization intense carbonate dissolution is evident by intervals with insufficient carbonate for $\delta^{18}O$ analysis. Using the conceptual framework presented in Figure 5.21 distances between distal (weak to no Au anomalism), proximal (strong Au anomalism) and Au mineralized zones at Goldstrike can be estimated. Figure 5.23 indicates that the distance between distal and proximal zones at Goldstrike are on the order of ~1 km, and the distance between mineralized and proximal samples is ~0.5 to 1 km. The distances represent haloes well outside of ore grade Au mineralization and could be used as a framework for vectoring fluid flow toward mineralized zone in carbonate hosted Carlin-type Au systems.

While trace element data shows similar patterns to $\delta^{18}O$ depletion, additional factors complicate the interpretation of trace element data related to Carlin-type mineralization. Individual Carlin-type Au deposits are variably enriched in many trace metals including Te, Cu, W, Mo, Se, Fe, Ag, Pb, Si, Ba, Cs, and Zn and consistently enriched in S, As, Au, Sb, Hg, and Tl (Cline et al., 2005). Before employing trace element vectoring in Carlin-type Au deposits, the specific chemical components associated with mineralization need to be identified. The lack of significant linear correlation between typical Carlin-type pathfinder elements in this study makes it difficult to define the specific chemical components associated with Carlin-type hydrothermal system at Goldstrike. De Almeida et al.'s (2010) determination that elemental associations change for different parts of the ore system at Goldstrike may explain the lack of correlation seen in the property-wide dataset presented in this chapter. Detailed studies of trace element metasomatism (e.g. Chapter 2 of this thesis) are likely more appropriate for evaluating trace element fluxes associated with Au mineralization. An additional problem is the difficulty in establishing appropriate background concentrations for trace elements. This study shows that at the distal extents of hydrothermal fluid flow, the magnitude of trace element enrichment can be low. Differentiating trace element enrichment from background becomes more important at low concentration and introduces greater uncertainty. A final concern in using trace elements in Carlin-type systems in Nevada is the occurrence of syn-sedimentary trace element enrichment (Emsbo et al., 1999; Large et al., 2009). While many of the syn-sedimentary suite of elements are not generally found in association with Carlin-type mineralization, As, Se, Ag, Zn, and Au are commonly associated with both the syn-sedimentary and Carlin-type event (Large et al., 2009).

Trace element sampling at Goldstrike was not sufficient to define the extent of lateral alteration haloes for Carlin-type metasomatism. However, down hole alteration in drill holes sampled for trace elements and $\delta^{18}O$ in carbonate provide some insight into the potential spatial relationships between $\delta^{18}O$ and trace element haloes. In the area of the Clydesdale anticline along the section A, drill holes exhibit both $\delta^{18}O$ depletion and trace element enrichment with Au values below background. The lack of Au mineralization in these drill holes indicates that they are outside of the Au mineralization halo. Figure 5.24 shows the down hole variation in $\delta^{18}O$, Ag, As, Hg, Tl, and Sb for drill hole CD-96-2C. Using background values for each chemical component to define the threshold at which alteration occurs, $\delta^{18}O$ alteration is the first indicator of hydrothermal alteration. Carlin-type pathfinder elements Hg and Sb are consistently enriched above background concentrations a further ~200 meters down the drill hole and anomalous Au occurs at ~100 meters below the first appearance of anomalous trace elements. In this example from the Clydesdales area, $\delta^{18}O$ forms an alteration halo well above trace element haloes and is the first down hole signal of hydrothermal alteration potentially associated with a Carlin-type Au system.

Several of the problems associated with trace element studies may be avoided when employing $\delta^{18}O$ in rock carbonates. The data from this study and the detailed study of the Banshee deposit show a range of values consistent with alteration by a hydrothermal fluid, and the degree of isotopic depletion is similar in both the near and far field. Additionally, background values for $\delta^{18}O$ isotopes in Devonian marine carbonates are well established (Veizer et al., 1999). In addition to the published background data, regional background samples collected from Lone Mountain near Eureka, NV have consistent values of 24-26.5‰ (VSMOW). Background values of essentially homogeneous composition increase the resolution of depletion patterns, and improve the accuracy of interpretation. Finally, syn-sedimentary enrichment will have little influence on $\delta^{18}O$ values. Several samples in this study show enrichment in syn-sedimentary related trace elements with no associated $\delta^{18}O$ depletion. Owing to the improved resolution of $\delta^{18}O$ isotopes over trace elements, $\delta^{18}O$ may be a better tool for vectoring hydrothermal fluid flow associated Carlin-type Au deposits.

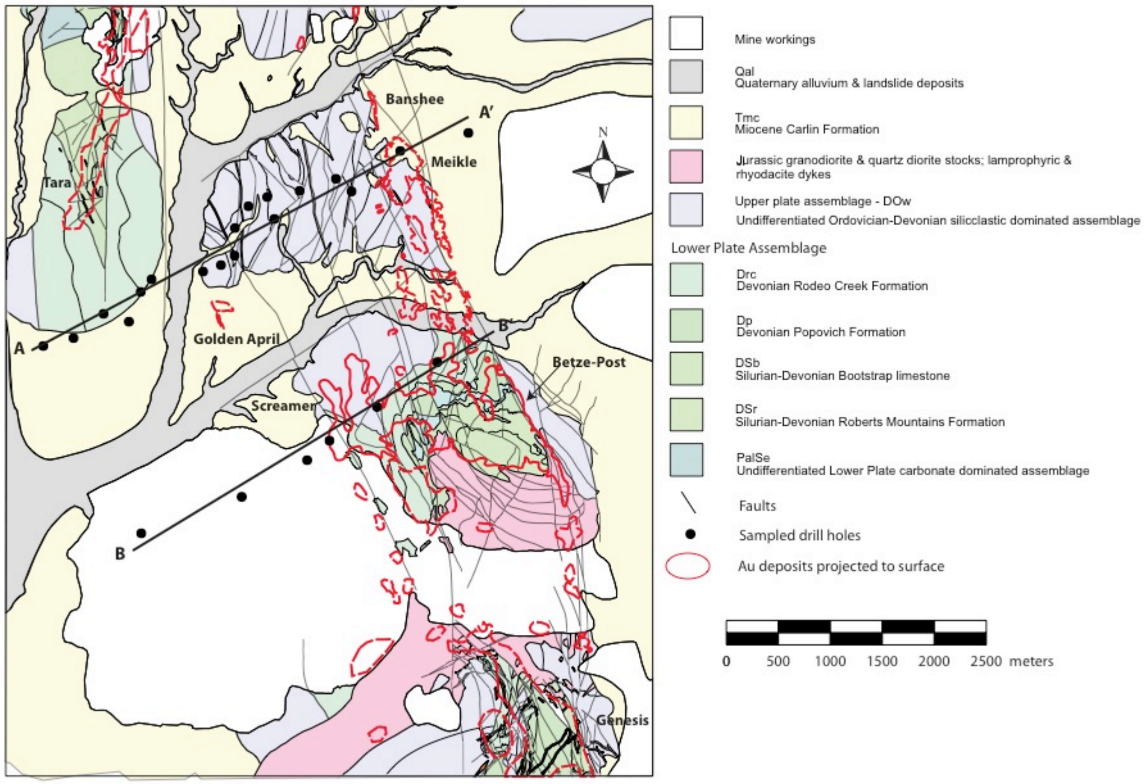

Figure 5.1 Geology map of the northern Carlin trend showing the distribution of known Au deposits and the location of the 2 cross sections of drill holes used in this study. The Golden April, Screamer, Betze-Post, Meikle, and Banshee deposits are labeled for reference. Data used to generate geology map from Thompson (2002).

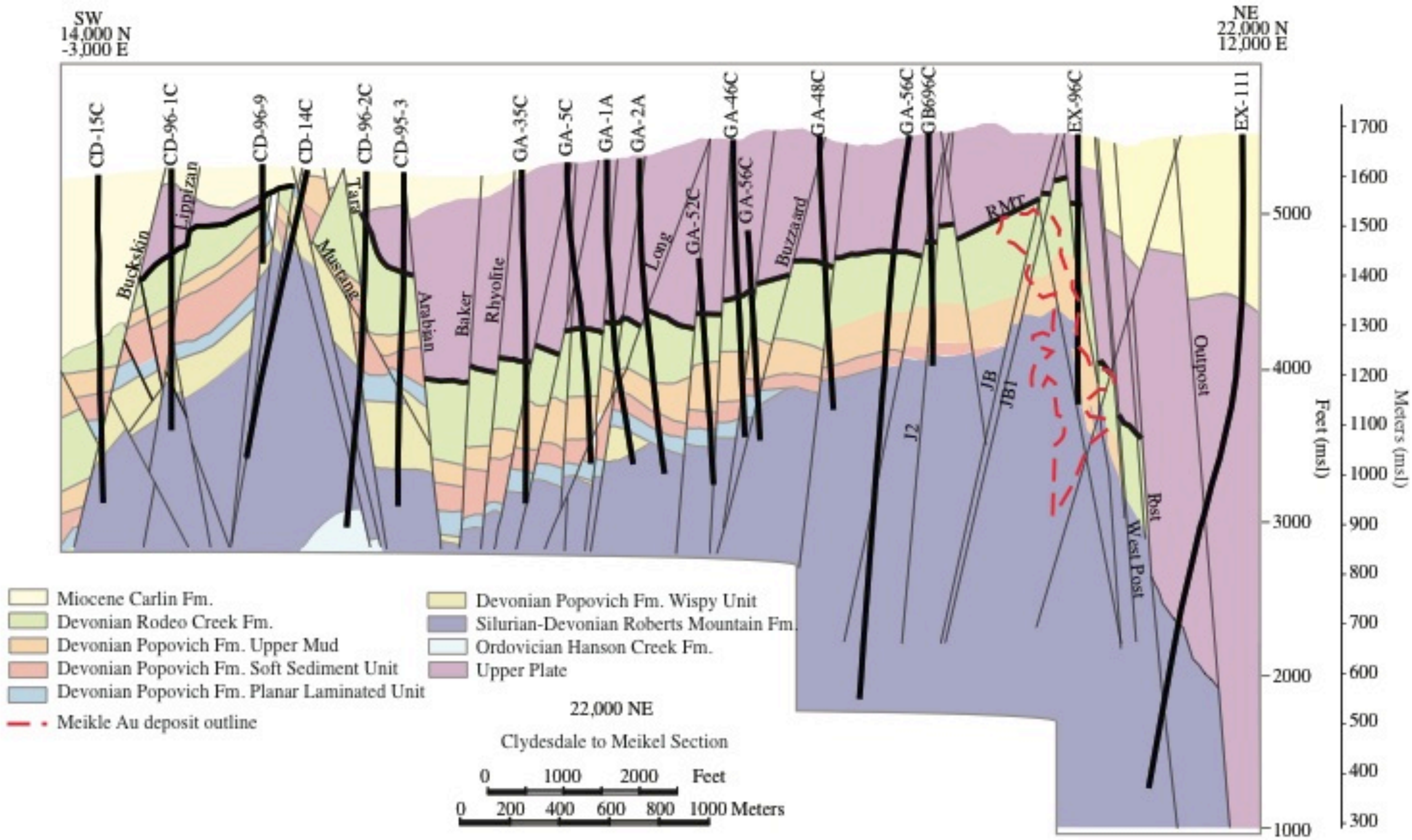

Figure 5.2 Geology of Section A showing the distribution of drill holes and structures with 2x vertical exaggeration. Modified from internal Barrick study.

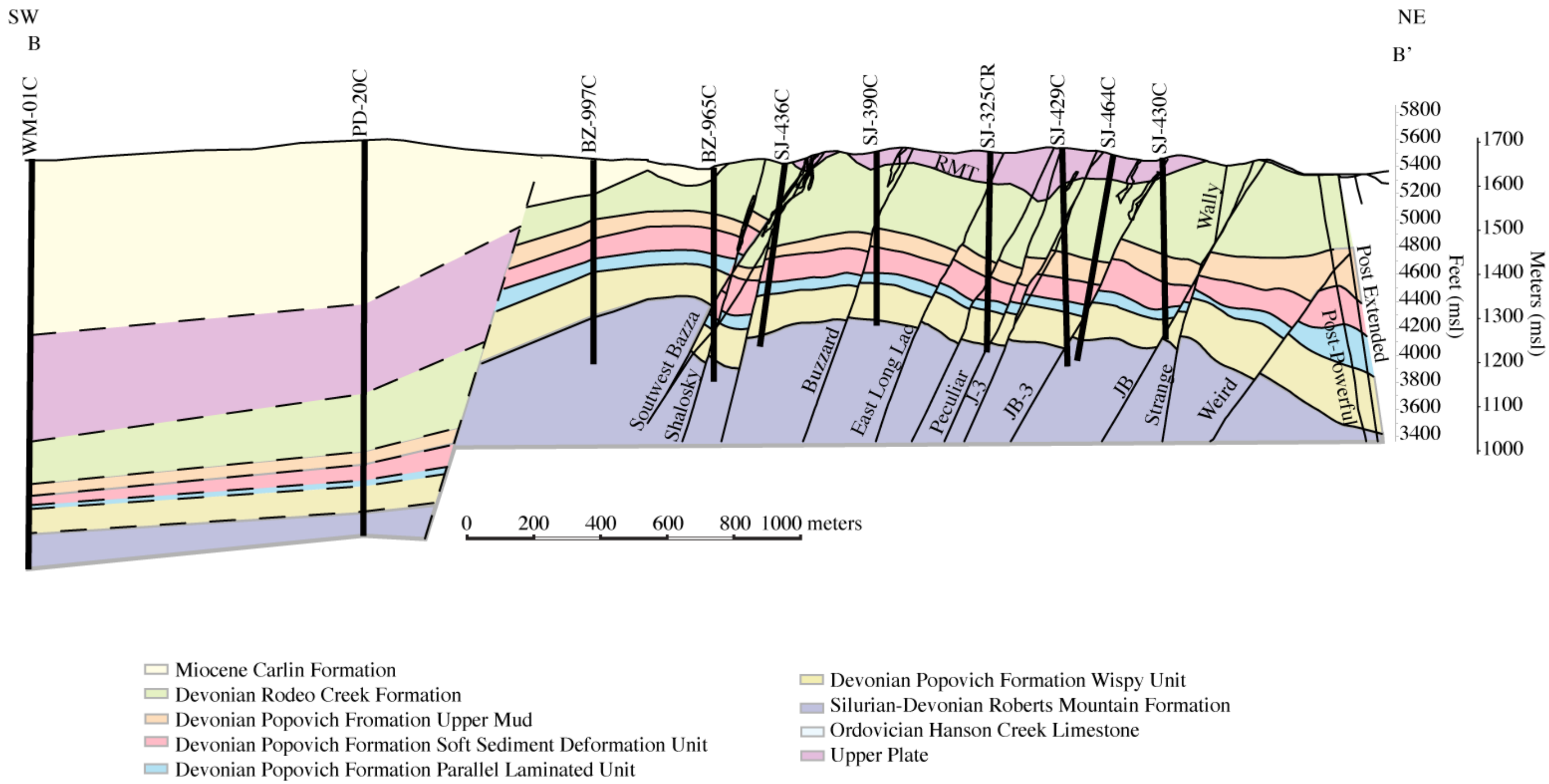

Figure 5.3 Geology of Section B showing the distribution of sampled drill holes and structure. Modified from Barrick geology modeling. Dashed fault and stratigraphy in the western portion of the section represent areas outside of current modeling. The lack of good drill control to the west makes the geology in the west area of the section poorly constrained based on the Barrick logs of the 2 western drill holes. The inferred fault that drops stratigraphy to the west has not been modeled or mapped and is interpreted here to account for the change of depth in stratigraphy.

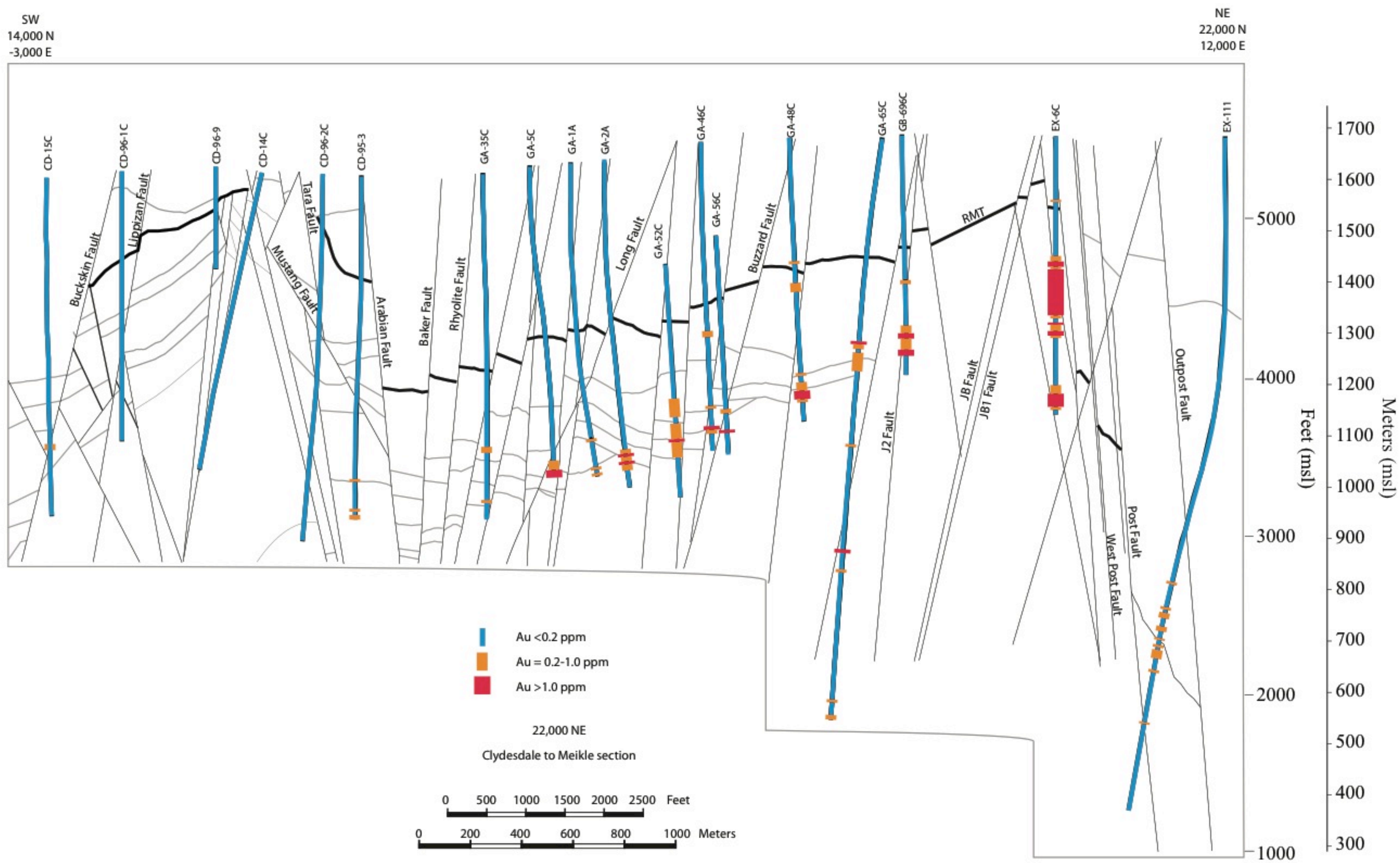

Figure 5.4 Cross-section A showing the distribution of Au intercepts in sampled drill holes (Au fire assay data provided by Barrick Gold Exploration). Au data is collected on 5 foot splits within the ore zone, and 20 foot chip assays outside of ore. Au concentrations are highest to the east nearer Meikle.

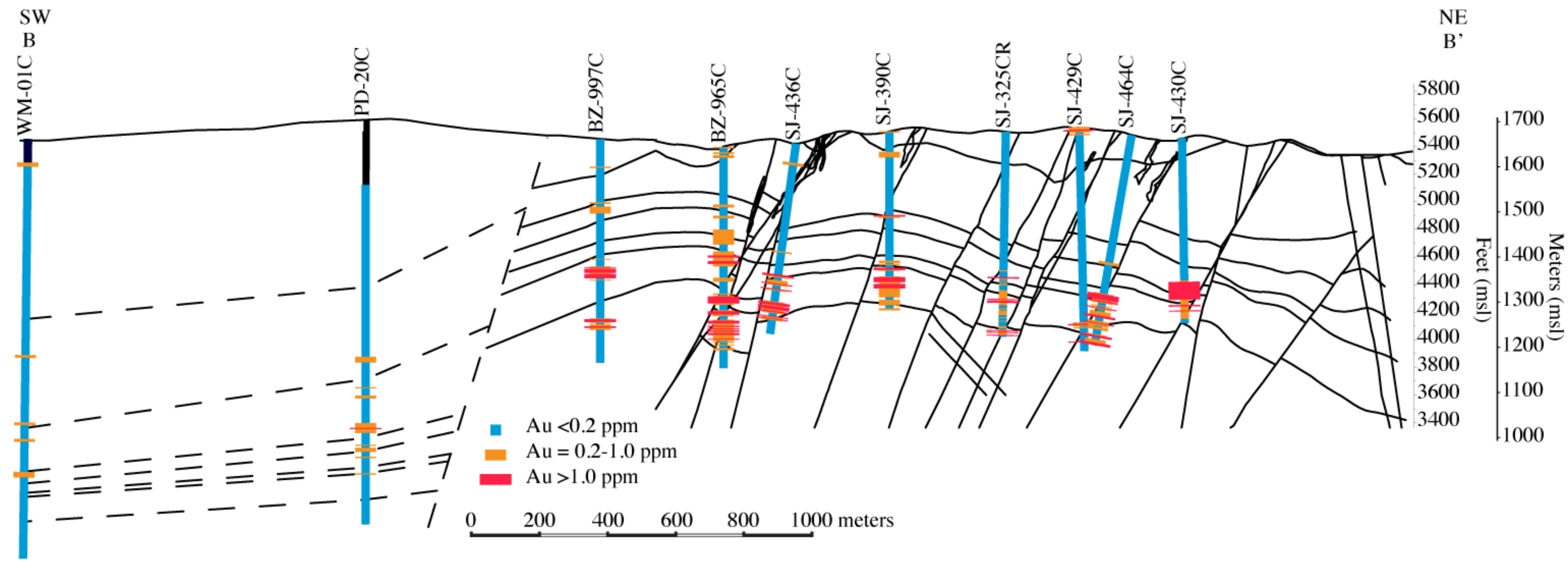

Figure 5.5 Cross-section B showing the distribution of Au intercepts in sampled drill holes (Au fire assay data provided by Barrick Gold Exploration, Inc.). Au data is collected on 5 foot splits within the ore zone, and 20 foot chip assays outside of ore.

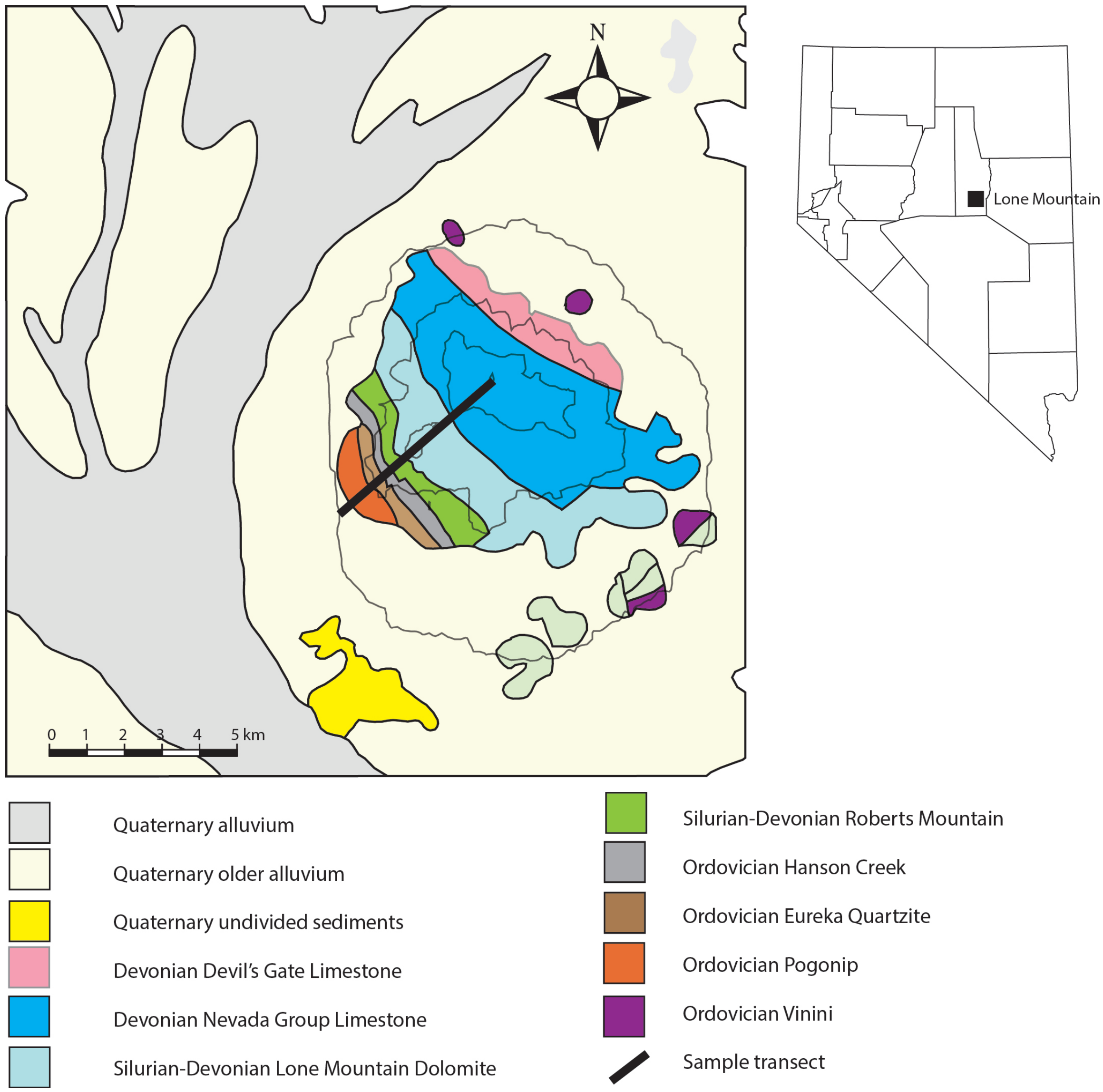

Figure 5.6 Simplified geology map of the Lone Mountain area near Eureka, NV. 14 samples were collected along the sample transect across the lower plate sequence. The Paleozoic carbonate sequence at Lone Mountain is correlative to the Paleozoic carbonate sequence on the northern Carlin trend with Silurian-Devonian Lone Mountain Dolomite being equivalent to Bootstrap Limestone and Devonian Nevada Group being correlative with the Devonian Popovich Formation (Cook and Corboy, 2004). Geology after Roberts et al. (1967).

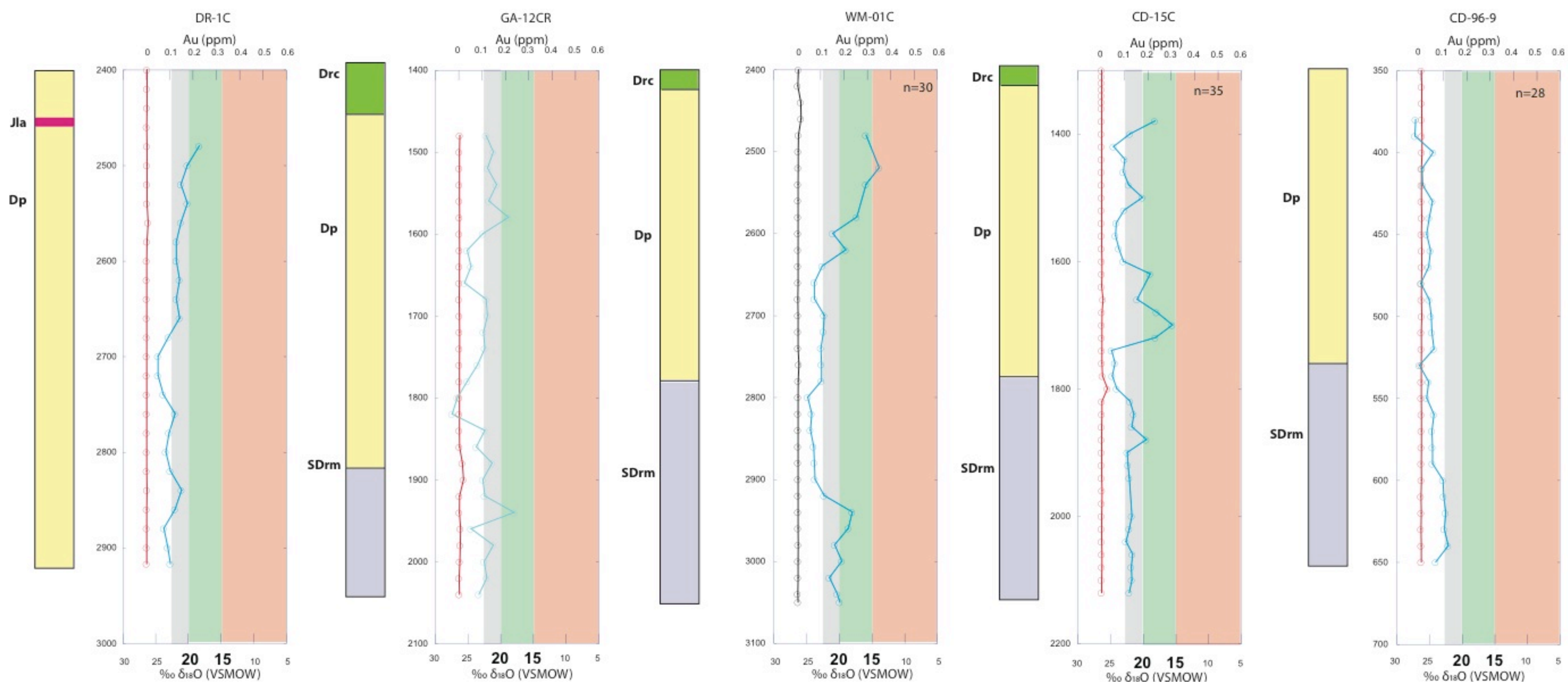

Figure 5.7 Down hole plots of δ^{18}O and Au assays for background holes in the Goldstrike district showing the down hole variation with lithology. Sampled intervals are considered non-depleted with δ^{18}O values of greater than 22‰, lightly to non-depleted with values of 20 to 22‰ (light grey zone), moderately depleted with values of 15 to 20‰ (light green zone), and extremely depleted with values of less than 15‰ (light red zone).

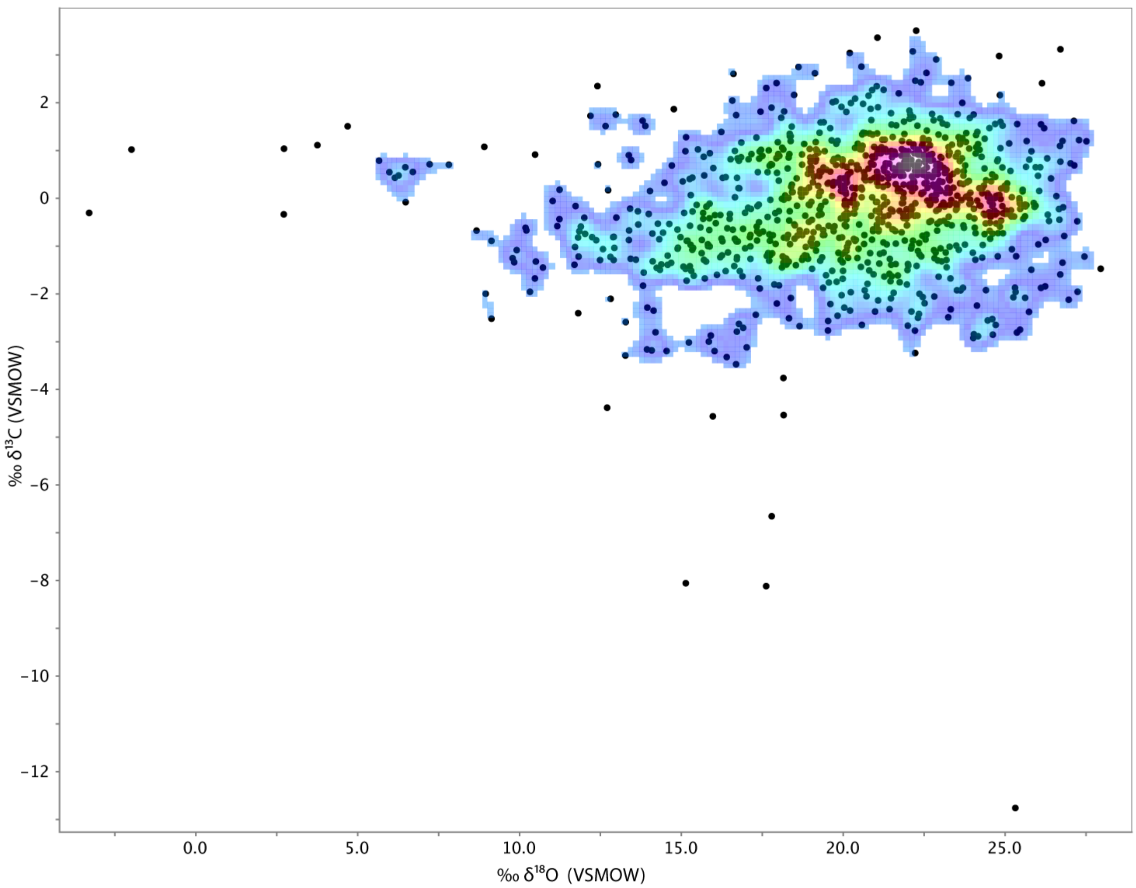

Figure 5.8 Scatter plot of all $\delta^{18}O$ and $\delta^{13}C$ data collected with this study (n=1586). The color overlay represents data density. Areas of high data density on the graph are red. Areas of lower data density are blue, and moderate data density is green.

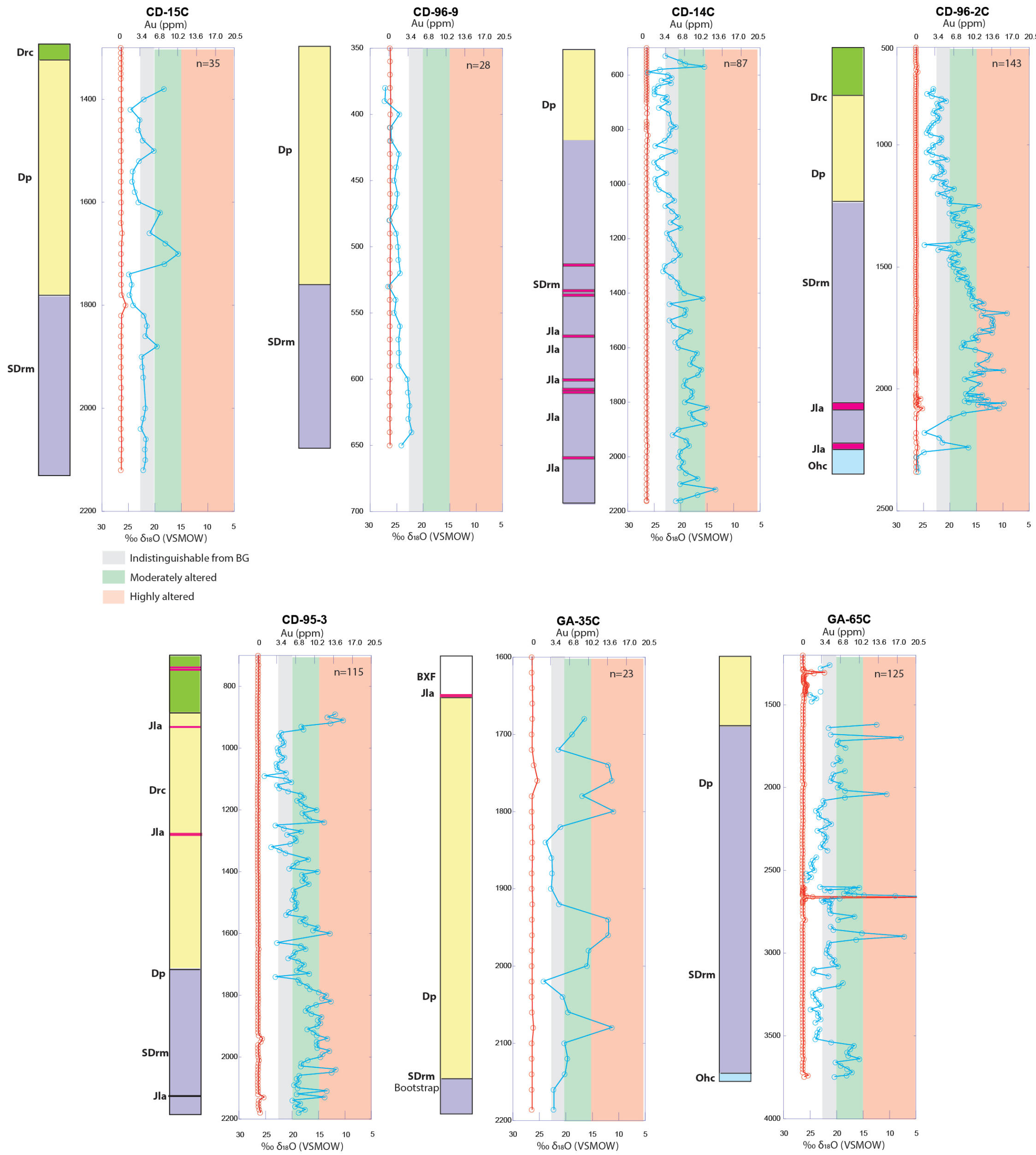

Figure 5.9 Down hole plots of $\delta^{18}O$ and Au assays for drill holes from cross-section A showing the down hole variation with lithology. Sampled intervals are considered non-depleted with $\delta^{18}O$ values of greater than 22‰, lightly to non-depleted with values of 20 to 22‰ (light grey zone), moderately depleted with values of 15 to 20‰ (light green zone), and extremely depleted with values of less than 15‰ (light red zone).

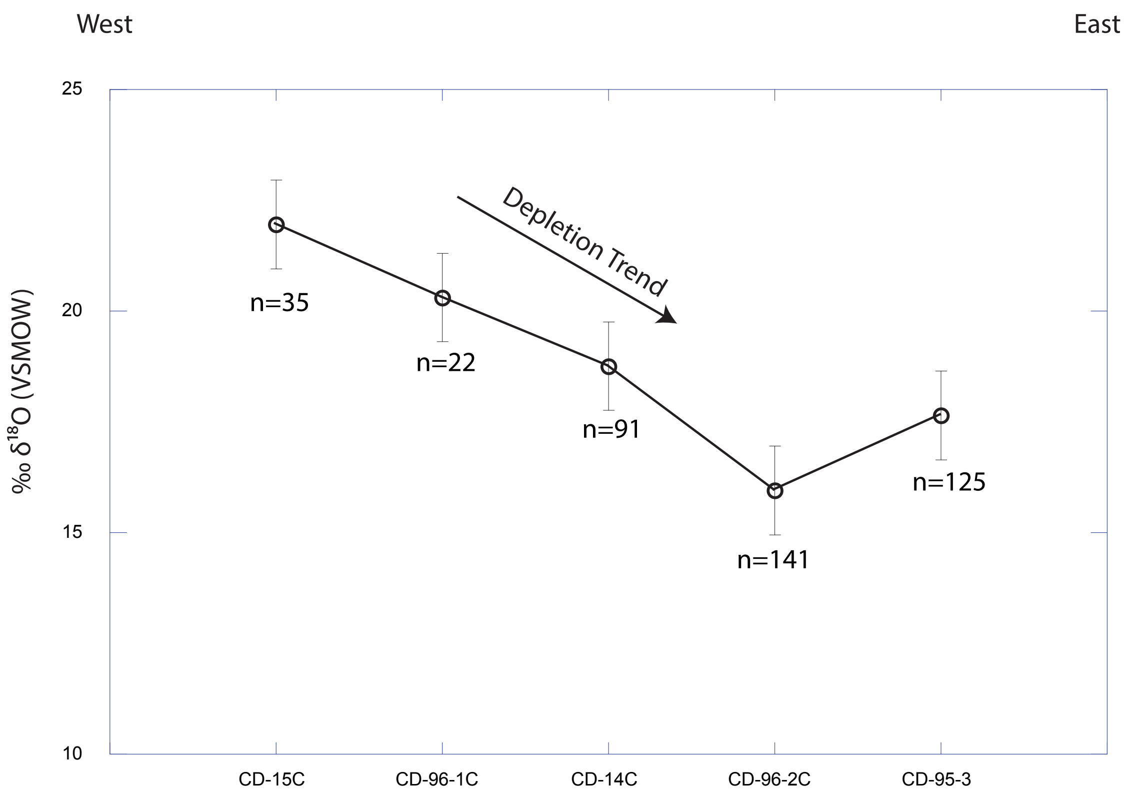

Figure 5.10 Plot of average δ^{18}O data ($\pm 2\sigma$) for drill holes through the western portion of cross-section A showing a trend of increasing δ^{18}O depletion towards CD-96-2C.

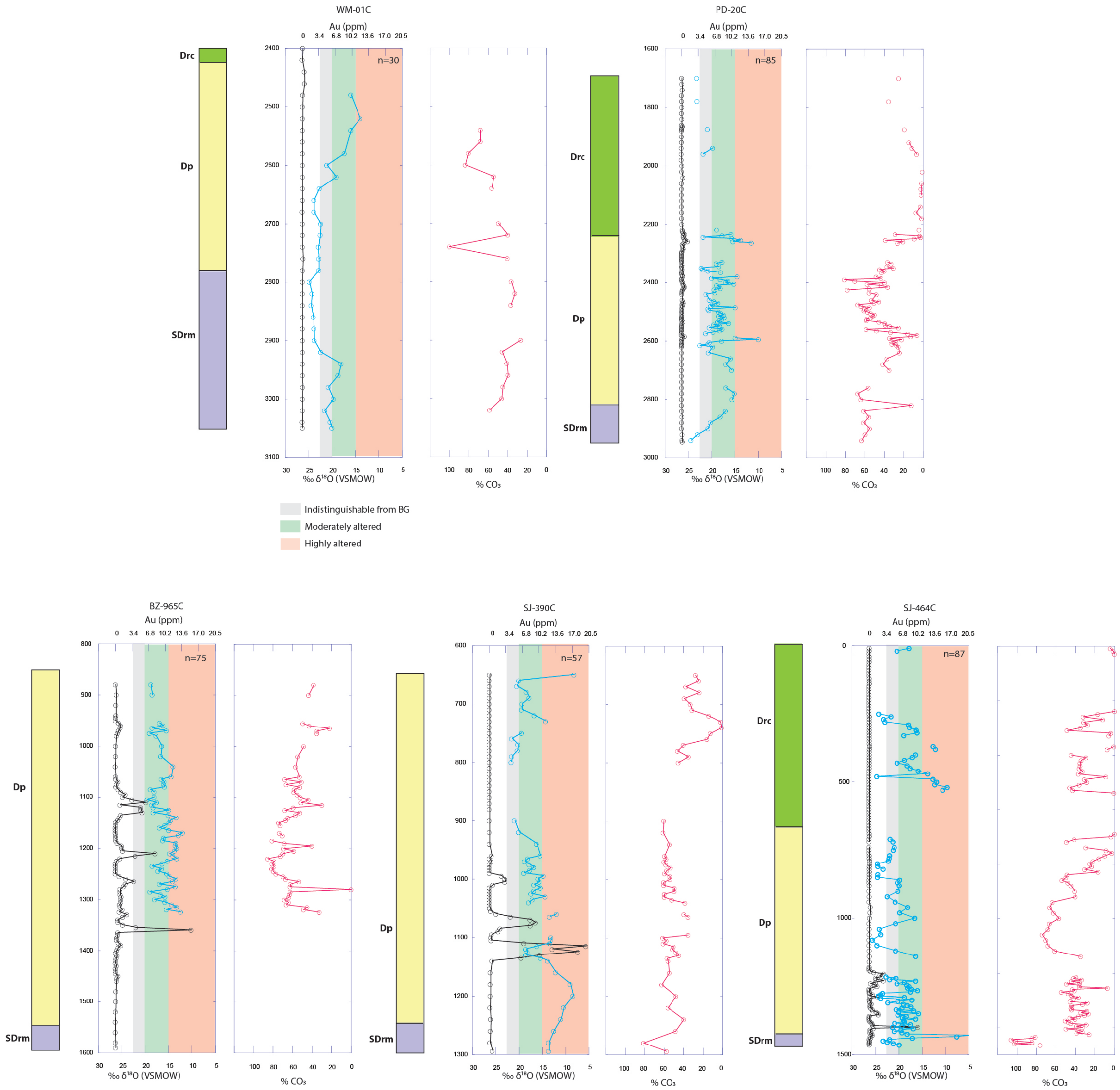

Figure 5.11 Down hole plots of δ^{18}O, Au assays, and %CO_3 content for drill holes from cross-section B showing the down hole variation with lithology. Sampled intervals are considered non-depleted with δ^{18}O values of greater than 22‰, lightly to non-depleted with values of 20 to 22‰ (light grey zone), moderately depleted with values of 15 to 20‰ (light green zone), and extremely depleted with values of less than 15‰ (light red zone).

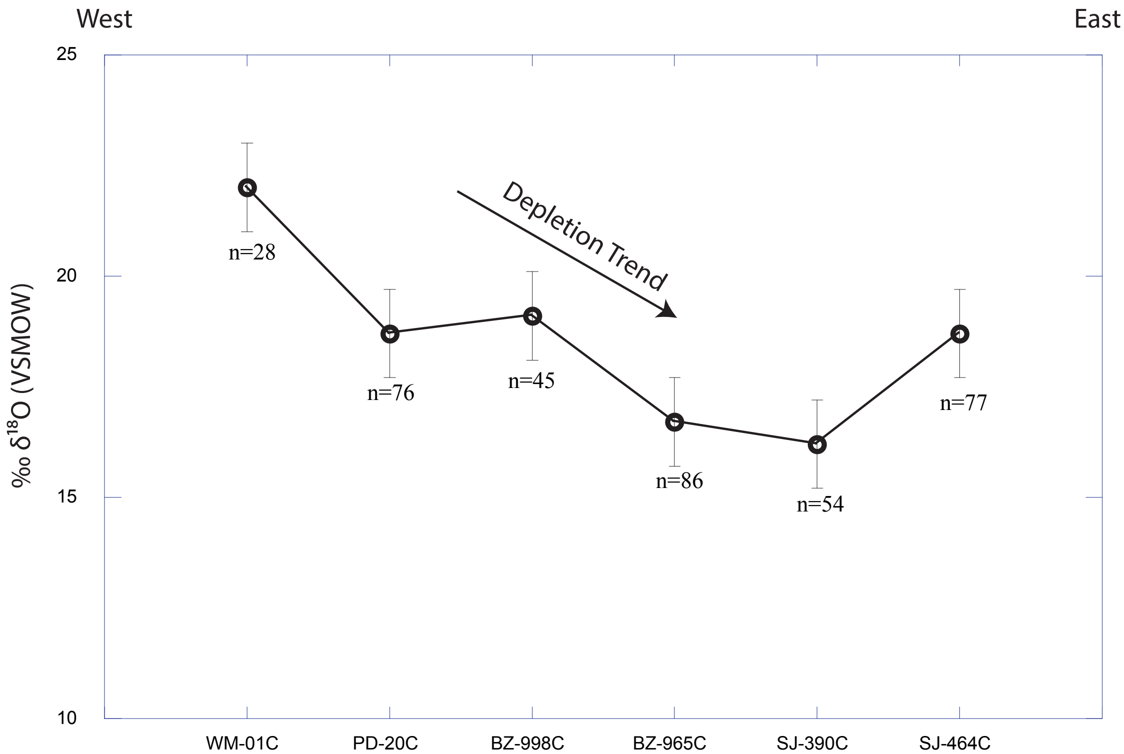

Figure 5.12 Plot of average $\delta^{18}O$ data ($\pm2\sigma$) for drill holes through cross-section B showing a trend of increasing $\delta^{18}O$ depletion towards SJ-390C.

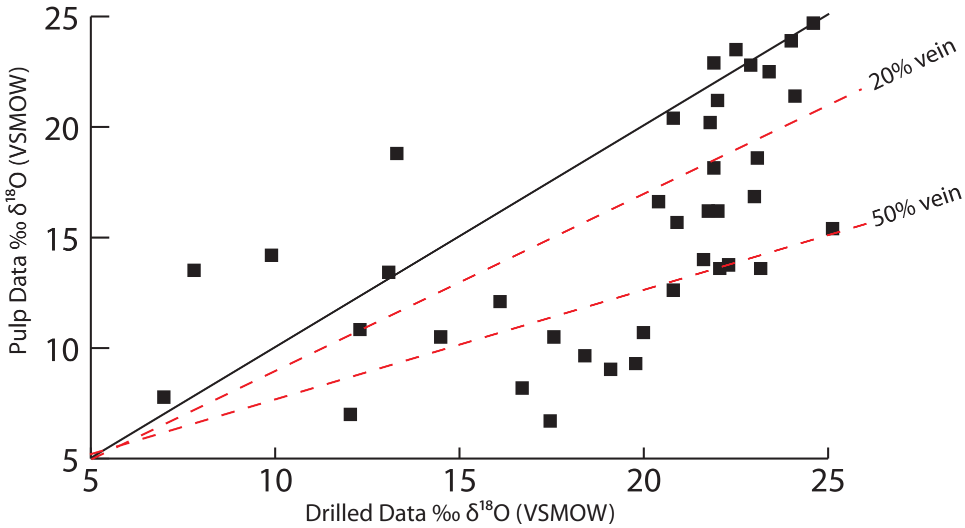

Figure 5.13 Scatter plot of $\delta^{18}O$ values from drilled hand specimens and 20-foot pulps for Goldstrike samples (See Appendix F for table of all data). Red dashed lines show the potential effect of late calcite vein contamination. A value of 5‰ $\delta^{18}O$ was used for late calcite vein material in all calculations (based on approximate $\delta^{18}O$ value for late calcite veins in Chapter 3).

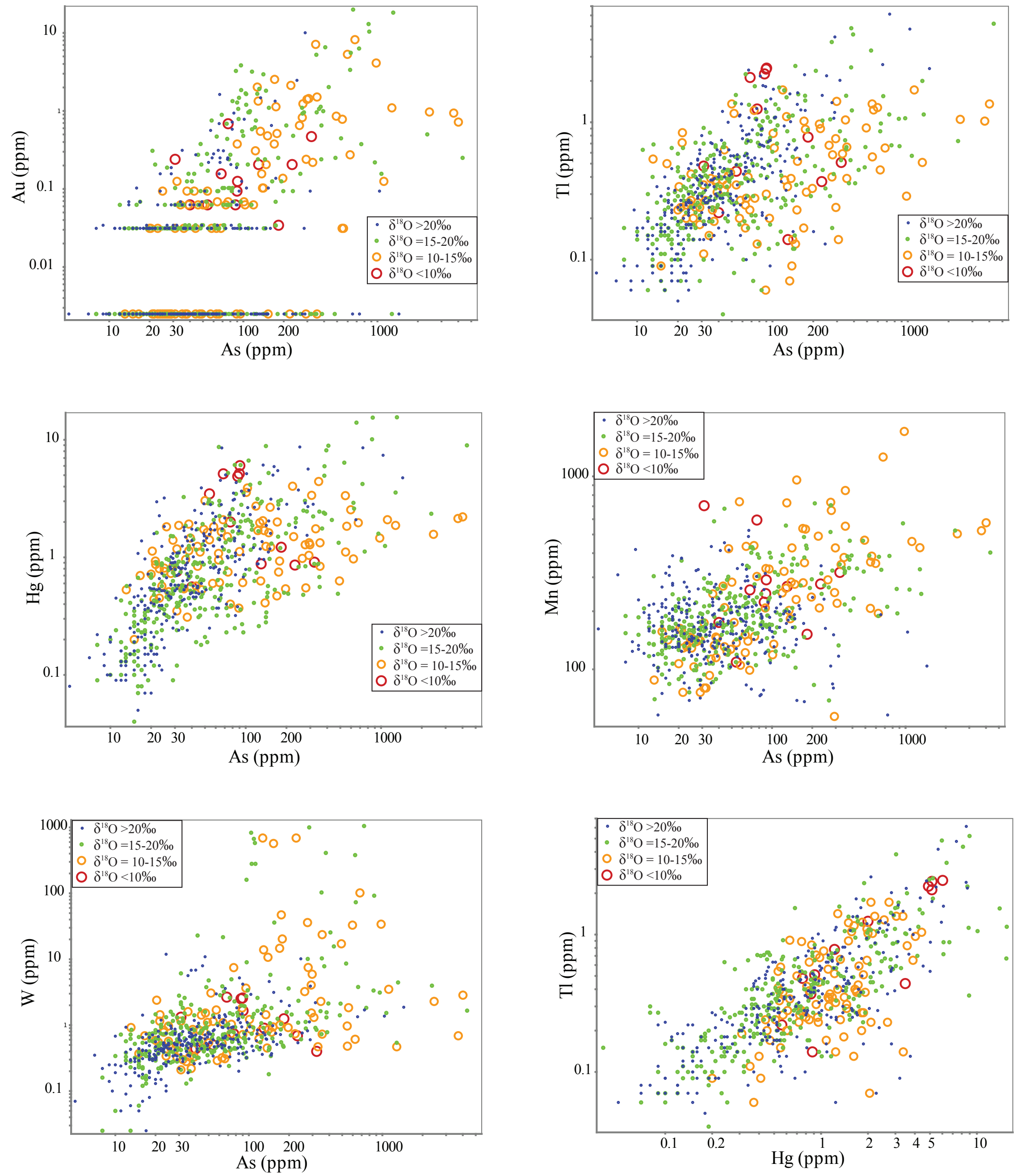

Figure 5.14 Trace element scatter plots for aqua regia data showing relative correlation of elements of interest. $\delta^{18}O$ values corresponding to each sample point are sized and colored according to degree of depletion. Samples with more depleted $\delta^{18}O$ values generally plot with elevated trace element contents. The correlation of Mn to As and $\delta^{18}O$ alteration is consistent with the interpretation from Chapter 3 that Mn enrichment is associated with dissolution-precipitation reaction in altered wall rock calcite. Au values less than detection limit are plotted at half detection (0.0025 ppm).

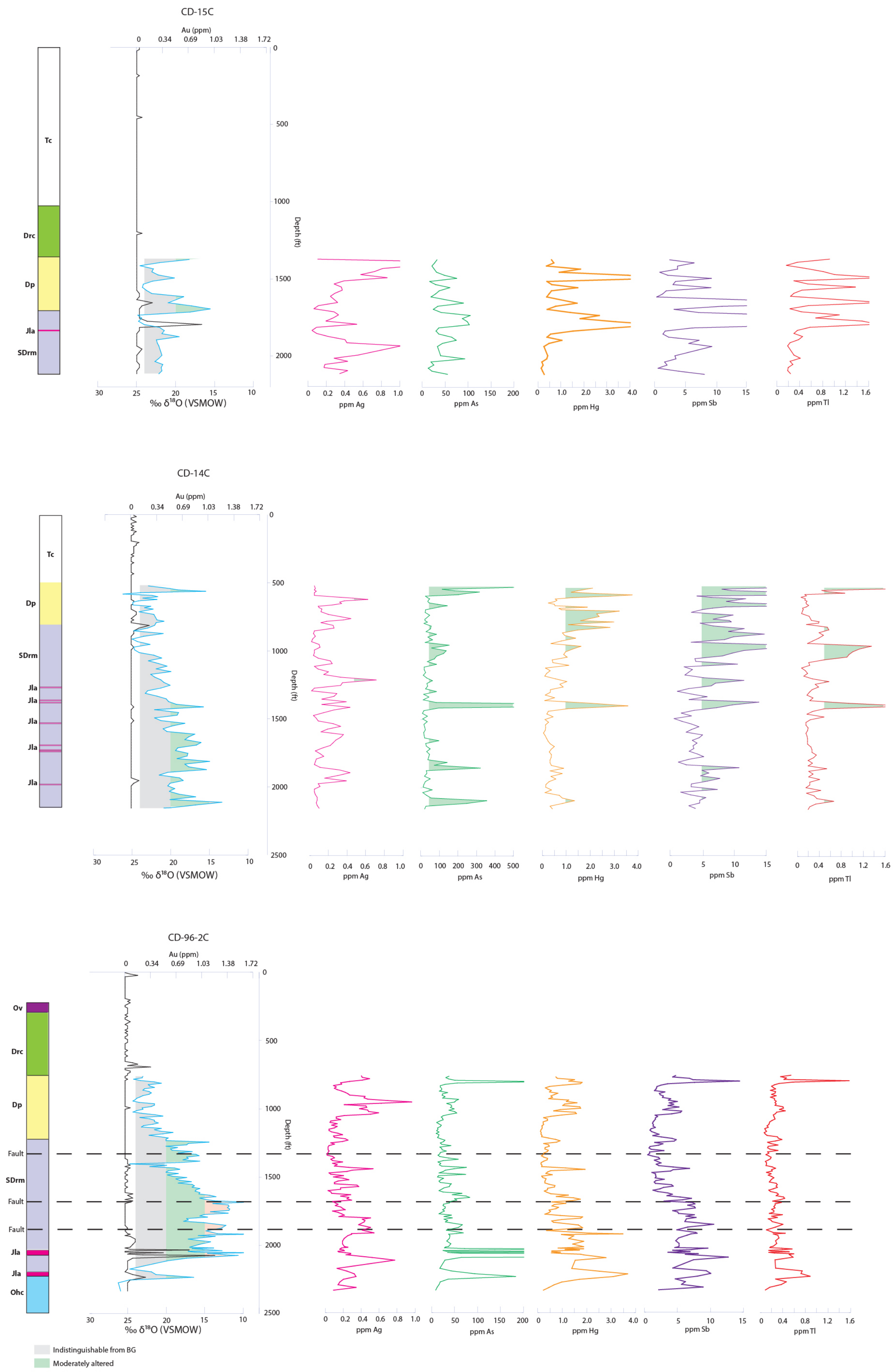

CD-15C
CD-14C
CD-96-2C
Au (ppm)
Depth (ft)
‰ δ18O (VSMOW)
ppm Ag
ppm As
ppm Hg
ppm Sb
ppm Tl
Tc
Drc
Dp
Jla
SDrm
Ov
Fault
Ohc
Indistinguishable from BG
Moderately altered
Highly altered

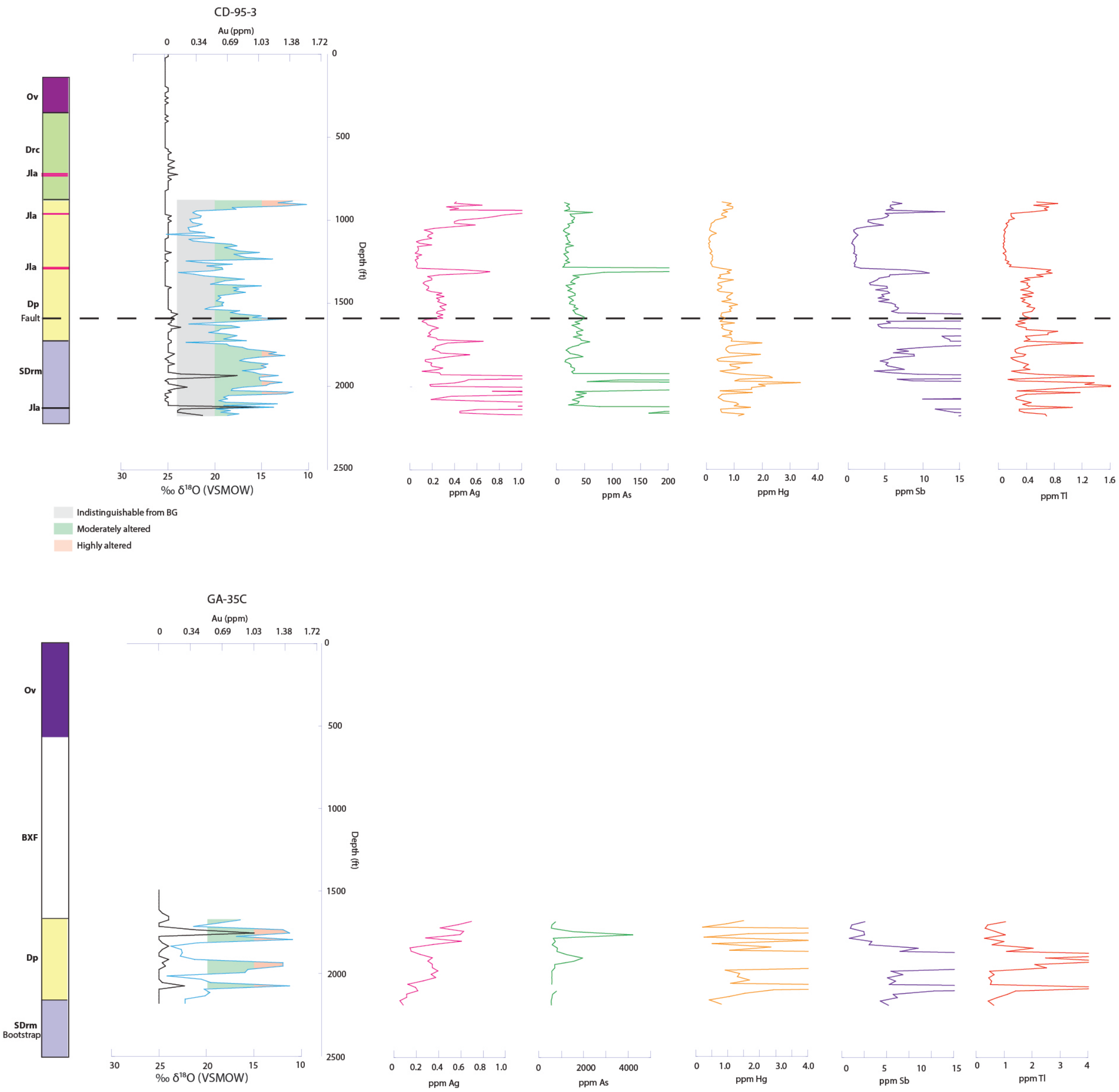

Figure 5.15 Down hole plots of $\delta^{18}O$, Au assays, Ag, As, Hg, Sb, and Tl for drill holes from section A. Green shaded zones highlight depleted $\delta^{18}O$ values between 15-20‰ and pink shaded zones highlight depleted $\delta^{18}O$ values <15‰.

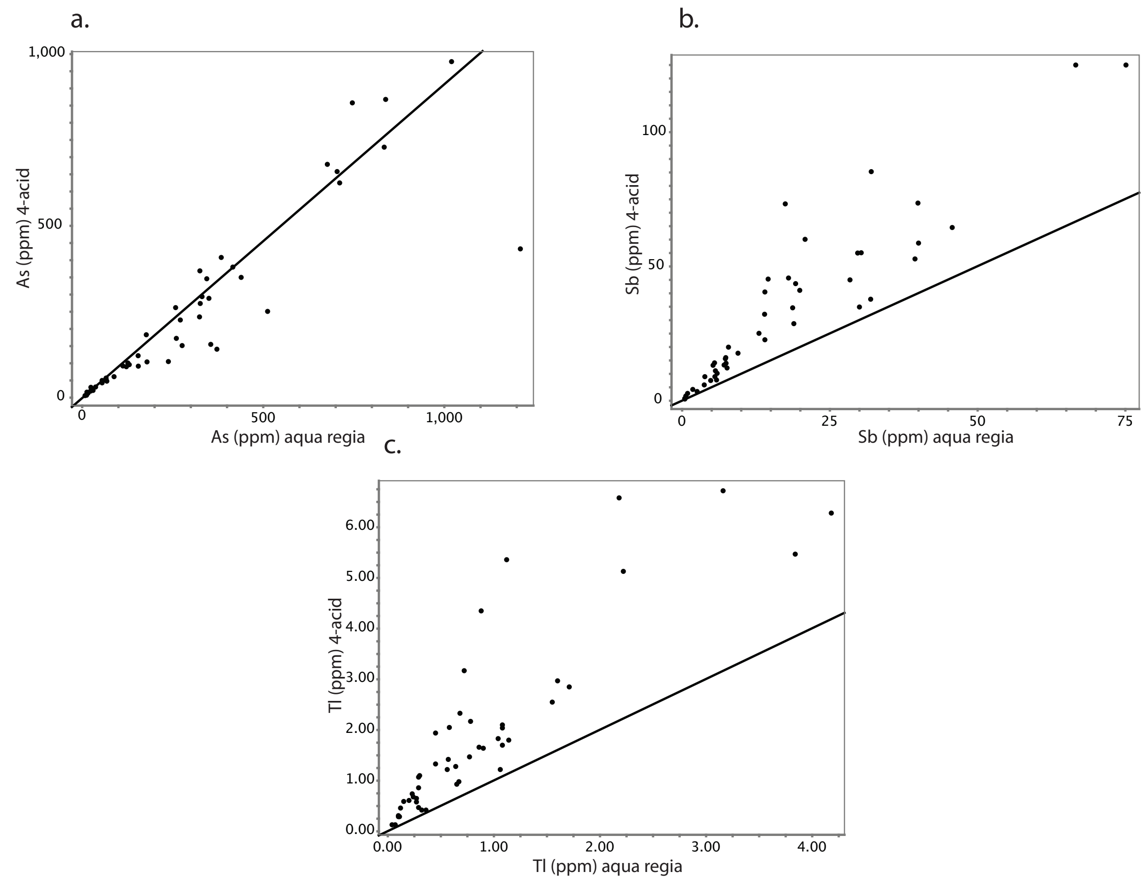

Figure 5.16 Comparison of aqua regia data versus four-acid data. Arsenic show a strong correlation between the two datasets. Tl (b) and Sb (C) show a poorer correlation with four-acid data consistently higher than aqua regia data for the same samples. Concentrations for both digestions were analyzed on an ICP-MS (see Appendix A for lab methods).

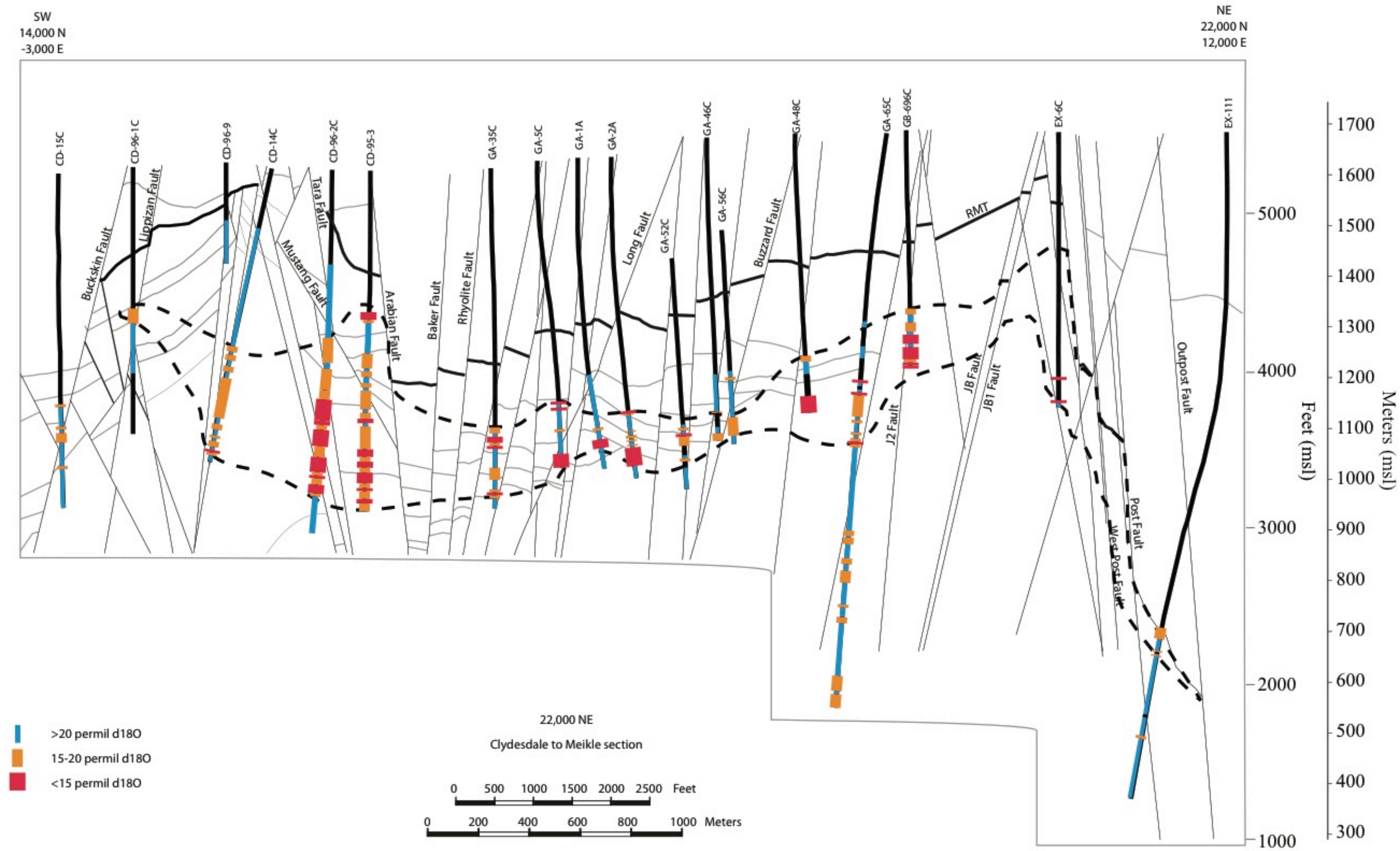

Figure 5.17 Section A with isotope data plotted by range of measured values from assay pulps. Light blue represents analyzed intervals with non-depleted to lightly depleted $\delta^{18}O$ values of greater than 20‰. Orange represents moderately depleted $\delta^{18}O$ values of 15 to 20‰. Red represents significantly depleted $\delta^{18}O$ values of less than 15‰. The black dashed line outlines the extent of $\delta^{18}O$ depletion along the cross-section.

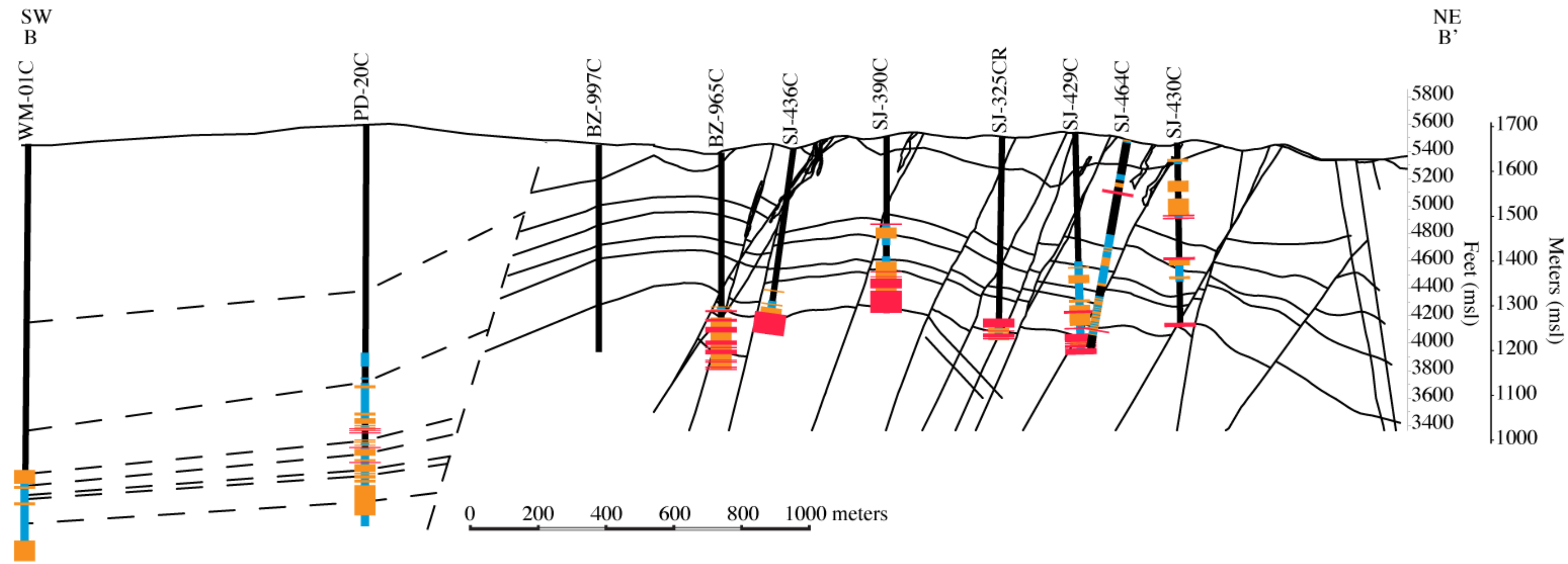

Figure 5.18 Section B with isotope data plotted by range of measured values from assay pulps. Light blue represents analyzed intervals with non-depleted to lightly depleted δ^{18}O values of greater than 20‰. Orange represents moderately depleted δ^{18}O values of 15 to 20‰. Red represents significantly depleted δ^{18}O values of less than 15‰.

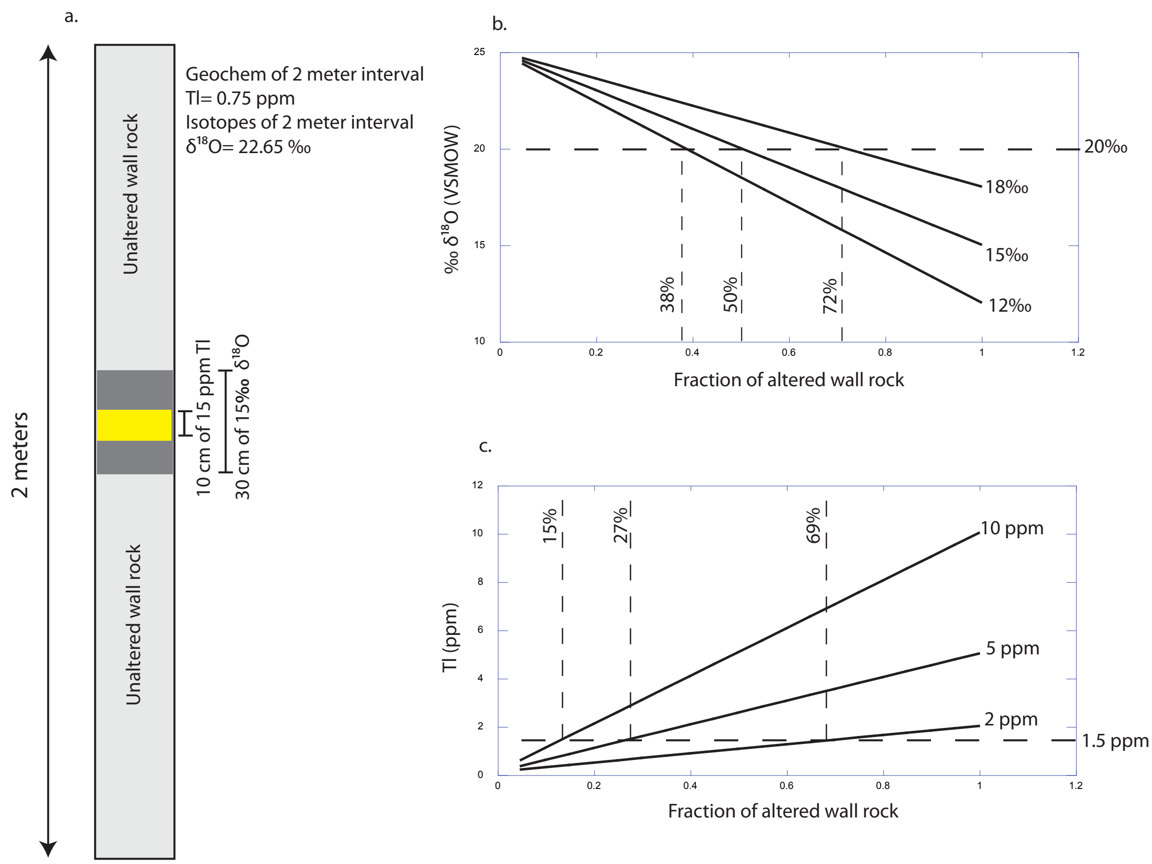

Figure 5.19 Diagrams showing the effect of discrete zones of alteration on measured values from bulk samples. a) Illustration of 2 meters of sampled drill core with a 10 cm zone of 15 ppm Tl and 30 cm interval of 15 δ^{18}O. If the entire 2 meter core interval is sampled for trace elements the measured values of Tl and δ^{18}O are diluted so that Tl=0.75 ppm and δ^{18}O = 22.65‰. Both the value for Tl and δ^{18}O are indistinguishable from background values even though they are altered over the discrete intervals. b) Graph showing the change in measured δ^{18}O over an assay interval at different fractions of altered wall rock versus unaltered wall rock. The three lines are calculated for different δ^{18}O values of altered wall rock. The percentages represent the fraction of altered wall rock necessary at specific δ^{18}O values for the assay interval to show alteration. c) Graph showing the change in measured Tl concentration over an assay interval at different fractions of altered wall rock versus unaltered wall rock. The three lines are calculated for different Tl concentrations in altered wall rock. The percentages represent the fraction of altered wall rock necessary at specific Tl concentrations for the assay interval to show alteration.

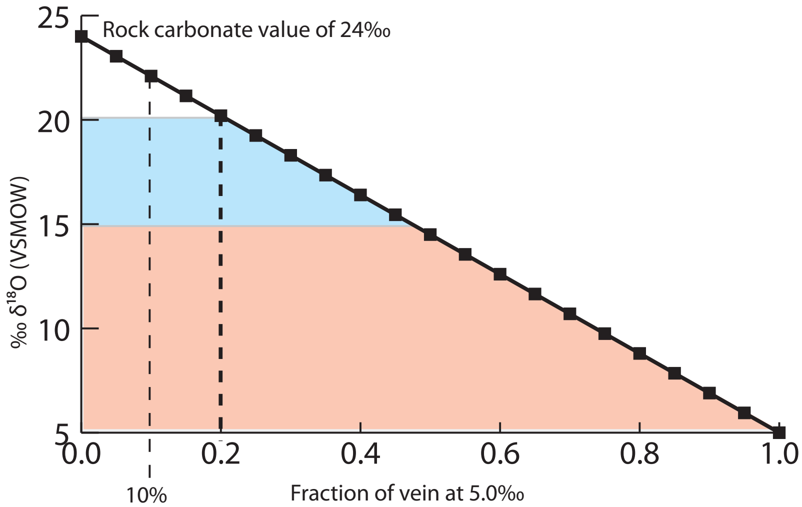

Figure 5.20 Plot showing the effects of increasing vein contamination on δ^{18}O values. A background sample with 20 % vein carbonate would produce a δ^{18}O value <20‰. A value of 5‰ δ^{18}O was used for vein material in all calculations (based on estimated value of late calcite vein from Chapter 3).

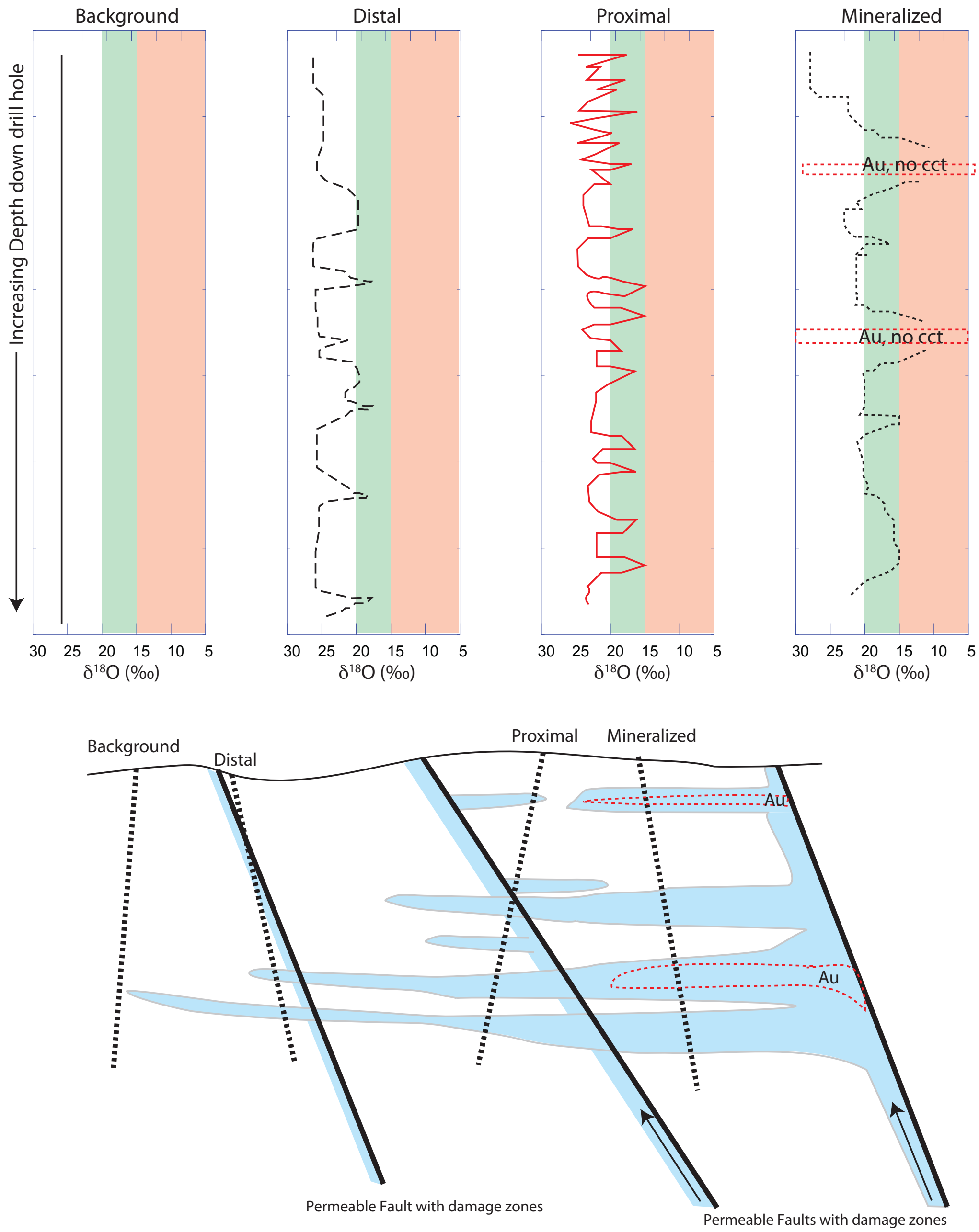

Figure 5.21 (A) Schematic diagrams of $\delta^{18}O$ alteration in a Carlin-type Au system illustrates how alteration is manifested in drill hole sampling. Background holes should have minimal to no alteration. Distal drill holes will show discrete narrow zones of alteration where fluid is channelized along high permeability zones. Drill holes proximal to mineralization will show increased frequency and larger intervals of isotopic alteration as well as more depleted $\delta^{18}O$ values. Drill holes through mineralized areas will show significant $\delta^{18}O$ depletion within large intervals of alteration with Au mineralization. (B) Schematic drill holes along a cross-section showing the spatial patterns of isotopic alteration and their relationship to mineralization.

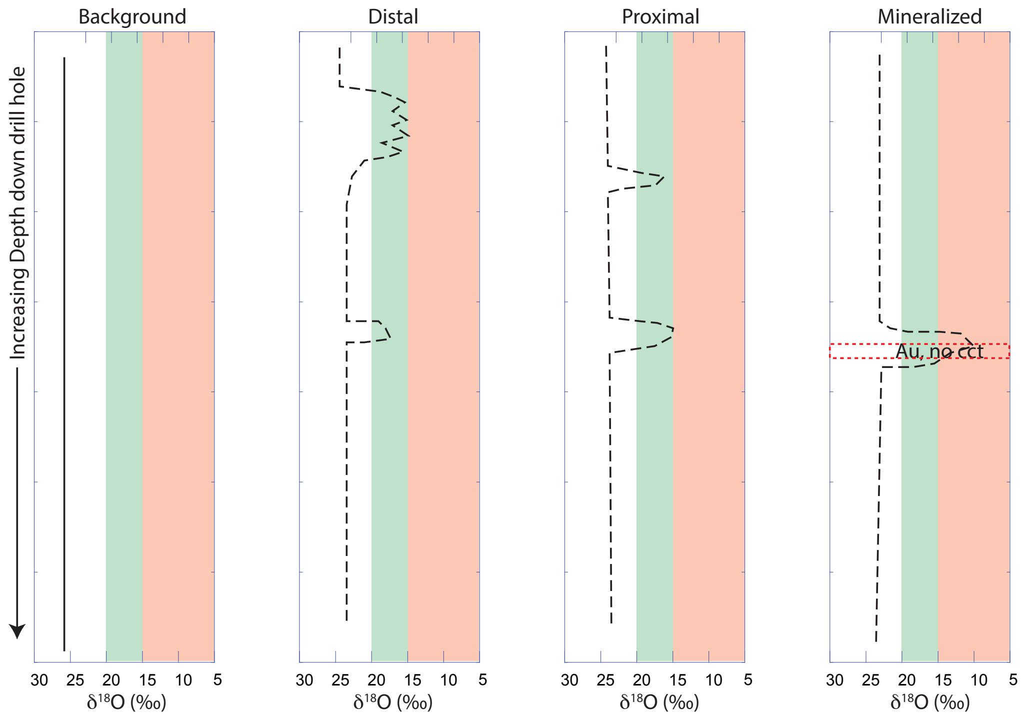

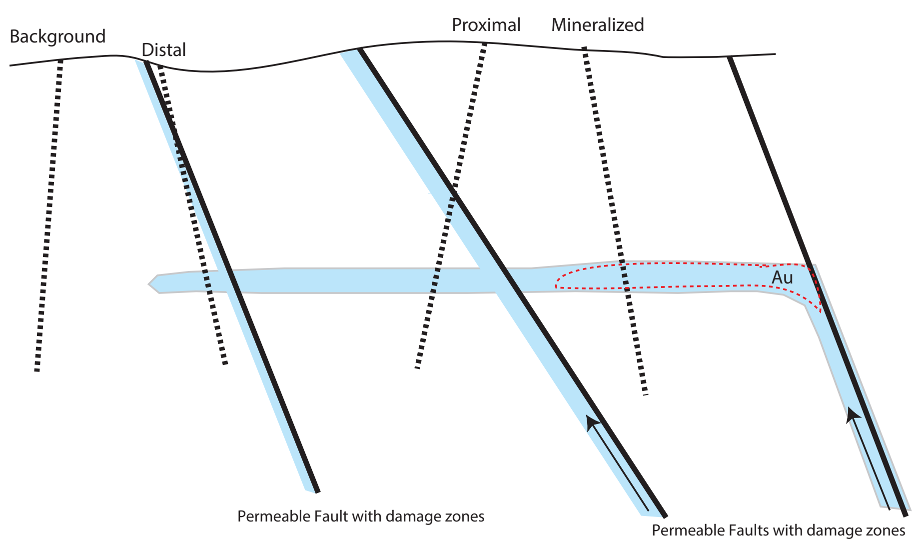

Figure 5.22 (A) Schematic diagram of $\delta^{18}O$ alteration in a Carlin-type Au system where fluid flow is controlled by a discrete breccia horizon within less permeable. Background holes should have minimal to no alteration. Distal drill holes will show discrete narrow zones of alteration where fluid is channelized along subvertical feeder structures and a high permeability breccia horizon. Drill holes proximal to mineralization will show increased intensity in isotopic alteration along the permeable flow path with little alteration in low permeability stratigraphy above and below the flow path. Drill holes through mineralized areas will show significant $\delta^{18}O$ depletion within a narrow zone of alteration with Au mineralization. (B) Schematic drill holes along a cross-section showing the spatial patterns of isotopic alteration and their relationship to mineralization.

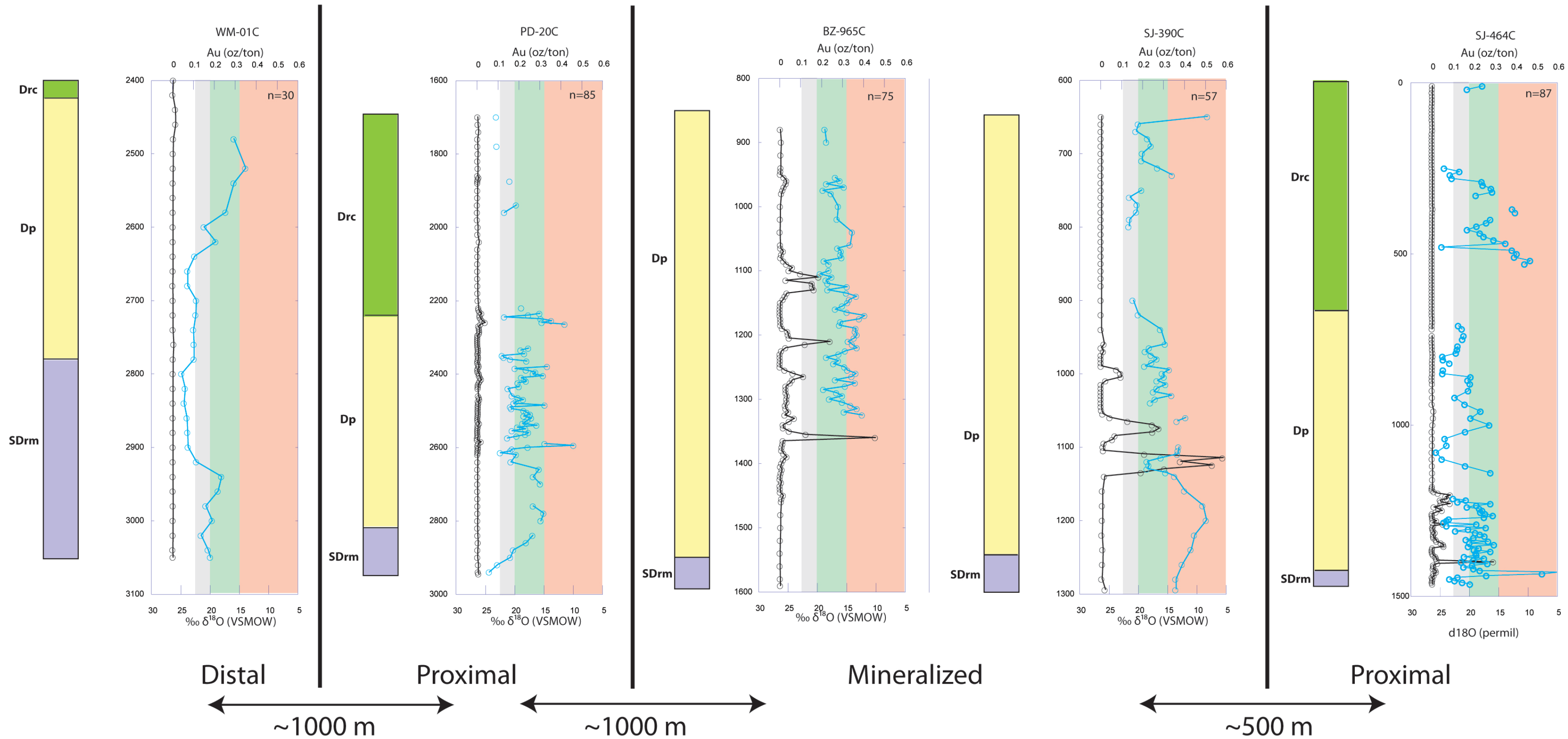

Figure 5.23 Down hole plots of $\delta^{18}O$ and Au assay data from Section A at Goldstrike showing the distances between distal, proximal and mineralized areas along the cross-section.

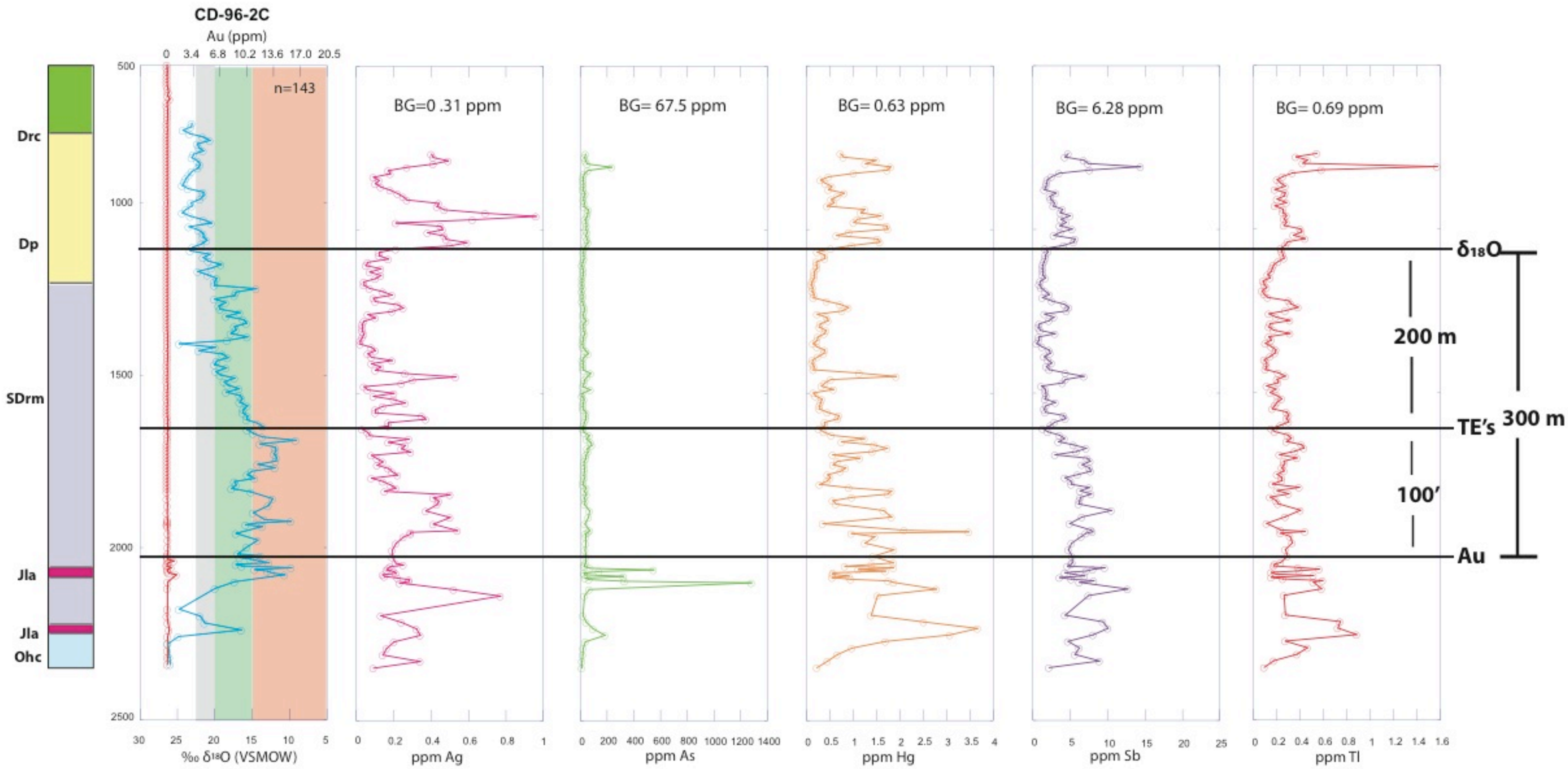

Figure 5.24 Down hole plots of δ^{18}O, Au assays, Ag, As, Hg, Sb, and Tl for CD-96-2C from section A shows the vertical distance between alteration haloes. The depth at which trace element concentrations occur above background threshold concentrations defines the trace element halo. The vertical distance between the isotope alteration halo and trace element halo is ~200 meters and the distance between the isotope alteration halo and the Au halo is ~300 meters.

Table 5.1 Background C and O isotopes from Lone Mountain, NV sampling of Paleozoic marine carbonates.

Sample ID	Easting (UTM NAD27 m)	Northing (UTM NAD27 m)	Sampled Formation	‰ $\delta^{18}O$ (VSMOW)	‰ $\delta^{13}C$ (VPDB)
LM-01	4381793	562025	Ordovician Pogonip	0.3	19.1
LM-02	4383145	563108	Devonian Nevada Group	-1.2	19.6
LM-03	4383134	563077	Devonian Nevada Group	-1.2	20.7
LM-04	4383087	563024	Devonian Nevada Group	3.5	26.2
LM-05	4382957	562844	Silurian-Devonian Lone Mountain Dolomite	-0.7	25.5
LM-06	4382630	562539	Silurian-Devonian Lone Mountain Dolomite	0.9	24.0
LM-08	4382357	562266	Silurian-Devonian Roberts Mountain	-0.1	24.3
LM-09	4382357	562266	Silurian-Devonian Roberts Mountain	0.5	26.2
LM-10	4382321	562191	Silurian-Devonian Roberts Mountain	0.9	24.1
LM-11	4382328	562179	Silurian-Devonian Roberts Mountain	1.2	26.7
LM-12	4382291	562116	Ordovician Hanson Creek	1.5	24.1

Table 5.2 Average and standard deviations of trace element concentrations for regional and local background samples. Background at Goldstrike is considered the average plus standard deviation.

	Regional Background (ppm)	Goldstrike Background (ppm)
Ag avg.	BDL	0.24
Ag Std.Dev.	BDL	0.07
Au avg.	0.029	0.016
Au Std.Dev.	0.053	0.4
As avg.	3.3	34
As Std.Dev.	5.1	33.5
Hg avg.	0.037	0.38
Hg Std.Dev.	0.041	0.25
Sb avg.	0.356	3.65
Sb Std.Dev.	0.255	2.63
Te avg.	0.02	0.02
Te Std.Dev.	0.14	0.01
Tl avg.	BDL	0.44
Tl Std. Dev.	BDL	0.25

Table 5.3 Correlation matrix for aqua regia geochemistry results and stable isotope results.

	Ag	As	Au (FA)	Au (aqua regia)	Bi	Ca	Cd
Ag	1						
As	0.148	1					
Au (FA)	0.247	0.396	1				
Au (aqua regia)	0.161	0.459	0.434	1			
Bi	0.068	0.279	0.284	0.297	1		
Ca	-0.280	-0.226	-0.290	-0.149	-0.397	1	
Cd	0.077	0.122	0.138	-0.018	0.045	-0.073	1
Cs	0.073	0.299	0.175	0.158	0.545	-0.441	0.063
Cu	0.386	0.257	0.343	0.048	0.262	-0.428	0.227
Fe	0.275	0.462	0.367	0.203	0.627	-0.555	0.079
Hg	0.338	0.286	0.360	0.034	0.197	-0.417	0.333
K	-0.051	0.264	0.099	0.185	0.455	-0.279	0.038
Li	-0.039	0.018	-0.082	-0.039	0.095	-0.113	-0.022
Mg	-0.076	-0.086	-0.120	-0.107	0.001	0.217	0.028
Mn	0.136	0.437	0.390	0.282	0.482	-0.202	0.091
Mo	0.177	-0.045	0.165	-0.053	-0.104	-0.283	0.132
Pb	0.192	0.130	0.076	0.019	0.161	-0.309	0.148
Rb	-0.009	0.236	0.114	0.138	0.399	-0.297	0.043
S	0.174	0.442	0.368	0.203	0.642	-0.413	0.137
Sb	0.197	0.026	0.015	-0.001	-0.044	-0.071	-0.002
Se	0.400	-0.048	0.274	-0.052	0.120	-0.324	0.173
Sn	0.196	0.019	0.054	-0.038	0.106	-0.183	0.018
Sr	-0.162	0.048	-0.172	0.019	-0.178	0.693	-0.036
Te	0.699	0.028	0.300	0.019	0.195	-0.332	0.089
Tl	0.286	0.383	0.298	0.041	0.205	-0.495	0.068
V	0.261	-0.027	0.348	-0.037	-0.072	-0.106	0.189
W	0.114	0.096	0.129	0.032	-0.016	-0.119	0.033
Zn	0.090	0.133	0.166	-0.017	0.078	-0.101	0.992
d18O	-0.226	-0.200	-0.110	-0.151	0.132	0.092	-0.184

	Cs	Cu	Fe	Hg	K	Li	Mg
Ag							
As							
Au (FA)							
Au (aqua regia)							
Bi							
Ca							
Cd							
Cs	1						
Cu	0.409	1					
Fe	0.639	0.459	1				
Hg	0.104	0.386	0.435	1			
K	0.616	0.086	0.386	-0.039	1		
Li	0.404	0.069	0.111	-0.114	0.680	1	
Mg	-0.036	0.020	-0.207	-0.224	0.112	0.146	1
Mn	0.505	0.285	0.622	0.110	0.405	0.181	0.093
Mo	-0.015	0.548	0.090	0.339	-0.278	-0.097	-0.070
Pb	0.086	0.200	0.236	0.284	-0.003	-0.107	-0.105
Rb	0.661	0.184	0.416	-0.016	0.944	0.798	0.087
S	0.458	0.451	0.811	0.426	0.253	-0.076	-0.055
Sb	-0.043	0.034	0.037	0.077	-0.055	-0.042	0.014
Se	0.238	0.683	0.249	0.376	0.001	0.022	0.008
Sn	0.211	0.408	0.230	0.086	0.032	0.130	-0.059
Sr	-0.065	-0.189	-0.234	-0.317	0.073	0.192	-0.009
Te	0.123	0.447	0.365	0.452	-0.157	-0.150	-0.182
Tl	0.212	0.373	0.560	0.768	-0.011	-0.075	-0.300
V	0.053	0.641	-0.007	0.252	-0.048	0.077	0.095
W	0.102	0.272	0.145	0.116	-0.055	-0.098	-0.037
Zn	0.087	0.261	0.117	0.358	0.044	-0.029	0.045
d18O	0.109	0.054	-0.115	-0.192	0.155	0.167	0.452

	Mn	Mo	Pb	Rb	S	Sb	Se
Ag							
As							
Au (FA)							
Au (aqua regia)							
Bi							
Ca							
Cd							
Cs							
Cu							
Fe							
Hg							
K							
Li							
Mg							
Mn	1						
Mo	-0.059	1					
Pb	0.046	0.152	1				
Rb	0.423	-0.167	-0.025	1			
S	0.454	0.094	0.256	0.215	1		
Sb	-0.009	0.066	0.043	-0.051	0.034	1	
Se	0.063	0.461	0.122	0.093	0.301	0.004	1
Sn	0.077	0.333	0.039	0.104	0.193	0.047	0.263
Sr	-0.017	-0.224	-0.272	0.092	-0.213	-0.071	-0.223
Te	0.097	0.377	0.198	-0.083	0.279	0.085	0.583
Tl	0.136	0.398	0.229	0.027	0.499	0.126	0.267
V	0.063	0.579	0.040	0.049	0.000	0.007	0.646
W	0.117	0.123	0.041	-0.032	0.072	0.080	0.085
Zn	0.121	0.141	0.182	0.046	0.184	0.005	0.193
d18O	-0.131	-0.071	-0.046	0.115	0.075	-0.137	0.008

	Sn	Sr	Te	Tl	W	Zn
Ag						
As						
Au (FA)						
Au (aqua regia)						
Bi						
Ca						
Cd						
Cs						
Cu						
Fe						
Hg						
K						
Li						
Mg						
Mn						
Mo						
Pb						
Rb						
S						
Sb						
Se						
Sn	1					
Sr	0.001	1				
Te	0.220	-0.256	1			
Tl	0.166	-0.348	0.402	1		
V	0.167	-0.061	0.315	0.161		
W	0.064	-0.082	0.067	0.121	1	
Zn	0.029	-0.069	0.108	0.095	0.034	1
d18O	-0.115	-0.074	-0.208	-0.161	-0.007	-0.115

Chapter 6 : Conclusions

This thesis investigates the physiochemical expression of low temperature sediment-hosted Carlin-type Au deposits using detailed studies of metasomatism, light stable isotope systematics, and their link to hydrothermal alteration. Metasomatism was investigated using a mass transfer study of the west Banshee lamprophyre dike where a single phase of lamprophyre intrusion was traced from unaltered to altered and mineralized. The west Banshee lamprophyre was also used to study stable isotope systematics of S, O, and H associated with clay alteration and sulfidation. Outside of the high-grade Au mineralization in the west Banshee lamprophyre dike, alteration of the breccia unit and limestone wall rocks were investigated using oxygen isotopes in calcite, cathodoluminescence textures, and mineral chemistry using LA-ICPMS. The recognition of syn-alteration calcite veining and non-equilibrium (i.e. kinetic) isotopic exchange at Banshee was the basis for reaction path modeling of oxygen isotope values that provided constraints on estimating integrated fluid fluxes based on oxygen isotope data. The result of the Banshee portion of this study is a detailed understanding of the manifestation of fluid-rock interaction in a relatively well-constrained Carlin-type Au deposit. The detailed study of alteration at the Banshee deposit formed the basis for a larger scale study in the Goldstrike district looking at the distal footprint of hydrothermal alteration associated with a giant Carlin-type Au system. Oxygen isotopes and geochemistry were analyzed from assay pulps along two cross-sections at Goldstrike from areas distal to mineralization through know mineralization.

6.1 Integration of Lithogeochemistry, Alteration Mineralogy and Light Stable Isotopes

Carlin-type Au deposits in northern Nevada were formed from acidic reduced fluids with less than 5wt% NaCL and temperatures estimated at 180-240°C (Cline and Hofstra, 2000; Cline et al., 2005; Hofstra and Cline, 2000; Lubben et al., 2012). Fluid-rock interaction lead to the dissolution of carbonate wall rock the precipitation of Au and trace elements through Fe-sulfidation reactions, argillic alteration of wall rocks with sufficient precursor minerals, and finally the precipitation of gangue minerals such as quartz, realgar, and orpiment (Cline et al., 2005; Hofstra and Cline, 2000). This study employed an integrated approach to define the alteration footprint of the hydrothermal system, leading to a comprehensive model for alteration in Carlin-type Au deposits.

Within mineralized lamprophyre at the Banshee deposit, alteration is characterized by addition of silica in the form of quartz, illitization with the addition of Cs, K, and Rb, and Fe-sulfidation with the addition of S and trace elements Au, As, Hg, Sb, Tl, and W (Chapter 2). Isotopic data from kaolinite and illite clay alteration minerals from west Banshee dike indicates that kaolinite alteration likely post-dates mineralization and illitization is the primary clay associated with Carlin-type alteration at Banshee. Additionally, $\delta^{34}S$ data from bulk samples of illite-altered and kaolinite-altered lamprophyre indicates a much lighter source of S in pyrite found in kaolinite-altered dike further suggesting a later stage alteration event that locally overprints the Carlin-type Au event.

Peripheral to the west Banshee lamprophyre, the breccia unit is intensely altered with near complete silicification of the wall rock, but the breccia unit does not host significant concentrations of Au. The reactive capacity for sulfidation is much greater in the lamprophyre relative to the breccia unit, adjacent limestones, and felsic dikes owing to the amount of reactive Fe available in hornblende (evidenced by pyrite replacement of hornblende). While the breccia unit does not host mineralization at Banshee it did serve as the backbone for fluid flow focusing the fluid across the permeable reactive barrier of lamprophyre.

Peripheral to Au mineralization and mineralogical alteration, isotopic alteration delineates a larger area of fluid-rock interaction than that defined by Au, and thus defines a distal footprint to hydrothermal alteration. Isotopic exchange occurred as fluids simultaneously dissolved and precipitated wall rock calcite as evidenced by CL textures in isotopically depleted calcite. As the fluid became progressively rock buffered, calcite veins precipitated along fractures (possibly caused by stresses related to massive carbonate dissolution). The veins are tied to the alteration system on the basis of positive Eu* anomalies, cross cutting relationships with early veins, and rock buffered $\delta^{18}O$ values similar to wall rock alteration. Syn-alteration veining is perhaps the most distal visible alteration feature in Carlin-type Au deposits. Syn-alteration veining was suggested at the original Carlin deposit on the basis of $\delta^{18}O$ values, but they were poorly described or constrained (Kuehn and Rose, 1992). Ilchik (1990) showed that calcite veining at the Alligator Ridge Carlin-type deposit is coincident with the edge of carbonate dissolution, contains realgar, and has $\delta^{18}O$ values similar to altered wall rock calcite. This thesis provides further criteria for evaluating the connection between calcite veins and hydrothermal alteration.

The fact that syn-alteration veins are more depleted than adjacent wall rock indicates that isoptopic exchange between the fluid and wall rock was out of equilibrium. Non-equilibrium (i.e. kinetic) exchange was investigated using a combination of one-dimensional reaction path modeling and the variance between wall rock calcite and veins. The modeling process lead to the develop of a new framework for estimating integrated fluid flux versus the reactive path length of the fluid where if either the infiltration distance or the integrated fluid flux are known the other can be estimated. Used in this way $\delta^{18}O$ data from syn-alteration-vein rock pairs could be used to evaluate the flux of the fluid and/or the infiltration distance along a flow path. It may also be used to evaluate the relative paleo-permeability network where multiple vein rock pairs can be compared to each other. At Banshee the results of reaction path modeling and vein-rock pair analysis is interpreted to define 2 distinct fluid pathways defined by permeability contrasts and could be used as an alteration vectoring tool to evaluate relative proximity to higher flow/permeability zones.

In combination the data presented in this thesis shows that while intense alteration is restricted to areas proximal to ore, distal alteration of wall rocks can extend >200 meters above mineralization and at least 2 km lateral to mineralization (see Chapter 5). The distal footprint of alteration is reliably defined by $\delta^{18}O$ alteration in calcite using bulk sampling of pulps, but the data also suggests that more careful sampling of calcite veined material at the distal margins of fluid-rock interaction may define alteration on an even larger scale potentially expanding the known footprint of Carlin-type Au systems. This study also emphasizes the complicated nature of hydrothermal fluid flow around Carlin-type Au deposits (as evidenced by stable isotope alteration), likely reflecting various controls on permeability around these deposits.

6.2 Scientific Contributions of the Dissertation

The two main goals of this thesis were to (i) better characterize the evolution of low temperature hydrothermal alteration in sediment-hosted Carlin-type Au systems; and (ii) better constrain the distal manifestations of hydrothermal fluid flow and identify physiochemical gradients that could provide exploration vectors toward Au mineralization in sediment hosted ore systems.

Low temperature (<350°C) sediment-hosted ore deposits present unique challenges in defining alteration zoning, and therefore lack context for evaluating the evolution of the hydrothermal fluid system. In Carlin-type Au systems, alteration mineralogy is restricted to arsenic-rich pyrite/marcasite, low temperature clays (i.e. illite), and silicification. The formation of these alteration phases can occur over a spectrum of physiochemical conditions and alteration is often poorly expressed in areas distal to mineralization. This study has established the key proximal alteration features associated with the ore system at west Banshee as well as defined alteration outside of visible indicators currently recorded during logging or other standard mineral exploration practices. Combining observations of proximal alteration with distal alteration establishes new constraints on the evolution of the Carlin-type Au system at Banshee. This thesis has gone beyond the mere recognition of $\delta^{18}O$ alteration both proximal and distal to mineralization in Carlin-type deposits noted by previous authors (Arehart and Donelick, 2006; Emsbo et al., 2003; Hofstra et al., 2011; Ilchik, 1990; Kuehn and Rose, 1992; Radtke et al., 1980; Stenger et al., 1998b) to also investigate the mechanism of isotopic alteration, the textural evidence for dissolution-precipitation reactions of calcite, and the recognition and modeling of non-equilibrium (i.e. rate limited) exchange.

By defining the distal signature of fluid-rock interaction in Carlin-type hydrothermal systems, criteria for distal vectoring have been established. Syn-alteration calcite veins, which precipitated from exchanged, reduced fluids at temperatures of ~200°C, are perhaps one of the more distal alteration features (Chapter 3). This thesis has established criteria for evaluating syn-alteration veining using a combination of textural description, $\delta^{18}O$ isotope analysis, and mineral chemistry (Chapter 3). Owing to rate limited exchange and fluid-rock buffering, syn-alteration calcite veins may be the more easily defined than minimal $\delta^{18}O$ depletion in coexisting wall rock calcite at the distal margins of hydrothermal fluid infiltration (Chapters 3 and 4). Vectoring in from syn-alteration veining $\delta^{18}O$ alteration of wall rocks averaged over set intervals may show progressive depletion vectoring towards areas proximal to mineralization (Chapter 5). The combination of $\delta^{18}O$ analysis with textural analysis and calcite mineral chemistry forms new criteria for vectoring towards a low-temperature limestone-hosted ore deposits such as Carlin-type Au deposits of Nevada.

6.3 Critical Results

6.3.1 Defining Oxygen Isotope Exchange Mechanisms

The two broad mechanisms for exchange between rock and fluid are diffusion and chemical reaction. Chapter 3 shows that significant diffusion is unlikely to occur within the temperature range and time scale of Carlin-type hydrothermal systems and, therefore, chemical reaction is the preferred mechanism of exchange. In order for exchange to occur by chemical reaction, the hydrothermal fluid must be capable of dissolving calcite and precipitating calcite in the same time and space. The process of dissolution-precipitation with pseudomorphic replacement is poorly understood and is generally described empirically. While $\delta^{18}O$ alteration of wall rock calcite has been recognized at a number of limestone-hosted Carlin-type Au deposits, the mechanism by which exchange occurs has not been characterized. Cathodoluminescence shows that samples of wall rock calcite that have $\delta^{18}O$ depletion have a unique CL response indicating a change in the mineral chemistry relative to unaltered limestone. Many of these samples show features suggesting near complete replacement and pseudomorphing of grains. The implication is that the fluid was capable of completely replacing calcite while preserving original grain textures. This observation suggests uniform alteration of wall rock rather than partial replacement or dissolution with precipitation of texturally distinct calcite. The chemical reactions resulting in isotopic exchange between the fluid and wall rock was a coupled process that is unrecognizable in transmitted light petrography and hand specimen.

6.3.2 Identification of Syn-alteration Calcite Veining

It is understandable that syn-alteration calcite veins have not been systematically described in Carlin-type Au deposits, as there is a lack of clear relationships tying them to mineralization. It is therefore critical to perform detailed analytical work on calcite veins prior to classification. This thesis developed criteria for evaluating calcite veining that can serve as a framework for identifying the key characteristics of the veining. Texturally the veins described in this thesis are similar to early calcite veining, but distinct from typically coarse late calcite common on the Carlin trend. Kuehn (1992) identified veins that had $\delta^{18}O$ values indicating precipitation from exchanged fluids, but he had no way of tying them back to alteration. In the present study, a combination of $\delta^{18}O$ isotope analysis, CL characterization, and mineral chemistry make it possible to identify veins that were precipitated from an exchanged, reduced (fO_2<-40), hydrothermal (180-240°C) fluid, thought to be characteristic of Carlin-type hydrothermal fluids.

6.3.3 Non-equilibrium Exchange in Low Temperature Hydrothermal Systems

A few previous authors have assumed equilibrium exchange can occur in low temperature carbonate-hosted hydrothermal systems (Stenger et al., 1998b; Zheng and Hoefs, 1993), and have used that assumption to model fluid-rock and fluid-fluid mixing processes to describe observed $\delta^{18}O$ alteration of rock calcite. Non-equilibrium exchange has been documented in low temperature experimental work (Kim and Oneil, 1997) and for low temperature hydrothermal systems (Frimmel, 1992) for the calcite-water system even where dissolution-precipitation reactions control the rate of $\delta^{18}O$ exchange. Without the ability to monitor both the fluid and rock values it is difficult to recognize non-equilibrium exchange between a hydrothermal fluid and wall rock. The recognition of syn-alteration calcite veins provide an ability to monitor relative differences between rock calcite and the alteration fluid since veins are precipitated directly from the fluid rather than through dissolution-precipitation reactions where pre-existing rock calcite mixes with fluid as precipitation is occurring. In the case of Banshee all recognized syn-alteration calcite veins show significant disequilibrium with adjacent rock calcite. Recognition of non-equilibrium exchange brings both challenges and opportunities to evaluating fluid-rock interaction. When equilibrium exchange is dominant simple titration models may be effective at describing W/R ratios that can be used to evaluate fluid-rock interaction processes, but the modeling is by nature dimensionless and does not consider incremental effects of fluid flow over distance. The recognition of kinetically controlled non-equilibrium exchange at Banshee allowed for 1D reactive transport modeling to evaluate the relationship between time integrated fluid flux (TIFF) and the reactive path length (i.e. geochemical reaction front) at variable N_D. A key learning from the work presented here is that equilibrium exchange should not be assumed, but rather the researcher should endeavor to evaluate the potential of non-equilibrium conditions.

6.3.4 Evaluating Integrated Fluid Fluxes and Fluid Infiltration

The approach defined in Chapter 4 of this thesis provides a framework for evaluating TIFF and distance in hydrothermal systems. A diagram similar to Figure 4.8 can be built if fluid temperature, fluid $\delta^{18}O$ value, unaltered wall rock $\delta^{18}O$ value, and porosity are known and vein-rock pairs related to alteration are defined. The diagram can then be used to evaluate the TIFF of a system if the path length is independently defined, or the path length if TIFF is independently defined. Even if the path length or TIFF cannot be defined, Figure 4.8 allows for the evaluation of different scenarios for both TIFF and path length.

6.3.5 Scale of Alteration in Carlin-type Au Deposits

Stenger et al. (1998) suggested that $\delta^{18}O$ alteration at the Twin Creeks Carlin-type Au deposit may extend for multiple kilometers based on sampling of distal outcrops and drilling in the district, but the lack of access to drilling and/or outcrop between the distal samples and samples collected proximal to the ore body did not allow for a critical assessment of the connection between regional scale alteration and alteration found within the immediate deposit area. The study of district scale alteration at Goldstrike presented in Chapter 5 allows for a far more precisely defined evaluation of $\delta^{18}O$ alteration outside of giant Carlin-type Au system. The data indicates that alteration extends at least 2 km outside of a defined ore body and shows that $\delta^{18}O$ values (in aggregate) show progressive depletion towards mineralization. In addition to the >2 km lateral extent of $\delta^{18}O$ depletion in limestone, alteration may extend vertically above the ore body. The data presented in Chapter 5 indicates that $\delta^{18}O$ isotope depletion can extend up to 300 meters above Au mineralization. Expanding the footprint of alteration in limestones, allows for better assessment of true extent of the hydrothermal system responsible for large Carlin-type Au systems.

6.4 Applications of Research Findings

6.4.1 Discrimination of Alteration in Carlin-type Au Deposits

As discussed in the introduction to this thesis, alteration patterns can be subtle in low temperature sediment-hosted hydrothermal systems. This thesis shows that careful analysis of potential alteration products is necessary to tie observed alteration to hydrothermal processes coeval with mineralization. This thesis defines a set of tools that can be applied to the alteration evaluation process. D and O stable isotopes in clay minerals can differentiate between different fluid sources responsible for alteration. However, plotting of fluid equivalent values of stable isotopes requires knowledge of the range of temperatures associated with distinct alteration events as well as modern groundwater conditions. In areas such as the northern Carlin trend, multiple episodes of alteration may have similar alteration products that are spatially coincident with Carlin-type alteration (Emsbo et al., 2006). Assuming a formation temperature for alteration can lead to misleading results when temperature-dependent fractionation is considered.

Calcite veining could be an important distal indicator of alteration in Carlin-type deposits, but it must first be linked genetically to hydrothermal alteration. Paleozoic limestones on the northern Carlin trend contain multiple generations of calcite and dolomite veining with a lack of clear paragenetic relationships to tie specific veins to hydrothermal alteration. Applying $\delta^{18}O$ analysis, mineral chemistry, and textural descriptions (using CL and transmitted light petrography) can provide confidence in the interpretation of calcite veining associated with hydrothermal fluid flow.

6.4.2 Use of Vein-Rock Pairs to Evaluate Integrated Fluid Flux and Reactive Path Length

The application of vein-rock pairs for defining non-equilibrium exchange processes has been used by previous researchers to define TIFF based on prior knowledge of estimated fluid path length. However, estimates of TIFF can be used to define path length as well. Independent estimates of TIFF can be made using a mass balance approach (Chapter 2). Once a TIFF estimate is made it can be input into the calculation of 1-dimensional reactive transport results to give a path length for fluid flow. Individual measurements of $\delta^{18}O$ in vein-rock pairs can then be placed at specific distances along the infiltration path providing a means of estimating the distance from both the isotopic exchange front and the fluid reservoir. As indicated by the data presented in Chapter 4, permeability contrasts can hinder interpretations of path length. However, if enough data is available from vein-rock pairs, groupings of data may help define contrasting permeability networks and better constrain path length interpretations.

6.4.3 Alteration Patterns in Carlin-type Au Deposits

This thesis defines the components of an integrated alteration model that zones outward from visible indicators to trace metal metasomatism, $\delta^{18}O$ alteration, and syn-alteration veining (Figure 6.1). The most proximal features of alteration are Au mineralization, silicification, and clay alteration. Massive carbonate dissolution occurred as acidic hydrothermal fluid infiltrated permeable carbonate-rich wall rocks. As dissolution of carbonate minerals occurred, Fe was released and reacted with bisulfide complexes to form trace element rich pyrite with Au. Where the fluid intersected dikes, mafic minerals released Fe for sulfidation reactions. In addition to sulfidation, primary minerals in dikes were progressively altered to illite. As the fluid became progressively rock buffered, carbonate dissolution-precipitation reactions began occurring at the fluid-mineral interface leading to mineral replacement textures and $\delta^{18}O$ exchange between the rock and fluid. At this point trace element metasomatism greatly diminished owing to a decrease in the amount of Fe available for sulfidation reactions or a lack of sulfur remaining in the fluid. As the difference between fluid and rock $\delta^{18}O$ values decreased through progressive rock buffering kinetic limits on exchange began to mask the $\delta^{18}O$

alteration in wall rock calcite. At this point $\delta^{18}O$ alteration is detectable in syn-alteration calcite veins that precipitated directly from the fluid within fractures and open space in the wall rocks. Once the fluid became completely rock buffered, detectable chemical modification of the wall rock ceased.

Creating a unified model for alteration that accounts for both proximal and distal expression of fluid-rock interaction provides a framework for establishing alteration in visibly unaltered wall rocks. By defining the relative patterns of alteration products it is possible to estimate the relative position of a rock sample to mineralization. By providing context to alteration patterns, the alteration model presented in this thesis could provide improved vectors to ore well outside mineralization.

6.4.4 Exploration Targeting Using Oxygen Isotopes

Exploration for Carlin-type deposits stands to benefit from an increased knowledge of the true scale of alteration footprints of Carlin-type Au deposits to more effectively explore for and evaluate targets. The two primary uses would be for (i) estimating the size potential of a Carlin-type Au deposit, and (ii) vectoring fluid pathways towards Au mineralization. Large gold companies need large deposits (>5 Moz's) to replenish Au reserves and develop efficient new mining operations. Evaluating the size potential early on in an exploration program can save both money and time. The study presented in Chapter 5 suggests that large systems such as found in the Goldstrike district have footprints with diameters of several km.'s. If a much smaller footprint of alteration is defined there might be less potential for a large Au discovery. Additionally if district scale sampling shows a much larger area of fluid-rock interaction, it may indicate greater size potential for an exploration target.

Vectoring fluid pathways is another potential benefit to the application of $\delta^{18}O$ isotope analyses in mineral exploration. Chapter 5 shows that the intensity of $\delta^{18}O$ alteration increases closer to mineralization. Using alteration intensity as a vector could lead to more refined drill target selection criteria. Once data is collected from 2-3 well place drill holes, $\delta^{18}O$ alteration may vector geologists in the direction of more intense alteration down the hydrothermal fluid flow path. While there is no direct correlation to the relative degree of $\delta^{18}O$ alteration and Au grade, this thesis shows that ore grade mineralization is associated with significant $\delta^{18}O$ alteration. Ore grade mineralization was not found in areas of minimal or no $\delta^{18}O$ alteration.

6.5 Future Research Directions

6.5.1 Dating of Alteration in Carlin-type Au Deposits

Dating of alteration minerals has proven elusive in Carlin-type deposits. Dating of galkhaite at the Getchell and Rodeo deposits has given Eocene ages believed to be coeval with mineralization (Arehart et al., 2003; Tretbar et al., 2000). However, galkhaite is rare and attempts at dating the more widespread illite alteration has consistently given ages much older than Eocene (Arehart et al., 2003; Arehart et al., 1993, 1995; Chakurian et al., 2003; DrewsArmitage et al., 1996; Folger et al., 1998; Groff et al., 1997; Hall et al., 2000; Hofstra et al., 1999; Ilchik, 1995). Arehart et al. (2003) note in their review of dating alteration in Carlin-type Au deposits that much of the illite is possibly older than mineralization and ore fluids were not sufficiently hot to reset $^{40}Ar/^{39}Ar$ in illite. Arehart et al. (2003) suggest that the best hope for dating illite is to define areas where potassic metasomatism is documented and linked with mineralization. This study identified potassic metasomatism associated with illitization and Au mineralization in the west Banshee dike potentially providing the ideal material for dating Carlin-type alteration. Samples of illite at west Banshee may represent the clearest link between illite and mineralization documented for Carlin-type deposits to date. Putting age constraints on the alteration at west Banshee could provide the first geochronologic evidence of Eocene illite/sericite on the Carlin trend outside of illite in an Eocene dike dated by Ressel et al. (2000a). The lack of Eocene dated illite in Carlin-type deposits is a missing link in the paragenesis of alteration.

6.5.2 Defining the Source of Fluid Components

The source of fluids and fluid components in Carlin-type deposits is debatable. The current literature has proponents of magmatic (Kesler et al., 2005; Muntean et al., 2011; Ressel, 2006) and amagmatic sources (Emsbo et al., 2006; Emsbo et al., 2003; Ilchik and Barton, 1997; Large et al., 2011). The west Banshee lamprophyre is a well constrained mineralized Jurassic dike that allows for further investigation of the source of fluid components. NanoSIMS analysis of ore stage pyrite from the west Banshee dike indicates depletion in $\delta^{34}S$ accompanies Au-rich rims. However, the specific values of $\delta^{34}S$ associated with Au could not be determined. Samples from the west Banshee dike should be used for more detailed work on $\delta^{34}S$ specifically within the Au rich rims in ore stage pyrite. Additionally, Pb isotopes could be measured within different stages of pyrite growth. Defining isotopic shifts related to Au rims might provide insight into the source of components directly precipitated with Au.

6.5.3 Testing of Alteration Models

An obvious future research direction is to test the alteration model developed in this paper at other occurrences of Carlin-type mineralization in Nevada. The lack of documentation of syn-alteration calcite veining argues for a reevaluation of the extensive calcite veining seen surrounding Carlin-type Au deposits. More detailed analysis of paragenetic relationships between veining, alteration, and mineralization should be investigated. However, this thesis provides a framework for evaluating calcite veining around Carlin-type Au deposits even when paragenesis is unclear. Alteration veining should be evaluated in each of the main Carlin-type Au deposit districts to test for the consistency of observations made at Banshee.

The footprint of $\delta^{18}O$ alteration surrounding Carlin-type deposits should also be tested at other known Carlin-type deposits to confirm the applicability of $\delta^{18}O$ alteration studies for defining distal footprints of hydrothermal alteration. Ideally testing would occur at both large and small deposits to evaluate the relationship between Au endowment, alteration, and fluid flow. The results of such studies should be measured against differences in host rock permeability and structural setting to put $\delta^{18}O$ alteration in context with differences between individual deposits.

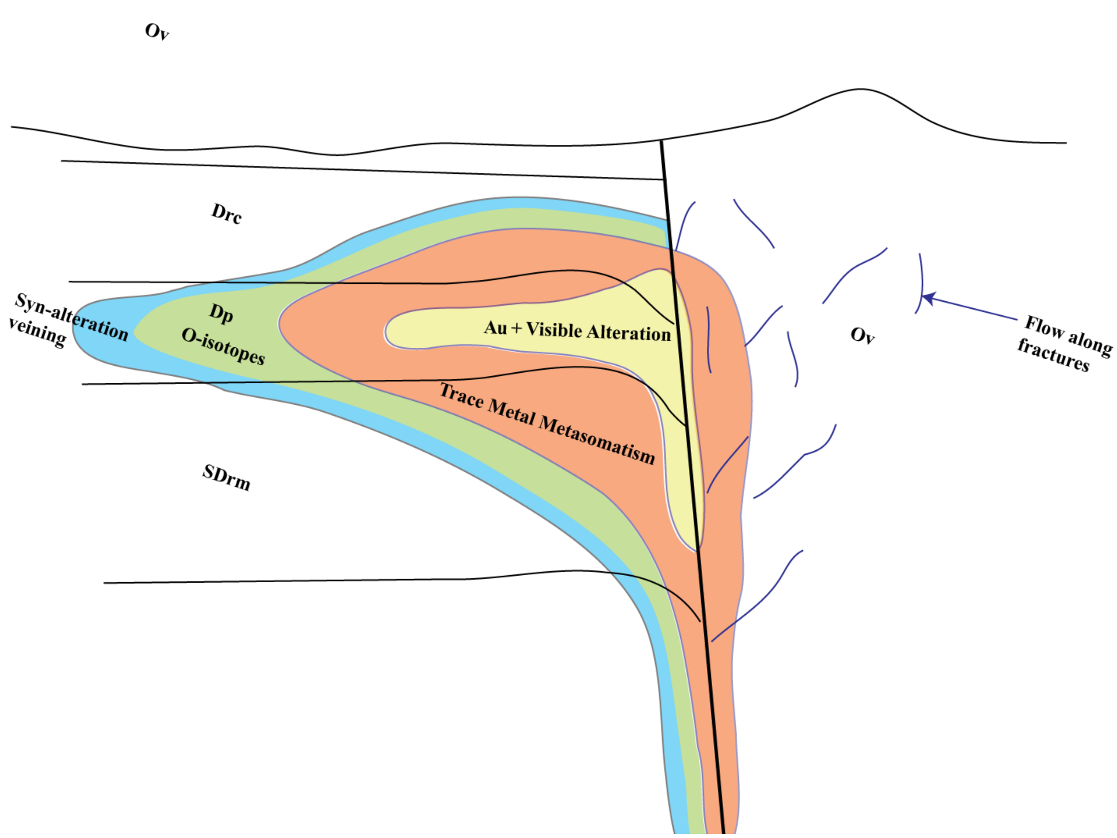

Figure 6.1 Proposed alteration model for Carlin-type Au deposits. Au deposition is restricted to within the zone of visible alteration proximal to the structural intersection with permeable stratigraphy.

References

Ahmed, A. D., 2010, Beyond the Confines of the Ore Deposit: Mapping Low Temperature Hydrothermal Alteration Above, Within, and Beneath Carlin-type Gold Deposits [M.S.: University of British Columbia, 197 p.

Albino, G. V., 1994, Geology and lithogeochemistry of the Ren gold prospect, Elko County, Nevada -- the role of rock sampling in exploration for deep Carlin-type deposits: Journal of Geochemical Exploration, v. 51, no. 1, p. 37-58.

Anna, L. O., Roberts, L. N. R., and Potter, C. J., 2007, Geologic Assessment of Undiscovered Oil and Gas in the Paleozoic-Tertiary Composite Total Petroleum System of the Eastern Great Basin, Nevada and Utah, *in* Interior, U. S. D. o. t., ed., Geologic Assessment of Undiscovered Oil and Gas Resources of the Eastern Great Basin Province, Nevada, Utah, Idaho, and Arizona, Volume U.S. Geological Reston, VA, USGS, p. 50.

Arehart, G. B., 1996, Characteristics and origin of sediment-hosted disseminated gold deposits: a review: Ore Geology Reviews, v. 11, no. 6, p. 383-403.

Arehart, G. B., Chakurian, A. M., Tretbar, D. R., Christensen, J. N., McInnes, B. A., and Donelick, R. A., 2003, Evaluation of radioisotope dating of Carlin-type deposits in the Great Basin, western North America, and implications for deposit genesis: Economic Geology and the Bulletin of the Society of Economic Geologists, v. 98, no. 2, p. 235-248.

Arehart, G. B., and Donelick, R. A., 2006, Thermal and isotopic profiling of the Pipeline hydrothermal system: Application to exploration for Carlin-type gold deposits: Journal of Geochemical Exploration, v. 91, no. 1-3, p. 27-40.

Arehart, G. B., Foland, K. A., Naeser, C. W., and Kesler, S. E., 1993, Ar-40/Ar-39, K/Ar, and fission-track geochronology of sediment-hosted disseminated gold deposits at Betze-Post, Carlin trend, northeastern Nevada: Economic Geology and the Bulletin of the Society of Economic Geologists, v. 88, no. 3, p. 622-646.

-, 1995, Ar-40/Ar-39, K/Ar, and fission-track geochronology of sediment-hosted disseminated gold deposits at Betze-Post, Carlin trend, northeastern Nevada - Reply: Economic Geology and the Bulletin of the Society of Economic Geologists, v. 90, no. 1, p. 210-212.

Armstrong, A. K., Theodore, T. G., Kotlyar, B. B., Lauha, E., Griffin, G. L., Lorge, D. L., and Abbot, E. W., 1997, Preliminary facies analysis of Devonian autochthonous rocks that host gold along the Carlin trend, Nevada, *in* Vikre, P., Thompson, T. B., Bettles, K., Christensen, O., and Parratt, R., eds., Carlin-Type Gold Deposits Field Conference: Society of Economic Geologists Guidebook Series: Fort Collins, CO, Society of Economic Geologists, p. 53-74.

Armstrong, A. K., Theodore, T. G., Oscarson, R. L., Kotlyar, B. B., Harris, A. G., Bettles, K. H., Lauha, E. A., Hipsley, R. A., Griffin, G. L., Abbot, E. W., and Cluer, J. K., 1998, Preliminary facies analysis of Silurian and Devonian autochthonous rocks that host gold along the Carlin trend, Nevada, *in* Tosdal, R. M., ed., Contributions to the gold metallogeny of northern Nevada, Volume 98-338: Menlo Park, CA, U.S. Geological Survey, p. 290.

Asquith, G., 1986, Microporosity in the O'Hara oolite zone of the Mississippian Ste. Genevieve Limestone, Hopkins County, Kentucky, and its implications for formation evaluation: Carbonates and Evaporites, v. 1, no. 1, p. 7-12.

Bakken, B. M., 1990, Gold mineralization, wall-rock alteration and the geochemical evolution of the hydrothermal system in the main ore body, Carlin Mine, Nevada [PhD: Stanford University, 236 p.

Bakken, B. M., and Einaudi, M. T., 1986, Spatial and temporal relations between wall rock alteration and gold mineralization, main pit, Carlin gold mine, Nevada, U.S.A., *in* Macdonald, A. J., ed., Proceedings of Gold '86, an International Symposium on the Geology of Gold: Toronto, Canada, Konsult International, p. 388-403.

Bakken, B. M., Hochella, M. F., Marshall, A. F., and Turner, A. M., 1989, High-resolution microscopy of gold in unoxidized ore from the Carlin Mine, Nevada: Economic Geology, v. 84, no. 1, p. 171-179.

Barker, S. L. L., Dipple, G. M., Dong, F., and Baer, D. S., 2011, Use of Laser Spectroscopy To Measure the 13C/12C and 18O/16O Compositions of Carbonate Minerals: Analytical Chemistry, p. null-null.

Barker, S. L. L., Dipple, G. M., Hickey, K. A., Lepore, W. A., and Vaughan, J. R., 2013, Applying Stable Isotopes to Mineral Exploration: Teaching an Old Dog New Tricks: Economic Geology, v. 108, no. 1, p. 1-9.

Barker, S. L. L., Hickey, K. A., Cline, J. S., Dipple, G. M., Kilburn, M. R., Vaughan, J. R., and Longo, A. A., 2009, Uncloaking Invisible Gold: Use of Nanosims to Evaluate Gold, Trace Elements, and Sulfur Isotopes in Pyrite from Carlin-Type Gold Deposits: Economic Geology, v. 104, no. 7, p. 897-904.

Bau, M., Balan, S., Schmidt, K., and Koschinsky, A., 2010, Rare earth elements in mussel shells of the Mytilidae family as tracers for hidden and fossil high-temperature hydrothermal systems: Earth and Planetary Science Letters, v. 299, no. 3-4, p. 310-316.

Bau, M., and Moller, P., 1992, Rare-earth element fractionation in metamorphogenic hydrothermal calcite, magnesite and siderite: Mineralogy and Petrology, v. 45, no. 3-4, p. 231-246.

Baumgartner, L. P., and Olsen, S. N., 1995, A least -squares approach to mass trasport calculations using the isocon method: Economic Geology and the Bulletin of the Society of Economic Geologists, v. 90, no. 5, p. 1261-1270.

Bettles, K., 2002, Exploration and geology, 1962 to 2002, at the Goldstrike property, Carlin Trend, Nevada, *in* Thompson, T. B., Teal, L., and Meeuwig, R. O., eds., Gold Deposits of the Carlin Trend, Volume Bulletin 111: Reno, Nevada Bureau of Mines and Geology, p. 54-75.

Bickle, M. J., and Baker, J., 1990, Migration of reaction and isotopic fronts in infiltration zones - assessments of fluid flux in metamorphic terrains: Earth and Planetary Science Letters, v. 98, no. 1, p. 1-13.

Bickle, M. J., and McKenzie, D., 1987, The transport of heat and matter by fluids during metamorphism: Contributions to Mineralogy and Petrology, v. 95, no. 3, p. 384-392.

Bilal, A. L., 1992, Thermodynamic study of Eu3+/Eu2+ redox reaction in aqueous solutions at elevated temperatures and pressures by means of cyclic voltammetry: Lanthan Actin Res.

Blattner, P., and Lassey, K. R., 1990, Transport of stable isotopes, kinetics, dispersive advection, and the isotopic fronts of baumgartner and rumble (1988): Contributions to Mineralogy and Petrology, v. 105, no. 4, p. 486-490.

Bons, P. D., Elburg, M. A., and Gomez-Rivas, E., 2012, A review of the formation of tectonic veins and their microstructures: Journal of Structural Geology, v. 43, p. 33-62.

Booden, M. A., Mauk, J. L., and Simpson, M. P., 2011, Quantifying Metasomatism in Epithermal Au-Ag Deposits: A Case Study from the Waitekauri Area, New Zealand: Economic Geology, v. 106, no. 6, p. 999-1030.

Bowman, J., Valley, J., and Kita, N., 2009, Mechanisms of oxygen isotopic exchange and isotopic evolution of O-18/O-16-depleted periclase zone marbles in the Alta aureole, Utah: insights from ion microprobe analysis of calcite: Contributions to Mineralogy and Petrology, v. 157, no. 1, p. 77-93.

Bowman, J. R., and Willett, S. D., 1991, Spatial patterns of oxygen isotope exchange during during one-dimensional fluid infiltration: Geophysical Research Letters, v. 18, no. 5, p. 971-974.

Bowman, J. R., Willett, S. D., and Cook, S. J., 1994, Oxygen isotopic transport and exchange during fluid flow: one-dimensional models and applications: American Journal of Science, v. 294, no. 1, p. 1-55.

Browne, P. R. L., 1978, Hydrothermal alteration in active geothermal fields: Annual Review of Earth and Planetary Sciences, v. 6, p. 229-250.

Cail, T. L., 1999, Alteration associated with gold deposition at the Getchell, Carlin-type gold deposit, north-central NevadaM.S.]: University of Nevada, Las Vegas.

Cail, T. L., and Cline, J. S., 2001, Alteration Associated with Gold Deposition at the Getchell Carlin-Type Gold Deposit, North-Central Nevada: Economic Geology, v. 96, no. 6, p. 1343-1359.

Carmichael, S. K., and Ferry, J. M., 2008, Formation of replacement dolomite in the Latemar carbonate buildup, Dolomites, northern Italy: Part 2. Origin of the dolomitizing fluid and the amount and duration of fluid flow: Am J Sci, v. 308, no. 8, p. 885-904.

Cartwright, I., and Buick, I. S., 1999, The flow of surface-derived fluids through Alice Springs age middle-crustal ductile shear zones, Reynolds Range, central Australia: Journal of Metamorphic Geology, v. 17, no. 4, p. 397-414.

Cathles, L. M., 1981, Fluid Flow and Genesis of Hydrothermal Ore Deposits, Economic Geology 75th Anniversary Volume, Society of Economic Geologists, p. 424-457.

Cathles, L. M., 1990, Scales and Effects of Fluid Flow in the Upper Crust: Science, v. 248, no. 4953, p. 323-329.

Cathles, L. M., 1993, Oxygen-Isotope Alteration in the Noranda Mining District, Abitibi Greenstone-Belt, Quebec: Economic Geology and the Bulletin of the Society of Economic Geologists, v. 88, no. 6, p. 1483-1511.

Cathles, L. M., 1997, Thermal aspects of ore deposition, *in* Barnes, H., ed., Geochemistry of Hydrthermal Ore Deposits: New York, Wiley and Sons, p. 191-227.

Cavarretta, G., Gianelli, G., Scandiffio, G., and Tecce, F., 1985, Evolution of the Latera geothermal sytem, 2. metamorphic, hydrothermal mineral assemblages and fluid chemistry: Journal of Volcanology and Geothermal Research, v. 26, no. 3-4, p. 337-364.
Chakurian, A. M., Arehart, G. B., Donelick, R. A., Zhang, X., and Reiners, P. W., 2003, Timing constraints of gold mineralization along the Carlin trend utilizing apatite fission-track, 40Ar/39Ar, and apatite (U-Th)/He methods: Economic Geology and the Bulletin of the Society of Economic Geologists, v. 98, no. 6, p. 1159-1171.
Christiansen, R. L., and Yeats, R. S., 1992, Post-Laramide geology of the U.S. Cordilleran region, *in* Burchfiel, B. C., Lipman, P. W., and Zoback, M. L., eds., Cordilleran orogen: Conterminous U.S.: Boulder, CO, Geological Society of America, p. 261-406.
Clayton, R. N., Goldsmith, J. R., and Mayeda, T. K., 1989, Oxygen isotope fractionation in quartz, albite, anorthite and calcite: Geochimica et Cosmochimica Acta, v. 53, no. 3, p. 725-733.
Clayton, R. N., Muffler, L. J. P., and White, D. E., 1968, Oxygen Isotope Study of Calcite and Silicates of River Ranch No 1 Well Salton Sea Goethermal Field California: American Journal of Science, v. 266, no. 10, p. 968-&.
Cline, J. S., and Hofstra, A. A., 2000, Ore-fluid evolution at the Getchell Carlin-type gold deposit, Nevada, USA: European Journal of Mineralogy, v. 12, no. 1, p. 195-212.
Cline, J. S., Hofstra, A. H., Muntean, J. L., Tosdal, R. M., and Hickey, K. A., 2005, Carlin-type gold deposits in Nevada: critical geologic characteristics and viable models., *in* Hedenquist, J. W., Thompson, J. F. H., Goldfarb, R. J., and Richards, J. P., eds., Economic Geology Geology 100th anniversary volume: Boulder, CO, Society of Economic Geologists, p. 451-484.
Cole, D. R., 1994, Evidence for Oxygen-Isotope Disequilibrium in Selected Geothermal and Hydrothermal Ore Deposit Systems: Chemical Geology, v. 111, no. 1-4, p. 283-296.
Cole, D. R., and Chakraborty, S., 2001, Rates and Mechanisms of Isotopic Exchange: Reviews in Mineralogy, v. 43, p. 83-224.
Cole, D. R., and Ohmoto, H., 1986, Kinetics of Isotopic Exchange at Elevated-Temperatures and Pressures: Reviews in Mineralogy, v. 16, p. 41-90.
Cole, D. R., Ohmoto, H., and Lasaga, A. C., 1983, Isotopic exchange in mineral-fluid systems. I. Theoretical evaluation of oxygen isotopic exchange accompanying surface reactions and diffusion: Geochimica et Cosmochimica Acta, v. 47, no. 10, p. 1681-1693.
Cook, H. E., and Corboy, J. J., 2004, Great Basin Paleozoic Carbonate Platform: Facies, Facies Transitions, Depositional Models, Platform Architecture, Sequence Stratigraphy, and Predictive Mineral Host Models, *in* USGS, ed.: Reston, VA, USGS, p. 135.
Coplen, T. B., Kendall, C., and Barnes, I. L., 1982, Comment on "two new carbonate stable isotope standards": Geostandards Newsletter, v. 6, no. 2, p. 257-258.
Coplen, T. B., Kendall, C., and Hopple, J., 1983, Comparison of stable isotope reference samples: Nature, v. 302, no. 5905, p. 236-238.
Cox, S. F., 2005, Coupling between deformation, fluid pressures, and fluid flow in ore-producing hydrothermal systems at depth in the crust, *in* Hedenquist, J. W.,

Thompson, J. F. H., Goldfarb, R. J., and Richards, J. P., eds., Economic Geology 100th Anniversary Volume: Littleton, CO, Society of Economic Geologists, p. 39-75.
-, 2007, Structural and isotopic constraints on fluid flow regimes and fluid pathways during upper crustal deformation: An example from the Taemas area of the Lachlan Orogen, SE Australia: Journal of Geophysical Research-Solid Earth, v. 112, no. B8.
Cox, S. F., Braun, J., and Knackstedt, M. A., 2001, Principles of structural control on permeability and fluid flow in hydrothermal systems: Reviews in Economic Geology, v. 14, p. 1-24.
Criss, R. E., and Campion, D. E., 1991, Oxygen isotopes study of the fossil hydrothermal system in the Comstock lode mining district, Nevada: Geochemical Society Special Publication 3, p. 437-447.
Criss, R. E., Fleck, R. J., and Taylor, H. P., 1991, Tertiary meteoric hydrothermal systems and their relation to ore deposition, northwestern United States and southern British Columbia: Journal of Geophysical Research-Solid Earth and Planets, v. 96, no. B8, p. 13335-13356.
Criss, R. E., and Taylor, H. P., 1983, An O-18/O-16 and D/H study of tertiary hydrothermal systems in the southern half of teh Idaho Batholith: Geological Society of America Bulletin, v. 94, no. 5, p. 640-663.
Cui, X. J., Nabelek, P. I., and Liu, M., 2001, Heat and fluid flow in contact metamorphic aureoles with layered and transient permeability, with application to the Notch Peak aureole, Utah: Journal of Geophysical Research-Solid Earth, v. 106, no. B4, p. 6477-6491.
Davies, A. G. S., Cooke, D. R., Gemmell, J. B., and Simpson, K. A., 2008, Diatreme Breccias at the Kelian Gold Mine, Kalimantan, Indonesia: Precursors to Epithermal Gold Mineralization: Economic Geology, v. 103, no. 4, p. 689-716.
de Almeida, C. M., Olivo, G. R., Chouinard, A., Weakly, C., and Poirier, G., 2010, Mineral Paragenesis, Alteration, and Geochemistry of the Two Types of Gold Ore and the Host Rocks from the Carlin-Type Deposits in the Southern Part of the Goldstrike Property, Northern Nevada: Implications for Sources of Ore-Forming Elements, Ore Genesis, and Mineral Exploration: Economic Geology, v. 105, no. 5, p. 971-1004.
Deniel, C., and Pin, C., 2001, Single-stage method for the simultaneous isolation of lead and strontium from silicate samples for isotopic measurements: Analytica Chimica Acta, v. 426, no. 1, p. 95-103.
DePaolo, D. J., 1988, Neodymium Isotope Geochemistry, Berlin, Springer-Verlag.
Dickinson, W. R., 2006, Geotectonic evolution of the Great Basin: Geosphere, v. 2, no. 7, p. 353-368.
Diehl, S. F., Hofstra, A. H., Koenig, A. E., Emsbo, P., Christiansen, W., and Johnson, C., 2010, Hydrothermal Zebra Dolomite in the Great Basin, Nevada--Attributes and Relation to Paleozoic Stratigraphy, Tectonics, and Ore Deposits: Geosphere, v. 6, no. 5, p. 663-690.
Dipple, G. M., and Ferry, J. M., 1992a, Fluid flow and stable isotopic alteration in rocks at elevated temperatures with applications to metamorphism: Geochimica et Cosmochimica Acta, v. 56, no. 9, p. 3539-3550.

Dipple, G. M., and Ferry, J. M., 1992b, Metasomatism and Fluid-Flow in Ductile Fault Zones: Contributions to Mineralogy and Petrology, v. 112, no. 2-3, p. 149-164.
Dobak, P. J., Arbonies, D., Hipsley, R., and Visher, M., 2002, Geology of the Storm gold deposits, *in* Thompson, T. B., Teal, L., and Meeuwig, R. O., eds., Gold deposits of the Carlin trend: Reno, NV, Nevada Bureau of Mines and Geology, p. 46-53.
Dobson, P. F., Kneafsey, T. J., Hulen, J., and Simmons, A., 2003, Porosity, permeability, and fluid flow in the Yellowstone geothermal system, Wyoming: Journal of Volcanology and Geothermal Research, v. 123, no. 3-4, p. 313-324.
Dodson, M., 1973, Closure temperature in cooling geochronological and petrological systems: Contributions to Mineralogy and Petrology, v. 40, no. 3, p. 259-274.
DrewsArmitage, S. P., Romberger, S. B., and Whitney, C. G., 1996, Clay alteration and gold deposition in the Genesis and Blue Star deposits, Eureka County, Nevada: Economic Geology and the Bulletin of the Society of Economic Geologists, v. 91, no. 8, p. 1383-1393.
Ehrenberg, S. N., Eberli, G. P., Keramati, M., and Moallemi, S. A., 2006, Porosity-permeability relationships in interlayered limestone-dolostone reservoirs: AAPG Bulletin, v. 90, no. 1, p. 91-114.
Eiler, J. M., 2001, Oxygen Isotope Variations of Basaltic Lavas and Upper Mantle Rocks: Reviews in Mineralogy and Geochemistry, v. 43, no. 1, p. 319-364.
Emsbo, F., Hutchinson, R. W., Hofstra, A. H., Volk, J. A., Bettles, K. H., Baschuk, G. J., and Johnson, C. A., 1999, Syngenetic Au on the Carlin trend: Implications for Carlin-type deposits: Geology, v. 27, no. 1, p. 59-62.
Emsbo, P., Groves, D. I., Hofstra, A. H., and Bierlein, F. P., 2006, The giant Carlin gold province: a protracted interplay of orogenic, basinal, and hydrothermal processes above a lithospheric boundary: Mineralium Deposita, v. 41, no. 6, p. 517-525.
Emsbo, P., and Hofstra, A. H., 2003, Origin and significance of postore dissolution collapse breccias cemented with calcite and barite at the Meikle gold deposit, northern Carlin trend, Nevada: Economic Geology and the Bulletin of the Society of Economic Geologists, v. 98, no. 6, p. 1243-1252.
Emsbo, P., Hofstra, A. H., Lauha, E. A., Griffin, G. L., and Hutchinson, R. W., 2003, Origin of high-grade gold ore, source of ore fluid components, and genesis of the Meikle and neighboring Carlin-type deposits, northern Carlin trend, Nevada: Economic Geology and the Bulletin of the Society of Economic Geologists, v. 98, no. 6, p. 1069-1105.
Emsbo, P., Hofstra, A. H., Park, D., Zimmerman, J. M., and Snee, L., 1996, A mid-Tertiary age constraint on alteration and mineralization in igneous dikes on the Goldstrike property, Carlin trend, Nevada [abs.]: Geological Society of America Abstracts with Programs, v. 28, no. 7, p. A476.
Engel, A. E. J., Clayton, R. N., and Epstein, S., 1958, Variations in Isotopic Composition of Oxygen and Carbon in Leadville Limestone (Mississippian, Colorado) and in its Hydrothermal and Metamorphic Phases: The Journal of Geology, v. 66, no. 4, p. 374-393.
Ettner, D. C., 1989, Stratigraphy and structure of the Devonian autochthonous rocks, north-central Carlin trend of the southern Tuscarora Mountains, northern Eureka County, Nevada [M.Sc.: Idaho State University, 177 p.

Evans, D., 2000, Carbonate-hosted breccias in the Meikle mine, Nevada and their relationship with gold mineralization [MSc: Colorado School of Mines, 266 p.
Evans, J. G., and Mullens, T. E., 1976, Bootstrap window, Elko and Eureka counties, Nevada: Journal of Research of the US Geological Survey, v. 4, no. 1, p. 119-125.
Ferry, J. M., and Dipple, G. M., 1991, Fluid flow, mineral reactions, and metasomatism: Geology, v. 19, no. 3, p. 211-214.
Folger, H. W., Hofstra, A. H., Eberl, D. D., and Snee, L. W., 1998, Importance of clay characterization to interpretation of 40Ar/39Ar dates on illite from Carlin-type gold deposits: Insights from Jerritt Canyon, Nevada, *in* Tosdal, R. M., ed., Contributions to the Gold Metallogeny of Northern Nevada, Volume 98-338: Menlo Park, CA, US Geological Survey, p. 176-192.
Fortuna, J., Kesler, S. E., and Stenger, D. P., 2003, Source of iron for sulfidation and gold deposition, Twin Creeks Carlin-type deposit, Nevada: Economic Geology and the Bulletin of the Society of Economic Geologists, v. 98, no. 6, p. 1213-1224.
Frimmel, H. E., 1992, Isotopic fronts in hydrothermally mineralized carbonate rocks: Mineralium Deposita, v. 27, no. 4, p. 257-267.
Furley, R., 2001, Sequence stratigraphic framework for the Silurian-Devonian bootstrap limestone, Roberts Mountains, and Devonian Popovich formations, northern Carlin trend, Elko and Eureka counties, Nevada [MSc: Colorado School of Mines, 194 p.
Gemmell, J. B., 2007, Hydrothermal alteration associated with the Gosowong epithermal Au-Ag deposit, Halmahera, Indonesia: Mineralogy, geochemistry, and exploration implications: Economic Geology, v. 102, no. 5, p. 893-922.
Giggenbach, W. F., 1992, Isotopic shifts in waters from geothermal and volcanic systems along convergent plate boundaries and their origin: Earth and Planetary Science Letters, v. 113, no. 4, p. 495-510.
Giggenbach, W. F., 1997, The origin and evolution of fluids inmagmatic-hydrothermal systems, *in* Barnes, H., ed., Geochemistry of hydrothermal ore deposits: New York, Wiley and Sons, p. 737-796.
Goff, F., and Gardner, J. N., 1994, Evolution of a mineralized geothermal system, Valles Caldera, New Mexico: Economic Geology and the Bulletin of the Society of Economic Geologists, v. 89, no. 8, p. 1803-1832.
Grant, J. A., 1986, The isocon diagram - a simple solution to Gresens equation for metasomatic alteration: Economic Geology, v. 81, no. 8, p. 1976-1982.
-, 2005, Isocon analysis: A brief review of the method and applications: Physics and Chemistry of the Earth, v. 30, no. 17-18, p. 997-1004.
Gresens, R. L., 1967, Composition-volume relationships of metasomatism: Chemical Geology, v. 2, p. 47-65.
Groff, J. A., Heizler, M. T., McIntosh, W. C., and Norman, D. I., 1997, Ar-40/Ar-39 dating and mineral paragenesis for Carlin-type gold deposits along the Getchell trend, Nevada: Evidence for Cretaceous and tertiary gold mineralization: Economic Geology and the Bulletin of the Society of Economic Geologists, v. 92, no. 5, p. 601-622.
Hall, C. M., Kesler, S. E., Simon, G., and Fortuna, J., 2000, Overlapping Cretaceous and Eocene alteration, Twin Creeks Carlin-type deposit, Nevada: Economic Geology

and the Bulletin of the Society of Economic Geologists, v. 95, no. 8, p. 1739-1752.
Harris, M., and Radtke, A. S., 1976, Statistical study of selected trace elements with reference to geology and genesis of the Carlin gold deposit, Nevada, Washington, U.S. Govt. Print. Off., iii, 21 p. p.:
Hausen, D. M., and Kerr, P. F., 1968, Fine gold occurrence at Carlin, Nevada, *in* Ridge, J. D., ed., Ore deposits of the United States, 1933-1967, Volume 1: New York, American Institute of Mining and Engineers, p. 908-940.
Hedenquist, J. W., Reyes, A. G., Simmons, S. F., and Taguchi, S., 1992, The thermal and geochemical structure of geothermal and epithermal systems - a framework for interpreting fluid inclusion data: European Journal of Mineralogy, v. 4, no. 5, p. 989-1015.
Hedenquist, J. W., Thompson, J. F. H., Goldfarb, R. J., and Richards, J. P., 2005, Economic Geology One Hundredth Anniversary Volume: Boulder, CO, Society of Economic Geologists, p. 1136.
Heinrich, C. A., Walshe, J. L., and Harrold, B. P., 1996, Chemical mass transfer modelling of ore-forming hydrothermal systems: Current practise and problems: Ore Geology Reviews, v. 10, no. 3-6, p. 319-338.
Heitt, D. G., Dunbar, W. W., Thompson, T. B., and Jackson, R. G., 2003, Geology and geochemistry of the deep star gold deposit, Carlin trend, Nevada: Economic Geology and the Bulletin of the Society of Economic Geologists, v. 98, no. 6, p. 1107-1135.
Henley, R., and Ellis, A., 1983, Geothermal Systems Ancient and Modern: A Geochemical Review, Earth Science Reviews: Amsterdam, Elsevier Scientific Publishing Company, p. 1-50.
Henley, R. W., 1984, Hydrolysis Reactions in Hydrothermal Fluids, *in* Robertson, J. M., ed., Fluid-Mineral Equilibria in Hydrothermal Systems, Volume 1: El Paso, TX, Society of Economic Gologists, p. 65-82.
Henry, C. D., and Boden, D. R., 1998, Eocene magmatism: The heat source for Carlin-type gold deposits of northern Nevada: Geology, v. 26, no. 12, p. 1067-1070.
Hickey, K. A., Barker, S. L. L., Dipple, G. M., Arehart, G. B., and Donelick, R. A., 2013, The brevity of hydrothermal fluid flow revealed by thermal haloes around giant Au-deposits: implications for Carlin-type gold systems: Economic Geology- in Review.
Hickman, S., Sibson, R., and Bruhn, R., 1995, Introduction to special section: mechanical involvement of fluids in faulting: Journal of Geophysical Research, v. 100, no. 12, p. 831-840.
Hofstra, A. H., 1994, Geology and genesis of the Carlin-type gold deposits in the Jeritt Canyon district, Nevada [PhD Unpublished PhD]: University of Colorado, 719 p.
Hofstra, A. H., Christiansen, W. D., Zohar, P. B., and Tousignant, G., 2011, Lithogeochemistry of the Devonian Popovich Formation in the Northern Carlin Trend, Nevada, Great Basin Evolution and Metallogeny, Vols I and Ii, 63-96 p.:
Hofstra, A. H., and Cline, J. S., 2000, Characteristics and models for Carlin-type gold deposits: Reviews in Economic Geology, v. 13, p. 163-220.
Hofstra, A. H., Leventhal, J. S., Northrop, H. R., Landis, G. P., Rye, R. O., Birak, D. J., and Dahl, A. R., 1991, Genesis of sediment-hosted disseminated-gold deposits by

fluid mixing and sulfidization; chemical-reaction-path modeling of ore-depositional processes documented in the Jerritt Canyon District, Nevada: Geology, v. 19, no. 1, p. 36-40.
Hofstra, A. H., Northrop, H. R., Rye, R. O., Landis, G. P., and Birak, D. J., Origin of sediment-hosted disseminated gold deposits by fluid mixing: Evidence from jasperoids in the Jerritt Canyon gold district, Nevada, USA, *in* Proceedings Geological Society of Australia Oral Programme 221988, p. 284-289.
Hofstra, A. H., Snee, L. W., Rye, R. O., Folger, H. W., Phinisey, J. D., Loranger, R. J., Dahl, A. R., Naeser, C. W., Stein, H. J., and Lewchuk, M., 1999, Age constraints on Jerritt Canyon and other Carlin-type gold deposits in the western United States-relationship to mid-tertiary extension and magmatism: Economic Geology and the Bulletin of the Society of Economic Geologists, v. 94, no. 6, p. 769-802.
Holland, P. T., Beaty, D. W., and Snow, G. G., 1988, Comparative elemental and oxygen isotope geochemistry of jasperoid in the northern Great Basin- evidence for distinctive fluid evolution in gold producing hydrothermal systems: Economic Geology, v. 83, no. 7, p. 1401-1423.
Huttrer, G. W., 2001, The status of world geothermal power generation 1995-2000: Geothermics, v. 30, no. 1, p. 1-27.
Ikramuddin, M., Besse, L., and Nordstrom, P. M., 1986, The relation between Tl, Rb, and K in the Carlin-type gold deposits: Journal of Geochemical Exploration, v. 25, no. 1-2, p. 253-253.
Ilchik, R. P., 1990, Geology and geochemistry of the Vantage gold deposits, Alligator Ridge-Bald Mountain mining district, Nevada: Economic Geology and the Bulletin of the Society of Economic Geologists, v. 85, no. 1, p. 50-75.
-, 1995, Ar-40/Ar-39, K/Ar, and fission track geochronology of sediment-hosted disseminated gold deposits at Post-Betze, Carlin trend, northeastern Nevada - Discussion: Economic Geology and the Bulletin of the Society of Economic Geologists, v. 90, no. 1, p. 208-210.
Ilchik, R. P., and Barton, M. D., 1997, An amagmatic origin of carlin-type gold deposits: Economic Geology, v. 92, no. 3, p. 269-288.
Ingebritsen, S., Sanford, W., and Neuzil, C., 2006, Groundwater in Geologic Processes, Cambridge, University Press, 536 p.:
Jennings, S., and Thompson, G. R., 1986, Diagenesis of Plio-Pleistocene sediments of teh Colorado River delta, southern California: Journal of Sedimentary Petrology, v. 56, p. 89-98.
Jory, J., 2002, Stratigraphy and host rock controls of gold deposits of the northern Carlin trend, *in* Thompson, T. B., Teal, L., and Meeuwiw, R., eds., Gold deposits of the Carlin trend, Volume 111: Reno, Nevada Bureau of Mines and Geology, p. 20-34.
Kelley, D. L., Kelley, K. D., Coker, W. B., Caughlin, B., and Doherty, M. E., 2006, Beyond the Obvious Limits of Ore Deposits: The Use of Mineralogical, Geochemical, and Biological Features for the Remote Detection of Mineralization: Economic Geology, v. 101, no. 4, p. 729-752.
Kennedy, B. M., and van Soest, M. C., 2006, A helium isotope perspective on the Dixie Valley, Nevada, hydrothermal system: Geothermics, v. 35, no. 1, p. 26-43.
Kesler, S. E., 2005, Ore-Forming Fluids: ELEMENTS, v. 1, no. 1, p. 13-18.

Kesler, S. E., Fortuna, J., Ye, Z. J., Alt, J. C., Core, D. P., Zohar, P., Borhauer, J., and Chryssoulis, S. L., 2003, Evaluation of the role of sulfidation in deposition of gold, Screamer section of the Betze-Post Carlin-type deposit, Nevada: Economic Geology and the Bulletin of the Society of Economic Geologists, v. 98, no. 6, p. 1137-1157.

Kesler, S. E., Riciputi, L. C., and Ye, Z. J., 2005, Evidence for a magmatic origin for Carlin-type gold deposits: isotopic composition of sulfur in the Betze-Post-Screamer deposit, Nevada, USA: Mineralium Deposita, v. 40, no. 2, p. 127-136.

Kesler, S. E., Vennemann, T. W., Vazquez, R., Stenger, D. P., and Frederickson, G. C., Application of large-scale oxygen isotope haloes to exploration for chimney-mano Pb-Zn-Cu-Ag deposits, *in* Proceedings Geology and ore deposits of the American Cordillera: Geological Society of Nevada Conference, Reno/Sparks, 1995, p. 1383-1396.

Khan, F. I., Husain, T., and Hejazi, R., 2004, An overview and analysis of site remediation technologies: Journal of Environmental Management, v. 71, no. 2, p. 95-122.

Kim, S. T., and Oneil, J. R., 1997, Equilibrium and nonequilibrium oxygen isotope effects in synthetic carbonates: Geochimica et Cosmochimica Acta, v. 61, no. 16, p. 3461-3475.

Knoop, S. R., Kennedy, L. A., and Dipple, G. M., 2002, New evidence for syntectonic fluid migration across the hinterland-foreland transition of the Canadian Cordillera: Journal of Geophysical Research-Solid Earth, v. 107, no. B4.

Kuehn, C. A., 1989, Studies of disseminated gold deposits near Carlin, Nevada: Evidence for a deep geologic setting of ore formation [PhD: Pennsylvania State University, 396 p.

Kuehn, C. A., and Rose, A. W., 1992, Geology and geochemistry of wall-rock alteration at the Carlin gold deposit, Nevada: Economic Geology and the Bulletin of the Society of Economic Geologists, v. 87, no. 7, p. 1697-1721.

-, 1995, Carlin gold deposits, Nevada - origin in a deep zone of mixing between normally pressured and overpressured fluids: Economic Geology and the Bulletin of the Society of Economic Geologists, v. 90, no. 1, p. 17-36.

Kühn, M., 2001, Concepts, Classification, and Chemistry of Geothermal Systems: Lecture Notes in Earth Sciences, Berlin Springer Verlag, v. 103, p. 11-46.

Labotka, T. C., Cole, D. R., Fayek, M. J., and Chacko, T., 2011, An experimental study of the diffusion of C and O in calcite in mixed CO2-H2O fluid: American Mineralogist, v. 96, no. 8-9, p. 1262-1269.

Large, R. R., Bull, S. W., and Maslennikov, V. V., 2011, A Carbonaceous Sedimentary Source-Rock Model for Carlin-Type and Orogenic Gold Deposits: Economic Geology, v. 106, no. 3, p. 331-358.

Large, R. R., Danyushevsky, L., Hollit, C., Maslennikov, V., Meffre, S., Gilbert, S., Bull, S., Scott, R., Emsbo, P., Thomas, H., Singh, B., and Foster, J., 2009, Gold and Trace Element Zonation in Pyrite Using a Laser Imaging Technique: Implications for the Timing of Gold in Orogenic and Carlin-Style Sediment-Hosted Deposits: Economic Geology, v. 104, no. 5, p. 635-668.

Lasaga, A. C., Rye, D. M., L¸ttge, A., and Bolton, E. W., 2001, Calculation of fluid fluxes in Earth's crust: Geochimica et Cosmochimica Acta, v. 65, no. 7, p. 1161-1185.
Lassey, K. R., 1982, On the Computation of Certain Integrals Containing the Modified Bessel-Function I0(Zeta): Mathematics of Computation, v. 39, no. 160, p. 625-637.
Lassey, K. R., and Blattner, P., 1988, Kinetically Controlled Oxygen Isotope Exchange between Fluid and Rock in One-Dimensional Advective Flow: Geochimica et Cosmochimica Acta, v. 52, no. 8, p. 2169-2175.
Le Bas, M. J., and Streckeisen, A. L., 1991, The IUGS systematics of igneous rocks: Journal of the Geological Society, v. 148, no. 5, p. 825-833.
Leach, D. L., Sangster, D. F., Kelley, K. D., Large, R. R., Garven, G., Allen, C. R., Gutzmer, J., and Walters, S., 2005, Sediment-Hosted Lead-Zinc Deposits: A Global Perspective, *in* Hedenquist, J. W., Thompson, J. F. H., Goldfarb, R. J., and Richards, J. P., eds., Economic Geology Geology 100th anniversary volume: Boulder, CO, Society of Economic Geologists, p. 561-608.
Leonardson, R. W., and Rahn, J. E., 1996, Geology of the Betze-Post gold deposits, Eureka county, Nevada, *in* Coyner, A. R., and Fahey, P. L., eds., Geology and ore deposits of the American Cordillera: Reno, Nevada, Gelogical Society of Nevada.
Loucks, R., 1999, Paleocave carbonate reservoirs: Origins, burial-depth modifications, spatial complexity, and reservoir implications: AAPG Bulletin, v. 83, p. 1795-1834.
Lubben, J. D., 2004, Silicification Across the Betze-Post Carlin-Type Au Deposit: Clues to Ore Fluid Properties and Sources, Northern Carlin Trend, Nevada [MS Unpublished MS Thesis]: University of Nevada, Las Vegas, 155 p.
Lubben, J. D., Cline, J. S., and Barker, S. L. L., 2012, Ore Fluid Properties and Sources from Quartz-Associated Gold at the Betze-Post Carlin-Type Gold Deposit, Nevada, United States: Economic Geology, v. 107, no. 7, p. 1351-1385.
Machel, H. G., and Burton, E. A., 1991, Factors Governing Cathodoluminescence in Calcite and Dolomite, and Their Implications for Studies of Carbonate Diagenesis: Luminescence Microscopy and Spectroscopy : Qualitative and Quantitative Applications, v. 25, p. 37-57.
Maclean, W. H., 1990, Mass change calculations in altered rock series: Mineralium Deposita, v. 25, no. 1, p. 44-49.
Maclean, W. H., and Barrett, T. J., 1993, Lithogeochemical techniques usng immobile elements: Journal of Geochemical Exploration, v. 48, no. 2, p. 109-133.
Maclean, W. H., and Kranidiotis, P., 1987, Immobile elements as monitors of mass transfer in hydrothermal alteration - Phelps Dodge massive sulfide deposit, Matagami, Quebec: Economic Geology, v. 82, no. 4, p. 951-962.
Manning, C. E., and Ingebritsen, S. E., 1999, Permeability of the continental crust: Implications of geothermal data and metamorphic systems: Reviews of Geophysics, v. 37, no. 1, p. 127-150.
Mauk, J. L., and Simpson, M. P., Geochemistry and Stable Isotope Composition of Altered Rocks at the Golden Cross Epithermal Au-Ag Deposit, New Zealand: Economic Geology, v. 102, no. 5, p. 841-871.

-, 2007, Geochemistry and Stable Isotope Composition of Altered Rocks at the Golden Cross Epithermal Au-Ag Deposit, New Zealand: Economic Geology, v. 102, no. 5, p. 841-871.
McLennan, S. M., 1989, Rare earth elements in sedimentary rocks - influence of provenance and sedimentary processes: Reviews in Mineralogy, v. 21, p. 169-200.
Meinert, L. D., 1992, Skarns and skarn deposits: Geoscience Canada, v. 19, no. 4, p. 145-162.
Meinert, L. D., Dipple, G. M., and Nicolescu, S., 2005, World skarn deposits, *in* Hedenquist, J. W., Thompson, J. F. H., Goldfarb, R. J., and Richards, J. P., eds., Economic Geology One Hundredth Anniversary Volume: Littleton, CO, Society of Economic Geologists, p. 299-336.
Merriam, C. W., and Anderson, C. A., 1942, Reconnaissance survey of the Roberts Mountains, Nevada: Geological Society of America Bulletin, v. 53, p. 1675-1728.
Meunier, A., 2005, Hydrothermal Process-Thermal Metamorphism, Clays: New York, Springer, p. 379-415.
Meyer, C., and Hemley, J. J., 1967, Wall rock alteration, *in* Barnes, H., ed., Geochemistry of Hydrothermal Ore Deposits: New York, Holt, Rinehart and Winston, p. 166-165.
Morgan, C. E., 2006, Alteration of the bootstrap limestone, northern Carlin trend, Elko county, Nevada [MSc: Colarado School of Mines, 135 p.
Morse, J. W., Arvidson, R. S., and Luttge, A., 2007, Calcium carbonate formation and dissolution: Chemical Reviews, v. 107, no. 2, p. 342-381.
Mortensen, J. K., Thompson, J. F. H., and Tosdal, R. M., U-Pb age constraints on magmatism and mineralization in the northern Great Basin, Nevada, *in* Proceedings The Great Basin and Beyond Symposium, Reno/Sparks, Nevada, May 15-18, 2000 2000, Geological Society of Nevada, p. 419-438.
Muntean, J. L., Cline, J. S., Simon, A. C., and Longo, A. A., 2011, Magmatic-hydrothermal origin of Nevada's Carlin-type gold deposits: Nature Geoscience, v. 4, no. 2, p. 122-127.
Nabelek, P. I., 1987, General Equations for Modeling Fluid Rock Interaction Using Trace-Elements and Isotopes: Geochimica et Cosmochimica Acta, v. 51, no. 6, p. 1765-1769.
Nelson, C. E., 1990, Comparative geochemistry of jasperoids from Carlin-type gold deposits of the western United States: Journal of Geochemical Exploration, v. 36, no. 1-3, p. 171-195.
Nesbitt, B. E., 1996, Applications of oxygen and hydrogen isotopes to exploration for hydrothermal mineralization: Society of Economic Geologists Newsletter, no. 27, p. 1, 8-13.
Norton, D. L., 1984, Theory of Hydrothermal Systems, Annual Reviews in Earth and Planetary Science, Annual Reviews, p. 155-177.
Nutt, C. J., and Hofstra, A. H., 2003, Alligator ridge district, east-central Nevada: Carlin-type gold mineralization at shallow depths: Economic Geology and the Bulletin of the Society of Economic Geologists, v. 98, no. 6, p. 1225-1241.
O'Neil, J. R., 1986, Theoretical and experimental aspects of isotopic fractionation: Reviews in Mineralogy and Geochemistry, v. 16, no. 1, p. 1-40.

O'Neil, J. R., Clayton, R. N., and Mayeda, T. K., 1969, Oxygen Isotope Fractionation in Divalent Metal Carbonates: The Journal of Chemical Physics, v. 51, no. 12, p. 5547-5558.

Ohmoto, H., 1986, Stable isotope geochemistry of ore deposits: Reviews in Mineralogy and Geochemistry, v. 16, no. 1, p. 491-559.

Ohmoto, H., and Rye, R., 1979, Isotopes of sulfur and carbon, *in* Barnes, H., ed., Geochemistry of Hydrothermal Ore Deposits: New York, John Wiley and Sons, p. 509-567.

Osterberg, M. W., and Guilbert, J. M., Geology, wall-rock alteration, and new exploration techniques at the Chimney Creek sediment-hosted gold deposit, Humboldt County, Nevada, *in* Proceedings Geology and ore deposits of the Great Basin. Symposium proceedings, Reno, Nevada, 1991, Geological Society of Nevada, p. 805-821.

Person, M., Banerjee, A., Hofstra, A., Sweetkind, D., and Gao, Y. L., 2008, Hydrologic models of modern and fossil geothermal systems in the Great Basin: Genetic implications for epithermal Au-Ag and Carlin-type gold deposits: Geosphere, v. 4, no. 5, p. 888-917.

Putnis, A., 2002, Mineral replacement reactions: from macroscopic observations to microscopic mechanisms: Mineralogical Magazine, v. 66, no. 5, p. 689-708.

Putnis, A., 2009, Mineral Replacement Reactions: Reviews in Mineralogy and Geochemistry, v. 70, no. 1, p. 87-124.

Pytte, A. M., and Reynolds, R. C., 1989, The Thermal Transformations of Smectite to Illite, *in* Naeser, N. D., and McCulloh, T. H., eds., Thermal History of Sedimentary Basins: New York, Springer-Verlag, p. 133-140.

Radtke, A. S., 1985, Geology of the Carlin gold deposit, Nevada : a detailed study of one of the largest disseminated-replacement gold deposits in North America, Washington, U.S. G.P.O., U.S. Geological Survey professional paper ;, v. 1267, vi, 124 p. p.:

Radtke, A. S., Rye, R. O., and Dickson, F. W., 1980, Geology and stable isotope studies of the Carlin trend gold deposit, Nevada: Economic Geology, v. 75, no. 5, p. 641-672.

Radtke, A. S., Scheiner, B. J., Heropoul.C, Essingto.M, and Fabbi, B. P., 1972, Data on major and minor elements in host rocks and ores, Carlin gold deposit, Nevada: Economic Geology, v. 67, no. 7, p. 975-&.

Raudsepp, M., Pani, E., and Dipple, G. M., 1999, Measuring mineral abundance in skarn. I. The Rietveld method using X-ray powder-diffraction data: Canadian Mineralogist, v. 37, p. 1-15.

Reed, M. H., 1997, Hydrothermal alteration and its relationship to ore fluid composition, *in* Barnes, H., ed., Geochemistry of Hydrothermal Ore Deposits: New York, John Wiley and Sons, p. 303-365.

Reiners, P. W., and Brandon, M. T., 2006, Using thermochronology to understand orogenic erosion, Annual Review of Earth and Planetary Sciences, Volume 34: Palo Alto, Annual Reviews, p. 419-466.

Ressel, M. W., and Henry, C. D., 2006, Igneous Geology of the Carlin Trend, Nevada: Development of the Eocene Plutonic Complex and Significance for Carlin-Type Gold Deposits: Economic Geology, v. 101, no. 2, p. 347-383.

Ressel, M. W., Jr., 2006, Igneous geology of the Carlin trend, Nevada: The importance of Eocene magmatism in gold mineralizationPh.D.]: University of Nevada, Reno.
Ressel, M. W., Jr., Noble, D. C., Volk, J. A., Lamb, J. B., Park, D. E., Conrad, J. E., Heizler, M. T., and Mortensen, J. K., Precious-metal mineralization in Eocene dikes at Griffin and Meikle; Bearin on the age and origin of gold deposits of the Carlin trend, Nevada, *in* Proceedings Geological Society of Nevada, Geology and Ore Deposits 2000: The Great Basin and Beyond Sympsium, Reno/Sparks, Nevada, 2000a, Geological Society of Nevada, p. 79-101.
Ressel, M. W., Noble, D. C., Henry, C. D., and Trudel, W. S., 2000b, Dike-nested ores of the Beast deposit and the importance of Eocene magmatism in gold mineralization of the Carlin Trend, Nevada: Economic Geology and the Bulletin of the Society of Economic Geologists, v. 95, no. 7, p. 1417-1444.
Richard, E., 1999, An explanation of the effect of seawater carbonate concentration on foraminiferal oxygen isotopes: Geochimica et Cosmochimica Acta, v. 63, no. 13,Äì14, p. 2001-2007.
Robert, F., Boullier, A. M., and Firdaous, K., 1995, GOLD-QUARTZ VEINS IN METAMORPHIC TERRANES AND THEIR BEARING ON THE ROLE OF FLUIDS IN FAULTING: Journal of Geophysical Research-Solid Earth, v. 100, no. B7, p. 12861-12879.
Roberts, R. J., Ferguson, H. G., Gilluly, J., and Hotz, P. E., 1958, Paleozoic rocks of north-central Nevada: AAPG Bulletin, v. 42, no. 12, p. 2813-2857.
Roberts, R. J., Montgomery, K. M., and Lehner, R. E., 1967, Geology and Mineral Resources of Eureka County, Nevada: Nevada Bureau of Mines and Geology.
Rock, N., 1991, Lamprophyres, Glasgow and London, Blackie.
Roedder, E., 1983, DISCUSSION OF A REASSESSMENT OF PHASE-EQUILIBRIA INVOLVING 2 LIQUIDS IN THE SYSTEM K2O-AL2O3-FEO-SIO2: Contributions to Mineralogy and Petrology, v. 82, no. 2-3, p. 284-290.
Roedder, E., and Bodnar, R., 1997, Fluid inclusion studies of hydrothermal ore deposits, *in* Barnes, H., ed., Geochemistry of Hydrothermal Ore Deposits: New York, John Wiley and Sons, p. 657-698.
Rojstaczer, S. A., and Bredehoeft, J. D., 1988, Ground water and fault strength, *in* Back, W., Rosenshein, J. S., and Seaber, P. R., eds., Hydrogeology, Volume O-2: Boulder, CO, Geological Soceity of America, p. 447-460.
Sachs, L., 1984, Applied statistics: a handbook of techniques, New York, Springer-Verlag.
Savard, M. M., Veizer, J., and Hinton, R., 1995, Cathodoluminescence at low Fe and Mn concentrations - a SIMS study of zones of natural calcites Journal of Sedimentary Research Section a-Sedimentary Petrology and Processes, v. 65, no. 1, p. 208-213.
Schwartz, F. W., and Longstaffe, F. J., 1988, Groundwater and clastic diagenesis, *in* Back, W., Rosenshein, J. S., and Seaber, P. R., eds., Hydrogeology, Volume O-2: Boulder, CO, Geological Soceity of America, p. 413-434.
Seward, T. M., 1973, Thio Complexes of Gold and Transport of Gold in Hydrothermal Ore Solutions: Geochimica et Cosmochimica Acta, v. 37, no. 3, p. 379-399.

Sharp, Z. D., 1990, A Laser-Based Microanalytical Method for the Insitu Determination of Oxygen Isotope Ratios of Silicates and Oxides: Geochimica et Cosmochimica Acta, v. 54, no. 5, p. 1353-1357.
Simmons, S. F., and Brown, K. L., 2006, Gold in Magmatic Hydrothermal Solutions and the Rapid Formation of a Giant Ore Deposit: Science, v. 314, no. 5797, p. 288-291.
-, 2007, The flux of gold and related metals through a volcanic arc, Taupo Volcanic Zone, New Zealand: Geology, v. 35, no. 12, p. 1099-1102.
Simon, G., Kesler, S. E., and Chryssoulis, S., 1999, Geochemistry and textures of gold-bearing arsenian pyrite, Twin Creeks, Nevada: Implications for deposition of gold in Carlin-type deposits: Economic Geology and the Bulletin of the Society of Economic Geologists, v. 94, no. 3, p. 405-421.
Spooner, E. T. C., Beckinsale, R. D., England, P. C., and Senior, A., 1977, Hydration, O-18 Enrichment and Oxidation during Ocean-Floor Hydrothermal Metamorphism of Ophiolitic Metabasic Rocks from E Liguria, Italy: Geochimica et Cosmochimica Acta, v. 41, no. 7, p. 857-871.
Spycher, N. F., and Reed, M. H., 1989, As(Iii) and Sb(Iii) Sulfide Complexes - an Evaluation of Stoichiometry and Stability from Existing Experimental-Data: Geochimica et Cosmochimica Acta, v. 53, no. 9, p. 2185-2194.
Stenger, D. P., Kesler, S. E., Peltonen, D. R., and Tapper, C. J., 1998a, Deposition of gold in Carlin-type deposits: The role of sulfidation and decarbonation at Twin Creeks, Nevada: Economic Geology and the Bulletin of the Society of Economic Geologists, v. 93, no. 2, p. 201-215.
Stenger, D. P., Kesler, S. E., and Vennemann, T., 1998b, Carbon and oxygen isotope zoning around Carlin-type gold deposits: a reconnaissance survey at Twin Creeks, Nevada: Journal of Geochemical Exploration, v. 63, no. 2, p. 105-121.
Stewart, J. H., 1980, Geology of Nevada: Nevada Bureau of Mines and Geology Special Publication, v. 4, p. 136.
Streckeisen, A., 1980, Classification and nomenclature of volcanic rocks, lamprophyres, carbonatites and melilitic rocks IUGS Subcommission on the Systematics of Igneous Rocks: Geologische Rundschau, v. 69, no. 1, p. 194-207.
Sverjensky, D. A., 1984, Europium Redox Equilibria in Aqueous-Solution: Earth and Planetary Science Letters, v. 67, no. 1, p. 70-78.
Taylor, H. P., 1974, The Application of Oxygen and Hydrogen Isotope Studies to Problems of Hydrothermal Alteration and Ore Deposition: Economic Geology, v. 69, no. 6, p. 843-883.
-, 1977, Water/rock interactions and the origins of H2O in granitic batholiths: Journal of the Geological Society of London, v. 133, p. 509-558.
-, 1997, Oxygen and Hydrogen Isotope Relationships in Hydrothermal Mineral Deposits, *in* Barnes, H., ed., Geochemistry of Hydrothermal Ore Deposits: New York, John Wiley & Sons, Inc., p. 229-302.
Taylor, S. R., and McLennan, S. M., 1985, The Continental Crust; Its Composition and Evolution, Oxford, U.K., Blackwell, 312 p.:
Taylor, W. R., Rock, N. M. S., Groves, D. I., Perring, C. S., and Golding, S. D., 1994, Geochemistry of Archean shoshonitic lamprophyres from the Yilgarn Block,

Western Australia: Au abundance and association with gold mineralization: Applied Geochemistry, v. 9, no. 2, p. 197-222.
Teagle, D. A. H., Bickle, M. J., and Alt, J. C., 2003, Recharge flux to ocean-ridge black smoker systems: a geochemical estimate from ODP Hole 504B: Earth and Planetary Science Letters, v. 210, no. 1-2, p. 81-89.
Teal, L. a. J., M., 2002, Geologic overview of the Carlin Trend gold deposits, *in* Thompson, T. B., Teal, L., and Meeuwig, R., eds., Gold deposits of the Carlin trend, Volume 111: Reno, Nevada Bureau of Mines and Geology, p. 9-19.
Toth, J., 1988, Groundwater and hydrocarbon migration, *in* Back, W., Rosenshein, J. S., and Seaber, P. R., eds., Hydrogeology, Volume 0-2: Boulder, CO, Geological Soceity of America, p. 485-502.
Tretbar, D. R., Arehart, G. B., and Christensen, J. N., 2000, Dating gold deposition in a Carlin-type gold deposit using Rb/Sr methods on the mineral galkhaite: Geology, v. 28, no. 10, p. 947-950.
Vaughan, J. R., Hickey, K., Barker, S., and Dipple, G. M., 2010, Stable Isotopes and Fluid Flow Pathways in the Banshee Carlin-type Gold Deposit, Townsville, James Cook Univ, Smart Science for Exploration and Mining, Vol 1 and 2, 266-268 p.:
Vazquez, R., Vennemann, T. W., Kesler, S. E., and Russell, N., 1998, Carbon and oxygen isotope halos in the host limestone, El Mochito Zn-Pb-(Ag) skarn massive sulfide-oxide deposit, Honduras: Economic Geology, v. 93, no. 1, p. 15-31.
Veizer, J. n., Ala, D., Azmy, K., Bruckschen, P., Buhl, D., Bruhn, F., Carden, G. A. F., Diener, A., Ebneth, S., Godderis, Y., Jasper, T., Korte, C., Pawellek, F., Podlaha, O. G., and Strauss, H., 1999, 87Sr/86Sr, [delta]13C and [delta]18O evolution of Phanerozoic seawater: Chemical Geology, v. 161, no. 1-3, p. 59-88.
Volk, J. A., Lauha, E., Leonardson, R. W., and Rahn, J. E., 1995, Structural geology of the Betze-Post and Meikle deposits, Elko and Eurkeka counties, Nevada, *in* Craig, S., ed., Structural Geology of the Carlin Trend, Volume Field Trip Guidebook, trip B: Reno, Nevada, Geological Society of Nevada, p. 18.
Volk, J. A., Weakly, C., Penick, M., and Lander, A., 2001, Structural geology of the Goldstrike property, North-Central Nevada, Regional Tectonics and Structural Control of Ore: The Major Gold Trends of Northern NV, Battle Mountain Spring Field Conference, Volume 33: Battle Mountain, NV, Geological Society of Nevada, p. 361-379.
Warren, I., Simmons, S. F., and Mauk, J. L., 2007, Whole-Rock Geochemical Techniques for Evaluating Hydrothermal Alteration, Mass Changes, and Compositional Gradients Associated with Epithermal Au-Ag Mineralization: Economic Geology, v. 102, no. 5, p. 923-948.
Weis, D., Kieffer, B., Maerschalk, C., Barling, J., de Jong, J., Williams, G. A., Hanano, D., Pretorius, W., Mattielli, N., Scoates, J. S., Goolaerts, A., Friedman, R. M., and Mahoney, J. B., 2006, High-precision isotopic characterization of USGS reference materials by TIMS and MC-ICP-MS: Geochemistry, Geophysics, Geosystems, v. 7, no. 8, p. Q08006.
Wells, J. D., and Mullens, T. E., 1973, Gold-bearing arsenian pyrite determined by microprobe analysis, Cortez and Carlin gold mines, Nevada: Economic Geology, v. 68, no. 2, p. 187-201.

Wilkinson, J. J., 2001, Fluid inclusions in hydrothermal ore deposits: Lithos, v. 55, no. 1-4, p. 229-272.
Williams, C., 1992, Breccia bodies in the Carlin trend, Elko and Eureka counties, Nevada [MSc: Colorado State University, 213 p.
Williams, C. L., Thompson, T. B., Powell, J. L., and Dunbar, W. W., 2000, Gold-bearing breccias of the Rain mine, Carlin trend, Nevada: Economic Geology and the Bulletin of the Society of Economic Geologists, v. 95, no. 2, p. 391-404.
Williams-Jones, A. E., Heinrich, C. A., and Migdisov, A. A., 2005, Vapor as a medium for the transport of metals: Implications for ore deposit modeling: Geochimica Et Cosmochimica Acta, v. 69, no. 10, p. A733-A733.
Williams-Jones, A. E., Migdisov, A. A., and Samson, I. M., 2012, Hydrothermal Mobilisation of the Rare Earth Elements - a Tale of "Ceria" and "Yttria": Elements, v. 8, no. 5, p. 355-360.
Woolley, A. R., Bergman, S. C., Edgar, A. D., Le Bas, M. J., Mitchell, R. H., Rock, N. M. S., and Scott Smith, B. H., 1996, Classification of lamprophyres, lamproites, kimberlites, and the kalsilitic, melilitic, and leucitic rocks: Can Mineral, v. 34, no. 2, p. 175-186.
Wright, J. E., and Wooden, J. L., 1991, New Sr, Nd, and Pb isotopic data from plutons in the northern Great Basin: Implications for crustal structure and granite petrogenesis in the hinterland of the Sevier thrust belt: Geology, v. 19, no. 5, p. 457-460.
Yardley, B. W. D., and Lloyd, G. E., 1995, Why metasomatic fronts are really metasomatic sides: Geology, v. 23, no. 1, p. 53-56.
Ye, Z. J., Kesler, S. E., Essene, E. J., Zohar, P. B., and Borhauer, J. L., 2003, Relation of Carlin-type gold mineralization to lithology, structure and alteration: Screamer zone, Betze-Post deposit, Nevada: Mineralium Deposita, v. 38, no. 1, p. 22-38.
Yigit, O., 2001, Structural controls and geochemistry of Carlin-type gold mineralization in the Gold Bar district, Eureka County, NevadaPh.D.]: Colorado School of Mines.
Yigit, O., and Hofstra, A. H., 2003, Lithogeochemistry of Carlin-type gold mineralization in the Gold Bar district, Battle Mountain-Eureka trend, Nevada: Ore Geology Reviews, v. 22, no. 3-4, p. 201-224.
Yigit, O., Hofstra, A. H., Hitzman, M. W., and Nelson, E. P., 2006, Geology and geochemistry of jasperoids from the Gold Bar district, Nevada: Mineralium Deposita, v. V41, no. 6, p. 527-547.
Zheng, Y. F., and Hoefs, J., 1993, Carbon and oxygen isotopic covariations in hydrothermal calcites: Mineralium Deposita, v. 28, no. 2, p. 79-89.

Appendices

Appendix A

A.1 Methods for Commercial Laboratory

PREP-31

Standard Sample Preparation: Dry, Crush, Split and Pulverize

Sample preparation is the most critical step in the entire laboratory operation. The purpose of preparation is to produce a homogeneous analytical sub-sample that is fully representative of the material submitted to the laboratory.

The sample is logged in the tracking system, weighed, dried and finely crushed to better than 70 % passing a 2 mm (Tyler 9 mesh, US Std. No.10) screen. A split of up to 250 g is taken and pulverized to better than 85 % passing a 75 micron (Tyler 200 mesh, US Std. No. 200) screen. This method is appropriate for rock chip or drill samples.

Method Code	Description
LOG-22	Sample is logged in tracking system and a bar code label is attached.
DRY-21	Drying of excessively wet samples in drying ovens. This is the default drying procedure for most rock chip and drill samples.
CRU-31	Fine crushing of rock chip and drill samples to better than 70 % of the sample passing 2 mm.
SPL-21	Split sample using riffle splitter.
PUL-31	A sample split of up to 250 g is pulverized to better than 85 % of the sample passing 75 microns.

Flow Chart - Sample Preparation Package – PREP-31
Standard Sample Preparation: Dry, Crush, Split and Pulverize

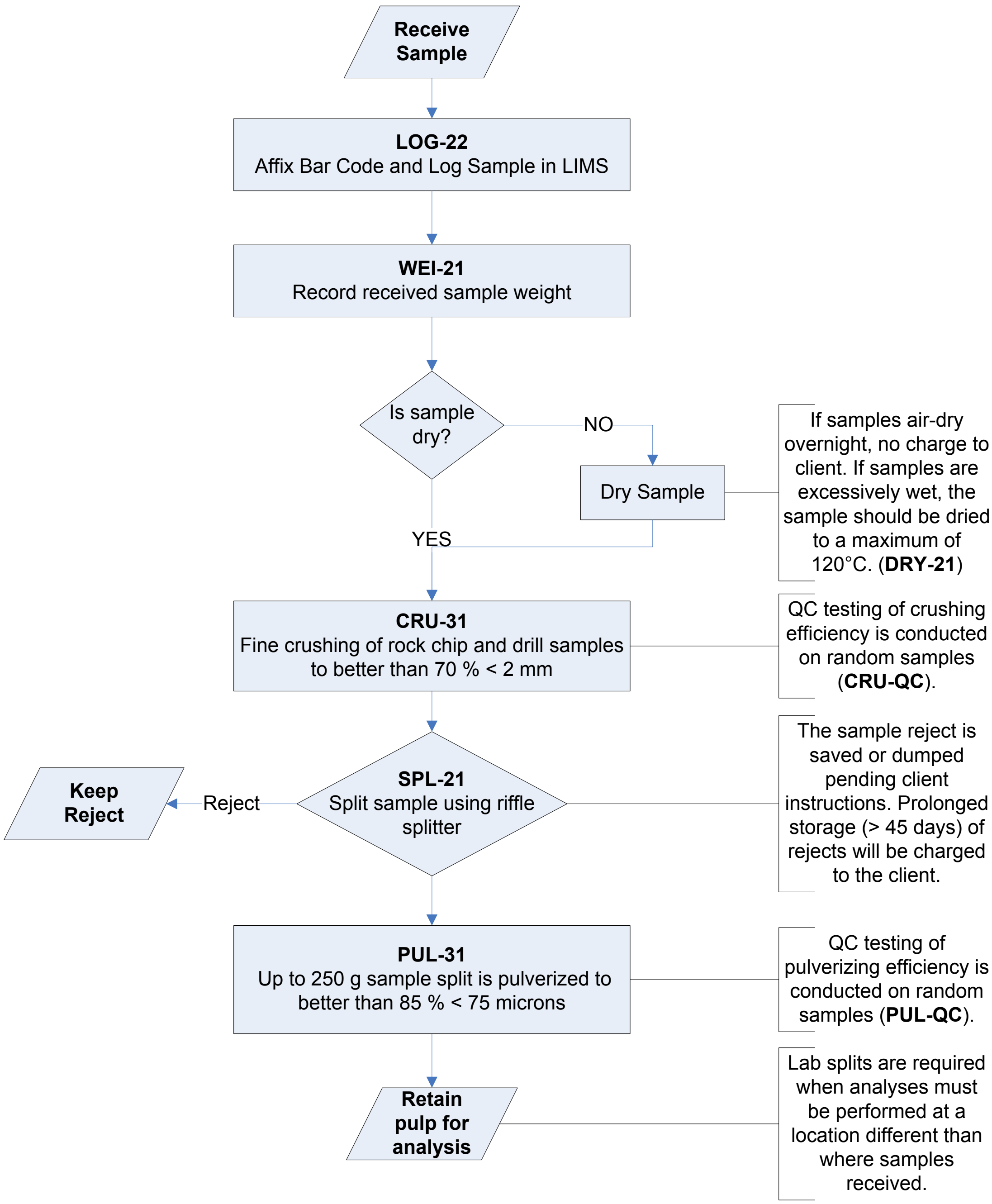

Au-ICP21 and Au-ICP22
Fire Assay Fusion ICP-AES Finish

Sample Decomposition:

Fire Assay Fusion (FA-FUSPG1 & FA-FUSPG2)

Analytical Method:

Inductively Coupled Plasma – Atomic Emission Spectrometry (ICP-AES)

A prepared sample is fused with a mixture of lead oxide, sodium carbonate, borax, silica and other reagents as required, inquarted with 6 mg of gold-free silver and then cupelled to yield a precious metal bead.

The bead is digested in 0.5 mL dilute nitric acid in the microwave oven. 0.5 mL concentrated hydrochloric acid is then added and the bead is further digested in the microwave at a lower power setting. The digested solution is cooled, diluted to a total volume of 4 mL with de-mineralized water, and analyzed by inductively coupled plasma atomic emission spectrometry against matrix-matched standards.

Method Code	Element	Symbol	Units	Sample Weight (g)	Lower Limit	Upper Limit	Default Overlimit Method
Au-ICP21	Gold	Au	ppm	30	0.001	10	Au-AA25
Au-ICP22	Gold	Au	ppm	50	0.001	10	Au-AA26

ME-MS41
Ultra-Trace Level Methods Using ICP-MS and ICP-AES

Sample Decomposition:

Aqua Regia Digestion (GEO-AR01)

Analytical Method:

Inductively Coupled Plasma-Atomic Emission Spectroscopy (ICP-AES) Inductively Coupled Plasma - Mass Spectrometry (ICP-MS)

A prepared sample (0.50 g) is digested with aqua regia in a graphite heating block. After cooling, the resulting solution is diluted to with deionized water, mixed and analyzed by inductively coupled plasma-atomic emission spectrometry. Following this analysis, the results are reviewed for high concentrations of bismuth, mercury, molybdenum, silver and tungsten and diluted accordingly. Samples are then analysed by ICP-MS for the remaining suite of elements. The analytical results are corrected for inter-element spectral interferences.

Element	Symbol	Units	Lower Limit	Upper Limit
Silver	Ag	ppm	0.01	100
Aluminum	Al	%	0.01	25
Arsenic	As	ppm	0.1	10 000
Gold	Au	ppm	0.2	25
Boron	B	ppm	10	10 000
Barium	Ba	ppm	10	10 000
Beryllium	Be	ppm	0.05	1 000
Bismuth	Bi	ppm	0.01	10 000
Calcium	Ca	%	0.01	25
Cadmium	Cd	ppm	0.01	1 000
Cerium	Ce	ppm	0.02	500

Element	Symbol	Units	Lower Limit	Upper Limit
Cobalt	Co	ppm	0.1	10 000
Chromium	Cr	ppm	1	10 000
Cesium	Cs	ppm	0.05	500
Copper	Cu	ppm	0.2	10 000
Iron	Fe	%	0.01	50
Gallium	Ga	ppm	0.05	10 000
Germanium	Ge	ppm	0.05	500
Hafnium	Hf	ppm	0.02	500
Mercury	Hg	ppm	0.01	10 000
Indium	In	ppm	0.005	500
Potassium	K	%	0.01	10
Lanthanum	La	ppm	0.2	10 000
Lithium	Li	ppm	0.1	10 000
Magnesium	Mg	%	0.01	25
Manganese	Mn	ppm	5	50 000
Molybdenum	Mo	ppm	0.05	10 000
Sodium	Na	%	0.01	10
Niobium	Nb	ppm	0.05	500
Nickel	Ni	ppm	0.2	10 000
Phosphorus	P	ppm	10	10 000
Lead	Pb	ppm	0.2	10 000
Rubidium	Rb	ppm	0.1	10 000
Rhenium	Re	ppm	0.001	50
Sulphur	S	%	0.01	10
Antimony	Sb	ppm	0.05	10 000
Scandium	Sc	ppm	0.1	10 000
Selenium	Se	ppm	0.2	1 000
Tin	Sn	ppm	0.2	500
Strontium	Sr	ppm	0.2	10 000
Tantalum	Ta	ppm	0.01	500
Tellurium	Te	ppm	0.01	500

Element	Symbol	Units	Lower Limit	Upper Limit
Thorium	Th	ppm	0.2	10000
Titanium	Ti	%	0.005	10
Thallium	Tl	ppm	0.02	10 000
Uranium	U	ppm	0.05	10 000
Vanadium	V	ppm	1	10 000
Tungsten	W	ppm	0.05	10 000
Yttrium	Y	ppm	0.05	500
Zinc	Zn	ppm	2	10 000
Zirconium	Zr	ppm	0.5	500

NOTE: In the majority of geological matrices, data reported from an aqua regia leach should be considered as representing only the leachable portion of the particular analyte.

ME-MS61m
Ultra-Trace Level Method Using ICP-MS and ICP-AES

ME-MS61m is a two-step package involving initial sample decomposition with a hydrofluoric, nitric, perchloric acid digestion and HCl leach. The sample digest is analyzed by ICP-AES or ICP-MS for all elements except mercury. Due to the high temperature (185°C) of the four acid digestion, significant amounts of mercury can be lost by evaporation. Use of the lower temperature aqua regia digestion (115°C) prevents this evaporation allowing for more accurate results.

Step I:

ICP AES/MS (ME-MS61)

Sample Decomposition:

HF-HNO_3-$HClO_4$ acid digestion, HCl leach (GEO-4A01)

Analytical Method:

Inductively Coupled Plasma - Atomic Emission Spectroscopy (ICP - AES) (ME-ICP61i)

Inductively Coupled Plasma - Mass Spectrometry (ICP-MS) (ME-MS61i)

A prepared sample (0.250 g) is digested with perchloric, nitric, and hydrofluoric acids to near dryness. The sample is then further digested in a small amount of hydrochloric acid. The solution is made up to a final volume of 12.5 mL with 11 % hydrochloric acid, homogenized, and analysed by inductively coupled plasma-atomic emission spectrometry.

Element	Symbol	Units	Lower Limit	Upper Limit
Silver	Ag	ppm	0.01	100
Aluminium	Al	%	0.01	50
Arsenic	As	ppm	0.2	10000

Element	Symbol	Units	Lower Limit	Upper Limit
Barium	Ba	ppm	10	10000
Beryllium	Be	ppm	0.05	1000
Bismuth	Bi	ppm	0.01	10000
Calcium	Ca	%	0.01	50
Cadmium	Cd	ppm	0.02	500
Cerium	Ce	ppm	0.01	500
Cobalt	Co	ppm	0.1	10000
Chromium	Cr	ppm	1	10000
Cesium	Cs	ppm	0.05	500
Copper	Cu	ppm	0.2	10000
Iron	Fe	%	0.01	50
Gallium	Ga	ppm	0.05	500
Germanium	Ge	ppm	0.05	500
Hafnium	Hf	ppm	0.1	500
Indium	In	ppm	0.005	500
Potassium	K	%	0.01	10
Lanthanum	La	ppm	0.5	500
Lithium	Li	ppm	0.2	500
Magnesium	Mg	%	0.01	50
Manganese	Mn	ppm	5	100000
Molybdenum	Mo	ppm	0.05	10000
Sodium	Na	%	0.01	10
Niobium	Nb	ppm	0.1	500
Nickel	Ni	ppm	0.2	10000
Phosphorous	P	ppm	10	10000
Lead	Pb	ppm	0.5	10000
Rubidium	Rb	ppm	0.1	500
Rhenium	Re	ppm	0.002	50
Sulphur	S	%	0.01	10
Antimony	Sb	ppm	0.05	1000
Selenium	Se	ppm	1	1000

Element	Symbol	Units	Lower Limit	Upper Limit
Tin	Sn	ppm	0.2	500
Strontium	Sr	ppm	0.2	10000
Tantalum	Ta	ppm	0.05	100
Tellurium	Te	ppm	0.05	500
Thorium	Th	ppm	0.2	500
Titanium	Ti	%	0.005	10
Thallium	Tl	ppm	0.02	500
Uranium	U	ppm	0.1	500
Vanadium	V	ppm	1	10000
Tungsten	W	ppm	0.1	10000
Yttrium	Y	ppm	0.1	500
Zinc	Zn	ppm	2	10000
Zirconium	Zr	ppm	0.5	500

Elements listed below are available upon request

Element	Symbol	Units	Lower Limit	Upper Limit
Scandium	Sc	ppm	0.1	250

Geochemical Procedure – ME-MS61m (con't)

Step II:

Detection of Mercury (Hg-CV41)

Sample Decomposition:

Nitric Aqua Regia Digestion (GEO-AR01)

Analytical Method:

Atomic Absorption Spectrometry (AES)

A prepared sample is digested with aqua regia for in a graphite heating block. After cooling, the resulting solution is diluted to 12.5 mL with deionized water and mixed well. A portion of the sample is treated with stannous chloride to reduce the mercury. The resulting mercury is volatilized by purging with an inert gas, such as argon or nitrogen, and measured by Atomic Absorption Spectrometry.

Element	**Symbol**	**Units**	**Detection Limit**	**Upper Limit**
Mercury	Hg	ppm	0.01	100

Geochemical Package – CCP-PKG01
Complete Characterization

By combining a number of methods into one cost effective package, a complete characterization is obtained. This package combines the whole rock package ME-ICP06 plus carbon and sulfur by combustion furnace (ME-IR08) to quantify the major elements in a sample. Trace elements including the full rare earth element suite are reported from three digestions with either ICP-AES or ICP-MS finish: A lithium borate fusion for the resistive and rare earth elements (ME-MS81), a four acid digestion for the basemetals (ME-4ACD81) and an aqua regia digestion for the volatile gold related trace elements (ME-MS42).

The nature of Lithophile elements and the matrices in which they occur require stronger dissolution procedures. The most accurate results will therefore be obtained using fusion as the dissolution procedure.

Whole Rock Geochemistry – ME-ICP06 and OA-GRA05
Analysis of major oxides by ICP-AES

ME-ICP06

Sample Decomposition:

Lithium Metaborate/Lithium Tetraborate ($LiBO_2$/Li_2B4O_7) Fusion* (FUS LI01)

Analytical Method:

Inductively Coupled Plasma - Atomic Emission Spectroscopy (ICP-AES)

A prepared sample (0.200 g) is added to lithium metaborate/lithium tetraborate flux (1.8 g), mixed well and fused in a furnace at 1025°C. The resulting melt is then cooled and dissolved in an acid mixture containing nitric, hydrochloric and hydrofluoric acids. This solution is then analyzed by ICP-AES. Results are corrected for spectral inter-element interferences and reported.

Element	Symbol	Units	Lower Limit	Upper Limit
Silica	SiO_2	%	0.01	100
Aluminum	Al_2O_3	%	0.01	100
Iron	Fe_2O_3	%	0.01	100
Calcium	CaO	%	0.01	100

Element	Symbol	Units	Lower Limit	Upper Limit
Magnesium	MgO	%	0.01	100
Sodium	Na_2O	%	0.01	100
Potassium	K_2O	%	0.01	100
Chromium	Cr_2O_3	%	0.01	100
Titanium	TiO_2	%	0.01	100
Manganese	MnO	%	0.01	100
Phosphorus	P_2O_5	%	0.01	100
Strontium	SrO	%	0.01	100
Barium	BaO	%	0.01	100

OA-GRA05
Loss on Ignition

Sample Decomposition:

Thermal decomposition Furnace (OA-GRA05)

Analytical Method:

Gravimetric

If required, the total oxide content is determined from the ICP analyte concentrations and loss on Ignition (L.O.I.) values. A prepared sample (1.0 g) is placed in an oven at 1000°C for one hour, cooled and then weighed. The percent loss on ignition is calculated from the difference in weight.

Method Code	Element	Symbol	Units	Lower Limit	Upper Limit
OA-GRA05	Loss on Ignition	LOI	%	0.01	100

Total Carbon – Method Code C-IR07

Sample Decomposition:

LECO Furnace

Analytical Method:

Infrared Spectroscopy

The sample is combusted in a LECO induction furnace. The generated CO2 is quantitatively detected by infrared spectrometry and reported as percent carbon.

Method Code	Element	Symbol	Units	Lower Limit	Upper Limit
C-IR07	Carbon	C	%	0.01	50

Specialty Assay Procedure – Total Sulphur S-IR08

Sample Decomposition:

Various

Analytical Method:

Leco sulphur analyzer, Gravimetric

The sample is analyzed for Total Sulphur using a Leco sulphur analyzer. Sulphur dioxide released from the sample is measured by an IR detection system and the Total Sulphur result is provided.

Method Code	Element	Symbol	Units	Lower Limit	Upper Limit
S-IR08	Sulphur	S	%	0.01	50

ME-MS81
Lithogeochemistry

Sample Decomposition:

Lithium Borate ($LiBO_2$/$Li_2B_4O_7$) Fusion (FUS-LI01)*

Analytical Method:

Inductively Coupled Plasma - Mass Spectroscopy (ICP - MS)

A prepared sample (0.200 g) is added to lithium metaborate/lithium tetraborate flux (1.8 g), mixed well and fused in a furnace at 1025°C. The resulting melt is then cooled and dissolved in an acid mixture containing nitric, hydrochloric and hydrofluoric acids. This solution is then analyzed by inductively coupled plasma - mass spectrometry.

Element	Symbol	Unit	Lower Limit	Upper Limit
Barium	Ba	ppm	0.5	10000
Cerium	Ce	ppm	0.5	10000
Chromium	Cr	ppm	10	10000
Cesium	Cs	ppm	0.01	10000
Dysprosium	Dy	ppm	0.05	1000
Erbium	Er	ppm	0.03	1000
Europium	Eu	ppm	0.03	1000
Gallium	Ga	ppm	0.1	1000
Gadolinium	Gd	ppm	0.05	1000
Hafnium	Hf	ppm	0.2	10000
Holmium	Ho	ppm	0.01	1000
Lanthanum	La	ppm	0.5	10000
Lutetium	Lu	ppm	0.01	1000
Niobium	Nb	ppm	0.2	2500
Neodymium	Nd	ppm	0.1	10000

Geochemical Package

Element	Symbol	Unit	Lower Limit	Upper Limit
Praseodymium	Pr	ppm	0.03	1000
Rubidium	Rb	ppm	0.2	10000
Samarium	Sm	ppm	0.03	1000
Tin	Sn	ppm	1	10000
Strontium	Sr	ppm	0.1	10000
Tantalum	Ta	ppm	0.1	2500
Terbium	Tb	ppm	0.01	1000
Thorium	Th	ppm	0.05	1000
Thallium	Tl	ppm	0.5	1000
Thullium	Tm	ppm	0.01	1000
Uranium	U	ppm	0.05	1000
Vanadium	V	ppm	5	10000
Tungsten	W	ppm	1	10000
Yttrium	Y	ppm	0.5	10000
Ytterbium	Yb	ppm	0.03	1000
Zirconium	Zr	ppm	2	10000

*__Note__: Minerals that may not recover fully using the lithium borate fusion include zircon, some metal oxides, some rare-earth phosphates and some sulphides. Basemetals also do not fully recover using this method.

ME-4ACD81 Addition of Basemetals

Sample Decomposition:

4-Acid (GEO-4ACID)

Analytical Method:

Inductively Coupled Plasma – Atomic Emission Spectroscopy (ICP-AES

A prepared sample (0.25 g) is digested with perchloric, nitric, hydrofluoric and hydrochloric acids. The residue is topped up with dilute hydrochloric acid and the resulting solution is analyzed by inductively coupled plasma-atomic emission spectrometry. Results are corrected for spectral inter-element interferences.

Element	Symbol	Units	Lower Limit	Upper Limit
Silver	Ag	ppm	0.5	100
Cadmium	Cd	ppm	0.5	1000
Cobalt	Co	ppm	1	10000
Copper	Cu	ppm	1	10000
Lithium	Li	ppm	10	10000
Molybdenum	Mo	ppm	1	10000
Nickel	Ni	ppm	1	10000
Lead	Pb	ppm	2	10000
Zinc	Zn	ppm	2	10000

Geochemical Procedure – ME-MS42
Single Element Trace Level Methods Using ICP-MS

Sample Decomposition:

Aqua Regia Digestion (GEO-AR01)

Analytical Method:

Inductively Coupled Plasma - Mass Spectrometry (ICP-MS)

A prepared sample (0.50 g) is digested with aqua regia for 45 minutes. After cooling, the resulting solution is diluted to 12.5 mL with de-ionized water, mixed and analyzed by inductively coupled plasma-mass spectrometry. The analytical results are corrected for inter element spectral interferences.

Element	Symbol	Units	Lower Limit	Upper Limit
Arsenic	As	ppm	0.1	250
Bismuth	Bi	ppm	0.01	250
Mercury	Hg	ppm	0.005	250
Antimony	Sb	ppm	0.05	250
Selenium	Se	ppm	0.2	250
Tellurium	Te	ppm	0.01	250

Appendix B

B.1 δD and $\delta^{18}O$ Data in Clay Minerals

STABLE ISOTOPE RESULTS

Sample Type: Minerals for $\delta^{18}O$ value analysis

SIL number	Sample number	Sample Type	$\delta^{18}O$ value	Duplicate $\delta^{18}O$ value
97487	1214	Illite	11.3	11.1
97488	1215	Illite	9.2	9.1
97489	1216	Kaolinite	1.1	
97490	1217	Kaolinite	0.7	
97491	AKS8	Illite	12.0	

Oxygen was extracted from sample powders for isotope analyses using a CO_2-laser and BrF_5 (Sharp, 1990). Oxygen isotope values are reported in the familiar $\delta^{18}O$ notation, relative to VSMOW. Samples were normalized to the international quartz standard NBS-28 using a value of +9.6 per mil (‰). Values for four NBS-28 analysed with the samples had values that varied by less than 0.15 ‰. Samples and standards were heated overnight to 150°C prior to loading into the vacuum extraction line. These were then evacuated for approx 6 hours. Blank BrF_5 runs were done until yield was less than 0.2 μmoles oxygen. Oxygen yields were recorded and CO_2 gas analysed on a Geo20-20 mass spectrometer.

Reference

Sharp, Z. D., 1990, Laser-based microanalytical method for the in situ determination of oxygen isotope ratios of silicates and oxides: Geochimica et Cosmochimica Acta, v. 54, p. 1353-1357.

Sample Type: Mineral for δD value analysis

SIL number	Sample number	Sample Type	δD value	std. dev.
97487	1214	Illite	-124.8	0.3
97488	1215	Illite	-120.5	1.1
97489	1216	Kaolinite	-151.8	1.5
97490	1217	Kaolinite	-157.0	1.5
97491	AKS8	Illite	-126.4	0.8

Mineral samples were analysed on a HEKAtech high temperature elemental analyser coupled with a GV Instruments IsoPrime mass spectrometer. Samples were pyrolyzed at 1450 deg C, in silver capsules. All samples were analysed in triplicate.

All results are reported with respect to VSMOW, normalized to international standards IAEA-CH-7, NBS30 and NBS22 with reported δD values of -100 ‰, 66‰ and 118‰ (www.ciaaw.org/Hydrogen.htm). The precision on the standards is 1.5‰.

Samples will be kept for 3 months from the date of the report and discarded unless we are otherwise notified.

Sample Type: Groundwater from Goldstrike dewatering wells

Sample #	Measured D/H	Meaured O 18/16	Actual D/H	dH (VSMOW)	Actual O 18/16	Measured d18O (VSMOW)
BW40	0.000133	0.00197	0.000135807	-128.1	0.001974266	-15.42666667
BW36	0.000133	0.00197	0.000135807	-128.1	0.001974266	-15.42666667
BW40-1	0.000133	0.00197	0.000135807	-128.1	0.001974266	-15.42666667
BW35	0.000133	0.00197	0.000135807	-128.1	0.001974266	-15.42666667
BW36-1	0.000132	0.00197	0.000135132	-132.4	0.001974266	-15.42666667
BW35-1	0.000133	0.00197	0.000135807	-128.1	0.001974266	-15.42666667

B.2 $\delta^{34}S$ Data

University of Ottawa, Faculty of Science (Earth Sciences)
G.G. Hatch Isotope Laboratories, 130 Louis Pasteur
Ottawa, Ontario, Canada K1N 6N5
Attn: P. Middlestead or W. Abdi

pmiddles@science.uottawa.ca
wabdi@science.uottawa.ca
Fax. (613) 562-5192
Office tel. (613) 562-5800 ext. 6839
Lab tel. (613) 562-5800 ext. 6836

Completed: 30-apr-2010
Cost: 21 x $45 = $945

Submitter Information	
Last Name:	Vaughan
First Name:	Jeremy
Initial:	0
Address (Line 1):	Dep't. of Earth and Ocean Science- UBC
Address (Line 2):	6339 Stores Road
City & State or Province:	Vancouver, BC
Postal Code:	V6T 1Z4
Country:	Canada
Email:	jvaughan@eos.ubc.ca
Telephone:	778-968-5053
Fax:	0
Supervisor (if applicable):	Ken Hickey

Billing Information	
Cost Center or PO:	JDNH
Last Name:	Dosanjh
First Name:	Manjit
Address (Line 1):	MDRU-UBC
Address (Line 2):	6339 Stores Road
City & State or Province:	Vancouver, BC
Postal Code:	V6T 1Z4
Country:	Canada
Email:	mdosanjh@eos.ubc.ca
Telephone:	604-822-6136
Fax:	604-822-8535

Samples (& their containers) will not be returned; plan accordingly.

Note: %S not quite as good as by off-line EA.

Samples are weighed into tin capsules with equal or greater amounts of tungstic oxide by either the researcher or the lab. Samples are loaded into a VarioEL II elemental analyser to be flash combusted at 1800C. Released gases are carried by helium through the EA to be cleaned, then separated and concentrated twice by "trap & purge". SO2 gas is carried into the DeltaPlus isotope ratio mass spectrometer (ThermoFinnigan, Germany) for analysis. Analytical precision is +/-0.2permil.

Submission Date:	1 April 2010
Project Title:	Carlin 3
Isotope Ratios Req:	Delta S-34
Numeric Media Code:	60

Optional Project	0
Comment:	0
	0

dup = QCD = quality control duplicate

OurLabID	Sample ID	Weight (mg)	Delta 34S cdt	%S	Comment	Hatch Lab ID
S-4025	NB-11C-1153	33.789	9.4	0.04	0	B1011-006-001
		121.761	7.2	0.12		
S-4026	NB-11C-1267	4.448	6.8	2.29	0	B1011-006-002
S-4027	NB-11C-1569	10.187	-8.9	0.46	0	B1011-006-003
S-4028	**NB-11C-1569 dup**	**10.051**	**-8.3**	**0.58**	**0**	**B1011-006-004**
		21.742	-9.5	0.95		
S-4029	NB-17C-1081	2.364	6.3	4.29	0	B1011-006-005
S-4030	NB-17C-1587	45.422	9.3	0.02	0	B1011-006-006
		186.509	7.5	0.02		
S-4031	NB-24C-1130	14.518	9.0	0.20	0	B1011-006-007
		62.607	9.2	0.37		
S-4032	NB-24C-1264	5.341	7.4	1.81	0	B1011-006-008
S-4033	NB-30C-1475	4.732	4.7	1.84	0	B1011-006-009
S-4034	H07-13b-436	1.672	3.5	5.87	0	B1011-006-010
S-4035	H07-13b-461	2.945	5.7	3.46	0	B1011-006-011
S-4036	H07-13b-476	1.399	6.7	6.63	0	B1011-006-012
S-4037	H07-13b-486	1.971	4.7	4.38	0	B1011-006-013
S-4038	H07-24-422	0.871	4.6	10.79	0	B1011-006-014
S-4039	H07-25-555	1.663	6.0	5.41	0	B1011-006-015
S-4040	**H07-25-555 dup**	**1.694**	**6.1**	**6.06**	**0**	**B1011-006-016**
S-4041	H07-34-537	50.767	2.3	0.01	0	B1011-006-017
		203.514	7.2	0.03		
S-4042	H07-54-298	20.781	5.2	0.04	0	B1011-006-018
		81.925	3.1	0.22		
S-4043	H07-54-332	14.995	-10.0	0.36	0	B1011-006-019
		31.333	-13.8	0.66		
S-4044	H07-63-976	33.166	9.9	.0.3	0	B1011-006-020
		141.165	7.9	0.07		
S-4045	H07-70-785	1.912	5.0	4.76	0	B1011-006-021
S-4046	H07-70-864	7.120	6.4	1.40	0	B1011-006-022
S-4047	H08-03-740	1.616	5.6	6.76	0	B1011-006-023

Part 1: the higher %S samples.
Part 2: the lower %S samples
Part 3: the lowest %S samples
Part 4: repeats

B.3 Nd and Sr Isotope Data

Sample #	$^{143}Nd/^{144}Nd$ Normalised	Error (+/-2s)	$^{87}Sr/^{86}Sr$ Normalised	Error (+/-2s)
NBC-11C-1267	Not Analyzed	Not Analyzed	0.726917	0.000009
NBC-11C-1305	Not Analyzed	Not Analyzed	0.721573	0.000006
NBC-24C-1264	Not Analyzed	Not Analyzed	0.725630	0.000009
NBC-24C-1320	Not Analyzed	Not Analyzed	0.743956	0.000010
U16-H07-25-510-515	Not Analyzed	Not Analyzed	0.721700	0.000008
U16-H07-25-555-560	Not Analyzed	Not Analyzed	0.718017	0.000009
U16-H07-63-1144	0.512457	0.000009	0.706016	0.000008
U16-H07-63-976	Not Analyzed	Not Analyzed	0.706124	0.000007
U16-H07-69-880	Not Analyzed	Not Analyzed	0.736462	0.000009
U16-H07-70-785	Not Analyzed	Not Analyzed	0.726426	0.000009
U16-H07-70-832A	0.512474	0.000008	0.718363	0.000009
U16-H07-70-864	Not Analyzed	Not Analyzed	0.707793	0.000006
U16-H07-13b-436-441	0.512547	0.000008	0.716664	0.000008
U16-H07-13b-476	0.512537	0.000007	0.712873	0.000007
U16-H07-13b-486	0.512546	0.000007	0.707552	0.000007
U16-H07-34-537	0.512555	0.000007	0.704461	0.000009
USGS Ref Mat				
G-2	0.512231	0.000008	0.709773	0.000009
Isotopes Duplicate				
U16-H07-34-537	Not Analyzed	Not Analyzed	0.704454	0.000007
U16-H07-63-1144 Dup	0.512467	0.000007	0.706015	0.000009

Appendix C

C.1 Banshee Drilled Isotope Data

hole ID	start depth (ft)	end depth (ft)		δ13C VPDB	δ18O VSMOW	Lihology
Bell-72	2603	2604		0.57	19.33	Stage 1 Breccia/Bootstrap Limestone
Bell-72	2625	2626		1.30	19.31	Stage 1 Breccia/Bootstrap Limestone
Bell-72	2666	2667		0.63	23.85	Stage 1 Breccia/Bootstrap Limestone
Bell-74A	2000	2001		-4.04	17.39	Ordovician Vinini
Bell-74A	2725	2726		-0.62	19.22	Stage 1 Breccia/Bootstrap Limestone
NBC-41C	1040	1041		-3.69	16.95	Ordovician Vinini
NBC-41C	1104	1105		-0.63	15.82	Ordovician Vinini
NBC-41C	1370	1371		2.72	13.96	Devonian Rodeo Creek
NBC-41C	1395	1396		1.21	18.96	Devonian Rodeo Creek
NBC-41C	1500	1501		0.03	26.07	Devonian Popovich Upper Mud
NBC-64C	2152	2153				Stage 2 Breccia
NBC-64C	2216	2217		1.29	18.66	Stage 1 Breccia/Bootstrap Limestone
NBC-64C	2228	2229		1.44	3.50	Calcite Vein
NBC-64C	2256	2257		1.16	9.63	Stage 1 Breccia/Bootstrap Limestone
U15-H08-29	72	73		2.19	19.35	Stage 1 Breccia/Bootstrap Limestone
U15-H08-29	100	101	A	2.64	12.94	Stage 1 Breccia/Bootstrap Limestone
U15-H08-29	100	101	B			Stage 1 Breccia/Bootstrap Limestone
U15-H08-29	120	121	A	-0.30	11.86	Stage 1 Breccia/Bootstrap Limestone
U15-H08-29	120	121	B			Stage 1 Breccia/Bootstrap Limestone
U15-H08-29	120	121	C			Calcite Vein
U15-H08-29	140	141	A	1.81	16.66	Stage 1 Breccia/Bootstrap Limestone
U15-H08-29	140	141	B	4.14	5.55	Calcite Vein
U15-H08-29	155	156		-1.36	13.88	Stage 1 Breccia/Bootstrap Limestone
U15-H08-29	167	168	A	-1.41	7.01	Stage 1 Breccia/Bootstrap Limestone
U15-H08-29	167	168	B	0.99	3.43	Calcite Vein
U15-H08-29	181	182	A	1.52	14.39	Stage 1 Breccia/Bootstrap Limestone
U15-H08-29	181	182	B	0.68	4.68	Calcite Vein
U15-H08-29	490	491				Devonian Popovich Upper Mud
U15-H08-29	502	503				Devonian Popovich Upper Mud
U15-H08-29	552	553				Devonian Rodeo Creek
U15-H08-29	651	652		0.80	20.14	Devonian Rodeo Creek
U16-h07-13B	11	12	A	1.86	20.78	Stage 1 Breccia/Bootstrap Limestone
U16-h07-13B	11	12	B	1.05	16.08	Stage 1 Breccia/Bootstrap Limestone
U16-h07-13B	11	12	C	-0.38	17.80	Calcite Vein
U16-h07-13B	31	32		0.69	12.31	Stage 1 Breccia/Bootstrap Limestone
U16-h07-13B	51	52		0.58	15.94	Stage 1 Breccia/Bootstrap Limestone
U16-h07-13B	81	82		0.75	10.94	Stage 1 Breccia/Bootstrap Limestone
U16-h07-13B	131	132		2.41	14.90	Stage 1 Breccia/Bootstrap Limestone
U16-h07-13B	141	142		2.54	13.13	Stage 1 Breccia/Bootstrap Limestone
U16-h07-13B	151	152	A	2.20	11.71	Stage 1 Breccia/Bootstrap Limestone
U16-h07-13B	151	152	B	1.10	14.95	Stage 1 Breccia/Bootstrap Limestone
U16-h07-13B	291	292	A			silicified Stage 2 Breccia in Stage 3 Breccia
U16-h07-13B	291	292	B			silicified Stage 2 Breccia in Stage 3 Breccia
U16-h07-13B	306	307		0.68	7.78	Stage 3 Breccia
U16-h07-13B	331	332		-0.68	4.71	Stage 3 Breccia
U16-h07-13B	391	392				silicified Stage 2 Breccia in Stage 3 Breccia
U16-h07-13B	451	452				silicfied Stage 2 Breccia
U16-h07-13B	503	504				Devonian Popovich Upper Mud
U16-h07-13B	515	516	A	-2.25	21.97	Devonian Popovich Upper Mud
U16-h07-13B	515	516	B	-2.97	23.15	Devonian Popovich Upper Mud

hole ID	start depth (ft)	end depth (ft)		δ13C VPDB	δ18O VSMOW	Lihology
U16-h07-13B	554	555		-1.20	12.90	Devonian Popovich Upper Mud
U16-h07-15	170	171				Stage 2 Breccia
U16-h07-15	440	441				silicified Stage 2 Breccia
U16-H07-24	5	6		1.98	23.45	Stage 1 Breccia/Bootstrap Limestone
U16-H07-24	40	41		-0.21	23.89	Stage 1 Breccia/Bootstrap Limestone
U16-H07-24	75	76		2.08	20.58	Stage 1 Breccia/Bootstrap Limestone
U16-H07-24	110	111	A	1.54	19.84	Stage 1 Breccia/Bootstrap Limestone
U16-H07-24	110	111	B	1.86	21.51	Calcite Vein
U16-H07-24	145	146	A	1.44	16.12	Stage 1 Breccia/Bootstrap Limestone
U16-H07-24	145	146	B	1.26	21.50	Calcite Vein
U16-H07-24	173	174		-2.02	9.04	Stage 1 Breccia/Bootstrap Limestone
U16-H07-24	181	182	A	-1.52	13.96	Stage 1 Breccia/Bootstrap Limestone
U16-H07-24	181	182	B	1.82	13.67	Stage 1 Breccia/Bootstrap Limestone
U16-H07-24	210	211		1.66	18.08	Stage 1 Breccia/Bootstrap Limestone
U16-H07-24	246	247		1.45	22.12	Stage 1 Breccia/Bootstrap Limestone
U16-H07-24	269	270		1.20	22.99	Stage 1 Breccia/Bootstrap Limestone
U16-H07-24	280	281		2.19	19.35	Stage 1 Breccia/Bootstrap Limestone
U16-H07-24	312	313	A	1.47	17.76	Stage 1 Breccia/Bootstrap Limestone
U16-H07-24	312	313	B			Calcite Vein
U16-H07-24	339	340		-0.21	7.43	Stage 1 Breccia/Bootstrap Limestone
U16-H07-24	367.5	368.5	A	2.99	11.37	Stage 1 Breccia/Bootstrap Limestone
U16-H07-24	367.5	368.5	B	2.12	9.32	Stage 1 Breccia/Bootstrap Limestone
U16-H07-24	392	393		0.71	12.61	Stage 1 Breccia/Bootstrap Limestone
U16-H07-24	694	695		-0.83	18.56	Devonian Popovich Upper Mud
U16-H07-24	757	758		-0.26	20.47	Devonian Popovich Upper Mud
U16-H07-24	823	824				Devonian Popovich Upper Mud
U16-h07-25	25	26	A	0.34	21.43	Stage 1 Breccia/Bootstrap Limestone
U16-h07-25	25	26	B	1.68	24.58	Calcite Vein
U16-h07-25	55	56		2.25	24.06	Stage 1 Breccia/Bootstrap Limestone
U16-h07-25	80	81	A	1.55	21.70	Stage 1 Breccia/Bootstrap Limestone clast
U16-h07-25	80	81	B	1.70	21.24	Stage 1 Breccia/Bootstrap Limestone matrix
U16-h07-25	80	81	C	0.71		Calcite Vein
U16-H07-25	137	138		0.74	19.62	Stage 1 Breccia/Bootstrap Limestone
U16-h07-25	167	168		0.70	18.43	Stage 1 Breccia/Bootstrap Limestone
U16-h07-25	199	200		-0.13	18.35	Stage 2 Breccia
U16-h07-25	246			2.40	16.03	Stage 2 Breccia
U16-h07-25	611			-1.81	22.33	Devonian Popovich Upper Mud
U16-h07-25	628			-0.88	22.46	Devonian Popovich Upper Mud
U16-H07-30	5	6		-0.06	24.20	Stage 1 Breccia/Bootstrap Limestone
U16-H07-30	35	36		2.06	24.30	Stage 1 Breccia/Bootstrap Limestone
U16-H07-30	65	66		1.02	23.94	Stage 1 Breccia/Bootstrap Limestone
U16-H07-30	90	91		1.58	25.91	Stage 1 Breccia/Bootstrap Limestone
U16-H07-30	120	121		1.35	24.57	Stage 1 Breccia/Bootstrap Limestone
U16-H07-30	150	151		2.27	24.47	Stage 1 Breccia/Bootstrap Limestone
U16-H07-30	180	181		1.57	24.71	Stage 1 Breccia/Bootstrap Limestone
U16-H07-30	210	211		1.34	24.36	Stage 1 Breccia/Bootstrap Limestone
U16-H07-30	240	241	B	2.19	23.25	Stage 1 Breccia/Bootstrap Limestone
U16-H07-30	240	241	A	1.36	22.07	Stage 1 Breccia/Bootstrap Limestone
U16-H07-30	270	271	A	1.85	21.81	Stage 1 Breccia/Bootstrap Limestone
U16-H07-30	270	271	B	0.34	19.23	Calcite Vein

hole ID	start depth (ft)	end depth (ft)		δ13C VPDB	δ18O VSMOW	Lihology
U16-H07-30	300	301				Stage 1 Breccia/Bootstrap Limestone
U16-H07-30	330	331		2.44	22.14	Stage 1 Breccia/Bootstrap Limestone
U16-H07-30	360	361		0.25	24.21	Stage 1 Breccia/Bootstrap Limestone
U16-H07-30	370	371		3.21	23.53	Stage 1 Breccia/Bootstrap Limestone
U16-H07-31	7	8		3.50	23.48	Stage 1 Breccia/Bootstrap Limestone
U16-H07-31	37	38		2.24	22.92	Stage 1 Breccia/Bootstrap Limestone
U16-H07-31	67	68		-0.21	23.93	Stage 1 Breccia/Bootstrap Limestone
U16-H07-31	97	98		2.65	23.67	Stage 1 Breccia/Bootstrap Limestone
U16-H07-31	127	128		1.49	24.13	Stage 1 Breccia/Bootstrap Limestone
U16-H07-31	157	158		2.63	24.30	Stage 1 Breccia/Bootstrap Limestone
U16-H07-31	187	188		1.26	25.08	Stage 1 Breccia/Bootstrap Limestone
U16-H07-31	217	218	A	1.01	23.29	Stage 1 Breccia/Bootstrap Limestone
U16-H07-31	217	218	B			Calcite Vein
U16-H07-31	247	248		-0.36	21.32	Stage 1 Breccia/Bootstrap Limestone
U16-H07-31	277	278	A	0.92	24.35	Stage 1 Breccia/Bootstrap Limestone
U16-H07-31	277	278	B	0.82	24.03	Stage 1 Breccia/Bootstrap Limestone
U16-H07-31	310	311		3.75	22.22	Stage 1 Breccia/Bootstrap Limestone
U16-H07-31	336	337		2.37	25.58	Stage 1 Breccia/Bootstrap Limestone
U16-H07-31	355	356	A	1.21	4.29	Calcite Vein
U16-H07-31	355	356	B	0.68	2.26	Calcite Vein
U16-H07-31	384	385		0.29	17.25	Stage 1 Breccia/Bootstrap Limestone
U16-H07-31	405	406			20.21	Stage 1 Breccia/Bootstrap Limestone
U16-h07-34	30	31	A	2.22	24.49	Stage 1 Breccia/Bootstrap Limestone
U16-h07-34	30	31	B	1.15	23.20	Calcite Vein
U16-H07-34	54	55	A	2.46	23.34	Stage 1 Breccia/Bootstrap Limestone
U16-H07-34	54	55	B	2.75	2.08	Calcite Vein
U16-H07-34	84	85	A	2.37	25.07	Stage 1 Breccia/Bootstrap Limestone
U16-H07-34	84	85	B	1.35	24.02	Stage 1 Breccia/Bootstrap Limestone
U16-h07-34	138	139	A	1.99	24.52	Stage 1 Breccia/Bootstrap Limestone
U16-h07-34	138	139	B	0.79	24.68	Stage 1 Breccia/Bootstrap Limestone
U16-h07-34	163	164		0.79	24.95	Stage 1 Breccia/Bootstrap Limestone
U16-h07-34	208	209	A	1.24	24.40	Stage 1 Breccia/Bootstrap Limestone
U16-h07-34	208	209	B	0.73	23.56	Stage 1 Breccia/Bootstrap Limestone
U16-H07-34	245	246	A	2.84	23.88	Stage 1 Breccia/Bootstrap Limestone
U16-H07-34	245	246	B	1.67	22.19	Stage 1 Breccia/Bootstrap Limestone
U16-h07-34	316	317	A	1.23	22.52	Stage 1 Breccia/Bootstrap Limestone clast
U16-h07-34	316	317	B		23.59	Stage 1 Breccia/Bootstrap Limestone matrix
U16-h07-34	405	406	A	1.70	21.64	Stage 1 Breccia/Bootstrap Limestone clast
U16-h07-34	405	406	B	1.34	20.84	Stage 1 Breccia/Bootstrap Limestone matrix
U16-h07-34	497	498	A	1.42	8.02	Stage 1 Breccia/Bootstrap Limestone
U16-h07-34	497	498	B	1.54	2.18	Calcite Vein
U16-h07-34	525	526		2.59	12.73	Stage 1 Breccia/Bootstrap Limestone
U16-h07-34	553	554	A	2.61	16.00	Stage 1 Breccia/Bootstrap Limestone
U16-h07-34	553	554	B	1.00	8.06	Calcite Vein
U16-h07-34	553	554	C	0.71	4.38	Calcite Vein
U16-H07-35	20	21		2.07	12.59	Stage 1 Breccia/Bootstrap Limestone
U16-H07-35	46	47		1.35	17.23	Stage 1 Breccia/Bootstrap Limestone
U16-H07-35	81	82		2.63	12.46	Stage 1 Breccia/Bootstrap Limestone
U16-H07-35	102	103		1.38	14.12	Stage 1 Breccia/Bootstrap Limestone
U16-H07-35	116	117		2.02	14.54	Stage 1 Breccia/Bootstrap Limestone

hole ID	start depth (ft)	end depth (ft)		δ13C VPDB	δ18O VSMOW	Lihology
U16-H07-35	145	146		3.42	4.62	Calcite Vein
U16-h07-35	458	459		-1.50	22.18	Devonian Popovich Upper Mud
U16-h07-54	5	6		2.32	15.64	Stage 1 Breccia/Bootstrap Limestone
U16-h07-54	17	18	A	2.77	15.33	Stage 1 Breccia/Bootstrap Limestone
U16-h07-54	17	18	B	1.69	13.30	Stage 1 Breccia/Bootstrap Limestone
U16-h07-54	17	18	C	-1.68	11.97	Calcite Vein
U16-h07-54	49.5	50.5	A	1.32	18.42	Stage 1 Breccia/Bootstrap Limestone
U16-h07-54	49.5	50.5	B	2.06	13.59	Stage 1 Breccia/Bootstrap Limestone
U16-h07-54	49.5	50.5	C	2.06	17.25	Stage 1 Breccia/Bootstrap Limestone
U16-h07-54	79	80		0.43	8.40	Stage 1 Breccia/Bootstrap Limestone
U16-h07-54	102	103	A	0.95	7.58	Stage 2 Breccia
U16-h07-54	102	103	B	2.38	5.45	Calcite Vein
U16-h07-54	135	136	C	3.04	3.44	Calcite Vein
U16-h07-54	157	158	A	1.13	8.26	Stage 2 Breccia
U16-h07-54	157	158	B	1.42	10.83	
U16-h07-54	157	158	C	1.32	18.42	Calcite Vein
U16-h07-54	168	169			18.68	Stage 1 Breccia/Bootstrap Limestone
U16-h07-54	200	201	A	0.87	19.99	Stage 1 Breccia/Bootstrap Limestone clast
U16-h07-54	200	201	B	2.33	24.71	Stage 1 Breccia/Bootstrap Limestone matrix
U16-h07-54	228	229		1.69	17.89	Stage 1 Breccia/Bootstrap Limestone
U16-h07-54	249	250		1.39	15.55	Stage 1 Breccia/Bootstrap Limestone
U16-h07-54	260	261	A	-1.19	4.73	Stage 1 Breccia/Bootstrap Limestone
U16-h07-54	260	261	B	2.11	4.47	Calcite Vein
U16-h07-54	375	376	A	1.24	17.11	Stage 2 Breccia
U16-h07-54	375	376	B	1.63	19.41	Stage 2 Breccia
U16-h07-54	422	423	A	0.86	5.15	Calcite Vein
U16-h07-54	422	423	B	0.95	5.05	Calcite Vein
U16-h07-54	441	442		1.24	8.33	silicified Stage 2 Breccia
U16-h07-54	460	461	A	-1.65	8.97	silicified Stage 2 Breccia
U16-h07-54	460	461	B	0.90	8.79	
U16-h07-54	483	484	A	-0.40	11.39	silicified Stage 2 Breccia clast in Stage 3 Breccia
U16-h07-54	483	484	B	-0.13	10.47	silicified Stage 2 Breccia matrix in Stage 3 Breccia
U16-h07-54	483	484	C	4.05	5.62	Calcite Vein
U16-h07-54	500	501		0.63	8.19	silicified Stage 2 Breccia in Stage 3 Breccia
U16-h07-54	520	521		0.80	4.37	Calcite Vein
U16-h07-61	10	11		-0.37	6.90	Stage 1 Breccia/Bootstrap Limestone
U16-h07-61	38	39		1.30	13.08	Stage 1 Breccia/Bootstrap Limestone
U16-h07-61	87	88		-0.85	17.46	cave fill Stage 1 Breccia/Bootstrap Limestone
U16-h07-61	112	113		0.89	18.40	Stage 1 Breccia/Bootstrap Limestone
U16-h07-61	138	139		1.56	21.92	Stage 1 Breccia/Bootstrap Limestone
U16-h07-61	164	165		-1.46	7.81	Stage 1 Breccia/Bootstrap Limestone
U16-h07-61	194	195		1.34	20.43	Stage 2 Breccia
U16-h07-61	244	245		1.79	9.94	Stage 1 Breccia/Bootstrap Limestone
U16-h07-61	267	268		1.71	20.85	Stage 1 Breccia/Bootstrap Limestone
U16-h07-61	295	296		1.55	23.09	Stage 1 Breccia/Bootstrap Limestone
U16-h07-61	352	353		1.98	12.35	Stage 1 Breccia/Bootstrap Limestone
U16-h07-61	382	383		2.67	19.08	Stage 1 Breccia/Bootstrap Limestone
U16-h07-61	410	411		2.38	20.93	Stage 1 Breccia/Bootstrap Limestone
U16-h07-61	435	436		2.57	22.31	Stage 1 Breccia/Bootstrap Limestone
U16-h07-61	463	464		1.47	20.79	Stage 1 Breccia/Bootstrap Limestone

hole ID	start depth (ft)	end depth (ft)		δ13C VPDB	δ18O VSMOW	Lihology
U16-h07-61	487	488		0.75	17.40	Stage 1 Breccia/Bootstrap Limestone
U16-h07-61	514	515		1.39	16.67	Stage 1 Breccia/Bootstrap Limestone
U16-h07-61	530	531		-0.38	6.08	Stage 2 Breccia
U16-h07-61	552	553		-3.23	10.79	cave fill Stage 1 Breccia/Bootstrap Limestone
U16-h07-61	570	571		0.88	8.73	Stage 1 Breccia/Bootstrap Limestone
U16-h07-61	605	606		0.74	6.12	Stage 2 Breccia
U16-h07-61	637	638		0.37	7.43	Stage 1 Breccia/Bootstrap Limestone
U16-h07-61	667	668		2.02	10.99	Stage 1 Breccia/Bootstrap Limestone
U16-h07-61	707	708		0.52	16.91	Stage 1 Breccia/Bootstrap Limestone
U16-h07-61	770	771		1.27	11.08	Stage 1 Breccia/Bootstrap Limestone
U16-h07-61	825	826		1.73	16.17	Stage 2 Breccia
U16-h07-61	865	866		2.15	14.23	Stage 1 Breccia/Bootstrap Limestone
U16-h07-61	883.5	884.5		-0.19	6.01	Stage 2 Breccia
U16-h07-61	1020	1021		-2.86	15.17	Stage 1 Breccia/Bootstrap Limestone
U16-H07-63	25	26	A	-0.86	11.08	Stage 1 Breccia/Bootstrap Limestone
U16-H07-63	25	26	B	-0.44	6.57	Stage 1 Breccia/Bootstrap Limestone
U16-H07-63	25	26	C	3.50	2.84	Calcite Vein
U16-H07-63	68	69				Stage 1 Breccia/Bootstrap Limestone
U16-H07-63	80	81		0.89	14.90	Stage 1 Breccia/Bootstrap Limestone
U16-H07-63	145	146		1.57	22.37	Stage 1 Breccia/Bootstrap Limestone
U16-H07-63	231	232		1.58	19.47	Stage 1 Breccia/Bootstrap Limestone
U16-H07-63	260	261		0.89	20.64	Stage 1 Breccia/Bootstrap Limestone
U16-H07-63	306	307				Stage 2 Breccia
U16-H07-63	400	401		1.14	19.38	Stage 1 Breccia/Bootstrap Limestone
U16-H07-63	450	451	A	1.11	17.71	Stage 1 Breccia/Bootstrap Limestone
U16-H07-63	450	451	B	1.02	14.49	Stage 1 Breccia/Bootstrap Limestone
U16-H07-63	450	451	C	1.24	4.26	Calcite Vein
U16-H07-63	491	492	A	0.79	17.56	Stage 1 Breccia/Bootstrap Limestone
U16-H07-63	491	492	B	0.26	5.35	Calcite Vein
U16-H07-63	552	553		0.95	18.83	Stage 1 Breccia/Bootstrap Limestone
U16-H07-63	602	603		2.62	21.62	Stage 1 Breccia/Bootstrap Limestone
U16-H07-63	632	633		-0.34	23.17	Stage 1 Breccia/Bootstrap Limestone
U16-H07-63	675	676		1.07	21.63	Stage 1 Breccia/Bootstrap Limestone
U16-H07-63	727	728		1.37	21.06	Stage 1 Breccia/Bootstrap Limestone
U16-H07-63	800	801		0.83	22.06	Stage 1 Breccia/Bootstrap Limestone
U16-H07-63	841	842		-0.89	23.08	Stage 1 Breccia/Bootstrap Limestone
U16-H07-63	889	890		1.38	22.01	Stage 1 Breccia/Bootstrap Limestone
U16-H07-63	922	923		1.80	25.12	Stage 1 Breccia/Bootstrap Limestone
U16-H07-63	956	957		1.53	18.36	Stage 1 Breccia/Bootstrap Limestone
U16-H07-63	975	976	A	2.25	20.38	Stage 1 Breccia/Bootstrap Limestone
U16-H07-63	975	976	B	2.54	20.32	Stage 1 Breccia/Bootstrap Limestone
U16-H07-63	976	977				Jurassic Lamprophyre
U16-H07-63	989	990		1.25	12.04	Stage 1 Breccia/Bootstrap Limestone
U16-H07-63	992	993		0.42	19.78	Stage 1 Breccia/Bootstrap Limestone
U16-H07-63	1030	1031				Jurassic Lamprophyre
U16-H07-63	1065	1066		0.56	21.75	Stage 1 Breccia/Bootstrap Limestone
U16-H07-63	1112	1113		1.50	19.99	Stage 1 Breccia/Bootstrap Limestone
U16-H07-63	1118	1119	A			Stage 1 Breccia/Bootstrap Limestone
U16-H07-63	1118	1119	B			Stage 1 Breccia/Bootstrap Limestone
U16-H07-63	1140	1141				Jurassic Lamprophyre

hole ID	start depth (ft)	end depth (ft)		δ13C VPDB	δ18O VSMOW	Lihology
U16-H07-63	1144	1145				Jurassic Lamprophyre
U16-H07-63	1183	1184	A	1.29	23.08	Stage 1 Breccia/Bootstrap Limestone
U16-H07-63	1183	1184	B	1.09	17.84	Stage 1 Breccia/Bootstrap Limestone
U16-h07-66	5	6		1.02	11.70	Stage 1 Breccia/Bootstrap Limestone
U16-h07-66	37	38		1.16	19.14	Stage 1 Breccia/Bootstrap Limestone
U16-h07-66	75	76		2.99	20.83	Stage 1 Breccia/Bootstrap Limestone
U16-h07-66	110	111		2.64	16.98	Stage 1 Breccia/Bootstrap Limestone
U16-h07-66	143	144		3.15	16.76	Stage 1 Breccia/Bootstrap Limestone
U16-h07-66	177	178		2.64	20.45	Stage 1 Breccia/Bootstrap Limestone
U16-h07-66	211	212		1.63	15.48	cave fill Stage 1 Breccia/Bootstrap Limestone
U16-h07-66	247	248		1.79	15.40	Stage 1 Breccia/Bootstrap Limestone
U16-H07-67	3	4		1.68	9.47	Stage 1 Breccia/Bootstrap Limestone
U16-H07-67	54	55		1.02	17.62	Stage 1 Breccia/Bootstrap Limestone
U16-H07-67	111	112		1.80	24.12	Stage 1 Breccia/Bootstrap Limestone
U16-H07-67	129	130	A	2.87	21.86	Stage 1 Breccia/Bootstrap Limestone
U16-H07-67	129	130	B	1.02	16.65	Calcite Vein
U16-H07-67	156	157		2.25	20.80	Stage 1 Breccia/Bootstrap Limestone
U16-h07-68	25	26		0.45	10.29	Stage 1 Breccia/Bootstrap Limestone
U16-h07-68	75	76		2.23	19.97	Stage 1 Breccia/Bootstrap Limestone
U16-h07-68	99	100		3.10	15.59	Stage 1 Breccia/Bootstrap Limestone
U16-h07-68	123	124		0.72	21.36	Stage 1 Breccia/Bootstrap Limestone
U16-h07-68	235	236		-0.98	22.79	Devonian Popovich Upper Mud
U16-h07-68	278	279				Devonian Popovich Upper Mud
U16-h07-68	293	294		-1.33	18.62	Devonian Popovich Upper Mud
U16-H07-69	5	6		1.05	9.02	Stage 1 Breccia/Bootstrap Limestone
U16-H07-69	30	31		1.55	14.10	Stage 1 Breccia/Bootstrap Limestone
U16-H07-69	109	110		0.60	20.55	Stage 1 Breccia/Bootstrap Limestone
U16-H07-69	130	131		1.85	20.32	Stage 1 Breccia/Bootstrap Limestone
U16-H07-69	155	156		0.92	21.69	Stage 1 Breccia/Bootstrap Limestone
U16-H07-69	180	181	A	0.34	11.25	Stage 1 Breccia/Bootstrap Limestone
U16-H07-69	180	181	B	0.33	-0.52	Calcite Vein
U16-H07-69	202	203		0.53	18.92	Stage 1 Breccia/Bootstrap Limestone
U16-H07-69	265	266		3.58	21.83	Stage 1 Breccia/Bootstrap Limestone
U16-H07-69	287	288	A	2.05	16.08	Stage 1 Breccia/Bootstrap Limestone
U16-H07-69	287	288	B	1.76	12.64	Stage 1 Breccia/Bootstrap Limestone
U16-H07-69	309	310		0.06	18.04	Stage 1 Breccia/Bootstrap Limestone
U16-H07-69	351	352				Stage 1 Breccia/Bootstrap Limestone
U16-H07-69	370	371		-0.55	16.80	Stage 1 Breccia/Bootstrap Limestone
U16-H07-69	383	384		2.99	13.26	Stage 2 Breccia
U16-H07-69	407	408		2.89	19.04	Stage 1 Breccia/Bootstrap Limestone
U16-H07-69	474	475		0.86	10.44	Stage 1 Breccia/Bootstrap Limestone
U16-H07-69	486.5	487.5	A	0.44	8.30	Stage 1 Breccia/Bootstrap Limestone
U16-H07-69	486.5	487.5	B	1.55	-0.25	Calcite Vein
U16-H07-69	510	511		-3.20	13.03	Stage 1 Breccia/Bootstrap Limestone
U16-H07-69	529	530	A	0.18	13.60	Stage 1 Breccia/Bootstrap Limestone
U16-H07-69	529	530	B			Calcite Vein
U16-H07-69	560	561		0.18	6.20	Stage 1 Breccia/Bootstrap Limestone
U16-H07-69	590	591	A	2.46	23.53	Stage 1 Breccia/Bootstrap Limestone
U16-H07-69	590	591	B	1.20	4.22	Calcite Vein
U16-H07-69	606	607		3.13	11.16	Stage 1 Breccia/Bootstrap Limestone

hole ID	start depth (ft)	end depth (ft)		δ13C VPDB	δ18O VSMOW	Lihology
U16-H07-69	630	631		0.72	17.68	Stage 1 Breccia/Bootstrap Limestone
U16-H07-69	655	656		1.01	15.50	Stage 1 Breccia/Bootstrap Limestone
U16-H07-69	705	706		1.90	11.47	Stage 1 Breccia/Bootstrap Limestone
U16-H07-69	720	721		-0.12	14.72	Stage 2 Breccia
U16-H07-69	740	741		1.60	13.53	Stage 1 Breccia/Bootstrap Limestone
U16-H07-69	765	766		0.93	12.16	Stage 1 Breccia/Bootstrap Limestone
U16-H07-69	780	781		1.30	11.13	Stage 1 Breccia/Bootstrap Limestone
U16-H07-69	805	806	A			Stage 1 Breccia/Bootstrap Limestone
U16-H07-69	805	806	B			Stage 1 Breccia/Bootstrap Limestone
U16-h07-70	47	48		1.45	10.83	Stage 1 Breccia/Bootstrap Limestone
U16-h07-70	77	78				cave fill Stage 1 Breccia/Bootstrap Limestone
U16-h07-70	120	121		2.08	20.78	Stage 1 Breccia/Bootstrap Limestone
U16-h07-70	157	158		0.44	24.01	Stage 1 Breccia/Bootstrap Limestone
U16-h07-70	190	191		2.11	20.13	Stage 1 Breccia/Bootstrap Limestone
U16-h07-70	277	278		3.25	21.81	Stage 1 Breccia/Bootstrap Limestone
U16-h07-70	420	421		2.90	17.55	Stage 1 Breccia/Bootstrap Limestone
U16-h07-70	445	446		-0.42	8.81	Stage 1 Breccia/Bootstrap Limestone
U16-h07-70	465	466		0.26	16.62	Stage 1 Breccia/Bootstrap Limestone
U16-h07-70	502	503		1.61	9.84	Stage 1 Breccia/Bootstrap Limestone
U16-h07-70	529	530		0.61	16.07	Stage 2 Breccia
U16-H07-70	540	541		1.87	8.52	Stage 1 Breccia/Bootstrap Limestone
U16-h07-70	590	591		-0.96	16.14	Stage 1 Breccia/Bootstrap Limestone
U16-h07-70	645	646		2.11	15.64	Stage 1 Breccia/Bootstrap Limestone
U16-H07-71	12	13	A			Stage 1 Breccia/Bootstrap Limestone
U16-H07-71	12	13	B			Stage 1 Breccia/Bootstrap Limestone
U16-H07-71	42	43		0.38	20.70	Stage 1 Breccia/Bootstrap Limestone
U16-H07-71	67	68	A	1.43	12.98	Stage 1 Breccia/Bootstrap Limestone
U16-H07-71	67	68	B			Stage 1 Breccia/Bootstrap Limestone
U16-H07-71	67	68	C	4.26	5.52	Calcite Vein
U16-H07-71	97	98		1.59	19.53	Stage 2 Breccia
U16-H07-71	100	101	B	2.37	16.04	Stage 1 Breccia/Bootstrap Limestone
U16-H07-71	100	101	A	2.25	15.62	Stage 1 Breccia/Bootstrap Limestone
U16-H07-71	136	137	A			Stage 3 Breccia
U16-H07-71	136	137	B	-1.77	7.25	Calcite Vein
U16-H07-71	172	173		0.72	20.41	Stage 1 Breccia/Bootstrap Limestone
U16-H07-71	230	231		2.46	8.11	Stage 1 Breccia/Bootstrap Limestone
U16-H07-71	257	258		3.31	21.74	Stage 1 Breccia/Bootstrap Limestone
U16-H07-71	286	287		2.97	21.95	Stage 1 Breccia/Bootstrap Limestone
U16-H07-71	314	315		4.26	21.49	Stage 1 Breccia/Bootstrap Limestone
U16-H07-71	327	328	B	2.32	16.60	Stage 1 Breccia/Bootstrap Limestone
U16-H07-71	327	328	A	3.00	16.49	Stage 2 Breccia
U16-H07-71	577.5	578.5		1.32	3.07	Calcite Vein
U16-H08-03	5	6		2.35	25.36	Stage 1 Breccia/Bootstrap Limestone
U16-H08-03	25	26		1.78	24.21	Stage 1 Breccia/Bootstrap Limestone
U16-H08-03	60	61		-0.06	24.20	Stage 1 Breccia/Bootstrap Limestone
U16-H08-03	100	101		0.93	23.38	Stage 1 Breccia/Bootstrap Limestone
U16-H08-03	140	141		2.01	25.26	Stage 1 Breccia/Bootstrap Limestone
U16-H08-03	180	181		2.55	24.01	Stage 1 Breccia/Bootstrap Limestone
U16-H08-03	220	221	B	1.50	23.60	Stage 1 Breccia/Bootstrap Limestone
U16-H08-03	220	221	A	1.55	23.56	Stage 1 Breccia/Bootstrap Limestone

hole ID	start depth (ft)	end depth (ft)		δ13C VPDB	δ18O VSMOW	Lihology
U16-H08-03	260	261		2.23	23.65	Stage 1 Breccia/Bootstrap Limestone
U16-H08-03	300	301		0.99	23.16	Stage 1 Breccia/Bootstrap Limestone
U16-H08-03	340	341		2.04	24.82	Stage 1 Breccia/Bootstrap Limestone
U16-H08-03	380	381		2.70	22.78	Stage 1 Breccia/Bootstrap Limestone
U16-H08-03	420	421		3.82	24.73	Stage 1 Breccia/Bootstrap Limestone
U16-H08-03	450	451		2.66	24.75	Stage 1 Breccia/Bootstrap Limestone
U16-H08-03	480	481		1.47	25.50	Stage 1 Breccia/Bootstrap Limestone
U16-H08-03	510	511	A	2.21	24.82	Stage 1 Breccia/Bootstrap Limestone
U16-H08-03	510	511	B	0.37	4.86	Calcite Vein
U16-H08-03	540	541	A	1.83	19.72	Stage 1 Breccia/Bootstrap Limestone
U16-H08-03	540	541	B			Calcite Vein
U16-H08-03	570	571		4.08	21.28	Stage 1 Breccia/Bootstrap Limestone
U16-H08-03	590	591	A	1.99	23.34	Stage 1 Breccia/Bootstrap Limestone
U16-H08-03	590	591	B	1.29	21.66	Stage 1 Breccia/Bootstrap Limestone
U16-H08-03	590	591	C	0.42	22.83	Calcite Vein
U16-H08-03	610	611		-0.50	17.09	Stage 1 Breccia/Bootstrap Limestone
U16-H08-27	202	203		2.96	24.86	Stage 1 Breccia/Bootstrap Limestone
U16-H08-27	233	234		1.06	23.60	Stage 1 Breccia/Bootstrap Limestone
U16-H08-27	270	271	B	1.48	24.39	Stage 1 Breccia/Bootstrap Limestone
U16-H08-27	270	271	A	1.72	23.77	Stage 1 Breccia/Bootstrap Limestone
U16-H08-27	302	303		1.73	24.51	Stage 1 Breccia/Bootstrap Limestone
U16-H08-27	337	338		3.57	23.98	Stage 1 Breccia/Bootstrap Limestone
U16-H08-27	372	373		1.53	25.50	Stage 1 Breccia/Bootstrap Limestone
U16-H08-27	402	403		2.15	22.89	Stage 1 Breccia/Bootstrap Limestone
U16-H08-27	429.5	430.5		1.82	26.12	Stage 1 Breccia/Bootstrap Limestone
U16-H08-27	459	460		2.32	25.41	Stage 1 Breccia/Bootstrap Limestone
U16-H08-27	488	489		4.09	25.68	Stage 1 Breccia/Bootstrap Limestone
U16-H08-27	521	522		3.46	23.20	Stage 1 Breccia/Bootstrap Limestone
U16-H08-27	529	530		1.35	25.76	Stage 1 Breccia/Bootstrap Limestone
U16-H08-27	561	562		1.71	23.17	Stage 1 Breccia/Bootstrap Limestone
U16-H08-27	592	593		2.35	20.59	Stage 1 Breccia/Bootstrap Limestone
U16-H08-27	621	622		0.85	19.12	Stage 1 Breccia/Bootstrap Limestone
U16-H08-27	638	639	B	1.67	10.70	Stage 1 Breccia/Bootstrap Limestone
U16-H08-27	638	639	A	2.99	6.84	Calcite Vein
U16-H08-27	687	688	B	0.74	19.62	Stage 1 Breccia/Bootstrap Limestone
U16-H08-27	687	688	A	1.75	8.89	Stage 1 Breccia/Bootstrap Limestone

Appendix D

D.1 LA-ICPMS Data

Sample ID	SampleType	‰ δ13C (VPDB)	‰ δ18O (VSMOW)	Mg (ppm)	2SE (ppm)	Mg LOD (ppm)	Si (ppm)	2SE (ppm)	Si LOD (ppm)	Sc (ppm)
U16-h07-13b-11	matrix	1.9	20.8	3249.090	321.985	1.505	18733.430	3932.249	718.720	0.490
U16-h07-13b-11	matrix	1.9	20.8	3049.463	188.346	1.342	460.311	203.419	621.320	0.091
U16-h07-13b-11	matrix	1.9	20.8	2710.608	109.347	1.268	458.406	230.664	613.680	0.113
U16-h07-13b-11	matrix	1.9	20.8	2259.765	99.367	1.307	792.496	232.229	605.360	0.788
U16-h07-13b-11	matrix	1.9	20.8	2221.102	81.620	1.314	1055.610	202.440	636.090	0.348
U16-h07-13b-11	matrix	1.9	20.8	2181.327	60.830	1.334	973.851	226.743	645.930	0.380
U16-h07-13b-11	matrix	1.9	20.8	2048.098	59.822	1.324	722.861	194.200	640.680	0.097
U16-h07-13b-11	matrix	1.9	20.8	2023.641	55.909	1.340	792.976	192.319	620.200	0.552
U16-h07-13b-11	matrix	1.9	20.8	2022.090	52.232	1.362	2953.230	441.082	650.140	0.619
U16-h07-13b-11	matrix	1.9	20.8	2016.938	80.501	1.332	1319.125	278.799	636.030	0.350
U16-h07-13b-11	matrix	1.9	20.8	1958.145	68.322	1.304	558.611	248.973	603.970	0.851
U16-h07-13b-11	matrix	1.9	20.8	1953.292	114.876	1.233	685.667	176.466	588.860	0.633
U16-h07-13b-11	matrix	1.9	20.8	1921.458	53.887	1.311	411.257	170.000	625.840	0.537
U16-h07-13b-11	matrix	1.9	20.8	1920.858	101.342	1.312	3389.686	767.610	607.370	1.177
U16-h07-13b-11	matrix	1.9	20.8	1878.974	103.590	1.287	462.424	173.603	595.980	0.510
U16-h07-13b-11	matrix	1.9	20.8	1840.096	69.253	1.304	937.608	194.448	622.570	0.718
U16-h07-13b-11	matrix	1.9	20.8	1795.514	67.662	1.321	637.576	219.020	611.520	0.595
U16-h07-13b-11	matrix	1.9	20.8	1769.188	72.640	1.296	626.076	170.504	618.850	0.182
U16-h07-13b-11	matrix	1.9	20.8	1739.461	79.254	1.339	2726.063	390.774	619.930	1.217
U16-h07-13b-11	matrix	1.9	20.8	1696.790	57.664	1.333	814.061	155.630	645.120	0.305
U16-h07-13b-11	matrix	1.9	20.8	1624.877	62.676	1.273	720.973	257.334	616.360	0.654
U16-h07-13b-11	vein 1	1	16.1	1732.642	43.297	1.234	415.589	203.762	608.030	0.272
U16-h07-13b-11	vein 1	1	16.1	1637.696	35.455	1.286	474.136	219.432	634.000	0.093
U16-h07-13b-11	vein 1	1	16.1	1591.753	40.934	1.241	573.836	162.971	611.430	0.055
U16-h07-13b-11	vein 1	1	16.1	1586.011	64.253	1.237	440.537	222.900	609.540	0.052
U16-h07-13b-11	vein 1	1	16.1	1527.452	40.127	1.225	81.035	235.381	603.920	0.024
U16-h07-13b-11	vein 1	1	16.1	1485.890	43.801	1.215	320.503	218.464	598.890	0.017
U16-h07-13b-11	vein 1	1	16.1	1368.663	36.734	1.245	364.941	170.270	613.560	0.091
U16-h07-13b-11	vein 2	-0.4	17.8	1790.425	90.793	1.257	422.938	178.662	604.420	0.065
U16-h07-13b-11	vein 2	-0.4	17.8	1555.004	32.374	1.329	145.456	225.638	639.020	0.060
U16-h07-13b-11	vein 2	-0.4	17.8	1526.953	44.079	1.302	49.718	164.240	625.970	0.016
U16-h07-13b-11	vein 2	-0.4	17.8	1482.255	46.976	1.352	383.912	249.798	650.130	0.104
U16-h07-13b-11	vein 2	-0.4	17.8	1448.802	35.468	1.365	393.117	178.142	656.340	0.050

Sample ID	SampleType	‰ δ13C (VPDB)	‰ δ18O (VSMOW)	Mg (ppm)	2SE (ppm)	Mg LOD (ppm)	Si (ppm)	2SE (ppm)	Si LOD (ppm)	Sc (ppm)
U16-h07-13b-11	vein 2	-0.4	17.8	1428.167	38.745	1.285	333.415	203.284	633.490	-0.012
U16-h07-13b-11	vein 3	1	16.1	1684.615	47.411	1.349	870.697	243.826	648.850	0.137
U16-h07-13b-11	vein 3	1	16.1	1545.535	53.802	1.320	827.216	228.942	634.650	0.232
U16-h07-13b-11	vein 3	1	16.1	1436.133	46.470	1.346	516.631	241.490	647.210	0.167
U16-h07-13b-31	dk ooid	0.7	12.3	2298.954	149.345	45.186	653.799	168.823	500.970	1.992
U16-h07-13b-31	dk ooid	0.7	12.3	1657.765	93.930	0.147	6831.471	1708.368	1014.700	4.013
U16-h07-13b-31	dk ooid	0.7	12.3	1525.841	59.386	45.121	1423.588	269.102	500.600	2.854
U16-h07-13b-31	dk ooid	0.7	12.3	1525.628	77.640	44.457	12836.730	4127.204	493.050	1.869
U16-h07-13b-31	dk ooid	0.7	12.3	1431.887	92.409	0.117	2135.342	236.887	813.140	4.409
U16-h07-13b-31	dk ooid	0.7	12.3	1346.420	55.007	0.139	3136.155	341.549	963.490	3.426
U16-h07-13b-31	matrix cement	0.7	12.3	2078.163	82.958	45.172	770.702	190.395	502.180	2.659
U16-h07-13b-31	matrix cement	0.7	12.3	1648.430	92.032	29.205	1828.348	217.030	682.800	3.306
U16-h07-13b-31	matrix cement	0.7	12.3	1301.519	70.348	44.768	5068.027	844.535	497.570	3.001
U16-h07-13b-31	matrix cement	0.7	12.3	1278.962	61.185	43.537	1398.409	246.735	483.190	3.119
U16-h07-13b-31	matrix cement	0.7	12.3	1240.215	85.166	29.747	7553.632	3383.497	695.130	2.281
U16-h07-13b-31	matrix cement	0.7	12.3	1227.658	81.116	45.669	3609.795	646.183	507.340	3.525
U16-h07-13b-31	matrix cement	0.7	12.3	1164.477	83.605	43.905	1403.338	183.487	487.390	3.719
U16-h07-13b-31	matrix cement	0.7	12.3	1152.520	50.530	28.399	572.373	211.904	664.130	4.385
U16-h07-13b-31	matrix cement	0.7	12.3	1122.157	28.699	8.074	2370.537	269.425	606.870	2.968
U16-h07-13b-31	matrix cement	0.7	12.3	1055.966	48.502	7.997	2741.779	284.115	600.930	2.831
U16-h07-13b-31	matrix cement	0.7	12.3	1002.724	27.500	28.951	1884.864	250.260	676.190	3.295
U16-h07-13b-31	matrix cement	0.7	12.3	911.059	28.259	29.263	1878.177	205.114	683.650	2.203
U16-h07-13b-31	ooid	0.7	12.3	2066.310	88.843	32.271	7415.721	699.956	633.640	3.106
U16-h07-13b-31	ooid	0.7	12.3	1748.505	89.469	108.810	789.019	217.799	725.840	1.948
U16-h07-13b-31	ooid	0.7	12.3	1730.953	70.969	32.475	5225.935	564.724	637.510	2.805
U16-h07-13b-31	ooid	0.7	12.3	1692.447	53.419	0.903	1143.913	225.334	778.980	1.640
U16-h07-13b-31	ooid	0.7	12.3	1690.618	63.864	29.336	434.900	184.198	379.820	1.716
U16-h07-13b-31	ooid	0.7	12.3	1686.232	101.286	25.793	809.449	205.472	614.840	3.891
U16-h07-13b-31	ooid	0.7	12.3	1578.989	96.016	31.534	8837.146	1081.390	408.140	2.897
U16-h07-13b-31	ooid	0.7	12.3	1505.845	62.495	0.876	2669.683	387.506	755.160	2.911
U16-h07-13b-31	ooid	0.7	12.3	1428.268	94.195	1.757	807.830	223.337	536.850	5.287
U16-h07-13b-31	ooid	0.7	12.3	1391.007	41.211	25.633	3780.509	375.772	611.360	3.551
U16-h07-13b-31	ooid	0.7	12.3	1328.794	98.414	32.786	3895.135	688.854	644.990	3.921

Sample ID	SampleType	‰ δ13C (VPDB)	‰ δ18O (VSMOW)	Mg (ppm)	2SE (ppm)	Mg LOD (ppm)	Si (ppm)	2SE (ppm)	Si LOD (ppm)	Sc (ppm)
U16-h07-13b-31	ooid	0.7	12.3	1304.201	55.846	108.540	3565.935	541.930	724.260	3.677
U16-h07-13b-31	ooid	0.7	12.3	1304.173	64.134	31.454	1101.489	216.911	618.000	4.323
U16-h07-13b-31	ooid	0.7	12.3	1281.494	91.121	32.000	4365.679	272.096	628.850	3.062
U16-h07-13b-31	ooid	0.7	12.3	1274.893	57.068	107.830	2590.921	276.941	719.020	3.953
U16-h07-13b-31	ooid	0.7	12.3	1265.926	56.819	25.642	3470.539	274.026	611.450	3.244
U16-h07-13b-31	ooid	0.7	12.3	1230.076	47.424	1.832	5363.064	525.276	559.420	3.830
U16-h07-13b-31	ooid	0.7	12.3	1217.608	55.727	1.763	2929.257	255.880	538.400	4.103
U16-h07-13b-31	ooid	0.7	12.3	1210.839	68.629	31.410	3057.563	225.687	617.660	3.208
U16-h07-13b-31	ooid	0.7	12.3	1188.764	56.215	31.329	3339.232	297.508	616.460	3.915
U16-h07-13b-31	ooid	0.7	12.3	1171.742	66.607	1.686	2780.197	430.344	515.410	5.098
U16-h07-13b-31	ooid	0.7	12.3	1157.805	44.151	1.676	1137.605	204.368	512.430	3.640
U16-h07-13b-31	ooid	0.7	12.3	1122.882	45.801	30.589	1255.411	200.304	600.820	3.176
U16-h07-13b-31	ooid	0.7	12.3	1097.293	42.468	0.876	2405.971	322.138	756.180	2.829
U16-h07-13b-31	vein-1			2651.231	180.700	35.672	15737.970	2194.393	598.220	3.796
U16-h07-13b-31	vein-1			1703.401	78.220	29.457	522.568	216.010	381.190	1.208
U16-h07-13b-31	vein-1			1642.230	45.012	32.208	673.158	149.606	540.020	0.045
U16-h07-13b-31	vein-1			1578.980	91.383	25.231	1221.933	212.403	515.910	0.473
U16-h07-13b-31	vein-1			1486.661	62.085	31.132	855.100	181.758	521.770	0.793
U16-h07-13b-31	vein-1			1328.192	59.317	29.133	1040.225	166.276	488.160	0.233
U16-h07-13b-81	coarse calcite	1.37	16.5	160.418	10.681	109.490	248.414	287.464	460.600	0.008
U16-h07-13b-81	coarse calcite	1.37	16.5	-36.033	21.245	113.140	1145.953	485.271	475.930	0.001
U16-h07-13b-81	coarse calcite	1.37	16.5	-56.884	15.215	105.050	689.775	511.569	441.910	0.062
U16-h07-13b-81	coarse calcite	1.37	16.5	-285.456	25.058	973.430	2388.850	762.970	490.060	0.104
U16-h07-13b-81	vein 1	4.03	7.96	2435.194	1144.678	1173.900	104077.900	50515.970	846.530	2.640
U16-h07-13b-81	vein 1	4.03	7.96	1914.117	154.941	431.420	-163.099	567.715	872.250	0.448
U16-h07-13b-81	vein 1	4.03	7.96	1714.718	240.811	902.660	439.662	212.142	650.940	0.184
U16-h07-13b-81	vein 1	4.03	7.96	1354.765	258.440	244.230	-204.037	292.827	574.950	4.915
U16-h07-13b-81	vein 1	4.03	7.96	1209.202	86.145	100.260	3456.415	722.766	421.740	0.949
U16-h07-13b-81	vein 1	4.03	7.96	908.308	158.905	246.520	2276.512	1075.156	794.870	1.298
U16-h07-13b-81	vein 1	4.03	7.96	892.555	131.568	212.550	183.856	339.623	557.270	1.077
U16-h07-13b-81	vein 1	4.03	7.96	94.903	198.646	217.610	191.217	349.771	570.550	3.849
U16-h07-13b-81	vein 1	4.03	7.96	-229.412	78.904	243.100	73.385	277.349	572.270	2.359
U16-h07-24-145	ooids and cement	1.9	18	2360.501	85.360	0.115	512.058	239.214	482.430	0.031

Sample ID	SampleType	‰ δ13C (VPDB)	‰ δ18O (VSMOW)	Mg (ppm)	2SE (ppm)	Mg LOD (ppm)	Si (ppm)	2SE (ppm)	Si LOD (ppm)	Sc (ppm)
U16-h07-24-145	ooids and cement	1.9	18	2043.095	43.026	0.149	580.891	236.545	411.130	0.095
U16-h07-24-145	ooids and cement	1.9	18	1993.533	74.061	0.152	1120.661	231.562	418.310	0.161
U16-h07-24-145	ooids and cement	1.9	18	1979.831	88.867	0.146	570.145	295.898	401.560	0.117
U16-h07-24-145	ooids and cement	1.9	18	1941.716	83.684	0.110	927.686	241.150	459.070	0.060
U16-h07-24-145	ooids and cement	1.9	18	1880.052	83.736	0.157	681.086	233.053	434.100	0.032
U16-h07-24-145	ooids and cement	1.9	18	1822.625	64.452	0.140	552.068	225.679	386.120	0.137
U16-h07-24-145	ooids and cement	1.9	18	1764.425	74.812	0.142	460.967	214.221	392.070	0.107
U16-h07-24-145	vein-1	1.9	21	3615.317	120.169	46.637	518.851	225.030	773.360	0.057
U16-h07-24-145	vein-1	1.9	21	3211.983	86.954	43.004	398.500	200.407	713.120	0.005
U16-h07-24-145	vein-1	1.9	21	3006.009	80.297	43.097	686.694	216.826	714.660	-0.017
U16-h07-24-145	vein-1	1.9	21	2809.776	69.989	43.395	897.738	221.195	719.600	0.012
U16-h07-24-145	vein-1	1.9	21	2797.353	98.933	41.869	671.860	199.293	694.310	0.043
U16-h07-24-145	vein-1	1.9	21	2393.237	64.933	0.199	619.421	242.775	1066.300	-0.018
U16-h07-24-145	vein-1	1.9	21	2239.574	57.350	0.199	1098.946	262.687	1064.400	0.029
U16-h07-24-145	vein-1	1.9	21	2100.488	59.827	0.187	1043.820	162.808	999.120	0.041
U16-h07-24-145	vein-2	1.9	21	984.221	43.475	46.394	1784.087	497.919	743.370	-0.014
U16-h07-24-145	vein-2	1.9	21	556.811	27.243	45.725	2118.211	1330.522	732.640	0.400
U16-h07-24-145	vein-2	1.9	21	435.959	11.918	46.944	-1456.762	1423.885	752.180	0.101
U16-h07-24-145	vein-3	1.9	21	797.043	66.597	278.450	5304.383	4389.474	783.380	1.921
U16-h07-24-145	vein-3	1.9	21	310.623	30.002	47.905	-1376.696	611.722	767.580	-0.029
U16-h07-24-145	vein-3	1.9	21	182.513	13.869	641.860	-204.385	374.010	583.860	-0.053
U16-h07-24-145	vein-3	1.9	21	162.331	5.117	46.731	-423.149	232.198	748.770	0.007
U16-h07-24-145	vein-3	1.9	21	156.319	7.965	636.330	-52.374	122.575	559.130	-0.025
U16-h07-24-145	vein-3	1.9	21	155.533	5.035	46.938	-251.580	199.222	752.090	-0.012
U16-h07-24-145	vein-3	1.9	21	93.098	3.013	48.488	-34.986	159.683	776.920	-0.023
U16-h07-24-145	vein-4	1.9	21	3416.111	3722.278	279.450	6206.357	19565.010	763.640	4.140
U16-h07-24-145	vein-4	1.9	21	2247.489	82.315	0.092	-167.030	217.933	770.490	0.157
U16-h07-24-145	vein-4	1.9	21	2086.774	69.799	0.089	-124.917	199.154	746.240	0.130
U16-h07-24-145	vein-4	1.9	21	1554.905	55.204	4.616	320.967	271.748	1221.900	0.035
U16-h07-24-145	vein-4	1.9	21	1418.351	3358.671	278.350	37571.100	109929.200	760.650	1.165
U16-h07-24-145	vein-4	1.9	21	799.540	29.261	4.505	559.738	317.093	1192.500	0.074
U16-h07-24-145	vein-4	1.9	21	739.253	41.136	297.250	-34066.020	121326.000	836.270	5.064
U16-h07-24-145	vein-4	1.9	21	724.155	45.946	4.523	562.048	557.719	1197.200	0.034

Sample ID	SampleType	‰ δ13C (VPDB)	‰ δ18O (VSMOW)	Mg (ppm)	2SE (ppm)	Mg LOD (ppm)	Si (ppm)	2SE (ppm)	Si LOD (ppm)	Sc (ppm)
U16-h07-24-145	vein-4	1.9	21	575.199	41.276	4.837	2111.628	2161.064	1280.500	-0.746
U16-h07-24-145	vein-4	1.9	21	543.689	56.352	268.920	-424.701	1017.281	734.880	0.261
U16-h07-24-145	vein-4	1.9	21	522.480	25.412	4.746	1769.555	1607.464	1256.300	-0.334
U16-h07-24-145	vein-4	1.9	21	496.789	47.395	4.845	8272.852	3999.228	1282.400	-0.356
U16-h07-24-145	vein-4	1.9	21	440.489	46.205	653.380	391.740	519.047	594.340	0.031
U16-h07-24-145	vein-4	1.9	21	308.245	22.854	623.950	-503.946	582.125	567.570	-0.033
U16-h07-24-145	vein-4	1.9	21	256.950	172.215	284.700	-3206.725	5366.268	778.000	-0.129
U16-h07-24-145	vein-4	1.9	21	230.100	1192.057	263.890	-2475.132	17090.460	721.130	-0.433
U16-h07-24-145	vein-6	1.9	21	2590.448	246.444	0.096	86.421	221.559	807.500	0.044
U16-h07-24-145	vein-6	1.9	21	2054.867	51.836	0.087	301.260	256.266	727.540	0.085
U16-h07-24-145	vein-6	1.9	21	2031.302	114.331	0.144	1028.009	259.028	400.020	0.130
U16-h07-24-145	vein-6	1.9	21	2026.526	94.229	0.088	458.334	208.007	735.110	0.103
U16-h07-24-145	vein-6	1.9	21	1757.839	76.437	0.083	72.236	204.159	698.320	0.123
U16-h07-24-145	vein-7	1.9	21	2223.856	92.673	0.157	523.291	238.368	436.400	0.064
U16-h07-25-167	coarse calcite			26005.570	48836.740	304.480	56.346	138.384	361.940	0.025
U16-h07-25-167	coarse calcite			4406.896	592.488	311.130	30.887	230.664	369.850	0.070
U16-h07-25-167	coarse calcite			1359.843	100.868	326.030	177.408	194.948	387.560	0.029
U16-h07-25-167	coarse calcite			-5729.678	912.902	322.370	235.700	125.248	383.210	0.003
U16-h07-25-167	dk ooid	0.7	18.4	7153.715	822.252	307.350	851.667	180.017	365.360	0.159
U16-h07-25-167	dk ooid	0.7	18.4	4296.341	473.744	22.264	2485.758	432.150	650.820	0.284
U16-h07-25-167	dk ooid	0.7	18.4	4004.424	537.082	23.557	2656.161	395.686	688.610	0.239
U16-h07-25-167	dk ooid	0.7	18.4	3166.577	213.314	17.993	1433.935	355.836	726.220	0.208
U16-h07-25-167	dk ooid	0.7	18.4	3094.869	441.532	0.313	1754.183	219.073	669.390	0.192
U16-h07-25-167	dk ooid	0.7	18.4	2941.999	335.188	3.055	2528.581	231.012	362.980	0.384
U16-h07-25-167	dk ooid	0.7	18.4	2823.091	303.158	17.721	807.259	346.067	730.850	0.078
U16-h07-25-167	dk ooid	0.7	18.4	2590.324	123.782	21.688	471.035	197.837	633.980	0.167
U16-h07-25-167	dk ooid	0.7	18.4	2410.398	113.001	17.547	1613.665	364.606	723.670	0.211
U16-h07-25-167	dk ooid	0.7	18.4	2388.609	114.889	0.299	707.432	199.075	638.280	0.115
U16-h07-25-167	dk ooid	0.7	18.4	2384.323	126.394	0.301	1568.599	267.642	643.990	0.137
U16-h07-25-167	dk ooid	0.7	18.4	2380.906	116.998	16.801	1139.899	260.878	692.920	0.109
U16-h07-25-167	dk ooid	0.7	18.4	2310.977	151.865	3.023	429.432	208.417	359.150	0.118
U16-h07-25-167	dk ooid	0.7	18.4	2218.971	95.149	17.159	1539.072	233.896	707.670	0.216
U16-h07-25-167	dk ooid	0.7	18.4	2199.270	92.101	0.301	873.796	206.022	647.110	0.129

Sample ID	SampleType	‰ δ13C (VPDB)	‰ δ18O (VSMOW)	Mg (ppm)	2SE (ppm)	Mg LOD (ppm)	Si (ppm)	2SE (ppm)	Si LOD (ppm)	Sc (ppm)
U16-h07-25-167	dk ooid	0.7	18.4	2199.045	111.101	17.208	1017.965	199.345	694.560	0.177
U16-h07-25-167	dk ooid	0.7	18.4	2100.373	88.628	0.297	757.416	209.230	637.810	0.100
U16-h07-25-167	dk ooid	0.7	18.4	2085.444	82.793	0.308	982.140	187.963	659.400	0.091
U16-h07-25-167	dk ooid	0.7	18.4	2079.790	101.344	2.702	1021.618	198.832	320.980	0.255
U16-h07-25-167	dk ooid	0.7	18.4	2078.750	110.578	0.306	1065.354	208.542	654.490	0.090
U16-h07-25-167	dk ooid	0.7	18.4	1939.427	57.395	16.932	396.557	159.921	698.320	0.151
U16-h07-25-167	dk ooid	0.7	18.4	1933.310	106.637	17.188	865.700	211.396	693.760	0.170
U16-h07-25-167	early vein			1600.856	106.269	0.230	143.222	100.941	665.760	0.014
U16-h07-25-167	early vein			1529.753	60.955	0.230	239.706	124.468	664.670	0.016
U16-h07-25-167	early vein			1407.500	59.747	0.234	344.465	105.960	675.350	0.060
U16-h07-25-167	early vein			1215.909	43.608	0.233	291.845	159.497	671.870	0.029
U16-h07-25-167	late vein			3122.341	490.752	0.245	3513.136	359.865	717.140	0.439
U16-h07-25-167	late vein			1794.375	243.131	0.233	2856.658	464.872	682.850	0.360
U16-h07-25-167	late vein			1556.526	121.391	0.226	1062.532	156.772	660.400	0.268
U16-h07-25-167	late vein			1517.071	74.940	0.223	1068.908	108.901	645.230	0.177
U16-h07-25-167	late vein			1248.302	42.693	0.233	789.413	119.405	673.250	0.134
U16-h07-25-167	lt ooid			2475.246	121.698	0.225	1327.379	209.562	653.400	0.092
U16-h07-25-167	lt ooid			2411.286	184.437	0.224	1395.374	217.378	630.800	0.088
U16-h07-25-167	lt ooid			2394.410	200.963	0.226	1102.261	228.108	635.740	0.120
U16-h07-25-167	lt ooid			2384.137	251.523	0.307	1750.355	186.377	659.180	0.221
U16-h07-25-167	lt ooid			2310.529	179.243	0.296	1371.927	237.203	635.920	0.233
U16-h07-25-167	lt ooid			2118.411	103.358	0.220	767.008	213.773	617.750	0.116
U16-h07-25-167	lt ooid			2036.857	162.996	0.211	1130.631	127.146	612.900	0.117
U16-h07-25-167	lt ooid			1920.435	81.060	0.308	1351.260	249.203	660.470	0.175
U16-h07-25-167	lt ooid			1723.726	97.219	0.216	515.012	201.832	607.650	0.140
U16-h07-25-167	lt ooid			1719.222	68.629	0.217	1136.268	185.975	629.970	0.162
U16-h07-25-167	matrix cement			3601.679	577.123	0.244	287.841	244.832	685.310	0.047
U16-h07-25-167	matrix cement			2524.523	139.697	0.228	740.655	212.427	657.450	0.119
U16-h07-25-167	matrix cement			2434.437	515.472	0.238	1519.926	982.823	687.250	0.142
U16-h07-25-167	matrix cement			2247.937	139.153	0.214	627.911	257.287	619.130	0.098
U16-h07-25-167	matrix cement			2221.725	113.035	0.221	761.522	190.508	637.060	0.051
U16-h07-25-167	matrix cement			2126.698	131.970	0.219	451.413	182.712	631.750	0.016
U16-h07-25-167	matrix cement			2039.669	90.055	0.230	256.332	195.394	646.870	0.064

Sample ID	SampleType	‰ δ13C (VPDB)	‰ δ18O (VSMOW)	Mg (ppm)	2SE (ppm)	Mg LOD (ppm)	Si (ppm)	2SE (ppm)	Si LOD (ppm)	Sc (ppm)
U16-h07-25-167	matrix cement			1947.261	107.973	0.219	413.563	133.116	631.700	0.118
U16-h07-25-167	matrix cement			1778.398	65.236	0.220	611.838	182.348	635.620	0.080
U16-h07-25-167	matrix cement			1745.028	73.462	0.211	301.500	156.538	610.310	0.113
U16-h07-25-167	matrix cement			1645.003	64.867	0.227	635.166	177.892	655.820	0.037
U16-h07-34-405	matrix cement			754.825	2400.309	798.160	-37237.890	84762.420	468.870	-0.315
U16-h07-34-405	matrix cement			416.744	190.708	592.220	-4758.801	6447.513	567.820	0.080
U16-h07-34-405	matrix cement			381.493	466.356	779.390	-3867.757	20614.930	460.360	1.585
U16-h07-34-405	matrix cement			324.621	26.858	863.570	-3958.423	1207.986	472.600	-0.087
U16-h07-34-405	matrix cement			291.736	73.637	929.140	-551.789	1718.013	508.480	0.118
U16-h07-34-405	matrix cement			287.573	259.937	721.620	-12551.650	11385.010	426.230	-0.587
U16-h07-34-405	matrix cement			143.153	351.447	721.660	-8277.174	13373.890	426.260	-0.757
U16-h07-34-405	matrix cement			136.037	43.529	930.100	-947.656	1614.881	509.010	0.047
U16-h07-34-405	matrix cement			134.495	126.504	601.160	13890.290	13537.800	576.400	-0.145
U16-h07-34-405	matrix cement			79.833	22.579	930.240	1695.287	1512.858	509.080	-0.174
U16-h07-34-405	matrix cement			44.382	132.747	762.140	-3677.793	3683.059	450.170	-0.045
U16-h07-34-405	matrix cement			13.994	608.710	720.940	-2762.104	5638.405	423.510	-0.004
U16-h07-34-405	matrix cement			3.008	121.996	758.240	1778.369	6369.524	447.860	-2.200
U16-h07-34-405	matrix cement			-37.318	163.921	781.750	8905.894	17841.790	459.230	-1.484
U16-h07-34-405	matrix cement			-499.224	1265.262	794.900	554.478	22293.670	469.520	-3.028
U16-h07-34-405	matrix cement			-511.186	1204.762	776.650	15699.870	42732.450	458.740	2.649
U16-h07-34-405	matrix cement			-592.220	309.242	799.350	-6034.196	8447.207	472.150	-0.874
U16-h07-34-405	ooid			520.673	31.059	850.190	584.325	1006.888	428.020	0.185
U16-h07-34-405	ooid			465.221	60.682	884.520	7767.826	3692.587	620.370	0.825
U16-h07-34-405	ooid			438.131	191.677	544.890	-16157.640	6441.375	522.440	-4.264
U16-h07-34-405	ooid			408.307	68.706	828.210	-3646.717	1820.747	462.600	-0.763
U16-h07-34-405	ooid			407.624	47.416	891.930	-4159.416	1510.314	412.250	0.154
U16-h07-34-405	ooid			406.851	44.368	849.530	-4912.640	1877.417	392.650	-0.771
U16-h07-34-405	ooid			400.903	66.936	903.390	-5177.729	1855.066	561.380	-1.316
U16-h07-34-405	ooid			381.618	47.960	802.210	-4400.972	1850.250	447.810	-0.131
U16-h07-34-405	ooid			333.178	82.650	851.150	-2537.041	2996.886	497.150	0.283
U16-h07-34-405	ooid			329.868	67.297	795.430	-1032.659	2301.862	464.600	-0.741
U16-h07-34-405	ooid			327.824	107.358	857.330	-2050.531	2976.125	478.870	0.358
U16-h07-34-405	ooid			327.208	42.260	826.500	-1214.122	1090.715	382.000	-0.303

Sample ID	SampleType	‰ δ13C (VPDB)	‰ δ18O (VSMOW)	Mg (ppm)	2SE (ppm)	Mg LOD (ppm)	Si (ppm)	2SE (ppm)	Si LOD (ppm)	Sc (ppm)
U16-h07-34-405	ooid			302.915	37.090	836.290	-5507.326	1649.637	466.840	-0.372
U16-h07-34-405	ooid			298.883	46.409	907.820	-3123.903	1272.474	419.590	-0.227
U16-h07-34-405	ooid			289.697	37.319	913.990	-551.032	1652.222	456.770	-0.387
U16-h07-34-405	ooid			286.503	97.334	923.760	-4885.290	2558.973	461.650	-0.426
U16-h07-34-405	ooid			281.750	34.562	906.380	-2319.374	1504.077	418.930	-0.097
U16-h07-34-405	ooid			272.415	46.894	840.950	-7095.853	3613.160	589.810	-0.730
U16-h07-34-405	ooid			257.518	48.753	837.110	-2275.213	1415.394	386.910	-0.602
U16-h07-34-405	ooid			182.544	30.323	901.300	-2099.419	1833.477	560.080	-0.039
U16-h07-34-405	ooid			-2054.681	1542.450	595.810	18193.930	20791.870	571.270	2.513
U16-h07-34-405	ooid and clast			3362.532	202.679	13.586	854105.400	195797.300	1408.200	5.274
U16-h07-34-405	ooid and clast			2907.849	109.448	0.098	1321.289	289.397	511.710	0.383
U16-h07-34-405	ooid and clast			2805.874	92.883	2.699	309.587	198.671	541.010	0.104
U16-h07-34-405	ooid and clast			2770.151	154.526	2.774	1245.620	271.015	555.880	0.115
U16-h07-34-405	ooid and clast			2657.686	168.758	3.471	2664.175	285.843	359.790	1.701
U16-h07-34-405	ooid and clast			2522.163	102.481	3.888	11495.900	1662.872	402.960	2.403
U16-h07-34-405	ooid and clast			2378.400	94.760	0.095	2211.613	301.200	495.470	3.033
U16-h07-34-405	ooid and clast			2354.697	116.827	3.389	1540.333	289.860	351.290	3.038
U16-h07-34-405	ooid and clast			2246.602	112.874	3.462	3561.254	360.868	358.810	1.579
U16-h07-34-405	ooid and clast			2131.904	73.967	3.552	5745.409	2645.001	368.230	1.807
U16-h07-34-405	ooid and clast			2090.455	105.959	2.638	3174.178	363.951	528.750	2.701
U16-h07-34-405	ooid and clast			644.617	26.918	0.690	1813.268	280.873	745.990	0.277
U16-h07-34-405	ooid and clast			553.334	14.802	0.694	6428.603	790.873	750.590	5.576
U16-h07-34-405	ooid and clast			537.563	25.792	81.692	5700.205	706.862	397.340	6.229
U16-h07-34-405	ooid and clast			469.075	26.702	0.080	3039.019	546.352	560.820	8.866
U16-h07-34-405	ooid and clast			398.650	18.498	0.689	12035.600	2123.299	744.630	9.962
U16-h07-34-405	ooid and clast			300.272	15.403	0.701	-6591.399	42859.950	758.240	22.854
U16-h07-34-405	ooid and clast			294.327	18.641	86.539	4803.928	13028.580	420.920	5.052
U16-h07-34-405	ooid and clast			292.521	10.519	2.034	-10756.010	39816.830	688.230	-22.339
U16-h07-34-405	ooid and clast			250.162	21.522	814.790	-292.329	264.696	385.820	0.144
U16-h07-34-405	ooid and clast			233.072	9.161	84.487	-11021.640	1252.574	410.940	-5.328
U16-h07-34-405	ooid and clast			231.233	8.304	0.722	-27757.420	4417.562	780.860	-7.498
U16-h07-34-405	ooid and clast			230.741	11.292	0.656	-9128.294	2177.118	709.170	-16.024
U16-h07-34-405	ooid and clast			212.736	11.794	11.240	-1361.511	423.173	480.190	-4.164

Sample ID	SampleType	‰ δ13C (VPDB)	‰ δ18O (VSMOW)	Mg (ppm)	2SE (ppm)	Mg LOD (ppm)	Si (ppm)	2SE (ppm)	Si LOD (ppm)	Sc (ppm)
U16-h07-34-405	ooid and clast			180.094	8.237	0.702	-7177.623	700.246	758.900	-2.656
U16-h07-34-405	ooid and clast			170.349	6.484	0.667	-940.617	381.632	721.230	-2.491
U16-h07-34-405	ooid and clast			169.353	22.564	635.740	-1106.688	1019.488	440.880	-3.369
U16-h07-34-405	ooid and clast			152.903	8.853	1.492	-3826.612	646.832	766.040	-2.377
U16-h07-34-405	ooid and clast			146.324	13.097	2.279	-12281.630	1971.607	501.640	-1.854
U16-h07-34-405	ooid and clast			137.305	14.086	643.750	-2148.278	457.203	446.440	-2.185
U16-h07-34-405	ooid and clast			108.126	4.649	2.026	-2484.001	218.120	445.790	-1.309
U16-h07-34-405	ooid and clast			85.434	3.363	1.976	-1124.554	146.137	434.770	-1.130
U16-h07-34-405	ooid and clast			85.329	6.766	751.610	-1683.401	409.840	355.910	-1.673
U16-h07-34-405	ooid and clast			79.221	10.467	1.554	-269.358	186.539	797.700	-0.299
U16-h07-34-405	vein 1			543.817	157.494	783.220	-1304.711	1876.636	555.240	0.326
U16-h07-34-405	vein 1			232.578	47.476	800.670	1401.459	4421.208	570.020	0.516
U16-h07-34-405	vein 1			192.177	140.634	825.410	7630.414	12663.420	587.630	-2.708
U16-h07-34-405	vein 1			63.598	74.929	757.270	-5275.501	4213.353	539.120	0.846
U16-h07-34-405	vein 1			-137.154	39.398	784.780	1699.528	3404.948	558.700	1.144
U16-h07-34-405	vein 2			158.461	14.454	902.620	-14807.590	2263.788	639.880	-0.902
U16-h07-34-405	vein 2			148.200	10.378	832.130	-1893.544	677.057	589.920	-0.622
U16-h07-34-405	vein 2			142.167	9.766	876.220	-4707.114	1177.776	621.170	-0.481
U16-h07-34-405	vein 2			114.126	22.340	892.930	-4261.403	1484.472	633.020	-0.843
U16-h07-34-405	vein 2			84.260	12.294	851.900	-1744.970	981.473	603.930	-1.019
U16-h07-34-405	vein 2			70.694	19.279	882.340	-1725.927	1602.180	625.510	-0.657
U16-h07-54-338	coarse calcite			2388.479	61.334	207.930	974.589	282.881	677.040	0.457
U16-h07-54-338	coarse calcite			2349.798	87.893	261.280	787.606	227.943	582.510	0.024
U16-h07-54-338	coarse calcite			2341.184	60.975	155.050	883.228	225.787	774.230	0.022
U16-h07-54-338	coarse calcite			2231.209	93.152	140.680	1086.484	282.097	580.220	0.488
U16-h07-54-338	coarse calcite			2147.542	67.970	250.800	976.738	200.113	559.060	2.406
U16-h07-54-338	coarse calcite			2111.470	94.293	128.860	-144.866	276.067	925.680	0.140
U16-h07-54-338	coarse calcite			2090.149	65.305	263.910	689.926	242.797	588.580	0.070
U16-h07-54-338	coarse calcite			2082.324	55.409	172.850	913.577	227.476	628.180	0.599
U16-h07-54-338	coarse calcite			1962.576	70.252	0.094	1461.143	247.711	855.690	2.030
U16-h07-54-338	coarse calcite			1947.118	89.477	241.070	1121.509	170.763	537.090	4.739
U16-h07-54-338	coarse calcite			1899.139	53.660	245.430	1135.712	195.180	546.960	2.274
U16-h07-54-338	coarse calcite			1842.245	55.312	105.330	-326.859	264.543	1105.500	1.652

Sample ID	SampleType	‰ δ13C (VPDB)	‰ δ18O (VSMOW)	Mg (ppm)	2SE (ppm)	Mg LOD (ppm)	Si (ppm)	2SE (ppm)	Si LOD (ppm)	Sc (ppm)
U16-h07-54-338	coarse calcite			1800.648	61.486	138.750	-683.417	226.526	715.820	0.357
U16-h07-54-338	coarse calcite			1718.988	95.755	0.092	1515.277	251.335	831.030	1.375
U16-h07-54-338	coarse calcite			1598.864	143.752	148.600	215.059	230.958	503.290	0.213
U16-h07-54-5	matrix cement	2.3	15.6	1695.420	107.773	6.401	444.586	182.331	664.300	0.522
U16-h07-54-5	matrix cement	2.3	15.6	1652.813	75.493	6.445	459.850	220.616	681.920	0.698
U16-h07-54-5	matrix cement	2.3	15.6	1637.490	111.194	6.687	1531.295	264.705	694.020	1.421
U16-h07-54-5	matrix cement	2.3	15.6	1531.226	62.014	6.229	1027.279	277.346	646.460	1.600
U16-h07-54-5	matrix cement	2.3	15.6	1428.398	47.807	4.575	1617.004	242.430	1078.000	3.562
U16-h07-54-5	matrix cement	2.3	15.6	1409.603	36.121	2.519	1354.549	209.500	673.420	2.628
U16-h07-54-5	matrix cement	2.3	15.6	1400.396	80.472	6.610	1594.543	374.972	699.460	1.767
U16-h07-54-5	matrix cement	2.3	15.6	1364.663	40.199	6.365	1055.082	257.024	660.530	3.508
U16-h07-54-5	matrix cement	2.3	15.6	1351.291	57.600	4.560	763.604	236.851	1074.600	1.264
U16-h07-54-5	matrix cement	2.3	15.6	1348.961	40.114	6.668	1848.765	204.551	692.010	1.686
U16-h07-54-5	matrix cement	2.3	15.6	1309.442	37.267	2.063	598.160	228.739	779.550	4.144
U16-h07-54-5	matrix cement	2.3	15.6	1239.802	55.614	6.527	957.709	269.573	677.400	1.422
U16-h07-54-5	matrix cement	2.3	15.6	1126.086	51.798	6.409	517.117	230.192	678.190	1.706
U16-h07-54-5	matrix cement	2.3	15.6	1029.213	35.740	6.618	636.507	201.558	686.800	1.256
U16-h07-54-5	matrix cement	2.3	15.6	1009.481	29.212	2.536	627.395	247.068	677.790	0.443
U16-h07-54-5	matrix cement	2.3	15.6	973.030	75.213	6.532	765.907	226.870	677.910	1.800
U16-h07-54-5	matrix cement	2.3	15.6	906.880	58.154	6.541	308.873	211.109	692.070	1.310
U16-h07-54-5	ooid	2.3	15.6	1725.587	68.480	7.797	5928.369	600.689	865.050	1.805
U16-h07-54-5	ooid	2.3	15.6	1676.419	63.449	3.870	750.190	265.398	877.250	3.462
U16-h07-54-5	ooid	2.3	15.6	1675.658	68.865	3.822	237.888	203.537	650.960	0.413
U16-h07-54-5	ooid	2.3	15.6	1624.496	60.146	5.021	1649.698	401.146	524.430	4.303
U16-h07-54-5	ooid	2.3	15.6	1579.998	46.889	4.199	3325.238	318.221	951.840	3.729
U16-h07-54-5	ooid	2.3	15.6	1497.534	78.264	6.622	531.078	238.699	734.700	0.690
U16-h07-54-5	ooid	2.3	15.6	1471.505	39.348	5.195	2267.324	310.578	542.610	3.572
U16-h07-54-5	ooid	2.3	15.6	1405.376	48.499	4.229	1691.852	471.655	958.680	3.980
U16-h07-54-5	ooid	2.3	15.6	1390.720	40.070	2.056	2188.656	275.594	777.050	2.438
U16-h07-54-5	ooid	2.3	15.6	1389.014	49.976	3.936	1417.581	318.941	649.620	2.625
U16-h07-54-5	ooid	2.3	15.6	1379.530	55.946	3.920	2128.555	237.033	647.030	2.769
U16-h07-54-5	ooid	2.3	15.6	1371.731	56.368	4.898	1070.016	243.329	511.590	3.210
U16-h07-54-5	ooid	2.3	15.6	1293.398	54.174	4.034	509.740	240.317	914.430	0.886

Sample ID	SampleType	‰ δ13C (VPDB)	‰ δ18O (VSMOW)	Mg (ppm)	2SE (ppm)	Mg LOD (ppm)	Si (ppm)	2SE (ppm)	Si LOD (ppm)	Sc (ppm)
U16-h07-54-5	ooid	2.3	15.6	1274.796	45.394	5.071	6770.912	1641.845	529.680	2.479
U16-h07-54-5	ooid	2.3	15.6	1274.601	94.023	4.937	-264.148	264.670	1119.000	1.212
U16-h07-54-5	ooid	2.3	15.6	1245.182	47.715	2.164	1153.405	396.508	817.750	1.405
U16-h07-54-5	ooid	2.3	15.6	1236.028	73.548	4.794	1096.303	237.672	501.290	3.114
U16-h07-54-5	ooid	2.3	15.6	1212.970	60.937	4.962	199.555	186.177	518.220	4.122
U16-h07-54-5	ooid	2.3	15.6	1189.867	49.618	6.315	427.972	193.532	700.670	3.330
U16-h07-54-5	ooid	2.3	15.6	1141.283	67.333	4.899	1754.982	357.412	511.690	3.242
U16-h07-54-5	ooid	2.3	15.6	1088.780	86.591	4.236	-83.958	182.192	960.150	1.807
U16-h07-54-5	ooid	2.3	15.6	1016.872	61.712	6.871	116.229	263.941	762.320	1.600
U16-h07-54-5	ooid	2.3	15.6	970.851	51.007	3.956	94.835	175.693	896.700	3.018
U16-h07-54-5	ooid	2.3	15.6	948.239	56.108	5.055	1548.334	637.673	527.950	3.595
U16-h07-54-5	ooid	2.3	15.6	874.330	37.620	6.701	213.835	271.626	743.530	0.881
U16-h07-54-5	vein 1			2048.589	233.557	0.873	285.875	213.664	741.730	0.578
U16-h07-54-5	vein 1			1253.274	98.867	6.337	389.096	212.025	736.720	1.301
U16-h07-54-5	vein 1			1137.854	90.339	9.683	260.431	205.317	992.930	0.374
U16-h07-54-5	vein 1			1051.591	76.874	9.267	502.878	250.967	950.250	0.674
U16-h07-54-5	vein 1			1021.644	81.932	9.767	649.487	230.787	1001.400	0.356
U16-h07-54-5	vein 1		17.7344357	632.800	42.669	9.475	164.031	170.370	971.540	1.561
U16-h07-54-5	vein 2		105.1279	2511.966	88.944	0.865	89.465	198.861	728.570	0.175
U16-h07-54-5	vein 2		76.1787036	1665.765	105.865	0.853	184.785	214.099	724.690	1.056
U16-h07-54-5	vein 2			1503.373	123.853	0.850	-130.839	253.782	721.970	0.151
U16-h07-67-129	darker vein	2.4	25.2	3023.248	282.358	2.018	674.553	157.735	541.030	0.111
U16-h07-67-129	darker vein	2.4	25.2	2871.152	98.166	193.760	499.889	175.844	680.110	0.037
U16-h07-67-129	darker vein	2.4	25.2	2796.988	75.975	42.650	984.585	217.516	609.300	0.003
U16-h07-67-129	darker vein	2.4	25.2	2678.867	157.695	194.050	559.934	183.815	681.250	0.076
U16-h07-67-129	darker vein	2.4	25.2	2552.695	122.840	2.075	699.254	220.141	556.180	0.051
U16-h07-67-129	darker vein	2.4	25.2	2535.090	76.388	2.045	825.549	229.343	548.150	0.013
U16-h07-67-129	darker vein	2.4	25.2	2053.852	76.508	43.177	897.927	156.686	616.720	0.024
U16-h07-67-129	lighter vein	1	16.7	1686.118	75.214	70.418	785.074	211.143	545.900	-0.019
U16-h07-67-129	lighter vein	1	16.7	1629.462	82.921	201.930	404.518	143.184	708.400	0.060
U16-h07-67-129	lighter vein	1	16.7	1549.149	64.969	42.225	59.778	220.638	820.560	-0.017
U16-h07-67-129	lighter vein	1	16.7	1470.442	56.007	69.076	337.111	180.661	535.780	0.057
U16-h07-67-129	lighter vein	1	16.7	1400.813	40.600	66.916	954.270	183.476	518.610	0.004

Sample ID	SampleType	‰ δ13C (VPDB)	‰ δ18O (VSMOW)	Mg (ppm)	2SE (ppm)	Mg LOD (ppm)	Si (ppm)	2SE (ppm)	Si LOD (ppm)	Sc (ppm)
U16-h07-67-129	lighter vein	1	16.7	1323.736	31.893	72.805	565.082	201.439	564.500	-0.001
U16-h07-67-129	lighter vein	1	16.7	1247.419	42.443	205.230	175.527	193.852	720.180	0.116
U16-h07-67-129	ooid and matrix	2.9	21.9	29431.550	3547.754	86.328	534385.700	61208.280	3122.600	14.524
U16-h07-67-129	ooid and matrix	2.9	21.9	15371.680	2250.113	28.162	5117.675	474.979	524.440	2.229
U16-h07-67-129	ooid and matrix	2.9	21.9	10274.760	1820.576	116.510	33142.900	5112.404	799.330	2.848
U16-h07-67-129	ooid and matrix	2.9	21.9	9637.393	1498.182	59.123	13543.060	1264.638	581.360	2.193
U16-h07-67-129	ooid and matrix	2.9	21.9	6893.238	1085.138	9.410	48999.010	16445.590	883.380	3.017
U16-h07-67-129	ooid and matrix	2.9	21.9	6163.883	522.749	44.866	11749.440	1743.174	710.830	2.130
U16-h07-67-129	ooid and matrix	2.9	21.9	5669.055	1419.071	36.451	2501.479	231.280	524.090	0.927
U16-h07-67-129	ooid and matrix	2.9	21.9	4637.440	623.992	862.950	5247.070	541.957	3751.000	1.179
U16-h07-67-129	ooid and matrix	2.9	21.9	4540.889	347.340	151.910	15476.530	1363.323	732.010	2.940
U16-h07-67-129	ooid and matrix	2.9	21.9	3974.154	175.721	49.793	22003.050	2133.205	789.030	3.559
U16-h07-67-129	ooid and matrix	2.9	21.9	3806.294	482.840	30.524	11008.020	3700.880	568.530	1.268
U16-h07-67-129	ooid and matrix	2.9	21.9	3610.652	348.637	138.380	3177.794	760.340	479.220	0.687
U16-h07-67-129	ooid and matrix	2.9	21.9	3371.549	179.391	63.611	4481.070	306.231	680.700	0.894
U16-h07-67-129	ooid and matrix	2.9	21.9	2915.782	232.279	43.665	743.618	211.180	843.630	0.257
U16-h07-67-129	ooid and matrix	2.9	21.9	2882.539	198.407	15.014	2807.042	257.123	542.840	0.998
U16-h07-67-129	ooid and matrix	2.9	21.9	2830.936	177.918	139.010	570.847	213.258	481.140	0.011
U16-h07-67-129	ooid and matrix	2.9	21.9	2647.628	257.968	44.460	2443.666	628.369	859.230	1.120
U16-h07-67-129	ooid and matrix	2.9	21.9	2533.716	137.752	143.610	894.507	202.177	692.170	0.118
U16-h07-67-129	ooid and matrix	2.9	21.9	2432.794	204.003	42.113	633.990	233.974	667.520	0.266
U16-h07-67-129	ooid and matrix	2.9	21.9	2373.024	144.810	28.268	985.788	196.534	526.610	2.909
U16-h07-67-129	ooid and matrix	2.9	21.9	2202.546	91.663	130.690	780.060	184.676	452.430	0.135
U16-h07-67-129	ooid and matrix	2.9	21.9	2165.907	115.683	10.968	1823.970	313.197	822.680	0.521
U16-h07-67-129	ooid and matrix	2.9	21.9	2063.540	77.602	62.691	1085.810	196.693	670.990	0.157
U16-h07-67-129	ooid and matrix	2.9	21.9	1836.892	58.845	57.564	885.303	227.348	504.210	0.158
U16-h07-67-129	ooid and matrix	2.9	21.9	1520.334	67.446	11.353	1131.900	179.504	851.330	0.093

Sample ID	SampleType	2SE (ppm)	Sc LOD (ppm)	Ti (ppm)	2SE (ppm)	Ti LOD (ppm)	V (ppm)	2SE (ppm)	V LOD (ppm)	Mn (ppm)	2SE (ppm)
U16-h07-13b-11	matrix	0.118	0.253	17.772	3.490	0.000	5.477	0.904	0.120	48.488	3.823
U16-h07-13b-11	matrix	0.049	0.225	0.251	0.178	0.000	0.365	0.068	0.104	19.383	1.153
U16-h07-13b-11	matrix	0.064	0.220	0.274	0.204	0.000	0.463	0.131	0.103	14.617	1.391
U16-h07-13b-11	matrix	0.131	0.219	12.310	2.782	0.000	1.752	0.146	0.101	39.240	3.359
U16-h07-13b-11	matrix	0.229	0.228	4.124	1.642	0.000	0.917	0.145	0.107	23.116	4.441
U16-h07-13b-11	matrix	0.128	0.232	0.252	0.198	0.000	0.659	0.096	0.108	20.469	1.903
U16-h07-13b-11	matrix	0.043	0.230	0.198	0.177	0.000	0.607	0.076	0.108	44.493	1.948
U16-h07-13b-11	matrix	0.114	0.225	20.490	4.698	0.000	2.240	0.264	0.104	41.877	2.651
U16-h07-13b-11	matrix	0.086	0.229	71.636	12.707	0.000	3.882	0.401	0.109	34.153	1.344
U16-h07-13b-11	matrix	0.097	0.224	22.329	4.377	0.000	2.022	0.281	0.106	35.845	2.623
U16-h07-13b-11	matrix	0.120	0.219	3.128	1.572	0.000	1.661	0.183	0.101	43.425	4.040
U16-h07-13b-11	matrix	0.121	0.207	2.548	0.719	0.000	1.609	0.230	0.098	28.646	2.168
U16-h07-13b-11	matrix	0.102	0.220	3.533	1.467	0.000	1.203	0.218	0.105	32.050	2.149
U16-h07-13b-11	matrix	0.147	0.220	18.908	5.130	0.000	7.289	1.565	0.102	53.130	4.302
U16-h07-13b-11	matrix	0.073	0.216	3.154	1.174	0.000	1.675	0.157	0.100	50.271	3.959
U16-h07-13b-11	matrix	0.092	0.219	21.512	6.284	0.000	1.950	0.253	0.104	38.527	1.762
U16-h07-13b-11	matrix	0.118	0.222	4.697	1.532	0.000	1.757	0.251	0.102	38.278	2.881
U16-h07-13b-11	matrix	0.053	0.218	5.672	1.732	0.000	6.759	0.602	0.104	30.581	1.790
U16-h07-13b-11	matrix	0.162	0.225	272.559	178.249	0.000	5.380	0.579	0.104	51.950	3.547
U16-h07-13b-11	matrix	0.084	0.232	0.590	0.303	0.000	1.636	0.160	0.108	95.343	4.799
U16-h07-13b-11	matrix	0.100	0.221	2.814	0.855	0.000	1.555	0.193	0.103	49.846	2.918
U16-h07-13b-11	vein 1	0.070	0.221	0.227	0.235	0.000	1.483	0.176	0.103	115.411	4.364
U16-h07-13b-11	vein 1	0.060	0.231	1.410	0.424	0.000	6.099	0.431	0.108	125.424	3.842
U16-h07-13b-11	vein 1	0.048	0.223	0.006	0.096	0.000	4.450	0.246	0.104	124.519	2.851
U16-h07-13b-11	vein 1	0.061	0.222	0.307	0.222	0.000	3.105	0.180	0.103	94.638	3.095
U16-h07-13b-11	vein 1	0.050	0.220	-0.019	0.074	0.000	1.337	0.173	0.102	122.334	4.402
U16-h07-13b-11	vein 1	0.042	0.218	0.571	0.367	0.000	2.464	0.241	0.102	120.057	3.946
U16-h07-13b-11	vein 1	0.046	0.223	0.358	0.280	0.000	4.121	0.326	0.104	117.317	3.651
U16-h07-13b-11	vein 2	0.053	0.214	0.897	0.650	0.000	0.888	0.140	0.101	53.907	1.947
U16-h07-13b-11	vein 2	0.063	0.227	-0.030	0.063	0.000	0.693	0.275	0.107	60.394	1.443
U16-h07-13b-11	vein 2	0.045	0.222	-0.065	0.003	0.000	0.614	0.115	0.104	65.137	2.003
U16-h07-13b-11	vein 2	0.068	0.230	0.016	0.120	0.000	0.118	0.051	0.108	61.095	1.157
U16-h07-13b-11	vein 2	0.047	0.233	0.078	0.133	0.000	0.008	0.037	0.109	63.446	2.004

Sample ID	SampleType	2SE (ppm)	Sc LOD (ppm)	Ti (ppm)	2SE (ppm)	Ti LOD (ppm)	V (ppm)	2SE (ppm)	V LOD (ppm)	Mn (ppm)	2SE (ppm)
U16-h07-13b-11	vein 2	0.045	0.231	0.254	0.240	0.000	0.030	0.034	0.107	59.741	1.775
U16-h07-13b-11	vein 3	0.052	0.230	4.668	4.117	0.000	1.454	0.321	0.108	117.878	3.582
U16-h07-13b-11	vein 3	0.067	0.225	0.220	0.213	0.000	2.270	0.212	0.106	115.099	5.347
U16-h07-13b-11	vein 3	0.053	0.229	0.267	0.216	0.000	1.937	0.258	0.108	58.860	2.028
U16-h07-13b-31	dk ooid	0.295	0.197	0.456	0.291	0.276	6.752	0.742	0.179	169.122	18.414
U16-h07-13b-31	dk ooid	0.289	0.150	82.351	14.088	0.000	25.260	2.443	0.169	390.418	24.769
U16-h07-13b-31	dk ooid	0.303	0.197	24.034	8.516	0.275	15.975	0.910	0.178	284.341	22.490
U16-h07-13b-31	dk ooid	0.161	0.194	53.897	11.425	0.271	15.431	1.426	0.176	390.253	20.706
U16-h07-13b-31	dk ooid	0.392	0.120	35.198	5.589	0.000	16.838	0.855	0.135	364.887	36.426
U16-h07-13b-31	dk ooid	0.227	0.142	57.569	7.769	0.000	24.097	1.724	0.160	514.336	25.369
U16-h07-13b-31	matrix cement	0.231	0.197	3.493	2.892	0.274	5.251	0.497	0.178	206.837	13.304
U16-h07-13b-31	matrix cement	0.323	0.337	33.687	6.953	2.152	11.706	0.820	0.391	337.268	24.520
U16-h07-13b-31	matrix cement	0.202	0.195	70.669	14.347	0.272	21.571	2.232	0.176	382.698	13.909
U16-h07-13b-31	matrix cement	0.199	0.190	6.265	1.577	0.265	9.210	0.801	0.172	396.397	24.821
U16-h07-13b-31	matrix cement	0.172	0.343	65.799	7.679	2.194	19.535	0.900	0.398	366.442	11.669
U16-h07-13b-31	matrix cement	0.246	0.199	60.800	15.705	0.277	18.681	2.166	0.180	515.090	35.403
U16-h07-13b-31	matrix cement	0.230	0.191	14.849	3.008	0.267	10.977	0.905	0.173	453.575	32.440
U16-h07-13b-31	matrix cement	0.200	0.328	3.778	2.140	2.092	10.734	0.910	0.380	523.781	31.662
U16-h07-13b-31	matrix cement	0.172	0.089	62.008	7.853	1.007	15.624	0.698	0.136	484.157	21.031
U16-h07-13b-31	matrix cement	0.215	0.088	57.593	7.688	0.998	16.234	0.871	0.135	486.751	18.227
U16-h07-13b-31	matrix cement	0.289	0.334	34.029	4.262	2.137	13.118	0.678	0.388	483.960	17.994
U16-h07-13b-31	matrix cement	0.215	0.338	40.625	5.752	2.159	15.171	0.658	0.392	466.480	23.654
U16-h07-13b-31	ooid	0.130	0.283	129.457	14.751	0.364	43.207	2.650	0.366	387.761	10.003
U16-h07-13b-31	ooid	0.234	0.219	0.470	0.258	0.630	5.002	0.449	0.333	219.695	12.438
U16-h07-13b-31	ooid	0.181	0.285	111.826	11.956	0.366	32.451	3.042	0.369	335.791	19.814
U16-h07-13b-31	ooid	0.207	0.144	0.174	0.236	0.580	9.056	0.843	0.203	110.821	5.966
U16-h07-13b-31	ooid	0.329	0.141	0.045	0.145	0.429	10.535	0.754	0.114	87.419	12.672
U16-h07-13b-31	ooid	0.293	0.267	8.687	2.770	1.522	9.967	0.770	0.322	347.044	17.474
U16-h07-13b-31	ooid	0.211	0.151	252.155	34.181	0.461	40.431	4.798	0.123	504.969	16.895
U16-h07-13b-31	ooid	0.312	0.140	48.008	10.547	0.562	17.392	1.128	0.197	329.878	20.458
U16-h07-13b-31	ooid	0.394	0.120	0.010	0.116	0.528	11.010	0.815	0.099	433.671	14.943
U16-h07-13b-31	ooid	0.224	0.265	193.768	20.506	1.511	26.180	1.582	0.320	402.514	18.930
U16-h07-13b-31	ooid	0.220	0.288	78.554	8.514	0.368	26.331	2.411	0.371	553.430	34.949

Sample ID	SampleType	2SE (ppm)	Sc LOD (ppm)	Ti (ppm)	2SE (ppm)	Ti LOD (ppm)	V (ppm)	2SE (ppm)	V LOD (ppm)	Mn (ppm)	2SE (ppm)
U16-h07-13b-31	ooid	0.247	0.219	190.671	31.232	0.628	25.302	2.611	0.332	436.240	16.007
U16-h07-13b-31	ooid	0.221	0.276	14.621	3.792	0.354	12.369	0.749	0.357	472.187	19.904
U16-h07-13b-31	ooid	0.235	0.281	87.852	11.410	0.360	31.289	1.896	0.363	445.273	15.234
U16-h07-13b-31	ooid	0.223	0.217	62.361	14.698	0.625	19.817	1.203	0.330	406.164	24.441
U16-h07-13b-31	ooid	0.226	0.265	106.780	18.100	1.512	23.949	1.162	0.320	470.541	19.879
U16-h07-13b-31	ooid	0.209	0.125	137.194	31.131	0.551	31.495	2.389	0.104	474.089	14.975
U16-h07-13b-31	ooid	0.211	0.121	74.663	8.887	0.530	21.736	1.648	0.100	471.474	24.931
U16-h07-13b-31	ooid	0.177	0.276	98.797	41.608	0.353	22.231	0.955	0.356	423.301	17.203
U16-h07-13b-31	ooid	0.234	0.275	67.802	8.272	0.352	22.120	0.984	0.355	456.186	16.333
U16-h07-13b-31	ooid	0.282	0.115	36.184	11.467	0.506	16.383	1.594	0.095	478.199	19.459
U16-h07-13b-31	ooid	0.210	0.115	19.718	7.656	0.503	12.844	0.655	0.095	492.505	21.106
U16-h07-13b-31	ooid	0.214	0.269	30.031	5.749	0.345	16.124	1.137	0.347	463.656	16.268
U16-h07-13b-31	ooid	0.166	0.140	67.644	14.915	0.562	20.036	1.268	0.197	482.951	20.338
U16-h07-13b-31	vein-1	0.178	0.144	422.835	89.857	1.066	90.401	12.617	0.163	286.058	11.988
U16-h07-13b-31	vein-1	0.484	0.141	0.203	0.250	0.431	2.454	0.720	0.115	179.927	25.569
U16-h07-13b-31	vein-1	0.042	0.130	0.059	0.135	0.962	1.251	0.170	0.147	110.392	3.978
U16-h07-13b-31	vein-1	0.126	0.082	0.044	0.131	0.422	6.244	0.593	0.071	81.353	15.305
U16-h07-13b-31	vein-1	0.167	0.126	30.713	3.851	0.931	19.425	0.943	0.143	104.859	11.280
U16-h07-13b-31	vein-1	0.072	0.118	5.425	1.273	0.872	6.589	0.786	0.133	68.679	6.267
U16-h07-13b-81	coarse calcite	0.052	0.070	-0.243	0.086	0.404	-0.012	0.037	0.057	18.717	1.174
U16-h07-13b-81	coarse calcite	0.094	0.072	-0.390	0.506	0.418	-0.057	0.057	0.059	-4.803	2.267
U16-h07-13b-81	coarse calcite	0.106	0.067	-2.196	0.583	0.388	-0.141	0.064	0.054	-7.296	2.162
U16-h07-13b-81	coarse calcite	0.124	0.083	-6.972	1.388	8.974	0.201	0.208	0.183	302.657	25.780
U16-h07-13b-81	vein 1	1.122	0.239	341.616	258.597	1.389	18.585	3.419	0.915	294.625	42.773
U16-h07-13b-81	vein 1	0.166	0.397	-2.291	0.342	4.943	-3.792	0.270	1.757	-122.295	12.250
U16-h07-13b-81	vein 1	0.091	0.184	2.512	0.906	1.068	2.154	0.399	0.704	93.848	12.884
U16-h07-13b-81	vein 1	1.089	1.608	0.112	0.234	0.387	5.893	1.822	5.240	68.683	47.053
U16-h07-13b-81	vein 1	0.174	0.064	32.113	7.455	0.370	8.301	0.828	0.052	145.925	12.249
U16-h07-13b-81	vein 1	0.209	1.098	15.019	9.308	6.163	6.921	0.672	7.264	162.677	13.579
U16-h07-13b-81	vein 1	0.256	0.893	1.488	2.090	6.424	7.395	1.238	5.143	552.137	138.965
U16-h07-13b-81	vein 1	0.714	0.915	-0.862	0.173	6.577	17.635	1.990	5.265	685.801	136.527
U16-h07-13b-81	vein 1	0.533	1.601	-0.603	0.160	0.385	14.424	1.734	5.216	747.719	163.471
U16-h07-24-145	ooids and cement	0.036	0.110	0.077	0.126	0.309	7.840	1.039	0.053	21.503	1.819

Sample ID	SampleType	2SE (ppm)	Sc LOD (ppm)	Ti (ppm)	2SE (ppm)	Ti LOD (ppm)	V (ppm)	2SE (ppm)	V LOD (ppm)	Mn (ppm)	2SE (ppm)
U16-h07-24-145	ooids and cement	0.041	0.093	2.358	1.443	0.548	0.359	0.117	0.087	20.008	2.589
U16-h07-24-145	ooids and cement	0.048	0.095	10.238	2.774	0.558	0.561	0.112	0.088	23.528	1.773
U16-h07-24-145	ooids and cement	0.053	0.091	0.205	0.185	0.536	0.251	0.059	0.085	20.967	0.945
U16-h07-24-145	ooids and cement	0.039	0.104	1.639	1.000	0.294	0.280	0.065	0.051	26.547	1.269
U16-h07-24-145	ooids and cement	0.034	0.098	0.019	0.089	0.579	0.018	0.031	0.092	7.870	1.661
U16-h07-24-145	ooids and cement	0.038	0.087	0.071	0.143	0.515	0.269	0.064	0.081	18.303	0.981
U16-h07-24-145	ooids and cement	0.048	0.089	0.072	0.120	0.523	0.205	0.048	0.083	16.018	0.817
U16-h07-24-145	vein-1	0.046	0.109	0.133	0.091	0.454	1.785	0.195	0.158	30.701	1.001
U16-h07-24-145	vein-1	0.029	0.101	0.118	0.088	0.418	1.735	0.169	0.146	32.667	1.502
U16-h07-24-145	vein-1	0.031	0.101	0.081	0.080	0.419	1.653	0.123	0.146	30.097	0.779
U16-h07-24-145	vein-1	0.034	0.101	0.126	0.101	0.422	2.052	0.134	0.147	29.737	0.852
U16-h07-24-145	vein-1	0.028	0.098	0.363	0.182	0.407	1.873	0.121	0.142	30.242	0.765
U16-h07-24-145	vein-1	0.027	0.175	0.231	0.162	0.393	1.878	0.109	0.161	32.215	0.898
U16-h07-24-145	vein-1	0.042	0.175	0.134	0.111	0.392	2.022	0.283	0.160	31.119	1.136
U16-h07-24-145	vein-1	0.037	0.164	0.564	0.214	0.368	1.344	0.118	0.150	33.163	1.315
U16-h07-24-145	vein-2	0.072	0.107	0.424	0.290	0.431	2.648	0.297	0.152	46.648	3.088
U16-h07-24-145	vein-2	0.278	0.105	1.221	0.950	0.425	11.032	2.735	0.150	111.443	9.651
U16-h07-24-145	vein-2	0.124	0.108	-1.051	0.758	0.436	-8.969	1.157	0.154	-339.916	383.021
U16-h07-24-145	vein-3	0.980	0.129	2.500	1.775	0.823	21.416	5.408	1.162	1426.344	2320.017
U16-h07-24-145	vein-3	0.075	0.110	-5.806	2.230	0.445	-3.601	0.301	0.157	-60.568	1.883
U16-h07-24-145	vein-3	0.062	0.097	-0.637	0.377	0.609	-0.221	0.152	0.545	-20.841	1.983
U16-h07-24-145	vein-3	0.040	0.107	-0.369	0.217	0.434	-0.788	0.097	0.153	-28.144	1.259
U16-h07-24-145	vein-3	0.021	0.096	-0.624	0.312	0.556	-1.262	0.094	0.510	-14.253	0.786
U16-h07-24-145	vein-3	0.028	0.108	-0.239	0.163	0.436	-0.910	0.091	0.154	-18.759	0.606
U16-h07-24-145	vein-3	0.021	0.112	-0.063	0.111	0.451	-0.028	0.034	0.159	-14.815	0.723
U16-h07-24-145	vein-4	6.471	0.130	-3.137	5.176	0.918	92.740	131.570	1.174	-157.741	119.631
U16-h07-24-145	vein-4	0.046	0.097	-0.059	0.168	0.581	0.734	0.083	0.079	18.182	0.801
U16-h07-24-145	vein-4	0.039	0.094	0.078	0.188	0.563	1.303	0.162	0.076	19.792	1.601
U16-h07-24-145	vein-4	0.054	0.152	-0.346	0.127	0.935	0.853	0.110	0.084	22.577	1.201
U16-h07-24-145	vein-4	12.352	0.129	-76.452	128.377	0.915	37.597	139.403	1.170	146.413	1054.014
U16-h07-24-145	vein-4	0.058	0.148	-0.247	0.341	0.912	1.408	0.195	0.082	57.721	1.938
U16-h07-24-145	vein-4	18.433	0.138	-28.166	31.251	0.879	90.393	155.880	1.240	367.015	30.037
U16-h07-24-145	vein-4	0.097	0.149	-0.515	0.369	0.916	0.083	0.280	0.082	71.733	2.973

Sample ID	SampleType	2SE (ppm)	Sc LOD (ppm)	Ti (ppm)	2SE (ppm)	Ti LOD (ppm)	V (ppm)	2SE (ppm)	V LOD (ppm)	Mn (ppm)	2SE (ppm)
U16-h07-24-145	vein-4	0.899	0.159	-0.010	2.203	0.979	-5.713	6.109	0.088	146.774	41.680
U16-h07-24-145	vein-4	0.269	0.125	-0.146	0.930	0.884	6.536	3.214	1.130	-61.970	11.541
U16-h07-24-145	vein-4	0.294	0.156	-1.366	0.805	0.961	-8.790	0.821	0.086	129.820	5.889
U16-h07-24-145	vein-4	0.842	0.159	4.213	7.672	0.981	-28.661	6.278	0.088	230.274	28.635
U16-h07-24-145	vein-4	0.099	0.099	0.519	0.240	0.620	1.675	0.675	0.554	-50.072	4.680
U16-h07-24-145	vein-4	0.072	0.094	-0.075	0.457	0.592	0.592	0.289	0.529	-36.370	2.984
U16-h07-24-145	vein-4	1.446	0.132	3.849	6.258	0.936	-3.131	8.888	1.196	-68.802	39.055
U16-h07-24-145	vein-4	2.250	0.123	2.788	11.744	0.867	-6.897	68.705	1.109	-81.193	87.350
U16-h07-24-145	vein-6	0.038	0.101	-0.083	0.151	0.609	0.054	0.033	0.083	33.592	2.189
U16-h07-24-145	vein-6	0.052	0.091	0.285	0.241	0.548	0.565	0.083	0.074	19.214	1.105
U16-h07-24-145	vein-6	0.052	0.089	20.788	4.543	0.572	0.917	0.148	0.086	20.861	1.234
U16-h07-24-145	vein-6	0.045	0.092	11.179	3.446	0.554	0.437	0.072	0.075	18.397	1.087
U16-h07-24-145	vein-6	0.042	0.088	0.193	0.208	0.526	0.333	0.066	0.071	22.818	0.951
U16-h07-24-145	vein-7	0.040	0.098	0.143	0.179	0.625	0.038	0.031	0.094	18.653	2.628
U16-h07-25-167	coarse calcite	0.035	0.088	3.462	0.849	3.574	4.809	0.434	1.087	17.018	1.349
U16-h07-25-167	coarse calcite	0.062	0.090	-0.695	0.288	3.652	0.341	0.106	1.111	14.977	1.832
U16-h07-25-167	coarse calcite	0.061	0.094	-0.854	0.131	3.827	-0.068	0.097	1.164	5.313	0.678
U16-h07-25-167	coarse calcite	0.036	0.093	-0.256	0.211	3.784	0.465	0.065	1.151	9.838	1.573
U16-h07-25-167	dk ooid	0.036	0.089	6.391	1.644	3.608	1.907	0.262	1.097	20.232	0.973
U16-h07-25-167	dk ooid	0.061	0.135	19.158	3.625	0.424	4.354	0.683	0.169	25.639	2.220
U16-h07-25-167	dk ooid	0.058	0.143	29.840	4.846	0.448	4.633	0.619	0.179	25.621	1.471
U16-h07-25-167	dk ooid	0.085	0.064	9.919	4.011	0.505	1.598	0.419	0.128	36.614	6.757
U16-h07-25-167	dk ooid	0.056	0.197	23.578	3.386	0.833	3.105	0.250	0.123	33.776	1.257
U16-h07-25-167	dk ooid	0.062	0.086	34.603	9.788	0.276	4.960	0.398	0.070	40.201	3.333
U16-h07-25-167	dk ooid	0.047	0.066	3.731	1.817	0.518	3.894	0.339	0.128	49.511	3.076
U16-h07-25-167	dk ooid	0.056	0.131	29.395	15.043	0.413	1.767	0.194	0.165	24.128	1.516
U16-h07-25-167	dk ooid	0.067	0.066	17.053	4.016	0.512	2.391	0.305	0.126	30.830	1.567
U16-h07-25-167	dk ooid	0.044	0.188	10.619	3.586	0.795	2.045	0.181	0.118	29.136	1.003
U16-h07-25-167	dk ooid	0.058	0.189	14.589	2.629	0.802	1.983	0.196	0.119	29.351	1.069
U16-h07-25-167	dk ooid	0.042	0.063	10.345	2.774	0.491	2.048	0.220	0.121	28.869	1.905
U16-h07-25-167	dk ooid	0.061	0.085	0.078	0.380	0.273	2.352	0.234	0.069	37.330	2.727
U16-h07-25-167	dk ooid	0.066	0.064	24.521	4.377	0.501	2.662	0.193	0.124	30.200	1.214
U16-h07-25-167	dk ooid	0.052	0.192	1.932	0.790	0.858	4.776	0.543	0.115	30.489	1.457

Sample ID	SampleType	2SE (ppm)	Sc LOD (ppm)	Ti (ppm)	2SE (ppm)	Ti LOD (ppm)	V (ppm)	2SE (ppm)	V LOD (ppm)	Mn (ppm)	2SE (ppm)
U16-h07-25-167	dk ooid	0.050	0.061	13.444	2.634	0.483	2.132	0.235	0.122	27.991	1.363
U16-h07-25-167	dk ooid	0.050	0.189	1.242	0.705	0.846	1.461	0.214	0.113	30.437	1.737
U16-h07-25-167	dk ooid	0.062	0.194	5.192	1.208	0.821	1.372	0.170	0.122	29.549	1.308
U16-h07-25-167	dk ooid	0.059	0.076	7.800	1.703	0.244	2.256	0.243	0.062	29.128	1.831
U16-h07-25-167	dk ooid	0.057	0.193	9.066	1.980	0.815	1.651	0.177	0.121	31.032	1.676
U16-h07-25-167	dk ooid	0.057	0.063	5.583	1.258	0.494	1.682	0.141	0.122	31.083	1.600
U16-h07-25-167	dk ooid	0.067	0.061	8.271	2.248	0.483	1.448	0.170	0.122	33.501	1.840
U16-h07-25-167	early vein	0.026	0.133	0.698	0.173	0.687	0.589	0.071	0.052	18.899	0.758
U16-h07-25-167	early vein	0.033	0.133	0.681	0.230	0.686	0.559	0.083	0.052	18.918	1.058
U16-h07-25-167	early vein	0.026	0.135	0.302	0.062	0.697	0.714	0.081	0.053	18.306	0.755
U16-h07-25-167	early vein	0.034	0.134	0.559	0.197	0.693	0.527	0.085	0.053	20.650	0.972
U16-h07-25-167	late vein	0.065	0.142	111.627	40.054	0.691	12.996	0.723	0.058	28.100	1.559
U16-h07-25-167	late vein	0.063	0.136	27.784	4.886	0.658	9.794	0.894	0.055	21.269	1.045
U16-h07-25-167	late vein	0.040	0.131	7.625	1.618	0.636	2.471	0.297	0.053	21.018	1.013
U16-h07-25-167	late vein	0.048	0.129	6.401	2.526	0.666	3.065	0.141	0.051	21.769	1.080
U16-h07-25-167	late vein	0.042	0.134	2.252	0.627	0.694	2.585	0.169	0.053	20.402	0.727
U16-h07-25-167	lt ooid	0.049	0.130	17.707	3.599	0.696	1.366	0.123	0.051	27.154	1.192
U16-h07-25-167	lt ooid	0.053	0.125	13.248	2.754	0.619	2.210	0.275	0.050	31.535	3.073
U16-h07-25-167	lt ooid	0.057	0.126	7.973	2.518	0.624	1.510	0.212	0.050	31.112	2.356
U16-h07-25-167	lt ooid	0.067	0.196	19.438	6.773	0.874	2.662	0.181	0.117	34.213	1.929
U16-h07-25-167	lt ooid	0.078	0.189	12.780	1.794	0.843	2.305	0.246	0.113	31.377	1.858
U16-h07-25-167	lt ooid	0.062	0.123	3.072	0.869	0.606	1.014	0.126	0.049	28.740	1.339
U16-h07-25-167	lt ooid	0.046	0.122	21.985	6.398	0.653	1.611	0.156	0.048	30.014	1.370
U16-h07-25-167	lt ooid	0.060	0.196	11.752	2.094	0.876	1.780	0.150	0.118	30.792	1.071
U16-h07-25-167	lt ooid	0.052	0.121	1.263	0.520	0.596	1.568	0.158	0.048	27.472	1.595
U16-h07-25-167	lt ooid	0.072	0.126	6.011	2.083	0.671	1.605	0.162	0.050	31.260	1.959
U16-h07-25-167	matrix cement	0.043	0.136	0.072	0.054	0.673	0.160	0.037	0.054	75.659	2.065
U16-h07-25-167	matrix cement	0.052	0.132	14.402	2.652	0.669	1.831	0.204	0.053	36.716	3.042
U16-h07-25-167	matrix cement	0.059	0.138	3.446	1.024	0.699	1.205	0.120	0.055	37.648	1.177
U16-h07-25-167	matrix cement	0.043	0.124	4.602	2.046	0.630	1.735	0.241	0.050	25.335	1.510
U16-h07-25-167	matrix cement	0.056	0.128	5.785	2.320	0.648	1.538	0.154	0.051	28.192	1.431
U16-h07-25-167	matrix cement	0.043	0.127	24.339	22.924	0.643	1.071	0.108	0.051	25.003	1.612
U16-h07-25-167	matrix cement	0.048	0.128	1.828	0.608	0.635	1.659	0.224	0.051	27.791	1.543

Sample ID	SampleType	2SE (ppm)	Sc LOD (ppm)	Ti (ppm)	2SE (ppm)	Ti LOD (ppm)	V (ppm)	2SE (ppm)	V LOD (ppm)	Mn (ppm)	2SE (ppm)
U16-h07-25-167	matrix cement	0.055	0.127	0.758	0.350	0.643	2.357	0.200	0.051	29.029	1.052
U16-h07-25-167	matrix cement	0.050	0.128	4.600	1.174	0.647	1.372	0.130	0.051	26.247	1.302
U16-h07-25-167	matrix cement	0.049	0.122	0.593	0.230	0.621	1.341	0.115	0.049	29.651	1.440
U16-h07-25-167	matrix cement	0.027	0.131	2.313	0.521	0.676	0.703	0.082	0.052	19.626	1.319
U16-h07-34-405	matrix cement	7.346	0.107	-15.144	26.379	0.372	-4.954	22.072	0.094	-141.365	324.682
U16-h07-34-405	matrix cement	1.287	0.108	37.143	10.899	0.450	4.195	1.392	0.076	-30.028	57.953
U16-h07-34-405	matrix cement	4.039	0.103	5.091	5.670	0.367	0.386	3.342	0.094	11.125	51.278
U16-h07-34-405	matrix cement	0.231	0.081	-38.377	9.642	4.128	-3.358	0.972	0.376	-68.690	8.835
U16-h07-34-405	matrix cement	0.427	0.087	25.972	4.553	4.441	2.465	0.523	0.404	-7.983	23.165
U16-h07-34-405	matrix cement	1.469	0.095	-103.652	207.011	0.340	-13.889	14.005	0.087	-367.741	181.288
U16-h07-34-405	matrix cement	2.172	0.095	-351.476	291.516	0.340	-14.772	11.884	0.087	-571.568	536.098
U16-h07-34-405	matrix cement	0.308	0.087	23.634	3.575	4.446	3.089	0.339	0.405	-264.018	33.498
U16-h07-34-405	matrix cement	3.540	0.110	-5.459	10.706	0.456	-0.973	2.412	0.078	-72.819	62.068
U16-h07-34-405	matrix cement	0.330	0.087	24.779	2.784	4.446	-6.157	1.234	0.405	-228.185	25.194
U16-h07-34-405	matrix cement	0.804	0.101	29.359	14.342	0.359	0.592	0.820	0.092	-69.419	35.961
U16-h07-34-405	matrix cement	1.423	0.097	-33.711	62.051	0.336	-7.348	3.984	0.085	-359.549	140.288
U16-h07-34-405	matrix cement	2.020	0.100	33.386	13.016	0.357	3.406	1.231	0.092	-894.477	517.218
U16-h07-34-405	matrix cement	2.898	0.105	-0.887	8.211	0.365	7.727	5.506	0.092	83.584	61.199
U16-h07-34-405	matrix cement	7.161	0.105	-16.962	11.064	0.374	-1.814	4.040	0.096	-100.763	298.485
U16-h07-34-405	matrix cement	4.324	0.103	49.765	67.405	0.365	1.309	4.899	0.094	-114.217	679.688
U16-h07-34-405	matrix cement	1.755	0.106	6.513	16.299	0.376	3.101	3.553	0.097	-191.333	110.591
U16-h07-34-405	ooid	0.230	0.073	8.409	9.512	7.838	0.977	0.417	0.160	-33.513	5.499
U16-h07-34-405	ooid	1.018	0.083	138.005	64.760	6.225	8.979	3.271	0.389	9.848	12.235
U16-h07-34-405	ooid	4.283	0.099	-414.970	410.638	0.414	-65.168	50.373	0.070	-963.789	654.989
U16-h07-34-405	ooid	0.482	0.082	-303.919	224.877	37.289	-5.046	1.490	0.534	-236.592	49.227
U16-h07-34-405	ooid	0.391	0.080	-154.475	333.017	6.340	-1.046	2.750	0.279	-88.808	16.991
U16-h07-34-405	ooid	0.274	0.077	-83.231	29.237	6.038	-4.273	0.934	0.266	-124.983	17.631
U16-h07-34-405	ooid	0.679	0.155	-179.230	67.103	4.787	-26.084	6.968	1.845	-339.888	43.178
U16-h07-34-405	ooid	0.269	0.081	-114.307	31.878	36.563	-5.571	1.168	0.504	-71.432	14.721
U16-h07-34-405	ooid	0.506	0.102	34.412	5.975	5.729	2.967	0.639	0.479	140.277	33.685
U16-h07-34-405	ooid	0.461	0.095	-69.831	28.609	5.354	-8.683	2.016	0.448	-283.218	33.926
U16-h07-34-405	ooid	0.419	0.085	45.800	10.990	38.600	-1.093	3.228	0.553	-97.194	46.435
U16-h07-34-405	ooid	0.299	0.075	-3.367	10.775	5.875	-1.335	0.476	0.259	-60.938	9.599

Sample ID	SampleType	2SE (ppm)	Sc LOD (ppm)	Ti (ppm)	2SE (ppm)	Ti LOD (ppm)	V (ppm)	2SE (ppm)	V LOD (ppm)	Mn (ppm)	2SE (ppm)
U16-h07-34-405	ooid	0.382	0.084	-16.841	13.637	38.116	-2.857	1.008	0.526	-148.797	27.842
U16-h07-34-405	ooid	0.308	0.082	-66.906	31.806	6.453	-3.532	1.394	0.284	-120.207	23.824
U16-h07-34-405	ooid	0.556	0.092	1.490	2.961	1.284	6.911	1.640	0.297	64.162	12.399
U16-h07-34-405	ooid	0.492	0.093	10.176	3.109	1.298	-1.560	1.003	0.300	-163.816	40.765
U16-h07-34-405	ooid	0.262	0.082	13.600	6.375	6.442	0.782	0.481	0.284	16.506	7.435
U16-h07-34-405	ooid	0.529	0.079	-103.381	76.056	5.918	-7.881	2.049	0.370	-373.649	311.704
U16-h07-34-405	ooid	0.208	0.075	-148.412	73.459	5.950	-2.474	0.926	0.262	-11.813	6.086
U16-h07-34-405	ooid	0.338	0.155	7.820	2.158	4.776	-5.772	2.127	1.841	-223.339	45.948
U16-h07-34-405	ooid	3.365	0.109	487.944	448.261	0.452	45.929	57.596	0.077	621.580	784.254
U16-h07-34-405	ooid and clast	0.635	0.610	2836.254	1627.703	0.000	36.362	4.759	0.350	142.887	15.105
U16-h07-34-405	ooid and clast	0.114	0.085	23.962	6.990	0.738	1.776	0.371	0.145	30.273	2.066
U16-h07-34-405	ooid and clast	0.067	0.108	0.379	0.266	0.453	0.254	0.083	0.088	7.112	1.138
U16-h07-34-405	ooid and clast	0.058	0.111	2.490	0.816	0.465	0.737	0.118	0.090	25.874	2.770
U16-h07-34-405	ooid and clast	0.187	0.156	78.966	13.421	0.000	5.673	0.858	0.089	96.592	8.739
U16-h07-34-405	ooid and clast	0.237	0.175	97.708	11.047	0.000	19.018	2.039	0.100	162.918	8.110
U16-h07-34-405	ooid and clast	0.369	0.083	48.753	8.354	0.715	11.781	1.498	0.140	287.812	34.423
U16-h07-34-405	ooid and clast	0.213	0.152	19.573	3.762	0.000	8.502	0.727	0.087	146.084	8.033
U16-h07-34-405	ooid and clast	0.131	0.155	118.375	16.828	0.000	8.314	0.702	0.089	101.157	5.783
U16-h07-34-405	ooid and clast	0.208	0.160	44.471	8.604	0.000	6.481	0.661	0.091	113.507	6.691
U16-h07-34-405	ooid and clast	0.214	0.105	72.591	12.360	0.443	10.938	0.649	0.086	128.942	8.146
U16-h07-34-405	ooid and clast	0.088	0.116	10.203	3.083	1.002	1.358	0.244	0.058	25.700	1.647
U16-h07-34-405	ooid and clast	0.449	0.116	176.036	30.010	1.009	17.860	1.098	0.058	261.779	15.651
U16-h07-34-405	ooid and clast	0.456	0.098	81.120	9.656	5.377	19.361	1.554	0.496	279.399	14.843
U16-h07-34-405	ooid and clast	0.723	0.130	25.014	4.848	0.000	21.153	1.870	0.063	400.267	28.609
U16-h07-34-405	ooid and clast	0.846	0.115	616.501	123.538	1.001	30.860	2.577	0.058	373.383	19.278
U16-h07-34-405	ooid and clast	13.684	0.118	38.675	31.903	1.019	120.831	122.730	0.059	1101.712	125.981
U16-h07-34-405	ooid and clast	23.690	0.103	23.438	89.112	5.696	3.334	102.507	0.525	970.084	1310.876
U16-h07-34-405	ooid and clast	31.126	0.199	53.369	1497.412	0.576	-119.733	101.231	0.077	-103.461	1354.134
U16-h07-34-405	ooid and clast	0.064	0.181	0.739	0.161	1.324	0.105	0.037	0.184	5.322	0.952
U16-h07-34-405	ooid and clast	0.580	0.101	-335.387	98.540	5.561	-23.779	2.257	0.513	-328.772	33.826
U16-h07-34-405	ooid and clast	0.719	0.121	-285.183	28.924	1.049	-25.713	1.792	0.061	-669.078	30.168
U16-h07-34-405	ooid and clast	1.265	0.110	-232.559	62.360	0.953	-32.692	2.120	0.055	-3089.136	662.075
U16-h07-34-405	ooid and clast	0.293	0.201	-12.237	3.661	0.836	-9.682	0.899	0.137	-283.533	19.843

Sample ID	SampleType	2SE (ppm)	Sc LOD (ppm)	Ti (ppm)	2SE (ppm)	Ti LOD (ppm)	V (ppm)	2SE (ppm)	V LOD (ppm)	Mn (ppm)	2SE (ppm)
U16-h07-34-405	ooid and clast	0.241	0.118	-164.012	21.319	1.020	-13.586	0.894	0.059	-167.520	13.265
U16-h07-34-405	ooid and clast	0.288	0.112	0.214	0.557	0.969	-8.873	1.196	0.056	-233.611	28.923
U16-h07-34-405	ooid and clast	0.916	0.961	-5.451	4.180	2.261	-8.042	1.414	2.295	-204.336	39.070
U16-h07-34-405	ooid and clast	0.216	0.196	-81.228	12.237	0.677	-8.583	0.561	0.079	-180.280	17.825
U16-h07-34-405	ooid and clast	0.335	0.164	-144.168	13.923	0.571	-14.708	1.285	0.101	-197.895	21.456
U16-h07-34-405	ooid and clast	0.281	0.973	-65.086	14.908	2.289	-6.180	0.911	2.324	-144.027	17.857
U16-h07-34-405	ooid and clast	0.096	0.146	-71.402	10.128	0.507	-4.526	0.274	0.089	-70.008	4.279
U16-h07-34-405	ooid and clast	0.103	0.142	-15.359	5.209	0.495	-3.053	0.150	0.087	-78.154	8.142
U16-h07-34-405	ooid and clast	0.167	0.167	-22.025	7.513	1.221	-4.667	0.388	0.170	-90.179	7.883
U16-h07-34-405	ooid and clast	0.087	0.204	-0.684	0.484	0.705	-0.268	0.069	0.082	-15.370	1.878
U16-h07-34-405	vein 1	0.356	0.104	1.939	1.125	0.414	2.126	0.562	0.390	82.689	30.121
U16-h07-34-405	vein 1	0.462	0.112	1.969	1.586	0.412	0.354	1.059	0.389	-707.505	83.798
U16-h07-34-405	vein 1	4.738	0.116	-6.873	13.355	0.425	-28.538	18.782	0.401	-1496.935	682.200
U16-h07-34-405	vein 1	0.631	0.106	1.651	2.250	0.390	4.146	1.201	0.368	6.935	43.115
U16-h07-34-405	vein 1	0.557	0.110	1.483	2.111	0.404	5.243	1.188	0.381	-281.587	57.844
U16-h07-34-405	vein 2	0.256	0.120	-158.051	35.636	0.478	-41.441	9.004	0.449	-327.073	39.137
U16-h07-34-405	vein 2	0.150	0.111	-4.450	1.840	0.440	-3.383	0.499	0.414	-78.127	5.786
U16-h07-34-405	vein 2	0.124	0.117	-55.469	10.150	0.464	-8.383	1.043	0.436	-168.364	16.549
U16-h07-34-405	vein 2	0.377	0.119	-12.749	5.678	0.472	-8.355	1.891	0.444	-189.744	24.522
U16-h07-34-405	vein 2	0.306	0.113	-33.616	22.574	0.451	-7.609	0.889	0.424	-148.298	8.709
U16-h07-34-405	vein 2	0.403	0.117	-1.882	2.204	0.467	-6.431	1.055	0.439	-246.108	28.462
U16-h07-54-338	coarse calcite	0.093	0.102	2.319	0.682	1.311	1.535	0.149	0.317	92.646	15.234
U16-h07-54-338	coarse calcite	0.041	0.207	5.706	2.031	0.615	2.180	0.319	0.197	8.193	0.433
U16-h07-54-338	coarse calcite	0.037	0.110	0.045	0.178	0.629	0.394	0.086	0.101	9.695	1.713
U16-h07-54-338	coarse calcite	0.094	0.145	7.152	2.093	1.030	3.804	1.000	0.652	42.657	3.284
U16-h07-54-338	coarse calcite	0.687	0.199	1.639	0.548	0.590	4.163	0.879	0.189	205.674	60.030
U16-h07-54-338	coarse calcite	0.050	0.089	3.876	1.311	0.533	0.711	0.137	0.127	15.787	1.521
U16-h07-54-338	coarse calcite	0.054	0.209	0.572	0.401	0.621	0.622	0.133	0.199	10.028	0.572
U16-h07-54-338	coarse calcite	0.089	0.133	0.390	0.244	0.778	0.928	0.105	0.165	45.396	5.249
U16-h07-54-338	coarse calcite	0.678	0.168	1.096	0.602	0.650	4.012	1.338	0.091	173.291	53.371
U16-h07-54-338	coarse calcite	1.056	0.191	2.084	0.685	0.568	5.892	1.150	0.182	342.050	70.166
U16-h07-54-338	coarse calcite	0.668	0.195	3.246	0.960	0.578	3.513	0.964	0.185	169.304	36.733
U16-h07-54-338	coarse calcite	0.253	0.189	0.364	0.250	0.566	2.169	0.211	0.092	156.712	15.714

Sample ID	SampleType	2SE (ppm)	Sc LOD (ppm)	Ti (ppm)	2SE (ppm)	Ti LOD (ppm)	V (ppm)	2SE (ppm)	V LOD (ppm)	Mn (ppm)	2SE (ppm)
U16-h07-54-338	coarse calcite	0.124	0.154	1.284	0.736	0.503	1.150	0.160	0.091	129.977	16.739
U16-h07-54-338	coarse calcite	0.607	0.163	1.019	0.473	0.632	2.670	0.648	0.088	164.316	39.500
U16-h07-54-338	coarse calcite	0.070	0.150	0.278	0.300	0.840	1.345	0.182	0.203	30.977	5.088
U16-h07-54-5	matrix cement	0.143	0.073	0.567	0.282	0.800	1.136	0.284	0.096	28.652	6.415
U16-h07-54-5	matrix cement	0.149	0.074	7.131	1.754	0.871	1.846	0.297	0.098	46.821	10.053
U16-h07-54-5	matrix cement	0.215	0.077	32.785	5.576	0.836	4.474	0.571	0.100	95.834	14.489
U16-h07-54-5	matrix cement	0.167	0.071	15.056	4.923	0.779	3.258	0.460	0.093	87.285	5.284
U16-h07-54-5	matrix cement	0.249	0.120	25.815	9.667	0.000	6.750	0.472	0.104	159.140	5.650
U16-h07-54-5	matrix cement	0.215	0.149	16.047	2.656	0.394	4.868	0.313	0.134	141.014	8.416
U16-h07-54-5	matrix cement	0.180	0.076	15.787	4.247	0.893	3.881	0.559	0.101	101.751	14.333
U16-h07-54-5	matrix cement	0.242	0.073	10.103	1.989	0.795	5.821	0.334	0.095	169.330	9.623
U16-h07-54-5	matrix cement	0.166	0.120	1.266	0.560	0.000	2.067	0.227	0.103	59.935	3.574
U16-h07-54-5	matrix cement	0.201	0.076	45.164	10.488	0.833	5.801	0.450	0.100	103.356	7.717
U16-h07-54-5	matrix cement	0.219	0.138	12.419	4.045	0.639	6.222	0.314	0.107	198.573	6.442
U16-h07-54-5	matrix cement	0.198	0.075	2.563	0.837	0.816	3.978	0.536	0.098	97.102	11.829
U16-h07-54-5	matrix cement	0.232	0.074	3.545	1.113	0.866	4.697	0.487	0.097	134.765	13.945
U16-h07-54-5	matrix cement	0.199	0.076	2.291	1.442	0.827	3.198	0.404	0.099	103.081	12.857
U16-h07-54-5	matrix cement	0.112	0.150	2.182	0.756	0.397	12.942	1.449	0.135	54.478	1.764
U16-h07-54-5	matrix cement	0.189	0.075	1.322	0.859	0.816	3.816	0.327	0.098	142.962	9.462
U16-h07-54-5	matrix cement	0.261	0.075	0.095	0.158	0.884	2.386	0.551	0.099	53.113	10.187
U16-h07-54-5	ooid	0.193	0.128	67.575	16.950	0.820	16.569	1.063	0.092	161.672	7.517
U16-h07-54-5	ooid	0.240	0.145	6.211	1.568	0.606	6.003	0.374	0.097	154.040	9.790
U16-h07-54-5	ooid	0.073	0.092	5.827	1.239	0.763	2.391	0.302	0.117	32.388	4.326
U16-h07-54-5	ooid	0.238	0.120	32.691	8.749	0.599	8.861	0.528	0.095	193.198	6.747
U16-h07-54-5	ooid	0.237	0.158	59.069	16.160	0.658	9.538	0.536	0.105	177.005	6.673
U16-h07-54-5	ooid	0.132	0.108	9.906	2.983	0.697	1.866	0.354	0.078	48.340	6.039
U16-h07-54-5	ooid	0.208	0.124	1008.983	432.629	0.619	13.619	2.373	0.098	182.945	5.926
U16-h07-54-5	ooid	0.233	0.159	57.379	8.646	0.662	10.054	0.558	0.106	186.787	7.130
U16-h07-54-5	ooid	0.224	0.137	34.743	5.313	0.637	6.705	0.442	0.106	142.232	8.484
U16-h07-54-5	ooid	0.196	0.092	37.996	7.460	0.679	7.463	0.664	0.119	140.426	7.457
U16-h07-54-5	ooid	0.186	0.092	75.793	36.036	0.676	9.201	0.450	0.118	153.104	7.380
U16-h07-54-5	ooid	0.207	0.117	31.269	13.195	0.584	5.609	0.259	0.093	143.219	6.255
U16-h07-54-5	ooid	0.126	0.151	7.491	2.146	0.632	1.754	0.265	0.101	55.826	7.936

Sample ID	SampleType	2SE (ppm)	Sc LOD (ppm)	Ti (ppm)	2SE (ppm)	Ti LOD (ppm)	V (ppm)	2SE (ppm)	V LOD (ppm)	Mn (ppm)	2SE (ppm)
U16-h07-54-5	ooid	0.229	0.121	8.123	2.029	0.605	4.369	0.377	0.096	116.350	7.293
U16-h07-54-5	ooid	0.225	0.185	1.858	0.767	0.773	2.282	0.305	0.124	63.116	6.539
U16-h07-54-5	ooid	0.238	0.145	9.618	1.929	0.670	3.038	0.436	0.112	86.768	11.717
U16-h07-54-5	ooid	0.201	0.113	17.135	4.562	0.512	8.008	0.709	0.089	163.134	17.293
U16-h07-54-5	ooid	0.365	0.118	0.262	0.222	0.591	10.045	1.092	0.094	226.421	25.435
U16-h07-54-5	ooid	0.214	0.103	1.147	0.633	0.664	4.866	0.413	0.075	149.868	5.594
U16-h07-54-5	ooid	0.249	0.117	20.492	4.917	0.584	7.021	0.426	0.093	161.617	7.702
U16-h07-54-5	ooid	0.174	0.159	0.501	0.299	0.663	2.577	0.228	0.106	78.463	5.122
U16-h07-54-5	ooid	0.386	0.112	0.816	0.471	0.723	5.817	1.357	0.081	163.330	37.132
U16-h07-54-5	ooid	0.366	0.148	1.147	0.337	0.620	4.925	0.648	0.099	171.397	16.556
U16-h07-54-5	ooid	0.217	0.121	7.938	2.822	0.603	7.171	0.472	0.095	182.713	9.342
U16-h07-54-5	ooid	0.141	0.110	0.053	0.158	0.705	3.729	0.807	0.079	48.757	2.458
U16-h07-54-5	vein 1	0.107	0.111	-0.081	0.118	0.582	5.925	0.364	0.115	54.834	2.150
U16-h07-54-5	vein 1	0.235	0.141	-0.068	0.114	0.719	12.211	0.608	0.186	133.545	12.089
U16-h07-54-5	vein 1	0.080	0.106	0.149	0.205	0.381	7.975	0.490	0.214	47.512	1.765
U16-h07-54-5	vein 1	0.109	0.102	0.216	0.252	0.364	6.668	0.451	0.205	53.557	3.340
U16-h07-54-5	vein 1	0.074	0.107	5.091	1.725	0.384	7.364	0.388	0.216	55.880	1.771
U16-h07-54-5	vein 1	0.240	0.104	0.111	0.196	0.372	7.669	0.766	0.210	217.900	27.122
U16-h07-54-5	vein 2	0.061	0.109	-0.036	0.126	0.609	6.218	0.324	0.115	35.994	0.942
U16-h07-54-5	vein 2	0.121	0.108	-0.078	0.113	0.569	10.117	0.827	0.112	197.424	15.443
U16-h07-54-5	vein 2	0.031	0.108	-0.039	0.133	0.567	4.003	0.414	0.112	39.420	1.195
U16-h07-67-129	darker vein	0.057	0.174	0.321	0.268	0.368	0.516	0.089	0.073	18.567	1.373
U16-h07-67-129	darker vein	0.049	0.140	0.248	0.243	0.727	0.381	0.092	0.110	17.851	1.321
U16-h07-67-129	darker vein	0.037	0.083	0.229	0.244	0.691	0.122	0.037	0.096	12.512	0.715
U16-h07-67-129	darker vein	0.048	0.140	0.395	0.277	0.728	1.920	0.260	0.111	14.989	1.023
U16-h07-67-129	darker vein	0.050	0.179	0.324	0.310	0.379	0.117	0.049	0.075	14.271	1.684
U16-h07-67-129	darker vein	0.039	0.177	0.310	0.273	0.373	0.312	0.074	0.074	21.834	1.784
U16-h07-67-129	darker vein	0.041	0.084	-0.006	0.152	0.700	0.189	0.049	0.098	24.116	1.315
U16-h07-67-129	lighter vein	0.039	0.141	-0.095	0.110	0.349	0.430	0.119	0.086	121.442	3.627
U16-h07-67-129	lighter vein	0.050	0.146	0.097	0.196	0.759	1.519	0.114	0.115	114.949	2.329
U16-h07-67-129	lighter vein	0.035	0.118	-0.036	0.175	0.685	0.478	0.075	0.067	99.667	4.256
U16-h07-67-129	lighter vein	0.038	0.138	1.134	0.568	0.342	1.692	0.150	0.084	85.751	2.344
U16-h07-67-129	lighter vein	0.036	0.134	-0.095	0.106	0.332	0.938	0.104	0.081	107.724	3.267

Sample ID	SampleType	2SE (ppm)	Sc LOD (ppm)	Ti (ppm)	2SE (ppm)	Ti LOD (ppm)	V (ppm)	2SE (ppm)	V LOD (ppm)	Mn (ppm)	2SE (ppm)
U16-h07-67-129	lighter vein	0.038	0.145	0.159	0.238	0.361	0.926	0.125	0.088	109.572	2.885
U16-h07-67-129	lighter vein	0.052	0.148	-0.100	0.110	0.771	0.742	0.127	0.117	96.791	2.736
U16-h07-67-129	ooid and matrix	1.806	0.840	18126.180	3036.338	0.000	723.790	90.585	0.689	365.282	53.684
U16-h07-67-129	ooid and matrix	0.208	0.120	137.974	16.546	0.000	15.232	1.192	0.111	117.817	7.030
U16-h07-67-129	ooid and matrix	0.383	0.164	697.829	137.569	8.681	48.297	6.208	0.233	167.356	22.487
U16-h07-67-129	ooid and matrix	0.278	0.121	557.522	76.136	9.283	23.870	2.634	0.359	84.834	11.459
U16-h07-67-129	ooid and matrix	0.616	0.092	1812.168	532.193	1.802	55.305	17.979	0.211	79.943	9.931
U16-h07-67-129	ooid and matrix	0.199	0.141	330.206	30.917	1.313	17.742	1.271	0.207	73.125	5.703
U16-h07-67-129	ooid and matrix	0.115	0.244	101.938	38.018	1.138	7.084	0.704	0.114	41.606	5.242
U16-h07-67-129	ooid and matrix	0.156	0.373	185.591	63.070	617.750	10.118	1.417	17.333	65.013	6.858
U16-h07-67-129	ooid and matrix	0.239	0.256	415.993	49.106	8.373	19.173	0.997	0.421	67.175	3.777
U16-h07-67-129	ooid and matrix	0.347	0.157	871.386	66.800	1.457	41.640	2.865	0.230	87.582	5.691
U16-h07-67-129	ooid and matrix	0.268	0.130	689.323	258.911	0.000	22.754	6.147	0.120	87.453	10.283
U16-h07-67-129	ooid and matrix	0.136	0.134	524.604	304.923	2.791	5.228	0.867	0.272	31.032	4.584
U16-h07-67-129	ooid and matrix	0.093	0.223	63.664	5.012	0.915	9.114	0.432	0.205	36.406	1.874
U16-h07-67-129	ooid and matrix	0.063	0.159	1.588	0.599	0.354	0.773	0.187	0.133	46.565	3.667
U16-h07-67-129	ooid and matrix	0.095	0.146	40.646	3.722	0.000	7.845	0.512	0.120	58.338	4.131
U16-h07-67-129	ooid and matrix	0.045	0.135	0.348	0.315	2.806	0.836	0.228	0.274	51.176	14.883
U16-h07-67-129	ooid and matrix	0.157	0.162	204.523	138.866	0.360	11.790	1.064	0.135	35.085	2.489
U16-h07-67-129	ooid and matrix	0.044	0.242	0.376	0.458	7.911	1.338	0.124	0.398	61.923	3.872
U16-h07-67-129	ooid and matrix	0.058	0.132	0.702	0.403	1.232	3.333	0.242	0.194	24.205	2.568
U16-h07-67-129	ooid and matrix	1.026	0.120	14.486	3.689	0.000	5.695	0.384	0.111	57.709	5.346
U16-h07-67-129	ooid and matrix	0.052	0.127	0.453	0.350	2.637	1.293	0.244	0.257	24.286	1.758
U16-h07-67-129	ooid and matrix	0.092	0.114	12.057	3.665	0.000	2.633	0.734	0.101	43.974	1.987
U16-h07-67-129	ooid and matrix	0.048	0.220	0.185	0.226	0.902	1.666	0.251	0.202	37.186	2.669
U16-h07-67-129	ooid and matrix	0.062	0.166	0.145	0.217	0.368	1.133	0.096	0.122	51.623	1.503
U16-h07-67-129	ooid and matrix	0.052	0.118	-0.147	0.006	0.000	1.720	0.203	0.105	107.775	3.224

Sample ID	SampleType	Mn LOD (ppm)	Fe(ppm)	2SE (ppm)	Fe LOD (ppm)	Rb (ppm)	2SE (ppm)	Rb LOD (ppm)	Sr (ppm)	2SE (ppm)
U16-h07-13b-11	matrix	1.243	91.890	27.569	4.190	21.638	4.600	0.064	521.611	94.385
U16-h07-13b-11	matrix	1.086	24.768	2.893	3.984	0.014	0.012	0.056	372.188	25.285
U16-h07-13b-11	matrix	1.072	20.920	3.129	3.510	0.108	0.155	0.055	239.943	9.859
U16-h07-13b-11	matrix	1.059	144.396	18.488	3.882	0.320	0.058	0.055	175.316	8.363
U16-h07-13b-11	matrix	1.111	81.385	14.551	3.638	0.171	0.056	0.057	156.262	6.000
U16-h07-13b-11	matrix	1.128	29.171	4.598	3.694	0.013	0.014	0.057	653.288	22.571
U16-h07-13b-11	matrix	1.119	24.585	3.842	3.664	0.013	0.011	0.057	316.390	18.999
U16-h07-13b-11	matrix	1.085	130.509	16.162	3.977	0.823	0.110	0.056	145.780	5.841
U16-h07-13b-11	matrix	1.125	377.643	114.920	3.790	3.115	0.338	0.058	133.999	3.971
U16-h07-13b-11	matrix	1.100	155.297	23.261	3.708	1.742	0.203	0.057	160.467	6.994
U16-h07-13b-11	matrix	1.056	51.411	8.344	3.873	0.119	0.079	0.055	140.119	5.622
U16-h07-13b-11	matrix	1.019	62.585	10.874	3.433	0.231	0.075	0.053	160.339	8.361
U16-h07-13b-11	matrix	1.083	70.626	13.724	3.649	0.116	0.032	0.056	135.013	3.136
U16-h07-13b-11	matrix	1.062	485.365	399.053	3.895	4.278	1.350	0.055	136.442	7.769
U16-h07-13b-11	matrix	1.042	55.519	6.461	3.822	0.130	0.041	0.054	133.453	5.794
U16-h07-13b-11	matrix	1.077	80.375	21.462	3.630	0.693	0.182	0.056	129.403	4.115
U16-h07-13b-11	matrix	1.069	46.599	7.031	3.921	0.194	0.045	0.055	131.009	4.995
U16-h07-13b-11	matrix	1.070	95.682	20.868	3.608	0.276	0.056	0.055	172.896	13.038
U16-h07-13b-11	matrix	1.084	173.433	67.116	3.975	3.339	0.612	0.056	129.297	5.325
U16-h07-13b-11	matrix	1.127	25.262	4.285	3.689	0.043	0.033	0.057	97.804	4.993
U16-h07-13b-11	matrix	1.077	52.480	8.622	3.525	0.193	0.062	0.055	122.640	5.619
U16-h07-13b-11	vein 1	1.063	38.687	3.847	3.714	0.016	0.011	0.056	145.566	7.404
U16-h07-13b-11	vein 1	1.108	50.013	5.110	3.873	0.203	0.062	0.058	126.937	4.436
U16-h07-13b-11	vein 1	1.069	49.652	2.780	3.735	0.023	0.017	0.056	124.149	2.937
U16-h07-13b-11	vein 1	1.065	47.193	5.473	3.724	0.038	0.019	0.056	221.187	15.941
U16-h07-13b-11	vein 1	1.056	36.157	3.844	3.689	0.069	0.021	0.055	106.393	3.444
U16-h07-13b-11	vein 1	1.047	46.817	3.738	3.658	0.150	0.039	0.055	129.450	3.072
U16-h07-13b-11	vein 1	1.072	48.692	3.511	3.748	0.090	0.038	0.056	125.603	4.289
U16-h07-13b-11	vein 2	1.043	32.439	3.816	3.726	0.020	0.014	0.054	299.055	21.126
U16-h07-13b-11	vein 2	1.103	30.008	4.641	3.940	-0.004	0.000	0.057	136.411	3.034
U16-h07-13b-11	vein 2	1.080	29.721	2.868	3.859	0.033	0.018	0.056	113.151	4.264
U16-h07-13b-11	vein 2	1.122	27.763	3.510	4.008	0.007	0.010	0.058	114.629	3.647
U16-h07-13b-11	vein 2	1.133	31.341	4.165	4.046	-0.005	0.000	0.058	101.468	2.470

Sample ID	SampleType	Mn LOD (ppm)	Fe(ppm)	2SE (ppm)	Fe LOD (ppm)	Rb (ppm)	2SE (ppm)	Rb LOD (ppm)	Sr (ppm)	2SE (ppm)
U16-h07-13b-11	vein 2	1.107	25.140	3.315	3.870	0.014	0.012	0.058	100.328	2.995
U16-h07-13b-11	vein 3	1.120	25.044	3.098	4.000	0.035	0.030	0.058	82.941	1.951
U16-h07-13b-11	vein 3	1.095	20.698	3.604	3.913	0.004	0.007	0.056	89.550	2.301
U16-h07-13b-11	vein 3	1.117	20.171	3.519	3.990	-0.004	0.000	0.058	93.927	5.131
U16-h07-13b-31	dk ooid	4.901	135.136	17.305	6.877	-0.001	0.005	0.014	225.008	19.914
U16-h07-13b-31	dk ooid	0.943	915.156	280.495	4.804	5.315	0.846	0.022	117.600	15.548
U16-h07-13b-31	dk ooid	4.888	349.325	47.546	6.860	1.245	0.325	0.014	121.820	6.618
U16-h07-13b-31	dk ooid	4.819	493.971	38.584	6.763	2.057	0.310	0.014	75.404	6.239
U16-h07-13b-31	dk ooid	0.754	417.097	48.043	3.845	2.133	0.162	0.018	144.748	10.725
U16-h07-13b-31	dk ooid	0.894	756.103	96.021	4.558	4.288	0.430	0.021	111.545	8.556
U16-h07-13b-31	matrix cement	4.874	230.926	31.459	6.844	0.031	0.016	0.014	280.825	39.603
U16-h07-13b-31	matrix cement	5.176	461.872	81.800	10.484	2.105	0.363	0.059	128.924	10.377
U16-h07-13b-31	matrix cement	4.833	1011.660	252.794	6.786	5.854	1.224	0.014	84.914	5.012
U16-h07-13b-31	matrix cement	4.713	327.761	25.758	6.615	0.667	0.133	0.014	87.927	5.669
U16-h07-13b-31	matrix cement	5.276	1356.970	325.882	10.689	4.148	0.356	0.060	54.282	2.222
U16-h07-13b-31	matrix cement	4.935	904.478	235.117	6.928	2.596	0.610	0.015	88.834	5.962
U16-h07-13b-31	matrix cement	4.751	1042.973	478.373	6.669	0.727	0.135	0.014	137.881	21.820
U16-h07-13b-31	matrix cement	5.030	412.519	55.441	10.189	0.134	0.077	0.057	147.343	12.807
U16-h07-13b-31	matrix cement	2.020	551.038	20.582	35.107	2.499	0.187	0.000	52.749	2.000
U16-h07-13b-31	matrix cement	2.001	652.570	57.316	34.791	3.406	0.307	0.000	47.629	2.624
U16-h07-13b-31	matrix cement	5.140	704.943	71.769	10.413	1.307	0.091	0.058	60.044	3.397
U16-h07-13b-31	matrix cement	5.193	774.679	80.711	10.520	1.571	0.177	0.059	34.286	1.401
U16-h07-13b-31	ooid	2.693	1210.315	240.217	4.957	9.294	0.802	0.057	70.721	2.747
U16-h07-13b-31	ooid	10.897	211.578	25.552	20.988	0.027	0.015	0.000	174.189	7.073
U16-h07-13b-31	ooid	2.711	1463.941	459.597	4.995	6.628	0.811	0.057	103.105	9.715
U16-h07-13b-31	ooid	1.048	124.986	9.866	6.584	0.007	0.008	0.138	169.703	11.040
U16-h07-13b-31	ooid	1.404	97.916	10.807	5.698	-0.004	0.000	0.034	146.542	6.767
U16-h07-13b-31	ooid	4.593	379.552	85.922	10.171	0.336	0.094	0.052	161.422	22.929
U16-h07-13b-31	ooid	1.510	1177.179	263.807	6.137	12.321	1.567	0.036	54.006	2.502
U16-h07-13b-31	ooid	1.017	498.205	69.998	6.399	2.143	0.447	0.134	110.000	11.194
U16-h07-13b-31	ooid	0.918	333.324	23.405	4.513	0.019	0.023	0.028	173.012	8.429
U16-h07-13b-31	ooid	4.559	877.523	174.327	10.100	5.108	0.393	0.051	84.426	3.743
U16-h07-13b-31	ooid	2.726	1271.601	389.020	4.984	4.774	0.876	0.058	55.155	4.396

Sample ID	SampleType	Mn LOD (ppm)	Fe(ppm)	2SE (ppm)	Fe LOD (ppm)	Rb (ppm)	2SE (ppm)	Rb LOD (ppm)	Sr (ppm)	2SE (ppm)
U16-h07-13b-31	ooid	10.866	697.800	99.634	20.930	4.525	0.666	0.000	57.941	2.613
U16-h07-13b-31	ooid	2.621	481.226	61.343	4.813	0.602	0.077	0.055	125.110	8.389
U16-h07-13b-31	ooid	2.666	2106.092	1272.130	4.890	5.176	0.463	0.056	53.594	3.974
U16-h07-13b-31	ooid	10.809	970.425	195.979	20.816	2.659	0.360	0.000	103.223	16.561
U16-h07-13b-31	ooid	4.563	1069.284	200.069	10.107	4.723	0.427	0.051	54.676	3.307
U16-h07-13b-31	ooid	0.958	1975.421	666.665	4.714	7.146	0.611	0.029	45.776	1.397
U16-h07-13b-31	ooid	0.922	1371.457	711.552	4.530	3.395	0.346	0.028	65.340	3.962
U16-h07-13b-31	ooid	2.613	710.225	114.061	4.784	3.133	0.212	0.055	62.795	4.321
U16-h07-13b-31	ooid	2.603	777.687	126.288	4.759	3.999	0.331	0.055	60.208	2.053
U16-h07-13b-31	ooid	0.880	687.028	228.154	4.326	2.548	0.714	0.026	107.094	15.025
U16-h07-13b-31	ooid	0.875	722.652	183.441	4.298	0.672	0.096	0.026	79.155	4.452
U16-h07-13b-31	ooid	2.551	603.335	83.829	4.689	0.903	0.092	0.054	61.612	3.531
U16-h07-13b-31	ooid	1.017	673.415	75.696	6.381	3.048	0.230	0.134	54.657	1.554
U16-h07-13b-31	vein-1	0.887	2759.497	421.759	5.700	20.644	3.202	0.000	123.556	6.659
U16-h07-13b-31	vein-1	1.411	65.962	14.381	5.741	0.018	0.013	0.034	92.225	4.468
U16-h07-13b-31	vein-1	0.801	31.212	4.116	5.154	0.047	0.027	0.000	101.109	2.990
U16-h07-13b-31	vein-1	0.747	79.795	20.011	5.714	0.017	0.014	0.054	168.477	8.597
U16-h07-13b-31	vein-1	0.775	232.364	182.491	4.995	0.026	0.014	0.000	60.712	1.823
U16-h07-13b-31	vein-1	0.725	47.458	4.870	4.680	0.026	0.014	0.000	135.838	11.407
U16-h07-13b-81	coarse calcite	3.809	96.881	15.602	27.027	0.001	0.003	0.009	0.330	0.087
U16-h07-13b-81	coarse calcite	3.936	57.913	11.471	27.927	-0.017	0.004	0.010	-17.818	3.594
U16-h07-13b-81	coarse calcite	3.654	205.197	23.587	25.931	-0.055	0.009	0.009	-53.059	4.786
U16-h07-13b-81	coarse calcite	16.322	102.728	23.508	70.806	-0.118	0.045	0.177	-135.039	15.055
U16-h07-13b-81	vein 1	27.153	3544.900	1980.081	18.798	3.510	0.928	0.136	56.531	3.248
U16-h07-13b-81	vein 1	31.834	-88.899	8.751	58.902	-0.125	0.022	0.133	175.610	10.174
U16-h07-13b-81	vein 1	20.880	71.926	15.283	14.454	0.261	0.036	0.105	39.187	2.675
U16-h07-13b-81	vein 1	89.540	70.730	15.597	30.232	-0.001	0.000	0.012	31.527	6.510
U16-h07-13b-81	vein 1	3.487	127.441	35.583	24.747	1.477	0.173	0.009	69.299	5.755
U16-h07-13b-81	vein 1	95.681	244.477	32.516	134.420	0.257	0.071	0.145	17.560	3.974
U16-h07-13b-81	vein 1	121.920	187.268	62.932	152.670	0.087	0.060	0.341	16.044	5.984
U16-h07-13b-81	vein 1	124.820	88.846	54.061	156.300	-0.052	0.007	0.349	-2.810	5.498
U16-h07-13b-81	vein 1	89.123	49.664	15.209	30.091	-0.017	0.005	0.012	-16.716	2.416
U16-h07-24-145	ooids and cement	0.536	29.588	3.205	2.854	0.008	0.006	0.006	90.275	3.881

Sample ID	SampleType	Mn LOD (ppm)	Fe(ppm)	2SE (ppm)	Fe LOD (ppm)	Rb (ppm)	2SE (ppm)	Rb LOD (ppm)	Sr (ppm)	2SE (ppm)
U16-h07-24-145	ooids and cement	0.812	65.224	6.655	3.399	0.068	0.038	0.000	161.432	7.730
U16-h07-24-145	ooids and cement	0.826	144.861	64.710	3.459	0.338	0.078	0.000	131.196	5.432
U16-h07-24-145	ooids and cement	0.793	35.960	3.141	3.320	0.000	1.000	0.000	124.284	7.408
U16-h07-24-145	ooids and cement	0.510	49.557	6.325	2.715	0.113	0.079	0.005	173.970	6.448
U16-h07-24-145	ooids and cement	0.857	29.349	2.646	3.589	0.026	0.011	0.000	259.404	53.517
U16-h07-24-145	ooids and cement	0.763	35.883	3.841	3.192	0.015	0.013	0.000	128.471	4.980
U16-h07-24-145	ooids and cement	0.774	31.208	3.111	3.242	0.001	0.002	0.000	142.324	5.159
U16-h07-24-145	vein-1	1.014	52.015	3.294	4.029	0.020	0.010	0.000	495.293	21.611
U16-h07-24-145	vein-1	0.935	62.259	4.335	3.715	0.025	0.013	0.000	502.626	21.862
U16-h07-24-145	vein-1	0.937	63.373	3.908	3.723	0.020	0.014	0.000	575.540	12.028
U16-h07-24-145	vein-1	0.944	81.882	3.828	3.749	-0.003	0.005	0.000	389.621	12.245
U16-h07-24-145	vein-1	0.911	57.314	4.279	3.617	0.041	0.018	0.000	442.440	14.662
U16-h07-24-145	vein-1	0.826	86.335	5.936	3.453	-0.004	0.010	0.062	407.337	7.817
U16-h07-24-145	vein-1	0.825	54.712	3.519	3.447	0.002	0.008	0.062	436.786	15.873
U16-h07-24-145	vein-1	0.774	46.080	4.720	3.236	0.045	0.019	0.058	376.201	10.114
U16-h07-24-145	vein-2	0.983	82.622	8.883	3.688	0.017	0.012	0.000	532.522	11.770
U16-h07-24-145	vein-2	0.968	152.682	14.590	3.635	0.189	0.125	0.000	384.505	23.632
U16-h07-24-145	vein-2	0.994	287.890	1596.250	3.731	-0.261	0.106	0.000	491.985	12.868
U16-h07-24-145	vein-3	3.080	410.254	980.618	86.916	0.729	0.104	0.242	1412.910	91.834
U16-h07-24-145	vein-3	1.015	-358.213	67.647	3.808	-0.145	0.042	0.000	211.717	5.809
U16-h07-24-145	vein-3	5.763	-32.149	6.111	14.882	0.004	0.003	0.011	415.474	14.098
U16-h07-24-145	vein-3	0.990	-61.372	7.061	3.715	-0.001	0.002	0.000	240.130	5.588
U16-h07-24-145	vein-3	5.436	-210.968	71.397	14.756	-0.048	0.013	0.011	251.423	10.418
U16-h07-24-145	vein-3	0.994	-41.079	4.539	3.731	0.000	1.000	0.000	316.577	7.746
U16-h07-24-145	vein-3	1.027	-33.079	2.903	3.854	0.000	1.000	0.000	160.581	7.629
U16-h07-24-145	vein-4	3.155	-975.371	1214.626	78.724	0.586	1.413	0.245	10092.670	11982.560
U16-h07-24-145	vein-4	0.714	29.816	3.378	3.206	0.014	0.010	0.000	208.472	7.225
U16-h07-24-145	vein-4	0.691	26.663	2.588	3.105	0.022	0.012	0.000	193.204	8.680
U16-h07-24-145	vein-4	0.723	31.266	4.081	6.426	0.026	0.015	0.000	169.779	4.046
U16-h07-24-145	vein-4	3.143	1337.781	1855.455	78.415	1.479	3.838	0.244	4461.508	6669.837
U16-h07-24-145	vein-4	0.705	37.004	4.527	6.271	0.001	0.007	0.000	299.713	9.265
U16-h07-24-145	vein-4	3.288	51.469	85.898	92.784	1.555	3.929	0.258	1352.905	108.026
U16-h07-24-145	vein-4	0.708	43.442	6.668	6.296	-0.018	0.001	0.000	316.703	8.025

Sample ID	SampleType	Mn LOD (ppm)	Fe(ppm)	2SE (ppm)	Fe LOD (ppm)	Rb (ppm)	2SE (ppm)	Rb LOD (ppm)	Sr (ppm)	2SE (ppm)
U16-h07-24-145	vein-4	0.757	54.213	16.841	6.734	-0.017	0.069	0.000	300.684	85.726
U16-h07-24-145	vein-4	3.036	-2579.420	1927.309	75.759	-0.085	0.100	0.236	1329.770	145.951
U16-h07-24-145	vein-4	0.743	55.560	15.881	6.606	-0.116	0.016	0.000	423.780	50.428
U16-h07-24-145	vein-4	0.758	161.384	69.234	6.744	-0.274	0.139	0.000	354.506	41.438
U16-h07-24-145	vein-4	5.867	-109.493	18.000	15.149	0.047	0.013	0.011	1206.179	127.284
U16-h07-24-145	vein-4	5.603	-127.688	50.845	14.467	-0.019	0.025	0.011	952.689	85.203
U16-h07-24-145	vein-4	3.214	-101.864	368.256	80.204	-0.828	0.448	0.249	410.417	398.952
U16-h07-24-145	vein-4	2.979	-289.986	456.238	74.342	1.226	2.194	0.231	129.443	4520.074
U16-h07-24-145	vein-6	0.748	25.089	2.747	3.360	0.007	0.006	0.000	78.098	1.978
U16-h07-24-145	vein-6	0.674	31.445	2.981	3.027	0.003	0.005	0.000	183.583	9.140
U16-h07-24-145	vein-6	0.783	381.729	147.160	3.257	0.920	0.173	0.000	173.963	11.931
U16-h07-24-145	vein-6	0.681	73.358	9.788	3.059	0.332	0.046	0.000	147.556	5.335
U16-h07-24-145	vein-6	0.647	34.305	3.955	2.905	0.002	0.003	0.000	124.277	4.928
U16-h07-24-145	vein-7	0.854	47.334	5.979	3.553	0.076	0.032	0.000	152.685	19.078
U16-h07-25-167	coarse calcite	3.890	6.200	2.721	53.603	0.040	0.024	0.156	-46.322	4.827
U16-h07-25-167	coarse calcite	3.975	12.925	3.686	54.774	-0.015	0.014	0.159	62.203	26.981
U16-h07-25-167	coarse calcite	4.165	5.063	2.243	57.397	-0.024	0.008	0.167	200.848	8.077
U16-h07-25-167	coarse calcite	4.118	4.409	1.455	56.752	0.017	0.018	0.165	202.922	10.432
U16-h07-25-167	dk ooid	3.927	249.523	130.154	54.109	0.559	0.098	0.157	128.321	9.332
U16-h07-25-167	dk ooid	0.655	270.498	92.968	4.796	2.790	0.432	0.000	163.705	10.273
U16-h07-25-167	dk ooid	0.693	204.212	39.794	5.074	3.552	0.459	0.000	153.968	3.968
U16-h07-25-167	dk ooid	1.505	167.431	54.274	2.424	1.206	0.470	0.050	197.259	9.528
U16-h07-25-167	dk ooid	0.848	253.838	90.769	2.858	2.159	0.287	0.056	185.011	4.662
U16-h07-25-167	dk ooid	0.622	88.656	10.671	2.138	2.959	0.187	0.027	215.957	14.487
U16-h07-25-167	dk ooid	1.507	466.884	310.030	2.168	1.092	0.431	0.051	299.518	15.606
U16-h07-25-167	dk ooid	0.638	83.903	27.708	4.672	0.426	0.099	0.000	157.077	6.304
U16-h07-25-167	dk ooid	1.492	122.482	17.187	2.146	1.507	0.431	0.051	178.580	6.628
U16-h07-25-167	dk ooid	0.809	88.180	12.947	2.725	0.319	0.052	0.054	170.179	6.580
U16-h07-25-167	dk ooid	0.816	170.504	66.200	2.750	1.254	0.192	0.054	194.737	8.678
U16-h07-25-167	dk ooid	1.429	68.821	7.720	2.055	0.519	0.115	0.049	170.540	8.642
U16-h07-25-167	dk ooid	0.615	32.410	4.158	2.116	-0.008	0.012	0.027	271.124	21.287
U16-h07-25-167	dk ooid	1.459	124.506	14.224	2.099	1.163	0.127	0.050	168.085	7.227
U16-h07-25-167	dk ooid	0.814	46.829	7.828	2.830	0.113	0.041	0.055	159.391	7.830

Sample ID	SampleType	Mn LOD (ppm)	Fe(ppm)	2SE (ppm)	Fe LOD (ppm)	Rb (ppm)	2SE (ppm)	Rb LOD (ppm)	Sr (ppm)	2SE (ppm)
U16-h07-25-167	dk ooid	1.440	127.974	26.913	2.318	0.976	0.104	0.048	173.311	8.945
U16-h07-25-167	dk ooid	0.803	86.083	61.107	2.789	0.046	0.023	0.054	187.088	6.873
U16-h07-25-167	dk ooid	0.836	153.932	49.386	2.816	0.333	0.063	0.055	171.596	4.932
U16-h07-25-167	dk ooid	0.550	84.321	17.902	1.891	0.646	0.153	0.024	168.946	6.855
U16-h07-25-167	dk ooid	0.829	79.884	13.293	2.795	0.680	0.092	0.055	176.359	5.581
U16-h07-25-167	dk ooid	1.440	48.574	6.323	2.071	0.221	0.042	0.049	179.899	6.689
U16-h07-25-167	dk ooid	1.438	51.003	7.731	2.315	0.475	0.075	0.048	179.553	10.336
U16-h07-25-167	early vein	0.898	17.066	1.160	3.301	0.020	0.006	0.016	29.357	1.723
U16-h07-25-167	early vein	0.897	14.327	1.487	3.295	0.027	0.009	0.016	51.949	2.440
U16-h07-25-167	early vein	0.911	14.948	1.039	3.348	0.030	0.009	0.016	36.633	2.657
U16-h07-25-167	early vein	0.906	19.905	2.372	3.331	0.018	0.005	0.016	42.420	5.194
U16-h07-25-167	late vein	0.971	217.154	69.158	3.672	3.645	0.396	0.017	248.403	5.852
U16-h07-25-167	late vein	0.924	90.714	30.557	3.497	2.092	0.361	0.016	292.200	6.388
U16-h07-25-167	late vein	0.894	18.994	1.952	3.382	0.761	0.169	0.015	289.609	9.933
U16-h07-25-167	late vein	0.871	17.770	1.490	3.199	0.780	0.066	0.015	157.507	4.113
U16-h07-25-167	late vein	0.908	15.272	0.848	3.338	0.399	0.048	0.016	179.105	4.227
U16-h07-25-167	lt ooid	0.892	78.545	12.733	3.390	0.820	0.156	0.015	201.677	6.718
U16-h07-25-167	lt ooid	0.852	78.300	12.157	3.024	0.635	0.124	0.015	203.144	9.014
U16-h07-25-167	lt ooid	0.858	78.667	15.926	3.047	0.389	0.098	0.015	200.907	8.600
U16-h07-25-167	lt ooid	0.830	91.054	14.279	2.883	1.364	0.118	0.056	180.790	5.789
U16-h07-25-167	lt ooid	0.800	224.408	54.936	2.781	0.971	0.155	0.054	170.689	7.689
U16-h07-25-167	lt ooid	0.834	63.181	18.191	2.961	0.174	0.040	0.015	187.898	6.689
U16-h07-25-167	lt ooid	0.837	58.754	9.353	3.180	0.496	0.072	0.014	171.613	5.913
U16-h07-25-167	lt ooid	0.831	174.232	37.463	2.888	0.673	0.091	0.056	182.644	8.460
U16-h07-25-167	lt ooid	0.820	45.260	9.741	2.913	0.162	0.035	0.014	155.618	9.650
U16-h07-25-167	lt ooid	0.860	56.887	7.649	3.269	0.387	0.096	0.015	168.144	5.203
U16-h07-25-167	matrix cement	0.925	597.361	21.047	3.285	0.041	0.015	0.016	153.110	7.018
U16-h07-25-167	matrix cement	0.894	273.942	126.097	3.034	0.649	0.079	0.015	198.894	6.141
U16-h07-25-167	matrix cement	0.934	25.689	4.725	3.171	0.219	0.069	0.016	276.525	7.815
U16-h07-25-167	matrix cement	0.842	95.748	39.677	2.857	0.453	0.259	0.014	182.933	10.320
U16-h07-25-167	matrix cement	0.866	66.399	14.195	2.940	0.248	0.063	0.015	174.775	5.405
U16-h07-25-167	matrix cement	0.859	37.589	3.980	2.915	0.061	0.032	0.015	174.818	9.698
U16-h07-25-167	matrix cement	0.873	43.406	5.145	3.101	0.112	0.038	0.015	215.584	15.773

Sample ID	SampleType	Mn LOD (ppm)	Fe(ppm)	2SE (ppm)	Fe LOD (ppm)	Rb (ppm)	2SE (ppm)	Rb LOD (ppm)	Sr (ppm)	2SE (ppm)
U16-h07-25-167	matrix cement	0.859	25.037	3.321	2.915	0.026	0.010	0.015	216.076	10.528
U16-h07-25-167	matrix cement	0.864	55.530	11.750	2.933	0.230	0.043	0.015	171.541	8.350
U16-h07-25-167	matrix cement	0.830	33.476	5.205	2.816	0.016	0.004	0.014	175.907	9.481
U16-h07-25-167	matrix cement	0.885	61.677	20.309	3.251	0.229	0.053	0.016	157.425	9.849
U16-h07-34-405	matrix cement	0.735	313.740	2810.774	9.518	-0.131	0.327	0.000	325.056	14201.730
U16-h07-34-405	matrix cement	1.123	-185.176	557.967	10.964	2.360	0.524	0.024	1714.966	553.023
U16-h07-34-405	matrix cement	0.722	-990.322	765.856	9.064	0.033	0.030	0.000	-79.726	399.473
U16-h07-34-405	matrix cement	4.115	-757.345	121.536	41.374	-2.218	0.624	0.250	207.736	20.334
U16-h07-34-405	matrix cement	4.428	26.355	134.226	44.516	1.176	0.231	0.269	259.584	37.938
U16-h07-34-405	matrix cement	0.668	-2780.137	1348.405	8.392	-7.015	7.665	0.000	-912.145	531.758
U16-h07-34-405	matrix cement	0.668	-1701.210	5493.800	8.393	-12.090	9.297	0.000	-903.147	839.038
U16-h07-34-405	matrix cement	4.432	398.474	139.659	44.562	1.234	0.155	0.269	-20.346	34.142
U16-h07-34-405	matrix cement	1.140	186.291	859.342	11.129	-0.154	0.286	0.024	-437.004	400.828
U16-h07-34-405	matrix cement	4.433	204.258	176.519	44.569	1.478	0.143	0.269	6.664	25.747
U16-h07-34-405	matrix cement	0.706	-63.497	507.955	8.864	1.468	0.325	0.000	407.067	88.571
U16-h07-34-405	matrix cement	0.664	-976.036	1116.685	8.598	-1.736	2.594	0.000	-633.287	358.545
U16-h07-34-405	matrix cement	0.702	-426.955	1699.603	8.818	1.376	0.553	0.000	-1127.269	793.574
U16-h07-34-405	matrix cement	0.720	-1032.978	661.851	9.323	0.073	0.045	0.000	6664.476	4342.875
U16-h07-34-405	matrix cement	0.736	578.365	993.786	9.245	-0.001	0.213	0.000	826.648	1777.638
U16-h07-34-405	matrix cement	0.719	1332.330	1553.341	9.033	-0.062	0.157	0.000	861.494	3731.214
U16-h07-34-405	matrix cement	0.740	-2332.885	1709.588	9.297	0.536	0.754	0.000	-2889.368	1786.454
U16-h07-34-405	ooid	14.256	237.833	111.209	61.842	0.373	0.245	0.155	345.892	28.795
U16-h07-34-405	ooid	3.436	331.172	119.527	48.571	7.990	3.260	0.194	371.792	22.273
U16-h07-34-405	ooid	1.033	-10747.580	5114.773	10.088	-24.962	9.929	0.022	-607.726	835.117
U16-h07-34-405	ooid	4.848	-2132.093	624.976	31.212	-2.735	0.854	0.128	362.973	58.098
U16-h07-34-405	ooid	3.337	-3971.890	4428.302	23.430	0.447	0.143	0.094	707.631	96.079
U16-h07-34-405	ooid	3.178	-5108.342	1453.377	22.316	-2.499	0.557	0.089	643.388	85.696
U16-h07-34-405	ooid	8.215	-6289.542	3711.435	20.955	-5.506	1.289	4.558	261.948	59.575
U16-h07-34-405	ooid	4.583	-5265.944	1985.643	27.814	-3.777	0.775	0.124	471.470	65.902
U16-h07-34-405	ooid	4.591	262.354	214.160	18.512	0.560	0.106	0.095	1110.245	245.829
U16-h07-34-405	ooid	4.290	-1570.607	361.181	17.300	-1.391	0.423	0.089	283.145	71.196
U16-h07-34-405	ooid	5.018	-89.800	757.414	32.309	1.024	0.303	0.133	508.241	65.550
U16-h07-34-405	ooid	3.092	-1219.350	437.810	21.711	0.088	0.128	0.087	649.124	79.482

Sample ID	SampleType	Mn LOD (ppm)	Fe(ppm)	2SE (ppm)	Fe LOD (ppm)	Rb (ppm)	2SE (ppm)	Rb LOD (ppm)	Sr (ppm)	2SE (ppm)
U16-h07-34-405	ooid	4.778	-3909.290	903.636	28.996	-2.000	0.539	0.129	408.434	76.388
U16-h07-34-405	ooid	3.396	-3256.004	594.055	23.847	-1.062	0.321	0.095	522.261	72.972
U16-h07-34-405	ooid	3.045	-465.592	130.628	11.810	0.471	0.143	0.011	510.990	58.720
U16-h07-34-405	ooid	3.078	-380.928	197.034	11.936	0.074	0.062	0.012	216.833	38.920
U16-h07-34-405	ooid	3.391	-785.898	848.327	23.810	0.096	0.184	0.095	550.757	44.395
U16-h07-34-405	ooid	3.267	755.932	310.107	46.179	-2.731	1.039	0.185	309.574	29.343
U16-h07-34-405	ooid	3.132	-4266.041	831.687	21.990	-2.837	0.942	0.088	592.640	31.364
U16-h07-34-405	ooid	8.196	-51.081	80.135	20.907	1.140	0.137	4.547	220.627	37.872
U16-h07-34-405	ooid	1.129	5954.127	8128.923	11.030	29.791	20.961	0.024	245.621	691.555
U16-h07-34-405	ooid and clast	1.819	411.400	51.482	17.657	28.511	4.423	0.064	192.710	7.042
U16-h07-34-405	ooid and clast	2.023	209.751	45.517	10.031	1.075	0.262	0.225	236.702	10.110
U16-h07-34-405	ooid and clast	0.540	37.156	5.268	3.995	0.042	0.017	0.038	185.825	6.243
U16-h07-34-405	ooid and clast	0.555	110.370	8.877	4.105	0.225	0.051	0.039	181.904	7.047
U16-h07-34-405	ooid and clast	0.465	225.806	24.014	4.511	2.700	0.381	0.016	191.605	7.271
U16-h07-34-405	ooid and clast	0.520	227.005	51.438	5.053	16.311	2.141	0.018	244.607	17.891
U16-h07-34-405	ooid and clast	1.959	322.107	37.907	9.712	2.079	0.264	0.218	151.698	4.747
U16-h07-34-405	ooid and clast	0.454	142.046	12.046	4.405	1.582	0.172	0.016	170.507	4.943
U16-h07-34-405	ooid and clast	0.463	649.778	304.198	4.499	4.420	0.575	0.016	189.300	10.763
U16-h07-34-405	ooid and clast	0.476	140.106	12.371	4.617	1.515	0.227	0.017	201.087	10.012
U16-h07-34-405	ooid and clast	0.528	274.819	74.855	3.905	3.778	0.351	0.037	169.156	8.176
U16-h07-34-405	ooid and clast	0.473	124.813	33.448	4.300	0.602	0.105	0.000	148.420	6.123
U16-h07-34-405	ooid and clast	0.476	333.188	37.806	4.327	7.067	0.851	0.000	192.599	7.765
U16-h07-34-405	ooid and clast	2.167	777.629	333.989	149.740	4.716	0.395	0.273	244.912	12.263
U16-h07-34-405	ooid and clast	0.894	204.621	43.458	4.470	1.284	0.221	0.000	245.065	12.011
U16-h07-34-405	ooid and clast	0.472	357.268	30.461	4.292	13.156	1.220	0.000	202.237	9.852
U16-h07-34-405	ooid and clast	0.481	518.958	86.313	4.371	3.603	1.847	0.000	162.895	16.357
U16-h07-34-405	ooid and clast	2.295	383.856	53.133	158.630	3.745	3.148	0.289	305.055	12.315
U16-h07-34-405	ooid and clast	0.795	1104.731	460.241	4.674	-13.758	55.499	0.027	409.822	26.220
U16-h07-34-405	ooid and clast	3.244	9.198	9.875	118.490	0.022	0.008	0.065	26.804	49.814
U16-h07-34-405	ooid and clast	2.241	-31289.690	18696.190	154.860	-15.782	1.900	0.282	578.411	34.065
U16-h07-34-405	ooid and clast	0.495	-2348.733	793.256	4.501	-14.589	1.314	0.000	231.594	10.339
U16-h07-34-405	ooid and clast	0.450	17001.760	32136.600	4.088	-7.818	1.930	0.000	190.707	9.610
U16-h07-34-405	ooid and clast	0.590	-4.994	1257.071	2.772	-0.632	0.162	0.000	934.748	74.240

Sample ID	SampleType	Mn LOD (ppm)	Fe(ppm)	2SE (ppm)	Fe LOD (ppm)	Rb (ppm)	2SE (ppm)	Rb LOD (ppm)	Sr (ppm)	2SE (ppm)
U16-h07-34-405	ooid and clast	0.481	-357.586	53.451	4.374	-9.137	0.579	0.000	196.470	6.139
U16-h07-34-405	ooid and clast	0.457	-175.800	24.978	4.157	0.000	0.006	0.000	216.739	15.159
U16-h07-34-405	ooid and clast	26.871	-251.524	59.772	26.371	-0.349	0.222	0.118	5343.549	3876.865
U16-h07-34-405	ooid and clast	0.879	-752.389	134.115	2.391	-4.104	0.981	0.016	-3668.646	6126.320
U16-h07-34-405	ooid and clast	0.867	-668.796	69.896	4.222	-13.020	1.810	0.024	-409.077	31.663
U16-h07-34-405	ooid and clast	27.209	-230.626	28.391	26.703	-3.450	0.530	0.119	-674.776	95.361
U16-h07-34-405	ooid and clast	0.770	-312.808	165.318	3.752	-3.241	0.315	0.021	-312.110	11.728
U16-h07-34-405	ooid and clast	0.751	-129.042	14.223	3.659	-0.989	0.217	0.021	-208.250	11.890
U16-h07-34-405	ooid and clast	2.992	-134.984	26.930	109.300	-1.709	0.532	0.060	-218.468	19.545
U16-h07-34-405	ooid and clast	0.915	-110.784	17.566	2.490	-0.043	0.027	0.017	-993.001	52.637
U16-h07-34-405	vein 1	5.741	-188.632	56.505	10.112	-0.278	0.128	0.022	-303.500	73.351
U16-h07-34-405	vein 1	5.834	-759.780	409.245	10.777	-0.077	0.103	0.022	-910.769	139.918
U16-h07-34-405	vein 1	6.014	-1263.772	590.140	11.110	-0.498	0.303	0.023	-2582.043	1453.454
U16-h07-34-405	vein 1	5.518	-545.781	151.006	10.193	-0.847	0.326	0.021	-1013.470	204.990
U16-h07-34-405	vein 1	5.718	-2237.448	440.646	10.563	-0.432	0.224	0.022	-767.044	126.307
U16-h07-34-405	vein 2	6.616	-95578.940	36996.880	11.654	-19.199	2.130	0.025	241.671	14.790
U16-h07-34-405	vein 2	6.099	-26.591	8.552	10.744	-1.688	0.411	0.023	723.701	45.860
U16-h07-34-405	vein 2	6.422	-155.381	25.611	11.313	-6.971	0.867	0.024	441.669	25.128
U16-h07-34-405	vein 2	6.545	-37.441	23.851	11.529	-4.298	1.333	0.025	615.489	57.408
U16-h07-34-405	vein 2	6.244	-37.044	15.105	10.999	-1.399	0.228	0.023	322.031	22.781
U16-h07-34-405	vein 2	6.467	6.145	38.103	11.392	0.047	0.007	0.024	1072.331	114.087
U16-h07-54-338	coarse calcite	4.864	88.577	7.682	4.559	0.064	0.021	0.055	173.188	6.260
U16-h07-54-338	coarse calcite	4.542	41.624	3.159	14.311	0.166	0.053	0.018	176.845	6.854
U16-h07-54-338	coarse calcite	1.072	35.078	4.694	3.583	-0.001	0.004	0.000	221.587	6.623
U16-h07-54-338	coarse calcite	1.777	101.729	8.092	4.218	0.163	0.058	0.068	183.817	7.446
U16-h07-54-338	coarse calcite	4.361	231.435	65.073	13.704	0.090	0.032	0.017	157.062	5.730
U16-h07-54-338	coarse calcite	1.223	40.667	3.221	4.855	0.052	0.023	0.000	166.729	7.446
U16-h07-54-338	coarse calcite	4.585	34.846	3.880	14.520	0.013	0.016	0.018	135.784	3.562
U16-h07-54-338	coarse calcite	1.978	87.067	6.957	5.611	-0.004	0.000	0.000	196.065	7.337
U16-h07-54-338	coarse calcite	0.873	331.729	92.823	4.662	0.035	0.025	0.045	139.081	5.700
U16-h07-54-338	coarse calcite	4.195	624.489	130.857	13.075	0.054	0.025	0.016	152.555	7.836
U16-h07-54-338	coarse calcite	4.269	595.937	199.008	13.363	0.149	0.049	0.017	167.839	6.458
U16-h07-54-338	coarse calcite	3.324	143.390	16.980	5.820	-0.001	0.004	0.000	132.907	3.448

Sample ID	SampleType	Mn LOD (ppm)	Fe(ppm)	2SE (ppm)	Fe LOD (ppm)	Rb (ppm)	2SE (ppm)	Rb LOD (ppm)	Sr (ppm)	2SE (ppm)
U16-h07-54-338	coarse calcite	6.350	101.323	10.332	8.238	0.013	0.012	0.011	115.545	3.750
U16-h07-54-338	coarse calcite	0.848	297.995	91.709	4.505	0.087	0.029	0.044	113.084	10.059
U16-h07-54-338	coarse calcite	5.553	40.290	4.213	5.413	-0.002	0.003	0.017	134.109	14.050
U16-h07-54-5	matrix cement	0.454	80.514	14.056	4.020	0.022	0.014	0.000	167.774	20.548
U16-h07-54-5	matrix cement	0.464	136.985	18.988	4.529	0.415	0.104	0.000	57.905	3.193
U16-h07-54-5	matrix cement	0.474	442.481	85.385	4.199	1.560	0.243	0.000	112.673	13.104
U16-h07-54-5	matrix cement	0.441	225.068	69.880	3.912	0.707	0.247	0.000	131.875	7.158
U16-h07-54-5	matrix cement	0.670	453.884	180.271	3.026	1.272	0.143	0.000	83.823	3.060
U16-h07-54-5	matrix cement	0.961	164.282	20.242	2.183	0.784	0.098	0.000	104.424	6.257
U16-h07-54-5	matrix cement	0.476	713.926	205.472	4.646	1.035	0.274	0.000	99.623	4.668
U16-h07-54-5	matrix cement	0.451	177.450	10.998	3.997	0.468	0.086	0.000	90.965	5.023
U16-h07-54-5	matrix cement	0.668	65.295	4.283	3.017	0.042	0.019	0.000	113.072	13.185
U16-h07-54-5	matrix cement	0.473	384.990	49.194	4.187	1.843	0.114	0.000	115.741	7.335
U16-h07-54-5	matrix cement	0.825	171.088	17.340	5.076	0.333	0.108	0.035	83.800	3.351
U16-h07-54-5	matrix cement	0.463	111.590	8.589	4.099	0.287	0.065	0.000	165.787	15.090
U16-h07-54-5	matrix cement	0.461	250.818	32.449	4.505	0.243	0.061	0.000	87.606	3.835
U16-h07-54-5	matrix cement	0.469	115.653	17.135	4.156	0.145	0.060	0.000	138.154	11.464
U16-h07-54-5	matrix cement	0.967	55.808	15.658	2.198	-0.003	0.000	0.000	52.817	5.865
U16-h07-54-5	matrix cement	0.463	112.002	8.178	4.102	0.065	0.030	0.000	130.892	7.490
U16-h07-54-5	matrix cement	0.471	52.803	6.155	4.597	0.002	0.008	0.000	94.962	8.658
U16-h07-54-5	ooid	0.963	2881.302	876.940	5.227	12.847	1.205	0.017	77.966	2.393
U16-h07-54-5	ooid	1.397	134.100	16.197	2.361	0.570	0.140	0.022	111.692	7.139
U16-h07-54-5	ooid	0.697	64.859	6.381	3.233	0.180	0.042	0.023	106.011	6.834
U16-h07-54-5	ooid	0.589	469.440	101.990	4.752	2.298	0.447	0.019	101.091	4.842
U16-h07-54-5	ooid	1.515	523.530	208.579	2.561	4.126	0.301	0.024	103.897	7.950
U16-h07-54-5	ooid	0.818	158.766	22.112	4.439	0.498	0.140	0.014	149.992	12.806
U16-h07-54-5	ooid	0.610	592.331	171.719	4.917	2.788	0.241	0.019	100.959	2.675
U16-h07-54-5	ooid	1.526	2367.615	617.812	2.580	2.521	0.437	0.024	128.838	3.683
U16-h07-54-5	ooid	0.822	355.735	65.751	5.060	2.416	0.245	0.034	83.752	3.400
U16-h07-54-5	ooid	0.697	621.736	157.386	3.315	1.783	0.259	0.023	95.693	3.711
U16-h07-54-5	ooid	0.694	625.755	66.846	3.302	2.937	0.248	0.023	122.796	5.118
U16-h07-54-5	ooid	0.575	191.811	29.759	4.636	0.990	0.163	0.018	87.050	3.442
U16-h07-54-5	ooid	1.456	120.176	15.129	2.461	0.494	0.113	0.023	86.698	5.130

Sample ID	SampleType	Mn LOD (ppm)	Fe(ppm)	2SE (ppm)	Fe LOD (ppm)	Rb (ppm)	2SE (ppm)	Rb LOD (ppm)	Sr (ppm)	2SE (ppm)
U16-h07-54-5	ooid	0.595	141.992	9.721	4.800	0.677	0.086	0.019	85.385	4.415
U16-h07-54-5	ooid	1.781	90.840	10.345	3.011	0.095	0.028	0.028	102.346	6.631
U16-h07-54-5	ooid	0.865	194.495	24.366	5.325	0.672	0.099	0.036	101.727	4.759
U16-h07-54-5	ooid	0.564	362.096	147.908	4.707	0.679	0.141	0.018	114.608	7.087
U16-h07-54-5	ooid	0.582	101.342	11.861	4.696	0.041	0.020	0.018	157.668	13.814
U16-h07-54-5	ooid	0.780	130.031	11.577	4.234	0.203	0.110	0.014	76.841	3.584
U16-h07-54-5	ooid	0.575	326.276	53.095	4.637	1.130	0.107	0.018	94.706	5.216
U16-h07-54-5	ooid	1.529	63.046	5.576	2.584	0.049	0.018	0.024	74.576	8.565
U16-h07-54-5	ooid	0.849	71.930	8.556	4.606	0.078	0.034	0.015	363.897	27.124
U16-h07-54-5	ooid	1.428	108.969	5.728	2.413	0.064	0.030	0.022	83.207	3.321
U16-h07-54-5	ooid	0.593	170.861	26.088	4.784	0.502	0.219	0.019	88.171	7.494
U16-h07-54-5	ooid	0.828	46.978	4.611	4.493	-0.004	0.000	0.015	93.135	7.606
U16-h07-54-5	vein 1	0.830	62.611	6.479	5.564	0.002	0.005	0.000	469.626	62.061
U16-h07-54-5	vein 1	1.542	99.564	9.438	4.402	-0.003	0.000	0.028	185.806	18.179
U16-h07-54-5	vein 1	2.790	85.348	8.329	2.402	0.002	0.005	0.015	178.624	19.529
U16-h07-54-5	vein 1	2.670	124.861	13.958	2.299	0.029	0.014	0.015	118.119	8.969
U16-h07-54-5	vein 1	2.814	78.471	6.443	2.423	0.733	0.082	0.016	149.873	14.872
U16-h07-54-5	vein 1	2.730	105.749	9.892	2.350	0.001	0.005	0.015	43.702	5.083
U16-h07-54-5	vein 2	0.789	47.658	3.939	5.560	0.001	0.005	0.000	515.863	15.189
U16-h07-54-5	vein 2	0.811	167.682	11.856	5.436	-0.003	0.000	0.000	209.396	15.641
U16-h07-54-5	vein 2	0.808	57.975	4.324	5.416	-0.003	0.000	0.000	186.506	16.331
U16-h07-67-129	darker vein	0.919	50.015	5.016	5.518	0.051	0.044	0.038	432.329	20.042
U16-h07-67-129	darker vein	0.933	99.348	9.101	10.554	0.014	0.010	0.000	476.630	28.488
U16-h07-67-129	darker vein	0.743	154.957	22.222	4.066	0.024	0.013	0.012	394.382	20.816
U16-h07-67-129	darker vein	0.934	167.069	13.882	10.587	0.032	0.016	0.000	684.814	34.360
U16-h07-67-129	darker vein	0.946	158.223	21.503	5.651	0.014	0.010	0.039	1326.284	64.186
U16-h07-67-129	darker vein	0.931	166.884	12.074	5.584	0.020	0.012	0.039	566.022	35.133
U16-h07-67-129	darker vein	0.753	253.240	14.153	4.110	0.000	0.005	0.012	405.790	28.193
U16-h07-67-129	lighter vein	3.171	53.083	5.529	5.909	0.001	0.005	0.036	85.680	3.302
U16-h07-67-129	lighter vein	0.973	47.619	4.172	10.945	0.053	0.023	0.000	126.213	3.130
U16-h07-67-129	lighter vein	1.489	49.886	5.081	3.482	0.011	0.014	0.009	80.958	2.565
U16-h07-67-129	lighter vein	3.108	47.779	4.473	5.828	0.066	0.028	0.036	106.779	3.496
U16-h07-67-129	lighter vein	3.014	44.860	3.815	5.600	0.037	0.017	0.035	97.079	3.625

Sample ID	SampleType	Mn LOD (ppm)	Fe(ppm)	2SE (ppm)	Fe LOD (ppm)	Rb (ppm)	2SE (ppm)	Rb LOD (ppm)	Sr (ppm)	2SE (ppm)
U16-h07-67-129	lighter vein	3.277	42.638	3.531	6.121	-0.004	0.000	0.038	138.204	4.250
U16-h07-67-129	lighter vein	0.988	34.722	3.856	11.152	-0.003	0.003	0.000	135.665	3.181
U16-h07-67-129	ooid and matrix	6.283	112307.300	25084.480	27.558	648.186	79.363	0.000	212.720	12.893
U16-h07-67-129	ooid and matrix	0.636	1584.135	624.294	3.467	5.782	0.724	0.016	128.324	6.059
U16-h07-67-129	ooid and matrix	1.088	10481.670	2960.191	16.694	34.326	5.972	0.292	141.855	8.352
U16-h07-67-129	ooid and matrix	1.260	802.962	256.024	1.476	19.463	1.377	0.298	201.387	20.192
U16-h07-67-129	ooid and matrix	1.292	4843.912	1986.684	12.576	50.721	19.555	0.118	202.795	13.401
U16-h07-67-129	ooid and matrix	1.150	2430.812	1157.292	10.418	12.471	0.994	0.128	184.334	7.631
U16-h07-67-129	ooid and matrix	1.308	429.031	113.952	4.740	1.965	0.139	0.035	192.924	8.534
U16-h07-67-129	ooid and matrix	11.621	497.465	98.868	1062.400	5.251	0.385	5.298	134.015	8.047
U16-h07-67-129	ooid and matrix	0.755	909.419	330.845	51.460	14.355	0.974	0.341	167.564	7.358
U16-h07-67-129	ooid and matrix	1.276	5193.666	1253.881	11.576	29.979	3.049	0.142	278.833	7.250
U16-h07-67-129	ooid and matrix	0.689	4200.025	1408.134	3.760	14.627	4.542	0.018	239.273	17.573
U16-h07-67-129	ooid and matrix	0.861	109.454	28.718	5.492	1.744	0.299	0.122	95.591	11.895
U16-h07-67-129	ooid and matrix	0.656	253.693	25.780	6.111	4.867	0.349	0.018	190.027	8.072
U16-h07-67-129	ooid and matrix	1.425	146.463	9.049	4.710	0.097	0.033	0.000	102.731	5.056
U16-h07-67-129	ooid and matrix	1.094	478.394	179.069	4.800	2.737	0.183	0.000	129.413	5.354
U16-h07-67-129	ooid and matrix	0.865	43.586	14.177	5.501	0.015	0.014	0.122	42.466	2.325
U16-h07-67-129	ooid and matrix	1.450	127.394	22.527	4.801	2.442	0.733	0.000	177.574	4.036
U16-h07-67-129	ooid and matrix	0.713	195.612	79.082	48.745	0.034	0.018	0.322	197.292	6.952
U16-h07-67-129	ooid and matrix	1.079	230.190	99.308	9.808	0.081	0.027	0.120	273.000	7.264
U16-h07-67-129	ooid and matrix	0.638	325.069	162.819	3.483	0.521	0.078	0.017	237.878	14.818
U16-h07-67-129	ooid and matrix	0.813	270.075	75.325	5.177	0.044	0.019	0.115	318.691	9.594
U16-h07-67-129	ooid and matrix	1.012	105.341	15.182	3.783	1.308	0.456	0.039	138.324	5.123
U16-h07-67-129	ooid and matrix	0.647	56.473	5.244	6.019	0.012	0.009	0.018	239.490	12.531
U16-h07-67-129	ooid and matrix	1.488	73.539	17.368	5.433	0.043	0.023	0.000	139.277	4.776
U16-h07-67-129	ooid and matrix	1.048	47.500	4.578	3.922	-0.002	0.005	0.041	127.266	3.488

Sample ID	SampleType	Sr LOD (ppm)	Y (ppm)	2SE (ppm)	Y LOD (ppm)	Ba (ppm)	2SE (ppm)	Ba LOD (ppm)	La (ppm)	La LOD (ppm)	2SE (ppm)
U16-h07-13b-11	matrix	0.166	3.282	0.341	0.015	161.860	17.175	0.000	4.886	0.000	0.762
U16-h07-13b-11	matrix	0.144	0.540	0.050	0.013	86.448	3.785	0.000	1.304	0.000	0.101
U16-h07-13b-11	matrix	0.144	0.897	0.104	0.013	30.662	2.623	0.000	1.096	0.000	0.066
U16-h07-13b-11	matrix	0.141	1.625	0.116	0.013	39.518	2.961	0.000	1.643	0.000	0.084
U16-h07-13b-11	matrix	0.149	1.051	0.071	0.014	35.599	2.244	0.000	1.056	0.000	0.093
U16-h07-13b-11	matrix	0.151	0.870	0.084	0.014	51.115	3.879	0.000	1.259	0.000	0.131
U16-h07-13b-11	matrix	0.150	1.712	0.212	0.014	18.458	1.612	0.000	2.989	0.000	0.404
U16-h07-13b-11	matrix	0.144	2.044	0.178	0.013	69.713	3.874	0.000	2.092	0.000	0.189
U16-h07-13b-11	matrix	0.150	4.250	0.283	0.014	81.410	4.148	0.000	2.829	0.000	0.152
U16-h07-13b-11	matrix	0.147	1.898	0.308	0.013	83.614	6.999	0.000	1.590	0.000	0.165
U16-h07-13b-11	matrix	0.140	2.453	0.150	0.013	75.208	4.241	0.000	2.466	0.000	0.129
U16-h07-13b-11	matrix	0.136	1.517	0.178	0.012	52.589	5.041	0.000	1.429	0.000	0.120
U16-h07-13b-11	matrix	0.145	1.917	0.116	0.013	72.071	3.060	0.000	1.721	0.000	0.073
U16-h07-13b-11	matrix	0.141	2.924	0.135	0.013	106.048	6.082	0.000	2.573	0.000	0.137
U16-h07-13b-11	matrix	0.139	2.102	0.129	0.013	80.866	4.960	0.000	3.160	0.000	0.194
U16-h07-13b-11	matrix	0.144	2.845	0.323	0.013	70.633	2.914	0.000	2.296	0.000	0.190
U16-h07-13b-11	matrix	0.142	2.008	0.133	0.013	80.827	3.729	0.000	2.193	0.000	0.126
U16-h07-13b-11	matrix	0.143	1.335	0.106	0.013	46.869	2.484	0.000	1.067	0.000	0.084
U16-h07-13b-11	matrix	0.144	3.810	0.218	0.013	120.950	8.629	0.000	3.019	0.000	0.222
U16-h07-13b-11	matrix	0.151	3.055	0.173	0.014	43.755	3.558	0.000	3.615	0.000	0.266
U16-h07-13b-11	matrix	0.144	2.166	0.141	0.013	73.520	2.815	0.000	2.931	0.000	0.172
U16-h07-13b-11	vein 1	0.141	3.215	0.317	0.013	313.274	10.214	0.000	5.683	0.000	0.449
U16-h07-13b-11	vein 1	0.147	15.724	0.535	0.013	16.972	1.362	0.000	15.778	0.000	0.438
U16-h07-13b-11	vein 1	0.142	15.099	0.484	0.013	15.403	0.928	0.000	19.617	0.000	0.665
U16-h07-13b-11	vein 1	0.142	8.865	0.398	0.013	198.405	10.256	0.000	12.622	0.000	0.566
U16-h07-13b-11	vein 1	0.140	5.441	0.524	0.013	39.950	2.231	0.000	15.681	0.000	1.656
U16-h07-13b-11	vein 1	0.139	12.888	0.438	0.013	39.625	2.989	0.000	36.092	0.000	1.309
U16-h07-13b-11	vein 1	0.143	10.794	0.576	0.013	43.157	4.982	0.000	13.157	0.000	0.514
U16-h07-13b-11	vein 2	0.140	0.816	0.187	0.013	160.805	6.285	0.000	1.085	0.000	0.149
U16-h07-13b-11	vein 2	0.148	0.533	0.270	0.014	52.040	1.510	0.000	0.191	0.000	0.092
U16-h07-13b-11	vein 2	0.145	0.314	0.040	0.013	79.378	7.574	0.000	0.375	0.000	0.067
U16-h07-13b-11	vein 2	0.151	0.037	0.011	0.014	4.481	1.085	0.000	0.014	0.000	0.006
U16-h07-13b-11	vein 2	0.152	0.102	0.023	0.014	5.396	0.652	0.000	0.076	0.000	0.019

Sample ID	SampleType	Sr LOD (ppm)	Y (ppm)	2SE (ppm)	Y LOD (ppm)	Ba (ppm)	2SE (ppm)	Ba LOD (ppm)	La (ppm)	La LOD (ppm)	2SE (ppm)
U16-h07-13b-11	vein 2	0.147	0.031	0.009	0.013	3.629	0.422	0.000	0.013	0.000	0.006
U16-h07-13b-11	vein 3	0.150	2.480	0.223	0.014	20.978	1.487	0.000	3.822	0.000	0.373
U16-h07-13b-11	vein 3	0.147	3.658	0.273	0.014	28.531	2.664	0.000	6.738	0.000	0.694
U16-h07-13b-11	vein 3	0.150	7.300	0.794	0.014	4.016	0.865	0.000	5.585	0.000	0.698
U16-h07-13b-31	dk ooid	2.569	3.289	0.375	0.153	10.888	1.547	0.187	2.799	0.123	0.217
U16-h07-13b-31	dk ooid	0.016	8.890	0.513	0.000	19.853	1.969	0.000	6.799	0.010	0.316
U16-h07-13b-31	dk ooid	2.562	5.409	0.686	0.152	10.093	1.608	0.187	4.832	0.123	0.472
U16-h07-13b-31	dk ooid	2.526	6.493	0.323	0.150	14.415	1.314	0.184	4.685	0.121	0.249
U16-h07-13b-31	dk ooid	0.013	8.213	0.392	0.000	19.376	1.765	0.000	5.363	0.008	0.241
U16-h07-13b-31	dk ooid	0.015	11.039	0.601	0.000	27.042	2.580	0.000	7.679	0.009	0.567
U16-h07-13b-31	matrix cement	2.555	3.821	0.344	0.152	11.286	1.166	0.186	3.768	0.122	0.333
U16-h07-13b-31	matrix cement	2.402	6.458	0.342	0.248	15.070	1.571	0.094	4.797	0.118	0.257
U16-h07-13b-31	matrix cement	2.533	14.754	1.781	0.150	16.221	2.227	0.184	9.000	0.121	1.102
U16-h07-13b-31	matrix cement	2.470	7.004	0.493	0.147	9.188	1.073	0.180	4.776	0.118	0.197
U16-h07-13b-31	matrix cement	2.449	8.355	0.521	0.252	20.105	2.101	0.096	4.819	0.120	0.406
U16-h07-13b-31	matrix cement	2.586	9.735	0.602	0.154	64.271	6.003	0.188	5.990	0.124	0.533
U16-h07-13b-31	matrix cement	2.490	7.645	0.777	0.148	23.199	1.904	0.181	5.389	0.119	0.324
U16-h07-13b-31	matrix cement	2.335	8.201	0.295	0.241	4.599	0.807	0.092	5.784	0.114	0.326
U16-h07-13b-31	matrix cement	0.479	8.641	0.330	0.064	11.632	0.736	0.000	5.120	0.093	0.205
U16-h07-13b-31	matrix cement	0.475	9.079	0.388	0.064	14.562	1.407	0.000	5.242	0.092	0.200
U16-h07-13b-31	matrix cement	2.386	8.821	0.277	0.246	11.139	1.077	0.094	5.128	0.117	0.199
U16-h07-13b-31	matrix cement	2.410	7.860	0.550	0.248	5.923	0.673	0.095	3.923	0.118	0.234
U16-h07-13b-31	ooid	1.756	9.424	0.489	0.142	55.014	4.269	0.177	6.637	0.099	0.342
U16-h07-13b-31	ooid	7.181	3.759	0.247	0.230	8.008	0.513	0.619	2.566	0.188	0.214
U16-h07-13b-31	ooid	1.768	12.278	1.106	0.143	52.015	4.596	0.178	7.735	0.100	0.693
U16-h07-13b-31	ooid	0.153	6.089	0.348	0.077	8.628	1.035	0.200	3.362	0.079	0.146
U16-h07-13b-31	ooid	1.463	13.887	0.889	0.000	1.813	0.377	0.000	5.837	0.016	0.303
U16-h07-13b-31	ooid	1.013	5.931	0.302	0.084	8.576	0.705	0.210	5.001	0.102	0.276
U16-h07-13b-31	ooid	1.573	10.458	0.717	0.000	45.675	4.294	0.000	5.959	0.017	0.409
U16-h07-13b-31	ooid	0.148	9.566	1.239	0.075	21.238	2.575	0.194	6.158	0.076	0.618
U16-h07-13b-31	ooid	0.077	6.991	0.345	0.026	4.078	0.492	0.000	6.260	0.017	0.371
U16-h07-13b-31	ooid	1.006	12.924	0.736	0.084	29.895	1.921	0.208	8.392	0.102	0.342
U16-h07-13b-31	ooid	1.778	7.681	0.375	0.143	28.573	2.821	0.178	4.866	0.100	0.224

Sample ID	SampleType	Sr LOD (ppm)	Y (ppm)	2SE (ppm)	Y LOD (ppm)	Ba (ppm)	2SE (ppm)	Ba LOD (ppm)	La (ppm)	La LOD (ppm)	2SE (ppm)
U16-h07-13b-31	ooid	7.161	9.381	0.494	0.229	30.441	3.053	0.618	5.719	0.187	0.378
U16-h07-13b-31	ooid	1.710	7.843	0.339	0.138	11.609	1.310	0.172	5.538	0.096	0.295
U16-h07-13b-31	ooid	1.739	9.542	0.579	0.140	30.971	3.427	0.175	5.523	0.098	0.344
U16-h07-13b-31	ooid	7.123	10.531	0.877	0.228	18.178	1.358	0.615	6.952	0.186	0.409
U16-h07-13b-31	ooid	1.007	8.804	0.473	0.084	21.179	1.280	0.208	5.426	0.102	0.271
U16-h07-13b-31	ooid	0.080	9.223	0.365	0.028	36.115	2.635	0.000	5.806	0.018	0.279
U16-h07-13b-31	ooid	0.077	11.067	0.729	0.027	22.446	2.174	0.000	7.137	0.017	0.497
U16-h07-13b-31	ooid	1.704	8.914	0.440	0.137	24.162	2.137	0.171	5.277	0.096	0.213
U16-h07-13b-31	ooid	1.698	9.237	0.284	0.137	23.230	1.320	0.170	6.181	0.095	0.220
U16-h07-13b-31	ooid	0.074	8.645	0.442	0.025	18.993	1.707	0.000	6.147	0.016	0.291
U16-h07-13b-31	ooid	0.073	7.705	0.369	0.025	10.682	0.893	0.000	5.046	0.016	0.225
U16-h07-13b-31	ooid	1.664	7.295	0.339	0.134	12.251	0.920	0.167	4.560	0.094	0.184
U16-h07-13b-31	ooid	0.148	8.394	0.429	0.075	21.433	1.427	0.194	4.659	0.076	0.230
U16-h07-13b-31	vein-1	1.242	13.648	1.543	0.024	61.703	11.390	1.158	9.969	0.051	0.860
U16-h07-13b-31	vein-1	1.470	1.684	0.447	0.000	9.799	1.139	0.000	1.655	0.016	0.411
U16-h07-13b-31	vein-1	1.122	1.316	0.112	0.022	61.967	5.494	1.046	1.849	0.046	0.155
U16-h07-13b-31	vein-1	1.649	1.699	0.197	0.312	148.881	10.708	0.366	1.058	0.273	0.120
U16-h07-13b-31	vein-1	1.086	1.694	0.138	0.021	127.955	8.634	1.012	1.086	0.045	0.105
U16-h07-13b-31	vein-1	1.016	1.426	0.165	0.020	89.008	6.114	0.948	1.578	0.042	0.182
U16-h07-13b-81	coarse calcite	0.412	-0.001	0.000	0.005	0.094	0.093	0.757	0.000	0.006	0.000
U16-h07-13b-81	coarse calcite	0.426	-0.085	0.016	0.005	-2.663	0.460	0.782	-0.065	0.006	0.013
U16-h07-13b-81	coarse calcite	0.395	-0.264	0.033	0.004	-7.588	0.762	0.726	-0.210	0.006	0.024
U16-h07-13b-81	coarse calcite	81.265	-0.596	0.152	0.343	-21.782	2.507	9.712	-0.572	0.272	0.100
U16-h07-13b-81	vein 1	49.058	18.976	1.620	2.824	32.160	8.990	1.999	5.460	3.316	0.840
U16-h07-13b-81	vein 1	44.394	20.902	2.111	5.573	0.253	1.206	2.699	17.069	4.610	1.293
U16-h07-13b-81	vein 1	37.724	3.107	0.310	2.171	5.116	0.615	1.538	2.686	2.550	0.457
U16-h07-13b-81	vein 1	15.632	3.575	1.421	2.992	0.420	0.266	0.516	6.403	2.507	1.322
U16-h07-13b-81	vein 1	0.377	5.254	0.529	0.004	9.285	0.782	0.693	3.957	0.005	0.315
U16-h07-13b-81	vein 1	8.939	7.186	0.727	5.220	2.065	0.406	1.346	4.126	3.181	0.461
U16-h07-13b-81	vein 1	12.349	7.027	1.175	4.132	1.917	0.545	1.195	3.242	2.441	0.603
U16-h07-13b-81	vein 1	12.643	4.778	1.231	4.230	0.241	0.267	1.223	2.410	2.499	0.835
U16-h07-13b-81	vein 1	15.559	1.336	0.311	2.978	0.205	0.308	0.514	0.933	2.495	0.234
U16-h07-24-145	ooids and cement	0.000	0.154	0.031	0.000	18.989	1.437	0.000	0.129	0.000	0.020

Sample ID	SampleType	Sr LOD (ppm)	Y (ppm)	2SE (ppm)	Y LOD (ppm)	Ba (ppm)	2SE (ppm)	Ba LOD (ppm)	La (ppm)	La LOD (ppm)	2SE (ppm)
U16-h07-24-145	ooids and cement	0.000	1.690	0.079	0.000	72.918	2.804	0.000	1.173	0.000	0.085
U16-h07-24-145	ooids and cement	0.000	1.320	0.088	0.000	51.092	3.457	0.000	1.087	0.000	0.071
U16-h07-24-145	ooids and cement	0.000	1.099	0.087	0.000	67.567	3.743	0.000	1.044	0.000	0.069
U16-h07-24-145	ooids and cement	0.000	1.757	0.107	0.000	38.962	2.862	0.000	1.643	0.000	0.098
U16-h07-24-145	ooids and cement	0.000	0.006	0.005	0.000	4.086	0.861	0.000	0.002	0.000	0.003
U16-h07-24-145	ooids and cement	0.000	1.280	0.103	0.000	63.590	3.068	0.000	1.099	0.000	0.064
U16-h07-24-145	ooids and cement	0.000	1.146	0.092	0.000	69.318	4.039	0.000	0.950	0.000	0.074
U16-h07-24-145	vein-1	7.006	0.700	0.057	0.014	63.175	5.426	0.628	0.909	0.067	0.129
U16-h07-24-145	vein-1	6.460	0.542	0.049	0.013	85.626	8.771	0.579	0.632	0.062	0.057
U16-h07-24-145	vein-1	6.474	0.779	0.061	0.013	61.540	2.507	0.580	1.082	0.062	0.104
U16-h07-24-145	vein-1	6.519	1.137	0.104	0.013	104.194	5.051	0.584	0.638	0.062	0.056
U16-h07-24-145	vein-1	6.290	0.688	0.039	0.013	75.923	9.645	0.564	0.586	0.060	0.058
U16-h07-24-145	vein-1	0.171	0.709	0.050	0.092	138.318	6.780	0.100	0.643	0.074	0.065
U16-h07-24-145	vein-1	0.171	0.608	0.073	0.092	156.510	23.940	0.100	0.581	0.074	0.093
U16-h07-24-145	vein-1	0.160	1.520	0.110	0.086	162.239	10.488	0.093	1.769	0.070	0.109
U16-h07-24-145	vein-2	6.796	1.165	0.096	0.014	71.169	3.758	0.595	1.344	0.064	0.119
U16-h07-24-145	vein-2	6.698	2.828	0.511	0.014	333.526	45.888	0.587	3.065	0.063	0.536
U16-h07-24-145	vein-2	6.876	-2.445	0.386	0.014	-447.669	58.996	0.603	-1.368	0.065	0.240
U16-h07-24-145	vein-3	43.618	-20.107	2.077	0.386	-123.522	21.565	17.318	5.768	0.258	1.461
U16-h07-24-145	vein-3	7.017	-0.691	0.087	0.014	-10.979	1.027	0.615	-0.698	0.066	0.093
U16-h07-24-145	vein-3	150.310	-0.637	0.072	0.380	-2.585	1.538	3.611	-0.715	0.445	0.114
U16-h07-24-145	vein-3	6.845	-0.360	0.049	0.014	-7.433	0.529	0.600	-0.394	0.064	0.037
U16-h07-24-145	vein-3	150.620	-0.696	0.058	0.371	-8.734	0.623	3.535	-0.557	0.441	0.049
U16-h07-24-145	vein-3	6.876	-0.611	0.062	0.014	-7.486	0.637	0.602	-0.548	0.065	0.059
U16-h07-24-145	vein-3	7.103	0.068	0.013	0.014	-3.758	0.420	0.622	0.049	0.067	0.014
U16-h07-24-145	vein-4	44.492	18.369	22.262	0.400	102.135	245.311	17.961	-2.226	0.265	1.801
U16-h07-24-145	vein-4	0.000	1.826	0.120	0.000	124.031	6.884	0.000	1.329	0.000	0.091
U16-h07-24-145	vein-4	0.000	1.405	0.085	0.000	152.763	10.714	0.000	0.842	0.000	0.101
U16-h07-24-145	vein-4	0.219	0.441	0.048	0.000	34.726	1.854	0.162	0.342	0.000	0.045
U16-h07-24-145	vein-4	44.318	-34.859	55.331	0.398	2079.077	6941.797	17.891	27.460	0.264	45.718
U16-h07-24-145	vein-4	0.214	3.764	0.240	0.000	117.382	6.486	0.158	4.045	0.000	0.183
U16-h07-24-145	vein-4	46.563	-128.962	174.430	0.412	65.764	30.332	18.487	-265.146	0.276	261.097
U16-h07-24-145	vein-4	0.215	5.150	0.389	0.000	203.618	30.683	0.159	5.863	0.000	0.519

Sample ID	SampleType	Sr LOD (ppm)	Y (ppm)	2SE (ppm)	Y LOD (ppm)	Ba (ppm)	2SE (ppm)	Ba LOD (ppm)	La (ppm)	La LOD (ppm)	2SE (ppm)
U16-h07-24-145	vein-4	0.230	5.577	0.764	0.000	186.784	43.202	0.170	5.374	0.000	2.288
U16-h07-24-145	vein-4	42.817	1.798	0.319	0.385	-29.751	32.789	17.285	2.256	0.255	0.319
U16-h07-24-145	vein-4	0.225	11.187	2.384	0.000	69.560	26.030	0.167	11.525	0.000	1.175
U16-h07-24-145	vein-4	0.230	21.559	3.147	0.000	111.126	38.046	0.170	24.780	0.000	4.257
U16-h07-24-145	vein-4	153.010	0.586	0.185	0.386	-32.369	4.077	3.676	0.797	0.453	0.145
U16-h07-24-145	vein-4	146.110	0.147	0.106	0.369	-57.523	4.041	3.511	-0.112	0.433	0.123
U16-h07-24-145	vein-4	45.329	1.761	3.251	0.407	-379.387	230.349	18.299	1.689	0.270	2.273
U16-h07-24-145	vein-4	42.016	-1.017	10.655	0.377	99.914	433.548	16.961	-0.500	0.250	4.383
U16-h07-24-145	vein-6	0.000	0.008	0.006	0.000	10.560	0.632	0.000	0.008	0.000	0.005
U16-h07-24-145	vein-6	0.000	1.029	0.082	0.000	54.796	4.511	0.000	0.803	0.000	0.063
U16-h07-24-145	vein-6	0.000	1.329	0.084	0.000	77.554	5.731	0.000	1.055	0.000	0.065
U16-h07-24-145	vein-6	0.000	1.520	0.086	0.000	62.210	3.373	0.000	1.273	0.000	0.097
U16-h07-24-145	vein-6	0.000	1.234	0.071	0.000	88.191	5.166	0.000	1.144	0.000	0.084
U16-h07-24-145	vein-7	0.000	1.660	0.240	0.000	12.385	1.338	0.000	0.921	0.000	0.109
U16-h07-25-167	coarse calcite	59.263	-0.410	0.059	0.831	21.326	3.395	7.696	1.943	0.492	0.141
U16-h07-25-167	coarse calcite	60.558	1.567	0.301	0.849	12.643	5.081	7.864	0.522	0.503	0.084
U16-h07-25-167	coarse calcite	63.458	3.631	0.213	0.890	4.623	0.765	8.240	0.580	0.527	0.088
U16-h07-25-167	coarse calcite	62.745	0.373	0.084	0.880	5.215	0.860	8.148	-0.046	0.521	0.022
U16-h07-25-167	dk ooid	59.823	0.882	0.075	0.839	38.865	3.749	7.768	0.913	0.497	0.077
U16-h07-25-167	dk ooid	0.120	1.799	0.221	0.000	72.522	6.617	0.000	1.548	0.000	0.146
U16-h07-25-167	dk ooid	0.126	1.983	0.146	0.000	45.713	2.714	0.000	1.684	0.000	0.100
U16-h07-25-167	dk ooid	1.712	1.542	0.361	0.000	31.641	2.111	0.424	1.397	0.022	0.217
U16-h07-25-167	dk ooid	0.155	2.497	0.105	0.026	45.242	2.416	0.000	2.083	0.069	0.117
U16-h07-25-167	dk ooid	0.293	3.372	0.565	0.016	66.486	3.097	0.092	3.374	0.009	0.625
U16-h07-25-167	dk ooid	1.725	1.337	0.112	0.000	24.482	2.815	0.439	1.391	0.023	0.112
U16-h07-25-167	dk ooid	0.116	1.334	0.092	0.000	31.543	1.475	0.000	1.275	0.000	0.087
U16-h07-25-167	dk ooid	1.708	1.440	0.071	0.000	52.106	3.730	0.435	1.315	0.023	0.086
U16-h07-25-167	dk ooid	0.147	1.426	0.085	0.025	40.766	2.386	0.000	1.300	0.066	0.097
U16-h07-25-167	dk ooid	0.149	2.164	0.133	0.025	33.264	2.511	0.000	2.075	0.066	0.100
U16-h07-25-167	dk ooid	1.635	1.454	0.106	0.000	56.486	3.184	0.416	1.218	0.022	0.085
U16-h07-25-167	dk ooid	0.289	1.346	0.124	0.016	16.010	1.383	0.091	1.019	0.009	0.105
U16-h07-25-167	dk ooid	1.670	1.587	0.127	0.000	42.981	2.463	0.425	1.324	0.022	0.085
U16-h07-25-167	dk ooid	0.150	1.523	0.097	0.025	34.803	2.900	0.000	1.247	0.067	0.088

Sample ID	SampleType	Sr LOD (ppm)	Y (ppm)	2SE (ppm)	Y LOD (ppm)	Ba (ppm)	2SE (ppm)	Ba LOD (ppm)	La (ppm)	La LOD (ppm)	2SE (ppm)
U16-h07-25-167	dk ooid	1.637	1.516	0.082	0.000	42.103	2.092	0.405	1.460	0.021	0.099
U16-h07-25-167	dk ooid	0.147	1.364	0.087	0.025	41.058	1.995	0.000	1.490	0.066	0.093
U16-h07-25-167	dk ooid	0.152	1.328	0.094	0.026	46.606	2.830	0.000	1.289	0.068	0.071
U16-h07-25-167	dk ooid	0.259	1.700	0.109	0.015	40.844	2.387	0.081	1.584	0.008	0.116
U16-h07-25-167	dk ooid	0.151	1.563	0.095	0.026	44.447	2.034	0.000	1.400	0.067	0.101
U16-h07-25-167	dk ooid	1.648	1.836	0.113	0.000	41.622	1.947	0.419	1.765	0.022	0.115
U16-h07-25-167	dk ooid	1.635	2.648	0.270	0.000	36.444	2.653	0.405	2.792	0.021	0.429
U16-h07-25-167	early vein	0.022	0.680	0.131	0.000	9.560	1.696	0.126	0.470	0.000	0.076
U16-h07-25-167	early vein	0.022	1.185	0.067	0.000	11.592	1.106	0.126	1.125	0.000	0.105
U16-h07-25-167	early vein	0.023	1.341	0.108	0.000	8.400	0.662	0.128	0.536	0.000	0.053
U16-h07-25-167	early vein	0.023	0.705	0.097	0.000	23.053	3.617	0.127	0.625	0.000	0.073
U16-h07-25-167	late vein	0.024	3.591	0.169	0.000	226.349	20.847	0.136	1.365	0.000	0.103
U16-h07-25-167	late vein	0.023	2.946	0.369	0.000	161.129	15.832	0.130	1.469	0.000	0.169
U16-h07-25-167	late vein	0.022	7.682	0.460	0.000	59.795	7.304	0.125	3.331	0.000	0.182
U16-h07-25-167	late vein	0.022	5.452	0.219	0.000	22.334	1.510	0.122	3.353	0.000	0.164
U16-h07-25-167	late vein	0.023	5.706	0.263	0.000	23.066	1.230	0.127	4.819	0.000	0.201
U16-h07-25-167	lt ooid	0.022	1.636	0.089	0.000	40.549	1.993	0.124	1.523	0.000	0.115
U16-h07-25-167	lt ooid	0.021	1.767	0.127	0.000	54.782	4.195	0.123	1.593	0.000	0.106
U16-h07-25-167	lt ooid	0.021	1.385	0.096	0.000	35.031	2.009	0.124	1.456	0.000	0.098
U16-h07-25-167	lt ooid	0.152	2.740	0.166	0.026	39.556	1.963	0.000	2.379	0.068	0.167
U16-h07-25-167	lt ooid	0.147	1.420	0.091	0.025	41.923	3.181	0.000	1.366	0.065	0.084
U16-h07-25-167	lt ooid	0.021	1.513	0.090	0.000	43.185	2.075	0.120	1.316	0.000	0.095
U16-h07-25-167	lt ooid	0.021	1.989	0.140	0.000	43.154	2.864	0.117	1.557	0.000	0.079
U16-h07-25-167	lt ooid	0.153	2.681	0.333	0.026	42.404	1.999	0.000	1.898	0.068	0.147
U16-h07-25-167	lt ooid	0.020	1.535	0.104	0.000	47.011	3.846	0.118	1.380	0.000	0.108
U16-h07-25-167	lt ooid	0.021	1.984	0.131	0.000	37.386	2.722	0.120	1.807	0.000	0.139
U16-h07-25-167	matrix cement	0.023	0.099	0.022	0.000	12.977	1.310	0.134	0.054	0.000	0.012
U16-h07-25-167	matrix cement	0.022	1.511	0.159	0.000	62.606	4.373	0.124	1.245	0.000	0.124
U16-h07-25-167	matrix cement	0.023	4.697	0.312	0.000	23.064	1.467	0.130	4.931	0.000	0.373
U16-h07-25-167	matrix cement	0.021	1.274	0.105	0.000	36.484	2.531	0.117	1.279	0.000	0.105
U16-h07-25-167	matrix cement	0.022	1.100	0.070	0.000	22.266	1.442	0.120	1.302	0.000	0.097
U16-h07-25-167	matrix cement	0.021	1.168	0.098	0.000	30.718	2.188	0.119	1.347	0.000	0.098
U16-h07-25-167	matrix cement	0.022	1.402	0.114	0.000	37.933	1.966	0.126	1.110	0.000	0.077

Sample ID	SampleType	Sr LOD (ppm)	Y (ppm)	2SE (ppm)	Y LOD (ppm)	Ba (ppm)	2SE (ppm)	Ba LOD (ppm)	La (ppm)	La LOD (ppm)	2SE (ppm)
U16-h07-25-167	matrix cement	0.021	1.431	0.108	0.000	109.209	7.031	0.119	1.103	0.000	0.086
U16-h07-25-167	matrix cement	0.022	1.072	0.054	0.000	36.862	1.982	0.120	1.051	0.000	0.074
U16-h07-25-167	matrix cement	0.021	2.055	0.168	0.000	31.656	2.220	0.115	1.688	0.000	0.091
U16-h07-25-167	matrix cement	0.022	0.665	0.059	0.000	12.406	0.686	0.124	0.587	0.000	0.059
U16-h07-34-405	matrix cement	151.410	7.424	7.606	0.091	-74.131	246.728	1.310	1.660	0.033	32.819
U16-h07-34-405	matrix cement	85.078	1.736	1.055	0.097	200.938	74.221	0.536	3.964	0.058	1.247
U16-h07-34-405	matrix cement	145.310	-0.787	3.742	0.090	-24.943	33.388	1.256	-0.017	0.033	0.961
U16-h07-34-405	matrix cement	71.573	-2.737	0.317	0.293	-134.252	15.412	9.217	-2.700	0.284	0.305
U16-h07-34-405	matrix cement	77.008	-2.156	0.575	0.315	41.649	27.711	9.917	0.145	0.305	0.378
U16-h07-34-405	matrix cement	134.530	-10.063	7.311	0.083	-612.808	335.479	1.163	-15.754	0.031	7.180
U16-h07-34-405	matrix cement	134.540	-20.515	18.072	0.083	-692.332	522.130	1.163	-15.795	0.031	13.923
U16-h07-34-405	matrix cement	77.088	-0.865	0.406	0.315	103.451	9.107	9.927	0.812	0.306	0.398
U16-h07-34-405	matrix cement	86.364	-0.861	1.499	0.098	-11.559	26.544	0.544	-1.747	0.059	1.642
U16-h07-34-405	matrix cement	77.100	-1.879	0.599	0.315	-94.739	11.726	9.929	0.593	0.306	0.192
U16-h07-34-405	matrix cement	142.090	-3.783	0.956	0.088	-111.497	44.614	1.229	-2.381	0.032	0.832
U16-h07-34-405	matrix cement	136.760	-13.854	7.217	0.082	-511.606	241.177	1.184	-6.887	0.030	2.212
U16-h07-34-405	matrix cement	141.360	-5.688	2.234	0.087	52.123	92.952	1.222	-1.791	0.032	1.115
U16-h07-34-405	matrix cement	148.290	5.594	6.961	0.089	-58.252	99.479	1.283	12.220	0.033	8.265
U16-h07-34-405	matrix cement	148.200	-1.482	4.659	0.092	-6.757	25.736	1.281	0.444	0.034	6.248
U16-h07-34-405	matrix cement	144.800	-2.647	6.394	0.089	27.045	86.070	1.252	-1.109	0.033	2.737
U16-h07-34-405	matrix cement	149.030	-9.731	6.084	0.092	52.710	37.245	1.288	-3.358	0.034	7.721
U16-h07-34-405	ooid	70.976	3.237	0.282	0.300	76.248	8.390	8.483	2.028	0.238	0.284
U16-h07-34-405	ooid	67.094	9.521	1.600	0.335	169.173	22.671	9.333	7.299	0.292	1.113
U16-h07-34-405	ooid	78.279	-19.456	14.562	0.089	-552.567	415.415	0.493	-23.972	0.053	14.471
U16-h07-34-405	ooid	67.145	-5.556	1.038	0.372	-172.422	40.676	8.252	-3.028	0.343	0.795
U16-h07-34-405	ooid	74.183	-0.548	0.377	0.293	-44.306	31.037	7.559	-0.093	0.260	0.495
U16-h07-34-405	ooid	70.656	-6.616	1.009	0.279	-171.978	21.757	7.200	-5.744	0.247	0.894
U16-h07-34-405	ooid	66.632	-7.059	0.859	0.453	-35.626	37.545	15.568	-8.076	0.459	1.307
U16-h07-34-405	ooid	64.241	-2.578	0.568	0.356	-180.045	30.748	7.742	-1.836	0.331	0.440
U16-h07-34-405	ooid	109.480	3.259	1.007	0.381	140.585	39.681	8.521	2.961	0.301	0.874
U16-h07-34-405	ooid	102.310	-7.148	1.238	0.356	-323.303	63.609	7.964	-5.304	0.282	1.033
U16-h07-34-405	ooid	69.506	-2.589	0.775	0.385	-128.687	47.178	8.542	-5.147	0.355	1.276
U16-h07-34-405	ooid	68.740	-1.938	0.435	0.271	-124.767	24.103	7.004	-2.137	0.241	0.432

Sample ID	SampleType	Sr LOD (ppm)	Y (ppm)	2SE (ppm)	Y LOD (ppm)	Ba (ppm)	2SE (ppm)	Ba LOD (ppm)	La (ppm)	La LOD (ppm)	2SE (ppm)
U16-h07-34-405	ooid	66.970	-1.825	0.590	0.371	-203.547	36.821	8.071	-2.033	0.345	0.560
U16-h07-34-405	ooid	75.504	-3.126	0.508	0.298	-116.200	36.626	7.694	-3.201	0.264	0.740
U16-h07-34-405	ooid	79.419	-1.993	0.612	0.332	-17.387	26.225	6.342	-2.226	0.303	0.714
U16-h07-34-405	ooid	80.268	-3.733	0.962	0.335	-168.775	42.117	6.410	-3.942	0.306	1.320
U16-h07-34-405	ooid	75.385	-1.528	0.361	0.297	-23.381	22.171	7.681	-0.147	0.264	0.306
U16-h07-34-405	ooid	63.789	-7.527	1.421	0.318	-81.652	661.074	8.874	-6.642	0.278	0.925
U16-h07-34-405	ooid	69.623	-2.822	0.543	0.275	-133.170	15.006	7.094	-2.455	0.244	0.521
U16-h07-34-405	ooid	66.478	-3.654	0.880	0.452	-275.914	38.041	15.532	-2.846	0.458	0.661
U16-h07-34-405	ooid	85.594	4.264	12.760	0.097	-61.919	244.812	0.539	6.013	0.058	13.188
U16-h07-34-405	ooid and clast	1.123	25.538	4.010	0.080	209.858	22.259	0.554	18.695	0.000	3.109
U16-h07-34-405	ooid and clast	5.050	0.995	0.232	0.242	11.319	1.356	1.884	1.328	0.137	0.376
U16-h07-34-405	ooid and clast	0.183	0.350	0.056	0.000	5.770	0.521	0.039	0.213	0.000	0.033
U16-h07-34-405	ooid and clast	0.188	0.752	0.087	0.000	10.045	0.695	0.040	0.629	0.000	0.056
U16-h07-34-405	ooid and clast	0.287	4.506	0.471	0.020	36.676	4.491	0.142	3.886	0.000	0.400
U16-h07-34-405	ooid and clast	0.321	8.543	0.552	0.023	69.895	6.117	0.159	6.443	0.000	0.374
U16-h07-34-405	ooid and clast	4.890	8.002	1.188	0.234	21.171	1.921	1.824	4.261	0.132	0.400
U16-h07-34-405	ooid and clast	0.280	4.290	0.193	0.020	44.219	1.677	0.138	3.588	0.000	0.178
U16-h07-34-405	ooid and clast	0.286	5.602	0.369	0.020	86.168	6.664	0.141	4.439	0.000	0.384
U16-h07-34-405	ooid and clast	0.294	4.468	0.270	0.021	89.349	4.877	0.145	3.438	0.000	0.213
U16-h07-34-405	ooid and clast	0.179	6.710	0.500	0.000	58.628	3.159	0.038	5.316	0.000	0.480
U16-h07-34-405	ooid and clast	0.093	1.366	0.112	0.000	17.345	1.484	0.000	1.039	0.000	0.094
U16-h07-34-405	ooid and clast	0.094	9.742	0.357	0.000	104.231	4.445	0.000	8.039	0.000	0.299
U16-h07-34-405	ooid and clast	5.260	9.312	0.586	0.168	77.804	4.899	2.090	7.623	0.145	0.431
U16-h07-34-405	ooid and clast	0.019	11.111	0.724	0.000	88.193	10.266	0.000	8.986	0.000	0.614
U16-h07-34-405	ooid and clast	0.093	19.614	1.295	0.000	187.605	14.056	0.000	16.707	0.000	1.167
U16-h07-34-405	ooid and clast	0.095	27.352	85.449	0.000	149.866	135.131	0.000	22.203	0.000	35.210
U16-h07-34-405	ooid and clast	5.572	10.791	39.546	0.178	480.490	730.001	2.214	19.029	0.154	52.642
U16-h07-34-405	ooid and clast	0.084	-22.025	53.993	0.000	-35.640	971.573	0.059	-29.492	0.000	50.699
U16-h07-34-405	ooid and clast	65.661	0.740	0.041	0.509	-1.575	1.609	2.071	1.078	0.756	0.066
U16-h07-34-405	ooid and clast	5.440	-12.004	1.102	0.174	-185.801	12.302	2.162	-10.204	0.150	0.695
U16-h07-34-405	ooid and clast	0.098	-16.983	1.093	0.000	-173.941	12.116	0.000	-13.639	0.000	1.080
U16-h07-34-405	ooid and clast	0.089	-21.622	1.375	0.000	-316.940	26.933	0.000	-19.083	0.000	1.385
U16-h07-34-405	ooid and clast	1.159	-6.553	0.376	0.016	-65.121	5.869	0.140	-5.640	0.021	0.395

Sample ID	SampleType	Sr LOD (ppm)	Y (ppm)	2SE (ppm)	Y LOD (ppm)	Ba (ppm)	2SE (ppm)	Ba LOD (ppm)	La (ppm)	La LOD (ppm)	2SE (ppm)
U16-h07-34-405	ooid and clast	0.095	-5.231	0.249	0.000	-119.314	5.184	0.000	-5.042	0.000	0.261
U16-h07-34-405	ooid and clast	0.090	-4.427	0.302	0.000	-81.756	4.511	0.000	-3.717	0.000	0.286
U16-h07-34-405	ooid and clast	58.202	-5.031	0.751	1.197	-45.290	9.857	16.134	-3.939	0.954	0.499
U16-h07-34-405	ooid and clast	0.161	-5.192	0.454	0.000	-70.494	10.847	0.142	-3.468	0.000	0.120
U16-h07-34-405	ooid and clast	0.498	-4.527	0.469	0.000	-89.078	13.740	0.143	-2.463	0.007	0.224
U16-h07-34-405	ooid and clast	58.935	-4.438	0.464	1.213	-34.510	3.591	16.337	-3.124	0.966	0.389
U16-h07-34-405	ooid and clast	0.443	-2.614	0.170	0.000	-35.713	2.142	0.127	-2.164	0.006	0.171
U16-h07-34-405	ooid and clast	0.432	-2.130	0.112	0.000	-21.818	2.112	0.124	-1.596	0.006	0.071
U16-h07-34-405	ooid and clast	60.570	-2.409	0.169	0.470	-33.409	2.515	1.910	-1.970	0.697	0.169
U16-h07-34-405	ooid and clast	0.168	-1.414	0.119	0.000	-3.558	0.537	0.148	-2.267	0.000	0.225
U16-h07-34-405	vein 1	91.947	5.303	0.874	0.569	-48.305	13.927	4.151	6.604	0.707	1.064
U16-h07-34-405	vein 1	96.211	4.127	1.073	0.602	-948.085	88.171	4.346	5.370	0.744	1.186
U16-h07-34-405	vein 1	99.183	17.002	9.861	0.620	19.777	34.913	4.480	16.418	0.767	8.424
U16-h07-34-405	vein 1	90.996	7.570	1.573	0.569	-222.669	49.415	4.110	8.968	0.703	1.788
U16-h07-34-405	vein 1	94.301	6.878	1.277	0.590	-314.551	58.422	4.260	8.042	0.729	1.435
U16-h07-34-405	vein 2	105.960	-3.819	0.483	0.655	-85.600	16.334	4.784	-5.706	0.815	0.565
U16-h07-34-405	vein 2	97.688	-3.150	0.365	0.604	-7.332	1.903	4.410	-2.164	0.752	0.278
U16-h07-34-405	vein 2	102.860	-4.201	0.461	0.636	-22.553	2.679	4.644	-4.767	0.791	0.307
U16-h07-34-405	vein 2	104.830	-8.444	1.440	0.648	-107.688	72.577	4.732	-8.602	0.807	1.247
U16-h07-34-405	vein 2	100.010	-8.434	1.184	0.619	-25.934	4.025	4.515	-15.338	0.770	2.218
U16-h07-34-405	vein 2	103.580	-9.089	1.243	0.641	6.896	3.377	4.676	-11.696	0.797	1.196
U16-h07-54-338	coarse calcite	11.478	1.300	0.111	0.042	28.965	2.488	1.875	0.643	0.047	0.064
U16-h07-54-338	coarse calcite	24.181	0.703	0.059	0.228	64.733	6.047	5.670	0.395	0.127	0.044
U16-h07-54-338	coarse calcite	11.584	0.421	0.052	0.020	5.107	0.531	0.193	0.242	0.010	0.033
U16-h07-54-338	coarse calcite	6.422	1.432	0.152	0.119	73.105	10.253	8.516	0.858	0.026	0.074
U16-h07-54-338	coarse calcite	23.219	6.516	1.822	0.219	31.303	3.576	5.445	2.900	0.122	0.652
U16-h07-54-338	coarse calcite	11.336	0.710	0.055	0.067	21.985	3.411	0.577	0.504	0.006	0.072
U16-h07-54-338	coarse calcite	24.408	0.876	0.082	0.230	46.724	2.543	5.720	0.435	0.128	0.051
U16-h07-54-338	coarse calcite	9.413	1.444	0.116	0.120	7.300	0.846	0.700	0.674	0.064	0.095
U16-h07-54-338	coarse calcite	0.038	3.765	1.247	0.008	60.828	5.499	0.000	1.962	0.015	0.540
U16-h07-54-338	coarse calcite	22.339	7.420	1.318	0.211	33.710	2.801	5.243	3.763	0.117	0.659
U16-h07-54-338	coarse calcite	22.733	5.212	1.034	0.214	40.567	6.158	5.333	2.784	0.119	0.227
U16-h07-54-338	coarse calcite	5.860	2.592	0.325	0.154	34.568	2.375	1.521	1.723	0.032	0.305

Sample ID	SampleType	Sr LOD (ppm)	Y (ppm)	2SE (ppm)	Y LOD (ppm)	Ba (ppm)	2SE (ppm)	Ba LOD (ppm)	La (ppm)	La LOD (ppm)	2SE (ppm)
U16-h07-54-338	coarse calcite	6.024	1.311	0.102	0.097	36.667	2.276	2.316	0.613	0.076	0.082
U16-h07-54-338	coarse calcite	0.037	4.275	1.449	0.008	17.462	2.455	0.000	2.072	0.015	0.830
U16-h07-54-338	coarse calcite	13.846	0.668	0.076	0.050	47.916	3.789	4.388	0.478	0.058	0.058
U16-h07-54-5	matrix cement	0.296	1.073	0.158	0.000	10.229	0.793	0.075	1.033	0.028	0.205
U16-h07-54-5	matrix cement	0.302	2.176	0.226	0.000	3.691	0.745	0.076	1.923	0.028	0.283
U16-h07-54-5	matrix cement	0.310	4.224	0.401	0.000	20.220	1.295	0.079	3.455	0.029	0.299
U16-h07-54-5	matrix cement	0.288	4.842	0.565	0.000	15.731	1.136	0.073	3.315	0.027	0.414
U16-h07-54-5	matrix cement	0.210	4.563	0.293	0.000	16.974	1.520	0.213	4.201	0.000	0.248
U16-h07-54-5	matrix cement	0.079	4.126	0.143	0.000	12.487	0.820	0.060	3.977	0.000	0.153
U16-h07-54-5	matrix cement	0.310	4.235	0.351	0.000	13.707	1.844	0.078	3.407	0.028	0.295
U16-h07-54-5	matrix cement	0.295	4.351	0.219	0.000	14.459	1.107	0.075	4.494	0.027	0.259
U16-h07-54-5	matrix cement	0.209	3.012	0.225	0.000	13.430	1.482	0.212	2.421	0.000	0.159
U16-h07-54-5	matrix cement	0.309	3.676	0.348	0.000	19.004	1.978	0.079	3.548	0.029	0.321
U16-h07-54-5	matrix cement	0.060	4.517	0.222	0.035	12.827	0.850	0.000	4.349	0.014	0.189
U16-h07-54-5	matrix cement	0.302	2.629	0.181	0.000	11.724	0.999	0.077	2.686	0.028	0.260
U16-h07-54-5	matrix cement	0.300	3.354	0.321	0.000	39.521	6.123	0.076	4.117	0.028	0.433
U16-h07-54-5	matrix cement	0.306	3.861	0.235	0.000	16.811	1.969	0.078	3.628	0.029	0.310
U16-h07-54-5	matrix cement	0.080	1.635	0.252	0.000	12.551	1.546	0.060	1.131	0.000	0.118
U16-h07-54-5	matrix cement	0.302	3.655	0.180	0.000	11.083	0.909	0.077	4.466	0.028	0.273
U16-h07-54-5	matrix cement	0.306	1.635	0.240	0.000	9.295	2.047	0.077	1.701	0.028	0.308
U16-h07-54-5	ooid	0.294	7.750	0.452	0.012	51.903	3.276	0.157	8.506	0.049	0.432
U16-h07-54-5	ooid	0.124	4.318	0.215	0.012	13.879	0.980	0.000	4.484	0.009	0.225
U16-h07-54-5	ooid	0.120	1.060	0.155	0.011	8.494	0.766	0.043	1.043	0.012	0.195
U16-h07-54-5	ooid	0.185	4.949	0.358	0.014	18.840	1.317	0.053	4.796	0.012	0.204
U16-h07-54-5	ooid	0.134	6.042	0.397	0.013	30.192	3.482	0.000	4.714	0.010	0.239
U16-h07-54-5	ooid	0.250	1.950	0.281	0.010	12.408	1.360	0.133	1.643	0.042	0.203
U16-h07-54-5	ooid	0.192	7.933	0.502	0.015	23.661	1.280	0.055	6.131	0.013	0.375
U16-h07-54-5	ooid	0.135	13.060	1.068	0.013	26.429	2.508	0.000	9.188	0.010	0.427
U16-h07-54-5	ooid	0.060	4.584	0.273	0.035	18.615	1.355	0.000	4.137	0.013	0.204
U16-h07-54-5	ooid	0.118	3.977	0.204	0.011	13.858	1.534	0.046	4.109	0.012	0.256
U16-h07-54-5	ooid	0.117	6.363	0.492	0.011	15.736	1.213	0.046	5.370	0.012	0.385
U16-h07-54-5	ooid	0.181	4.036	0.203	0.014	13.261	0.838	0.052	4.214	0.012	0.204
U16-h07-54-5	ooid	0.129	2.110	0.133	0.012	12.781	2.869	0.000	2.224	0.009	0.139

Sample ID	SampleType	Sr LOD (ppm)	Y (ppm)	2SE (ppm)	Y LOD (ppm)	Ba (ppm)	2SE (ppm)	Ba LOD (ppm)	La (ppm)	La LOD (ppm)	2SE (ppm)
U16-h07-54-5	ooid	0.187	3.323	0.193	0.015	16.151	1.616	0.054	3.724	0.012	0.222
U16-h07-54-5	ooid	0.158	2.342	0.217	0.015	3.841	0.529	0.000	2.707	0.011	0.222
U16-h07-54-5	ooid	0.063	2.888	0.195	0.037	14.293	0.692	0.000	2.610	0.014	0.315
U16-h07-54-5	ooid	0.171	4.610	0.293	0.013	8.559	0.750	0.052	5.926	0.011	0.609
U16-h07-54-5	ooid	0.183	4.427	0.386	0.014	5.671	0.767	0.053	5.771	0.012	0.518
U16-h07-54-5	ooid	0.238	3.703	0.176	0.010	20.798	1.236	0.127	3.860	0.040	0.218
U16-h07-54-5	ooid	0.181	3.991	0.267	0.014	15.214	1.173	0.052	4.685	0.012	0.366
U16-h07-54-5	ooid	0.136	2.956	0.163	0.013	4.514	0.464	0.000	2.884	0.010	0.175
U16-h07-54-5	ooid	0.259	3.472	0.706	0.011	5.638	1.243	0.138	4.176	0.044	0.955
U16-h07-54-5	ooid	0.127	4.272	0.344	0.012	3.673	0.368	0.000	4.716	0.009	0.357
U16-h07-54-5	ooid	0.186	4.432	0.315	0.014	8.048	1.045	0.054	5.392	0.012	0.352
U16-h07-54-5	ooid	0.253	1.235	0.124	0.011	11.126	1.152	0.135	1.601	0.042	0.215
U16-h07-54-5	vein 1	0.177	4.578	0.232	0.000	31.116	2.567	0.134	2.183	0.009	0.146
U16-h07-54-5	vein 1	0.473	17.650	1.309	0.356	78.043	7.546	0.207	16.844	0.026	2.187
U16-h07-54-5	vein 1	0.344	4.071	0.189	0.087	97.308	13.614	0.000	3.794	0.113	0.169
U16-h07-54-5	vein 1	0.330	3.362	0.182	0.083	44.794	9.386	0.000	2.153	0.108	0.151
U16-h07-54-5	vein 1	0.347	4.240	0.275	0.087	75.472	7.189	0.000	3.435	0.114	0.273
U16-h07-54-5	vein 1	0.337	7.205	0.289	0.085	10.960	1.998	0.000	6.267	0.110	0.845
U16-h07-54-5	vein 2	0.178	2.531	0.150	0.000	130.396	5.306	0.132	1.127	0.008	0.068
U16-h07-54-5	vein 2	0.173	9.680	0.438	0.000	96.855	7.095	0.131	9.074	0.008	0.896
U16-h07-54-5	vein 2	0.172	1.152	0.132	0.000	36.071	3.148	0.131	0.484	0.008	0.070
U16-h07-67-129	darker vein	0.000	1.574	0.271	0.000	37.062	5.423	0.000	0.747	0.000	0.076
U16-h07-67-129	darker vein	23.614	1.079	0.089	0.095	12.100	0.777	0.768	0.906	0.042	0.074
U16-h07-67-129	darker vein	8.448	0.903	0.110	0.011	7.657	0.685	0.106	0.577	0.009	0.051
U16-h07-67-129	darker vein	23.642	0.551	0.065	0.095	13.867	0.845	0.768	0.600	0.042	0.063
U16-h07-67-129	darker vein	0.000	1.111	0.165	0.000	14.164	1.458	0.000	0.658	0.000	0.091
U16-h07-67-129	darker vein	0.000	1.447	0.127	0.000	12.248	1.215	0.000	1.641	0.000	0.155
U16-h07-67-129	darker vein	8.555	2.808	0.300	0.011	11.229	0.652	0.107	1.951	0.009	0.167
U16-h07-67-129	lighter vein	2.221	6.920	1.785	0.013	3.656	1.582	0.168	2.606	0.000	0.647
U16-h07-67-129	lighter vein	24.634	24.655	0.598	0.099	10.005	0.777	0.801	13.017	0.044	0.466
U16-h07-67-129	lighter vein	1.539	8.021	0.623	0.110	2.768	0.408	0.000	3.600	0.019	0.360
U16-h07-67-129	lighter vein	2.177	24.450	0.678	0.013	11.257	1.639	0.165	10.835	0.000	0.737
U16-h07-67-129	lighter vein	2.112	5.797	0.386	0.013	12.428	0.855	0.160	4.992	0.000	0.313

Sample ID	SampleType	Sr LOD (ppm)	Y (ppm)	2SE (ppm)	Y LOD (ppm)	Ba (ppm)	2SE (ppm)	Ba LOD (ppm)	La (ppm)	La LOD (ppm)	2SE (ppm)
U16-h07-67-129	lighter vein	2.296	22.818	0.552	0.014	5.435	0.510	0.174	15.953	0.000	0.414
U16-h07-67-129	lighter vein	25.025	9.370	2.262	0.101	4.766	1.117	0.814	10.513	0.045	0.590
U16-h07-67-129	ooid and matrix	5.896	166.384	21.029	0.301	1495.863	161.808	1.671	86.223	0.139	10.941
U16-h07-67-129	ooid and matrix	2.792	22.494	1.671	0.028	52.160	3.585	0.495	14.332	0.022	0.980
U16-h07-67-129	ooid and matrix	1.023	33.012	2.882	0.181	124.256	11.009	1.594	16.970	0.100	1.113
U16-h07-67-129	ooid and matrix	1.511	16.927	0.977	0.102	89.417	6.551	0.826	9.865	0.104	0.580
U16-h07-67-129	ooid and matrix	0.065	23.214	5.044	0.000	215.642	55.682	0.487	12.945	0.077	2.713
U16-h07-67-129	ooid and matrix	0.963	14.915	0.939	0.086	72.811	5.121	0.315	9.247	0.118	0.602
U16-h07-67-129	ooid and matrix	1.877	6.663	0.250	0.102	41.174	2.306	0.894	5.357	0.049	0.264
U16-h07-67-129	ooid and matrix	28.287	11.357	0.586	4.440	52.335	2.325	40.593	7.648	3.641	0.421
U16-h07-67-129	ooid and matrix	2.996	19.477	0.733	0.366	113.128	4.737	0.914	13.773	0.164	0.558
U16-h07-67-129	ooid and matrix	1.068	21.705	1.312	0.095	111.966	8.392	0.349	12.422	0.131	0.740
U16-h07-67-129	ooid and matrix	3.025	11.129	2.174	0.030	47.707	11.890	0.536	7.370	0.024	1.202
U16-h07-67-129	ooid and matrix	1.159	3.028	0.407	0.065	65.423	21.928	0.223	2.008	0.035	0.159
U16-h07-67-129	ooid and matrix	0.849	9.495	0.362	0.125	37.805	2.106	0.103	6.484	0.056	0.353
U16-h07-67-129	ooid and matrix	1.171	1.282	0.140	0.052	5.065	0.878	0.243	1.985	0.052	0.160
U16-h07-67-129	ooid and matrix	1.026	10.006	0.358	0.052	40.391	2.080	0.291	7.032	0.024	0.303
U16-h07-67-129	ooid and matrix	1.166	0.681	0.204	0.066	12.000	1.585	0.224	0.356	0.035	0.061
U16-h07-67-129	ooid and matrix	1.191	5.293	0.824	0.053	42.868	2.161	0.247	4.413	0.053	0.248
U16-h07-67-129	ooid and matrix	2.830	3.247	0.553	0.346	14.072	1.350	0.864	2.504	0.154	0.383
U16-h07-67-129	ooid and matrix	0.903	8.652	0.362	0.080	15.596	0.918	0.295	6.425	0.110	0.314
U16-h07-67-129	ooid and matrix	2.800	12.161	1.635	0.028	17.894	0.964	0.496	3.869	0.022	0.168
U16-h07-67-129	ooid and matrix	1.096	5.090	0.317	0.062	22.944	1.930	0.211	3.877	0.033	0.322
U16-h07-67-129	ooid and matrix	0.836	22.326	2.794	0.086	31.376	2.838	0.254	16.887	0.150	2.031
U16-h07-67-129	ooid and matrix	0.836	7.391	0.526	0.124	20.887	1.093	0.101	6.808	0.055	0.303
U16-h07-67-129	ooid and matrix	3.681	12.713	0.916	0.286	38.432	8.921	0.926	13.935	0.279	0.938
U16-h07-67-129	ooid and matrix	0.866	16.034	1.311	0.089	14.014	1.329	0.263	14.611	0.155	0.713

Sample ID	SampleType	Ce (ppm)	2SE (ppm)	Ce LOD (ppm)	Pr (ppm)	2SE (ppm)	Pr LOD (ppm)	Nd (ppm)	2SE (ppm)	Nd LOD (ppm)	Sm (ppm)
U16-h07-13b-11	matrix	4.708	0.694	0.000	0.506	0.074	0.000	1.826	0.328	0.000	0.233
U16-h07-13b-11	matrix	0.940	0.078	0.000	0.086	0.017	0.000	0.342	0.070	0.000	0.027
U16-h07-13b-11	matrix	1.117	0.102	0.000	0.116	0.020	0.000	0.465	0.076	0.000	0.085
U16-h07-13b-11	matrix	1.787	0.125	0.000	0.177	0.016	0.000	0.711	0.124	0.000	0.084
U16-h07-13b-11	matrix	1.042	0.105	0.000	0.120	0.019	0.000	0.483	0.097	0.000	0.070
U16-h07-13b-11	matrix	1.100	0.099	0.000	0.112	0.014	0.000	0.472	0.098	0.000	0.046
U16-h07-13b-11	matrix	2.617	0.303	0.000	0.307	0.052	0.000	1.220	0.196	0.000	0.135
U16-h07-13b-11	matrix	2.267	0.200	0.000	0.217	0.025	0.000	0.995	0.107	0.000	0.154
U16-h07-13b-11	matrix	3.379	0.220	0.000	0.444	0.054	0.000	1.838	0.226	0.000	0.328
U16-h07-13b-11	matrix	1.828	0.200	0.000	0.233	0.036	0.000	0.894	0.156	0.000	0.156
U16-h07-13b-11	matrix	2.517	0.117	0.000	0.303	0.030	0.000	1.148	0.160	0.000	0.204
U16-h07-13b-11	matrix	1.504	0.114	0.000	0.161	0.022	0.000	0.530	0.105	0.000	0.141
U16-h07-13b-11	matrix	1.884	0.113	0.000	0.208	0.022	0.000	0.893	0.118	0.000	0.166
U16-h07-13b-11	matrix	2.646	0.119	0.000	0.302	0.042	0.000	1.172	0.126	0.000	0.116
U16-h07-13b-11	matrix	2.940	0.196	0.000	0.296	0.026	0.000	1.028	0.116	0.000	0.184
U16-h07-13b-11	matrix	2.564	0.180	0.000	0.286	0.037	0.000	1.182	0.153	0.000	0.215
U16-h07-13b-11	matrix	2.276	0.150	0.000	0.251	0.027	0.000	1.081	0.129	0.000	0.209
U16-h07-13b-11	matrix	1.040	0.107	0.000	0.104	0.017	0.000	0.504	0.105	0.000	0.064
U16-h07-13b-11	matrix	3.144	0.264	0.000	0.332	0.029	0.000	1.557	0.192	0.000	0.306
U16-h07-13b-11	matrix	3.522	0.206	0.000	0.370	0.036	0.000	1.357	0.141	0.000	0.205
U16-h07-13b-11	matrix	2.611	0.197	0.000	0.296	0.036	0.000	1.187	0.150	0.000	0.199
U16-h07-13b-11	vein 1	5.682	0.568	0.000	0.534	0.055	0.000	1.919	0.209	0.000	0.250
U16-h07-13b-11	vein 1	19.025	0.853	0.000	2.426	0.102	0.000	9.001	0.476	0.000	1.629
U16-h07-13b-11	vein 1	25.586	0.832	0.000	3.108	0.099	0.000	11.642	0.588	0.000	1.721
U16-h07-13b-11	vein 1	13.792	0.720	0.000	1.557	0.099	0.000	5.684	0.388	0.000	0.951
U16-h07-13b-11	vein 1	13.720	1.644	0.000	1.460	0.172	0.000	5.399	0.702	0.000	0.779
U16-h07-13b-11	vein 1	37.140	1.154	0.000	3.954	0.183	0.000	14.395	0.733	0.000	2.158
U16-h07-13b-11	vein 1	15.459	0.529	0.000	1.885	0.082	0.000	6.518	0.294	0.000	1.115
U16-h07-13b-11	vein 2	0.942	0.127	0.000	0.096	0.019	0.000	0.357	0.070	0.000	0.054
U16-h07-13b-11	vein 2	0.353	0.169	0.000	0.038	0.022	0.000	0.222	0.109	0.000	0.037
U16-h07-13b-11	vein 2	0.343	0.062	0.000	0.038	0.010	0.000	0.198	0.060	0.000	0.012
U16-h07-13b-11	vein 2	0.012	0.005	0.000	0.000	1.000	0.000	0.006	0.008	0.000	0.000
U16-h07-13b-11	vein 2	0.077	0.019	0.000	0.008	0.004	0.000	0.006	0.008	0.000	0.000

Sample ID	SampleType	Ce (ppm)	2SE (ppm)	Ce LOD (ppm)	Pr (ppm)	2SE (ppm)	Pr LOD (ppm)	Nd (ppm)	2SE (ppm)	Nd LOD (ppm)	Sm (ppm)
U16-h07-13b-11	vein 2	0.013	0.006	0.000	0.000	1.000	0.000	0.000	1.000	0.000	0.000
U16-h07-13b-11	vein 3	3.755	0.292	0.000	0.427	0.050	0.000	1.441	0.164	0.000	0.196
U16-h07-13b-11	vein 3	6.171	0.500	0.000	0.646	0.065	0.000	2.387	0.238	0.000	0.332
U16-h07-13b-11	vein 3	7.507	0.832	0.000	0.952	0.129	0.000	3.899	0.483	0.000	0.523
U16-h07-13b-31	dk ooid	3.000	0.296	0.093	0.308	0.048	0.013	1.211	0.171	0.133	0.144
U16-h07-13b-31	dk ooid	7.450	0.370	0.019	0.952	0.078	0.014	3.927	0.316	0.000	0.770
U16-h07-13b-31	dk ooid	5.857	0.476	0.093	0.751	0.090	0.012	2.226	0.276	0.132	0.498
U16-h07-13b-31	dk ooid	5.025	0.293	0.091	0.605	0.047	0.012	2.393	0.221	0.131	0.411
U16-h07-13b-31	dk ooid	5.973	0.260	0.015	0.698	0.051	0.012	2.724	0.202	0.000	0.451
U16-h07-13b-31	dk ooid	8.623	0.626	0.018	0.965	0.087	0.014	3.703	0.438	0.000	0.566
U16-h07-13b-31	matrix cement	4.136	0.337	0.092	0.444	0.046	0.012	1.537	0.198	0.132	0.235
U16-h07-13b-31	matrix cement	6.017	0.351	0.106	0.709	0.056	0.022	2.818	0.284	0.000	0.513
U16-h07-13b-31	matrix cement	12.212	1.575	0.091	1.529	0.236	0.012	6.738	0.987	0.131	1.169
U16-h07-13b-31	matrix cement	5.632	0.316	0.089	0.636	0.042	0.012	2.444	0.231	0.128	0.377
U16-h07-13b-31	matrix cement	6.163	0.554	0.108	0.835	0.099	0.022	3.196	0.437	0.000	0.638
U16-h07-13b-31	matrix cement	7.798	0.885	0.093	0.928	0.116	0.013	3.698	0.552	0.133	0.630
U16-h07-13b-31	matrix cement	6.432	0.348	0.090	0.734	0.066	0.012	2.570	0.337	0.129	0.518
U16-h07-13b-31	matrix cement	6.454	0.340	0.103	0.695	0.052	0.021	2.439	0.226	0.000	0.444
U16-h07-13b-31	matrix cement	6.306	0.294	0.112	0.849	0.050	0.000	2.992	0.266	0.046	0.598
U16-h07-13b-31	matrix cement	6.300	0.306	0.111	0.802	0.055	0.000	2.989	0.213	0.046	0.558
U16-h07-13b-31	matrix cement	6.017	0.221	0.106	0.697	0.042	0.022	2.776	0.191	0.000	0.418
U16-h07-13b-31	matrix cement	4.838	0.311	0.107	0.640	0.058	0.022	2.365	0.254	0.000	0.373
U16-h07-13b-31	ooid	8.163	0.434	0.050	1.047	0.077	0.012	4.321	0.306	0.000	0.774
U16-h07-13b-31	ooid	3.112	0.257	0.218	0.342	0.037	0.035	1.274	0.134	0.124	0.226
U16-h07-13b-31	ooid	10.367	1.055	0.050	1.444	0.151	0.012	6.284	0.819	0.000	1.189
U16-h07-13b-31	ooid	3.833	0.189	0.114	0.513	0.037	0.053	1.739	0.194	0.043	0.361
U16-h07-13b-31	ooid	6.346	0.257	0.007	0.780	0.052	0.000	2.754	0.159	0.000	0.558
U16-h07-13b-31	ooid	5.520	0.247	0.090	0.612	0.052	0.017	2.002	0.188	0.095	0.384
U16-h07-13b-31	ooid	7.003	0.475	0.008	0.977	0.111	0.000	4.102	0.514	0.000	0.704
U16-h07-13b-31	ooid	7.737	0.898	0.110	0.946	0.141	0.052	4.149	0.729	0.042	0.605
U16-h07-13b-31	ooid	7.021	0.362	0.011	0.711	0.056	0.000	2.489	0.189	0.000	0.343
U16-h07-13b-31	ooid	10.691	1.028	0.089	1.270	0.092	0.016	5.311	0.343	0.094	0.925
U16-h07-13b-31	ooid	5.669	0.355	0.051	0.642	0.044	0.012	2.180	0.158	0.000	0.362

Sample ID	SampleType	Ce (ppm)	2SE (ppm)	Ce LOD (ppm)	Pr (ppm)	2SE (ppm)	Pr LOD (ppm)	Nd (ppm)	2SE (ppm)	Nd LOD (ppm)	Sm (ppm)
U16-h07-13b-31	ooid	6.770	0.511	0.217	0.932	0.088	0.035	3.217	0.309	0.124	0.602
U16-h07-13b-31	ooid	6.061	0.296	0.049	0.705	0.054	0.012	2.294	0.198	0.000	0.426
U16-h07-13b-31	ooid	6.733	0.558	0.050	0.848	0.077	0.012	3.413	0.383	0.000	0.667
U16-h07-13b-31	ooid	8.049	0.575	0.216	1.007	0.084	0.035	4.596	0.372	0.124	0.789
U16-h07-13b-31	ooid	6.373	0.329	0.089	0.761	0.057	0.016	2.935	0.327	0.094	0.553
U16-h07-13b-31	ooid	7.374	0.583	0.011	0.875	0.092	0.000	3.332	0.204	0.000	0.616
U16-h07-13b-31	ooid	8.409	0.459	0.011	1.046	0.065	0.000	4.246	0.407	0.000	0.697
U16-h07-13b-31	ooid	7.021	0.466	0.049	0.947	0.063	0.012	3.395	0.193	0.000	0.598
U16-h07-13b-31	ooid	7.411	0.373	0.048	0.950	0.055	0.012	3.726	0.318	0.000	0.692
U16-h07-13b-31	ooid	7.174	0.452	0.010	0.789	0.051	0.000	2.863	0.237	0.000	0.503
U16-h07-13b-31	ooid	5.996	0.326	0.010	0.641	0.045	0.000	2.271	0.165	0.000	0.401
U16-h07-13b-31	ooid	5.375	0.302	0.047	0.584	0.040	0.012	2.066	0.169	0.000	0.365
U16-h07-13b-31	ooid	5.442	0.282	0.110	0.655	0.049	0.052	2.473	0.162	0.042	0.433
U16-h07-13b-31	vein-1	13.795	1.367	0.019	1.806	0.233	0.011	7.998	1.006	0.031	1.455
U16-h07-13b-31	vein-1	1.775	0.453	0.007	0.183	0.041	0.000	0.575	0.144	0.000	0.048
U16-h07-13b-31	vein-1	1.485	0.107	0.017	0.227	0.033	0.010	0.715	0.107	0.028	0.113
U16-h07-13b-31	vein-1	1.003	0.150	0.286	0.131	0.023	0.028	0.442	0.099	0.172	0.034
U16-h07-13b-31	vein-1	1.139	0.130	0.017	0.127	0.019	0.009	0.475	0.102	0.027	0.074
U16-h07-13b-31	vein-1	1.568	0.189	0.016	0.172	0.028	0.009	0.594	0.103	0.025	0.129
U16-h07-13b-81	coarse calcite	0.000	0.000	0.003	0.000	0.000	0.000	-0.001	0.000	0.012	0.000
U16-h07-13b-81	coarse calcite	-0.066	0.013	0.003	-0.007	0.001	0.000	-0.033	0.007	0.012	0.000
U16-h07-13b-81	coarse calcite	-0.223	0.022	0.003	-0.025	0.002	0.000	-0.114	0.011	0.011	-0.001
U16-h07-13b-81	coarse calcite	-0.572	0.103	0.262	-0.063	0.012	0.042	-0.331	0.046	0.148	-0.005
U16-h07-13b-81	vein 1	8.004	0.858	2.070	1.333	0.229	0.376	5.492	0.752	1.322	0.991
U16-h07-13b-81	vein 1	20.055	1.375	5.386	2.856	0.306	0.756	9.430	1.126	2.806	1.871
U16-h07-13b-81	vein 1	2.446	0.444	1.591	0.311	0.053	0.289	1.458	0.239	1.017	0.185
U16-h07-13b-81	vein 1	5.958	1.023	2.362	0.587	0.113	0.268	1.423	0.417	0.865	0.148
U16-h07-13b-81	vein 1	4.512	0.432	0.003	0.591	0.068	0.000	2.110	0.253	0.011	0.367
U16-h07-13b-81	vein 1	4.459	0.572	3.455	0.531	0.097	0.391	1.811	0.325	1.323	0.358
U16-h07-13b-81	vein 1	3.654	0.678	2.484	0.396	0.087	0.309	1.642	0.283	1.052	0.271
U16-h07-13b-81	vein 1	3.070	0.855	2.543	0.344	0.109	0.316	1.206	0.343	1.078	0.287
U16-h07-13b-81	vein 1	0.630	0.274	2.351	0.115	0.045	0.266	0.010	0.170	0.861	0.018
U16-h07-24-145	ooids and cement	0.128	0.017	0.000	0.015	0.007	0.000	0.047	0.025	0.000	0.000

Sample ID	SampleType	Ce (ppm)	2SE (ppm)	Ce LOD (ppm)	Pr (ppm)	2SE (ppm)	Pr LOD (ppm)	Nd (ppm)	2SE (ppm)	Nd LOD (ppm)	Sm (ppm)
U16-h07-24-145	ooids and cement	1.300	0.078	0.000	0.187	0.026	0.000	0.757	0.093	0.000	0.175
U16-h07-24-145	ooids and cement	1.270	0.087	0.000	0.158	0.030	0.000	0.640	0.111	0.000	0.059
U16-h07-24-145	ooids and cement	1.065	0.076	0.000	0.155	0.016	0.000	0.593	0.128	0.000	0.068
U16-h07-24-145	ooids and cement	1.731	0.083	0.000	0.239	0.022	0.000	0.910	0.102	0.000	0.188
U16-h07-24-145	ooids and cement	0.004	0.003	0.000	0.000	0.001	0.000	0.000	1.000	0.000	0.000
U16-h07-24-145	ooids and cement	1.238	0.089	0.000	0.148	0.019	0.000	0.631	0.107	0.000	0.089
U16-h07-24-145	ooids and cement	1.078	0.082	0.000	0.110	0.018	0.000	0.421	0.090	0.000	0.109
U16-h07-24-145	vein-1	0.981	0.111	0.029	0.087	0.015	0.000	0.353	0.067	0.054	0.028
U16-h07-24-145	vein-1	0.586	0.047	0.027	0.063	0.011	0.000	0.224	0.054	0.050	0.045
U16-h07-24-145	vein-1	1.143	0.061	0.027	0.109	0.016	0.000	0.474	0.084	0.050	0.061
U16-h07-24-145	vein-1	0.780	0.054	0.027	0.093	0.018	0.000	0.357	0.065	0.050	0.059
U16-h07-24-145	vein-1	0.552	0.040	0.026	0.066	0.014	0.000	0.197	0.045	0.048	0.024
U16-h07-24-145	vein-1	0.737	0.056	0.095	0.086	0.015	0.067	0.248	0.051	0.140	0.062
U16-h07-24-145	vein-1	0.626	0.088	0.095	0.065	0.010	0.067	0.188	0.029	0.140	0.017
U16-h07-24-145	vein-1	1.785	0.118	0.089	0.176	0.021	0.063	0.670	0.084	0.131	0.124
U16-h07-24-145	vein-2	1.527	0.109	0.027	0.168	0.018	0.000	0.687	0.112	0.052	0.125
U16-h07-24-145	vein-2	2.682	0.465	0.027	0.316	0.073	0.000	1.106	0.312	0.051	0.069
U16-h07-24-145	vein-2	-2.152	0.303	0.028	-0.271	0.063	0.000	-1.060	0.297	0.053	-0.108
U16-h07-24-145	vein-3	1.702	1.664	0.327	-0.187	0.333	0.045	-2.340	1.652	0.233	-1.010
U16-h07-24-145	vein-3	-0.639	0.091	0.028	-0.063	0.021	0.000	-0.335	0.108	0.054	-0.078
U16-h07-24-145	vein-3	-0.770	0.109	0.374	-0.092	0.023	0.049	-0.445	0.118	0.183	-0.042
U16-h07-24-145	vein-3	-0.391	0.042	0.028	-0.043	0.012	0.000	-0.170	0.049	0.052	-0.030
U16-h07-24-145	vein-3	-0.645	0.048	0.367	-0.076	0.012	0.049	-0.363	0.057	0.178	-0.057
U16-h07-24-145	vein-3	-0.605	0.059	0.028	-0.059	0.013	0.000	-0.250	0.051	0.053	-0.020
U16-h07-24-145	vein-3	0.065	0.013	0.029	0.007	0.004	0.000	0.023	0.017	0.054	0.011
U16-h07-24-145	vein-4	0.479	4.122	0.337	-0.358	0.475	0.046	0.231	2.073	0.246	1.388
U16-h07-24-145	vein-4	1.587	0.093	0.000	0.215	0.021	0.000	0.819	0.095	0.000	0.150
U16-h07-24-145	vein-4	0.963	0.138	0.000	0.129	0.018	0.000	0.452	0.085	0.000	0.089
U16-h07-24-145	vein-4	0.443	0.047	0.000	0.045	0.012	0.000	0.266	0.058	0.000	0.042
U16-h07-24-145	vein-4	18.931	40.394	0.336	0.691	3.701	0.046	6.537	11.255	0.245	-1.494
U16-h07-24-145	vein-4	4.303	0.215	0.000	0.516	0.054	0.000	2.069	0.253	0.000	0.325
U16-h07-24-145	vein-4	-264.266	296.629	0.349	-14.784	27.059	0.048	-140.021	86.210	0.248	-10.751
U16-h07-24-145	vein-4	5.784	0.604	0.000	0.674	0.066	0.000	2.730	0.381	0.000	0.481

Sample ID	SampleType	Ce (ppm)	2SE (ppm)	Ce LOD (ppm)	Pr (ppm)	2SE (ppm)	Pr LOD (ppm)	Nd (ppm)	2SE (ppm)	Nd LOD (ppm)	Sm (ppm)
U16-h07-24-145	vein-4	4.064	2.795	0.000	0.633	0.104	0.000	2.921	0.790	0.000	0.499
U16-h07-24-145	vein-4	2.362	0.340	0.325	0.160	0.049	0.045	0.787	0.302	0.237	0.117
U16-h07-24-145	vein-4	11.768	1.464	0.000	1.196	0.223	0.000	5.025	1.071	0.000	0.858
U16-h07-24-145	vein-4	23.124	3.439	0.000	3.270	0.634	0.000	11.558	2.610	0.000	2.215
U16-h07-24-145	vein-4	0.533	0.168	0.381	0.045	0.039	0.050	0.100	0.174	0.186	0.024
U16-h07-24-145	vein-4	-0.260	0.123	0.364	-0.057	0.026	0.048	-0.151	0.136	0.178	-0.004
U16-h07-24-145	vein-4	2.640	3.392	0.344	-0.196	0.415	0.047	1.200	2.502	0.251	-0.287
U16-h07-24-145	vein-4	2.508	6.938	0.319	-0.071	0.703	0.044	0.513	2.220	0.233	-0.192
U16-h07-24-145	vein-6	0.011	0.006	0.000	0.000	1.000	0.000	0.000	1.000	0.000	0.000
U16-h07-24-145	vein-6	0.925	0.065	0.000	0.101	0.015	0.000	0.436	0.088	0.000	0.065
U16-h07-24-145	vein-6	1.324	0.090	0.000	0.168	0.021	0.000	0.806	0.125	0.000	0.103
U16-h07-24-145	vein-6	1.421	0.096	0.000	0.176	0.024	0.000	0.763	0.098	0.000	0.102
U16-h07-24-145	vein-6	1.127	0.064	0.000	0.151	0.021	0.000	0.631	0.090	0.000	0.094
U16-h07-24-145	vein-7	1.144	0.110	0.000	0.144	0.023	0.000	0.724	0.120	0.000	0.099
U16-h07-25-167	coarse calcite	1.495	0.124	0.487	0.063	0.022	0.056	0.083	0.102	0.235	-0.033
U16-h07-25-167	coarse calcite	0.587	0.093	0.497	0.082	0.023	0.057	0.304	0.141	0.240	0.084
U16-h07-25-167	coarse calcite	1.101	0.096	0.521	0.161	0.026	0.060	0.668	0.116	0.251	0.162
U16-h07-25-167	coarse calcite	0.037	0.042	0.515	0.029	0.014	0.060	0.125	0.064	0.249	0.026
U16-h07-25-167	dk ooid	0.863	0.086	0.491	0.080	0.016	0.057	0.366	0.107	0.237	0.022
U16-h07-25-167	dk ooid	1.637	0.172	0.000	0.146	0.028	0.000	0.745	0.115	0.000	0.069
U16-h07-25-167	dk ooid	1.905	0.149	0.000	0.218	0.027	0.000	0.867	0.121	0.000	0.065
U16-h07-25-167	dk ooid	1.461	0.251	0.021	0.207	0.040	0.008	0.657	0.142	0.000	0.070
U16-h07-25-167	dk ooid	2.259	0.132	0.042	0.249	0.034	0.036	0.921	0.149	0.079	0.120
U16-h07-25-167	dk ooid	3.286	0.591	0.004	0.459	0.105	0.000	1.574	0.273	0.000	0.178
U16-h07-25-167	dk ooid	1.053	0.093	0.021	0.143	0.017	0.008	0.482	0.085	0.000	-0.013
U16-h07-25-167	dk ooid	1.258	0.076	0.000	0.165	0.017	0.000	0.583	0.085	0.000	0.013
U16-h07-25-167	dk ooid	1.367	0.089	0.021	0.170	0.019	0.008	0.646	0.092	0.000	0.045
U16-h07-25-167	dk ooid	1.309	0.079	0.040	0.156	0.023	0.035	0.533	0.079	0.075	0.092
U16-h07-25-167	dk ooid	2.059	0.144	0.040	0.236	0.027	0.035	1.011	0.119	0.076	0.142
U16-h07-25-167	dk ooid	1.241	0.111	0.020	0.152	0.018	0.008	0.629	0.106	0.000	0.052
U16-h07-25-167	dk ooid	0.826	0.069	0.004	0.144	0.020	0.000	0.538	0.096	0.000	0.022
U16-h07-25-167	dk ooid	1.386	0.085	0.020	0.179	0.022	0.008	0.676	0.080	0.000	0.043
U16-h07-25-167	dk ooid	1.076	0.071	0.042	0.113	0.017	0.035	0.414	0.073	0.078	0.109

Sample ID	SampleType	Ce (ppm)	2SE (ppm)	Ce LOD (ppm)	Pr (ppm)	2SE (ppm)	Pr LOD (ppm)	Nd (ppm)	2SE (ppm)	Nd LOD (ppm)	Sm (ppm)
U16-h07-25-167	dk ooid	1.431	0.081	0.020	0.152	0.021	0.008	0.602	0.095	0.000	0.102
U16-h07-25-167	dk ooid	1.502	0.095	0.041	0.158	0.023	0.034	0.676	0.100	0.077	0.127
U16-h07-25-167	dk ooid	1.344	0.080	0.041	0.148	0.022	0.036	0.555	0.076	0.078	0.014
U16-h07-25-167	dk ooid	1.690	0.106	0.004	0.193	0.025	0.000	0.890	0.125	0.000	0.051
U16-h07-25-167	dk ooid	1.287	0.080	0.041	0.135	0.018	0.036	0.505	0.087	0.077	0.098
U16-h07-25-167	dk ooid	1.808	0.157	0.020	0.232	0.025	0.008	0.842	0.100	0.000	0.062
U16-h07-25-167	dk ooid	2.639	0.402	0.020	0.310	0.057	0.008	1.214	0.175	0.000	0.159
U16-h07-25-167	early vein	0.363	0.044	0.000	0.046	0.007	0.000	0.160	0.033	0.000	0.066
U16-h07-25-167	early vein	0.919	0.084	0.000	0.126	0.014	0.000	0.494	0.088	0.000	0.087
U16-h07-25-167	early vein	0.594	0.054	0.000	0.071	0.010	0.000	0.294	0.047	0.000	0.085
U16-h07-25-167	early vein	0.555	0.066	0.000	0.068	0.011	0.000	0.299	0.053	0.000	0.093
U16-h07-25-167	late vein	1.896	0.104	0.000	0.272	0.022	0.000	1.740	0.153	0.000	0.256
U16-h07-25-167	late vein	1.559	0.193	0.000	0.190	0.027	0.000	1.050	0.207	0.000	0.198
U16-h07-25-167	late vein	4.083	0.202	0.000	0.526	0.029	0.000	2.444	0.187	0.000	0.378
U16-h07-25-167	late vein	4.401	0.187	0.000	0.562	0.043	0.000	2.216	0.120	0.000	0.373
U16-h07-25-167	late vein	5.675	0.299	0.000	0.674	0.036	0.000	2.594	0.190	0.000	0.419
U16-h07-25-167	lt ooid	1.548	0.078	0.000	0.173	0.021	0.000	0.545	0.081	0.000	0.107
U16-h07-25-167	lt ooid	1.528	0.113	0.000	0.183	0.023	0.000	0.659	0.095	0.000	0.133
U16-h07-25-167	lt ooid	1.352	0.089	0.000	0.167	0.019	0.000	0.604	0.092	0.000	0.109
U16-h07-25-167	lt ooid	2.349	0.168	0.043	0.240	0.021	0.035	1.019	0.116	0.080	0.116
U16-h07-25-167	lt ooid	1.489	0.096	0.041	0.177	0.021	0.034	0.592	0.097	0.077	0.129
U16-h07-25-167	lt ooid	1.336	0.087	0.000	0.143	0.018	0.000	0.603	0.085	0.000	0.116
U16-h07-25-167	lt ooid	1.535	0.094	0.000	0.182	0.023	0.000	0.769	0.096	0.000	0.118
U16-h07-25-167	lt ooid	1.823	0.147	0.043	0.217	0.033	0.036	0.850	0.104	0.080	0.149
U16-h07-25-167	lt ooid	1.371	0.087	0.000	0.160	0.020	0.000	0.651	0.104	0.000	0.129
U16-h07-25-167	lt ooid	1.996	0.148	0.000	0.206	0.028	0.000	0.827	0.106	0.000	0.115
U16-h07-25-167	matrix cement	0.098	0.020	0.000	0.015	0.005	0.000	0.020	0.013	0.000	0.044
U16-h07-25-167	matrix cement	1.339	0.158	0.000	0.171	0.028	0.000	0.677	0.119	0.000	0.126
U16-h07-25-167	matrix cement	4.957	0.427	0.000	0.580	0.069	0.000	2.222	0.248	0.000	0.389
U16-h07-25-167	matrix cement	1.208	0.088	0.000	0.150	0.021	0.000	0.580	0.092	0.000	0.136
U16-h07-25-167	matrix cement	1.355	0.090	0.000	0.146	0.019	0.000	0.615	0.106	0.000	0.128
U16-h07-25-167	matrix cement	1.234	0.068	0.000	0.169	0.020	0.000	0.595	0.105	0.000	0.146
U16-h07-25-167	matrix cement	1.184	0.087	0.000	0.133	0.018	0.000	0.531	0.067	0.000	0.120

Sample ID	SampleType	Ce (ppm)	2SE (ppm)	Ce LOD (ppm)	Pr (ppm)	2SE (ppm)	Pr LOD (ppm)	Nd (ppm)	2SE (ppm)	Nd LOD (ppm)	Sm (ppm)
U16-h07-25-167	matrix cement	1.157	0.092	0.000	0.158	0.017	0.000	0.472	0.077	0.000	0.171
U16-h07-25-167	matrix cement	1.099	0.055	0.000	0.144	0.020	0.000	0.402	0.078	0.000	0.138
U16-h07-25-167	matrix cement	1.676	0.124	0.000	0.215	0.021	0.000	0.827	0.099	0.000	0.171
U16-h07-25-167	matrix cement	0.647	0.033	0.000	0.084	0.013	0.000	0.318	0.054	0.000	0.101
U16-h07-34-405	matrix cement	1.563	64.734	0.032	-3.886	9.807	0.013	-0.220	22.277	0.070	0.027
U16-h07-34-405	matrix cement	4.959	1.162	0.059	0.447	0.229	0.018	1.852	0.832	0.095	0.296
U16-h07-34-405	matrix cement	-0.838	1.027	0.031	0.214	0.474	0.013	0.233	1.633	0.067	-0.003
U16-h07-34-405	matrix cement	-3.192	0.497	0.335	-0.302	0.121	0.048	-1.392	0.511	0.177	-0.131
U16-h07-34-405	matrix cement	-0.021	0.378	0.360	-0.137	0.117	0.051	-0.343	0.413	0.191	-0.037
U16-h07-34-405	matrix cement	-12.125	8.416	0.029	-1.215	1.114	0.012	-7.403	2.529	0.062	-1.470
U16-h07-34-405	matrix cement	-17.388	14.328	0.029	-1.543	1.356	0.012	-10.029	7.500	0.062	-1.285
U16-h07-34-405	matrix cement	0.321	0.331	0.361	-0.023	0.066	0.051	-0.073	0.380	0.191	-0.143
U16-h07-34-405	matrix cement	-0.661	1.421	0.060	-0.054	0.350	0.018	-0.156	1.776	0.097	0.147
U16-h07-34-405	matrix cement	0.283	0.278	0.361	-0.011	0.065	0.051	-0.273	0.319	0.191	0.022
U16-h07-34-405	matrix cement	-1.083	0.698	0.030	-0.574	0.305	0.013	-1.740	0.747	0.065	-0.126
U16-h07-34-405	matrix cement	-5.802	2.696	0.029	-0.389	0.348	0.012	-4.511	3.004	0.063	-0.046
U16-h07-34-405	matrix cement	-3.945	1.385	0.030	-0.340	0.594	0.013	-3.534	2.741	0.065	-0.271
U16-h07-34-405	matrix cement	23.110	13.924	0.031	2.530	1.183	0.013	7.985	5.183	0.068	0.617
U16-h07-34-405	matrix cement	-2.859	7.703	0.032	0.144	0.621	0.013	-0.758	3.066	0.068	-0.090
U16-h07-34-405	matrix cement	-4.523	7.343	0.031	-0.423	0.762	0.013	0.320	3.084	0.066	-0.074
U16-h07-34-405	matrix cement	-5.029	2.274	0.032	-0.239	0.528	0.013	-3.734	3.430	0.068	-0.669
U16-h07-34-405	ooid	2.240	0.231	0.229	0.294	0.076	0.037	1.013	0.280	0.129	0.288
U16-h07-34-405	ooid	8.933	1.729	0.340	1.790	0.682	0.047	5.181	1.816	0.191	0.532
U16-h07-34-405	ooid	-22.910	17.254	0.055	-2.751	1.982	0.016	-11.503	4.743	0.088	-0.481
U16-h07-34-405	ooid	-5.205	1.686	0.437	-0.441	0.160	0.048	-1.747	0.570	0.200	-0.356
U16-h07-34-405	ooid	-0.097	0.376	0.346	-0.077	0.103	0.041	-0.293	0.636	0.186	0.066
U16-h07-34-405	ooid	-6.066	0.894	0.329	-0.700	0.131	0.039	-2.455	0.660	0.177	-0.223
U16-h07-34-405	ooid	-10.358	2.012	0.534	-1.138	0.264	0.063	-4.015	0.972	0.219	-0.925
U16-h07-34-405	ooid	-2.799	0.556	0.420	-0.217	0.121	0.045	-0.495	0.412	0.197	-0.020
U16-h07-34-405	ooid	3.712	0.836	0.352	0.387	0.116	0.047	1.494	0.544	0.185	0.207
U16-h07-34-405	ooid	-6.489	1.268	0.328	-0.759	0.177	0.044	-3.260	0.970	0.173	-0.518
U16-h07-34-405	ooid	-3.973	1.297	0.453	-0.733	0.268	0.049	-2.055	0.827	0.207	0.149
U16-h07-34-405	ooid	-2.431	0.426	0.320	-0.278	0.080	0.038	-0.933	0.402	0.173	-0.047

Sample ID	SampleType	Ce (ppm)	2SE (ppm)	Ce LOD (ppm)	Pr (ppm)	2SE (ppm)	Pr LOD (ppm)	Nd (ppm)	2SE (ppm)	Nd LOD (ppm)	Sm (ppm)
U16-h07-34-405	ooid	-2.839	0.909	0.438	-0.381	0.164	0.047	-0.448	0.563	0.205	-0.280
U16-h07-34-405	ooid	-3.828	0.838	0.352	-0.473	0.116	0.042	-1.401	0.672	0.190	-0.252
U16-h07-34-405	ooid	-1.728	0.657	0.298	-0.206	0.162	0.045	-1.110	0.513	0.168	-0.478
U16-h07-34-405	ooid	-3.728	1.109	0.301	-0.423	0.164	0.046	-1.827	0.641	0.170	-0.059
U16-h07-34-405	ooid	-0.182	0.367	0.351	-0.023	0.070	0.041	-0.327	0.387	0.189	-0.044
U16-h07-34-405	ooid	-7.512	0.921	0.323	-0.886	0.218	0.045	-2.925	0.949	0.181	-0.891
U16-h07-34-405	ooid	-2.897	0.610	0.325	-0.502	0.101	0.038	-1.498	0.400	0.175	-0.063
U16-h07-34-405	ooid	-3.614	0.511	0.533	-0.318	0.164	0.063	-1.123	0.655	0.218	-0.163
U16-h07-34-405	ooid	10.914	16.350	0.060	0.899	2.175	0.018	2.397	8.277	0.096	0.538
U16-h07-34-405	ooid and clast	38.637	6.553	0.027	4.690	0.825	0.041	20.655	3.579	0.000	3.755
U16-h07-34-405	ooid and clast	2.126	0.473	0.274	0.237	0.075	0.072	0.967	0.296	0.124	0.140
U16-h07-34-405	ooid and clast	0.183	0.030	0.000	0.016	0.006	0.003	0.056	0.028	0.000	0.003
U16-h07-34-405	ooid and clast	0.770	0.112	0.000	0.074	0.013	0.003	0.259	0.063	0.000	0.040
U16-h07-34-405	ooid and clast	6.516	0.785	0.007	0.703	0.099	0.010	2.829	0.416	0.000	0.625
U16-h07-34-405	ooid and clast	12.552	1.244	0.008	1.520	0.136	0.012	5.888	0.675	0.000	1.046
U16-h07-34-405	ooid and clast	6.316	0.583	0.266	0.704	0.074	0.069	2.608	0.258	0.120	0.449
U16-h07-34-405	ooid and clast	5.039	0.320	0.007	0.492	0.039	0.010	1.756	0.205	0.000	0.346
U16-h07-34-405	ooid and clast	7.502	0.640	0.007	0.935	0.074	0.010	3.551	0.425	0.000	0.670
U16-h07-34-405	ooid and clast	4.926	0.291	0.007	0.604	0.047	0.011	1.990	0.187	0.000	0.389
U16-h07-34-405	ooid and clast	8.487	0.941	0.000	1.032	0.136	0.003	4.328	0.683	0.000	0.816
U16-h07-34-405	ooid and clast	1.591	0.118	0.000	0.189	0.029	0.000	0.732	0.151	0.000	0.090
U16-h07-34-405	ooid and clast	11.852	0.392	0.000	1.375	0.111	0.000	4.960	0.478	0.000	0.863
U16-h07-34-405	ooid and clast	11.190	0.739	0.225	1.229	0.096	0.021	4.383	0.495	0.068	0.845
U16-h07-34-405	ooid and clast	11.564	0.902	0.000	1.385	0.145	0.008	4.894	0.686	0.000	0.658
U16-h07-34-405	ooid and clast	26.420	2.041	0.000	3.165	0.322	0.000	11.647	1.338	0.000	2.260
U16-h07-34-405	ooid and clast	14.977	46.525	0.000	0.647	6.480	0.000	4.287	23.612	0.000	-0.658
U16-h07-34-405	ooid and clast	14.338	53.131	0.238	0.108	7.611	0.022	-4.874	29.882	0.073	2.074
U16-h07-34-405	ooid and clast	-62.049	112.423	0.000	-8.035	12.497	0.000	-35.855	11.121	0.000	-3.347
U16-h07-34-405	ooid and clast	0.951	0.167	1.304	0.193	0.016	0.151	0.549	0.049	0.600	0.094
U16-h07-34-405	ooid and clast	-16.081	1.340	0.233	-1.632	0.159	0.022	-5.780	0.725	0.071	-1.270
U16-h07-34-405	ooid and clast	-25.527	2.095	0.000	-2.963	0.316	0.000	-12.578	1.424	0.000	-2.253
U16-h07-34-405	ooid and clast	-28.628	2.214	0.000	-3.376	0.369	0.000	-11.452	1.320	0.000	-1.676
U16-h07-34-405	ooid and clast	-7.698	0.350	0.019	-0.825	0.069	0.000	-2.507	0.182	0.000	-0.656

Sample ID	SampleType	Ce (ppm)	2SE (ppm)	Ce LOD (ppm)	Pr (ppm)	2SE (ppm)	Pr LOD (ppm)	Nd (ppm)	2SE (ppm)	Nd LOD (ppm)	Sm (ppm)
U16-h07-34-405	ooid and clast	-7.966	0.359	0.000	-0.923	0.078	0.000	-3.816	0.386	0.000	-0.598
U16-h07-34-405	ooid and clast	-5.066	0.433	0.000	-0.611	0.077	0.000	-1.897	0.290	0.000	-0.360
U16-h07-34-405	ooid and clast	-5.115	1.038	1.315	-0.583	0.143	0.156	-1.423	0.371	0.504	-0.388
U16-h07-34-405	ooid and clast	-5.011	0.258	0.000	-0.574	0.050	0.011	-1.847	0.185	0.000	-0.357
U16-h07-34-405	ooid and clast	-3.936	0.418	0.011	-0.528	0.060	0.000	-1.519	0.201	0.042	-0.402
U16-h07-34-405	ooid and clast	-4.724	0.545	1.331	-0.491	0.082	0.158	-1.803	0.248	0.511	-0.498
U16-h07-34-405	ooid and clast	-3.504	0.313	0.010	-0.405	0.047	0.000	-1.334	0.169	0.038	-0.272
U16-h07-34-405	ooid and clast	-2.498	0.216	0.010	-0.254	0.026	0.000	-0.871	0.087	0.037	-0.172
U16-h07-34-405	ooid and clast	-2.431	0.216	1.203	-0.274	0.028	0.140	-0.987	0.116	0.553	-0.146
U16-h07-34-405	ooid and clast	-3.770	0.226	0.000	-0.418	0.044	0.011	-1.425	0.207	0.000	-0.305
U16-h07-34-405	vein 1	12.292	2.001	1.215	1.179	0.192	0.124	3.924	0.666	0.448	0.433
U16-h07-34-405	vein 1	11.285	2.312	1.266	0.933	0.254	0.125	3.733	1.060	0.454	0.187
U16-h07-34-405	vein 1	30.383	17.790	1.305	3.121	1.843	0.129	9.515	3.607	0.468	1.093
U16-h07-34-405	vein 1	17.419	3.608	1.197	1.632	0.340	0.118	5.274	1.176	0.430	0.632
U16-h07-34-405	vein 1	15.681	2.612	1.241	1.475	0.272	0.123	5.145	0.868	0.445	0.619
U16-h07-34-405	vein 2	-6.925	0.805	1.400	-0.845	0.116	0.143	-3.894	0.453	0.516	-0.458
U16-h07-34-405	vein 2	-4.282	0.498	1.291	-0.609	0.098	0.132	-1.935	0.355	0.476	-0.458
U16-h07-34-405	vein 2	-6.753	0.553	1.359	-0.803	0.080	0.139	-3.320	0.384	0.501	-0.590
U16-h07-34-405	vein 2	-13.430	2.128	1.385	-1.832	0.319	0.141	-6.407	1.276	0.511	-1.357
U16-h07-34-405	vein 2	-20.066	1.927	1.321	-1.995	0.240	0.135	-6.760	0.641	0.487	-0.846
U16-h07-34-405	vein 2	-20.800	2.594	1.369	-2.173	0.363	0.140	-7.667	1.195	0.505	-1.460
U16-h07-54-338	coarse calcite	0.752	0.081	0.024	0.095	0.020	0.005	0.321	0.079	0.000	0.082
U16-h07-54-338	coarse calcite	0.354	0.033	0.075	0.059	0.012	0.018	0.184	0.047	0.080	0.032
U16-h07-54-338	coarse calcite	0.212	0.024	0.010	0.021	0.008	0.008	0.169	0.052	0.043	0.007
U16-h07-54-338	coarse calcite	0.976	0.099	0.016	0.123	0.012	0.014	0.427	0.082	0.046	0.080
U16-h07-54-338	coarse calcite	4.119	0.988	0.072	0.463	0.117	0.018	1.945	0.542	0.077	0.376
U16-h07-54-338	coarse calcite	0.414	0.030	0.019	0.048	0.011	0.009	0.293	0.055	0.000	0.005
U16-h07-54-338	coarse calcite	0.384	0.048	0.075	0.062	0.012	0.019	0.192	0.055	0.081	0.046
U16-h07-54-338	coarse calcite	0.751	0.096	0.073	0.099	0.019	0.009	0.415	0.084	0.056	0.051
U16-h07-54-338	coarse calcite	2.257	0.531	0.020	0.281	0.076	0.010	1.147	0.306	0.000	0.156
U16-h07-54-338	coarse calcite	4.370	0.789	0.069	0.479	0.094	0.017	1.941	0.337	0.074	0.410
U16-h07-54-338	coarse calcite	3.428	0.288	0.070	0.359	0.031	0.017	1.401	0.197	0.075	0.343
U16-h07-54-338	coarse calcite	1.760	0.341	0.066	0.196	0.043	0.010	0.744	0.140	0.035	0.117

Sample ID	SampleType	Ce (ppm)	2SE (ppm)	Ce LOD (ppm)	Pr (ppm)	2SE (ppm)	Pr LOD (ppm)	Nd (ppm)	2SE (ppm)	Nd LOD (ppm)	Sm (ppm)
U16-h07-54-338	coarse calcite	0.709	0.108	0.078	0.074	0.020	0.004	0.309	0.060	0.028	0.044
U16-h07-54-338	coarse calcite	2.421	1.041	0.019	0.269	0.109	0.010	1.369	0.478	0.000	0.293
U16-h07-54-338	coarse calcite	0.472	0.064	0.027	0.066	0.016	0.009	0.281	0.061	0.049	0.009
U16-h07-54-5	matrix cement	1.038	0.180	0.014	0.106	0.023	0.000	0.382	0.101	0.000	0.062
U16-h07-54-5	matrix cement	2.525	0.262	0.014	0.292	0.039	0.000	1.352	0.165	0.000	0.229
U16-h07-54-5	matrix cement	4.427	0.381	0.014	0.520	0.055	0.000	2.222	0.278	0.000	0.401
U16-h07-54-5	matrix cement	3.898	0.457	0.013	0.433	0.076	0.000	2.071	0.332	0.000	0.392
U16-h07-54-5	matrix cement	4.572	0.223	0.007	0.540	0.045	0.000	2.106	0.184	0.000	0.388
U16-h07-54-5	matrix cement	4.309	0.192	0.000	0.482	0.036	0.000	1.832	0.198	0.000	0.282
U16-h07-54-5	matrix cement	4.186	0.309	0.014	0.547	0.051	0.000	2.003	0.220	0.000	0.419
U16-h07-54-5	matrix cement	4.775	0.250	0.014	0.510	0.043	0.000	1.873	0.196	0.000	0.346
U16-h07-54-5	matrix cement	2.671	0.174	0.007	0.278	0.033	0.000	1.056	0.157	0.000	0.160
U16-h07-54-5	matrix cement	3.901	0.351	0.014	0.511	0.059	0.000	1.495	0.142	0.000	0.334
U16-h07-54-5	matrix cement	4.425	0.176	0.000	0.512	0.043	0.000	1.698	0.158	0.000	0.359
U16-h07-54-5	matrix cement	3.012	0.308	0.014	0.279	0.031	0.000	1.005	0.122	0.000	0.182
U16-h07-54-5	matrix cement	4.121	0.435	0.014	0.443	0.058	0.000	1.475	0.175	0.000	0.154
U16-h07-54-5	matrix cement	4.994	0.386	0.014	0.597	0.046	0.000	2.377	0.219	0.000	0.368
U16-h07-54-5	matrix cement	0.932	0.130	0.000	0.095	0.018	0.000	0.349	0.074	0.000	0.072
U16-h07-54-5	matrix cement	4.978	0.333	0.014	0.506	0.056	0.000	1.838	0.280	0.000	0.315
U16-h07-54-5	matrix cement	1.763	0.326	0.014	0.172	0.026	0.000	0.808	0.150	0.000	0.120
U16-h07-54-5	ooid	9.511	0.591	0.007	1.182	0.097	0.010	5.453	0.610	0.000	0.916
U16-h07-54-5	ooid	5.136	0.268	0.019	0.578	0.045	0.000	1.974	0.186	0.039	0.354
U16-h07-54-5	ooid	1.047	0.169	0.000	0.112	0.025	0.003	0.415	0.093	0.000	0.079
U16-h07-54-5	ooid	5.127	0.207	0.011	0.564	0.045	0.006	2.303	0.178	0.000	0.351
U16-h07-54-5	ooid	5.419	0.256	0.020	0.625	0.056	0.000	2.636	0.253	0.042	0.541
U16-h07-54-5	ooid	2.025	0.279	0.006	0.222	0.037	0.009	0.850	0.139	0.000	0.076
U16-h07-54-5	ooid	7.516	0.458	0.011	0.925	0.062	0.006	3.922	0.324	0.000	0.860
U16-h07-54-5	ooid	10.155	0.560	0.020	1.349	0.088	0.000	5.807	0.517	0.042	1.069
U16-h07-54-5	ooid	4.536	0.233	0.000	0.484	0.044	0.000	2.206	0.236	0.000	0.388
U16-h07-54-5	ooid	4.393	0.263	0.000	0.485	0.044	0.003	2.048	0.214	0.000	0.316
U16-h07-54-5	ooid	5.785	0.394	0.000	0.729	0.082	0.003	2.896	0.301	0.000	0.556
U16-h07-54-5	ooid	4.691	0.276	0.011	0.496	0.036	0.006	1.998	0.212	0.000	0.357
U16-h07-54-5	ooid	2.461	0.172	0.020	0.267	0.029	0.000	1.031	0.109	0.040	0.178

Sample ID	SampleType	Ce (ppm)	2SE (ppm)	Ce LOD (ppm)	Pr (ppm)	2SE (ppm)	Pr LOD (ppm)	Nd (ppm)	2SE (ppm)	Nd LOD (ppm)	Sm (ppm)
U16-h07-54-5	ooid	3.700	0.198	0.011	0.392	0.028	0.006	1.520	0.146	0.000	0.234
U16-h07-54-5	ooid	3.001	0.295	0.024	0.311	0.034	0.000	1.151	0.154	0.049	0.277
U16-h07-54-5	ooid	2.919	0.358	0.000	0.311	0.048	0.000	1.172	0.171	0.000	0.249
U16-h07-54-5	ooid	5.647	0.353	0.010	0.601	0.059	0.005	2.073	0.254	0.000	0.359
U16-h07-54-5	ooid	5.924	0.575	0.011	0.621	0.062	0.006	1.991	0.199	0.000	0.346
U16-h07-54-5	ooid	4.112	0.172	0.006	0.456	0.034	0.008	1.576	0.197	0.000	0.287
U16-h07-54-5	ooid	4.620	0.337	0.011	0.491	0.052	0.006	1.781	0.186	0.000	0.329
U16-h07-54-5	ooid	2.969	0.175	0.021	0.330	0.035	0.000	1.239	0.156	0.042	0.230
U16-h07-54-5	ooid	4.227	0.911	0.006	0.436	0.092	0.009	1.486	0.333	0.000	0.241
U16-h07-54-5	ooid	4.897	0.377	0.019	0.551	0.049	0.000	1.983	0.144	0.040	0.321
U16-h07-54-5	ooid	5.827	0.427	0.011	0.637	0.061	0.006	2.078	0.183	0.000	0.207
U16-h07-54-5	ooid	1.549	0.214	0.006	0.181	0.029	0.009	0.682	0.124	0.000	0.087
U16-h07-54-5	vein 1	2.343	0.135	0.006	0.346	0.039	0.000	1.245	0.137	0.000	0.171
U16-h07-54-5	vein 1	15.517	1.804	0.026	1.514	0.158	0.014	5.093	0.608	0.052	0.654
U16-h07-54-5	vein 1	3.033	0.270	0.106	0.287	0.033	0.011	0.901	0.125	0.028	0.161
U16-h07-54-5	vein 1	1.992	0.138	0.101	0.219	0.023	0.010	0.836	0.120	0.027	0.147
U16-h07-54-5	vein 1	3.831	0.423	0.107	0.508	0.064	0.011	1.872	0.247	0.029	0.230
U16-h07-54-5	vein 1	6.246	0.740	0.103	0.682	0.087	0.011	2.125	0.238	0.028	0.388
U16-h07-54-5	vein 2	1.124	0.063	0.006	0.157	0.016	0.000	0.503	0.066	0.000	0.100
U16-h07-54-5	vein 2	9.633	0.637	0.006	1.048	0.065	0.000	3.541	0.298	0.000	0.550
U16-h07-54-5	vein 2	0.491	0.075	0.006	0.058	0.015	0.000	0.156	0.042	0.000	0.040
U16-h07-67-129	darker vein	0.529	0.070	0.000	0.056	0.011	0.000	0.235	0.059	0.000	0.025
U16-h07-67-129	darker vein	0.570	0.049	0.035	0.066	0.012	0.004	0.205	0.056	0.000	0.014
U16-h07-67-129	darker vein	0.471	0.042	0.010	0.047	0.011	0.000	0.169	0.046	0.000	0.019
U16-h07-67-129	darker vein	0.354	0.050	0.035	0.048	0.010	0.004	0.140	0.045	0.000	0.005
U16-h07-67-129	darker vein	0.518	0.095	0.000	0.055	0.015	0.000	0.168	0.052	0.000	0.036
U16-h07-67-129	darker vein	1.313	0.168	0.000	0.126	0.020	0.000	0.517	0.094	0.000	0.049
U16-h07-67-129	darker vein	1.760	0.180	0.010	0.189	0.023	0.000	0.662	0.105	0.000	0.051
U16-h07-67-129	lighter vein	3.423	0.816	0.000	0.494	0.130	0.000	1.891	0.490	0.000	0.380
U16-h07-67-129	lighter vein	14.880	0.600	0.037	2.155	0.118	0.004	8.467	0.438	0.000	1.353
U16-h07-67-129	lighter vein	4.337	0.385	0.035	0.614	0.074	0.006	2.385	0.242	0.017	0.342
U16-h07-67-129	lighter vein	12.338	0.610	0.000	1.825	0.112	0.000	7.249	0.488	0.000	1.208
U16-h07-67-129	lighter vein	4.800	0.274	0.000	0.589	0.053	0.000	2.457	0.229	0.000	0.314

Sample ID	SampleType	Ce (ppm)	2SE (ppm)	Ce LOD (ppm)	Pr (ppm)	2SE (ppm)	Pr LOD (ppm)	Nd (ppm)	2SE (ppm)	Nd LOD (ppm)	Sm (ppm)
U16-h07-67-129	lighter vein	16.184	0.402	0.000	2.442	0.133	0.000	8.819	0.391	0.000	1.305
U16-h07-67-129	lighter vein	8.173	1.053	0.038	1.105	0.184	0.004	3.483	0.669	0.000	0.389
U16-h07-67-129	ooid and matrix	125.865	16.496	0.162	21.003	2.866	0.032	96.733	12.573	0.363	18.034
U16-h07-67-129	ooid and matrix	16.728	1.388	0.045	2.413	0.266	0.005	9.948	1.057	0.000	1.611
U16-h07-67-129	ooid and matrix	22.607	1.904	0.276	3.282	0.300	0.023	14.157	1.185	0.253	2.408
U16-h07-67-129	ooid and matrix	11.907	0.632	0.077	1.835	0.128	0.052	7.345	0.623	0.101	1.160
U16-h07-67-129	ooid and matrix	17.331	4.025	0.040	2.357	0.510	0.020	12.098	3.294	0.000	1.968
U16-h07-67-129	ooid and matrix	11.702	1.193	0.066	1.632	0.117	0.028	6.690	0.511	0.211	0.994
U16-h07-67-129	ooid and matrix	5.091	0.283	0.056	0.622	0.053	0.000	2.397	0.223	0.000	0.295
U16-h07-67-129	ooid and matrix	8.257	0.377	5.231	1.162	0.107	0.639	4.356	0.271	2.268	0.677
U16-h07-67-129	ooid and matrix	14.646	0.668	0.256	2.260	0.133	0.064	8.942	0.466	0.182	1.334
U16-h07-67-129	ooid and matrix	16.378	1.573	0.073	2.584	0.279	0.031	11.191	1.307	0.234	1.880
U16-h07-67-129	ooid and matrix	8.011	1.428	0.048	1.189	0.234	0.006	4.551	0.927	0.000	0.769
U16-h07-67-129	ooid and matrix	2.761	0.239	0.047	0.346	0.032	0.000	1.238	0.141	0.000	0.149
U16-h07-67-129	ooid and matrix	7.667	0.581	0.046	1.124	0.053	0.012	4.443	0.315	0.067	0.684
U16-h07-67-129	ooid and matrix	2.307	0.194	0.079	0.240	0.026	0.012	0.975	0.155	0.000	0.078
U16-h07-67-129	ooid and matrix	7.768	0.470	0.028	1.109	0.093	0.006	4.162	0.260	0.063	0.695
U16-h07-67-129	ooid and matrix	0.299	0.059	0.047	0.037	0.011	0.000	0.122	0.046	0.000	0.011
U16-h07-67-129	ooid and matrix	4.021	0.566	0.080	0.477	0.078	0.012	2.070	0.435	0.000	0.369
U16-h07-67-129	ooid and matrix	2.557	0.399	0.242	0.372	0.059	0.061	1.342	0.280	0.172	0.204
U16-h07-67-129	ooid and matrix	6.656	0.337	0.062	0.838	0.079	0.026	3.168	0.311	0.198	0.563
U16-h07-67-129	ooid and matrix	3.615	0.194	0.045	0.482	0.046	0.005	1.799	0.217	0.000	0.289
U16-h07-67-129	ooid and matrix	3.580	0.326	0.044	0.630	0.065	0.000	2.479	0.245	0.000	0.358
U16-h07-67-129	ooid and matrix	17.017	2.012	0.052	2.234	0.293	0.023	8.564	1.164	0.077	1.180
U16-h07-67-129	ooid and matrix	7.244	0.394	0.045	0.885	0.055	0.012	2.852	0.204	0.066	0.459
U16-h07-67-129	ooid and matrix	12.597	0.872	0.339	1.617	0.119	0.036	6.488	0.552	0.197	0.803
U16-h07-67-129	ooid and matrix	14.775	0.998	0.054	2.061	0.201	0.024	7.286	0.705	0.080	1.204

Sample ID	SampleType	2SE (ppm)	Sm LOD (ppm)	Eu (ppm)	2SE (ppm)	Eu LOD (ppm)	Gd (ppm)	2SE (ppm)	Gd LOD (ppm)	Tb (ppm)
U16-h07-13b-11	matrix	0.068	0.043	0.195	0.047	0.000	0.318	0.080	0.000	0.054
U16-h07-13b-11	matrix	0.017	0.037	0.034	0.012	0.000	0.068	0.028	0.000	0.006
U16-h07-13b-11	matrix	0.037	0.036	0.010	0.006	0.000	0.082	0.030	0.000	0.008
U16-h07-13b-11	matrix	0.036	0.036	0.026	0.010	0.000	0.119	0.031	0.000	0.025
U16-h07-13b-11	matrix	0.026	0.038	0.019	0.009	0.000	0.048	0.022	0.000	0.013
U16-h07-13b-11	matrix	0.025	0.038	0.028	0.011	0.000	0.082	0.031	0.000	0.007
U16-h07-13b-11	matrix	0.053	0.038	0.061	0.015	0.000	0.166	0.042	0.000	0.015
U16-h07-13b-11	matrix	0.041	0.037	0.077	0.016	0.000	0.211	0.053	0.000	0.022
U16-h07-13b-11	matrix	0.090	0.039	0.085	0.020	0.000	0.418	0.083	0.000	0.049
U16-h07-13b-11	matrix	0.046	0.038	0.061	0.018	0.000	0.177	0.060	0.000	0.020
U16-h07-13b-11	matrix	0.051	0.036	0.063	0.016	0.000	0.251	0.056	0.000	0.031
U16-h07-13b-11	matrix	0.046	0.035	0.031	0.011	0.000	0.128	0.048	0.000	0.019
U16-h07-13b-11	matrix	0.051	0.037	0.045	0.015	0.000	0.151	0.050	0.000	0.029
U16-h07-13b-11	matrix	0.045	0.036	0.092	0.020	0.000	0.254	0.062	0.000	0.045
U16-h07-13b-11	matrix	0.052	0.036	0.109	0.025	0.000	0.220	0.056	0.000	0.023
U16-h07-13b-11	matrix	0.055	0.037	0.077	0.018	0.000	0.245	0.062	0.000	0.033
U16-h07-13b-11	matrix	0.046	0.037	0.076	0.016	0.000	0.163	0.045	0.000	0.028
U16-h07-13b-11	matrix	0.030	0.037	0.030	0.011	0.000	0.076	0.032	0.000	0.011
U16-h07-13b-11	matrix	0.072	0.037	0.093	0.017	0.000	0.330	0.071	0.000	0.047
U16-h07-13b-11	matrix	0.053	0.038	0.177	0.034	0.000	0.285	0.049	0.000	0.037
U16-h07-13b-11	matrix	0.054	0.036	0.089	0.016	0.000	0.208	0.061	0.000	0.025
U16-h07-13b-11	vein 1	0.059	0.036	0.270	0.046	0.000	0.299	0.070	0.000	0.038
U16-h07-13b-11	vein 1	0.177	0.038	1.322	0.083	0.000	1.532	0.136	0.000	0.199
U16-h07-13b-11	vein 1	0.194	0.036	1.940	0.109	0.000	2.021	0.186	0.000	0.207
U16-h07-13b-11	vein 1	0.124	0.036	0.698	0.063	0.000	0.887	0.109	0.000	0.108
U16-h07-13b-11	vein 1	0.147	0.036	0.993	0.153	0.000	0.587	0.115	0.000	0.058
U16-h07-13b-11	vein 1	0.159	0.036	2.391	0.175	0.000	1.868	0.181	0.000	0.180
U16-h07-13b-11	vein 1	0.143	0.036	1.138	0.080	0.000	1.208	0.148	0.000	0.127
U16-h07-13b-11	vein 2	0.023	0.035	0.035	0.013	0.000	0.043	0.022	0.000	0.010
U16-h07-13b-11	vein 2	0.025	0.037	0.026	0.017	0.000	0.014	0.010	0.000	0.003
U16-h07-13b-11	vein 2	0.011	0.037	0.011	0.005	0.000	0.022	0.016	0.000	0.002
U16-h07-13b-11	vein 2	1.000	0.038	0.000	1.000	0.000	0.005	0.000	0.000	0.000
U16-h07-13b-11	vein 2	1.000	0.038	0.002	0.002	0.000	0.007	0.005	0.000	0.000

Sample ID	SampleType	2SE (ppm)	Sm LOD (ppm)	Eu (ppm)	2SE (ppm)	Eu LOD (ppm)	Gd (ppm)	2SE (ppm)	Gd LOD (ppm)	Tb (ppm)
U16-h07-13b-11	vein 2	1.000	0.038	0.000	1.000	0.000	0.004	0.000	0.000	0.000
U16-h07-13b-11	vein 3	0.057	0.038	0.160	0.033	0.000	0.276	0.061	0.000	0.029
U16-h07-13b-11	vein 3	0.082	0.037	0.258	0.043	0.000	0.362	0.071	0.000	0.048
U16-h07-13b-11	vein 3	0.107	0.038	0.362	0.053	0.000	0.691	0.100	0.000	0.105
U16-h07-13b-31	dk ooid	0.046	0.000	0.053	0.016	0.000	0.212	0.055	0.026	0.051
U16-h07-13b-31	dk ooid	0.130	0.000	0.189	0.033	0.012	0.677	0.115	0.041	0.133
U16-h07-13b-31	dk ooid	0.098	0.000	0.123	0.021	0.000	0.461	0.094	0.026	0.068
U16-h07-13b-31	dk ooid	0.071	0.000	0.134	0.027	0.000	0.474	0.081	0.026	0.085
U16-h07-13b-31	dk ooid	0.106	0.000	0.154	0.030	0.010	0.550	0.102	0.033	0.103
U16-h07-13b-31	dk ooid	0.099	0.000	0.193	0.031	0.011	0.703	0.109	0.039	0.122
U16-h07-13b-31	matrix cement	0.069	0.000	0.077	0.018	0.000	0.218	0.071	0.026	0.054
U16-h07-13b-31	matrix cement	0.094	0.047	0.129	0.021	0.000	0.614	0.111	0.000	0.083
U16-h07-13b-31	matrix cement	0.223	0.000	0.390	0.080	0.000	1.361	0.252	0.026	0.229
U16-h07-13b-31	matrix cement	0.071	0.000	0.131	0.032	0.000	0.558	0.101	0.025	0.097
U16-h07-13b-31	matrix cement	0.123	0.047	0.171	0.033	0.000	0.703	0.128	0.000	0.124
U16-h07-13b-31	matrix cement	0.119	0.000	0.188	0.031	0.000	0.751	0.150	0.026	0.140
U16-h07-13b-31	matrix cement	0.088	0.000	0.165	0.036	0.000	0.547	0.091	0.025	0.113
U16-h07-13b-31	matrix cement	0.090	0.045	0.142	0.025	0.000	0.576	0.093	0.000	0.112
U16-h07-13b-31	matrix cement	0.107	0.000	0.187	0.030	0.000	0.728	0.112	0.000	0.114
U16-h07-13b-31	matrix cement	0.102	0.000	0.162	0.026	0.000	0.735	0.102	0.000	0.111
U16-h07-13b-31	matrix cement	0.091	0.046	0.136	0.031	0.000	0.577	0.087	0.000	0.093
U16-h07-13b-31	matrix cement	0.078	0.047	0.136	0.026	0.000	0.529	0.076	0.000	0.106
U16-h07-13b-31	ooid	0.110	0.000	0.230	0.035	0.000	0.912	0.113	0.000	0.133
U16-h07-13b-31	ooid	0.062	0.000	0.062	0.016	0.000	0.261	0.050	0.052	0.053
U16-h07-13b-31	ooid	0.212	0.000	0.316	0.051	0.000	1.376	0.164	0.000	0.194
U16-h07-13b-31	ooid	0.083	0.098	0.064	0.015	0.051	0.282	0.055	0.112	0.047
U16-h07-13b-31	ooid	0.098	0.000	0.151	0.022	0.000	0.705	0.100	0.000	0.131
U16-h07-13b-31	ooid	0.081	0.000	0.094	0.018	0.000	0.511	0.076	0.000	0.077
U16-h07-13b-31	ooid	0.124	0.000	0.175	0.032	0.000	0.853	0.128	0.000	0.115
U16-h07-13b-31	ooid	0.140	0.095	0.188	0.039	0.050	0.908	0.192	0.109	0.121
U16-h07-13b-31	ooid	0.083	0.000	0.140	0.032	0.000	0.500	0.088	0.000	0.091
U16-h07-13b-31	ooid	0.123	0.000	0.301	0.035	0.000	1.090	0.129	0.000	0.155
U16-h07-13b-31	ooid	0.091	0.000	0.121	0.026	0.000	0.422	0.082	0.000	0.087

Sample ID	SampleType	2SE (ppm)	Sm LOD (ppm)	Eu (ppm)	2SE (ppm)	Eu LOD (ppm)	Gd (ppm)	2SE (ppm)	Gd LOD (ppm)	Tb (ppm)
U16-h07-13b-31	ooid	0.118	0.000	0.141	0.030	0.000	0.767	0.098	0.052	0.118
U16-h07-13b-31	ooid	0.109	0.000	0.148	0.026	0.000	0.529	0.092	0.000	0.096
U16-h07-13b-31	ooid	0.116	0.000	0.203	0.030	0.000	0.755	0.112	0.000	0.119
U16-h07-13b-31	ooid	0.142	0.000	0.233	0.044	0.000	1.001	0.181	0.052	0.142
U16-h07-13b-31	ooid	0.107	0.000	0.158	0.030	0.000	0.655	0.114	0.000	0.109
U16-h07-13b-31	ooid	0.108	0.000	0.169	0.029	0.000	0.805	0.121	0.000	0.112
U16-h07-13b-31	ooid	0.153	0.000	0.208	0.037	0.000	0.785	0.100	0.000	0.122
U16-h07-13b-31	ooid	0.095	0.000	0.175	0.027	0.000	0.705	0.096	0.000	0.117
U16-h07-13b-31	ooid	0.114	0.000	0.191	0.029	0.000	0.715	0.090	0.000	0.132
U16-h07-13b-31	ooid	0.095	0.000	0.129	0.022	0.000	0.704	0.108	0.000	0.108
U16-h07-13b-31	ooid	0.091	0.000	0.112	0.021	0.000	0.602	0.090	0.000	0.089
U16-h07-13b-31	ooid	0.075	0.000	0.145	0.025	0.000	0.424	0.079	0.000	0.086
U16-h07-13b-31	ooid	0.077	0.095	0.140	0.020	0.050	0.696	0.064	0.109	0.103
U16-h07-13b-31	vein-1	0.239	0.000	0.422	0.066	0.000	1.650	0.213	0.000	0.225
U16-h07-13b-31	vein-1	0.027	0.000	0.051	0.015	0.000	0.105	0.047	0.000	0.021
U16-h07-13b-31	vein-1	0.043	0.000	0.059	0.014	0.000	0.102	0.031	0.000	0.014
U16-h07-13b-31	vein-1	0.021	0.038	0.012	0.007	0.000	0.095	0.034	0.060	0.012
U16-h07-13b-31	vein-1	0.033	0.000	0.028	0.012	0.000	0.114	0.039	0.000	0.011
U16-h07-13b-31	vein-1	0.041	0.000	0.025	0.011	0.000	0.110	0.036	0.000	0.010
U16-h07-13b-81	coarse calcite	1.000	0.005	0.000	1.000	0.001	0.000	1.000	0.008	0.000
U16-h07-13b-81	coarse calcite	0.000	0.005	0.000	1.000	0.001	-0.001	0.000	0.009	0.000
U16-h07-13b-81	coarse calcite	0.000	0.005	0.000	1.000	0.001	-0.005	0.000	0.008	-0.001
U16-h07-13b-81	coarse calcite	0.001	0.042	0.000	1.000	0.006	-0.014	0.002	0.031	-0.003
U16-h07-13b-81	vein 1	0.193	0.165	0.238	0.032	0.031	1.398	0.174	0.229	0.190
U16-h07-13b-81	vein 1	0.293	0.414	0.294	0.059	0.090	1.615	0.299	0.430	0.247
U16-h07-13b-81	vein 1	0.058	0.127	0.035	0.016	0.024	0.177	0.057	0.176	0.029
U16-h07-13b-81	vein 1	0.073	0.153	0.031	0.020	0.038	0.254	0.096	0.172	0.047
U16-h07-13b-81	vein 1	0.079	0.004	0.068	0.016	0.001	0.416	0.080	0.008	0.054
U16-h07-13b-81	vein 1	0.093	0.312	0.079	0.024	0.069	0.419	0.127	0.302	0.065
U16-h07-13b-81	vein 1	0.109	0.203	0.052	0.025	0.045	0.332	0.106	0.216	0.056
U16-h07-13b-81	vein 1	0.123	0.208	0.030	0.019	0.047	0.187	0.098	0.221	0.046
U16-h07-13b-81	vein 1	0.063	0.152	0.018	0.022	0.037	-0.033	0.072	0.171	0.010
U16-h07-24-145	ooids and cement	1.000	0.000	0.001	0.002	0.000	0.000	1.000	0.011	0.000

Sample ID	SampleType	2SE (ppm)	Sm LOD (ppm)	Eu (ppm)	2SE (ppm)	Eu LOD (ppm)	Gd (ppm)	2SE (ppm)	Gd LOD (ppm)	Tb (ppm)
U16-h07-24-145	ooids and cement	0.047	0.000	0.027	0.009	0.000	0.089	0.035	0.000	0.022
U16-h07-24-145	ooids and cement	0.033	0.000	0.014	0.008	0.000	0.125	0.071	0.000	0.020
U16-h07-24-145	ooids and cement	0.031	0.000	0.033	0.012	0.000	0.120	0.036	0.000	0.016
U16-h07-24-145	ooids and cement	0.049	0.000	0.047	0.015	0.000	0.162	0.040	0.010	0.028
U16-h07-24-145	ooids and cement	1.000	0.000	0.000	1.000	0.000	0.000	1.000	0.000	0.000
U16-h07-24-145	ooids and cement	0.032	0.000	0.026	0.010	0.000	0.101	0.042	0.000	0.009
U16-h07-24-145	ooids and cement	0.038	0.000	0.011	0.007	0.000	0.086	0.030	0.000	0.012
U16-h07-24-145	vein-1	0.016	0.000	0.012	0.006	0.000	0.030	0.017	0.000	0.010
U16-h07-24-145	vein-1	0.024	0.000	0.008	0.007	0.000	0.043	0.021	0.000	0.002
U16-h07-24-145	vein-1	0.024	0.000	0.022	0.008	0.000	0.074	0.029	0.000	0.010
U16-h07-24-145	vein-1	0.025	0.000	0.012	0.007	0.000	0.058	0.026	0.000	0.008
U16-h07-24-145	vein-1	0.017	0.000	0.003	0.005	0.000	0.047	0.022	0.000	0.006
U16-h07-24-145	vein-1	0.027	0.052	-0.005	0.006	0.070	0.054	0.023	0.055	0.002
U16-h07-24-145	vein-1	0.013	0.052	-0.005	0.004	0.070	0.049	0.023	0.055	0.002
U16-h07-24-145	vein-1	0.040	0.049	0.028	0.011	0.066	0.104	0.031	0.051	0.010
U16-h07-24-145	vein-2	0.043	0.000	0.035	0.012	0.000	0.079	0.038	0.000	0.012
U16-h07-24-145	vein-2	0.095	0.000	0.036	0.041	0.000	0.447	0.355	0.000	0.022
U16-h07-24-145	vein-2	0.085	0.000	-0.024	0.019	0.000	-0.066	0.052	0.000	-0.011
U16-h07-24-145	vein-3	0.704	0.058	0.097	0.172	0.032	-2.359	0.988	0.092	-0.097
U16-h07-24-145	vein-3	0.050	0.000	-0.018	0.010	0.000	-0.050	0.032	0.000	-0.007
U16-h07-24-145	vein-3	0.041	0.075	-0.016	0.011	0.016	-0.063	0.046	0.067	-0.016
U16-h07-24-145	vein-3	0.024	0.000	-0.007	0.005	0.000	-0.015	0.017	0.000	-0.005
U16-h07-24-145	vein-3	0.023	0.074	-0.015	0.006	0.015	-0.047	0.014	0.068	-0.006
U16-h07-24-145	vein-3	0.020	0.000	-0.005	0.005	0.000	-0.026	0.016	0.000	-0.007
U16-h07-24-145	vein-3	0.001	0.000	0.003	0.001	0.000	0.009	0.001	0.000	0.000
U16-h07-24-145	vein-4	1.747	0.060	0.624	0.878	0.033	0.813	1.086	0.096	0.209
U16-h07-24-145	vein-4	0.047	0.020	0.030	0.009	0.000	0.171	0.042	0.000	0.025
U16-h07-24-145	vein-4	0.029	0.019	0.020	0.007	0.000	0.069	0.031	0.000	0.013
U16-h07-24-145	vein-4	0.024	0.000	0.016	0.008	0.000	0.027	0.020	0.000	0.005
U16-h07-24-145	vein-4	12.817	0.060	0.996	1.885	0.033	0.566	3.590	0.095	0.556
U16-h07-24-145	vein-4	0.083	0.000	0.090	0.019	0.000	0.258	0.079	0.000	0.039
U16-h07-24-145	vein-4	27.767	0.062	2.479	8.330	0.034	-15.101	14.103	0.098	-1.252
U16-h07-24-145	vein-4	0.138	0.000	0.106	0.032	0.000	0.392	0.103	0.000	0.055

Sample ID	SampleType	2SE (ppm)	Sm LOD (ppm)	Eu (ppm)	2SE (ppm)	Eu LOD (ppm)	Gd (ppm)	2SE (ppm)	Gd LOD (ppm)	Tb (ppm)
U16-h07-24-145	vein-4	0.181	0.000	0.076	0.068	0.000	0.411	0.202	0.000	0.057
U16-h07-24-145	vein-4	0.155	0.058	0.041	0.025	0.032	0.112	0.085	0.092	0.014
U16-h07-24-145	vein-4	0.335	0.000	0.240	0.075	0.000	1.089	0.370	0.000	0.096
U16-h07-24-145	vein-4	0.822	0.000	0.541	0.233	0.000	2.650	1.185	0.000	0.320
U16-h07-24-145	vein-4	0.051	0.076	0.014	0.016	0.016	0.008	0.048	0.068	-0.003
U16-h07-24-145	vein-4	0.048	0.073	0.000	0.013	0.015	-0.032	0.043	0.065	-0.006
U16-h07-24-145	vein-4	0.578	0.061	-0.088	0.326	0.033	-0.276	0.972	0.098	0.042
U16-h07-24-145	vein-4	1.196	0.057	0.071	0.190	0.031	0.273	0.935	0.091	-0.110
U16-h07-24-145	vein-6	1.000	0.021	0.000	1.000	0.000	0.000	1.000	0.000	0.000
U16-h07-24-145	vein-6	0.037	0.019	0.017	0.007	0.000	0.112	0.030	0.000	0.013
U16-h07-24-145	vein-6	0.035	0.000	0.022	0.008	0.000	0.124	0.039	0.000	0.013
U16-h07-24-145	vein-6	0.038	0.019	0.030	0.010	0.000	0.105	0.041	0.000	0.017
U16-h07-24-145	vein-6	0.036	0.018	0.025	0.008	0.000	0.082	0.031	0.000	0.010
U16-h07-24-145	vein-7	0.034	0.000	0.033	0.011	0.000	0.172	0.043	0.000	0.017
U16-h07-25-167	coarse calcite	0.022	0.086	-0.003	0.007	0.017	-0.048	0.014	0.092	-0.009
U16-h07-25-167	coarse calcite	0.048	0.088	0.005	0.009	0.017	0.093	0.042	0.094	0.018
U16-h07-25-167	coarse calcite	0.072	0.092	0.026	0.014	0.018	0.268	0.080	0.099	0.039
U16-h07-25-167	coarse calcite	0.034	0.091	0.000	0.005	0.018	-0.005	0.021	0.097	0.001
U16-h07-25-167	dk ooid	0.031	0.087	0.016	0.010	0.017	0.026	0.028	0.093	0.007
U16-h07-25-167	dk ooid	0.035	0.000	0.013	0.010	0.000	0.053	0.033	0.000	0.013
U16-h07-25-167	dk ooid	0.039	0.000	0.021	0.012	0.000	0.105	0.046	0.000	0.013
U16-h07-25-167	dk ooid	0.042	0.000	0.012	0.008	0.000	0.054	0.039	0.000	0.009
U16-h07-25-167	dk ooid	0.041	0.000	0.029	0.011	0.059	0.160	0.054	0.074	0.017
U16-h07-25-167	dk ooid	0.075	0.000	0.042	0.015	0.000	0.189	0.073	0.000	0.018
U16-h07-25-167	dk ooid	0.019	0.000	0.005	0.008	0.000	0.009	0.028	0.000	-0.002
U16-h07-25-167	dk ooid	0.024	0.000	0.007	0.007	0.000	0.027	0.029	0.000	0.008
U16-h07-25-167	dk ooid	0.037	0.000	0.008	0.007	0.000	0.047	0.031	0.000	0.009
U16-h07-25-167	dk ooid	0.039	0.000	0.013	0.008	0.056	0.061	0.023	0.071	0.006
U16-h07-25-167	dk ooid	0.046	0.000	0.031	0.010	0.056	0.100	0.041	0.071	0.016
U16-h07-25-167	dk ooid	0.035	0.000	0.009	0.006	0.000	0.096	0.037	0.000	0.005
U16-h07-25-167	dk ooid	0.034	0.000	0.007	0.008	0.000	0.009	0.033	0.000	0.003
U16-h07-25-167	dk ooid	0.038	0.000	0.008	0.008	0.000	0.086	0.037	0.000	0.006
U16-h07-25-167	dk ooid	0.034	0.000	0.014	0.008	0.057	0.074	0.031	0.070	0.007

Sample ID	SampleType	2SE (ppm)	Sm LOD (ppm)	Eu (ppm)	2SE (ppm)	Eu LOD (ppm)	Gd (ppm)	2SE (ppm)	Gd LOD (ppm)	Tb (ppm)
U16-h07-25-167	dk ooid	0.046	0.000	0.012	0.009	0.000	0.062	0.027	0.000	0.011
U16-h07-25-167	dk ooid	0.050	0.000	0.015	0.008	0.056	0.098	0.033	0.069	0.014
U16-h07-25-167	dk ooid	0.020	0.000	0.010	0.008	0.058	0.029	0.020	0.073	0.010
U16-h07-25-167	dk ooid	0.035	0.000	0.015	0.010	0.000	0.080	0.039	0.000	0.014
U16-h07-25-167	dk ooid	0.038	0.000	0.009	0.007	0.057	0.025	0.022	0.072	0.013
U16-h07-25-167	dk ooid	0.037	0.000	0.010	0.009	0.000	0.085	0.047	0.000	0.009
U16-h07-25-167	dk ooid	0.060	0.000	0.042	0.014	0.000	0.203	0.061	0.000	0.017
U16-h07-25-167	early vein	0.010	0.000	0.009	0.002	0.000	0.083	0.014	0.055	0.008
U16-h07-25-167	early vein	0.021	0.000	0.018	0.005	0.000	0.093	0.016	0.055	0.019
U16-h07-25-167	early vein	0.018	0.000	0.014	0.004	0.000	0.110	0.020	0.056	0.012
U16-h07-25-167	early vein	0.019	0.000	0.014	0.005	0.000	0.082	0.012	0.055	0.010
U16-h07-25-167	late vein	0.039	0.000	0.056	0.012	0.000	0.296	0.044	0.060	0.031
U16-h07-25-167	late vein	0.045	0.000	0.035	0.008	0.000	0.189	0.034	0.057	0.024
U16-h07-25-167	late vein	0.045	0.000	0.099	0.016	0.000	0.457	0.052	0.055	0.060
U16-h07-25-167	late vein	0.064	0.000	0.115	0.013	0.000	0.416	0.043	0.053	0.050
U16-h07-25-167	late vein	0.067	0.000	0.111	0.015	0.000	0.498	0.067	0.055	0.063
U16-h07-25-167	lt ooid	0.035	0.000	0.025	0.009	0.000	0.096	0.030	0.054	0.017
U16-h07-25-167	lt ooid	0.038	0.000	0.036	0.011	0.000	0.117	0.029	0.052	0.017
U16-h07-25-167	lt ooid	0.033	0.000	0.025	0.008	0.000	0.101	0.030	0.052	0.015
U16-h07-25-167	lt ooid	0.047	0.000	0.041	0.012	0.058	0.154	0.036	0.072	0.018
U16-h07-25-167	lt ooid	0.044	0.000	0.026	0.010	0.056	0.102	0.034	0.069	0.018
U16-h07-25-167	lt ooid	0.033	0.000	0.032	0.011	0.000	0.105	0.028	0.051	0.017
U16-h07-25-167	lt ooid	0.042	0.000	0.014	0.007	0.000	0.117	0.029	0.051	0.015
U16-h07-25-167	lt ooid	0.054	0.000	0.043	0.014	0.058	0.131	0.028	0.072	0.017
U16-h07-25-167	lt ooid	0.032	0.000	0.026	0.010	0.000	0.120	0.034	0.050	0.017
U16-h07-25-167	lt ooid	0.044	0.000	0.020	0.008	0.000	0.157	0.034	0.052	0.017
U16-h07-25-167	matrix cement	0.002	0.000	0.003	0.000	0.000	0.054	0.010	0.056	0.003
U16-h07-25-167	matrix cement	0.028	0.000	0.017	0.006	0.000	0.134	0.030	0.054	0.015
U16-h07-25-167	matrix cement	0.078	0.000	0.083	0.020	0.000	0.380	0.058	0.057	0.047
U16-h07-25-167	matrix cement	0.036	0.000	0.025	0.008	0.000	0.143	0.029	0.051	0.017
U16-h07-25-167	matrix cement	0.034	0.000	0.016	0.006	0.000	0.132	0.026	0.052	0.012
U16-h07-25-167	matrix cement	0.033	0.000	0.018	0.007	0.000	0.146	0.033	0.052	0.018
U16-h07-25-167	matrix cement	0.035	0.000	0.018	0.007	0.000	0.126	0.033	0.053	0.016

Sample ID	SampleType	2SE (ppm)	Sm LOD (ppm)	Eu (ppm)	2SE (ppm)	Eu LOD (ppm)	Gd (ppm)	2SE (ppm)	Gd LOD (ppm)	Tb (ppm)
U16-h07-25-167	matrix cement	0.042	0.000	0.017	0.006	0.000	0.147	0.032	0.052	0.017
U16-h07-25-167	matrix cement	0.036	0.000	0.016	0.005	0.000	0.144	0.029	0.052	0.017
U16-h07-25-167	matrix cement	0.048	0.000	0.035	0.009	0.000	0.189	0.041	0.050	0.020
U16-h07-25-167	matrix cement	0.021	0.000	0.014	0.005	0.000	0.110	0.021	0.054	0.011
U16-h07-34-405	matrix cement	2.306	0.014	-0.478	1.070	0.006	-0.309	1.738	0.014	-0.373
U16-h07-34-405	matrix cement	0.159	0.047	0.093	0.040	0.013	0.279	0.218	0.043	0.019
U16-h07-34-405	matrix cement	0.014	0.013	0.000	0.003	0.006	0.001	0.011	0.014	-0.026
U16-h07-34-405	matrix cement	0.105	0.029	-0.043	0.043	0.012	-0.184	0.156	0.043	-0.032
U16-h07-34-405	matrix cement	0.122	0.032	0.023	0.026	0.013	-0.218	0.201	0.046	-0.046
U16-h07-34-405	matrix cement	0.738	0.012	-0.210	0.162	0.005	-1.377	0.690	0.013	-0.140
U16-h07-34-405	matrix cement	1.421	0.012	-0.262	0.197	0.005	-1.700	1.912	0.013	-0.297
U16-h07-34-405	matrix cement	0.137	0.032	0.030	0.017	0.013	-0.331	0.233	0.046	0.001
U16-h07-34-405	matrix cement	0.860	0.047	0.044	0.223	0.013	-0.632	0.930	0.043	-0.006
U16-h07-34-405	matrix cement	0.071	0.032	0.022	0.018	0.013	0.019	0.069	0.046	0.007
U16-h07-34-405	matrix cement	0.205	0.013	-0.033	0.065	0.006	-0.045	0.153	0.014	-0.055
U16-h07-34-405	matrix cement	1.366	0.012	-0.198	0.179	0.005	2.686	4.620	0.013	0.000
U16-h07-34-405	matrix cement	0.523	0.013	-0.083	0.103	0.006	-0.543	0.490	0.014	-0.161
U16-h07-34-405	matrix cement	0.526	0.013	0.091	0.157	0.006	0.536	0.418	0.014	0.122
U16-h07-34-405	matrix cement	0.243	0.013	-0.023	0.053	0.006	-0.327	0.604	0.014	-0.060
U16-h07-34-405	matrix cement	0.260	0.013	-0.016	0.056	0.006	-0.355	0.485	0.014	-0.021
U16-h07-34-405	matrix cement	0.751	0.013	-0.087	0.123	0.006	-0.459	0.545	0.014	-0.018
U16-h07-34-405	ooid	0.192	0.036	0.028	0.022	0.006	0.088	0.106	0.027	0.024
U16-h07-34-405	ooid	1.054	0.068	0.114	0.186	0.013	0.257	0.546	0.050	0.035
U16-h07-34-405	ooid	0.510	0.043	-0.145	0.190	0.012	-0.991	2.251	0.039	-0.146
U16-h07-34-405	ooid	0.443	0.064	-0.085	0.108	0.017	-0.283	0.285	0.051	0.001
U16-h07-34-405	ooid	0.160	0.058	-0.033	0.067	0.013	-0.134	0.190	0.049	0.019
U16-h07-34-405	ooid	0.188	0.055	-0.082	0.056	0.013	-0.233	0.170	0.047	-0.073
U16-h07-34-405	ooid	0.414	0.057	-0.197	0.109	0.014	-0.216	0.232	0.055	-0.085
U16-h07-34-405	ooid	0.148	0.063	0.008	0.043	0.016	-0.091	0.185	0.049	0.009
U16-h07-34-405	ooid	0.090	0.047	0.100	0.055	0.014	0.336	0.127	0.054	0.062
U16-h07-34-405	ooid	0.292	0.044	-0.114	0.086	0.013	-0.645	0.319	0.050	-0.079
U16-h07-34-405	ooid	0.230	0.066	-0.073	0.103	0.017	-0.522	0.353	0.053	-0.029
U16-h07-34-405	ooid	0.116	0.054	-0.006	0.031	0.012	-0.269	0.196	0.045	-0.038

Sample ID	SampleType	2SE (ppm)	Sm LOD (ppm)	Eu (ppm)	2SE (ppm)	Eu LOD (ppm)	Gd (ppm)	2SE (ppm)	Gd LOD (ppm)	Tb (ppm)
U16-h07-34-405	ooid	0.232	0.066	-0.036	0.074	0.017	-0.167	0.188	0.051	-0.052
U16-h07-34-405	ooid	0.233	0.059	-0.074	0.055	0.014	-0.247	0.231	0.050	-0.032
U16-h07-34-405	ooid	0.299	0.058	-0.036	0.088	0.023	-0.218	0.272	0.061	-0.029
U16-h07-34-405	ooid	0.240	0.059	-0.024	0.090	0.023	-0.232	0.326	0.061	-0.048
U16-h07-34-405	ooid	0.135	0.059	-0.025	0.040	0.013	-0.095	0.129	0.050	-0.014
U16-h07-34-405	ooid	0.496	0.064	-0.140	0.093	0.013	-0.330	0.301	0.047	-0.089
U16-h07-34-405	ooid	0.118	0.054	-0.004	0.029	0.012	-0.084	0.124	0.046	-0.039
U16-h07-34-405	ooid	0.213	0.057	-0.009	0.050	0.014	-0.315	0.258	0.055	-0.060
U16-h07-34-405	ooid	0.705	0.047	-0.115	0.270	0.013	0.177	1.289	0.043	-0.024
U16-h07-34-405	ooid and clast	0.711	0.000	0.683	0.167	0.000	3.325	0.693	0.000	0.461
U16-h07-34-405	ooid and clast	0.063	0.017	0.030	0.014	0.014	0.167	0.053	0.000	0.017
U16-h07-34-405	ooid and clast	0.006	0.000	0.000	1.000	0.000	0.003	0.005	0.000	0.001
U16-h07-34-405	ooid and clast	0.025	0.000	0.013	0.006	0.000	0.043	0.024	0.000	0.004
U16-h07-34-405	ooid and clast	0.114	0.000	0.110	0.026	0.000	0.542	0.108	0.000	0.068
U16-h07-34-405	ooid and clast	0.173	0.000	0.201	0.032	0.000	0.963	0.142	0.000	0.137
U16-h07-34-405	ooid and clast	0.069	0.017	0.127	0.027	0.013	0.498	0.091	0.000	0.098
U16-h07-34-405	ooid and clast	0.077	0.000	0.078	0.016	0.000	0.307	0.056	0.000	0.051
U16-h07-34-405	ooid and clast	0.124	0.000	0.148	0.025	0.000	0.657	0.095	0.000	0.097
U16-h07-34-405	ooid and clast	0.057	0.000	0.082	0.018	0.000	0.381	0.053	0.000	0.058
U16-h07-34-405	ooid and clast	0.147	0.000	0.158	0.033	0.000	0.692	0.131	0.000	0.088
U16-h07-34-405	ooid and clast	0.041	0.000	0.034	0.014	0.000	0.078	0.035	0.000	0.018
U16-h07-34-405	ooid and clast	0.160	0.000	0.208	0.036	0.000	0.816	0.157	0.000	0.120
U16-h07-34-405	ooid and clast	0.156	0.020	0.183	0.044	0.005	0.851	0.144	0.000	0.133
U16-h07-34-405	ooid and clast	0.142	0.050	0.228	0.042	0.000	0.764	0.193	0.000	0.143
U16-h07-34-405	ooid and clast	0.404	0.000	0.441	0.078	0.000	2.227	0.400	0.000	0.306
U16-h07-34-405	ooid and clast	7.112	0.000	0.768	0.799	0.000	-0.367	6.107	0.000	0.673
U16-h07-34-405	ooid and clast	3.671	0.021	0.213	1.260	0.005	-0.153	3.461	0.000	0.382
U16-h07-34-405	ooid and clast	6.717	0.000	-0.784	1.262	0.015	-5.733	4.663	0.000	-0.506
U16-h07-34-405	ooid and clast	0.005	0.124	0.028	0.002	0.030	0.090	0.010	0.114	0.012
U16-h07-34-405	ooid and clast	0.271	0.021	-0.259	0.063	0.005	-1.112	0.257	0.000	-0.149
U16-h07-34-405	ooid and clast	0.409	0.000	-0.439	0.086	0.000	-2.286	0.283	0.000	-0.327
U16-h07-34-405	ooid and clast	0.414	0.000	-0.449	0.107	0.000	-1.516	0.344	0.000	-0.240
U16-h07-34-405	ooid and clast	0.161	0.000	-0.132	0.027	0.000	-0.479	0.085	0.000	-0.078

Sample ID	SampleType	2SE (ppm)	Sm LOD (ppm)	Eu (ppm)	2SE (ppm)	Eu LOD (ppm)	Gd (ppm)	2SE (ppm)	Gd LOD (ppm)	Tb (ppm)
U16-h07-34-405	ooid and clast	0.125	0.000	-0.139	0.032	0.000	-0.713	0.122	0.000	-0.100
U16-h07-34-405	ooid and clast	0.111	0.000	-0.078	0.024	0.000	-0.371	0.118	0.000	-0.083
U16-h07-34-405	ooid and clast	0.299	0.146	-0.120	0.068	0.031	-0.438	0.192	0.133	-0.061
U16-h07-34-405	ooid and clast	0.069	0.000	-0.099	0.020	0.000	-0.321	0.079	0.000	-0.063
U16-h07-34-405	ooid and clast	0.110	0.049	-0.100	0.022	0.000	-0.308	0.072	0.042	-0.062
U16-h07-34-405	ooid and clast	0.134	0.147	-0.104	0.025	0.031	-0.376	0.124	0.135	-0.055
U16-h07-34-405	ooid and clast	0.055	0.044	-0.064	0.012	0.000	-0.253	0.044	0.038	-0.036
U16-h07-34-405	ooid and clast	0.032	0.043	-0.041	0.008	0.000	-0.144	0.028	0.037	-0.031
U16-h07-34-405	ooid and clast	0.045	0.114	-0.039	0.011	0.028	-0.131	0.036	0.105	-0.031
U16-h07-34-405	ooid and clast	0.071	0.000	-0.069	0.018	0.000	-0.242	0.055	0.000	-0.041
U16-h07-34-405	vein 1	0.071	0.101	0.096	0.015	0.021	0.321	0.051	0.092	0.068
U16-h07-34-405	vein 1	0.340	0.107	0.028	0.090	0.021	0.149	0.248	0.096	0.069
U16-h07-34-405	vein 1	0.691	0.110	0.242	0.150	0.022	0.875	0.492	0.099	0.188
U16-h07-34-405	vein 1	0.129	0.101	0.138	0.028	0.020	0.453	0.103	0.091	0.098
U16-h07-34-405	vein 1	0.139	0.105	0.132	0.021	0.021	0.449	0.071	0.094	0.088
U16-h07-34-405	vein 2	0.144	0.117	-0.108	0.038	0.024	-0.534	0.206	0.106	-0.071
U16-h07-34-405	vein 2	0.160	0.108	-0.059	0.032	0.022	-0.333	0.105	0.097	-0.072
U16-h07-34-405	vein 2	0.161	0.114	-0.110	0.034	0.024	-0.410	0.115	0.103	-0.060
U16-h07-34-405	vein 2	0.614	0.116	-0.197	0.093	0.024	-1.135	0.403	0.105	-0.202
U16-h07-34-405	vein 2	0.218	0.110	-0.298	0.073	0.023	-0.877	0.199	0.100	-0.153
U16-h07-34-405	vein 2	0.493	0.114	-0.288	0.113	0.024	-1.404	0.525	0.103	-0.166
U16-h07-54-338	coarse calcite	0.037	0.000	0.021	0.008	0.000	0.074	0.031	0.000	0.014
U16-h07-54-338	coarse calcite	0.023	0.000	0.004	0.004	0.000	0.007	0.011	0.000	0.005
U16-h07-54-338	coarse calcite	0.009	0.000	0.001	0.002	0.000	-0.004	0.000	0.000	0.000
U16-h07-54-338	coarse calcite	0.036	0.000	0.020	0.009	0.000	0.112	0.053	0.000	0.014
U16-h07-54-338	coarse calcite	0.116	0.000	0.132	0.035	0.000	0.491	0.137	0.000	0.079
U16-h07-54-338	coarse calcite	0.010	0.027	0.013	0.007	0.000	0.002	0.008	0.000	0.005
U16-h07-54-338	coarse calcite	0.024	0.000	0.013	0.007	0.000	0.048	0.028	0.000	0.007
U16-h07-54-338	coarse calcite	0.020	0.000	0.014	0.007	0.000	0.124	0.045	0.000	0.016
U16-h07-54-338	coarse calcite	0.061	0.000	0.067	0.027	0.029	0.339	0.135	0.000	0.060
U16-h07-54-338	coarse calcite	0.097	0.000	0.135	0.037	0.000	0.534	0.127	0.000	0.090
U16-h07-54-338	coarse calcite	0.095	0.000	0.083	0.023	0.000	0.434	0.085	0.000	0.065
U16-h07-54-338	coarse calcite	0.035	0.000	0.046	0.015	0.000	0.208	0.064	0.000	0.027

Sample ID	SampleType	2SE (ppm)	Sm LOD (ppm)	Eu (ppm)	2SE (ppm)	Eu LOD (ppm)	Gd (ppm)	2SE (ppm)	Gd LOD (ppm)	Tb (ppm)
U16-h07-54-338	coarse calcite	0.028	0.000	0.018	0.009	0.000	0.084	0.033	0.042	0.012
U16-h07-54-338	coarse calcite	0.125	0.000	0.069	0.030	0.028	0.271	0.117	0.000	0.057
U16-h07-54-338	coarse calcite	0.010	0.000	0.006	0.005	0.000	0.025	0.020	0.000	0.008
U16-h07-54-5	matrix cement	0.031	0.000	0.016	0.010	0.000	0.091	0.041	0.000	0.009
U16-h07-54-5	matrix cement	0.053	0.000	0.088	0.018	0.000	0.270	0.064	0.000	0.043
U16-h07-54-5	matrix cement	0.091	0.000	0.088	0.025	0.000	0.521	0.092	0.000	0.061
U16-h07-54-5	matrix cement	0.095	0.000	0.136	0.031	0.000	0.404	0.071	0.000	0.068
U16-h07-54-5	matrix cement	0.086	0.000	0.125	0.024	0.000	0.448	0.058	0.000	0.076
U16-h07-54-5	matrix cement	0.064	0.000	0.088	0.015	0.000	0.407	0.076	0.000	0.067
U16-h07-54-5	matrix cement	0.082	0.000	0.116	0.021	0.000	0.430	0.072	0.000	0.068
U16-h07-54-5	matrix cement	0.074	0.000	0.097	0.018	0.000	0.339	0.059	0.000	0.064
U16-h07-54-5	matrix cement	0.050	0.000	0.059	0.014	0.000	0.239	0.059	0.000	0.036
U16-h07-54-5	matrix cement	0.091	0.000	0.132	0.024	0.000	0.377	0.066	0.000	0.058
U16-h07-54-5	matrix cement	0.067	0.000	0.094	0.021	0.000	0.355	0.070	0.000	0.074
U16-h07-54-5	matrix cement	0.053	0.000	0.062	0.017	0.000	0.167	0.053	0.000	0.044
U16-h07-54-5	matrix cement	0.045	0.000	0.069	0.021	0.000	0.327	0.086	0.000	0.049
U16-h07-54-5	matrix cement	0.074	0.000	0.142	0.025	0.000	0.485	0.077	0.000	0.083
U16-h07-54-5	matrix cement	0.031	0.000	0.017	0.009	0.000	0.086	0.036	0.000	0.025
U16-h07-54-5	matrix cement	0.071	0.000	0.090	0.016	0.000	0.289	0.077	0.000	0.064
U16-h07-54-5	matrix cement	0.044	0.000	0.034	0.012	0.000	0.098	0.036	0.000	0.020
U16-h07-54-5	ooid	0.146	0.000	0.382	0.051	0.000	0.819	0.129	0.000	0.133
U16-h07-54-5	ooid	0.074	0.000	0.106	0.018	0.000	0.420	0.056	0.000	0.071
U16-h07-54-5	ooid	0.034	0.000	0.018	0.009	0.000	0.069	0.033	0.000	0.017
U16-h07-54-5	ooid	0.071	0.000	0.115	0.026	0.000	0.492	0.098	0.000	0.065
U16-h07-54-5	ooid	0.087	0.000	0.152	0.031	0.000	0.584	0.078	0.000	0.082
U16-h07-54-5	ooid	0.030	0.000	0.038	0.013	0.000	0.123	0.035	0.000	0.018
U16-h07-54-5	ooid	0.111	0.000	0.232	0.029	0.000	0.912	0.115	0.000	0.119
U16-h07-54-5	ooid	0.144	0.000	0.324	0.044	0.000	1.387	0.181	0.000	0.193
U16-h07-54-5	ooid	0.072	0.000	0.130	0.023	0.000	0.433	0.094	0.000	0.071
U16-h07-54-5	ooid	0.073	0.000	0.084	0.016	0.000	0.487	0.095	0.000	0.053
U16-h07-54-5	ooid	0.092	0.000	0.143	0.028	0.000	0.575	0.089	0.000	0.118
U16-h07-54-5	ooid	0.081	0.000	0.096	0.021	0.000	0.475	0.089	0.000	0.079
U16-h07-54-5	ooid	0.049	0.000	0.058	0.013	0.000	0.215	0.046	0.000	0.029

Sample ID	SampleType	2SE (ppm)	Sm LOD (ppm)	Eu (ppm)	2SE (ppm)	Eu LOD (ppm)	Gd (ppm)	2SE (ppm)	Gd LOD (ppm)	Tb (ppm)
U16-h07-54-5	ooid	0.056	0.000	0.073	0.021	0.000	0.295	0.068	0.000	0.051
U16-h07-54-5	ooid	0.070	0.000	0.060	0.015	0.000	0.182	0.059	0.000	0.035
U16-h07-54-5	ooid	0.068	0.000	0.055	0.013	0.000	0.214	0.055	0.000	0.043
U16-h07-54-5	ooid	0.067	0.000	0.133	0.025	0.000	0.493	0.075	0.000	0.079
U16-h07-54-5	ooid	0.080	0.000	0.094	0.017	0.000	0.402	0.077	0.000	0.079
U16-h07-54-5	ooid	0.070	0.000	0.087	0.020	0.000	0.291	0.049	0.000	0.048
U16-h07-54-5	ooid	0.074	0.000	0.094	0.017	0.000	0.438	0.096	0.000	0.071
U16-h07-54-5	ooid	0.060	0.000	0.073	0.018	0.000	0.200	0.071	0.000	0.037
U16-h07-54-5	ooid	0.082	0.000	0.098	0.025	0.000	0.354	0.111	0.000	0.063
U16-h07-54-5	ooid	0.065	0.000	0.099	0.020	0.000	0.399	0.072	0.000	0.079
U16-h07-54-5	ooid	0.072	0.000	0.104	0.021	0.000	0.341	0.057	0.000	0.059
U16-h07-54-5	ooid	0.040	0.000	0.042	0.014	0.000	0.089	0.042	0.000	0.017
U16-h07-54-5	vein 1	0.050	0.000	0.087	0.020	0.000	0.213	0.064	0.000	0.040
U16-h07-54-5	vein 1	0.124	0.000	0.245	0.044	0.008	0.873	0.134	0.000	0.184
U16-h07-54-5	vein 1	0.054	0.000	0.048	0.014	0.017	0.148	0.047	0.000	0.030
U16-h07-54-5	vein 1	0.052	0.000	0.046	0.013	0.016	0.224	0.068	0.000	0.037
U16-h07-54-5	vein 1	0.068	0.000	0.101	0.019	0.017	0.416	0.086	0.000	0.057
U16-h07-54-5	vein 1	0.086	0.000	0.138	0.022	0.016	0.484	0.087	0.000	0.109
U16-h07-54-5	vein 2	0.039	0.000	0.024	0.010	0.000	0.124	0.045	0.000	0.015
U16-h07-54-5	vein 2	0.112	0.000	0.194	0.024	0.000	0.661	0.115	0.000	0.139
U16-h07-54-5	vein 2	0.025	0.000	0.015	0.008	0.000	0.017	0.014	0.000	0.010
U16-h07-67-129	darker vein	0.021	0.000	0.007	0.005	0.000	0.006	0.009	0.000	0.004
U16-h07-67-129	darker vein	0.013	0.000	0.008	0.006	0.000	0.032	0.023	0.000	0.003
U16-h07-67-129	darker vein	0.015	0.000	0.000	0.001	0.000	0.015	0.014	0.000	0.003
U16-h07-67-129	darker vein	0.010	0.000	0.004	0.005	0.000	0.004	0.009	0.000	0.002
U16-h07-67-129	darker vein	0.024	0.000	0.007	0.005	0.000	0.016	0.013	0.000	0.001
U16-h07-67-129	darker vein	0.027	0.000	0.025	0.010	0.000	0.046	0.021	0.000	0.011
U16-h07-67-129	darker vein	0.026	0.000	0.022	0.007	0.000	0.119	0.038	0.000	0.011
U16-h07-67-129	lighter vein	0.137	0.000	0.105	0.035	0.000	0.361	0.123	0.000	0.056
U16-h07-67-129	lighter vein	0.178	0.000	0.469	0.045	0.000	1.658	0.170	0.000	0.215
U16-h07-67-129	lighter vein	0.066	0.000	0.083	0.023	0.000	0.471	0.095	0.017	0.066
U16-h07-67-129	lighter vein	0.136	0.000	0.364	0.040	0.000	1.553	0.148	0.000	0.224
U16-h07-67-129	lighter vein	0.070	0.000	0.095	0.022	0.000	0.333	0.060	0.000	0.046

Sample ID	SampleType	2SE (ppm)	Sm LOD (ppm)	Eu (ppm)	2SE (ppm)	Eu LOD (ppm)	Gd (ppm)	2SE (ppm)	Gd LOD (ppm)	Tb (ppm)
U16-h07-67-129	lighter vein	0.183	0.000	0.443	0.047	0.000	1.341	0.135	0.000	0.217
U16-h07-67-129	lighter vein	0.137	0.000	0.151	0.044	0.000	0.525	0.153	0.000	0.079
U16-h07-67-129	ooid and matrix	2.971	0.000	3.639	0.539	0.000	19.014	2.734	0.000	2.367
U16-h07-67-129	ooid and matrix	0.224	0.000	0.333	0.056	0.000	1.790	0.264	0.000	0.255
U16-h07-67-129	ooid and matrix	0.254	0.071	0.500	0.062	0.037	2.530	0.344	0.000	0.372
U16-h07-67-129	ooid and matrix	0.143	0.000	0.275	0.036	0.000	1.426	0.168	0.000	0.202
U16-h07-67-129	ooid and matrix	0.529	0.000	0.439	0.137	0.000	2.213	0.620	0.000	0.268
U16-h07-67-129	ooid and matrix	0.121	0.000	0.230	0.039	0.000	1.047	0.136	0.000	0.162
U16-h07-67-129	ooid and matrix	0.057	0.000	0.089	0.013	0.000	0.369	0.076	0.000	0.058
U16-h07-67-129	ooid and matrix	0.100	0.591	0.181	0.022	0.053	0.748	0.096	0.595	0.116
U16-h07-67-129	ooid and matrix	0.159	0.107	0.289	0.039	0.000	1.565	0.171	0.096	0.221
U16-h07-67-129	ooid and matrix	0.210	0.000	0.410	0.066	0.000	2.025	0.267	0.000	0.257
U16-h07-67-129	ooid and matrix	0.201	0.000	0.168	0.041	0.000	0.843	0.197	0.000	0.113
U16-h07-67-129	ooid and matrix	0.044	0.000	0.034	0.012	0.000	0.170	0.055	0.000	0.024
U16-h07-67-129	ooid and matrix	0.120	0.000	0.170	0.026	0.000	0.783	0.109	0.000	0.117
U16-h07-67-129	ooid and matrix	0.043	0.000	0.034	0.012	0.000	0.073	0.036	0.000	0.017
U16-h07-67-129	ooid and matrix	0.105	0.000	0.122	0.022	0.000	0.698	0.090	0.000	0.095
U16-h07-67-129	ooid and matrix	0.012	0.000	0.003	0.003	0.000	-0.001	0.006	0.000	0.001
U16-h07-67-129	ooid and matrix	0.110	0.000	0.076	0.024	0.000	0.322	0.099	0.000	0.052
U16-h07-67-129	ooid and matrix	0.059	0.101	0.037	0.012	0.000	0.175	0.059	0.090	0.022
U16-h07-67-129	ooid and matrix	0.119	0.000	0.116	0.022	0.000	0.628	0.109	0.000	0.081
U16-h07-67-129	ooid and matrix	0.062	0.000	0.064	0.016	0.000	0.372	0.059	0.000	0.068
U16-h07-67-129	ooid and matrix	0.060	0.000	0.090	0.025	0.000	0.417	0.084	0.000	0.060
U16-h07-67-129	ooid and matrix	0.173	0.000	0.346	0.066	0.000	1.412	0.246	0.000	0.196
U16-h07-67-129	ooid and matrix	0.075	0.000	0.141	0.027	0.000	0.543	0.097	0.000	0.069
U16-h07-67-129	ooid and matrix	0.125	0.000	0.237	0.040	0.010	0.944	0.131	0.000	0.122
U16-h07-67-129	ooid and matrix	0.177	0.000	0.299	0.052	0.000	1.200	0.153	0.000	0.168

Sample ID	SampleType	2SE (ppm)	Tb LOD (ppm)	Dy (ppm)	2SE (ppm)	Dy LOD (ppm)	Ho (ppm)	2SE (ppm)	Ho LOD (ppm)	Er (ppm)	2SE (ppm)
U16-h07-13b-11	matrix	0.012	0.000	0.255	0.056	0.000	0.049	0.009	0.000	0.193	0.039
U16-h07-13b-11	matrix	0.003	0.000	0.039	0.015	0.000	0.008	0.004	0.000	0.031	0.014
U16-h07-13b-11	matrix	0.004	0.000	0.053	0.022	0.000	0.014	0.006	0.000	0.048	0.015
U16-h07-13b-11	matrix	0.005	0.000	0.159	0.031	0.000	0.035	0.008	0.000	0.094	0.027
U16-h07-13b-11	matrix	0.004	0.000	0.101	0.023	0.000	0.024	0.009	0.000	0.084	0.022
U16-h07-13b-11	matrix	0.004	0.000	0.072	0.027	0.000	0.019	0.005	0.000	0.028	0.013
U16-h07-13b-11	matrix	0.006	0.000	0.136	0.031	0.000	0.032	0.008	0.000	0.081	0.028
U16-h07-13b-11	matrix	0.007	0.000	0.197	0.049	0.000	0.034	0.009	0.000	0.131	0.028
U16-h07-13b-11	matrix	0.011	0.000	0.423	0.072	0.000	0.083	0.012	0.000	0.209	0.041
U16-h07-13b-11	matrix	0.006	0.000	0.136	0.044	0.000	0.039	0.010	0.000	0.107	0.032
U16-h07-13b-11	matrix	0.009	0.000	0.253	0.036	0.000	0.047	0.010	0.000	0.177	0.026
U16-h07-13b-11	matrix	0.005	0.000	0.140	0.028	0.000	0.043	0.009	0.000	0.136	0.030
U16-h07-13b-11	matrix	0.006	0.000	0.201	0.046	0.000	0.038	0.007	0.000	0.102	0.027
U16-h07-13b-11	matrix	0.008	0.000	0.263	0.050	0.000	0.071	0.008	0.000	0.202	0.039
U16-h07-13b-11	matrix	0.006	0.000	0.186	0.027	0.000	0.039	0.010	0.000	0.132	0.028
U16-h07-13b-11	matrix	0.009	0.000	0.288	0.038	0.000	0.052	0.011	0.000	0.193	0.039
U16-h07-13b-11	matrix	0.007	0.000	0.192	0.032	0.000	0.052	0.010	0.000	0.167	0.030
U16-h07-13b-11	matrix	0.005	0.000	0.136	0.037	0.000	0.021	0.005	0.000	0.070	0.023
U16-h07-13b-11	matrix	0.010	0.000	0.404	0.065	0.000	0.081	0.012	0.000	0.266	0.035
U16-h07-13b-11	matrix	0.008	0.000	0.244	0.051	0.000	0.054	0.010	0.000	0.130	0.035
U16-h07-13b-11	matrix	0.008	0.000	0.197	0.040	0.000	0.045	0.010	0.000	0.114	0.031
U16-h07-13b-11	vein 1	0.008	0.000	0.225	0.042	0.000	0.054	0.012	0.000	0.142	0.034
U16-h07-13b-11	vein 1	0.015	0.000	1.295	0.107	0.000	0.271	0.023	0.000	0.831	0.072
U16-h07-13b-11	vein 1	0.021	0.000	1.164	0.099	0.000	0.225	0.027	0.000	0.581	0.052
U16-h07-13b-11	vein 1	0.014	0.000	0.751	0.082	0.000	0.124	0.016	0.000	0.390	0.048
U16-h07-13b-11	vein 1	0.014	0.000	0.405	0.066	0.000	0.075	0.015	0.000	0.209	0.045
U16-h07-13b-11	vein 1	0.018	0.000	0.955	0.085	0.000	0.171	0.020	0.000	0.387	0.049
U16-h07-13b-11	vein 1	0.016	0.000	0.838	0.070	0.000	0.175	0.020	0.000	0.428	0.046
U16-h07-13b-11	vein 2	0.004	0.000	0.071	0.025	0.000	0.011	0.005	0.000	0.027	0.013
U16-h07-13b-11	vein 2	0.002	0.000	0.027	0.018	0.000	0.005	0.004	0.000	0.018	0.012
U16-h07-13b-11	vein 2	0.001	0.000	0.008	0.006	0.000	0.005	0.003	0.000	0.015	0.010
U16-h07-13b-11	vein 2	1.000	0.000	0.000	1.000	0.000	0.000	1.000	0.000	0.000	1.000
U16-h07-13b-11	vein 2	1.000	0.000	0.002	0.003	0.000	0.002	0.002	0.000	0.000	1.000

Sample ID	SampleType	2SE (ppm)	Tb LOD (ppm)	Dy (ppm)	2SE (ppm)	Dy LOD (ppm)	Ho (ppm)	2SE (ppm)	Ho LOD (ppm)	Er (ppm)	2SE (ppm)
U16-h07-13b-11	vein 2	1.000	0.000	0.000	1.000	0.000	0.000	1.000	0.000	0.000	1.000
U16-h07-13b-11	vein 3	0.009	0.000	0.184	0.040	0.000	0.050	0.012	0.000	0.127	0.027
U16-h07-13b-11	vein 3	0.011	0.000	0.357	0.060	0.000	0.063	0.012	0.000	0.197	0.036
U16-h07-13b-11	vein 3	0.015	0.000	0.643	0.097	0.000	0.131	0.023	0.000	0.385	0.067
U16-h07-13b-31	dk ooid	0.009	0.000	0.363	0.068	0.000	0.072	0.015	0.004	0.227	0.054
U16-h07-13b-31	dk ooid	0.014	0.006	0.849	0.101	0.000	0.166	0.021	0.017	0.615	0.052
U16-h07-13b-31	dk ooid	0.018	0.000	0.610	0.092	0.000	0.130	0.020	0.004	0.371	0.050
U16-h07-13b-31	dk ooid	0.014	0.000	0.632	0.091	0.000	0.141	0.017	0.004	0.400	0.054
U16-h07-13b-31	dk ooid	0.016	0.005	0.783	0.086	0.000	0.191	0.019	0.014	0.541	0.066
U16-h07-13b-31	dk ooid	0.018	0.005	1.133	0.126	0.000	0.238	0.026	0.017	0.708	0.085
U16-h07-13b-31	matrix cement	0.012	0.000	0.378	0.068	0.000	0.091	0.014	0.004	0.247	0.045
U16-h07-13b-31	matrix cement	0.015	0.000	0.678	0.065	0.000	0.132	0.020	0.006	0.561	0.055
U16-h07-13b-31	matrix cement	0.031	0.000	1.584	0.187	0.000	0.283	0.037	0.004	0.822	0.089
U16-h07-13b-31	matrix cement	0.017	0.000	0.718	0.084	0.000	0.141	0.014	0.004	0.496	0.069
U16-h07-13b-31	matrix cement	0.017	0.000	0.860	0.102	0.000	0.163	0.021	0.006	0.447	0.062
U16-h07-13b-31	matrix cement	0.023	0.000	0.918	0.104	0.000	0.212	0.031	0.004	0.592	0.060
U16-h07-13b-31	matrix cement	0.021	0.000	0.777	0.115	0.000	0.161	0.026	0.004	0.552	0.078
U16-h07-13b-31	matrix cement	0.014	0.000	0.846	0.084	0.000	0.204	0.018	0.006	0.525	0.067
U16-h07-13b-31	matrix cement	0.018	0.000	0.861	0.104	0.053	0.188	0.026	0.000	0.609	0.069
U16-h07-13b-31	matrix cement	0.012	0.000	0.899	0.101	0.053	0.185	0.024	0.000	0.554	0.066
U16-h07-13b-31	matrix cement	0.013	0.000	0.897	0.078	0.000	0.172	0.020	0.006	0.585	0.048
U16-h07-13b-31	matrix cement	0.016	0.000	0.771	0.077	0.000	0.155	0.021	0.006	0.528	0.066
U16-h07-13b-31	ooid	0.015	0.000	0.916	0.080	0.000	0.215	0.019	0.005	0.550	0.053
U16-h07-13b-31	ooid	0.012	0.000	0.401	0.060	0.030	0.085	0.013	0.000	0.240	0.043
U16-h07-13b-31	ooid	0.027	0.000	1.254	0.125	0.000	0.265	0.033	0.005	0.742	0.099
U16-h07-13b-31	ooid	0.010	0.072	0.447	0.062	0.000	0.097	0.015	0.054	0.312	0.037
U16-h07-13b-31	ooid	0.015	0.000	0.963	0.099	0.000	0.232	0.034	0.000	0.819	0.088
U16-h07-13b-31	ooid	0.013	0.000	0.617	0.087	0.000	0.137	0.017	0.000	0.459	0.056
U16-h07-13b-31	ooid	0.018	0.000	1.013	0.103	0.000	0.183	0.018	0.000	0.569	0.062
U16-h07-13b-31	ooid	0.022	0.070	0.787	0.100	0.000	0.196	0.022	0.053	0.562	0.079
U16-h07-13b-31	ooid	0.012	0.000	0.718	0.094	0.000	0.167	0.021	0.000	0.563	0.077
U16-h07-13b-31	ooid	0.018	0.000	1.237	0.122	0.000	0.264	0.027	0.000	0.771	0.062
U16-h07-13b-31	ooid	0.013	0.000	0.720	0.094	0.000	0.175	0.025	0.005	0.578	0.069

Sample ID	SampleType	2SE (ppm)	Tb LOD (ppm)	Dy (ppm)	2SE (ppm)	Dy LOD (ppm)	Ho (ppm)	2SE (ppm)	Ho LOD (ppm)	Er (ppm)	2SE (ppm)
U16-h07-13b-31	ooid	0.017	0.000	0.756	0.099	0.030	0.206	0.021	0.000	0.607	0.068
U16-h07-13b-31	ooid	0.012	0.000	0.838	0.103	0.000	0.208	0.029	0.005	0.515	0.062
U16-h07-13b-31	ooid	0.019	0.000	0.936	0.103	0.000	0.199	0.016	0.005	0.625	0.059
U16-h07-13b-31	ooid	0.020	0.000	1.085	0.106	0.030	0.232	0.024	0.000	0.651	0.061
U16-h07-13b-31	ooid	0.018	0.000	0.828	0.072	0.000	0.181	0.020	0.000	0.603	0.051
U16-h07-13b-31	ooid	0.016	0.000	0.970	0.082	0.000	0.205	0.020	0.000	0.565	0.047
U16-h07-13b-31	ooid	0.015	0.000	1.056	0.105	0.000	0.253	0.029	0.000	0.686	0.067
U16-h07-13b-31	ooid	0.017	0.000	0.779	0.073	0.000	0.210	0.022	0.005	0.574	0.055
U16-h07-13b-31	ooid	0.018	0.000	0.975	0.091	0.000	0.213	0.023	0.005	0.592	0.057
U16-h07-13b-31	ooid	0.014	0.000	0.789	0.081	0.000	0.176	0.022	0.000	0.563	0.054
U16-h07-13b-31	ooid	0.014	0.000	0.775	0.079	0.000	0.173	0.018	0.000	0.547	0.043
U16-h07-13b-31	ooid	0.014	0.000	0.712	0.072	0.000	0.152	0.011	0.005	0.538	0.057
U16-h07-13b-31	ooid	0.016	0.070	0.764	0.063	0.000	0.170	0.017	0.053	0.562	0.047
U16-h07-13b-31	vein-1	0.034	0.000	1.539	0.223	0.000	0.296	0.042	0.000	0.789	0.104
U16-h07-13b-31	vein-1	0.006	0.000	0.121	0.053	0.000	0.038	0.015	0.000	0.085	0.038
U16-h07-13b-31	vein-1	0.005	0.000	0.083	0.025	0.000	0.011	0.004	0.000	0.049	0.014
U16-h07-13b-31	vein-1	0.005	0.003	0.113	0.032	0.021	0.022	0.006	0.008	0.063	0.018
U16-h07-13b-31	vein-1	0.005	0.000	0.116	0.034	0.000	0.043	0.011	0.000	0.094	0.027
U16-h07-13b-31	vein-1	0.004	0.000	0.100	0.025	0.000	0.028	0.007	0.000	0.049	0.015
U16-h07-13b-81	coarse calcite	1.000	0.000	0.000	1.000	0.000	0.000	1.000	0.001	0.000	1.000
U16-h07-13b-81	coarse calcite	0.000	0.000	-0.003	0.001	0.000	-0.001	0.000	0.001	-0.002	0.000
U16-h07-13b-81	coarse calcite	0.000	0.000	-0.012	0.001	0.000	-0.005	0.000	0.001	-0.006	0.001
U16-h07-13b-81	coarse calcite	0.000	0.004	-0.009	0.028	0.033	-0.014	0.002	0.013	-0.011	0.009
U16-h07-13b-81	vein 1	0.082	0.020	1.616	0.255	0.205	0.356	0.040	0.054	1.150	0.125
U16-h07-13b-81	vein 1	0.036	0.066	1.547	0.236	0.408	0.381	0.053	0.108	1.197	0.143
U16-h07-13b-81	vein 1	0.009	0.015	0.279	0.060	0.158	0.056	0.012	0.042	0.185	0.043
U16-h07-13b-81	vein 1	0.016	0.030	0.277	0.130	0.224	0.064	0.028	0.063	0.203	0.095
U16-h07-13b-81	vein 1	0.009	0.000	0.413	0.072	0.000	0.101	0.016	0.001	0.325	0.049
U16-h07-13b-81	vein 1	0.017	0.047	0.557	0.116	0.432	0.140	0.018	0.103	0.402	0.084
U16-h07-13b-81	vein 1	0.018	0.039	0.477	0.107	0.287	0.121	0.024	0.074	0.447	0.091
U16-h07-13b-81	vein 1	0.017	0.040	0.400	0.125	0.293	0.110	0.036	0.076	0.304	0.110
U16-h07-13b-81	vein 1	0.011	0.030	0.019	0.055	0.223	0.033	0.020	0.062	0.144	0.069
U16-h07-24-145	ooids and cement	1.000	0.000	0.002	0.004	0.000	0.000	1.000	0.003	0.013	0.010

Sample ID	SampleType	2SE (ppm)	Tb LOD (ppm)	Dy (ppm)	2SE (ppm)	Dy LOD (ppm)	Ho (ppm)	2SE (ppm)	Ho LOD (ppm)	Er (ppm)	2SE (ppm)
U16-h07-24-145	ooids and cement	0.007	0.000	0.156	0.033	0.000	0.030	0.008	0.000	0.075	0.019
U16-h07-24-145	ooids and cement	0.007	0.000	0.083	0.031	0.000	0.017	0.005	0.000	0.082	0.026
U16-h07-24-145	ooids and cement	0.007	0.000	0.084	0.023	0.000	0.020	0.005	0.000	0.047	0.016
U16-h07-24-145	ooids and cement	0.007	0.000	0.129	0.023	0.000	0.027	0.007	0.003	0.093	0.019
U16-h07-24-145	ooids and cement	1.000	0.000	0.000	1.000	0.000	0.000	1.000	0.000	0.000	1.000
U16-h07-24-145	ooids and cement	0.004	0.000	0.127	0.033	0.000	0.022	0.007	0.000	0.069	0.017
U16-h07-24-145	ooids and cement	0.005	0.000	0.128	0.028	0.000	0.024	0.009	0.000	0.058	0.018
U16-h07-24-145	vein-1	0.003	0.000	0.035	0.014	0.000	0.008	0.003	0.000	0.017	0.007
U16-h07-24-145	vein-1	0.002	0.000	0.039	0.016	0.000	0.007	0.003	0.000	0.012	0.009
U16-h07-24-145	vein-1	0.004	0.000	0.066	0.024	0.000	0.008	0.004	0.000	0.031	0.013
U16-h07-24-145	vein-1	0.004	0.000	0.069	0.022	0.000	0.011	0.004	0.000	0.052	0.016
U16-h07-24-145	vein-1	0.003	0.000	0.040	0.014	0.000	0.009	0.004	0.000	0.035	0.013
U16-h07-24-145	vein-1	0.003	0.067	0.021	0.016	0.101	0.002	0.003	0.060	0.019	0.011
U16-h07-24-145	vein-1	0.002	0.067	0.014	0.011	0.101	0.004	0.003	0.060	0.019	0.010
U16-h07-24-145	vein-1	0.004	0.063	0.102	0.029	0.095	0.019	0.005	0.056	0.074	0.020
U16-h07-24-145	vein-2	0.006	0.000	0.106	0.028	0.000	0.019	0.008	0.000	0.030	0.014
U16-h07-24-145	vein-2	0.013	0.000	0.133	0.083	0.000	0.042	0.025	0.000	0.140	0.079
U16-h07-24-145	vein-2	0.009	0.000	-0.055	0.051	0.000	-0.023	0.013	0.000	-0.082	0.055
U16-h07-24-145	vein-3	0.104	0.014	-1.787	0.536	0.073	-0.256	0.118	0.012	-0.598	0.344
U16-h07-24-145	vein-3	0.004	0.000	-0.049	0.028	0.000	-0.003	0.003	0.000	-0.021	0.014
U16-h07-24-145	vein-3	0.006	0.005	-0.052	0.027	0.029	-0.011	0.007	0.010	-0.022	0.016
U16-h07-24-145	vein-3	0.003	0.000	-0.038	0.017	0.000	-0.003	0.002	0.000	-0.014	0.010
U16-h07-24-145	vein-3	0.003	0.005	-0.046	0.014	0.030	-0.014	0.004	0.010	-0.029	0.009
U16-h07-24-145	vein-3	0.003	0.000	-0.060	0.018	0.000	-0.010	0.004	0.000	-0.028	0.011
U16-h07-24-145	vein-3	0.000	0.000	0.000	0.005	0.000	0.000	0.001	0.000	0.004	0.001
U16-h07-24-145	vein-4	0.333	0.015	0.985	1.194	0.075	0.042	0.138	0.013	1.229	1.545
U16-h07-24-145	vein-4	0.006	0.000	0.138	0.033	0.000	0.040	0.009	0.000	0.101	0.017
U16-h07-24-145	vein-4	0.005	0.000	0.091	0.020	0.000	0.024	0.006	0.000	0.060	0.015
U16-h07-24-145	vein-4	0.003	0.000	0.025	0.014	0.000	0.004	0.003	0.000	0.006	0.005
U16-h07-24-145	vein-4	0.686	0.015	-2.049	6.498	0.075	-0.410	0.790	0.013	-2.362	3.901
U16-h07-24-145	vein-4	0.012	0.000	0.332	0.065	0.000	0.060	0.013	0.000	0.172	0.033
U16-h07-24-145	vein-4	1.804	0.015	-14.089	9.362	0.078	-4.121	2.004	0.013	-4.555	7.979
U16-h07-24-145	vein-4	0.015	0.000	0.331	0.076	0.000	0.084	0.022	0.000	0.240	0.078

Sample ID	SampleType	2SE (ppm)	Tb LOD (ppm)	Dy (ppm)	2SE (ppm)	Dy LOD (ppm)	Ho (ppm)	2SE (ppm)	Ho LOD (ppm)	Er (ppm)	2SE (ppm)
U16-h07-24-145	vein-4	0.029	0.000	0.401	0.135	0.000	0.089	0.043	0.000	0.386	0.107
U16-h07-24-145	vein-4	0.011	0.014	0.103	0.073	0.072	0.008	0.015	0.012	0.068	0.043
U16-h07-24-145	vein-4	0.040	0.000	0.859	0.351	0.000	0.233	0.071	0.000	0.463	0.172
U16-h07-24-145	vein-4	0.125	0.000	1.113	0.444	0.000	0.297	0.121	0.000	0.992	0.392
U16-h07-24-145	vein-4	0.008	0.005	0.053	0.039	0.030	-0.004	0.008	0.010	0.013	0.027
U16-h07-24-145	vein-4	0.006	0.005	-0.033	0.034	0.029	-0.006	0.009	0.010	0.009	0.019
U16-h07-24-145	vein-4	0.109	0.015	0.431	0.604	0.077	-0.008	0.105	0.013	-0.106	0.512
U16-h07-24-145	vein-4	0.186	0.014	0.391	0.853	0.071	-0.261	0.229	0.012	-0.543	0.745
U16-h07-24-145	vein-6	1.000	0.000	0.000	1.000	0.000	0.000	1.000	0.000	0.000	1.000
U16-h07-24-145	vein-6	0.004	0.000	0.065	0.020	0.000	0.017	0.005	0.000	0.043	0.015
U16-h07-24-145	vein-6	0.005	0.000	0.096	0.026	0.000	0.025	0.005	0.000	0.049	0.016
U16-h07-24-145	vein-6	0.005	0.000	0.123	0.032	0.000	0.018	0.006	0.000	0.079	0.018
U16-h07-24-145	vein-6	0.004	0.000	0.131	0.027	0.000	0.017	0.005	0.000	0.060	0.019
U16-h07-24-145	vein-7	0.006	0.000	0.150	0.024	0.000	0.028	0.009	0.000	0.077	0.022
U16-h07-25-167	coarse calcite	0.002	0.014	-0.067	0.013	0.081	-0.014	0.003	0.023	-0.035	0.008
U16-h07-25-167	coarse calcite	0.008	0.014	0.122	0.051	0.083	0.028	0.012	0.024	0.080	0.030
U16-h07-25-167	coarse calcite	0.011	0.015	0.264	0.047	0.087	0.071	0.016	0.025	0.268	0.045
U16-h07-25-167	coarse calcite	0.004	0.015	0.006	0.015	0.086	0.002	0.005	0.024	-0.010	0.011
U16-h07-25-167	dk ooid	0.005	0.014	0.035	0.026	0.082	0.005	0.005	0.023	0.030	0.016
U16-h07-25-167	dk ooid	0.006	0.000	0.095	0.035	0.000	0.023	0.008	0.000	0.071	0.023
U16-h07-25-167	dk ooid	0.006	0.000	0.108	0.027	0.000	0.031	0.008	0.000	0.094	0.026
U16-h07-25-167	dk ooid	0.005	0.000	0.125	0.042	0.000	0.025	0.008	0.000	0.061	0.022
U16-h07-25-167	dk ooid	0.008	0.050	0.192	0.036	0.000	0.038	0.010	0.024	0.098	0.023
U16-h07-25-167	dk ooid	0.008	0.000	0.242	0.071	0.000	0.052	0.013	0.000	0.160	0.034
U16-h07-25-167	dk ooid	0.003	0.000	0.052	0.020	0.000	0.017	0.006	0.000	0.026	0.012
U16-h07-25-167	dk ooid	0.005	0.000	0.062	0.023	0.000	0.014	0.005	0.000	0.033	0.018
U16-h07-25-167	dk ooid	0.007	0.000	0.071	0.031	0.000	0.021	0.006	0.000	0.046	0.018
U16-h07-25-167	dk ooid	0.003	0.048	0.078	0.023	0.000	0.020	0.006	0.023	0.075	0.018
U16-h07-25-167	dk ooid	0.006	0.048	0.164	0.032	0.000	0.032	0.007	0.023	0.089	0.019
U16-h07-25-167	dk ooid	0.005	0.000	0.099	0.030	0.000	0.024	0.007	0.000	0.042	0.017
U16-h07-25-167	dk ooid	0.004	0.000	0.065	0.025	0.000	0.012	0.006	0.000	0.030	0.017
U16-h07-25-167	dk ooid	0.004	0.000	0.128	0.035	0.000	0.021	0.006	0.000	0.055	0.020
U16-h07-25-167	dk ooid	0.004	0.048	0.106	0.028	0.000	0.020	0.006	0.023	0.063	0.016

Sample ID	SampleType	2SE (ppm)	Tb LOD (ppm)	Dy (ppm)	2SE (ppm)	Dy LOD (ppm)	Ho (ppm)	2SE (ppm)	Ho LOD (ppm)	Er (ppm)	2SE (ppm)
U16-h07-25-167	dk ooid	0.006	0.000	0.099	0.031	0.000	0.024	0.007	0.000	0.065	0.021
U16-h07-25-167	dk ooid	0.005	0.048	0.107	0.025	0.000	0.026	0.006	0.023	0.084	0.022
U16-h07-25-167	dk ooid	0.005	0.049	0.112	0.031	0.000	0.021	0.007	0.023	0.071	0.020
U16-h07-25-167	dk ooid	0.006	0.000	0.103	0.033	0.000	0.022	0.007	0.000	0.067	0.025
U16-h07-25-167	dk ooid	0.005	0.049	0.132	0.033	0.000	0.018	0.006	0.023	0.111	0.026
U16-h07-25-167	dk ooid	0.005	0.000	0.124	0.033	0.000	0.031	0.009	0.000	0.075	0.024
U16-h07-25-167	dk ooid	0.009	0.000	0.158	0.045	0.000	0.040	0.009	0.000	0.099	0.032
U16-h07-25-167	early vein	0.002	0.004	0.032	0.012	0.000	0.014	0.004	0.000	0.048	0.010
U16-h07-25-167	early vein	0.005	0.004	0.072	0.020	0.000	0.018	0.005	0.000	0.083	0.016
U16-h07-25-167	early vein	0.003	0.004	0.081	0.022	0.000	0.015	0.004	0.000	0.085	0.014
U16-h07-25-167	early vein	0.002	0.004	0.041	0.020	0.000	0.011	0.004	0.000	0.070	0.011
U16-h07-25-167	late vein	0.005	0.004	0.226	0.037	0.000	0.056	0.009	0.000	0.247	0.029
U16-h07-25-167	late vein	0.006	0.004	0.188	0.030	0.000	0.049	0.009	0.000	0.202	0.030
U16-h07-25-167	late vein	0.006	0.004	0.434	0.040	0.000	0.098	0.008	0.000	0.359	0.035
U16-h07-25-167	late vein	0.007	0.004	0.403	0.038	0.000	0.088	0.011	0.000	0.233	0.026
U16-h07-25-167	late vein	0.009	0.004	0.375	0.047	0.000	0.085	0.010	0.000	0.254	0.035
U16-h07-25-167	lt ooid	0.006	0.004	0.083	0.022	0.000	0.027	0.008	0.000	0.082	0.021
U16-h07-25-167	lt ooid	0.006	0.004	0.102	0.028	0.000	0.028	0.008	0.000	0.083	0.020
U16-h07-25-167	lt ooid	0.005	0.004	0.118	0.033	0.000	0.018	0.006	0.000	0.077	0.017
U16-h07-25-167	lt ooid	0.006	0.049	0.154	0.032	0.000	0.044	0.008	0.023	0.146	0.031
U16-h07-25-167	lt ooid	0.006	0.048	0.105	0.027	0.000	0.026	0.006	0.023	0.082	0.021
U16-h07-25-167	lt ooid	0.005	0.004	0.079	0.021	0.000	0.024	0.007	0.000	0.089	0.019
U16-h07-25-167	lt ooid	0.005	0.004	0.149	0.035	0.000	0.031	0.007	0.000	0.080	0.016
U16-h07-25-167	lt ooid	0.005	0.049	0.161	0.034	0.000	0.040	0.008	0.023	0.156	0.035
U16-h07-25-167	lt ooid	0.005	0.003	0.087	0.023	0.000	0.019	0.006	0.000	0.107	0.026
U16-h07-25-167	lt ooid	0.006	0.004	0.124	0.033	0.000	0.029	0.008	0.000	0.090	0.020
U16-h07-25-167	matrix cement	0.000	0.004	0.005	0.006	0.000	0.001	0.001	0.000	0.019	0.001
U16-h07-25-167	matrix cement	0.005	0.004	0.080	0.022	0.000	0.022	0.008	0.000	0.093	0.020
U16-h07-25-167	matrix cement	0.009	0.004	0.297	0.054	0.000	0.080	0.012	0.000	0.190	0.027
U16-h07-25-167	matrix cement	0.004	0.004	0.098	0.024	0.000	0.021	0.006	0.000	0.096	0.016
U16-h07-25-167	matrix cement	0.003	0.004	0.063	0.019	0.000	0.024	0.007	0.000	0.088	0.017
U16-h07-25-167	matrix cement	0.004	0.004	0.066	0.020	0.000	0.023	0.007	0.000	0.093	0.019
U16-h07-25-167	matrix cement	0.005	0.004	0.091	0.024	0.000	0.023	0.006	0.000	0.082	0.022

Sample ID	SampleType	2SE (ppm)	Tb LOD (ppm)	Dy (ppm)	2SE (ppm)	Dy LOD (ppm)	Ho (ppm)	2SE (ppm)	Ho LOD (ppm)	Er (ppm)	2SE (ppm)
U16-h07-25-167	matrix cement	0.005	0.004	0.076	0.026	0.000	0.016	0.005	0.000	0.072	0.016
U16-h07-25-167	matrix cement	0.005	0.004	0.070	0.016	0.000	0.014	0.005	0.000	0.066	0.014
U16-h07-25-167	matrix cement	0.006	0.003	0.138	0.037	0.000	0.034	0.009	0.000	0.127	0.025
U16-h07-25-167	matrix cement	0.003	0.004	0.056	0.019	0.000	0.010	0.004	0.000	0.051	0.010
U16-h07-34-405	matrix cement	0.832	0.005	-0.628	2.918	0.019	0.065	0.612	0.004	-0.450	1.740
U16-h07-34-405	matrix cement	0.035	0.004	0.115	0.282	0.025	0.027	0.062	0.006	0.118	0.214
U16-h07-34-405	matrix cement	0.076	0.005	0.323	0.402	0.019	0.109	0.198	0.004	-0.464	0.495
U16-h07-34-405	matrix cement	0.023	0.007	-0.271	0.120	0.039	-0.044	0.027	0.009	-0.166	0.083
U16-h07-34-405	matrix cement	0.032	0.007	-0.051	0.130	0.041	-0.041	0.040	0.009	-0.077	0.100
U16-h07-34-405	matrix cement	0.094	0.005	-0.116	1.048	0.017	-0.235	0.091	0.004	-0.524	0.379
U16-h07-34-405	matrix cement	0.264	0.005	-1.447	0.977	0.017	-0.434	0.355	0.004	-0.599	0.896
U16-h07-34-405	matrix cement	0.017	0.007	0.027	0.106	0.042	-0.007	0.029	0.009	-0.084	0.083
U16-h07-34-405	matrix cement	0.007	0.004	-0.109	0.596	0.025	-0.007	0.052	0.006	-0.131	0.320
U16-h07-34-405	matrix cement	0.015	0.007	-0.114	0.117	0.042	-0.040	0.028	0.009	-0.173	0.101
U16-h07-34-405	matrix cement	0.052	0.005	-0.136	0.242	0.018	-0.073	0.076	0.004	-0.122	0.197
U16-h07-34-405	matrix cement	0.134	0.005	-1.255	1.009	0.017	-0.207	0.245	0.004	-0.786	0.538
U16-h07-34-405	matrix cement	0.122	0.005	-0.314	0.656	0.018	-0.117	0.164	0.004	-0.718	0.492
U16-h07-34-405	matrix cement	0.100	0.005	0.847	0.782	0.019	0.203	0.148	0.004	0.541	0.434
U16-h07-34-405	matrix cement	0.149	0.005	0.364	1.634	0.019	0.203	0.384	0.004	-0.357	0.384
U16-h07-34-405	matrix cement	0.080	0.005	-0.093	0.696	0.019	-0.053	0.166	0.004	-0.097	0.544
U16-h07-34-405	matrix cement	0.099	0.005	-0.707	0.700	0.019	-0.148	0.205	0.004	-0.129	0.306
U16-h07-34-405	ooid	0.018	0.004	0.112	0.096	0.029	0.069	0.033	0.011	0.151	0.073
U16-h07-34-405	ooid	0.083	0.008	0.466	0.469	0.045	0.417	0.244	0.012	0.526	0.547
U16-h07-34-405	ooid	0.170	0.004	-0.641	0.667	0.023	-0.259	0.292	0.005	-0.982	0.893
U16-h07-34-405	ooid	0.042	0.008	-0.388	0.258	0.050	-0.093	0.054	0.011	-0.138	0.189
U16-h07-34-405	ooid	0.020	0.008	-0.069	0.149	0.041	0.016	0.034	0.010	0.040	0.069
U16-h07-34-405	ooid	0.039	0.008	-0.354	0.192	0.039	-0.139	0.050	0.010	-0.505	0.140
U16-h07-34-405	ooid	0.041	0.009	-0.517	0.235	0.061	-0.150	0.075	0.016	-0.466	0.217
U16-h07-34-405	ooid	0.024	0.008	-0.141	0.182	0.048	-0.038	0.038	0.011	-0.173	0.116
U16-h07-34-405	ooid	0.021	0.009	0.213	0.130	0.030	0.058	0.035	0.010	0.210	0.086
U16-h07-34-405	ooid	0.045	0.009	-0.401	0.237	0.028	-0.132	0.059	0.010	-0.343	0.176
U16-h07-34-405	ooid	0.042	0.009	-0.255	0.314	0.051	-0.077	0.080	0.012	-0.277	0.133
U16-h07-34-405	ooid	0.027	0.007	0.027	0.102	0.038	-0.044	0.033	0.010	-0.142	0.081

Sample ID	SampleType	2SE (ppm)	Tb LOD (ppm)	Dy (ppm)	2SE (ppm)	Dy LOD (ppm)	Ho (ppm)	2SE (ppm)	Ho LOD (ppm)	Er (ppm)	2SE (ppm)
U16-h07-34-405	ooid	0.039	0.008	-0.221	0.234	0.050	-0.120	0.052	0.011	-0.090	0.120
U16-h07-34-405	ooid	0.037	0.008	-0.199	0.149	0.042	-0.044	0.039	0.011	-0.097	0.112
U16-h07-34-405	ooid	0.034	0.007	0.100	0.139	0.045	-0.021	0.044	0.010	-0.077	0.124
U16-h07-34-405	ooid	0.037	0.007	-0.253	0.231	0.046	-0.081	0.046	0.010	-0.133	0.134
U16-h07-34-405	ooid	0.023	0.008	-0.189	0.136	0.042	-0.020	0.025	0.011	-0.173	0.104
U16-h07-34-405	ooid	0.051	0.007	-0.674	0.391	0.043	-0.102	0.085	0.011	-0.305	0.201
U16-h07-34-405	ooid	0.023	0.007	-0.143	0.096	0.039	-0.070	0.027	0.010	-0.098	0.059
U16-h07-34-405	ooid	0.039	0.009	-0.455	0.266	0.060	-0.063	0.054	0.016	-0.192	0.156
U16-h07-34-405	ooid	0.117	0.004	-0.184	0.987	0.025	-0.017	0.197	0.006	0.619	1.182
U16-h07-34-405	ooid and clast	0.110	0.000	3.343	0.589	0.000	0.582	0.117	0.000	1.720	0.336
U16-h07-34-405	ooid and clast	0.007	0.011	0.112	0.042	0.082	0.024	0.008	0.008	0.089	0.028
U16-h07-34-405	ooid and clast	0.001	0.000	0.023	0.014	0.000	0.002	0.002	0.000	0.011	0.008
U16-h07-34-405	ooid and clast	0.003	0.000	0.049	0.020	0.000	0.011	0.005	0.000	0.029	0.013
U16-h07-34-405	ooid and clast	0.014	0.000	0.449	0.064	0.000	0.092	0.016	0.000	0.312	0.053
U16-h07-34-405	ooid and clast	0.015	0.000	0.900	0.091	0.000	0.201	0.027	0.000	0.560	0.070
U16-h07-34-405	ooid and clast	0.018	0.010	0.749	0.138	0.079	0.192	0.032	0.008	0.636	0.127
U16-h07-34-405	ooid and clast	0.008	0.000	0.425	0.053	0.000	0.113	0.016	0.000	0.343	0.045
U16-h07-34-405	ooid and clast	0.014	0.000	0.710	0.092	0.000	0.127	0.019	0.000	0.379	0.033
U16-h07-34-405	ooid and clast	0.011	0.000	0.480	0.065	0.000	0.100	0.016	0.000	0.298	0.042
U16-h07-34-405	ooid and clast	0.016	0.000	0.769	0.112	0.000	0.161	0.021	0.000	0.483	0.044
U16-h07-34-405	ooid and clast	0.007	0.000	0.130	0.037	0.000	0.030	0.009	0.000	0.099	0.021
U16-h07-34-405	ooid and clast	0.019	0.000	0.927	0.138	0.000	0.205	0.033	0.000	0.743	0.094
U16-h07-34-405	ooid and clast	0.027	0.004	0.934	0.137	0.027	0.212	0.033	0.002	0.664	0.094
U16-h07-34-405	ooid and clast	0.026	0.003	0.978	0.137	0.000	0.233	0.032	0.006	0.877	0.096
U16-h07-34-405	ooid and clast	0.062	0.000	2.281	0.291	0.000	0.526	0.067	0.000	1.628	0.224
U16-h07-34-405	ooid and clast	1.314	0.000	3.481	9.995	0.000	-0.138	2.134	0.000	1.356	5.465
U16-h07-34-405	ooid and clast	0.544	0.004	-0.489	4.195	0.029	-0.341	1.065	0.003	-0.706	6.229
U16-h07-34-405	ooid and clast	0.847	0.000	-1.726	8.275	0.000	-0.607	2.047	0.000	-1.093	5.788
U16-h07-34-405	ooid and clast	0.001	0.017	0.076	0.005	0.085	0.014	0.001	0.018	0.038	0.003
U16-h07-34-405	ooid and clast	0.034	0.004	-1.094	0.153	0.028	-0.261	0.055	0.003	-0.893	0.192
U16-h07-34-405	ooid and clast	0.050	0.000	-2.045	0.217	0.000	-0.411	0.041	0.000	-1.186	0.129
U16-h07-34-405	ooid and clast	0.057	0.000	-2.102	0.330	0.000	-0.522	0.090	0.000	-1.380	0.192
U16-h07-34-405	ooid and clast	0.014	0.000	-0.582	0.073	0.000	-0.154	0.022	0.000	-0.391	0.054

Sample ID	SampleType	2SE (ppm)	Tb LOD (ppm)	Dy (ppm)	2SE (ppm)	Dy LOD (ppm)	Ho (ppm)	2SE (ppm)	Ho LOD (ppm)	Er (ppm)	2SE (ppm)
U16-h07-34-405	ooid and clast	0.017	0.000	-0.604	0.087	0.000	-0.137	0.018	0.000	-0.347	0.055
U16-h07-34-405	ooid and clast	0.019	0.000	-0.485	0.091	0.000	-0.104	0.018	0.000	-0.351	0.061
U16-h07-34-405	ooid and clast	0.037	0.022	-0.409	0.254	0.165	-0.148	0.059	0.040	-0.278	0.153
U16-h07-34-405	ooid and clast	0.011	0.000	-0.428	0.049	0.000	-0.124	0.017	0.000	-0.336	0.055
U16-h07-34-405	ooid and clast	0.012	0.003	-0.307	0.068	0.000	-0.085	0.017	0.000	-0.262	0.052
U16-h07-34-405	ooid and clast	0.016	0.022	-0.354	0.090	0.167	-0.075	0.022	0.040	-0.346	0.086
U16-h07-34-405	ooid and clast	0.006	0.003	-0.245	0.027	0.000	-0.058	0.010	0.000	-0.177	0.024
U16-h07-34-405	ooid and clast	0.005	0.003	-0.204	0.028	0.000	-0.049	0.007	0.000	-0.169	0.019
U16-h07-34-405	ooid and clast	0.007	0.016	-0.240	0.041	0.079	-0.058	0.011	0.017	-0.156	0.019
U16-h07-34-405	ooid and clast	0.011	0.000	-0.199	0.043	0.000	-0.041	0.011	0.000	-0.106	0.027
U16-h07-34-405	vein 1	0.011	0.012	0.508	0.080	0.081	0.098	0.015	0.016	0.252	0.050
U16-h07-34-405	vein 1	0.031	0.012	0.403	0.217	0.083	0.079	0.050	0.017	0.312	0.097
U16-h07-34-405	vein 1	0.106	0.012	1.335	0.832	0.086	0.275	0.160	0.017	0.765	0.454
U16-h07-34-405	vein 1	0.022	0.011	0.740	0.167	0.079	0.134	0.036	0.016	0.400	0.097
U16-h07-34-405	vein 1	0.022	0.012	0.733	0.125	0.082	0.138	0.027	0.017	0.400	0.069
U16-h07-34-405	vein 2	0.025	0.013	-0.318	0.109	0.094	-0.099	0.035	0.019	-0.266	0.085
U16-h07-34-405	vein 2	0.025	0.012	-0.371	0.085	0.086	-0.099	0.025	0.017	-0.235	0.060
U16-h07-34-405	vein 2	0.013	0.013	-0.462	0.101	0.091	-0.109	0.026	0.018	-0.293	0.051
U16-h07-34-405	vein 2	0.059	0.013	-0.802	0.285	0.093	-0.203	0.061	0.019	-0.706	0.195
U16-h07-34-405	vein 2	0.036	0.013	-0.944	0.186	0.089	-0.171	0.038	0.018	-0.533	0.157
U16-h07-34-405	vein 2	0.062	0.013	-1.167	0.314	0.092	-0.210	0.073	0.018	-0.627	0.205
U16-h07-54-338	coarse calcite	0.005	0.000	0.102	0.034	0.030	0.030	0.009	0.004	0.056	0.017
U16-h07-54-338	coarse calcite	0.003	0.004	0.031	0.015	0.048	0.006	0.004	0.004	0.023	0.012
U16-h07-54-338	coarse calcite	0.001	0.000	0.016	0.010	0.000	0.005	0.004	0.000	0.013	0.008
U16-h07-54-338	coarse calcite	0.006	0.000	0.109	0.031	0.000	0.026	0.007	0.007	0.098	0.027
U16-h07-54-338	coarse calcite	0.028	0.004	0.636	0.201	0.046	0.157	0.046	0.004	0.562	0.174
U16-h07-54-338	coarse calcite	0.004	0.000	0.050	0.025	0.028	0.010	0.004	0.000	0.021	0.011
U16-h07-54-338	coarse calcite	0.004	0.004	0.043	0.018	0.049	0.012	0.005	0.004	0.035	0.013
U16-h07-54-338	coarse calcite	0.005	0.000	0.112	0.029	0.000	0.024	0.007	0.000	0.089	0.021
U16-h07-54-338	coarse calcite	0.020	0.026	0.412	0.150	0.017	0.094	0.033	0.018	0.276	0.082
U16-h07-54-338	coarse calcite	0.023	0.004	0.715	0.179	0.045	0.201	0.040	0.004	0.593	0.131
U16-h07-54-338	coarse calcite	0.012	0.004	0.543	0.128	0.046	0.116	0.019	0.004	0.376	0.082
U16-h07-54-338	coarse calcite	0.008	0.007	0.259	0.054	0.000	0.061	0.013	0.000	0.155	0.028

Sample ID	SampleType	2SE (ppm)	Tb LOD (ppm)	Dy (ppm)	2SE (ppm)	Dy LOD (ppm)	Ho (ppm)	2SE (ppm)	Ho LOD (ppm)	Er (ppm)	2SE (ppm)
U16-h07-54-338	coarse calcite	0.004	0.000	0.126	0.026	0.033	0.029	0.009	0.003	0.085	0.024
U16-h07-54-338	coarse calcite	0.024	0.025	0.401	0.163	0.016	0.106	0.038	0.018	0.320	0.125
U16-h07-54-338	coarse calcite	0.005	0.000	0.056	0.020	0.028	0.005	0.004	0.000	0.031	0.013
U16-h07-54-5	matrix cement	0.005	0.000	0.115	0.034	0.000	0.017	0.006	0.000	0.070	0.023
U16-h07-54-5	matrix cement	0.009	0.000	0.257	0.048	0.000	0.052	0.011	0.000	0.139	0.034
U16-h07-54-5	matrix cement	0.009	0.000	0.487	0.047	0.000	0.089	0.013	0.000	0.242	0.049
U16-h07-54-5	matrix cement	0.014	0.000	0.501	0.078	0.000	0.090	0.013	0.000	0.285	0.046
U16-h07-54-5	matrix cement	0.015	0.000	0.477	0.062	0.000	0.113	0.012	0.000	0.295	0.048
U16-h07-54-5	matrix cement	0.011	0.000	0.415	0.071	0.000	0.098	0.014	0.000	0.288	0.053
U16-h07-54-5	matrix cement	0.012	0.000	0.478	0.051	0.000	0.085	0.014	0.000	0.302	0.053
U16-h07-54-5	matrix cement	0.011	0.000	0.512	0.056	0.000	0.111	0.016	0.000	0.339	0.048
U16-h07-54-5	matrix cement	0.007	0.000	0.230	0.053	0.000	0.073	0.011	0.000	0.205	0.030
U16-h07-54-5	matrix cement	0.012	0.000	0.422	0.062	0.000	0.076	0.014	0.000	0.222	0.042
U16-h07-54-5	matrix cement	0.010	0.000	0.567	0.086	0.000	0.116	0.016	0.004	0.318	0.049
U16-h07-54-5	matrix cement	0.010	0.000	0.298	0.034	0.000	0.060	0.014	0.000	0.172	0.037
U16-h07-54-5	matrix cement	0.010	0.000	0.463	0.077	0.000	0.074	0.012	0.000	0.280	0.052
U16-h07-54-5	matrix cement	0.011	0.000	0.429	0.061	0.000	0.093	0.018	0.000	0.230	0.040
U16-h07-54-5	matrix cement	0.008	0.000	0.137	0.037	0.000	0.024	0.007	0.000	0.105	0.026
U16-h07-54-5	matrix cement	0.014	0.000	0.434	0.065	0.000	0.103	0.013	0.000	0.267	0.036
U16-h07-54-5	matrix cement	0.006	0.000	0.160	0.043	0.000	0.043	0.011	0.000	0.125	0.027
U16-h07-54-5	ooid	0.021	0.000	0.787	0.099	0.000	0.143	0.026	0.000	0.458	0.063
U16-h07-54-5	ooid	0.013	0.000	0.550	0.064	0.000	0.132	0.018	0.000	0.335	0.049
U16-h07-54-5	ooid	0.006	0.000	0.109	0.033	0.000	0.021	0.007	0.000	0.056	0.015
U16-h07-54-5	ooid	0.013	0.000	0.575	0.083	0.013	0.117	0.016	0.000	0.382	0.047
U16-h07-54-5	ooid	0.011	0.000	0.668	0.084	0.000	0.120	0.016	0.000	0.374	0.049
U16-h07-54-5	ooid	0.006	0.000	0.194	0.042	0.000	0.052	0.012	0.000	0.119	0.031
U16-h07-54-5	ooid	0.017	0.000	0.893	0.103	0.014	0.172	0.024	0.000	0.514	0.055
U16-h07-54-5	ooid	0.029	0.000	1.193	0.118	0.000	0.271	0.030	0.000	0.695	0.075
U16-h07-54-5	ooid	0.012	0.000	0.471	0.050	0.000	0.084	0.013	0.004	0.275	0.042
U16-h07-54-5	ooid	0.009	0.000	0.407	0.059	0.000	0.097	0.011	0.000	0.280	0.040
U16-h07-54-5	ooid	0.012	0.000	0.691	0.078	0.000	0.156	0.016	0.000	0.387	0.062
U16-h07-54-5	ooid	0.015	0.000	0.505	0.065	0.013	0.116	0.017	0.000	0.332	0.036
U16-h07-54-5	ooid	0.008	0.000	0.194	0.046	0.000	0.059	0.010	0.000	0.124	0.025

Sample ID	SampleType	2SE (ppm)	Tb LOD (ppm)	Dy (ppm)	2SE (ppm)	Dy LOD (ppm)	Ho (ppm)	2SE (ppm)	Ho LOD (ppm)	Er (ppm)	2SE (ppm)
U16-h07-54-5	ooid	0.008	0.000	0.348	0.061	0.013	0.087	0.012	0.000	0.249	0.040
U16-h07-54-5	ooid	0.009	0.000	0.283	0.051	0.000	0.052	0.013	0.000	0.161	0.028
U16-h07-54-5	ooid	0.010	0.000	0.325	0.060	0.000	0.060	0.010	0.004	0.189	0.045
U16-h07-54-5	ooid	0.015	0.000	0.640	0.069	0.012	0.130	0.016	0.000	0.368	0.050
U16-h07-54-5	ooid	0.012	0.000	0.598	0.089	0.013	0.126	0.015	0.000	0.421	0.055
U16-h07-54-5	ooid	0.011	0.000	0.473	0.060	0.000	0.088	0.013	0.000	0.298	0.038
U16-h07-54-5	ooid	0.012	0.000	0.475	0.068	0.013	0.108	0.018	0.000	0.372	0.041
U16-h07-54-5	ooid	0.010	0.000	0.293	0.061	0.000	0.065	0.012	0.000	0.200	0.039
U16-h07-54-5	ooid	0.016	0.000	0.400	0.107	0.000	0.113	0.033	0.000	0.306	0.079
U16-h07-54-5	ooid	0.014	0.000	0.530	0.071	0.000	0.103	0.016	0.000	0.333	0.052
U16-h07-54-5	ooid	0.013	0.000	0.526	0.074	0.013	0.123	0.015	0.000	0.320	0.043
U16-h07-54-5	ooid	0.005	0.000	0.097	0.030	0.000	0.031	0.009	0.000	0.078	0.024
U16-h07-54-5	vein 1	0.010	0.000	0.313	0.048	0.000	0.077	0.015	0.000	0.255	0.040
U16-h07-54-5	vein 1	0.024	0.000	1.790	0.192	0.000	0.419	0.050	0.000	1.446	0.149
U16-h07-54-5	vein 1	0.008	0.000	0.270	0.048	0.016	0.068	0.016	0.000	0.203	0.035
U16-h07-54-5	vein 1	0.008	0.000	0.239	0.049	0.016	0.053	0.010	0.000	0.203	0.036
U16-h07-54-5	vein 1	0.011	0.000	0.390	0.066	0.016	0.083	0.015	0.000	0.218	0.039
U16-h07-54-5	vein 1	0.016	0.000	0.777	0.083	0.016	0.145	0.017	0.000	0.452	0.066
U16-h07-54-5	vein 2	0.006	0.000	0.160	0.031	0.000	0.047	0.010	0.000	0.116	0.022
U16-h07-54-5	vein 2	0.020	0.000	1.030	0.076	0.000	0.245	0.023	0.000	0.746	0.081
U16-h07-54-5	vein 2	0.005	0.000	0.053	0.021	0.000	0.020	0.007	0.000	0.054	0.016
U16-h07-67-129	darker vein	0.003	0.000	0.058	0.019	0.000	0.022	0.009	0.000	0.077	0.022
U16-h07-67-129	darker vein	0.003	0.000	0.067	0.021	0.000	0.012	0.005	0.003	0.053	0.017
U16-h07-67-129	darker vein	0.003	0.000	0.020	0.012	0.000	0.012	0.006	0.000	0.032	0.013
U16-h07-67-129	darker vein	0.002	0.000	0.012	0.010	0.000	0.005	0.003	0.003	0.018	0.011
U16-h07-67-129	darker vein	0.002	0.000	0.045	0.019	0.000	0.004	0.004	0.000	0.015	0.010
U16-h07-67-129	darker vein	0.004	0.000	0.062	0.021	0.000	0.013	0.005	0.000	0.066	0.018
U16-h07-67-129	darker vein	0.004	0.000	0.157	0.032	0.000	0.030	0.009	0.000	0.117	0.030
U16-h07-67-129	lighter vein	0.015	0.000	0.435	0.115	0.000	0.087	0.030	0.000	0.281	0.087
U16-h07-67-129	lighter vein	0.018	0.000	1.357	0.120	0.000	0.349	0.025	0.004	1.065	0.086
U16-h07-67-129	lighter vein	0.013	0.002	0.556	0.072	0.000	0.134	0.018	0.000	0.324	0.054
U16-h07-67-129	lighter vein	0.020	0.000	1.522	0.114	0.000	0.378	0.023	0.000	1.212	0.071
U16-h07-67-129	lighter vein	0.008	0.000	0.355	0.052	0.000	0.079	0.013	0.000	0.271	0.040

Sample ID	SampleType	2SE (ppm)	Tb LOD (ppm)	Dy (ppm)	2SE (ppm)	Dy LOD (ppm)	Ho (ppm)	2SE (ppm)	Ho LOD (ppm)	Er (ppm)	2SE (ppm)
U16-h07-67-129	lighter vein	0.024	0.000	1.363	0.094	0.000	0.327	0.022	0.000	0.971	0.076
U16-h07-67-129	lighter vein	0.019	0.000	0.575	0.140	0.000	0.136	0.033	0.004	0.385	0.098
U16-h07-67-129	ooid and matrix	0.379	0.000	13.555	1.564	0.000	3.054	0.496	0.000	8.049	1.103
U16-h07-67-129	ooid and matrix	0.029	0.000	1.778	0.172	0.000	0.416	0.045	0.004	1.245	0.143
U16-h07-67-129	ooid and matrix	0.045	0.000	2.688	0.269	0.000	0.593	0.057	0.000	1.706	0.188
U16-h07-67-129	ooid and matrix	0.018	0.000	1.187	0.123	0.000	0.327	0.029	0.000	0.928	0.094
U16-h07-67-129	ooid and matrix	0.066	0.000	1.996	0.429	0.000	0.410	0.081	0.000	1.161	0.243
U16-h07-67-129	ooid and matrix	0.021	0.000	1.103	0.115	0.047	0.251	0.026	0.012	0.760	0.089
U16-h07-67-129	ooid and matrix	0.011	0.000	0.411	0.060	0.000	0.129	0.016	0.009	0.354	0.050
U16-h07-67-129	ooid and matrix	0.018	0.063	0.931	0.093	0.514	0.184	0.023	0.133	0.622	0.066
U16-h07-67-129	ooid and matrix	0.019	0.013	1.589	0.117	0.026	0.351	0.032	0.007	1.163	0.094
U16-h07-67-129	ooid and matrix	0.041	0.000	1.863	0.179	0.052	0.404	0.040	0.013	1.209	0.133
U16-h07-67-129	ooid and matrix	0.025	0.000	0.827	0.190	0.000	0.178	0.042	0.005	0.573	0.122
U16-h07-67-129	ooid and matrix	0.007	0.000	0.217	0.051	0.000	0.047	0.013	0.000	0.178	0.034
U16-h07-67-129	ooid and matrix	0.020	0.000	0.742	0.077	0.000	0.163	0.019	0.000	0.533	0.067
U16-h07-67-129	ooid and matrix	0.006	0.000	0.145	0.037	0.000	0.024	0.007	0.000	0.047	0.019
U16-h07-67-129	ooid and matrix	0.012	0.000	0.762	0.078	0.000	0.179	0.020	0.000	0.577	0.059
U16-h07-67-129	ooid and matrix	0.002	0.000	0.032	0.018	0.000	0.007	0.005	0.000	0.004	0.005
U16-h07-67-129	ooid and matrix	0.015	0.000	0.307	0.076	0.000	0.084	0.017	0.000	0.257	0.048
U16-h07-67-129	ooid and matrix	0.006	0.012	0.155	0.044	0.025	0.056	0.014	0.006	0.142	0.034
U16-h07-67-129	ooid and matrix	0.010	0.000	0.634	0.071	0.044	0.155	0.015	0.011	0.469	0.043
U16-h07-67-129	ooid and matrix	0.012	0.000	0.721	0.106	0.000	0.207	0.032	0.004	0.776	0.119
U16-h07-67-129	ooid and matrix	0.013	0.000	0.373	0.056	0.000	0.091	0.013	0.000	0.270	0.040
U16-h07-67-129	ooid and matrix	0.028	0.000	1.536	0.207	0.000	0.328	0.049	0.010	1.054	0.134
U16-h07-67-129	ooid and matrix	0.010	0.000	0.489	0.062	0.000	0.115	0.019	0.000	0.315	0.059
U16-h07-67-129	ooid and matrix	0.019	0.010	0.972	0.123	0.041	0.185	0.026	0.005	0.579	0.072
U16-h07-67-129	ooid and matrix	0.020	0.000	1.107	0.127	0.000	0.250	0.031	0.011	0.802	0.096

Sample ID	SampleType	Er LOD (ppm)	Tm(ppm)	2SE (ppm)	Tm LOD (ppm)	Yb (ppm)	2SE (ppm)	Yb LOD (ppm)	Lu (ppm)	2SE (ppm)	Lu LOD (ppm)
U16-h07-13b-11	matrix	0.000	0.018	0.007	0.000	0.120	0.032	0.000	0.011	0.004	0.000
U16-h07-13b-11	matrix	0.000	0.002	0.000	0.000	0.011	0.005	0.000	0.001	0.000	0.000
U16-h07-13b-11	matrix	0.000	0.004	0.002	0.000	0.062	0.024	0.000	0.003	0.002	0.000
U16-h07-13b-11	matrix	0.000	0.019	0.005	0.000	0.083	0.025	0.000	0.011	0.004	0.000
U16-h07-13b-11	matrix	0.000	0.012	0.005	0.000	0.049	0.019	0.000	0.014	0.005	0.000
U16-h07-13b-11	matrix	0.000	0.009	0.003	0.000	0.046	0.020	0.000	0.006	0.003	0.000
U16-h07-13b-11	matrix	0.000	0.012	0.004	0.000	0.054	0.019	0.000	0.008	0.003	0.000
U16-h07-13b-11	matrix	0.000	0.017	0.005	0.000	0.095	0.027	0.000	0.016	0.005	0.000
U16-h07-13b-11	matrix	0.000	0.027	0.006	0.000	0.199	0.044	0.000	0.022	0.006	0.000
U16-h07-13b-11	matrix	0.000	0.012	0.005	0.000	0.082	0.024	0.000	0.010	0.004	0.000
U16-h07-13b-11	matrix	0.000	0.022	0.006	0.000	0.139	0.027	0.000	0.025	0.005	0.000
U16-h07-13b-11	matrix	0.000	0.011	0.004	0.000	0.091	0.025	0.000	0.008	0.003	0.000
U16-h07-13b-11	matrix	0.000	0.015	0.005	0.000	0.117	0.037	0.000	0.016	0.006	0.000
U16-h07-13b-11	matrix	0.000	0.023	0.006	0.000	0.152	0.026	0.000	0.026	0.008	0.000
U16-h07-13b-11	matrix	0.000	0.011	0.004	0.000	0.113	0.026	0.000	0.012	0.004	0.000
U16-h07-13b-11	matrix	0.000	0.027	0.007	0.000	0.118	0.034	0.000	0.018	0.006	0.000
U16-h07-13b-11	matrix	0.000	0.017	0.006	0.000	0.112	0.030	0.000	0.013	0.005	0.000
U16-h07-13b-11	matrix	0.000	0.009	0.004	0.000	0.093	0.028	0.000	0.009	0.004	0.000
U16-h07-13b-11	matrix	0.000	0.027	0.007	0.000	0.172	0.044	0.000	0.023	0.006	0.000
U16-h07-13b-11	matrix	0.000	0.026	0.008	0.000	0.117	0.034	0.000	0.015	0.005	0.000
U16-h07-13b-11	matrix	0.000	0.023	0.007	0.000	0.138	0.032	0.000	0.019	0.006	0.000
U16-h07-13b-11	vein 1	0.000	0.020	0.007	0.000	0.087	0.031	0.000	0.014	0.006	0.000
U16-h07-13b-11	vein 1	0.000	0.081	0.011	0.000	0.551	0.063	0.000	0.059	0.010	0.000
U16-h07-13b-11	vein 1	0.000	0.051	0.009	0.000	0.229	0.038	0.000	0.027	0.007	0.000
U16-h07-13b-11	vein 1	0.000	0.044	0.010	0.000	0.246	0.061	0.000	0.036	0.008	0.000
U16-h07-13b-11	vein 1	0.000	0.023	0.007	0.000	0.101	0.024	0.000	0.013	0.005	0.000
U16-h07-13b-11	vein 1	0.000	0.035	0.007	0.000	0.136	0.025	0.000	0.023	0.007	0.000
U16-h07-13b-11	vein 1	0.000	0.048	0.012	0.000	0.277	0.050	0.000	0.034	0.008	0.000
U16-h07-13b-11	vein 2	0.000	0.005	0.003	0.000	0.026	0.014	0.000	0.003	0.001	0.000
U16-h07-13b-11	vein 2	0.000	0.002	0.001	0.000	0.004	0.000	0.000	0.002	0.001	0.000
U16-h07-13b-11	vein 2	0.000	0.001	0.000	0.000	0.006	0.003	0.000	0.001	0.000	0.000
U16-h07-13b-11	vein 2	0.000	0.001	0.000	0.000	0.004	0.000	0.000	0.001	0.000	0.000
U16-h07-13b-11	vein 2	0.000	0.001	0.000	0.000	0.004	0.000	0.000	0.001	0.000	0.000

Sample ID	SampleType	Er LOD (ppm)	Tm(ppm)	2SE (ppm)	Tm LOD (ppm)	Yb (ppm)	2SE (ppm)	Yb LOD (ppm)	Lu (ppm)	2SE (ppm)	Lu LOD (ppm)
U16-h07-13b-11	vein 2	0.000	0.001	0.000	0.000	0.004	0.000	0.000	0.001	0.000	0.000
U16-h07-13b-11	vein 3	0.000	0.014	0.005	0.000	0.072	0.025	0.000	0.009	0.004	0.000
U16-h07-13b-11	vein 3	0.000	0.016	0.006	0.000	0.098	0.030	0.000	0.015	0.005	0.000
U16-h07-13b-11	vein 3	0.000	0.037	0.008	0.000	0.268	0.056	0.000	0.032	0.009	0.000
U16-h07-13b-31	dk ooid	0.000	0.033	0.010	0.000	0.238	0.051	0.017	0.034	0.010	0.000
U16-h07-13b-31	dk ooid	0.000	0.087	0.012	0.006	0.575	0.093	0.000	0.074	0.013	0.000
U16-h07-13b-31	dk ooid	0.000	0.046	0.011	0.000	0.297	0.065	0.017	0.054	0.009	0.000
U16-h07-13b-31	dk ooid	0.000	0.062	0.015	0.000	0.302	0.062	0.017	0.047	0.010	0.000
U16-h07-13b-31	dk ooid	0.000	0.086	0.013	0.005	0.447	0.071	0.000	0.077	0.013	0.000
U16-h07-13b-31	dk ooid	0.000	0.099	0.015	0.005	0.695	0.094	0.000	0.094	0.015	0.000
U16-h07-13b-31	matrix cement	0.000	0.049	0.011	0.000	0.282	0.050	0.017	0.045	0.011	0.000
U16-h07-13b-31	matrix cement	0.034	0.056	0.010	0.000	0.453	0.073	0.000	0.059	0.011	0.005
U16-h07-13b-31	matrix cement	0.000	0.098	0.016	0.000	0.541	0.077	0.017	0.100	0.018	0.000
U16-h07-13b-31	matrix cement	0.000	0.061	0.010	0.000	0.483	0.066	0.016	0.055	0.009	0.000
U16-h07-13b-31	matrix cement	0.035	0.070	0.013	0.000	0.428	0.060	0.000	0.066	0.011	0.006
U16-h07-13b-31	matrix cement	0.000	0.091	0.013	0.000	0.611	0.109	0.017	0.077	0.011	0.000
U16-h07-13b-31	matrix cement	0.000	0.079	0.016	0.000	0.520	0.081	0.016	0.081	0.012	0.000
U16-h07-13b-31	matrix cement	0.033	0.090	0.016	0.000	0.634	0.070	0.000	0.098	0.014	0.005
U16-h07-13b-31	matrix cement	0.019	0.079	0.013	0.000	0.518	0.075	0.000	0.073	0.010	0.000
U16-h07-13b-31	matrix cement	0.019	0.079	0.011	0.000	0.562	0.067	0.000	0.078	0.014	0.000
U16-h07-13b-31	matrix cement	0.034	0.089	0.015	0.000	0.572	0.072	0.000	0.078	0.015	0.005
U16-h07-13b-31	matrix cement	0.034	0.071	0.012	0.000	0.519	0.079	0.000	0.054	0.012	0.005
U16-h07-13b-31	ooid	0.030	0.065	0.011	0.005	0.463	0.068	0.000	0.065	0.011	0.000
U16-h07-13b-31	ooid	0.000	0.041	0.008	0.000	0.298	0.042	0.033	0.036	0.008	0.000
U16-h07-13b-31	ooid	0.030	0.092	0.014	0.005	0.533	0.085	0.000	0.060	0.011	0.000
U16-h07-13b-31	ooid	0.107	0.044	0.010	0.068	0.187	0.046	0.072	0.033	0.008	0.079
U16-h07-13b-31	ooid	0.000	0.101	0.013	0.000	0.674	0.089	0.000	0.085	0.014	0.000
U16-h07-13b-31	ooid	0.038	0.069	0.013	0.000	0.457	0.078	0.000	0.077	0.012	0.000
U16-h07-13b-31	ooid	0.000	0.082	0.013	0.000	0.461	0.061	0.000	0.062	0.011	0.000
U16-h07-13b-31	ooid	0.104	0.074	0.013	0.066	0.545	0.084	0.070	0.058	0.010	0.077
U16-h07-13b-31	ooid	0.000	0.083	0.012	0.000	0.609	0.069	0.015	0.082	0.014	0.003
U16-h07-13b-31	ooid	0.038	0.094	0.015	0.000	0.562	0.076	0.000	0.084	0.015	0.000
U16-h07-13b-31	ooid	0.030	0.082	0.018	0.005	0.559	0.075	0.000	0.089	0.010	0.000

Sample ID	SampleType	Er LOD (ppm)	Tm(ppm)	2SE (ppm)	Tm LOD (ppm)	Yb (ppm)	2SE (ppm)	Yb LOD (ppm)	Lu (ppm)	2SE (ppm)	Lu LOD (ppm)
U16-h07-13b-31	ooid	0.000	0.080	0.015	0.000	0.575	0.079	0.033	0.065	0.009	0.000
U16-h07-13b-31	ooid	0.029	0.091	0.016	0.005	0.539	0.069	0.000	0.073	0.013	0.000
U16-h07-13b-31	ooid	0.029	0.071	0.014	0.005	0.525	0.072	0.000	0.077	0.012	0.000
U16-h07-13b-31	ooid	0.000	0.096	0.016	0.000	0.596	0.065	0.033	0.083	0.015	0.000
U16-h07-13b-31	ooid	0.038	0.094	0.017	0.000	0.582	0.070	0.000	0.070	0.014	0.000
U16-h07-13b-31	ooid	0.000	0.088	0.013	0.000	0.520	0.071	0.016	0.084	0.014	0.003
U16-h07-13b-31	ooid	0.000	0.109	0.016	0.000	0.613	0.085	0.015	0.081	0.011	0.003
U16-h07-13b-31	ooid	0.029	0.064	0.011	0.005	0.483	0.073	0.000	0.076	0.012	0.000
U16-h07-13b-31	ooid	0.028	0.081	0.011	0.005	0.560	0.067	0.000	0.072	0.009	0.000
U16-h07-13b-31	ooid	0.000	0.085	0.014	0.000	0.564	0.081	0.014	0.101	0.013	0.003
U16-h07-13b-31	ooid	0.000	0.072	0.011	0.000	0.549	0.060	0.014	0.081	0.016	0.003
U16-h07-13b-31	ooid	0.028	0.076	0.010	0.005	0.470	0.068	0.000	0.060	0.009	0.000
U16-h07-13b-31	ooid	0.104	0.107	0.013	0.066	0.490	0.051	0.070	0.075	0.013	0.077
U16-h07-13b-31	vein-1	0.000	0.087	0.017	0.000	0.576	0.071	0.000	0.090	0.013	0.000
U16-h07-13b-31	vein-1	0.000	0.006	0.003	0.000	0.077	0.039	0.000	0.010	0.006	0.000
U16-h07-13b-31	vein-1	0.000	0.002	0.002	0.000	0.029	0.018	0.000	0.001	0.002	0.000
U16-h07-13b-31	vein-1	0.010	0.008	0.004	0.000	0.076	0.024	0.000	0.008	0.003	0.000
U16-h07-13b-31	vein-1	0.000	0.011	0.005	0.000	0.132	0.031	0.000	0.009	0.004	0.000
U16-h07-13b-31	vein-1	0.000	0.005	0.003	0.000	0.031	0.015	0.000	0.006	0.003	0.000
U16-h07-13b-81	coarse calcite	0.000	0.000	1.000	0.000	0.000	1.000	0.000	0.000	1.000	0.002
U16-h07-13b-81	coarse calcite	0.000	0.000	0.000	0.000	-0.001	0.000	0.000	0.000	0.000	0.002
U16-h07-13b-81	coarse calcite	0.000	0.000	0.000	0.000	-0.004	0.000	0.000	0.000	0.000	0.002
U16-h07-13b-81	coarse calcite	0.022	-0.001	0.000	0.005	-0.013	0.002	0.016	-0.001	0.000	0.003
U16-h07-13b-81	vein 1	0.111	0.145	0.022	0.028	0.942	0.121	0.146	0.141	0.028	0.018
U16-h07-13b-81	vein 1	0.356	0.175	0.026	0.055	1.343	0.197	0.369	0.223	0.052	0.076
U16-h07-13b-81	vein 1	0.085	0.023	0.010	0.022	0.164	0.042	0.112	0.012	0.006	0.014
U16-h07-13b-81	vein 1	0.203	0.024	0.017	0.037	0.195	0.095	0.228	0.027	0.018	0.035
U16-h07-13b-81	vein 1	0.000	0.045	0.008	0.000	0.314	0.052	0.000	0.045	0.008	0.002
U16-h07-13b-81	vein 1	0.347	0.075	0.017	0.049	0.475	0.107	0.374	0.066	0.014	0.053
U16-h07-13b-81	vein 1	0.273	0.059	0.020	0.044	0.464	0.104	0.284	0.063	0.017	0.041
U16-h07-13b-81	vein 1	0.279	0.065	0.021	0.045	0.391	0.120	0.291	0.058	0.016	0.042
U16-h07-13b-81	vein 1	0.202	0.026	0.016	0.037	0.186	0.062	0.227	0.034	0.020	0.035
U16-h07-24-145	ooids and cement	0.000	0.000	1.000	0.004	0.011	0.013	0.000	0.000	1.000	0.000

Sample ID	SampleType	Er LOD (ppm)	Tm(ppm)	2SE (ppm)	Tm LOD (ppm)	Yb (ppm)	2SE (ppm)	Yb LOD (ppm)	Lu (ppm)	2SE (ppm)	Lu LOD (ppm)
U16-h07-24-145	ooids and cement	0.000	0.011	0.004	0.000	0.070	0.022	0.000	0.008	0.004	0.000
U16-h07-24-145	ooids and cement	0.000	0.006	0.004	0.000	0.022	0.016	0.000	0.008	0.005	0.000
U16-h07-24-145	ooids and cement	0.000	0.008	0.004	0.000	0.030	0.014	0.000	0.003	0.003	0.000
U16-h07-24-145	ooids and cement	0.000	0.012	0.004	0.004	0.068	0.019	0.000	0.008	0.003	0.000
U16-h07-24-145	ooids and cement	0.000	0.000	1.000	0.000	0.000	1.000	0.000	0.000	1.000	0.000
U16-h07-24-145	ooids and cement	0.000	0.006	0.003	0.000	0.050	0.017	0.000	0.009	0.004	0.000
U16-h07-24-145	ooids and cement	0.000	0.012	0.005	0.000	0.073	0.020	0.000	0.009	0.004	0.000
U16-h07-24-145	vein-1	0.000	0.000	0.000	0.000	0.015	0.008	0.000	0.001	0.001	0.000
U16-h07-24-145	vein-1	0.000	-0.001	0.001	0.000	0.002	0.004	0.000	0.001	0.001	0.000
U16-h07-24-145	vein-1	0.000	-0.003	0.001	0.000	0.000	0.002	0.000	0.000	0.001	0.000
U16-h07-24-145	vein-1	0.000	-0.001	0.003	0.000	0.010	0.008	0.000	0.002	0.001	0.000
U16-h07-24-145	vein-1	0.000	-0.003	0.002	0.000	0.031	0.015	0.000	0.002	0.002	0.000
U16-h07-24-145	vein-1	0.104	-0.010	0.001	0.045	0.010	0.010	0.058	0.001	0.001	0.027
U16-h07-24-145	vein-1	0.104	-0.003	0.003	0.045	0.005	0.006	0.058	0.001	0.001	0.027
U16-h07-24-145	vein-1	0.097	-0.004	0.003	0.042	0.039	0.017	0.054	0.005	0.002	0.026
U16-h07-24-145	vein-2	0.000	0.001	0.001	0.000	0.018	0.015	0.000	0.001	0.001	0.000
U16-h07-24-145	vein-2	0.000	0.006	0.006	0.000	0.095	0.070	0.000	0.021	0.015	0.000
U16-h07-24-145	vein-2	0.000	-0.009	0.007	0.000	-0.058	0.040	0.000	-0.001	0.002	0.000
U16-h07-24-145	vein-3	0.050	0.061	0.037	0.010	-0.441	0.412	0.046	-0.113	0.079	0.005
U16-h07-24-145	vein-3	0.000	-0.001	0.001	0.000	-0.007	0.008	0.000	0.000	1.000	0.000
U16-h07-24-145	vein-3	0.024	-0.004	0.003	0.003	-0.002	0.008	0.014	-0.001	0.001	0.002
U16-h07-24-145	vein-3	0.000	-0.001	0.001	0.000	0.000	1.000	0.000	0.000	0.001	0.000
U16-h07-24-145	vein-3	0.024	-0.005	0.002	0.003	-0.008	0.005	0.014	-0.001	0.001	0.002
U16-h07-24-145	vein-3	0.000	-0.001	0.001	0.000	-0.013	0.008	0.000	-0.001	0.001	0.000
U16-h07-24-145	vein-3	0.000	0.000	1.000	0.000	0.000	1.000	0.000	0.000	1.000	0.000
U16-h07-24-145	vein-4	0.051	0.133	0.189	0.010	0.842	1.187	0.047	0.084	0.116	0.005
U16-h07-24-145	vein-4	0.000	0.011	0.004	0.000	0.082	0.024	0.000	0.009	0.003	0.000
U16-h07-24-145	vein-4	0.000	0.010	0.004	0.000	0.036	0.016	0.000	0.008	0.003	0.000
U16-h07-24-145	vein-4	0.000	0.000	1.000	0.000	0.000	1.000	0.000	0.000	0.001	0.000
U16-h07-24-145	vein-4	0.051	0.098	0.532	0.010	-0.965	4.559	0.046	-0.174	0.432	0.005
U16-h07-24-145	vein-4	0.000	0.022	0.008	0.000	0.113	0.038	0.000	0.018	0.008	0.000
U16-h07-24-145	vein-4	0.053	0.014	0.836	0.011	-5.731	10.085	0.050	-0.214	0.589	0.005
U16-h07-24-145	vein-4	0.000	0.039	0.014	0.000	0.240	0.063	0.000	0.020	0.009	0.000

Sample ID	SampleType	Er LOD (ppm)	Tm(ppm)	2SE (ppm)	Tm LOD (ppm)	Yb (ppm)	2SE (ppm)	Yb LOD (ppm)	Lu (ppm)	2SE (ppm)	Lu LOD (ppm)
U16-h07-24-145	vein-4	0.000	0.030	0.021	0.000	0.235	0.127	0.000	0.035	0.020	0.000
U16-h07-24-145	vein-4	0.049	0.008	0.009	0.010	0.011	0.058	0.045	0.000	0.009	0.005
U16-h07-24-145	vein-4	0.000	0.040	0.029	0.000	0.408	0.178	0.000	0.025	0.022	0.000
U16-h07-24-145	vein-4	0.000	0.085	0.087	0.000	1.023	0.466	0.000	0.051	0.061	0.000
U16-h07-24-145	vein-4	0.025	-0.004	0.006	0.003	0.015	0.019	0.014	0.001	0.003	0.002
U16-h07-24-145	vein-4	0.023	0.003	0.001	0.003	-0.008	0.020	0.013	-0.002	0.003	0.002
U16-h07-24-145	vein-4	0.052	-0.063	0.085	0.010	-0.296	0.285	0.048	-0.018	0.046	0.005
U16-h07-24-145	vein-4	0.048	0.001	0.110	0.010	-0.239	0.698	0.044	-0.027	0.068	0.005
U16-h07-24-145	vein-6	0.000	0.000	1.000	0.000	0.000	1.000	0.000	0.000	1.000	0.000
U16-h07-24-145	vein-6	0.000	0.008	0.004	0.000	0.026	0.015	0.000	0.006	0.003	0.000
U16-h07-24-145	vein-6	0.000	0.010	0.003	0.000	0.036	0.014	0.000	0.006	0.003	0.000
U16-h07-24-145	vein-6	0.000	0.006	0.003	0.000	0.050	0.019	0.000	0.009	0.004	0.000
U16-h07-24-145	vein-6	0.000	0.007	0.003	0.000	0.053	0.022	0.000	0.004	0.002	0.000
U16-h07-24-145	vein-7	0.000	0.009	0.003	0.000	0.042	0.018	0.000	0.003	0.002	0.000
U16-h07-25-167	coarse calcite	0.069	-0.007	0.001	0.011	-0.027	0.014	0.066	-0.004	0.001	0.008
U16-h07-25-167	coarse calcite	0.070	0.013	0.007	0.012	0.051	0.037	0.067	0.008	0.005	0.009
U16-h07-25-167	coarse calcite	0.073	0.034	0.011	0.012	0.177	0.048	0.070	0.023	0.008	0.009
U16-h07-25-167	coarse calcite	0.073	-0.001	0.002	0.012	-0.015	0.012	0.070	-0.003	0.001	0.009
U16-h07-25-167	dk ooid	0.069	0.004	0.004	0.012	0.032	0.024	0.066	0.002	0.003	0.008
U16-h07-25-167	dk ooid	0.015	0.011	0.006	0.000	0.070	0.026	0.000	0.011	0.005	0.000
U16-h07-25-167	dk ooid	0.016	0.012	0.006	0.000	0.071	0.032	0.000	0.008	0.004	0.000
U16-h07-25-167	dk ooid	0.000	0.003	0.004	0.000	0.054	0.024	0.000	0.007	0.004	0.000
U16-h07-25-167	dk ooid	0.034	0.010	0.005	0.029	0.095	0.033	0.017	0.008	0.004	0.026
U16-h07-25-167	dk ooid	0.000	0.019	0.007	0.000	0.171	0.045	0.000	0.016	0.006	0.000
U16-h07-25-167	dk ooid	0.000	0.001	0.004	0.000	0.038	0.022	0.000	0.006	0.004	0.000
U16-h07-25-167	dk ooid	0.015	0.005	0.004	0.000	0.018	0.020	0.000	0.001	0.003	0.000
U16-h07-25-167	dk ooid	0.000	0.005	0.004	0.000	0.057	0.021	0.000	0.011	0.005	0.000
U16-h07-25-167	dk ooid	0.033	0.003	0.003	0.027	0.062	0.025	0.016	0.007	0.005	0.025
U16-h07-25-167	dk ooid	0.033	0.006	0.003	0.028	0.103	0.028	0.017	0.011	0.005	0.025
U16-h07-25-167	dk ooid	0.000	0.003	0.003	0.000	0.046	0.020	0.000	0.005	0.004	0.000
U16-h07-25-167	dk ooid	0.000	0.000	0.003	0.000	0.006	0.017	0.000	0.003	0.004	0.000
U16-h07-25-167	dk ooid	0.000	0.005	0.004	0.000	0.027	0.020	0.000	0.002	0.003	0.000
U16-h07-25-167	dk ooid	0.033	0.011	0.004	0.028	0.058	0.024	0.017	0.007	0.003	0.025

Sample ID	SampleType	Er LOD (ppm)	Tm(ppm)	2SE (ppm)	Tm LOD (ppm)	Yb (ppm)	2SE (ppm)	Yb LOD (ppm)	Lu (ppm)	2SE (ppm)	Lu LOD (ppm)
U16-h07-25-167	dk ooid	0.000	0.005	0.004	0.000	0.048	0.024	0.000	0.006	0.004	0.000
U16-h07-25-167	dk ooid	0.033	0.007	0.004	0.028	0.049	0.021	0.017	0.008	0.004	0.025
U16-h07-25-167	dk ooid	0.034	0.003	0.004	0.028	0.045	0.022	0.017	0.006	0.004	0.026
U16-h07-25-167	dk ooid	0.000	0.006	0.005	0.000	0.061	0.027	0.000	0.012	0.005	0.000
U16-h07-25-167	dk ooid	0.034	0.011	0.005	0.028	0.064	0.025	0.017	0.003	0.003	0.026
U16-h07-25-167	dk ooid	0.000	0.007	0.004	0.000	0.072	0.024	0.000	0.003	0.003	0.000
U16-h07-25-167	dk ooid	0.000	0.011	0.005	0.000	0.072	0.023	0.000	0.009	0.004	0.000
U16-h07-25-167	early vein	0.000	0.006	0.002	0.000	0.048	0.008	0.000	0.002	0.001	0.011
U16-h07-25-167	early vein	0.000	0.009	0.003	0.000	0.069	0.015	0.000	0.005	0.002	0.011
U16-h07-25-167	early vein	0.000	0.009	0.003	0.000	0.071	0.015	0.000	0.005	0.002	0.011
U16-h07-25-167	early vein	0.000	0.004	0.002	0.000	0.061	0.010	0.000	0.003	0.001	0.011
U16-h07-25-167	late vein	0.000	0.029	0.007	0.000	0.213	0.028	0.000	0.026	0.006	0.012
U16-h07-25-167	late vein	0.000	0.027	0.006	0.000	0.188	0.034	0.000	0.018	0.005	0.011
U16-h07-25-167	late vein	0.000	0.042	0.007	0.000	0.228	0.034	0.000	0.027	0.005	0.011
U16-h07-25-167	late vein	0.000	0.030	0.006	0.000	0.175	0.027	0.000	0.023	0.005	0.011
U16-h07-25-167	late vein	0.000	0.033	0.006	0.000	0.182	0.027	0.000	0.023	0.004	0.011
U16-h07-25-167	lt ooid	0.000	0.012	0.005	0.000	0.084	0.027	0.000	0.009	0.004	0.011
U16-h07-25-167	lt ooid	0.000	0.006	0.004	0.000	0.085	0.024	0.000	0.012	0.005	0.010
U16-h07-25-167	lt ooid	0.000	0.008	0.004	0.000	0.080	0.022	0.000	0.006	0.003	0.010
U16-h07-25-167	lt ooid	0.034	0.012	0.005	0.029	0.116	0.029	0.017	0.015	0.006	0.026
U16-h07-25-167	lt ooid	0.033	0.004	0.003	0.028	0.091	0.031	0.017	0.010	0.004	0.025
U16-h07-25-167	lt ooid	0.000	0.009	0.005	0.000	0.079	0.022	0.000	0.005	0.003	0.010
U16-h07-25-167	lt ooid	0.000	0.006	0.003	0.000	0.094	0.027	0.000	0.006	0.003	0.010
U16-h07-25-167	lt ooid	0.034	0.009	0.006	0.029	0.097	0.031	0.017	0.007	0.005	0.026
U16-h07-25-167	lt ooid	0.000	0.014	0.005	0.000	0.085	0.022	0.000	0.010	0.004	0.010
U16-h07-25-167	lt ooid	0.000	0.014	0.005	0.000	0.080	0.025	0.000	0.011	0.005	0.010
U16-h07-25-167	matrix cement	0.000	0.001	0.000	0.000	0.030	0.001	0.000	-0.001	0.000	0.011
U16-h07-25-167	matrix cement	0.000	0.008	0.003	0.000	0.114	0.024	0.000	0.008	0.004	0.011
U16-h07-25-167	matrix cement	0.000	0.026	0.006	0.000	0.184	0.035	0.000	0.025	0.006	0.011
U16-h07-25-167	matrix cement	0.000	0.011	0.004	0.000	0.109	0.023	0.000	0.012	0.004	0.010
U16-h07-25-167	matrix cement	0.000	0.009	0.004	0.000	0.066	0.015	0.000	0.007	0.003	0.011
U16-h07-25-167	matrix cement	0.000	0.010	0.003	0.000	0.070	0.015	0.000	0.005	0.003	0.011
U16-h07-25-167	matrix cement	0.000	0.008	0.004	0.000	0.093	0.023	0.000	0.009	0.003	0.011

Sample ID	SampleType	Er LOD (ppm)	Tm(ppm)	2SE (ppm)	Tm LOD (ppm)	Yb (ppm)	2SE (ppm)	Yb LOD (ppm)	Lu (ppm)	2SE (ppm)	Lu LOD (ppm)
U16-h07-25-167	matrix cement	0.000	0.010	0.004	0.000	0.122	0.024	0.000	0.012	0.004	0.011
U16-h07-25-167	matrix cement	0.000	0.010	0.004	0.000	0.095	0.022	0.000	0.009	0.004	0.011
U16-h07-25-167	matrix cement	0.000	0.015	0.004	0.000	0.137	0.026	0.000	0.015	0.005	0.010
U16-h07-25-167	matrix cement	0.000	0.004	0.001	0.000	0.059	0.010	0.000	0.006	0.003	0.011
U16-h07-34-405	matrix cement	0.020	-0.163	0.339	0.006	-0.174	1.233	0.012	-0.166	0.330	0.004
U16-h07-34-405	matrix cement	0.021	0.014	0.038	0.006	0.085	0.194	0.029	0.013	0.014	0.003
U16-h07-34-405	matrix cement	0.019	0.032	0.104	0.006	0.001	0.008	0.012	-0.106	0.147	0.004
U16-h07-34-405	matrix cement	0.029	-0.013	0.015	0.005	-0.226	0.119	0.029	-0.012	0.011	0.004
U16-h07-34-405	matrix cement	0.032	0.019	0.005	0.006	-0.070	0.124	0.032	-0.002	0.010	0.004
U16-h07-34-405	matrix cement	0.018	0.003	0.111	0.006	-0.496	0.609	0.011	-0.185	0.104	0.004
U16-h07-34-405	matrix cement	0.018	-0.185	0.225	0.006	-0.524	1.235	0.011	-0.207	0.141	0.004
U16-h07-34-405	matrix cement	0.032	0.005	0.014	0.006	0.071	0.053	0.032	0.006	0.005	0.004
U16-h07-34-405	matrix cement	0.021	-0.002	0.032	0.006	-0.015	0.377	0.030	-0.001	0.002	0.003
U16-h07-34-405	matrix cement	0.032	-0.031	0.026	0.006	-0.103	0.097	0.032	-0.049	0.026	0.004
U16-h07-34-405	matrix cement	0.019	0.001	0.025	0.006	0.008	0.113	0.012	-0.005	0.018	0.004
U16-h07-34-405	matrix cement	0.018	0.073	0.224	0.006	-0.658	1.014	0.011	-0.043	0.062	0.004
U16-h07-34-405	matrix cement	0.018	-0.020	0.055	0.006	-0.304	0.289	0.011	-0.091	0.079	0.004
U16-h07-34-405	matrix cement	0.019	0.061	0.090	0.006	0.177	0.368	0.012	0.040	0.069	0.004
U16-h07-34-405	matrix cement	0.019	0.014	0.060	0.006	-0.017	0.166	0.012	0.002	0.033	0.004
U16-h07-34-405	matrix cement	0.019	-0.027	0.068	0.006	-0.116	0.197	0.012	-0.025	0.039	0.004
U16-h07-34-405	matrix cement	0.019	0.020	0.082	0.006	0.075	0.693	0.012	-0.008	0.030	0.004
U16-h07-34-405	ooid	0.020	0.012	0.012	0.004	0.061	0.047	0.014	0.004	0.009	0.003
U16-h07-34-405	ooid	0.037	0.170	0.097	0.006	0.514	0.351	0.029	-0.004	0.055	0.006
U16-h07-34-405	ooid	0.019	-0.222	0.255	0.005	-1.008	0.847	0.027	-0.401	0.354	0.003
U16-h07-34-405	ooid	0.039	-0.055	0.041	0.006	-0.492	0.297	0.044	-0.096	0.061	0.007
U16-h07-34-405	ooid	0.026	-0.024	0.022	0.005	-0.046	0.131	0.035	0.005	0.016	0.005
U16-h07-34-405	ooid	0.024	-0.062	0.027	0.005	-0.193	0.139	0.033	-0.031	0.026	0.004
U16-h07-34-405	ooid	0.053	-0.049	0.043	0.011	-0.396	0.342	0.067	-0.143	0.061	0.011
U16-h07-34-405	ooid	0.037	-0.040	0.027	0.006	0.035	0.110	0.042	-0.002	0.016	0.007
U16-h07-34-405	ooid	0.032	0.051	0.014	0.006	0.235	0.069	0.039	0.040	0.009	0.007
U16-h07-34-405	ooid	0.030	-0.065	0.036	0.006	-0.529	0.227	0.037	-0.088	0.047	0.007
U16-h07-34-405	ooid	0.040	-0.011	0.039	0.006	-0.048	0.220	0.045	-0.006	0.031	0.007
U16-h07-34-405	ooid	0.024	-0.004	0.011	0.004	-0.091	0.089	0.032	-0.030	0.019	0.004

Sample ID	SampleType	Er LOD (ppm)	Tm(ppm)	2SE (ppm)	Tm LOD (ppm)	Yb (ppm)	2SE (ppm)	Yb LOD (ppm)	Lu (ppm)	2SE (ppm)	Lu LOD (ppm)
U16-h07-34-405	ooid	0.039	-0.037	0.032	0.006	-0.318	0.197	0.044	-0.037	0.028	0.007
U16-h07-34-405	ooid	0.026	-0.030	0.019	0.005	-0.140	0.167	0.035	-0.028	0.017	0.005
U16-h07-34-405	ooid	0.032	0.002	0.028	0.008	0.152	0.137	0.039	0.023	0.015	0.008
U16-h07-34-405	ooid	0.032	-0.044	0.039	0.008	-0.200	0.218	0.040	-0.029	0.035	0.008
U16-h07-34-405	ooid	0.026	-0.019	0.016	0.005	0.036	0.053	0.035	-0.004	0.012	0.005
U16-h07-34-405	ooid	0.035	-0.035	0.034	0.006	-0.430	0.209	0.027	-0.076	0.043	0.006
U16-h07-34-405	ooid	0.024	-0.020	0.016	0.004	-0.218	0.092	0.033	-0.025	0.016	0.004
U16-h07-34-405	ooid	0.053	-0.065	0.049	0.011	-0.490	0.220	0.067	-0.072	0.037	0.011
U16-h07-34-405	ooid	0.021	0.015	0.129	0.006	0.379	0.989	0.030	-0.012	0.149	0.003
U16-h07-34-405	ooid and clast	0.000	0.184	0.040	0.000	1.211	0.260	0.000	0.127	0.030	0.000
U16-h07-34-405	ooid and clast	0.033	0.010	0.004	0.004	0.067	0.031	0.043	0.005	0.003	0.003
U16-h07-34-405	ooid and clast	0.000	0.001	0.001	0.000	0.018	0.011	0.000	0.001	0.001	0.000
U16-h07-34-405	ooid and clast	0.000	0.008	0.004	0.000	0.034	0.018	0.000	0.003	0.002	0.000
U16-h07-34-405	ooid and clast	0.000	0.042	0.009	0.000	0.242	0.055	0.000	0.041	0.010	0.000
U16-h07-34-405	ooid and clast	0.000	0.070	0.011	0.000	0.469	0.061	0.000	0.071	0.009	0.000
U16-h07-34-405	ooid and clast	0.032	0.106	0.024	0.004	0.682	0.122	0.042	0.082	0.013	0.003
U16-h07-34-405	ooid and clast	0.000	0.044	0.008	0.000	0.352	0.056	0.000	0.050	0.009	0.000
U16-h07-34-405	ooid and clast	0.000	0.044	0.008	0.000	0.301	0.055	0.000	0.063	0.009	0.000
U16-h07-34-405	ooid and clast	0.000	0.050	0.007	0.000	0.391	0.069	0.000	0.037	0.007	0.000
U16-h07-34-405	ooid and clast	0.000	0.064	0.012	0.000	0.495	0.066	0.000	0.061	0.009	0.000
U16-h07-34-405	ooid and clast	0.000	0.010	0.006	0.003	0.111	0.033	0.000	0.006	0.004	0.000
U16-h07-34-405	ooid and clast	0.000	0.111	0.023	0.003	0.814	0.140	0.000	0.107	0.025	0.000
U16-h07-34-405	ooid and clast	0.015	0.108	0.022	0.002	0.723	0.111	0.011	0.088	0.017	0.000
U16-h07-34-405	ooid and clast	0.000	0.118	0.019	0.003	0.871	0.103	0.000	0.152	0.032	0.003
U16-h07-34-405	ooid and clast	0.000	0.230	0.046	0.003	1.524	0.340	0.000	0.126	0.038	0.000
U16-h07-34-405	ooid and clast	0.000	0.242	0.732	0.003	3.307	8.189	0.000	0.625	1.398	0.000
U16-h07-34-405	ooid and clast	0.015	0.003	0.929	0.003	0.987	3.079	0.012	0.083	0.576	0.000
U16-h07-34-405	ooid and clast	0.000	-0.488	0.632	0.000	-4.578	3.812	0.000	-0.311	0.563	0.000
U16-h07-34-405	ooid and clast	0.044	0.005	0.000	0.010	0.020	0.004	0.052	0.003	0.000	0.009
U16-h07-34-405	ooid and clast	0.015	-0.086	0.025	0.003	-0.710	0.170	0.011	-0.118	0.028	0.000
U16-h07-34-405	ooid and clast	0.000	-0.211	0.037	0.003	-0.948	0.142	0.000	-0.118	0.024	0.000
U16-h07-34-405	ooid and clast	0.000	-0.279	0.066	0.003	-1.537	0.241	0.000	-0.222	0.045	0.000
U16-h07-34-405	ooid and clast	0.000	-0.068	0.014	0.007	-0.513	0.089	0.000	-0.070	0.012	0.000

Sample ID	SampleType	Er LOD (ppm)	Tm(ppm)	2SE (ppm)	Tm LOD (ppm)	Yb (ppm)	2SE (ppm)	Yb LOD (ppm)	Lu (ppm)	2SE (ppm)	Lu LOD (ppm)
U16-h07-34-405	ooid and clast	0.000	-0.062	0.013	0.003	-0.437	0.072	0.000	-0.056	0.013	0.000
U16-h07-34-405	ooid and clast	0.000	-0.044	0.014	0.003	-0.406	0.092	0.000	-0.066	0.015	0.000
U16-h07-34-405	ooid and clast	0.099	-0.064	0.026	0.022	-0.422	0.194	0.142	-0.026	0.031	0.022
U16-h07-34-405	ooid and clast	0.000	-0.045	0.011	0.000	-0.446	0.068	0.019	-0.056	0.010	0.000
U16-h07-34-405	ooid and clast	0.018	-0.034	0.007	0.000	-0.294	0.057	0.041	-0.048	0.013	0.012
U16-h07-34-405	ooid and clast	0.100	-0.037	0.015	0.023	-0.330	0.083	0.144	-0.056	0.018	0.022
U16-h07-34-405	ooid and clast	0.016	-0.028	0.006	0.000	-0.187	0.031	0.037	-0.034	0.006	0.010
U16-h07-34-405	ooid and clast	0.016	-0.022	0.005	0.000	-0.157	0.023	0.036	-0.020	0.003	0.010
U16-h07-34-405	ooid and clast	0.041	-0.022	0.005	0.009	-0.227	0.035	0.048	-0.027	0.004	0.008
U16-h07-34-405	ooid and clast	0.000	-0.020	0.006	0.000	-0.065	0.028	0.020	-0.007	0.004	0.000
U16-h07-34-405	vein 1	0.053	0.046	0.007	0.009	0.211	0.045	0.052	0.033	0.005	0.010
U16-h07-34-405	vein 1	0.056	0.039	0.026	0.009	0.277	0.101	0.054	0.050	0.008	0.010
U16-h07-34-405	vein 1	0.058	0.132	0.074	0.009	0.562	0.370	0.056	0.086	0.052	0.011
U16-h07-34-405	vein 1	0.053	0.065	0.017	0.009	0.280	0.095	0.051	0.041	0.016	0.010
U16-h07-34-405	vein 1	0.055	0.067	0.012	0.009	0.339	0.070	0.053	0.046	0.008	0.010
U16-h07-34-405	vein 2	0.061	-0.028	0.018	0.010	-0.168	0.078	0.060	-0.027	0.017	0.011
U16-h07-34-405	vein 2	0.056	-0.039	0.013	0.009	-0.273	0.062	0.055	-0.059	0.016	0.010
U16-h07-34-405	vein 2	0.059	-0.027	0.011	0.010	-0.253	0.070	0.058	-0.027	0.012	0.011
U16-h07-34-405	vein 2	0.061	-0.104	0.045	0.010	-0.464	0.188	0.059	-0.113	0.046	0.011
U16-h07-34-405	vein 2	0.058	-0.081	0.023	0.009	-0.463	0.138	0.057	-0.057	0.023	0.011
U16-h07-34-405	vein 2	0.060	-0.095	0.048	0.010	-0.602	0.264	0.059	-0.091	0.042	0.011
U16-h07-54-338	coarse calcite	0.000	0.005	0.004	0.000	0.067	0.025	0.000	0.006	0.003	0.000
U16-h07-54-338	coarse calcite	0.045	0.001	0.002	0.006	0.027	0.017	0.048	0.000	0.001	0.003
U16-h07-54-338	coarse calcite	0.000	0.002	0.002	0.000	-0.001	0.003	0.000	0.000	0.001	0.000
U16-h07-54-338	coarse calcite	0.000	0.013	0.005	0.003	0.058	0.022	0.000	0.003	0.003	0.003
U16-h07-54-338	coarse calcite	0.043	0.061	0.020	0.006	0.481	0.151	0.046	0.070	0.022	0.003
U16-h07-54-338	coarse calcite	0.000	0.002	0.002	0.000	0.037	0.018	0.000	-0.002	0.000	0.000
U16-h07-54-338	coarse calcite	0.045	0.006	0.004	0.006	0.018	0.012	0.048	0.000	0.001	0.003
U16-h07-54-338	coarse calcite	0.000	0.014	0.005	0.000	0.121	0.030	0.000	0.011	0.005	0.000
U16-h07-54-338	coarse calcite	0.061	0.047	0.017	0.024	0.290	0.110	0.019	0.044	0.016	0.016
U16-h07-54-338	coarse calcite	0.041	0.087	0.019	0.005	0.581	0.119	0.044	0.091	0.024	0.003
U16-h07-54-338	coarse calcite	0.042	0.056	0.016	0.006	0.391	0.086	0.045	0.048	0.011	0.003
U16-h07-54-338	coarse calcite	0.022	0.022	0.007	0.004	0.178	0.047	0.000	0.035	0.011	0.000

Sample ID	SampleType	Er LOD (ppm)	Tm(ppm)	2SE (ppm)	Tm LOD (ppm)	Yb (ppm)	2SE (ppm)	Yb LOD (ppm)	Lu (ppm)	2SE (ppm)	Lu LOD (ppm)
U16-h07-54-338	coarse calcite	0.036	0.010	0.005	0.006	0.071	0.029	0.000	0.005	0.003	0.000
U16-h07-54-338	coarse calcite	0.060	0.055	0.022	0.024	0.284	0.124	0.018	0.053	0.019	0.015
U16-h07-54-338	coarse calcite	0.000	0.004	0.003	0.000	0.036	0.017	0.016	0.003	0.003	0.000
U16-h07-54-5	matrix cement	0.008	0.008	0.004	0.000	0.080	0.031	0.000	0.008	0.004	0.005
U16-h07-54-5	matrix cement	0.008	0.022	0.007	0.000	0.116	0.038	0.000	0.018	0.006	0.005
U16-h07-54-5	matrix cement	0.009	0.037	0.009	0.000	0.269	0.061	0.000	0.024	0.008	0.005
U16-h07-54-5	matrix cement	0.008	0.042	0.010	0.000	0.214	0.046	0.000	0.033	0.008	0.005
U16-h07-54-5	matrix cement	0.000	0.046	0.009	0.000	0.315	0.046	0.000	0.039	0.009	0.000
U16-h07-54-5	matrix cement	0.000	0.043	0.008	0.000	0.248	0.059	0.000	0.038	0.006	0.000
U16-h07-54-5	matrix cement	0.008	0.039	0.007	0.000	0.225	0.056	0.000	0.032	0.007	0.005
U16-h07-54-5	matrix cement	0.008	0.047	0.010	0.000	0.336	0.036	0.000	0.037	0.008	0.005
U16-h07-54-5	matrix cement	0.000	0.027	0.007	0.000	0.160	0.035	0.000	0.018	0.006	0.000
U16-h07-54-5	matrix cement	0.009	0.032	0.008	0.000	0.184	0.041	0.000	0.028	0.008	0.005
U16-h07-54-5	matrix cement	0.000	0.044	0.008	0.000	0.321	0.066	0.000	0.036	0.009	0.000
U16-h07-54-5	matrix cement	0.008	0.018	0.007	0.000	0.188	0.040	0.000	0.022	0.007	0.005
U16-h07-54-5	matrix cement	0.008	0.039	0.010	0.000	0.211	0.051	0.000	0.037	0.008	0.005
U16-h07-54-5	matrix cement	0.008	0.034	0.008	0.000	0.195	0.042	0.000	0.026	0.006	0.005
U16-h07-54-5	matrix cement	0.000	0.007	0.004	0.000	0.099	0.035	0.000	0.015	0.004	0.000
U16-h07-54-5	matrix cement	0.008	0.037	0.010	0.000	0.214	0.047	0.000	0.039	0.010	0.005
U16-h07-54-5	matrix cement	0.008	0.017	0.008	0.000	0.156	0.041	0.000	0.020	0.007	0.005
U16-h07-54-5	ooid	0.000	0.056	0.013	0.000	0.272	0.074	0.000	0.038	0.010	0.000
U16-h07-54-5	ooid	0.000	0.047	0.009	0.000	0.339	0.047	0.000	0.038	0.009	0.000
U16-h07-54-5	ooid	0.000	0.010	0.004	0.000	0.064	0.022	0.000	0.009	0.004	0.000
U16-h07-54-5	ooid	0.000	0.054	0.010	0.000	0.308	0.064	0.000	0.044	0.009	0.000
U16-h07-54-5	ooid	0.000	0.045	0.009	0.000	0.281	0.064	0.000	0.043	0.009	0.000
U16-h07-54-5	ooid	0.000	0.019	0.007	0.000	0.064	0.030	0.000	0.011	0.004	0.000
U16-h07-54-5	ooid	0.000	0.073	0.013	0.000	0.380	0.063	0.000	0.050	0.010	0.000
U16-h07-54-5	ooid	0.000	0.088	0.017	0.000	0.500	0.069	0.000	0.075	0.014	0.000
U16-h07-54-5	ooid	0.000	0.035	0.009	0.000	0.260	0.041	0.000	0.035	0.009	0.000
U16-h07-54-5	ooid	0.000	0.028	0.009	0.000	0.247	0.048	0.000	0.035	0.007	0.000
U16-h07-54-5	ooid	0.000	0.056	0.011	0.000	0.282	0.048	0.000	0.048	0.009	0.000
U16-h07-54-5	ooid	0.000	0.049	0.012	0.000	0.284	0.046	0.000	0.046	0.009	0.000
U16-h07-54-5	ooid	0.000	0.020	0.007	0.000	0.095	0.026	0.000	0.016	0.006	0.000

Sample ID	SampleType	Er LOD (ppm)	Tm(ppm)	2SE (ppm)	Tm LOD (ppm)	Yb (ppm)	2SE (ppm)	Yb LOD (ppm)	Lu (ppm)	2SE (ppm)	Lu LOD (ppm)
U16-h07-54-5	ooid	0.000	0.032	0.008	0.000	0.195	0.043	0.000	0.037	0.007	0.000
U16-h07-54-5	ooid	0.000	0.021	0.007	0.000	0.126	0.041	0.000	0.012	0.005	0.000
U16-h07-54-5	ooid	0.000	0.029	0.008	0.000	0.162	0.034	0.000	0.017	0.006	0.000
U16-h07-54-5	ooid	0.000	0.052	0.009	0.000	0.373	0.058	0.000	0.054	0.010	0.000
U16-h07-54-5	ooid	0.000	0.063	0.012	0.000	0.462	0.079	0.000	0.070	0.013	0.000
U16-h07-54-5	ooid	0.000	0.026	0.007	0.000	0.281	0.045	0.000	0.030	0.006	0.000
U16-h07-54-5	ooid	0.000	0.044	0.010	0.000	0.278	0.058	0.000	0.041	0.007	0.000
U16-h07-54-5	ooid	0.000	0.026	0.008	0.000	0.216	0.045	0.000	0.025	0.007	0.000
U16-h07-54-5	ooid	0.000	0.045	0.014	0.000	0.297	0.080	0.000	0.042	0.014	0.000
U16-h07-54-5	ooid	0.000	0.046	0.012	0.000	0.303	0.055	0.000	0.036	0.010	0.000
U16-h07-54-5	ooid	0.000	0.043	0.009	0.000	0.350	0.061	0.000	0.042	0.011	0.000
U16-h07-54-5	ooid	0.000	0.012	0.005	0.000	0.075	0.021	0.000	0.013	0.004	0.000
U16-h07-54-5	vein 1	0.000	0.033	0.008	0.004	0.185	0.048	0.000	0.023	0.006	0.000
U16-h07-54-5	vein 1	0.000	0.193	0.027	0.000	1.070	0.137	0.000	0.111	0.018	0.000
U16-h07-54-5	vein 1	0.025	0.023	0.008	0.000	0.184	0.039	0.000	0.024	0.007	0.000
U16-h07-54-5	vein 1	0.024	0.023	0.005	0.000	0.107	0.031	0.000	0.023	0.007	0.000
U16-h07-54-5	vein 1	0.026	0.029	0.008	0.000	0.184	0.042	0.000	0.025	0.007	0.000
U16-h07-54-5	vein 1	0.025	0.064	0.013	0.000	0.366	0.067	0.000	0.055	0.012	0.000
U16-h07-54-5	vein 2	0.000	0.013	0.005	0.004	0.064	0.026	0.000	0.015	0.006	0.000
U16-h07-54-5	vein 2	0.000	0.132	0.018	0.004	0.648	0.097	0.000	0.071	0.011	0.000
U16-h07-54-5	vein 2	0.000	0.010	0.004	0.004	0.027	0.015	0.000	0.002	0.003	0.000
U16-h07-67-129	darker vein	0.000	0.007	0.004	0.000	0.074	0.029	0.000	0.015	0.006	0.000
U16-h07-67-129	darker vein	0.000	0.005	0.003	0.000	0.032	0.016	0.000	0.009	0.003	0.009
U16-h07-67-129	darker vein	0.000	0.006	0.003	0.000	0.052	0.018	0.000	0.007	0.003	0.000
U16-h07-67-129	darker vein	0.000	0.006	0.003	0.000	0.021	0.014	0.000	0.001	0.002	0.009
U16-h07-67-129	darker vein	0.000	0.007	0.004	0.000	0.034	0.017	0.000	0.004	0.003	0.000
U16-h07-67-129	darker vein	0.000	0.006	0.003	0.000	0.036	0.017	0.000	0.005	0.003	0.000
U16-h07-67-129	darker vein	0.000	0.021	0.006	0.000	0.119	0.035	0.000	0.016	0.005	0.000
U16-h07-67-129	lighter vein	0.000	0.033	0.014	0.000	0.112	0.044	0.045	0.021	0.008	0.000
U16-h07-67-129	lighter vein	0.000	0.114	0.016	0.000	0.637	0.063	0.000	0.080	0.013	0.009
U16-h07-67-129	lighter vein	0.000	0.040	0.009	0.000	0.224	0.052	0.000	0.024	0.008	0.000
U16-h07-67-129	lighter vein	0.000	0.140	0.015	0.000	0.734	0.107	0.044	0.107	0.011	0.000
U16-h07-67-129	lighter vein	0.000	0.041	0.008	0.000	0.223	0.040	0.043	0.029	0.008	0.000

Sample ID	SampleType	Er LOD (ppm)	Tm(ppm)	2SE (ppm)	Tm LOD (ppm)	Yb (ppm)	2SE (ppm)	Yb LOD (ppm)	Lu (ppm)	2SE (ppm)	Lu LOD (ppm)
U16-h07-67-129	lighter vein	0.000	0.093	0.012	0.000	0.490	0.074	0.046	0.058	0.011	0.000
U16-h07-67-129	lighter vein	0.000	0.059	0.015	0.000	0.326	0.084	0.000	0.048	0.011	0.009
U16-h07-67-129	ooid and matrix	0.000	0.974	0.160	0.000	5.777	0.983	0.000	0.716	0.128	0.000
U16-h07-67-129	ooid and matrix	0.000	0.183	0.021	0.000	1.014	0.115	0.040	0.163	0.016	0.000
U16-h07-67-129	ooid and matrix	0.034	0.204	0.025	0.018	1.266	0.154	0.000	0.187	0.026	0.009
U16-h07-67-129	ooid and matrix	0.000	0.121	0.015	0.000	0.834	0.081	0.033	0.114	0.021	0.000
U16-h07-67-129	ooid and matrix	0.000	0.159	0.033	0.000	0.939	0.185	0.000	0.148	0.036	0.000
U16-h07-67-129	ooid and matrix	0.000	0.106	0.014	0.000	0.641	0.075	0.000	0.098	0.015	0.000
U16-h07-67-129	ooid and matrix	0.000	0.046	0.010	0.000	0.436	0.081	0.000	0.062	0.010	0.000
U16-h07-67-129	ooid and matrix	0.259	0.087	0.009	0.046	0.509	0.069	0.173	0.089	0.014	0.053
U16-h07-67-129	ooid and matrix	0.019	0.172	0.021	0.000	1.028	0.120	0.000	0.151	0.015	0.006
U16-h07-67-129	ooid and matrix	0.000	0.182	0.016	0.000	1.002	0.105	0.000	0.178	0.020	0.000
U16-h07-67-129	ooid and matrix	0.000	0.077	0.019	0.000	0.649	0.116	0.043	0.073	0.018	0.000
U16-h07-67-129	ooid and matrix	0.000	0.021	0.007	0.009	0.163	0.037	0.021	0.013	0.005	0.000
U16-h07-67-129	ooid and matrix	0.014	0.071	0.010	0.000	0.418	0.075	0.000	0.059	0.012	0.000
U16-h07-67-129	ooid and matrix	0.000	0.007	0.005	0.000	0.083	0.032	0.000	0.007	0.005	0.000
U16-h07-67-129	ooid and matrix	0.000	0.064	0.009	0.000	0.550	0.056	0.000	0.061	0.009	0.000
U16-h07-67-129	ooid and matrix	0.000	0.002	0.002	0.009	0.009	0.011	0.021	0.001	0.002	0.000
U16-h07-67-129	ooid and matrix	0.000	0.051	0.010	0.000	0.356	0.059	0.000	0.057	0.011	0.000
U16-h07-67-129	ooid and matrix	0.018	0.012	0.004	0.000	0.088	0.028	0.000	0.017	0.006	0.006
U16-h07-67-129	ooid and matrix	0.000	0.065	0.010	0.000	0.475	0.075	0.000	0.055	0.011	0.000
U16-h07-67-129	ooid and matrix	0.000	0.130	0.026	0.000	1.275	0.220	0.040	0.175	0.031	0.000
U16-h07-67-129	ooid and matrix	0.000	0.046	0.010	0.008	0.207	0.050	0.019	0.032	0.007	0.000
U16-h07-67-129	ooid and matrix	0.015	0.126	0.023	0.000	0.774	0.104	0.000	0.088	0.014	0.000
U16-h07-67-129	ooid and matrix	0.014	0.037	0.008	0.000	0.230	0.041	0.000	0.030	0.008	0.000
U16-h07-67-129	ooid and matrix	0.015	0.062	0.013	0.000	0.363	0.067	0.000	0.040	0.008	0.000
U16-h07-67-129	ooid and matrix	0.016	0.093	0.016	0.000	0.426	0.075	0.000	0.049	0.010	0.000

Sample ID	SampleType	Pb (ppm)	2SE (ppm)	Pb LOD (ppm)	Th (ppm)	2SE (ppm)	Th LOD (ppm)	U (ppm)	2SE (ppm)	U LOD (ppm)
U16-h07-13b-11	matrix	0.582	0.100	0.054	0.065	0.014	0.000	1.618	0.146	0.000
U16-h07-13b-11	matrix	0.219	0.046	0.047	0.014	0.006	0.000	0.184	0.020	0.000
U16-h07-13b-11	matrix	0.092	0.032	0.046	0.010	0.004	0.000	0.346	0.095	0.000
U16-h07-13b-11	matrix	0.866	0.134	0.045	0.073	0.010	0.000	1.033	0.095	0.000
U16-h07-13b-11	matrix	0.628	0.123	0.048	0.054	0.012	0.000	0.689	0.081	0.000
U16-h07-13b-11	matrix	0.238	0.046	0.048	0.019	0.006	0.000	0.358	0.049	0.000
U16-h07-13b-11	matrix	0.030	0.028	0.048	0.029	0.008	0.000	0.110	0.019	0.000
U16-h07-13b-11	matrix	0.536	0.073	0.047	0.124	0.016	0.000	1.521	0.166	0.000
U16-h07-13b-11	matrix	1.374	0.340	0.049	0.317	0.033	0.000	10.425	1.149	0.000
U16-h07-13b-11	matrix	0.785	0.168	0.048	0.095	0.024	0.000	2.502	0.424	0.000
U16-h07-13b-11	matrix	0.412	0.081	0.045	0.086	0.012	0.000	1.358	0.099	0.000
U16-h07-13b-11	matrix	0.292	0.049	0.045	0.079	0.014	0.000	0.863	0.105	0.000
U16-h07-13b-11	matrix	0.422	0.066	0.047	0.075	0.010	0.000	0.826	0.115	0.000
U16-h07-13b-11	matrix	2.089	1.988	0.046	0.064	0.012	0.000	2.328	1.060	0.000
U16-h07-13b-11	matrix	0.280	0.041	0.045	0.066	0.013	0.000	0.888	0.106	0.000
U16-h07-13b-11	matrix	0.494	0.081	0.047	0.133	0.023	0.000	2.207	0.553	0.000
U16-h07-13b-11	matrix	0.352	0.054	0.046	0.079	0.014	0.000	0.779	0.078	0.000
U16-h07-13b-11	matrix	0.579	0.153	0.047	0.048	0.014	0.000	1.793	0.191	0.000
U16-h07-13b-11	matrix	0.601	0.106	0.047	0.179	0.021	0.000	2.899	0.367	0.000
U16-h07-13b-11	matrix	0.024	0.020	0.048	0.039	0.009	0.000	0.548	0.066	0.000
U16-h07-13b-11	matrix	0.434	0.092	0.046	0.100	0.016	0.000	1.048	0.169	0.000
U16-h07-13b-11	vein 1	0.201	0.038	0.046	0.045	0.009	0.000	0.323	0.049	0.000
U16-h07-13b-11	vein 1	0.028	0.019	0.048	0.024	0.006	0.000	0.116	0.032	0.000
U16-h07-13b-11	vein 1	0.031	0.024	0.046	0.007	0.004	0.000	0.071	0.029	0.000
U16-h07-13b-11	vein 1	0.285	0.041	0.046	0.038	0.008	0.000	0.766	0.072	0.000
U16-h07-13b-11	vein 1	0.014	0.016	0.045	0.015	0.005	0.000	0.027	0.007	0.000
U16-h07-13b-11	vein 1	0.050	0.020	0.045	0.045	0.009	0.000	0.050	0.010	0.000
U16-h07-13b-11	vein 1	0.063	0.026	0.046	0.038	0.008	0.000	0.081	0.023	0.000
U16-h07-13b-11	vein 2	0.306	0.047	0.045	0.004	0.002	0.000	0.082	0.014	0.000
U16-h07-13b-11	vein 2	0.058	0.023	0.047	0.001	0.000	0.000	0.045	0.024	0.000
U16-h07-13b-11	vein 2	0.047	0.022	0.047	0.005	0.003	0.000	0.156	0.027	0.000
U16-h07-13b-11	vein 2	0.026	0.024	0.048	0.001	0.000	0.000	0.043	0.011	0.000
U16-h07-13b-11	vein 2	0.017	0.021	0.049	0.001	0.000	0.000	0.062	0.013	0.000

Sample ID	SampleType	Pb (ppm)	2SE (ppm)	Pb LOD (ppm)	Th (ppm)	2SE (ppm)	Th LOD (ppm)	U (ppm)	2SE (ppm)	U LOD (ppm)
U16-h07-13b-11	vein 2	0.033	0.024	0.048	0.001	0.000	0.000	-0.001	0.001	0.000
U16-h07-13b-11	vein 3	0.043	0.027	0.048	0.029	0.009	0.000	0.119	0.042	0.000
U16-h07-13b-11	vein 3	0.016	0.018	0.047	0.030	0.007	0.000	0.096	0.024	0.000
U16-h07-13b-11	vein 3	0.071	0.042	0.048	0.007	0.004	0.000	0.029	0.009	0.000
U16-h07-13b-31	dk ooid	0.433	0.062	0.142	0.035	0.010	0.009	0.737	0.063	4.244
U16-h07-13b-31	dk ooid	18.776	3.854	0.051	0.341	0.056	0.000	7.922	1.042	0.000
U16-h07-13b-31	dk ooid	5.386	1.114	0.141	0.188	0.034	0.009	5.520	1.147	4.225
U16-h07-13b-31	dk ooid	3.635	0.506	0.139	0.129	0.025	0.009	2.001	0.295	4.169
U16-h07-13b-31	dk ooid	5.278	0.701	0.041	0.177	0.026	0.000	2.724	0.263	0.000
U16-h07-13b-31	dk ooid	11.067	1.455	0.049	0.278	0.034	0.000	5.502	0.657	0.000
U16-h07-13b-31	matrix cement	1.206	0.140	0.140	0.058	0.011	0.009	0.519	0.055	4.193
U16-h07-13b-31	matrix cement	2.354	0.296	0.074	0.213	0.026	0.000	6.487	1.031	0.015
U16-h07-13b-31	matrix cement	5.890	1.296	0.139	0.675	0.125	0.009	42.835	8.738	4.159
U16-h07-13b-31	matrix cement	1.968	0.332	0.136	0.068	0.016	0.008	1.741	0.264	4.070
U16-h07-13b-31	matrix cement	6.209	0.985	0.075	0.406	0.076	0.000	10.581	2.308	0.015
U16-h07-13b-31	matrix cement	4.270	1.159	0.142	0.291	0.061	0.009	10.982	2.572	4.252
U16-h07-13b-31	matrix cement	4.206	1.465	0.137	0.146	0.024	0.008	4.307	1.114	4.100
U16-h07-13b-31	matrix cement	1.108	0.224	0.072	0.109	0.020	0.000	1.831	0.237	0.014
U16-h07-13b-31	matrix cement	2.536	0.253	0.031	0.192	0.022	0.000	7.068	0.796	0.078
U16-h07-13b-31	matrix cement	3.692	0.321	0.030	0.192	0.023	0.000	7.093	0.521	0.078
U16-h07-13b-31	matrix cement	3.904	0.490	0.073	0.112	0.016	0.000	3.688	0.349	0.015
U16-h07-13b-31	matrix cement	2.341	0.364	0.074	0.111	0.019	0.000	3.594	0.367	0.015
U16-h07-13b-31	ooid	8.306	1.318	0.041	0.464	0.059	0.000	3.831	0.319	0.015
U16-h07-13b-31	ooid	0.668	0.101	0.041	0.028	0.007	0.000	0.826	0.072	0.027
U16-h07-13b-31	ooid	6.179	1.288	0.041	1.897	0.283	0.000	6.460	0.736	0.015
U16-h07-13b-31	ooid	0.266	0.036	0.045	0.031	0.009	0.032	0.963	0.048	0.037
U16-h07-13b-31	ooid	0.145	0.031	0.049	0.020	0.006	0.000	0.744	0.048	0.000
U16-h07-13b-31	ooid	3.309	0.700	0.141	0.127	0.013	0.000	1.486	0.175	0.019
U16-h07-13b-31	ooid	2.912	0.381	0.052	0.385	0.058	0.000	7.003	1.004	0.000
U16-h07-13b-31	ooid	2.645	0.467	0.044	0.359	0.068	0.031	5.367	1.227	0.036
U16-h07-13b-31	ooid	0.637	0.069	0.026	0.092	0.013	0.000	1.779	0.171	0.010
U16-h07-13b-31	ooid	17.971	1.154	0.140	0.530	0.059	0.000	25.171	2.115	0.019
U16-h07-13b-31	ooid	5.260	0.930	0.041	0.141	0.020	0.000	2.095	0.085	0.015

Sample ID	SampleType	Pb (ppm)	2SE (ppm)	Pb LOD (ppm)	Th (ppm)	2SE (ppm)	Th LOD (ppm)	U (ppm)	2SE (ppm)	U LOD (ppm)
U16-h07-13b-31	ooid	12.131	1.644	0.041	0.262	0.054	0.000	10.476	2.080	0.027
U16-h07-13b-31	ooid	2.086	0.290	0.040	0.130	0.018	0.000	1.591	0.102	0.015
U16-h07-13b-31	ooid	5.396	1.496	0.040	0.320	0.052	0.000	3.320	0.264	0.015
U16-h07-13b-31	ooid	17.376	1.660	0.041	0.343	0.045	0.000	17.198	2.738	0.027
U16-h07-13b-31	ooid	11.638	0.924	0.140	0.243	0.033	0.000	9.177	1.128	0.019
U16-h07-13b-31	ooid	8.213	2.058	0.027	0.313	0.042	0.000	3.378	0.201	0.011
U16-h07-13b-31	ooid	13.840	1.366	0.026	0.330	0.044	0.000	17.051	2.841	0.010
U16-h07-13b-31	ooid	3.413	0.507	0.040	0.356	0.038	0.000	3.072	0.209	0.015
U16-h07-13b-31	ooid	5.102	0.723	0.039	0.334	0.032	0.000	3.428	0.236	0.014
U16-h07-13b-31	ooid	7.391	2.228	0.025	0.154	0.030	0.000	5.888	1.382	0.010
U16-h07-13b-31	ooid	5.660	0.862	0.025	0.096	0.018	0.000	3.136	0.743	0.010
U16-h07-13b-31	ooid	4.339	0.816	0.039	0.081	0.012	0.000	1.846	0.089	0.014
U16-h07-13b-31	ooid	2.585	0.341	0.044	0.164	0.023	0.031	2.441	0.189	0.036
U16-h07-13b-31	vein-1	58.873	9.772	0.031	1.495	0.321	0.000	11.263	1.087	0.000
U16-h07-13b-31	vein-1	0.124	0.160	0.049	0.008	0.005	0.000	0.083	0.041	0.000
U16-h07-13b-31	vein-1	0.035	0.016	0.028	0.005	0.004	0.000	0.023	0.007	0.000
U16-h07-13b-31	vein-1	0.049	0.018	0.025	0.001	0.002	0.000	0.446	0.046	0.007
U16-h07-13b-31	vein-1	0.009	0.014	0.027	0.002	0.002	0.000	0.375	0.054	0.000
U16-h07-13b-31	vein-1	0.076	0.018	0.026	0.007	0.003	0.000	0.150	0.022	0.000
U16-h07-13b-81	coarse calcite	0.012	0.020	0.086	0.000	1.000	0.001	-0.001	0.003	0.007
U16-h07-13b-81	coarse calcite	-0.105	0.037	0.089	-0.003	0.001	0.001	-0.007	0.013	0.007
U16-h07-13b-81	coarse calcite	-0.229	0.049	0.082	-0.011	0.001	0.001	-0.106	0.016	0.007
U16-h07-13b-81	coarse calcite	-0.597	0.148	0.306	-0.031	0.005	0.018	0.046	0.170	0.158
U16-h07-13b-81	vein 1	9.920	3.350	0.141	0.432	0.091	0.012	9.629	2.522	0.294
U16-h07-13b-81	vein 1	-0.156	0.032	0.358	-0.013	0.010	0.029	-0.798	0.072	0.733
U16-h07-13b-81	vein 1	0.359	0.125	0.109	0.055	0.017	0.009	1.447	0.425	0.226
U16-h07-13b-81	vein 1	-0.017	0.017	0.097	0.006	0.006	0.015	0.697	0.226	0.537
U16-h07-13b-81	vein 1	0.474	0.109	0.079	0.254	0.035	0.001	6.049	0.869	0.006
U16-h07-13b-81	vein 1	0.178	0.068	0.148	0.048	0.015	0.037	1.524	0.263	1.564
U16-h07-13b-81	vein 1	0.062	0.045	0.401	0.037	0.016	0.027	0.969	0.215	1.636
U16-h07-13b-81	vein 1	-0.049	0.019	0.411	0.020	0.012	0.028	2.069	0.592	1.675
U16-h07-13b-81	vein 1	-0.011	0.020	0.096	0.006	0.007	0.015	0.970	0.227	0.534
U16-h07-24-145	ooids and cement	0.064	0.033	0.034	0.000	0.001	0.000	7.288	1.507	0.000

Sample ID	SampleType	Pb (ppm)	2SE (ppm)	Pb LOD (ppm)	Th (ppm)	2SE (ppm)	Th LOD (ppm)	U (ppm)	2SE (ppm)	U LOD (ppm)
U16-h07-24-145	ooids and cement	0.585	0.057	0.061	0.050	0.010	0.000	0.707	0.061	0.000
U16-h07-24-145	ooids and cement	0.847	0.147	0.062	0.084	0.012	0.000	1.388	0.216	0.000
U16-h07-24-145	ooids and cement	0.378	0.050	0.060	0.056	0.014	0.000	0.891	0.075	0.000
U16-h07-24-145	ooids and cement	0.875	0.107	0.033	0.030	0.008	0.000	0.250	0.026	0.000
U16-h07-24-145	ooids and cement	0.214	0.051	0.065	0.000	1.000	0.000	0.008	0.004	0.000
U16-h07-24-145	ooids and cement	0.497	0.102	0.058	0.061	0.010	0.000	0.749	0.074	0.000
U16-h07-24-145	ooids and cement	0.310	0.045	0.058	0.042	0.011	0.000	0.633	0.048	0.000
U16-h07-24-145	vein-1	0.745	0.053	0.064	0.009	0.004	0.000	0.188	0.038	0.004
U16-h07-24-145	vein-1	0.668	0.099	0.059	0.004	0.003	0.000	0.245	0.029	0.003
U16-h07-24-145	vein-1	0.794	0.059	0.059	0.005	0.003	0.000	0.196	0.038	0.003
U16-h07-24-145	vein-1	0.714	0.060	0.060	-0.004	0.000	0.000	0.024	0.008	0.003
U16-h07-24-145	vein-1	0.473	0.043	0.058	0.004	0.003	0.000	0.163	0.029	0.003
U16-h07-24-145	vein-1	0.719	0.060	0.068	-0.003	0.002	0.042	0.096	0.014	0.037
U16-h07-24-145	vein-1	0.520	0.053	0.068	0.001	0.003	0.041	0.135	0.032	0.037
U16-h07-24-145	vein-1	0.340	0.054	0.064	0.019	0.009	0.039	0.377	0.046	0.035
U16-h07-24-145	vein-2	1.465	0.344	0.060	0.002	0.002	0.000	0.201	0.032	0.003
U16-h07-24-145	vein-2	5.477	1.796	0.059	0.069	0.025	0.000	0.789	0.172	0.003
U16-h07-24-145	vein-2	-3.883	0.909	0.061	-0.012	0.009	0.000	-0.165	0.063	0.004
U16-h07-24-145	vein-3	0.061	0.551	0.140	0.093	0.026	0.015	4.655	0.581	0.143
U16-h07-24-145	vein-3	-1.540	0.456	0.062	-0.016	0.009	0.000	-0.768	0.297	0.004
U16-h07-24-145	vein-3	-0.081	0.124	0.269	-0.001	0.002	0.005	-0.296	0.064	0.140
U16-h07-24-145	vein-3	-0.074	0.031	0.060	0.000	0.000	0.000	-0.093	0.015	0.004
U16-h07-24-145	vein-3	-2.704	1.291	0.267	-0.010	0.003	0.005	-0.488	0.043	0.141
U16-h07-24-145	vein-3	-0.031	0.033	0.061	-0.001	0.001	0.000	-0.292	0.045	0.004
U16-h07-24-145	vein-3	-0.024	0.031	0.063	0.000	0.000	0.000	0.039	0.005	0.004
U16-h07-24-145	vein-4	-15.788	18.997	0.145	-0.001	0.089	0.015	-0.873	2.079	0.147
U16-h07-24-145	vein-4	0.033	0.022	0.043	0.016	0.006	0.000	0.128	0.013	0.000
U16-h07-24-145	vein-4	0.031	0.021	0.042	0.010	0.004	0.000	0.280	0.033	0.000
U16-h07-24-145	vein-4	0.135	0.053	0.061	0.001	0.001	0.000	0.007	0.003	0.000
U16-h07-24-145	vein-4	3.570	4.067	0.145	-0.054	0.680	0.015	9.427	22.051	0.147
U16-h07-24-145	vein-4	0.179	0.088	0.060	0.022	0.009	0.000	0.337	0.042	0.000
U16-h07-24-145	vein-4	-3.587	12.003	0.150	-1.771	1.421	0.016	-112.519	63.158	0.152
U16-h07-24-145	vein-4	0.339	0.124	0.060	0.043	0.013	0.000	0.480	0.139	0.000

Sample ID	SampleType	Pb (ppm)	2SE (ppm)	Pb LOD (ppm)	Th (ppm)	2SE (ppm)	Th LOD (ppm)	U (ppm)	2SE (ppm)	U LOD (ppm)
U16-h07-24-145	vein-4	0.343	1.323	0.064	0.070	0.041	0.000	-0.012	0.416	0.000
U16-h07-24-145	vein-4	-2.818	1.420	0.140	-0.009	0.018	0.015	0.722	0.161	0.142
U16-h07-24-145	vein-4	0.822	1.063	0.063	0.075	0.036	0.000	-0.656	0.076	0.000
U16-h07-24-145	vein-4	4.829	2.957	0.064	0.365	0.142	0.000	-0.788	0.888	0.000
U16-h07-24-145	vein-4	-1.246	0.293	0.274	0.004	0.005	0.005	0.495	0.094	0.142
U16-h07-24-145	vein-4	-1.665	0.853	0.261	-0.007	0.006	0.005	0.209	0.042	0.136
U16-h07-24-145	vein-4	0.093	2.007	0.148	-0.040	0.089	0.016	0.186	1.329	0.150
U16-h07-24-145	vein-4	-1.771	13.609	0.137	0.300	0.659	0.015	4.323	7.050	0.139
U16-h07-24-145	vein-6	0.011	0.017	0.045	0.000	1.000	0.000	0.017	0.006	0.000
U16-h07-24-145	vein-6	0.310	0.049	0.041	0.040	0.010	0.000	0.737	0.059	0.000
U16-h07-24-145	vein-6	1.421	0.239	0.060	0.123	0.020	0.000	1.445	0.269	0.000
U16-h07-24-145	vein-6	0.652	0.073	0.041	0.085	0.015	0.000	1.671	0.212	0.000
U16-h07-24-145	vein-6	0.404	0.046	0.039	0.062	0.011	0.000	0.728	0.055	0.000
U16-h07-24-145	vein-7	1.401	0.177	0.066	0.050	0.014	0.000	0.004	0.003	0.000
U16-h07-25-167	coarse calcite	0.002	0.010	1.542	-0.001	0.000	0.021	0.089	0.016	0.177
U16-h07-25-167	coarse calcite	0.056	0.023	1.576	0.002	0.003	0.022	0.155	0.041	0.181
U16-h07-25-167	coarse calcite	0.005	0.015	1.651	-0.001	0.001	0.023	-0.024	0.007	0.189
U16-h07-25-167	coarse calcite	0.010	0.011	1.632	-0.001	0.000	0.022	-0.019	0.003	0.187
U16-h07-25-167	dk ooid	0.954	0.274	1.556	0.133	0.014	0.021	1.188	0.067	0.179
U16-h07-25-167	dk ooid	1.071	0.269	0.040	0.123	0.019	0.000	1.211	0.135	0.010
U16-h07-25-167	dk ooid	1.339	0.164	0.043	0.163	0.019	0.000	1.199	0.148	0.010
U16-h07-25-167	dk ooid	1.084	0.121	0.031	0.070	0.019	0.000	3.117	0.956	0.008
U16-h07-25-167	dk ooid	0.923	0.166	0.060	0.142	0.023	0.025	2.876	0.318	0.019
U16-h07-25-167	dk ooid	1.121	0.202	0.026	0.174	0.021	0.000	1.578	0.139	0.003
U16-h07-25-167	dk ooid	2.112	0.800	0.031	0.023	0.007	0.000	1.862	0.160	0.008
U16-h07-25-167	dk ooid	0.530	0.063	0.039	0.134	0.014	0.000	1.788	0.282	0.010
U16-h07-25-167	dk ooid	0.824	0.274	0.031	0.117	0.012	0.000	2.605	0.246	0.008
U16-h07-25-167	dk ooid	0.505	0.075	0.058	0.098	0.014	0.024	2.857	0.536	0.018
U16-h07-25-167	dk ooid	1.030	0.182	0.058	0.098	0.018	0.024	2.800	0.433	0.018
U16-h07-25-167	dk ooid	0.511	0.073	0.030	0.259	0.050	0.000	1.876	0.223	0.008
U16-h07-25-167	dk ooid	0.473	0.057	0.026	0.004	0.003	0.000	4.973	1.234	0.003
U16-h07-25-167	dk ooid	0.606	0.100	0.030	0.127	0.018	0.000	4.330	0.995	0.008
U16-h07-25-167	dk ooid	0.210	0.041	0.058	0.039	0.010	0.024	2.069	0.167	0.018

Sample ID	SampleType	Pb (ppm)	2SE (ppm)	Pb LOD (ppm)	Th (ppm)	2SE (ppm)	Th LOD (ppm)	U (ppm)	2SE (ppm)	U LOD (ppm)
U16-h07-25-167	dk ooid	0.652	0.082	0.029	0.137	0.017	0.000	1.951	0.146	0.007
U16-h07-25-167	dk ooid	0.359	0.123	0.058	0.124	0.020	0.024	2.079	0.144	0.018
U16-h07-25-167	dk ooid	0.648	0.112	0.060	0.072	0.013	0.024	2.288	0.258	0.018
U16-h07-25-167	dk ooid	0.470	0.064	0.023	0.155	0.018	0.000	1.499	0.162	0.003
U16-h07-25-167	dk ooid	0.446	0.068	0.059	0.105	0.015	0.024	2.457	0.371	0.018
U16-h07-25-167	dk ooid	0.499	0.087	0.030	0.151	0.024	0.000	1.299	0.072	0.008
U16-h07-25-167	dk ooid	0.338	0.061	0.029	0.077	0.016	0.000	1.216	0.113	0.007
U16-h07-25-167	early vein	-0.034	0.006	0.029	0.000	0.001	0.009	0.897	0.117	0.004
U16-h07-25-167	early vein	-0.010	0.012	0.029	0.000	0.001	0.009	0.436	0.052	0.004
U16-h07-25-167	early vein	-0.028	0.007	0.030	-0.001	0.001	0.009	0.292	0.029	0.004
U16-h07-25-167	early vein	-0.019	0.013	0.030	0.002	0.003	0.009	0.387	0.042	0.004
U16-h07-25-167	late vein	0.784	0.237	0.032	0.189	0.032	0.009	2.167	0.206	0.004
U16-h07-25-167	late vein	3.776	4.241	0.030	0.115	0.038	0.009	3.496	1.456	0.004
U16-h07-25-167	late vein	-0.010	0.013	0.029	0.053	0.009	0.009	0.748	0.128	0.004
U16-h07-25-167	late vein	-0.016	0.011	0.029	0.071	0.014	0.009	0.911	0.082	0.004
U16-h07-25-167	late vein	-0.009	0.011	0.030	0.075	0.026	0.009	0.757	0.035	0.004
U16-h07-25-167	lt ooid	0.759	0.134	0.029	0.077	0.011	0.009	1.066	0.112	0.004
U16-h07-25-167	lt ooid	0.374	0.044	0.028	0.085	0.012	0.008	2.696	0.241	0.003
U16-h07-25-167	lt ooid	0.469	0.063	0.028	0.104	0.014	0.008	2.740	0.191	0.004
U16-h07-25-167	lt ooid	0.768	0.197	0.059	0.190	0.022	0.024	2.520	0.390	0.018
U16-h07-25-167	lt ooid	0.896	0.161	0.057	0.332	0.028	0.023	2.326	0.226	0.018
U16-h07-25-167	lt ooid	0.333	0.060	0.027	0.067	0.011	0.008	1.970	0.137	0.003
U16-h07-25-167	lt ooid	0.468	0.078	0.028	0.090	0.015	0.008	1.768	0.148	0.003
U16-h07-25-167	lt ooid	0.714	0.122	0.060	0.111	0.016	0.024	1.810	0.146	0.018
U16-h07-25-167	lt ooid	0.249	0.051	0.027	0.084	0.012	0.008	1.466	0.086	0.003
U16-h07-25-167	lt ooid	0.222	0.054	0.028	0.090	0.011	0.009	0.955	0.158	0.004
U16-h07-25-167	matrix cement	0.127	0.027	0.030	0.000	0.001	0.009	0.014	0.005	0.004
U16-h07-25-167	matrix cement	0.969	0.231	0.029	0.063	0.012	0.009	3.209	0.855	0.004
U16-h07-25-167	matrix cement	0.060	0.035	0.030	0.044	0.009	0.009	0.187	0.050	0.004
U16-h07-25-167	matrix cement	0.696	0.241	0.027	0.070	0.014	0.008	2.484	0.419	0.003
U16-h07-25-167	matrix cement	0.688	0.099	0.028	0.054	0.013	0.009	2.196	0.283	0.004
U16-h07-25-167	matrix cement	0.419	0.042	0.028	0.074	0.013	0.009	2.792	0.534	0.004
U16-h07-25-167	matrix cement	0.334	0.044	0.028	0.060	0.011	0.009	1.474	0.147	0.004

Sample ID	SampleType	Pb (ppm)	2SE (ppm)	Pb LOD (ppm)	Th (ppm)	2SE (ppm)	Th LOD (ppm)	U (ppm)	2SE (ppm)	U LOD (ppm)
U16-h07-25-167	matrix cement	0.184	0.026	0.028	0.062	0.015	0.009	1.964	0.142	0.004
U16-h07-25-167	matrix cement	0.395	0.097	0.028	0.084	0.016	0.009	1.865	0.254	0.004
U16-h07-25-167	matrix cement	0.145	0.036	0.027	0.078	0.012	0.008	1.445	0.092	0.003
U16-h07-25-167	matrix cement	0.514	0.137	0.029	0.012	0.005	0.009	0.656	0.166	0.004
U16-h07-34-405	matrix cement	-1.134	12.232	0.241	0.004	0.152	0.002	0.568	24.038	0.015
U16-h07-34-405	matrix cement	1.159	1.490	0.145	0.235	0.048	0.000	1.833	0.729	0.021
U16-h07-34-405	matrix cement	-3.441	6.485	0.235	0.005	0.052	0.002	0.191	0.604	0.015
U16-h07-34-405	matrix cement	-1.501	0.487	0.544	-0.175	0.062	0.021	-1.545	0.182	0.171
U16-h07-34-405	matrix cement	-0.902	0.427	0.585	0.094	0.038	0.023	0.932	0.273	0.184
U16-h07-34-405	matrix cement	-1.589	1.698	0.218	-1.041	0.939	0.002	-9.257	6.295	0.014
U16-h07-34-405	matrix cement	-1.592	4.090	0.218	-1.568	1.221	0.002	-11.212	9.348	0.014
U16-h07-34-405	matrix cement	-6.860	3.490	0.586	0.119	0.020	0.023	1.469	0.118	0.184
U16-h07-34-405	matrix cement	-2.105	2.136	0.147	-0.012	0.023	0.000	-0.554	0.585	0.021
U16-h07-34-405	matrix cement	-1.639	0.627	0.586	0.148	0.013	0.023	0.804	0.136	0.184
U16-h07-34-405	matrix cement	-0.782	1.320	0.230	0.165	0.044	0.002	0.661	1.272	0.015
U16-h07-34-405	matrix cement	-2.127	5.793	0.218	-0.454	0.182	0.002	-10.140	5.063	0.014
U16-h07-34-405	matrix cement	-8.667	3.268	0.229	0.186	0.128	0.002	1.905	1.523	0.014
U16-h07-34-405	matrix cement	4.965	5.004	0.236	0.055	0.034	0.002	8.946	5.617	0.015
U16-h07-34-405	matrix cement	-3.506	7.271	0.240	-0.006	0.016	0.002	-0.894	2.646	0.015
U16-h07-34-405	matrix cement	-13.464	16.554	0.234	-0.006	0.018	0.002	-0.988	3.287	0.015
U16-h07-34-405	matrix cement	2.467	5.148	0.241	0.090	0.057	0.003	0.920	0.505	0.015
U16-h07-34-405	ooid	2.910	0.587	0.267	0.144	0.035	0.015	1.249	0.184	0.138
U16-h07-34-405	ooid	8.683	2.576	0.249	1.094	0.306	0.033	6.256	1.555	0.202
U16-h07-34-405	ooid	-10.372	5.102	0.133	-2.010	0.709	0.000	-17.334	5.615	0.019
U16-h07-34-405	ooid	-2.528	0.670	0.307	0.301	0.132	0.100	-4.052	0.693	0.221
U16-h07-34-405	ooid	-1.479	0.696	0.357	0.565	0.084	0.094	-0.497	0.706	0.163
U16-h07-34-405	ooid	-1.949	0.499	0.340	0.160	0.069	0.090	-2.789	0.427	0.155
U16-h07-34-405	ooid	-5.167	2.055	0.248	-0.962	0.167	0.034	-7.957	1.743	0.551
U16-h07-34-405	ooid	-1.713	0.423	0.300	-0.147	0.127	0.097	-1.917	0.336	0.213
U16-h07-34-405	ooid	-0.369	0.771	0.199	0.148	0.027	0.026	2.767	0.602	0.286
U16-h07-34-405	ooid	-2.280	0.568	0.186	-0.134	0.117	0.024	-5.282	0.992	0.268
U16-h07-34-405	ooid	-0.928	0.631	0.318	-2.171	0.368	0.104	-0.141	0.657	0.229
U16-h07-34-405	ooid	-0.696	0.254	0.330	-0.018	0.066	0.087	-1.196	0.216	0.151

Sample ID	SampleType	Pb (ppm)	2SE (ppm)	Pb LOD (ppm)	Th (ppm)	2SE (ppm)	Th LOD (ppm)	U (ppm)	2SE (ppm)	U LOD (ppm)
U16-h07-34-405	ooid	-2.743	0.592	0.313	-5.331	0.946	0.102	-1.773	0.531	0.222
U16-h07-34-405	ooid	-1.638	0.442	0.363	0.050	0.096	0.096	-2.367	0.394	0.166
U16-h07-34-405	ooid	-1.947	0.482	0.326	0.123	0.030	0.010	0.805	0.380	0.128
U16-h07-34-405	ooid	-0.624	0.391	0.330	-0.014	0.045	0.010	-1.448	0.443	0.129
U16-h07-34-405	ooid	-1.262	0.330	0.362	-1.110	0.335	0.096	0.518	0.144	0.166
U16-h07-34-405	ooid	-4.257	0.826	0.236	-0.687	0.172	0.031	-3.188	0.510	0.192
U16-h07-34-405	ooid	-1.234	0.253	0.335	-1.216	0.157	0.088	-0.770	0.155	0.153
U16-h07-34-405	ooid	-0.942	0.503	0.247	-0.012	0.064	0.034	-1.361	0.578	0.550
U16-h07-34-405	ooid	12.820	13.711	0.146	1.436	1.698	0.000	12.812	16.101	0.021
U16-h07-34-405	ooid and clast	1.337	0.267	0.166	4.528	0.818	0.000	37.114	6.322	0.000
U16-h07-34-405	ooid and clast	0.726	0.200	0.784	0.167	0.067	0.040	0.778	0.183	0.987
U16-h07-34-405	ooid and clast	0.265	0.038	0.045	0.000	0.001	0.000	0.251	0.050	0.000
U16-h07-34-405	ooid and clast	0.377	0.055	0.046	0.019	0.006	0.000	0.570	0.087	0.000
U16-h07-34-405	ooid and clast	0.489	0.069	0.042	0.520	0.068	0.000	5.093	0.693	0.000
U16-h07-34-405	ooid and clast	0.658	0.137	0.048	1.136	0.212	0.000	10.154	1.072	0.000
U16-h07-34-405	ooid and clast	0.914	0.086	0.759	0.281	0.033	0.039	6.783	0.942	0.955
U16-h07-34-405	ooid and clast	0.453	0.049	0.041	0.165	0.020	0.000	3.542	0.219	0.000
U16-h07-34-405	ooid and clast	0.888	0.257	0.042	1.069	0.118	0.000	7.824	0.920	0.000
U16-h07-34-405	ooid and clast	0.603	0.075	0.043	0.214	0.022	0.000	4.278	0.293	0.000
U16-h07-34-405	ooid and clast	0.805	0.198	0.044	0.475	0.081	0.000	7.465	0.847	0.000
U16-h07-34-405	ooid and clast	1.333	0.224	0.044	0.060	0.012	0.004	1.084	0.129	0.000
U16-h07-34-405	ooid and clast	1.651	0.222	0.044	1.241	0.148	0.004	11.022	0.616	0.000
U16-h07-34-405	ooid and clast	2.159	0.529	0.077	0.740	0.072	0.019	10.658	0.691	0.157
U16-h07-34-405	ooid and clast	1.812	0.454	0.053	0.512	0.050	0.007	12.416	1.166	0.000
U16-h07-34-405	ooid and clast	3.379	0.403	0.043	2.734	0.301	0.004	21.467	1.430	0.000
U16-h07-34-405	ooid and clast	4.808	9.025	0.044	1.916	1.678	0.004	21.442	101.916	0.000
U16-h07-34-405	ooid and clast	4.765	15.192	0.081	0.248	1.093	0.021	17.150	43.839	0.167
U16-h07-34-405	ooid and clast	-25.182	19.988	0.044	-3.470	12.902	0.000	-87.060	60.199	0.003
U16-h07-34-405	ooid and clast	0.317	0.037	0.295	0.069	0.012	0.076	0.056	0.004	0.072
U16-h07-34-405	ooid and clast	-3.116	1.021	0.079	-1.411	0.165	0.020	-11.332	1.305	0.163
U16-h07-34-405	ooid and clast	-3.667	0.872	0.046	-3.315	0.400	0.004	-19.907	1.714	0.000
U16-h07-34-405	ooid and clast	-2.791	0.590	0.041	-2.469	0.405	0.003	-19.659	1.877	0.000
U16-h07-34-405	ooid and clast	-0.776	0.091	0.043	-0.268	0.040	0.000	-5.818	0.381	0.025

Sample ID	SampleType	Pb (ppm)	2SE (ppm)	Pb LOD (ppm)	Th (ppm)	2SE (ppm)	Th LOD (ppm)	U (ppm)	2SE (ppm)	U LOD (ppm)
U16-h07-34-405	ooid and clast	-1.220	0.110	0.044	-0.827	0.088	0.004	-5.289	0.363	0.000
U16-h07-34-405	ooid and clast	-1.185	0.135	0.042	-0.189	0.033	0.003	-3.096	0.374	0.000
U16-h07-34-405	ooid and clast	-0.380	0.166	0.209	-0.235	0.065	0.055	-4.369	0.870	1.181
U16-h07-34-405	ooid and clast	-0.603	0.063	0.043	-0.452	0.056	0.000	-4.954	0.412	0.000
U16-h07-34-405	ooid and clast	-1.044	0.187	0.478	-0.449	0.078	0.037	-5.304	0.577	1.903
U16-h07-34-405	ooid and clast	-0.729	0.105	0.212	-0.489	0.079	0.056	-5.237	0.741	1.196
U16-h07-34-405	ooid and clast	-0.342	0.091	0.425	-0.293	0.034	0.033	-3.284	0.317	1.691
U16-h07-34-405	ooid and clast	-0.196	0.022	0.414	-0.152	0.028	0.032	-2.017	0.191	1.649
U16-h07-34-405	ooid and clast	-0.211	0.035	0.272	-0.149	0.031	0.070	-2.398	0.200	0.067
U16-h07-34-405	ooid and clast	-0.676	0.063	0.045	-0.212	0.029	0.000	-0.082	0.021	0.000
U16-h07-34-405	vein 1	-0.169	0.182	0.116	0.029	0.005	0.007	4.748	0.816	0.515
U16-h07-34-405	vein 1	1.131	0.386	0.121	0.030	0.021	0.007	6.480	0.944	0.532
U16-h07-34-405	vein 1	5.774	9.001	0.125	0.079	0.044	0.007	7.357	5.213	0.549
U16-h07-34-405	vein 1	1.639	0.332	0.114	0.047	0.011	0.006	5.990	1.144	0.503
U16-h07-34-405	vein 1	0.539	0.610	0.118	0.040	0.006	0.007	6.433	1.052	0.522
U16-h07-34-405	vein 2	-97.714	33.599	0.133	-0.501	0.078	0.008	-8.789	1.085	0.593
U16-h07-34-405	vein 2	-0.030	0.045	0.123	-0.127	0.047	0.007	-2.132	0.366	0.547
U16-h07-34-405	vein 2	-0.136	0.085	0.130	-0.276	0.049	0.007	-4.444	0.537	0.576
U16-h07-34-405	vein 2	-0.016	0.119	0.132	-0.564	0.194	0.008	-7.676	1.522	0.587
U16-h07-34-405	vein 2	0.082	0.045	0.126	-0.224	0.043	0.007	-4.359	0.539	0.560
U16-h07-34-405	vein 2	0.252	0.104	0.130	-0.053	0.033	0.007	-8.653	1.152	0.580
U16-h07-54-338	coarse calcite	0.507	0.083	0.029	0.018	0.008	0.000	1.298	0.495	0.126
U16-h07-54-338	coarse calcite	0.356	0.040	1.334	0.012	0.006	0.003	0.912	0.198	0.091
U16-h07-54-338	coarse calcite	0.242	0.035	0.014	0.000	0.001	0.000	0.248	0.051	0.011
U16-h07-54-338	coarse calcite	0.375	0.049	0.033	0.017	0.011	0.004	2.226	1.097	0.077
U16-h07-54-338	coarse calcite	0.312	0.038	1.281	0.024	0.009	0.003	1.187	0.210	0.088
U16-h07-54-338	coarse calcite	0.354	0.047	0.030	0.010	0.006	0.000	0.359	0.055	0.017
U16-h07-54-338	coarse calcite	0.295	0.041	1.345	0.000	0.002	0.003	0.369	0.087	0.092
U16-h07-54-338	coarse calcite	0.306	0.037	0.031	0.003	0.003	0.000	0.709	0.062	0.048
U16-h07-54-338	coarse calcite	0.286	0.043	0.063	0.016	0.008	0.006	1.253	0.310	0.018
U16-h07-54-338	coarse calcite	0.313	0.035	1.234	0.020	0.006	0.003	4.075	0.880	0.085
U16-h07-54-338	coarse calcite	0.396	0.052	1.255	0.009	0.005	0.003	1.963	0.488	0.086
U16-h07-54-338	coarse calcite	0.291	0.045	0.027	0.013	0.006	0.000	1.119	0.097	0.018

Sample ID	SampleType	Pb (ppm)	2SE (ppm)	Pb LOD (ppm)	Th (ppm)	2SE (ppm)	Th LOD (ppm)	U (ppm)	2SE (ppm)	U LOD (ppm)
U16-h07-54-338	coarse calcite	0.306	0.032	0.288	0.007	0.004	0.017	1.508	0.287	0.096
U16-h07-54-338	coarse calcite	0.368	0.072	0.061	0.007	0.005	0.006	2.015	0.338	0.017
U16-h07-54-338	coarse calcite	0.164	0.038	0.039	0.002	0.003	0.000	0.828	0.091	0.035
U16-h07-54-5	matrix cement	0.287	0.067	0.043	0.016	0.005	0.000	0.195	0.038	0.003
U16-h07-54-5	matrix cement	0.370	0.154	0.043	0.064	0.022	0.000	0.984	0.066	0.003
U16-h07-54-5	matrix cement	4.741	0.628	0.044	0.206	0.025	0.000	4.208	0.668	0.003
U16-h07-54-5	matrix cement	2.930	0.827	0.041	0.082	0.021	0.000	4.114	1.782	0.003
U16-h07-54-5	matrix cement	3.767	0.679	0.066	0.072	0.014	0.000	2.631	0.398	0.000
U16-h07-54-5	matrix cement	2.740	0.564	0.040	0.086	0.016	0.000	1.573	0.155	0.000
U16-h07-54-5	matrix cement	6.230	1.427	0.044	0.896	0.082	0.000	2.733	0.680	0.003
U16-h07-54-5	matrix cement	3.156	0.323	0.042	0.074	0.011	0.000	1.675	0.271	0.003
U16-h07-54-5	matrix cement	0.362	0.034	0.066	0.038	0.007	0.000	0.659	0.045	0.000
U16-h07-54-5	matrix cement	5.568	0.781	0.044	0.090	0.016	0.000	2.375	0.310	0.003
U16-h07-54-5	matrix cement	1.522	0.145	0.066	0.055	0.011	0.000	1.106	0.093	0.008
U16-h07-54-5	matrix cement	0.830	0.121	0.043	0.027	0.008	0.000	1.027	0.147	0.003
U16-h07-54-5	matrix cement	1.941	0.309	0.043	0.057	0.013	0.000	0.978	0.124	0.003
U16-h07-54-5	matrix cement	0.609	0.158	0.044	0.027	0.008	0.000	0.923	0.072	0.003
U16-h07-54-5	matrix cement	0.066	0.029	0.041	0.004	0.003	0.000	1.335	0.223	0.000
U16-h07-54-5	matrix cement	0.274	0.044	0.043	0.016	0.005	0.000	0.768	0.044	0.003
U16-h07-54-5	matrix cement	0.042	0.021	0.044	0.002	0.002	0.000	0.546	0.073	0.003
U16-h07-54-5	ooid	18.393	2.294	0.062	0.595	0.104	0.000	6.975	0.863	0.018
U16-h07-54-5	ooid	1.696	0.244	0.050	0.077	0.014	0.006	1.654	0.201	0.000
U16-h07-54-5	ooid	0.188	0.050	0.034	0.011	0.005	0.003	0.421	0.041	0.007
U16-h07-54-5	ooid	5.676	1.299	0.042	0.079	0.018	0.000	3.657	0.981	0.005
U16-h07-54-5	ooid	8.721	0.897	0.054	0.160	0.023	0.006	5.389	0.810	0.000
U16-h07-54-5	ooid	1.054	0.255	0.053	0.032	0.009	0.000	0.343	0.050	0.015
U16-h07-54-5	ooid	5.609	0.802	0.043	0.277	0.048	0.000	10.352	1.185	0.005
U16-h07-54-5	ooid	10.123	1.257	0.055	0.321	0.046	0.006	18.941	2.255	0.000
U16-h07-54-5	ooid	2.918	0.281	0.066	0.126	0.019	0.000	4.084	0.594	0.008
U16-h07-54-5	ooid	5.408	0.606	0.035	0.112	0.014	0.003	2.507	0.235	0.007
U16-h07-54-5	ooid	6.526	0.495	0.035	0.204	0.039	0.003	7.746	1.149	0.007
U16-h07-54-5	ooid	2.888	0.319	0.041	0.078	0.012	0.000	1.711	0.259	0.004
U16-h07-54-5	ooid	1.035	0.215	0.052	0.056	0.011	0.006	0.839	0.100	0.000

Sample ID	SampleType	Pb (ppm)	2SE (ppm)	Pb LOD (ppm)	Th (ppm)	2SE (ppm)	Th LOD (ppm)	U (ppm)	2SE (ppm)	U LOD (ppm)
U16-h07-54-5	ooid	2.009	0.223	0.042	0.064	0.012	0.000	1.073	0.062	0.005
U16-h07-54-5	ooid	0.950	0.118	0.064	0.089	0.017	0.007	0.700	0.081	0.000
U16-h07-54-5	ooid	1.713	0.207	0.069	0.057	0.011	0.000	1.001	0.082	0.008
U16-h07-54-5	ooid	3.481	0.803	0.039	0.050	0.011	0.000	1.982	0.218	0.004
U16-h07-54-5	ooid	0.347	0.064	0.041	0.027	0.007	0.000	0.787	0.068	0.004
U16-h07-54-5	ooid	1.676	0.266	0.051	0.131	0.051	0.000	1.067	0.122	0.014
U16-h07-54-5	ooid	3.919	0.425	0.041	0.090	0.025	0.000	2.502	0.437	0.004
U16-h07-54-5	ooid	0.621	0.068	0.055	0.048	0.009	0.006	0.776	0.061	0.000
U16-h07-54-5	ooid	0.462	0.132	0.055	0.011	0.006	0.000	0.562	0.113	0.016
U16-h07-54-5	ooid	0.856	0.119	0.051	0.087	0.017	0.006	0.929	0.095	0.000
U16-h07-54-5	ooid	2.363	0.522	0.042	0.032	0.011	0.000	1.281	0.160	0.005
U16-h07-54-5	ooid	0.127	0.026	0.054	0.008	0.004	0.000	0.768	0.102	0.015
U16-h07-54-5	vein 1	0.404	0.050	0.049	0.002	0.002	0.000	0.089	0.021	0.000
U16-h07-54-5	vein 1	0.180	0.021	0.050	0.004	0.003	0.000	0.205	0.030	0.004
U16-h07-54-5	vein 1	0.288	0.038	0.046	0.015	0.007	0.000	0.369	0.053	0.008
U16-h07-54-5	vein 1	0.178	0.025	0.044	0.013	0.006	0.000	0.378	0.044	0.007
U16-h07-54-5	vein 1	0.592	0.173	0.046	0.138	0.026	0.000	1.642	0.200	0.008
U16-h07-54-5	vein 1	0.056	0.019	0.045	0.015	0.006	0.000	1.015	0.100	0.008
U16-h07-54-5	vein 2	0.448	0.073	0.048	-0.001	0.000	0.000	0.006	0.003	0.000
U16-h07-54-5	vein 2	0.237	0.033	0.048	0.001	0.002	0.000	0.458	0.040	0.000
U16-h07-54-5	vein 2	0.386	0.045	0.048	-0.001	0.000	0.000	0.063	0.018	0.000
U16-h07-67-129	darker vein	0.297	0.044	0.056	-0.001	0.001	0.000	0.324	0.061	0.000
U16-h07-67-129	darker vein	0.420	0.056	0.018	-0.001	0.000	0.000	0.254	0.022	0.007
U16-h07-67-129	darker vein	0.424	0.065	0.020	-0.001	0.000	0.000	0.340	0.098	0.010
U16-h07-67-129	darker vein	0.464	0.063	0.018	-0.001	0.000	0.000	0.688	0.087	0.007
U16-h07-67-129	darker vein	0.361	0.047	0.058	-0.001	0.000	0.000	0.222	0.040	0.000
U16-h07-67-129	darker vein	0.425	0.047	0.057	-0.001	0.000	0.000	0.292	0.057	0.000
U16-h07-67-129	darker vein	0.233	0.030	0.020	-0.001	0.000	0.000	0.164	0.021	0.010
U16-h07-67-129	lighter vein	-0.004	0.007	0.038	-0.001	0.000	0.000	0.014	0.008	0.005
U16-h07-67-129	lighter vein	0.021	0.012	0.019	0.005	0.004	0.000	0.122	0.017	0.008
U16-h07-67-129	lighter vein	0.034	0.022	0.022	-0.001	0.000	0.000	-0.001	0.002	0.000
U16-h07-67-129	lighter vein	0.062	0.022	0.037	0.009	0.004	0.000	0.219	0.044	0.005
U16-h07-67-129	lighter vein	0.043	0.019	0.036	0.006	0.004	0.000	0.091	0.016	0.005

Sample ID	SampleType	Pb (ppm)	2SE (ppm)	Pb LOD (ppm)	Th (ppm)	2SE (ppm)	Th LOD (ppm)	U (ppm)	2SE (ppm)	U LOD (ppm)
U16-h07-67-129	lighter vein	0.053	0.023	0.039	-0.001	0.001	0.000	0.211	0.022	0.005
U16-h07-67-129	lighter vein	0.026	0.014	0.019	0.007	0.004	0.000	0.032	0.011	0.008
U16-h07-67-129	ooid and matrix	123.432	18.566	0.179	47.049	7.231	0.000	198.783	28.197	0.000
U16-h07-67-129	ooid and matrix	0.916	0.271	0.042	1.533	0.273	0.000	10.769	1.562	0.022
U16-h07-67-129	ooid and matrix	11.059	2.568	0.067	3.370	0.345	0.020	25.778	2.155	0.068
U16-h07-67-129	ooid and matrix	0.895	0.184	0.039	1.700	0.154	0.008	10.303	0.864	0.100
U16-h07-67-129	ooid and matrix	7.817	2.879	0.130	4.648	1.476	0.000	18.639	5.412	0.031
U16-h07-67-129	ooid and matrix	1.411	0.463	0.043	1.501	0.166	0.013	8.389	0.694	0.050
U16-h07-67-129	ooid and matrix	0.792	0.104	0.036	0.289	0.025	0.010	3.071	0.159	0.022
U16-h07-67-129	ooid and matrix	0.718	0.101	2.401	0.472	0.047	0.960	5.328	0.870	9.549
U16-h07-67-129	ooid and matrix	1.497	0.406	0.064	1.613	0.120	0.022	9.432	0.830	0.136
U16-h07-67-129	ooid and matrix	5.581	0.949	0.048	3.080	0.442	0.014	19.903	2.147	0.055
U16-h07-67-129	ooid and matrix	5.287	1.706	0.045	0.954	0.316	0.000	10.570	2.380	0.024
U16-h07-67-129	ooid and matrix	0.392	0.130	0.072	0.188	0.035	0.015	1.341	0.197	0.030
U16-h07-67-129	ooid and matrix	0.651	0.075	0.023	0.342	0.035	0.000	6.165	0.336	0.013
U16-h07-67-129	ooid and matrix	0.198	0.032	0.026	0.186	0.020	0.011	0.286	0.072	0.010
U16-h07-67-129	ooid and matrix	0.659	0.123	0.031	0.311	0.024	0.000	4.972	0.281	0.000
U16-h07-67-129	ooid and matrix	0.063	0.019	0.073	0.003	0.003	0.015	0.830	0.230	0.030
U16-h07-67-129	ooid and matrix	0.329	0.061	0.027	0.340	0.121	0.011	3.280	0.699	0.011
U16-h07-67-129	ooid and matrix	0.366	0.040	0.060	0.004	0.003	0.020	0.460	0.053	0.129
U16-h07-67-129	ooid and matrix	0.435	0.341	0.041	0.170	0.025	0.012	0.764	0.065	0.047
U16-h07-67-129	ooid and matrix	0.574	0.090	0.042	0.095	0.016	0.000	2.169	0.189	0.022
U16-h07-67-129	ooid and matrix	0.494	0.135	0.069	0.146	0.022	0.014	0.314	0.030	0.028
U16-h07-67-129	ooid and matrix	0.150	0.026	0.025	0.175	0.029	0.000	1.109	0.129	0.000
U16-h07-67-129	ooid and matrix	0.129	0.030	0.023	0.018	0.007	0.000	0.675	0.116	0.012
U16-h07-67-129	ooid and matrix	0.042	0.022	0.027	0.053	0.012	0.000	0.275	0.044	0.010
U16-h07-67-129	ooid and matrix	0.040	0.020	0.026	0.014	0.005	0.000	0.439	0.056	0.000

Appendix E

E.1 Reactive Transport Modeling Results at TIFF of $1x10^2$ (moles H_2O/cm^2)

z (km)	Nd=5 Rock ‰ δ18O	Fluid ‰ δ18O	Δr-fl	Nd=2 Rock ‰ δ18O	Fluid ‰ δ18O	Δr-fl	Nd=1 Rock ‰ δ18O	Fluid ‰ δ18O
0	4.1415	4	0.1415	6.842	4	2.842	11.7255	4
0.0001	4.1765	4.0073	0.1692	6.9526	4.0542	2.8984	11.8026	4.0729
0.0002	4.2141	4.016	0.1981	7.0632	4.1095	2.9537	11.8793	4.1459
0.0004	4.2542	4.0261	0.2281	7.1739	4.1658	3.0081	11.9557	4.2189
0.0005	4.2969	4.0377	0.2592	7.2847	4.2233	3.0614	12.0318	4.2921
0.0006	4.3421	4.0508	0.2913	7.3955	4.2818	3.1137	12.1075	4.3653
0.0007	4.39	4.0654	0.3246	7.5064	4.3414	3.165	12.1829	4.4385
0.0009	4.4404	4.0817	0.3587	7.6174	4.402	3.2154	12.2579	4.5118
0.001	4.4934	4.0997	0.3937	7.7283	4.4635	3.2648	12.3326	4.5852
0.0011	4.549	4.1194	0.4296	7.8393	4.5261	3.3132	12.407	4.6586
0.0012	4.6072	4.1408	0.4664	7.9503	4.5896	3.3607	12.481	4.7321
0.0014	4.668	4.164	0.504	8.0612	4.6541	3.4071	12.5547	4.8056
0.0015	4.7314	4.1891	0.5423	8.1721	4.7195	3.4526	12.6281	4.8791
0.0016	4.7973	4.2161	0.5812	8.2829	4.7858	3.4971	12.7011	4.9527
0.0017	4.8658	4.2449	0.6209	8.3937	4.853	3.5407	12.7738	5.0263
0.0019	4.9368	4.2757	0.6611	8.5044	4.9211	3.5833	12.8462	5.0999
0.002	5.0103	4.3085	0.7018	8.615	4.9901	3.6249	12.9182	5.1736
0.0021	5.0863	4.3433	0.743	8.7255	5.0598	3.6657	12.9899	5.2473
0.0023	5.1648	4.38	0.7848	8.8359	5.1304	3.7055	13.0613	5.321
0.0024	5.2458	4.4189	0.8269	8.9462	5.2018	3.7444	13.1323	5.3947
0.0025	5.3291	4.4598	0.8693	9.0563	5.274	3.7823	13.203	5.4684
0.0026	5.4149	4.5028	0.9121	9.1663	5.3469	3.8194	13.2734	5.5421
0.0028	5.503	4.5479	0.9551	9.2761	5.4206	3.8555	13.3434	5.6158
0.0029	5.5935	4.5951	0.9984	9.3858	5.4951	3.8907	13.4131	5.6895
0.003	5.6862	4.6444	1.0418	9.4953	5.5702	3.9251	13.4825	5.7632
0.0031	5.7812	4.6958	1.0854	9.6046	5.646	3.9586	13.5515	5.8369
0.0033	5.8785	4.7494	1.1291	9.7137	5.7225	3.9912	13.6203	5.9106
0.0034	5.9779	4.8052	1.1727	9.8225	5.7997	4.0228	13.6887	5.9843
0.0035	6.0795	4.8631	1.2164	9.9312	5.8776	4.0536	13.7567	6.0579
0.0036	6.1831	4.9231	1.26	10.0396	5.956	4.0836	13.8245	6.1316
0.0038	6.2889	4.9853	1.3036	10.1478	6.0351	4.1127	13.8919	6.2052
0.0039	6.3966	5.0496	1.347	10.2557	6.1148	4.1409	13.959	6.2787
0.004	6.5064	5.1161	1.3903	10.3634	6.195	4.1684	14.0258	6.3523
0.0041	6.618	5.1847	1.4333	10.4708	6.2758	4.195	14.0923	6.4258
0.0043	6.7316	5.2554	1.4762	10.5779	6.3572	4.2207	14.1584	6.4993
0.0044	6.8469	5.3283	1.5186	10.6847	6.4391	4.2456	14.2242	6.5727
0.0045	6.9641	5.4032	1.5609	10.7913	6.5215	4.2698	14.2897	6.6461
0.0046	7.083	5.4802	1.6028	10.8975	6.6044	4.2931	14.3549	6.7194
0.0047	7.2035	5.5593	1.6442	11.0035	6.6878	4.3157	14.4197	6.7927
0.0049	7.3258	5.6405	1.6853	11.1091	6.7717	4.3374	14.4843	6.866
0.005	7.4495	5.7236	1.7259	11.2144	6.856	4.3584	14.5485	6.9392
0.0051	7.5749	5.8088	1.7661	11.3193	6.9408	4.3785	14.6124	7.0123
0.0052	7.7017	5.896	1.8057	11.4239	7.0259	4.398	14.676	7.0854
0.0054	7.8299	5.9851	1.8448	11.5282	7.1115	4.4167	14.7393	7.1584
0.0055	7.9595	6.0762	1.8833	11.6321	7.1975	4.4346	14.8023	7.2313
0.0056	8.0904	6.1691	1.9213	11.7357	7.2839	4.4518	14.8649	7.3042
0.0057	8.2226	6.264	1.9586	11.8389	7.3706	4.4683	14.9273	7.377
0.0059	8.356	6.3607	1.9953	11.9417	7.4577	4.484	14.9893	7.4497
0.006	8.4906	6.4592	2.0314	12.0441	7.5451	4.499	15.051	7.5224
0.0061	8.6263	6.5595	2.0668	12.1462	7.6329	4.5133	15.1124	7.5949
0.0062	8.763	6.6616	2.1014	12.2478	7.721	4.5268	15.1736	7.6674

z (km)	Nd=5 Rock ‰ δ18O	Fluid ‰ δ18O	Δr-fl	Nd=2 Rock ‰ δ18O	Fluid ‰ δ18O	Δr-fl	Nd=1 Rock ‰ δ18O	Fluid ‰ δ18O
0.0064	8.9007	6.7654	2.1353	12.3491	7.8093	4.5398	15.2343	7.7398
0.0065	9.0394	6.8709	2.1685	12.4499	7.8979	4.552	15.2948	7.8122
0.0066	9.179	6.978	2.201	12.5504	7.9869	4.5635	15.355	7.8844
0.0067	9.3194	7.0868	2.2326	12.6504	8.076	4.5744	15.4149	7.9566
0.0069	9.4606	7.1971	2.2635	12.75	8.1654	4.5846	15.4745	8.0286
0.007	9.6026	7.309	2.2936	12.8492	8.2551	4.5941	15.5338	8.1006
0.0071	9.7452	7.4223	2.3229	12.948	8.3449	4.6031	15.5927	8.1724
0.0072	9.8885	7.5372	2.3513	13.0463	8.435	4.6113	15.6514	8.2442
0.0074	10.0323	7.6534	2.3789	13.1442	8.5252	4.619	15.7098	8.3159
0.0075	10.1767	7.7711	2.4056	13.2417	8.6156	4.6261	15.7679	8.3874
0.0076	10.3215	7.89	2.4315	13.3387	8.7062	4.6325	15.8256	8.4589
0.0077	10.4668	8.0103	2.4565	13.4353	8.797	4.6383	15.8831	8.5302
0.0079	10.6125	8.1318	2.4807	13.5314	8.8879	4.6435	15.9403	8.6015
0.008	10.7585	8.2546	2.5039	13.627	8.9789	4.6481	15.9972	8.6726
0.0081	10.9048	8.3785	2.5263	13.7222	9.07	4.6522	16.0538	8.7436
0.0082	11.0513	8.5035	2.5478	13.817	9.1613	4.6557	16.1101	8.8145
0.0084	11.198	8.6296	2.5684	13.9112	9.2526	4.6586	16.1661	8.8853
0.0085	11.3449	8.7568	2.5881	14.005	9.344	4.661	16.2218	8.9559
0.0086	11.4919	8.8849	2.607	14.0983	9.4356	4.6627	16.2772	9.0265
0.0087	11.6389	9.014	2.6249	14.1912	9.5271	4.6641	16.3323	9.0969
0.0089	11.7859	9.1441	2.6418	14.2835	9.6187	4.6648	16.3872	9.1672
0.009	11.9329	9.2749	2.658	14.3754	9.7104	4.665	16.4417	9.2373
0.0091	12.0798	9.4066	2.6732	14.4668	9.8021	4.6647	16.496	9.3074
0.0092	12.2266	9.5391	2.6875	14.5577	9.8938	4.6639	16.55	9.3773
0.0094	12.3732	9.6723	2.7009	14.6481	9.9855	4.6626	16.6037	9.447
0.0095	12.5196	9.8062	2.7134	14.738	10.0773	4.6607	16.6571	9.5167
0.0096	12.6658	9.9407	2.7251	14.8275	10.169	4.6585	16.7102	9.5862
0.0097	12.8117	10.0758	2.7359	14.9164	10.2607	4.6557	16.7631	9.6555
0.0099	12.9573	10.2115	2.7458	15.0048	10.3524	4.6524	16.8156	9.7248
0.01	13.1025	10.3477	2.7548	15.0928	10.444	4.6488	16.8679	9.7938
0.0101	13.2474	10.4844	2.763	15.1802	10.5356	4.6446	16.9199	9.8628
0.0102	13.3918	10.6215	2.7703	15.2671	10.6271	4.64	16.9716	9.9316
0.0104	13.5358	10.759	2.7768	15.3535	10.7186	4.6349	17.0231	10.0002
0.0105	13.6792	10.8969	2.7823	15.4394	10.81	4.6294	17.0743	10.0687
0.0106	13.8222	11.035	2.7872	15.5248	10.9013	4.6235	17.1252	10.1371
0.0107	13.9646	11.1734	2.7912	15.6097	10.9925	4.6172	17.1758	10.2053
0.0109	14.1063	11.312	2.7943	15.6941	11.0837	4.6104	17.2261	10.2734
0.011	14.2475	11.4508	2.7967	15.778	11.1747	4.6033	17.2762	10.3413
0.0111	14.388	11.5898	2.7982	15.8614	11.2656	4.5958	17.326	10.409
0.0112	14.5279	11.7288	2.7991	15.9442	11.3564	4.5878	17.3755	10.4766
0.0114	14.667	11.8679	2.7991	16.0265	11.447	4.5795	17.4248	10.5441
0.0115	14.8054	12.0071	2.7983	16.1084	11.5375	4.5709	17.4738	10.6113
0.0116	14.943	12.1462	2.7968	16.1897	11.6279	4.5618	17.5225	10.6785
0.0117	15.0799	12.2853	2.7946	16.2705	11.7181	4.5524	17.571	10.7454
0.0119	15.2159	12.4243	2.7916	16.3507	11.8081	4.5426	17.6192	10.8122
0.012	15.3511	12.5632	2.7879	16.4305	11.898	4.5325	17.6671	10.8789
0.0121	15.4855	12.7019	2.7836	16.5097	11.9877	4.522	17.7148	10.9454
0.0122	15.619	12.8404	2.7786	16.5884	12.0772	4.5112	17.7622	11.0117
0.0124	15.7516	12.9787	2.7729	16.6666	12.1665	4.5001	17.8093	11.0778
0.0125	15.8832	13.1167	2.7665	16.7443	12.2557	4.4886	17.8562	11.1438
0.0126	16.014	13.2545	2.7595	16.8215	12.3446	4.4769	17.9028	11.2096

z (km)	Nd=5 Rock ‰ δ18O	Fluid ‰ δ18O	Δr-fl	Nd=2 Rock ‰ δ18O	Fluid ‰ δ18O	Δr-fl	Nd=1 Rock ‰ δ18O	Fluid ‰ δ18O
0.0127	16.1438	13.3919	2.7519	16.8981	12.4333	4.4648	17.9492	11.2753
0.0129	16.2726	13.529	2.7436	16.9743	12.5218	4.4525	17.9953	11.3407
0.013	16.4004	13.6657	2.7347	17.0499	12.6101	4.4398	18.0411	11.406
0.0131	16.5272	13.8019	2.7253	17.125	12.6981	4.4269	18.0867	11.4712
0.0132	16.653	13.9377	2.7153	17.1996	12.786	4.4136	18.1321	11.5361
0.0134	16.7777	14.0731	2.7046	17.2736	12.8735	4.4001	18.1771	11.6009
0.0135	16.9014	14.2079	2.6935	17.3472	12.9609	4.3863	18.222	11.6655
0.0136	17.0241	14.3422	2.6819	17.4202	13.048	4.3722	18.2666	11.7299
0.0137	17.1456	14.476	2.6696	17.4927	13.1348	4.3579	18.3109	11.7942
0.0139	17.2661	14.6091	2.657	17.5647	13.2213	4.3434	18.355	11.8583
0.014	17.3855	14.7417	2.6438	17.6362	13.3076	4.3286	18.3988	11.9222
0.0141	17.5038	14.8736	2.6302	17.7072	13.3937	4.3135	18.4424	11.9859
0.0142	17.6209	15.0049	2.616	17.7777	13.4794	4.2983	18.4857	12.0494
0.0144	17.7369	15.1355	2.6014	17.8476	13.5649	4.2827	18.5288	12.1128
0.0145	17.8518	15.2653	2.5865	17.9171	13.65	4.2671	18.5716	12.1759
0.0146	17.9656	15.3945	2.5711	17.986	13.7349	4.2511	18.6143	12.2389
0.0147	18.0782	15.5229	2.5553	18.0545	13.8195	4.235	18.6566	12.3017
0.0149	18.1896	15.6506	2.539	18.1224	13.9038	4.2186	18.6987	12.3644
0.015	18.2999	15.7774	2.5225	18.1898	13.9878	4.202	18.7406	12.4268
0.0151	18.4091	15.9035	2.5056	18.2567	14.0715	4.1852	18.7823	12.489
0.0152	18.517	16.0287	2.4883	18.3232	14.1548	4.1684	18.8237	12.5511
0.0154	18.6238	16.1531	2.4707	18.3891	14.2379	4.1512	18.8648	12.613
0.0155	18.7294	16.2766	2.4528	18.4545	14.3206	4.1339	18.9057	12.6747
0.0156	18.8338	16.3993	2.4345	18.5194	14.403	4.1164	18.9464	12.7362
0.0157	18.937	16.5211	2.4159	18.5838	14.4851	4.0987	18.9869	12.7975
0.0159	19.0391	16.6419	2.3972	18.6477	14.5668	4.0809	19.0271	12.8586
0.016	19.14	16.7619	2.3781	18.7112	14.6482	4.063	19.0671	12.9195
0.0161	19.2397	16.8809	2.3588	18.7741	14.7293	4.0448	19.1069	12.9803
0.0162	19.3381	16.999	2.3391	18.8366	14.81	4.0266	19.1464	13.0408
0.0164	19.4355	17.1161	2.3194	18.8985	14.8904	4.0081	19.1857	13.1012
0.0165	19.5316	17.2322	2.2994	18.96	14.9704	3.9896	19.2248	13.1614
0.0166	19.6265	17.3474	2.2791	19.021	15.0501	3.9709	19.2636	13.2213
0.0167	19.7203	17.4615	2.2588	19.0814	15.1294	3.952	19.3022	13.2811
0.0169	19.8129	17.5747	2.2382	19.1415	15.2084	3.9331	19.3406	13.3407
0.017	19.9043	17.6869	2.2174	19.201	15.287	3.914	19.3788	13.4001
0.0171	19.9945	17.798	2.1965	19.26	15.3652	3.8948	19.4167	13.4593
0.0172	20.0835	17.9081	2.1754	19.3186	15.4431	3.8755	19.4544	13.5183
0.0174	20.1714	18.0172	2.1542	19.3767	15.5206	3.8561	19.4919	13.5771
0.0175	20.2581	18.1252	2.1329	19.4343	15.5978	3.8365	19.5292	13.6357
0.0176	20.3437	18.2322	2.1115	19.4915	15.6745	3.817	19.5663	13.6941
0.0177	20.4281	18.3381	2.09	19.5482	15.7509	3.7973	19.6031	13.7523
0.0179	20.5113	18.443	2.0683	19.6044	15.8269	3.7775	19.6397	13.8103
0.018	20.5934	18.5468	2.0466	19.6601	15.9026	3.7575	19.6761	13.8681
0.0181	20.6744	18.6495	2.0249	19.7154	15.9778	3.7376	19.7123	13.9258
0.0182	20.7542	18.7512	2.003	19.7703	16.0527	3.7176	19.7483	13.9832
0.0184	20.8329	18.8518	1.9811	19.8246	16.1272	3.6974	19.7841	14.0404
0.0185	20.9105	18.9513	1.9592	19.8785	16.2013	3.6772	19.8196	14.0974
0.0186	20.987	19.0497	1.9373	19.932	16.275	3.657	19.855	14.1543
0.0187	21.0623	19.147	1.9153	19.985	16.3483	3.6367	19.8901	14.2109
0.0189	21.1366	19.2433	1.8933	20.0375	16.4213	3.6162	19.925	14.2673
0.019	21.2097	19.3384	1.8713	20.0896	16.4938	3.5958	19.9597	14.3235

	Nd=5			Nd=2			Nd=1	
	Rock ‰	Fluid ‰		Rock ‰	Fluid ‰		Rock ‰	Fluid ‰
z (km)	**δ18O**	**δ18O**	**Δr-fl**	**δ18O**	**δ18O**	**Δr-fl**	**δ18O**	**δ18O**
0.0191	21.2818	19.4325	1.8493	20.1413	16.566	3.5753	19.9942	14.3796
0.0192	21.3528	19.5255	1.8273	20.1925	16.6377	3.5548	20.0285	14.4354
0.0194	21.4227	19.6174	1.8053	20.2433	16.7091	3.5342	20.0626	14.491
0.0195	21.4916	19.7082	1.7834	20.2936	16.7801	3.5135	20.0965	14.5465
0.0196	21.5594	19.7979	1.7615	20.3435	16.8506	3.4929	20.1301	14.6017
0.0197	21.6261	19.8865	1.7396	20.3929	16.9208	3.4721	20.1636	14.6567
0.0199	21.6919	19.974	1.7179	20.442	16.9905	3.4515	20.1969	14.7115
0.02	21.7566	20.0605	1.6961	20.4905	17.0599	3.4306	20.23	14.7661
0.0201	21.8202	20.1459	1.6743	20.5387	17.1289	3.4098	20.2628	14.8206
0.0202	21.8829	20.2302	1.6527	20.5864	17.1974	3.389	20.2955	14.8748
0.0204	21.9446	20.3134	1.6312	20.6338	17.2656	3.3682	20.328	14.9288
0.0205	22.0053	20.3956	1.6097	20.6807	17.3333	3.3474	20.3603	14.9826
0.0206	22.065	20.4767	1.5883	20.7271	17.4007	3.3264	20.3923	15.0362
0.0207	22.1237	20.5567	1.567	20.7732	17.4676	3.3056	20.4242	15.0896
0.0209	22.1814	20.6357	1.5457	20.8188	17.5342	3.2846	20.4559	15.1428
0.021	22.2383	20.7136	1.5247	20.8641	17.6003	3.2638	20.4874	15.1959
0.0211	22.2941	20.7905	1.5036	20.9089	17.666	3.2429	20.5187	15.2487
0.0212	22.3491	20.8663	1.4828	20.9533	17.7313	3.222	20.5498	15.3013
0.0214	22.4031	20.9411	1.462	20.9973	17.7962	3.2011	20.5808	15.3537
0.0215	22.4562	21.0148	1.4414	21.0409	17.8607	3.1802	20.6115	15.4059
0.0216	22.5084	21.0875	1.4209	21.0841	17.9248	3.1593	20.642	15.4579
0.0217	22.5597	21.1592	1.4005	21.1269	17.9885	3.1384	20.6724	15.5096
0.0219	22.6101	21.2299	1.3802	21.1694	18.0518	3.1176	20.7026	15.5612
0.022	22.6596	21.2996	1.36	21.2114	18.1147	3.0967	20.7325	15.6126
0.0221	22.7083	21.3683	1.34	21.253	18.1772	3.0758	20.7623	15.6638
0.0222	22.7562	21.436	1.3202	21.2943	18.2392	3.0551	20.792	15.7148
0.0224	22.8032	21.5027	1.3005	21.3351	18.3009	3.0342	20.8214	15.7656
0.0225	22.8493	21.5684	1.2809	21.3756	18.3621	3.0135	20.8506	15.8162
0.0226	22.8947	21.6331	1.2616	21.4157	18.423	2.9927	20.8797	15.8665
0.0227	22.9392	21.6969	1.2423	21.4555	18.4834	2.9721	20.9086	15.9167
0.0229	22.9829	21.7597	1.2232	21.4948	18.5434	2.9514	20.9373	15.9667
0.023	23.0259	21.8215	1.2044	21.5338	18.6031	2.9307	20.9658	16.0165
0.0231	23.068	21.8824	1.1856	21.5724	18.6623	2.9101	20.9942	16.066
0.0232	23.1094	21.9424	1.167	21.6106	18.7211	2.8895	21.0224	16.1154
0.0234	23.1501	22.0014	1.1487	21.6485	18.7795	2.869	21.0504	16.1646
0.0235	23.1899	22.0595	1.1304	21.686	18.8375	2.8485	21.0782	16.2136
0.0236	23.2291	22.1167	1.1124	21.7232	18.8951	2.8281	21.1058	16.2623
0.0237	23.2675	22.173	1.0945	21.76	18.9523	2.8077	21.1333	16.3109
0.0239	23.3052	22.2284	1.0768	21.7964	19.0092	2.7872	21.1606	16.3593
0.024	23.3422	22.2829	1.0593	21.8325	19.0656	2.7669	21.1877	16.4074
0.0241	23.3785	22.3366	1.0419	21.8683	19.1216	2.7467	21.2147	16.4554
0.0242	23.4141	22.3893	1.0248	21.9037	19.1772	2.7265	21.2415	16.5032
0.0244	23.449	22.4412	1.0078	21.9387	19.2324	2.7063	21.2681	16.5507
0.0245	23.4833	22.4923	0.991	21.9734	19.2872	2.6862	21.2946	16.5981
0.0246	23.5169	22.5425	0.9744	22.0078	19.3416	2.6662	21.3208	16.6453
0.0247	23.5499	22.5919	0.958	22.0418	19.3957	2.6461	21.347	16.6922
0.0249	23.5822	22.6405	0.9417	22.0755	19.4493	2.6262	21.3729	16.739
0.025	23.6139	22.6882	0.9257	22.1089	19.5025	2.6064	21.3987	16.7856
0.0251	23.6449	22.7352	0.9097	22.1419	19.5554	2.5865	21.4243	16.8319
0.0252	23.6754	22.7813	0.8941	22.1747	19.6078	2.5669	21.4498	16.8781
0.0254	23.7052	22.8266	0.8786	22.207	19.6599	2.5471	21.4751	16.9241

	Nd=5			Nd=2			Nd=1	
	Rock ‰	Fluid ‰		Rock ‰	Fluid ‰		Rock ‰	Fluid ‰
z (km)	δ18O	δ18O	Δr-fl	δ18O	δ18O	Δr-fl	δ18O	δ18O
0.0255	23.7345	22.8712	0.8633	22.2391	19.7116	2.5275	21.5002	16.9699
0.0256	23.7632	22.915	0.8482	22.2708	19.7629	2.5079	21.5252	17.0154
0.0257	23.7913	22.9581	0.8332	22.3023	19.8138	2.4885	21.55	17.0608
0.0259	23.8188	23.0004	0.8184	22.3334	19.8643	2.4691	21.5747	17.106
0.026	23.8458	23.0419	0.8039	22.3642	19.9144	2.4498	21.5992	17.151
0.0261	23.8723	23.0828	0.7895	22.3946	19.9642	2.4304	21.6235	17.1958
0.0262	23.8982	23.1229	0.7753	22.4248	20.0136	2.4112	21.6477	17.2404
0.0264	23.9236	23.1622	0.7614	22.4547	20.0625	2.3922	21.6718	17.2848
0.0265	23.9484	23.2009	0.7475	22.4843	20.1112	2.3731	21.6956	17.329
0.0266	23.9728	23.2389	0.7339	22.5135	20.1594	2.3541	21.7194	17.373
0.0267	23.9966	23.2762	0.7204	22.5425	20.2073	2.3352	21.7429	17.4168
0.0269	24.02	23.3128	0.7072	22.5712	20.2547	2.3165	21.7664	17.4604
0.027	24.0429	23.3488	0.6941	22.5996	20.3019	2.2977	21.7896	17.5038
0.0271	24.0653	23.3841	0.6812	22.6276	20.3486	2.279	21.8128	17.5471
0.0272	24.0872	23.4187	0.6685	22.6554	20.395	2.2604	21.8357	17.5901
0.0274	24.1086	23.4527	0.6559	22.683	20.441	2.242	21.8586	17.6329
0.0275	24.1297	23.4861	0.6436	22.7102	20.4866	2.2236	21.8812	17.6756
0.0276	24.1502	23.5189	0.6313	22.7371	20.5319	2.2052	21.9038	17.7181
0.0277	24.1704	23.551	0.6194	22.7638	20.5768	2.187	21.9261	17.7603
0.0279	24.1901	23.5825	0.6076	22.7902	20.6213	2.1689	21.9484	17.8024
0.028	24.2094	23.6135	0.5959	22.8163	20.6655	2.1508	21.9705	17.8443
0.0281	24.2282	23.6438	0.5844	22.8421	20.7093	2.1328	21.9924	17.886
0.0282	24.2467	23.6736	0.5731	22.8677	20.7528	2.1149	22.0142	17.9275
0.0284	24.2648	23.7028	0.562	22.893	20.7959	2.0971	22.0359	17.9688
0.0285	24.2824	23.7314	0.551	22.9181	20.8387	2.0794	22.0574	18.0099
0.0286	24.2997	23.7595	0.5402	22.9428	20.8811	2.0617	22.0788	18.0508
0.0287	24.3167	23.787	0.5297	22.9673	20.9231	2.0442	22.1	18.0916
0.0289	24.3332	23.814	0.5192	22.9916	20.9648	2.0268	22.1211	18.1321
0.029	24.3494	23.8405	0.5089	23.0156	21.0062	2.0094	22.1421	18.1725
0.0291	24.3652	23.8665	0.4987	23.0393	21.0472	1.9921	22.1629	18.2127
0.0292	24.3807	23.8919	0.4888	23.0628	21.0879	1.9749	22.1836	18.2526
0.0294	24.3958	23.9168	0.479	23.0861	21.1282	1.9579	22.2041	18.2925
0.0295	24.4106	23.9413	0.4693	23.109	21.1682	1.9408	22.2245	18.3321
0.0296	24.4251	23.9652	0.4599	23.1318	21.2078	1.924	22.2448	18.3715
0.0297	24.4392	23.9887	0.4505	23.1543	21.2471	1.9072	22.265	18.4107
0.0299	24.4531	24.0117	0.4414	23.1766	21.2861	1.8905	22.285	18.4498
0.03	24.4666	24.0344	0.4322	23.1986	21.3247	1.8739	22.3049	18.4887
0.0301	24.4798	24.0565	0.4233	23.2204	21.363	1.8574	22.3246	18.5274
0.0302	24.4927	24.0781	0.4146	23.2419	21.401	1.8409	22.3442	18.5659
0.0304	24.5053	24.0993	0.406	23.2632	21.4386	1.8246	22.3637	18.6042
0.0305	24.5177	24.1201	0.3976	23.2843	21.476	1.8083	22.3831	18.6423
0.0306	24.5297	24.1404	0.3893	23.3052	21.513	1.7922	22.4023	18.6803
0.0307	24.5415	24.1603	0.3812	23.3258	21.5496	1.7762	22.4214	18.718
0.0309	24.553	24.1798	0.3732	23.3462	21.586	1.7602	22.4404	18.7556
0.031	24.5643	24.1989	0.3654	23.3664	21.622	1.7444	22.4592	18.793
0.0311	24.5752	24.2176	0.3576	23.3863	21.6577	1.7286	22.478	18.8303
0.0312	24.586	24.2359	0.3501	23.4061	21.6931	1.713	22.4966	18.8673
0.0314	24.5964	24.2538	0.3426	23.4256	21.7282	1.6974	22.515	18.9042
0.0315	24.6067	24.2714	0.3353	23.4449	21.763	1.6819	22.5334	18.9409
0.0316	24.6167	24.2885	0.3282	23.464	21.7974	1.6666	22.5516	18.9774
0.0317	24.6264	24.3053	0.3211	23.4829	21.8316	1.6513	22.5697	19.0137

	Nd=5			Nd=2			Nd=1	
	Rock ‰	Fluid ‰		Rock ‰	Fluid ‰		Rock ‰	Fluid ‰
z (km)	δ18O	δ18O	Δr-fl	δ18O	δ18O	Δr-fl	δ18O	δ18O
0.0319	24.636	24.3218	0.3142	23.5015	21.8654	1.6361	22.5877	19.0499
0.032	24.6453	24.3379	0.3074	23.52	21.899	1.621	22.6056	19.0858
0.0321	24.6544	24.3536	0.3008	23.5383	21.9322	1.6061	22.6233	19.1216
0.0322	24.6632	24.369	0.2942	23.5563	21.9652	1.5911	22.6409	19.1573
0.0324	24.6719	24.3841	0.2878	23.5742	21.9978	1.5764	22.6584	19.1927
0.0325	24.6804	24.3989	0.2815	23.5918	22.0301	1.5617	22.6758	19.228
0.0326	24.6886	24.4133	0.2753	23.6093	22.0622	1.5471	22.6931	19.2631
0.0327	24.6967	24.4274	0.2693	23.6266	22.0939	1.5327	22.7102	19.298
0.0329	24.7045	24.4412	0.2633	23.6436	22.1254	1.5182	22.7273	19.3327
0.033	24.7122	24.4547	0.2575	23.6605	22.1566	1.5039	22.7442	19.3673
0.0331	24.7197	24.4679	0.2518	23.6772	22.1875	1.4897	22.761	19.4017
0.0332	24.727	24.4809	0.2461	23.6937	22.2181	1.4756	22.7777	19.4359
0.0334	24.7342	24.4935	0.2407	23.71	22.2484	1.4616	22.7943	19.47
0.0335	24.7411	24.5059	0.2352	23.7261	22.2784	1.4477	22.8107	19.5039
0.0336	24.7479	24.5179	0.23	23.7421	22.3082	1.4339	22.8271	19.5376
0.0337	24.7545	24.5297	0.2248	23.7579	22.3376	1.4203	22.8433	19.5711
0.0339	24.761	24.5413	0.2197	23.7734	22.3668	1.4066	22.8595	19.6045
0.034	24.7673	24.5526	0.2147	23.7888	22.3958	1.393	22.8755	19.6377
0.0341	24.7735	24.5636	0.2099	23.8041	22.4244	1.3797	22.8914	19.6708
0.0342	24.7795	24.5744	0.2051	23.8191	22.4528	1.3663	22.9072	19.7036
0.0344	24.7853	24.5849	0.2004	23.834	22.4809	1.3531	22.9229	19.7363
0.0345	24.791	24.5952	0.1958	23.8487	22.5088	1.3399	22.9385	19.7689
0.0346	24.7966	24.6053	0.1913	23.8633	22.5364	1.3269	22.954	19.8012
0.0347	24.802	24.6151	0.1869	23.8777	22.5637	1.314	22.9693	19.8334
0.0349	24.8073	24.6248	0.1825	23.8919	22.5907	1.3012	22.9846	19.8655
0.035	24.8125	24.6341	0.1784	23.9059	22.6175	1.2884	22.9998	19.8973
0.0351	24.8175	24.6433	0.1742	23.9198	22.6441	1.2757	23.0148	19.929
0.0352	24.8224	24.6523	0.1701	23.9335	22.6704	1.2631	23.0298	19.9606
0.0354	24.8272	24.661	0.1662	23.9471	22.6964	1.2507	23.0446	19.992
0.0355	24.8318	24.6696	0.1622	23.9605	22.7222	1.2383	23.0594	20.0232
0.0356	24.8364	24.6779	0.1585	23.9738	22.7477	1.2261	23.074	20.0542
0.0357	24.8408	24.6861	0.1547	23.9869	22.773	1.2139	23.0886	20.0851
0.0359	24.8451	24.6941	0.151	23.9998	22.798	1.2018	23.103	20.1158
0.036	24.8493	24.7019	0.1474	24.0126	22.8228	1.1898	23.1174	20.1464
0.0361	24.8534	24.7095	0.1439	24.0253	22.8473	1.178	23.1316	20.1768
0.0362	24.8574	24.7169	0.1405	24.0378	22.8717	1.1661	23.1458	20.2071
0.0364	24.8613	24.7241	0.1372	24.0501	22.8957	1.1544	23.1598	20.2372
0.0365	24.8651	24.7312	0.1339	24.0623	22.9196	1.1427	23.1738	20.2671
0.0366	24.8688	24.7381	0.1307	24.0744	22.9431	1.1313	23.1877	20.2969
0.0367	24.8724	24.7452	0.1272	24.0863	22.9665	1.1198	23.2014	20.3265
0.0369	24.8759	24.7514	0.1245	24.0981	22.9896	1.1085	23.2151	20.3559
0.037	24.8793	24.7578	0.1215	24.1097	23.0125	1.0972	23.2287	20.3853
0.0371	24.8826	24.7641	0.1185	24.1212	23.0352	1.086	23.2421	20.4144
0.0372	24.8859	24.7702	0.1157	24.1326	23.0577	1.0749	23.2555	20.4434
0.0374	24.889	24.7762	0.1128	24.1438	23.0799	1.0639	23.2688	20.4722
0.0375	24.8921	24.782	0.1101	24.1549	23.1019	1.053	23.282	20.5009
0.0376	24.8951	24.7877	0.1074	24.1659	23.1236	1.0423	23.2951	20.5294
0.0377	24.898	24.7933	0.1047	24.1767	23.1452	1.0315	23.3081	20.5578
0.0379	24.9009	24.7987	0.1022	24.1874	23.1665	1.0209	23.321	20.5861
0.038	24.9036	24.8039	0.0997	24.198	23.1877	1.0103	23.3339	20.6141
0.0381	24.9063	24.8091	0.0972	24.2084	23.2086	0.9998	23.3466	20.6421

	Nd=5			Nd=2			Nd=1	
	Rock ‰	Fluid ‰		Rock ‰	Fluid ‰		Rock ‰	Fluid ‰
z (km)	**δ18O**	**δ18O**	**Δr-fl**	**δ18O**	**δ18O**	**Δr-fl**	**δ18O**	**δ18O**
0.0382	24.9089	24.8141	0.0948	24.2188	23.2293	0.9895	23.3593	20.6698
0.0384	24.9115	24.819	0.0925	24.229	23.2497	0.9793	23.3718	20.6974
0.0385	24.914	24.8238	0.0902	24.239	23.27	0.969	23.3843	20.7249
0.0386	24.9164	24.8285	0.0879	24.249	23.2901	0.9589	23.3967	20.7522
0.0387	24.9187	24.833	0.0857	24.2588	23.3099	0.9489	23.409	20.7794
0.0389	24.921	24.8374	0.0836	24.2686	23.3296	0.939	23.4212	20.8064
0.039	24.9233	24.842	0.0813	24.2782	23.3491	0.9291	23.4333	20.8333
0.0391	24.9254	24.8462	0.0792	24.2876	23.3683	0.9193	23.4454	20.8601
0.0392	24.9275	24.8503	0.0772	24.297	23.3874	0.9096	23.4573	20.8867
0.0394	24.9296	24.8544	0.0752	24.3063	23.4062	0.9001	23.4692	20.9131
0.0395	24.9316	24.8583	0.0733	24.3154	23.4249	0.8905	23.481	20.9394
0.0396	24.9336	24.8621	0.0715	24.3244	23.4434	0.881	23.4927	20.9655
0.0397	24.9354	24.8658	0.0696	24.3334	23.4616	0.8718	23.5043	20.9916
0.0399	24.9373	24.8694	0.0679	24.3422	23.4797	0.8625	23.5158	21.0174
0.04	24.9391	24.8729	0.0662	24.3509	23.4976	0.8533	23.5273	21.0431
0.0401	24.9408	24.8764	0.0644	24.3595	23.5153	0.8442	23.5387	21.0687
0.0402	24.9425	24.8797	0.0628	24.368	23.5328	0.8352	23.55	21.0942
0.0404	24.9442	24.883	0.0612	24.3763	23.5502	0.8261	23.5612	21.1195
0.0405	24.9458	24.8862	0.0596	24.3846	23.5673	0.8173	23.5723	21.1446
0.0406	24.9473	24.8893	0.058	24.3928	23.5843	0.8085	23.5834	21.1697
0.0407	24.9489	24.8923	0.0566	24.4009	23.6011	0.7998	23.5943	21.1945
0.0409	24.9503	24.8952	0.0551	24.4089	23.6177	0.7912	23.6052	21.2193
0.041	24.9518	24.8981	0.0537	24.4168	23.6342	0.7826	23.616	21.2439
0.0411	24.9532	24.9009	0.0523	24.4246	23.6504	0.7742	23.6268	21.2683
0.0412	24.9545	24.9036	0.0509	24.4322	23.6665	0.7657	23.6375	21.2927
0.0414	24.9559	24.9062	0.0497	24.4398	23.6824	0.7574	23.648	21.3169
0.0415	24.9571	24.9088	0.0483	24.4473	23.6982	0.7491	23.6586	21.3409
0.0416	24.9584	24.9113	0.0471	24.4547	23.7138	0.7409	23.669	21.3648
0.0417	24.9596	24.9138	0.0458	24.4621	23.7292	0.7329	23.6793	21.3886
0.0419	24.9608	24.9162	0.0446	24.4693	23.7444	0.7249	23.6896	21.4123
0.042	24.9619	24.9185	0.0434	24.4764	23.7595	0.7169	23.6998	21.4358
0.0421	24.963	24.9208	0.0422	24.4835	23.7745	0.709	23.71	21.4592
0.0422	24.9641	24.923	0.0411	24.4904	23.7892	0.7012	23.7201	21.4824
0.0424	24.9652	24.9251	0.0401	24.4973	23.8038	0.6935	23.73	21.5056
0.0425	24.9662	24.9272	0.039	24.5041	23.8183	0.6858	23.74	21.5285
0.0426	24.9672	24.9292	0.038	24.5108	23.8325	0.6783	23.7498	21.5514
0.0427	24.9682	24.9312	0.037	24.5174	23.8467	0.6707	23.7596	21.5741
0.0429	24.9691	24.9331	0.036	24.5239	23.8607	0.6632	23.7693	21.5967
0.043	24.97	24.935	0.035	24.5304	23.8745	0.6559	23.7789	21.6192
0.0431	24.9709	24.9369	0.034	24.5367	23.8881	0.6486	23.7885	21.6415
0.0432	24.9718	24.9386	0.0332	24.543	23.9017	0.6413	23.798	21.6637
0.0434	24.9726	24.9404	0.0322	24.5492	23.915	0.6342	23.8074	21.6858
0.0435	24.9734	24.942	0.0314	24.5553	23.9283	0.627	23.8168	21.7078
0.0436	24.9742	24.9437	0.0305	24.5614	23.9414	0.62	23.8261	21.7296
0.0437	24.975	24.9453	0.0297	24.5674	23.9543	0.6131	23.8353	21.7513
0.0439	24.9757	24.9468	0.0289	24.5733	23.9671	0.6062	23.8445	21.7729
0.044	24.9765	24.9483	0.0282	24.5791	23.9797	0.5994	23.8536	21.7944
0.0441	24.9772	24.9502	0.027	24.5848	23.9922	0.5926	23.8626	21.8157
0.0442	24.9778	24.9516	0.0262	24.5905	24.0046	0.5859	23.8716	21.8369
0.0444	24.9785	24.953	0.0255	24.5961	24.0169	0.5792	23.8805	21.858
0.0445	24.9792	24.9543	0.0249	24.6016	24.029	0.5726	23.8893	21.879

z (km)	Nd=5 Rock ‰ δ18O	Nd=5 Fluid ‰ δ18O	Δr-fl	Nd=2 Rock ‰ δ18O	Nd=2 Fluid ‰ δ18O	Δr-fl	Nd=1 Rock ‰ δ18O	Nd=1 Fluid ‰ δ18O
0.0446	24.9798	24.9556	0.0242	24.6071	24.0409	0.5662	23.8981	21.8998
0.0447	24.9804	24.9569	0.0235	24.6125	24.0528	0.5597	23.9068	21.9205
0.0449	24.981	24.9582	0.0228	24.6178	24.0644	0.5534	23.9154	21.9411
0.045	24.9816	24.9594	0.0222	24.6231	24.076	0.5471	23.924	21.9616
0.0451	24.9821	24.9605	0.0216	24.6283	24.0875	0.5408	23.9325	21.982
0.0452	24.9827	24.9617	0.021	24.6334	24.0988	0.5346	23.9409	22.0022
0.0454	24.9832	24.9628	0.0204	24.6384	24.1099	0.5285	23.9493	22.0223
0.0455	24.9837	24.9639	0.0198	24.6434	24.121	0.5224	23.9576	22.0423
0.0456	24.9842	24.9649	0.0193	24.6483	24.1319	0.5164	23.9659	22.0622
0.0457	24.9847	24.9659	0.0188	24.6532	24.1427	0.5105	23.9741	22.082
0.0459	24.9851	24.9669	0.0182	24.658	24.1534	0.5046	23.9823	22.1016
0.046	24.9856	24.9679	0.0177	24.6627	24.164	0.4987	23.9903	22.1212
0.0461	24.986	24.9688	0.0172	24.6674	24.1744	0.493	23.9984	22.1406
0.0462	24.9865	24.9697	0.0168	24.672	24.1847	0.4873	24.0063	22.1599
0.0464	24.9869	24.9706	0.0163	24.6766	24.195	0.4816	24.0142	22.1791
0.0465	24.9873	24.9715	0.0158	24.6811	24.205	0.4761	24.0221	22.1982
0.0466	24.9877	24.9723	0.0154	24.6855	24.215	0.4705	24.0299	22.2171
0.0467	24.9881	24.9731	0.015	24.6899	24.2249	0.465	24.0376	22.236
0.0469	24.9884	24.9739	0.0145	24.6942	24.2346	0.4596	24.0453	22.2547
0.047	24.9888	24.9747	0.0141	24.6985	24.2443	0.4542	24.0529	22.2733
0.0471	24.9891	24.9754	0.0137	24.7027	24.2538	0.4489	24.0604	22.2919
0.0472	24.9895	24.9762	0.0133	24.7068	24.2632	0.4436	24.068	22.3103
0.0474	24.9898	24.9769	0.0129	24.7109	24.2725	0.4384	24.0754	22.3286
0.0475	24.9901	24.9776	0.0125	24.715	24.2817	0.4333	24.0828	22.3467
0.0476	24.9904	24.9782	0.0122	24.7189	24.2908	0.4281	24.0901	22.3648
0.0477	24.9907	24.9789	0.0118	24.7229	24.2998	0.4231	24.0974	22.3828
0.0479	24.991	24.9795	0.0115	24.7268	24.3086	0.4182	24.1046	22.4006
0.048	24.9913	24.9801	0.0112	24.7306	24.3174	0.4132	24.1118	22.4184
0.0481	24.9915	24.9807	0.0108	24.7344	24.3261	0.4083	24.1189	22.436
0.0482	24.9918	24.9817	0.0101	24.7381	24.3347	0.4034	24.126	22.4536
0.0484	24.9921	24.9823	0.0098	24.7418	24.3431	0.3987	24.133	22.471
0.0485	24.9923	24.9828	0.0095	24.7454	24.3515	0.3939	24.14	22.4883
0.0486	24.9926	24.9833	0.0093	24.749	24.3598	0.3892	24.1469	22.5056
0.0487	24.9928	24.9838	0.009	24.7526	24.368	0.3846	24.1538	22.5227
0.0489	24.993	24.9843	0.0087	24.7561	24.3761	0.38	24.1606	22.5397
0.049	24.9932	24.9848	0.0084	24.7595	24.3841	0.3754	24.1673	22.5566
0.0491	24.9934	24.9852	0.0082	24.7629	24.3919	0.371	24.174	22.5734
0.0492	24.9937	24.9857	0.008	24.7663	24.3997	0.3666	24.1807	22.5901
0.0494	24.9939	24.9861	0.0078	24.7696	24.4075	0.3621	24.1873	22.6067
0.0495	24.994	24.9865	0.0075	24.7729	24.4151	0.3578	24.1939	22.6232
0.0496	24.9942	24.987	0.0072	24.7761	24.4226	0.3535	24.2004	22.6396
0.0497	24.9944	24.9874	0.007	24.7793	24.43	0.3493	24.2068	22.6559
0.0499	24.9946	24.9877	0.0069	24.7824	24.4374	0.345	24.2132	22.6721
0.05	24.9948	24.9881	0.0067	24.7855	24.4447	0.3408	24.2196	22.6882

			Nd=0.75			Nd=0.5		
		Rock ‰	Fluid ‰		Rock ‰	Fluid ‰		
z (km)	Δr-fl	δ18O	δ18O	Δr-fl	δ18O	δ18O	Δr-fl	
0	7.7255	13.9197	4	9.9197	16.7371	4	12.7371	
0.0001	7.7297	13.9764	4.0701	9.9063	16.7707	4.06	12.7107	
0.0002	7.7334	14.0329	4.1402	9.8927	16.8042	4.1199	12.6843	
0.0004	7.7368	14.0892	4.2102	9.879	16.8376	4.1797	12.6579	
0.0005	7.7397	14.1452	4.2802	9.865	16.8708	4.2394	12.6314	
0.0006	7.7422	14.2009	4.35	9.8509	16.9039	4.299	12.6049	
0.0007	7.7444	14.2564	4.4198	9.8366	16.9369	4.3585	12.5784	
0.0009	7.7461	14.3117	4.4895	9.8222	16.9697	4.4178	12.5519	
0.001	7.7474	14.3667	4.5592	9.8075	17.0025	4.4771	12.5254	
0.0011	7.7484	14.4215	4.6288	9.7927	17.0351	4.5362	12.4989	
0.0012	7.7489	14.4761	4.6982	9.7779	17.0676	4.5953	12.4723	
0.0014	7.7491	14.5304	4.7677	9.7627	17.1	4.6542	12.4458	
0.0015	7.749	14.5845	4.837	9.7475	17.1323	4.713	12.4193	
0.0016	7.7484	14.6383	4.9062	9.7321	17.1644	4.7717	12.3927	
0.0017	7.7475	14.6919	4.9754	9.7165	17.1965	4.8303	12.3662	
0.0019	7.7463	14.7453	5.0445	9.7008	17.2284	4.8888	12.3396	
0.002	7.7446	14.7984	5.1135	9.6849	17.2602	4.9472	12.313	
0.0021	7.7426	14.8513	5.1824	9.6689	17.2919	5.0055	12.2864	
0.0023	7.7403	14.904	5.2512	9.6528	17.3234	5.0636	12.2598	
0.0024	7.7376	14.9564	5.32	9.6364	17.3549	5.1217	12.2332	
0.0025	7.7346	15.0086	5.3886	9.62	17.3862	5.1796	12.2066	
0.0026	7.7313	15.0606	5.4572	9.6034	17.4174	5.2375	12.1799	
0.0028	7.7276	15.1123	5.5257	9.5866	17.4486	5.2952	12.1534	
0.0029	7.7236	15.1638	5.594	9.5698	17.4795	5.3528	12.1267	
0.003	7.7193	15.2151	5.6623	9.5528	17.5104	5.4103	12.1001	
0.0031	7.7146	15.2661	5.7305	9.5356	17.5412	5.4677	12.0735	
0.0033	7.7097	15.317	5.7986	9.5184	17.5718	5.5249	12.0469	
0.0034	7.7044	15.3676	5.8665	9.5011	17.6024	5.5821	12.0203	
0.0035	7.6988	15.4179	5.9344	9.4835	17.6328	5.6392	11.9936	
0.0036	7.6929	15.4681	6.0022	9.4659	17.6631	5.6961	11.967	
0.0038	7.6867	15.518	6.0699	9.4481	17.6933	5.7529	11.9404	
0.0039	7.6803	15.5677	6.1375	9.4302	17.7234	5.8096	11.9138	
0.004	7.6735	15.6172	6.2049	9.4123	17.7534	5.8662	11.8872	
0.0041	7.6665	15.6664	6.2723	9.3941	17.7833	5.9227	11.8606	
0.0043	7.6591	15.7154	6.3396	9.3758	17.813	5.9791	11.8339	
0.0044	7.6515	15.7642	6.4067	9.3575	17.8427	6.0354	11.8073	
0.0045	7.6436	15.8128	6.4738	9.339	17.8722	6.0916	11.7806	
0.0046	7.6355	15.8612	6.5407	9.3205	17.9017	6.1476	11.7541	
0.0047	7.627	15.9093	6.6075	9.3018	17.931	6.2035	11.7275	
0.0049	7.6183	15.9573	6.6742	9.2831	17.9602	6.2594	11.7008	
0.005	7.6093	16.005	6.7408	9.2642	17.9893	6.3151	11.6742	
0.0051	7.6001	16.0525	6.8073	9.2452	18.0183	6.3707	11.6476	
0.0052	7.5906	16.0997	6.8737	9.226	18.0472	6.4261	11.6211	
0.0054	7.5809	16.1468	6.94	9.2068	18.076	6.4815	11.5945	
0.0055	7.571	16.1937	7.0061	9.1876	18.1046	6.5368	11.5678	
0.0056	7.5607	16.2403	7.0722	9.1681	18.1332	6.5919	11.5413	
0.0057	7.5503	16.2867	7.1381	9.1486	18.1617	6.647	11.5147	
0.0059	7.5396	16.3329	7.2039	9.129	18.19	6.7019	11.4881	
0.006	7.5286	16.3789	7.2695	9.1094	18.2183	6.7567	11.4616	
0.0061	7.5175	16.4247	7.3351	9.0896	18.2464	6.8114	11.435	
0.0062	7.5062	16.4703	7.4005	9.0698	18.2744	6.866	11.4084	

			Nd=0.75			Nd=0.5	
		Rock ‰	Fluid ‰		Rock ‰	Fluid ‰	
z (km)	**Δr-fl**	**δ18O**	**δ18O**	**Δr-fl**	**δ18O**	**δ18O**	**Δr-fl**
0.0064	7.4945	16.5156	7.4658	9.0498	18.3024	6.9204	11.382
0.0065	7.4826	16.5608	7.531	9.0298	18.3302	6.9748	11.3554
0.0066	7.4706	16.6058	7.5961	9.0097	18.3579	7.029	11.3289
0.0067	7.4583	16.6505	7.6611	8.9894	18.3856	7.0832	11.3024
0.0069	7.4459	16.695	7.7259	8.9691	18.4131	7.1372	11.2759
0.007	7.4332	16.7394	7.7906	8.9488	18.4405	7.1911	11.2494
0.0071	7.4203	16.7835	7.8551	8.9284	18.4678	7.2449	11.2229
0.0072	7.4072	16.8274	7.9196	8.9078	18.495	7.2985	11.1965
0.0074	7.3939	16.8711	7.9839	8.8872	18.5221	7.3521	11.17
0.0075	7.3805	16.9146	8.0481	8.8665	18.5491	7.4055	11.1436
0.0076	7.3667	16.9579	8.1121	8.8458	18.576	7.4589	11.1171
0.0077	7.3529	17.0011	8.176	8.8251	18.6028	7.5121	11.0907
0.0079	7.3388	17.044	8.2398	8.8042	18.6295	7.5652	11.0643
0.008	7.3246	17.0867	8.3035	8.7832	18.6561	7.6182	11.0379
0.0081	7.3102	17.1292	8.367	8.7622	18.6827	7.6711	11.0116
0.0082	7.2956	17.1715	8.4304	8.7411	18.7091	7.7239	10.9852
0.0084	7.2808	17.2136	8.4937	8.7199	18.7354	7.7765	10.9589
0.0085	7.2659	17.2555	8.5568	8.6987	18.7616	7.829	10.9326
0.0086	7.2507	17.2972	8.6198	8.6774	18.7877	7.8815	10.9062
0.0087	7.2354	17.3388	8.6827	8.6561	18.8137	7.9338	10.8799
0.0089	7.22	17.3801	8.7454	8.6347	18.8396	7.986	10.8536
0.009	7.2044	17.4212	8.808	8.6132	18.8654	8.0381	10.8273
0.0091	7.1886	17.4622	8.8705	8.5917	18.8911	8.09	10.8011
0.0092	7.1727	17.5029	8.9328	8.5701	18.9167	8.1419	10.7748
0.0094	7.1567	17.5435	8.995	8.5485	18.9423	8.1936	10.7487
0.0095	7.1404	17.5838	9.057	8.5268	18.9677	8.2453	10.7224
0.0096	7.124	17.624	9.1189	8.5051	18.993	8.2968	10.6962
0.0097	7.1076	17.664	9.1807	8.4833	19.0182	8.3482	10.67
0.0099	7.0908	17.7038	9.2423	8.4615	19.0434	8.3995	10.6439
0.01	7.0741	17.7434	9.3038	8.4396	19.0684	8.4507	10.6177
0.0101	7.0571	17.7828	9.3651	8.4177	19.0934	8.5017	10.5917
0.0102	7.04	17.822	9.4263	8.3957	19.1182	8.5527	10.5655
0.0104	7.0229	17.861	9.4874	8.3736	19.143	8.6035	10.5395
0.0105	7.0056	17.8999	9.5483	8.3516	19.1676	8.6542	10.5134
0.0106	6.9881	17.9386	9.609	8.3296	19.1922	8.7048	10.4874
0.0107	6.9705	17.9771	9.6697	8.3074	19.2167	8.7553	10.4614
0.0109	6.9527	18.0154	9.7302	8.2852	19.2411	8.8057	10.4354
0.011	6.9349	18.0535	9.7905	8.263	19.2653	8.856	10.4093
0.0111	6.917	18.0914	9.8507	8.2407	19.2895	8.9061	10.3834
0.0112	6.8989	18.1292	9.9107	8.2185	19.3136	8.9562	10.3574
0.0114	6.8807	18.1667	9.9706	8.1961	19.3377	9.0061	10.3316
0.0115	6.8625	18.2041	10.0304	8.1737	19.3616	9.0559	10.3057
0.0116	6.844	18.2413	10.09	8.1513	19.3854	9.1056	10.2798
0.0117	6.8256	18.2784	10.1495	8.1289	19.4091	9.1552	10.2539
0.0119	6.807	18.3152	10.2088	8.1064	19.4328	9.2047	10.2281
0.012	6.7882	18.3519	10.268	8.0839	19.4563	9.254	10.2023
0.0121	6.7694	18.3884	10.327	8.0614	19.4798	9.3033	10.1765
0.0122	6.7505	18.4247	10.3859	8.0388	19.5032	9.3524	10.1508
0.0124	6.7315	18.4609	10.4446	8.0163	19.5265	9.4014	10.1251
0.0125	6.7124	18.4968	10.5032	7.9936	19.5497	9.4503	10.0994
0.0126	6.6932	18.5326	10.5616	7.971	19.5728	9.4991	10.0737

z (km)	Δr-fl	Nd=0.75 Rock ‰ δ18O	Nd=0.75 Fluid ‰ δ18O	Δr-fl	Nd=0.5 Rock ‰ δ18O	Nd=0.5 Fluid ‰ δ18O	Δr-fl
0.0127	6.6739	18.5682	10.6199	7.9483	19.5958	9.5478	10.048
0.0129	6.6546	18.6037	10.678	7.9257	19.6187	9.5964	10.0223
0.013	6.6351	18.639	10.736	7.903	19.6416	9.6448	9.9968
0.0131	6.6155	18.6741	10.7938	7.8803	19.6643	9.6932	9.9711
0.0132	6.596	18.709	10.8515	7.8575	19.687	9.7414	9.9456
0.0134	6.5762	18.7438	10.909	7.8348	19.7096	9.7895	9.9201
0.0135	6.5565	18.7784	10.9664	7.812	19.7321	9.8375	9.8946
0.0136	6.5367	18.8128	11.0236	7.7892	19.7545	9.8854	9.8691
0.0137	6.5167	18.8471	11.0807	7.7664	19.7768	9.9332	9.8436
0.0139	6.4967	18.8811	11.1376	7.7435	19.799	9.9808	9.8182
0.014	6.4766	18.9151	11.1944	7.7207	19.8212	10.0284	9.7928
0.0141	6.4565	18.9488	11.251	7.6978	19.8433	10.0758	9.7675
0.0142	6.4363	18.9824	11.3074	7.675	19.8652	10.1231	9.7421
0.0144	6.416	19.0158	11.3638	7.652	19.8871	10.1704	9.7167
0.0145	6.3957	19.0491	11.4199	7.6292	19.9089	10.2175	9.6914
0.0146	6.3754	19.0822	11.4759	7.6063	19.9307	10.2645	9.6662
0.0147	6.3549	19.1151	11.5318	7.5833	19.9523	10.3113	9.641
0.0149	6.3343	19.1479	11.5875	7.5604	19.9739	10.3581	9.6158
0.015	6.3138	19.1805	11.643	7.5375	19.9953	10.4048	9.5905
0.0151	6.2933	19.213	11.6984	7.5146	20.0167	10.4513	9.5654
0.0152	6.2726	19.2452	11.7536	7.4916	20.038	10.4977	9.5403
0.0154	6.2518	19.2774	11.8087	7.4687	20.0593	10.544	9.5153
0.0155	6.231	19.3093	11.8636	7.4457	20.0804	10.5902	9.4902
0.0156	6.2102	19.3411	11.9184	7.4227	20.1015	10.6363	9.4652
0.0157	6.1894	19.3728	11.973	7.3998	20.1224	10.6823	9.4401
0.0159	6.1685	19.4043	12.0275	7.3768	20.1433	10.7282	9.4151
0.016	6.1476	19.4356	12.0818	7.3538	20.1642	10.774	9.3902
0.0161	6.1266	19.4668	12.1359	7.3309	20.1849	10.8196	9.3653
0.0162	6.1056	19.4978	12.1899	7.3079	20.2055	10.8651	9.3404
0.0164	6.0845	19.5287	12.2437	7.285	20.2261	10.9106	9.3155
0.0165	6.0634	19.5594	12.2974	7.262	20.2466	10.9559	9.2907
0.0166	6.0423	19.59	12.351	7.239	20.267	11.0011	9.2659
0.0167	6.0211	19.6204	12.4043	7.2161	20.2874	11.0462	9.2412
0.0169	5.9999	19.6507	12.4575	7.1932	20.3076	11.0912	9.2164
0.017	5.9787	19.6808	12.5106	7.1702	20.3278	11.136	9.1918
0.0171	5.9574	19.7107	12.5635	7.1472	20.3479	11.1808	9.1671
0.0172	5.9361	19.7405	12.6162	7.1243	20.3679	11.2254	9.1425
0.0174	5.9148	19.7702	12.6688	7.1014	20.3878	11.27	9.1178
0.0175	5.8935	19.7997	12.7213	7.0784	20.4077	11.3144	9.0933
0.0176	5.8722	19.8291	12.7735	7.0556	20.4275	11.3587	9.0688
0.0177	5.8508	19.8583	12.8257	7.0326	20.4472	11.4029	9.0443
0.0179	5.8294	19.8873	12.8776	7.0097	20.4668	11.447	9.0198
0.018	5.808	19.9163	12.9294	6.9869	20.4864	11.491	8.9954
0.0181	5.7865	19.945	12.9811	6.9639	20.5059	11.5349	8.971
0.0182	5.7651	19.9736	13.0326	6.941	20.5253	11.5787	8.9466
0.0184	5.7437	20.0021	13.0839	6.9182	20.5446	11.6223	8.9223
0.0185	5.7222	20.0305	13.1351	6.8954	20.5638	11.6659	8.8979
0.0186	5.7007	20.0587	13.1861	6.8726	20.583	11.7093	8.8737
0.0187	5.6792	20.0867	13.237	6.8497	20.6021	11.7526	8.8495
0.0189	5.6577	20.1146	13.2877	6.8269	20.6211	11.7958	8.8253
0.019	5.6362	20.1424	13.3383	6.8041	20.6401	11.839	8.8011

		Nd=0.75				Nd=0.5		
		Rock ‰	Fluid ‰		Rock ‰	Fluid ‰		
z (km)	**Δr-fl**	**δ18O**	**δ18O**	**Δr-fl**	**δ18O**	**δ18O**	**Δr-fl**	
0.0191	5.6146	20.17	13.3886	6.7814	20.6589	11.882	8.7769	
0.0192	5.5931	20.1975	13.4389	6.7586	20.6777	11.9249	8.7528	
0.0194	5.5716	20.2248	13.489	6.7358	20.6965	11.9676	8.7289	
0.0195	5.55	20.252	13.5389	6.7131	20.7151	12.0103	8.7048	
0.0196	5.5284	20.2791	13.5887	6.6904	20.7337	12.0529	8.6808	
0.0197	5.5069	20.306	13.6383	6.6677	20.7522	12.0953	8.6569	
0.0199	5.4854	20.3328	13.6877	6.6451	20.7706	12.1377	8.6329	
0.02	5.4639	20.3595	13.737	6.6225	20.789	12.1799	8.6091	
0.0201	5.4422	20.386	13.7862	6.5998	20.8073	12.2221	8.5852	
0.0202	5.4207	20.4124	13.8352	6.5772	20.8255	12.2641	8.5614	
0.0204	5.3992	20.4386	13.884	6.5546	20.8436	12.306	8.5376	
0.0205	5.3777	20.4647	13.9327	6.532	20.8617	12.3478	8.5139	
0.0206	5.3561	20.4907	13.9812	6.5095	20.8797	12.3895	8.4902	
0.0207	5.3346	20.5165	14.0296	6.4869	20.8976	12.4311	8.4665	
0.0209	5.3131	20.5423	14.0778	6.4645	20.9155	12.4726	8.4429	
0.021	5.2915	20.5678	14.1258	6.442	20.9333	12.514	8.4193	
0.0211	5.27	20.5933	14.1737	6.4196	20.951	12.5552	8.3958	
0.0212	5.2485	20.6186	14.2215	6.3971	20.9686	12.5964	8.3722	
0.0214	5.2271	20.6438	14.269	6.3748	20.9862	12.6375	8.3487	
0.0215	5.2056	20.6688	14.3165	6.3523	21.0037	12.6784	8.3253	
0.0216	5.1841	20.6938	14.3637	6.3301	21.0211	12.7193	8.3018	
0.0217	5.1628	20.7185	14.4108	6.3077	21.0385	12.76	8.2785	
0.0219	5.1414	20.7432	14.4578	6.2854	21.0558	12.8006	8.2552	
0.022	5.1199	20.7678	14.5046	6.2632	21.073	12.8412	8.2318	
0.0221	5.0985	20.7922	14.5513	6.2409	21.0902	12.8816	8.2086	
0.0222	5.0772	20.8164	14.5978	6.2186	21.1073	12.9219	8.1854	
0.0224	5.0558	20.8406	14.6441	6.1965	21.1243	12.9621	8.1622	
0.0225	5.0344	20.8646	14.6903	6.1743	21.1412	13.0022	8.139	
0.0226	5.0132	20.8885	14.7363	6.1522	21.1581	13.0422	8.1159	
0.0227	4.9919	20.9123	14.7822	6.1301	21.1749	13.0821	8.0928	
0.0229	4.9706	20.936	14.8279	6.1081	21.1917	13.1219	8.0698	
0.023	4.9493	20.9595	14.8735	6.086	21.2084	13.1615	8.0469	
0.0231	4.9282	20.9829	14.9189	6.064	21.225	13.2011	8.0239	
0.0232	4.907	21.0062	14.9641	6.0421	21.2415	13.2406	8.0009	
0.0234	4.8858	21.0294	15.0092	6.0202	21.258	13.2799	7.9781	
0.0235	4.8646	21.0524	15.0542	5.9982	21.2744	13.3192	7.9552	
0.0236	4.8435	21.0754	15.099	5.9764	21.2908	13.3583	7.9325	
0.0237	4.8224	21.0982	15.1436	5.9546	21.3071	13.3974	7.9097	
0.0239	4.8013	21.1209	15.1881	5.9328	21.3233	13.4363	7.887	
0.024	4.7803	21.1434	15.2325	5.9109	21.3395	13.4752	7.8643	
0.0241	4.7593	21.1659	15.2767	5.8892	21.3556	13.5139	7.8417	
0.0242	4.7383	21.1882	15.3207	5.8675	21.3716	13.5525	7.8191	
0.0244	4.7174	21.2104	15.3646	5.8458	21.3875	13.5911	7.7964	
0.0245	4.6965	21.2325	15.4083	5.8242	21.4034	13.6295	7.7739	
0.0246	4.6755	21.2545	15.4519	5.8026	21.4193	13.6678	7.7515	
0.0247	4.6548	21.2764	15.4953	5.7811	21.435	13.706	7.729	
0.0249	4.6339	21.2981	15.5386	5.7595	21.4508	13.7442	7.7066	
0.025	4.6131	21.3198	15.5817	5.7381	21.4664	13.7822	7.6842	
0.0251	4.5924	21.3413	15.6246	5.7167	21.482	13.8201	7.6619	
0.0252	4.5717	21.3627	15.6675	5.6952	21.4975	13.8579	7.6396	
0.0254	4.551	21.384	15.7101	5.6739	21.513	13.8956	7.6174	

z (km)	Δr-fl	Nd=0.75 Rock ‰ δ18O	Fluid ‰ δ18O	Δr-fl	Nd=0.5 Rock ‰ δ18O	Fluid ‰ δ18O	Δr-fl
0.0255	4.5303	21.4051	15.7526	5.6525	21.5284	13.9332	7.5952
0.0256	4.5098	21.4262	15.795	5.6312	21.5437	13.9707	7.573
0.0257	4.4892	21.4472	15.8372	5.61	21.559	14.0081	7.5509
0.0259	4.4687	21.468	15.8793	5.5887	21.5742	14.0454	7.5288
0.026	4.4482	21.4888	15.9212	5.5676	21.5893	14.0826	7.5067
0.0261	4.4277	21.5094	15.963	5.5464	21.6044	14.1197	7.4847
0.0262	4.4073	21.5299	16.0046	5.5253	21.6194	14.1566	7.4628
0.0264	4.387	21.5503	16.046	5.5043	21.6344	14.1935	7.4409
0.0265	4.3666	21.5706	16.0873	5.4833	21.6493	14.2303	7.419
0.0266	4.3464	21.5908	16.1285	5.4623	21.6641	14.267	7.3971
0.0267	4.3261	21.6109	16.1695	5.4414	21.6789	14.3036	7.3753
0.0269	4.306	21.6308	16.2104	5.4204	21.6936	14.3401	7.3535
0.027	4.2858	21.6507	16.2511	5.3996	21.7083	14.3764	7.3319
0.0271	4.2657	21.6705	16.2917	5.3788	21.7229	14.4127	7.3102
0.0272	4.2456	21.6901	16.3321	5.358	21.7374	14.4489	7.2885
0.0274	4.2257	21.7097	16.3724	5.3373	21.7519	14.485	7.2669
0.0275	4.2056	21.7291	16.4125	5.3166	21.7664	14.521	7.2454
0.0276	4.1857	21.7484	16.4525	5.2959	21.7807	14.5569	7.2238
0.0277	4.1658	21.7677	16.4923	5.2754	21.795	14.5926	7.2024
0.0279	4.146	21.7868	16.532	5.2548	21.8093	14.6283	7.181
0.028	4.1262	21.8058	16.5716	5.2342	21.8235	14.6639	7.1596
0.0281	4.1064	21.8248	16.611	5.2138	21.8376	14.6994	7.1382
0.0282	4.0867	21.8436	16.6502	5.1934	21.8517	14.7348	7.1169
0.0284	4.0671	21.8623	16.6893	5.173	21.8657	14.7701	7.0956
0.0285	4.0475	21.8809	16.7283	5.1526	21.8797	14.8052	7.0745
0.0286	4.028	21.8994	16.7671	5.1323	21.8936	14.8403	7.0533
0.0287	4.0084	21.9179	16.8058	5.1121	21.9074	14.8753	7.0321
0.0289	3.989	21.9362	16.8443	5.0919	21.9212	14.9102	7.011
0.029	3.9696	21.9544	16.8827	5.0717	21.935	14.945	6.99
0.0291	3.9502	21.9725	16.9209	5.0516	21.9486	14.9797	6.9689
0.0292	3.931	21.9906	16.959	5.0316	21.9623	15.0143	6.948
0.0294	3.9116	22.0085	16.9969	5.0116	21.9758	15.0488	6.927
0.0295	3.8924	22.0263	17.0347	4.9916	21.9894	15.0832	6.9062
0.0296	3.8733	22.0441	17.0724	4.9717	22.0028	15.1175	6.8853
0.0297	3.8543	22.0617	17.1099	4.9518	22.0162	15.1517	6.8645
0.0299	3.8352	22.0792	17.1473	4.9319	22.0296	15.1858	6.8438
0.03	3.8162	22.0967	17.1845	4.9122	22.0429	15.2198	6.8231
0.0301	3.7972	22.114	17.2216	4.8924	22.0561	15.2538	6.8023
0.0302	3.7783	22.1313	17.2586	4.8727	22.0693	15.2876	6.7817
0.0304	3.7595	22.1485	17.2954	4.8531	22.0824	15.3213	6.7611
0.0305	3.7408	22.1655	17.3321	4.8334	22.0955	15.3549	6.7406
0.0306	3.722	22.1825	17.3686	4.8139	22.1085	15.3885	6.72
0.0307	3.7034	22.1994	17.405	4.7944	22.1215	15.4219	6.6996
0.0309	3.6848	22.2162	17.4412	4.775	22.1344	15.4552	6.6792
0.031	3.6662	22.2329	17.4773	4.7556	22.1473	15.4885	6.6588
0.0311	3.6477	22.2495	17.5133	4.7362	22.1601	15.5216	6.6385
0.0312	3.6293	22.266	17.5491	4.7169	22.1728	15.5547	6.6181
0.0314	3.6108	22.2824	17.5848	4.6976	22.1855	15.5876	6.5979
0.0315	3.5925	22.2988	17.6204	4.6784	22.1982	15.6205	6.5777
0.0316	3.5742	22.315	17.6558	4.6592	22.2108	15.6533	6.5575
0.0317	3.556	22.3312	17.6911	4.6401	22.2233	15.686	6.5373

z (km)	Δr-fl	Nd=0.75 Rock ‰ δ18O	Fluid ‰ δ18O	Δr-fl	Nd=0.5 Rock ‰ δ18O	Fluid ‰ δ18O	Δr-fl
0.0319	3.5378	22.3472	17.7262	4.621	22.2358	15.7185	6.5173
0.032	3.5198	22.3632	17.7612	4.602	22.2483	15.751	6.4973
0.0321	3.5017	22.3791	17.7961	4.583	22.2607	15.7834	6.4773
0.0322	3.4836	22.3949	17.8308	4.5641	22.273	15.8157	6.4573
0.0324	3.4657	22.4106	17.8654	4.5452	22.2853	15.8479	6.4374
0.0325	3.4478	22.4263	17.8999	4.5264	22.2975	15.88	6.4175
0.0326	3.43	22.4418	17.9342	4.5076	22.3097	15.912	6.3977
0.0327	3.4122	22.4573	17.9684	4.4889	22.3219	15.944	6.3779
0.0329	3.3946	22.4726	18.0024	4.4702	22.3339	15.9758	6.3581
0.033	3.3769	22.4879	18.0363	4.4516	22.346	16.0075	6.3385
0.0331	3.3593	22.5031	18.0701	4.433	22.358	16.0392	6.3188
0.0332	3.3418	22.5182	18.1037	4.4145	22.3699	16.0707	6.2992
0.0334	3.3243	22.5333	18.1372	4.3961	22.3818	16.1022	6.2796
0.0335	3.3068	22.5482	18.1706	4.3776	22.3936	16.1336	6.26
0.0336	3.2895	22.5631	18.2039	4.3592	22.4054	16.1649	6.2405
0.0337	3.2722	22.5779	18.237	4.3409	22.4172	16.196	6.2212
0.0339	3.255	22.5926	18.27	4.3226	22.4289	16.2271	6.2018
0.034	3.2378	22.6072	18.3028	4.3044	22.4405	16.2581	6.1824
0.0341	3.2206	22.6218	18.3355	4.2863	22.4521	16.2891	6.163
0.0342	3.2036	22.6362	18.3681	4.2681	22.4636	16.3199	6.1437
0.0344	3.1866	22.6506	18.4005	4.2501	22.4751	16.3506	6.1245
0.0345	3.1696	22.6649	18.4329	4.232	22.4866	16.3813	6.1053
0.0346	3.1528	22.6791	18.465	4.2141	22.498	16.4118	6.0862
0.0347	3.1359	22.6933	18.4971	4.1962	22.5094	16.4423	6.0671
0.0349	3.1191	22.7073	18.529	4.1783	22.5207	16.4726	6.0481
0.035	3.1025	22.7213	18.5608	4.1605	22.5319	16.5029	6.029
0.0351	3.0858	22.7352	18.5925	4.1427	22.5431	16.5331	6.01
0.0352	3.0692	22.749	18.624	4.125	22.5543	16.5632	5.9911
0.0354	3.0526	22.7628	18.6555	4.1073	22.5654	16.5932	5.9722
0.0355	3.0362	22.7765	18.6867	4.0898	22.5765	16.6231	5.9534
0.0356	3.0198	22.7901	18.7179	4.0722	22.5875	16.653	5.9345
0.0357	3.0035	22.8036	18.7489	4.0547	22.5985	16.6827	5.9158
0.0359	2.9872	22.817	18.7798	4.0372	22.6095	16.7124	5.8971
0.036	2.971	22.8304	18.8106	4.0198	22.6203	16.7419	5.8784
0.0361	2.9548	22.8437	18.8412	4.0025	22.6312	16.7714	5.8598
0.0362	2.9387	22.8569	18.8717	3.9852	22.642	16.8008	5.8412
0.0364	2.9226	22.87	18.9021	3.9679	22.6527	16.8301	5.8226
0.0365	2.9067	22.8831	18.9324	3.9507	22.6635	16.8593	5.8042
0.0366	2.8908	22.8961	18.9625	3.9336	22.6741	16.8884	5.7857
0.0367	2.8749	22.909	18.9926	3.9164	22.6847	16.9175	5.7672
0.0369	2.8592	22.9219	19.0225	3.8994	22.6953	16.9464	5.7489
0.037	2.8434	22.9347	19.0522	3.8825	22.7058	16.9753	5.7305
0.0371	2.8277	22.9474	19.0819	3.8655	22.7163	17.0041	5.7122
0.0372	2.8121	22.96	19.1114	3.8486	22.7268	17.0328	5.694
0.0374	2.7966	22.9726	19.1408	3.8318	22.7372	17.0614	5.6758
0.0375	2.7811	22.985	19.1701	3.8149	22.7475	17.0899	5.6576
0.0376	2.7657	22.9975	19.1992	3.7983	22.7578	17.1183	5.6395
0.0377	2.7503	23.0098	19.2282	3.7816	22.7681	17.1466	5.6215
0.0379	2.7349	23.0221	19.2571	3.765	22.7783	17.1749	5.6034
0.038	2.7198	23.0343	19.2859	3.7484	22.7885	17.2031	5.5854
0.0381	2.7045	23.0464	19.3146	3.7318	22.7986	17.2312	5.5674

		Nd=0.75				Nd=0.5	
		Rock ‰	Fluid ‰		Rock ‰	Fluid ‰	
z (km)	**Δr-fl**	**δ18O**	**δ18O**	**Δr-fl**	**δ18O**	**δ18O**	**Δr-fl**
0.0382	2.6895	23.0585	19.3431	3.7154	22.8087	17.2592	5.5495
0.0384	2.6744	23.0705	19.3716	3.6989	22.8188	17.2871	5.5317
0.0385	2.6594	23.0825	19.3999	3.6826	22.8288	17.3149	5.5139
0.0386	2.6445	23.0943	19.428	3.6663	22.8388	17.3427	5.4961
0.0387	2.6296	23.1061	19.4561	3.65	22.8487	17.3703	5.4784
0.0389	2.6148	23.1178	19.484	3.6338	22.8586	17.3979	5.4607
0.039	2.6	23.1295	19.5119	3.6176	22.8684	17.4254	5.443
0.0391	2.5853	23.1411	19.5396	3.6015	22.8782	17.4528	5.4254
0.0392	2.5706	23.1526	19.5672	3.5854	22.888	17.4801	5.4079
0.0394	2.5561	23.1641	19.5946	3.5695	22.8977	17.5074	5.3903
0.0395	2.5416	23.1755	19.622	3.5535	22.9074	17.5345	5.3729
0.0396	2.5272	23.1868	19.6492	3.5376	22.917	17.5616	5.3554
0.0397	2.5127	23.1981	19.6763	3.5218	22.9266	17.5886	5.338
0.0399	2.4984	23.2093	19.7033	3.506	22.9362	17.6155	5.3207
0.04	2.4842	23.2205	19.7302	3.4903	22.9457	17.6423	5.3034
0.0401	2.47	23.2315	19.757	3.4745	22.9551	17.6691	5.286
0.0402	2.4558	23.2426	19.7836	3.459	22.9646	17.6957	5.2689
0.0404	2.4417	23.2535	19.8102	3.4433	22.974	17.7223	5.2517
0.0405	2.4277	23.2644	19.8366	3.4278	22.9833	17.7488	5.2345
0.0406	2.4137	23.2752	19.8629	3.4123	22.9926	17.7752	5.2174
0.0407	2.3998	23.286	19.8891	3.3969	23.0019	17.8016	5.2003
0.0409	2.3859	23.2967	19.9152	3.3815	23.0111	17.8278	5.1833
0.041	2.3721	23.3073	19.9412	3.3661	23.0203	17.854	5.1663
0.0411	2.3585	23.3179	19.967	3.3509	23.0295	17.8801	5.1494
0.0412	2.3448	23.3284	19.9928	3.3356	23.0386	17.9061	5.1325
0.0414	2.3311	23.3389	20.0184	3.3205	23.0477	17.932	5.1157
0.0415	2.3177	23.3493	20.0439	3.3054	23.0567	17.9579	5.0988
0.0416	2.3042	23.3596	20.0693	3.2903	23.0657	17.9836	5.0821
0.0417	2.2907	23.3699	20.0946	3.2753	23.0747	18.0093	5.0654
0.0419	2.2773	23.3801	20.1198	3.2603	23.0836	18.0349	5.0487
0.042	2.264	23.3903	20.1449	3.2454	23.0925	18.0604	5.0321
0.0421	2.2508	23.4004	20.1699	3.2305	23.1013	18.0859	5.0154
0.0422	2.2377	23.4104	20.1947	3.2157	23.1101	18.1112	4.9989
0.0424	2.2244	23.4204	20.2195	3.2009	23.1189	18.1365	4.9824
0.0425	2.2115	23.4303	20.2441	3.1862	23.1277	18.1617	4.966
0.0426	2.1984	23.4402	20.2686	3.1716	23.1363	18.1869	4.9494
0.0427	2.1855	23.45	20.293	3.157	23.145	18.2119	4.9331
0.0429	2.1726	23.4597	20.3174	3.1423	23.1536	18.2369	4.9167
0.043	2.1597	23.4694	20.3416	3.1278	23.1622	18.2618	4.9004
0.0431	2.147	23.4791	20.3657	3.1134	23.1708	18.2866	4.8842
0.0432	2.1343	23.4886	20.3896	3.099	23.1793	18.3113	4.868
0.0434	2.1216	23.4982	20.4135	3.0847	23.1877	18.336	4.8517
0.0435	2.109	23.5076	20.4373	3.0703	23.1962	18.3606	4.8356
0.0436	2.0965	23.5171	20.461	3.0561	23.2046	18.3851	4.8195
0.0437	2.084	23.5264	20.4845	3.0419	23.213	18.4095	4.8035
0.0439	2.0716	23.5357	20.508	3.0277	23.2213	18.4338	4.7875
0.044	2.0592	23.545	20.5314	3.0136	23.2296	18.4581	4.7715
0.0441	2.0469	23.5542	20.5546	2.9996	23.2378	18.4823	4.7555
0.0442	2.0347	23.5633	20.5778	2.9855	23.2461	18.5064	4.7397
0.0444	2.0225	23.5724	20.6008	2.9716	23.2543	18.5305	4.7238
0.0445	2.0103	23.5814	20.6237	2.9577	23.2624	18.5544	4.708

		Nd=0.75				Nd=0.5	
		Rock ‰	Fluid ‰		Rock ‰	Fluid ‰	
z (km)	**Δr-fl**	**δ18O**	**δ18O**	**Δr-fl**	**δ18O**	**δ18O**	**Δr-fl**
0.0446	1.9983	23.5904	20.6466	2.9438	23.2705	18.5783	4.6922
0.0447	1.9863	23.5994	20.6693	2.9301	23.2786	18.6021	4.6765
0.0449	1.9743	23.6082	20.6919	2.9163	23.2867	18.6259	4.6608
0.045	1.9624	23.6171	20.7145	2.9026	23.2947	18.6495	4.6452
0.0451	1.9505	23.6258	20.7369	2.8889	23.3026	18.6731	4.6295
0.0452	1.9387	23.6346	20.7592	2.8754	23.3106	18.6966	4.614
0.0454	1.927	23.6432	20.7814	2.8618	23.3185	18.7201	4.5984
0.0455	1.9153	23.6519	20.8036	2.8483	23.3264	18.7434	4.583
0.0456	1.9037	23.6604	20.8256	2.8348	23.3342	18.7667	4.5675
0.0457	1.8921	23.669	20.8475	2.8215	23.342	18.7899	4.5521
0.0459	1.8807	23.6774	20.8693	2.8081	23.3498	18.813	4.5368
0.046	1.8691	23.6858	20.8911	2.7947	23.3575	18.8361	4.5214
0.0461	1.8578	23.6942	20.9127	2.7815	23.3652	18.8591	4.5061
0.0462	1.8464	23.7025	20.9342	2.7683	23.3729	18.882	4.4909
0.0464	1.8351	23.7108	20.9556	2.7552	23.3806	18.9049	4.4757
0.0465	1.8239	23.719	20.977	2.742	23.3882	18.9276	4.4606
0.0466	1.8128	23.7272	20.9982	2.729	23.3957	18.9503	4.4454
0.0467	1.8016	23.7353	21.0193	2.716	23.4033	18.9729	4.4304
0.0469	1.7906	23.7434	21.0404	2.703	23.4108	18.9955	4.4153
0.047	1.7796	23.7514	21.0613	2.6901	23.4183	19.018	4.4003
0.0471	1.7685	23.7594	21.0822	2.6772	23.4257	19.0404	4.3853
0.0472	1.7577	23.7674	21.1029	2.6645	23.4331	19.0627	4.3704
0.0474	1.7468	23.7752	21.1236	2.6516	23.4405	19.0849	4.3556
0.0475	1.7361	23.7831	21.1441	2.639	23.4478	19.1071	4.3407
0.0476	1.7253	23.7909	21.1646	2.6263	23.4552	19.1292	4.326
0.0477	1.7146	23.7986	21.185	2.6136	23.4624	19.1513	4.3111
0.0479	1.704	23.8063	21.2052	2.6011	23.4697	19.1733	4.2964
0.048	1.6934	23.814	21.2254	2.5886	23.4769	19.1952	4.2817
0.0481	1.6829	23.8216	21.2455	2.5761	23.4841	19.217	4.2671
0.0482	1.6724	23.8292	21.2655	2.5637	23.4913	19.2387	4.2526
0.0484	1.662	23.8367	21.2854	2.5513	23.4984	19.2604	4.238
0.0485	1.6517	23.8442	21.3052	2.539	23.5055	19.282	4.2235
0.0486	1.6413	23.8516	21.3249	2.5267	23.5125	19.3036	4.2089
0.0487	1.6311	23.859	21.3445	2.5145	23.5196	19.3251	4.1945
0.0489	1.6209	23.8663	21.3641	2.5022	23.5266	19.3465	4.1801
0.049	1.6107	23.8736	21.3835	2.4901	23.5335	19.3678	4.1657
0.0491	1.6006	23.8809	21.4029	2.478	23.5405	19.3891	4.1514
0.0492	1.5906	23.8881	21.4221	2.466	23.5474	19.4103	4.1371
0.0494	1.5806	23.8953	21.4413	2.454	23.5543	19.4314	4.1229
0.0495	1.5707	23.9024	21.4604	2.442	23.5611	19.4524	4.1087
0.0496	1.5608	23.9095	21.4794	2.4301	23.5679	19.4734	4.0945
0.0497	1.5509	23.9165	21.4983	2.4182	23.5747	19.4943	4.0804
0.0499	1.5411	23.9235	21.5171	2.4064	23.5815	19.5152	4.0663
0.05	1.5314	23.9305	21.5358	2.3947	23.5882	19.536	4.0522

E.2 Reactive Transport Modeling Results at TIFF of $1x10^3$ (moles H_2O/cm^2)

z (km)	Nd=5 Rock ‰ δ18O	Fluid ‰ δ18O	Δr-fl	Nd=2 Rock ‰ δ18O	Fluid ‰ δ18O	Δr-fl	Nd=1 Rock ‰ δ18O	Fluid ‰ δ18O
0	4.1415	4	0.1415	6.842	4	2.842	11.7255	4
0.0012	4.1765	4.0073	0.1692	6.9526	4.0542	2.8984	11.8026	4.0729
0.0025	4.2141	4.016	0.1981	7.0632	4.1095	2.9537	11.8793	4.1459
0.0037	4.2542	4.0261	0.2281	7.1739	4.1658	3.0081	11.9557	4.2189
0.005	4.2969	4.0377	0.2592	7.2847	4.2233	3.0614	12.0318	4.2921
0.0062	4.3421	4.0508	0.2913	7.3955	4.2818	3.1137	12.1075	4.3653
0.0075	4.39	4.0654	0.3246	7.5064	4.3414	3.165	12.1829	4.4385
0.0088	4.4404	4.0817	0.3587	7.6174	4.402	3.2154	12.2579	4.5118
0.01	4.4934	4.0997	0.3937	7.7283	4.4635	3.2648	12.3326	4.5852
0.0112	4.549	4.1194	0.4296	7.8393	4.5261	3.3132	12.407	4.6586
0.0125	4.6072	4.1408	0.4664	7.9503	4.5896	3.3607	12.481	4.7321
0.0137	4.668	4.164	0.504	8.0612	4.6541	3.4071	12.5547	4.8056
0.015	4.7314	4.1891	0.5423	8.1721	4.7195	3.4526	12.6281	4.8791
0.0162	4.7973	4.2161	0.5812	8.2829	4.7858	3.4971	12.7011	4.9527
0.0175	4.8658	4.2449	0.6209	8.3937	4.853	3.5407	12.7738	5.0263
0.0188	4.9368	4.2757	0.6611	8.5044	4.9211	3.5833	12.8462	5.0999
0.02	5.0103	4.3085	0.7018	8.615	4.9901	3.6249	12.9182	5.1736
0.0213	5.0863	4.3433	0.743	8.7255	5.0598	3.6657	12.9899	5.2473
0.0225	5.1648	4.38	0.7848	8.8359	5.1304	3.7055	13.0613	5.321
0.0238	5.2458	4.4189	0.8269	8.9462	5.2018	3.7444	13.1323	5.3947
0.025	5.3291	4.4598	0.8693	9.0563	5.274	3.7823	13.203	5.4684
0.0263	5.4149	4.5028	0.9121	9.1663	5.3469	3.8194	13.2734	5.5421
0.0275	5.503	4.5479	0.9551	9.2761	5.4206	3.8555	13.3434	5.6158
0.0288	5.5935	4.5951	0.9984	9.3858	5.4951	3.8907	13.4131	5.6895
0.03	5.6862	4.6444	1.0418	9.4953	5.5702	3.9251	13.4825	5.7632
0.0313	5.7812	4.6958	1.0854	9.6046	5.646	3.9586	13.5515	5.8369
0.0325	5.8785	4.7494	1.1291	9.7137	5.7225	3.9912	13.6203	5.9106
0.0338	5.9779	4.8052	1.1727	9.8225	5.7997	4.0228	13.6887	5.9843
0.035	6.0795	4.8631	1.2164	9.9312	5.8776	4.0536	13.7567	6.0579
0.0363	6.1831	4.9231	1.26	10.0396	5.956	4.0836	13.8245	6.1316
0.0375	6.2889	4.9853	1.3036	10.1478	6.0351	4.1127	13.8919	6.2052
0.0388	6.3966	5.0496	1.347	10.2557	6.1148	4.1409	13.959	6.2787
0.04	6.5064	5.1161	1.3903	10.3634	6.195	4.1684	14.0258	6.3523
0.0413	6.618	5.1847	1.4333	10.4708	6.2758	4.195	14.0923	6.4258
0.0425	6.7316	5.2554	1.4762	10.5779	6.3572	4.2207	14.1584	6.4993
0.0438	6.8469	5.3283	1.5186	10.6847	6.4391	4.2456	14.2242	6.5727
0.045	6.9641	5.4032	1.5609	10.7913	6.5215	4.2698	14.2897	6.6461
0.0463	7.083	5.4802	1.6028	10.8975	6.6044	4.2931	14.3549	6.7194
0.0475	7.2035	5.5593	1.6442	11.0035	6.6878	4.3157	14.4197	6.7927
0.0487	7.3258	5.6405	1.6853	11.1091	6.7717	4.3374	14.4843	6.866
0.05	7.4495	5.7236	1.7259	11.2144	6.856	4.3584	14.5485	6.9392
0.0512	7.5749	5.8088	1.7661	11.3193	6.9408	4.3785	14.6124	7.0123
0.0525	7.7017	5.896	1.8057	11.4239	7.0259	4.398	14.676	7.0854

z (km)	Nd=5 Rock ‰ δ18O	Fluid ‰ δ18O	Δr-fl	Nd=2 Rock ‰ δ18O	Fluid ‰ δ18O	Δr-fl	Nd=1 Rock ‰ δ18O	Fluid ‰ δ18O
0.0537	7.8299	5.9851	1.8448	11.5282	7.1115	4.4167	14.7393	7.1584
0.055	7.9595	6.0762	1.8833	11.6321	7.1975	4.4346	14.8023	7.2313
0.0562	8.0904	6.1691	1.9213	11.7357	7.2839	4.4518	14.8649	7.3042
0.0575	8.2226	6.264	1.9586	11.8389	7.3706	4.4683	14.9273	7.377
0.0587	8.356	6.3607	1.9953	11.9417	7.4577	4.484	14.9893	7.4497
0.06	8.4906	6.4592	2.0314	12.0441	7.5451	4.499	15.051	7.5224
0.0612	8.6263	6.5595	2.0668	12.1462	7.6329	4.5133	15.1124	7.5949
0.0625	8.763	6.6616	2.1014	12.2478	7.721	4.5268	15.1736	7.6674
0.0637	8.9007	6.7654	2.1353	12.3491	7.8093	4.5398	15.2343	7.7398
0.065	9.0394	6.8709	2.1685	12.4499	7.8979	4.552	15.2948	7.8122
0.0662	9.179	6.978	2.201	12.5504	7.9869	4.5635	15.355	7.8844
0.0675	9.3194	7.0868	2.2326	12.6504	8.076	4.5744	15.4149	7.9566
0.0687	9.4606	7.1971	2.2635	12.75	8.1654	4.5846	15.4745	8.0286
0.07	9.6026	7.309	2.2936	12.8492	8.2551	4.5941	15.5338	8.1006
0.0712	9.7452	7.4223	2.3229	12.948	8.3449	4.6031	15.5927	8.1724
0.0725	9.8885	7.5372	2.3513	13.0463	8.435	4.6113	15.6514	8.2442
0.0737	10.0323	7.6534	2.3789	13.1442	8.5252	4.619	15.7098	8.3159
0.075	10.1767	7.7711	2.4056	13.2417	8.6156	4.6261	15.7679	8.3874
0.0762	10.3215	7.89	2.4315	13.3387	8.7062	4.6325	15.8256	8.4589
0.0775	10.4668	8.0103	2.4565	13.4353	8.797	4.6383	15.8831	8.5302
0.0787	10.6125	8.1318	2.4807	13.5314	8.8879	4.6435	15.9403	8.6015
0.08	10.7585	8.2546	2.5039	13.627	8.9789	4.6481	15.9972	8.6726
0.0812	10.9048	8.3785	2.5263	13.7222	9.07	4.6522	16.0538	8.7436
0.0825	11.0513	8.5035	2.5478	13.817	9.1613	4.6557	16.1101	8.8145
0.0837	11.198	8.6296	2.5684	13.9112	9.2526	4.6586	16.1661	8.8853
0.085	11.3449	8.7568	2.5881	14.005	9.344	4.661	16.2218	8.9559
0.0862	11.4919	8.8849	2.607	14.0983	9.4356	4.6627	16.2772	9.0265
0.0875	11.6389	9.014	2.6249	14.1912	9.5271	4.6641	16.3323	9.0969
0.0887	11.7859	9.1441	2.6418	14.2835	9.6187	4.6648	16.3872	9.1672
0.09	11.9329	9.2749	2.658	14.3754	9.7104	4.665	16.4417	9.2373
0.0912	12.0798	9.4066	2.6732	14.4668	9.8021	4.6647	16.496	9.3074
0.0925	12.2266	9.5391	2.6875	14.5577	9.8938	4.6639	16.55	9.3773
0.0937	12.3732	9.6723	2.7009	14.6481	9.9855	4.6626	16.6037	9.447
0.095	12.5196	9.8062	2.7134	14.738	10.0773	4.6607	16.6571	9.5167
0.0962	12.6658	9.9407	2.7251	14.8275	10.169	4.6585	16.7102	9.5862
0.0975	12.8117	10.0758	2.7359	14.9164	10.2607	4.6557	16.7631	9.6555
0.0987	12.9573	10.2115	2.7458	15.0048	10.3524	4.6524	16.8156	9.7248
0.1	13.1025	10.3477	2.7548	15.0928	10.444	4.6488	16.8679	9.7938
0.1012	13.2474	10.4844	2.763	15.1802	10.5356	4.6446	16.9199	9.8628
0.1025	13.3918	10.6215	2.7703	15.2671	10.6271	4.64	16.9716	9.9316
0.1037	13.5358	10.759	2.7768	15.3535	10.7186	4.6349	17.0231	10.0002
0.105	13.6792	10.8969	2.7823	15.4394	10.81	4.6294	17.0743	10.0687
0.1062	13.8222	11.035	2.7872	15.5248	10.9013	4.6235	17.1252	10.1371

z (km)	Nd=5 Rock ‰ δ18O	Fluid ‰ δ18O	Δr-fl	Nd=2 Rock ‰ δ18O	Fluid ‰ δ18O	Δr-fl	Nd=1 Rock ‰ δ18O	Fluid ‰ δ18O
0.1075	13.9646	11.1734	2.7912	15.6097	10.9925	4.6172	17.1758	10.2053
0.1087	14.1063	11.312	2.7943	15.6941	11.0837	4.6104	17.2261	10.2734
0.11	14.2475	11.4508	2.7967	15.778	11.1747	4.6033	17.2762	10.3413
0.1112	14.388	11.5898	2.7982	15.8614	11.2656	4.5958	17.326	10.409
0.1125	14.5279	11.7288	2.7991	15.9442	11.3564	4.5878	17.3755	10.4766
0.1137	14.667	11.8679	2.7991	16.0265	11.447	4.5795	17.4248	10.5441
0.115	14.8054	12.0071	2.7983	16.1084	11.5375	4.5709	17.4738	10.6113
0.1162	14.943	12.1462	2.7968	16.1897	11.6279	4.5618	17.5225	10.6785
0.1175	15.0799	12.2853	2.7946	16.2705	11.7181	4.5524	17.571	10.7454
0.1187	15.2159	12.4243	2.7916	16.3507	11.8081	4.5426	17.6192	10.8122
0.12	15.3511	12.5632	2.7879	16.4305	11.898	4.5325	17.6671	10.8789
0.1212	15.4855	12.7019	2.7836	16.5097	11.9877	4.522	17.7148	10.9454
0.1225	15.619	12.8404	2.7786	16.5884	12.0772	4.5112	17.7622	11.0117
0.1237	15.7516	12.9787	2.7729	16.6666	12.1665	4.5001	17.8093	11.0778
0.125	15.8832	13.1167	2.7665	16.7443	12.2557	4.4886	17.8562	11.1438
0.1262	16.014	13.2545	2.7595	16.8215	12.3446	4.4769	17.9028	11.2096
0.1275	16.1438	13.3919	2.7519	16.8981	12.4333	4.4648	17.9492	11.2753
0.1287	16.2726	13.529	2.7436	16.9743	12.5218	4.4525	17.9953	11.3407
0.13	16.4004	13.6657	2.7347	17.0499	12.6101	4.4398	18.0411	11.406
0.1312	16.5272	13.8019	2.7253	17.125	12.6981	4.4269	18.0867	11.4712
0.1325	16.653	13.9377	2.7153	17.1996	12.786	4.4136	18.1321	11.5361
0.1337	16.7777	14.0731	2.7046	17.2736	12.8735	4.4001	18.1771	11.6009
0.135	16.9014	14.2079	2.6935	17.3472	12.9609	4.3863	18.222	11.6655
0.1362	17.0241	14.3422	2.6819	17.4202	13.048	4.3722	18.2666	11.7299
0.1375	17.1456	14.476	2.6696	17.4927	13.1348	4.3579	18.3109	11.7942
0.1387	17.2661	14.6091	2.657	17.5647	13.2213	4.3434	18.355	11.8583
0.14	17.3855	14.7417	2.6438	17.6362	13.3076	4.3286	18.3988	11.9222
0.1412	17.5038	14.8736	2.6302	17.7072	13.3937	4.3135	18.4424	11.9859
0.1425	17.6209	15.0049	2.616	17.7777	13.4794	4.2983	18.4857	12.0494
0.1437	17.7369	15.1355	2.6014	17.8476	13.5649	4.2827	18.5288	12.1128
0.145	17.8518	15.2653	2.5865	17.9171	13.65	4.2671	18.5716	12.1759
0.1462	17.9656	15.3945	2.5711	17.986	13.7349	4.2511	18.6143	12.2389
0.1475	18.0782	15.5229	2.5553	18.0545	13.8195	4.235	18.6566	12.3017
0.1487	18.1896	15.6506	2.539	18.1224	13.9038	4.2186	18.6987	12.3644
0.15	18.2999	15.7774	2.5225	18.1898	13.9878	4.202	18.7406	12.4268
0.1512	18.4091	15.9035	2.5056	18.2567	14.0715	4.1852	18.7823	12.489
0.1525	18.517	16.0287	2.4883	18.3232	14.1548	4.1684	18.8237	12.5511
0.1537	18.6238	16.1531	2.4707	18.3891	14.2379	4.1512	18.8648	12.613
0.155	18.7294	16.2766	2.4528	18.4545	14.3206	4.1339	18.9057	12.6747
0.1562	18.8338	16.3993	2.4345	18.5194	14.403	4.1164	18.9464	12.7362
0.1575	18.937	16.5211	2.4159	18.5838	14.4851	4.0987	18.9869	12.7975
0.1587	19.0391	16.6419	2.3972	18.6477	14.5668	4.0809	19.0271	12.8586
0.16	19.14	16.7619	2.3781	18.7112	14.6482	4.063	19.0671	12.9195

z (km)	Nd=5 Rock ‰ δ18O	Fluid ‰ δ18O	Δr-fl	Nd=2 Rock ‰ δ18O	Fluid ‰ δ18O	Δr-fl	Nd=1 Rock ‰ δ18O	Fluid ‰ δ18O
0.1612	19.2397	16.8809	2.3588	18.7741	14.7293	4.0448	19.1069	12.9803
0.1625	19.3381	16.999	2.3391	18.8366	14.81	4.0266	19.1464	13.0408
0.1637	19.4355	17.1161	2.3194	18.8985	14.8904	4.0081	19.1857	13.1012
0.165	19.5316	17.2322	2.2994	18.96	14.9704	3.9896	19.2248	13.1614
0.1662	19.6265	17.3474	2.2791	19.021	15.0501	3.9709	19.2636	13.2213
0.1675	19.7203	17.4615	2.2588	19.0814	15.1294	3.952	19.3022	13.2811
0.1687	19.8129	17.5747	2.2382	19.1415	15.2084	3.9331	19.3406	13.3407
0.17	19.9043	17.6869	2.2174	19.201	15.287	3.914	19.3788	13.4001
0.1712	19.9945	17.798	2.1965	19.26	15.3652	3.8948	19.4167	13.4593
0.1725	20.0835	17.9081	2.1754	19.3186	15.4431	3.8755	19.4544	13.5183
0.1737	20.1714	18.0172	2.1542	19.3767	15.5206	3.8561	19.4919	13.5771
0.175	20.2581	18.1252	2.1329	19.4343	15.5978	3.8365	19.5292	13.6357
0.1762	20.3437	18.2322	2.1115	19.4915	15.6745	3.817	19.5663	13.6941
0.1775	20.4281	18.3381	2.09	19.5482	15.7509	3.7973	19.6031	13.7523
0.1787	20.5113	18.443	2.0683	19.6044	15.8269	3.7775	19.6397	13.8103
0.18	20.5934	18.5468	2.0466	19.6601	15.9026	3.7575	19.6761	13.8681
0.1812	20.6744	18.6495	2.0249	19.7154	15.9778	3.7376	19.7123	13.9258
0.1825	20.7542	18.7512	2.003	19.7703	16.0527	3.7176	19.7483	13.9832
0.1837	20.8329	18.8518	1.9811	19.8246	16.1272	3.6974	19.7841	14.0404
0.185	20.9105	18.9513	1.9592	19.8785	16.2013	3.6772	19.8196	14.0974
0.1862	20.987	19.0497	1.9373	19.932	16.275	3.657	19.855	14.1543
0.1875	21.0623	19.147	1.9153	19.985	16.3483	3.6367	19.8901	14.2109
0.1887	21.1366	19.2433	1.8933	20.0375	16.4213	3.6162	19.925	14.2673
0.19	21.2097	19.3384	1.8713	20.0896	16.4938	3.5958	19.9597	14.3235
0.1912	21.2818	19.4325	1.8493	20.1413	16.566	3.5753	19.9942	14.3796
0.1925	21.3528	19.5255	1.8273	20.1925	16.6377	3.5548	20.0285	14.4354
0.1937	21.4227	19.6174	1.8053	20.2433	16.7091	3.5342	20.0626	14.491
0.195	21.4916	19.7082	1.7834	20.2936	16.7801	3.5135	20.0965	14.5465
0.1962	21.5594	19.7979	1.7615	20.3435	16.8506	3.4929	20.1301	14.6017
0.1975	21.6261	19.8865	1.7396	20.3929	16.9208	3.4721	20.1636	14.6567
0.1987	21.6919	19.974	1.7179	20.442	16.9905	3.4515	20.1969	14.7115
0.2	21.7566	20.0605	1.6961	20.4905	17.0599	3.4306	20.23	14.7661
0.2012	21.8202	20.1459	1.6743	20.5387	17.1289	3.4098	20.2628	14.8206
0.2025	21.8829	20.2302	1.6527	20.5864	17.1974	3.389	20.2955	14.8748
0.2037	21.9446	20.3134	1.6312	20.6338	17.2656	3.3682	20.328	14.9288
0.205	22.0053	20.3956	1.6097	20.6807	17.3333	3.3474	20.3603	14.9826
0.2062	22.065	20.4767	1.5883	20.7271	17.4007	3.3264	20.3923	15.0362
0.2075	22.1237	20.5567	1.567	20.7732	17.4676	3.3056	20.4242	15.0896
0.2087	22.1814	20.6357	1.5457	20.8188	17.5342	3.2846	20.4559	15.1428
0.21	22.2383	20.7136	1.5247	20.8641	17.6003	3.2638	20.4874	15.1959
0.2112	22.2941	20.7905	1.5036	20.9089	17.666	3.2429	20.5187	15.2487
0.2125	22.3491	20.8663	1.4828	20.9533	17.7313	3.222	20.5498	15.3013
0.2137	22.4031	20.9411	1.462	20.9973	17.7962	3.2011	20.5808	15.3537

	Nd=5			Nd=2			Nd=1	
z (km)	Rock ‰ δ18O	Fluid ‰ δ18O	Δr-fl	Rock ‰ δ18O	Fluid ‰ δ18O	Δr-fl	Rock ‰ δ18O	Fluid ‰ δ18O
0.215	22.4562	21.0148	1.4414	21.0409	17.8607	3.1802	20.6115	15.4059
0.2162	22.5084	21.0875	1.4209	21.0841	17.9248	3.1593	20.642	15.4579
0.2175	22.5597	21.1592	1.4005	21.1269	17.9885	3.1384	20.6724	15.5096
0.2187	22.6101	21.2299	1.3802	21.1694	18.0518	3.1176	20.7026	15.5612
0.22	22.6596	21.2996	1.36	21.2114	18.1147	3.0967	20.7325	15.6126
0.2212	22.7083	21.3683	1.34	21.253	18.1772	3.0758	20.7623	15.6638
0.2225	22.7562	21.436	1.3202	21.2943	18.2392	3.0551	20.792	15.7148
0.2237	22.8032	21.5027	1.3005	21.3351	18.3009	3.0342	20.8214	15.7656
0.225	22.8493	21.5684	1.2809	21.3756	18.3621	3.0135	20.8506	15.8162
0.2262	22.8947	21.6331	1.2616	21.4157	18.423	2.9927	20.8797	15.8665
0.2275	22.9392	21.6969	1.2423	21.4555	18.4834	2.9721	20.9086	15.9167
0.2287	22.9829	21.7597	1.2232	21.4948	18.5434	2.9514	20.9373	15.9667
0.23	23.0259	21.8215	1.2044	21.5338	18.6031	2.9307	20.9658	16.0165
0.2312	23.068	21.8824	1.1856	21.5724	18.6623	2.9101	20.9942	16.066
0.2325	23.1094	21.9424	1.167	21.6106	18.7211	2.8895	21.0224	16.1154
0.2337	23.1501	22.0014	1.1487	21.6485	18.7795	2.869	21.0504	16.1646
0.235	23.1899	22.0595	1.1304	21.686	18.8375	2.8485	21.0782	16.2136
0.2362	23.2291	22.1167	1.1124	21.7232	18.8951	2.8281	21.1058	16.2623
0.2375	23.2675	22.173	1.0945	21.76	18.9523	2.8077	21.1333	16.3109
0.2387	23.3052	22.2284	1.0768	21.7964	19.0092	2.7872	21.1606	16.3593
0.24	23.3422	22.2829	1.0593	21.8325	19.0656	2.7669	21.1877	16.4074
0.2412	23.3785	22.3366	1.0419	21.8683	19.1216	2.7467	21.2147	16.4554
0.2425	23.4141	22.3893	1.0248	21.9037	19.1772	2.7265	21.2415	16.5032
0.2437	23.449	22.4412	1.0078	21.9387	19.2324	2.7063	21.2681	16.5507
0.245	23.4833	22.4923	0.991	21.9734	19.2872	2.6862	21.2946	16.5981
0.2462	23.5169	22.5425	0.9744	22.0078	19.3416	2.6662	21.3208	16.6453
0.2475	23.5499	22.5919	0.958	22.0418	19.3957	2.6461	21.347	16.6922
0.2487	23.5822	22.6405	0.9417	22.0755	19.4493	2.6262	21.3729	16.739
0.25	23.6139	22.6882	0.9257	22.1089	19.5025	2.6064	21.3987	16.7856
0.2512	23.6449	22.7352	0.9097	22.1419	19.5554	2.5865	21.4243	16.8319
0.2525	23.6754	22.7813	0.8941	22.1747	19.6078	2.5669	21.4498	16.8781
0.2537	23.7052	22.8266	0.8786	22.207	19.6599	2.5471	21.4751	16.9241
0.255	23.7345	22.8712	0.8633	22.2391	19.7116	2.5275	21.5002	16.9699
0.2562	23.7632	22.915	0.8482	22.2708	19.7629	2.5079	21.5252	17.0154
0.2575	23.7913	22.9581	0.8332	22.3023	19.8138	2.4885	21.55	17.0608
0.2587	23.8188	23.0004	0.8184	22.3334	19.8643	2.4691	21.5747	17.106
0.26	23.8458	23.0419	0.8039	22.3642	19.9144	2.4498	21.5992	17.151
0.2612	23.8723	23.0828	0.7895	22.3946	19.9642	2.4304	21.6235	17.1958
0.2625	23.8982	23.1229	0.7753	22.4248	20.0136	2.4112	21.6477	17.2404
0.2637	23.9236	23.1622	0.7614	22.4547	20.0625	2.3922	21.6718	17.2848
0.265	23.9484	23.2009	0.7475	22.4843	20.1112	2.3731	21.6956	17.329
0.2662	23.9728	23.2389	0.7339	22.5135	20.1594	2.3541	21.7194	17.373
0.2675	23.9966	23.2762	0.7204	22.5425	20.2073	2.3352	21.7429	17.4168

		Nd=5			Nd=2			Nd=1
z (km)	Rock ‰ δ18O	Fluid ‰ δ18O	Δr-fl	Rock ‰ δ18O	Fluid ‰ δ18O	Δr-fl	Rock ‰ δ18O	Fluid ‰ δ18O
0.2687	24.02	23.3128	0.7072	22.5712	20.2547	2.3165	21.7664	17.4604
0.27	24.0429	23.3488	0.6941	22.5996	20.3019	2.2977	21.7896	17.5038
0.2712	24.0653	23.3841	0.6812	22.6276	20.3486	2.279	21.8128	17.5471
0.2725	24.0872	23.4187	0.6685	22.6554	20.395	2.2604	21.8357	17.5901
0.2737	24.1086	23.4527	0.6559	22.683	20.441	2.242	21.8586	17.6329
0.275	24.1297	23.4861	0.6436	22.7102	20.4866	2.2236	21.8812	17.6756
0.2762	24.1502	23.5189	0.6313	22.7371	20.5319	2.2052	21.9038	17.7181
0.2775	24.1704	23.551	0.6194	22.7638	20.5768	2.187	21.9261	17.7603
0.2787	24.1901	23.5825	0.6076	22.7902	20.6213	2.1689	21.9484	17.8024
0.28	24.2094	23.6135	0.5959	22.8163	20.6655	2.1508	21.9705	17.8443
0.2812	24.2282	23.6438	0.5844	22.8421	20.7093	2.1328	21.9924	17.886
0.2825	24.2467	23.6736	0.5731	22.8677	20.7528	2.1149	22.0142	17.9275
0.2837	24.2648	23.7028	0.562	22.893	20.7959	2.0971	22.0359	17.9688
0.285	24.2824	23.7314	0.551	22.9181	20.8387	2.0794	22.0574	18.0099
0.2862	24.2997	23.7595	0.5402	22.9428	20.8811	2.0617	22.0788	18.0508
0.2875	24.3167	23.787	0.5297	22.9673	20.9231	2.0442	22.1	18.0916
0.2887	24.3332	23.814	0.5192	22.9916	20.9648	2.0268	22.1211	18.1321
0.29	24.3494	23.8405	0.5089	23.0156	21.0062	2.0094	22.1421	18.1725
0.2912	24.3652	23.8665	0.4987	23.0393	21.0472	1.9921	22.1629	18.2127
0.2925	24.3807	23.8919	0.4888	23.0628	21.0879	1.9749	22.1836	18.2526
0.2937	24.3958	23.9168	0.479	23.0861	21.1282	1.9579	22.2041	18.2925
0.295	24.4106	23.9413	0.4693	23.109	21.1682	1.9408	22.2245	18.3321
0.2962	24.4251	23.9652	0.4599	23.1318	21.2078	1.924	22.2448	18.3715
0.2975	24.4392	23.9887	0.4505	23.1543	21.2471	1.9072	22.265	18.4107
0.2987	24.4531	24.0117	0.4414	23.1766	21.2861	1.8905	22.285	18.4498
0.3	24.4666	24.0344	0.4322	23.1986	21.3247	1.8739	22.3049	18.4887
0.3012	24.4798	24.0565	0.4233	23.2204	21.363	1.8574	22.3246	18.5274
0.3025	24.4927	24.0781	0.4146	23.2419	21.401	1.8409	22.3442	18.5659
0.3037	24.5053	24.0993	0.406	23.2632	21.4386	1.8246	22.3637	18.6042
0.305	24.5177	24.1201	0.3976	23.2843	21.476	1.8083	22.3831	18.6423
0.3062	24.5297	24.1404	0.3893	23.3052	21.513	1.7922	22.4023	18.6803
0.3075	24.5415	24.1603	0.3812	23.3258	21.5496	1.7762	22.4214	18.718
0.3087	24.553	24.1798	0.3732	23.3462	21.586	1.7602	22.4404	18.7556
0.31	24.5643	24.1989	0.3654	23.3664	21.622	1.7444	22.4592	18.793
0.3112	24.5752	24.2176	0.3576	23.3863	21.6577	1.7286	22.478	18.8303
0.3125	24.586	24.2359	0.3501	23.4061	21.6931	1.713	22.4966	18.8673
0.3137	24.5964	24.2538	0.3426	23.4256	21.7282	1.6974	22.515	18.9042
0.315	24.6067	24.2714	0.3353	23.4449	21.763	1.6819	22.5334	18.9409
0.3162	24.6167	24.2885	0.3282	23.464	21.7974	1.6666	22.5516	18.9774
0.3175	24.6264	24.3053	0.3211	23.4829	21.8316	1.6513	22.5697	19.0137
0.3187	24.636	24.3218	0.3142	23.5015	21.8654	1.6361	22.5877	19.0499
0.32	24.6453	24.3379	0.3074	23.52	21.899	1.621	22.6056	19.0858
0.3212	24.6544	24.3536	0.3008	23.5383	21.9322	1.6061	22.6233	19.1216

z (km)	Nd=5 Rock ‰ δ18O	Fluid ‰ δ18O	Δr-fl	Nd=2 Rock ‰ δ18O	Fluid ‰ δ18O	Δr-fl	Nd=1 Rock ‰ δ18O	Fluid ‰ δ18O
0.3225	24.6632	24.369	0.2942	23.5563	21.9652	1.5911	22.6409	19.1573
0.3237	24.6719	24.3841	0.2878	23.5742	21.9978	1.5764	22.6584	19.1927
0.325	24.6804	24.3989	0.2815	23.5918	22.0301	1.5617	22.6758	19.228
0.3262	24.6886	24.4133	0.2753	23.6093	22.0622	1.5471	22.6931	19.2631
0.3275	24.6967	24.4274	0.2693	23.6266	22.0939	1.5327	22.7102	19.298
0.3287	24.7045	24.4412	0.2633	23.6436	22.1254	1.5182	22.7273	19.3327
0.33	24.7122	24.4547	0.2575	23.6605	22.1566	1.5039	22.7442	19.3673
0.3312	24.7197	24.4679	0.2518	23.6772	22.1875	1.4897	22.761	19.4017
0.3325	24.727	24.4809	0.2461	23.6937	22.2181	1.4756	22.7777	19.4359
0.3337	24.7342	24.4935	0.2407	23.71	22.2484	1.4616	22.7943	19.47
0.335	24.7411	24.5059	0.2352	23.7261	22.2784	1.4477	22.8107	19.5039
0.3362	24.7479	24.5179	0.23	23.7421	22.3082	1.4339	22.8271	19.5376
0.3375	24.7545	24.5297	0.2248	23.7579	22.3376	1.4203	22.8433	19.5711
0.3387	24.761	24.5413	0.2197	23.7734	22.3668	1.4066	22.8595	19.6045
0.34	24.7673	24.5526	0.2147	23.7888	22.3958	1.393	22.8755	19.6377
0.3412	24.7735	24.5636	0.2099	23.8041	22.4244	1.3797	22.8914	19.6708
0.3425	24.7795	24.5744	0.2051	23.8191	22.4528	1.3663	22.9072	19.7036
0.3437	24.7853	24.5849	0.2004	23.834	22.4809	1.3531	22.9229	19.7363
0.345	24.791	24.5952	0.1958	23.8487	22.5088	1.3399	22.9385	19.7689
0.3462	24.7966	24.6053	0.1913	23.8633	22.5364	1.3269	22.954	19.8012
0.3475	24.802	24.6151	0.1869	23.8777	22.5637	1.314	22.9693	19.8334
0.3487	24.8073	24.6248	0.1825	23.8919	22.5907	1.3012	22.9846	19.8655
0.35	24.8125	24.6341	0.1784	23.9059	22.6175	1.2884	22.9998	19.8973
0.3512	24.8175	24.6433	0.1742	23.9198	22.6441	1.2757	23.0148	19.929
0.3525	24.8224	24.6523	0.1701	23.9335	22.6704	1.2631	23.0298	19.9606
0.3537	24.8272	24.661	0.1662	23.9471	22.6964	1.2507	23.0446	19.992
0.355	24.8318	24.6696	0.1622	23.9605	22.7222	1.2383	23.0594	20.0232
0.3562	24.8364	24.6779	0.1585	23.9738	22.7477	1.2261	23.074	20.0542
0.3575	24.8408	24.6861	0.1547	23.9869	22.773	1.2139	23.0886	20.0851
0.3587	24.8451	24.6941	0.151	23.9998	22.798	1.2018	23.103	20.1158
0.36	24.8493	24.7019	0.1474	24.0126	22.8228	1.1898	23.1174	20.1464
0.3612	24.8534	24.7095	0.1439	24.0253	22.8473	1.178	23.1316	20.1768
0.3625	24.8574	24.7169	0.1405	24.0378	22.8717	1.1661	23.1458	20.2071
0.3637	24.8613	24.7241	0.1372	24.0501	22.8957	1.1544	23.1598	20.2372
0.365	24.8651	24.7312	0.1339	24.0623	22.9196	1.1427	23.1738	20.2671
0.3662	24.8688	24.7381	0.1307	24.0744	22.9431	1.1313	23.1877	20.2969
0.3675	24.8724	24.7452	0.1272	24.0863	22.9665	1.1198	23.2014	20.3265
0.3687	24.8759	24.7514	0.1245	24.0981	22.9896	1.1085	23.2151	20.3559
0.37	24.8793	24.7578	0.1215	24.1097	23.0125	1.0972	23.2287	20.3853
0.3712	24.8826	24.7641	0.1185	24.1212	23.0352	1.086	23.2421	20.4144
0.3725	24.8859	24.7702	0.1157	24.1326	23.0577	1.0749	23.2555	20.4434
0.3737	24.889	24.7762	0.1128	24.1438	23.0799	1.0639	23.2688	20.4722
0.375	24.8921	24.782	0.1101	24.1549	23.1019	1.053	23.282	20.5009

z (km)	Nd=5 Rock ‰ δ18O	Fluid ‰ δ18O	Δr-fl	Nd=2 Rock ‰ δ18O	Fluid ‰ δ18O	Δr-fl	Nd=1 Rock ‰ δ18O	Fluid ‰ δ18O
0.3762	24.8951	24.7877	0.1074	24.1659	23.1236	1.0423	23.2951	20.5294
0.3775	24.898	24.7933	0.1047	24.1767	23.1452	1.0315	23.3081	20.5578
0.3787	24.9009	24.7987	0.1022	24.1874	23.1665	1.0209	23.321	20.5861
0.38	24.9036	24.8039	0.0997	24.198	23.1877	1.0103	23.3339	20.6141
0.3812	24.9063	24.8091	0.0972	24.2084	23.2086	0.9998	23.3466	20.6421
0.3825	24.9089	24.8141	0.0948	24.2188	23.2293	0.9895	23.3593	20.6698
0.3837	24.9115	24.819	0.0925	24.229	23.2497	0.9793	23.3718	20.6974
0.385	24.914	24.8238	0.0902	24.239	23.27	0.969	23.3843	20.7249
0.3862	24.9164	24.8285	0.0879	24.249	23.2901	0.9589	23.3967	20.7522
0.3875	24.9187	24.833	0.0857	24.2588	23.3099	0.9489	23.409	20.7794
0.3887	24.921	24.8374	0.0836	24.2686	23.3296	0.939	23.4212	20.8064
0.39	24.9233	24.842	0.0813	24.2782	23.3491	0.9291	23.4333	20.8333
0.3912	24.9254	24.8462	0.0792	24.2876	23.3683	0.9193	23.4454	20.8601
0.3925	24.9275	24.8503	0.0772	24.297	23.3874	0.9096	23.4573	20.8867
0.3937	24.9296	24.8544	0.0752	24.3063	23.4062	0.9001	23.4692	20.9131
0.395	24.9316	24.8583	0.0733	24.3154	23.4249	0.8905	23.481	20.9394
0.3962	24.9336	24.8621	0.0715	24.3244	23.4434	0.881	23.4927	20.9655
0.3975	24.9354	24.8658	0.0696	24.3334	23.4616	0.8718	23.5043	20.9916
0.3987	24.9373	24.8694	0.0679	24.3422	23.4797	0.8625	23.5158	21.0174
0.4	24.9391	24.8729	0.0662	24.3509	23.4976	0.8533	23.5273	21.0431
0.4012	24.9408	24.8764	0.0644	24.3595	23.5153	0.8442	23.5387	21.0687
0.4025	24.9425	24.8797	0.0628	24.368	23.5328	0.8352	23.55	21.0942
0.4037	24.9442	24.883	0.0612	24.3763	23.5502	0.8261	23.5612	21.1195
0.405	24.9458	24.8862	0.0596	24.3846	23.5673	0.8173	23.5723	21.1446
0.4062	24.9473	24.8893	0.058	24.3928	23.5843	0.8085	23.5834	21.1697
0.4075	24.9489	24.8923	0.0566	24.4009	23.6011	0.7998	23.5943	21.1945
0.4087	24.9503	24.8952	0.0551	24.4089	23.6177	0.7912	23.6052	21.2193
0.41	24.9518	24.8981	0.0537	24.4168	23.6342	0.7826	23.616	21.2439
0.4112	24.9532	24.9009	0.0523	24.4246	23.6504	0.7742	23.6268	21.2683
0.4125	24.9545	24.9036	0.0509	24.4322	23.6665	0.7657	23.6375	21.2927
0.4137	24.9559	24.9062	0.0497	24.4398	23.6824	0.7574	23.648	21.3169
0.415	24.9571	24.9088	0.0483	24.4473	23.6982	0.7491	23.6586	21.3409
0.4162	24.9584	24.9113	0.0471	24.4547	23.7138	0.7409	23.669	21.3648
0.4175	24.9596	24.9138	0.0458	24.4621	23.7292	0.7329	23.6793	21.3886
0.4187	24.9608	24.9162	0.0446	24.4693	23.7444	0.7249	23.6896	21.4123
0.42	24.9619	24.9185	0.0434	24.4764	23.7595	0.7169	23.6998	21.4358
0.4212	24.963	24.9208	0.0422	24.4835	23.7745	0.709	23.71	21.4592
0.4225	24.9641	24.923	0.0411	24.4904	23.7892	0.7012	23.7201	21.4824
0.4237	24.9652	24.9251	0.0401	24.4973	23.8038	0.6935	23.73	21.5056
0.425	24.9662	24.9272	0.039	24.5041	23.8183	0.6858	23.74	21.5285
0.4262	24.9672	24.9292	0.038	24.5108	23.8325	0.6783	23.7498	21.5514
0.4275	24.9682	24.9312	0.037	24.5174	23.8467	0.6707	23.7596	21.5741
0.4287	24.9691	24.9331	0.036	24.5239	23.8607	0.6632	23.7693	21.5967

		Nd=5			Nd=2			Nd=1
z (km)	Rock ‰ δ18O	Fluid ‰ δ18O	Δr-fl	Rock ‰ δ18O	Fluid ‰ δ18O	Δr-fl	Rock ‰ δ18O	Fluid ‰ δ18O
0.43	24.97	24.935	0.035	24.5304	23.8745	0.6559	23.7789	21.6192
0.4312	24.9709	24.9369	0.034	24.5367	23.8881	0.6486	23.7885	21.6415
0.4325	24.9718	24.9386	0.0332	24.543	23.9017	0.6413	23.798	21.6637
0.4337	24.9726	24.9404	0.0322	24.5492	23.915	0.6342	23.8074	21.6858
0.435	24.9734	24.942	0.0314	24.5553	23.9283	0.627	23.8168	21.7078
0.4362	24.9742	24.9437	0.0305	24.5614	23.9414	0.62	23.8261	21.7296
0.4375	24.975	24.9453	0.0297	24.5674	23.9543	0.6131	23.8353	21.7513
0.4387	24.9757	24.9468	0.0289	24.5733	23.9671	0.6062	23.8445	21.7729
0.44	24.9765	24.9483	0.0282	24.5791	23.9797	0.5994	23.8536	21.7944
0.4412	24.9772	24.9502	0.027	24.5848	23.9922	0.5926	23.8626	21.8157
0.4425	24.9778	24.9516	0.0262	24.5905	24.0046	0.5859	23.8716	21.8369
0.4437	24.9785	24.953	0.0255	24.5961	24.0169	0.5792	23.8805	21.858
0.445	24.9792	24.9543	0.0249	24.6016	24.029	0.5726	23.8893	21.879
0.4462	24.9798	24.9556	0.0242	24.6071	24.0409	0.5662	23.8981	21.8998
0.4475	24.9804	24.9569	0.0235	24.6125	24.0528	0.5597	23.9068	21.9205
0.4487	24.981	24.9582	0.0228	24.6178	24.0644	0.5534	23.9154	21.9411
0.45	24.9816	24.9594	0.0222	24.6231	24.076	0.5471	23.924	21.9616
0.4512	24.9821	24.9605	0.0216	24.6283	24.0875	0.5408	23.9325	21.982
0.4525	24.9827	24.9617	0.021	24.6334	24.0988	0.5346	23.9409	22.0022
0.4537	24.9832	24.9628	0.0204	24.6384	24.1099	0.5285	23.9493	22.0223
0.455	24.9837	24.9639	0.0198	24.6434	24.121	0.5224	23.9576	22.0423
0.4562	24.9842	24.9649	0.0193	24.6483	24.1319	0.5164	23.9659	22.0622
0.4575	24.9847	24.9659	0.0188	24.6532	24.1427	0.5105	23.9741	22.082
0.4587	24.9851	24.9669	0.0182	24.658	24.1534	0.5046	23.9823	22.1016
0.46	24.9856	24.9679	0.0177	24.6627	24.164	0.4987	23.9903	22.1212
0.4612	24.986	24.9688	0.0172	24.6674	24.1744	0.493	23.9984	22.1406
0.4625	24.9865	24.9697	0.0168	24.672	24.1847	0.4873	24.0063	22.1599
0.4637	24.9869	24.9706	0.0163	24.6766	24.195	0.4816	24.0142	22.1791
0.465	24.9873	24.9715	0.0158	24.6811	24.205	0.4761	24.0221	22.1982
0.4662	24.9877	24.9723	0.0154	24.6855	24.215	0.4705	24.0299	22.2171
0.4675	24.9881	24.9731	0.015	24.6899	24.2249	0.465	24.0376	22.236
0.4687	24.9884	24.9739	0.0145	24.6942	24.2346	0.4596	24.0453	22.2547
0.47	24.9888	24.9747	0.0141	24.6985	24.2443	0.4542	24.0529	22.2733
0.4712	24.9891	24.9754	0.0137	24.7027	24.2538	0.4489	24.0604	22.2919
0.4725	24.9895	24.9762	0.0133	24.7068	24.2632	0.4436	24.068	22.3103
0.4737	24.9898	24.9769	0.0129	24.7109	24.2725	0.4384	24.0754	22.3286
0.475	24.9901	24.9776	0.0125	24.715	24.2817	0.4333	24.0828	22.3467
0.4762	24.9904	24.9782	0.0122	24.7189	24.2908	0.4281	24.0901	22.3648
0.4775	24.9907	24.9789	0.0118	24.7229	24.2998	0.4231	24.0974	22.3828
0.4787	24.991	24.9795	0.0115	24.7268	24.3086	0.4182	24.1046	22.4006
0.48	24.9913	24.9801	0.0112	24.7306	24.3174	0.4132	24.1118	22.4184
0.4812	24.9915	24.9807	0.0108	24.7344	24.3261	0.4083	24.1189	22.436
0.4825	24.9918	24.9817	0.0101	24.7381	24.3347	0.4034	24.126	22.4536

	Nd=5			Nd=2			Nd=1	
z (km)	Rock ‰ δ18O	Fluid ‰ δ18O	Δr-fl	Rock ‰ δ18O	Fluid ‰ δ18O	Δr-fl	Rock ‰ δ18O	Fluid ‰ δ18O
0.4837	24.9921	24.9823	0.0098	24.7418	24.3431	0.3987	24.133	22.471
0.485	24.9923	24.9828	0.0095	24.7454	24.3515	0.3939	24.14	22.4883
0.4862	24.9926	24.9833	0.0093	24.749	24.3598	0.3892	24.1469	22.5056
0.4875	24.9928	24.9838	0.009	24.7526	24.368	0.3846	24.1538	22.5227
0.4887	24.993	24.9843	0.0087	24.7561	24.3761	0.38	24.1606	22.5397
0.49	24.9932	24.9848	0.0084	24.7595	24.3841	0.3754	24.1673	22.5566
0.4912	24.9934	24.9852	0.0082	24.7629	24.3919	0.371	24.174	22.5734
0.4925	24.9937	24.9857	0.008	24.7663	24.3997	0.3666	24.1807	22.5901
0.4937	24.9939	24.9861	0.0078	24.7696	24.4075	0.3621	24.1873	22.6067
0.495	24.994	24.9865	0.0075	24.7729	24.4151	0.3578	24.1939	22.6232
0.4962	24.9942	24.987	0.0072	24.7761	24.4226	0.3535	24.2004	22.6396
0.4975	24.9944	24.9874	0.007	24.7793	24.43	0.3493	24.2068	22.6559
0.4987	24.9946	24.9877	0.0069	24.7824	24.4374	0.345	24.2132	22.6721
0.5	24.9948	24.9881	0.0067	24.7855	24.4447	0.3408	24.2196	22.6882

z (km)	Δr-fl	Nd=0.75 Rock ‰ δ18O	Fluid ‰ δ18O	Δr-fl	Nd=0.5 Rock ‰ δ18O	Fluid ‰ δ18O	Δr-fl
0	7.7255	13.9197	4	9.9197	16.7371	4	12.7371
0.0012	7.7297	13.9764	4.0701	9.9063	16.7707	4.06	12.7107
0.0025	7.7334	14.0329	4.1402	9.8927	16.8042	4.1199	12.6843
0.0037	7.7368	14.0892	4.2102	9.879	16.8376	4.1797	12.6579
0.005	7.7397	14.1452	4.2802	9.865	16.8708	4.2394	12.6314
0.0062	7.7422	14.2009	4.35	9.8509	16.9039	4.299	12.6049
0.0075	7.7444	14.2564	4.4198	9.8366	16.9369	4.3585	12.5784
0.0088	7.7461	14.3117	4.4895	9.8222	16.9697	4.4178	12.5519
0.01	7.7474	14.3667	4.5592	9.8075	17.0025	4.4771	12.5254
0.0112	7.7484	14.4215	4.6288	9.7927	17.0351	4.5362	12.4989
0.0125	7.7489	14.4761	4.6982	9.7779	17.0676	4.5953	12.4723
0.0137	7.7491	14.5304	4.7677	9.7627	17.1	4.6542	12.4458
0.015	7.749	14.5845	4.837	9.7475	17.1323	4.713	12.4193
0.0162	7.7484	14.6383	4.9062	9.7321	17.1644	4.7717	12.3927
0.0175	7.7475	14.6919	4.9754	9.7165	17.1965	4.8303	12.3662
0.0188	7.7463	14.7453	5.0445	9.7008	17.2284	4.8888	12.3396
0.02	7.7446	14.7984	5.1135	9.6849	17.2602	4.9472	12.313
0.0213	7.7426	14.8513	5.1824	9.6689	17.2919	5.0055	12.2864
0.0225	7.7403	14.904	5.2512	9.6528	17.3234	5.0636	12.2598
0.0238	7.7376	14.9564	5.32	9.6364	17.3549	5.1217	12.2332
0.025	7.7346	15.0086	5.3886	9.62	17.3862	5.1796	12.2066
0.0263	7.7313	15.0606	5.4572	9.6034	17.4174	5.2375	12.1799
0.0275	7.7276	15.1123	5.5257	9.5866	17.4486	5.2952	12.1534
0.0288	7.7236	15.1638	5.594	9.5698	17.4795	5.3528	12.1267
0.03	7.7193	15.2151	5.6623	9.5528	17.5104	5.4103	12.1001
0.0313	7.7146	15.2661	5.7305	9.5356	17.5412	5.4677	12.0735
0.0325	7.7097	15.317	5.7986	9.5184	17.5718	5.5249	12.0469
0.0338	7.7044	15.3676	5.8665	9.5011	17.6024	5.5821	12.0203
0.035	7.6988	15.4179	5.9344	9.4835	17.6328	5.6392	11.9936
0.0363	7.6929	15.4681	6.0022	9.4659	17.6631	5.6961	11.967
0.0375	7.6867	15.518	6.0699	9.4481	17.6933	5.7529	11.9404
0.0388	7.6803	15.5677	6.1375	9.4302	17.7234	5.8096	11.9138
0.04	7.6735	15.6172	6.2049	9.4123	17.7534	5.8662	11.8872
0.0413	7.6665	15.6664	6.2723	9.3941	17.7833	5.9227	11.8606
0.0425	7.6591	15.7154	6.3396	9.3758	17.813	5.9791	11.8339
0.0438	7.6515	15.7642	6.4067	9.3575	17.8427	6.0354	11.8073
0.045	7.6436	15.8128	6.4738	9.339	17.8722	6.0916	11.7806
0.0463	7.6355	15.8612	6.5407	9.3205	17.9017	6.1476	11.7541
0.0475	7.627	15.9093	6.6075	9.3018	17.931	6.2035	11.7275
0.0487	7.6183	15.9573	6.6742	9.2831	17.9602	6.2594	11.7008
0.05	7.6093	16.005	6.7408	9.2642	17.9893	6.3151	11.6742
0.0512	7.6001	16.0525	6.8073	9.2452	18.0183	6.3707	11.6476
0.0525	7.5906	16.0997	6.8737	9.226	18.0472	6.4261	11.6211

z (km)	Δr-fl	Rock ‰ δ18O	Nd=0.75 Fluid ‰ δ18O	Δr-fl	Rock ‰ δ18O	Nd=0.5 Fluid ‰ δ18O	Δr-fl
0.0537	7.5809	16.1468	6.94	9.2068	18.076	6.4815	11.5945
0.055	7.571	16.1937	7.0061	9.1876	18.1046	6.5368	11.5678
0.0562	7.5607	16.2403	7.0722	9.1681	18.1332	6.5919	11.5413
0.0575	7.5503	16.2867	7.1381	9.1486	18.1617	6.647	11.5147
0.0587	7.5396	16.3329	7.2039	9.129	18.19	6.7019	11.4881
0.06	7.5286	16.3789	7.2695	9.1094	18.2183	6.7567	11.4616
0.0612	7.5175	16.4247	7.3351	9.0896	18.2464	6.8114	11.435
0.0625	7.5062	16.4703	7.4005	9.0698	18.2744	6.866	11.4084
0.0637	7.4945	16.5156	7.4658	9.0498	18.3024	6.9204	11.382
0.065	7.4826	16.5608	7.531	9.0298	18.3302	6.9748	11.3554
0.0662	7.4706	16.6058	7.5961	9.0097	18.3579	7.029	11.3289
0.0675	7.4583	16.6505	7.6611	8.9894	18.3856	7.0832	11.3024
0.0687	7.4459	16.695	7.7259	8.9691	18.4131	7.1372	11.2759
0.07	7.4332	16.7394	7.7906	8.9488	18.4405	7.1911	11.2494
0.0712	7.4203	16.7835	7.8551	8.9284	18.4678	7.2449	11.2229
0.0725	7.4072	16.8274	7.9196	8.9078	18.495	7.2985	11.1965
0.0737	7.3939	16.8711	7.9839	8.8872	18.5221	7.3521	11.17
0.075	7.3805	16.9146	8.0481	8.8665	18.5491	7.4055	11.1436
0.0762	7.3667	16.9579	8.1121	8.8458	18.576	7.4589	11.1171
0.0775	7.3529	17.0011	8.176	8.8251	18.6028	7.5121	11.0907
0.0787	7.3388	17.044	8.2398	8.8042	18.6295	7.5652	11.0643
0.08	7.3246	17.0867	8.3035	8.7832	18.6561	7.6182	11.0379
0.0812	7.3102	17.1292	8.367	8.7622	18.6827	7.6711	11.0116
0.0825	7.2956	17.1715	8.4304	8.7411	18.7091	7.7239	10.9852
0.0837	7.2808	17.2136	8.4937	8.7199	18.7354	7.7765	10.9589
0.085	7.2659	17.2555	8.5568	8.6987	18.7616	7.829	10.9326
0.0862	7.2507	17.2972	8.6198	8.6774	18.7877	7.8815	10.9062
0.0875	7.2354	17.3388	8.6827	8.6561	18.8137	7.9338	10.8799
0.0887	7.22	17.3801	8.7454	8.6347	18.8396	7.986	10.8536
0.09	7.2044	17.4212	8.808	8.6132	18.8654	8.0381	10.8273
0.0912	7.1886	17.4622	8.8705	8.5917	18.8911	8.09	10.8011
0.0925	7.1727	17.5029	8.9328	8.5701	18.9167	8.1419	10.7748
0.0937	7.1567	17.5435	8.995	8.5485	18.9423	8.1936	10.7487
0.095	7.1404	17.5838	9.057	8.5268	18.9677	8.2453	10.7224
0.0962	7.124	17.624	9.1189	8.5051	18.993	8.2968	10.6962
0.0975	7.1076	17.664	9.1807	8.4833	19.0182	8.3482	10.67
0.0987	7.0908	17.7038	9.2423	8.4615	19.0434	8.3995	10.6439
0.1	7.0741	17.7434	9.3038	8.4396	19.0684	8.4507	10.6177
0.1012	7.0571	17.7828	9.3651	8.4177	19.0934	8.5017	10.5917
0.1025	7.04	17.822	9.4263	8.3957	19.1182	8.5527	10.5655
0.1037	7.0229	17.861	9.4874	8.3736	19.143	8.6035	10.5395
0.105	7.0056	17.8999	9.5483	8.3516	19.1676	8.6542	10.5134
0.1062	6.9881	17.9386	9.609	8.3296	19.1922	8.7048	10.4874

z (km)	Δr-fl	Nd=0.75 Rock ‰ δ18O	Fluid ‰ δ18O	Δr-fl	Nd=0.5 Rock ‰ δ18O	Fluid ‰ δ18O	Δr-fl
0.1075	6.9705	17.9771	9.6697	8.3074	19.2167	8.7553	10.4614
0.1087	6.9527	18.0154	9.7302	8.2852	19.2411	8.8057	10.4354
0.11	6.9349	18.0535	9.7905	8.263	19.2653	8.856	10.4093
0.1112	6.917	18.0914	9.8507	8.2407	19.2895	8.9061	10.3834
0.1125	6.8989	18.1292	9.9107	8.2185	19.3136	8.9562	10.3574
0.1137	6.8807	18.1667	9.9706	8.1961	19.3377	9.0061	10.3316
0.115	6.8625	18.2041	10.0304	8.1737	19.3616	9.0559	10.3057
0.1162	6.844	18.2413	10.09	8.1513	19.3854	9.1056	10.2798
0.1175	6.8256	18.2784	10.1495	8.1289	19.4091	9.1552	10.2539
0.1187	6.807	18.3152	10.2088	8.1064	19.4328	9.2047	10.2281
0.12	6.7882	18.3519	10.268	8.0839	19.4563	9.254	10.2023
0.1212	6.7694	18.3884	10.327	8.0614	19.4798	9.3033	10.1765
0.1225	6.7505	18.4247	10.3859	8.0388	19.5032	9.3524	10.1508
0.1237	6.7315	18.4609	10.4446	8.0163	19.5265	9.4014	10.1251
0.125	6.7124	18.4968	10.5032	7.9936	19.5497	9.4503	10.0994
0.1262	6.6932	18.5326	10.5616	7.971	19.5728	9.4991	10.0737
0.1275	6.6739	18.5682	10.6199	7.9483	19.5958	9.5478	10.048
0.1287	6.6546	18.6037	10.678	7.9257	19.6187	9.5964	10.0223
0.13	6.6351	18.639	10.736	7.903	19.6416	9.6448	9.9968
0.1312	6.6155	18.6741	10.7938	7.8803	19.6643	9.6932	9.9711
0.1325	6.596	18.709	10.8515	7.8575	19.687	9.7414	9.9456
0.1337	6.5762	18.7438	10.909	7.8348	19.7096	9.7895	9.9201
0.135	6.5565	18.7784	10.9664	7.812	19.7321	9.8375	9.8946
0.1362	6.5367	18.8128	11.0236	7.7892	19.7545	9.8854	9.8691
0.1375	6.5167	18.8471	11.0807	7.7664	19.7768	9.9332	9.8436
0.1387	6.4967	18.8811	11.1376	7.7435	19.799	9.9808	9.8182
0.14	6.4766	18.9151	11.1944	7.7207	19.8212	10.0284	9.7928
0.1412	6.4565	18.9488	11.251	7.6978	19.8433	10.0758	9.7675
0.1425	6.4363	18.9824	11.3074	7.675	19.8652	10.1231	9.7421
0.1437	6.416	19.0158	11.3638	7.652	19.8871	10.1704	9.7167
0.145	6.3957	19.0491	11.4199	7.6292	19.9089	10.2175	9.6914
0.1462	6.3754	19.0822	11.4759	7.6063	19.9307	10.2645	9.6662
0.1475	6.3549	19.1151	11.5318	7.5833	19.9523	10.3113	9.641
0.1487	6.3343	19.1479	11.5875	7.5604	19.9739	10.3581	9.6158
0.15	6.3138	19.1805	11.643	7.5375	19.9953	10.4048	9.5905
0.1512	6.2933	19.213	11.6984	7.5146	20.0167	10.4513	9.5654
0.1525	6.2726	19.2452	11.7536	7.4916	20.038	10.4977	9.5403
0.1537	6.2518	19.2774	11.8087	7.4687	20.0593	10.544	9.5153
0.155	6.231	19.3093	11.8636	7.4457	20.0804	10.5902	9.4902
0.1562	6.2102	19.3411	11.9184	7.4227	20.1015	10.6363	9.4652
0.1575	6.1894	19.3728	11.973	7.3998	20.1224	10.6823	9.4401
0.1587	6.1685	19.4043	12.0275	7.3768	20.1433	10.7282	9.4151
0.16	6.1476	19.4356	12.0818	7.3538	20.1642	10.774	9.3902

z (km)	Δr-fl	Nd=0.75 Rock ‰ δ18O	Fluid ‰ δ18O	Δr-fl	Nd=0.5 Rock ‰ δ18O	Fluid ‰ δ18O	Δr-fl
0.1612	6.1266	19.4668	12.1359	7.3309	20.1849	10.8196	9.3653
0.1625	6.1056	19.4978	12.1899	7.3079	20.2055	10.8651	9.3404
0.1637	6.0845	19.5287	12.2437	7.285	20.2261	10.9106	9.3155
0.165	6.0634	19.5594	12.2974	7.262	20.2466	10.9559	9.2907
0.1662	6.0423	19.59	12.351	7.239	20.267	11.0011	9.2659
0.1675	6.0211	19.6204	12.4043	7.2161	20.2874	11.0462	9.2412
0.1687	5.9999	19.6507	12.4575	7.1932	20.3076	11.0912	9.2164
0.17	5.9787	19.6808	12.5106	7.1702	20.3278	11.136	9.1918
0.1712	5.9574	19.7107	12.5635	7.1472	20.3479	11.1808	9.1671
0.1725	5.9361	19.7405	12.6162	7.1243	20.3679	11.2254	9.1425
0.1737	5.9148	19.7702	12.6688	7.1014	20.3878	11.27	9.1178
0.175	5.8935	19.7997	12.7213	7.0784	20.4077	11.3144	9.0933
0.1762	5.8722	19.8291	12.7735	7.0556	20.4275	11.3587	9.0688
0.1775	5.8508	19.8583	12.8257	7.0326	20.4472	11.4029	9.0443
0.1787	5.8294	19.8873	12.8776	7.0097	20.4668	11.447	9.0198
0.18	5.808	19.9163	12.9294	6.9869	20.4864	11.491	8.9954
0.1812	5.7865	19.945	12.9811	6.9639	20.5059	11.5349	8.971
0.1825	5.7651	19.9736	13.0326	6.941	20.5253	11.5787	8.9466
0.1837	5.7437	20.0021	13.0839	6.9182	20.5446	11.6223	8.9223
0.185	5.7222	20.0305	13.1351	6.8954	20.5638	11.6659	8.8979
0.1862	5.7007	20.0587	13.1861	6.8726	20.583	11.7093	8.8737
0.1875	5.6792	20.0867	13.237	6.8497	20.6021	11.7526	8.8495
0.1887	5.6577	20.1146	13.2877	6.8269	20.6211	11.7958	8.8253
0.19	5.6362	20.1424	13.3383	6.8041	20.6401	11.839	8.8011
0.1912	5.6146	20.17	13.3886	6.7814	20.6589	11.882	8.7769
0.1925	5.5931	20.1975	13.4389	6.7586	20.6777	11.9249	8.7528
0.1937	5.5716	20.2248	13.489	6.7358	20.6965	11.9676	8.7289
0.195	5.55	20.252	13.5389	6.7131	20.7151	12.0103	8.7048
0.1962	5.5284	20.2791	13.5887	6.6904	20.7337	12.0529	8.6808
0.1975	5.5069	20.306	13.6383	6.6677	20.7522	12.0953	8.6569
0.1987	5.4854	20.3328	13.6877	6.6451	20.7706	12.1377	8.6329
0.2	5.4639	20.3595	13.737	6.6225	20.789	12.1799	8.6091
0.2012	5.4422	20.386	13.7862	6.5998	20.8073	12.2221	8.5852
0.2025	5.4207	20.4124	13.8352	6.5772	20.8255	12.2641	8.5614
0.2037	5.3992	20.4386	13.884	6.5546	20.8436	12.306	8.5376
0.205	5.3777	20.4647	13.9327	6.532	20.8617	12.3478	8.5139
0.2062	5.3561	20.4907	13.9812	6.5095	20.8797	12.3895	8.4902
0.2075	5.3346	20.5165	14.0296	6.4869	20.8976	12.4311	8.4665
0.2087	5.3131	20.5423	14.0778	6.4645	20.9155	12.4726	8.4429
0.21	5.2915	20.5678	14.1258	6.442	20.9333	12.514	8.4193
0.2112	5.27	20.5933	14.1737	6.4196	20.951	12.5552	8.3958
0.2125	5.2485	20.6186	14.2215	6.3971	20.9686	12.5964	8.3722
0.2137	5.2271	20.6438	14.269	6.3748	20.9862	12.6375	8.3487

z (km)	Δr-fl	Nd=0.75 Rock ‰ δ18O	Fluid ‰ δ18O	Δr-fl	Nd=0.5 Rock ‰ δ18O	Fluid ‰ δ18O	Δr-fl
0.215	5.2056	20.6688	14.3165	6.3523	21.0037	12.6784	8.3253
0.2162	5.1841	20.6938	14.3637	6.3301	21.0211	12.7193	8.3018
0.2175	5.1628	20.7185	14.4108	6.3077	21.0385	12.76	8.2785
0.2187	5.1414	20.7432	14.4578	6.2854	21.0558	12.8006	8.2552
0.22	5.1199	20.7678	14.5046	6.2632	21.073	12.8412	8.2318
0.2212	5.0985	20.7922	14.5513	6.2409	21.0902	12.8816	8.2086
0.2225	5.0772	20.8164	14.5978	6.2186	21.1073	12.9219	8.1854
0.2237	5.0558	20.8406	14.6441	6.1965	21.1243	12.9621	8.1622
0.225	5.0344	20.8646	14.6903	6.1743	21.1412	13.0022	8.139
0.2262	5.0132	20.8885	14.7363	6.1522	21.1581	13.0422	8.1159
0.2275	4.9919	20.9123	14.7822	6.1301	21.1749	13.0821	8.0928
0.2287	4.9706	20.936	14.8279	6.1081	21.1917	13.1219	8.0698
0.23	4.9493	20.9595	14.8735	6.086	21.2084	13.1615	8.0469
0.2312	4.9282	20.9829	14.9189	6.064	21.225	13.2011	8.0239
0.2325	4.907	21.0062	14.9641	6.0421	21.2415	13.2406	8.0009
0.2337	4.8858	21.0294	15.0092	6.0202	21.258	13.2799	7.9781
0.235	4.8646	21.0524	15.0542	5.9982	21.2744	13.3192	7.9552
0.2362	4.8435	21.0754	15.099	5.9764	21.2908	13.3583	7.9325
0.2375	4.8224	21.0982	15.1436	5.9546	21.3071	13.3974	7.9097
0.2387	4.8013	21.1209	15.1881	5.9328	21.3233	13.4363	7.887
0.24	4.7803	21.1434	15.2325	5.9109	21.3395	13.4752	7.8643
0.2412	4.7593	21.1659	15.2767	5.8892	21.3556	13.5139	7.8417
0.2425	4.7383	21.1882	15.3207	5.8675	21.3716	13.5525	7.8191
0.2437	4.7174	21.2104	15.3646	5.8458	21.3875	13.5911	7.7964
0.245	4.6965	21.2325	15.4083	5.8242	21.4034	13.6295	7.7739
0.2462	4.6755	21.2545	15.4519	5.8026	21.4193	13.6678	7.7515
0.2475	4.6548	21.2764	15.4953	5.7811	21.435	13.706	7.729
0.2487	4.6339	21.2981	15.5386	5.7595	21.4508	13.7442	7.7066
0.25	4.6131	21.3198	15.5817	5.7381	21.4664	13.7822	7.6842
0.2512	4.5924	21.3413	15.6246	5.7167	21.482	13.8201	7.6619
0.2525	4.5717	21.3627	15.6675	5.6952	21.4975	13.8579	7.6396
0.2537	4.551	21.384	15.7101	5.6739	21.513	13.8956	7.6174
0.255	4.5303	21.4051	15.7526	5.6525	21.5284	13.9332	7.5952
0.2562	4.5098	21.4262	15.795	5.6312	21.5437	13.9707	7.573
0.2575	4.4892	21.4472	15.8372	5.61	21.559	14.0081	7.5509
0.2587	4.4687	21.468	15.8793	5.5887	21.5742	14.0454	7.5288
0.26	4.4482	21.4888	15.9212	5.5676	21.5893	14.0826	7.5067
0.2612	4.4277	21.5094	15.963	5.5464	21.6044	14.1197	7.4847
0.2625	4.4073	21.5299	16.0046	5.5253	21.6194	14.1566	7.4628
0.2637	4.387	21.5503	16.046	5.5043	21.6344	14.1935	7.4409
0.265	4.3666	21.5706	16.0873	5.4833	21.6493	14.2303	7.419
0.2662	4.3464	21.5908	16.1285	5.4623	21.6641	14.267	7.3971
0.2675	4.3261	21.6109	16.1695	5.4414	21.6789	14.3036	7.3753

z (km)	Δr-fl	Nd=0.75 Rock ‰ δ18O	Fluid ‰ δ18O	Δr-fl	Nd=0.5 Rock ‰ δ18O	Fluid ‰ δ18O	Δr-fl
0.2687	4.306	21.6308	16.2104	5.4204	21.6936	14.3401	7.3535
0.27	4.2858	21.6507	16.2511	5.3996	21.7083	14.3764	7.3319
0.2712	4.2657	21.6705	16.2917	5.3788	21.7229	14.4127	7.3102
0.2725	4.2456	21.6901	16.3321	5.358	21.7374	14.4489	7.2885
0.2737	4.2257	21.7097	16.3724	5.3373	21.7519	14.485	7.2669
0.275	4.2056	21.7291	16.4125	5.3166	21.7664	14.521	7.2454
0.2762	4.1857	21.7484	16.4525	5.2959	21.7807	14.5569	7.2238
0.2775	4.1658	21.7677	16.4923	5.2754	21.795	14.5926	7.2024
0.2787	4.146	21.7868	16.532	5.2548	21.8093	14.6283	7.181
0.28	4.1262	21.8058	16.5716	5.2342	21.8235	14.6639	7.1596
0.2812	4.1064	21.8248	16.611	5.2138	21.8376	14.6994	7.1382
0.2825	4.0867	21.8436	16.6502	5.1934	21.8517	14.7348	7.1169
0.2837	4.0671	21.8623	16.6893	5.173	21.8657	14.7701	7.0956
0.285	4.0475	21.8809	16.7283	5.1526	21.8797	14.8052	7.0745
0.2862	4.028	21.8994	16.7671	5.1323	21.8936	14.8403	7.0533
0.2875	4.0084	21.9179	16.8058	5.1121	21.9074	14.8753	7.0321
0.2887	3.989	21.9362	16.8443	5.0919	21.9212	14.9102	7.011
0.29	3.9696	21.9544	16.8827	5.0717	21.935	14.945	6.99
0.2912	3.9502	21.9725	16.9209	5.0516	21.9486	14.9797	6.9689
0.2925	3.931	21.9906	16.959	5.0316	21.9623	15.0143	6.948
0.2937	3.9116	22.0085	16.9969	5.0116	21.9758	15.0488	6.927
0.295	3.8924	22.0263	17.0347	4.9916	21.9894	15.0832	6.9062
0.2962	3.8733	22.0441	17.0724	4.9717	22.0028	15.1175	6.8853
0.2975	3.8543	22.0617	17.1099	4.9518	22.0162	15.1517	6.8645
0.2987	3.8352	22.0792	17.1473	4.9319	22.0296	15.1858	6.8438
0.3	3.8162	22.0967	17.1845	4.9122	22.0429	15.2198	6.8231
0.3012	3.7972	22.114	17.2216	4.8924	22.0561	15.2538	6.8023
0.3025	3.7783	22.1313	17.2586	4.8727	22.0693	15.2876	6.7817
0.3037	3.7595	22.1485	17.2954	4.8531	22.0824	15.3213	6.7611
0.305	3.7408	22.1655	17.3321	4.8334	22.0955	15.3549	6.7406
0.3062	3.722	22.1825	17.3686	4.8139	22.1085	15.3885	6.72
0.3075	3.7034	22.1994	17.405	4.7944	22.1215	15.4219	6.6996
0.3087	3.6848	22.2162	17.4412	4.775	22.1344	15.4552	6.6792
0.31	3.6662	22.2329	17.4773	4.7556	22.1473	15.4885	6.6588
0.3112	3.6477	22.2495	17.5133	4.7362	22.1601	15.5216	6.6385
0.3125	3.6293	22.266	17.5491	4.7169	22.1728	15.5547	6.6181
0.3137	3.6108	22.2824	17.5848	4.6976	22.1855	15.5876	6.5979
0.315	3.5925	22.2988	17.6204	4.6784	22.1982	15.6205	6.5777
0.3162	3.5742	22.315	17.6558	4.6592	22.2108	15.6533	6.5575
0.3175	3.556	22.3312	17.6911	4.6401	22.2233	15.686	6.5373
0.3187	3.5378	22.3472	17.7262	4.621	22.2358	15.7185	6.5173
0.32	3.5198	22.3632	17.7612	4.602	22.2483	15.751	6.4973
0.3212	3.5017	22.3791	17.7961	4.583	22.2607	15.7834	6.4773

z (km)	Δr-fl	Nd=0.75 Rock ‰ δ18O	Fluid ‰ δ18O	Δr-fl	Nd=0.5 Rock ‰ δ18O	Fluid ‰ δ18O	Δr-fl
0.3225	3.4836	22.3949	17.8308	4.5641	22.273	15.8157	6.4573
0.3237	3.4657	22.4106	17.8654	4.5452	22.2853	15.8479	6.4374
0.325	3.4478	22.4263	17.8999	4.5264	22.2975	15.88	6.4175
0.3262	3.43	22.4418	17.9342	4.5076	22.3097	15.912	6.3977
0.3275	3.4122	22.4573	17.9684	4.4889	22.3219	15.944	6.3779
0.3287	3.3946	22.4726	18.0024	4.4702	22.3339	15.9758	6.3581
0.33	3.3769	22.4879	18.0363	4.4516	22.346	16.0075	6.3385
0.3312	3.3593	22.5031	18.0701	4.433	22.358	16.0392	6.3188
0.3325	3.3418	22.5182	18.1037	4.4145	22.3699	16.0707	6.2992
0.3337	3.3243	22.5333	18.1372	4.3961	22.3818	16.1022	6.2796
0.335	3.3068	22.5482	18.1706	4.3776	22.3936	16.1336	6.26
0.3362	3.2895	22.5631	18.2039	4.3592	22.4054	16.1649	6.2405
0.3375	3.2722	22.5779	18.237	4.3409	22.4172	16.196	6.2212
0.3387	3.255	22.5926	18.27	4.3226	22.4289	16.2271	6.2018
0.34	3.2378	22.6072	18.3028	4.3044	22.4405	16.2581	6.1824
0.3412	3.2206	22.6218	18.3355	4.2863	22.4521	16.2891	6.163
0.3425	3.2036	22.6362	18.3681	4.2681	22.4636	16.3199	6.1437
0.3437	3.1866	22.6506	18.4005	4.2501	22.4751	16.3506	6.1245
0.345	3.1696	22.6649	18.4329	4.232	22.4866	16.3813	6.1053
0.3462	3.1528	22.6791	18.465	4.2141	22.498	16.4118	6.0862
0.3475	3.1359	22.6933	18.4971	4.1962	22.5094	16.4423	6.0671
0.3487	3.1191	22.7073	18.529	4.1783	22.5207	16.4726	6.0481
0.35	3.1025	22.7213	18.5608	4.1605	22.5319	16.5029	6.029
0.3512	3.0858	22.7352	18.5925	4.1427	22.5431	16.5331	6.01
0.3525	3.0692	22.749	18.624	4.125	22.5543	16.5632	5.9911
0.3537	3.0526	22.7628	18.6555	4.1073	22.5654	16.5932	5.9722
0.355	3.0362	22.7765	18.6867	4.0898	22.5765	16.6231	5.9534
0.3562	3.0198	22.7901	18.7179	4.0722	22.5875	16.653	5.9345
0.3575	3.0035	22.8036	18.7489	4.0547	22.5985	16.6827	5.9158
0.3587	2.9872	22.817	18.7798	4.0372	22.6095	16.7124	5.8971
0.36	2.971	22.8304	18.8106	4.0198	22.6203	16.7419	5.8784
0.3612	2.9548	22.8437	18.8412	4.0025	22.6312	16.7714	5.8598
0.3625	2.9387	22.8569	18.8717	3.9852	22.642	16.8008	5.8412
0.3637	2.9226	22.87	18.9021	3.9679	22.6527	16.8301	5.8226
0.365	2.9067	22.8831	18.9324	3.9507	22.6635	16.8593	5.8042
0.3662	2.8908	22.8961	18.9625	3.9336	22.6741	16.8884	5.7857
0.3675	2.8749	22.909	18.9926	3.9164	22.6847	16.9175	5.7672
0.3687	2.8592	22.9219	19.0225	3.8994	22.6953	16.9464	5.7489
0.37	2.8434	22.9347	19.0522	3.8825	22.7058	16.9753	5.7305
0.3712	2.8277	22.9474	19.0819	3.8655	22.7163	17.0041	5.7122
0.3725	2.8121	22.96	19.1114	3.8486	22.7268	17.0328	5.694
0.3737	2.7966	22.9726	19.1408	3.8318	22.7372	17.0614	5.6758
0.375	2.7811	22.985	19.1701	3.8149	22.7475	17.0899	5.6576

z (km)	Δr-fl	Nd=0.75 Rock ‰ δ18O	Fluid ‰ δ18O	Δr-fl	Nd=0.5 Rock ‰ δ18O	Fluid ‰ δ18O	Δr-fl
0.3762	2.7657	22.9975	19.1992	3.7983	22.7578	17.1183	5.6395
0.3775	2.7503	23.0098	19.2282	3.7816	22.7681	17.1466	5.6215
0.3787	2.7349	23.0221	19.2571	3.765	22.7783	17.1749	5.6034
0.38	2.7198	23.0343	19.2859	3.7484	22.7885	17.2031	5.5854
0.3812	2.7045	23.0464	19.3146	3.7318	22.7986	17.2312	5.5674
0.3825	2.6895	23.0585	19.3431	3.7154	22.8087	17.2592	5.5495
0.3837	2.6744	23.0705	19.3716	3.6989	22.8188	17.2871	5.5317
0.385	2.6594	23.0825	19.3999	3.6826	22.8288	17.3149	5.5139
0.3862	2.6445	23.0943	19.428	3.6663	22.8388	17.3427	5.4961
0.3875	2.6296	23.1061	19.4561	3.65	22.8487	17.3703	5.4784
0.3887	2.6148	23.1178	19.484	3.6338	22.8586	17.3979	5.4607
0.39	2.6	23.1295	19.5119	3.6176	22.8684	17.4254	5.443
0.3912	2.5853	23.1411	19.5396	3.6015	22.8782	17.4528	5.4254
0.3925	2.5706	23.1526	19.5672	3.5854	22.888	17.4801	5.4079
0.3937	2.5561	23.1641	19.5946	3.5695	22.8977	17.5074	5.3903
0.395	2.5416	23.1755	19.622	3.5535	22.9074	17.5345	5.3729
0.3962	2.5272	23.1868	19.6492	3.5376	22.917	17.5616	5.3554
0.3975	2.5127	23.1981	19.6763	3.5218	22.9266	17.5886	5.338
0.3987	2.4984	23.2093	19.7033	3.506	22.9362	17.6155	5.3207
0.4	2.4842	23.2205	19.7302	3.4903	22.9457	17.6423	5.3034
0.4012	2.47	23.2315	19.757	3.4745	22.9551	17.6691	5.286
0.4025	2.4558	23.2426	19.7836	3.459	22.9646	17.6957	5.2689
0.4037	2.4417	23.2535	19.8102	3.4433	22.974	17.7223	5.2517
0.405	2.4277	23.2644	19.8366	3.4278	22.9833	17.7488	5.2345
0.4062	2.4137	23.2752	19.8629	3.4123	22.9926	17.7752	5.2174
0.4075	2.3998	23.286	19.8891	3.3969	23.0019	17.8016	5.2003
0.4087	2.3859	23.2967	19.9152	3.3815	23.0111	17.8278	5.1833
0.41	2.3721	23.3073	19.9412	3.3661	23.0203	17.854	5.1663
0.4112	2.3585	23.3179	19.967	3.3509	23.0295	17.8801	5.1494
0.4125	2.3448	23.3284	19.9928	3.3356	23.0386	17.9061	5.1325
0.4137	2.3311	23.3389	20.0184	3.3205	23.0477	17.932	5.1157
0.415	2.3177	23.3493	20.0439	3.3054	23.0567	17.9579	5.0988
0.4162	2.3042	23.3596	20.0693	3.2903	23.0657	17.9836	5.0821
0.4175	2.2907	23.3699	20.0946	3.2753	23.0747	18.0093	5.0654
0.4187	2.2773	23.3801	20.1198	3.2603	23.0836	18.0349	5.0487
0.42	2.264	23.3903	20.1449	3.2454	23.0925	18.0604	5.0321
0.4212	2.2508	23.4004	20.1699	3.2305	23.1013	18.0859	5.0154
0.4225	2.2377	23.4104	20.1947	3.2157	23.1101	18.1112	4.9989
0.4237	2.2244	23.4204	20.2195	3.2009	23.1189	18.1365	4.9824
0.425	2.2115	23.4303	20.2441	3.1862	23.1277	18.1617	4.966
0.4262	2.1984	23.4402	20.2686	3.1716	23.1363	18.1869	4.9494
0.4275	2.1855	23.45	20.293	3.157	23.145	18.2119	4.9331
0.4287	2.1726	23.4597	20.3174	3.1423	23.1536	18.2369	4.9167

z (km)	Δr-fl	Nd=0.75 Rock ‰ δ18O	Fluid ‰ δ18O	Δr-fl	Nd=0.5 Rock ‰ δ18O	Fluid ‰ δ18O	Δr-fl
0.43	2.1597	23.4694	20.3416	3.1278	23.1622	18.2618	4.9004
0.4312	2.147	23.4791	20.3657	3.1134	23.1708	18.2866	4.8842
0.4325	2.1343	23.4886	20.3896	3.099	23.1793	18.3113	4.868
0.4337	2.1216	23.4982	20.4135	3.0847	23.1877	18.336	4.8517
0.435	2.109	23.5076	20.4373	3.0703	23.1962	18.3606	4.8356
0.4362	2.0965	23.5171	20.461	3.0561	23.2046	18.3851	4.8195
0.4375	2.084	23.5264	20.4845	3.0419	23.213	18.4095	4.8035
0.4387	2.0716	23.5357	20.508	3.0277	23.2213	18.4338	4.7875
0.44	2.0592	23.545	20.5314	3.0136	23.2296	18.4581	4.7715
0.4412	2.0469	23.5542	20.5546	2.9996	23.2378	18.4823	4.7555
0.4425	2.0347	23.5633	20.5778	2.9855	23.2461	18.5064	4.7397
0.4437	2.0225	23.5724	20.6008	2.9716	23.2543	18.5305	4.7238
0.445	2.0103	23.5814	20.6237	2.9577	23.2624	18.5544	4.708
0.4462	1.9983	23.5904	20.6466	2.9438	23.2705	18.5783	4.6922
0.4475	1.9863	23.5994	20.6693	2.9301	23.2786	18.6021	4.6765
0.4487	1.9743	23.6082	20.6919	2.9163	23.2867	18.6259	4.6608
0.45	1.9624	23.6171	20.7145	2.9026	23.2947	18.6495	4.6452
0.4512	1.9505	23.6258	20.7369	2.8889	23.3026	18.6731	4.6295
0.4525	1.9387	23.6346	20.7592	2.8754	23.3106	18.6966	4.614
0.4537	1.927	23.6432	20.7814	2.8618	23.3185	18.7201	4.5984
0.455	1.9153	23.6519	20.8036	2.8483	23.3264	18.7434	4.583
0.4562	1.9037	23.6604	20.8256	2.8348	23.3342	18.7667	4.5675
0.4575	1.8921	23.669	20.8475	2.8215	23.342	18.7899	4.5521
0.4587	1.8807	23.6774	20.8693	2.8081	23.3498	18.813	4.5368
0.46	1.8691	23.6858	20.8911	2.7947	23.3575	18.8361	4.5214
0.4612	1.8578	23.6942	20.9127	2.7815	23.3652	18.8591	4.5061
0.4625	1.8464	23.7025	20.9342	2.7683	23.3729	18.882	4.4909
0.4637	1.8351	23.7108	20.9556	2.7552	23.3806	18.9049	4.4757
0.465	1.8239	23.719	20.977	2.742	23.3882	18.9276	4.4606
0.4662	1.8128	23.7272	20.9982	2.729	23.3957	18.9503	4.4454
0.4675	1.8016	23.7353	21.0193	2.716	23.4033	18.9729	4.4304
0.4687	1.7906	23.7434	21.0404	2.703	23.4108	18.9955	4.4153
0.47	1.7796	23.7514	21.0613	2.6901	23.4183	19.018	4.4003
0.4712	1.7685	23.7594	21.0822	2.6772	23.4257	19.0404	4.3853
0.4725	1.7577	23.7674	21.1029	2.6645	23.4331	19.0627	4.3704
0.4737	1.7468	23.7752	21.1236	2.6516	23.4405	19.0849	4.3556
0.475	1.7361	23.7831	21.1441	2.639	23.4478	19.1071	4.3407
0.4762	1.7253	23.7909	21.1646	2.6263	23.4552	19.1292	4.326
0.4775	1.7146	23.7986	21.185	2.6136	23.4624	19.1513	4.3111
0.4787	1.704	23.8063	21.2052	2.6011	23.4697	19.1733	4.2964
0.48	1.6934	23.814	21.2254	2.5886	23.4769	19.1952	4.2817
0.4812	1.6829	23.8216	21.2455	2.5761	23.4841	19.217	4.2671
0.4825	1.6724	23.8292	21.2655	2.5637	23.4913	19.2387	4.2526

z (km)	Δr-fl	Nd=0.75 Rock ‰ δ18O	Fluid ‰ δ18O	Δr-fl	Nd=0.5 Rock ‰ δ18O	Fluid ‰ δ18O	Δr-fl
0.4837	1.662	23.8367	21.2854	2.5513	23.4984	19.2604	4.238
0.485	1.6517	23.8442	21.3052	2.539	23.5055	19.282	4.2235
0.4862	1.6413	23.8516	21.3249	2.5267	23.5125	19.3036	4.2089
0.4875	1.6311	23.859	21.3445	2.5145	23.5196	19.3251	4.1945
0.4887	1.6209	23.8663	21.3641	2.5022	23.5266	19.3465	4.1801
0.49	1.6107	23.8736	21.3835	2.4901	23.5335	19.3678	4.1657
0.4912	1.6006	23.8809	21.4029	2.478	23.5405	19.3891	4.1514
0.4925	1.5906	23.8881	21.4221	2.466	23.5474	19.4103	4.1371
0.4937	1.5806	23.8953	21.4413	2.454	23.5543	19.4314	4.1229
0.495	1.5707	23.9024	21.4604	2.442	23.5611	19.4524	4.1087
0.4962	1.5608	23.9095	21.4794	2.4301	23.5679	19.4734	4.0945
0.4975	1.5509	23.9165	21.4983	2.4182	23.5747	19.4943	4.0804
0.4987	1.5411	23.9235	21.5171	2.4064	23.5815	19.5152	4.0663
0.5	1.5314	23.9305	21.5358	2.3947	23.5882	19.536	4.0522

E.3 Reactive Transport Modeling Results at TIFF of $1x10^4$ (moles H_2O/cm^2)

	Nd=5			Nd=2			Nd=1	
	Rock ‰	**Fluid ‰**		**Rock ‰**	**Fluid ‰**		**Rock ‰**	**Fluid ‰**
z (km)	**δ18O**	**δ18O**	**Δr-fl**	**δ18O**	**δ18O**	**Δr-fl**	**δ18O**	**δ18O**
0	4.1415	4	0.1415	6.842	4	2.842	11.7255	4
0.0125	4.1765	4.0073	0.1692	6.9526	4.0542	2.8984	11.8026	4.0729
0.025	4.2141	4.016	0.1981	7.0632	4.1095	2.9537	11.8793	4.1459
0.0375	4.2542	4.0261	0.2281	7.1739	4.1658	3.0081	11.9557	4.2189
0.05	4.2969	4.0377	0.2592	7.2847	4.2233	3.0614	12.0318	4.2921
0.0625	4.3421	4.0508	0.2913	7.3955	4.2818	3.1137	12.1075	4.3653
0.075	4.39	4.0654	0.3246	7.5064	4.3414	3.165	12.1829	4.4385
0.0875	4.4404	4.0817	0.3587	7.6174	4.402	3.2154	12.2579	4.5118
0.1	4.4934	4.0997	0.3937	7.7283	4.4635	3.2648	12.3326	4.5852
0.1125	4.549	4.1194	0.4296	7.8393	4.5261	3.3132	12.407	4.6586
0.125	4.6072	4.1408	0.4664	7.9503	4.5896	3.3607	12.481	4.7321
0.1375	4.668	4.164	0.504	8.0612	4.6541	3.4071	12.5547	4.8056
0.15	4.7314	4.1891	0.5423	8.1721	4.7195	3.4526	12.6281	4.8791
0.1625	4.7973	4.2161	0.5812	8.2829	4.7858	3.4971	12.7011	4.9527
0.175	4.8658	4.2449	0.6209	8.3937	4.853	3.5407	12.7738	5.0263
0.1875	4.9368	4.2757	0.6611	8.5044	4.9211	3.5833	12.8462	5.0999
0.2	5.0103	4.3085	0.7018	8.615	4.9901	3.6249	12.9182	5.1736
0.2125	5.0863	4.3433	0.743	8.7255	5.0598	3.6657	12.9899	5.2473
0.225	5.1648	4.38	0.7848	8.8359	5.1304	3.7055	13.0613	5.321
0.2375	5.2458	4.4189	0.8269	8.9462	5.2018	3.7444	13.1323	5.3947
0.25	5.3291	4.4598	0.8693	9.0563	5.274	3.7823	13.203	5.4684
0.2625	5.4149	4.5028	0.9121	9.1663	5.3469	3.8194	13.2734	5.5421
0.275	5.503	4.5479	0.9551	9.2761	5.4206	3.8555	13.3434	5.6158
0.2875	5.5935	4.5951	0.9984	9.3858	5.4951	3.8907	13.4131	5.6895
0.3	5.6862	4.6444	1.0418	9.4953	5.5702	3.9251	13.4825	5.7632
0.3125	5.7812	4.6958	1.0854	9.6046	5.646	3.9586	13.5515	5.8369
0.325	5.8785	4.7494	1.1291	9.7137	5.7225	3.9912	13.6203	5.9106
0.3375	5.9779	4.8052	1.1727	9.8225	5.7997	4.0228	13.6887	5.9843
0.35	6.0795	4.8631	1.2164	9.9312	5.8776	4.0536	13.7567	6.0579
0.3625	6.1831	4.9231	1.26	10.0396	5.956	4.0836	13.8245	6.1316
0.375	6.2889	4.9853	1.3036	10.1478	6.0351	4.1127	13.8919	6.2052
0.3875	6.3966	5.0496	1.347	10.2557	6.1148	4.1409	13.959	6.2787
0.4	6.5064	5.1161	1.3903	10.3634	6.195	4.1684	14.0258	6.3523
0.4125	6.618	5.1847	1.4333	10.4708	6.2758	4.195	14.0923	6.4258
0.425	6.7316	5.2554	1.4762	10.5779	6.3572	4.2207	14.1584	6.4993
0.4375	6.8469	5.3283	1.5186	10.6847	6.4391	4.2456	14.2242	6.5727
0.45	6.9641	5.4032	1.5609	10.7913	6.5215	4.2698	14.2897	6.6461
0.4625	7.083	5.4802	1.6028	10.8975	6.6044	4.2931	14.3549	6.7194
0.475	7.2035	5.5593	1.6442	11.0035	6.6878	4.3157	14.4197	6.7927
0.4875	7.3258	5.6405	1.6853	11.1091	6.7717	4.3374	14.4843	6.866
0.5	7.4495	5.7236	1.7259	11.2144	6.856	4.3584	14.5485	6.9392
0.5125	7.5749	5.8088	1.7661	11.3193	6.9408	4.3785	14.6124	7.0123
0.525	7.7017	5.896	1.8057	11.4239	7.0259	4.398	14.676	7.0854

z (km)	Nd=5 Rock ‰ δ18O	Fluid ‰ δ18O	Δr-fl	Nd=2 Rock ‰ δ18O	Fluid ‰ δ18O	Δr-fl	Nd=1 Rock ‰ δ18O	Fluid ‰ δ18O
0.5375	7.8299	5.9851	1.8448	11.5282	7.1115	4.4167	14.7393	7.1584
0.55	7.9595	6.0762	1.8833	11.6321	7.1975	4.4346	14.8023	7.2313
0.5625	8.0904	6.1691	1.9213	11.7357	7.2839	4.4518	14.8649	7.3042
0.575	8.2226	6.264	1.9586	11.8389	7.3706	4.4683	14.9273	7.377
0.5875	8.356	6.3607	1.9953	11.9417	7.4577	4.484	14.9893	7.4497
0.6	8.4906	6.4592	2.0314	12.0441	7.5451	4.499	15.051	7.5224
0.6125	8.6263	6.5595	2.0668	12.1462	7.6329	4.5133	15.1124	7.5949
0.625	8.763	6.6616	2.1014	12.2478	7.721	4.5268	15.1736	7.6674
0.6375	8.9007	6.7654	2.1353	12.3491	7.8093	4.5398	15.2343	7.7398
0.65	9.0394	6.8709	2.1685	12.4499	7.8979	4.552	15.2948	7.8122
0.6625	9.179	6.978	2.201	12.5504	7.9869	4.5635	15.355	7.8844
0.675	9.3194	7.0868	2.2326	12.6504	8.076	4.5744	15.4149	7.9566
0.6875	9.4606	7.1971	2.2635	12.75	8.1654	4.5846	15.4745	8.0286
0.7	9.6026	7.309	2.2936	12.8492	8.2551	4.5941	15.5338	8.1006
0.7125	9.7452	7.4223	2.3229	12.948	8.3449	4.6031	15.5927	8.1724
0.725	9.8885	7.5372	2.3513	13.0463	8.435	4.6113	15.6514	8.2442
0.7375	10.0323	7.6534	2.3789	13.1442	8.5252	4.619	15.7098	8.3159
0.75	10.1767	7.7711	2.4056	13.2417	8.6156	4.6261	15.7679	8.3874
0.7625	10.3215	7.89	2.4315	13.3387	8.7062	4.6325	15.8256	8.4589
0.775	10.4668	8.0103	2.4565	13.4353	8.797	4.6383	15.8831	8.5302
0.7875	10.6125	8.1318	2.4807	13.5314	8.8879	4.6435	15.9403	8.6015
0.8	10.7585	8.2546	2.5039	13.627	8.9789	4.6481	15.9972	8.6726
0.8125	10.9048	8.3785	2.5263	13.7222	9.07	4.6522	16.0538	8.7436
0.825	11.0513	8.5035	2.5478	13.817	9.1613	4.6557	16.1101	8.8145
0.8375	11.198	8.6296	2.5684	13.9112	9.2526	4.6586	16.1661	8.8853
0.85	11.3449	8.7568	2.5881	14.005	9.344	4.661	16.2218	8.9559
0.8625	11.4919	8.8849	2.607	14.0983	9.4356	4.6627	16.2772	9.0265
0.875	11.6389	9.014	2.6249	14.1912	9.5271	4.6641	16.3323	9.0969
0.8875	11.7859	9.1441	2.6418	14.2835	9.6187	4.6648	16.3872	9.1672
0.9	11.9329	9.2749	2.658	14.3754	9.7104	4.665	16.4417	9.2373
0.9125	12.0798	9.4066	2.6732	14.4668	9.8021	4.6647	16.496	9.3074
0.925	12.2266	9.5391	2.6875	14.5577	9.8938	4.6639	16.55	9.3773
0.9375	12.3732	9.6723	2.7009	14.6481	9.9855	4.6626	16.6037	9.447
0.95	12.5196	9.8062	2.7134	14.738	10.0773	4.6607	16.6571	9.5167
0.9625	12.6658	9.9407	2.7251	14.8275	10.169	4.6585	16.7102	9.5862
0.975	12.8117	10.0758	2.7359	14.9164	10.2607	4.6557	16.7631	9.6555
0.9875	12.9573	10.2115	2.7458	15.0048	10.3524	4.6524	16.8156	9.7248
1	13.1025	10.3477	2.7548	15.0928	10.444	4.6488	16.8679	9.7938
1.0125	13.2474	10.4844	2.763	15.1802	10.5356	4.6446	16.9199	9.8628
1.025	13.3918	10.6215	2.7703	15.2671	10.6271	4.64	16.9716	9.9316
1.0375	13.5358	10.759	2.7768	15.3535	10.7186	4.6349	17.0231	10.0002
1.05	13.6792	10.8969	2.7823	15.4394	10.81	4.6294	17.0743	10.0687
1.0625	13.8222	11.035	2.7872	15.5248	10.9013	4.6235	17.1252	10.1371

		Nd=5			Nd=2			Nd=1
	Rock ‰	Fluid ‰		Rock ‰	Fluid ‰		Rock ‰	Fluid ‰
z (km)	**δ18O**	**δ18O**	**Δr-fl**	**δ18O**	**δ18O**	**Δr-fl**	**δ18O**	**δ18O**
1.075	13.9646	11.1734	2.7912	15.6097	10.9925	4.6172	17.1758	10.2053
1.0875	14.1063	11.312	2.7943	15.6941	11.0837	4.6104	17.2261	10.2734
1.1	14.2475	11.4508	2.7967	15.778	11.1747	4.6033	17.2762	10.3413
1.1125	14.388	11.5898	2.7982	15.8614	11.2656	4.5958	17.326	10.409
1.125	14.5279	11.7288	2.7991	15.9442	11.3564	4.5878	17.3755	10.4766
1.1375	14.667	11.8679	2.7991	16.0265	11.447	4.5795	17.4248	10.5441
1.15	14.8054	12.0071	2.7983	16.1084	11.5375	4.5709	17.4738	10.6113
1.1625	14.943	12.1462	2.7968	16.1897	11.6279	4.5618	17.5225	10.6785
1.175	15.0799	12.2853	2.7946	16.2705	11.7181	4.5524	17.571	10.7454
1.1875	15.2159	12.4243	2.7916	16.3507	11.8081	4.5426	17.6192	10.8122
1.2	15.3511	12.5632	2.7879	16.4305	11.898	4.5325	17.6671	10.8789
1.2125	15.4855	12.7019	2.7836	16.5097	11.9877	4.522	17.7148	10.9454
1.225	15.619	12.8404	2.7786	16.5884	12.0772	4.5112	17.7622	11.0117
1.2375	15.7516	12.9787	2.7729	16.6666	12.1665	4.5001	17.8093	11.0778
1.25	15.8832	13.1167	2.7665	16.7443	12.2557	4.4886	17.8562	11.1438
1.2625	16.014	13.2545	2.7595	16.8215	12.3446	4.4769	17.9028	11.2096
1.275	16.1438	13.3919	2.7519	16.8981	12.4333	4.4648	17.9492	11.2753
1.2875	16.2726	13.529	2.7436	16.9743	12.5218	4.4525	17.9953	11.3407
1.3	16.4004	13.6657	2.7347	17.0499	12.6101	4.4398	18.0411	11.406
1.3125	16.5272	13.8019	2.7253	17.125	12.6981	4.4269	18.0867	11.4712
1.325	16.653	13.9377	2.7153	17.1996	12.786	4.4136	18.1321	11.5361
1.3375	16.7777	14.0731	2.7046	17.2736	12.8735	4.4001	18.1771	11.6009
1.35	16.9014	14.2079	2.6935	17.3472	12.9609	4.3863	18.222	11.6655
1.3625	17.0241	14.3422	2.6819	17.4202	13.048	4.3722	18.2666	11.7299
1.375	17.1456	14.476	2.6696	17.4927	13.1348	4.3579	18.3109	11.7942
1.3875	17.2661	14.6091	2.657	17.5647	13.2213	4.3434	18.355	11.8583
1.4	17.3855	14.7417	2.6438	17.6362	13.3076	4.3286	18.3988	11.9222
1.4125	17.5038	14.8736	2.6302	17.7072	13.3937	4.3135	18.4424	11.9859
1.425	17.6209	15.0049	2.616	17.7777	13.4794	4.2983	18.4857	12.0494
1.4375	17.7369	15.1355	2.6014	17.8476	13.5649	4.2827	18.5288	12.1128
1.45	17.8518	15.2653	2.5865	17.9171	13.65	4.2671	18.5716	12.1759
1.4625	17.9656	15.3945	2.5711	17.986	13.7349	4.2511	18.6143	12.2389
1.475	18.0782	15.5229	2.5553	18.0545	13.8195	4.235	18.6566	12.3017
1.4875	18.1896	15.6506	2.539	18.1224	13.9038	4.2186	18.6987	12.3644
1.5	18.2999	15.7774	2.5225	18.1898	13.9878	4.202	18.7406	12.4268
1.5125	18.4091	15.9035	2.5056	18.2567	14.0715	4.1852	18.7823	12.489
1.525	18.517	16.0287	2.4883	18.3232	14.1548	4.1684	18.8237	12.5511
1.5375	18.6238	16.1531	2.4707	18.3891	14.2379	4.1512	18.8648	12.613
1.55	18.7294	16.2766	2.4528	18.4545	14.3206	4.1339	18.9057	12.6747
1.5625	18.8338	16.3993	2.4345	18.5194	14.403	4.1164	18.9464	12.7362
1.575	18.937	16.5211	2.4159	18.5838	14.4851	4.0987	18.9869	12.7975
1.5875	19.0391	16.6419	2.3972	18.6477	14.5668	4.0809	19.0271	12.8586
1.6	19.14	16.7619	2.3781	18.7112	14.6482	4.063	19.0671	12.9195

	Nd=5			Nd=2			Nd=1	
z (km)	Rock ‰ δ18O	Fluid ‰ δ18O	Δr-fl	Rock ‰ δ18O	Fluid ‰ δ18O	Δr-fl	Rock ‰ δ18O	Fluid ‰ δ18O
1.6125	19.2397	16.8809	2.3588	18.7741	14.7293	4.0448	19.1069	12.9803
1.625	19.3381	16.999	2.3391	18.8366	14.81	4.0266	19.1464	13.0408
1.6375	19.4355	17.1161	2.3194	18.8985	14.8904	4.0081	19.1857	13.1012
1.65	19.5316	17.2322	2.2994	18.96	14.9704	3.9896	19.2248	13.1614
1.6625	19.6265	17.3474	2.2791	19.021	15.0501	3.9709	19.2636	13.2213
1.675	19.7203	17.4615	2.2588	19.0814	15.1294	3.952	19.3022	13.2811
1.6875	19.8129	17.5747	2.2382	19.1415	15.2084	3.9331	19.3406	13.3407
1.7	19.9043	17.6869	2.2174	19.201	15.287	3.914	19.3788	13.4001
1.7125	19.9945	17.798	2.1965	19.26	15.3652	3.8948	19.4167	13.4593
1.725	20.0835	17.9081	2.1754	19.3186	15.4431	3.8755	19.4544	13.5183
1.7375	20.1714	18.0172	2.1542	19.3767	15.5206	3.8561	19.4919	13.5771
1.75	20.2581	18.1252	2.1329	19.4343	15.5978	3.8365	19.5292	13.6357
1.7625	20.3437	18.2322	2.1115	19.4915	15.6745	3.817	19.5663	13.6941
1.775	20.4281	18.3381	2.09	19.5482	15.7509	3.7973	19.6031	13.7523
1.7875	20.5113	18.443	2.0683	19.6044	15.8269	3.7775	19.6397	13.8103
1.8	20.5934	18.5468	2.0466	19.6601	15.9026	3.7575	19.6761	13.8681
1.8125	20.6744	18.6495	2.0249	19.7154	15.9778	3.7376	19.7123	13.9258
1.825	20.7542	18.7512	2.003	19.7703	16.0527	3.7176	19.7483	13.9832
1.8375	20.8329	18.8518	1.9811	19.8246	16.1272	3.6974	19.7841	14.0404
1.85	20.9105	18.9513	1.9592	19.8785	16.2013	3.6772	19.8196	14.0974
1.8625	20.987	19.0497	1.9373	19.932	16.275	3.657	19.855	14.1543
1.875	21.0623	19.147	1.9153	19.985	16.3483	3.6367	19.8901	14.2109
1.8875	21.1366	19.2433	1.8933	20.0375	16.4213	3.6162	19.925	14.2673
1.9	21.2097	19.3384	1.8713	20.0896	16.4938	3.5958	19.9597	14.3235
1.9125	21.2818	19.4325	1.8493	20.1413	16.566	3.5753	19.9942	14.3796
1.925	21.3528	19.5255	1.8273	20.1925	16.6377	3.5548	20.0285	14.4354
1.9375	21.4227	19.6174	1.8053	20.2433	16.7091	3.5342	20.0626	14.491
1.95	21.4916	19.7082	1.7834	20.2936	16.7801	3.5135	20.0965	14.5465
1.9625	21.5594	19.7979	1.7615	20.3435	16.8506	3.4929	20.1301	14.6017
1.975	21.6261	19.8865	1.7396	20.3929	16.9208	3.4721	20.1636	14.6567
1.9875	21.6919	19.974	1.7179	20.442	16.9905	3.4515	20.1969	14.7115
2	21.7566	20.0605	1.6961	20.4905	17.0599	3.4306	20.23	14.7661
2.0125	21.8202	20.1459	1.6743	20.5387	17.1289	3.4098	20.2628	14.8206
2.025	21.8829	20.2302	1.6527	20.5864	17.1974	3.389	20.2955	14.8748
2.0375	21.9446	20.3134	1.6312	20.6338	17.2656	3.3682	20.328	14.9288
2.05	22.0053	20.3956	1.6097	20.6807	17.3333	3.3474	20.3603	14.9826
2.0625	22.065	20.4767	1.5883	20.7271	17.4007	3.3264	20.3923	15.0362
2.075	22.1237	20.5567	1.567	20.7732	17.4676	3.3056	20.4242	15.0896
2.0875	22.1814	20.6357	1.5457	20.8188	17.5342	3.2846	20.4559	15.1428
2.1	22.2383	20.7136	1.5247	20.8641	17.6003	3.2638	20.4874	15.1959
2.1125	22.2941	20.7905	1.5036	20.9089	17.666	3.2429	20.5187	15.2487
2.125	22.3491	20.8663	1.4828	20.9533	17.7313	3.222	20.5498	15.3013
2.1375	22.4031	20.9411	1.462	20.9973	17.7962	3.2011	20.5808	15.3537

z (km)	Nd=5 Rock ‰ δ18O	Fluid ‰ δ18O	Δr-fl	Nd=2 Rock ‰ δ18O	Fluid ‰ δ18O	Δr-fl	Nd=1 Rock ‰ δ18O	Fluid ‰ δ18O
2.15	22.4562	21.0148	1.4414	21.0409	17.8607	3.1802	20.6115	15.4059
2.1625	22.5084	21.0875	1.4209	21.0841	17.9248	3.1593	20.642	15.4579
2.175	22.5597	21.1592	1.4005	21.1269	17.9885	3.1384	20.6724	15.5096
2.1875	22.6101	21.2299	1.3802	21.1694	18.0518	3.1176	20.7026	15.5612
2.2	22.6596	21.2996	1.36	21.2114	18.1147	3.0967	20.7325	15.6126
2.2125	22.7083	21.3683	1.34	21.253	18.1772	3.0758	20.7623	15.6638
2.225	22.7562	21.436	1.3202	21.2943	18.2392	3.0551	20.792	15.7148
2.2375	22.8032	21.5027	1.3005	21.3351	18.3009	3.0342	20.8214	15.7656
2.25	22.8493	21.5684	1.2809	21.3756	18.3621	3.0135	20.8506	15.8162
2.2625	22.8947	21.6331	1.2616	21.4157	18.423	2.9927	20.8797	15.8665
2.275	22.9392	21.6969	1.2423	21.4555	18.4834	2.9721	20.9086	15.9167
2.2875	22.9829	21.7597	1.2232	21.4948	18.5434	2.9514	20.9373	15.9667
2.3	23.0259	21.8215	1.2044	21.5338	18.6031	2.9307	20.9658	16.0165
2.3125	23.068	21.8824	1.1856	21.5724	18.6623	2.9101	20.9942	16.066
2.325	23.1094	21.9424	1.167	21.6106	18.7211	2.8895	21.0224	16.1154
2.3375	23.1501	22.0014	1.1487	21.6485	18.7795	2.869	21.0504	16.1646
2.35	23.1899	22.0595	1.1304	21.686	18.8375	2.8485	21.0782	16.2136
2.3625	23.2291	22.1167	1.1124	21.7232	18.8951	2.8281	21.1058	16.2623
2.375	23.2675	22.173	1.0945	21.76	18.9523	2.8077	21.1333	16.3109
2.3875	23.3052	22.2284	1.0768	21.7964	19.0092	2.7872	21.1606	16.3593
2.4	23.3422	22.2829	1.0593	21.8325	19.0656	2.7669	21.1877	16.4074
2.4125	23.3785	22.3366	1.0419	21.8683	19.1216	2.7467	21.2147	16.4554
2.425	23.4141	22.3893	1.0248	21.9037	19.1772	2.7265	21.2415	16.5032
2.4375	23.449	22.4412	1.0078	21.9387	19.2324	2.7063	21.2681	16.5507
2.45	23.4833	22.4923	0.991	21.9734	19.2872	2.6862	21.2946	16.5981
2.4625	23.5169	22.5425	0.9744	22.0078	19.3416	2.6662	21.3208	16.6453
2.475	23.5499	22.5919	0.958	22.0418	19.3957	2.6461	21.347	16.6922
2.4875	23.5822	22.6405	0.9417	22.0755	19.4493	2.6262	21.3729	16.739
2.5	23.6139	22.6882	0.9257	22.1089	19.5025	2.6064	21.3987	16.7856
2.5125	23.6449	22.7352	0.9097	22.1419	19.5554	2.5865	21.4243	16.8319
2.525	23.6754	22.7813	0.8941	22.1747	19.6078	2.5669	21.4498	16.8781
2.5375	23.7052	22.8266	0.8786	22.207	19.6599	2.5471	21.4751	16.9241
2.55	23.7345	22.8712	0.8633	22.2391	19.7116	2.5275	21.5002	16.9699
2.5625	23.7632	22.915	0.8482	22.2708	19.7629	2.5079	21.5252	17.0154
2.575	23.7913	22.9581	0.8332	22.3023	19.8138	2.4885	21.55	17.0608
2.5875	23.8188	23.0004	0.8184	22.3334	19.8643	2.4691	21.5747	17.106
2.6	23.8458	23.0419	0.8039	22.3642	19.9144	2.4498	21.5992	17.151
2.6125	23.8723	23.0828	0.7895	22.3946	19.9642	2.4304	21.6235	17.1958
2.625	23.8982	23.1229	0.7753	22.4248	20.0136	2.4112	21.6477	17.2404
2.6375	23.9236	23.1622	0.7614	22.4547	20.0625	2.3922	21.6718	17.2848
2.65	23.9484	23.2009	0.7475	22.4843	20.1112	2.3731	21.6956	17.329
2.6625	23.9728	23.2389	0.7339	22.5135	20.1594	2.3541	21.7194	17.373
2.675	23.9966	23.2762	0.7204	22.5425	20.2073	2.3352	21.7429	17.4168

z (km)	Nd=5 Rock ‰ δ18O	Fluid ‰ δ18O	Δr-fl	Nd=2 Rock ‰ δ18O	Fluid ‰ δ18O	Δr-fl	Nd=1 Rock ‰ δ18O	Fluid ‰ δ18O
2.6875	24.02	23.3128	0.7072	22.5712	20.2547	2.3165	21.7664	17.4604
2.7	24.0429	23.3488	0.6941	22.5996	20.3019	2.2977	21.7896	17.5038
2.7125	24.0653	23.3841	0.6812	22.6276	20.3486	2.279	21.8128	17.5471
2.725	24.0872	23.4187	0.6685	22.6554	20.395	2.2604	21.8357	17.5901
2.7375	24.1086	23.4527	0.6559	22.683	20.441	2.242	21.8586	17.6329
2.75	24.1297	23.4861	0.6436	22.7102	20.4866	2.2236	21.8812	17.6756
2.7625	24.1502	23.5189	0.6313	22.7371	20.5319	2.2052	21.9038	17.7181
2.775	24.1704	23.551	0.6194	22.7638	20.5768	2.187	21.9261	17.7603
2.7875	24.1901	23.5825	0.6076	22.7902	20.6213	2.1689	21.9484	17.8024
2.8	24.2094	23.6135	0.5959	22.8163	20.6655	2.1508	21.9705	17.8443
2.8125	24.2282	23.6438	0.5844	22.8421	20.7093	2.1328	21.9924	17.886
2.825	24.2467	23.6736	0.5731	22.8677	20.7528	2.1149	22.0142	17.9275
2.8375	24.2648	23.7028	0.562	22.893	20.7959	2.0971	22.0359	17.9688
2.85	24.2824	23.7314	0.551	22.9181	20.8387	2.0794	22.0574	18.0099
2.8625	24.2997	23.7595	0.5402	22.9428	20.8811	2.0617	22.0788	18.0508
2.875	24.3167	23.787	0.5297	22.9673	20.9231	2.0442	22.1	18.0916
2.8875	24.3332	23.814	0.5192	22.9916	20.9648	2.0268	22.1211	18.1321
2.9	24.3494	23.8405	0.5089	23.0156	21.0062	2.0094	22.1421	18.1725
2.9125	24.3652	23.8665	0.4987	23.0393	21.0472	1.9921	22.1629	18.2127
2.925	24.3807	23.8919	0.4888	23.0628	21.0879	1.9749	22.1836	18.2526
2.9375	24.3958	23.9168	0.479	23.0861	21.1282	1.9579	22.2041	18.2925
2.95	24.4106	23.9413	0.4693	23.109	21.1682	1.9408	22.2245	18.3321
2.9625	24.4251	23.9652	0.4599	23.1318	21.2078	1.924	22.2448	18.3715
2.975	24.4392	23.9887	0.4505	23.1543	21.2471	1.9072	22.265	18.4107
2.9875	24.4531	24.0117	0.4414	23.1766	21.2861	1.8905	22.285	18.4498
3	24.4666	24.0344	0.4322	23.1986	21.3247	1.8739	22.3049	18.4887
3.0125	24.4798	24.0565	0.4233	23.2204	21.363	1.8574	22.3246	18.5274
3.025	24.4927	24.0781	0.4146	23.2419	21.401	1.8409	22.3442	18.5659
3.0375	24.5053	24.0993	0.406	23.2632	21.4386	1.8246	22.3637	18.6042
3.05	24.5177	24.1201	0.3976	23.2843	21.476	1.8083	22.3831	18.6423
3.0625	24.5297	24.1404	0.3893	23.3052	21.513	1.7922	22.4023	18.6803
3.075	24.5415	24.1603	0.3812	23.3258	21.5496	1.7762	22.4214	18.718
3.0875	24.553	24.1798	0.3732	23.3462	21.586	1.7602	22.4404	18.7556
3.1	24.5643	24.1989	0.3654	23.3664	21.622	1.7444	22.4592	18.793
3.1125	24.5752	24.2176	0.3576	23.3863	21.6577	1.7286	22.478	18.8303
3.125	24.586	24.2359	0.3501	23.4061	21.6931	1.713	22.4966	18.8673
3.1375	24.5964	24.2538	0.3426	23.4256	21.7282	1.6974	22.515	18.9042
3.15	24.6067	24.2714	0.3353	23.4449	21.763	1.6819	22.5334	18.9409
3.1625	24.6167	24.2885	0.3282	23.464	21.7974	1.6666	22.5516	18.9774
3.175	24.6264	24.3053	0.3211	23.4829	21.8316	1.6513	22.5697	19.0137
3.1875	24.636	24.3218	0.3142	23.5015	21.8654	1.6361	22.5877	19.0499
3.2	24.6453	24.3379	0.3074	23.52	21.899	1.621	22.6056	19.0858
3.2125	24.6544	24.3536	0.3008	23.5383	21.9322	1.6061	22.6233	19.1216

z (km)	Nd=5 Rock ‰ δ18O	Fluid ‰ δ18O	Δr-fl	Nd=2 Rock ‰ δ18O	Fluid ‰ δ18O	Δr-fl	Nd=1 Rock ‰ δ18O	Fluid ‰ δ18O
3.225	24.6632	24.369	0.2942	23.5563	21.9652	1.5911	22.6409	19.1573
3.2375	24.6719	24.3841	0.2878	23.5742	21.9978	1.5764	22.6584	19.1927
3.25	24.6804	24.3989	0.2815	23.5918	22.0301	1.5617	22.6758	19.228
3.2625	24.6886	24.4133	0.2753	23.6093	22.0622	1.5471	22.6931	19.2631
3.275	24.6967	24.4274	0.2693	23.6266	22.0939	1.5327	22.7102	19.298
3.2875	24.7045	24.4412	0.2633	23.6436	22.1254	1.5182	22.7273	19.3327
3.3	24.7122	24.4547	0.2575	23.6605	22.1566	1.5039	22.7442	19.3673
3.3125	24.7197	24.4679	0.2518	23.6772	22.1875	1.4897	22.761	19.4017
3.325	24.727	24.4809	0.2461	23.6937	22.2181	1.4756	22.7777	19.4359
3.3375	24.7342	24.4935	0.2407	23.71	22.2484	1.4616	22.7943	19.47
3.35	24.7411	24.5059	0.2352	23.7261	22.2784	1.4477	22.8107	19.5039
3.3625	24.7479	24.5179	0.23	23.7421	22.3082	1.4339	22.8271	19.5376
3.375	24.7545	24.5297	0.2248	23.7579	22.3376	1.4203	22.8433	19.5711
3.3875	24.761	24.5413	0.2197	23.7734	22.3668	1.4066	22.8595	19.6045
3.4	24.7673	24.5526	0.2147	23.7888	22.3958	1.393	22.8755	19.6377
3.4125	24.7735	24.5636	0.2099	23.8041	22.4244	1.3797	22.8914	19.6708
3.425	24.7795	24.5744	0.2051	23.8191	22.4528	1.3663	22.9072	19.7036
3.4375	24.7853	24.5849	0.2004	23.834	22.4809	1.3531	22.9229	19.7363
3.45	24.791	24.5952	0.1958	23.8487	22.5088	1.3399	22.9385	19.7689
3.4625	24.7966	24.6053	0.1913	23.8633	22.5364	1.3269	22.954	19.8012
3.475	24.802	24.6151	0.1869	23.8777	22.5637	1.314	22.9693	19.8334
3.4875	24.8073	24.6248	0.1825	23.8919	22.5907	1.3012	22.9846	19.8655
3.5	24.8125	24.6341	0.1784	23.9059	22.6175	1.2884	22.9998	19.8973
3.5125	24.8175	24.6433	0.1742	23.9198	22.6441	1.2757	23.0148	19.929
3.525	24.8224	24.6523	0.1701	23.9335	22.6704	1.2631	23.0298	19.9606
3.5375	24.8272	24.661	0.1662	23.9471	22.6964	1.2507	23.0446	19.992
3.55	24.8318	24.6696	0.1622	23.9605	22.7222	1.2383	23.0594	20.0232
3.5625	24.8364	24.6779	0.1585	23.9738	22.7477	1.2261	23.074	20.0542
3.575	24.8408	24.6861	0.1547	23.9869	22.773	1.2139	23.0886	20.0851
3.5875	24.8451	24.6941	0.151	23.9998	22.798	1.2018	23.103	20.1158
3.6	24.8493	24.7019	0.1474	24.0126	22.8228	1.1898	23.1174	20.1464
3.6125	24.8534	24.7095	0.1439	24.0253	22.8473	1.178	23.1316	20.1768
3.625	24.8574	24.7169	0.1405	24.0378	22.8717	1.1661	23.1458	20.2071
3.6375	24.8613	24.7241	0.1372	24.0501	22.8957	1.1544	23.1598	20.2372
3.65	24.8651	24.7312	0.1339	24.0623	22.9196	1.1427	23.1738	20.2671
3.6625	24.8688	24.7381	0.1307	24.0744	22.9431	1.1313	23.1877	20.2969
3.675	24.8724	24.7452	0.1272	24.0863	22.9665	1.1198	23.2014	20.3265
3.6875	24.8759	24.7514	0.1245	24.0981	22.9896	1.1085	23.2151	20.3559
3.7	24.8793	24.7578	0.1215	24.1097	23.0125	1.0972	23.2287	20.3853
3.7125	24.8826	24.7641	0.1185	24.1212	23.0352	1.086	23.2421	20.4144
3.725	24.8859	24.7702	0.1157	24.1326	23.0577	1.0749	23.2555	20.4434
3.7375	24.889	24.7762	0.1128	24.1438	23.0799	1.0639	23.2688	20.4722
3.75	24.8921	24.782	0.1101	24.1549	23.1019	1.053	23.282	20.5009

z (km)	Nd=5 Rock ‰ δ18O	Fluid ‰ δ18O	Δr-fl	Nd=2 Rock ‰ δ18O	Fluid ‰ δ18O	Δr-fl	Nd=1 Rock ‰ δ18O	Fluid ‰ δ18O
3.7625	24.8951	24.7877	0.1074	24.1659	23.1236	1.0423	23.2951	20.5294
3.775	24.898	24.7933	0.1047	24.1767	23.1452	1.0315	23.3081	20.5578
3.7875	24.9009	24.7987	0.1022	24.1874	23.1665	1.0209	23.321	20.5861
3.8	24.9036	24.8039	0.0997	24.198	23.1877	1.0103	23.3339	20.6141
3.8125	24.9063	24.8091	0.0972	24.2084	23.2086	0.9998	23.3466	20.6421
3.825	24.9089	24.8141	0.0948	24.2188	23.2293	0.9895	23.3593	20.6698
3.8375	24.9115	24.819	0.0925	24.229	23.2497	0.9793	23.3718	20.6974
3.85	24.914	24.8238	0.0902	24.239	23.27	0.969	23.3843	20.7249
3.8625	24.9164	24.8285	0.0879	24.249	23.2901	0.9589	23.3967	20.7522
3.875	24.9187	24.833	0.0857	24.2588	23.3099	0.9489	23.409	20.7794
3.8875	24.921	24.8374	0.0836	24.2686	23.3296	0.939	23.4212	20.8064
3.9	24.9233	24.842	0.0813	24.2782	23.3491	0.9291	23.4333	20.8333
3.9125	24.9254	24.8462	0.0792	24.2876	23.3683	0.9193	23.4454	20.8601
3.925	24.9275	24.8503	0.0772	24.297	23.3874	0.9096	23.4573	20.8867
3.9375	24.9296	24.8544	0.0752	24.3063	23.4062	0.9001	23.4692	20.9131
3.95	24.9316	24.8583	0.0733	24.3154	23.4249	0.8905	23.481	20.9394
3.9625	24.9336	24.8621	0.0715	24.3244	23.4434	0.881	23.4927	20.9655
3.975	24.9354	24.8658	0.0696	24.3334	23.4616	0.8718	23.5043	20.9916
3.9875	24.9373	24.8694	0.0679	24.3422	23.4797	0.8625	23.5158	21.0174
4	24.9391	24.8729	0.0662	24.3509	23.4976	0.8533	23.5273	21.0431
4.0125	24.9408	24.8764	0.0644	24.3595	23.5153	0.8442	23.5387	21.0687
4.025	24.9425	24.8797	0.0628	24.368	23.5328	0.8352	23.55	21.0942
4.0375	24.9442	24.883	0.0612	24.3763	23.5502	0.8261	23.5612	21.1195
4.05	24.9458	24.8862	0.0596	24.3846	23.5673	0.8173	23.5723	21.1446
4.0625	24.9473	24.8893	0.058	24.3928	23.5843	0.8085	23.5834	21.1697
4.075	24.9489	24.8923	0.0566	24.4009	23.6011	0.7998	23.5943	21.1945
4.0875	24.9503	24.8952	0.0551	24.4089	23.6177	0.7912	23.6052	21.2193
4.1	24.9518	24.8981	0.0537	24.4168	23.6342	0.7826	23.616	21.2439
4.1125	24.9532	24.9009	0.0523	24.4246	23.6504	0.7742	23.6268	21.2683
4.125	24.9545	24.9036	0.0509	24.4322	23.6665	0.7657	23.6375	21.2927
4.1375	24.9559	24.9062	0.0497	24.4398	23.6824	0.7574	23.648	21.3169
4.15	24.9571	24.9088	0.0483	24.4473	23.6982	0.7491	23.6586	21.3409
4.1625	24.9584	24.9113	0.0471	24.4547	23.7138	0.7409	23.669	21.3648
4.175	24.9596	24.9138	0.0458	24.4621	23.7292	0.7329	23.6793	21.3886
4.1875	24.9608	24.9162	0.0446	24.4693	23.7444	0.7249	23.6896	21.4123
4.2	24.9619	24.9185	0.0434	24.4764	23.7595	0.7169	23.6998	21.4358
4.2125	24.963	24.9208	0.0422	24.4835	23.7745	0.709	23.71	21.4592
4.225	24.9641	24.923	0.0411	24.4904	23.7892	0.7012	23.7201	21.4824
4.2375	24.9652	24.9251	0.0401	24.4973	23.8038	0.6935	23.73	21.5056
4.25	24.9662	24.9272	0.039	24.5041	23.8183	0.6858	23.74	21.5285
4.2625	24.9672	24.9292	0.038	24.5108	23.8325	0.6783	23.7498	21.5514
4.275	24.9682	24.9312	0.037	24.5174	23.8467	0.6707	23.7596	21.5741
4.2875	24.9691	24.9331	0.036	24.5239	23.8607	0.6632	23.7693	21.5967

z (km)	Nd=5 Rock ‰ δ18O	Nd=5 Fluid ‰ δ18O	Δr-fl	Nd=2 Rock ‰ δ18O	Nd=2 Fluid ‰ δ18O	Δr-fl	Nd=1 Rock ‰ δ18O	Nd=1 Fluid ‰ δ18O
4.3	24.97	24.935	0.035	24.5304	23.8745	0.6559	23.7789	21.6192
4.3125	24.9709	24.9369	0.034	24.5367	23.8881	0.6486	23.7885	21.6415
4.325	24.9718	24.9386	0.0332	24.543	23.9017	0.6413	23.798	21.6637
4.3375	24.9726	24.9404	0.0322	24.5492	23.915	0.6342	23.8074	21.6858
4.35	24.9734	24.942	0.0314	24.5553	23.9283	0.627	23.8168	21.7078
4.3625	24.9742	24.9437	0.0305	24.5614	23.9414	0.62	23.8261	21.7296
4.375	24.975	24.9453	0.0297	24.5674	23.9543	0.6131	23.8353	21.7513
4.3875	24.9757	24.9468	0.0289	24.5733	23.9671	0.6062	23.8445	21.7729
4.4	24.9765	24.9483	0.0282	24.5791	23.9797	0.5994	23.8536	21.7944
4.4125	24.9772	24.9502	0.027	24.5848	23.9922	0.5926	23.8626	21.8157
4.425	24.9778	24.9516	0.0262	24.5905	24.0046	0.5859	23.8716	21.8369
4.4375	24.9785	24.953	0.0255	24.5961	24.0169	0.5792	23.8805	21.858
4.45	24.9792	24.9543	0.0249	24.6016	24.029	0.5726	23.8893	21.879
4.4625	24.9798	24.9556	0.0242	24.6071	24.0409	0.5662	23.8981	21.8998
4.475	24.9804	24.9569	0.0235	24.6125	24.0528	0.5597	23.9068	21.9205
4.4875	24.981	24.9582	0.0228	24.6178	24.0644	0.5534	23.9154	21.9411
4.5	24.9816	24.9594	0.0222	24.6231	24.076	0.5471	23.924	21.9616
4.5125	24.9821	24.9605	0.0216	24.6283	24.0875	0.5408	23.9325	21.982
4.525	24.9827	24.9617	0.021	24.6334	24.0988	0.5346	23.9409	22.0022
4.5375	24.9832	24.9628	0.0204	24.6384	24.1099	0.5285	23.9493	22.0223
4.55	24.9837	24.9639	0.0198	24.6434	24.121	0.5224	23.9576	22.0423
4.5625	24.9842	24.9649	0.0193	24.6483	24.1319	0.5164	23.9659	22.0622
4.575	24.9847	24.9659	0.0188	24.6532	24.1427	0.5105	23.9741	22.082
4.5875	24.9851	24.9669	0.0182	24.658	24.1534	0.5046	23.9823	22.1016
4.6	24.9856	24.9679	0.0177	24.6627	24.164	0.4987	23.9903	22.1212
4.6125	24.986	24.9688	0.0172	24.6674	24.1744	0.493	23.9984	22.1406
4.625	24.9865	24.9697	0.0168	24.672	24.1847	0.4873	24.0063	22.1599
4.6375	24.9869	24.9706	0.0163	24.6766	24.195	0.4816	24.0142	22.1791
4.65	24.9873	24.9715	0.0158	24.6811	24.205	0.4761	24.0221	22.1982
4.6625	24.9877	24.9723	0.0154	24.6855	24.215	0.4705	24.0299	22.2171
4.675	24.9881	24.9731	0.015	24.6899	24.2249	0.465	24.0376	22.236
4.6875	24.9884	24.9739	0.0145	24.6942	24.2346	0.4596	24.0453	22.2547
4.7	24.9888	24.9747	0.0141	24.6985	24.2443	0.4542	24.0529	22.2733
4.7125	24.9891	24.9754	0.0137	24.7027	24.2538	0.4489	24.0604	22.2919
4.725	24.9895	24.9762	0.0133	24.7068	24.2632	0.4436	24.068	22.3103
4.7375	24.9898	24.9769	0.0129	24.7109	24.2725	0.4384	24.0754	22.3286
4.75	24.9901	24.9776	0.0125	24.715	24.2817	0.4333	24.0828	22.3467
4.7625	24.9904	24.9782	0.0122	24.7189	24.2908	0.4281	24.0901	22.3648
4.775	24.9907	24.9789	0.0118	24.7229	24.2998	0.4231	24.0974	22.3828
4.7875	24.991	24.9795	0.0115	24.7268	24.3086	0.4182	24.1046	22.4006
4.8	24.9913	24.9801	0.0112	24.7306	24.3174	0.4132	24.1118	22.4184
4.8125	24.9915	24.9807	0.0108	24.7344	24.3261	0.4083	24.1189	22.436
4.825	24.9918	24.9817	0.0101	24.7381	24.3347	0.4034	24.126	22.4536

	Nd=5			Nd=2			Nd=1	
z (km)	Rock ‰ δ18O	Fluid ‰ δ18O	Δr-fl	Rock ‰ δ18O	Fluid ‰ δ18O	Δr-fl	Rock ‰ δ18O	Fluid ‰ δ18O
4.8375	24.9921	24.9823	0.0098	24.7418	24.3431	0.3987	24.133	22.471
4.85	24.9923	24.9828	0.0095	24.7454	24.3515	0.3939	24.14	22.4883
4.8625	24.9926	24.9833	0.0093	24.749	24.3598	0.3892	24.1469	22.5056
4.875	24.9928	24.9838	0.009	24.7526	24.368	0.3846	24.1538	22.5227
4.8875	24.993	24.9843	0.0087	24.7561	24.3761	0.38	24.1606	22.5397
4.9	24.9932	24.9848	0.0084	24.7595	24.3841	0.3754	24.1673	22.5566
4.9125	24.9934	24.9852	0.0082	24.7629	24.3919	0.371	24.174	22.5734
4.925	24.9937	24.9857	0.008	24.7663	24.3997	0.3666	24.1807	22.5901
4.9375	24.9939	24.9861	0.0078	24.7696	24.4075	0.3621	24.1873	22.6067
4.95	24.994	24.9865	0.0075	24.7729	24.4151	0.3578	24.1939	22.6232
4.9625	24.9942	24.987	0.0072	24.7761	24.4226	0.3535	24.2004	22.6396
4.975	24.9944	24.9874	0.007	24.7793	24.43	0.3493	24.2068	22.6559
4.9875	24.9946	24.9877	0.0069	24.7824	24.4374	0.345	24.2132	22.6721
5	24.9948	24.9881	0.0067	24.7855	24.4447	0.3408	24.2196	22.6882

z (km)	Δr-fl	Nd=0.75 Rock ‰ δ18O	Fluid ‰ δ18O	Δr-fl	Nd=0.5 Rock ‰ δ18O	Fluid ‰ δ18O	Δr-fl
0	7.7255	13.9197	4	9.9197	16.7371	4	12.7371
0.0125	7.7297	13.9764	4.0701	9.9063	16.7707	4.06	12.7107
0.025	7.7334	14.0329	4.1402	9.8927	16.8042	4.1199	12.6843
0.0375	7.7368	14.0892	4.2102	9.879	16.8376	4.1797	12.6579
0.05	7.7397	14.1452	4.2802	9.865	16.8708	4.2394	12.6314
0.0625	7.7422	14.2009	4.35	9.8509	16.9039	4.299	12.6049
0.075	7.7444	14.2564	4.4198	9.8366	16.9369	4.3585	12.5784
0.0875	7.7461	14.3117	4.4895	9.8222	16.9697	4.4178	12.5519
0.1	7.7474	14.3667	4.5592	9.8075	17.0025	4.4771	12.5254
0.1125	7.7484	14.4215	4.6288	9.7927	17.0351	4.5362	12.4989
0.125	7.7489	14.4761	4.6982	9.7779	17.0676	4.5953	12.4723
0.1375	7.7491	14.5304	4.7677	9.7627	17.1	4.6542	12.4458
0.15	7.749	14.5845	4.837	9.7475	17.1323	4.713	12.4193
0.1625	7.7484	14.6383	4.9062	9.7321	17.1644	4.7717	12.3927
0.175	7.7475	14.6919	4.9754	9.7165	17.1965	4.8303	12.3662
0.1875	7.7463	14.7453	5.0445	9.7008	17.2284	4.8888	12.3396
0.2	7.7446	14.7984	5.1135	9.6849	17.2602	4.9472	12.313
0.2125	7.7426	14.8513	5.1824	9.6689	17.2919	5.0055	12.2864
0.225	7.7403	14.904	5.2512	9.6528	17.3234	5.0636	12.2598
0.2375	7.7376	14.9564	5.32	9.6364	17.3549	5.1217	12.2332
0.25	7.7346	15.0086	5.3886	9.62	17.3862	5.1796	12.2066
0.2625	7.7313	15.0606	5.4572	9.6034	17.4174	5.2375	12.1799
0.275	7.7276	15.1123	5.5257	9.5866	17.4486	5.2952	12.1534
0.2875	7.7236	15.1638	5.594	9.5698	17.4795	5.3528	12.1267
0.3	7.7193	15.2151	5.6623	9.5528	17.5104	5.4103	12.1001
0.3125	7.7146	15.2661	5.7305	9.5356	17.5412	5.4677	12.0735
0.325	7.7097	15.317	5.7986	9.5184	17.5718	5.5249	12.0469
0.3375	7.7044	15.3676	5.8665	9.5011	17.6024	5.5821	12.0203
0.35	7.6988	15.4179	5.9344	9.4835	17.6328	5.6392	11.9936
0.3625	7.6929	15.4681	6.0022	9.4659	17.6631	5.6961	11.967
0.375	7.6867	15.518	6.0699	9.4481	17.6933	5.7529	11.9404
0.3875	7.6803	15.5677	6.1375	9.4302	17.7234	5.8096	11.9138
0.4	7.6735	15.6172	6.2049	9.4123	17.7534	5.8662	11.8872
0.4125	7.6665	15.6664	6.2723	9.3941	17.7833	5.9227	11.8606
0.425	7.6591	15.7154	6.3396	9.3758	17.813	5.9791	11.8339
0.4375	7.6515	15.7642	6.4067	9.3575	17.8427	6.0354	11.8073
0.45	7.6436	15.8128	6.4738	9.339	17.8722	6.0916	11.7806
0.4625	7.6355	15.8612	6.5407	9.3205	17.9017	6.1476	11.7541
0.475	7.627	15.9093	6.6075	9.3018	17.931	6.2035	11.7275
0.4875	7.6183	15.9573	6.6742	9.2831	17.9602	6.2594	11.7008
0.5	7.6093	16.005	6.7408	9.2642	17.9893	6.3151	11.6742
0.5125	7.6001	16.0525	6.8073	9.2452	18.0183	6.3707	11.6476
0.525	7.5906	16.0997	6.8737	9.226	18.0472	6.4261	11.6211

			Nd=0.75			Nd=0.5	
		Rock ‰	Fluid ‰		Rock ‰	Fluid ‰	
z (km)	**Δr-fl**	**δ18O**	**δ18O**	**Δr-fl**	**δ18O**	**δ18O**	**Δr-fl**
0.5375	7.5809	16.1468	6.94	9.2068	18.076	6.4815	11.5945
0.55	7.571	16.1937	7.0061	9.1876	18.1046	6.5368	11.5678
0.5625	7.5607	16.2403	7.0722	9.1681	18.1332	6.5919	11.5413
0.575	7.5503	16.2867	7.1381	9.1486	18.1617	6.647	11.5147
0.5875	7.5396	16.3329	7.2039	9.129	18.19	6.7019	11.4881
0.6	7.5286	16.3789	7.2695	9.1094	18.2183	6.7567	11.4616
0.6125	7.5175	16.4247	7.3351	9.0896	18.2464	6.8114	11.435
0.625	7.5062	16.4703	7.4005	9.0698	18.2744	6.866	11.4084
0.6375	7.4945	16.5156	7.4658	9.0498	18.3024	6.9204	11.382
0.65	7.4826	16.5608	7.531	9.0298	18.3302	6.9748	11.3554
0.6625	7.4706	16.6058	7.5961	9.0097	18.3579	7.029	11.3289
0.675	7.4583	16.6505	7.6611	8.9894	18.3856	7.0832	11.3024
0.6875	7.4459	16.695	7.7259	8.9691	18.4131	7.1372	11.2759
0.7	7.4332	16.7394	7.7906	8.9488	18.4405	7.1911	11.2494
0.7125	7.4203	16.7835	7.8551	8.9284	18.4678	7.2449	11.2229
0.725	7.4072	16.8274	7.9196	8.9078	18.495	7.2985	11.1965
0.7375	7.3939	16.8711	7.9839	8.8872	18.5221	7.3521	11.17
0.75	7.3805	16.9146	8.0481	8.8665	18.5491	7.4055	11.1436
0.7625	7.3667	16.9579	8.1121	8.8458	18.576	7.4589	11.1171
0.775	7.3529	17.0011	8.176	8.8251	18.6028	7.5121	11.0907
0.7875	7.3388	17.044	8.2398	8.8042	18.6295	7.5652	11.0643
0.8	7.3246	17.0867	8.3035	8.7832	18.6561	7.6182	11.0379
0.8125	7.3102	17.1292	8.367	8.7622	18.6827	7.6711	11.0116
0.825	7.2956	17.1715	8.4304	8.7411	18.7091	7.7239	10.9852
0.8375	7.2808	17.2136	8.4937	8.7199	18.7354	7.7765	10.9589
0.85	7.2659	17.2555	8.5568	8.6987	18.7616	7.829	10.9326
0.8625	7.2507	17.2972	8.6198	8.6774	18.7877	7.8815	10.9062
0.875	7.2354	17.3388	8.6827	8.6561	18.8137	7.9338	10.8799
0.8875	7.22	17.3801	8.7454	8.6347	18.8396	7.986	10.8536
0.9	7.2044	17.4212	8.808	8.6132	18.8654	8.0381	10.8273
0.9125	7.1886	17.4622	8.8705	8.5917	18.8911	8.09	10.8011
0.925	7.1727	17.5029	8.9328	8.5701	18.9167	8.1419	10.7748
0.9375	7.1567	17.5435	8.995	8.5485	18.9423	8.1936	10.7487
0.95	7.1404	17.5838	9.057	8.5268	18.9677	8.2453	10.7224
0.9625	7.124	17.624	9.1189	8.5051	18.993	8.2968	10.6962
0.975	7.1076	17.664	9.1807	8.4833	19.0182	8.3482	10.67
0.9875	7.0908	17.7038	9.2423	8.4615	19.0434	8.3995	10.6439
1	7.0741	17.7434	9.3038	8.4396	19.0684	8.4507	10.6177
1.0125	7.0571	17.7828	9.3651	8.4177	19.0934	8.5017	10.5917
1.025	7.04	17.822	9.4263	8.3957	19.1182	8.5527	10.5655
1.0375	7.0229	17.861	9.4874	8.3736	19.143	8.6035	10.5395
1.05	7.0056	17.8999	9.5483	8.3516	19.1676	8.6542	10.5134
1.0625	6.9881	17.9386	9.609	8.3296	19.1922	8.7048	10.4874

z (km)	Nd=0.75 Δr-fl	Nd=0.75 Rock ‰ δ18O	Nd=0.75 Fluid ‰ δ18O	Nd=0.75 Δr-fl	Nd=0.5 Rock ‰ δ18O	Nd=0.5 Fluid ‰ δ18O	Nd=0.5 Δr-fl
1.075	6.9705	17.9771	9.6697	8.3074	19.2167	8.7553	10.4614
1.0875	6.9527	18.0154	9.7302	8.2852	19.2411	8.8057	10.4354
1.1	6.9349	18.0535	9.7905	8.263	19.2653	8.856	10.4093
1.1125	6.917	18.0914	9.8507	8.2407	19.2895	8.9061	10.3834
1.125	6.8989	18.1292	9.9107	8.2185	19.3136	8.9562	10.3574
1.1375	6.8807	18.1667	9.9706	8.1961	19.3377	9.0061	10.3316
1.15	6.8625	18.2041	10.0304	8.1737	19.3616	9.0559	10.3057
1.1625	6.844	18.2413	10.09	8.1513	19.3854	9.1056	10.2798
1.175	6.8256	18.2784	10.1495	8.1289	19.4091	9.1552	10.2539
1.1875	6.807	18.3152	10.2088	8.1064	19.4328	9.2047	10.2281
1.2	6.7882	18.3519	10.268	8.0839	19.4563	9.254	10.2023
1.2125	6.7694	18.3884	10.327	8.0614	19.4798	9.3033	10.1765
1.225	6.7505	18.4247	10.3859	8.0388	19.5032	9.3524	10.1508
1.2375	6.7315	18.4609	10.4446	8.0163	19.5265	9.4014	10.1251
1.25	6.7124	18.4968	10.5032	7.9936	19.5497	9.4503	10.0994
1.2625	6.6932	18.5326	10.5616	7.971	19.5728	9.4991	10.0737
1.275	6.6739	18.5682	10.6199	7.9483	19.5958	9.5478	10.048
1.2875	6.6546	18.6037	10.678	7.9257	19.6187	9.5964	10.0223
1.3	6.6351	18.639	10.736	7.903	19.6416	9.6448	9.9968
1.3125	6.6155	18.6741	10.7938	7.8803	19.6643	9.6932	9.9711
1.325	6.596	18.709	10.8515	7.8575	19.687	9.7414	9.9456
1.3375	6.5762	18.7438	10.909	7.8348	19.7096	9.7895	9.9201
1.35	6.5565	18.7784	10.9664	7.812	19.7321	9.8375	9.8946
1.3625	6.5367	18.8128	11.0236	7.7892	19.7545	9.8854	9.8691
1.375	6.5167	18.8471	11.0807	7.7664	19.7768	9.9332	9.8436
1.3875	6.4967	18.8811	11.1376	7.7435	19.799	9.9808	9.8182
1.4	6.4766	18.9151	11.1944	7.7207	19.8212	10.0284	9.7928
1.4125	6.4565	18.9488	11.251	7.6978	19.8433	10.0758	9.7675
1.425	6.4363	18.9824	11.3074	7.675	19.8652	10.1231	9.7421
1.4375	6.416	19.0158	11.3638	7.652	19.8871	10.1704	9.7167
1.45	6.3957	19.0491	11.4199	7.6292	19.9089	10.2175	9.6914
1.4625	6.3754	19.0822	11.4759	7.6063	19.9307	10.2645	9.6662
1.475	6.3549	19.1151	11.5318	7.5833	19.9523	10.3113	9.641
1.4875	6.3343	19.1479	11.5875	7.5604	19.9739	10.3581	9.6158
1.5	6.3138	19.1805	11.643	7.5375	19.9953	10.4048	9.5905
1.5125	6.2933	19.213	11.6984	7.5146	20.0167	10.4513	9.5654
1.525	6.2726	19.2452	11.7536	7.4916	20.038	10.4977	9.5403
1.5375	6.2518	19.2774	11.8087	7.4687	20.0593	10.544	9.5153
1.55	6.231	19.3093	11.8636	7.4457	20.0804	10.5902	9.4902
1.5625	6.2102	19.3411	11.9184	7.4227	20.1015	10.6363	9.4652
1.575	6.1894	19.3728	11.973	7.3998	20.1224	10.6823	9.4401
1.5875	6.1685	19.4043	12.0275	7.3768	20.1433	10.7282	9.4151
1.6	6.1476	19.4356	12.0818	7.3538	20.1642	10.774	9.3902

z (km)	Δr-fl	Nd=0.75 Rock ‰ δ18O	Fluid ‰ δ18O	Δr-fl	Nd=0.5 Rock ‰ δ18O	Fluid ‰ δ18O	Δr-fl
1.6125	6.1266	19.4668	12.1359	7.3309	20.1849	10.8196	9.3653
1.625	6.1056	19.4978	12.1899	7.3079	20.2055	10.8651	9.3404
1.6375	6.0845	19.5287	12.2437	7.285	20.2261	10.9106	9.3155
1.65	6.0634	19.5594	12.2974	7.262	20.2466	10.9559	9.2907
1.6625	6.0423	19.59	12.351	7.239	20.267	11.0011	9.2659
1.675	6.0211	19.6204	12.4043	7.2161	20.2874	11.0462	9.2412
1.6875	5.9999	19.6507	12.4575	7.1932	20.3076	11.0912	9.2164
1.7	5.9787	19.6808	12.5106	7.1702	20.3278	11.136	9.1918
1.7125	5.9574	19.7107	12.5635	7.1472	20.3479	11.1808	9.1671
1.725	5.9361	19.7405	12.6162	7.1243	20.3679	11.2254	9.1425
1.7375	5.9148	19.7702	12.6688	7.1014	20.3878	11.27	9.1178
1.75	5.8935	19.7997	12.7213	7.0784	20.4077	11.3144	9.0933
1.7625	5.8722	19.8291	12.7735	7.0556	20.4275	11.3587	9.0688
1.775	5.8508	19.8583	12.8257	7.0326	20.4472	11.4029	9.0443
1.7875	5.8294	19.8873	12.8776	7.0097	20.4668	11.447	9.0198
1.8	5.808	19.9163	12.9294	6.9869	20.4864	11.491	8.9954
1.8125	5.7865	19.945	12.9811	6.9639	20.5059	11.5349	8.971
1.825	5.7651	19.9736	13.0326	6.941	20.5253	11.5787	8.9466
1.8375	5.7437	20.0021	13.0839	6.9182	20.5446	11.6223	8.9223
1.85	5.7222	20.0305	13.1351	6.8954	20.5638	11.6659	8.8979
1.8625	5.7007	20.0587	13.1861	6.8726	20.583	11.7093	8.8737
1.875	5.6792	20.0867	13.237	6.8497	20.6021	11.7526	8.8495
1.8875	5.6577	20.1146	13.2877	6.8269	20.6211	11.7958	8.8253
1.9	5.6362	20.1424	13.3383	6.8041	20.6401	11.839	8.8011
1.9125	5.6146	20.17	13.3886	6.7814	20.6589	11.882	8.7769
1.925	5.5931	20.1975	13.4389	6.7586	20.6777	11.9249	8.7528
1.9375	5.5716	20.2248	13.489	6.7358	20.6965	11.9676	8.7289
1.95	5.55	20.252	13.5389	6.7131	20.7151	12.0103	8.7048
1.9625	5.5284	20.2791	13.5887	6.6904	20.7337	12.0529	8.6808
1.975	5.5069	20.306	13.6383	6.6677	20.7522	12.0953	8.6569
1.9875	5.4854	20.3328	13.6877	6.6451	20.7706	12.1377	8.6329
2	5.4639	20.3595	13.737	6.6225	20.789	12.1799	8.6091
2.0125	5.4422	20.386	13.7862	6.5998	20.8073	12.2221	8.5852
2.025	5.4207	20.4124	13.8352	6.5772	20.8255	12.2641	8.5614
2.0375	5.3992	20.4386	13.884	6.5546	20.8436	12.306	8.5376
2.05	5.3777	20.4647	13.9327	6.532	20.8617	12.3478	8.5139
2.0625	5.3561	20.4907	13.9812	6.5095	20.8797	12.3895	8.4902
2.075	5.3346	20.5165	14.0296	6.4869	20.8976	12.4311	8.4665
2.0875	5.3131	20.5423	14.0778	6.4645	20.9155	12.4726	8.4429
2.1	5.2915	20.5678	14.1258	6.442	20.9333	12.514	8.4193
2.1125	5.27	20.5933	14.1737	6.4196	20.951	12.5552	8.3958
2.125	5.2485	20.6186	14.2215	6.3971	20.9686	12.5964	8.3722
2.1375	5.2271	20.6438	14.269	6.3748	20.9862	12.6375	8.3487

z (km)	Δr-fl	Nd=0.75 Rock ‰ δ18O	Fluid ‰ δ18O	Δr-fl	Nd=0.5 Rock ‰ δ18O	Fluid ‰ δ18O	Δr-fl
2.15	5.2056	20.6688	14.3165	6.3523	21.0037	12.6784	8.3253
2.1625	5.1841	20.6938	14.3637	6.3301	21.0211	12.7193	8.3018
2.175	5.1628	20.7185	14.4108	6.3077	21.0385	12.76	8.2785
2.1875	5.1414	20.7432	14.4578	6.2854	21.0558	12.8006	8.2552
2.2	5.1199	20.7678	14.5046	6.2632	21.073	12.8412	8.2318
2.2125	5.0985	20.7922	14.5513	6.2409	21.0902	12.8816	8.2086
2.225	5.0772	20.8164	14.5978	6.2186	21.1073	12.9219	8.1854
2.2375	5.0558	20.8406	14.6441	6.1965	21.1243	12.9621	8.1622
2.25	5.0344	20.8646	14.6903	6.1743	21.1412	13.0022	8.139
2.2625	5.0132	20.8885	14.7363	6.1522	21.1581	13.0422	8.1159
2.275	4.9919	20.9123	14.7822	6.1301	21.1749	13.0821	8.0928
2.2875	4.9706	20.936	14.8279	6.1081	21.1917	13.1219	8.0698
2.3	4.9493	20.9595	14.8735	6.086	21.2084	13.1615	8.0469
2.3125	4.9282	20.9829	14.9189	6.064	21.225	13.2011	8.0239
2.325	4.907	21.0062	14.9641	6.0421	21.2415	13.2406	8.0009
2.3375	4.8858	21.0294	15.0092	6.0202	21.258	13.2799	7.9781
2.35	4.8646	21.0524	15.0542	5.9982	21.2744	13.3192	7.9552
2.3625	4.8435	21.0754	15.099	5.9764	21.2908	13.3583	7.9325
2.375	4.8224	21.0982	15.1436	5.9546	21.3071	13.3974	7.9097
2.3875	4.8013	21.1209	15.1881	5.9328	21.3233	13.4363	7.887
2.4	4.7803	21.1434	15.2325	5.9109	21.3395	13.4752	7.8643
2.4125	4.7593	21.1659	15.2767	5.8892	21.3556	13.5139	7.8417
2.425	4.7383	21.1882	15.3207	5.8675	21.3716	13.5525	7.8191
2.4375	4.7174	21.2104	15.3646	5.8458	21.3875	13.5911	7.7964
2.45	4.6965	21.2325	15.4083	5.8242	21.4034	13.6295	7.7739
2.4625	4.6755	21.2545	15.4519	5.8026	21.4193	13.6678	7.7515
2.475	4.6548	21.2764	15.4953	5.7811	21.435	13.706	7.729
2.4875	4.6339	21.2981	15.5386	5.7595	21.4508	13.7442	7.7066
2.5	4.6131	21.3198	15.5817	5.7381	21.4664	13.7822	7.6842
2.5125	4.5924	21.3413	15.6246	5.7167	21.482	13.8201	7.6619
2.525	4.5717	21.3627	15.6675	5.6952	21.4975	13.8579	7.6396
2.5375	4.551	21.384	15.7101	5.6739	21.513	13.8956	7.6174
2.55	4.5303	21.4051	15.7526	5.6525	21.5284	13.9332	7.5952
2.5625	4.5098	21.4262	15.795	5.6312	21.5437	13.9707	7.573
2.575	4.4892	21.4472	15.8372	5.61	21.559	14.0081	7.5509
2.5875	4.4687	21.468	15.8793	5.5887	21.5742	14.0454	7.5288
2.6	4.4482	21.4888	15.9212	5.5676	21.5893	14.0826	7.5067
2.6125	4.4277	21.5094	15.963	5.5464	21.6044	14.1197	7.4847
2.625	4.4073	21.5299	16.0046	5.5253	21.6194	14.1566	7.4628
2.6375	4.387	21.5503	16.046	5.5043	21.6344	14.1935	7.4409
2.65	4.3666	21.5706	16.0873	5.4833	21.6493	14.2303	7.419
2.6625	4.3464	21.5908	16.1285	5.4623	21.6641	14.267	7.3971
2.675	4.3261	21.6109	16.1695	5.4414	21.6789	14.3036	7.3753

z (km)	Δr-fl	Nd=0.75 Rock ‰ δ18O	Fluid ‰ δ18O	Δr-fl	Nd=0.5 Rock ‰ δ18O	Fluid ‰ δ18O	Δr-fl
2.6875	4.306	21.6308	16.2104	5.4204	21.6936	14.3401	7.3535
2.7	4.2858	21.6507	16.2511	5.3996	21.7083	14.3764	7.3319
2.7125	4.2657	21.6705	16.2917	5.3788	21.7229	14.4127	7.3102
2.725	4.2456	21.6901	16.3321	5.358	21.7374	14.4489	7.2885
2.7375	4.2257	21.7097	16.3724	5.3373	21.7519	14.485	7.2669
2.75	4.2056	21.7291	16.4125	5.3166	21.7664	14.521	7.2454
2.7625	4.1857	21.7484	16.4525	5.2959	21.7807	14.5569	7.2238
2.775	4.1658	21.7677	16.4923	5.2754	21.795	14.5926	7.2024
2.7875	4.146	21.7868	16.532	5.2548	21.8093	14.6283	7.181
2.8	4.1262	21.8058	16.5716	5.2342	21.8235	14.6639	7.1596
2.8125	4.1064	21.8248	16.611	5.2138	21.8376	14.6994	7.1382
2.825	4.0867	21.8436	16.6502	5.1934	21.8517	14.7348	7.1169
2.8375	4.0671	21.8623	16.6893	5.173	21.8657	14.7701	7.0956
2.85	4.0475	21.8809	16.7283	5.1526	21.8797	14.8052	7.0745
2.8625	4.028	21.8994	16.7671	5.1323	21.8936	14.8403	7.0533
2.875	4.0084	21.9179	16.8058	5.1121	21.9074	14.8753	7.0321
2.8875	3.989	21.9362	16.8443	5.0919	21.9212	14.9102	7.011
2.9	3.9696	21.9544	16.8827	5.0717	21.935	14.945	6.99
2.9125	3.9502	21.9725	16.9209	5.0516	21.9486	14.9797	6.9689
2.925	3.931	21.9906	16.959	5.0316	21.9623	15.0143	6.948
2.9375	3.9116	22.0085	16.9969	5.0116	21.9758	15.0488	6.927
2.95	3.8924	22.0263	17.0347	4.9916	21.9894	15.0832	6.9062
2.9625	3.8733	22.0441	17.0724	4.9717	22.0028	15.1175	6.8853
2.975	3.8543	22.0617	17.1099	4.9518	22.0162	15.1517	6.8645
2.9875	3.8352	22.0792	17.1473	4.9319	22.0296	15.1858	6.8438
3	3.8162	22.0967	17.1845	4.9122	22.0429	15.2198	6.8231
3.0125	3.7972	22.114	17.2216	4.8924	22.0561	15.2538	6.8023
3.025	3.7783	22.1313	17.2586	4.8727	22.0693	15.2876	6.7817
3.0375	3.7595	22.1485	17.2954	4.8531	22.0824	15.3213	6.7611
3.05	3.7408	22.1655	17.3321	4.8334	22.0955	15.3549	6.7406
3.0625	3.722	22.1825	17.3686	4.8139	22.1085	15.3885	6.72
3.075	3.7034	22.1994	17.405	4.7944	22.1215	15.4219	6.6996
3.0875	3.6848	22.2162	17.4412	4.775	22.1344	15.4552	6.6792
3.1	3.6662	22.2329	17.4773	4.7556	22.1473	15.4885	6.6588
3.1125	3.6477	22.2495	17.5133	4.7362	22.1601	15.5216	6.6385
3.125	3.6293	22.266	17.5491	4.7169	22.1728	15.5547	6.6181
3.1375	3.6108	22.2824	17.5848	4.6976	22.1855	15.5876	6.5979
3.15	3.5925	22.2988	17.6204	4.6784	22.1982	15.6205	6.5777
3.1625	3.5742	22.315	17.6558	4.6592	22.2108	15.6533	6.5575
3.175	3.556	22.3312	17.6911	4.6401	22.2233	15.686	6.5373
3.1875	3.5378	22.3472	17.7262	4.621	22.2358	15.7185	6.5173
3.2	3.5198	22.3632	17.7612	4.602	22.2483	15.751	6.4973
3.2125	3.5017	22.3791	17.7961	4.583	22.2607	15.7834	6.4773

z (km)	Δr-fl	Rock ‰ δ18O	Nd=0.75 Fluid ‰ δ18O	Δr-fl	Rock ‰ δ18O	Nd=0.5 Fluid ‰ δ18O	Δr-fl
3.225	3.4836	22.3949	17.8308	4.5641	22.273	15.8157	6.4573
3.2375	3.4657	22.4106	17.8654	4.5452	22.2853	15.8479	6.4374
3.25	3.4478	22.4263	17.8999	4.5264	22.2975	15.88	6.4175
3.2625	3.43	22.4418	17.9342	4.5076	22.3097	15.912	6.3977
3.275	3.4122	22.4573	17.9684	4.4889	22.3219	15.944	6.3779
3.2875	3.3946	22.4726	18.0024	4.4702	22.3339	15.9758	6.3581
3.3	3.3769	22.4879	18.0363	4.4516	22.346	16.0075	6.3385
3.3125	3.3593	22.5031	18.0701	4.433	22.358	16.0392	6.3188
3.325	3.3418	22.5182	18.1037	4.4145	22.3699	16.0707	6.2992
3.3375	3.3243	22.5333	18.1372	4.3961	22.3818	16.1022	6.2796
3.35	3.3068	22.5482	18.1706	4.3776	22.3936	16.1336	6.26
3.3625	3.2895	22.5631	18.2039	4.3592	22.4054	16.1649	6.2405
3.375	3.2722	22.5779	18.237	4.3409	22.4172	16.196	6.2212
3.3875	3.255	22.5926	18.27	4.3226	22.4289	16.2271	6.2018
3.4	3.2378	22.6072	18.3028	4.3044	22.4405	16.2581	6.1824
3.4125	3.2206	22.6218	18.3355	4.2863	22.4521	16.2891	6.163
3.425	3.2036	22.6362	18.3681	4.2681	22.4636	16.3199	6.1437
3.4375	3.1866	22.6506	18.4005	4.2501	22.4751	16.3506	6.1245
3.45	3.1696	22.6649	18.4329	4.232	22.4866	16.3813	6.1053
3.4625	3.1528	22.6791	18.465	4.2141	22.498	16.4118	6.0862
3.475	3.1359	22.6933	18.4971	4.1962	22.5094	16.4423	6.0671
3.4875	3.1191	22.7073	18.529	4.1783	22.5207	16.4726	6.0481
3.5	3.1025	22.7213	18.5608	4.1605	22.5319	16.5029	6.029
3.5125	3.0858	22.7352	18.5925	4.1427	22.5431	16.5331	6.01
3.525	3.0692	22.749	18.624	4.125	22.5543	16.5632	5.9911
3.5375	3.0526	22.7628	18.6555	4.1073	22.5654	16.5932	5.9722
3.55	3.0362	22.7765	18.6867	4.0898	22.5765	16.6231	5.9534
3.5625	3.0198	22.7901	18.7179	4.0722	22.5875	16.653	5.9345
3.575	3.0035	22.8036	18.7489	4.0547	22.5985	16.6827	5.9158
3.5875	2.9872	22.817	18.7798	4.0372	22.6095	16.7124	5.8971
3.6	2.971	22.8304	18.8106	4.0198	22.6203	16.7419	5.8784
3.6125	2.9548	22.8437	18.8412	4.0025	22.6312	16.7714	5.8598
3.625	2.9387	22.8569	18.8717	3.9852	22.642	16.8008	5.8412
3.6375	2.9226	22.87	18.9021	3.9679	22.6527	16.8301	5.8226
3.65	2.9067	22.8831	18.9324	3.9507	22.6635	16.8593	5.8042
3.6625	2.8908	22.8961	18.9625	3.9336	22.6741	16.8884	5.7857
3.675	2.8749	22.909	18.9926	3.9164	22.6847	16.9175	5.7672
3.6875	2.8592	22.9219	19.0225	3.8994	22.6953	16.9464	5.7489
3.7	2.8434	22.9347	19.0522	3.8825	22.7058	16.9753	5.7305
3.7125	2.8277	22.9474	19.0819	3.8655	22.7163	17.0041	5.7122
3.725	2.8121	22.96	19.1114	3.8486	22.7268	17.0328	5.694
3.7375	2.7966	22.9726	19.1408	3.8318	22.7372	17.0614	5.6758
3.75	2.7811	22.985	19.1701	3.8149	22.7475	17.0899	5.6576

			Nd=0.75			Nd=0.5	
		Rock ‰	Fluid ‰		Rock ‰	Fluid ‰	
z (km)	**Δr-fl**	**δ18O**	**δ18O**	**Δr-fl**	**δ18O**	**δ18O**	**Δr-fl**
3.7625	2.7657	22.9975	19.1992	3.7983	22.7578	17.1183	5.6395
3.775	2.7503	23.0098	19.2282	3.7816	22.7681	17.1466	5.6215
3.7875	2.7349	23.0221	19.2571	3.765	22.7783	17.1749	5.6034
3.8	2.7198	23.0343	19.2859	3.7484	22.7885	17.2031	5.5854
3.8125	2.7045	23.0464	19.3146	3.7318	22.7986	17.2312	5.5674
3.825	2.6895	23.0585	19.3431	3.7154	22.8087	17.2592	5.5495
3.8375	2.6744	23.0705	19.3716	3.6989	22.8188	17.2871	5.5317
3.85	2.6594	23.0825	19.3999	3.6826	22.8288	17.3149	5.5139
3.8625	2.6445	23.0943	19.428	3.6663	22.8388	17.3427	5.4961
3.875	2.6296	23.1061	19.4561	3.65	22.8487	17.3703	5.4784
3.8875	2.6148	23.1178	19.484	3.6338	22.8586	17.3979	5.4607
3.9	2.6	23.1295	19.5119	3.6176	22.8684	17.4254	5.443
3.9125	2.5853	23.1411	19.5396	3.6015	22.8782	17.4528	5.4254
3.925	2.5706	23.1526	19.5672	3.5854	22.888	17.4801	5.4079
3.9375	2.5561	23.1641	19.5946	3.5695	22.8977	17.5074	5.3903
3.95	2.5416	23.1755	19.622	3.5535	22.9074	17.5345	5.3729
3.9625	2.5272	23.1868	19.6492	3.5376	22.917	17.5616	5.3554
3.975	2.5127	23.1981	19.6763	3.5218	22.9266	17.5886	5.338
3.9875	2.4984	23.2093	19.7033	3.506	22.9362	17.6155	5.3207
4	2.4842	23.2205	19.7302	3.4903	22.9457	17.6423	5.3034
4.0125	2.47	23.2315	19.757	3.4745	22.9551	17.6691	5.286
4.025	2.4558	23.2426	19.7836	3.459	22.9646	17.6957	5.2689
4.0375	2.4417	23.2535	19.8102	3.4433	22.974	17.7223	5.2517
4.05	2.4277	23.2644	19.8366	3.4278	22.9833	17.7488	5.2345
4.0625	2.4137	23.2752	19.8629	3.4123	22.9926	17.7752	5.2174
4.075	2.3998	23.286	19.8891	3.3969	23.0019	17.8016	5.2003
4.0875	2.3859	23.2967	19.9152	3.3815	23.0111	17.8278	5.1833
4.1	2.3721	23.3073	19.9412	3.3661	23.0203	17.854	5.1663
4.1125	2.3585	23.3179	19.967	3.3509	23.0295	17.8801	5.1494
4.125	2.3448	23.3284	19.9928	3.3356	23.0386	17.9061	5.1325
4.1375	2.3311	23.3389	20.0184	3.3205	23.0477	17.932	5.1157
4.15	2.3177	23.3493	20.0439	3.3054	23.0567	17.9579	5.0988
4.1625	2.3042	23.3596	20.0693	3.2903	23.0657	17.9836	5.0821
4.175	2.2907	23.3699	20.0946	3.2753	23.0747	18.0093	5.0654
4.1875	2.2773	23.3801	20.1198	3.2603	23.0836	18.0349	5.0487
4.2	2.264	23.3903	20.1449	3.2454	23.0925	18.0604	5.0321
4.2125	2.2508	23.4004	20.1699	3.2305	23.1013	18.0859	5.0154
4.225	2.2377	23.4104	20.1947	3.2157	23.1101	18.1112	4.9989
4.2375	2.2244	23.4204	20.2195	3.2009	23.1189	18.1365	4.9824
4.25	2.2115	23.4303	20.2441	3.1862	23.1277	18.1617	4.966
4.2625	2.1984	23.4402	20.2686	3.1716	23.1363	18.1869	4.9494
4.275	2.1855	23.45	20.293	3.157	23.145	18.2119	4.9331
4.2875	2.1726	23.4597	20.3174	3.1423	23.1536	18.2369	4.9167

		Nd=0.75				Nd=0.5	
		Rock ‰	Fluid ‰		Rock ‰	Fluid ‰	
z (km)	Δr-fl	δ18O	δ18O	Δr-fl	δ18O	δ18O	Δr-fl
4.3	2.1597	23.4694	20.3416	3.1278	23.1622	18.2618	4.9004
4.3125	2.147	23.4791	20.3657	3.1134	23.1708	18.2866	4.8842
4.325	2.1343	23.4886	20.3896	3.099	23.1793	18.3113	4.868
4.3375	2.1216	23.4982	20.4135	3.0847	23.1877	18.336	4.8517
4.35	2.109	23.5076	20.4373	3.0703	23.1962	18.3606	4.8356
4.3625	2.0965	23.5171	20.461	3.0561	23.2046	18.3851	4.8195
4.375	2.084	23.5264	20.4845	3.0419	23.213	18.4095	4.8035
4.3875	2.0716	23.5357	20.508	3.0277	23.2213	18.4338	4.7875
4.4	2.0592	23.545	20.5314	3.0136	23.2296	18.4581	4.7715
4.4125	2.0469	23.5542	20.5546	2.9996	23.2378	18.4823	4.7555
4.425	2.0347	23.5633	20.5778	2.9855	23.2461	18.5064	4.7397
4.4375	2.0225	23.5724	20.6008	2.9716	23.2543	18.5305	4.7238
4.45	2.0103	23.5814	20.6237	2.9577	23.2624	18.5544	4.708
4.4625	1.9983	23.5904	20.6466	2.9438	23.2705	18.5783	4.6922
4.475	1.9863	23.5994	20.6693	2.9301	23.2786	18.6021	4.6765
4.4875	1.9743	23.6082	20.6919	2.9163	23.2867	18.6259	4.6608
4.5	1.9624	23.6171	20.7145	2.9026	23.2947	18.6495	4.6452
4.5125	1.9505	23.6258	20.7369	2.8889	23.3026	18.6731	4.6295
4.525	1.9387	23.6346	20.7592	2.8754	23.3106	18.6966	4.614
4.5375	1.927	23.6432	20.7814	2.8618	23.3185	18.7201	4.5984
4.55	1.9153	23.6519	20.8036	2.8483	23.3264	18.7434	4.583
4.5625	1.9037	23.6604	20.8256	2.8348	23.3342	18.7667	4.5675
4.575	1.8921	23.669	20.8475	2.8215	23.342	18.7899	4.5521
4.5875	1.8807	23.6774	20.8693	2.8081	23.3498	18.813	4.5368
4.6	1.8691	23.6858	20.8911	2.7947	23.3575	18.8361	4.5214
4.6125	1.8578	23.6942	20.9127	2.7815	23.3652	18.8591	4.5061
4.625	1.8464	23.7025	20.9342	2.7683	23.3729	18.882	4.4909
4.6375	1.8351	23.7108	20.9556	2.7552	23.3806	18.9049	4.4757
4.65	1.8239	23.719	20.977	2.742	23.3882	18.9276	4.4606
4.6625	1.8128	23.7272	20.9982	2.729	23.3957	18.9503	4.4454
4.675	1.8016	23.7353	21.0193	2.716	23.4033	18.9729	4.4304
4.6875	1.7906	23.7434	21.0404	2.703	23.4108	18.9955	4.4153
4.7	1.7796	23.7514	21.0613	2.6901	23.4183	19.018	4.4003
4.7125	1.7685	23.7594	21.0822	2.6772	23.4257	19.0404	4.3853
4.725	1.7577	23.7674	21.1029	2.6645	23.4331	19.0627	4.3704
4.7375	1.7468	23.7752	21.1236	2.6516	23.4405	19.0849	4.3556
4.75	1.7361	23.7831	21.1441	2.639	23.4478	19.1071	4.3407
4.7625	1.7253	23.7909	21.1646	2.6263	23.4552	19.1292	4.326
4.775	1.7146	23.7986	21.185	2.6136	23.4624	19.1513	4.3111
4.7875	1.704	23.8063	21.2052	2.6011	23.4697	19.1733	4.2964
4.8	1.6934	23.814	21.2254	2.5886	23.4769	19.1952	4.2817
4.8125	1.6829	23.8216	21.2455	2.5761	23.4841	19.217	4.2671
4.825	1.6724	23.8292	21.2655	2.5637	23.4913	19.2387	4.2526

		Nd=0.75				Nd=0.5	
		Rock ‰	Fluid ‰		Rock ‰	Fluid ‰	
z (km)	Δr-fl	δ18O	δ18O	Δr-fl	δ18O	δ18O	Δr-fl
4.8375	1.662	23.8367	21.2854	2.5513	23.4984	19.2604	4.238
4.85	1.6517	23.8442	21.3052	2.539	23.5055	19.282	4.2235
4.8625	1.6413	23.8516	21.3249	2.5267	23.5125	19.3036	4.2089
4.875	1.6311	23.859	21.3445	2.5145	23.5196	19.3251	4.1945
4.8875	1.6209	23.8663	21.3641	2.5022	23.5266	19.3465	4.1801
4.9	1.6107	23.8736	21.3835	2.4901	23.5335	19.3678	4.1657
4.9125	1.6006	23.8809	21.4029	2.478	23.5405	19.3891	4.1514
4.925	1.5906	23.8881	21.4221	2.466	23.5474	19.4103	4.1371
4.9375	1.5806	23.8953	21.4413	2.454	23.5543	19.4314	4.1229
4.95	1.5707	23.9024	21.4604	2.442	23.5611	19.4524	4.1087
4.9625	1.5608	23.9095	21.4794	2.4301	23.5679	19.4734	4.0945
4.975	1.5509	23.9165	21.4983	2.4182	23.5747	19.4943	4.0804
4.9875	1.5411	23.9235	21.5171	2.4064	23.5815	19.5152	4.0663
5	1.5314	23.9305	21.5358	2.3947	23.5882	19.536	4.0522

E.4 Reactive Transport Modeling Results at TIFF of $1x10^5$ (moles H_2O/cm^2)

z (km)	Rock ‰ δ18O	Nd=50000 Fluid ‰ δ18O	Δr-fl	Rock ‰ δ18O	Nd=5000 Fluid ‰ δ18O	Δr-fl	Rock ‰ δ18O	Nd=50 Fluid ‰ δ18O
0	4	4	0	4	4	0	4	4
0.125	4	4	0	4	4	0	4	4
0.25	4	4	0	4	4	0	4	4
0.375	4	4	0	4	4	0	4	4
0.5	4	4	0	4	4	0	4	4
0.625	4	4	0	4	4	0	4	4
0.75	4	4	0	4	4	0	4	4
0.875	4	4	0	4	4	0	4	4
1	4	4	0	4	4	0	4	4
1.125	4	4	0	4	4	0	4	4
1.25	4	4	0	4	4	0	4	4
1.375	4	4	0	4	4	0	4	4
1.5	4	4	0	4	4	0	4	4
1.625	4	4	0	4	4	0	4	4
1.75	4	4	0	4	4	0	4	4
1.875	4	4	0	4	4	0	4	4
2	4	4	0	4	4	0	4	4
2.125	4	4	0	4	4	0	4	4
2.25	4	4	0	4	4	0	4	4
2.375	4	4	0	4	4	0	4	4
2.5	4	4	0	4	4	0	4	4
2.625	4	4	0	4	4	0	4	4
2.75	4	4	0	4	4	0	4	4
2.875	4	4	0	4	4	0	4	4
3	4	4	0	4	4	0	4	4
3.125	4	4	0	4	4	0	4	4
3.25	4	4	0	4	4	0	4	4
3.375	4	4	0	4	4	0	4	4
3.5	4	4	0	4	4	0	4	4
3.625	4	4	0	4	4	0	4	4
3.75	4	4	0	4	4	0	4	4
3.875	4	4	0	4	4	0	4	4.0001
4	4	4	0	4	4	0	4	4.0001
4.125	4	4	0	4	4	0	4	4.0001
4.25	4	4	0	4	4	0	4	4.0002
4.375	4	4	0	4	4	0	4	4.0003
4.5	4	4	0	4	4	0	4	4.0004
4.625	4	4	0	4	4	0	4	4.0005
4.75	4	4	0	4	4	0	4	4.0008
4.875	4	4	0	4	4	0	4	4.0011
5	4	4	0	4	4	0	4	4.0015
5.125	4	4	0	4	4	0	4.0021	4.002
5.25	4	4	0	4	4	0	4.0028	4.0028

z (km)	Rock ‰ δ18O	Nd=50000 Fluid ‰ δ18O	Δr-fl	Rock ‰ δ18O	Nd=5000 Fluid ‰ δ18O	Δr-fl	Rock ‰ δ18O	Nd=50 Fluid ‰ δ18O
5.375	4	4	0	4	4	0	4.0046	4.0037
5.5	4	4	0	4	4	0	4.0068	4.005
5.625	4	4	0	4	4	0	4.0088	4.0066
5.75	4	4	0	4	4	0	4.0122	4.0087
5.875	4	4	0	4	4	0	4.0163	4.0113
6	4	4	0	4	4	0	4.0214	4.0147
6.125	4	4	0	4	4	0	4.0275	4.0188
6.25	4	4	0	4	4	0	4.0351	4.024
6.375	4	4	0	4	4	0	4.0439	4.0304
6.5	4	4	0	4	4	0	4.055	4.0382
6.625	4	4	0	4	4	0	4.0683	4.0477
6.75	4	4	0	4	4	0	4.0842	4.0592
6.875	4	4	0	4	4	0	4.1031	4.0729
7	4	4	0	4	4	0	4.1254	4.0894
7.125	4	4	0	4	4	0	4.1515	4.1089
7.25	4	4	0	4	4	0	4.1821	4.1318
7.375	4	4	0	4	4	0	4.2175	4.1587
7.5	4	4	0	4	4	0	4.2585	4.1901
7.625	4	4	0	4	4	0	4.3054	4.2264
7.75	4	4	0	4	4	0	4.3592	4.2683
7.875	4	4	0	4	4	0	4.4203	4.3164
8	4	4	0	4	4	0	4.4894	4.3712
8.125	4	4	0	4	4	0	4.5672	4.4334
8.25	4	4	0	4	4	0	4.6544	4.5036
8.375	4	4	0	4	4	0	4.7516	4.5826
8.5	4	4	0	4	4	0	4.8596	4.671
8.625	4	4	0	4	4	0	4.979	4.7694
8.75	4	4	0	4	4	0	5.1103	4.8786
8.875	4	4	0	4	4	0	5.2543	4.9991
9	4	4	0	4	4	0	5.4113	5.1315
9.125	4	4	0	4	4	0	5.582	5.2765
9.25	4	4	0	4	4	0	5.7668	5.4345
9.375	4	4	0	4	4	0	5.9659	5.606
9.5	4	4	0	4	4	0	6.1798	5.7915
9.625	4	4	0	4	4	0	6.4086	5.9913
9.75	4	4	0	4	4	0	6.6524	6.2057
9.875	4	4	0	4	4	0	6.9113	6.4348
10	4	4	0	4	4	0	7.1852	6.6788
10.125	4	4	0	4	4	0	7.4739	6.9378
10.25	4	4	0	4	4	0	7.7772	7.2116
10.375	4	4	0	4	4	0	8.0948	7.5
10.5	4	4	0	4	4	0	8.4262	7.8029
10.625	4	4	0	4	4	0	8.7708	8.1199

z (km)	Nd=50000 Rock ‰ δ18O	Fluid ‰ δ18O	Δr-fl	Nd=5000 Rock ‰ δ18O	Fluid ‰ δ18O	Δr-fl	Nd=50 Rock ‰ δ18O	Fluid ‰ δ18O
10.75	4	4	0	4	4	0	9.1281	8.4505
10.875	4	4	0	4	4	0	9.4972	8.7941
11	4	4	0	4	4	0	9.8774	9.1502
11.125	4	4	0	4	4	0	10.2678	9.5181
11.25	4	4	0	4	4	0	10.6674	9.8969
11.375	4	4	0	4	4	0	11.0753	10.2857
11.5	4	4	0	4	4.0003	-0.0003	11.4903	10.6837
11.625	4	4	0	4.0007	4.0025	-0.0018	11.9114	11.0898
11.75	4	4	0	4.0172	4.0178	-0.0006	12.3375	11.503
11.875	4	4	0	4.0975	4.0949	0.0026	12.7673	11.9221
12	4	4	0	4.3999	4.3899	0.01	13.1997	12.3462
12.125	4	4	0	5.2709	5.245	0.0259	13.6335	12.774
12.25	4.0098	4.0112	-0.0014	14.5436	14.4564	0.0872	14.0676	13.2043
12.375	5.0818	5.0745	0.0073	10.3987	10.323	0.0757	14.5008	13.6361
12.5	14.5136	14.4864	0.0272	14.5431	14.4569	0.0862	14.9319	14.0681
12.625	23.908	23.9008	0.0072	18.6586	18.5832	0.0754	15.3598	14.4992
12.75	24.9876	24.9888	-0.0012	14.5432	14.4568	0.0864	15.7836	14.9283
12.875	25	25	0	23.6997	23.6733	0.0264	16.2021	15.3544
13	25	25	0	24.5715	24.5609	0.0106	16.6145	15.7763
13.125	25	25	0	24.8868	24.8838	0.003	17.0198	16.193
13.25	25	25	0	24.9761	24.9764	-0.0003	17.4171	16.6037
13.375	25	25	0	24.996	24.9976	-0.0016	17.8057	17.0073
13.5	25	25	0	24.9995	25	-0.0005	18.1849	17.4032
13.625	25	25	0	24.9999	25	-1E-04	18.554	17.7904
13.75	25	25	0	25	25	0	18.9126	18.1684
13.875	25	25	0	25	25	0	19.26	18.5364
14	25	25	0	25	25	0	19.5959	18.8939
14.125	25	25	0	25	25	0	19.92	19.2405
14.25	25	25	0	25	25	0	20.232	19.5757
14.375	25	25	0	25	25	0	20.5317	19.8992
14.5	25	25	0	25	25	0	20.8189	20.2107
14.625	25	25	0	25	25	0	21.0936	20.51
14.75	25	25	0	25	25	0	21.3559	20.797
14.875	25	25	0	25	25	0	21.6056	21.0716
15	25	25	0	25	25	0	21.8431	21.3338
15.125	25	25	0	25	25	0	22.0683	21.5837
15.25	25	25	0	25	25	0	22.2816	21.8213
15.375	25	25	0	25	25	0	22.4831	22.0468
15.5	25	25	0	25	25	0	22.6732	22.2604
15.625	25	25	0	25	25	0	22.852	22.4624
15.75	25	25	0	25	25	0	23.0201	22.6529
15.875	25	25	0	25	25	0	23.1777	22.8323
16	25	25	0	25	25	0	23.3252	23.001

z (km)	Rock ‰ δ18O	Nd=50000 Fluid ‰ δ18O	Δr-fl	Rock ‰ δ18O	Nd=5000 Fluid ‰ δ18O	Δr-fl	Rock ‰ δ18O	Nd=50 Fluid ‰ δ18O
16.125	25	25	0	25	25	0	23.463	23.1592
16.25	25	25	0	25	25	0	23.5915	23.3074
16.375	25	25	0	25	25	0	23.7112	23.4458
16.5	25	25	0	25	25	0	23.8223	23.5751
16.625	25	25	0	25	25	0	23.9254	23.6954
16.75	25	25	0	25	25	0	24.0209	23.8073
16.875	25	25	0	25	25	0	24.1091	23.9111
17	25	25	0	25	25	0	24.1906	24.0073
17.125	25	25	0	25	25	0	24.2656	24.0963
17.25	25	25	0	25	25	0	24.3346	24.1785
17.375	25	25	0	25	25	0	24.3979	24.2542
17.5	25	25	0	25	25	0	24.456	24.3239
17.625	25	25	0	25	25	0	24.5091	24.3879
17.75	25	25	0	25	25	0	24.5576	24.4466
17.875	25	25	0	25	25	0	24.6019	24.5003
18	25	25	0	25	25	0	24.6423	24.5495
18.125	25	25	0	25	25	0	24.6789	24.5944
18.25	25	25	0	25	25	0	24.7122	24.6352
18.375	25	25	0	25	25	0	24.7424	24.6724
18.5	25	25	0	25	25	0	24.7697	24.7062
18.625	25	25	0	25	25	0	24.7944	24.7369
18.75	25	25	0	25	25	0	24.8167	24.7647
18.875	25	25	0	25	25	0	24.8368	24.7898
19	25	25	0	25	25	0	24.8548	24.8125
19.125	25	25	0	25	25	0	24.871	24.833
19.25	25	25	0	25	25	0	24.8856	24.8515
19.375	25	25	0	25	25	0	24.8986	24.868
19.5	25	25	0	25	25	0	24.9103	24.8829
19.625	25	25	0	25	25	0	24.9207	24.8963
19.75	25	25	0	25	25	0	24.93	24.9083
19.875	25	25	0	25	25	0	24.9383	24.9189
20	25	25	0	25	25	0	24.9457	24.9285
20.125	25	25	0	25	25	0	24.9522	24.9371
20.25	25	25	0	25	25	0	24.958	24.9447
20.375	25	25	0	25	25	0	24.9632	24.9513
20.5	25	25	0	25	25	0	24.9677	24.9575
20.625	25	25	0	25	25	0	24.9718	24.9626
20.75	25	25	0	25	25	0	24.9753	24.9675
20.875	25	25	0	25	25	0	24.9784	24.9718
21	25	25	0	25	25	0	24.9812	24.9753
21.125	25	25	0	25	25	0	24.9836	24.9787
21.25	25	25	0	25	25	0	24.9857	24.9814
21.375	25	25	0	25	25	0	24.9876	24.9841

		Nd=50000			Nd=5000			Nd=50
z (km)	Rock ‰ δ18O	Fluid ‰ δ18O	Δr-fl	Rock ‰ δ18O	Fluid ‰ δ18O	Δr-fl	Rock ‰ δ18O	Fluid ‰ δ18O
21.5	25	25	0	25	25	0	24.9892	24.9866
21.625	25	25	0	25	25	0	24.9907	24.9883
21.75	25	25	0	25	25	0	24.9919	24.9902
21.875	25	25	0	25	25	0	24.993	24.9915
22	25	25	0	25	25	0	24.9939	24.9931
22.125	25	25	0	25	25	0	24.9948	24.994
22.25	25	25	0	25	25	0	24.9955	24.9953
22.375	25	25	0	25	25	0	24.9961	24.9959
22.5	25	25	0	25	25	0	24.9967	24.9969
22.625	25	25	0	25	25	0	24.9971	24.9974
22.75	25	25	0	25	25	0	24.9975	24.9982
22.875	25	25	0	25	25	0	24.9979	24.9985
23	25	25	0	25	25	0	24.9982	25
23.125	25	25	0	25	25	0	24.9984	25
23.25	25	25	0	25	25	0	24.9987	25
23.375	25	25	0	25	25	0	24.9989	25
23.5	25	25	0	25	25	0	24.999	25
23.625	25	25	0	25	25	0	24.9992	25
23.75	25	25	0	25	25	0	24.9993	25
23.875	25	25	0	25	25	0	24.9994	25
24	25	25	0	25	25	0	24.9995	25
24.125	25	25	0	25	25	0	24.9996	25
24.25	25	25	0	25	25	0	24.9996	25
24.375	25	25	0	25	25	0	24.9997	25
24.5	25	25	0	25	25	0	24.9997	25
24.625	25	25	0	25	25	0	24.9998	25
24.75	25	25	0	25	25	0	24.9998	25
24.875	25	25	0	25	25	0	24.9998	25
25	25	25	0	25	25	0	24.9999	25
25.125	25	25	0	25	25	0	24.9999	25
25.25	25	25	0	25	25	0	24.9999	25
25.375	25	25	0	25	25	0	24.9999	25
25.5	25	25	0	25	25	0	24.9999	25
25.625	25	25	0	25	25	0	24.9999	25
25.75	25	25	0	25	25	0	25	25
25.875	25	25	0	25	25	0	25	25
26	25	25	0	25	25	0	25	25
26.125	25	25	0	25	25	0	25	25
26.25	25	25	0	25	25	0	25	25
26.375	25	25	0	25	25	0	25	25
26.5	25	25	0	25	25	0	25	25
26.625	25	25	0	25	25	0	25	25
26.75	25	25	0	25	25	0	25	25

		Nd=50000			Nd=5000			Nd=50
z (km)	Rock ‰ δ18O	Fluid ‰ δ18O	Δr-fl	Rock ‰ δ18O	Fluid ‰ δ18O	Δr-fl	Rock ‰ δ18O	Fluid ‰ δ18O
26.875	25	25	0	25	25	0	25	25
27	25	25	0	25	25	0	25	25
27.125	25	25	0	25	25	0	25	25
27.25	25	25	0	25	25	0	25	25
27.375	25	25	0	25	25	0	25	25
27.5	25	25	0	25	25	0	25	25
27.625	25	25	0	25	25	0	25	25
27.75	25	25	0	25	25	0	25	25
27.875	25	25	0	25	25	0	25	25
28	25	25	0	25	25	0	25	25
28.125	25	25	0	25	25	0	25	25
28.25	25	25	0	25	25	0	25	25
28.375	25	25	0	25	25	0	25	25
28.5	25	25	0	25	25	0	25	25
28.625	25	25	0	25	25	0	25	25
28.75	25	25	0	25	25	0	25	25
28.875	25	25	0	25	25	0	25	25
29	25	25	0	25	25	0	25	25
29.125	25	25	0	25	25	0	25	25
29.25	25	25	0	25	25	0	25	25
29.375	25	25	0	25	25	0	25	25
29.5	25	25	0	25	25	0	25	25
29.625	25	25	0	25	25	0	25	25
29.75	25	25	0	25	25	0	25	25
29.875	25	25	0	25	25	0	25	25
30	25	25	0	25	25	0	25	25
30.125	25	25	0	25	25	0	25	25
30.25	25	25	0	25	25	0	25	25
30.375	25	25	0	25	25	0	25	25
30.5	25	25	0	25	25	0	25	25
30.625	25	25	0	25	25	0	25	25
30.75	25	25	0	25	25	0	25	25
30.875	25	25	0	25	25	0	25	25
31	25	25	0	25	25	0	25	25
31.125	25	25	0	25	25	0	25	25
31.25	25	25	0	25	25	0	25	25
31.375	25	25	0	25	25	0	25	25
31.5	25	25	0	25	25	0	25	25
31.625	25	25	0	25	25	0	25	25
31.75	25	25	0	25	25	0	25	25
31.875	25	25	0	25	25	0	25	25
32	25	25	0	25	25	0	25	25
32.125	25	25	0	25	25	0	25	25

z (km)	Rock ‰ δ18O	Nd=50000 Fluid ‰ δ18O	Δr-fl	Rock ‰ δ18O	Nd=5000 Fluid ‰ δ18O	Δr-fl	Rock ‰ δ18O	Nd=50 Fluid ‰ δ18O
32.25	25	25	0	25	25	0	25	25
32.375	25	25	0	25	25	0	25	25
32.5	25	25	0	25	25	0	25	25
32.625	25	25	0	25	25	0	25	25
32.75	25	25	0	25	25	0	25	25
32.875	25	25	0	25	25	0	25	25
33	25	25	0	25	25	0	25	25
33.125	25	25	0	25	25	0	25	25
33.25	25	25	0	25	25	0	25	25
33.375	25	25	0	25	25	0	25	25
33.5	25	25	0	25	25	0	25	25
33.625	25	25	0	25	25	0	25	25
33.75	25	25	0	25	25	0	25	25
33.875	25	25	0	25	25	0	25	25
34	25	25	0	25	25	0	25	25
34.125	25	25	0	25	25	0	25	25
34.25	25	25	0	25	25	0	25	25
34.375	25	25	0	25	25	0	25	25
34.5	25	25	0	25	25	0	25	25
34.625	25	25	0	25	25	0	25	25
34.75	25	25	0	25	25	0	25	25
34.875	25	25	0	25	25	0	25	25
35	25	25	0	25	25	0	25	25
35.125	25	25	0	25	25	0	25	25
35.25	25	25	0	25	25	0	25	25
35.375	25	25	0	25	25	0	25	25
35.5	25	25	0	25	25	0	25	25
35.625	25	25	0	25	25	0	25	25
35.75	25	25	0	25	25	0	25	25
35.875	25	25	0	25	25	0	25	25
36	25	25	0	25	25	0	25	25
36.125	25	25	0	25	25	0	25	25
36.25	25	25	0	25	25	0	25	25
36.375	25	25	0	25	25	0	25	25
36.5	25	25	0	25	25	0	25	25
36.625	25	25	0	25	25	0	25	25
36.75	25	25	0	25	25	0	25	25
36.875	25	25	0	25	25	0	25	25
37	25	25	0	25	25	0	25	25
37.125	25	25	0	25	25	0	25	25
37.25	25	25	0	25	25	0	25	25
37.375	25	25	0	25	25	0	25	25
37.5	25	25	0	25	25	0	25	25

		Nd=50000			Nd=5000			Nd=50
	Rock ‰	Fluid ‰		Rock ‰	Fluid ‰		Rock ‰	Fluid ‰
z (km)	δ18O	δ18O	Δr-fl	δ18O	δ18O	Δr-fl	δ18O	δ18O
37.625	25	25	0	25	25	0	25	25
37.75	25	25	0	25	25	0	25	25
37.875	25	25	0	25	25	0	25	25
38	25	25	0	25	25	0	25	25
38.125	25	25	0	25	25	0	25	25
38.25	25	25	0	25	25	0	25	25
38.375	25	25	0	25	25	0	25	25
38.5	25	25	0	25	25	0	25	25
38.625	25	25	0	25	25	0	25	25
38.75	25	25	0	25	25	0	25	25
38.875	25	25	0	25	25	0	25	25
39	25	25	0	25	25	0	25	25
39.125	25	25	0	25	25	0	25	25
39.25	25	25	0	25	25	0	25	25
39.375	25	25	0	25	25	0	25	25
39.5	25	25	0	25	25	0	25	25
39.625	25	25	0	25	25	0	25	25
39.75	25	25	0	25	25	0	25	25
39.875	25	25	0	25	25	0	25	25
40	25	25	0	25	25	0	25	25
40.125	25	25	0	25	25	0	25	25
40.25	25	25	0	25	25	0	25	25
40.375	25	25	0	25	25	0	25	25
40.5	25	25	0	25	25	0	25	25
40.625	25	25	0	25	25	0	25	25
40.75	25	25	0	25	25	0	25	25
40.875	25	25	0	25	25	0	25	25
41	25	25	0	25	25	0	25	25
41.125	25	25	0	25	25	0	25	25
41.25	25	25	0	25	25	0	25	25
41.375	25	25	0	25	25	0	25	25
41.5	25	25	0	25	25	0	25	25
41.625	25	25	0	25	25	0	25	25
41.75	25	25	0	25	25	0	25	25
41.875	25	25	0	25	25	0	25	25
42	25	25	0	25	25	0	25	25
42.125	25	25	0	25	25	0	25	25
42.25	25	25	0	25	25	0	25	25
42.375	25	25	0	25	25	0	25	25
42.5	25	25	0	25	25	0	25	25
42.625	25	25	0	25	25	0	25	25
42.75	25	25	0	25	25	0	25	25
42.875	25	25	0	25	25	0	25	25

z (km)	Rock ‰ δ18O	Nd=50000 Fluid ‰ δ18O	Δr-fl	Rock ‰ δ18O	Nd=5000 Fluid ‰ δ18O	Δr-fl	Rock ‰ δ18O	Nd=50 Fluid ‰ δ18O
43	25	25	0	25	25	0	25	25
43.125	25	25	0	25	25	0	25	25
43.25	25	25	0	25	25	0	25	25
43.375	25	25	0	25	25	0	25	25
43.5	25	25	0	25	25	0	25	25
43.625	25	25	0	25	25	0	25	25
43.75	25	25	0	25	25	0	25	25
43.875	25	25	0	25	25	0	25	25
44	25	25	0	25	25	0	25	25
44.125	25	25	0	25	25	0	25	25
44.25	25	25	0	25	25	0	25	25
44.375	25	25	0	25	25	0	25	25
44.5	25	25	0	25	25	0	25	25
44.625	25	25	0	25	25	0	25	25
44.75	25	25	0	25	25	0	25	25
44.875	25	25	0	25	25	0	25	25
45	25	25	0	25	25	0	25	25
45.125	25	25	0	25	25	0	25	25
45.25	25	25	0	25	25	0	25	25
45.375	25	25	0	25	25	0	25	25
45.5	25	25	0	25	25	0	25	25
45.625	25	25	0	25	25	0	25	25
45.75	25	25	0	25	25	0	25	25
45.875	25	25	0	25	25	0	25	25
46	25	25	0	25	25	0	25	25
46.125	25	25	0	25	25	0	25	25
46.25	25	25	0	25	25	0	25	25
46.375	25	25	0	25	25	0	25	25
46.5	25	25	0	25	25	0	25	25
46.625	25	25	0	25	25	0	25	25
46.75	25	25	0	25	25	0	25	25
46.875	25	25	0	25	25	0	25	25
47	25	25	0	25	25	0	25	25
47.125	25	25	0	25	25	0	25	25
47.25	25	25	0	25	25	0	25	25
47.375	25	25	0	25	25	0	25	25
47.5	25	25	0	25	25	0	25	25
47.625	25	25	0	25	25	0	25	25
47.75	25	25	0	25	25	0	25	25
47.875	25	25	0	25	25	0	25	25
48	25	25	0	25	25	0	25	25
48.125	25	25	0	25	25	0	25	25
48.25	25	25	0	25	25	0	25	25

		Nd=50000			Nd=5000			Nd=50
	Rock ‰	Fluid ‰		Rock ‰	Fluid ‰		Rock ‰	Fluid ‰
z (km)	δ18O	δ18O	Δr-fl	δ18O	δ18O	Δr-fl	δ18O	δ18O
48.375	25	25	0	25	25	0	25	25
48.5	25	25	0	25	25	0	25	25
48.625	25	25	0	25	25	0	25	25
48.75	25	25	0	25	25	0	25	25
48.875	25	25	0	25	25	0	25	25
49	25	25	0	25	25	0	25	25
49.125	25	25	0	25	25	0	25	25
49.25	25	25	0	25	25	0	25	25
49.375	25	25	0	25	25	0	25	25
49.5	25	25	0	25	25	0	25	25
49.625	25	25	0	25	25	0	25	25
49.75	25	25	0	25	25	0	25	25
49.875	25	25	0	25	25	0	25	25
50	25	25	0	25	25	0	25	25

		Nd=5				Nd=1		
z (km)	Δr-fl	Rock ‰ δ18O	Fluid ‰ δ18O	Δr-fl	Rock ‰ δ18O	Fluid ‰ δ18O	Δr-fl	Rock ‰ δ18O
0	0	4.1415	4	0.1415	11.7255	4	7.7255	13.9197
0.125	0	4.1765	4.0073	0.1692	11.8026	4.0729	7.7297	13.9764
0.25	0	4.2141	4.016	0.1981	11.8793	4.1459	7.7334	14.0329
0.375	0	4.2542	4.0261	0.2281	11.9557	4.2189	7.7368	14.0892
0.5	0	4.2969	4.0377	0.2592	12.0318	4.2921	7.7397	14.1452
0.625	0	4.3421	4.0508	0.2913	12.1075	4.3653	7.7422	14.2009
0.75	0	4.39	4.0654	0.3246	12.1829	4.4385	7.7444	14.2564
0.875	0	4.4404	4.0817	0.3587	12.2579	4.5118	7.7461	14.3117
1	0	4.4934	4.0997	0.3937	12.3326	4.5852	7.7474	14.3667
1.125	0	4.549	4.1194	0.4296	12.407	4.6586	7.7484	14.4215
1.25	0	4.6072	4.1408	0.4664	12.481	4.7321	7.7489	14.4761
1.375	0	4.668	4.164	0.504	12.5547	4.8056	7.7491	14.5304
1.5	0	4.7314	4.1891	0.5423	12.6281	4.8791	7.749	14.5845
1.625	0	4.7973	4.2161	0.5812	12.7011	4.9527	7.7484	14.6383
1.75	0	4.8658	4.2449	0.6209	12.7738	5.0263	7.7475	14.6919
1.875	0	4.9368	4.2757	0.6611	12.8462	5.0999	7.7463	14.7453
2	0	5.0103	4.3085	0.7018	12.9182	5.1736	7.7446	14.7984
2.125	0	5.0863	4.3433	0.743	12.9899	5.2473	7.7426	14.8513
2.25	0	5.1648	4.38	0.7848	13.0613	5.321	7.7403	14.904
2.375	0	5.2458	4.4189	0.8269	13.1323	5.3947	7.7376	14.9564
2.5	0	5.3291	4.4598	0.8693	13.203	5.4684	7.7346	15.0086
2.625	0	5.4149	4.5028	0.9121	13.2734	5.5421	7.7313	15.0606
2.75	0	5.503	4.5479	0.9551	13.3434	5.6158	7.7276	15.1123
2.875	0	5.5935	4.5951	0.9984	13.4131	5.6895	7.7236	15.1638
3	0	5.6862	4.6444	1.0418	13.4825	5.7632	7.7193	15.2151
3.125	0	5.7812	4.6958	1.0854	13.5515	5.8369	7.7146	15.2661
3.25	0	5.8785	4.7494	1.1291	13.6203	5.9106	7.7097	15.317
3.375	0	5.9779	4.8052	1.1727	13.6887	5.9843	7.7044	15.3676
3.5	0	6.0795	4.8631	1.2164	13.7567	6.0579	7.6988	15.4179
3.625	0	6.1831	4.9231	1.26	13.8245	6.1316	7.6929	15.4681
3.75	0	6.2889	4.9853	1.3036	13.8919	6.2052	7.6867	15.518
3.875	-1E-04	6.3966	5.0496	1.347	13.959	6.2787	7.6803	15.5677
4	-1E-04	6.5064	5.1161	1.3903	14.0258	6.3523	7.6735	15.6172
4.125	-1E-04	6.618	5.1847	1.4333	14.0923	6.4258	7.6665	15.6664
4.25	-0.0002	6.7316	5.2554	1.4762	14.1584	6.4993	7.6591	15.7154
4.375	-0.0003	6.8469	5.3283	1.5186	14.2242	6.5727	7.6515	15.7642
4.5	-0.0004	6.9641	5.4032	1.5609	14.2897	6.6461	7.6436	15.8128
4.625	-0.0005	7.083	5.4802	1.6028	14.3549	6.7194	7.6355	15.8612
4.75	-0.0008	7.2035	5.5593	1.6442	14.4197	6.7927	7.627	15.9093
4.875	-0.0011	7.3258	5.6405	1.6853	14.4843	6.866	7.6183	15.9573
5	-0.0015	7.4495	5.7236	1.7259	14.5485	6.9392	7.6093	16.005
5.125	0.0001	7.5749	5.8088	1.7661	14.6124	7.0123	7.6001	16.0525
5.25	0	7.7017	5.896	1.8057	14.676	7.0854	7.5906	16.0997

			Nd=5			Nd=1		
		Rock ‰	Fluid ‰		Rock ‰	Fluid ‰		Rock ‰
z (km)	Δr-fl	δ18O	δ18O	Δr-fl	δ18O	δ18O	Δr-fl	δ18O
5.375	0.0009	7.8299	5.9851	1.8448	14.7393	7.1584	7.5809	16.1468
5.5	0.0018	7.9595	6.0762	1.8833	14.8023	7.2313	7.571	16.1937
5.625	0.0022	8.0904	6.1691	1.9213	14.8649	7.3042	7.5607	16.2403
5.75	0.0035	8.2226	6.264	1.9586	14.9273	7.377	7.5503	16.2867
5.875	0.005	8.356	6.3607	1.9953	14.9893	7.4497	7.5396	16.3329
6	0.0067	8.4906	6.4592	2.0314	15.051	7.5224	7.5286	16.3789
6.125	0.0087	8.6263	6.5595	2.0668	15.1124	7.5949	7.5175	16.4247
6.25	0.0111	8.763	6.6616	2.1014	15.1736	7.6674	7.5062	16.4703
6.375	0.0135	8.9007	6.7654	2.1353	15.2343	7.7398	7.4945	16.5156
6.5	0.0168	9.0394	6.8709	2.1685	15.2948	7.8122	7.4826	16.5608
6.625	0.0206	9.179	6.978	2.201	15.355	7.8844	7.4706	16.6058
6.75	0.025	9.3194	7.0868	2.2326	15.4149	7.9566	7.4583	16.6505
6.875	0.0302	9.4606	7.1971	2.2635	15.4745	8.0286	7.4459	16.695
7	0.036	9.6026	7.309	2.2936	15.5338	8.1006	7.4332	16.7394
7.125	0.0426	9.7452	7.4223	2.3229	15.5927	8.1724	7.4203	16.7835
7.25	0.0503	9.8885	7.5372	2.3513	15.6514	8.2442	7.4072	16.8274
7.375	0.0588	10.0323	7.6534	2.3789	15.7098	8.3159	7.3939	16.8711
7.5	0.0684	10.1767	7.7711	2.4056	15.7679	8.3874	7.3805	16.9146
7.625	0.079	10.3215	7.89	2.4315	15.8256	8.4589	7.3667	16.9579
7.75	0.0909	10.4668	8.0103	2.4565	15.8831	8.5302	7.3529	17.0011
7.875	0.1039	10.6125	8.1318	2.4807	15.9403	8.6015	7.3388	17.044
8	0.1182	10.7585	8.2546	2.5039	15.9972	8.6726	7.3246	17.0867
8.125	0.1338	10.9048	8.3785	2.5263	16.0538	8.7436	7.3102	17.1292
8.25	0.1508	11.0513	8.5035	2.5478	16.1101	8.8145	7.2956	17.1715
8.375	0.169	11.198	8.6296	2.5684	16.1661	8.8853	7.2808	17.2136
8.5	0.1886	11.3449	8.7568	2.5881	16.2218	8.9559	7.2659	17.2555
8.625	0.2096	11.4919	8.8849	2.607	16.2772	9.0265	7.2507	17.2972
8.75	0.2317	11.6389	9.014	2.6249	16.3323	9.0969	7.2354	17.3388
8.875	0.2552	11.7859	9.1441	2.6418	16.3872	9.1672	7.22	17.3801
9	0.2798	11.9329	9.2749	2.658	16.4417	9.2373	7.2044	17.4212
9.125	0.3055	12.0798	9.4066	2.6732	16.496	9.3074	7.1886	17.4622
9.25	0.3323	12.2266	9.5391	2.6875	16.55	9.3773	7.1727	17.5029
9.375	0.3599	12.3732	9.6723	2.7009	16.6037	9.447	7.1567	17.5435
9.5	0.3883	12.5196	9.8062	2.7134	16.6571	9.5167	7.1404	17.5838
9.625	0.4173	12.6658	9.9407	2.7251	16.7102	9.5862	7.124	17.624
9.75	0.4467	12.8117	10.0758	2.7359	16.7631	9.6555	7.1076	17.664
9.875	0.4765	12.9573	10.2115	2.7458	16.8156	9.7248	7.0908	17.7038
10	0.5064	13.1025	10.3477	2.7548	16.8679	9.7938	7.0741	17.7434
10.125	0.5361	13.2474	10.4844	2.763	16.9199	9.8628	7.0571	17.7828
10.25	0.5656	13.3918	10.6215	2.7703	16.9716	9.9316	7.04	17.822
10.375	0.5948	13.5358	10.759	2.7768	17.0231	10.0002	7.0229	17.861
10.5	0.6233	13.6792	10.8969	2.7823	17.0743	10.0687	7.0056	17.8999
10.625	0.6509	13.8222	11.035	2.7872	17.1252	10.1371	6.9881	17.9386

z (km)	Δr-fl	Rock ‰ δ18O	Nd=5 Fluid ‰ δ18O	Δr-fl	Rock ‰ δ18O	Nd=1 Fluid ‰ δ18O	Δr-fl	Rock ‰ δ18O
10.75	0.6776	13.9646	11.1734	2.7912	17.1758	10.2053	6.9705	17.9771
10.875	0.7031	14.1063	11.312	2.7943	17.2261	10.2734	6.9527	18.0154
11	0.7272	14.2475	11.4508	2.7967	17.2762	10.3413	6.9349	18.0535
11.125	0.7497	14.388	11.5898	2.7982	17.326	10.409	6.917	18.0914
11.25	0.7705	14.5279	11.7288	2.7991	17.3755	10.4766	6.8989	18.1292
11.375	0.7896	14.667	11.8679	2.7991	17.4248	10.5441	6.8807	18.1667
11.5	0.8066	14.8054	12.0071	2.7983	17.4738	10.6113	6.8625	18.2041
11.625	0.8216	14.943	12.1462	2.7968	17.5225	10.6785	6.844	18.2413
11.75	0.8345	15.0799	12.2853	2.7946	17.571	10.7454	6.8256	18.2784
11.875	0.8452	15.2159	12.4243	2.7916	17.6192	10.8122	6.807	18.3152
12	0.8535	15.3511	12.5632	2.7879	17.6671	10.8789	6.7882	18.3519
12.125	0.8595	15.4855	12.7019	2.7836	17.7148	10.9454	6.7694	18.3884
12.25	0.8633	15.619	12.8404	2.7786	17.7622	11.0117	6.7505	18.4247
12.375	0.8647	15.7516	12.9787	2.7729	17.8093	11.0778	6.7315	18.4609
12.5	0.8638	15.8832	13.1167	2.7665	17.8562	11.1438	6.7124	18.4968
12.625	0.8606	16.014	13.2545	2.7595	17.9028	11.2096	6.6932	18.5326
12.75	0.8553	16.1438	13.3919	2.7519	17.9492	11.2753	6.6739	18.5682
12.875	0.8477	16.2726	13.529	2.7436	17.9953	11.3407	6.6546	18.6037
13	0.8382	16.4004	13.6657	2.7347	18.0411	11.406	6.6351	18.639
13.125	0.8268	16.5272	13.8019	2.7253	18.0867	11.4712	6.6155	18.6741
13.25	0.8134	16.653	13.9377	2.7153	18.1321	11.5361	6.596	18.709
13.375	0.7984	16.7777	14.0731	2.7046	18.1771	11.6009	6.5762	18.7438
13.5	0.7817	16.9014	14.2079	2.6935	18.222	11.6655	6.5565	18.7784
13.625	0.7636	17.0241	14.3422	2.6819	18.2666	11.7299	6.5367	18.8128
13.75	0.7442	17.1456	14.476	2.6696	18.3109	11.7942	6.5167	18.8471
13.875	0.7236	17.2661	14.6091	2.657	18.355	11.8583	6.4967	18.8811
14	0.702	17.3855	14.7417	2.6438	18.3988	11.9222	6.4766	18.9151
14.125	0.6795	17.5038	14.8736	2.6302	18.4424	11.9859	6.4565	18.9488
14.25	0.6563	17.6209	15.0049	2.616	18.4857	12.0494	6.4363	18.9824
14.375	0.6325	17.7369	15.1355	2.6014	18.5288	12.1128	6.416	19.0158
14.5	0.6082	17.8518	15.2653	2.5865	18.5716	12.1759	6.3957	19.0491
14.625	0.5836	17.9656	15.3945	2.5711	18.6143	12.2389	6.3754	19.0822
14.75	0.5589	18.0782	15.5229	2.5553	18.6566	12.3017	6.3549	19.1151
14.875	0.534	18.1896	15.6506	2.539	18.6987	12.3644	6.3343	19.1479
15	0.5093	18.2999	15.7774	2.5225	18.7406	12.4268	6.3138	19.1805
15.125	0.4846	18.4091	15.9035	2.5056	18.7823	12.489	6.2933	19.213
15.25	0.4603	18.517	16.0287	2.4883	18.8237	12.5511	6.2726	19.2452
15.375	0.4363	18.6238	16.1531	2.4707	18.8648	12.613	6.2518	19.2774
15.5	0.4128	18.7294	16.2766	2.4528	18.9057	12.6747	6.231	19.3093
15.625	0.3896	18.8338	16.3993	2.4345	18.9464	12.7362	6.2102	19.3411
15.75	0.3672	18.937	16.5211	2.4159	18.9869	12.7975	6.1894	19.3728
15.875	0.3454	19.0391	16.6419	2.3972	19.0271	12.8586	6.1685	19.4043
16	0.3242	19.14	16.7619	2.3781	19.0671	12.9195	6.1476	19.4356

z (km)	Δr-fl	Rock ‰ δ18O	Nd=5 Fluid ‰ δ18O	Δr-fl	Rock ‰ δ18O	Nd=1 Fluid ‰ δ18O	Δr-fl	Rock ‰ δ18O
16.125	0.3038	19.2397	16.8809	2.3588	19.1069	12.9803	6.1266	19.4668
16.25	0.2841	19.3381	16.999	2.3391	19.1464	13.0408	6.1056	19.4978
16.375	0.2654	19.4355	17.1161	2.3194	19.1857	13.1012	6.0845	19.5287
16.5	0.2472	19.5316	17.2322	2.2994	19.2248	13.1614	6.0634	19.5594
16.625	0.23	19.6265	17.3474	2.2791	19.2636	13.2213	6.0423	19.59
16.75	0.2136	19.7203	17.4615	2.2588	19.3022	13.2811	6.0211	19.6204
16.875	0.198	19.8129	17.5747	2.2382	19.3406	13.3407	5.9999	19.6507
17	0.1833	19.9043	17.6869	2.2174	19.3788	13.4001	5.9787	19.6808
17.125	0.1693	19.9945	17.798	2.1965	19.4167	13.4593	5.9574	19.7107
17.25	0.1561	20.0835	17.9081	2.1754	19.4544	13.5183	5.9361	19.7405
17.375	0.1437	20.1714	18.0172	2.1542	19.4919	13.5771	5.9148	19.7702
17.5	0.1321	20.2581	18.1252	2.1329	19.5292	13.6357	5.8935	19.7997
17.625	0.1212	20.3437	18.2322	2.1115	19.5663	13.6941	5.8722	19.8291
17.75	0.111	20.4281	18.3381	2.09	19.6031	13.7523	5.8508	19.8583
17.875	0.1016	20.5113	18.443	2.0683	19.6397	13.8103	5.8294	19.8873
18	0.0928	20.5934	18.5468	2.0466	19.6761	13.8681	5.808	19.9163
18.125	0.0845	20.6744	18.6495	2.0249	19.7123	13.9258	5.7865	19.945
18.25	0.077	20.7542	18.7512	2.003	19.7483	13.9832	5.7651	19.9736
18.375	0.07	20.8329	18.8518	1.9811	19.7841	14.0404	5.7437	20.0021
18.5	0.0635	20.9105	18.9513	1.9592	19.8196	14.0974	5.7222	20.0305
18.625	0.0575	20.987	19.0497	1.9373	19.855	14.1543	5.7007	20.0587
18.75	0.052	21.0623	19.147	1.9153	19.8901	14.2109	5.6792	20.0867
18.875	0.047	21.1366	19.2433	1.8933	19.925	14.2673	5.6577	20.1146
19	0.0423	21.2097	19.3384	1.8713	19.9597	14.3235	5.6362	20.1424
19.125	0.038	21.2818	19.4325	1.8493	19.9942	14.3796	5.6146	20.17
19.25	0.0341	21.3528	19.5255	1.8273	20.0285	14.4354	5.5931	20.1975
19.375	0.0306	21.4227	19.6174	1.8053	20.0626	14.491	5.5716	20.2248
19.5	0.0274	21.4916	19.7082	1.7834	20.0965	14.5465	5.55	20.252
19.625	0.0244	21.5594	19.7979	1.7615	20.1301	14.6017	5.5284	20.2791
19.75	0.0217	21.6261	19.8865	1.7396	20.1636	14.6567	5.5069	20.306
19.875	0.0194	21.6919	19.974	1.7179	20.1969	14.7115	5.4854	20.3328
20	0.0172	21.7566	20.0605	1.6961	20.23	14.7661	5.4639	20.3595
20.125	0.0151	21.8202	20.1459	1.6743	20.2628	14.8206	5.4422	20.386
20.25	0.0133	21.8829	20.2302	1.6527	20.2955	14.8748	5.4207	20.4124
20.375	0.0119	21.9446	20.3134	1.6312	20.328	14.9288	5.3992	20.4386
20.5	0.0102	22.0053	20.3956	1.6097	20.3603	14.9826	5.3777	20.4647
20.625	0.0092	22.065	20.4767	1.5883	20.3923	15.0362	5.3561	20.4907
20.75	0.0078	22.1237	20.5567	1.567	20.4242	15.0896	5.3346	20.5165
20.875	0.0066	22.1814	20.6357	1.5457	20.4559	15.1428	5.3131	20.5423
21	0.0059	22.2383	20.7136	1.5247	20.4874	15.1959	5.2915	20.5678
21.125	0.0049	22.2941	20.7905	1.5036	20.5187	15.2487	5.27	20.5933
21.25	0.0043	22.3491	20.8663	1.4828	20.5498	15.3013	5.2485	20.6186
21.375	0.0035	22.4031	20.9411	1.462	20.5808	15.3537	5.2271	20.6438

			Nd=5			Nd=1		
		Rock ‰	Fluid ‰		Rock ‰	Fluid ‰		Rock ‰
z (km)	**Δr-fl**	**δ18O**	**δ18O**	**Δr-fl**	**δ18O**	**δ18O**	**Δr-fl**	**δ18O**
21.5	0.0026	22.4562	21.0148	1.4414	20.6115	15.4059	5.2056	20.6688
21.625	0.0024	22.5084	21.0875	1.4209	20.642	15.4579	5.1841	20.6938
21.75	0.0017	22.5597	21.1592	1.4005	20.6724	15.5096	5.1628	20.7185
21.875	0.0015	22.6101	21.2299	1.3802	20.7026	15.5612	5.1414	20.7432
22	0.0008	22.6596	21.2996	1.36	20.7325	15.6126	5.1199	20.7678
22.125	0.0008	22.7083	21.3683	1.34	20.7623	15.6638	5.0985	20.7922
22.25	0.0002	22.7562	21.436	1.3202	20.792	15.7148	5.0772	20.8164
22.375	0.0002	22.8032	21.5027	1.3005	20.8214	15.7656	5.0558	20.8406
22.5	-0.0002	22.8493	21.5684	1.2809	20.8506	15.8162	5.0344	20.8646
22.625	-0.0003	22.8947	21.6331	1.2616	20.8797	15.8665	5.0132	20.8885
22.75	-0.0007	22.9392	21.6969	1.2423	20.9086	15.9167	4.9919	20.9123
22.875	-0.0006	22.9829	21.7597	1.2232	20.9373	15.9667	4.9706	20.936
23	-0.0018	23.0259	21.8215	1.2044	20.9658	16.0165	4.9493	20.9595
23.125	-0.0016	23.068	21.8824	1.1856	20.9942	16.066	4.9282	20.9829
23.25	-0.0013	23.1094	21.9424	1.167	21.0224	16.1154	4.907	21.0062
23.375	-0.0011	23.1501	22.0014	1.1487	21.0504	16.1646	4.8858	21.0294
23.5	-0.001	23.1899	22.0595	1.1304	21.0782	16.2136	4.8646	21.0524
23.625	-0.0008	23.2291	22.1167	1.1124	21.1058	16.2623	4.8435	21.0754
23.75	-0.0007	23.2675	22.173	1.0945	21.1333	16.3109	4.8224	21.0982
23.875	-0.0006	23.3052	22.2284	1.0768	21.1606	16.3593	4.8013	21.1209
24	-0.0005	23.3422	22.2829	1.0593	21.1877	16.4074	4.7803	21.1434
24.125	-0.0004	23.3785	22.3366	1.0419	21.2147	16.4554	4.7593	21.1659
24.25	-0.0004	23.4141	22.3893	1.0248	21.2415	16.5032	4.7383	21.1882
24.375	-0.0003	23.449	22.4412	1.0078	21.2681	16.5507	4.7174	21.2104
24.5	-0.0003	23.4833	22.4923	0.991	21.2946	16.5981	4.6965	21.2325
24.625	-0.0002	23.5169	22.5425	0.9744	21.3208	16.6453	4.6755	21.2545
24.75	-0.0002	23.5499	22.5919	0.958	21.347	16.6922	4.6548	21.2764
24.875	-0.0002	23.5822	22.6405	0.9417	21.3729	16.739	4.6339	21.2981
25	-1E-04	23.6139	22.6882	0.9257	21.3987	16.7856	4.6131	21.3198
25.125	-1E-04	23.6449	22.7352	0.9097	21.4243	16.8319	4.5924	21.3413
25.25	-1E-04	23.6754	22.7813	0.8941	21.4498	16.8781	4.5717	21.3627
25.375	-1E-04	23.7052	22.8266	0.8786	21.4751	16.9241	4.551	21.384
25.5	-1E-04	23.7345	22.8712	0.8633	21.5002	16.9699	4.5303	21.4051
25.625	-1E-04	23.7632	22.915	0.8482	21.5252	17.0154	4.5098	21.4262
25.75	0	23.7913	22.9581	0.8332	21.55	17.0608	4.4892	21.4472
25.875	0	23.8188	23.0004	0.8184	21.5747	17.106	4.4687	21.468
26	0	23.8458	23.0419	0.8039	21.5992	17.151	4.4482	21.4888
26.125	0	23.8723	23.0828	0.7895	21.6235	17.1958	4.4277	21.5094
26.25	0	23.8982	23.1229	0.7753	21.6477	17.2404	4.4073	21.5299
26.375	0	23.9236	23.1622	0.7614	21.6718	17.2848	4.387	21.5503
26.5	0	23.9484	23.2009	0.7475	21.6956	17.329	4.3666	21.5706
26.625	0	23.9728	23.2389	0.7339	21.7194	17.373	4.3464	21.5908
26.75	0	23.9966	23.2762	0.7204	21.7429	17.4168	4.3261	21.6109

		Nd=5			Nd=1			
z (km)	Δr-fl	Rock ‰ δ18O	Fluid ‰ δ18O	Δr-fl	Rock ‰ δ18O	Fluid ‰ δ18O	Δr-fl	Rock ‰ δ18O
26.875	0	24.02	23.3128	0.7072	21.7664	17.4604	4.306	21.6308
27	0	24.0429	23.3488	0.6941	21.7896	17.5038	4.2858	21.6507
27.125	0	24.0653	23.3841	0.6812	21.8128	17.5471	4.2657	21.6705
27.25	0	24.0872	23.4187	0.6685	21.8357	17.5901	4.2456	21.6901
27.375	0	24.1086	23.4527	0.6559	21.8586	17.6329	4.2257	21.7097
27.5	0	24.1297	23.4861	0.6436	21.8812	17.6756	4.2056	21.7291
27.625	0	24.1502	23.5189	0.6313	21.9038	17.7181	4.1857	21.7484
27.75	0	24.1704	23.551	0.6194	21.9261	17.7603	4.1658	21.7677
27.875	0	24.1901	23.5825	0.6076	21.9484	17.8024	4.146	21.7868
28	0	24.2094	23.6135	0.5959	21.9705	17.8443	4.1262	21.8058
28.125	0	24.2282	23.6438	0.5844	21.9924	17.886	4.1064	21.8248
28.25	0	24.2467	23.6736	0.5731	22.0142	17.9275	4.0867	21.8436
28.375	0	24.2648	23.7028	0.562	22.0359	17.9688	4.0671	21.8623
28.5	0	24.2824	23.7314	0.551	22.0574	18.0099	4.0475	21.8809
28.625	0	24.2997	23.7595	0.5402	22.0788	18.0508	4.028	21.8994
28.75	0	24.3167	23.787	0.5297	22.1	18.0916	4.0084	21.9179
28.875	0	24.3332	23.814	0.5192	22.1211	18.1321	3.989	21.9362
29	0	24.3494	23.8405	0.5089	22.1421	18.1725	3.9696	21.9544
29.125	0	24.3652	23.8665	0.4987	22.1629	18.2127	3.9502	21.9725
29.25	0	24.3807	23.8919	0.4888	22.1836	18.2526	3.931	21.9906
29.375	0	24.3958	23.9168	0.479	22.2041	18.2925	3.9116	22.0085
29.5	0	24.4106	23.9413	0.4693	22.2245	18.3321	3.8924	22.0263
29.625	0	24.4251	23.9652	0.4599	22.2448	18.3715	3.8733	22.0441
29.75	0	24.4392	23.9887	0.4505	22.265	18.4107	3.8543	22.0617
29.875	0	24.4531	24.0117	0.4414	22.285	18.4498	3.8352	22.0792
30	0	24.4666	24.0344	0.4322	22.3049	18.4887	3.8162	22.0967
30.125	0	24.4798	24.0565	0.4233	22.3246	18.5274	3.7972	22.114
30.25	0	24.4927	24.0781	0.4146	22.3442	18.5659	3.7783	22.1313
30.375	0	24.5053	24.0993	0.406	22.3637	18.6042	3.7595	22.1485
30.5	0	24.5177	24.1201	0.3976	22.3831	18.6423	3.7408	22.1655
30.625	0	24.5297	24.1404	0.3893	22.4023	18.6803	3.722	22.1825
30.75	0	24.5415	24.1603	0.3812	22.4214	18.718	3.7034	22.1994
30.875	0	24.553	24.1798	0.3732	22.4404	18.7556	3.6848	22.2162
31	0	24.5643	24.1989	0.3654	22.4592	18.793	3.6662	22.2329
31.125	0	24.5752	24.2176	0.3576	22.478	18.8303	3.6477	22.2495
31.25	0	24.586	24.2359	0.3501	22.4966	18.8673	3.6293	22.266
31.375	0	24.5964	24.2538	0.3426	22.515	18.9042	3.6108	22.2824
31.5	0	24.6067	24.2714	0.3353	22.5334	18.9409	3.5925	22.2988
31.625	0	24.6167	24.2885	0.3282	22.5516	18.9774	3.5742	22.315
31.75	0	24.6264	24.3053	0.3211	22.5697	19.0137	3.556	22.3312
31.875	0	24.636	24.3218	0.3142	22.5877	19.0499	3.5378	22.3472
32	0	24.6453	24.3379	0.3074	22.6056	19.0858	3.5198	22.3632
32.125	0	24.6544	24.3536	0.3008	22.6233	19.1216	3.5017	22.3791

		Nd=5				Nd=1		
		Rock ‰	Fluid ‰		Rock ‰	Fluid ‰		Rock ‰
z (km)	Δr-fl	δ18O	δ18O	Δr-fl	δ18O	δ18O	Δr-fl	δ18O
32.25	0	24.6632	24.369	0.2942	22.6409	19.1573	3.4836	22.3949
32.375	0	24.6719	24.3841	0.2878	22.6584	19.1927	3.4657	22.4106
32.5	0	24.6804	24.3989	0.2815	22.6758	19.228	3.4478	22.4263
32.625	0	24.6886	24.4133	0.2753	22.6931	19.2631	3.43	22.4418
32.75	0	24.6967	24.4274	0.2693	22.7102	19.298	3.4122	22.4573
32.875	0	24.7045	24.4412	0.2633	22.7273	19.3327	3.3946	22.4726
33	0	24.7122	24.4547	0.2575	22.7442	19.3673	3.3769	22.4879
33.125	0	24.7197	24.4679	0.2518	22.761	19.4017	3.3593	22.5031
33.25	0	24.727	24.4809	0.2461	22.7777	19.4359	3.3418	22.5182
33.375	0	24.7342	24.4935	0.2407	22.7943	19.47	3.3243	22.5333
33.5	0	24.7411	24.5059	0.2352	22.8107	19.5039	3.3068	22.5482
33.625	0	24.7479	24.5179	0.23	22.8271	19.5376	3.2895	22.5631
33.75	0	24.7545	24.5297	0.2248	22.8433	19.5711	3.2722	22.5779
33.875	0	24.761	24.5413	0.2197	22.8595	19.6045	3.255	22.5926
34	0	24.7673	24.5526	0.2147	22.8755	19.6377	3.2378	22.6072
34.125	0	24.7735	24.5636	0.2099	22.8914	19.6708	3.2206	22.6218
34.25	0	24.7795	24.5744	0.2051	22.9072	19.7036	3.2036	22.6362
34.375	0	24.7853	24.5849	0.2004	22.9229	19.7363	3.1866	22.6506
34.5	0	24.791	24.5952	0.1958	22.9385	19.7689	3.1696	22.6649
34.625	0	24.7966	24.6053	0.1913	22.954	19.8012	3.1528	22.6791
34.75	0	24.802	24.6151	0.1869	22.9693	19.8334	3.1359	22.6933
34.875	0	24.8073	24.6248	0.1825	22.9846	19.8655	3.1191	22.7073
35	0	24.8125	24.6341	0.1784	22.9998	19.8973	3.1025	22.7213
35.125	0	24.8175	24.6433	0.1742	23.0148	19.929	3.0858	22.7352
35.25	0	24.8224	24.6523	0.1701	23.0298	19.9606	3.0692	22.749
35.375	0	24.8272	24.661	0.1662	23.0446	19.992	3.0526	22.7628
35.5	0	24.8318	24.6696	0.1622	23.0594	20.0232	3.0362	22.7765
35.625	0	24.8364	24.6779	0.1585	23.074	20.0542	3.0198	22.7901
35.75	0	24.8408	24.6861	0.1547	23.0886	20.0851	3.0035	22.8036
35.875	0	24.8451	24.6941	0.151	23.103	20.1158	2.9872	22.817
36	0	24.8493	24.7019	0.1474	23.1174	20.1464	2.971	22.8304
36.125	0	24.8534	24.7095	0.1439	23.1316	20.1768	2.9548	22.8437
36.25	0	24.8574	24.7169	0.1405	23.1458	20.2071	2.9387	22.8569
36.375	0	24.8613	24.7241	0.1372	23.1598	20.2372	2.9226	22.87
36.5	0	24.8651	24.7312	0.1339	23.1738	20.2671	2.9067	22.8831
36.625	0	24.8688	24.7381	0.1307	23.1877	20.2969	2.8908	22.8961
36.75	0	24.8724	24.7452	0.1272	23.2014	20.3265	2.8749	22.909
36.875	0	24.8759	24.7514	0.1245	23.2151	20.3559	2.8592	22.9219
37	0	24.8793	24.7578	0.1215	23.2287	20.3853	2.8434	22.9347
37.125	0	24.8826	24.7641	0.1185	23.2421	20.4144	2.8277	22.9474
37.25	0	24.8859	24.7702	0.1157	23.2555	20.4434	2.8121	22.96
37.375	0	24.889	24.7762	0.1128	23.2688	20.4722	2.7966	22.9726
37.5	0	24.8921	24.782	0.1101	23.282	20.5009	2.7811	22.985

		Nd=5			Nd=1			
z (km)	Δr-fl	Rock ‰ δ18O	Fluid ‰ δ18O	Δr-fl	Rock ‰ δ18O	Fluid ‰ δ18O	Δr-fl	Rock ‰ δ18O
37.625	0	24.8951	24.7877	0.1074	23.2951	20.5294	2.7657	22.9975
37.75	0	24.898	24.7933	0.1047	23.3081	20.5578	2.7503	23.0098
37.875	0	24.9009	24.7987	0.1022	23.321	20.5861	2.7349	23.0221
38	0	24.9036	24.8039	0.0997	23.3339	20.6141	2.7198	23.0343
38.125	0	24.9063	24.8091	0.0972	23.3466	20.6421	2.7045	23.0464
38.25	0	24.9089	24.8141	0.0948	23.3593	20.6698	2.6895	23.0585
38.375	0	24.9115	24.819	0.0925	23.3718	20.6974	2.6744	23.0705
38.5	0	24.914	24.8238	0.0902	23.3843	20.7249	2.6594	23.0825
38.625	0	24.9164	24.8285	0.0879	23.3967	20.7522	2.6445	23.0943
38.75	0	24.9187	24.833	0.0857	23.409	20.7794	2.6296	23.1061
38.875	0	24.921	24.8374	0.0836	23.4212	20.8064	2.6148	23.1178
39	0	24.9233	24.842	0.0813	23.4333	20.8333	2.6	23.1295
39.125	0	24.9254	24.8462	0.0792	23.4454	20.8601	2.5853	23.1411
39.25	0	24.9275	24.8503	0.0772	23.4573	20.8867	2.5706	23.1526
39.375	0	24.9296	24.8544	0.0752	23.4692	20.9131	2.5561	23.1641
39.5	0	24.9316	24.8583	0.0733	23.481	20.9394	2.5416	23.1755
39.625	0	24.9336	24.8621	0.0715	23.4927	20.9655	2.5272	23.1868
39.75	0	24.9354	24.8658	0.0696	23.5043	20.9916	2.5127	23.1981
39.875	0	24.9373	24.8694	0.0679	23.5158	21.0174	2.4984	23.2093
40	0	24.9391	24.8729	0.0662	23.5273	21.0431	2.4842	23.2205
40.125	0	24.9408	24.8764	0.0644	23.5387	21.0687	2.47	23.2315
40.25	0	24.9425	24.8797	0.0628	23.55	21.0942	2.4558	23.2426
40.375	0	24.9442	24.883	0.0612	23.5612	21.1195	2.4417	23.2535
40.5	0	24.9458	24.8862	0.0596	23.5723	21.1446	2.4277	23.2644
40.625	0	24.9473	24.8893	0.058	23.5834	21.1697	2.4137	23.2752
40.75	0	24.9489	24.8923	0.0566	23.5943	21.1945	2.3998	23.286
40.875	0	24.9503	24.8952	0.0551	23.6052	21.2193	2.3859	23.2967
41	0	24.9518	24.8981	0.0537	23.616	21.2439	2.3721	23.3073
41.125	0	24.9532	24.9009	0.0523	23.6268	21.2683	2.3585	23.3179
41.25	0	24.9545	24.9036	0.0509	23.6375	21.2927	2.3448	23.3284
41.375	0	24.9559	24.9062	0.0497	23.648	21.3169	2.3311	23.3389
41.5	0	24.9571	24.9088	0.0483	23.6586	21.3409	2.3177	23.3493
41.625	0	24.9584	24.9113	0.0471	23.669	21.3648	2.3042	23.3596
41.75	0	24.9596	24.9138	0.0458	23.6793	21.3886	2.2907	23.3699
41.875	0	24.9608	24.9162	0.0446	23.6896	21.4123	2.2773	23.3801
42	0	24.9619	24.9185	0.0434	23.6998	21.4358	2.264	23.3903
42.125	0	24.963	24.9208	0.0422	23.71	21.4592	2.2508	23.4004
42.25	0	24.9641	24.923	0.0411	23.7201	21.4824	2.2377	23.4104
42.375	0	24.9652	24.9251	0.0401	23.73	21.5056	2.2244	23.4204
42.5	0	24.9662	24.9272	0.039	23.74	21.5285	2.2115	23.4303
42.625	0	24.9672	24.9292	0.038	23.7498	21.5514	2.1984	23.4402
42.75	0	24.9682	24.9312	0.037	23.7596	21.5741	2.1855	23.45
42.875	0	24.9691	24.9331	0.036	23.7693	21.5967	2.1726	23.4597

		Nd=5				Nd=1		
z (km)	Δr-fl	Rock ‰ δ18O	Fluid ‰ δ18O	Δr-fl	Rock ‰ δ18O	Fluid ‰ δ18O	Δr-fl	Rock ‰ δ18O
43	0	24.97	24.935	0.035	23.7789	21.6192	2.1597	23.4694
43.125	0	24.9709	24.9369	0.034	23.7885	21.6415	2.147	23.4791
43.25	0	24.9718	24.9386	0.0332	23.798	21.6637	2.1343	23.4886
43.375	0	24.9726	24.9404	0.0322	23.8074	21.6858	2.1216	23.4982
43.5	0	24.9734	24.942	0.0314	23.8168	21.7078	2.109	23.5076
43.625	0	24.9742	24.9437	0.0305	23.8261	21.7296	2.0965	23.5171
43.75	0	24.975	24.9453	0.0297	23.8353	21.7513	2.084	23.5264
43.875	0	24.9757	24.9468	0.0289	23.8445	21.7729	2.0716	23.5357
44	0	24.9765	24.9483	0.0282	23.8536	21.7944	2.0592	23.545
44.125	0	24.9772	24.9502	0.027	23.8626	21.8157	2.0469	23.5542
44.25	0	24.9778	24.9516	0.0262	23.8716	21.8369	2.0347	23.5633
44.375	0	24.9785	24.953	0.0255	23.8805	21.858	2.0225	23.5724
44.5	0	24.9792	24.9543	0.0249	23.8893	21.879	2.0103	23.5814
44.625	0	24.9798	24.9556	0.0242	23.8981	21.8998	1.9983	23.5904
44.75	0	24.9804	24.9569	0.0235	23.9068	21.9205	1.9863	23.5994
44.875	0	24.981	24.9582	0.0228	23.9154	21.9411	1.9743	23.6082
45	0	24.9816	24.9594	0.0222	23.924	21.9616	1.9624	23.6171
45.125	0	24.9821	24.9605	0.0216	23.9325	21.982	1.9505	23.6258
45.25	0	24.9827	24.9617	0.021	23.9409	22.0022	1.9387	23.6346
45.375	0	24.9832	24.9628	0.0204	23.9493	22.0223	1.927	23.6432
45.5	0	24.9837	24.9639	0.0198	23.9576	22.0423	1.9153	23.6519
45.625	0	24.9842	24.9649	0.0193	23.9659	22.0622	1.9037	23.6604
45.75	0	24.9847	24.9659	0.0188	23.9741	22.082	1.8921	23.669
45.875	0	24.9851	24.9669	0.0182	23.9823	22.1016	1.8807	23.6774
46	0	24.9856	24.9679	0.0177	23.9903	22.1212	1.8691	23.6858
46.125	0	24.986	24.9688	0.0172	23.9984	22.1406	1.8578	23.6942
46.25	0	24.9865	24.9697	0.0168	24.0063	22.1599	1.8464	23.7025
46.375	0	24.9869	24.9706	0.0163	24.0142	22.1791	1.8351	23.7108
46.5	0	24.9873	24.9715	0.0158	24.0221	22.1982	1.8239	23.719
46.625	0	24.9877	24.9723	0.0154	24.0299	22.2171	1.8128	23.7272
46.75	0	24.9881	24.9731	0.015	24.0376	22.236	1.8016	23.7353
46.875	0	24.9884	24.9739	0.0145	24.0453	22.2547	1.7906	23.7434
47	0	24.9888	24.9747	0.0141	24.0529	22.2733	1.7796	23.7514
47.125	0	24.9891	24.9754	0.0137	24.0604	22.2919	1.7685	23.7594
47.25	0	24.9895	24.9762	0.0133	24.068	22.3103	1.7577	23.7674
47.375	0	24.9898	24.9769	0.0129	24.0754	22.3286	1.7468	23.7752
47.5	0	24.9901	24.9776	0.0125	24.0828	22.3467	1.7361	23.7831
47.625	0	24.9904	24.9782	0.0122	24.0901	22.3648	1.7253	23.7909
47.75	0	24.9907	24.9789	0.0118	24.0974	22.3828	1.7146	23.7986
47.875	0	24.991	24.9795	0.0115	24.1046	22.4006	1.704	23.8063
48	0	24.9913	24.9801	0.0112	24.1118	22.4184	1.6934	23.814
48.125	0	24.9915	24.9807	0.0108	24.1189	22.436	1.6829	23.8216
48.25	0	24.9918	24.9817	0.0101	24.126	22.4536	1.6724	23.8292

		Nd=5			Nd=1			
		Rock ‰	Fluid ‰		Rock ‰	Fluid ‰		Rock ‰
z (km)	**Δr-fl**	**δ18O**	**δ18O**	**Δr-fl**	**δ18O**	**δ18O**	**Δr-fl**	**δ18O**
48.375	0	24.9921	24.9823	0.0098	24.133	22.471	1.662	23.8367
48.5	0	24.9923	24.9828	0.0095	24.14	22.4883	1.6517	23.8442
48.625	0	24.9926	24.9833	0.0093	24.1469	22.5056	1.6413	23.8516
48.75	0	24.9928	24.9838	0.009	24.1538	22.5227	1.6311	23.859
48.875	0	24.993	24.9843	0.0087	24.1606	22.5397	1.6209	23.8663
49	0	24.9932	24.9848	0.0084	24.1673	22.5566	1.6107	23.8736
49.125	0	24.9934	24.9852	0.0082	24.174	22.5734	1.6006	23.8809
49.25	0	24.9937	24.9857	0.008	24.1807	22.5901	1.5906	23.8881
49.375	0	24.9939	24.9861	0.0078	24.1873	22.6067	1.5806	23.8953
49.5	0	24.994	24.9865	0.0075	24.1939	22.6232	1.5707	23.9024
49.625	0	24.9942	24.987	0.0072	24.2004	22.6396	1.5608	23.9095
49.75	0	24.9944	24.9874	0.007	24.2068	22.6559	1.5509	23.9165
49.875	0	24.9946	24.9877	0.0069	24.2132	22.6721	1.5411	23.9235
50	0	24.9948	24.9881	0.0067	24.2196	22.6882	1.5314	23.9305

z (km)	Nd=0.75 Fluid ‰ δ18O	Δr-fl	Rock ‰ δ18O	Nd=0.5 Fluid ‰ δ18O	Δr-fl
0	4	9.9197	16.7371	4	12.7371
0.125	4.0701	9.9063	16.7707	4.06	12.7107
0.25	4.1402	9.8927	16.8042	4.1199	12.6843
0.375	4.2102	9.879	16.8376	4.1797	12.6579
0.5	4.2802	9.865	16.8708	4.2394	12.6314
0.625	4.35	9.8509	16.9039	4.299	12.6049
0.75	4.4198	9.8366	16.9369	4.3585	12.5784
0.875	4.4895	9.8222	16.9697	4.4178	12.5519
1	4.5592	9.8075	17.0025	4.4771	12.5254
1.125	4.6288	9.7927	17.0351	4.5362	12.4989
1.25	4.6982	9.7779	17.0676	4.5953	12.4723
1.375	4.7677	9.7627	17.1	4.6542	12.4458
1.5	4.837	9.7475	17.1323	4.713	12.4193
1.625	4.9062	9.7321	17.1644	4.7717	12.3927
1.75	4.9754	9.7165	17.1965	4.8303	12.3662
1.875	5.0445	9.7008	17.2284	4.8888	12.3396
2	5.1135	9.6849	17.2602	4.9472	12.313
2.125	5.1824	9.6689	17.2919	5.0055	12.2864
2.25	5.2512	9.6528	17.3234	5.0636	12.2598
2.375	5.32	9.6364	17.3549	5.1217	12.2332
2.5	5.3886	9.62	17.3862	5.1796	12.2066
2.625	5.4572	9.6034	17.4174	5.2375	12.1799
2.75	5.5257	9.5866	17.4486	5.2952	12.1534
2.875	5.594	9.5698	17.4795	5.3528	12.1267
3	5.6623	9.5528	17.5104	5.4103	12.1001
3.125	5.7305	9.5356	17.5412	5.4677	12.0735
3.25	5.7986	9.5184	17.5718	5.5249	12.0469
3.375	5.8665	9.5011	17.6024	5.5821	12.0203
3.5	5.9344	9.4835	17.6328	5.6392	11.9936
3.625	6.0022	9.4659	17.6631	5.6961	11.967
3.75	6.0699	9.4481	17.6933	5.7529	11.9404
3.875	6.1375	9.4302	17.7234	5.8096	11.9138
4	6.2049	9.4123	17.7534	5.8662	11.8872
4.125	6.2723	9.3941	17.7833	5.9227	11.8606
4.25	6.3396	9.3758	17.813	5.9791	11.8339
4.375	6.4067	9.3575	17.8427	6.0354	11.8073
4.5	6.4738	9.339	17.8722	6.0916	11.7806
4.625	6.5407	9.3205	17.9017	6.1476	11.7541
4.75	6.6075	9.3018	17.931	6.2035	11.7275
4.875	6.6742	9.2831	17.9602	6.2594	11.7008
5	6.7408	9.2642	17.9893	6.3151	11.6742
5.125	6.8073	9.2452	18.0183	6.3707	11.6476
5.25	6.8737	9.226	18.0472	6.4261	11.6211

z (km)	Nd=0.75 Fluid ‰ δ18O	Δr-fl	Rock ‰ δ18O	Nd=0.5 Fluid ‰ δ18O	Δr-fl
5.375	6.94	9.2068	18.076	6.4815	11.5945
5.5	7.0061	9.1876	18.1046	6.5368	11.5678
5.625	7.0722	9.1681	18.1332	6.5919	11.5413
5.75	7.1381	9.1486	18.1617	6.647	11.5147
5.875	7.2039	9.129	18.19	6.7019	11.4881
6	7.2695	9.1094	18.2183	6.7567	11.4616
6.125	7.3351	9.0896	18.2464	6.8114	11.435
6.25	7.4005	9.0698	18.2744	6.866	11.4084
6.375	7.4658	9.0498	18.3024	6.9204	11.382
6.5	7.531	9.0298	18.3302	6.9748	11.3554
6.625	7.5961	9.0097	18.3579	7.029	11.3289
6.75	7.6611	8.9894	18.3856	7.0832	11.3024
6.875	7.7259	8.9691	18.4131	7.1372	11.2759
7	7.7906	8.9488	18.4405	7.1911	11.2494
7.125	7.8551	8.9284	18.4678	7.2449	11.2229
7.25	7.9196	8.9078	18.495	7.2985	11.1965
7.375	7.9839	8.8872	18.5221	7.3521	11.17
7.5	8.0481	8.8665	18.5491	7.4055	11.1436
7.625	8.1121	8.8458	18.576	7.4589	11.1171
7.75	8.176	8.8251	18.6028	7.5121	11.0907
7.875	8.2398	8.8042	18.6295	7.5652	11.0643
8	8.3035	8.7832	18.6561	7.6182	11.0379
8.125	8.367	8.7622	18.6827	7.6711	11.0116
8.25	8.4304	8.7411	18.7091	7.7239	10.9852
8.375	8.4937	8.7199	18.7354	7.7765	10.9589
8.5	8.5568	8.6987	18.7616	7.829	10.9326
8.625	8.6198	8.6774	18.7877	7.8815	10.9062
8.75	8.6827	8.6561	18.8137	7.9338	10.8799
8.875	8.7454	8.6347	18.8396	7.986	10.8536
9	8.808	8.6132	18.8654	8.0381	10.8273
9.125	8.8705	8.5917	18.8911	8.09	10.8011
9.25	8.9328	8.5701	18.9167	8.1419	10.7748
9.375	8.995	8.5485	18.9423	8.1936	10.7487
9.5	9.057	8.5268	18.9677	8.2453	10.7224
9.625	9.1189	8.5051	18.993	8.2968	10.6962
9.75	9.1807	8.4833	19.0182	8.3482	10.67
9.875	9.2423	8.4615	19.0434	8.3995	10.6439
10	9.3038	8.4396	19.0684	8.4507	10.6177
10.125	9.3651	8.4177	19.0934	8.5017	10.5917
10.25	9.4263	8.3957	19.1182	8.5527	10.5655
10.375	9.4874	8.3736	19.143	8.6035	10.5395
10.5	9.5483	8.3516	19.1676	8.6542	10.5134
10.625	9.609	8.3296	19.1922	8.7048	10.4874

z (km)	Nd=0.75 Fluid ‰ δ18O	Δr-fl	Rock ‰ δ18O	Nd=0.5 Fluid ‰ δ18O	Δr-fl
10.75	9.6697	8.3074	19.2167	8.7553	10.4614
10.875	9.7302	8.2852	19.2411	8.8057	10.4354
11	9.7905	8.263	19.2653	8.856	10.4093
11.125	9.8507	8.2407	19.2895	8.9061	10.3834
11.25	9.9107	8.2185	19.3136	8.9562	10.3574
11.375	9.9706	8.1961	19.3377	9.0061	10.3316
11.5	10.0304	8.1737	19.3616	9.0559	10.3057
11.625	10.09	8.1513	19.3854	9.1056	10.2798
11.75	10.1495	8.1289	19.4091	9.1552	10.2539
11.875	10.2088	8.1064	19.4328	9.2047	10.2281
12	10.268	8.0839	19.4563	9.254	10.2023
12.125	10.327	8.0614	19.4798	9.3033	10.1765
12.25	10.3859	8.0388	19.5032	9.3524	10.1508
12.375	10.4446	8.0163	19.5265	9.4014	10.1251
12.5	10.5032	7.9936	19.5497	9.4503	10.0994
12.625	10.5616	7.971	19.5728	9.4991	10.0737
12.75	10.6199	7.9483	19.5958	9.5478	10.048
12.875	10.678	7.9257	19.6187	9.5964	10.0223
13	10.736	7.903	19.6416	9.6448	9.9968
13.125	10.7938	7.8803	19.6643	9.6932	9.9711
13.25	10.8515	7.8575	19.687	9.7414	9.9456
13.375	10.909	7.8348	19.7096	9.7895	9.9201
13.5	10.9664	7.812	19.7321	9.8375	9.8946
13.625	11.0236	7.7892	19.7545	9.8854	9.8691
13.75	11.0807	7.7664	19.7768	9.9332	9.8436
13.875	11.1376	7.7435	19.799	9.9808	9.8182
14	11.1944	7.7207	19.8212	10.0284	9.7928
14.125	11.251	7.6978	19.8433	10.0758	9.7675
14.25	11.3074	7.675	19.8652	10.1231	9.7421
14.375	11.3638	7.652	19.8871	10.1704	9.7167
14.5	11.4199	7.6292	19.9089	10.2175	9.6914
14.625	11.4759	7.6063	19.9307	10.2645	9.6662
14.75	11.5318	7.5833	19.9523	10.3113	9.641
14.875	11.5875	7.5604	19.9739	10.3581	9.6158
15	11.643	7.5375	19.9953	10.4048	9.5905
15.125	11.6984	7.5146	20.0167	10.4513	9.5654
15.25	11.7536	7.4916	20.038	10.4977	9.5403
15.375	11.8087	7.4687	20.0593	10.544	9.5153
15.5	11.8636	7.4457	20.0804	10.5902	9.4902
15.625	11.9184	7.4227	20.1015	10.6363	9.4652
15.75	11.973	7.3998	20.1224	10.6823	9.4401
15.875	12.0275	7.3768	20.1433	10.7282	9.4151
16	12.0818	7.3538	20.1642	10.774	9.3902

	Nd=0.75			Nd=0.5	
	Fluid ‰		Rock ‰	Fluid ‰	
z (km)	δ18O	Δr-fl	δ18O	δ18O	Δr-fl
16.125	12.1359	7.3309	20.1849	10.8196	9.3653
16.25	12.1899	7.3079	20.2055	10.8651	9.3404
16.375	12.2437	7.285	20.2261	10.9106	9.3155
16.5	12.2974	7.262	20.2466	10.9559	9.2907
16.625	12.351	7.239	20.267	11.0011	9.2659
16.75	12.4043	7.2161	20.2874	11.0462	9.2412
16.875	12.4575	7.1932	20.3076	11.0912	9.2164
17	12.5106	7.1702	20.3278	11.136	9.1918
17.125	12.5635	7.1472	20.3479	11.1808	9.1671
17.25	12.6162	7.1243	20.3679	11.2254	9.1425
17.375	12.6688	7.1014	20.3878	11.27	9.1178
17.5	12.7213	7.0784	20.4077	11.3144	9.0933
17.625	12.7735	7.0556	20.4275	11.3587	9.0688
17.75	12.8257	7.0326	20.4472	11.4029	9.0443
17.875	12.8776	7.0097	20.4668	11.447	9.0198
18	12.9294	6.9869	20.4864	11.491	8.9954
18.125	12.9811	6.9639	20.5059	11.5349	8.971
18.25	13.0326	6.941	20.5253	11.5787	8.9466
18.375	13.0839	6.9182	20.5446	11.6223	8.9223
18.5	13.1351	6.8954	20.5638	11.6659	8.8979
18.625	13.1861	6.8726	20.583	11.7093	8.8737
18.75	13.237	6.8497	20.6021	11.7526	8.8495
18.875	13.2877	6.8269	20.6211	11.7958	8.8253
19	13.3383	6.8041	20.6401	11.839	8.8011
19.125	13.3886	6.7814	20.6589	11.882	8.7769
19.25	13.4389	6.7586	20.6777	11.9249	8.7528
19.375	13.489	6.7358	20.6965	11.9676	8.7289
19.5	13.5389	6.7131	20.7151	12.0103	8.7048
19.625	13.5887	6.6904	20.7337	12.0529	8.6808
19.75	13.6383	6.6677	20.7522	12.0953	8.6569
19.875	13.6877	6.6451	20.7706	12.1377	8.6329
20	13.737	6.6225	20.789	12.1799	8.6091
20.125	13.7862	6.5998	20.8073	12.2221	8.5852
20.25	13.8352	6.5772	20.8255	12.2641	8.5614
20.375	13.884	6.5546	20.8436	12.306	8.5376
20.5	13.9327	6.532	20.8617	12.3478	8.5139
20.625	13.9812	6.5095	20.8797	12.3895	8.4902
20.75	14.0296	6.4869	20.8976	12.4311	8.4665
20.875	14.0778	6.4645	20.9155	12.4726	8.4429
21	14.1258	6.442	20.9333	12.514	8.4193
21.125	14.1737	6.4196	20.951	12.5552	8.3958
21.25	14.2215	6.3971	20.9686	12.5964	8.3722
21.375	14.269	6.3748	20.9862	12.6375	8.3487

z (km)	Nd=0.75 Fluid ‰ δ18O	Δr-fl	Rock ‰ δ18O	Nd=0.5 Fluid ‰ δ18O	Δr-fl
21.5	14.3165	6.3523	21.0037	12.6784	8.3253
21.625	14.3637	6.3301	21.0211	12.7193	8.3018
21.75	14.4108	6.3077	21.0385	12.76	8.2785
21.875	14.4578	6.2854	21.0558	12.8006	8.2552
22	14.5046	6.2632	21.073	12.8412	8.2318
22.125	14.5513	6.2409	21.0902	12.8816	8.2086
22.25	14.5978	6.2186	21.1073	12.9219	8.1854
22.375	14.6441	6.1965	21.1243	12.9621	8.1622
22.5	14.6903	6.1743	21.1412	13.0022	8.139
22.625	14.7363	6.1522	21.1581	13.0422	8.1159
22.75	14.7822	6.1301	21.1749	13.0821	8.0928
22.875	14.8279	6.1081	21.1917	13.1219	8.0698
23	14.8735	6.086	21.2084	13.1615	8.0469
23.125	14.9189	6.064	21.225	13.2011	8.0239
23.25	14.9641	6.0421	21.2415	13.2406	8.0009
23.375	15.0092	6.0202	21.258	13.2799	7.9781
23.5	15.0542	5.9982	21.2744	13.3192	7.9552
23.625	15.099	5.9764	21.2908	13.3583	7.9325
23.75	15.1436	5.9546	21.3071	13.3974	7.9097
23.875	15.1881	5.9328	21.3233	13.4363	7.887
24	15.2325	5.9109	21.3395	13.4752	7.8643
24.125	15.2767	5.8892	21.3556	13.5139	7.8417
24.25	15.3207	5.8675	21.3716	13.5525	7.8191
24.375	15.3646	5.8458	21.3875	13.5911	7.7964
24.5	15.4083	5.8242	21.4034	13.6295	7.7739
24.625	15.4519	5.8026	21.4193	13.6678	7.7515
24.75	15.4953	5.7811	21.435	13.706	7.729
24.875	15.5386	5.7595	21.4508	13.7442	7.7066
25	15.5817	5.7381	21.4664	13.7822	7.6842
25.125	15.6246	5.7167	21.482	13.8201	7.6619
25.25	15.6675	5.6952	21.4975	13.8579	7.6396
25.375	15.7101	5.6739	21.513	13.8956	7.6174
25.5	15.7526	5.6525	21.5284	13.9332	7.5952
25.625	15.795	5.6312	21.5437	13.9707	7.573
25.75	15.8372	5.61	21.559	14.0081	7.5509
25.875	15.8793	5.5887	21.5742	14.0454	7.5288
26	15.9212	5.5676	21.5893	14.0826	7.5067
26.125	15.963	5.5464	21.6044	14.1197	7.4847
26.25	16.0046	5.5253	21.6194	14.1566	7.4628
26.375	16.046	5.5043	21.6344	14.1935	7.4409
26.5	16.0873	5.4833	21.6493	14.2303	7.419
26.625	16.1285	5.4623	21.6641	14.267	7.3971
26.75	16.1695	5.4414	21.6789	14.3036	7.3753

z (km)	Nd=0.75 Fluid ‰ δ18O	Δr-fl	Rock ‰ δ18O	Nd=0.5 Fluid ‰ δ18O	Δr-fl
26.875	16.2104	5.4204	21.6936	14.3401	7.3535
27	16.2511	5.3996	21.7083	14.3764	7.3319
27.125	16.2917	5.3788	21.7229	14.4127	7.3102
27.25	16.3321	5.358	21.7374	14.4489	7.2885
27.375	16.3724	5.3373	21.7519	14.485	7.2669
27.5	16.4125	5.3166	21.7664	14.521	7.2454
27.625	16.4525	5.2959	21.7807	14.5569	7.2238
27.75	16.4923	5.2754	21.795	14.5926	7.2024
27.875	16.532	5.2548	21.8093	14.6283	7.181
28	16.5716	5.2342	21.8235	14.6639	7.1596
28.125	16.611	5.2138	21.8376	14.6994	7.1382
28.25	16.6502	5.1934	21.8517	14.7348	7.1169
28.375	16.6893	5.173	21.8657	14.7701	7.0956
28.5	16.7283	5.1526	21.8797	14.8052	7.0745
28.625	16.7671	5.1323	21.8936	14.8403	7.0533
28.75	16.8058	5.1121	21.9074	14.8753	7.0321
28.875	16.8443	5.0919	21.9212	14.9102	7.011
29	16.8827	5.0717	21.935	14.945	6.99
29.125	16.9209	5.0516	21.9486	14.9797	6.9689
29.25	16.959	5.0316	21.9623	15.0143	6.948
29.375	16.9969	5.0116	21.9758	15.0488	6.927
29.5	17.0347	4.9916	21.9894	15.0832	6.9062
29.625	17.0724	4.9717	22.0028	15.1175	6.8853
29.75	17.1099	4.9518	22.0162	15.1517	6.8645
29.875	17.1473	4.9319	22.0296	15.1858	6.8438
30	17.1845	4.9122	22.0429	15.2198	6.8231
30.125	17.2216	4.8924	22.0561	15.2538	6.8023
30.25	17.2586	4.8727	22.0693	15.2876	6.7817
30.375	17.2954	4.8531	22.0824	15.3213	6.7611
30.5	17.3321	4.8334	22.0955	15.3549	6.7406
30.625	17.3686	4.8139	22.1085	15.3885	6.72
30.75	17.405	4.7944	22.1215	15.4219	6.6996
30.875	17.4412	4.775	22.1344	15.4552	6.6792
31	17.4773	4.7556	22.1473	15.4885	6.6588
31.125	17.5133	4.7362	22.1601	15.5216	6.6385
31.25	17.5491	4.7169	22.1728	15.5547	6.6181
31.375	17.5848	4.6976	22.1855	15.5876	6.5979
31.5	17.6204	4.6784	22.1982	15.6205	6.5777
31.625	17.6558	4.6592	22.2108	15.6533	6.5575
31.75	17.6911	4.6401	22.2233	15.686	6.5373
31.875	17.7262	4.621	22.2358	15.7185	6.5173
32	17.7612	4.602	22.2483	15.751	6.4973
32.125	17.7961	4.583	22.2607	15.7834	6.4773

	Nd=0.75			Nd=0.5	
	Fluid ‰		Rock ‰	Fluid ‰	
z (km)	δ18O	Δr-fl	δ18O	δ18O	Δr-fl
32.25	17.8308	4.5641	22.273	15.8157	6.4573
32.375	17.8654	4.5452	22.2853	15.8479	6.4374
32.5	17.8999	4.5264	22.2975	15.88	6.4175
32.625	17.9342	4.5076	22.3097	15.912	6.3977
32.75	17.9684	4.4889	22.3219	15.944	6.3779
32.875	18.0024	4.4702	22.3339	15.9758	6.3581
33	18.0363	4.4516	22.346	16.0075	6.3385
33.125	18.0701	4.433	22.358	16.0392	6.3188
33.25	18.1037	4.4145	22.3699	16.0707	6.2992
33.375	18.1372	4.3961	22.3818	16.1022	6.2796
33.5	18.1706	4.3776	22.3936	16.1336	6.26
33.625	18.2039	4.3592	22.4054	16.1649	6.2405
33.75	18.237	4.3409	22.4172	16.196	6.2212
33.875	18.27	4.3226	22.4289	16.2271	6.2018
34	18.3028	4.3044	22.4405	16.2581	6.1824
34.125	18.3355	4.2863	22.4521	16.2891	6.163
34.25	18.3681	4.2681	22.4636	16.3199	6.1437
34.375	18.4005	4.2501	22.4751	16.3506	6.1245
34.5	18.4329	4.232	22.4866	16.3813	6.1053
34.625	18.465	4.2141	22.498	16.4118	6.0862
34.75	18.4971	4.1962	22.5094	16.4423	6.0671
34.875	18.529	4.1783	22.5207	16.4726	6.0481
35	18.5608	4.1605	22.5319	16.5029	6.029
35.125	18.5925	4.1427	22.5431	16.5331	6.01
35.25	18.624	4.125	22.5543	16.5632	5.9911
35.375	18.6555	4.1073	22.5654	16.5932	5.9722
35.5	18.6867	4.0898	22.5765	16.6231	5.9534
35.625	18.7179	4.0722	22.5875	16.653	5.9345
35.75	18.7489	4.0547	22.5985	16.6827	5.9158
35.875	18.7798	4.0372	22.6095	16.7124	5.8971
36	18.8106	4.0198	22.6203	16.7419	5.8784
36.125	18.8412	4.0025	22.6312	16.7714	5.8598
36.25	18.8717	3.9852	22.642	16.8008	5.8412
36.375	18.9021	3.9679	22.6527	16.8301	5.8226
36.5	18.9324	3.9507	22.6635	16.8593	5.8042
36.625	18.9625	3.9336	22.6741	16.8884	5.7857
36.75	18.9926	3.9164	22.6847	16.9175	5.7672
36.875	19.0225	3.8994	22.6953	16.9464	5.7489
37	19.0522	3.8825	22.7058	16.9753	5.7305
37.125	19.0819	3.8655	22.7163	17.0041	5.7122
37.25	19.1114	3.8486	22.7268	17.0328	5.694
37.375	19.1408	3.8318	22.7372	17.0614	5.6758
37.5	19.1701	3.8149	22.7475	17.0899	5.6576

	Nd=0.75			Nd=0.5	
z (km)	Fluid ‰ δ18O	Δr-fl	Rock ‰ δ18O	Fluid ‰ δ18O	Δr-fl
37.625	19.1992	3.7983	22.7578	17.1183	5.6395
37.75	19.2282	3.7816	22.7681	17.1466	5.6215
37.875	19.2571	3.765	22.7783	17.1749	5.6034
38	19.2859	3.7484	22.7885	17.2031	5.5854
38.125	19.3146	3.7318	22.7986	17.2312	5.5674
38.25	19.3431	3.7154	22.8087	17.2592	5.5495
38.375	19.3716	3.6989	22.8188	17.2871	5.5317
38.5	19.3999	3.6826	22.8288	17.3149	5.5139
38.625	19.428	3.6663	22.8388	17.3427	5.4961
38.75	19.4561	3.65	22.8487	17.3703	5.4784
38.875	19.484	3.6338	22.8586	17.3979	5.4607
39	19.5119	3.6176	22.8684	17.4254	5.443
39.125	19.5396	3.6015	22.8782	17.4528	5.4254
39.25	19.5672	3.5854	22.888	17.4801	5.4079
39.375	19.5946	3.5695	22.8977	17.5074	5.3903
39.5	19.622	3.5535	22.9074	17.5345	5.3729
39.625	19.6492	3.5376	22.917	17.5616	5.3554
39.75	19.6763	3.5218	22.9266	17.5886	5.338
39.875	19.7033	3.506	22.9362	17.6155	5.3207
40	19.7302	3.4903	22.9457	17.6423	5.3034
40.125	19.757	3.4745	22.9551	17.6691	5.286
40.25	19.7836	3.459	22.9646	17.6957	5.2689
40.375	19.8102	3.4433	22.974	17.7223	5.2517
40.5	19.8366	3.4278	22.9833	17.7488	5.2345
40.625	19.8629	3.4123	22.9926	17.7752	5.2174
40.75	19.8891	3.3969	23.0019	17.8016	5.2003
40.875	19.9152	3.3815	23.0111	17.8278	5.1833
41	19.9412	3.3661	23.0203	17.854	5.1663
41.125	19.967	3.3509	23.0295	17.8801	5.1494
41.25	19.9928	3.3356	23.0386	17.9061	5.1325
41.375	20.0184	3.3205	23.0477	17.932	5.1157
41.5	20.0439	3.3054	23.0567	17.9579	5.0988
41.625	20.0693	3.2903	23.0657	17.9836	5.0821
41.75	20.0946	3.2753	23.0747	18.0093	5.0654
41.875	20.1198	3.2603	23.0836	18.0349	5.0487
42	20.1449	3.2454	23.0925	18.0604	5.0321
42.125	20.1699	3.2305	23.1013	18.0859	5.0154
42.25	20.1947	3.2157	23.1101	18.1112	4.9989
42.375	20.2195	3.2009	23.1189	18.1365	4.9824
42.5	20.2441	3.1862	23.1277	18.1617	4.966
42.625	20.2686	3.1716	23.1363	18.1869	4.9494
42.75	20.293	3.157	23.145	18.2119	4.9331
42.875	20.3174	3.1423	23.1536	18.2369	4.9167

z (km)	Nd=0.75 Fluid ‰ δ18O	Δr-fl	Rock ‰ δ18O	Nd=0.5 Fluid ‰ δ18O	Δr-fl
43	20.3416	3.1278	23.1622	18.2618	4.9004
43.125	20.3657	3.1134	23.1708	18.2866	4.8842
43.25	20.3896	3.099	23.1793	18.3113	4.868
43.375	20.4135	3.0847	23.1877	18.336	4.8517
43.5	20.4373	3.0703	23.1962	18.3606	4.8356
43.625	20.461	3.0561	23.2046	18.3851	4.8195
43.75	20.4845	3.0419	23.213	18.4095	4.8035
43.875	20.508	3.0277	23.2213	18.4338	4.7875
44	20.5314	3.0136	23.2296	18.4581	4.7715
44.125	20.5546	2.9996	23.2378	18.4823	4.7555
44.25	20.5778	2.9855	23.2461	18.5064	4.7397
44.375	20.6008	2.9716	23.2543	18.5305	4.7238
44.5	20.6237	2.9577	23.2624	18.5544	4.708
44.625	20.6466	2.9438	23.2705	18.5783	4.6922
44.75	20.6693	2.9301	23.2786	18.6021	4.6765
44.875	20.6919	2.9163	23.2867	18.6259	4.6608
45	20.7145	2.9026	23.2947	18.6495	4.6452
45.125	20.7369	2.8889	23.3026	18.6731	4.6295
45.25	20.7592	2.8754	23.3106	18.6966	4.614
45.375	20.7814	2.8618	23.3185	18.7201	4.5984
45.5	20.8036	2.8483	23.3264	18.7434	4.583
45.625	20.8256	2.8348	23.3342	18.7667	4.5675
45.75	20.8475	2.8215	23.342	18.7899	4.5521
45.875	20.8693	2.8081	23.3498	18.813	4.5368
46	20.8911	2.7947	23.3575	18.8361	4.5214
46.125	20.9127	2.7815	23.3652	18.8591	4.5061
46.25	20.9342	2.7683	23.3729	18.882	4.4909
46.375	20.9556	2.7552	23.3806	18.9049	4.4757
46.5	20.977	2.742	23.3882	18.9276	4.4606
46.625	20.9982	2.729	23.3957	18.9503	4.4454
46.75	21.0193	2.716	23.4033	18.9729	4.4304
46.875	21.0404	2.703	23.4108	18.9955	4.4153
47	21.0613	2.6901	23.4183	19.018	4.4003
47.125	21.0822	2.6772	23.4257	19.0404	4.3853
47.25	21.1029	2.6645	23.4331	19.0627	4.3704
47.375	21.1236	2.6516	23.4405	19.0849	4.3556
47.5	21.1441	2.639	23.4478	19.1071	4.3407
47.625	21.1646	2.6263	23.4552	19.1292	4.326
47.75	21.185	2.6136	23.4624	19.1513	4.3111
47.875	21.2052	2.6011	23.4697	19.1733	4.2964
48	21.2254	2.5886	23.4769	19.1952	4.2817
48.125	21.2455	2.5761	23.4841	19.217	4.2671
48.25	21.2655	2.5637	23.4913	19.2387	4.2526

	Nd=0.75			Nd=0.5	
z (km)	Fluid ‰ δ18O	Δr-fl	Rock ‰ δ18O	Fluid ‰ δ18O	Δr-fl
48.375	21.2854	2.5513	23.4984	19.2604	4.238
48.5	21.3052	2.539	23.5055	19.282	4.2235
48.625	21.3249	2.5267	23.5125	19.3036	4.2089
48.75	21.3445	2.5145	23.5196	19.3251	4.1945
48.875	21.3641	2.5022	23.5266	19.3465	4.1801
49	21.3835	2.4901	23.5335	19.3678	4.1657
49.125	21.4029	2.478	23.5405	19.3891	4.1514
49.25	21.4221	2.466	23.5474	19.4103	4.1371
49.375	21.4413	2.454	23.5543	19.4314	4.1229
49.5	21.4604	2.442	23.5611	19.4524	4.1087
49.625	21.4794	2.4301	23.5679	19.4734	4.0945
49.75	21.4983	2.4182	23.5747	19.4943	4.0804
49.875	21.5171	2.4064	23.5815	19.5152	4.0663
50	21.5358	2.3947	23.5882	19.536	4.0522

E.5 Reactive Transport Modeling Results at TIFF of $1x10^6$ (moles H_2O/cm^2)

	Nd=5			Nd=2			Nd=1	
z (km)	Rock ‰ δ18O	Fluid ‰ δ18O	Δr-fl	Rock ‰ δ18O	Fluid ‰ δ18O	Δr-fl	Rock ‰ δ18O	Fluid ‰ δ18O
0	4.1415	4	0.1415	6.842	4	2.842	11.7255	4
1.25	4.1765	4.0073	0.1692	6.9526	4.0542	2.8984	11.8026	4.0729
2.5	4.2141	4.016	0.1981	7.0632	4.1095	2.9537	11.8793	4.1459
3.75	4.2542	4.0261	0.2281	7.1739	4.1658	3.0081	11.9557	4.2189
5	4.2969	4.0377	0.2592	7.2847	4.2233	3.0614	12.0318	4.2921
6.25	4.3421	4.0508	0.2913	7.3955	4.2818	3.1137	12.1075	4.3653
7.5	4.39	4.0654	0.3246	7.5064	4.3414	3.165	12.1829	4.4385
8.75	4.4404	4.0817	0.3587	7.6174	4.402	3.2154	12.2579	4.5118
10	4.4934	4.0997	0.3937	7.7283	4.4635	3.2648	12.3326	4.5852
11.25	4.549	4.1194	0.4296	7.8393	4.5261	3.3132	12.407	4.6586
12.5	4.6072	4.1408	0.4664	7.9503	4.5896	3.3607	12.481	4.7321
13.75	4.668	4.164	0.504	8.0612	4.6541	3.4071	12.5547	4.8056
15	4.7314	4.1891	0.5423	8.1721	4.7195	3.4526	12.6281	4.8791
16.25	4.7973	4.2161	0.5812	8.2829	4.7858	3.4971	12.7011	4.9527
17.5	4.8658	4.2449	0.6209	8.3937	4.853	3.5407	12.7738	5.0263
18.75	4.9368	4.2757	0.6611	8.5044	4.9211	3.5833	12.8462	5.0999
20	5.0103	4.3085	0.7018	8.615	4.9901	3.6249	12.9182	5.1736
21.25	5.0863	4.3433	0.743	8.7255	5.0598	3.6657	12.9899	5.2473
22.5	5.1648	4.38	0.7848	8.8359	5.1304	3.7055	13.0613	5.321
23.75	5.2458	4.4189	0.8269	8.9462	5.2018	3.7444	13.1323	5.3947
25	5.3291	4.4598	0.8693	9.0563	5.274	3.7823	13.203	5.4684
26.25	5.4149	4.5028	0.9121	9.1663	5.3469	3.8194	13.2734	5.5421
27.5	5.503	4.5479	0.9551	9.2761	5.4206	3.8555	13.3434	5.6158
28.75	5.5935	4.5951	0.9984	9.3858	5.4951	3.8907	13.4131	5.6895
30	5.6862	4.6444	1.0418	9.4953	5.5702	3.9251	13.4825	5.7632
31.25	5.7812	4.6958	1.0854	9.6046	5.646	3.9586	13.5515	5.8369
32.5	5.8785	4.7494	1.1291	9.7137	5.7225	3.9912	13.6203	5.9106
33.75	5.9779	4.8052	1.1727	9.8225	5.7997	4.0228	13.6887	5.9843
35	6.0795	4.8631	1.2164	9.9312	5.8776	4.0536	13.7567	6.0579
36.25	6.1831	4.9231	1.26	10.0396	5.956	4.0836	13.8245	6.1316
37.5	6.2889	4.9853	1.3036	10.1478	6.0351	4.1127	13.8919	6.2052
38.75	6.3966	5.0496	1.347	10.2557	6.1148	4.1409	13.959	6.2787
40	6.5064	5.1161	1.3903	10.3634	6.195	4.1684	14.0258	6.3523
41.25	6.618	5.1847	1.4333	10.4708	6.2758	4.195	14.0923	6.4258
42.5	6.7316	5.2554	1.4762	10.5779	6.3572	4.2207	14.1584	6.4993
43.75	6.8469	5.3283	1.5186	10.6847	6.4391	4.2456	14.2242	6.5727
45	6.9641	5.4032	1.5609	10.7913	6.5215	4.2698	14.2897	6.6461
46.25	7.083	5.4802	1.6028	10.8975	6.6044	4.2931	14.3549	6.7194
47.5	7.2035	5.5593	1.6442	11.0035	6.6878	4.3157	14.4197	6.7927
48.75	7.3258	5.6405	1.6853	11.1091	6.7717	4.3374	14.4843	6.866
50	7.4495	5.7236	1.7259	11.2144	6.856	4.3584	14.5485	6.9392
51.25	7.5749	5.8088	1.7661	11.3193	6.9408	4.3785	14.6124	7.0123
52.5	7.7017	5.896	1.8057	11.4239	7.0259	4.398	14.676	7.0854

	Nd=5			Nd=2			Nd=1	
z (km)	Rock ‰ δ18O	Fluid ‰ δ18O	Δr-fl	Rock ‰ δ18O	Fluid ‰ δ18O	Δr-fl	Rock ‰ δ18O	Fluid ‰ δ18O
53.75	7.8299	5.9851	1.8448	11.5282	7.1115	4.4167	14.7393	7.1584
55	7.9595	6.0762	1.8833	11.6321	7.1975	4.4346	14.8023	7.2313
56.25	8.0904	6.1691	1.9213	11.7357	7.2839	4.4518	14.8649	7.3042
57.5	8.2226	6.264	1.9586	11.8389	7.3706	4.4683	14.9273	7.377
58.75	8.356	6.3607	1.9953	11.9417	7.4577	4.484	14.9893	7.4497
60	8.4906	6.4592	2.0314	12.0441	7.5451	4.499	15.051	7.5224
61.25	8.6263	6.5595	2.0668	12.1462	7.6329	4.5133	15.1124	7.5949
62.5	8.763	6.6616	2.1014	12.2478	7.721	4.5268	15.1736	7.6674
63.75	8.9007	6.7654	2.1353	12.3491	7.8093	4.5398	15.2343	7.7398
65	9.0394	6.8709	2.1685	12.4499	7.8979	4.552	15.2948	7.8122
66.25	9.179	6.978	2.201	12.5504	7.9869	4.5635	15.355	7.8844
67.5	9.3194	7.0868	2.2326	12.6504	8.076	4.5744	15.4149	7.9566
68.75	9.4606	7.1971	2.2635	12.75	8.1654	4.5846	15.4745	8.0286
70	9.6026	7.309	2.2936	12.8492	8.2551	4.5941	15.5338	8.1006
71.25	9.7452	7.4223	2.3229	12.948	8.3449	4.6031	15.5927	8.1724
72.5	9.8885	7.5372	2.3513	13.0463	8.435	4.6113	15.6514	8.2442
73.75	10.0323	7.6534	2.3789	13.1442	8.5252	4.619	15.7098	8.3159
75	10.1767	7.7711	2.4056	13.2417	8.6156	4.6261	15.7679	8.3874
76.25	10.3215	7.89	2.4315	13.3387	8.7062	4.6325	15.8256	8.4589
77.5	10.4668	8.0103	2.4565	13.4353	8.797	4.6383	15.8831	8.5302
78.75	10.6125	8.1318	2.4807	13.5314	8.8879	4.6435	15.9403	8.6015
80	10.7585	8.2546	2.5039	13.627	8.9789	4.6481	15.9972	8.6726
81.25	10.9048	8.3785	2.5263	13.7222	9.07	4.6522	16.0538	8.7436
82.5	11.0513	8.5035	2.5478	13.817	9.1613	4.6557	16.1101	8.8145
83.75	11.198	8.6296	2.5684	13.9112	9.2526	4.6586	16.1661	8.8853
85	11.3449	8.7568	2.5881	14.005	9.344	4.661	16.2218	8.9559
86.25	11.4919	8.8849	2.607	14.0983	9.4356	4.6627	16.2772	9.0265
87.5	11.6389	9.014	2.6249	14.1912	9.5271	4.6641	16.3323	9.0969
88.75	11.7859	9.1441	2.6418	14.2835	9.6187	4.6648	16.3872	9.1672
90	11.9329	9.2749	2.658	14.3754	9.7104	4.665	16.4417	9.2373
91.25	12.0798	9.4066	2.6732	14.4668	9.8021	4.6647	16.496	9.3074
92.5	12.2266	9.5391	2.6875	14.5577	9.8938	4.6639	16.55	9.3773
93.75	12.3732	9.6723	2.7009	14.6481	9.9855	4.6626	16.6037	9.447
95	12.5196	9.8062	2.7134	14.738	10.0773	4.6607	16.6571	9.5167
96.25	12.6658	9.9407	2.7251	14.8275	10.169	4.6585	16.7102	9.5862
97.5	12.8117	10.0758	2.7359	14.9164	10.2607	4.6557	16.7631	9.6555
98.75	12.9573	10.2115	2.7458	15.0048	10.3524	4.6524	16.8156	9.7248
100	13.1025	10.3477	2.7548	15.0928	10.444	4.6488	16.8679	9.7938
101.25	13.2474	10.4844	2.763	15.1802	10.5356	4.6446	16.9199	9.8628
102.5	13.3918	10.6215	2.7703	15.2671	10.6271	4.64	16.9716	9.9316
103.75	13.5358	10.759	2.7768	15.3535	10.7186	4.6349	17.0231	10.0002
105	13.6792	10.8969	2.7823	15.4394	10.81	4.6294	17.0743	10.0687
106.25	13.8222	11.035	2.7872	15.5248	10.9013	4.6235	17.1252	10.1371

z (km)	Rock ‰ δ18O	Nd=5 Fluid ‰ δ18O	Δr-fl	Rock ‰ δ18O	Nd=2 Fluid ‰ δ18O	Δr-fl	Rock ‰ δ18O	Nd=1 Fluid ‰ δ18O
107.5	13.9646	11.1734	2.7912	15.6097	10.9925	4.6172	17.1758	10.2053
108.75	14.1063	11.312	2.7943	15.6941	11.0837	4.6104	17.2261	10.2734
110	14.2475	11.4508	2.7967	15.778	11.1747	4.6033	17.2762	10.3413
111.25	14.388	11.5898	2.7982	15.8614	11.2656	4.5958	17.326	10.409
112.5	14.5279	11.7288	2.7991	15.9442	11.3564	4.5878	17.3755	10.4766
113.75	14.667	11.8679	2.7991	16.0265	11.447	4.5795	17.4248	10.5441
115	14.8054	12.0071	2.7983	16.1084	11.5375	4.5709	17.4738	10.6113
116.25	14.943	12.1462	2.7968	16.1897	11.6279	4.5618	17.5225	10.6785
117.5	15.0799	12.2853	2.7946	16.2705	11.7181	4.5524	17.571	10.7454
118.75	15.2159	12.4243	2.7916	16.3507	11.8081	4.5426	17.6192	10.8122
120	15.3511	12.5632	2.7879	16.4305	11.898	4.5325	17.6671	10.8789
121.25	15.4855	12.7019	2.7836	16.5097	11.9877	4.522	17.7148	10.9454
122.5	15.619	12.8404	2.7786	16.5884	12.0772	4.5112	17.7622	11.0117
123.75	15.7516	12.9787	2.7729	16.6666	12.1665	4.5001	17.8093	11.0778
125	15.8832	13.1167	2.7665	16.7443	12.2557	4.4886	17.8562	11.1438
126.25	16.014	13.2545	2.7595	16.8215	12.3446	4.4769	17.9028	11.2096
127.5	16.1438	13.3919	2.7519	16.8981	12.4333	4.4648	17.9492	11.2753
128.75	16.2726	13.529	2.7436	16.9743	12.5218	4.4525	17.9953	11.3407
130	16.4004	13.6657	2.7347	17.0499	12.6101	4.4398	18.0411	11.406
131.25	16.5272	13.8019	2.7253	17.125	12.6981	4.4269	18.0867	11.4712
132.5	16.653	13.9377	2.7153	17.1996	12.786	4.4136	18.1321	11.5361
133.75	16.7777	14.0731	2.7046	17.2736	12.8735	4.4001	18.1771	11.6009
135	16.9014	14.2079	2.6935	17.3472	12.9609	4.3863	18.222	11.6655
136.25	17.0241	14.3422	2.6819	17.4202	13.048	4.3722	18.2666	11.7299
137.5	17.1456	14.476	2.6696	17.4927	13.1348	4.3579	18.3109	11.7942
138.75	17.2661	14.6091	2.657	17.5647	13.2213	4.3434	18.355	11.8583
140	17.3855	14.7417	2.6438	17.6362	13.3076	4.3286	18.3988	11.9222
141.25	17.5038	14.8736	2.6302	17.7072	13.3937	4.3135	18.4424	11.9859
142.5	17.6209	15.0049	2.616	17.7777	13.4794	4.2983	18.4857	12.0494
143.75	17.7369	15.1355	2.6014	17.8476	13.5649	4.2827	18.5288	12.1128
145	17.8518	15.2653	2.5865	17.9171	13.65	4.2671	18.5716	12.1759
146.25	17.9656	15.3945	2.5711	17.986	13.7349	4.2511	18.6143	12.2389
147.5	18.0782	15.5229	2.5553	18.0545	13.8195	4.235	18.6566	12.3017
148.75	18.1896	15.6506	2.539	18.1224	13.9038	4.2186	18.6987	12.3644
150	18.2999	15.7774	2.5225	18.1898	13.9878	4.202	18.7406	12.4268
151.25	18.4091	15.9035	2.5056	18.2567	14.0715	4.1852	18.7823	12.489
152.5	18.517	16.0287	2.4883	18.3232	14.1548	4.1684	18.8237	12.5511
153.75	18.6238	16.1531	2.4707	18.3891	14.2379	4.1512	18.8648	12.613
155	18.7294	16.2766	2.4528	18.4545	14.3206	4.1339	18.9057	12.6747
156.25	18.8338	16.3993	2.4345	18.5194	14.403	4.1164	18.9464	12.7362
157.5	18.937	16.5211	2.4159	18.5838	14.4851	4.0987	18.9869	12.7975
158.75	19.0391	16.6419	2.3972	18.6477	14.5668	4.0809	19.0271	12.8586
160	19.14	16.7619	2.3781	18.7112	14.6482	4.063	19.0671	12.9195

z (km)	Nd=5 Rock ‰ δ18O	Fluid ‰ δ18O	Δr-fl	Nd=2 Rock ‰ δ18O	Fluid ‰ δ18O	Δr-fl	Nd=1 Rock ‰ δ18O	Fluid ‰ δ18O
161.25	19.2397	16.8809	2.3588	18.7741	14.7293	4.0448	19.1069	12.9803
162.5	19.3381	16.999	2.3391	18.8366	14.81	4.0266	19.1464	13.0408
163.75	19.4355	17.1161	2.3194	18.8985	14.8904	4.0081	19.1857	13.1012
165	19.5316	17.2322	2.2994	18.96	14.9704	3.9896	19.2248	13.1614
166.25	19.6265	17.3474	2.2791	19.021	15.0501	3.9709	19.2636	13.2213
167.5	19.7203	17.4615	2.2588	19.0814	15.1294	3.952	19.3022	13.2811
168.75	19.8129	17.5747	2.2382	19.1415	15.2084	3.9331	19.3406	13.3407
170	19.9043	17.6869	2.2174	19.201	15.287	3.914	19.3788	13.4001
171.25	19.9945	17.798	2.1965	19.26	15.3652	3.8948	19.4167	13.4593
172.5	20.0835	17.9081	2.1754	19.3186	15.4431	3.8755	19.4544	13.5183
173.75	20.1714	18.0172	2.1542	19.3767	15.5206	3.8561	19.4919	13.5771
175	20.2581	18.1252	2.1329	19.4343	15.5978	3.8365	19.5292	13.6357
176.25	20.3437	18.2322	2.1115	19.4915	15.6745	3.817	19.5663	13.6941
177.5	20.4281	18.3381	2.09	19.5482	15.7509	3.7973	19.6031	13.7523
178.75	20.5113	18.443	2.0683	19.6044	15.8269	3.7775	19.6397	13.8103
180	20.5934	18.5468	2.0466	19.6601	15.9026	3.7575	19.6761	13.8681
181.25	20.6744	18.6495	2.0249	19.7154	15.9778	3.7376	19.7123	13.9258
182.5	20.7542	18.7512	2.003	19.7703	16.0527	3.7176	19.7483	13.9832
183.75	20.8329	18.8518	1.9811	19.8246	16.1272	3.6974	19.7841	14.0404
185	20.9105	18.9513	1.9592	19.8785	16.2013	3.6772	19.8196	14.0974
186.25	20.987	19.0497	1.9373	19.932	16.275	3.657	19.855	14.1543
187.5	21.0623	19.147	1.9153	19.985	16.3483	3.6367	19.8901	14.2109
188.75	21.1366	19.2433	1.8933	20.0375	16.4213	3.6162	19.925	14.2673
190	21.2097	19.3384	1.8713	20.0896	16.4938	3.5958	19.9597	14.3235
191.25	21.2818	19.4325	1.8493	20.1413	16.566	3.5753	19.9942	14.3796
192.5	21.3528	19.5255	1.8273	20.1925	16.6377	3.5548	20.0285	14.4354
193.75	21.4227	19.6174	1.8053	20.2433	16.7091	3.5342	20.0626	14.491
195	21.4916	19.7082	1.7834	20.2936	16.7801	3.5135	20.0965	14.5465
196.25	21.5594	19.7979	1.7615	20.3435	16.8506	3.4929	20.1301	14.6017
197.5	21.6261	19.8865	1.7396	20.3929	16.9208	3.4721	20.1636	14.6567
198.75	21.6919	19.974	1.7179	20.442	16.9905	3.4515	20.1969	14.7115
200	21.7566	20.0605	1.6961	20.4905	17.0599	3.4306	20.23	14.7661
201.25	21.8202	20.1459	1.6743	20.5387	17.1289	3.4098	20.2628	14.8206
202.5	21.8829	20.2302	1.6527	20.5864	17.1974	3.389	20.2955	14.8748
203.75	21.9446	20.3134	1.6312	20.6338	17.2656	3.3682	20.328	14.9288
205	22.0053	20.3956	1.6097	20.6807	17.3333	3.3474	20.3603	14.9826
206.25	22.065	20.4767	1.5883	20.7271	17.4007	3.3264	20.3923	15.0362
207.5	22.1237	20.5567	1.567	20.7732	17.4676	3.3056	20.4242	15.0896
208.75	22.1814	20.6357	1.5457	20.8188	17.5342	3.2846	20.4559	15.1428
210	22.2383	20.7136	1.5247	20.8641	17.6003	3.2638	20.4874	15.1959
211.25	22.2941	20.7905	1.5036	20.9089	17.666	3.2429	20.5187	15.2487
212.5	22.3491	20.8663	1.4828	20.9533	17.7313	3.222	20.5498	15.3013
213.75	22.4031	20.9411	1.462	20.9973	17.7962	3.2011	20.5808	15.3537

	Nd=5			Nd=2			Nd=1	
z (km)	Rock ‰ δ18O	Fluid ‰ δ18O	Δr-fl	Rock ‰ δ18O	Fluid ‰ δ18O	Δr-fl	Rock ‰ δ18O	Fluid ‰ δ18O
215	22.4562	21.0148	1.4414	21.0409	17.8607	3.1802	20.6115	15.4059
216.25	22.5084	21.0875	1.4209	21.0841	17.9248	3.1593	20.642	15.4579
217.5	22.5597	21.1592	1.4005	21.1269	17.9885	3.1384	20.6724	15.5096
218.75	22.6101	21.2299	1.3802	21.1694	18.0518	3.1176	20.7026	15.5612
220	22.6596	21.2996	1.36	21.2114	18.1147	3.0967	20.7325	15.6126
221.25	22.7083	21.3683	1.34	21.253	18.1772	3.0758	20.7623	15.6638
222.5	22.7562	21.436	1.3202	21.2943	18.2392	3.0551	20.792	15.7148
223.75	22.8032	21.5027	1.3005	21.3351	18.3009	3.0342	20.8214	15.7656
225	22.8493	21.5684	1.2809	21.3756	18.3621	3.0135	20.8506	15.8162
226.25	22.8947	21.6331	1.2616	21.4157	18.423	2.9927	20.8797	15.8665
227.5	22.9392	21.6969	1.2423	21.4555	18.4834	2.9721	20.9086	15.9167
228.75	22.9829	21.7597	1.2232	21.4948	18.5434	2.9514	20.9373	15.9667
230	23.0259	21.8215	1.2044	21.5338	18.6031	2.9307	20.9658	16.0165
231.25	23.068	21.8824	1.1856	21.5724	18.6623	2.9101	20.9942	16.066
232.5	23.1094	21.9424	1.167	21.6106	18.7211	2.8895	21.0224	16.1154
233.75	23.1501	22.0014	1.1487	21.6485	18.7795	2.869	21.0504	16.1646
235	23.1899	22.0595	1.1304	21.686	18.8375	2.8485	21.0782	16.2136
236.25	23.2291	22.1167	1.1124	21.7232	18.8951	2.8281	21.1058	16.2623
237.5	23.2675	22.173	1.0945	21.76	18.9523	2.8077	21.1333	16.3109
238.75	23.3052	22.2284	1.0768	21.7964	19.0092	2.7872	21.1606	16.3593
240	23.3422	22.2829	1.0593	21.8325	19.0656	2.7669	21.1877	16.4074
241.25	23.3785	22.3366	1.0419	21.8683	19.1216	2.7467	21.2147	16.4554
242.5	23.4141	22.3893	1.0248	21.9037	19.1772	2.7265	21.2415	16.5032
243.75	23.449	22.4412	1.0078	21.9387	19.2324	2.7063	21.2681	16.5507
245	23.4833	22.4923	0.991	21.9734	19.2872	2.6862	21.2946	16.5981
246.25	23.5169	22.5425	0.9744	22.0078	19.3416	2.6662	21.3208	16.6453
247.5	23.5499	22.5919	0.958	22.0418	19.3957	2.6461	21.347	16.6922
248.75	23.5822	22.6405	0.9417	22.0755	19.4493	2.6262	21.3729	16.739
250	23.6139	22.6882	0.9257	22.1089	19.5025	2.6064	21.3987	16.7856
251.25	23.6449	22.7352	0.9097	22.1419	19.5554	2.5865	21.4243	16.8319
252.5	23.6754	22.7813	0.8941	22.1747	19.6078	2.5669	21.4498	16.8781
253.75	23.7052	22.8266	0.8786	22.207	19.6599	2.5471	21.4751	16.9241
255	23.7345	22.8712	0.8633	22.2391	19.7116	2.5275	21.5002	16.9699
256.25	23.7632	22.915	0.8482	22.2708	19.7629	2.5079	21.5252	17.0154
257.5	23.7913	22.9581	0.8332	22.3023	19.8138	2.4885	21.55	17.0608
258.75	23.8188	23.0004	0.8184	22.3334	19.8643	2.4691	21.5747	17.106
260	23.8458	23.0419	0.8039	22.3642	19.9144	2.4498	21.5992	17.151
261.25	23.8723	23.0828	0.7895	22.3946	19.9642	2.4304	21.6235	17.1958
262.5	23.8982	23.1229	0.7753	22.4248	20.0136	2.4112	21.6477	17.2404
263.75	23.9236	23.1622	0.7614	22.4547	20.0625	2.3922	21.6718	17.2848
265	23.9484	23.2009	0.7475	22.4843	20.1112	2.3731	21.6956	17.329
266.25	23.9728	23.2389	0.7339	22.5135	20.1594	2.3541	21.7194	17.373
267.5	23.9966	23.2762	0.7204	22.5425	20.2073	2.3352	21.7429	17.4168

	Nd=5			Nd=2			Nd=1	
	Rock ‰	**Fluid ‰**		**Rock ‰**	**Fluid ‰**		**Rock ‰**	**Fluid ‰**
z (km)	**δ18O**	**δ18O**	**Δr-fl**	**δ18O**	**δ18O**	**Δr-fl**	**δ18O**	**δ18O**
268.75	24.02	23.3128	0.7072	22.5712	20.2547	2.3165	21.7664	17.4604
270	24.0429	23.3488	0.6941	22.5996	20.3019	2.2977	21.7896	17.5038
271.25	24.0653	23.3841	0.6812	22.6276	20.3486	2.279	21.8128	17.5471
272.5	24.0872	23.4187	0.6685	22.6554	20.395	2.2604	21.8357	17.5901
273.75	24.1086	23.4527	0.6559	22.683	20.441	2.242	21.8586	17.6329
275	24.1297	23.4861	0.6436	22.7102	20.4866	2.2236	21.8812	17.6756
276.25	24.1502	23.5189	0.6313	22.7371	20.5319	2.2052	21.9038	17.7181
277.5	24.1704	23.551	0.6194	22.7638	20.5768	2.187	21.9261	17.7603
278.75	24.1901	23.5825	0.6076	22.7902	20.6213	2.1689	21.9484	17.8024
280	24.2094	23.6135	0.5959	22.8163	20.6655	2.1508	21.9705	17.8443
281.25	24.2282	23.6438	0.5844	22.8421	20.7093	2.1328	21.9924	17.886
282.5	24.2467	23.6736	0.5731	22.8677	20.7528	2.1149	22.0142	17.9275
283.75	24.2648	23.7028	0.562	22.893	20.7959	2.0971	22.0359	17.9688
285	24.2824	23.7314	0.551	22.9181	20.8387	2.0794	22.0574	18.0099
286.25	24.2997	23.7595	0.5402	22.9428	20.8811	2.0617	22.0788	18.0508
287.5	24.3167	23.787	0.5297	22.9673	20.9231	2.0442	22.1	18.0916
288.75	24.3332	23.814	0.5192	22.9916	20.9648	2.0268	22.1211	18.1321
290	24.3494	23.8405	0.5089	23.0156	21.0062	2.0094	22.1421	18.1725
291.25	24.3652	23.8665	0.4987	23.0393	21.0472	1.9921	22.1629	18.2127
292.5	24.3807	23.8919	0.4888	23.0628	21.0879	1.9749	22.1836	18.2526
293.75	24.3958	23.9168	0.479	23.0861	21.1282	1.9579	22.2041	18.2925
295	24.4106	23.9413	0.4693	23.109	21.1682	1.9408	22.2245	18.3321
296.25	24.4251	23.9652	0.4599	23.1318	21.2078	1.924	22.2448	18.3715
297.5	24.4392	23.9887	0.4505	23.1543	21.2471	1.9072	22.265	18.4107
298.75	24.4531	24.0117	0.4414	23.1766	21.2861	1.8905	22.285	18.4498
300	24.4666	24.0344	0.4322	23.1986	21.3247	1.8739	22.3049	18.4887
301.25	24.4798	24.0565	0.4233	23.2204	21.363	1.8574	22.3246	18.5274
302.5	24.4927	24.0781	0.4146	23.2419	21.401	1.8409	22.3442	18.5659
303.75	24.5053	24.0993	0.406	23.2632	21.4386	1.8246	22.3637	18.6042
305	24.5177	24.1201	0.3976	23.2843	21.476	1.8083	22.3831	18.6423
306.25	24.5297	24.1404	0.3893	23.3052	21.513	1.7922	22.4023	18.6803
307.5	24.5415	24.1603	0.3812	23.3258	21.5496	1.7762	22.4214	18.718
308.75	24.553	24.1798	0.3732	23.3462	21.586	1.7602	22.4404	18.7556
310	24.5643	24.1989	0.3654	23.3664	21.622	1.7444	22.4592	18.793
311.25	24.5752	24.2176	0.3576	23.3863	21.6577	1.7286	22.478	18.8303
312.5	24.586	24.2359	0.3501	23.4061	21.6931	1.713	22.4966	18.8673
313.75	24.5964	24.2538	0.3426	23.4256	21.7282	1.6974	22.515	18.9042
315	24.6067	24.2714	0.3353	23.4449	21.763	1.6819	22.5334	18.9409
316.25	24.6167	24.2885	0.3282	23.464	21.7974	1.6666	22.5516	18.9774
317.5	24.6264	24.3053	0.3211	23.4829	21.8316	1.6513	22.5697	19.0137
318.75	24.636	24.3218	0.3142	23.5015	21.8654	1.6361	22.5877	19.0499
320	24.6453	24.3379	0.3074	23.52	21.899	1.621	22.6056	19.0858
321.25	24.6544	24.3536	0.3008	23.5383	21.9322	1.6061	22.6233	19.1216

z (km)	Nd=5 Rock ‰ δ18O	Fluid ‰ δ18O	Δr-fl	Nd=2 Rock ‰ δ18O	Fluid ‰ δ18O	Δr-fl	Nd=1 Rock ‰ δ18O	Fluid ‰ δ18O
322.5	24.6632	24.369	0.2942	23.5563	21.9652	1.5911	22.6409	19.1573
323.75	24.6719	24.3841	0.2878	23.5742	21.9978	1.5764	22.6584	19.1927
325	24.6804	24.3989	0.2815	23.5918	22.0301	1.5617	22.6758	19.228
326.25	24.6886	24.4133	0.2753	23.6093	22.0622	1.5471	22.6931	19.2631
327.5	24.6967	24.4274	0.2693	23.6266	22.0939	1.5327	22.7102	19.298
328.75	24.7045	24.4412	0.2633	23.6436	22.1254	1.5182	22.7273	19.3327
330	24.7122	24.4547	0.2575	23.6605	22.1566	1.5039	22.7442	19.3673
331.25	24.7197	24.4679	0.2518	23.6772	22.1875	1.4897	22.761	19.4017
332.5	24.727	24.4809	0.2461	23.6937	22.2181	1.4756	22.7777	19.4359
333.75	24.7342	24.4935	0.2407	23.71	22.2484	1.4616	22.7943	19.47
335	24.7411	24.5059	0.2352	23.7261	22.2784	1.4477	22.8107	19.5039
336.25	24.7479	24.5179	0.23	23.7421	22.3082	1.4339	22.8271	19.5376
337.5	24.7545	24.5297	0.2248	23.7579	22.3376	1.4203	22.8433	19.5711
338.75	24.761	24.5413	0.2197	23.7734	22.3668	1.4066	22.8595	19.6045
340	24.7673	24.5526	0.2147	23.7888	22.3958	1.393	22.8755	19.6377
341.25	24.7735	24.5636	0.2099	23.8041	22.4244	1.3797	22.8914	19.6708
342.5	24.7795	24.5744	0.2051	23.8191	22.4528	1.3663	22.9072	19.7036
343.75	24.7853	24.5849	0.2004	23.834	22.4809	1.3531	22.9229	19.7363
345	24.791	24.5952	0.1958	23.8487	22.5088	1.3399	22.9385	19.7689
346.25	24.7966	24.6053	0.1913	23.8633	22.5364	1.3269	22.954	19.8012
347.5	24.802	24.6151	0.1869	23.8777	22.5637	1.314	22.9693	19.8334
348.75	24.8073	24.6248	0.1825	23.8919	22.5907	1.3012	22.9846	19.8655
350	24.8125	24.6341	0.1784	23.9059	22.6175	1.2884	22.9998	19.8973
351.25	24.8175	24.6433	0.1742	23.9198	22.6441	1.2757	23.0148	19.929
352.5	24.8224	24.6523	0.1701	23.9335	22.6704	1.2631	23.0298	19.9606
353.75	24.8272	24.661	0.1662	23.9471	22.6964	1.2507	23.0446	19.992
355	24.8318	24.6696	0.1622	23.9605	22.7222	1.2383	23.0594	20.0232
356.25	24.8364	24.6779	0.1585	23.9738	22.7477	1.2261	23.074	20.0542
357.5	24.8408	24.6861	0.1547	23.9869	22.773	1.2139	23.0886	20.0851
358.75	24.8451	24.6941	0.151	23.9998	22.798	1.2018	23.103	20.1158
360	24.8493	24.7019	0.1474	24.0126	22.8228	1.1898	23.1174	20.1464
361.25	24.8534	24.7095	0.1439	24.0253	22.8473	1.178	23.1316	20.1768
362.5	24.8574	24.7169	0.1405	24.0378	22.8717	1.1661	23.1458	20.2071
363.75	24.8613	24.7241	0.1372	24.0501	22.8957	1.1544	23.1598	20.2372
365	24.8651	24.7312	0.1339	24.0623	22.9196	1.1427	23.1738	20.2671
366.25	24.8688	24.7381	0.1307	24.0744	22.9431	1.1313	23.1877	20.2969
367.5	24.8724	24.7452	0.1272	24.0863	22.9665	1.1198	23.2014	20.3265
368.75	24.8759	24.7514	0.1245	24.0981	22.9896	1.1085	23.2151	20.3559
370	24.8793	24.7578	0.1215	24.1097	23.0125	1.0972	23.2287	20.3853
371.25	24.8826	24.7641	0.1185	24.1212	23.0352	1.086	23.2421	20.4144
372.5	24.8859	24.7702	0.1157	24.1326	23.0577	1.0749	23.2555	20.4434
373.75	24.889	24.7762	0.1128	24.1438	23.0799	1.0639	23.2688	20.4722
375	24.8921	24.782	0.1101	24.1549	23.1019	1.053	23.282	20.5009

	Nd=5			Nd=2			Nd=1	
z (km)	Rock ‰ δ18O	Fluid ‰ δ18O	Δr-fl	Rock ‰ δ18O	Fluid ‰ δ18O	Δr-fl	Rock ‰ δ18O	Fluid ‰ δ18O
376.25	24.8951	24.7877	0.1074	24.1659	23.1236	1.0423	23.2951	20.5294
377.5	24.898	24.7933	0.1047	24.1767	23.1452	1.0315	23.3081	20.5578
378.75	24.9009	24.7987	0.1022	24.1874	23.1665	1.0209	23.321	20.5861
380	24.9036	24.8039	0.0997	24.198	23.1877	1.0103	23.3339	20.6141
381.25	24.9063	24.8091	0.0972	24.2084	23.2086	0.9998	23.3466	20.6421
382.5	24.9089	24.8141	0.0948	24.2188	23.2293	0.9895	23.3593	20.6698
383.75	24.9115	24.819	0.0925	24.229	23.2497	0.9793	23.3718	20.6974
385	24.914	24.8238	0.0902	24.239	23.27	0.969	23.3843	20.7249
386.25	24.9164	24.8285	0.0879	24.249	23.2901	0.9589	23.3967	20.7522
387.5	24.9187	24.833	0.0857	24.2588	23.3099	0.9489	23.409	20.7794
388.75	24.921	24.8374	0.0836	24.2686	23.3296	0.939	23.4212	20.8064
390	24.9233	24.842	0.0813	24.2782	23.3491	0.9291	23.4333	20.8333
391.25	24.9254	24.8462	0.0792	24.2876	23.3683	0.9193	23.4454	20.8601
392.5	24.9275	24.8503	0.0772	24.297	23.3874	0.9096	23.4573	20.8867
393.75	24.9296	24.8544	0.0752	24.3063	23.4062	0.9001	23.4692	20.9131
395	24.9316	24.8583	0.0733	24.3154	23.4249	0.8905	23.481	20.9394
396.25	24.9336	24.8621	0.0715	24.3244	23.4434	0.881	23.4927	20.9655
397.5	24.9354	24.8658	0.0696	24.3334	23.4616	0.8718	23.5043	20.9916
398.75	24.9373	24.8694	0.0679	24.3422	23.4797	0.8625	23.5158	21.0174
400	24.9391	24.8729	0.0662	24.3509	23.4976	0.8533	23.5273	21.0431
401.25	24.9408	24.8764	0.0644	24.3595	23.5153	0.8442	23.5387	21.0687
402.5	24.9425	24.8797	0.0628	24.368	23.5328	0.8352	23.55	21.0942
403.75	24.9442	24.883	0.0612	24.3763	23.5502	0.8261	23.5612	21.1195
405	24.9458	24.8862	0.0596	24.3846	23.5673	0.8173	23.5723	21.1446
406.25	24.9473	24.8893	0.058	24.3928	23.5843	0.8085	23.5834	21.1697
407.5	24.9489	24.8923	0.0566	24.4009	23.6011	0.7998	23.5943	21.1945
408.75	24.9503	24.8952	0.0551	24.4089	23.6177	0.7912	23.6052	21.2193
410	24.9518	24.8981	0.0537	24.4168	23.6342	0.7826	23.616	21.2439
411.25	24.9532	24.9009	0.0523	24.4246	23.6504	0.7742	23.6268	21.2683
412.5	24.9545	24.9036	0.0509	24.4322	23.6665	0.7657	23.6375	21.2927
413.75	24.9559	24.9062	0.0497	24.4398	23.6824	0.7574	23.648	21.3169
415	24.9571	24.9088	0.0483	24.4473	23.6982	0.7491	23.6586	21.3409
416.25	24.9584	24.9113	0.0471	24.4547	23.7138	0.7409	23.669	21.3648
417.5	24.9596	24.9138	0.0458	24.4621	23.7292	0.7329	23.6793	21.3886
418.75	24.9608	24.9162	0.0446	24.4693	23.7444	0.7249	23.6896	21.4123
420	24.9619	24.9185	0.0434	24.4764	23.7595	0.7169	23.6998	21.4358
421.25	24.963	24.9208	0.0422	24.4835	23.7745	0.709	23.71	21.4592
422.5	24.9641	24.923	0.0411	24.4904	23.7892	0.7012	23.7201	21.4824
423.75	24.9652	24.9251	0.0401	24.4973	23.8038	0.6935	23.73	21.5056
425	24.9662	24.9272	0.039	24.5041	23.8183	0.6858	23.74	21.5285
426.25	24.9672	24.9292	0.038	24.5108	23.8325	0.6783	23.7498	21.5514
427.5	24.9682	24.9312	0.037	24.5174	23.8467	0.6707	23.7596	21.5741
428.75	24.9691	24.9331	0.036	24.5239	23.8607	0.6632	23.7693	21.5967

	Nd=5			Nd=2			Nd=1	
z (km)	Rock ‰ δ18O	Fluid ‰ δ18O	Δr-fl	Rock ‰ δ18O	Fluid ‰ δ18O	Δr-fl	Rock ‰ δ18O	Fluid ‰ δ18O
430	24.97	24.935	0.035	24.5304	23.8745	0.6559	23.7789	21.6192
431.25	24.9709	24.9369	0.034	24.5367	23.8881	0.6486	23.7885	21.6415
432.5	24.9718	24.9386	0.0332	24.543	23.9017	0.6413	23.798	21.6637
433.75	24.9726	24.9404	0.0322	24.5492	23.915	0.6342	23.8074	21.6858
435	24.9734	24.942	0.0314	24.5553	23.9283	0.627	23.8168	21.7078
436.25	24.9742	24.9437	0.0305	24.5614	23.9414	0.62	23.8261	21.7296
437.5	24.975	24.9453	0.0297	24.5674	23.9543	0.6131	23.8353	21.7513
438.75	24.9757	24.9468	0.0289	24.5733	23.9671	0.6062	23.8445	21.7729
440	24.9765	24.9483	0.0282	24.5791	23.9797	0.5994	23.8536	21.7944
441.25	24.9772	24.9502	0.027	24.5848	23.9922	0.5926	23.8626	21.8157
442.5	24.9778	24.9516	0.0262	24.5905	24.0046	0.5859	23.8716	21.8369
443.75	24.9785	24.953	0.0255	24.5961	24.0169	0.5792	23.8805	21.858
445	24.9792	24.9543	0.0249	24.6016	24.029	0.5726	23.8893	21.879
446.25	24.9798	24.9556	0.0242	24.6071	24.0409	0.5662	23.8981	21.8998
447.5	24.9804	24.9569	0.0235	24.6125	24.0528	0.5597	23.9068	21.9205
448.75	24.981	24.9582	0.0228	24.6178	24.0644	0.5534	23.9154	21.9411
450	24.9816	24.9594	0.0222	24.6231	24.076	0.5471	23.924	21.9616
451.25	24.9821	24.9605	0.0216	24.6283	24.0875	0.5408	23.9325	21.982
452.5	24.9827	24.9617	0.021	24.6334	24.0988	0.5346	23.9409	22.0022
453.75	24.9832	24.9628	0.0204	24.6384	24.1099	0.5285	23.9493	22.0223
455	24.9837	24.9639	0.0198	24.6434	24.121	0.5224	23.9576	22.0423
456.25	24.9842	24.9649	0.0193	24.6483	24.1319	0.5164	23.9659	22.0622
457.5	24.9847	24.9659	0.0188	24.6532	24.1427	0.5105	23.9741	22.082
458.75	24.9851	24.9669	0.0182	24.658	24.1534	0.5046	23.9823	22.1016
460	24.9856	24.9679	0.0177	24.6627	24.164	0.4987	23.9903	22.1212
461.25	24.986	24.9688	0.0172	24.6674	24.1744	0.493	23.9984	22.1406
462.5	24.9865	24.9697	0.0168	24.672	24.1847	0.4873	24.0063	22.1599
463.75	24.9869	24.9706	0.0163	24.6766	24.195	0.4816	24.0142	22.1791
465	24.9873	24.9715	0.0158	24.6811	24.205	0.4761	24.0221	22.1982
466.25	24.9877	24.9723	0.0154	24.6855	24.215	0.4705	24.0299	22.2171
467.5	24.9881	24.9731	0.015	24.6899	24.2249	0.465	24.0376	22.236
468.75	24.9884	24.9739	0.0145	24.6942	24.2346	0.4596	24.0453	22.2547
470	24.9888	24.9747	0.0141	24.6985	24.2443	0.4542	24.0529	22.2733
471.25	24.9891	24.9754	0.0137	24.7027	24.2538	0.4489	24.0604	22.2919
472.5	24.9895	24.9762	0.0133	24.7068	24.2632	0.4436	24.068	22.3103
473.75	24.9898	24.9769	0.0129	24.7109	24.2725	0.4384	24.0754	22.3286
475	24.9901	24.9776	0.0125	24.715	24.2817	0.4333	24.0828	22.3467
476.25	24.9904	24.9782	0.0122	24.7189	24.2908	0.4281	24.0901	22.3648
477.5	24.9907	24.9789	0.0118	24.7229	24.2998	0.4231	24.0974	22.3828
478.75	24.991	24.9795	0.0115	24.7268	24.3086	0.4182	24.1046	22.4006
480	24.9913	24.9801	0.0112	24.7306	24.3174	0.4132	24.1118	22.4184
481.25	24.9915	24.9807	0.0108	24.7344	24.3261	0.4083	24.1189	22.436
482.5	24.9918	24.9817	0.0101	24.7381	24.3347	0.4034	24.126	22.4536

	Nd=5			Nd=2			Nd=1	
z (km)	Rock ‰ δ18O	Fluid ‰ δ18O	Δr-fl	Rock ‰ δ18O	Fluid ‰ δ18O	Δr-fl	Rock ‰ δ18O	Fluid ‰ δ18O
483.75	24.9921	24.9823	0.0098	24.7418	24.3431	0.3987	24.133	22.471
485	24.9923	24.9828	0.0095	24.7454	24.3515	0.3939	24.14	22.4883
486.25	24.9926	24.9833	0.0093	24.749	24.3598	0.3892	24.1469	22.5056
487.5	24.9928	24.9838	0.009	24.7526	24.368	0.3846	24.1538	22.5227
488.75	24.993	24.9843	0.0087	24.7561	24.3761	0.38	24.1606	22.5397
490	24.9932	24.9848	0.0084	24.7595	24.3841	0.3754	24.1673	22.5566
491.25	24.9934	24.9852	0.0082	24.7629	24.3919	0.371	24.174	22.5734
492.5	24.9937	24.9857	0.008	24.7663	24.3997	0.3666	24.1807	22.5901
493.75	24.9939	24.9861	0.0078	24.7696	24.4075	0.3621	24.1873	22.6067
495	24.994	24.9865	0.0075	24.7729	24.4151	0.3578	24.1939	22.6232
496.25	24.9942	24.987	0.0072	24.7761	24.4226	0.3535	24.2004	22.6396
497.5	24.9944	24.9874	0.007	24.7793	24.43	0.3493	24.2068	22.6559
498.75	24.9946	24.9877	0.0069	24.7824	24.4374	0.345	24.2132	22.6721
500	24.9948	24.9881	0.0067	24.7855	24.4447	0.3408	24.2196	22.6882

		Nd=0.75				Nd=0.5	
z (km)	Δr-fl	Rock ‰ δ18O	Fluid ‰ δ18O	Δr-fl	Rock ‰ δ18O	Fluid ‰ δ18O	Δr-fl
0	7.7255	13.9197	4	9.9197	16.7371	4	12.7371
1.25	7.7297	13.9764	4.0701	9.9063	16.7707	4.06	12.7107
2.5	7.7334	14.0329	4.1402	9.8927	16.8042	4.1199	12.6843
3.75	7.7368	14.0892	4.2102	9.879	16.8376	4.1797	12.6579
5	7.7397	14.1452	4.2802	9.865	16.8708	4.2394	12.6314
6.25	7.7422	14.2009	4.35	9.8509	16.9039	4.299	12.6049
7.5	7.7444	14.2564	4.4198	9.8366	16.9369	4.3585	12.5784
8.75	7.7461	14.3117	4.4895	9.8222	16.9697	4.4178	12.5519
10	7.7474	14.3667	4.5592	9.8075	17.0025	4.4771	12.5254
11.25	7.7484	14.4215	4.6288	9.7927	17.0351	4.5362	12.4989
12.5	7.7489	14.4761	4.6982	9.7779	17.0676	4.5953	12.4723
13.75	7.7491	14.5304	4.7677	9.7627	17.1	4.6542	12.4458
15	7.749	14.5845	4.837	9.7475	17.1323	4.713	12.4193
16.25	7.7484	14.6383	4.9062	9.7321	17.1644	4.7717	12.3927
17.5	7.7475	14.6919	4.9754	9.7165	17.1965	4.8303	12.3662
18.75	7.7463	14.7453	5.0445	9.7008	17.2284	4.8888	12.3396
20	7.7446	14.7984	5.1135	9.6849	17.2602	4.9472	12.313
21.25	7.7426	14.8513	5.1824	9.6689	17.2919	5.0055	12.2864
22.5	7.7403	14.904	5.2512	9.6528	17.3234	5.0636	12.2598
23.75	7.7376	14.9564	5.32	9.6364	17.3549	5.1217	12.2332
25	7.7346	15.0086	5.3886	9.62	17.3862	5.1796	12.2066
26.25	7.7313	15.0606	5.4572	9.6034	17.4174	5.2375	12.1799
27.5	7.7276	15.1123	5.5257	9.5866	17.4486	5.2952	12.1534
28.75	7.7236	15.1638	5.594	9.5698	17.4795	5.3528	12.1267
30	7.7193	15.2151	5.6623	9.5528	17.5104	5.4103	12.1001
31.25	7.7146	15.2661	5.7305	9.5356	17.5412	5.4677	12.0735
32.5	7.7097	15.317	5.7986	9.5184	17.5718	5.5249	12.0469
33.75	7.7044	15.3676	5.8665	9.5011	17.6024	5.5821	12.0203
35	7.6988	15.4179	5.9344	9.4835	17.6328	5.6392	11.9936
36.25	7.6929	15.4681	6.0022	9.4659	17.6631	5.6961	11.967
37.5	7.6867	15.518	6.0699	9.4481	17.6933	5.7529	11.9404
38.75	7.6803	15.5677	6.1375	9.4302	17.7234	5.8096	11.9138
40	7.6735	15.6172	6.2049	9.4123	17.7534	5.8662	11.8872
41.25	7.6665	15.6664	6.2723	9.3941	17.7833	5.9227	11.8606
42.5	7.6591	15.7154	6.3396	9.3758	17.813	5.9791	11.8339
43.75	7.6515	15.7642	6.4067	9.3575	17.8427	6.0354	11.8073
45	7.6436	15.8128	6.4738	9.339	17.8722	6.0916	11.7806
46.25	7.6355	15.8612	6.5407	9.3205	17.9017	6.1476	11.7541
47.5	7.627	15.9093	6.6075	9.3018	17.931	6.2035	11.7275
48.75	7.6183	15.9573	6.6742	9.2831	17.9602	6.2594	11.7008
50	7.6093	16.005	6.7408	9.2642	17.9893	6.3151	11.6742
51.25	7.6001	16.0525	6.8073	9.2452	18.0183	6.3707	11.6476
52.5	7.5906	16.0997	6.8737	9.226	18.0472	6.4261	11.6211

z (km)	Δr-fl	Rock ‰ δ18O	Nd=0.75 Fluid ‰ δ18O	Δr-fl	Rock ‰ δ18O	Nd=0.5 Fluid ‰ δ18O	Δr-fl
53.75	7.5809	16.1468	6.94	9.2068	18.076	6.4815	11.5945
55	7.571	16.1937	7.0061	9.1876	18.1046	6.5368	11.5678
56.25	7.5607	16.2403	7.0722	9.1681	18.1332	6.5919	11.5413
57.5	7.5503	16.2867	7.1381	9.1486	18.1617	6.647	11.5147
58.75	7.5396	16.3329	7.2039	9.129	18.19	6.7019	11.4881
60	7.5286	16.3789	7.2695	9.1094	18.2183	6.7567	11.4616
61.25	7.5175	16.4247	7.3351	9.0896	18.2464	6.8114	11.435
62.5	7.5062	16.4703	7.4005	9.0698	18.2744	6.866	11.4084
63.75	7.4945	16.5156	7.4658	9.0498	18.3024	6.9204	11.382
65	7.4826	16.5608	7.531	9.0298	18.3302	6.9748	11.3554
66.25	7.4706	16.6058	7.5961	9.0097	18.3579	7.029	11.3289
67.5	7.4583	16.6505	7.6611	8.9894	18.3856	7.0832	11.3024
68.75	7.4459	16.695	7.7259	8.9691	18.4131	7.1372	11.2759
70	7.4332	16.7394	7.7906	8.9488	18.4405	7.1911	11.2494
71.25	7.4203	16.7835	7.8551	8.9284	18.4678	7.2449	11.2229
72.5	7.4072	16.8274	7.9196	8.9078	18.495	7.2985	11.1965
73.75	7.3939	16.8711	7.9839	8.8872	18.5221	7.3521	11.17
75	7.3805	16.9146	8.0481	8.8665	18.5491	7.4055	11.1436
76.25	7.3667	16.9579	8.1121	8.8458	18.576	7.4589	11.1171
77.5	7.3529	17.0011	8.176	8.8251	18.6028	7.5121	11.0907
78.75	7.3388	17.044	8.2398	8.8042	18.6295	7.5652	11.0643
80	7.3246	17.0867	8.3035	8.7832	18.6561	7.6182	11.0379
81.25	7.3102	17.1292	8.367	8.7622	18.6827	7.6711	11.0116
82.5	7.2956	17.1715	8.4304	8.7411	18.7091	7.7239	10.9852
83.75	7.2808	17.2136	8.4937	8.7199	18.7354	7.7765	10.9589
85	7.2659	17.2555	8.5568	8.6987	18.7616	7.829	10.9326
86.25	7.2507	17.2972	8.6198	8.6774	18.7877	7.8815	10.9062
87.5	7.2354	17.3388	8.6827	8.6561	18.8137	7.9338	10.8799
88.75	7.22	17.3801	8.7454	8.6347	18.8396	7.986	10.8536
90	7.2044	17.4212	8.808	8.6132	18.8654	8.0381	10.8273
91.25	7.1886	17.4622	8.8705	8.5917	18.8911	8.09	10.8011
92.5	7.1727	17.5029	8.9328	8.5701	18.9167	8.1419	10.7748
93.75	7.1567	17.5435	8.995	8.5485	18.9423	8.1936	10.7487
95	7.1404	17.5838	9.057	8.5268	18.9677	8.2453	10.7224
96.25	7.124	17.624	9.1189	8.5051	18.993	8.2968	10.6962
97.5	7.1076	17.664	9.1807	8.4833	19.0182	8.3482	10.67
98.75	7.0908	17.7038	9.2423	8.4615	19.0434	8.3995	10.6439
100	7.0741	17.7434	9.3038	8.4396	19.0684	8.4507	10.6177
101.25	7.0571	17.7828	9.3651	8.4177	19.0934	8.5017	10.5917
102.5	7.04	17.822	9.4263	8.3957	19.1182	8.5527	10.5655
103.75	7.0229	17.861	9.4874	8.3736	19.143	8.6035	10.5395
105	7.0056	17.8999	9.5483	8.3516	19.1676	8.6542	10.5134
106.25	6.9881	17.9386	9.609	8.3296	19.1922	8.7048	10.4874

		Nd=0.75				Nd=0.5	
		Rock ‰	Fluid ‰		Rock ‰	Fluid ‰	
z (km)	Δr-fl	δ18O	δ18O	Δr-fl	δ18O	δ18O	Δr-fl
107.5	6.9705	17.9771	9.6697	8.3074	19.2167	8.7553	10.4614
108.75	6.9527	18.0154	9.7302	8.2852	19.2411	8.8057	10.4354
110	6.9349	18.0535	9.7905	8.263	19.2653	8.856	10.4093
111.25	6.917	18.0914	9.8507	8.2407	19.2895	8.9061	10.3834
112.5	6.8989	18.1292	9.9107	8.2185	19.3136	8.9562	10.3574
113.75	6.8807	18.1667	9.9706	8.1961	19.3377	9.0061	10.3316
115	6.8625	18.2041	10.0304	8.1737	19.3616	9.0559	10.3057
116.25	6.844	18.2413	10.09	8.1513	19.3854	9.1056	10.2798
117.5	6.8256	18.2784	10.1495	8.1289	19.4091	9.1552	10.2539
118.75	6.807	18.3152	10.2088	8.1064	19.4328	9.2047	10.2281
120	6.7882	18.3519	10.268	8.0839	19.4563	9.254	10.2023
121.25	6.7694	18.3884	10.327	8.0614	19.4798	9.3033	10.1765
122.5	6.7505	18.4247	10.3859	8.0388	19.5032	9.3524	10.1508
123.75	6.7315	18.4609	10.4446	8.0163	19.5265	9.4014	10.1251
125	6.7124	18.4968	10.5032	7.9936	19.5497	9.4503	10.0994
126.25	6.6932	18.5326	10.5616	7.971	19.5728	9.4991	10.0737
127.5	6.6739	18.5682	10.6199	7.9483	19.5958	9.5478	10.048
128.75	6.6546	18.6037	10.678	7.9257	19.6187	9.5964	10.0223
130	6.6351	18.639	10.736	7.903	19.6416	9.6448	9.9968
131.25	6.6155	18.6741	10.7938	7.8803	19.6643	9.6932	9.9711
132.5	6.596	18.709	10.8515	7.8575	19.687	9.7414	9.9456
133.75	6.5762	18.7438	10.909	7.8348	19.7096	9.7895	9.9201
135	6.5565	18.7784	10.9664	7.812	19.7321	9.8375	9.8946
136.25	6.5367	18.8128	11.0236	7.7892	19.7545	9.8854	9.8691
137.5	6.5167	18.8471	11.0807	7.7664	19.7768	9.9332	9.8436
138.75	6.4967	18.8811	11.1376	7.7435	19.799	9.9808	9.8182
140	6.4766	18.9151	11.1944	7.7207	19.8212	10.0284	9.7928
141.25	6.4565	18.9488	11.251	7.6978	19.8433	10.0758	9.7675
142.5	6.4363	18.9824	11.3074	7.675	19.8652	10.1231	9.7421
143.75	6.416	19.0158	11.3638	7.652	19.8871	10.1704	9.7167
145	6.3957	19.0491	11.4199	7.6292	19.9089	10.2175	9.6914
146.25	6.3754	19.0822	11.4759	7.6063	19.9307	10.2645	9.6662
147.5	6.3549	19.1151	11.5318	7.5833	19.9523	10.3113	9.641
148.75	6.3343	19.1479	11.5875	7.5604	19.9739	10.3581	9.6158
150	6.3138	19.1805	11.643	7.5375	19.9953	10.4048	9.5905
151.25	6.2933	19.213	11.6984	7.5146	20.0167	10.4513	9.5654
152.5	6.2726	19.2452	11.7536	7.4916	20.038	10.4977	9.5403
153.75	6.2518	19.2774	11.8087	7.4687	20.0593	10.544	9.5153
155	6.231	19.3093	11.8636	7.4457	20.0804	10.5902	9.4902
156.25	6.2102	19.3411	11.9184	7.4227	20.1015	10.6363	9.4652
157.5	6.1894	19.3728	11.973	7.3998	20.1224	10.6823	9.4401
158.75	6.1685	19.4043	12.0275	7.3768	20.1433	10.7282	9.4151
160	6.1476	19.4356	12.0818	7.3538	20.1642	10.774	9.3902

z (km)	Δr-fl	Rock ‰ δ18O	Nd=0.75 Fluid ‰ δ18O	Δr-fl	Rock ‰ δ18O	Nd=0.5 Fluid ‰ δ18O	Δr-fl
161.25	6.1266	19.4668	12.1359	7.3309	20.1849	10.8196	9.3653
162.5	6.1056	19.4978	12.1899	7.3079	20.2055	10.8651	9.3404
163.75	6.0845	19.5287	12.2437	7.285	20.2261	10.9106	9.3155
165	6.0634	19.5594	12.2974	7.262	20.2466	10.9559	9.2907
166.25	6.0423	19.59	12.351	7.239	20.267	11.0011	9.2659
167.5	6.0211	19.6204	12.4043	7.2161	20.2874	11.0462	9.2412
168.75	5.9999	19.6507	12.4575	7.1932	20.3076	11.0912	9.2164
170	5.9787	19.6808	12.5106	7.1702	20.3278	11.136	9.1918
171.25	5.9574	19.7107	12.5635	7.1472	20.3479	11.1808	9.1671
172.5	5.9361	19.7405	12.6162	7.1243	20.3679	11.2254	9.1425
173.75	5.9148	19.7702	12.6688	7.1014	20.3878	11.27	9.1178
175	5.8935	19.7997	12.7213	7.0784	20.4077	11.3144	9.0933
176.25	5.8722	19.8291	12.7735	7.0556	20.4275	11.3587	9.0688
177.5	5.8508	19.8583	12.8257	7.0326	20.4472	11.4029	9.0443
178.75	5.8294	19.8873	12.8776	7.0097	20.4668	11.447	9.0198
180	5.808	19.9163	12.9294	6.9869	20.4864	11.491	8.9954
181.25	5.7865	19.945	12.9811	6.9639	20.5059	11.5349	8.971
182.5	5.7651	19.9736	13.0326	6.941	20.5253	11.5787	8.9466
183.75	5.7437	20.0021	13.0839	6.9182	20.5446	11.6223	8.9223
185	5.7222	20.0305	13.1351	6.8954	20.5638	11.6659	8.8979
186.25	5.7007	20.0587	13.1861	6.8726	20.583	11.7093	8.8737
187.5	5.6792	20.0867	13.237	6.8497	20.6021	11.7526	8.8495
188.75	5.6577	20.1146	13.2877	6.8269	20.6211	11.7958	8.8253
190	5.6362	20.1424	13.3383	6.8041	20.6401	11.839	8.8011
191.25	5.6146	20.17	13.3886	6.7814	20.6589	11.882	8.7769
192.5	5.5931	20.1975	13.4389	6.7586	20.6777	11.9249	8.7528
193.75	5.5716	20.2248	13.489	6.7358	20.6965	11.9676	8.7289
195	5.55	20.252	13.5389	6.7131	20.7151	12.0103	8.7048
196.25	5.5284	20.2791	13.5887	6.6904	20.7337	12.0529	8.6808
197.5	5.5069	20.306	13.6383	6.6677	20.7522	12.0953	8.6569
198.75	5.4854	20.3328	13.6877	6.6451	20.7706	12.1377	8.6329
200	5.4639	20.3595	13.737	6.6225	20.789	12.1799	8.6091
201.25	5.4422	20.386	13.7862	6.5998	20.8073	12.2221	8.5852
202.5	5.4207	20.4124	13.8352	6.5772	20.8255	12.2641	8.5614
203.75	5.3992	20.4386	13.884	6.5546	20.8436	12.306	8.5376
205	5.3777	20.4647	13.9327	6.532	20.8617	12.3478	8.5139
206.25	5.3561	20.4907	13.9812	6.5095	20.8797	12.3895	8.4902
207.5	5.3346	20.5165	14.0296	6.4869	20.8976	12.4311	8.4665
208.75	5.3131	20.5423	14.0778	6.4645	20.9155	12.4726	8.4429
210	5.2915	20.5678	14.1258	6.442	20.9333	12.514	8.4193
211.25	5.27	20.5933	14.1737	6.4196	20.951	12.5552	8.3958
212.5	5.2485	20.6186	14.2215	6.3971	20.9686	12.5964	8.3722
213.75	5.2271	20.6438	14.269	6.3748	20.9862	12.6375	8.3487

		Nd=0.75				Nd=0.5	
		Rock ‰	Fluid ‰		Rock ‰	Fluid ‰	
z (km)	Δr-fl	δ18O	δ18O	Δr-fl	δ18O	δ18O	Δr-fl
215	5.2056	20.6688	14.3165	6.3523	21.0037	12.6784	8.3253
216.25	5.1841	20.6938	14.3637	6.3301	21.0211	12.7193	8.3018
217.5	5.1628	20.7185	14.4108	6.3077	21.0385	12.76	8.2785
218.75	5.1414	20.7432	14.4578	6.2854	21.0558	12.8006	8.2552
220	5.1199	20.7678	14.5046	6.2632	21.073	12.8412	8.2318
221.25	5.0985	20.7922	14.5513	6.2409	21.0902	12.8816	8.2086
222.5	5.0772	20.8164	14.5978	6.2186	21.1073	12.9219	8.1854
223.75	5.0558	20.8406	14.6441	6.1965	21.1243	12.9621	8.1622
225	5.0344	20.8646	14.6903	6.1743	21.1412	13.0022	8.139
226.25	5.0132	20.8885	14.7363	6.1522	21.1581	13.0422	8.1159
227.5	4.9919	20.9123	14.7822	6.1301	21.1749	13.0821	8.0928
228.75	4.9706	20.936	14.8279	6.1081	21.1917	13.1219	8.0698
230	4.9493	20.9595	14.8735	6.086	21.2084	13.1615	8.0469
231.25	4.9282	20.9829	14.9189	6.064	21.225	13.2011	8.0239
232.5	4.907	21.0062	14.9641	6.0421	21.2415	13.2406	8.0009
233.75	4.8858	21.0294	15.0092	6.0202	21.258	13.2799	7.9781
235	4.8646	21.0524	15.0542	5.9982	21.2744	13.3192	7.9552
236.25	4.8435	21.0754	15.099	5.9764	21.2908	13.3583	7.9325
237.5	4.8224	21.0982	15.1436	5.9546	21.3071	13.3974	7.9097
238.75	4.8013	21.1209	15.1881	5.9328	21.3233	13.4363	7.887
240	4.7803	21.1434	15.2325	5.9109	21.3395	13.4752	7.8643
241.25	4.7593	21.1659	15.2767	5.8892	21.3556	13.5139	7.8417
242.5	4.7383	21.1882	15.3207	5.8675	21.3716	13.5525	7.8191
243.75	4.7174	21.2104	15.3646	5.8458	21.3875	13.5911	7.7964
245	4.6965	21.2325	15.4083	5.8242	21.4034	13.6295	7.7739
246.25	4.6755	21.2545	15.4519	5.8026	21.4193	13.6678	7.7515
247.5	4.6548	21.2764	15.4953	5.7811	21.435	13.706	7.729
248.75	4.6339	21.2981	15.5386	5.7595	21.4508	13.7442	7.7066
250	4.6131	21.3198	15.5817	5.7381	21.4664	13.7822	7.6842
251.25	4.5924	21.3413	15.6246	5.7167	21.482	13.8201	7.6619
252.5	4.5717	21.3627	15.6675	5.6952	21.4975	13.8579	7.6396
253.75	4.551	21.384	15.7101	5.6739	21.513	13.8956	7.6174
255	4.5303	21.4051	15.7526	5.6525	21.5284	13.9332	7.5952
256.25	4.5098	21.4262	15.795	5.6312	21.5437	13.9707	7.573
257.5	4.4892	21.4472	15.8372	5.61	21.559	14.0081	7.5509
258.75	4.4687	21.468	15.8793	5.5887	21.5742	14.0454	7.5288
260	4.4482	21.4888	15.9212	5.5676	21.5893	14.0826	7.5067
261.25	4.4277	21.5094	15.963	5.5464	21.6044	14.1197	7.4847
262.5	4.4073	21.5299	16.0046	5.5253	21.6194	14.1566	7.4628
263.75	4.387	21.5503	16.046	5.5043	21.6344	14.1935	7.4409
265	4.3666	21.5706	16.0873	5.4833	21.6493	14.2303	7.419
266.25	4.3464	21.5908	16.1285	5.4623	21.6641	14.267	7.3971
267.5	4.3261	21.6109	16.1695	5.4414	21.6789	14.3036	7.3753

z (km)	Δr-fl	Rock ‰ δ18O	Nd=0.75 Fluid ‰ δ18O	Δr-fl	Rock ‰ δ18O	Nd=0.5 Fluid ‰ δ18O	Δr-fl
268.75	4.306	21.6308	16.2104	5.4204	21.6936	14.3401	7.3535
270	4.2858	21.6507	16.2511	5.3996	21.7083	14.3764	7.3319
271.25	4.2657	21.6705	16.2917	5.3788	21.7229	14.4127	7.3102
272.5	4.2456	21.6901	16.3321	5.358	21.7374	14.4489	7.2885
273.75	4.2257	21.7097	16.3724	5.3373	21.7519	14.485	7.2669
275	4.2056	21.7291	16.4125	5.3166	21.7664	14.521	7.2454
276.25	4.1857	21.7484	16.4525	5.2959	21.7807	14.5569	7.2238
277.5	4.1658	21.7677	16.4923	5.2754	21.795	14.5926	7.2024
278.75	4.146	21.7868	16.532	5.2548	21.8093	14.6283	7.181
280	4.1262	21.8058	16.5716	5.2342	21.8235	14.6639	7.1596
281.25	4.1064	21.8248	16.611	5.2138	21.8376	14.6994	7.1382
282.5	4.0867	21.8436	16.6502	5.1934	21.8517	14.7348	7.1169
283.75	4.0671	21.8623	16.6893	5.173	21.8657	14.7701	7.0956
285	4.0475	21.8809	16.7283	5.1526	21.8797	14.8052	7.0745
286.25	4.028	21.8994	16.7671	5.1323	21.8936	14.8403	7.0533
287.5	4.0084	21.9179	16.8058	5.1121	21.9074	14.8753	7.0321
288.75	3.989	21.9362	16.8443	5.0919	21.9212	14.9102	7.011
290	3.9696	21.9544	16.8827	5.0717	21.935	14.945	6.99
291.25	3.9502	21.9725	16.9209	5.0516	21.9486	14.9797	6.9689
292.5	3.931	21.9906	16.959	5.0316	21.9623	15.0143	6.948
293.75	3.9116	22.0085	16.9969	5.0116	21.9758	15.0488	6.927
295	3.8924	22.0263	17.0347	4.9916	21.9894	15.0832	6.9062
296.25	3.8733	22.0441	17.0724	4.9717	22.0028	15.1175	6.8853
297.5	3.8543	22.0617	17.1099	4.9518	22.0162	15.1517	6.8645
298.75	3.8352	22.0792	17.1473	4.9319	22.0296	15.1858	6.8438
300	3.8162	22.0967	17.1845	4.9122	22.0429	15.2198	6.8231
301.25	3.7972	22.114	17.2216	4.8924	22.0561	15.2538	6.8023
302.5	3.7783	22.1313	17.2586	4.8727	22.0693	15.2876	6.7817
303.75	3.7595	22.1485	17.2954	4.8531	22.0824	15.3213	6.7611
305	3.7408	22.1655	17.3321	4.8334	22.0955	15.3549	6.7406
306.25	3.722	22.1825	17.3686	4.8139	22.1085	15.3885	6.72
307.5	3.7034	22.1994	17.405	4.7944	22.1215	15.4219	6.6996
308.75	3.6848	22.2162	17.4412	4.775	22.1344	15.4552	6.6792
310	3.6662	22.2329	17.4773	4.7556	22.1473	15.4885	6.6588
311.25	3.6477	22.2495	17.5133	4.7362	22.1601	15.5216	6.6385
312.5	3.6293	22.266	17.5491	4.7169	22.1728	15.5547	6.6181
313.75	3.6108	22.2824	17.5848	4.6976	22.1855	15.5876	6.5979
315	3.5925	22.2988	17.6204	4.6784	22.1982	15.6205	6.5777
316.25	3.5742	22.315	17.6558	4.6592	22.2108	15.6533	6.5575
317.5	3.556	22.3312	17.6911	4.6401	22.2233	15.686	6.5373
318.75	3.5378	22.3472	17.7262	4.621	22.2358	15.7185	6.5173
320	3.5198	22.3632	17.7612	4.602	22.2483	15.751	6.4973
321.25	3.5017	22.3791	17.7961	4.583	22.2607	15.7834	6.4773

		Nd=0.75				Nd=0.5	
z (km)	Δr-fl	Rock ‰ δ18O	Fluid ‰ δ18O	Δr-fl	Rock ‰ δ18O	Fluid ‰ δ18O	Δr-fl
322.5	3.4836	22.3949	17.8308	4.5641	22.273	15.8157	6.4573
323.75	3.4657	22.4106	17.8654	4.5452	22.2853	15.8479	6.4374
325	3.4478	22.4263	17.8999	4.5264	22.2975	15.88	6.4175
326.25	3.43	22.4418	17.9342	4.5076	22.3097	15.912	6.3977
327.5	3.4122	22.4573	17.9684	4.4889	22.3219	15.944	6.3779
328.75	3.3946	22.4726	18.0024	4.4702	22.3339	15.9758	6.3581
330	3.3769	22.4879	18.0363	4.4516	22.346	16.0075	6.3385
331.25	3.3593	22.5031	18.0701	4.433	22.358	16.0392	6.3188
332.5	3.3418	22.5182	18.1037	4.4145	22.3699	16.0707	6.2992
333.75	3.3243	22.5333	18.1372	4.3961	22.3818	16.1022	6.2796
335	3.3068	22.5482	18.1706	4.3776	22.3936	16.1336	6.26
336.25	3.2895	22.5631	18.2039	4.3592	22.4054	16.1649	6.2405
337.5	3.2722	22.5779	18.237	4.3409	22.4172	16.196	6.2212
338.75	3.255	22.5926	18.27	4.3226	22.4289	16.2271	6.2018
340	3.2378	22.6072	18.3028	4.3044	22.4405	16.2581	6.1824
341.25	3.2206	22.6218	18.3355	4.2863	22.4521	16.2891	6.163
342.5	3.2036	22.6362	18.3681	4.2681	22.4636	16.3199	6.1437
343.75	3.1866	22.6506	18.4005	4.2501	22.4751	16.3506	6.1245
345	3.1696	22.6649	18.4329	4.232	22.4866	16.3813	6.1053
346.25	3.1528	22.6791	18.465	4.2141	22.498	16.4118	6.0862
347.5	3.1359	22.6933	18.4971	4.1962	22.5094	16.4423	6.0671
348.75	3.1191	22.7073	18.529	4.1783	22.5207	16.4726	6.0481
350	3.1025	22.7213	18.5608	4.1605	22.5319	16.5029	6.029
351.25	3.0858	22.7352	18.5925	4.1427	22.5431	16.5331	6.01
352.5	3.0692	22.749	18.624	4.125	22.5543	16.5632	5.9911
353.75	3.0526	22.7628	18.6555	4.1073	22.5654	16.5932	5.9722
355	3.0362	22.7765	18.6867	4.0898	22.5765	16.6231	5.9534
356.25	3.0198	22.7901	18.7179	4.0722	22.5875	16.653	5.9345
357.5	3.0035	22.8036	18.7489	4.0547	22.5985	16.6827	5.9158
358.75	2.9872	22.817	18.7798	4.0372	22.6095	16.7124	5.8971
360	2.971	22.8304	18.8106	4.0198	22.6203	16.7419	5.8784
361.25	2.9548	22.8437	18.8412	4.0025	22.6312	16.7714	5.8598
362.5	2.9387	22.8569	18.8717	3.9852	22.642	16.8008	5.8412
363.75	2.9226	22.87	18.9021	3.9679	22.6527	16.8301	5.8226
365	2.9067	22.8831	18.9324	3.9507	22.6635	16.8593	5.8042
366.25	2.8908	22.8961	18.9625	3.9336	22.6741	16.8884	5.7857
367.5	2.8749	22.909	18.9926	3.9164	22.6847	16.9175	5.7672
368.75	2.8592	22.9219	19.0225	3.8994	22.6953	16.9464	5.7489
370	2.8434	22.9347	19.0522	3.8825	22.7058	16.9753	5.7305
371.25	2.8277	22.9474	19.0819	3.8655	22.7163	17.0041	5.7122
372.5	2.8121	22.96	19.1114	3.8486	22.7268	17.0328	5.694
373.75	2.7966	22.9726	19.1408	3.8318	22.7372	17.0614	5.6758
375	2.7811	22.985	19.1701	3.8149	22.7475	17.0899	5.6576

		Nd=0.75				Nd=0.5	
		Rock ‰	Fluid ‰		Rock ‰	Fluid ‰	
z (km)	**Δr-fl**	**δ18O**	**δ18O**	**Δr-fl**	**δ18O**	**δ18O**	**Δr-fl**
376.25	2.7657	22.9975	19.1992	3.7983	22.7578	17.1183	5.6395
377.5	2.7503	23.0098	19.2282	3.7816	22.7681	17.1466	5.6215
378.75	2.7349	23.0221	19.2571	3.765	22.7783	17.1749	5.6034
380	2.7198	23.0343	19.2859	3.7484	22.7885	17.2031	5.5854
381.25	2.7045	23.0464	19.3146	3.7318	22.7986	17.2312	5.5674
382.5	2.6895	23.0585	19.3431	3.7154	22.8087	17.2592	5.5495
383.75	2.6744	23.0705	19.3716	3.6989	22.8188	17.2871	5.5317
385	2.6594	23.0825	19.3999	3.6826	22.8288	17.3149	5.5139
386.25	2.6445	23.0943	19.428	3.6663	22.8388	17.3427	5.4961
387.5	2.6296	23.1061	19.4561	3.65	22.8487	17.3703	5.4784
388.75	2.6148	23.1178	19.484	3.6338	22.8586	17.3979	5.4607
390	2.6	23.1295	19.5119	3.6176	22.8684	17.4254	5.443
391.25	2.5853	23.1411	19.5396	3.6015	22.8782	17.4528	5.4254
392.5	2.5706	23.1526	19.5672	3.5854	22.888	17.4801	5.4079
393.75	2.5561	23.1641	19.5946	3.5695	22.8977	17.5074	5.3903
395	2.5416	23.1755	19.622	3.5535	22.9074	17.5345	5.3729
396.25	2.5272	23.1868	19.6492	3.5376	22.917	17.5616	5.3554
397.5	2.5127	23.1981	19.6763	3.5218	22.9266	17.5886	5.338
398.75	2.4984	23.2093	19.7033	3.506	22.9362	17.6155	5.3207
400	2.4842	23.2205	19.7302	3.4903	22.9457	17.6423	5.3034
401.25	2.47	23.2315	19.757	3.4745	22.9551	17.6691	5.286
402.5	2.4558	23.2426	19.7836	3.459	22.9646	17.6957	5.2689
403.75	2.4417	23.2535	19.8102	3.4433	22.974	17.7223	5.2517
405	2.4277	23.2644	19.8366	3.4278	22.9833	17.7488	5.2345
406.25	2.4137	23.2752	19.8629	3.4123	22.9926	17.7752	5.2174
407.5	2.3998	23.286	19.8891	3.3969	23.0019	17.8016	5.2003
408.75	2.3859	23.2967	19.9152	3.3815	23.0111	17.8278	5.1833
410	2.3721	23.3073	19.9412	3.3661	23.0203	17.854	5.1663
411.25	2.3585	23.3179	19.967	3.3509	23.0295	17.8801	5.1494
412.5	2.3448	23.3284	19.9928	3.3356	23.0386	17.9061	5.1325
413.75	2.3311	23.3389	20.0184	3.3205	23.0477	17.932	5.1157
415	2.3177	23.3493	20.0439	3.3054	23.0567	17.9579	5.0988
416.25	2.3042	23.3596	20.0693	3.2903	23.0657	17.9836	5.0821
417.5	2.2907	23.3699	20.0946	3.2753	23.0747	18.0093	5.0654
418.75	2.2773	23.3801	20.1198	3.2603	23.0836	18.0349	5.0487
420	2.264	23.3903	20.1449	3.2454	23.0925	18.0604	5.0321
421.25	2.2508	23.4004	20.1699	3.2305	23.1013	18.0859	5.0154
422.5	2.2377	23.4104	20.1947	3.2157	23.1101	18.1112	4.9989
423.75	2.2244	23.4204	20.2195	3.2009	23.1189	18.1365	4.9824
425	2.2115	23.4303	20.2441	3.1862	23.1277	18.1617	4.966
426.25	2.1984	23.4402	20.2686	3.1716	23.1363	18.1869	4.9494
427.5	2.1855	23.45	20.293	3.157	23.145	18.2119	4.9331
428.75	2.1726	23.4597	20.3174	3.1423	23.1536	18.2369	4.9167

			Nd=0.75			Nd=0.5	
		Rock ‰	Fluid ‰		Rock ‰	Fluid ‰	
z (km)	Δr-fl	δ18O	δ18O	Δr-fl	δ18O	δ18O	Δr-fl
430	2.1597	23.4694	20.3416	3.1278	23.1622	18.2618	4.9004
431.25	2.147	23.4791	20.3657	3.1134	23.1708	18.2866	4.8842
432.5	2.1343	23.4886	20.3896	3.099	23.1793	18.3113	4.868
433.75	2.1216	23.4982	20.4135	3.0847	23.1877	18.336	4.8517
435	2.109	23.5076	20.4373	3.0703	23.1962	18.3606	4.8356
436.25	2.0965	23.5171	20.461	3.0561	23.2046	18.3851	4.8195
437.5	2.084	23.5264	20.4845	3.0419	23.213	18.4095	4.8035
438.75	2.0716	23.5357	20.508	3.0277	23.2213	18.4338	4.7875
440	2.0592	23.545	20.5314	3.0136	23.2296	18.4581	4.7715
441.25	2.0469	23.5542	20.5546	2.9996	23.2378	18.4823	4.7555
442.5	2.0347	23.5633	20.5778	2.9855	23.2461	18.5064	4.7397
443.75	2.0225	23.5724	20.6008	2.9716	23.2543	18.5305	4.7238
445	2.0103	23.5814	20.6237	2.9577	23.2624	18.5544	4.708
446.25	1.9983	23.5904	20.6466	2.9438	23.2705	18.5783	4.6922
447.5	1.9863	23.5994	20.6693	2.9301	23.2786	18.6021	4.6765
448.75	1.9743	23.6082	20.6919	2.9163	23.2867	18.6259	4.6608
450	1.9624	23.6171	20.7145	2.9026	23.2947	18.6495	4.6452
451.25	1.9505	23.6258	20.7369	2.8889	23.3026	18.6731	4.6295
452.5	1.9387	23.6346	20.7592	2.8754	23.3106	18.6966	4.614
453.75	1.927	23.6432	20.7814	2.8618	23.3185	18.7201	4.5984
455	1.9153	23.6519	20.8036	2.8483	23.3264	18.7434	4.583
456.25	1.9037	23.6604	20.8256	2.8348	23.3342	18.7667	4.5675
457.5	1.8921	23.669	20.8475	2.8215	23.342	18.7899	4.5521
458.75	1.8807	23.6774	20.8693	2.8081	23.3498	18.813	4.5368
460	1.8691	23.6858	20.8911	2.7947	23.3575	18.8361	4.5214
461.25	1.8578	23.6942	20.9127	2.7815	23.3652	18.8591	4.5061
462.5	1.8464	23.7025	20.9342	2.7683	23.3729	18.882	4.4909
463.75	1.8351	23.7108	20.9556	2.7552	23.3806	18.9049	4.4757
465	1.8239	23.719	20.977	2.742	23.3882	18.9276	4.4606
466.25	1.8128	23.7272	20.9982	2.729	23.3957	18.9503	4.4454
467.5	1.8016	23.7353	21.0193	2.716	23.4033	18.9729	4.4304
468.75	1.7906	23.7434	21.0404	2.703	23.4108	18.9955	4.4153
470	1.7796	23.7514	21.0613	2.6901	23.4183	19.018	4.4003
471.25	1.7685	23.7594	21.0822	2.6772	23.4257	19.0404	4.3853
472.5	1.7577	23.7674	21.1029	2.6645	23.4331	19.0627	4.3704
473.75	1.7468	23.7752	21.1236	2.6516	23.4405	19.0849	4.3556
475	1.7361	23.7831	21.1441	2.639	23.4478	19.1071	4.3407
476.25	1.7253	23.7909	21.1646	2.6263	23.4552	19.1292	4.326
477.5	1.7146	23.7986	21.185	2.6136	23.4624	19.1513	4.3111
478.75	1.704	23.8063	21.2052	2.6011	23.4697	19.1733	4.2964
480	1.6934	23.814	21.2254	2.5886	23.4769	19.1952	4.2817
481.25	1.6829	23.8216	21.2455	2.5761	23.4841	19.217	4.2671
482.5	1.6724	23.8292	21.2655	2.5637	23.4913	19.2387	4.2526

			Nd=0.75			Nd=0.5	
		Rock ‰	Fluid ‰		Rock ‰	Fluid ‰	
z (km)	Δr-fl	δ18O	δ18O	Δr-fl	δ18O	δ18O	Δr-fl
483.75	1.662	23.8367	21.2854	2.5513	23.4984	19.2604	4.238
485	1.6517	23.8442	21.3052	2.539	23.5055	19.282	4.2235
486.25	1.6413	23.8516	21.3249	2.5267	23.5125	19.3036	4.2089
487.5	1.6311	23.859	21.3445	2.5145	23.5196	19.3251	4.1945
488.75	1.6209	23.8663	21.3641	2.5022	23.5266	19.3465	4.1801
490	1.6107	23.8736	21.3835	2.4901	23.5335	19.3678	4.1657
491.25	1.6006	23.8809	21.4029	2.478	23.5405	19.3891	4.1514
492.5	1.5906	23.8881	21.4221	2.466	23.5474	19.4103	4.1371
493.75	1.5806	23.8953	21.4413	2.454	23.5543	19.4314	4.1229
495	1.5707	23.9024	21.4604	2.442	23.5611	19.4524	4.1087
496.25	1.5608	23.9095	21.4794	2.4301	23.5679	19.4734	4.0945
497.5	1.5509	23.9165	21.4983	2.4182	23.5747	19.4943	4.0804
498.75	1.5411	23.9235	21.5171	2.4064	23.5815	19.5152	4.0663
500	1.5314	23.9305	21.5358	2.3947	23.5882	19.536	4.0522

Appendix F

F.1 Isotope Data Assay Pulps

Sample	CO2 (ppm)	+/-	δ13C (VPDB) (IRMS)	δ13C (VPDB) (LGR)	+/-	δ18O (VSMOW) (IRMS)	δ18O (VSMOW) (LGR)	+/-
BZ-965C-0880	112,434	112.4		-1	1.2		18.8	3.4
BZ-965C-0885	130,384	94.6		-0.9	0.9		20.5	2.7
BZ-965C-0885	54,632	82.6		-0.8	1.8		23.8	6.9
BZ-965C-0890	146,044	112.3		-1.3	0.8		22.6	2.4
BZ-965C-0895	148,031	116.2		-1.4	0.8		21.4	2.6
BZ-965C-0900	126,716	95		-0.7	1		18.5	2.8
BZ-965C-0905	87,538	93.2		-0.2	1.2		13.3	4.2
BZ-965C-0955	62,682	90		0.3	1.7		17	5.4
BZ-965C-0960	53,509	93.6		0.1	1.9		16.2	5.6
BZ-965C-0960-0980	47,126	90.7		-0.7	2.2		13	7.1
BZ-965C-0965	66,453	96.1		-2	1.7		18.5	4.6
BZ-965C-0970	44,518	82		-1	2.1		15.5	7.2
BZ-965C-0975	44,792	81		-0.7	2.1		19.1	7.9
BZ-965C-0980	67,131	94.3		-0.5	1.7		17.7	5.4
BZ-965C-1000	60,455	89.4		-0.6	1.8		16.5	5.1
BZ-965C-1020	69,154	90.4		0.2	1.5		16.7	5.1
BZ-965C-1040	70,569	87.3		1.6	1.5		14.1	4.9
BZ-965C-1060	63,861	93.1		1.8	1.7		14.5	5.3
BZ-965C-1060-1080	60,060	99.8		2	1.9		15.4	5.4
BZ-965C-1065	80,309	96.6		2.5	1.4		16.6	4.2
BZ-965C-1070	61,317	79.1		1.8	1.5		16	5.4
BZ-965C-1075	75,880	86.9		2.3	1.3		16.1	4.2
BZ-965C-1080	53,281	81.9		2	1.8		15.9	6.4
BZ-965C-1080-1100	66,613	90.7		2.2	1.5		18.5	5.3
BZ-965C-1085	72,370	87.3		2.1	1.4		18.9	5.3
BZ-965C-1090	73,938	91.9		2.3	1.4		18.1	4.8
BZ-965C-1095-1110	68,776	85.9		2.2	1.4		18.1	5
BZ-965C-1095-1110	62,083	87.1		1.7	1.5		19.2	5.4
BZ-965C-1100-1120	60,670	84.4		2.2	1.6		17.5	5.7
BZ-965C-1105	52,912	77.9		2.2	1.6		19.6	7
BZ-965C-1110	63,915	87.1		2.4	1.5		17.6	5.1
BZ-965C-1115	35,599	76.1		1.6	2.6		18.6	9.1
BZ-965C-1120	85,087	94.6		2.7	1.3		18.3	4.2
BZ-965C-1120-1140	71,101	1797.2		1.2	2.1		12.5	16.7
BZ-965C-1125	81,642	87		1.4	1.2		15	4.3
BZ-965C-1130	63,344	93.8		2.8	1.7		18.3	4.9
BZ-965C-1135	71,987	90.8		1	1.5		15.1	4.8
BZ-965C-1140	88,749	88.2		2	1.1		13.4	4
BZ-965C-1140-1160	64,818	86.1		1.3	1.5		15.9	5.5
BZ-965C-1145	67,089	79.1		1.4	1.3		14.6	4.7
BZ-965C-1150	77,130	82		1.3	1.3		14.9	4.9
BZ-965C-1155	71,206	91.6		1.6	1.5		15.8	5.3
BZ-965C-1160	76,423	87.8		2.1	1.2		17	4.9
BZ-965C-1165	66,418	88.2		1.3	1.5		15	4.8
BZ-965C-1170	75,013	1837.5		1.7	2.1		12	15.8
BZ-965C-1175	70,472	80.4		1	1.4		12.9	4.1
BZ-965C-1180	81,382	84.6		1.8	1.3		16.1	4.2
BZ-965C-1185	77,770	87.1		1.9	1.3		16.3	4.4
BZ-965C-1190	68,594	90.2		1.2	1.6		13.5	5.3
BZ-965C-1195	40,367	74.8		1.1	2.2		13.6	9.1

Sample	CO2 (ppm)	+/-	δ13C (VPDB) (IRMS)	δ13C (VPDB) (LGR)	+/-	δ18O (VSMOW) (IRMS)	δ18O (VSMOW) (LGR)	+/-
BZ-965C-1200	67,769	87.8		1.1	1.4		13.3	4.8
BZ-965C-1205	61,069	77.1		0.7	1.5		13.8	5.2
BZ-965C-1210	75,379	93.5		1.2	1.5		14.8	4.3
BZ-965C-1215	81,203	81.8		1.2	1.2		14.1	4.1
BZ-965C-1220	94,542	95.4		1.1	1.1		13.3	3.8
BZ-965C-1225	89,811	90.1		1.4	1.1		15.3	3.8
BZ-965C-1230	89,114	82.4		1.7	1.1		16.4	3.9
BZ-965C-1235	83,587	85.3		1.7	1.1		18.5	4.4
BZ-965C-1240	81,277	91.7		1.8	1.2		16.5	4.8
BZ-965C-1245	90,757	105.8		1.5	1.2		17.3	4.1
BZ-965C-1250	92,275	91.3		1.5	1.2		15.4	3.9
BZ-965C-1255	118,267	95.7		0.6	0.9		14.9	2.8
BZ-965C-1260-1280	119,549	105.2		0.1	1		13.5	2.7
BZ-965C-1260-1280	114,322	106.5		0.4	1.1		17	3.4
BZ-965C-1265	90,298	90.8		0.2	1.2		14.2	3.9
BZ-965C-1270	106,364	88.4		-0.1	1		17	3.3
BZ-965C-1275	106,649	2986.4		0.5	2		13.6	14.7
BZ-965C-1280	104,847	87.1		0.5	1		15.3	3.5
BZ-965C-1285	80,348	95.9		0.4	1.5		19	4.3
BZ-965C-1285	160,375	129.5		-0.2	0.8		24.1	2.5
BZ-965C-1290	73,818	92.2		0.2	1.5		16.8	4.4
BZ-965C-1290	160,793	137.1		0.3	0.9		22.3	2.5
BZ-965C-1295	95,840	98.9		0.1	1.2		15.8	3.5
BZ-965C-1295	156,573	110.1		0.3	0.8		22	2.3
BZ-965C-1300	103,702	107.5		0.5	1.2		18	3.2
BZ-965C-1300	121,712	99.7		-0.2	0.9		19	2.8
BZ-965C-1300	173,966	133.4		-0.1	0.8		25.2	2
BZ-965C-1305	89,961	98.4		0.9	1.3		15.8	3.3
BZ-965C-1305	123,434	109.1		0.2	1.1		18.2	2.9
BZ-965C-1305	165,381	134		0.5	0.9		22.9	2.5
BZ-965C-1310	97,101	103.2		0.7	1.2		14.4	3.2
BZ-965C-1310	168,897	119		0.5	0.8		23.4	2.2
BZ-965C-1315	63,403	96.2		0.4	1.7		13.3	4.8
BZ-965C-1315	129,873	93.8		0.7	0.8		16.3	3
BZ-965C-1320	68,545	97.3		-1.4	1.7		15.5	4.8
BZ-965C-1325	63,758	74.4		-1.7	1.5		12.4	5.3
BZ-997C-0620	52,756	77.7		0.1	1.7		22.3	6.8
BZ-997C-0630	69,297	87.4		0.3	1.5		20	4.4
BZ-997C-0640	58,732	75.1		1.3	1.6		17.8	5.9
BZ-997C-0650	33,917	71		1.5	2.7		17.8	10.2
BZ-997C-0660	39,788	77.9		1.3	2.3		19.5	9.1
BZ-997C-0670	33,240	82.8		1.4	3		20.5	9.7
BZ-997C-0680	52,664	79.9		2.2	1.7		11.8	6.3
BZ-997C-0700	89,159	90.1		2	1.2		18	3.8
BZ-997C-0710	100,290	104		1.6	1.1		16.9	3.2
BZ-997C-0720	87,766	88		1.4	1.3		16.2	4.3
BZ-997C-0820	98,038	100.1		0.7	1.1		13.3	3.5
BZ-997C-0840	72,773	91.2		0.6	1.3		2.9	4.4
BZ-997C-0850	60,665	93.5		1.2	1.8		12.2	5.6
BZ-997C-0855	60,236	88.5		0.8	1.8		11.5	5.8

Sample	CO2 (ppm)	+/-	δ13C (VPDB) (IRMS)	δ13C (VPDB) (LGR)	+/-	δ18O (VSMOW) (IRMS)	δ18O (VSMOW) (LGR)	+/-
BZ-997C-0870	32,883	66.9		-0.3	2.7		13.3	11
BZ-997C-0875	47,112	73		-0.2	2		14.3	7.2
BZ-997C-0915	94,139	83.2		-0.4	1		18.2	3.8
BZ-997C-0920	90,485	81.9		-0.7	1		15.6	3.5
BZ-997C-0925	95,818	88.2		-0.9	1.1		16.9	3.5
BZ-997C-0930	49,415	67.9		-1.4	1.7		16	7.8
BZ-997C-0935	31,406	69.6		-2.2	2.8		16.6	11.9
BZ-997C-0945	76,410	84.2		-1.7	1.3		14	4.7
BZ-997C-0960	54,750	81.4		-1.5	1.6		23.2	6.7
BZ-997C-0975	33,016	67		-1.4	2.8		15	9.3
BZ-997C-1010	56,175	84.1		-0.2	1.6		13.8	6.3
BZ-997C-1020	59,080	83.1		0.2	1.7		16	5.2
BZ-997C-1020	95,502	97.4		0.5	1.1		16.7	4
BZ-997C-1080	139,641	104.6		-0.4	0.9		26.3	3
BZ-997C-1100	122,549	112		0.5	1		24.3	3.3
BZ-997C-1160	138,266	108.4		1.5	0.9		24	2.8
BZ-997C-1180	153,423	121.4		1.2	0.9		24.8	2.5
BZ-997C-1200	47,066	72.9		1.6	2		15.2	7.7
BZ-997C-1240	30,148	71.3		2.1	2.9		21.1	10.2
BZ-997C-1280	78,509	96		3.3	1.3		19	4.6
BZ-997C-1290	84,611	92.9		3	1.3		17.7	3.9
BZ-997C-1305	40,108	65.9		3.4	2		29.3	8.9
BZ-997C-1315	102,950	2683		1.8	2.2		24.1	14.8
BZ-997C-1320	146,954	121.2		1.8	0.9		29.9	2.4
BZ-997C-1325	126,008	96.8		1.6	0.9		29.9	2.9
BZ-997C-1340	79,973	87.5		1.8	1.2		24.5	4.1
BZ-997C-1355	31,812	67.9		0.5	2.7		26.1	10.9
BZ-997C-1560	48,561	82.3		-0.6	2.1		16.9	7.5
BZ-997C-1580	50,240	73.6		-0.2	1.8		13.6	7.2
BZ-997C-1600	66,445	88.5		0.9	1.5		13.7	6
BZ-997C-1620	50,889	90.3		2.4	2		13.4	6
BZ-998C-0650	47,533	86.2		1.2	2.1		17.4	7.9
BZ-998C-0660	66,191	87.5		1	1.5		15.9	5.2
BZ-998C-0670	70,701	83.5		1.2	1.5		14.7	5.3
BZ-998C-0680	91,923	96.6		1.7	1.3		20.2	4.2
BZ-998C-0690	97,284	109.2		1.9	1.3		19.3	4.1
BZ-998C-0700	85,458	95.9		1.9	1.3		22.2	4.1
BZ-998C-0710	75,497	90.7		2	1.4		21.8	4.8
BZ-998C-0720	70,419	92.5		2.1	1.5		19.4	5
BZ-998C-0720	71,281	86.1		2.1	1.4		22.4	4.7
BZ-998C-0730	60,564	85.6		1.2	1.8		21.7	6
BZ-998C-0730	68,978	91.3		1.7	1.5		21.7	5
BZ-998C-0740	71,008	84.6		1.1	1.5		20.6	5.1
BZ-998C-0740	105,096	103.9		0.8	1.2		23.7	3.3
BZ-998C-0750	82,413	94.7		0.8	1.4		20.5	3.8
BZ-998C-0750	83,365	92.9		0.8	1.3		21.5	4.2
BZ-998C-0760	74,169	89.8		0.8	1.5		23.5	4.9
BZ-998C-0760	77,578	105.8		0.9	1.5		23.5	4.5
BZ-998C-0780	83,248	99.7		1.9	1.4		19	4.5
BZ-998C-0800	61,169	97.8		0.4	1.8		19.7	6.2

Sample	CO2 (ppm)	+/-	δ13C (VPDB) (IRMS)	δ13C (VPDB) (LGR)	+/-	δ18O (VSMOW) (IRMS)	δ18O (VSMOW) (LGR)	+/-
BZ-998C-0840	54,184	92.1		0.5	2		25.1	6.5
BZ-998C-0860	47,170	79.8		-0.3	1.9		23.9	7.2
BZ-998C-0880	48,355	88.2		0	2.2		22.6	7
BZ-998C-0900	61,031	91.3		0	1.8		22	5.9
BZ-998C-0920	53,880	81.5		-0.4	1.8		19.1	6.3
BZ-998C-0940	48,813	81.9		0	2.1		18.4	7
BZ-998C-0960	63,888	78		-0.4	1.5		17.3	5.7
BZ-998C-0980	48,084	82.8		-0.4	2		17.9	6.8
BZ-998C-1000	46,470	79.8		-0.2	2		19.3	7.9
BZ-998C-1020	57,490	97.8		0.7	1.9		16.8	6.4
BZ-998C-1040	46,944	79.5		0.9	2.1		20.6	6.9
BZ-998C-1060	36,186	77.4		0.2	2.5		19.8	9
BZ-998C-1240	43,523	77.6		1.5	2.1		17.8	8
BZ-998C-1260	37,316	70.6		0	2.3		17.7	9.6
BZ-998C-1280	39,138	76.5		-0.3	2.3		14.8	9.3
BZ-998C-1300	53,736	89		0.2	1.9		16.7	6.8
BZ-998C-1320	55,069	90.9		0.5	1.9		17.3	6.4
BZ-998C-1340	42,779	84.1		0.2	2.3		15.8	8.1
BZ-998C-1360	44,172	79.5		0.3	2.1		13	7.4
BZ-998C-1380	51,606	84.6		-1	1.9		10.7	6.9
BZ-998C-1400	53,266	80.6		-1.5	1.8		11.5	6.4
BZ-998C-1420	48,554	89		-0.7	2		3.3	6.7
BZ-998C-1440	58,257	81.1		-0.1	1.7		11.1	5.5
BZ-998C-1460	50,369	84.3		0.1	2.2		12.1	6.7
BZ-998C-1480	42,568	80.7		-1.2	2.3		13.8	8.4
BZ-998C-1500	32,936	72.5		-2.1	2.6		8.7	10.4
CD-14C-0530	50,157	69.7		2.9	1.8		22.9	6.7
CD-14C-0550	40,257	72.6		1.8	2.1		20.1	8.6
CD-14C-0560	66,828	76.9		2.6	1.4		19.1	5.3
CD-14C-0570	34,823	76.7		1	2.6		15.5	9.4
CD-14C-0580	64,491	82.3		2.5	1.5		23.9	5.5
CD-14C-0590	69,676	88.6		2.4	1.4		26.2	5
CD-14C-0600	73,865	75.7		2.4	1.4		22.4	5.1
CD-14C-0610	61,687	84.9		2.2	1.7		21.7	5.4
CD-14C-0620	97,443	90.9		1.7	1		23.6	3.9
CD-14C-0630	89,538	91		1.2	1.2		21.8	4.1
CD-14C-0640	102,793	93.9		1.4	1		24.2	3.6
CD-14C-0650	101,164	89.7		1.6	1		24.9	3.2
CD-14C-0660	95,215	87		1.5	1.1		24.9	3.4
CD-14C-0670	85,066	86.3		2.1	1.2		24.9	4.9
CD-14C-0680	71,955	83.3		2.6	1.3		22.6	5.6
CD-14C-0690	72,693	88.5		2.4	1.4		23.4	4.7
CD-14C-0700	61,784	83.4		1.5	1.6		22.3	5.7
CD-14C-0720	54,963	71.2		1.7	1.5		24.1	6.8
CD-14C-0740	63,321	73.3		1.1	1.3		22.2	5.6
CD-14C-0770	83,147	81.1		1	1.2		21.8	4.5
CD-14C-0780	76,793	84.9		1.3	1.3		20.9	4.4
CD-14C-0790	76,559	75.7		0.9	1.3		21.9	4.7
CD-14C-0800	70,587	79.7		1.2	1.3		22.1	5.4
CD-14C-0820	69,671	87.7		1.3	1.3		23	5.7

Sample	CO2 (ppm)	+/-	δ13C (VPDB) (IRMS)	δ13C (VPDB) (LGR)	+/-	δ18O (VSMOW) (IRMS)	δ18O (VSMOW) (LGR)	+/-
CD-14C-0840	48,367	73		0.8	1.9		24.8	7.3
CD-14C-0860	48,473	85		-0.3	2.1		21	5.9
CD-14C-0880	41,838	68.5		0	1.8		23.5	7.7
CD-14C-0900	38,461	64.4		0.2	2.3		25	9.6
CD-14C-0920	55,538	78.7		0.9	1.7		24.3	6.7
CD-14C-0940	61,833	76.8		0.9	1.5		22.7	5.8
CD-14C-0960	44,957	63.5		0.8	1.8		24.8	7.3
CD-14C-0980	45,012	70.8		0.4	1.8		24.7	7.9
CD-14C-1000	48,901	64.5		1.1	1.8		24.1	7.1
CD-14C-1020	50,580	69.9		0.9	1.8		22.2	7.1
CD-14C-1040	58,250	67.1		1.1	1.4		21.2	5.7
CD-14C-1060	62,615	74.6		0.7	1.5		22.9	5.3
CD-14C-1080	81,164	74.6		1.3	1.1		21.6	4.5
CD-14C-1100	63,546	68.8		1	1.4		20.5	5.5
CD-14C-1120	70,119	79.2		1.3	1.3		21.9	5.1
CD-14C-1140	68,184	83.6		0.8	1.4		20	4.9
CD-14C-1160	82,651	85.1		1	1.2		22.6	4
CD-14C-1180	72,215	78.3		0.2	1.3		22.1	4.4
CD-14C-1200	65,230	72.3		-0.2	1.3		21.3	5.3
CD-14C-1220	61,000	75.3		-0.4	1.5		20.9	5
CD-14C-1240	68,727	77.3		-0.3	1.3		20.1	4.6
CD-14C-1260	67,031	76		0.2	1.4		21.3	4.3
CD-14C-1280	63,806	71.1		0.1	1.3		23	4.6
CD-14C-1300	55,073	69.5		0.1	1.7		23.3	5.8
CD-14C-1320	46,283	72.2		0.1	2		21.8	6.9
CD-14C-1340	67,881	84.8		0.2	1.4		20.6	4.4
CD-14C-1360	57,765	73.1		0	1.6		20.3	5.1
CD-14C-1380	50,463	76		0.1	1.9		19.3	6.2
CD-14C-1400	59,751	73.8		-0.2	1.5		15.8	4.9
CD-14C-1420	61,208	91		-0.4	1.7		22.1	6.1
CD-14C-1440	52,513	80.2		-0.5	1.8		19	6.1
CD-14C-1460	51,559	87.2		-1.1	2.1		19.2	6.3
CD-14C-1480	51,189	81.1		-1	2		22.1	5.8
CD-14C-1500	50,286	68.3		-1.2	1.7		21.3	5.5
CD-14C-1520	60,016	88.1		-1.3	1.7		18.2	5.7
CD-14C-1540	82,138	106.7		-1.2	1.5		19.9	4.6
CD-14C-1560	60,135	83.6		-1.6	1.9		21	6.3
CD-14C-1580	51,942	85.9		-1.3	2.3		20.5	7.4
CD-14C-1600	58,305	92		-1.6	2.1		16.9	6.2
CD-14C-1620	76,350	103.6		-1.2	1.6		17.7	5.4
CD-14C-1640	80,609	97.7		-1.2	1.6		18.2	4.7
CD-14C-1660	50,512	96.8		-1.6	2.4		16.1	7.2
CD-14C-1680	60,862	87.6		-1.3	1.9		16.7	6.3
CD-14C-1700	46,596	86.7		-1.5	2.5		19.1	7.4
CD-14C-1720	41,770	84		-1.9	2.6		19.4	9.1
CD-14C-1740	44,399	89.6		-1.2	2.6		17.8	8.5
CD-14C-1760	43,589	89		-1	2.5		17.9	8
CD-14C-1780	58,178	80.1		-1	2		19.2	6.3
CD-14C-1800	54,104	91.4		-0.8	2		15	6.6
CD-14C-1820	56,597	68.7		-0.8	1.4		18.2	5.2

Sample	CO2 (ppm)	+/-	δ13C (VPDB) (IRMS)	δ13C (VPDB) (LGR)	+/-	δ18O (VSMOW) (IRMS)	δ18O (VSMOW) (LGR)	+/-
CD-14C-1840	49,314	79.9		-0.4	2		17.7	6
CD-14C-1860	44,935	83.2		-0.3	2.2		15.4	6.8
CD-14C-1880	96,021	93.9		-0.3	1.1		20.4	3.5
CD-14C-1900	92,450	87.4		-0.3	1.1		21.5	3.4
CD-14C-1920	78,510	84.5		0.1	1.2		18.9	3.9
CD-14C-1940	59,442	75		-0.5	1.5		18.4	5.8
CD-14C-1960	65,194	84.8		-0.4	1.6		20.1	4.5
CD-14C-1980	56,449	75.5		-0.9	1.7		20.4	5.2
CD-14C-2000	78,875	91.6		-0.1	1.4		19.5	4.5
CD-14C-2020	63,427	85.5		-0.3	1.6		20.2	5.2
CD-14C-2040	69,126	82.6		-0.2	1.5		19	4.4
CD-14C-2060	73,184	82.7		0.2	1.5		16.8	4.3
CD-14C-2080	84,307	92.9		0.3	1.3		20.1	4
CD-14C-2100	41,600	80		-0.2	2.3		13.4	8.5
CD-14C-2120	92,264	94.2		0.8	1.2		16.8	3.6
CD-14C-2140	73,217	87		0.1	1.5		20	4.1
CD-14C-2160	88,714	91.7		0.4	1.4		20.9	3.9
CD-15C-1380	38,089	80.1	-0.3	-1.2	2.4	18.3	17.8	7.8
CD-15C-1400	54,904	91.9	-1.1	-1.5	2	22.1	20.8	6.9
CD-15C-1420	55,150	86.9	-1.9	-2.2	2	24.6	22.5	6.5
CD-15C-1440	61,582	88.7	-2.2	-2.4	1.9	22.9	21	6.1
CD-15C-1460	75,394	91.1	-1.5	-1.8	1.5	23.1	21.8	5.2
CD-15C-1480	80,852	81.1	-0.9	-1.4	1.3	22.3	21.6	5.3
CD-15C-1500	58,219	86.5	-0.7	-1.5	1.9	20.2	20	7.1
CD-15C-1520	43,854	87.7	-0.7	-1.3	2.3	23	20.2	9.1
CD-15C-1540	42,443	86.8	0.5	-0.9	2.4	24.2	21.9	9.9
CD-15C-1560	78,011	86.9	-0.2	-0.3	1.5	24.3	24.7	5.3
CD-15C-1580	70,138	88	0.2	-0.1	1.8	23.8	23.7	5.1
CD-15C-1600	61,307	86.5	0.6	0.3	1.7	23.1	23.6	6.9
CD-15C-1620	58,711	92.6	-0.1	0.8	2	19	22.7	6.9
CD-15C-1660	79,798	92.1	1.3	1	1.5	21	21.3	5
CD-15C-1680	51,716	76		0.9	1.8	18	18	5.9
CD-15C-1700	43,870	74.7	1.2	0.9	2.2	15.6	15.9	10.2
CD-15C-1720	63,631	80.4	0.9	0.5	1.8	18.2	20.3	6.8
CD-15C-1740	38,834	86.3	0.1	-0.3	2.7	24.9	25.2	9.2
CD-15C-1760	71,080	74.6	-0.3	0.3	1.4	24.4	23.9	5.2
CD-15C-1780	86,853	88.5	0.2	0.7	1.2	24.8	23.8	3.9
CD-15C-1800	58,034	74.7	-0.3	1.2	1.4	24.1	23.6	5.9
CD-15C-1820	46,194	77.3	-1.9	0.1	2	22.1	20	6.6
CD-15C-1840	50,528	95.3	-2.2	0.3	2.2	21.5	19.1	6.3
CD-15C-1860	60,926	69.2	-1.5	0.6	1.5	21.8	22.9	6.2
CD-15C-1880	39,832	67	-0.9	-0.1	2.1	19.6	20.1	9.5
CD-15C-1900	71,332	84.5	-0.7	0.5	1.4	22.5	22.5	5.2
CD-15C-1920	65,480	74.3	0.5	-0.2	1.5	22.4	22	5.2
CD-15C-1940	48,771	65.7	0.2	0	1.7	22.2	21.3	6.9
CD-15C-2000	55,515	75.8	0.6	-0.1	1.6	21.8	21.8	5.9
CD-15C-2020	36,134	68.3	-0.1	-0.6	2.4	22.2	19.7	9.3
CD-15C-2040	36,309	63.8	1.3	-0.6	2.3	22.7	20.1	9.8
CD-15C-2060	32,410	71.7	1.1	0.1	2.7	21.7	20.1	11.5
CD-15C-2080	50,957	72.6	1.1	-0.6	1.7	21.9	20.5	7.4

Sample	CO2 (ppm)	+/-	δ13C (VPDB) (IRMS)	δ13C (VPDB) (LGR)	+/-	δ18O (VSMOW) (IRMS)	δ18O (VSMOW) (LGR)	+/-
CD-15C-2100	63,859	74.6	1.2	-0.4	1.4	21.8	18.9	4.8
CD-15C-2120	44,293	76.6	1.2	-0.6	2.1	22.2	21.1	8.4
CD-94-3-1230	36,211	64.8		-3.8	2.4		18.2	10.6
CD-94-3-1350	150,647	156.4		0.1	1.2		29.1	3.1
CD-94-3-1360	36,918	67.5		-0.5	2.3		21.2	9.6
CD-94-3-1360	131,048	114		0.4	0.9		26.9	2.9
CD-94-3-1370	44,202	67.9		-0.2	1.8		24.1	8
CD-94-3-1380	54,872	69		0.6	1.6		22.4	7.1
CD-94-3-1390	37,319	72.7		-0.2	2.3		23.1	10.2
CD-94-3-1390	153,567	122.3		0.1	0.9		30	2.5
CD-94-3-1400	48,539	73		0.3	1.8		23.8	7.2
CD-95-3-0890	35,883	81.3		-2.4	2.6		11.8	8.7
CD-95-3-0900	44,418	95		-2.6	2.3		13.3	6.4
CD-95-3-0910	39,139	86.2		-2	2.3		10.3	5.6
CD-95-3-0920	37,739	85		-4.4	2.6		12.7	7.1
CD-95-3-0930	41,926	89		-4.6	2.5		18.2	7.2
CD-95-3-0940	44,019	95		-6.7	2.4		17.8	6.6
CD-95-3-0950	69,970	95.7		-2.7	1.6		22	4.7
CD-95-3-0960	81,789	85.2		-2.4	1.3		22.4	3.8
CD-95-3-0970	91,505	91.6		-1.5	1.3		22	3.4
CD-95-3-0980	94,118	93.5		-1.6	1.2		21.5	3.7
CD-95-3-0990	84,083	91.5		-2	1.2		21.6	3.7
CD-95-3-1000	88,330	88.8		-0.5	1.2		22.7	3.4
CD-95-3-1010	80,990	81.1		-0.8	1.2		22.6	3.7
CD-95-3-1020	99,045	92.6		-1	1.3		22.4	3
CD-95-3-1030	84,567	86.9		-0.6	1.2		21.4	3.9
CD-95-3-1040	87,490	85.6		-0.3	1.3		21.9	3.1
CD-95-3-1050	88,515	91.4		0.1	1.2		22.9	3.6
CD-95-3-1060	95,745	90.3		0	1.2		22.8	3.4
CD-95-3-1070	90,594	97.3		-0.2	1.2		22.7	3.9
CD-95-3-1080	69,959	80.7		-0.3	1.4		21.1	4.4
CD-95-3-1090	80,783	94		0.6	1.4		25.2	3.7
CD-95-3-1100	84,908	102.6		0.5	1.4		21.1	4
CD-95-3-1110	76,118	96.7		0.4	1.5		20.1	4.3
CD-95-3-1120	95,415	106.2		0.2	1.2		22.8	3.6
CD-95-3-1130	109,381	112.4		0.1	1.1		22.4	3.5
CD-95-3-1140	96,182	111		0.5	1.2		20.7	3.5
CD-95-3-1150	62,903	99.9		0	2		18.3	5.6
CD-95-3-1160	89,987	102.7		0.5	1.3		17.7	4.1
CD-95-3-1170	86,246	131.9		0.8	1.6		19	4.5
CD-95-3-1180	89,747	111.9		1	1.6		18.2	4.1
CD-95-3-1190	81,553	106.8		1	1.5		17.5	4.6
CD-95-3-1200	72,875	307.3		-1	2.1		15.3	5.1
CD-95-3-1210	81,281	110.1		1.2	1.6		18	4.9
CD-95-3-1220	88,622	113.4		0.8	1.6		17.4	4.5
CD-95-3-1230	76,906	111.5		1	1.8		16.7	5.3
CD-95-3-1240	83,234	1711.9		1.5	3.4		13.9	12.9
CD-95-3-1250	88,888	86.9		1.5	1.1		23.1	3.6
CD-95-3-1260	83,829	100.4		1.8	1.3		21.5	3.3
CD-95-3-1270	77,346	73.8		1.8	1.2		18.2	4

Sample	CO2 (ppm)	+/-	δ13C (VPDB) (IRMS)	δ13C (VPDB) (LGR)	+/-	δ18O (VSMOW) (IRMS)	δ18O (VSMOW) (LGR)	+/-
CD-95-3-1280	79,137	76.6		1.6	1.1		20.9	4.1
CD-95-3-1290	51,052	81.2		1.4	1.8		19.3	6
CD-95-3-1300	81,792	93.6		1	1.3		19.2	3.6
CD-95-3-1310	100,675	91.4		0.7	1		20.3	3.1
CD-95-3-1320	135,838	221.7		-0.4	1		23.9	2.5
CD-95-3-1330	57,034	77.8		0.7	1.6		22.3	5.3
CD-95-3-1340	53,159	76.4		1.2	1.9		21.2	5.3
CD-95-3-1360	89,448	1752.9		1.1	3		16.9	11.9
CD-95-3-1370	74,013	80		1	1.4		19	3.7
CD-95-3-1380	72,649	78.8		1.2	1.3		19.7	4.4
CD-95-3-1390	87,274	94.1		1.1	1.2		20.5	3.6
CD-95-3-1400	73,319	79.9		1	1.2		15.1	3.8
CD-95-3-1410	68,628	87.3		1	1.6		18.1	3.7
CD-95-3-1420	82,249	81		0.9	1.2		17.5	3.6
CD-95-3-1430	96,403	96.7		0.8	1.1		18	3.3
CD-95-3-1440	65,614	81.2		0.8	1.4		16.8	4.9
CD-95-3-1460	73,902	88.9		0.3	1.6		19.7	5.1
CD-95-3-1470	75,940	78.5		0.6	1.2		19.4	3.9
CD-95-3-1480	65,301	82.5		0.3	1.5		19.6	4.4
CD-95-3-1490	69,179	78.8		0.4	1.4		19.9	3.9
CD-95-3-1500	72,211	86.2		0.8	1.3		19.1	4.4
CD-95-3-1510	68,912	78		0.5	1.3		19.3	4.5
CD-95-3-1520	74,642	90.2		0.2	1.5		19.2	3.9
CD-95-3-1530	68,977	80.9		0	1.5		20.6	4.9
CD-95-3-1540	78,154	85.6		-0.1	1.2		21.1	4.2
CD-95-3-1550	66,476	78.8		-0.2	1.5		17.4	4.1
CD-95-3-1560	64,984	82.1		0.2	1.5		18.4	4.5
CD-95-3-1570	30,490	71.5		-0.9	2.8		17.4	9.7
CD-95-3-1580	59,045	82.8		0.3	1.6		15.1	4.9
CD-95-3-1590	43,959	74		0.6	2		16	7
CD-95-3-1600	63,985	90.1		0.2	1.8		12.8	5.1
CD-95-3-1630	30,003	65		-2.1	2.8		22.8	9.4
CD-95-3-1640	36,608	69.8		-2.5	2.6		18.3	7.2
CD-95-3-1650	43,905	68.8		-1.9	1.8		17.4	6.3
CD-95-3-1660	53,582	76.9		-1.3	1.6		19.4	5.1
CD-95-3-1670	46,522	74.9		-1.5	1.8		19.7	5.6
CD-95-3-1680	42,211	70.5		-2.1	2.1		20.7	6.3
CD-95-3-1690	58,238	80.9		-1.3	1.7		18.8	4.9
CD-95-3-1700	56,050	67.5		-0.8	1.5		17.7	4.7
CD-95-3-1710	66,246	81.7		-1	1.5		18.4	4.6
CD-95-3-1720	70,932	83.7		-0.9	1.4		19.1	4.3
CD-95-3-1730	68,062	74		-1.4	1.5		16.7	4.2
CD-95-3-1740	37,753	75		-1.3	2.4		23.1	8.3
CD-95-3-1750	60,136	77		-1.2	1.4		18.8	4.5
CD-95-3-1760	78,251	81.7		-0.6	1.2		18.5	4.3
CD-95-3-1770	94,712	96.3		-0.8	1.2		17.1	3.3
CD-95-3-1780	78,429	85		-0.7	1.2		16.6	3.8
CD-95-3-1790	75,500	84.2		-1.1	1.4		14.9	4.1
CD-95-3-1800	85,372	89.6		-1.3	1.3		13.5	3.5
CD-95-3-1810	85,140	91.6		-0.9	1.2		14.3	3.6

Sample	CO2 (ppm)	+/-	δ13C (VPDB) (IRMS)	δ13C (VPDB) (LGR)	+/-	δ18O (VSMOW) (IRMS)	δ18O (VSMOW) (LGR)	+/-
CD-95-3-1820	82,902	82.3		-1.1	1.3		12.6	3.4
CD-95-3-1830	95,312	87.2		-1.1	1.1		15.4	3.2
CD-95-3-1840	85,207	85.2		-0.7	1.1		16.9	3.7
CD-95-3-1850	88,499	89.9		-0.8	1.2		17.4	3.6
CD-95-3-1860	90,349	101.9		-1.2	1.2		16.3	3.5
CD-95-3-1870	78,686	83.2		-1.4	1.2		14.4	3.8
CD-95-3-1880	86,652	87.7		-1.4	1.2		15.1	3.7
CD-95-3-1890	73,761	78.3		-1.2	1.3		14.6	3.9
CD-95-3-1900	79,171	81.4		-0.9	1.2		15.2	3.7
CD-95-3-1910	75,338	82.8		-0.2	1.2		17.1	4.1
CD-95-3-1920	80,018	78.7		-1	1.2		15.9	4
CD-95-3-1930	72,158	82.6		-0.6	1.4		15.3	3.8
CD-95-3-1940	37,668	74.7		-3.3	2.2		13.3	7.1
CD-95-3-1950	34,301	72		-3	2.5		15.3	9
CD-95-3-1960	81,692	87.1		-1.5	1.3		15.3	3.6
CD-95-3-1970	73,855	82.6		-1.5	1.3		15.2	3.8
CD-95-3-1980	75,031	84.9		-1.3	1.4		12.9	3.7
CD-95-3-1990	33,954	72.1		-2.8	2.3		14.2	8.8
CD-95-3-2000	32,390	66.9		-3.2	2.6		14.6	9
CD-95-3-2010	33,114	72.8		-3.1	2.7		17	8.1
CD-95-3-2020	46,929	70.6		-1.4	1.8		18.2	5.6
CD-95-3-2030	79,776	95.8		-0.9	1.4		18.3	3.6
CD-95-3-2040	69,447	96.3		-1	1.6		11.7	4.6
CD-95-3-2050	76,896	98.1		-1.3	1.3		12.5	3.9
CD-95-3-2060	88,588	104.4		-0.8	1.4		18.6	3.4
CD-95-3-2070	84,135	97.4		-0.5	1.4		19.1	3.4
CD-95-3-2080	81,807	90.3		-0.8	1.2		18.7	3.5
CD-95-3-2090	72,651	90.3		-0.6	1.4		19.6	4.6
CD-95-3-2100	76,083	97.6		-0.7	1.3		18.9	4.1
CD-95-3-2110	44,930	76.7		-0.9	2		13.4	7
CD-95-3-2130	56,081	81.6		-1.8	1.7		13.8	5.7
CD-95-3-2140	89,009	106.3		-0.4	1.4		19.9	3.8
CD-95-3-2150	80,218	98.5		-0.3	1.4		18.4	3.5
CD-95-3-2160	98,743	103.2		-0.4	1.2		19.4	3.3
CD-95-3-2170	86,821	105.3		-0.7	1.4		17.5	3.6
CD-95-3-2180	61,904	89.8		-0.7	1.8		18.7	4.8
CD-96-1C-0870	59,378	76.6		-4.6	1.6		16	5.8
CD-96-1C-0880	51,781	91.5		-8.1	2.2		17.6	5.6
CD-96-1C-0890	34,356	74.4		-8.1	2.6		15.2	8.4
CD-96-1C-0900	45,846	88.3		-3.5	2.6		16.7	8.8
CD-96-1C-0920	83,032	97.9		-2.5	1.4		17.3	5
CD-96-1C-0940	54,682	87.8		-2.4	1.8		14.2	5.2
CD-96-1C-0960	76,197	92.3		-1.6	1.4		15.4	4
CD-96-1C-0980	111,410	131		0.5	1.4		22.8	3.8
CD-96-1C-1000	104,642	111.2		0.8	1.4		23.7	4.4
CD-96-1C-1020	107,530	114.8		0.9	1.3		22.3	3.7
CD-96-1C-1040	113,629	109.6		1.3	1.2		23.2	3.1
CD-96-1C-1060	110,950	112.3		1	1.3		23.3	3.8
CD-96-1C-1080	87,773	104.3		1.2	1.6		22.5	4.3
CD-96-1C-1100	118,098	119.7		1.3	1.2		23.6	3

Sample	CO2 (ppm)	+/-	δ13C (VPDB) (IRMS)	δ13C (VPDB) (LGR)	+/-	δ18O (VSMOW) (IRMS)	δ18O (VSMOW) (LGR)	+/-
CD-96-1C-1120	115,289	110.2		1.3	1.1		20.8	2.9
CD-96-1C-1160	109,786	96.3		0.9	1.1		20.9	2.7
CD-96-1C-1180	109,626	87.9		1	0.9		21.6	3.1
CD-96-1C-1200	95,204	97.3		1.5	1.1		21.7	3.2
CD-96-1C-1220	94,469	86.1		1.6	1		22.1	3.3
CD-96-1C-1240	85,899	88.3		0.9	1.2		21.8	3.8
CD-96-1C-1260	75,317	83.7		0.7	1.4		21.5	4.2
CD-96-1C-1280	88,820	97.1		0.1	1.3		22.2	3.7
CD-96-2C-0770	77,167	103.5		-0.5	1.5		23.1	4.1
CD-96-2C-0780	64,515	89		-0.6	1.6		23.2	4.9
CD-96-2C-0790	76,557	87.8		-0.2	1.4		24.3	3.9
CD-96-2C-0800	64,322	77.3		-0.1	1.6		23.4	4.4
CD-96-2C-0810	82,142	97.8		0.9	1.4		21.6	4
CD-96-2C-0820	82,742	111		0.9	1.6		20.7	4.1
CD-96-2C-0830	77,654	93.6		0.7	1.4		22.4	3.8
CD-96-2C-0840	100,405	108.4		0.7	1.3		22.2	3.3
CD-96-2C-0850	91,902	114.9		0.6	1.4		21.6	3.7
CD-96-2C-0860	97,260	100.6		0.7	1.3		22.9	3
CD-96-2C-0870	94,033	99.2		0.6	1.3		23.1	3.2
CD-96-2C-0880	77,130	106.4		0.7	1.6		22.3	4.3
CD-96-2C-0890	81,559	108.8		0.7	1.6		22	4.1
CD-96-2C-0900	77,445	95.8		0.5	1.5		22.3	4.5
CD-96-2C-0910	78,121	104.7		0.3	1.5		23.1	3.9
CD-96-2C-0920	66,989	86.2		-0.2	1.6		23.5	4.7
CD-96-2C-0930	75,781	93		-0.4	1.4		23.9	4.6
CD-96-2C-0940	62,617	85.2		-0.7	1.6		24.1	5.1
CD-96-2C-0950	72,115	83.3		-0.8	1.4		24.4	4.8
CD-96-2C-0960	79,435	101		-1.1	1.5		23.6	4.2
CD-96-2C-0970	80,367	87.6		-1	1.2		21.6	3.8
CD-96-2C-0980	46,591	79.3		-0.7	2		21.6	6.5
CD-96-2C-0990	69,202	83.3		-0.4	1.4		22	4.5
CD-96-2C-1000	73,819	95.2		-0.2	1.6		23.2	4.1
CD-96-2C-1010	66,041	86		-0.2	1.5		23.1	4.7
CD-96-2C-1020	69,284	91.3		0	1.5		23.9	4.6
CD-96-2C-1030	54,400	79.8		0.6	1.9		24.4	5.5
CD-96-2C-1040	51,627	80.1		0.4	1.9		23.3	5.9
CD-96-2C-1050	52,993	79.1		-0.3	1.8		21.5	5.9
CD-96-2C-1060	76,305	95.9		0.6	1.5		20.5	3.8
CD-96-2C-1070	38,799	87		-0.1	2.8		23.5	8.3
CD-96-2C-1080	83,600	92.5		0.6	1.3		22.2	4.1
CD-96-2C-1090	80,496	85.5		0.6	1.2		21.6	4.1
CD-96-2C-1100	86,359	93.5		0.5	1.4		21.6	3.9
CD-96-2C-1110	81,398	91.7		0.5	1.3		21.1	3.7
CD-96-2C-1120	77,114	93.2		0.6	1.4		21.8	3.7
CD-96-2C-1130	92,991	92.9		0.3	1.1		23	3.8
CD-96-2C-1140	88,122	92.7		0.4	1.3		23.3	3.7
CD-96-2C-1150	88,883	89.8		0.5	1.2		20.7	3.6
CD-96-2C-1160	98,322	96		0.9	1.1		21.6	3.1
CD-96-2C-1170	102,301	97.1		0.7	1.1		20.9	3.3
CD-96-2C-1180	63,837	81.4		0.8	1.5		19.2	4.9

Sample	CO2 (ppm)	+/-	δ13C (VPDB) (IRMS)	δ13C (VPDB) (LGR)	+/-	δ18O (VSMOW) (IRMS)	δ18O (VSMOW) (LGR)	+/-
CD-96-2C-1190	89,395	93.3		0.6	1.3		20.5	3.8
CD-96-2C-1200	93,183	103.7		0.6	1.3		22.3	3.7
CD-96-2C-1210	90,184	89.2		0.7	1.2		21	3.5
CD-96-2C-1220	83,765	92.6		0.3	1.3		19.8	3.4
CD-96-2C-1230	85,713	93.3		-0.2	1.4		20.1	3.5
CD-96-2C-1240	78,767	88.9		-0.5	1.4		20.1	4.2
CD-96-2C-1250	77,259	92.6		0.3	1.4		14.5	4.2
CD-96-2C-1260	74,822	95.1		0.9	1.4		17.2	4.6
CD-96-2C-1270	70,104	94.1		1	1.7		17.4	4.7
CD-96-2C-1280	51,931	78.4		0.1	2.1		20.1	6.2
CD-96-2C-1290	55,831	92.1		0.4	2		18.6	5.7
CD-96-2C-1300	50,456	81.4		0.3	2.1		19.5	6.7
CD-96-2C-1310	58,551	84.1		0.1	1.7		19.3	5.3
CD-96-2C-1320	65,024	89.6		0	1.6		16.7	4.7
CD-96-2C-1330	77,507	94.9		0.1	1.5		18.5	4.4
CD-96-2C-1340	64,528	91.8		-0.4	1.7		16.2	4.9
CD-96-2C-1350	72,352	91.2		-0.2	1.5		15.8	4.4
CD-96-2C-1360	66,729	85.6		-0.2	1.4		17.4	4.8
CD-96-2C-1370	57,599	94.5		-0.2	1.8		17.2	5.1
CD-96-2C-1380	64,482	90.8		-0.3	1.6		17.9	5.2
CD-96-2C-1390	66,536	98.9		-0.4	1.7		15.7	4.5
CD-96-2C-1400	76,557	85.2		0.1	1.4		18.4	3.9
CD-96-2C-1420	80,770	94.4		0.2	1.4		20	4.1
CD-96-2C-1430	76,171	55.5		-0.2	1		22.2	5.5
CD-96-2C-1440	76,979	95.9		-0.9	1.5		19	4
CD-96-2C-1450	50,039	86.8		-1.3	2		18.3	6.3
CD-96-2C-1460	73,915	95.3		-0.6	1.5		19.8	4.1
CD-96-2C-1470	34,634	72.7		-1	2.8		20.1	9.2
CD-96-2C-1480	70,890	92		-0.6	1.6		18.5	4.6
CD-96-2C-1490	56,957	83.9		-0.8	1.8		19.9	5.3
CD-96-2C-1500	79,254	97.8		-0.6	1.5		19.3	3.6
CD-96-2C-1510	54,956	86		-0.7	2		17.4	5.7
CD-96-2C-1520	61,159	85.1		-1.3	1.7		18.8	4.8
CD-96-2C-1530	74,067	94.3		-0.8	1.5		18.3	4.3
CD-96-2C-1540	63,125	96.2		-0.9	1.7		16.8	5.1
CD-96-2C-1550	46,557	92.7		-0.9	2.3		18.5	6.8
CD-96-2C-1560	55,563	81.7		-0.9	1.8		16.7	5.5
CD-96-2C-1570	62,210	96.1		-0.6	1.7		16.4	5.3
CD-96-2C-1580	76,038	95.8		-0.9	1.4		16.7	4.1
CD-96-2C-1590	57,876	99.2		-0.9	1.9		15.7	6.3
CD-96-2C-1600	56,700	88.5		-1.3	1.8		16.2	6
CD-96-2C-1610	54,461	86		-0.9	1.9		16.3	6.1
CD-96-2C-1620	49,776	76.8		-1.2	2		15.7	6.1
CD-96-2C-1630	65,657	90.9		-1	1.7		15.8	5.3
CD-96-2C-1640	74,058	102.4		-1.5	1.6		14.4	4.4
CD-96-2C-1650	44,455	97.4		-1.3	2.6		13.6	7.3
CD-96-2C-1660	77,221	96		-1.3	1.4		15.7	3.8
CD-96-2C-1670	78,016	85.4		-1.1	1.3		14.9	4.2
CD-96-2C-1680	67,696	101.9		-0.6	1.9		13.7	5.1
CD-96-2C-1690	86,541	108		-0.9	1.5		9.2	4

Sample	CO2 (ppm)	+/-	δ13C (VPDB) (IRMS)	δ13C (VPDB) (LGR)	+/-	δ18O (VSMOW) (IRMS)	δ18O (VSMOW) (LGR)	+/-
CD-96-2C-1700	83,365	102.4		-0.3	1.5		14	3.8
CD-96-2C-1720	61,286	76.2		-0.6	1.5		11.9	5.5
CD-96-2C-1730	70,815	89.3		-0.8	1.5		12.1	4.3
CD-96-2C-1740	77,813	91.6		-0.8	1.5		11.8	3.9
CD-96-2C-1750	72,089	96.4		-0.7	1.6		11.9	4.3
CD-96-2C-1760	58,463	98.1		-0.5	1.9		14.3	5.4
CD-96-2C-1770	50,035	90.1		-0.4	2.1		12	6.3
CD-96-2C-1780	80,436	92.3		-0.3	1.4		15.1	3.9
CD-96-2C-1790	60,395	92.8		-0.3	1.8		15.7	4.6
CD-96-2C-1800	87,698	88.7		-0.6	1.2		14.7	3.4
CD-96-2C-1810	74,896	89.4		-0.5	1.4		17.4	4.1
CD-96-2C-1820	87,141	87.9		-1	1.2		17.2	3.4
CD-96-2C-1830	97,864	100.8		-0.8	1.2		17.8	3.3
CD-96-2C-1840	99,429	94.7		-0.9	1.2		15.2	2.9
CD-96-2C-1860	62,976	82.3		-0.8	1.5		12.3	4.7
CD-96-2C-1880	75,311	95.5		-0.8	1.4		12.9	3.7
CD-96-2C-1900	86,210	90.6		-0.7	1.2		14.9	3.6
CD-96-2C-1920	78,454	94		-0.7	1.4		13.4	3.6
CD-96-2C-1925	61,839	93.7		-1.1	1.8		9.9	4.3
CD-96-2C-1930	65,337	91.7		-0.7	1.6		14.5	4.4
CD-96-2C-1935	51,335	85.9		0	1.9		15.3	5.4
CD-96-2C-1935	77,792	89.8		-0.1	1.3		15.9	3.8
CD-96-2C-1940	54,184	82		-0.3	1.7		13.7	5.2
CD-96-2C-1960	81,124	90.7		-0.8	1.4		17.2	3.8
CD-96-2C-1980	79,611	94.6		-1.5	1.3		14.3	3.7
CD-96-2C-2000	76,368	101.8		-1.3	1.5		15.8	4.1
CD-96-2C-2020	68,225	93.4		-1.1	1.7		17	4.4
CD-96-2C-2025	98,135	105.6		-1.6	1.3		13.9	3.2
CD-96-2C-2030	103,566	107.8		-1.2	1.2		16.7	3.1
CD-96-2C-2035	101,180	98.6		-1.4	1.1		15.3	3.4
CD-96-2C-2040	69,473	88.2		-0.8	1.6		14.1	4.8
CD-96-2C-2045	80,949	94.7		-1.2	1.5		12.8	3.8
CD-96-2C-2050	108,644	103.8		-1.3	1.1		17.2	3.2
CD-96-2C-2055	115,286	110		-1.5	1.1		16.4	2.6
CD-96-2C-2060	43,606	80		-1.3	2.4		9.8	8.2
CD-96-2C-2065	106,252	106		-1.4	1.2		14.7	3.5
CD-96-2C-2070	95,477	103.4		-1.1	1.3		13	3.6
CD-96-2C-2075	43,480	85.5		-0.9	2.5		12.4	7.6
CD-96-2C-2080	68,944	79.8		-1.5	1.6		10.7	4.4
CD-96-2C-2100	84,139	94.5		-1.7	1.3		17.4	3.6
CD-96-2C-2120	69,679	101.2		-1.7	1.7		20	4.8
CD-96-2C-2180	116,012	106.9		-0.7	1.1		24.8	2.9
CD-96-2C-2200	92,033	109.6		-0.6	1.3		22	3.7
CD-96-2C-2220	69,183	91.5		-0.4	1.6		21.4	4.2
CD-96-2C-2240	101,973	103.7		-1.2	1.2		16.5	2.9
CD-96-2C-2260	113,801	112.3		-0.6	1.2		24.9	3.1
CD-96-2C-2280	122,952	120.3		-0.4	1.1		26.3	2.9
CD-96-2C-2320	126,288	101.8		0.1	1		26.1	2.7
CD-96-2C-2340	127,718	110.1		0.5	1.1		26	2.7
CD-96-9-0380	58,144	92		1.6	1.9		27.2	5.9

Sample	CO2 (ppm)	+/-	δ13C (VPDB) (IRMS)	δ13C (VPDB) (LGR)	+/-	δ18O (VSMOW) (IRMS)	δ18O (VSMOW) (LGR)	+/-
CD-96-9-0390	57,840	96		1.2	2.2		27.3	6.6
CD-96-9-0400	67,704	100.9		1.5	1.8		24.5	5.7
CD-96-9-0410	82,792	97.7		1.4	1.4		26.2	4.7
CD-96-9-0420	66,373	85.7		1.5	1.6		26.1	5.5
CD-96-9-0430	58,418	81.1		0.3	1.7		24.6	4.7
CD-96-9-0440	83,060	89.3		0.2	1.2		25.1	3.1
CD-96-9-0450	63,012	84.6		-0.2	1.5		25.5	4.7
CD-96-9-0460	67,894	80.3		-0.5	1.3		24.9	4.5
CD-96-9-0470	47,993	68		-0.4	1.7		25.2	5.7
CD-96-9-0480	57,742	78		-0.5	1.6		26.4	4.9
CD-96-9-0490	67,822	77.9		0.2	1.4		25.1	4
CD-96-9-0500	59,060	77.6		-0.3	1.6		24.8	5.2
CD-96-9-0510	67,225	80		0	1.4		24.7	4.1
CD-96-9-0520	75,701	72		-0.4	1.1		24.4	4.1
CD-96-9-0530	52,046	76		0	1.8		26.6	5.1
CD-96-9-0540	63,639	79.4		-0.4	1.6		25.2	4.4
CD-96-9-0550	64,389	78.4		-0.1	1.4		25.5	5
CD-96-9-0560	62,238	77.3		-0.5	1.5		24.4	5.4
CD-96-9-0570	53,808	82.4		-0.5	1.8		24.7	5.9
CD-96-9-0580	48,473	89.7		0	2.2		24.6	6.8
CD-96-9-0590	56,216	91.5		-0.1	2		24.6	7
CD-96-9-0600	60,685	83.5		0.3	1.8		23	5.8
CD-96-9-0610	68,403	84.4		-0.3	1.4		22.9	4.6
CD-96-9-0620	74,037	95.8		-0.1	1.8		22.6	4.6
CD-96-9-0630	47,308	84		0.3	2.2		22.8	7.8
CD-96-9-0640	50,976	94.3		0.2	2		22.2	6.7
CD-96-9-0650	67,876	98.7		-0.4	1.8		24.1	5.1
DR-1C-2480	54,258	72.6	-0.7	-0.3	1.7	18.4	17	6.6
DR-1C-2500	47,254	67.7	-0.2	-0.3	1.6	20.2	18	7
DR-1C-2520	49,866	73.2	0.1	0	2	21.2	17.8	7
DR-1C-2540	51,706	70.5	-0.2	1	1.6	20.2	17.7	6.2
DR-1C-2560	52,191	70.7	0.1	0.8	1.6	21.2	19	7
DR-1C-2580	52,390	67.4	-0.1	-0.2	1.6	21.9	18.6	7.2
DR-1C-2600	53,440	75	0.2	-0.2	1.6	21.9	19.3	6.3
DR-1C-2620	58,750	77.8	0.3	0.4	1.6	21.4	19.3	6.1
DR-1C-2640	57,979	69.3	0.2	0.8	1.4	21.9	20	6.1
DR-1C-2660	50,133	70.3	0.3	0.6	1.8	21.4	19.5	7.2
DR-1C-2680	52,261	71.8	0.2	0.7	1.6	23.1	19.8	6.3
DR-1C-2700	61,718	68.2	-0.1	0.5	1.4	24.7	21.9	5.6
DR-1C-2720	61,839	72.2	-0.1	0	1.4	24.7	20.9	6.3
DR-1C-2740	50,871	69.8	0.1	1.1	1.7	23.9	20.6	6.5
DR-1C-2760	50,256	69.7	0.5	1.2	1.7	22.1	19.9	6.8
DR-1C-2780	71,202	74.2	-0.1	1	1.3	23	19.5	5.2
DR-1C-2800	47,021	70.5	-0.3	0.6	1.9	23.5	20.1	7.2
DR-1C-2820	69,862	88.6	-0.1	0.1	1.6	22.8	20.1	5.1
DR-1C-2840	74,696	84.5	-0.3	0	1.4	21.1	18.2	4.7
DR-1C-2860	79,929	89.6	-0.9	-0.2	1.4	22.1	20.4	5
DR-1C-2880	60,440	95.7	-0.4	-0.1	1.9	23.8	20.4	6.4
DR-1C-2900	64,448	81	-0.4	-0.2	1.5	23.2	22.1	5.2
DR-1C-2917	68,094	90	-1	-0.4	1.7	22.8	19.3	6

Sample	CO2 (ppm)	+/-	δ13C (VPDB) (IRMS)	δ13C (VPDB) (LGR)	+/-	δ18O (VSMOW) (IRMS)	δ18O (VSMOW) (LGR)	+/-
EX-104-1380	44,285	75.5		-2.6	1.9		23.6	7.7
EX-104-1400	128,421	92.5		-2.5	0.9		26.1	2.9
EX-104-1420	74,079	75		-1.3	1.2		22.9	4.6
EX-104-1440	65,712	78.9		-0.4	1.4		24.7	5.4
EX-104-1500	47,804	70.5		-0.7	1.7		21.1	7.6
EX-104-1580	58,126	71		0	1.4		13.7	6.1
EX-104-1600	54,520	66.9		0.8	1.5		18.4	5.9
EX-104-1612	66,887	72.4		0.9	1.3		17	5.1
EX-111C-2180	36,497	80.7		-9.2	2.5		18.9	7.3
EX-111C-3425	61,368	97.2		0.9	1.8		18.4	4.5
EX-111C-3430	59,161	98.2		1.1	1.8		18.8	4.9
EX-111C-3435	33,683	84.5		0	2.8		18.1	8.6
EX-111C-3440	50,670	96.8		0.4	2.2		18	6
EX-111C-3445	37,371	88		-0.6	2.5		17.4	7.6
EX-111C-3490	34,607	79.2		0.5	2.7		22.7	7.5
EX-111C-3520	63,240	101.7		0.4	1.9		20.7	4.4
EX-111C-3525	55,687	103.1		0.7	2		20	5
EX-111C-3535	41,022	89.1		-0.1	2.3		20.3	6.7
EX-111C-3540	73,164	104.6		0.9	1.6		22	3.6
EX-111C-3545	32,046	90.1		1.1	3.1		22.2	9.4
EX-111C-3550	90,341	94.2		0.9	1.2		23.5	3.7
EX-111C-3555	89,052	107.1		1	1.4		24.2	3.5
EX-111C-3560	58,570	97.1		0.3	1.8		22.2	4.9
EX-111C-3565	88,618	104.8		0.5	1.3		23.3	3.5
EX-111C-3570	60,434	96		0.3	1.8		21.9	5.3
EX-111C-3575	70,783	97.8		-0.9	1.5		17.8	4.1
EX-111C-3590	76,324	91.6		0.3	1.4		22.2	4
EX-111C-3595	95,379	110.7		0.5	1.3		21.7	3.2
EX-111C-3600	75,289	99.1		-1.7	1.4		15.2	4.1
EX-111C-3620	80,683	99.2		0.5	1.3		22.4	3.4
EX-111C-3640	72,863	105.5		0.7	1.5		23	3.8
EX-111C-3660	92,264	111.7		0.7	1.3		22.1	3.4
EX-111C-3680	75,463	101		0.7	1.5		22	4.4
EX-111C-3700	84,440	94.8		0.6	1.3		22.6	3.6
EX-111C-3720	84,627	107.6		0.6	1.4		22	3.6
EX-111C-3740	77,953	106.6		0.6	1.5		21.9	4.2
EX-111C-3760	70,024	92		0.9	1.5		22.4	4.4
EX-111C-3780	72,239	97		0.7	1.5		22.2	4.2
EX-111C-3800	86,497	119		0.8	1.4		23.6	3.8
EX-111C-3820	64,966	90.7		0.9	1.7		23.3	4.4
EX-111C-3840	87,125	100.8		1	1.4		22	3.7
EX-111C-3880	82,170	107.1		0.8	1.5		22.6	4
EX-111C-3900	86,346	98.6		0.8	1.3		23.1	4
EX-111C-3920	68,947	95.9		1	1.6		21.9	4.5
EX-111C-3940	71,254	90.7		0.9	1.4		22.4	3.7
EX-111C-3960	90,377	100.1		0.7	1.1		23	3.3
EX-111C-3980	67,624	88.7		0.2	1.6		20.3	4.4
EX-111C-4020	65,647	102.2		0.5	1.7		23.7	4.3
EX-111C-4020	146,404	129.9		-0.7	1		28	2.4
EX-111C-4040	69,971	99.5		0.5	1.6		23.7	4.3

Sample	CO2 (ppm)	+/-	δ13C (VPDB) (IRMS)	δ13C (VPDB) (LGR)	+/-	δ18O (VSMOW) (IRMS)	δ18O (VSMOW) (LGR)	+/-
EX-111C-4040	142,765	117.5		-0.6	0.9		27.5	2.6
EX-111C-4060	86,695	96.4		0.8	1.4		26.3	3.5
EX-111C-4080	76,206	101.8		0.6	1.4		26	4
EX-111C-4100	78,494	103		0.6	1.4		25.7	3.7
EX-111C-4120	89,068	91.7		1	1.3		25.8	3.8
EX-111C-4140	78,233	110.4		0.4	1.6		15.4	4.4
EX-111C-4160	79,578	93		0.8	1.3		25.8	3.6
EX-111C-4180	80,656	111.3		0.6	1.5		24.9	3.7
EX-111C-4200	76,384	104.9		0.5	1.4		24.6	4.2
EX-111C-4220	62,894	95.3		-0.5	1.6		23	4.9
EX-111C-4240	67,084	100.1		-0.3	1.7		24.4	4.9
EX-111C-4260	72,972	101.2		-0.1	1.5		23.9	4.2
EX-111C-4280	67,710	96.5		-0.3	1.7		24.5	4.2
EX-111C-4300	76,254	97.7		0.6	1.5		26.1	3.8
EX-111C-4320	90,282	97.6		0.7	1.2		27.2	3.2
EX-111C-4340	91,462	97		0.7	1.2		26.7	3.1
EX-111C-4360	83,144	100.8		0.7	1.4		27	3.7
EX-111C-4380	84,740	93.9		-0.4	1.4		24.7	4
EX-111C-4400	95,436	98.7		-0.3	1.1		25	3.7
EX-111C-4420	88,068	98.5		0	1.3		24.8	3.7
EX-111C-4440	87,758	91.2		0.1	1.2		25.6	4.1
EX-111C-4460	86,466	94.8		-0.1	1.2		25.5	3.9
EX-111C-4480	96,005	102.8		-0.2	1.2		25.7	3.4
EX-111C-4500	84,993	105.8		0	1.4		25.5	4.6
EX-111C-4520	70,731	95.1		-0.2	1.6		24.6	5.1
EX-111C-4528	75,887	89.5		0.3	1.4		25.1	4.4
EX-112C-3850	81,867	96.6		1.1	1.4		21	3.5
EX-112C-3855	76,911	91.5		1	1.3		21.1	4
EX-112C-3860	58,640	88.1		1	1.7		20.4	4.8
EX-112C-3865	73,687	84.7		0.5	1.3		20.2	4.9
EX-112C-3870	57,320	92.4		0	1.7		18.2	5.5
EX-112C-3875	83,807	98.9		0.4	1.3		21.1	3.9
EX-112C-3880	79,777	109.9		0.5	1.5		21.8	3.8
EX-6C-1375	70,311	120.6		0.2	1.8		18.9	4.8
EX-6C-1380	72,554	114.1		-0.5	1.6		22.7	4.4
EX-6C-1385	70,333	108.6		-0.3	1.8		20.3	4.6
EX-6C-1390	57,588	95.9		0.6	1.9		21.3	5.3
EX-6C-1395	42,240	99		0	2.5		19.7	7.7
EX-6C-1400	61,235	90.2		0.2	1.7		18.7	5.1
EX-6C-1410	72,055	111.1		0.8	1.7		19.2	4.9
EX-6C-1420	73,426	102.2		0.7	1.6		12.5	4.6
EX-6C-1425	78,604	106.2		0.5	1.5		6	3.8
EX-6C-1440	72,275	104.8		0.4	1.6		19.1	4.5
EX-6C-1445	76,536	121		0.7	1.7		21.9	4.5
EX-6C-1450	67,033	90.9		0.2	1.6		20	4.5
EX-6C-1455	68,014	102.6		0.6	1.7		21.6	4.9
EX-6C-1460	73,169	121		0.9	1.8		21.2	4.7
EX-6C-1465	47,834	111.8		0.6	2.5		19.3	7.8
EX-6C-1470	55,069	114.4		0.7	2.2		18.8	6.1
EX-6C-1470	39,681	90.4		0.2	2.6		20.4	8

Sample	CO2 (ppm)	+/-	δ13C (VPDB) (IRMS)	δ13C (VPDB) (LGR)	+/-	δ18O (VSMOW) (IRMS)	δ18O (VSMOW) (LGR)	+/-
EX-6C-1475	71,900	107.9		0	1.6		19.3	4.4
EX-6C-1475	75,927	106.9		0	1.6		20.4	4.4
EX-6C-1480	78,001	113.4		1.3	1.6		24.1	4.5
EX-6C-1480	83,144	103.4		0.9	1.4		24.1	3.7
EX-6C-1485	80,960	112.8		-0.7	1.5		21.5	4.2
EX-6C-1485	87,497	119.7		-1.1	1.6		22.8	4.3
EX-6C-1490	75,159	105.1		0.7	1.6		20.9	4.4
EX-6C-1490	91,236	130.3		0.4	1.5		21.4	3.9
EX-6C-1495	86,228	115.4		0.6	1.5		23	3.9
EX-6C-1500	72,097	96.3		-0.1	1.7		21	4.7
EX-6C-1505	77,114	114.9		0	1.7		21.9	4.4
EX-6C-1510	80,595	100.2		-0.1	1.4		20.2	4.3
EX-6C-1515	81,248	112.2		0.7	1.6		22.5	4.5
EX-6C-1520	84,142	104.9		0.9	1.4		19.3	4
EX-6C-1525	72,776	112.3		0.2	1.8		19	4.5
EX-6C-1530	76,714	88.4		0.2	1.3		21.1	4.1
EX-6C-1535	74,878	111		1.7	1.7		22.2	4.5
EX-6C-1540	73,497	117.8		0.3	1.8		22.5	4.8
EX-6C-1545	51,170	101		0.3	2.3		22.6	6
EX-6C-1550	36,185	90		-0.5	2.9		18	9.4
EX-6C-1555	80,099	95.2		0.6	1.5		19	3.9
EX-6C-1560	58,441	101.3		1.6	1.9		13.8	5.3
EX-6C-1565	55,947	130.9		0.8	2.1		13.5	5.5
EX-6C-1575	55,088	97.4		1.9	1.9		17.8	5.9
EX-6C-1710	66,733	92.8		-1.3	1.6		10.5	4.7
EX-6C-1715	62,014	98.1		-1.7	1.8		10.5	5.3
EX-6C-1720	44,692	90.3		0.1	2.3		14.1	6.5
EX-6C-1725	58,544	106.6		1.5	1.9		18.4	5.7
EX-6C-1730	63,294	92.7		1	1.6		20.6	4.8
EX-6C-1735	65,683	101		1.6	1.8		19.3	4.9
EX-6C-1740	64,908	108.6		1.9	1.8		20	4.7
EX-6C-1745	67,615	107.1		1.8	1.8		17.5	4.9
EX-6C-1750	71,643	97.1		1.6	1.5		22.8	4.8
EX-6C-1753	62,778	104.8		2	1.9		23.7	5.1
EX-98-1310	49,503	67.7		0.9	1.8		18.9	6.8
EX-98-1320	70,427	82.7		0.4	1.4		23.1	5.3
EX-98-1340	50,956	67.1		1.1	1.6		23.3	7.3
EX-98-1360	59,201	77.3		0.1	1.7		23.2	6.2
EX-98-1365	71,519	64.6		0.8	1.2		23	5.1
GA-12CR-1480	75,160	78.2		-0.1	1.2		22.3	4.8
GA-12CR-1500	68,351	73.5		-0.2	1.4		21.2	5.3
GA-12CR-1520	81,479	79.6		-1.1	1.1		22.1	4.3
GA-12CR-1540	72,791	77		-0.8	1.2		20.7	5.7
GA-12CR-1560	70,386	79.6		-0.4	1.4		21.9	4.8
GA-12CR-1580	80,246	73.1		-1.2	1.1		18.9	4.9
GA-12CR-1600	52,352	68.7		-1.3	1.6		22.8	7.1
GA-12CR-1620	81,206	81.6		-1.1	1.2		25.2	4.6
GA-12CR-1640	76,163	75.9		-0.4	1.2		24.6	5.4
GA-12CR-1660	75,637	87.7		-0.1	1.4		25.6	5
GA-12CR-1680	84,576	80.7		-0.4	1.1		22.3	4.6

Sample	CO2 (ppm)	+/-	δ13C (VPDB) (IRMS)	δ13C (VPDB) (LGR)	+/-	δ18O (VSMOW) (IRMS)	δ18O (VSMOW) (LGR)	+/-
GA-12CR-1700	72,587	81.6		0.8	1.3		22.1	5.7
GA-12CR-1720	70,882	79.1		1.1	1.2		22.7	5.8
GA-12CR-1740	78,927	79.9		0.9	1.1		22.5	4.6
GA-12CR-1760	89,142	84.7		1.1	1.1		23.6	4
GA-12CR-1780	76,584	76.2		1.1	1.2		25.2	4.8
GA-12CR-1800	82,170	80.1		1.1	1.1		26.7	4.3
GA-12CR-1820	90,666	86		1.2	1.1		27.5	4.6
GA-12CR-1840	68,963	82.4		1.1	1.4		22.5	5.3
GA-12CR-1860	70,315	97.8		1.2	1.5		23.8	5.2
GA-12CR-1880	68,004	84.5		0.5	1.5		21.4	5.3
GA-12CR-1900	74,923	77.5		0.8	1.1		22.8	4.5
GA-12CR-1920	95,249	96.7		0.6	1.1		22.5	3.8
GA-12CR-1940	114,819	390.6		-2.2	1.8		18	4.1
GA-12CR-1960	105,009	95.6		-0.1	1.1		24.6	3.7
GA-12CR-1980	102,220	96.9		0.4	1.1		21.2	4.1
GA-12CR-2000	99,969	93.1		0.4	1.1		22.6	3.9
GA-12CR-2020	55,022	73.4		0.3	1.6		22.2	5.9
GA-12CR-2040	105,571	120.2		0.2	1.2		23.4	3.9
GA-1A-1460	39,787	83.1		-2.5	2.3		19.8	8.5
GA-1A-1470	45,268	91.2		-1.7	2.3		23.3	7.3
GA-1A-1480	36,442	89.9		-1.8	2.9		17.9	8.6
GA-1A-1490	32,308	86.6		-1.2	3.3		22.4	9.7
GA-1A-1500	45,141	87.8		-1.4	2.3		18.3	7.2
GA-1A-1510	33,308	84.7		-1.3	3		19.9	9.8
GA-1A-1520	36,297	89.2		-2.2	2.9		19.6	8.7
GA-1A-1530	32,748	82.8		-1.6	3.3		21.4	9.8
GA-1A-1540	35,393	94.9		-2	3.1		22.4	8.6
GA-1A-1580	65,858	94.8		-1.3	1.7		23.2	4.5
GA-1A-1610	103,645	99.3		-2.9	1.1		24.6	2.6
GA-1A-1620	66,984	94		-2.3	1.6		23.3	4.4
GA-1A-1630	55,742	99.4		-2.9	2		24.1	5.2
GA-1A-1640	70,815	93.4		-2.5	1.5		24.6	4.6
GA-1A-1650	75,494	95.6		-2.8	1.4		25.5	4.1
GA-1A-1660	80,147	97.4		-2.9	1.5		24.2	3.9
GA-1A-1670	57,251	76.3		-2.2	1.6		21.1	5.9
GA-1A-1680	64,222	94.8		-2.3	1.7		20.1	4.4
GA-1A-1690	47,777	78.5		-1.9	2		20.7	6.6
GA-1A-1700	77,421	107.9		-2.9	1.5		24	4
GA-1A-1710	48,206	78.1		-2.8	2.1		25.4	6
GA-1A-1720	75,605	94.8		-2.4	1.5		22.1	4.2
GA-1A-1730	41,713	80		-2.5	2.3		23.3	6.7
GA-1A-1740	57,466	93.4		-2.3	1.8		21.5	4.9
GA-1A-1750	60,673	87.9		-1.7	1.8		23	4.9
GA-1A-1760	82,394	115.3		-1.2	1.6		22.9	4.1
GA-1A-1770	98,976	109.9		-1.1	1.1		22.3	3.3
GA-1A-1780	65,475	97.4		-1.1	1.8		20.5	5.2
GA-1A-1790	68,572	96.2		-0.9	1.5		20.9	4.3
GA-1A-1800	86,927	104.4		-0.4	1.3		22.3	3.8
GA-1A-1810	63,836	90.9		-1.2	1.8		20	4.8
GA-1A-1820	68,038	86		-1.2	1.5		17.7	4.5

Sample	CO2 (ppm)	+/-	δ13C (VPDB) (IRMS)	δ13C (VPDB) (LGR)	+/-	δ18O (VSMOW) (IRMS)	δ18O (VSMOW) (LGR)	+/-
GA-1A-1830	43,765	83.4		-1	2.3		20.7	6.9
GA-1A-1840	50,560	77.7		-0.6	1.9		20.1	6.8
GA-1A-1850	45,040	80.7		-0.7	2.3		21.1	6.6
GA-1A-1860	73,898	95.5		-0.6	1.5		23.7	4.3
GA-1A-1870	42,990	94.2		-1.7	2.6		21.3	7.5
GA-1A-1880	80,039	97.5		-0.7	1.5		21.1	3.6
GA-1A-1890	49,400	76.4		-0.7	1.9		21.6	6.8
GA-1A-1900	45,763	79.6		1.7	2.1		13	6.2
GA-1A-1950	71,742	87.7		-1.4	1.5		14.6	4.2
GA-1A-1960	99,294	120.9		-1.6	1.4		19.5	3.3
GA-1A-1970	65,150	81.6		-0.4	1.5		22.2	4.5
GA-1A-1970	125,298	133.3		-1.9	1.2		23.6	2.7
GA-1A-1980	64,379	91.2		-1	1.6		23.8	4.4
GA-1A-1980	124,392	100.2		-2.1	1		25.6	2.4
GA-1A-1990	77,821	87.6		-1	1.3		21.4	3.6
GA-1A-2000	73,569	89.1		-0.1	1.5		19	4.1
GA-1A-2010	56,103	74.8		0.1	1.7		22.4	5
GA-1A-2020	65,875	87.6		-0.2	1.4		22.1	4.5
GA-1A-2030	59,522	79.4		0.4	1.6		21.1	4.8
GA-1A-2040	62,713	81.8		-0.2	1.5		23.5	4.7
GA-1A-2050	65,829	92.1		-0.1	1.7		22.9	4.3
GA-1A-2060	73,005	83.3		-0.1	1.3		22.8	4.4
GA-1A-2070	66,181	92		0.5	1.6		23.2	4.4
GA-1A-2080	71,947	89.7		0.3	1.3		18.4	4.2
GA-2A-1680	49,894	1134.3		-2.3	2.8		14	14.8
GA-2A-1690	52,007	95.9		-0.7	2.1		10.2	6.7
GA-2A-1700	51,210	91.5		-0.8	2.1		19.4	6.4
GA-2A-1710	53,944	95.1		-1.2	2		24	7.1
GA-2A-1720	70,059	104.8		-1.5	1.6		16.8	5
GA-2A-1730	70,287	120.6		-0.7	1.8		20.9	5.6
GA-2A-1740	58,362	96.2		-1.2	2		22.4	5.8
GA-2A-1750	77,435	101.3		-1.9	1.4		23.7	4.9
GA-2A-1760	84,433	109.5		-2	1.4		20	4
GA-2A-1770	83,379	113.3		-2.5	1.4		22.3	4
GA-2A-1780	87,227	97.4		-2.1	1.3		22.5	4
GA-2A-1790	101,125	109.7		-2.4	1.2		25.8	3.6
GA-2A-1800	110,586	120.5		-2.6	1.1		24.5	3.4
GA-2A-1810	40,221	90.5		-1.8	2.6		22	8.4
GA-2A-1820	53,537	1244.1		-1	2.8		19.1	14.6
GA-2A-1830	66,834	133		-1.8	2.3		20.8	6
GA-2A-1840	72,881	118.7		-1	1.9		20.2	4.8
GA-2A-1850	38,145	94.1		-1.8	2.6		19.8	8.6
GA-2A-1860	57,864	110.2		-1.3	2.1		18.9	7.5
GA-2A-1870	55,751	103.7		-0.2	2.1		20.1	7.8
GA-2A-1880	51,724	110.5		0.1	2.4		18.7	7.7
GA-2A-1890	68,651	116		0.4	1.8		20.1	4.7
GA-2A-1900	40,178	114.9		-0.3	3.2		21.8	9.3
GA-2A-1910	77,764	1625.4		0.8	3.2		16.5	13.9
GA-2A-1920	55,532	102.2		0.7	2.1		20.4	6.8
GA-2A-1930	36,072	144.8		-0.8	3.1		12.9	8.6

Sample	CO2 (ppm)	+/-	δ13C (VPDB) (IRMS)	δ13C (VPDB) (LGR)	+/-	δ18O (VSMOW) (IRMS)	δ18O (VSMOW) (LGR)	+/-
GA-2A-1970	74,626	103.9		1	1.7		2.8	4.8
GA-2A-1980	73,571	112.9		0.8	1.8		5.7	5.7
GA-2A-1990	59,954	110.4		0.6	2.2		6.5	8.4
GA-2A-2000	74,895	112.9		1.1	1.8		3.8	5.4
GA-2A-2030	58,641	108.5		0.7	2.1		14.7	5.6
GA-2A-2040	55,564	104.1		0.4	2.2		15.3	5.8
GA-2A-2050	102,946	156.3		0.1	1.7		23.2	3.6
GA-2A-2060	118,767	132.9		-0.3	1.3		25.1	2.8
GA-2A-2070	107,977	124.4		0.1	1.4		24.3	3.4
GA-2A-2080	114,991	138.9		-0.6	1.3		23.4	3.5
GA-2A-2100	113,570	135.1		-0.7	1.4		25	3.1
GA-2A-2110	119,048	145.9		-0.5	1.3		27.3	3.3
GA-2A-2120	107,756	125.6		-0.2	1.3		26	3.6
GA-35C-1680	66,745	95.5		-0.4	1.6		16.5	4.9
GA-35C-1700	62,381	85.6		-0.8	1.6		18.8	5.3
GA-35C-1720	72,071	100.8		-0.1	1.6		21.4	4.4
GA-35C-1760	66,605	94		0.2	1.7		11.3	5.1
GA-35C-1780	91,527	94.7		0.8	1.2		16.9	3.7
GA-35C-1800	97,000	100		-0.1	1.3		11	3.3
GA-35C-1820	72,612	89.3		0.8	1.5		21	4.6
GA-35C-1840	60,960	97.2		1.3	1.7		23.8	4.5
GA-35C-1860	54,452	87		1.2	1.9		22.7	5.5
GA-35C-1880	63,668	84.9		1.4	1.7		22.6	4.3
GA-35C-1900	48,522	88.6		0.9	2		22.8	6
GA-35C-1920	49,291	77.7		-0.4	1.9		21.3	6.4
GA-35C-2020	51,611	86.7		1.1	2		24.2	5.9
GA-35C-2040	69,186	81.2		2	1.5		20.6	4.9
GA-35C-2060	92,091	98		1.4	1.3		19.6	3.5
GA-35C-2100	30,141	71.6		2	3.1		20.3	9.8
GA-35C-2120	68,249	97.6		0.8	1.6		19.7	4.7
GA-35C-2140	72,026	80.6		3	1.4		20.2	5
GA-35C-2160	102,786	96.9		3.5	1.1		22.3	2.9
GA-35C-2186	77,607	89.6		2.4	1.4		22.3	3.7
GA-38-1250	60,135	75.9		-1.4	1.4		22.3	5.7
GA-38-1260	49,638	69.6		-1.2	1.7		21.2	6.6
GA-38-1270	57,903	71.2		-0.1	1.5		19	5.8
GA-38-1280	61,717	39.3		-0.9	0.7		22.6	2.4
GA-38-1290	84,432	88		-0.9	1.2		22.2	4.2
GA-38-1300	45,316	60.3		-2.6	1.9		19.6	8.2
GA-38-1310	44,486	39.6		-2.8	0.9		19.6	3.6
GA-38-1320	46,250	32.4		-2.7	0.8		20.6	3.2
GA-38-1340	62,322	38.2		-1.9	0.8		24.4	2.5
GA-38-1350	54,401	36.8		-2.1	0.9		25.3	2.4
GA-38-1360	73,581	44.2		-1.9	0.7		26.1	2.2
GA-38-1370	60,709	35.6		-1.4	0.8		26.8	2.4
GA-38-1390	66,805	42.5		-1	0.7		26.1	2.3
GA-38-1400	55,540	38.3		-0.4	0.8		25.6	2.9
GA-38-1410	68,267	43.4		-0.8	0.6		26.9	2.3
GA-38-1420	54,402	35.4		-0.2	0.7		26.8	2.9
GA-38-1430	53,996	38.5		-0.1	0.8		25.9	2.4

Sample	CO2 (ppm)	+/-	δ13C (VPDB) (IRMS)	δ13C (VPDB) (LGR)	+/-	δ18O (VSMOW) (IRMS)	δ18O (VSMOW) (LGR)	+/-
GA-38-1440	52,003	32.8		0	0.8		25.2	3.2
GA-38-1450	46,567	68.8		0.2	1.8		24.3	7.2
GA-38-1460	54,951	68.1		1	1.4		21.5	7.1
GA-38-1470	61,248	70.8		1	1.4		24.9	5.7
GA-38-1480	56,349	71.6		1.2	1.5		25.7	6.7
GA-38-1490	40,132	71.8		0.9	2.2		22.5	8.4
GA-38-1500	58,703	79.2		1.5	1.4		25.4	6.2
GA-38-1510	71,387	75.1	0.9	-0.7	1.2	24	22.9	5.1
GA-38-1520	51,561	71	1.7	0	1.6	20.8	18.7	7.3
GA-38-1530	78,712	69.8	0.4	-1	1	25.2	24.3	4.5
GA-38-1540	84,420	80.2	0.7	-0.9	1.2	24	24.6	4.4
GA-38-1550	59,650	73	0.7	-0.7	1.6	26.3	21.8	6.2
GA-38-1560	69,749	71.5	0.6	-0.9	1.2	26.9	26.3	5
GA-38-1570	74,136	81.2	0.6	-0.7	1.4	25.7	24.6	5
GA-38-1580	54,240	77.4	0.6	-0.5	1.8	24.2	22.9	6.4
GA-38-1590	59,141	78.8	1	-0.2	1.6	27.1	24.9	6.1
GA-38-1600	63,423	71.9	1.1	-0.1	1.4	26.7	24.6	5.5
GA-38-1610	60,438	65.8	1	-0.2	1.4	24.6	23.3	5.5
GA-38-1620	68,415	74.5	0.4	-1.2	1.4	25.8	23.2	5.2
GA-38-1630	69,261	76	-0.1	-0.8	1.4	24.7	24.6	4.9
GA-38-1640	87,086	78.2	0	-1.4	1.1	22	21.1	4.4
GA-38-1650	77,246	77.8	0.1	-0.6	1.2	21.8	10.2	5
GA-38-1660	59,210	70.9	0.3	0.2	1.6	22.5	16.8	6
GA-38-1670	67,470	82.7	0.2	-1	1.4	22.6	18.9	5.4
GA-38-1680	43,349	64.2	0	-2.1	1.7	17.2	12.8	8.1
GA-38-1690	61,739	76.4	-0.6	-2	1.4	21.4	20.3	5.9
GA-38-1700	75,610	75.3	-0.2	-1.8	1.2	20	19.6	5.1
GA-46C-1600	57,257	100		-0.6	2		24.1	6.4
GA-46C-1620	64,841	99.4		-0.3	1.9		22.1	5.8
GA-46C-1640	99,683	105.2		-1.9	1.2		26.3	3.8
GA-46C-1660	97,240	114.3		-1.5	1.3		28	4.2
GA-46C-1680	92,240	110		-2	1.3		25.3	4.1
GA-46C-1680	108,229	115.5		-2	1.2		27.3	3.4
GA-46C-1700	97,354	107.8		-1.2	1.3		27.5	3.5
GA-46C-1720	31,159	87		-1.6	3.3		26.7	11.6
GA-46C-1740	49,876	100.6		-1	2.3		23.3	7.1
GA-46C-1760	44,639	97.3		-1.5	2.5		25.8	8.4
GA-46C-1800	45,628	94.2		0.3	2.5		21.6	7.8
GA-46C-1800-1820	51,248	96.6		0.1	2.1		24.5	7.5
GA-46C-1805	44,788	97		-0.4	2.4		25.3	8.2
GA-46C-1810	40,592	94.3		-0.2	2.6		25.9	8.7
GA-46C-1815	35,945	87.1		0.4	2.9		26.4	9.9
GA-46C-1815-1820	48,545	95.7		0.8	2.5		23	8.2
GA-46C-1825	47,986	6775.6		0.4			20	
GA-46C-1920	40,435	92.1		-0.4	2.3		23.3	8.7
GA-46C-1940	41,848	87.4		0	2.3		24.7	9
GA-46C-1990	62,179	11394.8		0.6			19	
GA-48C-1680	44,687	81.5		-0.7	2.2		20.9	7.8
GA-48C-1700	67,458	98.5		-0.7	1.9		19.4	5.4
GA-48C-1720	93,936	120.7		-0.4	1.5		24.6	4.4

Sample	CO2 (ppm)	+/-	δ13C (VPDB) (IRMS)	δ13C (VPDB) (LGR)	+/-	δ18O (VSMOW) (IRMS)	δ18O (VSMOW) (LGR)	+/-
GA-48C-1740	113,237	127.5		-2.3	1.1		24.2	3.4
GA-48C-1760	119,589	115.8		-2.1	1.1		27	3.1
GA-48C-1780	54,908	96		-1.2	2		25.4	7.1
GA-48C-1930	42,131	80.6		-0.4	2.4		13	8.5
GA-48C-1940	67,074	106.6		-0.4	1.7		2.7	5.8
GA-48C-1960	64,683	104.6		-1.2	1.8		11.8	6.3
GA-48C-1980	54,573	89		0.5	1.8		6.7	7.2
GA-48C-2000	63,943	109.3		0.4	1.9		6.2	6
GA-48C-2031	69,835	97.6		0.5	1.5		6.3	5.8
GA-52C-1460	106,455	112.3		-2.8	1.1		22.2	3.6
GA-52C-1480	62,645	96.7		-2.7	1.8		18.7	4.9
GA-52C-1500	53,378	88.8		-1.5	1.9		23.2	7.4
GA-52C-1520	36,601	89.4		-3.2	2.9		14	10.6
GA-52C-1540	40,672	82.8		-2.9	2.4		15.9	9.1
GA-52C-1580	48,072	86.5		-2.7	2		16.9	8.3
GA-52C-1660	55,852	89.3		-0.8	1.8		22.5	6.8
GA-52C-1680	67,880	100.2		-1.3	1.6		19.3	5.1
GA-52C-1740	84,872	106.6		-1.4	1.3		22	4.3
GA-52C-1760	88,867	101.1		-1.4	1.3		21.5	4.4
GA-52C-1780	73,192	100.7		-1	1.6		23.5	4.7
GA-52C-1800	60,943	95.1		-1.3	1.8		22.9	5.9
GA-52C-1820	73,601	107.1		-0.3	1.6		21.6	5.2
GA-52C-1840	63,229	97.3		0.1	1.8		23.3	5.7
GA-52C-1860	53,270	84.4		0.2	1.9		24.2	7.4
GA-58-1720	38,264	71.5		-2.7	2.5		24.7	9.9
GA-58-1740	63,492	80.7		-1.3	1.6		24.3	5.4
GA-58-1760	76,231	95.4		0.2	1.4		24.9	4.6
GA-58-1780	46,313	77.5		0.2	2.1		22.2	7.6
GA-58-1800	80,339	91.9		-0.4	1.3		25.6	4.6
GA-58-1820	65,254	83.7		-1.2	1.6		24.8	5.6
GA-58-1840	86,247	100.6		-1.9	1.3		25.3	4.3
GA-58C-1580	48,935	79.7		-1.2	2		20.1	7
GA-58C-1600	78,462	107.3		-0.9	1.5		20.4	4.9
GA-58C-1620	48,115	90.2		0.7	2.2		17.8	7.1
GA-58C-1640	94,312	101.9		-0.1	1.3		22.7	3.9
GA-58C-1660	114,989	107.7		-0.2	1.1		26.7	3.4
GA-58C-1680	123,166	3094.4		-0.5	2.6		26.7	13.5
GA-58C-1700	39,701	86		0.3	2.4		22.1	9.2
GA-58C-1860	76,366	91.7		-0.1	1.3		21.9	5.3
GA-58C-1880	61,634	80.3		0.3	1.5		19.9	6.2
GA-58C-1900	81,215	97.8		0.5	1.4		19	4.5
GA-58C-1920	84,345	107.6		0.7	1.4		17.8	4.6
GA-58C-1940	91,253	103.4		0.8	1.3		18.3	4.1
GA-58C-1960	73,058	93.1		1.3	1.4		18.4	4.9
GA-58C-1980	50,675	96		1.3	2.2		17.3	7.1
GA-58C-2000	55,420	86.7		1.2	1.9		23.7	6.5
GA-58C-2025	32,988	76		1.1	2.8		23.4	11.9
GA-58C-2035	45,312	75.1		1	2		21.4	7.5
GA-5C-1640	81,632	102		-2	1.4		9	4.5
GA-5C-1660	128,429	135.8		-3.3	1.2		22.2	3

Sample	CO2 (ppm)	+/-	δ13C (VPDB) (IRMS)	δ13C (VPDB) (LGR)	+/-	δ18O (VSMOW) (IRMS)	δ18O (VSMOW) (LGR)	+/-
GA-5C-1680	75,894	96.5		-2.5	1.5		9.2	5
GA-5C-1720	79,542	110.9		-1.9	1.6		23.5	5.3
GA-5C-1740	79,905	98.7		-1.3	1.5		24.1	4.7
GA-5C-1760	64,221	103.4		-0.8	1.7		20	6.3
GA-5C-1780	71,006	99.4		-0.7	1.6		19.7	5.4
GA-5C-1800	60,291	100.5		-0.2	1.9		15.5	5.8
GA-5C-1820	77,091	92.8		0.5	1.3		19.3	4.4
GA-5C-1840	92,881	94.9		0.8	1.1		22.1	3.2
GA-5C-1860	97,871	108.6		0.7	1.2		21.8	3.4
GA-5C-1920	74,679	83.8		1.5	1.4		23.2	3.9
GA-5C-1960	105,896	147.6		1.2	1.2		24.4	3.2
GA-5C-1980	33,857	77.3		1.5	2.9		12.7	8.7
GA-65C-1260	44,585	83.6		-0.9	2.2		21.3	7.1
GA-65C-1280	42,148	77.5		-0.2	2.2		23	7.3
GA-65C-1420	37,806	96.1		0.2	2.9		23	8
GA-65C-1440	38,314	94.7		-0.3	2.7		25	7.8
GA-65C-1460	41,241	93.9		-0.6	2.7		23.8	7
GA-65C-1620	78,147	106.1		2.3	1.6		12.4	4
GA-65C-1640	56,066	99.6		1.5	2.1		21.5	5.3
GA-65C-1680	65,902	107.9		0.9	1.9		21.1	5
GA-65C-1700	73,620	104.8		0.7	1.7		7.8	4.3
GA-65C-1720	75,150	112.1		0.8	1.7		19.7	4.1
GA-65C-1740	74,480	106.7		0.8	1.6		19.9	4.5
GA-65C-1760	70,187	105.3		0.6	1.8		18.3	4.6
GA-65C-1820	69,410	105.2		2	1.6		19.8	4.9
GA-65C-1840	67,999	112.1		1	1.8		19.2	5.1
GA-65C-1860	71,662	98.7		1.3	1.7		20.6	4.3
GA-65C-1900	64,124	95.4		1.2	1.7		18.4	4.2
GA-65C-1920	67,458	113.2		1.4	1.9		20.6	4.9
GA-65C-1940	59,420	97.7		2.2	1.9		20.9	5.2
GA-65C-1960	92,743	114.9		1	1.3		21.1	3.6
GA-65C-1980	78,318	96		2.1	1.3		18.5	4.3
GA-65C-1980	61,916	88.7		1	1.6		19.2	5.3
GA-65C-2000	70,697	100.9		1.1	1.7		19.8	4.5
GA-65C-2000	74,829	109.3		2.1	1.6		20.8	4.4
GA-65C-2020	79,610	110		1.3	1.5		18.4	4.2
GA-65C-2040	72,869	104.1		0.9	1.7		10.5	4.6
GA-65C-2060	74,911	99.5		1.3	1.6		18.4	4.2
GA-65C-2080	73,255	114.8		1.1	1.7		22.5	4.5
GA-65C-2100	80,939	106.6		1	1.4		22.3	4.4
GA-65C-2120	78,716	110.5		1.7	1.6		23	4.2
GA-65C-2140	64,514	126.8		1.7	2.3		23.9	5.2
GA-65C-2160	71,289	108.8		1.1	1.7		23.3	4.9
GA-65C-2180	82,505	124.7		0.9	1.6		23.3	3.7
GA-65C-2200	69,301	99		0.9	1.8		21.9	4.2
GA-65C-2220	73,125	113.2		0.9	1.7		21	4.4
GA-65C-2240	78,848	106.1		0.4	1.6		22.1	4.2
GA-65C-2260	74,319	108.9		0.9	1.5		23.6	4
GA-65C-2280	73,612	110.2		1	1.7		22.4	4.3
GA-65C-2300	73,531	99.2		1.6	1.6		21.9	4.7

Sample	CO2 (ppm)	+/-	δ13C (VPDB) (IRMS)	δ13C (VPDB) (LGR)	+/-	δ18O (VSMOW) (IRMS)	δ18O (VSMOW) (LGR)	+/-
GA-65C-2320	76,337	112.5		1.8	1.8		22.1	4.1
GA-65C-2340	78,491	107.7		0.7	1.5		22.6	4.4
GA-65C-2360	68,582	97.3		0.5	1.6		23	4.7
GA-65C-2380	82,872	123.5		0.2	1.7		21.7	4.2
GA-65C-2420	68,758	96.4		0	1.5		23.8	4.8
GA-65C-2440	74,164	115.4		0	1.7		24.5	4.3
GA-65C-2460	74,487	111.2		0	1.7		24.8	4.4
GA-65C-2480	69,784	123.8		-0.5	1.9		24.6	5.3
GA-65C-2500	67,325	104.7		-0.2	1.9		24.2	5
GA-65C-2520	72,435	100.6		-0.2	1.6		25.7	4.6
GA-65C-2540	77,873	106.8		0.1	1.5		24.8	4.2
GA-65C-2560	66,106	109.5		0.2	1.8		25.6	5.5
GA-65C-2600	61,599	102.7		-0.1	1.9		23.1	5.7
GA-65C-2605	83,128	123.3		0.9	1.6		15.7	4.2
GA-65C-2610	69,323	89.8		1.7	1.4		16.7	4.5
GA-65C-2615	79,723	104.4		2.4	1.6		18	3.7
GA-65C-2620	69,718	102.8		3.1	1.6		22.2	4.2
GA-65C-2625	74,176	101.6		3.3	1.5		21.1	4.1
GA-65C-2635	76,547	101.1		2.3	1.4		17.6	3.5
GA-65C-2640	72,523	105.7		2.7	1.6		18.6	4.3
GA-65C-2645	74,350	93.4		2.6	1.4		16.6	4.1
GA-65C-2650	69,076	100.9		1.8	1.6		14.8	4.6
GA-65C-2655	53,032	91.3		1.1	1.9		8.9	5.1
GA-65C-2660	51,018	87.9		1.5	2		4.7	6
GA-65C-2670	74,023	90.1		1.6	1.3		19.4	4.4
GA-65C-2675	67,706	86.3		1.9	1.4		20.9	4.5
GA-65C-2680	81,525	103.8		1.7	1.4		22.8	4.1
GA-65C-2685	79,397	103.7		1.7	1.4		22.1	3.9
GA-65C-2690	77,871	99.7		1.2	1.4		22.5	3.7
GA-65C-2695	72,634	96.5		0.6	1.6		21.3	3.7
GA-65C-2700	71,379	109.7		1.3	1.7		21.1	4.5
GA-65C-2720	83,469	108.9		1.2	1.3		21.3	3.8
GA-65C-2740	76,848	94.6		2.3	1.5		21.3	4.1
GA-65C-2760	73,017	100.7		2.3	1.5		21.1	4.7
GA-65C-2780	61,968	97.9		2	1.6		16.6	5.5
GA-65C-2800	71,453	108.3		2	1.7		19.7	4.2
GA-65C-2840	77,014	105		1.9	1.5		21.1	4.3
GA-65C-2860	75,999	92.8		2.7	1.4		20.6	4.4
GA-65C-2880	73,469	97.8		1.3	1.4		15.2	4
GA-65C-2900	70,319	100.1		0.7	1.6		7.2	4.7
GA-65C-2920	76,528	104.9		0.4	1.5		16.3	4.5
GA-65C-2940	56,723	102.9		0.7	2		21.4	5.4
GA-65C-2960	74,264	102.5		0.8	1.6		21.5	4.7
GA-65C-2980	68,736	97.3		0.6	1.6		21.8	4.7
GA-65C-3000	74,632	102		0.5	1.6		21.9	4.5
GA-65C-3020	71,750	107.5		0.6	1.8		21.3	4.7
GA-65C-3040	74,348	98.4		0.2	1.5		20.4	4.4
GA-65C-3060	87,953	112.5		0.6	1.4		20.8	3.4
GA-65C-3080	85,997	107.5		0.3	1.5		19.7	3.4
GA-65C-3100	86,623	112.1		-0.1	1.4		24.2	3.8

Sample	CO2 (ppm)	+/-	δ13C (VPDB) (IRMS)	δ13C (VPDB) (LGR)	+/-	δ18O (VSMOW) (IRMS)	δ18O (VSMOW) (LGR)	+/-
GA-65C-3120	86,895	106		0.2	1.4		24.4	3.5
GA-65C-3140	55,856	97.3		1	1.8		21.5	5.1
GA-65C-3180	90,357	99.8		0.9	1.2		18.8	3.4
GA-65C-3200	85,259	104.2		0.5	1.3		19.6	3.7
GA-65C-3220	84,722	100.8		0.2	1.2		23.2	3.7
GA-65C-3240	86,750	96.9		0	1.3		24.5	3.3
GA-65C-3260	84,795	99.9		0.4	1.4		24.4	3.6
GA-65C-3280	86,554	99		0	1.4		23.9	3.4
GA-65C-3300	86,687	106.2		0.5	1.4		23.4	3.2
GA-65C-3320	95,472	110.5		0.1	1.3		22.9	3.2
GA-65C-3340	80,711	104.6		0	1.5		24.9	4.1
GA-65C-3360	84,174	113.8		-0.3	1.4		23.5	3.5
GA-65C-3380	86,009	116.3		-0.1	1.5		23.5	3.6
GA-65C-3400	78,271	95.3		0.2	1.4		23	3.9
GA-65C-3420	86,128	117.8		0.1	1.5		24	3.9
GA-65C-3460	80,257	101		0.6	1.5		23.2	3.7
GA-65C-3480	87,478	96.4		0.5	1.3		23.6	3.6
GA-65C-3500	93,113	106.7		0.3	1.2		23.7	3.1
GA-65C-3520	89,228	106.1		-0.1	1.4		24	3.5
GA-65C-3540	94,921	110.5		0.4	1.2		21	3.3
GA-65C-3560	80,524	106.5		0.4	1.5		16.7	4
GA-65C-3580	80,887	108.5		0.5	1.5		17.4	3.9
GA-65C-3600	74,007	94		0.5	1.4		18	3.9
GA-65C-3620	76,854	105.9		0.7	1.5		17.8	4.2
GA-65C-3640	67,458	90.7		0.5	1.4		15.7	5.1
GA-65C-3660	88,815	108.9		0.5	1.4		20.2	3.9
GA-65C-3680	70,315	93.4		1.2	1.4		19.2	4.3
GA-65C-3700	72,213	107.4		0.9	1.6		18	4.6
GA-65C-3720	82,018	108.9		0.8	1.4		17.1	3.7
GA-65C-3740	57,578	101.8		1.7	1.9		18.1	5.1
GA-65C-3748	64,716	90.5		2.1	1.6		20.4	4.7
GB-696-1160	96,185	108.6		-3	1.2		15.9	3.4
GB-696-1180	111,196	99.1		-1.3	1.1		18.3	2.9
GB-696-1200	107,554	107.2		-1.4	1.1		22	2.9
GB-696-1210	72,734	96.9		-1.3	1.4		21.5	4
GB-696-1215	80,809	104.8		-1.5	1.5		20.6	3.8
GB-696-1220	56,556	82.3		-2.4	1.8		20.2	5.7
GB-696-1225	83,387	1698.5		-1.4	3.3		20.8	12.6
GB-696-1230	66,478	97.2		-2.1	1.7		21.5	5
GB-696-1235	44,063	90.6		-2.6	2.4		16.8	6.2
GB-696-1260	32,264	92.5		-2.8	3.3		16.7	9.8
GB-696-1260	87,662	106.4		-1.8	1.3		21.5	3.8
GB-696-1265	73,546	102.3		-1.7	1.6		15.7	4.2
GB-696-1270	79,750	92.8		-1.4	1.5		20	3.8
GB-696-1275	69,631	105.6		-1.8	1.8		18	4.4
GB-696-1280	67,903	82.1		-1.6	1.5		21.7	5
GB-696-1285	58,566	86.8		-1.3	1.9		17.7	5.5
GB-696-1290	61,692	105.2		-0.2	1.9		19.3	5.1
GB-696-1295	37,505	86.3		-2.1	2.8		18.4	8.5
GB-696-1300	67,750	93.1		-1.2	1.6		20.9	4

Sample	CO2 (ppm)	+/-	δ13C (VPDB) (IRMS)	δ13C (VPDB) (LGR)	+/-	δ18O (VSMOW) (IRMS)	δ18O (VSMOW) (LGR)	+/-
GB-696-1310	65,034	89.6		-0.9	1.6		20.4	4.6
GB-696-1315	57,971	85		-0.5	1.7		21.1	5
GB-696-1345	65,787	105.1		-0.6	1.9		15.6	6.1
GB-696-1350	72,003	107		-0.3	1.9		16.5	5.2
GB-696-1380	40,772	72.3		0.1	1.9		21.9	7.2
GB-696-1460	81,952	92.9		-0.1	1.4		6.5	4
GB-696-1460	38,377	86.6		-0.6	2.6		11.2	7.6
GB-696-1480	125,218	104.8		-0.4	1		16.1	2.7
GB-696-1480	67,942	93.5		0.4	1.6		16.4	4.5
GB-696-1500	66,192	96.9		0.9	1.7		13.4	4.6
GB-696-1500	154,490	131.2		-0.2	1		17.3	2.1
GB-696-1521	50,764	79.7		-0.7	1.9		8.7	5.8
GB-696-1521	119,044	119.4		-1.4	1.1		9.9	2.9
NBC-32-1060	56,144	75.7		-1.2	1.7		19.1	6.9
NBC-32-1080	49,327	68.1		-1.5	1.7		22	6.8
NBC-32-1100	61,125	76.6		0.9	1.4		23.3	6.2
NBC-32-1120	61,165	73.2		0.5	1.5		24.6	5.2
NBC-32-1140	50,400	72.7		1.2	1.8		23.4	7.2
NBC-32-1160	70,056	80.1		1.4	1.3		25.3	5.4
NBC-33-1195	50,823	69		0.7	1.7		20	7.4
NBC-33-1200	92,944	92.6		0.9	1.1		21.2	4.2
NBC-33-1200	57,010	75.5		0.5	1.6		23.9	6.4
NBC-33-1206	69,143	81.2		-0.6	1.5		21.2	5
NBC-48-1300	62,674	77.5		1.1	1.6		9.3	5.8
NBC-48-1340	72,404	77.6		1.5	1.3		3.3	5.6
NBC-48-1370	87,785	75.8		0.2	1.1		16.4	3.8
PD-20C-1700	39,362	88.4		-0.4	2.5		23.2	9.9
PD-20C-1780	50,146	91.9		-0.2	2.1		23.1	6.9
PD-20C-1875	42,317	95.3		-3.1	2.6		20.9	8.7
PD-20C-1940	82,938	109.3		-3.5	1.5		19.8	4.4
PD-20C-1960	46,330	98.9		-3.8	2.4		21.8	7.4
PD-20C-2220	34,643	91.5		-2.3	2.9		18.9	10.2
PD-20C-2235	70,994	96.2		-5.1	1.5		15.8	5.6
PD-20C-2240	30,313	779.4		-3	3.3		17.7	21.8
PD-20C-2240	32,637	92.1		-3.5	3.2		20.5	11.3
PD-20C-2255	97,760	102.7		-4.9	1.2		13.8	3.9
PD-20C-2260	57,953	90.3		-3.2	1.8		15.4	6.1
PD-20C-2265	32,786	73.3		1.4	2.7		11.5	10.7
PD-20C-2280	42,638	90.1		-2.2	2.5		4	8.4
PD-20C-2330	40,442	91.3		1.2	2.6		17.7	9.2
PD-20C-2335	36,000	90.1		1.1	3		19	9.6
PD-20C-2345	39,893	83.7		1.2	2.4		18.4	9
PD-20C-2350	31,575	85.7		-2.1	3.3		22.2	11.5
PD-20C-2355	50,547	102.7		-1.1	2.2		21.9	7.3
PD-20C-2360	44,465	87.4		-1.4	2.3		20.8	8
PD-20C-2365	49,156	1174.9		-1.5	2.7		18	18.3
PD-20C-2380	51,458	100.7		-1.3	2		14.5	7.2
PD-20C-2385	45,204	78.7		-1.1	2.2		20	7.7
PD-20C-2390	82,840	107.8		-1.3	1.5		18.1	4.6
PD-20C-2395	82,888	109.2		-1.4	1.4		16.5	4.5

Sample	CO2 (ppm)	+/-	δ13C (VPDB) (IRMS)	δ13C (VPDB) (LGR)	+/-	δ18O (VSMOW) (IRMS)	δ18O (VSMOW) (LGR)	+/-
PD-20C-2400	45,351	94.3		-1.5	2.3		16.9	9.3
PD-20C-2405	68,132	100.6		-1.7	1.5		15.2	5.9
PD-20C-2410	49,358	101.6		-0.8	2.2		18.9	7.6
PD-20C-2415	44,041	87.5		-2.1	2.4		18.4	8
PD-20C-2420	64,368	97.6		-1.7	1.7		18.1	5.5
PD-20C-2425	94,110	114.6		-1	1.3		19.5	4
PD-20C-2435	57,257	92.8		1.3	2.1		19.3	5.9
PD-20C-2440	96,824	108.5		-1.5	1.3		21.2	3.7
PD-20C-2460	97,883	117.8		-0.9	1.3		20.5	4.4
PD-20C-2465	83,327	98.7		-1	1.3		19.5	4.4
PD-20C-2470	95,391	114.7		-1.4	1.4		18.6	3.9
PD-20C-2475	76,609	105		-1.9	1.5		19.8	4.9
PD-20C-2480	60,469	97.9		-2.1	1.9		20.2	6.6
PD-20C-2485	99,827	108.4		-1.4	1.3		14.9	3.8
PD-20C-2490	62,433	88.9		-1.3	1.7		20.8	5.6
PD-20C-2495	68,138	102		-1.4	1.6		20.6	5.5
PD-20C-2500	106,369	125.4		-1.6	1.3		18.5	3.8
PD-20C-2505	100,787	110.2		-1.2	1.3		18	4.4
PD-20C-2510	92,482	116.8		-1	1.4		17.4	4
PD-20C-2515	95,266	113.3		-0.9	1.4		18.5	4.1
PD-20C-2520	97,258	129.9		-1.1	1.3		17.2	4.4
PD-20C-2525	104,420	114		-1.8	1.2		17.8	3.6
PD-20C-2530	105,325	110		-1.5	1.3		18.2	3.5
PD-20C-2535	82,231	112.7		-0.9	1.5		18.7	4.5
PD-20C-2540	71,312	1677.9		-0.4	2.5		16.3	15.3
PD-20C-2545	70,013	103.7		-0.5	1.7		19.6	5.7
PD-20C-2550	62,247	94.1		-0.3	1.8		18.2	5.8
PD-20C-2555	32,913	89.4		-1.3	3		20.5	9.7
PD-20C-2560	84,557	104.2		-0.9	1.3		17.7	4.6
PD-20C-2565	68,348	109		-0.4	1.7		18.2	5.6
PD-20C-2570	45,207	85.2		-0.6	2.2		19.7	7.7
PD-20C-2575	31,099	80.6		-1.5	3.2		21.3	11
PD-20C-2590	49,900	94.3		-1	2.3		14.9	6.7
PD-20C-2595	32,204	81.1		0.3	2.8		10	11.2
PD-20C-2600	45,108	95.4		-0.9	2.4		17.8	8.2
PD-20C-2605	37,353	86.4		-1.2	2.7		20.5	9.7
PD-20C-2610	44,062	90.6		-1.2	2.4		20.8	7.7
PD-20C-2615	37,225	79.2		-1.2	2.7		22.5	9.9
PD-20C-2620	33,604	77.1		-0.2	2.6		19.8	11.5
PD-20C-2640	33,513	87.4		-0.3	2.8		20.7	11
PD-20C-2660	50,920	90		0.3	2.2		15.9	6.9
PD-20C-2680	54,042	88		0.5	1.9		16.9	6.7
PD-20C-2700	48,026	100.1		0.8	2.3		15.7	7
PD-20C-2760	74,608	103.1		0.3	1.6		16.9	4.8
PD-20C-2780	88,652	116.3		-0.1	1.5		15.1	4.2
PD-20C-2800	85,768	108.8		-0.5	1.4		15.6	4.5
PD-20C-2840	83,047	87.5		-1.6	1.4		17	4.5
PD-20C-2860	77,220	99.7		-1.7	1.5		18.1	5.2
PD-20C-2880	83,306	115.1		-1.4	1.6		20.3	4.6
PD-20C-2900	78,535	95.5		-1.9	1.4		20.8	4.9

Sample	CO2 (ppm)	+/-	δ13C (VPDB) (IRMS)	δ13C (VPDB) (LGR)	+/-	δ18O (VSMOW) (IRMS)	δ18O (VSMOW) (LGR)	+/-
PD-20C-2920	83,532	115.1		-1.7	1.5		23	4.2
PD-20C-2940	96,272	117.3		-0.1	1.4		24.4	4
SJ-325CR-1350	52,941	45		1.3	0.9		5.8	3.6
SJ-325CR-1355	60,021	38.7		0.4	0.8		10.4	2.7
SJ-325CR-1360	42,314	37.5		-0.8	1		9.1	3.2
SJ-325CR-1375	48,228	44.1		0	1		5.7	3.4
SJ-325CR-1380	43,679	44.9		-2.3	1.2		5.7	3.5
SJ-325CR-1385	42,035	40.5		-1.5	1.1		6.9	3.9
SJ-325CR-1390	43,811	34.5		0.6	1.1		2.8	3.6
SJ-325CR-1395	51,365	39		1.7	0.9		6.1	3.4
SJ-325CR-1400	43,379	37.5		0.3	1.1		4.7	4.4
SJ-325CR-1405	59,868	42.4		1.2	0.9		8.1	2.9
SJ-325CR-1410	51,544	39.7		1.9	1		6.9	3.3
SJ-325CR-1415	99,409	55.1		0.8	0.6		20.3	1.7
SJ-325CR-1420	74,808	50.3		0.2	0.7		15.1	2.2
SJ-325CR-1425	85,012	49.8		0.5	0.7		18.6	2
SJ-325CR-1430	77,764	47.1		0.2	0.7		16.6	2.3
SJ-325CR-1435	63,896	45.7		1.4	0.8		9	2.4
SJ-325CR-1440	79,295	54.4		1.3	0.7		18	2.2
SJ-325CR-1445	65,691	44.8		1.4	0.8		18.2	2.8
SJ-325CR-1450	71,259	50.8		1.5	0.8		20.3	2.5
SJ-325CR-1455	44,992	39.2		-0.5	1.2		9.9	3.6
SJ-325CR-1460	37,402	43.5		0.9	1.3		6.4	4.5
SJ-325CR-1465	45,031	43		-0.1	1.1		8.2	3.2
SJ-325CR-1475	52,159	47		-0.4	0.9		6.9	3.4
SJ-325CR-1480	71,750	46.5		0.8	0.7		17.7	2.1
SJ-325CR-1485	60,963	47.2		0.2	0.9		10.5	2.8
SJ-325CR-1490	54,471	47.2		0.5	1		7.7	3.2
SJ-390C-0650	40,114	74.6		-3.1	2.3		8.3	8.1
SJ-390C-0660	32,519	74.5		-2.5	2.5		20.1	9.3
SJ-390C-0670	51,362	74.9		-1.7	1.9		20.5	5.8
SJ-390C-0680	96,399	90.1		-0.9	1.1		18.5	3.5
SJ-390C-0690	54,977	79		-0.3	1.7		17.9	5.9
SJ-390C-0700	82,969	84.4		0.6	1.2		19.4	4.1
SJ-390C-0710	39,614	76.9		-0.4	2.4		19.5	9.7
SJ-390C-0720	41,518	74.8		0.1	2.2		16.8	8.4
SJ-390C-0750	37,386	77		0.1	2.4		19.5	8.7
SJ-390C-0770	49,196	87		2.2	2.2		20.3	7.6
SJ-390C-0780	55,445	86		1.7	1.8		20.4	6.8
SJ-390C-0790	44,149	87.5		2	2.2		21.6	8.6
SJ-390C-0800	56,436	86.7		2.7	1.9		21.7	6.6
SJ-390C-0900	80,068	101		2.3	1.5		21	4.8
SJ-390C-0920	78,434	99		1.4	1.5		20.1	5.2
SJ-390C-0940	71,070	95.6		1.5	1.6		16.3	5.5
SJ-390C-0960	80,438	87.9		0.8	1.3		15.5	3.9
SJ-390C-0965	75,642	88.6		0.4	1.4		18.2	5
SJ-390C-0970	77,545	89.4		0.1	1.3		18.9	4.6
SJ-390C-0975	72,571	89.7		1.7	1.4		17.9	5.2
SJ-390C-0980	68,542	90.4		2.4	1.6		16.9	5.5
SJ-390C-0985	74,959	92.8		1.1	1.4		17.8	5.1

Sample	CO2 (ppm)	+/-	δ13C (VPDB) (IRMS)	δ13C (VPDB) (LGR)	+/-	δ18O (VSMOW) (IRMS)	δ18O (VSMOW) (LGR)	+/-
SJ-390C-0990	75,306	94.7		1.1	1.4		19	5.1
SJ-390C-0995	67,278	84.8		2	1.5		14.8	4.8
SJ-390C-1000	67,163	87.4		1.4	1.6		16	5.3
SJ-390C-1005	79,206	83.9		1.2	1.2		15.7	4.6
SJ-390C-1010	75,279	86.8		1.5	1.4		16.9	4.8
SJ-390C-1015	67,323	95.8		1.7	1.8		15.4	5.5
SJ-390C-1020	65,482	85.1		1	1.7		16.9	5.5
SJ-390C-1025	80,527	101.6		-1.2	1.5		17.5	5.2
SJ-390C-1030	76,912	96.5		-0.4	1.5		14.4	4.6
SJ-390C-1035	72,069	102.2		-1.8	1.6		17.2	4.8
SJ-390C-1040	50,072	87.4		-1.5	2.2		18	8.3
SJ-390C-1060	49,958	86.6		0.1	2		12	8.1
SJ-390C-1095	46,069	97		1.4	2.4		11.6	8.5
SJ-390C-1095	46,713	87.6		0.9	2.4		13.5	8.1
SJ-390C-1100	80,145	104.2		1	1.6		13.2	4.9
SJ-390C-1100	79,776	96.9		0.7	1.5		14.2	4.7
SJ-390C-1105	74,356	81.5		2	1.4		13.3	4.8
SJ-390C-1110	75,857	90.1		0.8	1.4		13.4	4.9
SJ-390C-1115	68,790	89.2		1.9	1.5		16.2	5.5
SJ-390C-1120	61,847	87.2		1.6	1.7		18.6	5.9
SJ-390C-1125	71,688	91.7		0.6	1.5		18.3	5.1
SJ-390C-1130	55,514	83.5		1.3	1.8		18.6	5.9
SJ-390C-1135	73,376	94.1		1.1	1.6		15.4	4.8
SJ-390C-1140	71,999	87.4		1.2	1.5		13.9	4.7
SJ-390C-1160	65,764	93		1.4	1.6		12.2	6
SJ-390C-1180	80,438	101.7		1.7	1.4		9.1	4.4
SJ-390C-1200	55,529	86.3		1.7	1.7		8.5	6.7
SJ-390C-1220	64,043	86.1		1.1	1.7		10.5	5.8
SJ-390C-1240	46,237	69.4		1.7	1.9		11.1	7.6
SJ-390C-1260	61,036	86.8		1.5	1.6		12.6	5.6
SJ-390C-1280	108,828	106.4		2	1.2		13.7	3.5
SJ-390C-1294.5	78,629	85.6		2.4	1.3		13.7	4.8
SJ-429C-0950	85,582	42.5		-0.6	0.7		21.9	1.9
SJ-429C-0960	74,776	54.1		-0.1	0.9		21.4	2.3
SJ-429C-0970	77,776	54.6		0	0.8		22.4	2.1
SJ-429C-0980	76,445	55.2		0.3	0.8		20.9	2.1
SJ-429C-0990	73,801	47.5		0.4	0.7		18.8	2.4
SJ-429C-1000	65,059	44		1.1	0.8		22.1	2.7
SJ-429C-1020	95,424	69.2		1.3	0.7		22.3	2.2
SJ-429C-1040	82,813	52.7		0.7	0.7		20	2.3
SJ-429C-1040	105,392	56.2		1.1	0.6		21.5	1.6
SJ-429C-1060	119,390	242.7		-0.6	1		19.9	2
SJ-429C-1080	76,718	74.1		1.6	1.1		18.7	2.6
SJ-429C-1100	39,484	43.2		1.5	1.2		16.6	4.5
SJ-429C-1120	90,929	62.5		1.7	0.7		21.6	1.9
SJ-429C-1140	92,260	76.7		1.6	0.8		22.7	2
SJ-429C-1160	74,536	60.5		1.2	0.7		21.2	2.5
SJ-429C-1180	48,728	43.4		0.6	1.1		22.2	3.6
SJ-429C-1240	36,566	40.4		0.7	1.3		15.8	4
SJ-429C-1260	65,269	47.2		1.3	0.7		21.1	2.6

Sample	CO2 (ppm)	+/-	δ13C (VPDB) (IRMS)	δ13C (VPDB) (LGR)	+/-	δ18O (VSMOW) (IRMS)	δ18O (VSMOW) (LGR)	+/-
SJ-429C-1280	33,783	39.6		0.7	1.2		18.9	4.3
SJ-429C-1300	51,143	41.5		0.6	1		17.9	3.4
SJ-429C-1320	75,610	75.4		-0.3	1.1		11	2.4
SJ-429C-1320	32,560	39.5		-0.4	1.4		14	4.9
SJ-429C-1380	92,353	62.8		-0.2	0.7		15.2	2.1
SJ-429C-1405	38,839	42		-0.4	1.4		17.8	4.3
SJ-429C-1410	49,034	49.2		-0.3	1.3		16.5	3.7
SJ-429C-1415	62,631	48.7		-0.3	0.8		21.6	2.7
SJ-429C-1420	64,617	45.5		0.2	0.8		24.3	2.4
SJ-429C-1425	59,016	39.2		-0.3	0.8		23.2	2.8
SJ-429C-1430	33,227	43.5		-0.7	1.4		14.2	4.9
SJ-429C-1445	65,066	62.5		-0.3	1.1		20.9	2.6
SJ-429C-1450	44,639	41.1		-0.7	1.1		23.2	4.7
SJ-429C-1455	41,025	32.6		-1	1		22.5	4.2
SJ-429C-1465	60,212	51.7		0.6	0.9		21.3	2.9
SJ-429C-1470	43,113	40.1		-1	1		22.8	3.9
SJ-429C-1475	73,907	47.2		-0.6	0.8		24.7	2.3
SJ-429C-1480	35,999	48.4		0.1	1.3		10	4.6
SJ-429C-1500	106,587	78.8		1.6	0.8		14.5	2
SJ-429C-1520	98,364	57.4		1.5	0.7		10.5	1.8
SJ-429C-1540	61,416	41.7		1.3	0.9		5.8	2.9
SJ-429C-1545	41,257	47.4		0	1.3		15.4	4.4
SJ-429C-1550	103,685	67.5		1.8	0.6		11.3	1.8
SJ-429C-1555	123,008	66.1		1.2	0.5		15.5	1.6
SJ-429C-1560	119,651	102.4		1.6	0.9		11.5	1.7
SJ-429C-1575	106,076	52.8		1.9	0.5		15.1	1.6
SJ-429C-1580	118,252	75.2		1.2	0.6		20	1.5
SJ-429C-1600	92,945	58.6		1.8	0.6		13.6	2.1
SJ-429C-1620	65,224	63.5		1.2	1.2		9.4	2.7
SJ-429C-1624	70,632	39.2		1.1	0.7		8	2.1
SJ-430C-0130	49,074	46.6		-1.6	1.1		16.7	3.3
SJ-430C-0130	53,266	48.6		-2.4	1.2		16.7	3.3
SJ-430C-0140	57,150	36.9		-2.3	0.9		19.8	3
SJ-430C-0290	58,781	47.8		-1	0.9		18.8	2.6
SJ-430C-0300	36,888	38.9		-1.6	1.2		16.6	4.6
SJ-430C-0310	48,171	48.7		-0.7	1		16.9	3.8
SJ-430C-0320	54,912	41.8		-0.4	0.9		17.6	3.1
SJ-430C-0330	78,700	54.4		-0.1	0.7		17.9	2.4
SJ-430C-0340	53,187	35.8		-0.7	0.9		15.9	2.8
SJ-430C-0350	60,212	46.5		-0.1	0.9		16.8	2.6
SJ-430C-0360	79,665	48.5		-0.4	0.8		17	2.2
SJ-430C-0420	50,110	36.2		-0.4	1		15.6	3.3
SJ-430C-0430	68,932	55.5		-0.7	0.8		18.9	2.7
SJ-430C-0440	79,436	48.9		-0.7	0.7		18.1	2.4
SJ-430C-0450	66,275	44.4		-1.1	0.8		17.1	2.4
SJ-430C-0460	68,052	44.3		-1.3	0.8		16.4	2.7
SJ-430C-0470	50,541	49.3		-1.4	1.1		17.3	3.3
SJ-430C-0500	49,060	42		-1.2	1		17.2	3.9
SJ-430C-0510	49,838	39.5		-1.1	1		19	3.2
SJ-430C-0520	53,431	38.7		-1.8	0.9		18.9	3.1

Sample	CO2 (ppm)	+/-	δ13C (VPDB) (IRMS)	δ13C (VPDB) (LGR)	+/-	δ18O (VSMOW) (IRMS)	δ18O (VSMOW) (LGR)	+/-
SJ-430C-0530	49,089	41.3		-1.9	1		16.9	4
SJ-430C-0540	53,821	49.9		-2.5	0.9		13.3	3.3
SJ-430C-0860	33,984	41		-0.7	1.5		13	4.7
SJ-430C-0880	51,781	42.5		-0.6	0.9		18.2	3.4
SJ-430C-0900	61,044	46.8		-2.1	0.8		17.2	3.1
SJ-430C-0920	99,524	51.1		-2.3	0.6		21.4	1.9
SJ-430C-0940	90,109	65.3		-2.2	0.6		22.8	2
SJ-430C-0960	94,741	64.4		-0.3	0.6		21.8	1.7
SJ-430C-0980	87,924	59.8		0	0.7		20.5	2.1
SJ-430C-1000	80,450	68.8		0	0.8		18.6	2.1
SJ-430C-1020	90,956	51		1.4	0.6		20.1	1.7
SJ-430C-1340	39,592	37.7		1.6	1.3		10	4.3
SJ-430C-1350	58,761	48		1.4	0.9		13.6	2.6
SJ-436C-1050	59,471	42.1		0.8	0.8		16.1	3.1
SJ-436C-1130	75,364	37.1		0.2	0.6		22	2.5
SJ-436C-1135	60,164	43.3		0.5	0.8		22.5	2.6
SJ-436C-1140	60,477	49.7		0.1	0.8		19.9	2.5
SJ-436C-1145	76,835	41.4		0.3	0.7		20.3	2.2
SJ-436C-1150	79,826	48.6		1.2	0.7		17.1	2.1
SJ-436C-1155	66,486	42.4		-0.3	0.8		19.1	2.7
SJ-436C-1160	59,009	38.6		0.4	0.8		18.7	2.8
SJ-436C-1180	58,976	35.7		1	0.8		20.6	3
SJ-436C-1200	46,639	45.1		1.3	1		15.9	3.4
SJ-436C-1220	40,378	40		1	1.1		15.3	3.8
SJ-436C-1240	39,701	1133.3		0.5	3.5		14.5	19.1
SJ-436C-1300	37,773	34.4		1.5	1.2		11.8	4.4
SJ-436C-1320	52,250	37.3		1.7	0.9		4.7	3.6
SJ-436C-1340	39,756	37.3		1.4	1.2		7.1	3.9
SJ-436C-1360	46,262	42.8		0.4	1.1		11.9	3.7
SJ-436C-1374.1	48,272	41.9		-0.5	1.1		12.8	3.8
SJ-464C-0010	44,386	75.2		-4.5	1.9		17.6	7.1
SJ-464C-0260	57,660	83.8		-0.3	1.7		21.5	5.8
SJ-464C-0280	55,517	93.2		-0.2	1.8		22.8	5.9
SJ-464C-0310	81,153	97.4		0.7	1.5		16.1	4.4
SJ-464C-0320	65,777	89.6		0	1.6		15.9	5.4
SJ-464C-0330	66,048	93.4		-0.4	1.6		18.7	5.2
SJ-464C-0380	84,565	81.5		-1.5	1.2		12	4.3
SJ-464C-0790	36,515	77.3		-2.1	2.5		22.1	9.3
SJ-464C-0800	43,402	83.4		-1.9	2.6		24.4	6.6
SJ-464C-0810	39,726	83.2		-1.9	2.5		24.3	8.2
SJ-464C-0820	53,013	81.1		-2.9	1.8		23.2	5.9
SJ-464C-0840	84,987	101.2		-2.2	1.2		24.3	3.9
SJ-464C-0850	86,107	98.1		-2.2	1.4		24.4	4
SJ-464C-0860	93,070	102.5		-1.3	1.3		19.6	3.4
SJ-464C-0870	85,346	100.4		-0.9	1.4		20.1	3.7
SJ-464C-0880	76,340	96.8		-0.1	1.6		19.7	4.3
SJ-464C-0900	71,904	93.8		0.5	1.6		20	4.6
SJ-464C-0940	113,996	105.7		0.6	1.1		20.6	2.9
SJ-464C-0960	113,346	110.8		0.5	1.1		17.9	3.1
SJ-464C-0980	87,867	99.1		0.6	1.2		19.6	3.7

Sample	CO2 (ppm)	+/-	δ13C (VPDB) (IRMS)	δ13C (VPDB) (LGR)	+/-	δ18O (VSMOW) (IRMS)	δ18O (VSMOW) (LGR)	+/-
SJ-464C-1000	101,955	104.6		0.5	1.2		16.4	3.2
SJ-464C-1020	57,561	79.8		1	1.7		20.5	5
SJ-464C-1040	119,002	98.5		1.7	1		24	3
SJ-464C-1060	124,408	115.1		2.1	1.1		23.7	2.9
SJ-464C-1080	121,288	98		2.2	1		25.5	3
SJ-464C-1100	117,581	115.7		2	1.1		24.5	3.1
SJ-464C-1120	67,503	97.2		0.9	1.7		20.5	4.5
SJ-464C-1140	57,782	95.2		2.2	2		16.2	7
SJ-464C-1215	59,126	83.1		-0.8	1.6		22.6	5.1
SJ-464C-1220	63,865	91.1		-0.4	1.6		20.4	5.1
SJ-464C-1225	46,992	81.7		1	2.1		21.8	7.7
SJ-464C-1230	77,320	112.3		1.8	1.7		16.2	5.6
SJ-464C-1235	60,468	102.6		1.5	2		18.6	6.7
SJ-464C-1240	82,003	96.8		1.6	1.5		20.2	4.8
SJ-464C-1245	62,117	91.7		1.1	1.8		18.1	7
SJ-464C-1250	61,456	99.2		1.1	1.9		17.6	6
SJ-464C-1260	77,419	96.8		1.7	1.6		17.1	5.4
SJ-464C-1265	71,480	96.1		1.4	1.6		15.8	5.5
SJ-464C-1270	93,017	110.1		1.5	1.4		17.3	4.4
SJ-464C-1275	87,805	92.3		0.1	1.3		23.3	4
SJ-464C-1280	82,696	86.7		0.6	1.1		23.7	4.1
SJ-464C-1285	78,678	91.8		0.5	1.2		24.2	4.3
SJ-464C-1290	65,561	87.6		1.3	1.6		18.6	5.2
SJ-464C-1295	75,433	45.8		1.2	0.6		23.7	2
SJ-464C-1300	69,060	82.6		0.9	1.4		17	5.4
SJ-464C-1305	47,558	93.1		1.1	2.3		20	7.2
SJ-464C-1310	31,055	77.5		1.4	3		22.2	11.2
SJ-464C-1315	35,769	79.3		0.9	2.5		18.8	10.5
SJ-464C-1320	48,668	76.3		1.1	1.9		18	7
SJ-464C-1325	47,376	81		1.2	2		17.2	7.7
SJ-464C-1330	51,106	91.6		1	2		19.1	7.2
SJ-464C-1335	47,798	80.7		0.8	2.1		20.4	6.8
SJ-464C-1340	30,998	74		1.4	2.9		16.6	12.1
SJ-464C-1345	36,430	67.7		0.7	2.3		19.8	10.1
SJ-464C-1350	30,899	802.3		1.4	3.3		15.6	20.9
SJ-464C-1355	58,031	98.5		-0.4	1.7		20	6
SJ-464C-1360	38,271	79.9		1.4	2.4		18.2	9.7
SJ-464C-1365	88,128	94.8		1.7	1.1		19	3.5
SJ-464C-1370	63,026	83.7		1.4	1.5		16.2	5.6
SJ-464C-1375	76,033	91.4		1.3	1.4		18.7	4.2
SJ-464C-1380	73,242	90.6		1.2	1.4		18.6	5.4
SJ-464C-1385	69,245	95.4		1	1.6		20.7	5.6
SJ-464C-1390	42,104	78.8		1.7	2.2		17.3	7.9
SJ-464C-1395	56,569	85		0	1.9		19.1	5.8
SJ-464C-1400	52,840	87		0.1	1.9		21.2	6
SJ-464C-1405	74,966	97.5		2.6	1.5		16.7	4.8
SJ-464C-1410	55,700	81.4		2.2	1.8		19.3	6.4
SJ-464C-1415	50,088	79.1		2.1	1.9		20.8	6.6
SJ-464C-1420	56,589	92.8		2.2	1.7		19.1	6.3
SJ-464C-1425	40,375	74.2		0.6	2.4		18	8.1

Sample	CO2 (ppm)	+/-	δ13C (VPDB) (IRMS)	δ13C (VPDB) (LGR)	+/-	δ18O (VSMOW) (IRMS)	δ18O (VSMOW) (LGR)	+/-
SJ-464C-1430	80,515	89		2.4	1.4		4.9	4.3
SJ-464C-1435	97,466	2765.6		0.3	2.7		7.4	14.5
SJ-464C-1440	98,552	95.3		1	1.1		16.9	3.7
SJ-464C-1445	118,915	99.4		0.5	0.9		21.8	3.4
SJ-464C-1450	119,874	102.8		1.3	1		23.2	3.1
SJ-464C-1455	96,340	89.4		1.7	1.2		22.3	3.6
SJ-464C-1460	119,295	98.3		1.9	0.9		21	2.8
SJ-464C-1465	88,576	95.9		2.2	1.2		19.7	4.2
WM-01C-2460	50,522	81.8		-3.2	1.9		16	7.8
WM-01C-2500	64,747	79.8		-3.3	1.5		16.4	5.9
WM-01C-2520	46,396	74.5		-3.2	2		14.1	7.9
WM-01C-2580	73,415	79.4	0.7	1.4	1.3	17.4	16.3	5.3
WM-01C-2600	68,782	92.2	0.8	1.3	1.5	21.1	20.7	6
WM-01C-2620	92,704	85.5	0.2	0.7	1.1	19.1	19	4
WM-01C-2640	82,038	85.6	-0.1	0.4	1.3	22.7	20.7	5
WM-01C-2660	86,604	88.9	-0.3	0.7	1.2	23.9	21.3	5.2
WM-01C-2680	66,764	75.3	-0.5	0.1	1.4	23.9	22.5	5.7
WM-01C-2700	79,499	81	-0.6	0.3	1.2	22.4	21.4	5.1
WM-01C-2720	75,726	86.3	-0.3	0.3	1.2	22.5	21.1	5.1
WM-01C-2740	73,000	82.5	-0.1	0.5	1.5	22.9	18.9	5.4
WM-01C-2760	73,566	82.5	-0.8	0.2	1.4	22.8	20.1	5.5
WM-01C-2780	67,366	86.6	-0.6	0.1	1.6	22.8	21.7	5.4
WM-01C-2800	56,117	71.2	-0.3	0.1	1.6	24.9	22.9	6.3
WM-01C-2820	58,301	74.3	-0.3	0.2	1.4	24.3	22.6	6.3
WM-01C-2840	66,935	72.6	-0.6	0.2	1.4	24.5	22.2	5.3
WM-01C-2860	69,550	74.8	-0.5	0.2	1.3	24	20.6	4.9
WM-01C-2880	58,860	73.7	-0.3	0.4	1.6	23.9	22.8	6.1
WM-01C-2900	46,497	107.9	-0.7	-12.8	2.6	23.8	25.3	11.8
WM-01C-2920	72,043	83.6	-0.1	-1.5	1.5	22.4	18.1	5.9
WM-01C-2940	55,109	90.7	0.1	-0.5	2	18.1	16.1	6.8
WM-01C-2960	56,997	74.2	-0.3	-0.4	1.6	18.7	15.9	7
WM-01C-2980	57,004	88.4	-0.2	-0.7	1.9	20.8	15.9	6.6
WM-01C-3000	62,493	236.8	-0.6	-1.1	1.6	19.7	15.4	7
WM-01C-3020	61,255	86.2	-0.2	-0.8	1.7	21.6	19.4	6.3
WM-01C-3040	73,303	99.7	-0.3	-1	1.8	20.4	15.8	5.6
WM-01C-3050	67,614	84.8		-0.9	1.6		16.3	5.8

Appendix G

G.1 Aqua Regia Multi-element Geochemistry

SAMPLE	Depth (ft)	d13C ‰	d18O ‰	Ag ppm	Al ppm	As ppm	Au (FA) ppm	Au (aqua regia) ppm	B ppm	Ba ppm	Be ppm
BZ-965C	880	-1	18.8	0.58	0.23	174.5	0.034	<0.2	<10	20	0.52
BZ-965C	885	-0.9	23.8	0.83	0.26	64.2		<0.2	<10	20	0.49
BZ-965C	905	-0.7	18.5	1.11	0.15	67		<0.2	<10	70	0.22
BZ-965C	910	-0.2	13.3	1.76	0.21	73.2		<0.2	<10	20	0.33
BZ-965C	955	0.3	17	0.44	0.29	209	0.651	<0.2	<10	30	0.36
BZ-965C	960	0.1	16.2	1.11	0.28	274	1.097	<0.2	<10	40	0.37
BZ-965C	965	-2	18.5	3.16	0.37	394	0.994	<0.2	<10	50	0.44
BZ-965C	970	-1	15.5	2.84	0.27	382	0.651	<0.2	<10	10	0.39
BZ-965C	975	-0.7	19.1	2.31	0.4	535	0.446	<0.2	<10	10	0.43
BZ-965C	980	-0.5	17.7	3.08	0.26	381	0.240	<0.2	<10	5	0.54
BZ-965C	1000	-0.6	16.5	2.15	0.66	71	0.034	<0.2	<10	100	0.6
BZ-965C	1020	0.2	16.7	1.04	0.49	72	0.034	<0.2	<10	20	0.6
BZ-965C	1040	1.6	14.1	0.56	0.35	57	<0.005	<0.2	<10	20	0.52
BZ-965C	1060	1.8	14.5	0.47	0.4	64	0.069	<0.2	<10	70	0.63
BZ-965C	1065	2.5	16.6	0.42	0.38	70	0.103	<0.2	<10	20	0.57
BZ-965C	1070	1.8	16	0.38	0.47	98	0.549	<0.2	<10	20	0.51
BZ-965C	1075	2.3	16.1	0.4	0.42	78	0.240	<0.2	<10	50	0.67
BZ-965C	1080	2	15.9	0.4	0.56	79	0.103	<0.2	<10	30	0.47
BZ-965C	1085	2.1	18.9	0.43	0.38	116	0.583	<0.2	<10	30	0.57
BZ-965C	1090	2.3	18.1	0.46	0.36	367	1.063	<0.2	<10	30	0.43
BZ-965C	1095	2.2	18.1	0.41	0.31	433	2.023	<0.2	<10	30	0.45
BZ-965C	1100			0.29	0.43	222	1.474	<0.2	<10	30	0.67
BZ-965C	1105	2.2	19.6	0.32	0.51	625	3.360	<0.2	<10	30	0.61
BZ-965C	1110	2.4	17.6	0.25	0.45	729	6.309	0.3	<10	90	0.91
BZ-965C	1115	1.6	18.6	0.12	0.39	283	0.960	<0.2	<10	60	0.58
BZ-965C	1120	2.7	18.3	0.15	0.4	350	5.246	0.2	<10	40	0.57
BZ-965C	1125	1.4	15	0.15	0.26	597	5.314	0.4	<10	130	0.59
BZ-965C	1130	2.8	18.3	0.2	0.31	632	5.554	0.3	<10	50	0.62
BZ-965C	1135	1	15.1	0.13	0.3	377	1.131	<0.2	<10	40	0.53
BZ-965C	1140	2	13.4	0.07	0.26	275	0.823	<0.2	<10	30	0.48
BZ-965C	1145	1.4	14.6	0.06	0.19	178	0.514	<0.2	<10	60	0.37
BZ-965C	1150	1.3	14.9	0.04	0.18	77	0.069	<0.2	<10	50	0.37
BZ-965C	1155	1.6	15.8	0.05	0.18	61	0.034	<0.2	<10	60	0.39
BZ-965C	1160	2.1	17	0.04	0.16	43	<0.005	<0.2	<10	70	0.4
BZ-965C	1165	1.3	15	0.04	0.21	95	<0.005	<0.2	<10	70	0.47
BZ-965C	1170	1.7	12	0.04	0.24	89	<0.005	<0.2	<10	120	0.42
BZ-965C	1175	1	12.9	0.04	0.26	139	0.103	<0.2	<10	60	0.49
BZ-965C	1180	1.8	16.1	0.03	0.17	83	0.103	<0.2	<10	70	0.43
BZ-965C	1185	1.9	16.3	0.03	0.15	72	0.103	<0.2	<10	60	0.42
BZ-965C	1190	1.2	13.5	0.05	0.2	170	0.377	<0.2	<10	40	0.52
BZ-965C	1195	1.1	13.6	0.04	0.2	278	1.234	<0.2	<10	80	0.4
BZ-965C	1200	1.1	13.3	0.04	0.16	129	1.337	<0.2	<10	40	0.41
BZ-965C	1205	0.7	13.8	0.05	0.2	354	1.509	<0.2	<10	40	0.39
BZ-965C	1215	1.2	14.1	0.08	0.32	679	8.194	0.4	<10	40	0.54
BZ-965C	1220	1.1	13.3	0.04	0.27	978	4.114	<0.2	<10	40	0.55
BZ-965C	1225	1.4	15.3	0.06	0.33	276	0.926	<0.2	<10	40	0.5
BZ-965C	1230	1.7	16.4	0.04	0.28	145	0.240	<0.2	<10	50	0.5
BZ-965C	1235	1.7	18.5	0.04	0.34	74	<0.005	<0.2	<10	70	0.55
BZ-965C	1240	1.8	16.5	0.04	0.29	31	<0.005	<0.2	<10	90	0.47
BZ-965C	1245	1.5	17.3	0.04	0.26	50	0.034	<0.2	<10	70	0.52
BZ-965C	1250	1.5	15.4	0.04	0.32	125	<0.005	<0.2	<10	60	0.52

SAMPLE	Depth (ft)	d13C ‰	d18O ‰	Ag ppm	Al ppm	As ppm	Au (FA) ppm	Au (aqua regia) ppm	B ppm	Ba ppm	Be ppm
BZ-965C	1255	0.6	14.9	0.05	0.3	153	<0.005	<0.2	<10	40	0.54
BZ-965C	1260			0.07	0.39	228	0.789	0.2	<10	50	0.59
BZ-965C	1265	0.2	14.2	0.08	0.36	226	2.126	0.2	<10	40	0.58
BZ-965C	1270	-0.1	17	0.99	0.32	96	3.840	<0.2	<10	40	0.55
BZ-965C	1275	0.5	13.6	1.1	0.23	127	2.023	<0.2	<10	20	0.49
BZ-965C	1280	0.5	15.3	1.51	0.22	104	1.680	<0.2	<10	40	0.46
BZ-965C	1285	0.4	19	1.05	0.25	109	0.960	<0.2	<10	50	0.47
BZ-965C	1290	0.2	16.8	1.09	0.18	111	0.960	<0.2	<10	60	0.45
BZ-965C	1295	0.1	15.8	0.77	0.19	112	0.994	<0.2	<10	40	0.44
BZ-965C	1300	0.5	18	0.57	0.2	105	1.200	<0.2	<10	30	0.48
BZ-965C	1305	0.9	15.8	0.44	0.17	155	1.097	<0.2	<10	20	0.43
BZ-965C	1310	0.7	14.4	0.29	0.16	175	1.131	<0.2	<10	50	0.42
BZ-965C	1315	0.4	13.3	0.17	0.23	493	0.857	<0.2	<10	40	0.42
BZ-965C	1320	-1.4	15.5	0.15	0.17	352	0.960	<0.2	<10	30	0.48
BZ-965C	1325	-1.7	12.4	0.18	0.42	298	1.406	<0.2	<10	30	0.42
CD-14	530	2.9	22.9	0.05	0.51	652	<0.005	<0.2	<10	70	0.53
CD-14	550	1.8	20.1	0.06	0.36	115	<0.005	<0.2	<10	440	0.42
CD-14	560	2.6	19.1	0.05	0.26	180	<0.005	<0.2	<10	190	0.35
CD-14	570	1	15.5	0.07	0.37	315	<0.005	<0.2	<10	130	0.47
CD-14	580	2.5	23.9	0.05	0.34	245	<0.005	<0.2	10	120	0.54
CD-14	590	2.4	26.2	0.05	0.32	201	<0.005	<0.2	10	120	0.44
CD-14	600	2.4	22.4	0.05	0.23	24	<0.005	<0.2	<10	230	0.53
CD-14	610	2.2	21.7	0.25	0.4	35	<0.005	<0.2	10	490	0.49
CD-14	620	1.7	23.6	0.46	0.25	47	<0.005	<0.2	<10	400	0.55
CD-14	630	1.2	21.8	0.62	0.22	40	<0.005	<0.2	<10	340	0.7
CD-14	640	1.4	24.2	0.37	0.21	37	0.031	<0.2	<10	330	0.65
CD-14	650	1.6	24.9	0.32	0.19	45	0.031	<0.2	<10	200	0.54
CD-14	660	1.5	24.9	0.34	0.23	90	0.031	<0.2	<10	110	0.71
CD-14	670	2.1	24.9	0.24	0.3	142	<0.005	<0.2	<10	220	0.84
CD-14	680	2.6	22.6	0.09	0.19	96	<0.005	<0.2	<10	160	0.45
CD-14	690	2.4	23.4	0.1	0.24	64	<0.005	<0.2	<10	150	0.51
CD-14	700	1.5	22.3	0.13	0.2	25	<0.005	<0.2	<10	90	0.49
CD-14	720	1.7	24.1	0.12	0.23	23	0.063	<0.2	<10	110	0.39
CD-14	740	1.1	22.2	0.2	0.21	47	0.063	<0.2	<10	150	0.3
CD-14	770	1	21.8	0.44	0.2	21	<0.005	<0.2	<10	230	0.47
CD-14	780	1.3	20.9	0.36	0.15	22	0.031	<0.2	<10	110	0.41
CD-14	790	0.9	21.9	0.18	0.19	35	<0.005	<0.2	<10	100	0.34
CD-14	800	1.2	22.1	0.12	0.2	16	<0.005	<0.2	<10	90	0.32
CD-14	820	1.3	23	0.25	0.26	55	0.219	<0.2	<10	280	0.44
CD-14	840	0.8	24.8	0.26	0.36	51.5	0.094	<0.2	<10	70	0.45
CD-14	860	-0.3	21	0.05	0.45	27.6	0.031	<0.2	<10	480	0.41
CD-14	880	0	23.5	0.04	0.48	83.6	0.031	<0.2	<10	230	0.51
CD-14	900	0.2	25	0.06	0.47	37.2	<0.005	<0.2	<10	110	0.41
CD-14	920	0.9	24.3	0.03	0.43	63.3	<0.005	<0.2	<10	250	0.48
CD-14	940	0.9	22.7	0.02	0.42	23	<0.005	<0.2	<10	270	0.42
CD-14	960	0.8	24.8	0.1	0.45	152.5	<0.005	<0.2	<10	250	0.55
CD-14	980	0.4	24.7	0.11	0.39	57.6	0.031	<0.2	<10	160	0.42
CD-14	1000	1.1	24.1	0.05	0.31	136	<0.005	<0.2	<10	290	0.33
CD-14	1020	0.9	22.2	0.05	0.36	122	<0.005	<0.2	<10	130	0.35
CD-14	1040	1.1	21.2	0.04	0.39	84	<0.005	<0.2	<10	80	0.39
CD-14	1060	0.7	22.9	0.09	0.47	72	<0.005	<0.2	<10	50	0.47

SAMPLE	Depth (ft)	d13C ‰	d18O ‰	Ag ppm	Al ppm	As ppm	Au (FA) ppm	Au (aqua regia) ppm	B ppm	Ba ppm	Be ppm
CD-14	1080	1.3	21.6	0.22	0.27	34	<0.005	<0.2	<10	70	0.45
CD-14	1100	1	20.5	0.24	0.35	84	<0.005	<0.2	<10	150	0.42
CD-14	1120	1.3	21.9	0.05	0.4	18	<0.005	<0.2	<10	300	0.36
CD-14	1140	0.8	20	0.09	0.35	18	<0.005	<0.2	<10	60	0.41
CD-14	1160	1	22.6	0.2	0.31	25	<0.005	<0.2	<10	70	0.4
CD-14	1180	0.2	22.1	0.15	0.28	13	<0.005	<0.2	<10	70	0.37
CD-14	1200	-0.2	21.3	0.33	0.24	31	<0.005	<0.2	<10	90	0.4
CD-14	1220	-0.4	20.9	0.71	0.29	62	<0.005	<0.2	<10	60	0.5
CD-14	1240	-0.3	20.1	0.35	0.23	32	<0.005	<0.2	<10	40	0.46
CD-14	1260	0.2	21.3	0.33	0.38	36	<0.005	<0.2	<10	250	0.55
CD-14	1280	0.1	23	0.05	0.32	25	<0.005	<0.2	<10	120	0.47
CD-14	1300	0.1	23.3	0.02	0.48	84	<0.005	<0.2	<10	40	0.6
CD-14	1320	0.1	21.8	0.29	0.46	15	<0.005	<0.2	<10	90	0.44
CD-14	1340	0.2	20.6	0.26	0.41	43	<0.005	<0.2	<10	50	0.49
CD-14	1360	0	20.3	0.13	0.48	12	<0.005	<0.2	<10	60	0.53
CD-14	1380	0.1	19.3	0.39	0.32	82	<0.005	<0.2	<10	30	0.5
CD-14	1400	-0.2	15.8	0.13	1.07	1280	<0.005	<0.2	<10	190	0.83
CD-14	1420	-0.4	22.1	0.43	0.35	96	0.031	<0.2	<10	340	0.52
CD-14	1440	-0.5	19	0.26	0.6	16	<0.005	<0.2	<10	160	0.63
CD-14	1460	-1.1	19.2	0.15	0.44	8	<0.005	<0.2	<10	40	0.5
CD-14	1480	-1	22.1	0.04	1.56	35.1	<0.005	<0.2	<10	640	1.15
CD-14	1500	-1.2	21.3	0.07	1.9	9.5	<0.005	<0.2	<10	690	1.21
CD-14	1520	-1.3	18.2	0.09	0.62	34	0.031	<0.2	<10	310	0.53
CD-14	1540	-1.2	19.9	0.25	0.24	16	<0.005	<0.2	<10	50	0.31
CD-14	1560	-1.6	21	0.33	0.36	20	<0.005	<0.2	<10	290	0.42
CD-14	1580	-1.3	20.5	0.19	0.36	24	<0.005	<0.2	<10	140	0.43
CD-14	1600	-1.6	16.9	0.12	0.47	15	<0.005	<0.2	<10	100	0.44
CD-14	1620	-1.2	17.7	0.36	0.26	17	<0.005	<0.2	<10	40	0.39
CD-14	1640	-1.2	18.2	0.33	0.23	20	<0.005	<0.2	<10	130	0.46
CD-14	1660	-1.6	16.1	0.28	0.86	96	<0.005	<0.2	<10	470	1.06
CD-14	1680	-1.3	16.7	0.25	0.28	26	<0.005	<0.2	<10	70	0.43
CD-14	1700	-1.5	19.1	0.22	0.32	29	<0.005	<0.2	<10	100	0.52
CD-14	1720	-1.9	19.4	0.13	0.3	50	<0.005	<0.2	<10	100	0.52
CD-14	1740	-1.2	17.8	0.06	0.29	31	<0.005	<0.2	<10	30	0.49
CD-14	1760	-1	17.9	0.11	0.34	46	<0.005	<0.2	<10	60	0.62
CD-14	1780	-1	19.2	0.15	0.3	42	<0.005	<0.2	<10	70	0.51
CD-14	1800	-0.8	15	0.07	0.28	37	<0.005	<0.2	<10	50	0.45
CD-14	1820	-0.8	18.2	0.06	1.19	141	<0.005	<0.2	<10	160	0.6
CD-14	1840	-0.4	17.7	0.05	0.47	72	<0.005	<0.2	<10	290	0.48
CD-14	1860	-0.3	15.4	0.11	0.86	321	<0.005	<0.2	<10	120	0.8
CD-14	1880	-0.3	20.4	0.32	0.24	29	<0.005	<0.2	<10	80	0.42
CD-14	1900	-0.3	21.5	0.43	0.27	32	<0.005	<0.2	<10	60	0.4
CD-14	1920	0.1	18.9	0.3	0.23	19	<0.005	<0.2	<10	30	0.39
CD-14	1940	-0.5	18.4	0.16	0.27	50	<0.005	<0.2	<10	70	0.43
CD-14	1960	-0.4	20.1	0.39	0.38	24	0.094	<0.2	<10	410	0.5
CD-14	1980	-0.9	20.4	0.09	0.64	16	0.031	<0.2	<10	230	0.53
CD-14	2000	-0.1	19.5	0.11	0.42	12	<0.005	<0.2	<10	220	0.43
CD-14	2020	-0.3	20.2	0.05	0.36	61	<0.005	<0.2	<10	170	0.48
CD-14	2040	-0.2	19	0.05	0.3	10	<0.005	<0.2	<10	180	0.37
CD-14	2060	0.2	16.8	0.06	0.27	30	<0.005	<0.2	<10	410	0.43
CD-14	2080	0.3	20.1	0.08	0.28	55	<0.005	<0.2	<10	60	0.43

SAMPLE	Depth (ft)	d13C ‰	d18O ‰	Ag ppm	Al ppm	As ppm	Au (FA) ppm	Au (aqua regia) ppm	B ppm	Ba ppm	Be ppm
CD-14	2100	-0.2	13.4	0.08	0.97	354	<0.005	<0.2	<10	150	0.72
CD-14	2120	0.8	16.8	0.07	0.28	246	<0.005	<0.2	<10	80	0.43
CD-14	2140	0.1	20	0.08	0.38	27	<0.005	<0.2	<10	90	0.5
CD-14	2160	0.4	20.9	0.1	0.37	20	<0.005	<0.2	<10	180	0.45
CD-15C	1380	-1.2	17.8	0.1	0.36	31	<0.005	<0.2	<10	120	0.53
CD-15C	1400	-1.5	20.8	1.76	0.47	26	<0.005	<0.2	<10	140	0.76
CD-15C	1420	-2.2	22.5	1.2	0.55	20	<0.005	<0.2	10	140	0.86
CD-15C	1440	-2.4	21	0.81	0.37	25	<0.005	<0.2	<10	150	0.7
CD-15C	1460	-1.8	21.8	0.72	0.44	30	<0.005	<0.2	<10	90	0.81
CD-15C	1480	-1.4	21.6	0.57	0.51	47	<0.005	<0.2	<10	100	0.69
CD-15C	1500	-1.5	20	0.86	0.48	74	<0.005	<0.2	<10	50	0.58
CD-15C	1520	-1.3	20.2	0.39	0.36	15	<0.005	<0.2	<10	60	0.68
CD-15C	1540	-0.9	21.9	0.28	0.37	28	<0.005	<0.2	<10	180	0.67
CD-15C	1560	-0.3	24.7	0.36	0.35	59	<0.005	<0.2	<10	160	0.78
CD-15C	1580	-0.1	23.7	0.37	0.56	36	<0.005	<0.2	10	120	0.88
CD-15C	1600	0.3	23.6	0.29	0.52	28	0.031	<0.2	10	140	0.86
CD-15C	1620	0.8	22.7	0.24	0.83	18	0.031	<0.2	10	150	0.77
CD-15C	1660	1	21.3	0.32	0.4	89	0.188	<0.2	<10	250	0.55
CD-15C	1680	0.9	18	0.11	0.3	33	0.063	<0.2	<10	490	0.44
CD-15C	1700	0.9	15.9	0.06	0.2	23	0.031	<0.2	<10	210	0.39
CD-15C	1720	0.5	20.3	0.28	0.29	40	0.031	<0.2	<10	100	0.52
CD-15C	1740	-0.3	25.2	0.33	0.51	103.5	0.031	<0.2	<10	130	0.68
CD-15C	1760	0.3	23.9	0.27	0.38	86.4	0.031	<0.2	<10	160	0.6
CD-15C	1780	0.7	23.8	0.19	0.47	97.1	0.125	<0.2	<10	100	0.5
CD-15C	1800	1.2	23.6	0.53	0.37	101.5	0.783	<0.2	<10	260	0.49
CD-15C	1820	0.1	20	0.09	0.35	34.8	0.031	<0.2	<10	60	0.51
CD-15C	1840	0.3	19.1	0.04	0.3	29	0.031	<0.2	<10	220	0.46
CD-15C	1860	0.6	22.9	0.09	0.25	35	<0.005	<0.2	<10	180	0.4
CD-15C	1880	-0.1	20.1	0.22	0.67	63	<0.005	<0.2	<10	210	0.58
CD-15C	1900	0.5	22.5	0.4	0.29	73	<0.005	<0.2	<10	80	0.47
CD-15C	1920	-0.2	22	0.42	0.32	43	<0.005	<0.2	<10	100	0.46
CD-15C	1940	0	21.3	1.01	0.29	32	<0.005	<0.2	<10	180	0.44
CD-15C	2000	-0.1	21.8	0.54	0.46	39	<0.005	<0.2	<10	270	0.48
CD-15C	2020	-0.6	19.7	0.28	0.57	91.4	<0.005	<0.2	<10	300	0.55
CD-15C	2040	-0.6	20.1	0.43	0.86	18	<0.005	<0.2	10	90	0.51
CD-15C	2060	0.1	20.1	0.18	0.38	24	0.031	<0.2	<10	90	0.37
CD-15C	2080	-0.6	20.5	0.17	0.54	12	0.031	<0.2	<10	80	0.44
CD-15C	2100	-0.4	18.9	0.43	0.42	20	<0.005	<0.2	<10	60	0.39
CD-15C	2120	-0.6	21.1	0.34	0.61	54	<0.005	<0.2	<10	80	0.49
CD-95-3	890	-2.4	11.8	0.41	0.15	13.1	<0.005	<0.2	<10	60	0.31
CD-95-3	900	-2.6	13.3	0.39	0.16	21.6	<0.005	<0.2	<10	90	0.26
CD-95-3	910	-2	10.3	0.64	0.2	16.6	<0.005	<0.2	<10	60	0.28
CD-95-3	920	-4.4	12.7	0.32	0.11	21.5	<0.005	<0.2	<10	100	0.21
CD-95-3	930	-4.6	18.2	0.43	0.19	21.8	<0.005	<0.2	<10	130	0.34
CD-95-3	940	-6.7	17.8	0.35	0.09	13.2	<0.005	<0.2	<10	360	0.18
CD-95-3	950	-2.7	22	3.13	0.4	63	<0.005	<0.2	10	110	0.68
CD-95-3	960	-2.4	22.4	0.99	0.34	23	<0.005	<0.2	<10	130	0.7
CD-95-3	970	-1.5	22	0.83	0.36	25	<0.005	<0.2	<10	100	0.69
CD-95-3	980	-1.6	21.5	0.74	0.36	31	0.063	<0.2	10	150	0.68
CD-95-3	990	-2	21.6	0.63	0.33	30	0.031	<0.2	10	200	0.56
CD-95-3	1000	-0.5	22.7	0.43	0.33	26	0.031	<0.2	10	80	1.19

SAMPLE	Depth (ft)	d13C ‰	d18O ‰	Ag ppm	Al ppm	As ppm	Au (FA) ppm	Au (aqua regia) ppm	B ppm	Ba ppm	Be ppm
CD-95-3	1010	-0.8	22.6	0.39	0.37	29	0.063	<0.2	10	70	1.09
CD-95-3	1020	-1	22.4	0.39	0.28	19	0.031	<0.2	10	100	0.6
CD-95-3	1030	-0.6	21.4	0.58	0.25	22	0.031	<0.2	10	80	0.62
CD-95-3	1040	-0.3	21.9	0.38	0.34	20	0.031	<0.2	10	100	0.57
CD-95-3	1050	0.1	22.9	0.21	0.29	13	0.031	<0.2	10	70	0.99
CD-95-3	1060	0	22.8	0.12	0.3	11	0.031	<0.2	10	130	0.57
CD-95-3	1070	-0.2	22.7	0.17	0.36	15	0.031	<0.2	10	100	0.57
CD-95-3	1080	-0.3	21.1	0.2	0.43	22	0.031	<0.2	10	140	0.68
CD-95-3	1090	0.6	25.2	0.16	0.38	15	0.031	<0.2	10	140	0.72
CD-95-3	1100	0.5	21.1	0.15	0.31	18	0.031	<0.2	10	160	0.66
CD-95-3	1110	0.4	20.1	0.19	0.36	18	0.031	<0.2	10	220	0.78
CD-95-3	1120	0.2	22.8	0.1	0.36	20	<0.005	<0.2	10	120	0.66
CD-95-3	1130	0.1	22.4	0.05	0.25	23	<0.005	<0.2	<10	200	0.54
CD-95-3	1140	0.5	20.7	0.08	0.26	16	<0.005	<0.2	10	230	0.64
CD-95-3	1150	0	18.3	0.19	0.33	29	<0.005	<0.2	10	90	0.66
CD-95-3	1160	0.5	17.7	0.06	0.22	16	<0.005	<0.2	<10	140	0.45
CD-95-3	1170	0.8	19	0.07	0.23	15	<0.005	<0.2	<10	160	0.46
CD-95-3	1180	1	18.2	0.07	0.19	15	<0.005	<0.2	<10	220	0.46
CD-95-3	1190	1	17.5	0.06	0.21	20	<0.005	<0.2	<10	180	0.44
CD-95-3	1200	-1	15.3	0.04	0.19	12	0.063	<0.2	<10	480	0.4
CD-95-3	1210	1.2	18	0.1	0.23	15	<0.005	<0.2	<10	250	0.38
CD-95-3	1220	0.8	17.4	0.05	0.21	18	<0.005	<0.2	<10	250	0.42
CD-95-3	1230	1	16.7	0.07	0.19	20	<0.005	<0.2	<10	180	0.42
CD-95-3	1240	1.5	13.9	0.04	0.19	15	<0.005	<0.2	<10	160	0.37
CD-95-3	1250	1.5	23.1	0.05	0.26	22	0.031	<0.2	10	140	0.39
CD-95-3	1260	1.8	21.5	0.06	0.24	13	<0.005	<0.2	<10	220	0.39
CD-95-3	1270	1.8	18.2	0.06	0.22	13	<0.005	<0.2	<10	230	0.4
CD-95-3	1280	1.6	20.9	0.05	0.17	10	<0.005	<0.2	<10	200	0.41
CD-95-3	1290	1.4	19.3	0.06	0.52	480	<0.005	<0.2	<10	180	0.46
CD-95-3	1300	1	19.2	0.48	0.35	344	<0.005	<0.2	<10	100	0.46
CD-95-3	1310	0.7	20.3	0.71	0.21	84	<0.005	<0.2	<10	110	0.39
CD-95-3	1320	-0.4	23.9	0.61	0.23	60	<0.005	<0.2	<10	80	0.42
CD-95-3	1330	0.7	22.3	0.26	0.19	28	<0.005	<0.2	<10	260	0.41
CD-95-3	1340	1.2	21.2	0.15	0.2	39	<0.005	<0.2	<10	210	0.39
CD-95-3	1350			0.19	0.16	31	<0.005	<0.2	<10	110	0.34
CD-95-3	1360	1.1	16.9	0.19	0.13	27	<0.005	<0.2	<10	160	0.36
CD-95-3	1370	1	19	0.13	0.17	24	<0.005	<0.2	<10	320	0.33
CD-95-3	1380	1.2	19.7	0.11	0.16	32	<0.005	<0.2	<10	230	0.32
CD-95-3	1390	1.1	20.5	0.13	0.17	16	<0.005	<0.2	<10	220	0.41
CD-95-3	1400	1	15.1	0.16	0.13	20	<0.005	<0.2	<10	170	0.3
CD-95-3	1410	1	18.1	0.16	0.17	26	0.063	<0.2	<10	330	0.32
CD-95-3	1420	0.9	17.5	0.14	0.14	19	0.031	<0.2	<10	170	0.31
CD-95-3	1430	0.8	18	0.18	0.19	27	0.031	<0.2	<10	190	0.39
CD-95-3	1440	0.8	16.8	0.28	0.18	32	0.031	<0.2	<10	190	0.39
CD-95-3	1450			0.23	0.28	32	0.031	<0.2	<10	220	0.37
CD-95-3	1460	0.3	19.7	0.3	0.28	20	0.031	<0.2	<10	150	0.49
CD-95-3	1470	0.6	19.4	0.23	0.27	25	0.031	<0.2	<10	150	0.43
CD-95-3	1480	0.3	19.6	0.26	0.22	29	0.031	<0.2	<10	50	0.41
CD-95-3	1490	0.4	19.9	0.24	0.23	23	0.031	<0.2	<10	220	0.25
CD-95-3	1500	0.8	19.1	0.28	0.22	22	0.031	<0.2	<10	210	0.22
CD-95-3	1510	0.5	19.3	0.32	0.23	32	0.031	<0.2	<10	120	0.24

SAMPLE	Depth (ft)	d13C ‰	d18O ‰	Ag ppm	Al ppm	As ppm	Au (FA) ppm	Au (aqua regia) ppm	B ppm	Ba ppm	Be ppm
CD-95-3	1520	0.2	19.2	0.26	0.22	30	0.031	<0.2	<10	130	0.19
CD-95-3	1530	0	20.6	0.28	0.27	37	0.031	<0.2	<10	110	0.25
CD-95-3	1540	-0.1	21.1	0.31	0.25	28	0.031	<0.2	<10	240	0.23
CD-95-3	1550	-0.2	17.4	0.24	0.2	31	0.063	<0.2	<10	230	0.15
CD-95-3	1560	0.2	18.4	0.23	0.2	33	0.063	<0.2	<10	310	0.17
CD-95-3	1570	-0.9	17.4	0.29	0.3	41.3	0.125	<0.2	<10	330	0.22
CD-95-3	1580	0.3	15.1	0.24	0.23	48	0.094	<0.2	<10	170	0.19
CD-95-3	1590	0.6	16	0.29	0.35	47	0.063	<0.2	<10	360	0.23
CD-95-3	1600	0.2	12.8	0.13	0.2	43	0.094	<0.2	<10	270	0.14
CD-95-3	1610			0.1	0.2	32	0.063	<0.2	<10	130	0.18
CD-95-3	1620			0.14	0.27	40	0.063	<0.2	<10	130	0.22
CD-95-3	1630	-2.1	22.8	0.15	0.35	26.3	0.031	<0.2	<10	330	0.28
CD-95-3	1640	-2.5	18.3	0.2	0.42	34	0.063	<0.2	<10	400	0.31
CD-95-3	1650	-1.9	17.4	0.25	0.37	39	0.157	<0.2	<10	320	0.27
CD-95-3	1660	-1.3	19.4	0.19	0.32	46	0.063	<0.2	<10	360	0.28
CD-95-3	1670	-1.5	19.7	0.18	0.33	34.5	0.063	<0.2	<10	360	0.26
CD-95-3	1680	-2.1	20.7	0.16	0.33	35.8	0.031	<0.2	<10	360	0.23
CD-95-3	1690	-1.3	18.8	0.18	0.26	44	0.031	<0.2	<10	340	0.25
CD-95-3	1700	-0.8	17.7	0.15	0.28	29	0.031	<0.2	<10	360	0.22
CD-95-3	1710	-1	18.4	0.23	0.26	41	0.031	<0.2	<10	310	0.2
CD-95-3	1720	-0.9	19.1	0.24	0.26	43	0.031	<0.2	<10	320	0.19
CD-95-3	1730	-1.4	16.7	0.65	0.19	58	0.063	<0.2	<10	270	0.18
CD-95-3	1740	-1.3	23.1	0.33	0.21	42.7	0.063	<0.2	<10	200	0.17
CD-95-3	1750	-1.2	18.8	0.27	0.26	38	0.031	<0.2	<10	330	0.22
CD-95-3	1760	-0.6	18.5	0.22	0.2	27	0.031	<0.2	<10	400	0.17
CD-95-3	1770	-0.8	17.1	0.22	0.14	20	0.031	<0.2	<10	550	0.13
CD-95-3	1780	-0.7	16.6	0.19	0.15	16	0.031	<0.2	<10	200	0.13
CD-95-3	1790	-1.1	14.9	0.25	0.15	20	0.031	<0.2	<10	240	0.16
CD-95-3	1800	-1.3	13.5	0.27	0.14	23	0.031	<0.2	<10	150	0.17
CD-95-3	1810	-0.9	14.3	0.53	0.16	38	0.094	<0.2	<10	350	0.17
CD-95-3	1820	-1.1	12.6	0.38	0.16	46	0.063	<0.2	<10	110	0.15
CD-95-3	1830	-1.1	15.4	0.27	0.14	21	0.031	<0.2	<10	70	0.17
CD-95-3	1840	-0.7	16.9	0.13	0.17	15	<0.005	<0.2	<10	70	0.13
CD-95-3	1850	-0.8	17.4	0.13	0.12	14	0.031	<0.2	<10	120	0.19
CD-95-3	1860	-1.2	16.3	0.19	0.11	22	0.031	<0.2	<10	50	0.24
CD-95-3	1870	-1.4	14.4	0.18	0.16	25	0.094	<0.2	<10	60	0.25
CD-95-3	1880	-1.4	15.1	0.19	0.1	24	0.031	<0.2	<10	50	0.26
CD-95-3	1890	-1.2	14.6	0.29	0.15	31	0.031	<0.2	<10	230	0.28
CD-95-3	1900	-0.9	15.2	0.24	0.16	31	0.031	<0.2	<10	180	0.27
CD-95-3	1910	-0.2	17.1	0.1	0.14	26	0.031	<0.2	<10	370	0.2
CD-95-3	1920	-1	15.9	0.26	0.15	29	0.031	<0.2	<10	160	0.25
CD-95-3	1930	-0.6	15.3	0.27	0.26	1070	0.157	<0.2	<10	290	0.36
CD-95-3	1940	-3.3	13.3	1.17	0.46	4010	0.720	0.6	<10	30	0.5
CD-95-3	1950	-3	15.3	1.69	0.53	2350	0.501	0.3	<10	80	0.54
CD-95-3	1960	-1.5	15.3	0.52	0.14	109	0.031	<0.2	<10	70	0.27
CD-95-3	1970	-1.5	15.2	0.48	0.19	54	<0.005	<0.2	<10	300	0.33
CD-95-3	1980	-1.3	12.9	0.39	0.21	545	0.031	<0.2	<10	90	0.3
CD-95-3	1990	-2.8	14.2	0.17	0.57	558	0.031	<0.2	<10	60	0.57
CD-95-3	2000	-3.2	14.6	0.18	0.6	1115	0.125	<0.2	<10	30	0.6
CD-95-3	2010	-3.1	17	1.44	0.58	956	0.219	<0.2	<10	30	0.56
CD-95-3	2020	-1.4	18.2	4.99	0.24	198.5	0.094	<0.2	<10	230	0.34

SAMPLE	Depth (ft)	d13C ‰	d18O ‰	Ag ppm	Al ppm	As ppm	Au (FA) ppm	Au (aqua regia) ppm	B ppm	Ba ppm	Be ppm
CD-95-3	2030	-0.9	18.3	0.73	0.16	33	0.031	<0.2	<10	200	0.36
CD-95-3	2040	-1	11.7	1.68	0.18	52	0.063	<0.2	<10	130	0.3
CD-95-3	2050	-1.3	12.5	1.12	0.21	35	<0.005	<0.2	<10	90	0.35
CD-95-3	2060	-0.8	18.6	0.36	0.2	47	<0.005	<0.2	<10	110	0.39
CD-95-3	2070	-0.5	19.1	0.27	0.19	36	0.031	<0.2	<10	130	0.42
CD-95-3	2080	-0.8	18.7	0.18	0.24	27	<0.005	<0.2	<10	290	0.37
CD-95-3	2090	-0.6	19.6	0.66	0.24	39	<0.005	<0.2	<10	270	0.34
CD-95-3	2100	-0.7	18.9	1.3	0.22	37	0.031	<0.2	<10	160	0.37
CD-95-3	2110	-0.9	13.4	1.27	0.17	20.4	0.031	<0.2	<10	70	0.22
CD-95-3	2120			0.96	0.27	75.8	0.031	<0.2	<10	190	0.37
CD-95-3	2130	-1.8	13.8	4.53	0.44	2440	0.970	0.8	<10	70	0.42
CD-95-3	2140	-0.4	19.9	0.61	0.21	266	0.157	<0.2	<10	110	0.29
CD-95-3	2150	-0.3	18.4	0.44	0.26	192	0.125	<0.2	<10	150	0.37
CD-95-3	2160	-0.4	19.4	0.44	0.21	164	0.125	<0.2	<10	140	0.33
CD-95-3	2170	-0.7	17.5	0.8	0.39	486	0.250	<0.2	<10	150	0.47
CD-95-3	2180	-0.7	18.7	1.73	0.5	757	0.376	0.2	<10	110	0.5
CD-96-2C	770	-0.5	23.1	0.4	0.39	37	<0.005	<0.2	140	90	0.65
CD-96-2C	780	-0.6	23.2	0.41	0.46	30.1	<0.005	<0.2	<10	80	0.82
CD-96-2C	790	-0.2	24.3	0.49	0.35	35.9	0.031	<0.2	<10	70	0.71
CD-96-2C	800	-0.1	23.4	0.41	0.39	50	<0.005	<0.2	<10	90	0.61
CD-96-2C	810	0.9	21.6	0.27	0.3	233	<0.005	<0.2	<10	60	0.49
CD-96-2C	820	0.9	20.7	0.17	0.3	55	<0.005	<0.2	<10	120	0.89
CD-96-2C	830	0.7	22.4	0.18	0.36	28	<0.005	<0.2	<10	140	1.06
CD-96-2C	840	0.7	22.2	0.09	0.28	18	<0.005	<0.2	<10	90	0.91
CD-96-2C	850	0.6	21.6	0.12	0.24	18	<0.005	<0.2	<10	100	0.77
CD-96-2C	860	0.7	22.9	0.1	0.29	21	<0.005	<0.2	<10	90	0.94
CD-96-2C	870	0.6	23.1	0.13	0.32	21	<0.005	<0.2	10	160	1.09
CD-96-2C	880	0.7	22.3	0.18	0.34	16	<0.005	<0.2	<10	70	1.09
CD-96-2C	890	0.7	22	0.22	0.34	34	<0.005	<0.2	<10	170	1.17
CD-96-2C	900	0.5	22.3	0.25	0.31	23	<0.005	<0.2	<10	80	1.04
CD-96-2C	910	0.3	23.1	0.27	0.38	22	<0.005	<0.2	<10	130	1.02
CD-96-2C	920	-0.2	23.5	0.44	0.35	28	<0.005	<0.2	<10	70	1.31
CD-96-2C	930	-0.4	23.9	0.43	0.36	23	<0.005	<0.2	<10	70	1.11
CD-96-2C	940	-0.7	24.1	0.47	0.4	58	<0.005	<0.2	10	100	1.16
CD-96-2C	950	-0.8	24.4	0.69	0.48	52	<0.005	<0.2	10	140	1.14
CD-96-2C	960	-1.1	23.6	0.96	0.41	49	<0.005	<0.2	10	140	1.25
CD-96-2C	970	-1	21.6	0.62	0.34	32	<0.005	<0.2	<10	190	0.98
CD-96-2C	980	-0.7	21.6	0.21	0.55	41	<0.005	<0.2	<10	200	1.19
CD-96-2C	990	-0.4	22	0.45	0.43	43	<0.005	<0.2	<10	130	0.71
CD-96-2C	1000	-0.2	23.2	0.46	0.31	40	0.063	<0.2	<10	130	0.63
CD-96-2C	1010	-0.2	23.1	0.38	0.32	48	<0.005	<0.2	<10	70	0.78
CD-96-2C	1020	0	23.9	0.47	0.3	37	<0.005	<0.2	<10	70	0.85
CD-96-2C	1030	0.6	24.4	0.48	0.55	49.5	<0.005	<0.2	<10	70	0.63
CD-96-2C	1040	0.4	23.3	0.59	0.45	54	<0.005	<0.2	<10	130	0.58
CD-96-2C	1050	-0.3	21.5	0.5	0.7	37	<0.005	<0.2	<10	180	0.82
CD-96-2C	1060	0.6	20.5	0.21	0.26	24	<0.005	<0.2	<10	110	0.5
CD-96-2C	1070	-0.1	23.5	0.12	0.3	20	<0.005	<0.2	<10	90	0.71
CD-96-2C	1080	0.6	22.2	0.12	0.26	23	<0.005	<0.2	<10	120	0.58
CD-96-2C	1090	0.6	21.6	0.17	0.3	24	<0.005	<0.2	<10	100	0.74
CD-96-2C	1100	0.5	21.6	0.06	0.27	16	<0.005	<0.2	<10	190	0.64
CD-96-2C	1110	0.5	21.1	0.05	0.23	10	<0.005	<0.2	<10	150	0.64

SAMPLE	Depth (ft)	d13C ‰	d18O ‰	Ag ppm	Al ppm	As ppm	Au (FA) ppm	Au (aqua regia) ppm	B ppm	Ba ppm	Be ppm
CD-96-2C	1120	0.6	21.8	0.13	0.26	15	<0.005	<0.2	<10	140	0.6
CD-96-2C	1130	0.3	23	0.07	0.26	20	<0.005	<0.2	<10	100	0.62
CD-96-2C	1140	0.4	23.3	0.13	0.3	18	<0.005	<0.2	<10	100	0.77
CD-96-2C	1150	0.5	20.7	0.1	0.24	12	<0.005	<0.2	<10	90	0.58
CD-96-2C	1160	0.9	21.6	0.04	0.13	13	<0.005	<0.2	<10	200	0.29
CD-96-2C	1170	0.7	20.9	0.04	0.14	10	<0.005	<0.2	<10	190	0.39
CD-96-2C	1180	0.8	19.2	0.07	0.19	15	<0.005	<0.2	<10	220	0.4
CD-96-2C	1190	0.6	20.5	0.14	0.22	9	<0.005	<0.2	<10	170	0.47
CD-96-2C	1200	0.6	22.3	0.19	0.26	15	<0.005	<0.2	<10	130	0.57
CD-96-2C	1210	0.7	21	0.09	0.24	14	<0.005	<0.2	<10	220	0.63
CD-96-2C	1220	0.3	19.8	0.1	0.2	12	<0.005	<0.2	<10	320	0.43
CD-96-2C	1230	-0.2	20.1	0.22	0.23	19	<0.005	<0.2	<10	180	0.46
CD-96-2C	1240	-0.5	20.1	0.25	0.22	28	<0.005	<0.2	<10	230	0.41
CD-96-2C	1250	0.3	14.5	0.19	0.17	25	<0.005	<0.2	<10	160	0.33
CD-96-2C	1260	0.9	17.2	0.06	0.22	18	<0.005	<0.2	<10	110	0.48
CD-96-2C	1270	1	17.4	0.1	0.25	21	<0.005	<0.2	<10	130	0.46
CD-96-2C	1280	0.1	20.1	0.04	0.29	41	<0.005	<0.2	<10	80	0.53
CD-96-2C	1290	0.4	18.6	0.03	0.26	17	<0.005	<0.2	<10	130	0.54
CD-96-2C	1300	0.3	19.5	0.03	0.27	21	<0.005	<0.2	<10	120	0.57
CD-96-2C	1310	0.1	19.3	0.03	0.27	22	<0.005	<0.2	<10	50	0.66
CD-96-2C	1320	0	16.7	0.04	0.27	31	<0.005	<0.2	<10	100	0.58
CD-96-2C	1330	0.1	18.5	0.03	0.26	18	<0.005	<0.2	<10	80	0.48
CD-96-2C	1340	-0.4	16.2	0.02	0.27	17	<0.005	<0.2	<10	80	0.57
CD-96-2C	1350	-0.2	15.8	0.02	0.28	13	<0.005	<0.2	<10	80	0.34
CD-96-2C	1360	-0.2	17.4	0.08	0.33	17	<0.005	<0.2	<10	60	0.41
CD-96-2C	1370	-0.2	17.2	0.1	0.28	36	<0.005	<0.2	<10	120	0.35
CD-96-2C	1380	-0.3	17.9	0.06	0.32	57	0.031	<0.2	<10	150	0.67
CD-96-2C	1390	-0.4	15.7	0.08	0.37	24	0.031	<0.2	<10	70	0.67
CD-96-2C	1400	0.1	18.4	0.19	0.23	13	0.031	<0.2	<10	90	0.43
CD-96-2C	1410			0.08	0.28	19	0.031	<0.2	<10	110	0.5
CD-96-2C	1420	0.2	20	0.13	0.22	16	0.063	<0.2	<10	60	0.51
CD-96-2C	1430	-0.2	22.2	0.1	0.23	21	<0.005	<0.2	<10	60	0.43
CD-96-2C	1440	-0.9	19	0.26	0.21	75	0.063	<0.2	<10	90	0.42
CD-96-2C	1450	-1.3	18.3	0.53	0.22	48	0.031	<0.2	<10	30	0.39
CD-96-2C	1460	-0.6	19.8	0.3	0.19	29	0.031	<0.2	<10	30	0.39
CD-96-2C	1470	-1	20.1	0.24	0.25	24	<0.005	<0.2	<10	60	0.56
CD-96-2C	1480	-0.6	18.5	0.04	0.24	15	<0.005	<0.2	<10	70	0.48
CD-96-2C	1490	-0.8	19.9	0.06	0.36	73	0.031	<0.2	<10	150	0.72
CD-96-2C	1500	-0.6	19.3	0.2	0.26	14	<0.005	<0.2	<10	90	0.38
CD-96-2C	1510	-0.7	17.4	0.09	0.38	12	<0.005	<0.2	<10	140	0.52
CD-96-2C	1520	-1.3	18.8	0.2	0.41	25	<0.005	<0.2	<10	110	0.63
CD-96-2C	1530	-0.8	18.3	0.26	0.32	19	0.031	<0.2	<10	230	0.53
CD-96-2C	1540	-0.9	16.8	0.14	0.27	15	0.031	<0.2	<10	120	0.51
CD-96-2C	1550	-0.9	18.5	0.1	0.39	18	<0.005	<0.2	<10	210	0.61
CD-96-2C	1560	-0.9	16.7	0.1	0.45	42	<0.005	<0.2	<10	150	0.8
CD-96-2C	1570	-0.6	16.4	0.35	0.42	39	<0.005	<0.2	<10	260	0.78
CD-96-2C	1580	-0.9	16.7	0.37	0.27	38	0.031	<0.2	<10	80	0.52
CD-96-2C	1590	-0.9	15.7	0.17	0.31	26	<0.005	<0.2	<10	210	0.54
CD-96-2C	1600	-1.3	16.2	0.17	0.31	21	<0.005	<0.2	<10	100	0.57
CD-96-2C	1610	-0.9	16.3	0.03	0.37	15	<0.005	<0.2	<10	80	0.67
CD-96-2C	1620	-1.2	15.7	0.06	0.38	24	<0.005	<0.2	<10	80	0.71

SAMPLE	Depth (ft)	d13C ‰	d18O ‰	Ag ppm	Al ppm	As ppm	Au (FA) ppm	Au (aqua regia) ppm	B ppm	Ba ppm	Be ppm
CD-96-2C	1630	-1	15.8	0.07	0.26	65	0.094	<0.2	<10	120	0.53
CD-96-2C	1640	-1.5	14.4	0.28	0.27	44	0.031	<0.2	<10	60	0.57
CD-96-2C	1650	-1.3	13.6	0.17	0.27	74	0.063	<0.2	<10	90	0.48
CD-96-2C	1660	-1.3	15.7	0.26	0.27	82	0.094	<0.2	<10	90	0.43
CD-96-2C	1670	-1.1	14.9	0.24	0.24	49	<0.005	<0.2	<10	170	0.39
CD-96-2C	1680	-0.6	13.7	0.29	0.24	54	0.094	<0.2	<10	70	0.34
CD-96-2C	1690	-0.9	9.2	0.08	0.15	40	0.063	<0.2	<10	240	0.21
CD-96-2C	1700	-0.3	14	0.11	0.22	38	<0.005	<0.2	<10	170	0.36
CD-96-2C	1710			0.14	0.22	25	<0.005	<0.2	<10	150	0.34
CD-96-2C	1720	-0.6	11.9	0.11	0.29	24	<0.005	<0.2	<10	110	0.35
CD-96-2C	1730	-0.8	12.1	0.17	0.21	29	<0.005	<0.2	<10	100	0.28
CD-96-2C	1740	-0.8	11.8	0.19	0.22	28	<0.005	<0.2	<10	90	0.32
CD-96-2C	1750	-0.7	11.9	0.22	0.23	23	<0.005	<0.2	<10	140	0.32
CD-96-2C	1760	-0.5	14.3	0.08	0.28	27	<0.005	<0.2	<10	170	0.35
CD-96-2C	1770	-0.4	12	0.14	0.33	21	<0.005	<0.2	<10	130	0.45
CD-96-2C	1780	-0.3	15.1	0.18	0.23	15	<0.005	<0.2	<10	100	0.37
CD-96-2C	1790	-0.3	15.7	0.21	0.25	42	<0.005	<0.2	10	240	0.39
CD-96-2C	1800	-0.6	14.7	0.15	0.15	26	<0.005	<0.2	<10	130	0.27
CD-96-2C	1810	-0.5	17.4	0.5	0.21	44	<0.005	<0.2	<10	180	0.35
CD-96-2C	1820	-1	17.2	0.41	0.17	26	<0.005	<0.2	<10	70	0.31
CD-96-2C	1830	-0.8	17.8	0.44	0.21	34	<0.005	<0.2	<10	230	0.3
CD-96-2C	1840	-0.9	15.2	0.43	0.18	29	<0.005	<0.2	<10	250	0.33
CD-96-2C	1860	-0.8	12.3	0.37	0.23	66	<0.005	<0.2	<10	70	0.3
CD-96-2C	1880	-0.8	12.9	0.5	0.23	58	0.031	<0.2	<10	90	0.3
CD-96-2C	1900	-0.7	14.9	0.41	0.19	31	<0.005	<0.2	<10	230	0.36
CD-96-2C	1920	-0.7	13.4	0.54	0.16	68	0.031	<0.2	<10	70	0.26
CD-96-2C	1925	-1.1	9.9	0.29	0.18	54	0.063	<0.2	<10	120	0.29
CD-96-2C	1930	-0.7	14.5	0.29	0.16	36	0.031	<0.2	<10	80	0.23
CD-96-2C	1940	-0.3	13.7	0.25	0.2	39	0.063	<0.2	<10	180	0.36
CD-96-2C	1960	-0.8	17.2	0.21	0.22	38	0.125	<0.2	<10	140	0.34
CD-96-2C	1980	-1.5	14.3	0.19	0.2	32	0.125	<0.2	<10	240	0.32
CD-96-2C	2000	-1.3	15.8	0.19	0.22	41	0.094	<0.2	<10	150	0.32
CD-96-2C	2020	-1.1	17	0.21	0.26	36	0.063	<0.2	<10	380	0.34
CD-96-2C	2025	-1.6	13.9	0.25	0.14	29	<0.005	<0.2	<10	350	0.27
CD-96-2C	2030	-1.2	16.7	0.18	0.16	27	0.031	<0.2	<10	70	0.3
CD-96-2C	2035	-1.4	15.3	0.17	0.16	71	0.063	<0.2	<10	140	0.27
CD-96-2C	2040	-0.8	14.1	0.16	0.41	547	0.783	0.3	<10	70	0.45
CD-96-2C	2045	-1.2	12.8	0.2	0.29	137	0.157	<0.2	<10	130	0.4
CD-96-2C	2050	-1.3	17.2	0.21	0.15	24	<0.005	<0.2	<10	60	0.38
CD-96-2C	2055	-1.5	16.4	0.14	0.11	31	<0.005	<0.2	<10	40	0.22
CD-96-2C	2060	-1.3	9.8	0.15	0.42	322	0.470	<0.2	<10	60	0.45
CD-96-2C	2065	-1.4	14.7	0.22	0.21	34	0.063	<0.2	<10	50	0.36
CD-96-2C	2070	-1.1	13	0.28	0.21	63	0.031	<0.2	<10	40	0.39
CD-96-2C	2075	-0.9	12.4	0.28	0.38	329	0.219	<0.2	<10	70	0.35
CD-96-2C	2080	-1.5	10.7	0.23	0.42	1280	1.096	1.2	<10	100	0.35
CD-96-2C	2100	-1.7	17.4	0.52	0.31	64	0.094	<0.2	<10	110	0.41
CD-96-2C	2120	-1.7	20	0.77	0.53	28	0.031	<0.2	10	60	0.52
CD-96-2C	2180	-0.7	24.8	0.13	0.28	17	0.031	<0.2	<10	30	0.42
CD-96-2C	2200	-0.6	22	0.24	0.33	42	<0.005	<0.2	<10	50	0.5
CD-96-2C	2220	-0.4	21.4	0.32	0.29	93	0.094	<0.2	<10	30	0.34
CD-96-2C	2240	-1.2	16.5	0.34	0.49	182	0.250	0.2	<10	50	0.39

SAMPLE	Depth (ft)	d13C ‰	d18O ‰	Ag ppm	Al ppm	As ppm	Au (FA) ppm	Au (aqua regia) ppm	B ppm	Ba ppm	Be ppm
CD-96-2C	2260	-0.6	24.9	0.2	0.17	35	0.063	<0.2	<10	30	0.17
CD-96-2C	2280	-0.4	26.3	0.16	0.08	18	0.031	<0.2	<10	20	0.18
CD-96-2C	2300			0.14	0.05	15	0.031	<0.2	<10	210	0.14
CD-96-2C	2320	0.1	26.1	0.34	0.04	11	0.031	<0.2	<10	120	0.15
CD-96-2C	2340	0.5	26	0.09	0.03	8	0.031	<0.2	<10	140	0.11
DR-1C	2480	-0.3	17	0.31	0.3	65	0.031	<0.2	<10	130	0.65
DR-1C	2500	-0.3	18	0.32	0.28	144	0.031	<0.2	<10	310	0.53
DR-1C	2520	0	17.8	0.26	0.24	38	0.031	<0.2	<10	170	0.47
DR-1C	2540	1	17.7	0.21	0.25	31	0.031	<0.2	<10	220	0.49
DR-1C	2560	0.8	19	0.2	0.18	27	0.188	<0.2	<10	160	0.45
DR-1C	2580	-0.2	18.6	0.2	0.24	20	0.031	<0.2	<10	140	0.45
DR-1C	2600	-0.2	19.3	0.33	0.34	21	<0.005	<0.2	<10	200	0.5
DR-1C	2620	0.4	19.3	0.32	0.21	18	<0.005	<0.2	<10	170	0.47
DR-1C	2640	0.8	20	0.14	0.25	11	<0.005	<0.2	<10	80	0.4
DR-1C	2660	0.6	19.5	0.17	0.27	13	<0.005	<0.2	<10	180	0.49
DR-1C	2680	0.7	19.8	0.28	0.27	25	<0.005	<0.2	<10	60	0.56
DR-1C	2700	0.5	21.9	0.33	0.37	18	<0.005	<0.2	<10	50	0.68
DR-1C	2720	0	20.9	0.36	0.4	96	<0.005	<0.2	10	60	0.73
DR-1C	2740	1.1	20.6	0.27	0.37	51	<0.005	<0.2	<10	100	0.56
DR-1C	2760	1.2	19.9	0.17	0.32	13	<0.005	<0.2	<10	130	0.4
DR-1C	2780	1	19.5	0.15	0.32	8	<0.005	<0.2	<10	60	0.45
DR-1C	2800	0.6	20.1	0.16	0.37	5	<0.005	<0.2	<10	60	0.51
DR-1C	2820	0.1	20.1	0.17	0.41	63	<0.005	<0.2	<10	50	0.76
DR-1C	2840	0	18.2	0.16	0.31	64	0.031	<0.2	<10	30	0.51
DR-1C	2860	-0.2	20.4	0.16	0.54	12	<0.005	<0.2	<10	50	0.59
DR-1C	2880	-0.1	20.4	0.26	0.44	17	<0.005	<0.2	<10	40	0.73
DR-1C	2900	-0.2	22.1	0.23	0.4	12	<0.005	<0.2	<10	30	0.69
DR-1C	2917	-0.4	19.3	0.35	0.37	10	<0.005	<0.2	<10	30	0.74
GA-2A	1680	-2.3	14	0.54	0.23	44.1	<0.005	<0.2	<10	130	0.32
GA-2A	1690	-0.7	10.2	0.31	0.35	47.3	<0.005	<0.2	<10	240	0.29
GA-2A	1700	-0.8	19.4	0.19	0.36	43.8	<0.005	<0.2	<10	120	0.36
GA-2A	1710	-1.2	24	0.14	0.46	47.6	<0.005	<0.2	<10	110	0.33
GA-2A	1720	-1.5	16.8	1.06	0.77	48.2	<0.005	<0.2	10	150	0.64
GA-2A	1730	-0.7	20.9	1.04	0.61	44	<0.005	<0.2	10	160	0.48
GA-2A	1740	-1.2	22.4	0.24	0.35	41	<0.005	<0.2	10	110	0.59
GA-2A	1750	-1.9	23.7	0.08	0.36	41	<0.005	<0.2	10	190	0.54
GA-2A	1760	-2	20	0.13	0.21	43	0.157	<0.2	<10	90	0.54
GA-2A	1770	-2.5	22.3	0.25	0.3	60	0.282	<0.2	<10	180	0.53
GA-2A	1780	-2.1	22.5	0.19	0.39	57	0.563	<0.2	10	160	0.49
GA-2A	1790	-2.4	25.8	0.16	0.41	67	0.250	<0.2	10	200	0.63
GA-2A	1800	-2.6	24.5	0.8	0.35	85	0.939	<0.2	<10	190	0.46
GA-2A	1810	-1.8	22	2.26	0.3	66.6	1.628	<0.2	<10	260	0.41
GA-2A	1820	-1	19.1	2.73	0.24	63.3	0.470	<0.2	<10	210	0.35
GA-2A	1830	-1.8	20.8	2.08	0.53	65	0.313	<0.2	10	170	0.58
GA-2A	1840	-1	20.2	0.73	0.37	66	0.689	<0.2	<10	130	0.54
GA-2A	1850	-1.8	19.8	0.83	0.35	127	1.659	<0.2	<10	80	0.41
GA-2A	1860	-1.3	18.9	0.6	0.34	89.9	1.283	<0.2	<10	60	0.33
GA-2A	1870	-0.2	20.1	0.32	0.3	76.5	0.250	<0.2	<10	110	0.27
GA-2A	1880	0.1	18.7	0.29	0.21	53.6	0.282	<0.2	<10	150	0.19
GA-2A	1890	0.4	20.1	0.28	0.33	67	0.219	<0.2	<10	190	0.22
GA-2A	1900	-0.3	21.8	0.33	0.23	58.5	0.250	<0.2	<10	160	0.22

SAMPLE	Depth (ft)	d13C ‰	d18O ‰	Ag ppm	Al ppm	As ppm	Au (FA) ppm	Au (aqua regia) ppm	B ppm	Ba ppm	Be ppm
GA-2A	1910	0.8	16.5	0.28	0.24	80	0.063	<0.2	<10	130	0.19
GA-2A	1920	0.7	20.4	0.31	0.15	88.5	0.063	<0.2	<10	130	0.13
GA-2A	1930	-0.8	12.9	0.36	0.17	119	0.063	<0.2	<10	100	0.16
GA-2A	1940			0.2	0.17	97	0.125	<0.2	<10	110	0.16
GA-2A	1950			0.53	0.21	217	0.125	<0.2	<10	80	0.16
GA-2A	1960			0.53	0.15	155.5	0.219	<0.2	<10	80	0.13
GA-2A	1970	1	2.8	0.41	0.18	90.5	0.125	<0.2	<10	110	0.14
GA-2A	1980	0.8	5.7	0.52	0.15	89.7	0.094	<0.2	<10	110	0.15
GA-2A	1990	0.6	6.5	0.47	0.21	87.3	0.063	<0.2	<10	120	0.16
GA-2A	2000	1.1	3.8	0.73	0.13	68.3	0.157	<0.2	<10	170	0.12
GA-2A	2010			8.01	0.08	98.7	0.157	<0.2	<10	220	0.13
GA-2A	2020			9.69	0.06	67.1	0.094	<0.2	<10	210	0.1
GA-2A	2030	0.7	14.7	1.13	0.09	50	0.063	<0.2	<10	210	0.08
GA-2A	2040	0.4	15.3	1.41	0.12	53	0.094	<0.2	<10	310	0.07
GA-2A	2050	0.1	23.2	0.08	0.11	14	0.063	<0.2	<10	210	0.05
GA-2A	2060	-0.3	25.1	0.04	0.09	14	<0.005	<0.2	<10	140	0.09
GA-2A	2070	0.1	24.3	0.12	0.1	15	<0.005	<0.2	<10	200	0.08
GA-2A	2080	-0.6	23.4	0.23	0.21	29	0.188	<0.2	<10	340	0.1
GA-2A	2100	-0.7	25	0.18	0.13	29	0.157	<0.2	<10	240	0.1
GA-2A	2110	-0.5	27.3	0.15	0.13	24	0.157	<0.2	<10	240	0.07
GA-2A	2120	-0.2	26	0.21	0.13	35	0.313	<0.2	<10	220	0.07
GA-35C	1680	-0.4	16.5	0.69	0.34	234	0.094	<0.2	<10	50	0.48
GA-35C	1700	-0.8	18.8	0.57	0.38	63	<0.005	<0.2	<10	40	0.76
GA-35C	1720	-0.1	21.4	0.41	0.42	38	<0.005	<0.2	<10	100	0.74
GA-35C	1740			0.62	0.45	995	0.344	<0.2	<10	90	1
GA-35C	1760	0.2	11.3	0.59	0.48	3700	0.939	<0.2	<10	120	0.89
GA-35C	1780	0.8	16.9	0.28	0.33	120	<0.005	<0.2	<10	50	0.83
GA-35C	1800	-0.1	11	0.6	0.22	222	<0.005	<0.2	<10	50	0.52
GA-35C	1820	0.8	21	0.35	0.19	74	0.031	<0.2	<10	80	0.41
GA-35C	1840	1.3	23.8	0.14	0.18	315	0.094	<0.2	<10	20	0.26
GA-35C	1860	1.2	22.7	0.15	0.18	284	0.031	<0.2	<10	190	0.19
GA-35C	1880	1.4	22.6	0.23	0.3	734	<0.005	<0.2	<10	30	0.31
GA-35C	1900	0.9	22.8	0.34	0.42	1445	<0.005	<0.2	<10	20	0.47
GA-35C	1920	-0.4	21.3	0.3	0.44	1035	0.094	<0.2	<10	20	0.39
GA-35C	1940			0.34	0.26	185	0.031	<0.2	<10	90	0.29
GA-35C	1960			0.34	0.28	192	0.063	<0.2	<10	40	0.26
GA-35C	1980			0.39	0.25	60.4	<0.005	<0.2	<10	110	0.25
GA-35C	2000			0.33	0.23	65.2	<0.005	<0.2	<10	170	0.19
GA-35C	2020			0.37	0.28	60.8	<0.005	<0.2	<10	50	0.24
GA-35C	2040	1.1	24.2	0.26	0.23	70	<0.005	<0.2	<10	120	0.21
GA-35C	2060	2	20.6	0.12	0.15	54	0.031	<0.2	<10	180	0.2
GA-35C	2080	1.4	19.6	0.19	0.63	4310	0.250	<0.2	<10	60	0.75
GA-35C	2100	2	20.3	0.21	0.41	275	<0.005	<0.2	<10	80	0.37
GA-35C	2120	0.8	19.7	0.11	0.51	92.1	<0.005	<0.2	<10	80	0.5
GA-35C	2140	3	20.2	0.11	0.32	66	<0.005	<0.2	<10	60	0.34
GA-35C	2160	3.5	22.3	0.05	0.19	29	<0.005	<0.2	<10	60	0.28
GA-35C	2186	2.4	22.3	0.08	0.35	41	<0.005	<0.2	<10	180	0.4
SJ-390C	640			2.38	0.44	380	0.069	<0.2	<10	110	0.36
SJ-390C	650	-3.1	8.3	4.2	1.02	183	0.034	<0.2	<10	90	0.82
SJ-390C	660	-2.5	20.1	3.04	0.94	123.5	<0.005	<0.2	<10	120	0.75
SJ-390C	670	-1.7	20.5	1.92	0.77	151	<0.005	<0.2	<10	110	0.63

SAMPLE	Depth (ft)	d13C ‰	d18O ‰	Ag ppm	Al ppm	As ppm	Au (FA) ppm	Au (aqua regia) ppm	B ppm	Ba ppm	Be ppm
SJ-390C	680	-0.9	18.5	1.02	0.52	106.5	<0.005	<0.2	<10	140	0.63
SJ-390C	690	-0.3	17.9	0.6	0.56	59.2	<0.005	<0.2	<10	120	0.66
SJ-390C	700	0.6	19.4	0.5	0.77	44.8	<0.005	<0.2	<10	80	0.63
SJ-390C	710	-0.4	19.5	0.5	1.15	46.8	<0.005	<0.2	<10	80	0.68
SJ-390C	720	0.1	16.8	0.57	0.7	206	<0.005	<0.2	<10	70	0.46
SJ-390C	730	0.5	14.3	0.7	0.44	293	<0.005	<0.2	<10	50	0.37
SJ-390C	740			0.78	0.77	277	<0.005	<0.2	<10	40	0.49
SJ-390C	750	0.1	19.5	0.32	0.58	267	<0.005	<0.2	<10	70	0.41
SJ-390C	760	1.7	21.6	0.32	0.45	288	<0.005	<0.2	<10	40	0.31
SJ-390C	770	2.2	20.3	0.14	0.38	128	<0.005	<0.2	<10	200	0.32
SJ-390C	780	1.7	20.4	0.13	0.43	132	<0.005	<0.2	<10	160	0.36
SJ-390C	790	2	21.6	0.12	0.39	100	<0.005	<0.2	<10	170	0.31
SJ-390C	800	2.7	21.7	0.1	0.37	114	<0.005	<0.2	<10	220	0.3
SJ-390C	900	2.3	21	0.06	1.72	17	<0.005	<0.2	<10	160	0.51
SJ-390C	920	1.4	20.1	0.48	1.38	30	<0.005	<0.2	<10	190	0.62
SJ-390C	940	1.5	16.3	0.73	0.81	350	<0.005	<0.2	<10	40	0.57
SJ-390C	960	0.8	16.2	0.42	0.47	235	0.480	<0.2	<10	40	0.54
SJ-390C	965	0.4	18.2	0.2	0.4	66	<0.005	<0.2	<10	110	0.57
SJ-390C	970	0.1	18.9	0.15	0.18	48	0.377	<0.2	<10	50	0.47
SJ-390C	975	1.7	17.9	0.1	0.21	22	<0.005	<0.2	<10	120	0.37
SJ-390C	980	2.4	16.9	0.11	0.23	19	<0.005	<0.2	<10	200	0.36
SJ-390C	985	1.1	17.8	0.08	0.42	17	<0.005	<0.2	<10	30	0.41
SJ-390C	990	1.1	19	0.1	0.47	78	<0.005	<0.2	<10	70	0.51
SJ-390C	995	2	14.8	0.19	0.25	171	2.537	<0.2	<10	20	0.49
SJ-390C	1000	1.4	16	0.08	0.16	116	3.189	<0.2	<10	20	0.34
SJ-390C	1005	1.2	15.7	0.09	0.14	88	3.257	<0.2	<10	30	0.35
SJ-390C	1010	1.5	16.9	0.16	0.19	124	0.754	<0.2	<10	20	0.39
SJ-390C	1015	1.7	15.4	0.23	0.26	386	<0.005	<0.2	<10	80	0.63
SJ-390C	1020	1	16.9	0.24	0.51	141	<0.005	<0.2	<10	70	0.54
SJ-390C	1025	-1.2	17.5	0.35	1.14	33	<0.005	<0.2	<10	80	0.76
SJ-390C	1030	-0.4	14.4	0.28	0.59	63	<0.005	<0.2	<10	50	0.74
SJ-390C	1035	-1.8	17.2	0.18	1.82	22	<0.005	<0.2	<10	110	0.84
SJ-390C	1040	-1.5	18	0.1	2.06	16	<0.005	<0.2	<10	110	0.82
SJ-390C	1060	0.1	12	0.24	0.59	307	1.440	<0.2	<10	70	0.55
SJ-390C	1095	0.9	13.5	0.16	0.21	151.5	0.480	<0.2	<10	20	0.2
SJ-390C	1100	0.7	13.2	0.17	0.39	123	0.309	<0.2	<10	20	0.4
SJ-390C	1105	2	13.3	0.12	0.28	90	0.377	<0.2	<10	20	0.42
SJ-390C	1110	0.8	13.4	0.21	0.35	346	7.131	0.7	<10	20	0.43
SJ-390C	1115	1.9	16.2	0.14	0.31	658	19.920	0.8	<10	20	0.33
SJ-390C	1120	1.6	18.6	0.14	0.5	858	12.994	4.1	<10	70	0.32
SJ-390C	1125	0.6	18.3	0.14	0.36	1310	18.206	5.5	<10	30	0.3
SJ-390C	1130	1.3	18.6	0.16	0.41	868	10.389	0.7	<10	80	0.27
SJ-390C	1135	1.1	15.4	0.13	0.39	408	6.549	1.2	<10	30	0.46
SJ-390C	1140	1.2	13.9	0.17	0.76	134	0.549	<0.2	<10	60	0.49
SJ-390C	1160	1.4	12.2	0.18	0.32	148	0.206	<0.2	<10	50	0.42
SJ-390C	1180	1.7	9.1	0.11	0.32	130	0.206	<0.2	<10	20	0.37
SJ-390C	1200	1.7	8.5	0.3	0.39	231	0.206	<0.2	<10	40	0.33
SJ-390C	1220	1.1	10.5	0.3	0.44	197	0.137	<0.2	<10	190	0.47
SJ-390C	1240	1.7	11.1	0.88	0.27	625	0.274	<0.2	<10	250	0.26
SJ-390C	1260	1.5	12.6	0.25	0.3	294	0.240	<0.2	<10	70	0.34
SJ-390C	1280	2	13.7	0.07	0.11	141	0.103	<0.2	<10	30	0.09

SAMPLE	Depth (ft)	d13C ‰	d18O ‰	Ag ppm	Al ppm	As ppm	Au (FA) ppm	Au (aqua regia) ppm	B ppm	Ba ppm	Be ppm
SJ-390C	1295	2.4	13.7	0.15	0.22	262	0.651	<0.2	<10	20	0.23
SJ-464C	10	-4.5	17.6	0.46	1.02	173.5	0.034	<0.2	10	530	0.74
SJ-464C	20			0.3	1.06	369	0.034	<0.2	10	1180	1.01
SJ-464C	30			0.1	0.84	75.1	<0.005	<0.2	10	220	1.02
SJ-464C	240			0.12	0.3	63.1	<0.005	<0.2	<10	140	0.46
SJ-464C	250	-1.3	24.1	0.07	0.36	34.3	<0.005	<0.2	<10	160	0.57
SJ-464C	260	-0.3	21.5	0.05	0.37	17	0.069	<0.2	<10	190	0.58
SJ-464C	270	-1.4	23.1	0.06	0.45	31.9	0.034	<0.2	<10	170	0.61
SJ-464C	280	-0.2	22.8	0.05	0.34	27	0.034	<0.2	<10	140	0.58
SJ-464C	290			0.06	0.43	25.1	0.034	<0.2	<10	270	0.77
SJ-464C	300			0.05	0.42	21.8	0.034	<0.2	<10	170	0.44
SJ-464C	310	0.7	16.1	0.03	0.39	44	0.034	<0.2	<10	150	0.5
SJ-464C	320	0	15.9	0.04	0.37	36.8	0.034	<0.2	10	200	0.65
SJ-464C	330	-0.4	18.7	0.21	0.37	93.7	0.034	<0.2	<10	60	0.38
SJ-464C	370			0.79	0.39	143.5	0.137	<0.2	<10	170	0.31
SJ-464C	380	-1.5	12	0.72	0.45	101	0.069	<0.2	<10	130	0.41
SJ-464C	390			0.18	0.38	25.9	0.034	<0.2	<10	110	0.45
SJ-464C	400			0.06	0.35	19.7	0.034	<0.2	<10	230	0.42
SJ-464C	410			0.1	0.33	12.2	0.034	<0.2	<10	330	0.31
SJ-464C	420			0.1	0.35	15	0.034	<0.2	<10	310	0.37
SJ-464C	430			0.04	0.37	6.9	0.034	<0.2	<10	250	0.32
SJ-464C	440			0.03	0.41	5.9	0.034	<0.2	<10	320	0.37
SJ-464C	450			0.03	0.28	23	0.034	<0.2	<10	250	0.28
SJ-464C	460			0.05	0.25	38	<0.005	<0.2	<10	230	0.21
SJ-464C	470			0.09	0.32	113.5	<0.005	<0.2	<10	260	0.34
SJ-464C	480			0.09	0.3	107	<0.005	<0.2	10	80	0.39
SJ-464C	490			0.22	0.38	76.6	<0.005	<0.2	10	70	0.48
SJ-464C	500			0.26	0.4	58.4	<0.005	<0.2	10	90	0.38
SJ-464C	510			0.05	0.42	27.8	<0.005	<0.2	<10	50	0.5
SJ-464C	520			0.04	0.48	25	<0.005	<0.2	10	100	0.57
SJ-464C	530			0.06	0.47	27.8	<0.005	<0.2	10	80	0.49
SJ-464C	540			0.13	0.37	23.8	<0.005	<0.2	<10	180	0.43
SJ-464C	690			0.22	0.11	61.2	0.034	<0.2	<10	160	0.09
SJ-464C	700			0.29	0.18	113	0.069	<0.2	<10	120	0.15
SJ-464C	710			0.11	0.4	122.5	<0.005	<0.2	<10	50	0.5
SJ-464C	720			0.05	0.39	121	<0.005	<0.2	<10	50	0.51
SJ-464C	740			0.1	0.51	71.3	<0.005	<0.2	<10	110	0.46
SJ-464C	750			1.68	0.38	50.4	<0.005	<0.2	<10	70	0.4
SJ-464C	760			3.32	0.43	101	<0.005	<0.2	<10	80	0.46
SJ-464C	770			2.65	0.6	126	0.034	<0.2	10	100	0.48
SJ-464C	780	-1.4	21.9	2.44	0.36	81.2	0.034	<0.2	<10	190	0.4
SJ-464C	790	-2.1	22.1	3.54	0.56	153.5	0.103	<0.2	10	90	0.4
SJ-464C	800	-1.9	24.4	3.24	0.75	174.5	0.137	<0.2	10	60	0.5
SJ-464C	810	-1.9	24.3	2.37	0.73	82.9	0.069	<0.2	10	60	0.51
SJ-464C	820	-2.9	23.2	1.97	0.69	64.1	0.034	<0.2	10	70	0.56
SJ-464C	830			1.36	0.55	72	0.069	<0.2	10	50	0.49
SJ-464C	840	-2.2	24.3	1.16	0.43	49	0.034	<0.2	10	60	0.55
SJ-464C	850	-2.2	24.4	0.98	0.42	34	0.069	<0.2	10	30	0.59
SJ-464C	860	-1.3	19.6	0.61	0.43	24	<0.005	<0.2	10	40	0.64
SJ-464C	870	-0.9	20.1	0.59	0.33	33	<0.005	<0.2	10	60	0.79
SJ-464C	880	-0.1	19.7	0.5	0.33	39.4	0.034	<0.2	10	30	0.84

SAMPLE	Depth (ft)	d13C ‰	d18O ‰	Ag ppm	Al ppm	As ppm	Au (FA) ppm	Au (aqua regia) ppm	B ppm	Ba ppm	Be ppm
SJ-464C	900	0.5	20	0.55	0.3	150	<0.005	<0.2	<10	80	0.56
SJ-464C	920			0.37	0.27	99.9	0.034	<0.2	10	60	0.55
SJ-464C	940	0.6	20.6	0.18	0.24	87	<0.005	<0.2	<10	130	0.67
SJ-464C	960	0.5	17.9	0.14	0.37	46	0.274	<0.2	10	90	1.01
SJ-464C	980	0.6	19.6	0.11	0.28	22	0.206	<0.2	10	110	0.86
SJ-464C	1000	0.5	16.4	0.16	0.29	31	0.103	<0.2	10	70	0.94
SJ-464C	1020	1	20.5	0.09	0.23	20	<0.005	<0.2	<10	140	0.6
SJ-464C	1040	1.7	24	0.07	0.28	19	0.034	<0.2	<10	170	0.55
SJ-464C	1060	2.1	23.7	0.04	0.16	9	0.034	<0.2	<10	140	0.38
SJ-464C	1080	2.2	25.5	0.05	0.24	18	<0.005	<0.2	<10	100	0.49
SJ-464C	1100	2	24.5	0.13	0.28	13	<0.005	<0.2	10	50	0.64
SJ-464C	1120	0.9	20.5	0.53	0.23	30	0.034	<0.2	<10	20	0.47
SJ-464C	1140	2.2	16.2	0.44	0.18	174	0.069	<0.2	<10	130	0.33
SJ-464C	1215	-0.8	22.6	0.47	0.34	251	2.469	<0.2	<10	20	0.51
SJ-464C	1220	-0.4	20.4	0.27	0.21	172.5	1.337	<0.2	<10	20	0.37
SJ-464C	1225	1	21.8	0.19	0.2	134.5	1.474	<0.2	<10	70	0.35
SJ-464C	1230	1.8	16.2	0.26	0.25	141	2.949	<0.2	<10	140	0.34
SJ-464C	1235	1.5	18.6	0.23	0.24	83	1.337	<0.2	<10	30	0.29
SJ-464C	1240	1.6	20.2	0.16	0.29	71	0.309	<0.2	<10	20	0.44
SJ-464C	1245	1.1	18.1	0.28	0.24	91.6	1.063	<0.2	<10	20	0.38
SJ-464C	1250	1.1	17.6	0.22	0.21	105	1.646	<0.2	<10	20	0.29
SJ-464C	1255			0.26	0.29	93.3	0.651	<0.2	<10	130	0.4
SJ-464C	1260	1.7	17.1	0.15	0.31	56.3	<0.005	<0.2	<10	80	0.47
SJ-464C	1265	1.4	15.8	0.19	0.33	63.8	<0.005	<0.2	<10	40	0.48
SJ-464C	1270	1.5	17.3	0.16	0.28	53	0.069	<0.2	<10	100	0.48
SJ-464C	1275	0.1	23.3	0.16	0.31	49.1	0.069	<0.2	<10	60	0.46
SJ-464C	1280	0.6	23.7	0.11	0.26	82.6	0.720	<0.2	<10	10	0.44
SJ-464C	1285	0.5	24.2	0.15	0.34	105.5	0.103	<0.2	<10	50	0.49
SJ-464C	1290	1.3	18.6	0.16	0.29	147.5	1.817	<0.2	<10	20	0.43
SJ-464C	1295	1.2	23.7	0.15	0.31	76.2	0.240	<0.2	<10	20	0.45
SJ-464C	1300	0.9	17	0.23	0.31	84.7	0.069	<0.2	<10	10	0.39
SJ-464C	1305	1.1	20	0.2	0.32	77.6	0.103	<0.2	<10	60	0.5
SJ-464C	1310	1.4	22.2	0.29	0.27	80.7	0.206	<0.2	<10	20	0.38
SJ-464C	1315	0.9	18.8	0.19	0.33	99.8	0.480	<0.2	<10	30	0.5
SJ-464C	1320	1.1	18	0.17	0.4	128.5	0.240	<0.2	<10	70	0.55
SJ-464C	1325	1.2	17.2	0.17	0.43	108	0.206	<0.2	<10	30	0.53
SJ-464C	1330	1	19.1	0.17	0.36	80	0.274	<0.2	<10	60	0.56
SJ-464C	1335	0.8	20.4	0.23	0.44	162	0.651	<0.2	<10	60	0.64
SJ-464C	1340	1.4	16.6	0.17	0.33	58	0.754	<0.2	<10	230	0.37
SJ-464C	1345	0.7	19.8	0.23	0.28	92.8	1.474	0.2	<10	160	0.37
SJ-464C	1350	1.4	15.6	0.19	0.2	96.3	1.851	0.2	<10	490	0.25
SJ-464C	1355	-0.4	20	0.25	0.29	131.5	1.920	0.2	<10	90	0.34
SJ-464C	1360	1.4	18.2	0.23	0.28	95.6	0.069	0.2	<10	250	0.43
SJ-464C	1365	1.7	19	0.26	0.53	67	<0.005	<0.2	<10	60	0.63
SJ-464C	1370	1.4	16.2	0.27	0.37	46	<0.005	<0.2	<10	40	0.45
SJ-464C	1375	1.3	18.7	0.37	0.43	49	0.034	<0.2	<10	50	0.46
SJ-464C	1380	1.2	18.6	0.46	0.37	90	0.206	<0.2	<10	140	0.44
SJ-464C	1385	1	20.7	0.38	0.34	82.6	0.583	<0.2	<10	160	0.39
SJ-464C	1390	1.7	17.3	0.25	0.18	75.1	0.686	<0.2	<10	90	0.2
SJ-464C	1395	0	19.1	0.29	0.26	92.2	0.789	<0.2	<10	50	0.26
SJ-464C	1400	0.1	21.2	1.1	0.32	289	10.046	0.5	<10	60	0.29

SAMPLE	Depth (ft)	d13C ‰	d18O ‰	Ag ppm	Al ppm	As ppm	Au (FA) ppm	Au (aqua regia) ppm	B ppm	Ba ppm	Be ppm
SJ-464C	1405	2.6	16.7	0.26	0.24	69	0.891	<0.2	<10	70	0.23
SJ-464C	1410	2.2	19.3	0.2	0.24	48.6	0.206	<0.2	<10	120	0.27
SJ-464C	1415	2.1	20.8	0.25	0.28	44.2	0.274	<0.2	<10	130	0.3
SJ-464C	1420	2.2	19.1	0.34	0.32	54.3	0.171	<0.2	<10	60	0.34
SJ-464C	1425	0.6	18	0.53	0.29	122	0.617	<0.2	<10	50	0.25
SJ-464C	1430	2.4	4.9	0.48	0.06	77	0.686	<0.2	<10	810	0.08
SJ-464C	1435	0.3	7.4	0.21	0.03	31	0.240	<0.2	<10	170	0.07
SJ-464C	1440	1	16.9	0.23	0.02	21	0.309	<0.2	<10	50	0.1
SJ-464C	1445	0.5	21.8	0.03	0.02	7	<0.005	<0.2	<10	40	0.1
SJ-464C	1450	1.3	23.2	0.03	0.06	16	0.103	<0.2	<10	40	0.12
SJ-464C	1455	1.7	22.3	0.06	0.16	14	0.069	<0.2	<10	90	0.19
SJ-464C	1460	1.9	21	0.04	0.08	24	<0.005	<0.2	<10	230	0.15
SJ-464C	1465	2.2	19.7	0.04	0.09	17	0.069	<0.2	<10	270	0.16
WM-01C	2440			0.78	0.39	51.3	0.407	<0.2	<10	160	0.34
WM-01C	2460	-3.2	16	0.81	0.27	75.8	0.438	<0.2	<10	170	0.26
WM-01C	2480			0.52	0.23	91.5	0.094	<0.2	<10	220	0.27
WM-01C	2500	-3.3	16.4	0.54	0.22	77	0.063	<0.2	<10	170	0.29
WM-01C	2520	-3.2	14.1	0.47	0.34	103	0.063	<0.2	<10	160	0.3
WM-01C	2540			0.53	0.27	152.5	0.031	<0.2	<10	170	0.42
WM-01C	2560			0.16	0.17	58	0.031	<0.2	<10	140	0.41
WM-01C	2580	1.4	16.3	0.1	0.2	39	0.031	<0.2	<10	90	0.51
WM-01C	2600	1.3	20.7	0.46	0.24	159	0.031	<0.2	<10	160	0.57
WM-01C	2620	0.7	19	0.47	0.22	64	0.031	<0.2	<10	90	0.47
WM-01C	2640	0.4	20.7	0.21	0.28	108	0.031	<0.2	<10	230	0.54
WM-01C	2660	0.7	21.3	0.26	0.31	116	0.031	<0.2	<10	240	0.39
WM-01C	2680	0.1	22.5	0.16	0.36	148	<0.005	<0.2	<10	240	0.41
WM-01C	2700	0.3	21.4	0.16	0.57	21	0.031	<0.2	<10	140	0.51
WM-01C	2720	0.3	21.1	0.18	0.41	36	0.031	<0.2	<10	180	0.41
WM-01C	2740	0.5	18.9	0.2	0.56	21	0.031	<0.2	<10	200	0.54
WM-01C	2760	0.2	20.1	0.21	0.55	66	0.157	<0.2	<10	160	0.46
WM-01C	2780	0.1	21.7	0.28	0.46	90	0.063	<0.2	<10	60	0.39
WM-01C	2800	0.1	22.9	0.22	0.45	126	0.031	<0.2	<10	200	0.41
WM-01C	2820	0.2	22.6	0.2	0.42	147	0.031	<0.2	<10	60	0.39
WM-01C	2840	0.2	22.2	0.33	0.4	20.2	0.031	<0.2	<10	50	0.39
WM-01C	2860	0.2	20.6	0.47	0.41	19.5	0.031	<0.2	<10	40	0.41
WM-01C	2880	0.4	22.8	0.49	0.43	31	0.031	<0.2	<10	60	0.36
WM-01C	2900	-12.8	25.3	0.29	0.64	58	0.031	<0.2	<10	90	0.46
WM-01C	2920	-1.5	18.1	0.15	0.35	62.1	0.031	<0.2	<10	60	0.34
WM-01C	2940	-0.5	16.1	0.11	0.32	66	0.031	<0.2	<10	370	0.35
WM-01C	2960	-0.4	15.9	0.12	0.31	55	0.031	<0.2	<10	300	0.33
WM-01C	2980	-0.7	15.9	0.08	0.45	115	0.063	<0.2	<10	80	0.45
WM-01C	3000	-1.1	15.4	0.05	0.38	94	0.031	<0.2	<10	70	0.38
WM-01C	3020	-0.8	19.4	0.08	0.39	142	0.031	<0.2	<10	60	0.42
WM-01C	3040	-1	15.8	0.12	0.35	52	<0.005	<0.2	<10	90	0.38
WM-01C	3050	-0.9	16.3	0.23	0.51	146	0.031	<0.2	<10	100	0.43

SAMPLE	Depth (ft)	Bi ppm	Ca ppm	Cd ppm	Ce ppm	Co ppm	Cr ppm	Cs ppm	Cu ppm	Fe ppm	Ga ppm
BZ-965C	880	0.06	8.88	1.56	11.75	5.3	27	0.94	22.6	1.18	0.85
BZ-965C	885	0.06	9.69	1.44	11.1	5.3	35	0.61	22.6	1.16	0.9
BZ-965C	905	0.02	6.53	1.25	13.4	3.7	70	0.5	11.1	0.79	0.52
BZ-965C	910	0.05	9.15	1.11	11.5	5.5	40	0.76	18.9	1.2	0.7
BZ-965C	955	0.08	11	2.82	8.14	6.3	32	0.91	19.9	1.65	0.97
BZ-965C	960	0.06	10	14.2	6.75	4.8	53	1.02	42.5	1.31	1.36
BZ-965C	965	0.08	4.81	39.5	5.57	3.7	124	1.41	110	0.97	2.06
BZ-965C	970	0.07	7.49	27.1	4.66	2.5	91	1.12	97.5	0.95	1.41
BZ-965C	975	0.13	7	23.7	12.25	9.3	93	2.64	105	2.05	1.76
BZ-965C	980	0.07	11.25	28.3	7.16	2.9	74	2.21	82.9	0.82	1.23
BZ-965C	1000	0.09	11.5	4.69	17.35	3.5	86	2.4	49.6	1.25	1.88
BZ-965C	1020	0.08	12.45	0.92	15.6	3.9	57	1.47	33.4	1.32	1.35
BZ-965C	1040	0.09	12.3	0.49	11.15	3.8	38	0.6	22.2	1.78	0.82
BZ-965C	1060	0.11	11.2	0.18	11.3	5.7	29	0.76	21.9	1.81	0.9
BZ-965C	1065	0.1	13.25	1.16	14.3	4.2	39	0.77	20.9	1.58	0.84
BZ-965C	1070	0.09	12.2	0.49	17.8	4.1	41	0.66	17.7	1.44	1.08
BZ-965C	1075	0.1	13.7	0.2	16.65	3.8	42	0.53	23.9	1.42	0.91
BZ-965C	1080	0.11	10.35	2.02	19.45	4.6	41	0.89	40.9	1.54	1.37
BZ-965C	1085	0.11	12.1	0.09	12.1	4.9	28	0.58	18.8	1.72	0.82
BZ-965C	1090	0.07	13.2	1.99	15.45	3.1	38	0.54	22.2	1.4	0.88
BZ-965C	1095	0.05	12.75	1.9	16.35	2.8	43	0.58	24.6	1.28	0.86
BZ-965C	1100	0.13	11.65	0.08	10.5	6.5	35	0.77	15.2	2.19	0.95
BZ-965C	1105	0.15	9.96	0.08	10.9	6.7	37	0.85	18.7	2.31	1.12
BZ-965C	1110	0.16	11.25	0.02	11.85	9	32	0.66	27.8	2.13	1.2
BZ-965C	1115	0.13	13.7	0.06	15.9	5.6	30	0.75	10.1	1.97	0.79
BZ-965C	1120	0.11	13.55	0.04	16.55	4.8	30	0.79	9.1	1.75	0.8
BZ-965C	1125	0.08	13.2	0.71	16.9	3.3	32	0.71	9.5	1.5	0.55
BZ-965C	1130	0.13	12.3	0.11	11.85	5.3	29	0.83	12.9	1.81	0.67
BZ-965C	1135	0.12	12.2	0.29	11.8	5.7	31	0.72	11.7	1.72	0.69
BZ-965C	1140	0.06	11.95	0.11	13.95	3.1	30	0.67	5.6	1.35	0.61
BZ-965C	1145	0.05	19.4	0.08	14.75	2.2	21	0.51	3.7	0.97	0.4
BZ-965C	1150	0.03	23.2	0.06	19.95	1.8	20	0.26	2.5	0.74	0.4
BZ-965C	1155	0.05	22.4	0.08	21.1	2.2	19	0.72	3.6	0.83	0.49
BZ-965C	1160	0.03	24.6	0.04	20.2	1.6	18	0.29	2.5	0.62	0.36
BZ-965C	1165	0.05	22.5	0.05	23.8	2.4	19	0.32	3.4	1.06	0.48
BZ-965C	1170	0.06	21.7	0.08	25.5	2.8	18	0.28	3.6	0.91	0.58
BZ-965C	1175	0.07	20.4	0.16	23.6	3.5	31	0.24	5.5	0.97	0.8
BZ-965C	1180	0.04	24.1	0.05	19	1.9	15	0.15	3.1	0.62	0.52
BZ-965C	1185	0.03	23.8	0.04	18.95	1.7	15	0.13	2.7	0.54	0.47
BZ-965C	1190	0.04	18.6	0.09	20.4	2.2	16	0.29	4.8	0.89	0.61
BZ-965C	1195	0.05	20.1	0.03	17.3	2.9	11	0.53	7.1	0.93	0.63
BZ-965C	1200	0.03	20.4	0.06	16.85	1.7	12	0.38	3.6	0.8	0.51
BZ-965C	1205	0.05	18	0.05	16.25	2.2	11	0.48	4.9	1.05	0.62
BZ-965C	1215	0.08	18	0.07	19.45	3.3	19	0.37	7.4	1.44	0.89
BZ-965C	1220	0.05	19.3	0.04	20.3	2.8	18	0.23	5.2	1.47	0.9
BZ-965C	1225	0.08	19.4	0.06	25	3.8	24	0.23	6	1.33	1.02
BZ-965C	1230	0.06	22	0.06	20.5	3.3	19	0.21	4.8	1.04	0.88
BZ-965C	1235	0.07	20.8	0.05	25.1	3.4	16	0.94	5.2	0.93	1.12
BZ-965C	1240	0.06	21.3	0.05	24.5	3.3	13	0.86	4.9	0.86	0.91
BZ-965C	1245	0.06	22.1	0.06	25.8	3.1	13	1.08	4.7	0.84	0.83
BZ-965C	1250	0.07	22.3	0.07	27	3.2	15	1.12	5.2	0.87	1.03

SAMPLE	Depth (ft)	Bi ppm	Ca ppm	Cd ppm	Ce ppm	Co ppm	Cr ppm	Cs ppm	Cu ppm	Fe ppm	Ga ppm
BZ-965C	1255	0.07	16	0.03	24.8	3.3	20	0.49	6	1.42	0.85
BZ-965C	1260	0.13	14.55	0.05	35.4	5.6	21	0.58	9.6	1.71	1.1
BZ-965C	1265	0.18	12.9	0.15	24.5	7.7	24	0.32	14.3	2.23	1.02
BZ-965C	1270	0.11	13.45	3.81	19.3	5.3	15	0.3	27.1	1.57	1.08
BZ-965C	1275	0.05	13	6.25	10.35	3.5	27	0.33	42	1.04	0.91
BZ-965C	1280	0.04	12.65	7.45	9.36	3.1	30	0.33	43.6	0.95	0.99
BZ-965C	1285	0.05	13	5.6	10.25	3.5	38	0.35	45.9	0.98	1.03
BZ-965C	1290	0.04	12.85	3.51	10.4	3.1	36	0.4	36.8	0.9	0.8
BZ-965C	1295	0.05	11.8	7.05	11.75	3.2	34	0.51	49	0.89	0.93
BZ-965C	1300	0.06	13.45	5.43	13.85	3.3	30	0.5	42	0.95	0.87
BZ-965C	1305	0.04	12.85	5.3	11.5	3	30	0.43	43.9	0.88	0.77
BZ-965C	1310	0.05	13.7	3.76	12.8	3	28	0.38	31.2	0.86	0.68
BZ-965C	1315	0.11	11.15	1.81	17.5	5.7	32	0.81	25.9	1.36	0.78
BZ-965C	1320	0.06	10.1	1.28	17.4	3.9	35	0.67	21.6	1.04	0.63
BZ-965C	1325	0.2	7.98	0.51	21.1	10.8	27	0.9	37.5	2.22	1.27
CD-14	530	0.1	15.8	0.12	30.4	3.1	25	1.03	8.3	2.92	1.8
CD-14	550	0.06	13.6	0.16	24.5	3.7	19	0.95	8	0.76	1.25
CD-14	560	0.03	23	0.06	22.4	2.2	15	0.6	4.7	0.99	0.86
CD-14	570	0.07	8.02	0.21	26.3	4.6	20	1	9.6	1.5	1.36
CD-14	580	0.07	20.5	0.11	22.2	5.2	12	0.99	7.8	2.64	0.88
CD-14	590	0.08	18.5	0.14	22.5	6.3	11	1.06	8.3	2.33	0.82
CD-14	600	0.05	23.9	0.39	19.25	3.2	12	0.6	10.7	1.03	0.69
CD-14	610	0.05	15.35	3.49	27.7	3.3	17	1.07	55.3	0.79	1.21
CD-14	620	0.05	15.9	7.76	11.55	2.3	13	0.67	60.3	0.86	0.81
CD-14	630	0.04	17.45	8.84	12.05	3.1	14	0.81	75.4	0.59	0.82
CD-14	640	0.04	15.9	9.24	13.8	2.9	14	0.69	50.8	0.7	0.76
CD-14	650	0.06	17.05	6.57	16.25	2.2	12	0.8	49	0.8	0.63
CD-14	660	0.04	16.7	6.54	13.9	2.4	12	0.86	38.2	0.76	0.73
CD-14	670	0.09	16.2	4.37	21.3	2.7	13	1.02	27.3	1.38	0.98
CD-14	680	0.05	20.3	0.33	18.8	2.8	11	1	7.2	1.25	0.48
CD-14	690	0.08	21.2	0.55	23.1	3.4	11	1.15	9.8	1.16	0.69
CD-14	700	0.05	16.8	1.14	16.7	2.7	10	0.77	15.5	0.49	0.62
CD-14	720	0.05	14.9	1.38	15.75	2.5	21	0.7	21	0.59	0.67
CD-14	740	0.04	12.25	2.34	9.32	3.6	41	0.44	29.1	0.63	0.64
CD-14	770	0.05	18.6	5.51	10.6	3.9	21	0.63	59.4	0.54	0.67
CD-14	780	0.05	15.1	5.23	9.42	3.3	17	0.63	50.7	0.52	0.58
CD-14	790	0.04	14.4	2.6	9.88	2.8	19	0.55	33.5	0.63	0.65
CD-14	800	0.04	16.65	1.61	10.9	3.5	23	0.45	20.1	0.5	0.59
CD-14	820	0.05	16.65	2.02	11.95	4.4	36	0.71	21.4	0.79	0.76
CD-14	840	0.07	9.35	1.06	14.65	4.9	48	0.88	20.9	1.11	1.05
CD-14	860	0.06	5.39	0.2	23	4	56	0.57	8.6	0.76	1.31
CD-14	880	0.07	6.04	0.14	22.1	4	52	0.67	8.7	1.05	1.38
CD-14	900	0.06	6.31	0.5	26.7	3.6	58	0.62	8.2	0.86	1.38
CD-14	920	0.06	7.85	0.18	21.9	4.3	44	0.68	8.7	1.03	1.24
CD-14	940	0.05	12.3	0.09	18.55	3.3	34	0.75	7.2	0.74	1.04
CD-14	960	0.07	6.29	1.02	19.15	3.9	44	0.92	9.4	1	1.44
CD-14	980	0.06	6.98	1.17	20.9	3.7	56	0.72	9.3	0.92	1.19
CD-14	1000	0.06	12.7	0.74	21.6	3.8	30	0.61	8.8	0.89	0.9
CD-14	1020	0.05	13.25	0.62	20.6	3.7	26	0.72	8.6	0.72	0.98
CD-14	1040	0.05	12.9	0.56	22.2	4.1	25	0.78	7.5	0.79	1.11
CD-14	1060	0.07	12.75	1.05	19.45	4.7	19	0.78	9.3	0.98	1.33

SAMPLE	Depth (ft)	Bi ppm	Ca ppm	Cd ppm	Ce ppm	Co ppm	Cr ppm	Cs ppm	Cu ppm	Fe ppm	Ga ppm
CD-14	1080	0.05	17.2	1.89	16.35	3.6	15	0.62	9.1	0.68	0.74
CD-14	1100	0.05	14.45	2.06	17.15	2.6	29	0.72	8.8	1.03	1.09
CD-14	1120	0.04	17.55	0.66	20	2.9	18	0.57	6.2	0.7	1.04
CD-14	1140	0.06	16.3	0.78	17.65	3.8	24	0.61	9.4	0.81	0.98
CD-14	1160	0.06	16.75	1.71	17.45	3.6	25	0.56	9.4	0.82	0.82
CD-14	1180	0.05	16.95	1.64	24.7	3.5	19	0.74	9.1	0.74	0.74
CD-14	1200	0.06	15.1	5.08	15.65	3.8	13	0.59	10.6	0.76	0.69
CD-14	1220	0.07	13.25	9.22	11.6	5	22	0.63	13.2	1.05	0.89
CD-14	1240	0.05	14.7	4.27	8.91	3.5	41	0.39	7.6	0.8	0.67
CD-14	1260	0.06	12.6	4.46	13.9	4.1	41	0.56	10	0.83	1.08
CD-14	1280	0.06	17.4	0.52	21.5	3.9	29	0.77	6.2	0.69	0.92
CD-14	1300	0.07	12.5	0.14	21.9	5.6	27	1.03	7.5	1.06	1.38
CD-14	1320	0.06	16.9	1.85	17.75	4.3	33	0.76	9	0.82	1.4
CD-14	1340	0.06	17.3	3.69	17.55	4	50	0.73	9	0.72	1.27
CD-14	1360	0.07	13.2	1.66	16.95	4.9	36	0.7	8.1	0.94	1.42
CD-14	1380	0.06	14.5	4.1	12.6	4.2	29	0.8	9	0.93	0.98
CD-14	1400	0.1	10.15	1.93	68.4	15.6	86	2.16	23.6	2.26	4.17
CD-14	1420	0.06	15.75	4.34	20.3	5.2	28	0.94	10.2	1.11	1.09
CD-14	1440	0.08	11.9	2.85	26.1	6.6	35	1.68	12.7	1.19	2.02
CD-14	1460	0.06	10.8	1.1	18.7	4.2	23	1.32	7	0.83	1.35
CD-14	1480	0.11	9.06	0.16	82.3	15.5	117	3.46	25.3	2.33	6.62
CD-14	1500	0.11	8.85	0.83	89	17.3	127	3.74	28.2	2.5	8.38
CD-14	1520	0.08	16.1	0.91	39.4	7.3	32	0.97	11.5	1.07	2.28
CD-14	1540	0.04	18.65	3.87	17.1	3	12	0.75	6	0.57	0.71
CD-14	1560	0.06	15.65	4.37	17.75	4.4	11	0.92	7.7	0.82	1.15
CD-14	1580	0.05	13.25	2.57	21.4	4.3	21	1.23	7	0.79	1.17
CD-14	1600	0.06	14.05	1.25	27.3	5.3	24	1.58	8.2	1	1.59
CD-14	1620	0.06	17.95	5.57	17.45	4	8	0.86	8.7	0.74	0.77
CD-14	1640	0.05	19.15	3.68	17.45	3.6	8	0.55	7.6	0.69	0.63
CD-14	1660	0.09	12	3.9	62.6	17.1	71	2.39	28.1	2.14	3.58
CD-14	1680	0.05	15.7	3.66	17.9	3.3	15	1.07	7.2	0.66	0.78
CD-14	1700	0.06	12.45	1.97	22.2	3.4	18	0.97	7.2	0.72	0.89
CD-14	1720	0.06	10.65	1.16	16.75	4	20	0.95	6.4	0.87	0.77
CD-14	1740	0.05	11.5	0.3	21.4	4	16	0.98	5	0.8	0.84
CD-14	1760	0.07	10.65	1.11	17.65	5.6	14	0.89	7.7	1.02	0.92
CD-14	1780	0.07	12.9	2.05	15.2	5.3	12	0.79	10.4	1	0.79
CD-14	1800	0.06	13.65	0.99	13.05	4	17	0.71	6.6	0.8	0.66
CD-14	1820	0.12	9.03	0.37	32.5	11.2	39	1.74	14.7	2.09	3.63
CD-14	1840	0.07	12.85	0.39	19.05	5.9	19	0.87	7.8	1.14	1.35
CD-14	1860	0.11	10.4	1.11	38.7	13.3	38	1.81	18	2.5	2.88
CD-14	1880	0.05	18.1	4.78	18.65	4.1	8	0.54	7.9	0.77	0.71
CD-14	1900	0.06	18.35	6.38	16.2	4.1	10	0.63	10.1	0.75	0.73
CD-14	1920	0.05	16.7	4.34	14	3.5	10	0.61	7.5	0.65	0.69
CD-14	1940	0.05	12.6	1.72	17.15	3.4	15	0.87	6.3	0.81	0.76
CD-14	1960	0.06	13.25	5.12	17.9	3.6	55	1.15	9.9	0.74	1.13
CD-14	1980	0.06	12.05	1.1	21.2	4	41	1.26	6.2	0.83	1.83
CD-14	2000	0.05	16.05	1.69	17.75	3.8	23	1.17	6.9	0.8	1.17
CD-14	2020	0.06	11.45	0.49	18.2	3.8	30	0.95	6.1	0.89	1.05
CD-14	2040	0.06	14.2	0.65	19.65	4.2	29	1.17	7.1	0.87	0.83
CD-14	2060	0.06	15.4	0.69	18.5	3.8	25	0.97	6.6	0.79	0.71
CD-14	2080	0.06	15.15	1.74	20	4.3	12	0.43	8.3	0.93	0.83

SAMPLE	Depth (ft)	Bi ppm	Ca ppm	Cd ppm	Ce ppm	Co ppm	Cr ppm	Cs ppm	Cu ppm	Fe ppm	Ga ppm
CD-14	2100	0.04	9.23	0.26	52.2	18.3	27	1.56	24.8	2.63	2.93
CD-14	2120	0.05	18.35	0.74	18.6	3.6	11	0.56	6.6	0.91	0.75
CD-14	2140	0.06	13.4	1.61	18.15	4.2	16	1.09	7.2	0.93	0.92
CD-14	2160	0.05	17.45	1.36	19.3	3.9	13	0.91	6.8	0.87	0.9
CD-15C	1380	0.11	16.75	0.33	18.5	8.7	13	1.12	17.9	1.86	0.89
CD-15C	1400	0.09	10.25	3.15	16.3	5.2	53	1.8	50.1	1.69	1.66
CD-15C	1420	0.07	12.85	1.18	26.3	3.7	62	1.69	39.5	1.12	1.92
CD-15C	1440	0.08	13.5	0.5	17.85	3.9	45	1.42	37.9	1.18	1.07
CD-15C	1460	0.1	12.1	0.3	19.2	4.9	45	1.66	41.8	1.5	1.23
CD-15C	1480	0.08	12.5	0.31	26.1	4.3	45	1.68	31	1.23	1.37
CD-15C	1500	0.07	10.4	0.4	15.1	3.9	53	1.46	36.5	1.42	1.33
CD-15C	1520	0.1	11.85	0.52	14.85	5.2	38	1.68	27.9	1.57	0.98
CD-15C	1540	0.1	12.75	0.11	15.65	4.8	16	1.32	16.1	1.33	0.86
CD-15C	1560	0.11	10.9	0.12	13.2	6.2	27	1.48	24.1	1.63	0.85
CD-15C	1580	0.13	12.85	0.05	13.65	6.6	23	1.34	24.1	1.63	1.31
CD-15C	1600	0.14	13.35	0.07	20.2	6.5	17	1.46	18.9	1.63	1.22
CD-15C	1620	0.12	14.1	0.07	20.3	5.7	33	1.22	14.3	1.46	1.86
CD-15C	1660	0.1	14.9	0.18	24.3	5.5	35	1.06	13.2	1.38	1.05
CD-15C	1680	0.06	18.5	0.12	25.2	3.2	19	0.76	5.7	0.88	0.81
CD-15C	1700	0.05	23.4	0.06	18.95	2.7	13	0.74	4.3	0.72	0.54
CD-15C	1720	0.09	15.2	0.15	14	5.8	16	1.1	18	1.28	0.86
CD-15C	1740	0.1	7.29	0.15	21.4	7	24	1.04	21.9	1.77	1.53
CD-15C	1760	0.1	4.03	0.22	20.7	6.1	31	1.09	22.1	1.38	1.18
CD-15C	1780	0.07	4.79	1.25	21.2	4.9	24	0.87	14	1.28	1.33
CD-15C	1800	0.07	5.95	2.21	16.4	4.4	24	0.88	12.7	1.14	1.05
CD-15C	1820	0.07	9.57	0.54	18	4.8	18	0.83	9.3	1	0.98
CD-15C	1840	0.06	13.65	0.17	21.3	4.1	14	0.8	6.6	0.81	0.8
CD-15C	1860	0.07	14.2	0.61	21.2	4.1	12	1.1	7.7	0.76	0.69
CD-15C	1880	0.09	11.65	0.71	33.6	11	62	1.93	18.9	1.34	2.69
CD-15C	1900	0.08	11.95	2.21	14.45	4.9	16	0.95	11.8	0.99	0.9
CD-15C	1920	0.07	14.85	3.7	14.95	4.9	15	0.99	11.8	0.91	0.9
CD-15C	1940	0.09	10.35	12.15	12.55	4.6	15	1.54	20.9	0.84	0.89
CD-15C	2000	0.1	12.4	2.59	18.75	5.6	19	1.34	13.4	0.95	1.4
CD-15C	2020	0.09	7.99	1.89	20.7	5.8	27	1.4	10.8	1.05	1.74
CD-15C	2040	0.1	13.05	3.25	17	6.8	25	1.6	14.3	1.48	2.28
CD-15C	2060	0.08	10.75	2.2	17.55	4.7	16	1.37	10.2	0.93	1.11
CD-15C	2080	0.07	12.25	1.57	20.4	4.6	17	1.52	8.2	0.88	1.59
CD-15C	2100	0.07	13.95	4.65	18.6	3.9	14	1.16	8.8	0.75	1.26
CD-15C	2120	0.07	13.9	4.57	18.25	5.6	15	1.11	11.1	1.14	1.79
CD-95-3	890	0.09	1.4	6.41	8.48	3.6	138	1.22	79.5	0.84	1.13
CD-95-3	900	0.09	2.05	2.75	9.22	6.1	114	1.06	34	1.31	0.67
CD-95-3	910	0.11	2.07	2.94	11.1	4	141	1.18	39.4	1.01	1.03
CD-95-3	920	0.08	1.92	2.75	6.88	3.9	139	0.84	35.4	0.87	0.66
CD-95-3	930	0.1	2.84	3.28	10.5	4.9	128	1.22	38	1.13	0.99
CD-95-3	940	0.07	3.71	2.79	7.06	3.5	135	0.51	33.2	0.72	0.56
CD-95-3	950	0.07	11.75	10.15	22.9	4.5	131	1.56	78.3	1.02	1.91
CD-95-3	960	0.06	13.65	1.17	19.3	3.4	71	1.13	32.9	0.97	1.07
CD-95-3	970	0.09	11.25	0.51	15.45	4.2	47	1.63	35.5	1.23	1.1
CD-95-3	980	0.07	12.45	0.61	16.05	4.2	47	1.34	34.7	1.19	1.06
CD-95-3	990	0.07	11.3	1.31	16.75	4	74	1.34	32.2	1.11	1.09
CD-95-3	1000	0.13	11.15	0.19	15	6.6	21	1.73	23.2	1.59	1

SAMPLE	Depth (ft)	Bi ppm	Ca ppm	Cd ppm	Ce ppm	Co ppm	Cr ppm	Cs ppm	Cu ppm	Fe ppm	Ga ppm
CD-95-3	1010	0.12	12.05	0.18	18.3	6.3	22	1.7	22.2	1.61	1.11
CD-95-3	1020	0.09	16.55	0.62	24.4	4.9	23	1.29	34.1	1.25	0.92
CD-95-3	1030	0.05	20.1	1.93	24.3	3.1	34	0.87	45.8	0.71	0.85
CD-95-3	1040	0.07	19.05	1.12	21.5	4.4	24	1.34	28	1.15	0.76
CD-95-3	1050	0.13	14.65	0.17	19.8	6	12	1.74	13.6	1.47	0.73
CD-95-3	1060	0.09	20.7	0.11	22.7	5.3	14	1.12	11.7	1.28	0.59
CD-95-3	1070	0.14	15.8	0.14	20.1	7.3	13	1.49	15.8	1.91	0.74
CD-95-3	1080	0.13	13.55	0.24	29	10	16	1.74	16.7	2.27	0.99
CD-95-3	1090	0.13	16.45	0.29	21.8	6.8	15	1.85	16.3	1.64	0.83
CD-95-3	1100	0.12	16.1	0.28	20.5	6.4	27	1.56	14.8	1.55	0.68
CD-95-3	1110	0.13	15	0.16	17	6.4	13	1.83	12.3	1.54	0.72
CD-95-3	1120	0.12	19.1	0.14	23.3	6.3	15	1.61	12	1.53	0.72
CD-95-3	1130	0.08	21.2	0.14	21	3.8	16	1.5	9.6	1.1	0.58
CD-95-3	1140	0.09	20	0.09	22.5	4.3	11	1.48	9.3	1.33	0.56
CD-95-3	1150	0.14	14	0.11	17.4	5.7	9	1.96	13.2	1.68	0.67
CD-95-3	1160	0.06	21.4	0.08	22.2	3.1	11	0.86	6.7	0.91	0.48
CD-95-3	1170	0.18	20	0.2	23.2	3.2	14	0.99	8.8	0.93	0.52
CD-95-3	1180	0.06	22	0.24	21.4	3.2	15	0.97	30.5	0.86	0.48
CD-95-3	1190	0.07	20.1	0.3	20.5	3.1	17	1.4	12.9	0.92	0.56
CD-95-3	1200	0.05	22.5	0.07	24.2	2.4	12	0.72	4.9	0.72	0.44
CD-95-3	1210	0.1	19.6	0.28	21.2	3.3	28	1.11	20.9	0.87	0.61
CD-95-3	1220	0.05	21.5	0.21	22.5	2.7	19	0.73	8.5	0.88	0.52
CD-95-3	1230	0.05	20.1	0.2	20.1	2.6	24	0.71	10.1	0.89	0.54
CD-95-3	1240	0.06	20.9	0.16	18.75	2.9	16	0.93	8.9	0.88	0.49
CD-95-3	1250	0.09	17.35	0.11	19.25	4.1	13	1.06	9.4	1.23	0.56
CD-95-3	1260	0.05	23.1	0.21	17.55	3.4	21	1	14.5	0.95	0.57
CD-95-3	1270	0.05	21.3	0.13	18.25	2.7	19	1.03	10.3	0.86	0.56
CD-95-3	1280	0.04	22	0.12	17.75	2.3	15	0.59	7.6	0.74	0.4
CD-95-3	1290	0.09	14.15	0.29	62.7	14.1	37	2.64	17.7	2.61	2
CD-95-3	1300	0.07	13.85	4.41	42.9	11.8	24	1.43	36.5	2.06	1.28
CD-95-3	1310	0.05	17.45	6.2	14.05	3.9	25	0.98	47	0.97	0.82
CD-95-3	1320	0.06	14.7	5.99	12.55	4	29	0.91	50.5	0.97	0.86
CD-95-3	1330	0.04	10.85	2.5	10.3	3.2	31	0.63	25.9	0.75	0.67
CD-95-3	1340	0.06	10.3	2.31	7.28	3.6	28	0.54	27.4	0.9	0.6
CD-95-3	1350	0.04	14	2.41	9.34	3	28	0.57	27.1	0.68	0.5
CD-95-3	1360	0.04	19.45	2.57	10.35	3.2	23	0.43	29	0.61	0.42
CD-95-3	1370	0.04	17	1.74	9.93	3.4	29	0.62	25.3	0.68	0.52
CD-95-3	1380	0.04	15.45	1.23	11.2	3	18	0.61	20.1	0.69	0.5
CD-95-3	1390	0.04	16.95	1.92	12.1	3.7	18	0.54	23.6	0.7	0.55
CD-95-3	1400	0.04	14.6	2.3	11.05	2.8	22	0.48	28.1	0.61	0.52
CD-95-3	1410	0.05	14.55	2	9.18	3.2	36	0.89	27.1	0.78	0.6
CD-95-3	1420	0.03	19.2	2.09	12.8	2.4	21	0.58	19.9	0.55	0.49
CD-95-3	1430	0.05	16.05	1.82	12.2	3.8	25	1.19	29.4	0.92	0.72
CD-95-3	1440	0.06	14.3	2.89	10.2	3.8	31	0.76	31.8	0.85	0.66
CD-95-3	1450	0.06	10.9	1.76	13.6	4.8	43	1.99	35.3	1.21	0.9
CD-95-3	1460	0.06	13.2	2.36	17.45	4.9	29	0.77	31.6	1.05	0.82
CD-95-3	1470	0.06	13.45	1.26	15.3	5	28	1.42	28.7	1.22	0.79
CD-95-3	1480	0.06	13	1.05	11.8	4.7	25	0.98	27.3	1.09	0.69
CD-95-3	1490	0.06	11.75	1.57	12.45	3.9	21	1.25	22.3	1.08	0.6
CD-95-3	1500	0.05	12.35	1.32	11.6	3.9	21	0.83	19.2	1.03	0.59
CD-95-3	1510	0.07	13.05	1.38	12.45	4.3	24	0.83	24.3	1.2	0.61

SAMPLE	Depth (ft)	Bi ppm	Ca ppm	Cd ppm	Ce ppm	Co ppm	Cr ppm	Cs ppm	Cu ppm	Fe ppm	Ga ppm
CD-95-3	1520	0.06	13.4	1.2	13.75	3.8	21	0.66	19.6	1.1	0.56
CD-95-3	1530	0.08	11.5	1.72	13.3	4.9	20	1.18	27.7	1.42	0.68
CD-95-3	1540	0.07	12.35	1.95	14.25	4.8	19	0.91	24.8	1.2	0.68
CD-95-3	1550	0.05	12.85	0.5	12.75	3.1	90	0.93	15.4	0.99	0.55
CD-95-3	1560	0.05	11.65	0.4	15.6	3.8	34	0.75	15	0.98	0.52
CD-95-3	1570	0.07	6.12	0.67	12.7	5.1	59	2.48	23.5	1.55	0.85
CD-95-3	1580	0.06	12.9	0.28	14.75	4.2	41	0.96	13.8	1.11	0.62
CD-95-3	1590	0.08	10.25	1.63	16.3	4.9	47	2.86	26.5	1.49	0.97
CD-95-3	1600	0.04	13.4	0.3	12.15	2.4	35	0.69	7.5	0.7	0.49
CD-95-3	1610	0.04	11.4	0.21	20.8	2.9	33	0.82	8	0.79	0.48
CD-95-3	1620	0.06	13.7	1.39	18.05	3.5	27	0.8	10.3	0.94	0.65
CD-95-3	1630	0.08	8.56	0.66	18.75	4.8	40	2.48	24	1.46	0.94
CD-95-3	1640	0.08	8.92	0.79	17.8	4.8	49	2.41	25.3	1.51	1.07
CD-95-3	1650	0.08	10	0.57	15.55	5.4	33	2.66	22.8	1.69	0.93
CD-95-3	1660	0.08	11.5	0.93	17.7	5.1	31	1.75	18.3	1.59	0.79
CD-95-3	1670	0.07	9.68	1.01	13.2	5.5	35	2.58	19.5	1.81	0.82
CD-95-3	1680	0.07	9.47	1.26	13.9	5.1	47	2.44	22.4	1.78	0.83
CD-95-3	1690	0.06	14.7	2.07	16.15	3.7	31	1.11	13.7	1.11	0.61
CD-95-3	1700	0.05	11.55	0.44	24.2	2.8	26	0.68	7.6	0.8	0.65
CD-95-3	1710	0.05	12.2	2.02	19.4	3.3	24	0.76	10.7	0.97	0.59
CD-95-3	1720	0.07	12.5	2.07	19.6	3.4	24	0.83	11.4	1.02	0.62
CD-95-3	1730	0.05	13.85	3.22	9.62	2.6	30	0.4	8.3	0.76	0.47
CD-95-3	1740	0.06	5.84	1	26.4	2.9	31	0.4	8.8	0.91	0.61
CD-95-3	1750	0.06	11.85	1.64	18.6	2.9	34	0.59	11	0.95	0.63
CD-95-3	1760	0.05	13.8	1.25	10.35	2.5	27	0.39	9.2	0.72	0.5
CD-95-3	1770	0.03	19.3	1.43	11.8	1.7	21	0.38	8.4	0.49	0.32
CD-95-3	1780	0.03	18.7	0.5	18.6	1.6	35	0.32	6.9	0.44	0.36
CD-95-3	1790	0.04	16.5	1.32	15.2	1.8	27	0.46	9	0.51	0.37
CD-95-3	1800	0.03	18.15	2.18	16.05	1.9	19	0.27	6.6	0.52	0.32
CD-95-3	1810	0.05	16.6	4.61	13.7	2.4	31	0.38	10.9	0.7	0.4
CD-95-3	1820	0.04	16.3	3.84	14.05	2.3	16	0.4	9.1	0.65	0.38
CD-95-3	1830	0.04	19.2	3.45	15.35	2.1	13	0.27	7.1	0.55	0.33
CD-95-3	1840	0.03	19	1.47	20.1	1.8	12	0.27	5.5	0.49	0.38
CD-95-3	1850	0.03	18.15	1.23	17.55	1.7	14	0.23	11.5	0.5	0.38
CD-95-3	1860	0.03	20.7	3.06	8.71	1.9	24	0.16	10	0.4	0.35
CD-95-3	1870	0.03	16.45	0.44	5.89	1.9	13	0.21	5.9	0.53	0.4
CD-95-3	1880	0.03	14.25	1.91	8.77	1.8	17	0.2	6.8	0.41	0.35
CD-95-3	1890	0.03	16.2	4.02	7.2	2.6	23	0.3	10.1	0.65	0.44
CD-95-3	1900	0.03	17.45	1.67	13.95	2.8	18	0.28	9.5	0.67	0.46
CD-95-3	1910	0.03	17.8	0.4	19.6	2.4	15	0.24	11.9	0.56	0.38
CD-95-3	1920	0.03	16.4	2.28	12.65	2.2	17	0.28	7.6	0.59	0.45
CD-95-3	1930	0.06	13.6	1.14	17.8	6.9	22	1.22	17.8	1.31	0.71
CD-95-3	1940	0.16	6.06	0.43	29	19.8	33	2	46.6	3.41	1.33
CD-95-3	1950	0.14	6.38	0.95	28	18.5	38	1.57	47.3	3.27	1.43
CD-95-3	1960	0.04	18.35	2.74	12	3.3	30	0.28	13.1	0.64	0.41
CD-95-3	1970	0.06	17.8	1.36	14.1	3.6	22	0.53	16.5	0.8	0.51
CD-95-3	1980	0.07	15.45	12.5	14.25	4.5	33	0.64	17.1	1.1	0.62
CD-95-3	1990	0.18	5.86	0.93	44.3	19.3	48	2.6	46.1	2.5	1.8
CD-95-3	2000	0.16	5.58	1.14	34.7	20.6	51	2.77	48.4	3.29	1.77
CD-95-3	2010	0.16	5.47	0.46	30.4	20.4	67	1.59	47.6	3.42	1.59
CD-95-3	2020	0.08	6.72	3.98	11.05	5.4	62	0.82	47.9	1.43	0.78

SAMPLE	Depth (ft)	Bi ppm	Ca ppm	Cd ppm	Ce ppm	Co ppm	Cr ppm	Cs ppm	Cu ppm	Fe ppm	Ga ppm
CD-95-3	2030	0.03	15.5	1.59	12.55	3	33	0.36	13.9	0.69	0.46
CD-95-3	2040	0.04	11.8	1.38	10.55	3.5	37	0.46	17.4	1.04	0.57
CD-95-3	2050	0.04	12.85	1.19	11.55	3.6	28	0.4	12.8	0.86	0.64
CD-95-3	2060	0.06	16.05	1.27	13.95	4.2	23	0.41	12.8	0.92	0.56
CD-95-3	2070	0.05	16.85	1.15	14.35	3.9	17	0.3	9.3	0.79	0.53
CD-95-3	2080	0.05	16.55	1.39	14.1	4.4	33	0.81	18.1	0.97	0.69
CD-95-3	2090	0.05	16.25	1.16	13.8	4.4	45	0.77	21	1.1	0.71
CD-95-3	2100	0.04	14.05	2.01	11.1	4.4	60	0.77	29.3	1.2	0.7
CD-95-3	2110	0.03	7.67	2.41	8.16	2.6	54	0.53	14	0.78	0.55
CD-95-3	2120	0.05	9.88	1.46	13.05	3.8	82	1.14	19.2	1.14	0.85
CD-95-3	2130	0.13	5.12	0.56	30.4	17.9	55	1.52	46.7	3.35	1.39
CD-95-3	2140	0.03	14.85	0.36	8.57	4.1	28	0.94	14.4	0.86	0.61
CD-95-3	2150	0.04	13.7	0.47	9.41	3.9	30	1.42	16	1.02	0.72
CD-95-3	2160	0.03	14.95	0.46	7.64	3.4	31	1.18	15	0.96	0.61
CD-95-3	2170	0.05	13.6	0.51	19.95	8.1	33	1.71	17.1	1.26	1.33
CD-95-3	2180	0.07	9.93	0.46	25.3	11.5	36	2.82	22.9	1.86	1.82
CD-96-2C	770	0.1	11.8	0.56	22.6	4.7	33	1.54	23.1	1.55	1.16
CD-96-2C	780	0.14	9.49	0.22	19.2	6.9	19	1.42	29.3	1.82	1.28
CD-96-2C	790	0.14	9.39	0.1	13.85	7.9	17	1.05	32.2	2.05	0.99
CD-96-2C	800	0.14	10.95	0.16	19.45	6.9	19	1.08	30.5	1.92	1.13
CD-96-2C	810	0.09	15.9	0.17	25.4	4.6	18	0.77	19.7	2.17	0.91
CD-96-2C	820	0.34	18.85	0.05	22.6	4.5	13	0.8	11.1	1.31	0.96
CD-96-2C	830	0.19	14.8	0.11	17.95	6.4	11	1.29	15.9	1.75	1.1
CD-96-2C	840	0.16	20.8	0.09	22	5	11	0.86	9.9	1.39	0.9
CD-96-2C	850	0.1	22.9	0.1	19.5	3.7	11	0.81	9.8	1.03	0.75
CD-96-2C	860	0.13	21.1	0.11	18.8	4.9	10	1.24	9	1.43	0.83
CD-96-2C	870	0.15	18.35	0.05	16.7	6	11	1.49	11.8	1.51	0.84
CD-96-2C	880	0.11	17.4	0.16	15	5.2	12	1.11	12.8	1.36	0.92
CD-96-2C	890	0.13	16.4	0.26	18.85	5.3	13	1.08	14.6	1.5	0.98
CD-96-2C	900	0.14	15.75	0.18	14.75	5.3	11	1.21	16.9	1.44	0.81
CD-96-2C	910	0.12	16.05	0.33	18.9	5.1	14	1.18	20.6	1.35	1.11
CD-96-2C	920	0.25	11.55	0.15	10.9	6.8	14	1.26	27.1	1.71	0.93
CD-96-2C	930	0.09	14.25	0.22	17.05	4.6	26	1.02	24.2	1.35	1.12
CD-96-2C	940	0.15	13	0.18	15.85	4.7	28	1.06	25.7	1.48	1.27
CD-96-2C	950	0.1	12.1	0.3	21.2	4.3	39	1.39	32.8	1.37	1.61
CD-96-2C	960	0.09	13.6	0.48	23.5	4.1	53	1.25	35	1.25	1.51
CD-96-2C	970	0.09	15.05	0.3	18.2	3.8	39	0.94	30.8	1.17	1.04
CD-96-2C	980	0.1	9.67	0.61	28	4.2	41	2.51	23.4	1.39	1.99
CD-96-2C	990	0.11	12.6	0.26	21.1	4.8	28	0.86	33.7	1.53	1.45
CD-96-2C	1000	0.11	12.9	0.24	15.3	5.5	18	0.8	24.2	1.6	1.02
CD-96-2C	1010	0.11	12.9	0.07	14.6	6.1	15	0.83	19.9	1.58	0.93
CD-96-2C	1020	0.13	11.4	0.06	10.4	7.5	12	0.96	23.6	1.7	0.84
CD-96-2C	1030	0.13	9.37	0.17	25.4	6.2	28	1.23	32.9	1.73	1.81
CD-96-2C	1040	0.1	10.45	0.23	22.2	5.2	31	0.98	43.8	1.43	1.48
CD-96-2C	1050	0.14	12.2	0.34	40	5.1	29	1.22	49.2	1.74	2.47
CD-96-2C	1060	0.09	19.7	0.42	20.1	4.6	12	0.8	13.6	1.26	0.75
CD-96-2C	1070	0.14	16.05	0.06	18.25	6.1	10	0.98	11.5	1.69	0.72
CD-96-2C	1080	0.12	17.3	0.07	14	5.7	12	0.79	9.6	1.53	0.69
CD-96-2C	1090	0.14	14.7	0.19	13.65	6.9	11	0.98	12	1.74	0.76
CD-96-2C	1100	0.12	19.1	0.12	17.7	5.6	10	0.79	8	1.67	0.68
CD-96-2C	1110	0.1	21.1	0.08	17.8	4.6	11	0.65	8.5	1.43	0.61

SAMPLE	Depth (ft)	Bi ppm	Ca ppm	Cd ppm	Ce ppm	Co ppm	Cr ppm	Cs ppm	Cu ppm	Fe ppm	Ga ppm
CD-96-2C	1120	0.12	18.45	0.1	15.25	5.6	11	0.77	9.6	1.47	0.7
CD-96-2C	1130	0.13	19	0.05	16.2	5.9	10	0.93	10.4	1.48	0.71
CD-96-2C	1140	0.13	17.8	0.09	15.6	6.4	11	1.05	10.7	1.55	0.73
CD-96-2C	1150	0.13	19.85	0.08	12.2	5.3	10	0.91	8.3	1.36	0.59
CD-96-2C	1160	0.04	>25.0	0.23	8.72	2.2	20	0.36	4.1	0.6	0.34
CD-96-2C	1170	0.04	>25.0	0.05	15.15	2.2	11	0.37	3.6	0.65	0.39
CD-96-2C	1180	0.05	25	0.11	15.85	2.4	12	0.42	7	0.88	0.54
CD-96-2C	1190	0.05	22.5	0.19	17.4	2.8	13	0.49	9.9	0.77	0.63
CD-96-2C	1200	0.08	20.3	0.15	19.1	3.9	14	0.75	14.9	1.02	0.72
CD-96-2C	1210	0.09	23.6	0.1	18.85	4.2	13	0.73	8.4	1.11	0.67
CD-96-2C	1220	0.05	19.2	1.38	12.5	3.2	17	0.57	13.2	0.7	0.65
CD-96-2C	1230	0.06	15.05	1.85	13.15	4.2	21	0.59	21.6	1	0.83
CD-96-2C	1240	0.06	14.5	1.91	12.75	4.3	21	0.66	20.7	0.95	0.85
CD-96-2C	1250	0.03	18.8	0.95	15.85	2.7	22	0.49	12.2	0.72	0.67
CD-96-2C	1260	0.04	15.4	0.69	17.85	3.1	16	0.5	5.8	0.67	0.65
CD-96-2C	1270	0.05	13.65	0.68	16.45	3.4	17	0.55	8.4	0.79	0.74
CD-96-2C	1280	0.05	10	0.42	18.7	4.2	20	0.75	7.1	1	0.9
CD-96-2C	1290	0.05	12.35	0.28	19.5	3.5	18	0.57	6	0.74	0.8
CD-96-2C	1300	0.05	10.4	0.16	18.2	3.6	18	0.86	6	0.77	0.78
CD-96-2C	1310	0.06	12.1	0.13	18.85	4.2	15	1.02	6.9	0.81	0.81
CD-96-2C	1320	0.05	14.2	0.28	17.05	3.7	12	0.71	6	0.79	0.8
CD-96-2C	1330	0.05	15.6	0.23	19.8	3.5	12	0.65	5.9	0.72	0.76
CD-96-2C	1340	0.05	14.3	0.12	21.3	4	11	0.74	6.1	0.78	0.86
CD-96-2C	1350	0.04	17.6	0.07	18.95	2.9	10	0.63	5.7	0.72	0.71
CD-96-2C	1360	0.05	13.55	0.77	19.35	3.8	25	0.73	7.7	0.88	0.84
CD-96-2C	1370	0.05	14.4	0.9	14.55	3.3	15	0.62	7.6	0.79	0.7
CD-96-2C	1380	0.06	14.65	0.4	16.05	4.3	12	0.82	8.1	0.87	0.85
CD-96-2C	1390	0.07	13.7	0.73	18.25	5.2	11	0.99	9.9	1.04	1.02
CD-96-2C	1400	0.05	18.7	1.54	13.5	3.7	8	0.63	9.4	0.74	0.61
CD-96-2C	1410	0.05	16.9	0.71	17.4	4.1	10	0.63	9.3	0.84	0.8
CD-96-2C	1420	0.05	18.5	0.99	12.25	3.8	8	0.43	8.9	0.79	0.62
CD-96-2C	1430	0.05	18.4	1.08	13.15	3.7	9	0.45	9.2	0.78	0.64
CD-96-2C	1440	0.05	17.5	3.54	12.75	2.9	8	0.47	7.4	0.76	0.47
CD-96-2C	1450	0.05	13	8.18	8.23	3.1	25	0.51	15	0.76	0.72
CD-96-2C	1460	0.04	18.7	4.17	9.81	2.9	18	0.48	9.9	0.61	0.62
CD-96-2C	1470	0.05	15.6	2.91	12.1	3.3	17	0.64	10.8	0.76	0.7
CD-96-2C	1480	0.05	18.5	0.41	16.2	3.5	9	0.67	6.6	0.71	0.69
CD-96-2C	1490	0.07	14.7	0.61	17.65	5.7	12	1.1	10.4	1.12	1.05
CD-96-2C	1500	0.05	19.15	1.95	12.1	3.6	13	0.69	9.6	0.74	0.69
CD-96-2C	1510	0.07	14.5	0.63	15.45	4.7	21	1.29	17	1.11	1.08
CD-96-2C	1520	0.08	12.35	1.62	16.55	5.7	16	0.97	14.7	1.2	1.11
CD-96-2C	1530	0.05	18.15	2.95	13.35	3.5	16	0.65	15.1	0.84	0.9
CD-96-2C	1540	0.05	16.55	1.46	15.1	3.7	13	0.79	8.8	0.83	0.74
CD-96-2C	1550	0.06	13.35	1.19	17.7	4.3	19	1.07	13.7	1.02	1.04
CD-96-2C	1560	0.08	12.15	1.02	19.25	5.8	15	1.1	12.1	1.25	1.22
CD-96-2C	1570	0.07	14.55	3.79	13.3	5.4	14	0.98	17.4	1.35	1.22
CD-96-2C	1580	0.06	17.25	5.48	10.65	4.3	13	0.48	13.7	1.01	0.76
CD-96-2C	1590	0.06	14.3	1.78	13.7	3.9	15	0.78	14.2	0.94	0.83
CD-96-2C	1600	0.06	13.15	1.78	13.35	4.3	12	0.82	10.5	0.91	0.82
CD-96-2C	1610	0.06	11.75	0.21	18.4	3.9	13	0.94	8.4	0.86	0.97
CD-96-2C	1620	0.06	10.85	0.6	17.9	4	14	0.92	8.7	0.87	0.94

SAMPLE	Depth (ft)	Bi ppm	Ca ppm	Cd ppm	Ce ppm	Co ppm	Cr ppm	Cs ppm	Cu ppm	Fe ppm	Ga ppm
CD-96-2C	1630	0.05	15.05	0.43	18.35	3.6	9	0.58	8.6	0.82	0.69
CD-96-2C	1640	0.05	17.3	3.55	12.4	3.6	9	0.51	9.1	0.75	0.72
CD-96-2C	1650	0.05	11.35	1.51	14.2	3.4	13	0.44	8.7	0.85	0.73
CD-96-2C	1660	0.05	16.3	2.42	13.35	4	10	0.36	11.5	1	0.78
CD-96-2C	1670	0.05	18.25	3.59	12.8	3.3	13	0.35	11.1	0.83	0.65
CD-96-2C	1680	0.04	16.5	3.2	14.4	2.4	15	0.38	7.4	0.65	0.67
CD-96-2C	1690	0.02	23	0.26	11.55	2	7	0.23	4.4	0.47	0.43
CD-96-2C	1700	0.05	20.5	2.13	16.6	3.3	6	0.29	8.8	0.82	0.62
CD-96-2C	1710	0.05	18.65	3.38	17.15	3.6	5	0.38	8.2	0.76	0.68
CD-96-2C	1720	0.04	16.45	3.39	17.6	4.5	6	0.48	8.7	0.97	0.9
CD-96-2C	1730	0.08	17.95	5.8	15.3	3.2	9	0.37	9.2	0.7	0.75
CD-96-2C	1740	0.04	18.1	5.4	15.9	3.5	9	0.38	8.8	0.79	0.66
CD-96-2C	1750	0.04	17.95	6.04	15.3	3.5	9	0.44	11.2	0.85	0.64
CD-96-2C	1760	0.04	14.2	1.05	18	4.2	9	0.5	7.9	0.84	0.76
CD-96-2C	1770	0.05	13.6	2.85	16.15	5.5	14	0.53	11.6	1.15	0.92
CD-96-2C	1780	0.04	18.45	3.41	16.1	4.1	6	0.43	8.4	0.87	0.61
CD-96-2C	1790	0.05	14.45	3.91	15	4.6	23	0.67	18.4	1.2	0.84
CD-96-2C	1800	0.03	21.2	5.11	12.05	2.9	7	0.26	8.3	0.62	0.43
CD-96-2C	1810	0.05	16.85	8.13	12.7	3.6	12	0.41	14.6	0.94	0.67
CD-96-2C	1820	0.04	21	6.13	14.2	3.2	6	0.26	9.3	0.68	0.48
CD-96-2C	1830	0.04	18.85	6.92	14.3	3.3	11	0.4	13.5	0.77	0.59
CD-96-2C	1840	0.04	18.65	6.5	13.5	3.3	11	0.38	11.7	0.77	0.53
CD-96-2C	1860	0.05	17.7	4	17.75	3.7	8	0.48	13.2	1.9	0.69
CD-96-2C	1880	0.05	17.75	6.35	12.45	3.9	8	0.52	10.7	0.83	0.59
CD-96-2C	1900	0.04	21.3	5.27	15.65	3	7	0.4	10.3	0.61	0.51
CD-96-2C	1920	0.04	20	9.67	10.3	2.9	11	0.42	11.3	0.67	0.49
CD-96-2C	1925	0.04	15.6	7.36	11.25	3.5	18	0.38	9.1	0.75	0.53
CD-96-2C	1930	0.04	18.4	3.42	23.2	2.8	13	0.28	8.1	0.67	0.52
CD-96-2C	1940	0.04	17.8	2.29	18.75	3.3	9	0.34	7	0.73	0.54
CD-96-2C	1960	0.03	20.1	3.06	17.9	2.8	10	0.31	6.5	0.54	0.58
CD-96-2C	1980	0.03	20.4	3.08	16.25	2.4	11	0.31	5.9	0.49	0.53
CD-96-2C	2000	0.03	20.3	2.74	19.75	2.4	11	0.4	5.9	0.51	0.6
CD-96-2C	2020	0.03	19	3.11	17.3	2.5	18	0.36	6.4	0.54	0.69
CD-96-2C	2025	0.02	23.3	4.17	11.5	2.2	16	0.3	6	0.41	0.39
CD-96-2C	2030	0.03	21.7	2.62	14.45	2.4	10	0.23	5.1	0.47	0.45
CD-96-2C	2035	0.03	19.3	1.04	15.1	2.4	7	0.32	4.3	0.63	0.47
CD-96-2C	2040	0.14	7.45	0.82	36.2	5.6	32	1.56	6.9	1.68	1.2
CD-96-2C	2045	0.05	18.3	2.07	20.9	3.3	7	0.82	5.5	0.77	0.79
CD-96-2C	2050	0.02	24.6	2.88	12.55	2.1	8	0.32	5.3	0.38	0.41
CD-96-2C	2055	0.02	24.4	1.79	9.66	1.7	11	0.21	3.4	0.31	0.33
CD-96-2C	2060	0.09	10.5	1.38	26.7	4.6	4	1.17	6.5	1.36	1.11
CD-96-2C	2065	0.02	22.9	2.6	12.55	2.2	8	0.31	5.7	0.4	0.55
CD-96-2C	2070	0.04	19.85	2.21	18.4	2.7	7	0.79	7.2	0.65	0.53
CD-96-2C	2075	0.12	10.1	1.55	27.6	4.4	9	1.16	6.4	1.47	0.98
CD-96-2C	2080	0.3	3.14	0.34	52.4	5.5	6	2.16	6.3	2.09	1.26
CD-96-2C	2100	0.07	14.8	1.11	16.25	2.3	35	0.53	9.9	0.71	0.88
CD-96-2C	2120	0.06	12.45	1.93	25.6	2.6	70	0.93	16.8	0.66	1.66
CD-96-2C	2180	0.07	16.5	0.32	17.65	2.1	36	0.4	9.4	0.41	0.8
CD-96-2C	2200	0.1	15.35	1.58	25	3.6	54	0.64	11.3	0.58	1.15
CD-96-2C	2220	0.25	12	0.97	27.4	3.9	66	0.76	5	0.73	0.94
CD-96-2C	2240	0.32	2.54	0.18	38.1	5	24	2.21	6.1	2.12	1.37

SAMPLE	Depth (ft)	Bi ppm	Ca ppm	Cd ppm	Ce ppm	Co ppm	Cr ppm	Cs ppm	Cu ppm	Fe ppm	Ga ppm
CD-96-2C	2260	0.16	18.25	0.69	9.47	1.3	9	0.49	2.6	0.36	0.55
CD-96-2C	2280	0.02	19.8	0.06	4.43	1	7	0.12	1.8	0.16	0.23
CD-96-2C	2300	0.01	18.95	0.03	2.92	0.9	8	0.08	1.5	0.14	0.16
CD-96-2C	2320	0.01	18.2	0.13	2.66	0.8	10	0.05	2	0.1	0.16
CD-96-2C	2340	0.01	18.8	0.02	2.09	0.7	8	<0.05	1.4	0.07	0.12
DR-1C	2480	0.07	17.25	2.64	35.5	12.9	60	1.27	48.2	1.65	1.25
DR-1C	2500	0.07	16.05	3.75	16	3.5	26	1.14	45.2	0.67	0.91
DR-1C	2520	0.05	16.9	2.77	14.75	3.4	22	0.6	35.8	0.67	0.77
DR-1C	2540	0.08	17.15	2.85	14.05	3.5	24	0.58	41.4	0.67	0.78
DR-1C	2560	0.05	15.75	2.63	14.45	3.2	55	0.39	30.4	0.75	0.6
DR-1C	2580	0.04	17.65	1.58	19.05	3.6	52	0.52	25.6	0.71	0.76
DR-1C	2600	0.06	13.6	1.85	16.7	5.2	81	0.7	27.7	1.18	0.98
DR-1C	2620	0.05	16.15	3.31	13.85	3.6	56	0.51	29.2	0.81	0.67
DR-1C	2640	0.05	16.65	2.18	14.6	3.5	38	0.51	26.2	0.7	0.76
DR-1C	2660	0.05	18.05	2.06	11.7	3.8	38	0.62	23.6	0.88	0.93
DR-1C	2680	0.05	16.8	1.95	14.2	4.1	36	0.84	28.8	0.83	0.93
DR-1C	2700	0.07	13.75	2.8	14.35	6	25	1.15	28.4	1.13	1.1
DR-1C	2720	0.08	11.25	0.93	13.9	6.3	20	0.99	26.3	1.73	1.26
DR-1C	2740	0.08	14.05	0.58	16.2	5.4	38	0.81	22.6	1.15	1.08
DR-1C	2760	0.07	18.75	0.6	19.2	4.7	18	1.07	15.4	1	0.92
DR-1C	2780	0.05	16.75	0.17	24.6	4	17	1.36	11.8	1.07	0.92
DR-1C	2800	0.07	13.6	0.11	18.1	4.9	14	1.37	14.5	1.01	1.05
DR-1C	2820	0.08	11.9	0.26	16.35	5.9	14	1.17	15.9	1.36	1.38
DR-1C	2840	0.06	12.75	0.09	15.25	5.4	15	0.8	13.6	1.19	1.01
DR-1C	2860	0.08	13.95	0.15	22.5	6	14	1.72	14.2	1.31	1.54
DR-1C	2880	0.09	10.3	0.2	20.6	7.2	13	1.5	17.9	1.52	1.45
DR-1C	2900	0.09	11.4	0.17	20.5	6.3	19	1.18	14.3	1.1	1.35
DR-1C	2917	0.08	11.5	1.46	19.4	6.5	12	1.19	18.5	1.12	1.19
GA-2A	1680	0.11	1.35	7.4	5.46	5.8	12	1.56	37	2.38	0.87
GA-2A	1690	0.09	1.08	5.31	7.66	5.7	19	1.21	42.5	3.29	1.35
GA-2A	1700	0.15	2.92	2.49	7.91	8.8	13	1.95	35.7	2.91	1.12
GA-2A	1710	0.14	6.37	1.56	9.38	9.5	16	2.75	28.4	2.78	1.17
GA-2A	1720	0.11	7.75	21.2	13.6	7.7	25	3.55	58	2.58	2.12
GA-2A	1730	0.09	8.91	10.4	17.35	5.5	27	1.68	55.2	2.53	1.91
GA-2A	1740	0.07	13.15	5.21	9.94	6.3	12	1.64	31	1.78	1.01
GA-2A	1750	0.07	13.05	1.03	10.65	5.9	11	1.25	37	1.78	0.95
GA-2A	1760	0.08	14.35	4.34	8.95	5.8	10	1.35	25	1.56	0.63
GA-2A	1770	0.08	10.85	11.2	7.56	5.6	15	1.48	40.1	1.72	1.05
GA-2A	1780	0.07	11.55	8.92	5.31	4.8	19	1.17	34.7	1.82	1.26
GA-2A	1790	0.08	13.6	1.78	9.87	6.7	18	1.63	28.7	1.84	1.15
GA-2A	1800	0.07	12.5	13.95	6.09	4.8	30	1.19	44.9	1.36	1.17
GA-2A	1810	0.09	5.91	24.1	10.65	4	55	1.26	127	1.74	1.68
GA-2A	1820	0.08	7.84	20.5	7.55	3.5	56	1.1	85.6	1.28	1.56
GA-2A	1830	0.09	10.2	4.73	22.9	4.2	79	1.52	71.1	1.57	1.83
GA-2A	1840	0.11	10.35	0.77	12.5	5.7	33	1.16	41.4	1.91	1.05
GA-2A	1850	0.19	2.44	1.63	8.77	8.1	20	1.49	54.2	3.76	1.07
GA-2A	1860	0.17	1.17	0.79	14.1	6.6	19	1.28	36	3.39	1.16
GA-2A	1870	0.16	5.9	0.56	21.1	6.5	12	1.57	24.8	2.61	0.97
GA-2A	1880	0.11	0.9	0.3	10.25	4.8	12	1.19	20.8	1.84	0.88
GA-2A	1890	0.12	13.1	1.26	25.1	5	19	1.46	23.9	1.79	1.09
GA-2A	1900	0.12	5.41	1.28	14.05	5.2	13	1.25	27.1	2.28	0.87

SAMPLE	Depth (ft)	Bi ppm	Ca ppm	Cd ppm	Ce ppm	Co ppm	Cr ppm	Cs ppm	Cu ppm	Fe ppm	Ga ppm
GA-2A	1910	0.13	13.5	0.59	17.4	5.9	12	1.4	20.8	2.48	0.75
GA-2A	1920	0.1	3.42	0.21	10.75	4.2	12	0.97	14.3	1.93	0.63
GA-2A	1930	0.12	14.05	0.67	15.1	5.1	17	1.09	17	2.9	0.67
GA-2A	1940	0.11	0.64	0.37	18.8	4.6	15	1.12	20.5	2.99	0.86
GA-2A	1950	0.11	2.63	1.7	19.95	4.5	14	1.39	27.8	2.73	0.97
GA-2A	1960	0.08	0.86	2.97	28.4	4.3	17	1.1	39.6	3.22	0.98
GA-2A	1970	0.07	3.55	2.54	13.75	4.2	18	0.97	43.8	3.55	1.04
GA-2A	1980	0.12	3.69	1.15	13.35	5.2	16	1.14	31.6	3.7	0.83
GA-2A	1990	0.11	3.03	0.79	17.2	5.1	17	1.13	31.4	3.7	1.02
GA-2A	2000	0.06	3.58	1.48	12.55	3.3	16	0.8	31.5	3.01	0.82
GA-2A	2010	0.07	0.88	1.68	13.35	3.1	18	0.87	35.6	2.92	0.74
GA-2A	2020	0.07	2.02	1.22	10.35	2.9	28	0.58	31.3	2.91	0.59
GA-2A	2030	0.03	16.25	0.65	9.58	1.8	12	0.43	11.7	1.13	0.42
GA-2A	2040	0.03	15.9	0.63	9.56	1.8	12	0.48	12.2	1.17	0.53
GA-2A	2050	0.01	>25.0	0.21	5.97	1.1	4	0.24	3.1	0.26	0.29
GA-2A	2060	0.02	>25.0	0.1	8.56	1.4	4	0.29	2.8	0.29	0.24
GA-2A	2070	0.02	>25.0	0.11	8.38	1.5	5	0.37	4.1	0.37	0.29
GA-2A	2080	0.03	24.5	0.26	12.15	2.2	8	0.56	8.1	1	0.53
GA-2A	2100	0.04	23.8	0.35	11.9	2.5	7	0.55	8	1.05	0.38
GA-2A	2110	0.03	>25.0	0.26	9.12	2	7	0.48	7	0.87	0.36
GA-2A	2120	0.05	24.6	0.38	11.15	2.6	8	0.55	9.5	1.36	0.4
GA-35C	1680	0.07	11	4.05	9.99	5.9	48	0.8	32.7	1.5	0.9
GA-35C	1700	0.13	10.65	8.27	8.18	6.8	34	0.76	26	1.65	1.15
GA-35C	1720	0.11	12.2	0.59	11.45	5.5	26	1.04	25.3	1.4	1.05
GA-35C	1740	0.15	9.65	220	18.7	15.5	55	1.93	53.3	2.38	2.1
GA-35C	1760	0.14	12	18.85	17.5	12	33	1.14	32.7	2.66	1.4
GA-35C	1780	0.11	14.5	1.16	15.7	6.1	17	0.81	15	1.67	0.89
GA-35C	1800	0.05	15.55	41.9	8.54	3.5	22	0.52	34.5	1.63	1.07
GA-35C	1820	0.05	12.95	4.47	9.26	3.2	27	0.44	30	0.76	0.7
GA-35C	1840	0.05	7.07	1.26	12.3	6.1	45	0.74	24.8	1.2	0.74
GA-35C	1860	0.05	4.21	0.57	23.4	7.7	64	0.71	22.5	1.09	0.75
GA-35C	1880	0.1	4.08	0.62	33.5	12.4	69	1.19	35.5	1.91	1.31
GA-35C	1900	0.12	3.63	0.75	68.3	24.6	71	2.81	60	3.13	1.88
GA-35C	1920	0.13	3.55	0.7	31.1	21.9	70	2.09	52.3	3.43	2.09
GA-35C	1940	0.08	0.24	40.1	16.35	5.4	79	1.03	22	1.5	1.58
GA-35C	1960	0.07	0.32	22.4	20.2	4.9	100	0.95	19.4	1.72	1.57
GA-35C	1980	0.07	0.96	1	18.2	5.8	69	0.9	21.5	1.36	1.13
GA-35C	2000	0.06	0.61	0.98	15.6	4.3	73	0.75	17.6	1.17	0.98
GA-35C	2020	0.07	2.95	2.04	20.7	4.5	65	0.91	16.2	1.13	1.15
GA-35C	2040	0.05	16.05	2.32	18.35	3.7	45	0.62	12	0.82	0.95
GA-35C	2060	0.04	22.5	1.24	18.45	2.7	20	0.43	6.9	0.61	0.55
GA-35C	2080	0.16	5.93	0.24	65.8	31.5	138	2.98	64.4	3.89	2.54
GA-35C	2100	0.06	3.96	0.17	20.4	4.6	71	0.88	10.8	0.98	1.28
GA-35C	2120	0.05	5.92	0.08	30.9	4.4	45	0.83	8.7	1.02	1.42
GA-35C	2140	0.04	17.15	0.12	14.9	3.3	21	0.52	6.2	0.63	0.92
GA-35C	2160	0.03	>25.0	0.08	12.4	2.3	10	0.37	4	0.4	0.54
GA-35C	2186	0.06	14.45	0.09	14.9	4.1	18	0.46	6.6	0.81	1
SJ-390C	640	9.47	0.72	23.2	11.05	4.3	51	2.26	89.7	2.28	2.47
SJ-390C	650	0.57	8.49	25.3	23	4.3	100	2.39	105.5	1.77	4.1
SJ-390C	660	2.59	8.79	8.96	29.2	4.6	131	1.96	92.9	1.86	4.4
SJ-390C	670	0.18	10.35	2.21	29.2	4.4	104	1.47	51.8	1.95	3.69

SAMPLE	Depth (ft)	Bi ppm	Ca ppm	Cd ppm	Ce ppm	Co ppm	Cr ppm	Cs ppm	Cu ppm	Fe ppm	Ga ppm
SJ-390C	680	0.19	8.66	0.79	19.1	5.5	63	1.24	43.1	1.85	3.16
SJ-390C	690	0.16	7.91	0.39	20.7	5.7	52	1.13	28.5	1.96	3.18
SJ-390C	700	0.13	7.77	0.31	17.6	5.9	51	1.56	26.3	1.97	3.83
SJ-390C	710	0.17	5.99	0.28	15.5	7.7	55	2.37	27.9	2.31	5.3
SJ-390C	720	0.22	3.58	0.36	24.1	9.5	45	1.69	35.6	3.34	4.02
SJ-390C	730	0.24	1.47	0.3	27.1	9.6	31	1.3	39	3.31	2.85
SJ-390C	740	0.71	2.17	1.66	25.6	11	46	1.9	51.2	3.8	4.18
SJ-390C	750	0.2	3.35	0.56	45.1	7.8	38	1.13	32.4	2.94	2.97
SJ-390C	760	0.18	3.99	0.48	41.7	8.5	35	0.77	26.4	3.4	2.32
SJ-390C	770	0.55	15.4	0.38	32.7	4.1	27	0.56	11.9	1.64	1.73
SJ-390C	780	0.11	16.75	0.3	33.6	4.1	28	0.56	10.7	1.73	1.81
SJ-390C	790	0.09	16.75	0.35	31	4.1	26	0.58	11.3	1.46	1.56
SJ-390C	800	0.08	16.7	0.2	32.1	3.5	23	0.46	9.1	1.34	1.45
SJ-390C	900	0.08	23.2	0.07	36.3	4	36	2.7	6.3	1.11	4.34
SJ-390C	920	0.09	21.3	4.68	27.6	3.9	33	2.8	34.4	1.09	3.8
SJ-390C	940	0.08	16.15	8.1	22.4	4.4	29	1.71	55.1	1.6	3.08
SJ-390C	960	0.09	18.15	4.59	17.05	3.7	23	1.59	44.1	0.99	1.52
SJ-390C	965	0.04	19.3	2.84	17.1	3.4	35	1.14	33	0.62	1.22
SJ-390C	970	0.04	18.25	1.97	16.3	3	18	0.51	29	0.6	0.51
SJ-390C	975	0.03	14.8	1.54	14.1	2.9	17	0.5	16.3	0.59	0.72
SJ-390C	980	0.04	12.05	1.72	14.2	3.4	19	0.47	17.4	0.66	0.87
SJ-390C	985	0.03	17	1.36	13.45	3	14	0.74	17.8	0.83	1.5
SJ-390C	990	0.04	17.7	1.85	15.35	3.1	14	1.05	17.3	0.86	1.56
SJ-390C	995	0.04	12.4	1.98	9.22	3.4	17	0.69	19.9	1.2	0.83
SJ-390C	1000	0.03	16.05	1.2	10.15	2.5	19	0.39	12.3	0.54	0.47
SJ-390C	1005	0.02	17.4	1.5	8.21	2.3	28	0.64	11.6	0.46	0.45
SJ-390C	1010	0.05	14.8	1.91	6.62	3.3	31	0.77	18.2	0.7	0.55
SJ-390C	1015	0.05	13.75	1.76	15.4	4.7	24	1.21	22.3	1.41	1.2
SJ-390C	1020	0.04	18.45	2.63	15.25	3.7	27	1.29	18.7	0.86	1.61
SJ-390C	1025	0.04	20.1	3.86	19.4	4.1	30	2.38	26.1	0.83	3
SJ-390C	1030	0.09	19.1	2.39	23.1	4.4	28	1.75	22.5	0.91	1.58
SJ-390C	1035	0.44	17.3	2.63	32.1	5.1	34	3.79	19.8	1.01	4.8
SJ-390C	1040	1.45	16.15	1.2	32	4.8	31	4.64	17.9	0.96	5.23
SJ-390C	1060	1	11.95	4.52	29.8	4.6	29	1.16	58.1	1.5	1.74
SJ-390C	1095	0.05	8.44	0.75	6.98	4.4	27	0.3	14.9	1.51	0.68
SJ-390C	1100	0.05	13.35	0.15	13.15	4.3	31	1.03	9.5	1.42	1.01
SJ-390C	1105	0.04	14.9	0.05	11.85	4.5	26	1.13	7.6	1.49	0.71
SJ-390C	1110	0.06	13.1	0.13	11.85	5.1	28	1.37	16.4	1.68	0.94
SJ-390C	1115	0.07	11.05	0.9	7.23	4.6	23	0.51	29.8	1.69	0.83
SJ-390C	1120	0.05	12.1	0.13	8.76	4.3	17	0.24	19.8	1.2	1.05
SJ-390C	1125	0.06	11.8	0.24	7.12	4.8	16	0.24	25.7	1.43	0.85
SJ-390C	1130	0.07	9.83	0.4	6.24	4.7	15	0.25	24.4	1.37	1
SJ-390C	1135	0.06	16.2	0.06	14.35	5.3	20	0.23	13	1.34	1.07
SJ-390C	1140	0.07	14.55	0.07	16.35	6.1	25	0.18	12.6	1.39	1.91
SJ-390C	1160	0.07	14.6	0.38	12.6	5.1	29	0.2	13.2	1.76	0.88
SJ-390C	1180	0.06	14.1	0.14	13.15	5.3	29	0.23	10	1.85	0.79
SJ-390C	1200	0.06	15.15	0.15	17.6	5	23	0.82	13.1	1.62	1.17
SJ-390C	1220	0.07	13.95	0.12	17.65	5.1	23	0.85	11.2	1.73	1.2
SJ-390C	1240	0.08	13.75	0.25	15.85	4.5	28	1.41	24.1	1.04	0.83
SJ-390C	1260	0.04	17.3	1.66	11.4	3.3	26	0.59	17.6	1.12	0.88
SJ-390C	1280	0.02	25	1.07	5.5	1.8	6	0.6	7.4	0.31	0.31

SAMPLE	Depth (ft)	Bi ppm	Ca ppm	Cd ppm	Ce ppm	Co ppm	Cr ppm	Cs ppm	Cu ppm	Fe ppm	Ga ppm
SJ-390C	1295	0.05	23.1	0.15	15	3.5	13	1.46	9.1	0.76	0.46
SJ-464C	10	0.17	2.52	3.52	38.9	17.6	73	2.36	83.1	3.59	2.74
SJ-464C	20	0.22	1.56	3.66	62.6	87.2	26	3.33	55.2	6.31	3.19
SJ-464C	30	0.19	0.21	0.35	63.2	3	17	5.92	54.5	3.55	2.35
SJ-464C	240	0.14	0.13	0.61	25.9	15.6	64	3.2	23.7	1.99	1.08
SJ-464C	250	0.13	4.41	0.78	25	12.2	41	3.06	18.8	1.75	1.19
SJ-464C	260	0.1	7.86	0.61	20.5	10.3	28	3.05	14.4	1.77	1.05
SJ-464C	270	0.12	3.24	0.81	26.4	12.1	31	4.73	18.6	1.99	1.37
SJ-464C	280	0.1	6.63	0.53	27.2	9.1	32	3.81	13.3	1.55	1.21
SJ-464C	290	0.14	6.13	1.58	34.8	11.6	28	5.62	17.6	1.62	1.66
SJ-464C	300	0.09	7.99	2.01	21.8	8.5	25	3.22	13	1.64	1.11
SJ-464C	310	0.11	11	0.6	30	9.2	14	2.71	12.7	1.63	1.06
SJ-464C	320	0.12	9.82	0.73	21.9	10.7	15	3.06	14.8	1.88	0.99
SJ-464C	330	0.09	1.68	3.03	14.85	7.5	82	3.05	19.5	1.21	1.11
SJ-464C	370	0.08	0.83	42.3	9.57	6.6	125	2.74	31.6	1.13	1.38
SJ-464C	380	0.07	2.36	32.3	14.85	6.1	127	3.23	27.1	1.19	1.54
SJ-464C	390	0.09	7.36	4.69	13.9	6.4	76	2.58	15.8	1.32	1.16
SJ-464C	400	0.08	9.04	1.43	19.65	6.6	47	2.19	13.6	1.37	0.98
SJ-464C	410	0.06	6.75	0.89	19.05	5.2	54	1.45	10.5	1.02	0.96
SJ-464C	420	0.08	7.98	1.25	15.5	6.6	64	1.52	11.8	1.25	0.98
SJ-464C	430	0.06	8.57	0.43	21.8	4.5	42	1.25	8.4	1.07	0.99
SJ-464C	440	0.07	8.75	0.31	23.9	6.1	35	1.35	9.2	1.22	1.13
SJ-464C	450	0.06	8.74	0.23	18.35	5.1	36	1.14	7.2	0.99	0.8
SJ-464C	460	0.04	7.94	0.44	14.25	4.6	69	0.74	6.9	0.87	0.7
SJ-464C	470	0.08	8.53	1.08	14.55	7.5	44	1.4	12.5	1.43	0.93
SJ-464C	480	0.08	10	0.61	15.55	6.2	29	1.15	9.5	1.35	0.82
SJ-464C	490	0.1	7.94	2.33	15.15	7.9	47	1.77	18.8	1.56	1.01
SJ-464C	500	0.08	6.34	2.61	20.2	6.4	73	1.68	17.8	1.25	1.15
SJ-464C	510	0.1	8.59	0.7	25.5	8.4	28	1.98	13.5	1.71	1.1
SJ-464C	520	0.11	9.69	0.62	26.8	8.9	27	2.07	13.9	1.81	1.28
SJ-464C	530	0.1	9.1	0.81	27.2	8	29	2.16	13.5	1.71	1.24
SJ-464C	540	0.1	3.52	1.86	22.2	7.4	122	2.2	20.7	1.3	1.13
SJ-464C	690	0.03	0.12	2.18	1.61	2.4	170	0.57	16.6	0.64	0.41
SJ-464C	700	0.06	0.99	1.14	2.27	5.2	84	0.79	16.1	1.5	0.55
SJ-464C	710	0.12	8.71	0.51	16.9	9.2	26	1.52	15.6	2.23	1.19
SJ-464C	720	0.1	12.5	0.73	16.7	8.6	13	1.33	13.5	2.08	1.13
SJ-464C	740	0.12	8.41	1.72	20.8	6.8	37	1.54	18.5	1.76	1.72
SJ-464C	750	0.05	3.24	28.7	11	3.2	188	1.65	97.1	1.03	2.34
SJ-464C	760	0.08	1.39	42.1	11.95	3.4	203	2.76	153	1.18	3.4
SJ-464C	770	0.09	3.09	26.3	15.85	5.1	166	2.86	120	1.54	3.26
SJ-464C	780	0.07	3.79	24.3	13.95	3.4	160	2.37	119.5	1.01	2.87
SJ-464C	790	0.08	6.63	26.9	21.6	3.8	152	3.15	115	1.21	3.93
SJ-464C	800	0.08	7.8	13.8	24.5	4.2	154	3.16	94.4	1.44	3.8
SJ-464C	810	0.09	6.64	4.43	23.3	4.7	144	2.69	61.4	1.72	3.88
SJ-464C	820	0.08	8.75	3.27	28	4.2	124	2.66	49.2	1.5	3.87
SJ-464C	830	0.07	11.05	1.81	28.3	3.9	96	2.11	36.9	1.22	2.69
SJ-464C	840	0.07	11.65	0.91	23	4.1	83	1.6	38.1	1.24	2.49
SJ-464C	850	0.08	11.2	0.67	18.55	4.3	78	1.44	37.2	1.33	2.36
SJ-464C	860	0.07	11.8	0.45	20.6	4.3	53	1.21	26.6	1.27	2.05
SJ-464C	870	0.1	10.15	0.42	17.9	5.2	39	0.97	27.7	1.53	1.58
SJ-464C	880	0.12	9.56	0.34	18.35	7	30	0.85	26.2	1.77	1.4

SAMPLE	Depth (ft)	Bi ppm	Ca ppm	Cd ppm	Ce ppm	Co ppm	Cr ppm	Cs ppm	Cu ppm	Fe ppm	Ga ppm
SJ-464C	900	0.13	8.41	0.56	23.2	7	44	0.99	43	1.93	1.43
SJ-464C	920	0.16	9.25	0.18	16.25	8	28	0.86	25.3	1.94	1.11
SJ-464C	940	0.13	14.3	0.08	14.45	6.6	15	0.9	12.1	1.7	0.86
SJ-464C	960	0.16	15	0.07	18.75	7.7	16	1.32	13.9	1.96	1.17
SJ-464C	980	0.13	16.75	0.06	20.7	6.4	12	1.46	10	1.58	0.89
SJ-464C	1000	0.15	14.8	0.08	24.4	7.3	21	1.62	12.5	1.67	1.02
SJ-464C	1020	0.06	22.5	0.08	23.2	3	13	0.71	5	0.85	0.79
SJ-464C	1040	0.07	19.7	0.11	23.6	3.5	16	0.78	5.2	0.96	1.03
SJ-464C	1060	0.04	21.9	0.05	19.7	1.9	13	0.39	2.9	0.58	0.61
SJ-464C	1080	0.07	21.7	0.06	24.1	3.8	12	0.83	4.9	0.98	0.78
SJ-464C	1100	0.12	17.85	0.06	24.1	6	11	1.16	8.5	1.3	0.91
SJ-464C	1120	0.06	15.2	5.88	14.95	3.9	14	0.84	38.5	0.98	0.95
SJ-464C	1140	0.05	10.35	3.89	9.44	3.7	42	0.92	45.3	0.95	0.92
SJ-464C	1215	0.07	8.38	2.6	7.24	6.2	42	0.51	24.2	1.62	1.39
SJ-464C	1220	0.05	9.66	0.88	12.05	4.6	56	0.39	16.8	1.05	0.89
SJ-464C	1225	0.05	9.38	0.71	10.4	4.2	44	0.34	15.1	0.99	0.83
SJ-464C	1230	0.05	9.71	0.71	9.51	4.5	42	0.36	17.1	1.03	1.01
SJ-464C	1235	0.04	7.76	1.37	17.55	3.4	53	0.56	17.8	0.94	0.92
SJ-464C	1240	0.06	10.6	0.2	23	4.3	30	0.36	15.4	1.11	1.1
SJ-464C	1245	0.05	8.14	0.57	17.85	3.9	60	0.5	21	1.15	0.97
SJ-464C	1250	0.04	7.33	0.87	10.8	3.5	64	0.38	15.3	0.92	0.86
SJ-464C	1255	0.06	8.54	1.27	17.85	4.9	39	0.52	19.4	1.15	1.12
SJ-464C	1260	0.06	9.32	0.48	14.05	4.9	18	0.44	14	1.15	1.06
SJ-464C	1265	0.07	8.83	0.42	15.35	5.4	26	0.44	17.3	1.27	1.21
SJ-464C	1270	0.06	11.85	0.17	16.4	5.1	16	0.35	11.2	1.03	0.94
SJ-464C	1275	0.07	9.99	0.16	16.75	5.3	14	0.41	12.1	1.16	1.08
SJ-464C	1280	0.07	9.89	0.08	14.9	5.2	14	0.48	9.7	1.03	0.89
SJ-464C	1285	0.08	9.51	0.05	22.6	6.1	14	0.54	12.4	1.27	1.24
SJ-464C	1290	0.06	8.08	0.18	21.7	4.7	24	0.62	11.9	1.18	1.11
SJ-464C	1295	0.07	9.9	0.08	19.1	5.3	27	0.53	11.3	1.13	1.17
SJ-464C	1300	0.06	9.06	0.27	18.75	4.8	27	0.52	13.9	1.12	1.18
SJ-464C	1305	0.07	9.94	0.06	20	5.8	20	0.67	13.3	1.2	1.22
SJ-464C	1310	0.07	6.33	0.58	12.55	4.8	72	0.56	23.4	1.12	1.12
SJ-464C	1315	0.07	8.32	0.19	18.1	5	39	0.79	12.5	1.15	1.26
SJ-464C	1320	0.08	9.59	0.16	14.75	5.9	34	1.34	16.2	1.43	1.47
SJ-464C	1325	0.07	10	0.2	15.15	5.3	28	1.17	15.7	1.28	1.56
SJ-464C	1330	0.07	10.3	0.18	14.3	5.7	15	1.16	15.6	1.14	1.36
SJ-464C	1335	0.08	10.4	0.17	12.55	6.2	13	1.37	18	1.36	1.56
SJ-464C	1340	0.05	10.35	0.28	10.9	3.7	42	0.99	11.5	0.83	1.13
SJ-464C	1345	0.05	9.39	0.34	12.15	4.2	26	1.04	11.1	0.96	0.97
SJ-464C	1350	0.04	6.89	0.85	16.5	2.8	52	0.79	9.9	0.7	0.77
SJ-464C	1355	0.05	7.64	0.23	22.2	3.6	53	1.09	13.2	0.85	1.13
SJ-464C	1360	0.06	9	0.25	15.7	4.3	49	1.03	12.1	0.96	1.01
SJ-464C	1365	0.08	10.25	0.2	22.7	5.2	15	1.25	14	1.03	1.87
SJ-464C	1370	0.06	10.6	0.13	26.7	3.9	26	0.88	14.2	0.77	1.38
SJ-464C	1375	0.07	12.55	0.4	22	4.8	19	0.73	17.3	0.9	1.47
SJ-464C	1380	0.07	10.2	0.34	25.7	5.1	27	0.8	16.6	1.17	1.4
SJ-464C	1385	0.09	9.62	0.34	19.7	4.8	27	0.75	18.9	1.16	1.25
SJ-464C	1390	0.03	8.52	0.2	18	3.5	61	0.55	11.6	0.71	0.76
SJ-464C	1395	0.06	9.12	0.23	36.4	4.6	70	0.82	18.3	1	1.11
SJ-464C	1400	0.07	8.32	1.45	30.4	5.6	51	0.97	31.2	1.4	1.41

SAMPLE	Depth (ft)	Bi ppm	Ca ppm	Cd ppm	Ce ppm	Co ppm	Cr ppm	Cs ppm	Cu ppm	Fe ppm	Ga ppm
SJ-464C	1405	0.03	17.1	0.9	23	2.7	43	0.65	17.7	0.7	0.91
SJ-464C	1410	0.04	9.19	0.41	22.9	3.1	46	0.54	18.3	0.74	0.93
SJ-464C	1415	0.05	8.27	0.26	14.35	3.3	45	0.62	19.1	0.83	0.96
SJ-464C	1420	0.06	9.51	1.44	14.2	3.4	44	0.62	26.2	0.84	1.09
SJ-464C	1425	0.11	7.27	0.82	14.7	2.6	64	0.73	17.5	0.9	1.13
SJ-464C	1430	0.02	21.6	0.43	5.72	1	43	0.23	6.2	0.33	0.31
SJ-464C	1435	0.05	25	0.41	3.27	0.7	25	0.09	3.5	0.12	0.15
SJ-464C	1440	0.01	25	0.53	3.49	0.7	19	0.08	2.8	0.11	0.14
SJ-464C	1445	0.01	25	0.05	3.04	0.5	5	0.07	0.9	0.06	0.08
SJ-464C	1450	0.01	25	0.22	6.34	0.8	16	0.26	1.8	0.15	0.18
SJ-464C	1455	0.02	23.9	0.17	14.25	1.5	9	0.53	3.4	0.36	0.41
SJ-464C	1460	0.01	25	0.1	9.2	0.9	4	0.25	1.7	0.18	0.21
SJ-464C	1465	0.01	25	0.13	9.31	0.9	4	0.25	1.7	0.18	0.24
WM-01C	2440	0.1	0.95	2.36	18	5.3	122	1.32	28	1.11	1.46
WM-01C	2460	0.09	0.97	4.84	12.35	5.2	145	1.01	35.2	1.15	1.14
WM-01C	2480	0.08	0.8	8.51	10.35	4.5	138	0.97	22.6	1.07	0.91
WM-01C	2500	0.08	2.41	4.04	9.5	4.2	105	0.81	23.5	1.09	0.87
WM-01C	2520	0.1	1.7	1.21	12.9	4.9	85	0.86	21.9	1.25	1.12
WM-01C	2540	0.11	8.04	3.96	11.65	5.5	66	0.89	30.2	1.21	1.15
WM-01C	2560	0.04	23.3	0.34	10.4	2.9	26	0.62	8.4	0.75	0.55
WM-01C	2580	0.06	22.7	0.1	19.7	3.2	21	0.82	5.3	0.78	0.6
WM-01C	2600	0.09	16.25	5.88	16.7	5.5	17	0.86	37.8	1.37	0.7
WM-01C	2620	0.06	18.75	4.15	13.4	4.9	16	0.55	39.4	0.91	0.73
WM-01C	2640	0.09	12.3	0.36	13.5	6.7	28	0.84	18.6	1.45	0.96
WM-01C	2660	0.07	12.7	0.19	13.05	5.5	31	0.59	17.1	1.28	0.93
WM-01C	2680	0.08	10.05	0.25	15.6	5.9	20	0.77	15.9	1.2	1.16
WM-01C	2700	0.07	13.15	0.25	16.7	6.1	30	0.83	19	1.22	1.67
WM-01C	2720	0.09	13.1	0.27	16.9	6.4	27	0.62	19.5	1.32	1.32
WM-01C	2740	0.11	11	0.13	17	7.5	20	0.75	17.1	1.53	1.63
WM-01C	2760	0.1	11	0.19	17.2	8.2	32	0.76	20.2	1.81	1.61
WM-01C	2780	0.11	10.95	0.39	15.85	8.2	25	0.73	20.1	1.79	1.51
WM-01C	2800	0.09	8.43	0.21	17.1	7.6	23	0.74	18.5	1.51	1.5
WM-01C	2820	0.07	8.01	0.21	18.05	5.9	32	0.61	14.9	1.27	1.36
WM-01C	2840	0.12	8.2	0.44	20.1	6.7	22	0.57	18	1.15	1.26
WM-01C	2860	0.11	8.69	0.28	19.7	6.2	24	0.71	19.6	0.98	1.39
WM-01C	2880	0.08	7.04	0.8	19.35	5.6	56	0.99	30.3	1.1	1.46
WM-01C	2900	0.07	7.35	0.89	35.8	5.1	47	1.11	27.7	1.2	1.88
WM-01C	2920	0.07	6.58	0.59	19.2	3.8	33	0.67	15.3	0.99	0.95
WM-01C	2940	0.05	11.55	0.42	16.5	3.9	31	0.76	11.3	0.97	0.79
WM-01C	2960	0.06	12.15	0.32	16.95	4.3	26	0.57	11.5	0.95	0.8
WM-01C	2980	0.06	10.1	0.32	16	4.8	32	0.5	13.8	0.93	1.2
WM-01C	3000	0.06	11.95	0.32	17.45	4.3	19	0.44	11.5	0.82	1.1
WM-01C	3020	0.07	10.35	0.79	16.15	4.7	16	0.42	10.2	0.89	1.18
WM-01C	3040	0.08	13.75	1.23	16.15	5.1	39	0.4	9.3	0.95	1.05
WM-01C	3050	0.06	16.8	1.29	21.1	4.3	18	0.59	14.8	0.89	1.44

SAMPLE	Depth (ft)	Ge ppm	Hf ppm	Hg ppm	In ppm	K ppm	La ppm	Li ppm	Mg ppm	Mn ppm	Mo ppm
BZ-965C	880	0.025	0.11	2.81	0.018	0.13	6.2	2.1	4.54	380	24.4
BZ-965C	885	0.025	0.12	1.42	0.012	0.16	5.6	2.7	5.38	330	22
BZ-965C	905	0.025	0.07	1.7	0.016	0.09	7.2	1.2	3.45	338	13.25
BZ-965C	910	0.025	0.1	1.5	0.022	0.14	5.7	1.6	4.94	438	8.96
BZ-965C	955	0.025	0.08	1.89	0.023	0.17	3.9	2.3	6.28	725	24.1
BZ-965C	960	0.05	0.09	3.03	0.021	0.16	3.7	2.6	5.71	515	61
BZ-965C	965	0.17	0.12	8.14	0.018	0.21	3.9	2.1	2.86	389	120.5
BZ-965C	970	0.13	0.1	5.96	0.017	0.16	3.8	1.7	4.31	464	100.5
BZ-965C	975	0.14	0.13	6.39	0.022	0.21	7	3.4	4.23	389	73.7
BZ-965C	980	0.13	0.09	4.95	0.014	0.15	6	2.4	6.56	370	84.8
BZ-965C	1000	0.13	0.14	1.34	0.02	0.23	15.6	4.4	5.69	430	14.8
BZ-965C	1020	0.09	0.08	0.81	0.023	0.19	13.2	3.7	6.76	422	3.71
BZ-965C	1040	0.06	0.08	0.6	0.034	0.09	8	3.5	6.41	739	2.17
BZ-965C	1060	0.05	0.07	0.61	0.031	0.13	6.3	3.7	6.06	434	2.36
BZ-965C	1065	0.025	0.06	0.74	0.047	0.1	8.2	4.3	7.18	402	5.43
BZ-965C	1070	0.05	0.09	0.71	0.026	0.11	10.6	5.5	6.12	380	4.83
BZ-965C	1075	0.025	0.07	0.58	0.022	0.09	9.6	4.1	7.34	395	2.94
BZ-965C	1080	0.06	0.09	1.01	0.046	0.15	13.9	4.8	4.93	304	3.68
BZ-965C	1085	0.025	0.06	0.63	0.024	0.11	6.5	3.7	6.57	359	2.87
BZ-965C	1090	0.025	0.07	1.76	0.022	0.1	10.4	4.9	6.88	385	21.1
BZ-965C	1095	0.05	0.08	2.08	0.027	0.1	12.5	4.1	6.62	333	27.9
BZ-965C	1100	0.05	0.05	1.66	0.032	0.15	5.5	4	6.34	280	2.57
BZ-965C	1105	0.05	0.05	2.91	0.036	0.2	5.3	4	5.35	189	3.78
BZ-965C	1110	0.08	0.05	4.21	0.013	0.2	5.9	4	6.08	211	2.49
BZ-965C	1115	0.05	0.04	2.46	0.031	0.18	8.1	3.5	7.32	325	1.22
BZ-965C	1120	0.025	0.04	2.45	0.025	0.18	9.3	3.3	7.21	316	2.47
BZ-965C	1125	0.025	0.04	2.54	0.085	0.12	9.1	1.5	7	354	6.8
BZ-965C	1130	0.025	0.04	2.6	0.025	0.15	5.8	2.9	6.6	383	5.91
BZ-965C	1135	0.05	0.04	2.4	0.048	0.14	5.5	3.4	6.48	335	2.09
BZ-965C	1140	0.025	0.03	1.28	0.021	0.1	8.2	5.9	6.3	734	1.84
BZ-965C	1145	0.025	0.03	0.93	0.016	0.07	10.9	5.1	3.89	533	1.14
BZ-965C	1150	0.025	0.03	0.4	0.015	0.04	15.7	2.6	3.45	303	0.6
BZ-965C	1155	0.025	0.03	0.32	0.019	0.07	16	1.5	3.36	213	0.5
BZ-965C	1160	0.025	0.03	0.19	0.012	0.04	17.2	1.5	2.98	165	0.52
BZ-965C	1165	0.025	0.04	0.61	0.018	0.05	17	2	3.68	331	0.66
BZ-965C	1170	0.025	0.03	0.37	0.019	0.06	18.2	2	3.3	208	0.45
BZ-965C	1175	0.05	0.03	0.41	0.015	0.08	16.2	3.1	3.29	283	0.63
BZ-965C	1180	0.05	0.03	0.25	0.01	0.05	16.3	2.2	2.2	246	0.41
BZ-965C	1185	0.025	0.03	0.23	0.008	0.03	16.1	1.9	2.2	228	0.45
BZ-965C	1190	0.025	0.03	0.47	0.015	0.08	16	2.5	3.23	537	1.07
BZ-965C	1195	0.06	0.04	0.55	0.012	0.08	12.4	1.8	2.66	666	1.96
BZ-965C	1200	0.025	0.03	0.63	0.013	0.07	12.3	1.7	2.99	729	0.73
BZ-965C	1205	0.05	0.03	0.84	0.013	0.09	11.6	2.3	3.66	845	2.17
BZ-965C	1215	0.05	0.04	1.97	0.018	0.11	12	4.8	5.35	1260	1.17
BZ-965C	1220	0.05	0.04	1.46	0.015	0.06	13.6	5.1	5.29	1710	0.72
BZ-965C	1225	0.05	0.04	0.84	0.02	0.09	16.5	6	4.46	709	0.56
BZ-965C	1230	0.05	0.03	0.5	0.017	0.08	13.7	4.1	4.02	375	0.39
BZ-965C	1235	0.05	0.04	0.32	0.017	0.12	16.8	3.6	3.85	276	0.34
BZ-965C	1240	0.05	0.03	0.24	0.016	0.14	16.5	2.8	3.73	179	0.38
BZ-965C	1245	0.06	0.03	0.21	0.015	0.13	18.1	2.3	3.18	173	0.37
BZ-965C	1250	0.05	0.03	0.26	0.018	0.15	19.9	2.8	2.7	158	0.56

SAMPLE	Depth (ft)	Ge ppm	Hf ppm	Hg ppm	In ppm	K ppm	La ppm	Li ppm	Mg ppm	Mn ppm	Mo ppm
BZ-965C	1255	0.06	0.03	1.22	0.02	0.15	16.4	1.2	7.03	958	1.06
BZ-965C	1260	0.07	0.03	1.29	0.022	0.19	20.2	1.2	7.56	458	1.41
BZ-965C	1265	0.07	0.04	1.5	0.028	0.2	12.1	1.1	7.08	208	2.72
BZ-965C	1270	0.06	0.06	1.27	0.023	0.18	9.7	1.9	7.41	235	21.5
BZ-965C	1275	0.05	0.06	1.97	0.019	0.12	5.5	2	7.36	263	50.8
BZ-965C	1280	0.05	0.06	2.09	0.017	0.12	5.4	1.8	6.84	249	53.6
BZ-965C	1285	0.06	0.06	2.01	0.013	0.13	6.2	2.1	7.55	253	56.2
BZ-965C	1290	0.05	0.06	1.72	0.013	0.1	6.2	1.4	6.92	309	64.2
BZ-965C	1295	0.06	0.07	1.87	0.015	0.11	6.9	1.3	6.68	268	81.3
BZ-965C	1300	0.06	0.07	1.5	0.035	0.11	7.7	1.7	7.71	319	60.5
BZ-965C	1305	0.025	0.06	1.31	0.014	0.09	6.8	1.5	7.21	349	72.4
BZ-965C	1310	0.025	0.06	0.75	0.015	0.08	8.1	1.6	7.59	357	66.1
BZ-965C	1315	0.05	0.06	0.63	0.02	0.12	9.1	4.1	5.48	467	40.7
BZ-965C	1320	0.05	0.06	0.56	0.013	0.1	9.4	1.8	5.41	323	30.1
BZ-965C	1325	0.06	0.08	1.28	0.03	0.16	9.9	5.8	3.6	426	22.9
CD-14	530	0.09	0.38	2.09	0.029	0.16	17.4	2.3	1.99	192	1.21
CD-14	550	0.06	0.13	1.45	0.024	0.17	16.2	1.5	2.17	238	0.44
CD-14	560	0.07	0.13	1.2	0.015	0.1	15.7	1.6	1.05	438	0.41
CD-14	570	0.07	0.11	2.23	0.029	0.2	15.9	1.6	2.76	133	0.45
CD-14	580	0.09	0.08	3.74	0.021	0.18	12.4	1.3	3.64	231	1.01
CD-14	590	0.07	0.09	2.83	0.022	0.17	11.4	1.6	4.88	236	0.57
CD-14	600	0.06	0.08	1.24	0.013	0.12	13.1	1.1	2.87	232	1.7
CD-14	610	0.08	0.22	0.53	0.013	0.18	21.9	2	4.68	167	3.15
CD-14	620	0.06	0.15	0.6	0.014	0.11	7.3	2	5.15	131	20.9
CD-14	630	0.08	0.14	0.5	0.013	0.11	8	2	4.21	136	17.4
CD-14	640	0.05	0.13	0.24	0.013	0.1	9	1.9	5.03	144	21.1
CD-14	650	0.06	0.13	0.49	0.013	0.1	10.9	1.6	4.31	127	19.8
CD-14	660	0.05	0.13	0.52	0.011	0.12	9.4	1.8	5.18	123	38.3
CD-14	670	0.06	0.24	1.87	0.029	0.12	12.5	1.9	4.23	165	17.8
CD-14	680	0.05	0.06	0.68	0.014	0.11	12.4	1.6	2.99	164	1.76
CD-14	690	0.05	0.1	0.79	0.016	0.12	15.1	1.8	3.02	176	1.74
CD-14	700	0.05	0.08	3.2	0.019	0.11	11.2	1.8	3.51	148	1.84
CD-14	720	0.05	0.1	2.26	0.011	0.11	10.4	2.4	4.04	137	4.22
CD-14	740	<0.05	0.1	2.36	0.013	0.08	5.5	2.3	4.03	178	24.8
CD-14	770	0.07	0.1	1.59	0.013	0.09	7.5	2.3	4.7	124	20.4
CD-14	780	0.07	0.08	2.97	0.01	0.07	6.4	1.9	4.46	96	23.4
CD-14	790	<0.05	0.07	1.8	0.012	0.08	6.8	2.3	3.95	109	31
CD-14	800	0.05	0.08	1.08	0.008	0.08	7.1	2.6	4.97	131	21.1
CD-14	820	0.06	0.09	2.81	0.013	0.11	8.2	2.9	5.06	116	48.4
CD-14	840	<0.05	0.09	1.46	0.017	0.17	7.8	2.8	4.44	137	20.8
CD-14	860	<0.05	0.07	0.83	0.015	0.18	12.4	3.1	2.97	119	9.08
CD-14	880	<0.05	0.08	0.92	0.014	0.21	12.1	3.2	3.35	139	6.4
CD-14	900	0.05	0.07	1.38	0.016	0.2	14.5	3.4	3.52	129	4.82
CD-14	920	<0.05	0.07	0.78	0.017	0.22	12	3.4	4.35	169	3.66
CD-14	940	<0.05	0.07	0.35	0.013	0.22	9.3	3.3	4.11	194	2.93
CD-14	960	<0.05	0.09	1.6	0.014	0.24	9.3	4.1	3.45	143	7.91
CD-14	980	0.05	0.07	1.25	0.016	0.2	10.5	2.9	3.76	145	26.5
CD-14	1000	<0.05	0.07	0.96	0.018	0.16	11.4	2.5	3.18	187	3.34
CD-14	1020	<0.05	0.06	0.88	0.015	0.18	11	3.7	3.2	194	2.05
CD-14	1040	<0.05	0.07	1.03	0.014	0.16	12.2	3.9	3.7	188	2.79
CD-14	1060	<0.05	0.08	0.4	0.015	0.22	10.3	4.4	4.51	200	3.07

SAMPLE	Depth (ft)	Ge ppm	Hf ppm	Hg ppm	In ppm	K ppm	La ppm	Li ppm	Mg ppm	Mn ppm	Mo ppm
CD-14	1080	<0.05	0.08	0.43	0.013	0.17	10	3.3	3.76	150	4.46
CD-14	1100	<0.05	0.08	1.09	0.011	0.18	9.9	3.6	3.3	142	3.59
CD-14	1120	<0.05	0.06	0.12	0.012	0.14	11.5	4.7	3.19	149	2.8
CD-14	1140	<0.05	0.08	0.32	0.015	0.2	9.7	3.5	3.74	163	4.37
CD-14	1160	<0.05	0.09	0.17	0.013	0.19	10.7	3.2	4.58	117	7.56
CD-14	1180	0.05	0.07	0.09	0.013	0.15	14.2	3.9	3.47	118	5.54
CD-14	1200	<0.05	0.08	0.54	0.015	0.15	9.6	2.6	4.41	113	12.8
CD-14	1220	0.05	0.09	1.01	0.015	0.16	7	3.1	4.38	114	14.65
CD-14	1240	<0.05	0.07	0.72	0.011	0.13	5.5	2.5	4.55	116	11.8
CD-14	1260	0.05	0.09	0.86	0.015	0.21	7.5	4.2	3.97	132	12.3
CD-14	1280	<0.05	0.06	0.33	0.014	0.17	11.5	4.8	2.9	140	4.67
CD-14	1300	0.05	0.07	0.32	0.015	0.21	11	8.5	4.13	184	4.96
CD-14	1320	0.05	0.08	0.11	0.013	0.2	10.1	6.2	3.46	139	10.25
CD-14	1340	0.05	0.09	0.5	0.019	0.2	10.4	4.8	3.55	157	12.7
CD-14	1360	<0.05	0.1	0.09	0.015	0.2	9	5.6	4.4	162	8.24
CD-14	1380	0.05	0.08	1.97	0.014	0.19	7.1	3.2	3.8	171	9.5
CD-14	1400	0.1	0.26	3.56	0.03	0.39	34.7	14.9	2.83	330	5
CD-14	1420	0.06	0.1	1.05	0.016	0.2	11.2	3.8	4.21	160	7.7
CD-14	1440	0.06	0.21	0.24	0.018	0.28	13.3	7.9	4.35	189	11.5
CD-14	1460	<0.05	0.06	0.18	0.014	0.16	9.5	7	4.25	154	5.78
CD-14	1480	0.13	0.75	0.44	0.028	0.74	38.7	24.5	4.47	433	4.6
CD-14	1500	0.16	0.73	0.1	0.032	0.72	43.1	34	4.55	418	4.78
CD-14	1520	0.07	0.11	0.25	0.017	0.15	21.7	10.3	3.52	214	5.37
CD-14	1540	<0.05	0.09	0.12	0.01	0.14	10.5	4.3	3.91	115	7.2
CD-14	1560	0.06	0.09	0.13	0.014	0.15	10	5.5	4.22	143	7.36
CD-14	1580	0.05	0.12	0.11	0.014	0.17	11.3	5.9	3.38	143	6.54
CD-14	1600	0.05	0.12	0.04	0.016	0.2	14	7.6	3.98	176	4.54
CD-14	1620	0.05	0.09	0.11	0.014	0.16	10.6	3.6	4.64	130	8.99
CD-14	1640	0.05	0.09	0.17	0.012	0.15	10.2	2.7	4.48	126	8.94
CD-14	1660	0.1	0.18	0.23	0.028	0.43	32.5	13.9	4.69	402	7.5
CD-14	1680	0.05	0.07	0.32	0.013	0.16	10.4	4.2	3.92	133	8
CD-14	1700	0.05	0.09	0.49	0.015	0.16	11.4	4.1	3.39	150	7.71
CD-14	1720	0.05	0.07	0.36	0.013	0.16	8.5	4.3	3.34	158	5.61
CD-14	1740	0.05	0.07	0.28	0.014	0.15	10.7	3	2.85	158	3.69
CD-14	1760	0.05	0.08	0.37	0.017	0.18	8.8	3.3	3.47	171	5.92
CD-14	1780	<0.05	0.1	0.36	0.016	0.18	8	3	4.26	151	10.6
CD-14	1800	<0.05	0.08	0.31	0.013	0.16	6.5	2.5	3.28	133	8.54
CD-14	1820	0.07	0.26	0.31	0.026	0.2	15.2	8.2	3.4	349	5.54
CD-14	1840	0.05	0.09	0.37	0.017	0.17	9.1	3.2	3.93	190	6.64
CD-14	1860	0.08	0.31	0.88	0.027	0.27	18.9	8.4	2.78	350	5.78
CD-14	1880	0.05	0.09	0.31	0.015	0.14	11.3	3	4.71	152	9.76
CD-14	1900	0.05	0.09	0.82	0.013	0.16	9.4	2.9	4.18	151	10.05
CD-14	1920	<0.05	0.09	0.35	0.013	0.15	8.2	2.4	3.93	201	8.31
CD-14	1940	<0.05	0.06	0.55	0.012	0.14	9.1	2.8	3.01	166	4.33
CD-14	1960	0.05	0.1	0.27	0.012	0.17	9.7	5.3	3.98	127	8.87
CD-14	1980	0.05	0.08	0.14	0.013	0.17	10.8	9.9	2.93	153	4.73
CD-14	2000	<0.05	0.09	0.13	0.014	0.16	10.2	6.6	4.04	165	6.99
CD-14	2020	<0.05	0.08	0.37	0.013	0.19	9.4	4.8	3.45	178	7
CD-14	2040	<0.05	0.06	0.1	0.011	0.17	10.2	3.7	4.03	151	6.67
CD-14	2060	<0.05	0.07	0.7	0.019	0.15	9.8	2.8	3.25	139	7.51
CD-14	2080	0.05	0.09	0.82	0.016	0.19	10.7	2.6	4.54	200	10.6

SAMPLE	Depth (ft)	Ge ppm	Hf ppm	Hg ppm	In ppm	K ppm	La ppm	Li ppm	Mg ppm	Mn ppm	Mo ppm
CD-14	2100	0.08	0.34	1.33	0.035	0.16	24.9	5	2.23	552	3.28
CD-14	2120	<0.05	0.08	0.83	0.01	0.16	10	2.2	3.55	272	7.68
CD-14	2140	<0.05	0.1	0.31	0.016	0.23	9.3	3.7	3.96	140	8.73
CD-14	2160	0.05	0.09	0.41	0.011	0.23	11	4	4.43	131	7.17
CD-15C	1380	0.06	0.06	0.57	0.021	0.21	8.3	2.4	1.63	296	2.64
CD-15C	1400	0.11	0.14	0.67	0.029	0.25	11.8	5.2	3.48	166	6.81
CD-15C	1420	0.13	0.15	0.35	0.02	0.27	22.2	6.2	6.41	134	4.16
CD-15C	1440	0.09	0.13	1.83	0.023	0.18	14.7	3.7	5.75	143	5.76
CD-15C	1460	0.11	0.13	0.91	0.022	0.21	15.1	3.6	5.77	132	2.79
CD-15C	1480	0.11	0.14	3.9	0.025	0.22	18.9	3.9	5.45	173	4.8
CD-15C	1500	0.11	0.15	5.22	0.023	0.22	11.4	3.6	4.96	221	5.06
CD-15C	1520	0.06	0.11	0.37	0.03	0.2	10.3	2.8	4.6	267	2.95
CD-15C	1540	0.05	0.1	0.58	0.02	0.21	10.5	2.9	4.59	175	10.5
CD-15C	1560	0.06	0.12	1.71	0.029	0.21	8.3	2.4	4.93	182	11.5
CD-15C	1580	0.05	0.12	0.57	0.023	0.33	8.2	3.2	5.04	223	3.55
CD-15C	1600	0.05	0.11	0.46	0.022	0.31	12.4	3	4.96	261	3.03
CD-15C	1620	0.06	0.12	0.36	0.022	0.45	12.7	4	4.51	273	3.12
CD-15C	1660	0.06	0.1	1.68	0.023	0.24	15.4	2.7	3.87	314	8.16
CD-15C	1680	0.06	0.08	0.75	0.019	0.16	18.7	2.5	2.69	255	3.4
CD-15C	1700	0.05	0.05	0.38	0.015	0.11	14.2	1.3	2.05	200	1.84
CD-15C	1720	<0.05	0.08	1.39	0.015	0.17	7.8	2.1	4.08	232	5.92
CD-15C	1740	0.06	0.11	2.65	0.018	0.29	10.6	3.7	3.91	131	5.19
CD-15C	1760	0.05	0.09	1.82	0.018	0.21	10.1	2.5	2.15	78	4.7
CD-15C	1780	0.05	0.11	3.36	0.017	0.22	10.2	3.9	2.69	108	6.98
CD-15C	1800	<0.05	0.09	5.15	0.017	0.19	7.7	2.9	3.21	147	7.21
CD-15C	1820	<0.05	0.09	3.26	0.015	0.17	8.6	3.3	4.39	280	4.6
CD-15C	1840	<0.05	0.07	1.51	0.011	0.14	10.5	2.5	3.58	195	2.79
CD-15C	1860	<0.05	0.08	0.53	0.012	0.14	10.9	1.8	3.76	163	4.25
CD-15C	1880	0.06	0.11	0.37	0.024	0.22	18.1	4.1	3.48	287	4.31
CD-15C	1900	<0.05	0.1	1.02	0.015	0.19	8.4	2.5	4.33	143	8.51
CD-15C	1920	<0.05	0.09	0.46	0.013	0.19	9.1	3.1	5.04	134	12.25
CD-15C	1940	<0.05	0.12	0.24	0.019	0.19	7.8	3.2	4.6	107	15.85
CD-15C	2000	0.05	0.12	0.4	0.016	0.23	10.2	4.2	4.11	171	9
CD-15C	2020	<0.05	0.09	0.36	0.017	0.2	10.5	6	3.15	166	6.26
CD-15C	2040	0.05	0.12	0.15	0.018	0.27	9.5	8.3	4.9	184	7.98
CD-15C	2060	<0.05	0.08	0.2	0.016	0.14	9.2	4.2	3.65	143	8.68
CD-15C	2080	<0.05	0.08	0.12	0.015	0.17	10.8	6.4	4.13	158	6.12
CD-15C	2100	<0.05	0.11	0.18	0.014	0.18	10.9	4.8	3.67	136	7.42
CD-15C	2120	<0.05	0.1	0.25	0.018	0.2	10.5	6.6	4.45	153	7.24
CD-95-3	890	0.06	0.08	0.53	0.014	0.07	7.1	1.1	0.3	88	32.2
CD-95-3	900	0.08	0.09	0.87	0.01	0.08	6.5	1.3	0.59	129	45.4
CD-95-3	910	0.07	0.06	0.7	0.012	0.08	7.6	1.6	0.29	142	18.65
CD-95-3	920	0.05	0.05	0.93	0.011	0.05	4.7	3.7	0.45	76	39.9
CD-95-3	930	0.06	0.07	0.91	0.012	0.09	6.7	1.7	0.96	113	28.3
CD-95-3	940	0.05	0.04	0.57	0.008	0.04	4.6	1.1	0.6	70	35.5
CD-95-3	950	0.14	0.16	0.74	0.015	0.16	22.2	7.7	4.81	151	29.5
CD-95-3	960	0.08	0.11	0.54	0.019	0.15	17.5	3.9	6.9	136	5.5
CD-95-3	970	0.07	0.11	0.52	0.022	0.18	12.7	3.4	5.68	118	2.81
CD-95-3	980	0.08	0.1	0.7	0.021	0.17	13.6	3.2	6.21	139	3.72
CD-95-3	990	0.06	0.1	0.52	0.02	0.15	13.8	3.2	4.48	134	10.5
CD-95-3	1000	<0.05	0.11	0.29	0.027	0.2	8.8	3.2	4.91	145	2.14

SAMPLE	Depth (ft)	Ge ppm	Hf ppm	Hg ppm	In ppm	K ppm	La ppm	Li ppm	Mg ppm	Mn ppm	Mo ppm
CD-95-3	1010	<0.05	0.1	0.25	0.025	0.22	10.8	3.3	4.87	150	2.22
CD-95-3	1020	0.07	0.1	0.15	0.022	0.15	19.5	2.5	4.03	130	5.18
CD-95-3	1030	0.06	0.11	0.15	0.012	0.13	22.6	2.5	3.61	85	18.5
CD-95-3	1040	0.05	0.1	0.13	0.018	0.18	16.7	1.9	4.51	136	9.5
CD-95-3	1050	<0.05	0.07	0.1	0.024	0.19	11.3	2.1	4.51	168	1.44
CD-95-3	1060	0.06	0.07	0.09	0.02	0.18	15.2	1.9	4.44	197	1.16
CD-95-3	1070	0.06	0.08	0.19	0.028	0.22	12	2	5.09	186	1.56
CD-95-3	1080	0.06	0.09	0.34	0.033	0.25	16.7	2.4	5.18	283	2.51
CD-95-3	1090	0.06	0.08	0.16	0.026	0.23	13.2	1.9	4.62	211	1.94
CD-95-3	1100	<0.05	0.08	0.1	0.028	0.19	12.3	1.9	5.17	204	1.63
CD-95-3	1110	<0.05	0.08	0.07	0.029	0.23	10.1	1.7	4.65	188	1.63
CD-95-3	1120	<0.05	0.07	0.07	0.033	0.23	14.1	2	5.04	221	1.17
CD-95-3	1130	<0.05	0.07	0.12	0.022	0.17	12.5	1.3	2.98	202	1.59
CD-95-3	1140	0.06	0.07	0.05	0.026	0.17	14.4	1.5	3.67	209	1.15
CD-95-3	1150	0.05	0.09	0.09	0.031	0.22	10.2	1.5	4.18	164	1.9
CD-95-3	1160	0.05	0.06	0.07	0.018	0.14	16.5	1.4	2.93	142	0.71
CD-95-3	1170	0.05	0.06	0.1	0.018	0.13	17.6	1.7	2.67	138	1.34
CD-95-3	1180	<0.05	0.06	0.15	0.016	0.11	15.5	1.8	2.63	140	1.71
CD-95-3	1190	0.05	0.07	0.18	0.015	0.12	14.7	2	2.39	132	2.13
CD-95-3	1200	<0.05	0.05	0.1	0.016	0.1	19	2	2.28	117	0.69
CD-95-3	1210	<0.05	0.07	0.19	0.02	0.12	16.3	2	2.16	125	3.1
CD-95-3	1220	<0.05	0.05	0.2	0.017	0.11	16.9	1.9	2.37	245	2.12
CD-95-3	1230	0.05	0.06	0.18	0.015	0.09	15.9	1.8	2.34	231	2.85
CD-95-3	1240	0.05	0.05	0.2	0.015	0.1	13.3	1.6	2.91	157	1.81
CD-95-3	1250	0.05	0.06	0.15	0.022	0.14	11	2.2	5.15	153	1.12
CD-95-3	1260	<0.05	0.06	0.13	0.014	0.1	13.1	2.3	2.95	168	2.4
CD-95-3	1270	<0.05	0.08	0.17	0.018	0.11	14.4	2.1	2.3	156	2.17
CD-95-3	1280	<0.05	0.05	0.19	0.014	0.09	14.5	1.2	2.14	133	1.47
CD-95-3	1290	0.09	0.12	0.49	0.031	0.14	33.2	5.3	1.92	464	3.66
CD-95-3	1300	0.08	0.12	0.88	0.028	0.13	25.6	3.4	4.05	336	29.4
CD-95-3	1310	0.06	0.1	0.71	0.015	0.1	8.7	2	4.75	186	44.4
CD-95-3	1320	0.06	0.11	0.83	0.016	0.11	7.7	2.2	5.19	158	56.5
CD-95-3	1330	0.05	0.07	0.45	0.016	0.09	5.7	1.9	5.83	141	32.3
CD-95-3	1340	<0.05	0.09	0.49	0.014	0.1	4.3	1.5	4.7	117	49.7
CD-95-3	1350	<0.05	0.08	0.39	0.012	0.08	6.5	1.3	4.06	120	45.9
CD-95-3	1360	<0.05	0.07	0.95	0.012	0.06	7.5	1.2	4.06	146	45.7
CD-95-3	1370	<0.05	0.06	0.62	0.01	0.08	6.8	1.4	4.06	147	36.5
CD-95-3	1380	<0.05	0.07	0.39	0.011	0.07	7	1.6	4.18	149	29.5
CD-95-3	1390	<0.05	0.07	0.39	0.011	0.07	8.4	2.3	4.86	135	46.7
CD-95-3	1400	<0.05	0.08	0.53	0.01	0.05	8.2	1.6	3.5	130	49.3
CD-95-3	1410	<0.05	0.09	0.51	0.009	0.08	6.6	1.6	3.77	162	42.6
CD-95-3	1420	<0.05	0.06	0.36	0.011	0.06	9.8	1.2	2.83	212	30.6
CD-95-3	1430	<0.05	0.09	0.44	0.012	0.08	8	2.1	3.75	222	31.1
CD-95-3	1440	0.05	0.1	0.92	0.014	0.09	6.5	1.6	4.24	162	42
CD-95-3	1450	0.06	0.1	0.83	0.016	0.13	8.2	2	4.01	161	20.2
CD-95-3	1460	0.06	0.1	0.72	0.019	0.14	10.4	2.4	5.04	132	34.1
CD-95-3	1470	0.06	0.1	0.7	0.015	0.13	8.6	2	4.56	170	19.55
CD-95-3	1480	0.05	0.1	0.86	0.014	0.11	6.4	1.9	5.12	176	23
CD-95-3	1490	<0.05	0.09	0.52	0.019	0.1	6.6	1	4.87	154	22.4
CD-95-3	1500	<0.05	0.09	0.88	0.013	0.11	6.1	0.9	5.09	165	21.4
CD-95-3	1510	<0.05	0.1	1.1	0.017	0.12	6.7	0.9	4.93	171	18.85

SAMPLE	Depth (ft)	Ge ppm	Hf ppm	Hg ppm	In ppm	K ppm	La ppm	Li ppm	Mg ppm	Mn ppm	Mo ppm
CD-95-3	1520	<0.05	0.08	0.79	0.015	0.11	7.8	1.1	5.43	193	13.85
CD-95-3	1530	<0.05	0.1	0.9	0.019	0.14	7.4	1	5.39	164	17.8
CD-95-3	1540	<0.05	0.09	0.8	0.018	0.13	7.5	1.1	5.69	152	18.25
CD-95-3	1550	<0.05	0.06	0.86	0.011	0.1	6.9	0.8	3.89	262	4.66
CD-95-3	1560	<0.05	0.06	0.52	0.013	0.1	7.6	0.8	4.59	281	3.21
CD-95-3	1570	0.05	0.09	0.51	0.016	0.14	6.3	0.8	2.36	250	5.62
CD-95-3	1580	<0.05	0.06	0.49	0.013	0.12	7	0.7	3.92	237	3.65
CD-95-3	1590	0.05	0.1	0.65	0.018	0.16	8.3	1.1	3.06	302	6.37
CD-95-3	1600	<0.05	0.05	0.57	0.011	0.1	5.7	0.6	3.1	270	4.86
CD-95-3	1610	<0.05	0.05	0.46	0.011	0.11	9.7	0.8	5.22	275	3.84
CD-95-3	1620	<0.05	0.07	0.99	0.014	0.14	8.9	1	3.6	170	5.84
CD-95-3	1630	<0.05	0.08	0.5	0.02	0.17	9.2	1.1	2.53	219	8.23
CD-95-3	1640	<0.05	0.09	0.58	0.019	0.2	9	1.2	2.7	214	7.83
CD-95-3	1650	0.05	0.1	0.52	0.022	0.19	7.6	1	2.56	235	7.28
CD-95-3	1660	0.05	0.09	0.62	0.021	0.16	8.6	1	3.27	233	9.77
CD-95-3	1670	0.06	0.08	0.91	0.022	0.16	6.3	0.9	2.91	251	18.1
CD-95-3	1680	0.05	0.09	0.8	0.018	0.15	6.8	1	2.51	232	15.6
CD-95-3	1690	<0.05	0.08	0.88	0.014	0.14	9.2	1.1	3.61	169	16.35
CD-95-3	1700	<0.05	0.06	0.54	0.013	0.14	12	1.3	3.27	160	4.29
CD-95-3	1710	<0.05	0.06	0.87	0.015	0.14	9.8	1.2	4.33	204	8.97
CD-95-3	1720	<0.05	0.07	0.9	0.016	0.13	10.1	1.2	4.35	210	9.55
CD-95-3	1730	<0.05	0.07	0.86	0.014	0.11	5	0.7	3.92	146	6.17
CD-95-3	1740	<0.05	0.06	1.97	0.01	0.13	13.5	1	3.52	104	12.35
CD-95-3	1750	<0.05	0.08	1.17	0.012	0.16	9.6	1.1	3.38	123	10.05
CD-95-3	1760	<0.05	0.06	0.78	0.011	0.13	5.7	1	3.91	104	8.86
CD-95-3	1770	<0.05	0.05	0.69	0.007	0.08	7.2	0.7	3.13	89	6.54
CD-95-3	1780	<0.05	0.05	0.67	0.008	0.09	9.9	0.8	3.33	107	4.29
CD-95-3	1790	<0.05	0.06	0.72	0.008	0.08	8.7	0.7	3.08	107	6.61
CD-95-3	1800	<0.05	0.04	0.8	0.01	0.08	8.9	0.6	3.12	131	5.32
CD-95-3	1810	<0.05	0.05	1.92	0.01	0.1	7.8	0.9	2.97	115	6.22
CD-95-3	1820	<0.05	0.05	1.11	0.011	0.1	7.1	0.7	2.66	123	5.22
CD-95-3	1830	<0.05	0.04	0.52	0.01	0.09	8.8	0.9	3.33	92	6.45
CD-95-3	1840	<0.05	0.05	0.35	0.01	0.1	11.3	0.9	2.62	94	7.04
CD-95-3	1850	0.05	0.04	0.41	0.008	0.08	9.7	1.1	2.93	102	6.92
CD-95-3	1860	<0.05	0.04	1.62	0.009	0.07	5.7	1.3	4.49	146	9.45
CD-95-3	1870	<0.05	0.04	0.81	0.006	0.1	3	1.3	3.23	145	6.86
CD-95-3	1880	<0.05	0.04	0.86	0.009	0.07	5	1.1	2.76	128	5.08
CD-95-3	1890	<0.05	0.05	1.18	0.014	0.09	4	1.3	4.64	174	7.32
CD-95-3	1900	<0.05	0.04	1.03	0.011	0.1	7.6	1.2	3.38	166	5.52
CD-95-3	1910	<0.05	0.03	0.46	0.008	0.08	10.1	1	2.8	156	2.6
CD-95-3	1920	<0.05	0.04	0.74	0.012	0.09	6.9	1.3	3.2	164	4.09
CD-95-3	1930	0.05	0.05	1.25	0.017	0.16	9.2	1.5	3.4	259	5
CD-95-3	1940	0.08	0.09	2.21	0.037	0.27	12.9	2.4	2.48	575	3.27
CD-95-3	1950	0.08	0.1	2.35	0.037	0.32	13	2.8	2.68	524	4.78
CD-95-3	1960	<0.05	0.04	1.16	0.009	0.08	8	1.1	3	165	5.74
CD-95-3	1970	0.05	0.05	0.99	0.011	0.11	8.9	1.5	2.98	143	6.52
CD-95-3	1980	0.05	0.07	3.35	0.027	0.12	7.6	1.8	2.57	207	9.31
CD-95-3	1990	0.09	0.11	1.84	0.037	0.24	21.9	4.4	1.81	386	4.49
CD-95-3	2000	0.09	0.11	2.09	0.04	0.26	16.4	4	1.82	460	4.61
CD-95-3	2010	0.08	0.11	1.59	0.038	0.26	13.8	5.4	2.32	571	5.38
CD-95-3	2020	0.05	0.08	1.6	0.018	0.14	5.6	1.9	3.22	293	13.75

SAMPLE	Depth (ft)	Ge ppm	Hf ppm	Hg ppm	In ppm	K ppm	La ppm	Li ppm	Mg ppm	Mn ppm	Mo ppm
CD-95-3	2030	<0.05	0.06	0.46	0.009	0.09	7.7	1.5	5.12	198	10.05
CD-95-3	2040	<0.05	0.06	1.63	0.012	0.1	6.2	1.7	5.06	175	17
CD-95-3	2050	<0.05	0.07	0.54	0.009	0.12	6.8	2.2	5.53	113	21.2
CD-95-3	2060	<0.05	0.06	0.46	0.012	0.12	8.9	1.8	5.48	125	22.7
CD-95-3	2070	<0.05	0.06	0.39	0.01	0.11	9.4	1.9	6.21	107	19.25
CD-95-3	2080	<0.05	0.06	0.5	0.012	0.13	8.8	1.9	5.04	138	15.95
CD-95-3	2090	<0.05	0.06	0.59	0.009	0.13	8.8	1.9	4.88	137	19.45
CD-95-3	2100	<0.05	0.07	1.03	0.015	0.12	6.5	1.9	5.87	187	21.5
CD-95-3	2110	<0.05	0.04	1.13	0.016	0.1	3.9	1.2	3.34	163	7.92
CD-95-3	2120	<0.05	0.06	0.96	0.014	0.14	7.2	1.7	4.88	214	10.1
CD-95-3	2130	0.08	0.08	1.57	0.035	0.26	12.8	2	2.38	504	4.37
CD-95-3	2140	<0.05	0.04	0.48	0.01	0.11	4.3	1.8	8.43	266	3.65
CD-95-3	2150	0.05	0.05	0.5	0.012	0.12	4.6	1.9	7.46	264	5.1
CD-95-3	2160	<0.05	0.04	0.53	0.01	0.1	3.8	2	8.29	272	7.41
CD-95-3	2170	<0.05	0.13	1.33	0.02	0.09	9.6	3.5	7.19	321	5.08
CD-95-3	2180	0.06	0.16	1.12	0.023	0.17	11.9	3.8	5.36	387	3.14
CD-96-2C	770	0.07	0.15	0.73	0.027	0.18	15.4	3.7	4.5	138	4.22
CD-96-2C	780	0.06	0.25	0.79	0.034	0.17	9.8	3	4.96	175	2.18
CD-96-2C	790	0.06	0.1	1.49	0.03	0.17	6.7	2.1	5.52	191	2.49
CD-96-2C	800	0.06	0.1	1.26	0.032	0.17	10.1	2.2	5.64	197	2.35
CD-96-2C	810	0.06	0.16	1.8	0.021	0.11	13.2	2.5	5.86	344	5.59
CD-96-2C	820	<0.05	0.07	1.73	0.023	0.14	13.7	2.8	4.76	333	2.11
CD-96-2C	830	<0.05	0.13	1.01	0.028	0.18	9.5	2.5	5.04	329	1.8
CD-96-2C	840	<0.05	0.06	0.47	0.022	0.14	12.7	2.3	4.37	279	1.24
CD-96-2C	850	<0.05	0.07	0.3	0.016	0.12	13.1	1.9	3.09	388	1.19
CD-96-2C	860	<0.05	0.06	0.4	0.022	0.16	10.4	1.9	3.98	376	0.92
CD-96-2C	870	<0.05	0.07	0.54	0.026	0.19	9	2	4.75	377	1.09
CD-96-2C	880	<0.05	0.07	0.47	0.025	0.18	9.1	2.3	4.56	315	1.07
CD-96-2C	890	<0.05	0.08	0.81	0.025	0.18	10.1	3.1	5.38	311	3.05
CD-96-2C	900	<0.05	0.07	0.66	0.022	0.17	8.1	2.2	5.26	267	1.72
CD-96-2C	910	<0.05	0.16	0.53	0.023	0.18	10	2.9	5.22	229	3.78
CD-96-2C	920	<0.05	0.11	0.59	0.03	0.2	6.1	2.2	5.52	187	1.86
CD-96-2C	930	<0.05	0.12	0.44	0.024	0.17	11.7	2.8	5.86	186	2.04
CD-96-2C	940	<0.05	0.1	1.25	0.026	0.21	10.9	3	5.57	183	1.9
CD-96-2C	950	<0.05	0.26	1.16	0.026	0.19	15.2	4.5	5.89	174	2.46
CD-96-2C	960	<0.05	0.12	1.59	0.025	0.19	18.5	4.3	7.18	153	3.12
CD-96-2C	970	<0.05	0.12	1.09	0.022	0.15	13.6	3.3	6.02	164	3.71
CD-96-2C	980	<0.05	0.46	1.01	0.021	0.15	18.3	6.6	2.9	177	7.38
CD-96-2C	990	0.08	0.39	1.71	0.027	0.14	13.5	2.9	5.36	182	3.13
CD-96-2C	1000	0.08	0.09	1.74	0.027	0.16	10.2	1.8	5.08	203	2.09
CD-96-2C	1010	0.07	0.1	0.91	0.028	0.17	8.5	1.9	4.93	220	2
CD-96-2C	1020	0.06	0.09	0.64	0.029	0.17	5.5	1.8	5.59	194	1.99
CD-96-2C	1030	0.09	0.16	1.52	0.028	0.22	16.1	3.3	4.79	211	3.03
CD-96-2C	1040	0.09	0.12	1.57	0.023	0.19	13.9	2.7	5.45	211	3.42
CD-96-2C	1050	0.1	0.09	0.97	0.026	0.18	25.2	6	3.37	267	7.31
CD-96-2C	1060	0.06	0.08	0.52	0.02	0.15	12.4	1.3	3.88	253	2.94
CD-96-2C	1070	0.06	0.11	0.23	0.028	0.17	9.4	1.4	4.86	211	1.28
CD-96-2C	1080	0.05	0.07	0.39	0.024	0.16	7.2	1.2	4.91	219	1.22
CD-96-2C	1090	0.05	0.08	0.39	0.03	0.19	6.5	1.3	5.28	215	1.44
CD-96-2C	1100	0.07	0.06	0.21	0.024	0.16	9.6	1.3	4.66	230	0.56
CD-96-2C	1110	0.06	0.06	0.21	0.022	0.13	10.1	1.3	4.44	229	0.73

SAMPLE	Depth (ft)	Ge ppm	Hf ppm	Hg ppm	In ppm	K ppm	La ppm	Li ppm	Mg ppm	Mn ppm	Mo ppm
CD-96-2C	1120	0.06	0.07	0.23	0.027	0.16	8.2	1.3	4.54	219	0.98
CD-96-2C	1130	0.06	0.08	0.16	0.026	0.16	9	1.4	4.81	208	1.17
CD-96-2C	1140	0.06	0.07	0.17	0.027	0.18	8.6	1.4	4.48	206	1.26
CD-96-2C	1150	0.05	0.07	0.16	0.023	0.15	6.7	1.3	4.54	215	1.23
CD-96-2C	1160	<0.05	0.04	0.12	0.01	0.07	6.2	0.8	1.83	105	2.46
CD-96-2C	1170	<0.05	0.05	0.1	0.012	0.07	12.2	1.1	1.96	127	0.81
CD-96-2C	1180	0.05	0.09	0.13	0.015	0.09	12.5	1.3	2.21	145	1.36
CD-96-2C	1190	0.05	0.07	0.12	0.016	0.11	13.2	1.4	3.09	139	1.11
CD-96-2C	1200	0.06	0.07	0.16	0.019	0.13	12.4	1.5	4.34	167	1.23
CD-96-2C	1210	0.06	0.07	0.15	0.021	0.14	11.3	1.5	3.63	200	1.06
CD-96-2C	1220	0.05	0.07	0.43	0.012	0.08	7.9	1.8	3.55	136	32.4
CD-96-2C	1230	0.06	0.12	0.72	0.013	0.09	7.5	2.4	4.7	160	28.7
CD-96-2C	1240	0.06	0.12	0.9	0.014	0.09	6.9	2.4	4.79	161	24.2
CD-96-2C	1250	0.06	0.07	0.76	0.01	0.07	9.2	1.6	2.76	129	11.05
CD-96-2C	1260	0.05	0.06	0.23	0.013	0.11	9.5	2.3	3.47	145	4.51
CD-96-2C	1270	0.05	0.07	0.43	0.014	0.12	8.7	2.2	3.53	157	5.5
CD-96-2C	1280	0.05	0.08	0.46	0.014	0.15	9.2	3	3.3	171	3.96
CD-96-2C	1290	<0.05	0.07	0.29	0.013	0.13	10	2.1	3.78	162	3.6
CD-96-2C	1300	<0.05	0.06	0.28	0.013	0.15	9.2	1.9	3.5	165	2.87
CD-96-2C	1310	0.05	0.07	0.42	0.014	0.16	9.6	2.6	4.15	177	3.28
CD-96-2C	1320	0.05	0.06	0.38	0.013	0.14	8.6	2.3	3.77	166	3.27
CD-96-2C	1330	<0.05	0.07	0.24	0.013	0.13	10.3	2.3	4.13	164	3.36
CD-96-2C	1340	0.05	0.07	0.23	0.013	0.14	10.7	2.5	4.92	181	3.03
CD-96-2C	1350	<0.05	0.02	0.14	0.01	0.13	9.7	2.1	3.83	157	2.4
CD-96-2C	1360	<0.05	0.05	0.23	0.015	0.17	9.8	2.4	4.55	166	5.17
CD-96-2C	1370	<0.05	0.03	0.39	0.013	0.16	7.6	3.2	3.9	169	4.4
CD-96-2C	1380	<0.05	0.04	0.37	0.013	0.18	7.8	2.7	4.5	209	3.64
CD-96-2C	1390	0.05	0.06	0.24	0.015	0.21	9	3.2	5.16	203	3.34
CD-96-2C	1400	<0.05	0.06	0.13	0.009	0.14	7.7	1.8	4	135	5.93
CD-96-2C	1410	<0.05	0.06	0.12	0.01	0.15	9	2.7	4.3	167	4.69
CD-96-2C	1420	<0.05	0.06	0.16	0.01	0.13	7	2	4.48	133	6.23
CD-96-2C	1430	<0.05	0.05	0.15	0.01	0.13	7.2	1.9	3.84	124	5.52
CD-96-2C	1440	<0.05	0.07	1.13	0.013	0.12	7.1	2	4.8	120	8.76
CD-96-2C	1450	<0.05	0.07	1.92	0.011	0.11	4.8	1.8	3.81	102	14.75
CD-96-2C	1460	<0.05	0.06	0.52	0.01	0.11	6	1.8	3.54	88	10.3
CD-96-2C	1470	<0.05	0.07	0.39	0.011	0.15	6.9	2.2	4.03	123	8.6
CD-96-2C	1480	<0.05	0.04	0.32	0.01	0.13	8.2	2.1	3.13	159	3.22
CD-96-2C	1490	0.05	0.06	0.58	0.014	0.2	8.8	3.3	3.76	174	6.37
CD-96-2C	1500	<0.05	0.06	0.15	0.009	0.15	7.1	2	3.91	120	9.08
CD-96-2C	1510	0.05	0.07	0.19	0.012	0.19	7.8	3	3.8	175	11.75
CD-96-2C	1520	0.05	0.08	0.33	0.014	0.23	8.1	2.6	4.77	187	8.43
CD-96-2C	1530	0.05	0.1	0.3	0.011	0.17	7.4	2.1	3.49	149	7.86
CD-96-2C	1540	<0.05	0.05	0.28	0.011	0.15	8.1	1.9	2.85	151	5.24
CD-96-2C	1550	0.05	0.06	0.28	0.014	0.21	8.8	2.9	3.31	181	5.03
CD-96-2C	1560	0.05	0.06	0.45	0.016	0.24	9.4	3.6	4.59	205	6.59
CD-96-2C	1570	0.06	0.08	0.69	0.016	0.24	6.9	2.5	4.42	173	8.89
CD-96-2C	1580	0.05	0.06	0.67	0.013	0.16	6	1.8	4.49	140	12.6
CD-96-2C	1590	0.05	0.06	0.39	0.015	0.16	7.1	1.8	3.01	143	7.59
CD-96-2C	1600	<0.05	0.06	0.39	0.013	0.18	6.9	1.9	4.12	150	7.6
CD-96-2C	1610	<0.05	0.05	0.26	0.011	0.19	8.9	2.7	4.26	168	5.03
CD-96-2C	1620	<0.05	0.06	0.37	0.012	0.21	8.6	2.9	4.47	170	6.07

SAMPLE	Depth (ft)	Ge ppm	Hf ppm	Hg ppm	In ppm	K ppm	La ppm	Li ppm	Mg ppm	Mn ppm	Mo ppm
CD-96-2C	1630	0.05	0.06	0.53	0.012	0.15	9.2	1.7	3.73	159	6.37
CD-96-2C	1640	<0.05	0.07	1.24	0.009	0.16	6.9	1.7	4.18	131	7.29
CD-96-2C	1650	<0.05	0.06	0.75	0.012	0.16	6.7	1.3	3.54	148	5.59
CD-96-2C	1660	<0.05	0.06	1.45	0.011	0.16	6.6	1.7	4.22	168	7.15
CD-96-2C	1670	<0.05	0.07	1.73	0.012	0.13	7.1	1.8	4.2	127	10.7
CD-96-2C	1680	<0.05	0.06	1.41	0.01	0.14	7.7	1.5	3.51	137	6.26
CD-96-2C	1690	<0.05	0.03	0.56	0.013	0.08	5.1	0.8	2.14	175	2.51
CD-96-2C	1700	0.05	0.05	1.14	0.012	0.13	8.8	2	3.68	147	8.36
CD-96-2C	1710	<0.05	0.06	0.66	0.011	0.14	9.7	2.9	3.64	137	10.25
CD-96-2C	1720	0.06	0.06	0.57	0.015	0.18	9.7	3.6	3	147	8.56
CD-96-2C	1730	<0.05	0.06	0.84	0.011	0.13	9.3	3.1	3.52	141	10.05
CD-96-2C	1740	<0.05	0.06	0.73	0.011	0.14	9.2	3.4	3.14	143	10.1
CD-96-2C	1750	0.05	0.06	0.45	0.011	0.14	9	2.7	2.5	133	11.35
CD-96-2C	1760	<0.05	0.05	0.51	0.01	0.15	9.3	2.9	2.06	139	7.57
CD-96-2C	1770	0.05	0.06	0.44	0.016	0.18	8.7	3.3	2.57	160	8.94
CD-96-2C	1780	0.05	0.05	0.28	0.014	0.15	9.3	3	2.84	120	9.46
CD-96-2C	1790	0.06	0.08	0.91	0.015	0.14	8.8	2.2	2.61	173	13.35
CD-96-2C	1800	<0.05	0.05	1.82	0.008	0.1	7.7	2.1	3.25	103	13.3
CD-96-2C	1810	0.06	0.07	1.74	0.013	0.12	8.1	2.8	3.93	128	11.9
CD-96-2C	1820	0.05	0.06	0.97	0.01	0.11	8.7	2.7	4.02	99	7.07
CD-96-2C	1830	0.05	0.07	0.56	0.012	0.12	8.9	2.9	3.16	107	9.43
CD-96-2C	1840	0.05	0.07	0.63	0.011	0.11	8.4	2.7	3.08	106	9.09
CD-96-2C	1860	0.07	0.06	1.65	0.015	0.14	9.6	3	2.54	140	6.52
CD-96-2C	1880	0.05	0.05	1.82	0.012	0.14	6.8	2.5	2.94	105	9.27
CD-96-2C	1900	0.05	0.06	0.35	0.009	0.12	9.4	3.1	2.87	80	8.11
CD-96-2C	1920	0.05	0.06	2.09	0.01	0.1	5.8	2.1	2.82	99	10.6
CD-96-2C	1925	0.05	0.06	3.47	0.013	0.12	5.1	1.7	2.66	109	10.75
CD-96-2C	1930	0.06	0.06	0.96	0.01	0.11	12.9	2.9	3.18	246	7.42
CD-96-2C	1940	<0.05	0.06	1.46	0.012	0.13	9.4	3.1	2.92	145	7.79
CD-96-2C	1960	0.05	0.05	1.25	0.011	0.13	9.9	3.6	2.4	89	7.78
CD-96-2C	1980	<0.05	0.05	1.87	0.009	0.13	8.5	3.5	2.01	80	7.26
CD-96-2C	2000	<0.05	0.06	1.42	0.012	0.14	10.5	3.6	2.26	96	6.58
CD-96-2C	2020	0.05	0.06	1.86	0.011	0.16	9.1	4.2	2.58	86	7.14
CD-96-2C	2025	<0.05	0.05	1.4	0.009	0.09	6.8	2.1	1.94	76	8.23
CD-96-2C	2030	<0.05	0.05	0.82	0.009	0.11	8.3	2.2	3.32	112	6.74
CD-96-2C	2035	0.05	0.04	1.86	0.009	0.1	8.4	1.5	3.35	161	6.3
CD-96-2C	2040	0.07	0.04	1.11	0.019	0.28	17.1	1	1.17	360	4.75
CD-96-2C	2045	0.06	0.05	1.69	0.012	0.19	11.6	1.4	2.42	183	7.18
CD-96-2C	2050	<0.05	0.05	0.57	0.008	0.09	8.7	1.9	3.23	76	7.85
CD-96-2C	2055	<0.05	0.04	0.56	0.006	0.07	6.6	1.5	2.41	94	6.06
CD-96-2C	2060	0.07	0.05	0.91	0.02	0.28	14.5	1	1.09	318	4.22
CD-96-2C	2065	<0.05	0.05	0.55	0.009	0.12	8.3	1.6	3	93	6.85
CD-96-2C	2070	0.05	0.05	0.95	0.009	0.13	11.1	1.4	2.63	151	7.33
CD-96-2C	2075	0.07	0.04	1.75	0.016	0.25	15	0.9	2.42	349	4.88
CD-96-2C	2080	0.08	0.05	1.87	0.022	0.34	25.4	0.8	0.64	427	2.54
CD-96-2C	2100	0.06	0.07	2.78	0.008	0.16	9	2.7	6.55	185	9.37
CD-96-2C	2120	0.08	0.12	1.52	0.011	0.27	16.1	5.7	5.45	88	9.67
CD-96-2C	2180	0.06	0.08	1.38	0.008	0.1	10.9	3.8	9.34	99	12.25
CD-96-2C	2200	0.06	0.1	2.51	0.009	0.16	15.2	3.4	8.38	109	34.7
CD-96-2C	2220	0.05	0.07	3.66	0.016	0.16	14.7	2.1	6.82	223	6.52
CD-96-2C	2240	0.05	0.07	3.07	0.019	0.31	18.3	1.3	0.74	423	5.85

SAMPLE	Depth (ft)	Ge ppm	Hf ppm	Hg ppm	In ppm	K ppm	La ppm	Li ppm	Mg ppm	Mn ppm	Mo ppm
CD-96-2C	2260	<0.05	0.03	1.69	0.014	0.09	6.5	1.5	11.05	171	1.77
CD-96-2C	2280	0.06	<0.02	0.97	<0.005	0.03	3.1	2.1	12.35	130	1.19
CD-96-2C	2300	0.08	<0.02	0.66	<0.005	0.02	1.7	1.8	11.95	129	1.13
CD-96-2C	2320	0.07	<0.02	0.45	<0.005	0.02	1.5	1.6	11.8	121	0.89
CD-96-2C	2340	0.08	<0.02	0.22	<0.005	0.01	1.2	1.3	12.1	109	0.8
DR-1C	2480	0.09	0.1	0.45	0.023	0.12	19.9	2.9	4.37	344	43.1
DR-1C	2500	0.06	0.08	0.46	0.01	0.11	11.1	2.7	3.93	124	67.2
DR-1C	2520	0.05	0.09	0.45	0.01	0.09	10.8	2.7	4.24	130	59.1
DR-1C	2540	0.05	0.09	0.41	0.014	0.09	9.9	2.7	4.04	125	55.9
DR-1C	2560	0.05	0.08	0.47	0.01	0.08	10.2	2.2	3.06	99	58.2
DR-1C	2580	0.06	0.1	0.67	0.013	0.11	11.9	2.6	3.99	139	39.5
DR-1C	2600	0.05	0.12	0.59	0.018	0.16	8.4	3.1	5.01	157	34.5
DR-1C	2620	0.06	0.09	0.34	0.015	0.09	8.7	2.4	4.03	107	44
DR-1C	2640	0.05	0.09	0.24	0.011	0.1	9.5	3.8	4.03	207	46.2
DR-1C	2660	0.05	0.1	0.33	0.012	0.12	8	2.9	3.94	304	37
DR-1C	2680	0.05	0.13	0.36	0.011	0.14	9.6	3.3	4.09	159	37
DR-1C	2700	0.05	0.16	0.39	0.023	0.19	8.3	4.9	5.29	158	41.3
DR-1C	2720	0.05	0.15	1.23	0.017	0.22	7.3	4.6	6	186	13.2
DR-1C	2740	<0.05	0.11	0.53	0.016	0.2	8.9	4.4	4.9	152	11.15
DR-1C	2760	0.05	0.1	0.15	0.013	0.17	11.5	3.4	3.61	134	2.9
DR-1C	2780	0.06	0.08	0.09	0.013	0.17	14.2	3.9	4.57	189	1.79
DR-1C	2800	<0.05	0.1	0.08	0.013	0.21	9.3	4.4	4.66	162	1.5
DR-1C	2820	<0.05	0.13	0.44	0.016	0.23	8.1	3.9	5.35	208	9.55
DR-1C	2840	<0.05	0.08	0.43	0.014	0.16	7.3	2.7	4.18	219	2.19
DR-1C	2860	0.05	0.08	0.13	0.018	0.19	11.5	6.3	4.15	184	1.86
DR-1C	2880	0.05	0.09	0.21	0.017	0.21	9.2	5.1	4.66	195	4.47
DR-1C	2900	<0.05	0.08	0.16	0.017	0.21	10	4.1	4.11	191	1.63
DR-1C	2917	0.05	0.08	0.2	0.017	0.2	8.9	4	4.54	186	4.1
GA-2A	1680	0.07	0.1	0.84	0.017	0.11	3.3	0.9	0.59	209	36.5
GA-2A	1690	0.09	0.11	0.53	0.015	0.14	4.4	1.3	0.46	422	40.6
GA-2A	1700	0.07	0.13	0.68	0.026	0.16	4.3	1.1	1.49	270	30.5
GA-2A	1710	0.06	0.13	0.51	0.029	0.23	5.3	1.3	3.86	415	34.1
GA-2A	1720	0.15	0.14	1.29	0.026	0.36	9.1	3.6	4.23	248	33.3
GA-2A	1730	0.13	0.13	0.55	0.018	0.21	11.2	4.3	4.76	453	24.8
GA-2A	1740	0.07	0.1	0.46	0.018	0.17	6	2.5	7.82	251	41.8
GA-2A	1750	0.07	0.1	0.57	0.017	0.18	6.2	2.7	7.49	413	27.5
GA-2A	1760	0.08	0.09	1.16	0.016	0.11	5.2	1.9	8.49	271	28.3
GA-2A	1770	0.08	0.12	2.22	0.017	0.15	4.7	2.4	6.43	349	33.6
GA-2A	1780	0.08	0.12	2.38	0.017	0.18	3.9	3.5	6.98	210	33
GA-2A	1790	0.08	0.15	1.23	0.018	0.2	6.4	4.2	8.16	525	31
GA-2A	1800	0.1	0.11	4.33	0.018	0.17	5.1	3.3	7.49	163	53
GA-2A	1810	0.12	0.12	8.53	0.014	0.15	6.9	3.3	3.22	488	86.2
GA-2A	1820	0.1	0.1	8.69	0.017	0.11	5.4	2.5	4.47	234	71.3
GA-2A	1830	0.12	0.12	4.52	0.022	0.2	18.4	5.1	5.17	303	12.4
GA-2A	1840	0.08	0.07	2.81	0.025	0.16	7.9	2.4	6.02	288	4.59
GA-2A	1850	0.08	0.1	4.29	0.049	0.16	4.1	1.8	1.04	556	10
GA-2A	1860	0.08	0.07	4.48	0.041	0.16	6	1.3	0.36	204	9.4
GA-2A	1870	0.07	0.06	2.4	0.033	0.14	10.3	1.1	3.61	303	6.42
GA-2A	1880	0.05	0.06	3.09	0.019	0.1	5.1	0.7	0.36	109	43.2
GA-2A	1890	0.08	0.07	1.75	0.028	0.14	14.8	1.2	3.3	238	4.8
GA-2A	1900	0.07	0.07	1.96	0.025	0.11	7.1	0.9	2.31	263	26.7

SAMPLE	Depth (ft)	Ge ppm	Hf ppm	Hg ppm	In ppm	K ppm	La ppm	Li ppm	Mg ppm	Mn ppm	Mo ppm
GA-2A	1910	0.06	0.06	1.66	0.029	0.11	8.7	0.8	2.13	379	7.28
GA-2A	1920	0.05	0.05	2.36	0.019	0.08	5	0.4	0.56	121	9.23
GA-2A	1930	0.07	0.05	2.73	0.029	0.08	7.5	0.5	0.67	249	10.15
GA-2A	1940	0.08	0.06	6.34	0.023	0.08	10.1	0.5	0.16	134	49.6
GA-2A	1950	0.09	0.07	7.7	0.021	0.1	11.3	0.9	0.21	126	36.8
GA-2A	1960	0.12	0.08	12.4	0.018	0.07	15.1	0.7	0.17	145	87
GA-2A	1970	0.07	0.1	6.03	0.017	0.08	7.3	0.6	0.23	291	39.4
GA-2A	1980	0.08	0.07	5.15	0.023	0.07	6.6	0.5	0.21	247	21.6
GA-2A	1990	0.08	0.07	4.89	0.026	0.1	8.7	0.6	0.14	223	19.6
GA-2A	2000	0.07	0.08	5.14	0.013	0.06	6.8	0.5	0.13	258	31.1
GA-2A	2010	0.09	0.06	9.52	0.014	0.04	7	0.5	0.2	173	22.8
GA-2A	2020	0.08	0.06	6.19	0.009	0.03	5.6	0.3	0.16	209	27.5
GA-2A	2030	<0.05	0.04	3.04	0.005	0.04	5.4	0.3	0.29	283	13.95
GA-2A	2040	<0.05	0.05	2.93	0.006	0.05	5.5	0.4	0.2	239	16
GA-2A	2050	<0.05	0.02	0.58	<0.005	0.05	3.6	0.4	0.3	102	3.57
GA-2A	2060	<0.05	0.02	0.25	<0.005	0.04	5.5	0.4	1.11	58	1.23
GA-2A	2070	<0.05	0.03	0.46	0.005	0.05	6	0.4	0.84	75	1.92
GA-2A	2080	0.05	0.04	1.08	0.011	0.09	7.6	0.5	0.63	83	3.89
GA-2A	2100	<0.05	0.03	0.98	0.015	0.06	7.6	0.4	1.01	71	4.14
GA-2A	2110	<0.05	0.03	0.73	0.008	0.06	6.3	0.4	0.55	69	3.49
GA-2A	2120	0.05	0.03	1.11	0.015	0.06	6.8	0.4	0.63	85	4.39
GA-35C	1680	0.06	0.07	1.98	0.027	0.17	4.4	1.8	6.4	314	13.2
GA-35C	1700	0.06	0.09	1.44	0.026	0.18	4.1	2.3	6.04	237	6.45
GA-35C	1720	0.06	0.09	0.69	0.019	0.21	6.7	1.9	6.69	276	5.93
GA-35C	1740	0.09	0.11	10.8	0.049	0.25	8	1.7	5.03	382	4.16
GA-35C	1760	0.09	0.09	2.14	0.044	0.27	7.7	1.7	6.31	523	2.33
GA-35C	1780	0.07	0.06	0.74	0.02	0.18	8.2	1.4	7.22	391	3.54
GA-35C	1800	0.07	0.09	4.03	0.016	0.11	4.2	1.3	8.15	490	48.6
GA-35C	1820	0.05	0.08	0.99	0.011	0.09	5.5	1.4	6.49	267	53.2
GA-35C	1840	0.05	0.08	2.83	0.013	0.07	5.9	1.7	3.78	117	35
GA-35C	1860	0.06	0.1	1.54	0.013	0.07	11.5	1.6	2.28	84	28.7
GA-35C	1880	0.08	0.14	8.55	0.022	0.1	14.5	3	2.15	58	33.1
GA-35C	1900	0.14	0.14	4.75	0.04	0.21	30.5	3.8	1.77	104	21
GA-35C	1920	0.11	0.11	7.39	0.042	0.24	13.3	3.8	1.69	156	8.75
GA-35C	1940	0.05	0.09	6.62	0.018	0.15	7.8	1.1	0.01	22	18.2
GA-35C	1960	0.06	0.08	6.72	0.017	0.15	10	1.3	0.03	31	30.5
GA-35C	1980	0.06	0.09	1.4	0.013	0.13	9.8	1.6	0.2	51	19.95
GA-35C	2000	0.05	0.07	1.85	0.011	0.12	8.2	1.3	0.1	22	21.2
GA-35C	2020	0.06	0.07	1.78	0.015	0.15	10.9	1.4	1.44	46	22.7
GA-35C	2040	0.05	0.06	2.16	0.013	0.12	10	1.3	1.67	79	13.2
GA-35C	2060	0.05	0.04	1.57	0.011	0.08	10.5	0.9	1.67	128	4.9
GA-35C	2080	0.16	0.15	8.97	0.059	0.34	29.3	2	2.6	403	9.32
GA-35C	2100	<0.05	0.06	2.9	0.014	0.22	10.2	1.6	2.04	104	6.34
GA-35C	2120	0.05	0.05	2.02	0.014	0.28	15.6	2.5	3.08	190	4.54
GA-35C	2140	<0.05	0.04	1.53	0.01	0.18	7.6	2.1	2.19	107	3.43
GA-35C	2160	<0.05	0.03	0.9	0.007	0.1	6.5	1.4	1.7	88	2.76
GA-35C	2186	0.05	0.05	1.28	0.014	0.18	7.1	3.9	4.03	144	3.75
SJ-390C	640	0.16	0.14	2.5	0.027	0.27	9.3	5.3	0.55	96	88.3
SJ-390C	650	0.27	0.18	1.22	0.023	0.6	22.1	14.3	5.22	152	58
SJ-390C	660	0.24	0.2	0.88	0.032	0.47	25.7	12.8	4.6	129	21.8
SJ-390C	670	0.16	0.2	1.18	0.052	0.31	24.5	9.8	5.37	134	7.78

SAMPLE	Depth (ft)	Ge ppm	Hf ppm	Hg ppm	In ppm	K ppm	La ppm	Li ppm	Mg ppm	Mn ppm	Mo ppm
SJ-390C	680	0.12	0.13	0.79	0.032	0.25	15.6	8.3	4.78	124	4.81
SJ-390C	690	0.1	0.12	0.46	0.031	0.27	15.9	9	4.52	179	3.06
SJ-390C	700	0.08	0.09	0.31	0.032	0.46	12	10.4	5.27	194	2.73
SJ-390C	710	0.08	0.11	0.18	0.056	0.75	9.4	15.7	4.94	119	3.22
SJ-390C	720	0.1	0.07	0.49	0.044	0.43	14.5	8.6	2.55	83	4.7
SJ-390C	730	0.09	0.07	1.04	0.032	0.23	16.1	3.8	0.82	57	5.07
SJ-390C	740	0.11	0.09	1.76	0.04	0.4	15	10.6	1.63	91	10.6
SJ-390C	750	0.1	0.08	2.5	0.042	0.19	30.8	12.2	2.07	69	6.46
SJ-390C	760	0.09	0.06	2.7	0.046	0.14	29.2	10.2	2.23	80	5.26
SJ-390C	770	0.06	0.05	1.18	0.026	0.12	25.5	7.5	2.28	173	2.75
SJ-390C	780	0.06	0.06	1.36	0.025	0.13	26.4	8	2.38	180	2.38
SJ-390C	790	0.07	0.05	0.79	0.023	0.12	24.5	7.2	2.21	157	3.39
SJ-390C	800	0.06	0.05	1.21	0.023	0.1	25.8	7.1	1.73	165	2.56
SJ-390C	900	0.05	0.06	0.42	0.021	0.85	26	12.4	3.32	340	0.63
SJ-390C	920	0.07	0.08	0.33	0.049	0.81	19.3	14.6	4.76	185	29.6
SJ-390C	940	0.07	0.11	0.68	0.025	0.49	15	8.1	6.04	217	74.6
SJ-390C	960	0.05	0.08	2.15	0.016	0.2	11.4	5.2	5.52	246	77
SJ-390C	965	0.025	0.08	0.9	0.014	0.26	11.7	3.7	4.59	108	54.9
SJ-390C	970	0.025	0.07	1.16	0.014	0.1	11.2	2.4	3.99	105	47.7
SJ-390C	975	0.025	0.05	0.3	0.008	0.07	9.4	2.9	4.26	148	26.5
SJ-390C	980	0.025	0.05	0.09	0.013	0.06	9.4	3.2	4.9	172	29.8
SJ-390C	985	0.025	0.06	0.08	0.01	0.22	9	5.3	3.36	146	33.4
SJ-390C	990	0.025	0.07	0.39	0.011	0.27	10.7	5.6	3.9	154	41.6
SJ-390C	995	0.025	0.05	2	0.013	0.09	5.9	4.6	5.05	281	45.4
SJ-390C	1000	0.025	0.05	1.27	0.012	0.07	7	2.7	3.56	180	41.2
SJ-390C	1005	0.025	0.05	1.6	0.011	0.07	6.1	1.2	3.11	169	45.9
SJ-390C	1010	0.025	0.05	1.67	0.011	0.09	4.1	2.2	5.57	200	39.7
SJ-390C	1015	0.06	0.09	2.35	0.013	0.11	10.4	3	4.12	202	30.2
SJ-390C	1020	0.05	0.08	0.28	0.011	0.31	10.9	4.9	3.83	184	30
SJ-390C	1025	0.1	0.1	0.42	0.021	0.82	13.9	12.3	4.77	116	45.2
SJ-390C	1030	0.06	0.1	1.08	0.015	0.32	15.1	6.1	4.69	122	28.7
SJ-390C	1035	0.09	0.13	0.23	0.023	1.31	18.8	21.8	5.2	132	29.1
SJ-390C	1040	0.1	0.12	0.08	0.01	1.4	18	23.9	4.96	129	21.7
SJ-390C	1060	0.06	0.12	3.37	0.042	0.19	17.5	6.5	4.42	220	62.4
SJ-390C	1095	0.025	0.05	2.67	0.024	0.05	3.8	4.1	4.33	230	4.14
SJ-390C	1100	0.025	0.06	1.69	0.021	0.15	7	7.4	7.17	322	6.24
SJ-390C	1105	0.025	0.05	1.12	0.016	0.11	6.1	6.7	7.34	333	1.55
SJ-390C	1110	0.025	0.06	4.42	0.023	0.15	6.2	2.8	6.71	380	7.12
SJ-390C	1115	0.025	0.06	14	0.046	0.08	3.9	6.1	5.96	328	12.75
SJ-390C	1120	0.025	0.06	10.1	0.025	0.05	4.4	7.2	6.39	261	8.08
SJ-390C	1125	0.025	0.06	15.55	0.035	0.04	3.6	5.7	6.51	246	3.55
SJ-390C	1130	0.025	0.07	15.45	0.046	0.04	3.2	6.5	5.43	195	3.97
SJ-390C	1135	0.025	0.06	8.91	0.018	0.03	7.4	5.2	6.08	233	1.48
SJ-390C	1140	0.025	0.08	2.05	0.018	0.05	8.2	6.4	6.03	202	3.89
SJ-390C	1160	0.05	0.06	1.62	0.028	0.02	6.3	4.3	6.68	276	3.21
SJ-390C	1180	0.025	0.06	0.88	0.018	0.02	6.6	4	6.18	269	2.67
SJ-390C	1200	0.05	0.06	0.86	0.013	0.08	8.6	3.5	2.81	277	3.48
SJ-390C	1220	0.05	0.07	0.54	0.011	0.06	8.6	4.8	4.67	237	2.27
SJ-390C	1240	0.025	0.06	0.97	0.01	0.1	8.5	1.7	2.2	195	2.87
SJ-390C	1260	0.025	0.06	1.33	0.018	0.05	6.5	2.8	2.72	250	6.86
SJ-390C	1280	0.025	0.03	1.24	0.012	0.04	3.3	0.7	0.28	426	5.62

SAMPLE	Depth (ft)	Ge ppm	Hf ppm	Hg ppm	In ppm	K ppm	La ppm	Li ppm	Mg ppm	Mn ppm	Mo ppm
SJ-390C	1295	0.025	0.04	0.98	0.012	0.11	8.1	3.3	1.03	291	6
SJ-464C	10	0.1	0.13	1.5	0.031	0.31	20	6.5	0.21	485	5.57
SJ-464C	20	0.15	0.12	1.22	0.038	0.37	33.7	31.1	0.11	8760	9.81
SJ-464C	30	0.11	0.1	0.16	0.037	0.33	33.3	1.8	0.08	153	2.82
SJ-464C	240	0.08	0.17	1.13	0.017	0.17	12.2	1.8	0.06	35	22.7
SJ-464C	250	0.07	0.18	0.63	0.023	0.21	11.4	2.8	2.36	156	17.05
SJ-464C	260	0.05	0.16	0.54	0.018	0.21	10.1	3.9	4.27	307	14.55
SJ-464C	270	0.06	0.17	0.58	0.022	0.25	12.6	3.7	1.7	165	21.4
SJ-464C	280	0.06	0.18	0.47	0.02	0.2	11.9	4.1	3.91	325	14.05
SJ-464C	290	0.07	0.22	0.6	0.028	0.26	15.8	5.3	3.58	310	14.3
SJ-464C	300	0.025	0.11	0.48	0.021	0.25	10	3.4	4.35	377	7.99
SJ-464C	310	0.05	0.11	0.56	0.022	0.2	12.3	4.7	5.91	680	3.03
SJ-464C	320	0.05	0.13	0.72	0.022	0.2	9.6	4.5	5.2	585	6.28
SJ-464C	330	0.025	0.14	1.61	0.02	0.18	7.3	2.8	0.76	125	18.8
SJ-464C	370	0.09	0.15	5.39	0.023	0.19	5.6	3.4	0.21	60	16.3
SJ-464C	380	0.1	0.15	3.57	0.018	0.21	8	4	0.96	119	13.7
SJ-464C	390	0.025	0.11	1.25	0.019	0.2	6.3	4.4	4.07	298	10.75
SJ-464C	400	0.025	0.1	0.89	0.016	0.17	7.6	4.4	5.02	457	8.05
SJ-464C	410	0.025	0.09	0.55	0.015	0.14	7.3	4.2	3.95	390	3.47
SJ-464C	420	0.025	0.09	0.87	0.015	0.15	6	4.7	4.39	541	3.16
SJ-464C	430	0.025	0.08	1.69	0.015	0.14	7.8	4.3	4.8	617	1.15
SJ-464C	440	0.025	0.09	2.13	0.016	0.15	8.5	5.5	4.83	617	1.07
SJ-464C	450	0.025	0.07	0.7	0.013	0.11	6.5	3.5	4.82	620	0.91
SJ-464C	460	0.025	0.07	0.67	0.013	0.09	5.5	3	4.36	524	1.6
SJ-464C	470	0.025	0.09	1	0.02	0.16	5.6	3	4.69	736	4.2
SJ-464C	480	0.025	0.08	0.97	0.017	0.15	5.7	2.7	5.38	1060	1.64
SJ-464C	490	0.025	0.1	1.45	0.02	0.19	6.4	3.4	4.25	799	6.14
SJ-464C	500	0.025	0.12	0.87	0.017	0.19	8.3	3.2	3.55	600	7.7
SJ-464C	510	0.025	0.09	0.33	0.021	0.2	10	4	4.48	742	2.8
SJ-464C	520	0.025	0.09	0.31	0.023	0.23	10.4	4.6	5.05	814	1.75
SJ-464C	530	0.025	0.09	0.28	0.022	0.21	10.2	4.3	4.81	931	2.88
SJ-464C	540	0.025	0.1	0.27	0.018	0.17	10.3	3	1.7	314	12.6
SJ-464C	690	0.025	0.04	1.5	0.015	0.06	0.9	0.7	0.03	30	15.05
SJ-464C	700	0.025	0.05	1.21	0.013	0.11	1	1	0.46	98	12.4
SJ-464C	710	0.025	0.1	0.49	0.027	0.23	6.8	4.5	4.77	521	8.46
SJ-464C	720	0.025	0.07	0.2	0.024	0.23	7	6.2	4.73	586	7.82
SJ-464C	740	0.025	0.12	0.42	0.03	0.23	9.4	13.7	2.04	335	22.2
SJ-464C	750	0.07	0.11	2.06	0.015	0.21	7.6	12	0.79	90	71.7
SJ-464C	760	0.14	0.14	4.52	0.017	0.25	10	11.8	0.66	47	126
SJ-464C	770	0.08	0.15	3.93	0.023	0.37	10.8	11	1.3	94	108
SJ-464C	780	0.07	0.15	3.52	0.018	0.16	10.7	7.6	2.04	73	85.3
SJ-464C	790	0.12	0.18	3.13	0.022	0.29	20	6.8	2.76	69	61.6
SJ-464C	800	0.12	0.19	2.59	0.025	0.39	23.3	6.4	3.3	68	31.3
SJ-464C	810	0.11	0.19	1.45	0.032	0.47	20.8	10.5	2.86	74	10.9
SJ-464C	820	0.09	0.18	1.41	0.027	0.41	24.6	12.2	4.02	83	8.05
SJ-464C	830	0.06	0.13	1.39	0.024	0.36	24.2	8.8	5.45	93	5.73
SJ-464C	840	0.06	0.12	1.38	0.024	0.38	19.6	9.9	6.25	103	3.81
SJ-464C	850	0.05	0.12	1.25	0.025	0.42	15.5	12.2	6.1	123	3.19
SJ-464C	860	0.025	0.1	0.89	0.021	0.55	15.3	12	6.26	160	2.1
SJ-464C	870	0.025	0.1	0.8	0.02	0.18	13.2	8.3	5.43	140	2.67
SJ-464C	880	0.025	0.1	0.75	0.026	0.19	11.9	6.8	5.26	136	2.37

SAMPLE	Depth (ft)	Ge ppm	Hf ppm	Hg ppm	In ppm	K ppm	La ppm	Li ppm	Mg ppm	Mn ppm	Mo ppm
SJ-464C	900	0.025	0.11	0.97	0.035	0.18	14.9	5.5	4.02	102	6.76
SJ-464C	920	0.025	0.08	0.6	0.029	0.17	9.3	3.8	3.99	107	4.27
SJ-464C	940	0.025	0.06	0.38	0.021	0.15	8.2	3.2	3.98	259	2.11
SJ-464C	960	0.025	0.07	0.32	0.027	0.24	10.2	4.2	4.99	291	1.39
SJ-464C	980	0.025	0.07	0.17	0.021	0.18	12	3.4	4.25	234	0.85
SJ-464C	1000	0.025	0.09	0.12	0.023	0.2	14.3	4.4	4.35	212	1.16
SJ-464C	1020	0.025	0.05	0.18	0.011	0.13	17.8	4.6	2.77	169	0.52
SJ-464C	1040	0.025	0.07	0.37	0.014	0.16	19.1	5.4	3.06	148	0.54
SJ-464C	1060	0.025	0.05	0.15	0.008	0.07	17.9	3.6	2.39	124	0.39
SJ-464C	1080	0.025	0.05	0.22	0.012	0.12	17.6	4.2	3.56	180	0.38
SJ-464C	1100	0.025	0.06	0.13	0.017	0.17	14.1	4.4	4.68	218	0.53
SJ-464C	1120	0.05	0.08	0.58	0.016	0.13	9.1	4.9	6.53	177	49.2
SJ-464C	1140	0.025	0.07	2.99	0.014	0.1	5.5	2.6	3.62	147	58.1
SJ-464C	1215	0.025	0.09	8.69	0.041	0.18	3.6	2.3	4.77	163	30.6
SJ-464C	1220	0.025	0.07	5.47	0.013	0.11	6.9	2.4	5.36	173	11.35
SJ-464C	1225	0.025	0.06	6.1	0.023	0.09	5.4	3	5.26	199	9.3
SJ-464C	1230	0.025	0.06	8.85	0.046	0.11	4.5	4.4	4.82	322	18.45
SJ-464C	1235	0.05	0.05	6.11	0.032	0.12	8.7	3.1	4.72	185	12.9
SJ-464C	1240	0.025	0.07	5.03	0.014	0.12	13.2	3.7	5.92	211	2.76
SJ-464C	1245	0.025	0.06	6.1	0.016	0.11	9.6	2.3	4.49	145	6.23
SJ-464C	1250	0.025	0.05	6.66	0.037	0.1	5.5	2.3	4.2	155	7.38
SJ-464C	1255	0.025	0.06	7.1	0.021	0.15	9	2.8	4.71	177	12.15
SJ-464C	1260	0.025	0.06	2.89	0.013	0.14	6.9	3.6	5.2	193	11.3
SJ-464C	1265	0.025	0.07	3.02	0.011	0.15	7.8	4.1	4.87	192	14.05
SJ-464C	1270	0.025	0.06	2.88	0.011	0.13	8.3	3.9	6.53	223	1.82
SJ-464C	1275	0.025	0.07	2.86	0.013	0.14	8.5	4.1	5.47	196	2.07
SJ-464C	1280	0.025	0.05	3.12	0.013	0.15	7.2	3	5.12	193	1.23
SJ-464C	1285	0.025	0.07	3.72	0.014	0.18	11.6	4.5	5.17	199	1.77
SJ-464C	1290	0.025	0.06	5.22	0.016	0.16	11.5	3.2	4.37	165	2.2
SJ-464C	1295	0.025	0.06	2.33	0.012	0.15	9.6	4.9	5.34	215	2.11
SJ-464C	1300	0.025	0.07	3.47	0.01	0.14	9.4	4.5	4.53	176	2.72
SJ-464C	1305	0.025	0.07	2.09	0.011	0.16	10.1	4.9	5.32	199	1.61
SJ-464C	1310	0.025	0.07	3.07	0.011	0.13	6.2	3.7	3.53	138	16.2
SJ-464C	1315	0.025	0.07	2.05	0.01	0.16	8.8	4.1	3.9	170	3.54
SJ-464C	1320	0.05	0.06	2.88	0.018	0.22	7.2	6.2	5.39	203	2.73
SJ-464C	1325	0.05	0.07	4.15	0.02	0.24	7.6	6.4	5.73	197	3.7
SJ-464C	1330	0.025	0.05	2.57	0.016	0.2	7	6.5	5.8	203	2.48
SJ-464C	1335	0.025	0.07	5.92	0.023	0.26	6.5	7	6.03	206	2.95
SJ-464C	1340	0.025	0.06	2.08	0.027	0.16	5.2	4.5	3.88	242	3.16
SJ-464C	1345	0.025	0.04	2.8	0.017	0.14	5.8	4.4	4.67	190	2.74
SJ-464C	1350	0.025	0.04	3.52	0.034	0.11	8.7	2.6	2.99	111	6.39
SJ-464C	1355	0.05	0.06	2.98	0.021	0.15	12	4	3.61	117	3.77
SJ-464C	1360	0.025	0.05	2.29	0.02	0.15	8	4.6	4.83	171	2.41
SJ-464C	1365	0.05	0.08	0.91	0.015	0.27	11.7	9.2	5.77	164	2.51
SJ-464C	1370	0.05	0.07	0.9	0.015	0.18	14.1	6.4	4.41	155	3.06
SJ-464C	1375	0.025	0.06	0.87	0.02	0.22	11.4	7.1	6.04	200	3.28
SJ-464C	1380	0.06	0.07	1.81	0.018	0.22	13.6	5.4	5.41	170	5.3
SJ-464C	1385	0.05	0.06	1.38	0.053	0.2	10.1	4.8	5.23	170	9.21
SJ-464C	1390	0.025	0.05	1.42	0.015	0.11	9.8	2.4	2.84	153	7.65
SJ-464C	1395	0.06	0.06	1.63	0.021	0.15	20.3	3.1	4.22	168	9.37
SJ-464C	1400	0.07	0.06	5.64	0.059	0.18	15.8	3.6	4.07	151	7.68

SAMPLE	Depth (ft)	Ge ppm	Hf ppm	Hg ppm	In ppm	K ppm	La ppm	Li ppm	Mg ppm	Mn ppm	Mo ppm
SJ-464C	1405	0.025	0.05	1.17	0.023	0.12	12.9	3.4	3	429	5.76
SJ-464C	1410	0.025	0.05	0.64	0.013	0.12	12.9	4.6	3.54	204	3.73
SJ-464C	1415	0.025	0.05	0.57	0.012	0.14	8.1	6	3.74	120	3.22
SJ-464C	1420	0.025	0.06	0.91	0.019	0.18	8.2	4.7	4.43	119	7.94
SJ-464C	1425	0.08	0.05	3.14	0.037	0.15	7.1	3.1	2.77	119	7.6
SJ-464C	1430	0.025	0.02	2	0.018	0.03	3.3	0.6	0.62	594	3.88
SJ-464C	1435	0.025	0.02	0.76	0.03	0.01	1.7	0.2	0.3	705	2.48
SJ-464C	1440	0.025	0.02	0.48	0.02	0.01	2	0.3	0.54	366	1.61
SJ-464C	1445	0.025	0.02	0.14	0.005	0.01	2	0.4	0.6	309	1.12
SJ-464C	1450	0.025	0.01	0.27	0.005	0.03	3.9	0.7	1.21	90	3.46
SJ-464C	1455	0.025	0.02	0.25	0.005	0.08	7.8	1.8	2.97	98	4.33
SJ-464C	1460	0.025	0.01	0.39	0.0025	0.04	5.2	0.8	1.02	80	2.6
SJ-464C	1465	0.025	0.01	0.43	0.0025	0.05	5.3	0.8	1.13	84	2.61
WM-01C	2440	0.07	0.11	2.7	0.014	0.15	11.3	3.5	0.19	63	16.9
WM-01C	2460	0.08	0.12	2.29	0.015	0.11	7.3	2.3	0.31	105	31.8
WM-01C	2480	0.08	0.11	1.38	0.013	0.1	6.8	2.1	0.21	67	40.1
WM-01C	2500	0.08	0.09	1.4	0.013	0.1	5.1	1.8	1.16	236	27.1
WM-01C	2520	0.06	0.12	3.89	0.012	0.13	7.9	2.3	0.67	135	17.85
WM-01C	2540	0.08	0.11	17.7	0.028	0.14	7.8	2	2.89	145	36.1
WM-01C	2560	0.05	0.07	2.77	0.012	0.08	7.4	1.4	3.23	280	1.61
WM-01C	2580	0.06	0.08	1.53	0.013	0.11	15	1.5	3.01	261	1.44
WM-01C	2600	0.07	0.12	5.01	0.023	0.13	9.5	2.2	5.5	214	29.8
WM-01C	2620	0.06	0.12	2.25	0.016	0.12	8.5	1.8	4.57	186	29.1
WM-01C	2640	0.05	0.11	2.31	0.019	0.14	6.8	3	6.23	208	2.57
WM-01C	2660	<0.05	0.11	2.67	0.013	0.15	6.4	3	6.04	218	2.47
WM-01C	2680	<0.05	0.11	2.04	0.012	0.16	7.5	3	5.05	183	2.46
WM-01C	2700	<0.05	0.11	0.21	0.013	0.2	8.8	5.5	4.93	197	4.92
WM-01C	2720	<0.05	0.09	0.56	0.017	0.17	8.4	3.3	4.62	214	2.89
WM-01C	2740	<0.05	0.1	0.12	0.015	0.2	7.8	5.1	5.39	204	1.92
WM-01C	2760	<0.05	0.09	0.48	0.014	0.17	8.1	5.7	4.74	210	2.36
WM-01C	2780	0.05	0.09	0.96	0.018	0.19	7.5	4	4.65	208	4.12
WM-01C	2800	<0.05	0.09	0.97	0.016	0.19	7.7	3.8	4.4	200	2.33
WM-01C	2820	<0.05	0.08	1.11	0.016	0.18	8.3	3.3	4.09	192	2.11
WM-01C	2840	<0.05	0.08	0.54	0.021	0.19	9.3	2.9	4.69	180	1.72
WM-01C	2860	<0.05	0.11	0.55	0.014	0.2	9.1	3.2	4.81	155	1.78
WM-01C	2880	<0.05	0.11	1.09	0.015	0.2	10	3	3.96	127	8.94
WM-01C	2900	0.05	0.16	0.81	0.016	0.25	16.6	3.6	3.81	144	4.05
WM-01C	2920	<0.05	0.08	0.64	0.018	0.14	9.4	2.4	3.47	153	3.43
WM-01C	2940	<0.05	0.07	0.55	0.015	0.12	7.9	2.4	3.46	222	2.46
WM-01C	2960	<0.05	0.08	0.54	0.012	0.13	8.3	2.3	3.73	199	5.08
WM-01C	2980	<0.05	0.08	0.41	0.015	0.19	7.6	2.8	4.02	192	3.19
WM-01C	3000	<0.05	0.07	0.27	0.012	0.16	8.5	2.7	4.51	228	2.41
WM-01C	3020	<0.05	0.08	0.34	0.014	0.17	7.7	2.8	4.76	208	3.43
WM-01C	3040	<0.05	0.07	0.19	0.016	0.16	8.2	2.8	5.23	234	4.55
WM-01C	3050	0.05	0.08	0.57	0.014	0.2	11	3.8	4.21	183	5.4

SAMPLE	Depth (ft)	Na ppm	Nb ppm	Ni ppm	P ppm	Pb ppm	Rb ppm	Re ppm	S ppm	Sb ppm
BZ-965C	880	0.01	0.09	51	410	8.5	6.4	0.049	1.29	15.4
BZ-965C	885	0.01	0.09	49.7	390	7.3	7.1	0.042	1.36	9.01
BZ-965C	905	0.01	0.06	55.4	400	5.3	3.9	0.052	0.8	9.84
BZ-965C	910	0.01	0.08	70.5	380	8.4	6	0.056	1.34	11.05
BZ-965C	955	0.02	0.11	98.1	390	11.6	7.9	0.318	1.84	16.6
BZ-965C	960	0.02	0.1	175	400	8.1	8.4	0.812	1.57	20.8
BZ-965C	965	0.01	0.025	223	790	18.5	15	1.09	1.24	38.7
BZ-965C	970	0.01	0.025	197.5	720	18.6	10.5	0.414	1.22	36.4
BZ-965C	975	0.02	0.025	179.5	1050	13.6	14.7	0.219	2.6	15.55
BZ-965C	980	0.03	0.025	139.5	630	8.7	9.5	0.155	1.02	11.15
BZ-965C	1000	0.02	0.025	85.4	7120	9.2	10.7	0.073	1.51	7.9
BZ-965C	1020	0.01	0.025	70.4	5230	10.3	7.6	0.04	1.58	7.84
BZ-965C	1040	0.02	0.025	40.6	1280	10.6	3.6	0.019	1.76	5.92
BZ-965C	1060	0.02	0.025	37.2	270	13.9	4.5	0.014	1.85	2.82
BZ-965C	1065	0.02	0.025	35.7	880	8.8	4.1	0.025	1.59	2.2
BZ-965C	1070	0.02	0.025	29.6	2550	8.5	4.7	0.018	1.42	2.77
BZ-965C	1075	0.02	0.025	27.8	590	7.9	3.9	0.018	1.34	3.18
BZ-965C	1080	0.02	0.025	37.9	3940	9.5	6.5	0.018	1.62	3.34
BZ-965C	1085	0.02	0.025	26.3	320	10.8	4.4	0.009	1.72	1.81
BZ-965C	1090	0.01	0.025	36.3	1960	8.1	4.8	0.024	1.44	5.1
BZ-965C	1095	0.02	0.025	39.2	2720	6.4	5.2	0.029	1.36	7.43
BZ-965C	1100	0.02	0.025	28.8	310	13.7	6.5	0.006	2.36	4.29
BZ-965C	1105	0.02	0.025	31.4	740	17	7.6	0.01	2.54	7.38
BZ-965C	1110	0.02	0.025	36.4	310	14.3	8.1	0.008	2.29	7.84
BZ-965C	1115	0.03	0.025	18.6	310	12.9	7.3	0.008	1.95	2.31
BZ-965C	1120	0.02	0.025	18.2	390	11.3	7.6	0.005	1.54	5.48
BZ-965C	1125	0.02	0.025	13.7	390	6.5	5.2	0.005	1.15	9.64
BZ-965C	1130	0.02	0.025	19	330	10.1	6.4	0.004	1.61	7.7
BZ-965C	1135	0.03	0.025	21.4	330	12.2	6.5	0.008	1.71	5.1
BZ-965C	1140	0.02	0.025	12.1	470	6	5.4	0.002	0.94	3.02
BZ-965C	1145	0.02	0.025	7.9	290	5.4	3.5	0.002	0.76	2.16
BZ-965C	1150	0.02	0.025	5.8	290	4.1	2	0.001	0.55	1.33
BZ-965C	1155	0.02	0.025	8.2	340	4.4	2.9	0.002	0.68	0.66
BZ-965C	1160	0.02	0.025	5.8	260	3.4	1.8	0.001	0.4	0.46
BZ-965C	1165	0.02	0.025	7.9	180	5.2	2	0.001	0.92	1.77
BZ-965C	1170	0.02	0.025	8.9	230	5.3	2.5	0.001	0.79	0.54
BZ-965C	1175	0.005	0.06	10.2	270	26.8	3.2	0.002	0.84	1.11
BZ-965C	1180	0.005	0.09	3.6	160	11.7	1.9	0.001	0.53	0.68
BZ-965C	1185	0.005	0.09	3.8	220	3.6	1.4	0.001	0.43	0.65
BZ-965C	1190	0.005	0.07	7.3	150	5.9	3.3	0.002	0.69	2.87
BZ-965C	1195	0.005	0.08	5	290	3.3	3.8	0.001	0.7	6.91
BZ-965C	1200	0.005	0.05	5.5	170	3.3	3.3	0.001	0.6	3.33
BZ-965C	1205	0.005	0.06	6.8	230	5.1	4.2	0.001	0.84	4.29
BZ-965C	1215	0.005	0.05	12	380	8.9	5	0.004	1.09	5.82
BZ-965C	1220	0.005	0.07	8	200	6.9	3	0.002	1.16	2.53
BZ-965C	1225	0.005	0.07	11.5	260	7.1	3.9	0.002	1.32	1.2
BZ-965C	1230	0.005	0.08	9	280	5	3.3	0.001	1	0.86
BZ-965C	1235	0.005	0.08	9	320	5.8	5.1	0.001	0.88	0.52
BZ-965C	1240	0.005	0.09	8.6	210	5.6	6.2	0.001	0.8	0.45
BZ-965C	1245	0.005	0.08	8.4	200	5.2	5.7	0.001	0.78	0.44
BZ-965C	1250	0.005	0.09	9.2	170	6.2	7.2	0.001	0.89	0.88

SAMPLE	Depth (ft)	Na ppm	Nb ppm	Ni ppm	P ppm	Pb ppm	Rb ppm	Re ppm	S ppm	Sb ppm
BZ-965C	1255	0.005	0.05	11.8	340	6	6.6	0.007	1.21	5.05
BZ-965C	1260	0.005	0.07	18.5	380	11.3	8.7	0.006	1.92	5.36
BZ-965C	1265	0.005	0.05	25.7	280	14.9	7.7	0.005	2.68	9.45
BZ-965C	1270	0.005	0.025	41.7	550	11.8	6.8	0.023	1.94	14
BZ-965C	1275	0.01	0.025	68.9	430	8.8	5.3	0.047	1.25	16.15
BZ-965C	1280	0.01	0.025	73.4	460	8.6	5.4	0.045	1.14	17.45
BZ-965C	1285	0.005	0.025	75.6	370	9.9	6	0.04	1.15	17.65
BZ-965C	1290	0.005	0.025	74.4	350	7.4	4.8	0.04	1.04	19.7
BZ-965C	1295	0.01	0.025	92.2	390	9.1	5.4	0.053	1.05	21.4
BZ-965C	1300	0.005	0.025	68.9	390	7.2	5.5	0.034	1.09	13.8
BZ-965C	1305	0.005	0.05	76.1	380	7.1	4.6	0.039	0.99	14.55
BZ-965C	1310	0.01	0.05	70.9	270	6.8	4.1	0.036	0.91	7.62
BZ-965C	1315	0.005	0.025	47.6	700	19.4	6.3	0.022	1.27	11.65
BZ-965C	1320	0.005	0.025	42.5	460	11.1	4.7	0.011	0.98	14.35
BZ-965C	1325	0.005	0.025	35.6	1040	16	7.5	0.007	2.17	48.1
CD-14	530	0.02	0.16	16.5	340	12.8	7.3	0.001	3.71	23.2
CD-14	550	0.02	0.08	22.7	380	10.9	6.6	0.007	0.91	8.06
CD-14	560	0.02	0.15	14.2	230	8.8	4.4	0.004	1.41	9.48
CD-14	570	0.02	0.06	30.8	300	13.9	7.2	0.009	2	15.65
CD-14	580	0.02	0.19	18.9	250	9.4	6.9	0.001	2.81	15.35
CD-14	590	0.03	0.15	16.8	240	8.3	6.7	0.001	3.06	23.7
CD-14	600	0.02	0.21	15.1	300	5.7	4.7	<0.001	0.27	4.16
CD-14	610	0.02	0.2	92.2	5230	13.4	8.6	0.001	0.22	6.42
CD-14	620	0.02	0.17	63.2	700	9.3	5.6	0.001	0.08	11.75
CD-14	630	0.03	0.22	120.5	600	12.2	5.8	0.002	0.15	10.3
CD-14	640	0.03	0.19	72.7	510	7.6	5.2	0.001	0.09	8.75
CD-14	650	0.03	0.22	49.4	700	8.4	5	0.001	0.28	10.6
CD-14	660	0.03	0.17	80.8	580	12.1	5.9	0.001	0.61	17.15
CD-14	670	0.02	0.19	43.8	450	11.8	5.8	0.001	1.17	20.8
CD-14	680	0.02	0.12	15.9	190	8.8	4.7	0.004	1.27	8.65
CD-14	690	0.02	0.14	17.1	220	10.8	5.2	0.003	1.18	6.58
CD-14	700	0.02	0.09	41.1	390	9.4	4.7	0.002	0.43	4.97
CD-14	720	0.02	0.1	38.9	420	15.3	5.2	0.003	0.22	3.29
CD-14	740	0.02	0.11	66.1	400	36.6	3.9	0.016	0.61	9.77
CD-14	770	0.02	0.1	80.9	450	52.6	4.4	0.026	0.54	6.7
CD-14	780	0.02	0.09	71.6	340	33.8	4.1	0.031	0.56	9.2
CD-14	790	0.01	0.08	59.5	390	31.1	4.3	0.043	0.68	9.5
CD-14	800	0.02	0.09	58	370	10.5	3.6	0.022	0.55	4.67
CD-14	820	0.02	0.11	78	560	7.2	5.2	0.054	1	6.69
CD-14	840	0.02	0.07	42.9	340	13.8	7.5	0.052	1.16	11.5
CD-14	860	0.02	0.05	20.3	290	9.6	7	0.086	0.53	9.07
CD-14	880	0.02	0.06	21.3	290	8.6	8.2	0.009	0.78	14.65
CD-14	900	0.02	0.06	20.1	240	7.8	8	0.009	0.55	9.86
CD-14	920	0.02	0.06	18.8	260	6.9	8.5	0.007	0.71	8.45
CD-14	940	0.02	0.06	14.2	220	6.9	8.6	0.002	0.37	3.26
CD-14	960	0.02	0.06	27.1	240	13	10.6	0.046	0.82	17.35
CD-14	980	0.02	0.07	21	270	10.6	8.3	0.144	0.59	16.3
CD-14	1000	0.02	0.07	17.6	200	7.7	6.9	0.011	0.67	11.45
CD-14	1020	0.02	0.07	17.3	190	7.8	7.9	0.004	0.45	9.6
CD-14	1040	0.02	0.07	17	200	6.5	7.6	0.005	0.44	8.13
CD-14	1060	0.02	0.06	20.1	250	7.6	9.5	0.003	0.5	3.84

SAMPLE	Depth (ft)	Na ppm	Nb ppm	Ni ppm	P ppm	Pb ppm	Rb ppm	Re ppm	S ppm	Sb ppm
CD-14	1080	0.02	0.09	16.3	160	7	7.8	0.005	0.46	3.97
CD-14	1100	0.02	0.08	16	190	7.8	8.5	0.004	0.87	10.45
CD-14	1120	0.02	0.09	12.8	180	5.5	6.6	0.002	0.4	2.17
CD-14	1140	0.02	0.09	19.2	200	6.9	9.2	0.003	0.4	3.45
CD-14	1160	0.02	0.08	22.9	150	7.8	8.6	0.006	0.62	2.86
CD-14	1180	0.02	0.09	18.5	160	6.2	7.4	0.004	0.49	2.29
CD-14	1200	0.02	0.08	24.1	190	8.2	7.1	0.019	0.51	5.16
CD-14	1220	0.02	0.06	30.8	270	11.1	8.2	0.033	0.89	11.45
CD-14	1240	0.02	0.1	20.1	150	8.3	6	0.015	0.66	7.05
CD-14	1260	0.03	0.07	21.4	200	9.5	9.5	0.015	0.58	6.38
CD-14	1280	0.03	0.09	11.8	190	7.5	7.8	0.003	0.43	2.89
CD-14	1300	0.03	0.07	15.5	280	7.7	10.8	0.001	0.54	1.12
CD-14	1320	0.03	0.1	19	230	8	10.3	0.012	0.48	3.28
CD-14	1340	0.02	0.1	20	430	7.9	10	0.012	0.52	5.73
CD-14	1360	0.02	0.08	19.6	210	7.7	9.8	0.011	0.5	2.94
CD-14	1380	0.02	0.09	19.9	220	8.6	9.4	0.016	0.74	13.8
CD-14	1400	0.03	0.14	76.5	1130	9.2	26.3	0.004	1.16	9.69
CD-14	1420	0.03	0.07	21.3	460	8	10.1	0.014	0.7	7.2
CD-14	1440	0.03	0.16	29	380	8.3	16.6	0.014	0.55	3.73
CD-14	1460	0.03	0.06	16.8	260	7.1	9.1	0.004	0.42	1.72
CD-14	1480	0.05	0.22	52.6	1390	6.6	46.4	0.002	0.38	3.3
CD-14	1500	0.05	0.19	62.7	1510	6.9	45.4	0.002	0.46	0.61
CD-14	1520	0.03	0.1	22.3	460	6.2	8.3	0.006	0.44	1.83
CD-14	1540	0.03	0.1	12.8	160	6	7.3	0.018	0.35	3.32
CD-14	1560	0.03	0.09	16.4	200	7.8	8.4	0.016	0.47	4.46
CD-14	1580	0.02	0.12	15.8	250	7	9.5	0.011	0.45	3.32
CD-14	1600	0.03	0.13	16.6	350	6.5	11.2	0.006	0.42	2.48
CD-14	1620	0.03	0.1	16.7	170	7.4	8.2	0.017	0.46	5.02
CD-14	1640	0.03	0.1	16.3	170	7.5	6.8	0.017	0.44	4.53
CD-14	1660	0.04	0.16	84.8	1390	7.1	25.7	0.013	0.6	3.44
CD-14	1680	0.03	0.09	15.9	160	6.7	8.6	0.013	0.43	4.16
CD-14	1700	0.03	0.07	14	760	8.7	7.8	0.011	0.46	3.55
CD-14	1720	0.02	0.06	14.8	200	9	7.3	0.006	0.53	3.68
CD-14	1740	0.02	0.07	12.1	220	7.3	6.8	0.004	0.47	2.95
CD-14	1760	0.02	0.06	17.4	240	9.3	8.2	0.007	0.64	4.21
CD-14	1780	0.02	0.05	29.3	250	8	7.9	0.011	0.69	5.21
CD-14	1800	0.03	0.07	18.6	200	8.2	7	0.006	0.59	2.85
CD-14	1820	0.12	0.14	36	700	6.7	11.9	0.002	0.42	1.28
CD-14	1840	0.05	0.16	21	310	7.9	8.2	0.001	0.63	2.51
CD-14	1860	0.05	0.17	48	900	10.7	14.6	0.006	1.62	10.7
CD-14	1880	0.03	0.11	19	180	7.8	6.6	0.017	0.49	4.95
CD-14	1900	0.03	0.1	18.8	180	7.5	7.5	0.024	0.48	6.01
CD-14	1920	0.02	0.09	15.5	230	6.9	6.6	0.017	0.44	4.72
CD-14	1940	0.02	0.05	14.2	220	6.5	5.9	0.007	0.61	7.72
CD-14	1960	0.02	0.08	23	680	8.2	8.6	0.019	0.52	5.77
CD-14	1980	0.03	0.06	15.3	230	6.7	8.7	0.004	0.5	3.27
CD-14	2000	0.02	0.09	17.9	210	5.9	8.4	0.008	0.5	3.25
CD-14	2020	0.02	0.07	16.6	210	6.7	8.8	0.003	0.72	7.34
CD-14	2040	0.03	0.09	16.5	180	6.4	8.3	0.005	0.59	1.62
CD-14	2060	0.02	0.07	15.9	160	6.2	7	0.01	0.51	3.17
CD-14	2080	0.02	0.07	21.6	210	7.5	7.7	0.015	0.71	5.55

SAMPLE	Depth (ft)	Na ppm	Nb ppm	Ni ppm	P ppm	Pb ppm	Rb ppm	Re ppm	S ppm	Sb ppm
CD-14	2100	0.09	0.14	52.6	1320	7.2	8.1	0.004	0.58	4.59
CD-14	2120	0.02	0.06	17	190	6.5	6.9	0.013	0.71	4.58
CD-14	2140	0.02	0.06	20.3	220	6.2	10	0.013	0.55	2.9
CD-14	2160	0.02	0.09	18.7	190	5.9	9.4	0.013	0.7	3.92
CD-15C	1380	0.03	0.1	34	330	12.4	9	0.006	2.35	4.09
CD-15C	1400	0.02	0.08	80.4	2620	7.2	11.7	0.05	2.28	7.55
CD-15C	1420	0.03	0.1	63.1	7090	7.6	12.3	0.042	1.55	5.21
CD-15C	1440	0.03	0.09	60.1	2890	6.6	8.5	0.028	1.62	5.21
CD-15C	1460	0.03	0.08	64.8	3350	8.5	10	0.023	2.04	2.69
CD-15C	1480	0.03	0.08	56.5	4930	7.4	10.8	0.023	1.66	3.83
CD-15C	1500	0.02	0.08	69.6	4520	9.9	11	0.033	1.86	10
CD-15C	1520	0.02	0.08	49.9	690	16	8.7	0.014	1.9	4.91
CD-15C	1540	0.02	0.07	35.8	140	12.7	8.1	0.024	1.42	4.56
CD-15C	1560	0.02	0.07	52.9	110	9.6	8.5	0.023	1.62	9.95
CD-15C	1580	0.03	0.07	42.9	280	13.7	12.5	0.013	1.66	3.6
CD-15C	1600	0.03	0.07	39.1	420	16.8	11.8	0.011	1.68	3.1
CD-15C	1620	0.03	0.07	33.8	340	14.7	15.8	0.01	1.43	2.24
CD-15C	1660	0.03	0.07	32.9	370	10.8	9.1	0.009	1.26	29.1
CD-15C	1680	0.03	0.09	22.3	320	7.2	6.1	0.006	0.76	11.5
CD-15C	1700	0.03	0.11	12.7	210	7.1	4.2	0.002	0.76	4.72
CD-15C	1720	0.03	0.08	28.8	400	19.8	6.8	0.005	1.44	8.18
CD-15C	1740	0.02	0.05	31.7	550	18.5	11.6	0.005	2.04	21.5
CD-15C	1760	0.02	<0.05	36.6	530	17.1	8.6	0.006	1.67	22.6
CD-15C	1780	0.02	<0.05	25.4	540	11.9	8.5	0.006	1.48	22.3
CD-15C	1800	0.02	<0.05	22	500	11.1	7.5	0.005	1.19	22.9
CD-15C	1820	0.03	0.05	18	330	10.4	6.7	0.002	0.83	7.3
CD-15C	1840	0.02	0.06	12.9	280	8.4	6.1	0.001	0.64	3.44
CD-15C	1860	0.01	0.06	14	300	8.7	6.5	0.003	0.48	3.14
CD-15C	1880	0.02	0.08	34.2	850	8.4	12	0.004	0.57	3.95
CD-15C	1900	0.01	0.06	24.1	220	10.8	8.6	0.006	0.79	8.25
CD-15C	1920	0.02	0.07	24.5	200	10.3	8.9	0.018	0.69	6.79
CD-15C	1940	0.01	0.06	32.7	210	12.4	9.5	0.037	0.63	10.05
CD-15C	2000	0.02	0.07	25.4	240	11.1	10.8	0.02	0.56	4.83
CD-15C	2020	0.02	0.06	23.1	260	10.5	9.4	0.006	0.62	4.98
CD-15C	2040	0.02	0.07	33.1	270	11.3	12.7	0.017	0.92	3.37
CD-15C	2060	0.01	0.06	23.6	190	9.4	6.7	0.009	0.62	3.73
CD-15C	2080	0.02	0.07	19.2	190	8.8	8.4	0.008	0.47	2.44
CD-15C	2100	0.02	0.07	20.1	180	9	8.7	0.02	0.54	5.4
CD-15C	2120	0.02	0.07	27.2	230	8.8	9.4	0.013	0.87	9
CD-95-3	890	0.01	0.08	62.1	770	7.8	4.7	0.02	0.79	5.83
CD-95-3	900	0.01	0.07	72.9	440	10.3	4.1	0.035	1.31	7.09
CD-95-3	910	0.01	0.08	50.5	1960	8.7	4.7	0.02	1.02	5.57
CD-95-3	920	0.01	0.08	60.2	300	9.4	2.9	0.025	0.85	5.52
CD-95-3	930	0.01	0.08	55.4	840	8.5	5	0.019	1.15	5.93
CD-95-3	940	0.01	0.09	51.4	220	7.1	2.3	0.024	0.69	5.03
CD-95-3	950	0.03	0.14	88.4	7890	6.4	9.4	0.075	1.23	12.85
CD-95-3	960	0.03	0.1	57.9	4540	5.1	6.9	0.037	1.25	4.87
CD-95-3	970	0.02	0.09	53.9	2520	7.1	8.3	0.025	1.52	5.33
CD-95-3	980	0.02	0.09	55.9	3010	6.5	7.7	0.026	1.55	5.09
CD-95-3	990	0.03	0.08	52.1	2760	7.4	7.2	0.026	1.27	4.44
CD-95-3	1000	0.02	0.2	39.5	540	8.9	8.6	0.012	1.78	2.59

SAMPLE	Depth (ft)	Na ppm	Nb ppm	Ni ppm	P ppm	Pb ppm	Rb ppm	Re ppm	S ppm	Sb ppm
CD-95-3	1010	0.02	0.22	34.6	610	10.2	9.1	0.008	1.82	2.55
CD-95-3	1020	0.02	0.1	44.1	2070	8	7.1	0.016	1.63	3.25
CD-95-3	1030	0.03	0.13	49.8	3550	6.7	6	0.027	0.91	4.62
CD-95-3	1040	0.03	0.12	35.3	2930	7	7.7	0.015	1.46	2.38
CD-95-3	1050	0.02	0.22	22.2	270	10.4	7.7	0.005	1.64	1.05
CD-95-3	1060	0.03	0.13	22.8	400	8.9	6.8	0.003	1.48	0.62
CD-95-3	1070	0.02	0.1	27.7	340	13.4	8.5	0.004	2.09	0.67
CD-95-3	1080	0.02	0.1	28.7	480	12.1	9.8	0.006	1.89	0.9
CD-95-3	1090	0.02	0.11	25	600	13	9.4	0.005	1.42	1.19
CD-95-3	1100	0.02	0.1	23	360	11.2	7.9	0.004	1.24	0.97
CD-95-3	1110	0.02	0.06	28.9	210	10	8.9	0.005	1.13	0.79
CD-95-3	1120	0.03	0.1	21.6	310	11.6	8.8	0.002	1.22	0.56
CD-95-3	1130	0.01	0.11	15.2	350	17.2	7	0.002	0.79	0.49
CD-95-3	1140	0.01	0.09	17.9	230	19.6	7.4	0.003	0.96	0.36
CD-95-3	1150	0.01	0.06	27.7	210	13.9	9.1	0.005	1.16	0.62
CD-95-3	1160	0.01	0.09	13.6	240	7.6	5.5	0.003	0.6	0.74
CD-95-3	1170	0.01	0.09	14.8	290	22.6	5.6	0.002	0.64	0.74
CD-95-3	1180	0.01	0.11	13.4	270	6.1	5	0.003	0.62	0.71
CD-95-3	1190	0.01	0.1	13.2	370	12.9	5.6	0.003	0.58	0.77
CD-95-3	1200	0.01	0.1	10	170	5.3	4.2	0.002	0.58	0.61
CD-95-3	1210	0.01	0.1	19.8	370	14.9	5.5	0.002	0.56	1.03
CD-95-3	1220	<0.01	0.05	11.9	320	5.3	4.8	0.002	0.65	0.88
CD-95-3	1230	<0.01	0.09	13.3	280	5.4	4.3	0.002	0.62	0.97
CD-95-3	1240	0.01	0.09	11.7	270	5.7	4.6	0.001	0.73	0.95
CD-95-3	1250	0.01	0.08	15.2	240	10.4	5.9	0.001	1.24	0.86
CD-95-3	1260	0.02	0.13	15.2	450	6.7	4.5	0.002	0.73	0.69
CD-95-3	1270	0.01	0.09	12.3	200	7.1	5	0.002	0.7	0.8
CD-95-3	1280	<0.01	0.09	10.6	230	5.6	3.9	0.002	0.71	0.73
CD-95-3	1290	<0.01	0.09	12.2	1010	25.3	7.5	0.003	1.38	1.57
CD-95-3	1300	0.01	0.09	38.4	800	8	6.4	0.02	1.8	7.55
CD-95-3	1310	0.01	0.09	55.4	430	7.1	5.2	0.03	1.07	9.81
CD-95-3	1320	0.02	0.08	65	590	7.1	5.6	0.028	1.06	10.75
CD-95-3	1330	0.01	0.05	49.8	550	10.3	4	0.016	0.94	5.51
CD-95-3	1340	0.01	0.05	71.2	450	8.1	4.1	0.019	1.11	5.4
CD-95-3	1350	0.01	0.07	58.4	390	7.9	3.5	0.019	0.77	4.05
CD-95-3	1360	0.03	0.11	58.8	380	7.3	2.7	0.022	0.77	3.8
CD-95-3	1370	0.02	0.11	55.3	470	9.3	3.4	0.017	0.78	3.29
CD-95-3	1380	0.01	0.07	44	390	6.7	3.5	0.011	0.73	2.76
CD-95-3	1390	0.03	0.1	68	420	9	3.4	0.016	0.9	2.87
CD-95-3	1400	0.01	0.07	61.4	350	6.2	3	0.021	0.72	5.08
CD-95-3	1410	0.01	0.08	56.4	410	10.3	4.2	0.02	0.75	5.15
CD-95-3	1420	<0.01	0.08	42.2	690	5.5	3.2	0.015	0.64	3.6
CD-95-3	1430	0.01	0.09	45.7	560	14.8	4.7	0.017	0.91	5.19
CD-95-3	1440	0.01	0.07	55.9	610	11.4	4.7	0.025	0.9	5.44
CD-95-3	1450	<0.01	0.07	40.1	1080	13.1	7.2	0.014	0.87	4.4
CD-95-3	1460	0.01	0.06	49.5	550	8	6.6	0.019	1.29	4.67
CD-95-3	1470	0.01	0.07	35.9	670	10.7	6.5	0.016	1.1	3.92
CD-95-3	1480	<0.01	0.06	39.7	440	13	5.4	0.015	1.18	5.36
CD-95-3	1490	0.01	0.07	32	620	9.2	4.6	0.017	1.09	4
CD-95-3	1500	0.01	0.08	28.6	520	11.7	4.4	0.013	1.22	5.68
CD-95-3	1510	0.01	0.09	27.3	490	20.2	4.9	0.014	1.32	6.23

SAMPLE	Depth (ft)	Na ppm	Nb ppm	Ni ppm	P ppm	Pb ppm	Rb ppm	Re ppm	S ppm	Sb ppm
CD-95-3	1520	0.01	0.09	24.1	360	10.7	4.3	0.009	1.27	6.19
CD-95-3	1530	0.01	0.09	29.1	630	8.5	5.8	0.01	1.49	6.64
CD-95-3	1540	0.01	0.09	27	490	8.5	5.3	0.012	1.3	6.46
CD-95-3	1550	0.01	0.14	16.5	480	8.2	4	0.004	0.77	5.72
CD-95-3	1560	0.01	0.09	14.2	400	9.3	3.9	0.003	0.86	6.62
CD-95-3	1570	<0.01	0.09	19.7	1100	8.5	6.8	0.006	0.71	18.3
CD-95-3	1580	0.01	0.08	15.8	440	9.3	4.8	0.004	0.81	101.5
CD-95-3	1590	0.01	0.1	20.7	960	9.4	7.8	0.007	0.79	15.9
CD-95-3	1600	0.01	0.09	12	360	7	3.9	0.003	0.53	52.8
CD-95-3	1610	0.01	0.08	11.3	280	8.7	4	0.003	0.51	5.05
CD-95-3	1620	0.01	0.09	15.3	250	9.9	5.4	0.008	0.6	5.54
CD-95-3	1630	0.01	0.09	18.9	780	9.2	7.7	0.006	0.52	3.87
CD-95-3	1640	0.01	0.09	21.4	1120	10.2	8.8	0.008	0.6	3.99
CD-95-3	1650	0.01	0.1	20.7	1080	9.4	8.2	0.008	0.77	4.42
CD-95-3	1660	0.01	0.09	21.2	810	11.1	6.9	0.01	0.78	22.1
CD-95-3	1670	0.01	0.08	19.8	870	19.5	7.1	0.012	0.67	23.4
CD-95-3	1680	0.01	0.1	20.7	1060	10.9	6.9	0.01	0.74	35.9
CD-95-3	1690	0.01	0.09	19.9	490	15.1	5.3	0.015	0.72	25.1
CD-95-3	1700	0.01	0.07	13	810	9.7	4.8	0.007	0.65	12.5
CD-95-3	1710	0.01	0.09	17.1	380	11.4	4.8	0.011	0.83	12.85
CD-95-3	1720	0.01	0.08	17.3	380	13.9	4.8	0.011	0.87	13.5
CD-95-3	1730	0.01	0.08	18.8	230	10.6	3.6	0.031	0.69	13.6
CD-95-3	1740	0.01	0.05	19.2	220	12	5.1	0.01	0.92	30.7
CD-95-3	1750	0.01	0.08	17.7	340	22.9	5.8	0.011	0.84	19.65
CD-95-3	1760	0.01	0.09	15.6	200	10.6	4.7	0.01	0.71	12.95
CD-95-3	1770	0.01	0.11	12.4	240	7.3	3.1	0.012	0.51	9.42
CD-95-3	1780	0.01	0.12	9.1	380	7.4	3.1	0.007	0.48	6.46
CD-95-3	1790	0.01	0.11	14.1	660	6.8	3.2	0.015	0.52	7.96
CD-95-3	1800	0.01	0.11	11.5	140	8.2	2.6	0.01	0.46	5.97
CD-95-3	1810	0.01	0.11	15.1	230	8.5	3.7	0.018	0.62	8.73
CD-95-3	1820	0.01	0.1	13.4	190	8.1	3.4	0.012	0.59	8.76
CD-95-3	1830	0.01	0.1	13.5	140	6.2	3.2	0.013	0.45	5.72
CD-95-3	1840	0.01	0.1	11.5	140	6	3.2	0.006	0.45	5.23
CD-95-3	1850	0.02	0.09	7.9	150	7.3	2.9	0.006	0.51	4.19
CD-95-3	1860	0.02	0.11	18.6	170	6.4	2.4	0.012	0.45	5.26
CD-95-3	1870	0.02	0.09	9.6	140	5	3.9	0.006	0.56	4.94
CD-95-3	1880	<0.01	0.11	9.7	120	5.5	2.7	0.007	0.39	5.2
CD-95-3	1890	0.02	0.09	19.5	330	7.1	3.3	0.01	0.65	6.42
CD-95-3	1900	0.02	0.1	17.3	160	9.5	3.3	0.007	0.75	7.42
CD-95-3	1910	0.02	0.11	9.8	190	13.4	2.6	0.002	0.61	3.41
CD-95-3	1920	0.03	0.11	11.2	230	6.7	3.1	0.009	0.65	5.42
CD-95-3	1930	0.02	0.11	16.8	810	7.8	8.1	0.005	0.93	9.26
CD-95-3	1940	0.02	0.07	37.1	2350	10.5	14.3	0.002	2.67	25.8
CD-95-3	1950	0.02	0.09	35.5	2140	14.5	16.9	0.003	2.7	24.9
CD-95-3	1960	0.01	0.12	21.8	300	5.7	3.8	0.018	0.55	6.47
CD-95-3	1970	0.02	0.12	24.1	440	8.8	4.7	0.02	0.7	8.56
CD-95-3	1980	0.02	0.13	24.1	420	6.4	5.8	0.022	1.15	29.9
CD-95-3	1990	0.02	0.09	37.6	2310	13.3	14.5	0.003	1.79	30
CD-95-3	2000	0.02	0.09	42.1	2380	12.3	14.8	0.003	2.46	32.5
CD-95-3	2010	0.02	0.1	42.2	2360	15.5	14.3	0.001	3.05	31.8
CD-95-3	2020	0.02	0.09	26.5	620	11.2	6.7	0.019	1.12	428

SAMPLE	Depth (ft)	Na ppm	Nb ppm	Ni ppm	P ppm	Pb ppm	Rb ppm	Re ppm	S ppm	Sb ppm
CD-95-3	2030	0.02	0.1	22.7	310	7.3	3.5	0.008	0.58	16.45
CD-95-3	2040	0.02	0.09	24	210	15.1	4.5	0.014	1.1	3450
CD-95-3	2050	0.02	0.1	26.8	230	10.3	5	0.021	0.86	1425
CD-95-3	2060	0.02	0.1	29.1	310	8.5	4.3	0.019	0.83	147
CD-95-3	2070	0.02	0.1	30.1	190	7.8	4.1	0.014	0.77	22.8
CD-95-3	2080	0.02	0.12	26.9	570	9.7	5.5	0.017	0.72	9.88
CD-95-3	2090	0.02	0.11	24.3	430	10	5.5	0.016	0.67	292
CD-95-3	2100	0.02	0.1	26.9	340	9.8	5.3	0.015	0.75	506
CD-95-3	2110	0.02	0.06	14.9	280	9.3	4.3	0.007	0.59	51.1
CD-95-3	2120	0.02	0.09	30.6	1200	7.6	6.7	0.012	0.64	22.4
CD-95-3	2130	0.02	0.08	37.2	2390	15.1	12	0.001	3.62	45.8
CD-95-3	2140	0.03	0.11	9	770	4.7	5.7	0.002	0.65	11.6
CD-95-3	2150	0.03	0.11	10.1	1090	5.5	6.4	0.003	0.58	12.9
CD-95-3	2160	0.03	0.12	8.9	820	6.9	5.2	0.003	0.61	14.2
CD-95-3	2170	0.02	0.13	21.6	1040	16.2	5.2	0.002	1.07	18.15
CD-95-3	2180	0.02	0.12	26.5	1560	12	9.5	0.001	1.77	14.75
CD-96-2C	770	0.02	0.07	38.3	2420	14.3	8.3	0.012	1.79	4.68
CD-96-2C	780	0.01	0.11	40.9	600	11.5	7.9	0.011	2.05	4.25
CD-96-2C	790	<0.01	0.08	43.5	320	13.2	7.5	0.01	2.32	6.77
CD-96-2C	800	<0.01	0.08	39.5	1210	12.6	8	0.012	2.29	7.32
CD-96-2C	810	0.01	0.17	22	500	10.1	5.3	0.007	2.73	14.35
CD-96-2C	820	0.02	0.21	18.3	480	10.5	6.3	0.002	1.63	7.54
CD-96-2C	830	0.02	0.18	29.5	510	10.7	8.2	0.004	2.01	3.47
CD-96-2C	840	0.02	0.18	16.9	330	8.4	6.2	0.002	1.79	2.48
CD-96-2C	850	0.02	0.19	14.9	420	6.2	5.2	0.003	1.23	1.87
CD-96-2C	860	0.02	0.18	17.2	340	8.1	7.1	0.001	1.72	1.8
CD-96-2C	870	0.02	0.15	22.2	240	10	8.2	0.003	1.79	1.7
CD-96-2C	880	0.02	0.15	22.6	420	7.8	7.4	0.003	1.64	1.49
CD-96-2C	890	0.02	0.09	23.8	460	9.9	8.1	0.004	1.78	3.05
CD-96-2C	900	0.02	0.12	24.4	470	9.4	7.6	0.004	1.75	2.23
CD-96-2C	910	0.02	0.16	29.5	1060	8.6	7.7	0.008	1.66	2.35
CD-96-2C	920	0.01	0.1	45.3	490	9.7	8.4	0.01	2.13	2.82
CD-96-2C	930	0.02	0.14	44.2	1530	6.6	7.5	0.013	1.75	2.7
CD-96-2C	940	0.02	0.11	44.2	1280	7.5	8.7	0.013	2	3.93
CD-96-2C	950	0.02	0.19	54.6	2960	6.7	8.7	0.02	1.79	3.61
CD-96-2C	960	0.02	0.13	58.7	3970	6.5	8.9	0.027	1.71	4.93
CD-96-2C	970	0.02	0.16	48.7	2110	6.6	6.6	0.019	1.52	3.71
CD-96-2C	980	0.02	0.24	28.4	1350	8.3	8.7	0.009	0.99	4.4
CD-96-2C	990	0.02	0.22	45.8	1530	18.1	7	0.017	1.61	3.56
CD-96-2C	1000	0.01	0.11	43.9	1160	45.9	7.6	0.013	1.77	5.19
CD-96-2C	1010	0.02	0.11	35.6	350	11.3	7.7	0.01	1.53	3.64
CD-96-2C	1020	0.01	0.1	42.1	280	12.7	8	0.011	1.67	2.75
CD-96-2C	1030	0.02	0.15	44.8	3860	11.8	11.5	0.014	1.87	5.6
CD-96-2C	1040	0.01	0.11	53	3050	10.8	9.7	0.02	1.57	5.42
CD-96-2C	1050	0.04	0.4	48.4	3200	18.2	9	0.024	1.43	4.1
CD-96-2C	1060	0.01	0.13	21.5	720	18.5	6.6	0.006	1.3	1.59
CD-96-2C	1070	0.02	0.14	20.7	340	12.5	7.4	0.003	1.65	1.96
CD-96-2C	1080	0.01	0.11	20.1	300	10.5	6.6	0.003	1.43	1.62
CD-96-2C	1090	0.02	0.1	25.9	350	12.2	7.6	0.004	1.5	1.62
CD-96-2C	1100	0.02	0.13	16.2	440	11.7	6.6	0.002	1.45	1.44
CD-96-2C	1110	0.02	0.17	13.4	340	12.1	5.7	0.002	1.01	1.28

SAMPLE	Depth (ft)	Na ppm	Nb ppm	Ni ppm	P ppm	Pb ppm	Rb ppm	Re ppm	S ppm	Sb ppm
CD-96-2C	1120	0.02	0.13	19.5	280	10.2	6.4	0.005	1.04	1.2
CD-96-2C	1130	0.02	0.17	19.7	250	12.4	6.8	0.003	1.1	1.32
CD-96-2C	1140	0.02	0.13	22.8	220	11.5	7.8	0.005	1.1	1.28
CD-96-2C	1150	0.02	0.14	16.3	170	48.5	6.4	0.003	0.89	1.61
CD-96-2C	1160	0.01	0.18	6.7	170	3.4	3.1	0.003	0.39	0.97
CD-96-2C	1170	0.01	0.19	5.2	120	4	3.2	0.001	0.44	0.81
CD-96-2C	1180	0.02	0.21	8.7	160	7.7	3.7	0.002	0.53	1.05
CD-96-2C	1190	0.01	0.17	12.8	610	4.7	4.6	0.004	0.56	1.57
CD-96-2C	1200	0.02	0.14	18.6	850	7.1	5.9	0.005	0.83	2.17
CD-96-2C	1210	0.02	0.18	14.9	410	12.1	5.6	0.002	0.94	1.24
CD-96-2C	1220	0.02	0.14	43	360	5.4	4.2	0.011	0.75	2.52
CD-96-2C	1230	0.02	0.17	41.6	370	10	4.8	0.015	1.03	4.13
CD-96-2C	1240	0.02	0.13	36.8	470	9.8	4.9	0.016	1.07	4.77
CD-96-2C	1250	0.01	0.2	20.9	400	6.8	3.9	0.007	0.69	4.46
CD-96-2C	1260	0.01	0.1	13.1	220	6.6	4.9	0.002	0.49	1.52
CD-96-2C	1270	0.02	0.1	15.7	330	7.3	5.4	0.004	0.61	2.76
CD-96-2C	1280	0.01	0.08	14.3	270	8.3	6.6	0.002	0.65	2.1
CD-96-2C	1290	0.01	0.09	11.3	230	9.1	5.9	0.002	0.43	0.82
CD-96-2C	1300	0.02	0.07	11	240	8.1	6.7	0.001	0.45	0.66
CD-96-2C	1310	0.02	0.09	12.4	220	7.5	7.5	0.002	0.46	0.98
CD-96-2C	1320	0.01	0.1	11.3	220	6.7	6.6	0.002	0.46	2.92
CD-96-2C	1330	0.01	0.1	11.3	200	6.4	6.3	0.002	0.36	0.74
CD-96-2C	1340	0.02	0.1	11.9	230	7.1	7.1	0.002	0.38	0.75
CD-96-2C	1350	0.02	0.08	9.9	230	6.1	5.6	0.001	0.41	0.47
CD-96-2C	1360	0.02	0.07	14.7	210	6.7	7.5	0.003	0.49	1.18
CD-96-2C	1370	0.02	0.08	13.7	200	7.5	6.6	0.003	0.48	2.11
CD-96-2C	1380	0.02	0.08	15.9	220	7.6	8.9	0.003	0.55	2.28
CD-96-2C	1390	0.02	0.08	18.8	260	7.6	10.5	0.002	0.57	1.47
CD-96-2C	1400	0.02	0.1	18.2	190	7	6.9	0.004	0.55	1.96
CD-96-2C	1410	0.02	0.1	17.6	200	6.6	7.5	0.003	0.52	2.48
CD-96-2C	1420	0.02	0.11	19.5	160	6.8	6.6	0.004	0.59	1.75
CD-96-2C	1430	0.02	0.12	17.9	170	6.5	6.6	0.003	0.5	2.16
CD-96-2C	1440	0.02	0.07	17.8	190	7.2	5.4	0.012	0.62	4.31
CD-96-2C	1450	0.01	0.08	24.5	310	8.3	6.2	0.029	0.55	6.79
CD-96-2C	1460	0.02	0.1	20.5	160	6.4	6.1	0.018	0.49	4.3
CD-96-2C	1470	0.02	0.11	20.4	160	8.2	7.3	0.01	0.5	3.92
CD-96-2C	1480	0.02	0.11	13.9	180	5.8	6.2	0.002	0.46	1.1
CD-96-2C	1490	0.02	0.09	23	280	7.4	10.4	0.004	0.64	1.63
CD-96-2C	1500	0.02	0.12	19.8	210	6.4	8.2	0.009	0.51	1.66
CD-96-2C	1510	0.02	0.16	25	310	22	10.2	0.004	0.66	1.72
CD-96-2C	1520	0.02	0.1	24.2	350	11.1	11.5	0.011	0.6	1.59
CD-96-2C	1530	0.02	0.19	20.6	280	23.4	8.2	0.012	0.45	2.96
CD-96-2C	1540	0.02	0.11	17.1	200	7.6	7.2	0.005	0.44	1.7
CD-96-2C	1550	0.02	0.12	19.8	340	17.8	9.6	0.004	0.47	1.45
CD-96-2C	1560	0.02	0.09	23.3	270	9.4	11.8	0.008	0.63	1.63
CD-96-2C	1570	0.02	0.11	28.3	350	15.6	12.3	0.016	0.91	4.06
CD-96-2C	1580	0.02	0.12	25.8	200	12.7	7.7	0.023	0.71	4.32
CD-96-2C	1590	0.02	0.11	21.6	290	12.8	8.1	0.008	0.61	2.85
CD-96-2C	1600	0.02	0.09	20.9	190	8.2	8.7	0.007	0.52	2.31
CD-96-2C	1610	0.02	0.07	15.7	200	7.7	9.4	0.002	0.49	1.27
CD-96-2C	1620	0.02	0.07	16.4	210	7.6	9.6	0.003	0.46	1.98

SAMPLE	Depth (ft)	Na ppm	Nb ppm	Ni ppm	P ppm	Pb ppm	Rb ppm	Re ppm	S ppm	Sb ppm
CD-96-2C	1630	0.02	0.11	17.2	210	6.7	7.1	0.007	0.49	3.5
CD-96-2C	1640	0.02	0.11	19.2	180	7.2	7.8	0.017	0.52	4.19
CD-96-2C	1650	0.02	0.09	15.9	220	8.1	6.9	0.008	0.57	3.39
CD-96-2C	1660	0.02	0.15	21.3	210	8.9	7.2	0.011	0.76	5.37
CD-96-2C	1670	0.02	0.09	24	250	7.9	6	0.023	0.81	7.09
CD-96-2C	1680	0.02	0.1	17.3	520	6.4	6.2	0.018	0.58	5.77
CD-96-2C	1690	0.02	0.14	9.3	300	3.4	3.7	0.003	0.45	2.93
CD-96-2C	1700	0.02	0.16	20.5	190	6.9	5.9	0.01	0.77	7.22
CD-96-2C	1710	0.02	0.14	15.8	160	6.8	6.5	0.013	0.54	7.61
CD-96-2C	1720	0.01	0.17	15.6	170	6.5	8.5	0.009	0.62	6.52
CD-96-2C	1730	0.02	0.18	14.8	190	6.2	6.5	0.013	0.51	7.52
CD-96-2C	1740	0.02	0.19	15.8	140	6.9	6.6	0.013	0.55	7.67
CD-96-2C	1750	0.02	0.25	17.6	220	7	6.4	0.013	0.56	5.95
CD-96-2C	1760	0.02	0.17	13.5	180	5.7	6.8	0.006	0.52	4.26
CD-96-2C	1770	0.02	0.18	18.6	340	7.4	8.3	0.008	0.71	5
CD-96-2C	1780	0.02	0.18	15.4	150	6.6	6.9	0.011	0.59	5.12
CD-96-2C	1790	0.01	0.23	26.3	600	10.3	6.9	0.018	1.01	7.51
CD-96-2C	1800	0.01	0.16	15.4	130	5	4.8	0.016	0.47	6.26
CD-96-2C	1810	0.02	0.23	22.4	400	11.6	6.3	0.022	0.75	7.77
CD-96-2C	1820	0.02	0.22	13.9	130	6.6	5.4	0.018	0.53	6.33
CD-96-2C	1830	0.02	0.22	17.2	270	6.8	6.1	0.018	0.67	6.2
CD-96-2C	1840	0.02	0.25	17.5	270	6.9	5.5	0.018	0.65	6.09
CD-96-2C	1860	0.01	0.16	17.5	190	23.9	6.4	0.016	2.1	10.45
CD-96-2C	1880	0.02	0.15	20.8	180	8.9	6.5	0.021	0.83	6.53
CD-96-2C	1900	0.02	0.18	18.1	210	5.9	5.9	0.02	0.57	4.88
CD-96-2C	1920	0.01	0.16	20.7	300	7.9	4.9	0.024	0.71	7.73
CD-96-2C	1925	0.01	0.14	19.1	170	7.8	5.1	0.016	0.72	7.93
CD-96-2C	1930	0.02	0.12	16.1	150	6.1	4.9	0.014	0.64	7.02
CD-96-2C	1940	0.02	0.14	15.3	160	5.8	5.6	0.012	0.66	6.41
CD-96-2C	1960	0.02	0.18	13.3	150	5.5	5.8	0.008	0.48	5.13
CD-96-2C	1980	0.02	0.19	11.6	130	5.3	5.7	0.008	0.47	4.71
CD-96-2C	2000	0.02	0.19	11.5	120	4.7	6.3	0.009	0.48	5.21
CD-96-2C	2020	0.02	0.18	12	120	5.2	7.1	0.009	0.51	5.22
CD-96-2C	2025	0.02	0.2	11.3	150	4.8	4.4	0.015	0.47	5.06
CD-96-2C	2030	0.02	0.2	11.2	120	6.2	4.9	0.008	0.5	4.57
CD-96-2C	2035	0.01	0.19	9.8	140	6.9	4.6	0.008	0.63	9.56
CD-96-2C	2040	0.01	0.13	5.4	660	10.3	12.1	0.003	1.2	7.99
CD-96-2C	2045	0.01	0.21	10.7	320	6.6	8.6	0.01	0.7	7.1
CD-96-2C	2050	0.02	0.23	12.1	130	4.4	4.5	0.012	0.46	4.26
CD-96-2C	2055	0.02	0.23	7.8	110	4.1	3.3	0.009	0.35	5.37
CD-96-2C	2060	0.01	0.16	5.1	610	7.7	11.5	0.004	1.07	6.87
CD-96-2C	2065	0.02	0.26	11.8	180	5.5	5.6	0.016	0.47	3.54
CD-96-2C	2070	0.02	0.24	12.5	270	8.3	6	0.017	0.76	5.11
CD-96-2C	2075	0.01	0.14	6.9	550	15.9	9.7	0.006	1.64	8.1
CD-96-2C	2080	0.01	0.05	3.1	730	13.8	12.9	0.001	2.03	6.17
CD-96-2C	2100	0.02	0.07	24.1	1540	11.6	6.4	0.027	0.88	12.65
CD-96-2C	2120	0.02	0.07	38.9	6970	13.7	10.5	0.051	0.85	7.4
CD-96-2C	2180	0.02	0.08	22.2	2500	7.1	3.5	0.016	0.53	4.27
CD-96-2C	2200	0.02	0.07	45.1	3830	14	5.8	0.057	0.76	9.33
CD-96-2C	2220	0.02	0.08	13.2	2330	14.3	6.7	0.007	0.79	10
CD-96-2C	2240	0.01	<0.05	4.4	730	20	13.2	0.001	2.3	8

SAMPLE	Depth (ft)	Na ppm	Nb ppm	Ni ppm	P ppm	Pb ppm	Rb ppm	Re ppm	S ppm	Sb ppm
CD-96-2C	2260	0.02	0.09	4.5	710	7.3	3.6	0.005	0.47	4.65
CD-96-2C	2280	0.02	0.09	3.8	240	5	1.3	0.004	0.21	6.16
CD-96-2C	2300	0.02	0.08	3	40	2.7	0.8	0.001	0.17	5.58
CD-96-2C	2320	0.02	0.08	2.1	70	37.3	0.5	0.001	0.13	8.85
CD-96-2C	2340	0.02	0.08	1.9	50	7.3	0.4	0.001	0.08	2.12
DR-1C	2480	0.02	0.11	107	910	54.9	5.3	0.023	1.57	5.19
DR-1C	2500	0.03	0.08	86.5	480	11.1	5.2	0.035	0.81	6.37
DR-1C	2520	0.02	0.08	76.4	300	13.3	4.2	0.03	0.89	5.2
DR-1C	2540	0.02	0.09	74.3	400	7.1	4	0.026	0.9	4.89
DR-1C	2560	0.01	0.12	79.1	510	11.5	3.3	0.026	0.99	3.77
DR-1C	2580	0.02	0.12	59	510	8	4.4	0.021	0.91	4.38
DR-1C	2600	0.01	0.1	54.7	590	8.8	6.4	0.023	1.33	5.41
DR-1C	2620	0.02	0.11	62.1	420	10	3.9	0.023	1.03	4.32
DR-1C	2640	0.02	0.09	69.2	520	5.6	4.7	0.018	0.95	2.92
DR-1C	2660	0.02	0.09	56.1	360	6.7	5.7	0.018	1.2	3.61
DR-1C	2680	0.02	0.08	56.2	420	6.9	6.4	0.028	1.07	4.18
DR-1C	2700	0.02	0.06	53.8	500	8.5	8.5	0.031	1.37	6.23
DR-1C	2720	0.02	0.05	39.2	370	10.4	9.5	0.014	1.75	11.95
DR-1C	2740	0.02	0.06	30.5	460	7.6	8.8	0.011	0.92	4.76
DR-1C	2760	0.02	0.08	22.6	620	6.3	7.8	0.006	0.76	1.61
DR-1C	2780	0.01	0.07	17.2	630	5.2	8.2	0.004	0.58	0.55
DR-1C	2800	0.01	0.05	19.1	420	6.5	9.5	0.003	0.49	0.47
DR-1C	2820	0.02	0.06	26.1	400	9	10.2	0.007	0.99	2.14
DR-1C	2840	0.01	0.05	19	280	7.8	7.2	0.002	0.86	2.06
DR-1C	2860	0.01	0.07	18.8	400	10.4	9.9	0.003	0.8	0.7
DR-1C	2880	0.02	0.05	23.9	460	8.9	10	0.007	1	1.24
DR-1C	2900	0.02	0.05	20.7	420	8.9	9.9	0.003	0.65	1.02
DR-1C	2917	0.02	0.05	23.9	480	8.2	9.2	0.008	0.63	1.05
GA-2A	1680	0.01	0.21	52.9	700	8.7	6.4	0.023	1.41	9.07
GA-2A	1690	0.02	0.32	51.7	680	10.5	7.2	0.022	1.21	6.84
GA-2A	1700	0.03	0.24	56.6	670	11.3	9.1	0.021	2.02	6.49
GA-2A	1710	0.03	0.16	68.2	850	11	12.4	0.03	2.3	5.64
GA-2A	1720	0.02	0.13	75.9	3530	8.5	21.6	0.045	2.31	15.75
GA-2A	1730	0.02	0.21	61.2	4350	9.6	11.5	0.035	1.75	15.5
GA-2A	1740	0.02	0.12	84.7	620	8.6	10.1	0.053	2.01	11.25
GA-2A	1750	0.02	0.13	56.3	450	17.3	10	0.036	1.55	4.86
GA-2A	1760	0.02	0.14	62.5	400	17.6	7.4	0.071	1.7	8.26
GA-2A	1770	0.02	0.15	72.3	560	12.2	9.2	0.047	1.52	13.05
GA-2A	1780	0.02	0.19	76.2	370	9.1	11.1	0.062	1.43	11.85
GA-2A	1790	0.03	0.15	73.7	590	20.4	11.9	0.067	1.69	9.16
GA-2A	1800	0.02	0.13	162	870	17.2	10.7	0.147	1.59	16.55
GA-2A	1810	0.02	0.2	130	1170	10.5	9.6	0.164	0.93	29.7
GA-2A	1820	0.02	0.18	114	1660	16.9	7.3	0.115	1.09	24.8
GA-2A	1830	0.03	0.16	79.6	8080	8.8	10.7	0.06	1.6	14.25
GA-2A	1840	0.02	0.12	57.2	1860	10.4	8	0.025	2.15	7.33
GA-2A	1850	0.01	0.14	64.2	1330	17.5	8.7	0.02	3.78	20.7
GA-2A	1860	0.01	0.08	47	1790	15	9	0.012	3.68	21.1
GA-2A	1870	0.02	0.15	35.3	1390	12	7.2	0.007	2.56	20
GA-2A	1880	0.01	0.11	29.2	1040	9.6	5.8	0.007	1.63	33
GA-2A	1890	0.04	0.17	33.6	3670	9.7	7.4	0.01	1.92	20
GA-2A	1900	0.02	0.21	34.8	1050	10	5.9	0.012	1.78	19.2

SAMPLE	Depth (ft)	Na ppm	Nb ppm	Ni ppm	P ppm	Pb ppm	Rb ppm	Re ppm	S ppm	Sb ppm
GA-2A	1910	0.02	0.26	29.5	1010	11.2	6	0.006	2.27	18
GA-2A	1920	0.02	0.19	21	670	8.3	4.3	0.003	1.64	29
GA-2A	1930	0.02	0.26	28.5	930	11.1	4.5	0.006	3.15	33.4
GA-2A	1940	0.01	0.28	30	640	14.8	4.7	0.01	2.13	66.2
GA-2A	1950	0.01	0.22	40.7	1610	9.9	5.4	0.018	2.49	139
GA-2A	1960	0.01	0.4	52.4	1000	9.9	4	0.023	2.13	130.5
GA-2A	1970	0.01	0.49	47.6	430	14.4	4.5	0.031	1.5	56
GA-2A	1980	0.01	0.62	45	640	17.9	4.2	0.006	2.49	60.5
GA-2A	1990	0.01	0.43	40.4	1440	16.1	5.2	0.01	2.38	51.2
GA-2A	2000	0.01	0.48	37.2	560	26.1	3.3	0.007	1	78.1
GA-2A	2010	0.01	0.4	41.4	660	44.8	2.5	0.003	1.11	219
GA-2A	2020	0.01	0.55	35	730	39.7	1.7	0.005	0.77	136
GA-2A	2030	0.02	0.26	14.8	470	15.9	1.8	0.002	0.53	56.8
GA-2A	2040	0.02	0.23	16.3	590	15.7	2.3	0.005	0.63	51.5
GA-2A	2050	0.02	0.28	5.3	240	4.6	2	0.002	0.21	9.09
GA-2A	2060	0.02	0.27	5.6	330	2.9	1.8	0.001	0.25	4.94
GA-2A	2070	0.03	0.33	6.7	570	3.8	2	0.002	0.33	7.35
GA-2A	2080	0.02	0.41	12.6	960	6.2	3.7	0.005	1.01	10.1
GA-2A	2100	0.02	0.47	14.2	860	4.8	2.7	0.007	1.11	8.07
GA-2A	2110	0.02	0.53	10.9	1190	4.7	2.5	0.004	0.88	7.26
GA-2A	2120	0.02	0.59	15.7	1420	5.5	2.7	0.005	1.46	9.26
GA-35C	1680	0.02	0.06	49.3	740	27.3	6	0.027	1.83	9.98
GA-35C	1700	0.02	0.06	45.7	290	37.7	7.3	0.015	2.02	4.17
GA-35C	1720	0.02	0.07	36.2	1490	27.1	9.3	0.012	1.62	3.47
GA-35C	1740	0.02	0.08	80	910	29.8	10.8	0.004	2.97	9.55
GA-35C	1760	0.02	0.08	57.8	810	38.1	10.2	0.002	2.86	9.78
GA-35C	1780	0.02	0.09	25.3	300	31.9	7.2	0.004	1.9	3.07
GA-35C	1800	0.03	0.1	59.3	310	35.8	4.6	0.023	2.21	13.1
GA-35C	1820	0.02	0.08	68.6	410	18.7	3.8	0.029	0.94	11.85
GA-35C	1840	0.02	0.06	70.6	660	16.1	3.8	0.013	1.43	33.9
GA-35C	1860	0.01	0.06	84.3	720	26.1	3.5	0.013	1.23	25.7
GA-35C	1880	0.01	0.06	94.9	1290	20	5.1	0.013	2.27	94.7
GA-35C	1900	0.01	0.09	130.5	2280	22.6	10.2	0.016	3.58	73.9
GA-35C	1920	0.01	0.07	115.5	2130	27.4	11.6	0.008	3.85	79.5
GA-35C	1940	0.01	<0.05	27.8	840	54.9	6.2	0.01	1.74	57
GA-35C	1960	0.01	<0.05	28.7	950	53.1	6.3	0.01	1.9	70.3
GA-35C	1980	0.01	<0.05	45	1390	155	5.9	0.022	1.33	21.7
GA-35C	2000	0.01	<0.05	34.9	1310	43.3	5.2	0.013	1.25	27
GA-35C	2020	0.01	<0.05	36.4	1330	87.4	6	0.015	1.28	20.1
GA-35C	2040	0.02	0.1	25.3	970	34.1	5.1	0.009	0.96	23.7
GA-35C	2060	0.02	0.12	12.6	400	26.1	3	0.003	0.68	20.9
GA-35C	2080	0.01	0.1	151.5	3010	20.8	14	0.002	3.41	139.5
GA-35C	2100	0.01	<0.05	24.2	660	13.8	7.8	0.002	0.98	40.8
GA-35C	2120	0.02	<0.05	17.3	560	11.5	9.4	0.001	0.71	22.6
GA-35C	2140	0.02	0.08	14	340	8.7	6.3	0.002	0.59	24.5
GA-35C	2160	0.02	0.12	8.8	200	6	3.7	0.001	0.39	16.85
GA-35C	2186	0.02	0.07	15.2	290	10.7	6.5	0.002	0.69	20.5
SJ-390C	640	0.005	0.07	209	960	26.4	17.6	0.18	1.41	28.4
SJ-390C	650	0.02	0.11	160.5	9210	22.1	26	0.195	1.56	40
SJ-390C	660	0.02	0.12	138	10000	32.9	23.5	0.113	1.98	32
SJ-390C	670	0.02	0.11	101.5	10000	22.5	16.2	0.064	2.21	43.9

SAMPLE	Depth (ft)	Na ppm	Nb ppm	Ni ppm	P ppm	Pb ppm	Rb ppm	Re ppm	S ppm	Sb ppm
SJ-390C	680	0.01	0.14	86.6	5320	40.2	13.1	0.034	2.15	33.4
SJ-390C	690	0.01	0.1	62.5	3620	17.6	13.2	0.021	2.26	24.3
SJ-390C	700	0.01	0.07	48.7	1640	15	21.2	0.017	2.32	19.05
SJ-390C	710	0.01	0.06	49.4	510	16.6	34.6	0.015	2.7	33
SJ-390C	720	0.01	0.06	59.9	1130	28.2	20.6	0.014	3.98	133.5
SJ-390C	730	0.005	0.07	58.1	1540	19.5	11	0.015	3.75	148
SJ-390C	740	0.01	0.06	73.7	1390	539	18.7	0.021	3.97	124.5
SJ-390C	750	0.01	0.05	43.9	1040	166.5	9.5	0.008	3.15	130.5
SJ-390C	760	0.01	0.05	43.2	860	65.5	6.6	0.007	3.81	149
SJ-390C	770	0.01	0.06	20.9	660	21.9	5.2	0.004	1.67	55.2
SJ-390C	780	0.02	0.06	19.9	530	28.8	5.7	0.004	1.98	55
SJ-390C	790	0.01	0.05	18.9	490	37.9	5.2	0.003	1.57	37.1
SJ-390C	800	0.01	0.05	16.1	430	15.7	4.3	0.003	1.52	49.6
SJ-390C	900	0.02	0.07	13.9	220	7.9	31.3	0.002	1.22	1.64
SJ-390C	920	0.02	0.05	49.4	410	15.6	30.9	0.031	1.49	7.1
SJ-390C	940	0.02	0.05	102.5	450	11.6	21.3	0.059	2.13	80.8
SJ-390C	960	0.02	0.05	96.8	390	16.7	8.3	0.054	1.2	13.95
SJ-390C	965	0.02	0.06	70.5	380	12.4	9.7	0.036	0.84	7.93
SJ-390C	970	0.01	0.025	61.8	400	10.4	4.1	0.032	0.85	5.54
SJ-390C	975	0.02	0.025	44	420	6.3	3.5	0.016	0.79	4.31
SJ-390C	980	0.02	0.025	50.7	420	8.1	3.1	0.013	0.86	5.23
SJ-390C	985	0.01	0.06	54	350	9.1	9.3	0.019	0.78	3.98
SJ-390C	990	0.02	0.06	65.9	470	8.5	10.8	0.02	0.99	20.8
SJ-390C	995	0.01	0.05	74	480	7.6	4.4	0.019	1.05	29.8
SJ-390C	1000	0.01	0.025	62.8	450	5.9	3.3	0.013	0.75	8.53
SJ-390C	1005	0.01	0.025	61.3	450	4.7	3.7	0.021	0.57	4.74
SJ-390C	1010	0.01	0.025	59.2	390	6.3	5.6	0.022	0.87	11.65
SJ-390C	1015	0.01	0.11	54	400	8	6.7	0.027	1.8	142
SJ-390C	1020	0.01	0.05	44.3	420	6.5	12	0.026	1.21	28
SJ-390C	1025	0.01	0.06	54.2	400	8.7	28.9	0.039	1.17	5.74
SJ-390C	1030	0.01	0.06	41.9	360	7.6	11.8	0.027	1.2	7
SJ-390C	1035	0.01	0.06	39.7	440	5.8	47.3	0.024	1.2	2.23
SJ-390C	1040	0.01	0.05	31.5	400	2.4	52.3	0.018	0.84	0.62
SJ-390C	1060	0.01	0.06	79.4	930	17.1	7.8	0.05	0.81	20.8
SJ-390C	1095	0.005	0.05	22.7	400	5.3	3.1	0.005	1.13	7.31
SJ-390C	1100	0.01	0.06	19.2	380	5.4	8.2	0.002	1.09	6.67
SJ-390C	1105	0.01	0.06	10.7	360	4.1	5.9	0.001	1.08	3.84
SJ-390C	1110	0.01	0.06	22.9	320	4.7	7.7	0.001	1.37	14
SJ-390C	1115	0.01	0.025	22.7	370	7.9	4.1	0.006	1.48	45.7
SJ-390C	1120	0.01	0.06	16.9	280	5.4	2.5	0.0005	0.96	31.9
SJ-390C	1125	0.01	0.05	11.2	470	7.2	1.8	0.001	1.22	45.5
SJ-390C	1130	0.005	0.06	18.5	610	6.9	2.2	0.005	1.15	39.4
SJ-390C	1135	0.01	0.06	11.6	390	6.4	1.8	0.001	0.94	30
SJ-390C	1140	0.01	0.06	18.3	300	7	2.6	0.001	0.95	8.23
SJ-390C	1160	0.01	0.08	16.3	280	6.5	1.3	0.003	0.91	7.4
SJ-390C	1180	0.01	0.07	15.4	530	5.5	1.2	0.002	1	5.83
SJ-390C	1200	0.01	0.08	19.8	1090	6.8	3.9	0.004	0.97	16.65
SJ-390C	1220	0.01	0.07	17.1	940	6.5	3.6	0.004	0.88	6.21
SJ-390C	1240	0.01	0.05	29.8	1480	4.7	5.9	0.01	0.69	14.4
SJ-390C	1260	0.01	0.07	26.2	360	4	2.5	0.015	0.71	7.6
SJ-390C	1280	0.01	0.09	2.9	410	2.5	2.1	0.003	0.39	4.1

SAMPLE	Depth (ft)	Na ppm	Nb ppm	Ni ppm	P ppm	Pb ppm	Rb ppm	Re ppm	S ppm	Sb ppm
SJ-390C	1295	0.01	0.06	17.8	540	4.6	5.5	0.002	0.87	5.63
SJ-464C	10	0.08	0.25	84.2	2200	13	14.7	0.0005	0.08	3.1
SJ-464C	20	0.09	0.12	239	2980	19	15.4	0.0005	0.04	1.8
SJ-464C	30	0.01	0.025	19.4	1060	7.9	15.9	0.0005	0.05	0.5
SJ-464C	240	0.005	0.025	54.3	300	9.5	9.6	0.067	1.81	1.82
SJ-464C	250	0.005	0.025	44.4	460	7.5	10.6	0.043	1.52	1.08
SJ-464C	260	0.01	0.025	33.6	330	6.2	10.9	0.027	1.31	0.85
SJ-464C	270	0.005	0.025	45.5	360	8.9	14	0.058	1.65	1.9
SJ-464C	280	0.01	0.025	31.8	580	6.1	11.2	0.035	1.04	0.69
SJ-464C	290	0.02	0.05	38.3	550	7.5	17.1	0.035	1.05	1.1
SJ-464C	300	0.01	0.025	29.4	610	5.9	10.6	0.019	1.08	0.93
SJ-464C	310	0.02	0.025	22.2	610	6.4	9.3	0.006	1.05	1.76
SJ-464C	320	0.02	0.025	27.2	480	7.1	9.4	0.019	1.44	1.95
SJ-464C	330	0.005	0.025	54.8	1100	7.5	10.3	0.089	1.2	3.96
SJ-464C	370	0.005	0.025	52.2	2150	9.8	11	0.048	1.14	16.9
SJ-464C	380	0.005	0.05	45.4	2800	8.3	12.3	0.041	1.2	16.85
SJ-464C	390	0.01	0.06	34.5	700	4.9	9.5	0.014	1.24	3.77
SJ-464C	400	0.02	0.06	28.1	650	4.7	7.6	0.007	1.2	2.54
SJ-464C	410	0.02	0.06	19.6	920	4.2	6.2	0.009	0.87	1.62
SJ-464C	420	0.02	0.06	20.2	830	5.2	6.8	0.007	1	1.5
SJ-464C	430	0.01	0.06	16.7	650	4.9	6.1	0.002	0.53	1.31
SJ-464C	440	0.02	0.06	17.4	640	7.1	6.6	0.002	0.83	0.92
SJ-464C	450	0.01	0.06	12.9	560	4.7	4.9	0.002	0.65	1.71
SJ-464C	460	0.01	0.06	13.9	570	5	3.9	0.003	0.56	2.69
SJ-464C	470	0.01	0.07	26	760	6.3	6.5	0.009	1.04	3.75
SJ-464C	480	0.01	0.07	18.9	810	6.3	6	0.004	0.77	2.91
SJ-464C	490	0.01	0.07	33.2	1080	7.7	7.9	0.019	0.99	3.44
SJ-464C	500	0.01	0.07	34.6	1900	6.7	8	0.024	0.82	3.43
SJ-464C	510	0.01	0.06	25.2	720	6.3	8.3	0.007	0.93	1.45
SJ-464C	520	0.01	0.07	25.5	600	5.8	9.5	0.005	0.94	1.17
SJ-464C	530	0.01	0.07	23.8	970	6	8.7	0.006	0.85	1.35
SJ-464C	540	0.01	0.05	37.1	930	7.2	8	0.027	0.9	1.72
SJ-464C	690	0.005	0.05	30.9	270	9.4	3.1	0.016	0.54	3.77
SJ-464C	700	0.005	0.06	34.8	380	9.7	5.4	0.012	1.57	6.27
SJ-464C	710	0.02	0.1	35.6	510	11.2	9.8	0.008	2.15	6.06
SJ-464C	720	0.01	0.1	29.9	430	8.7	9.6	0.006	2.19	5.35
SJ-464C	740	0.07	0.12	47.5	490	9.4	10.6	0.027	1.84	4.66
SJ-464C	750	0.01	0.08	124	610	5.6	12.8	0.143	1.13	18.65
SJ-464C	760	0.01	0.09	210	1050	8.6	16	0.255	1.38	30.3
SJ-464C	770	0.01	0.09	178.5	1020	9.3	14.9	0.216	1.63	20
SJ-464C	780	0.02	0.09	140.5	1860	7.5	12.9	0.19	1.11	14.5
SJ-464C	790	0.02	0.1	132	6700	7.8	15.8	0.184	1.49	16.3
SJ-464C	800	0.03	0.1	120	9350	7.2	15.5	0.137	1.81	13.35
SJ-464C	810	0.02	0.09	103.5	7340	6.9	15	0.079	2.14	8.34
SJ-464C	820	0.02	0.1	86.3	8780	6.3	15.9	0.069	1.91	6.3
SJ-464C	830	0.02	0.1	69.2	8080	5.9	12.8	0.055	1.6	5.3
SJ-464C	840	0.02	0.1	69.4	5270	6.1	10.8	0.047	1.69	4.19
SJ-464C	850	0.02	0.1	67.9	4000	6.5	10.7	0.036	1.76	2.93
SJ-464C	860	0.02	0.09	47	2390	6.2	9.9	0.021	1.62	2.06
SJ-464C	870	0.02	0.025	52.3	1850	7	9.6	0.019	1.81	3.15
SJ-464C	880	0.01	0.025	48.9	1280	9	9.2	0.015	2.08	3.39

SAMPLE	Depth (ft)	Na ppm	Nb ppm	Ni ppm	P ppm	Pb ppm	Rb ppm	Re ppm	S ppm	Sb ppm
SJ-464C	900	0.02	0.025	68.8	1220	9.6	9.3	0.028	2.29	36.4
SJ-464C	920	0.02	0.025	40.5	390	12.1	8.6	0.01	2.25	60.1
SJ-464C	940	0.01	0.025	22.5	320	10.3	7.6	0.004	1.76	27
SJ-464C	960	0.02	0.05	22.6	340	13.3	11	0.004	1.78	3.08
SJ-464C	980	0.02	0.06	13.4	280	10.1	8.7	0.004	1.21	1.97
SJ-464C	1000	0.02	0.05	20.2	250	11	9.6	0.004	1.27	6.21
SJ-464C	1020	0.01	0.06	0.1	280	4.9	6.4	0.001	0.65	2.32
SJ-464C	1040	0.02	0.06	4.1	240	6	7.7	0.002	0.82	5.25
SJ-464C	1060	0.02	0.06	0.1	190	3.2	3.9	0.001	0.45	1.79
SJ-464C	1080	0.02	0.07	3	250	5.9	6.2	0.001	0.95	1.69
SJ-464C	1100	0.02	0.06	10.9	290	9	8.1	0.001	1.45	4.83
SJ-464C	1120	0.02	0.025	67	380	7	5.9	0.037	1.32	13.7
SJ-464C	1140	0.01	0.025	107	450	6.5	4.8	0.041	1.21	28.7
SJ-464C	1215	0.01	0.025	47.3	460	8.2	8.8	0.021	2.01	32
SJ-464C	1220	0.01	0.025	29	310	5.7	5.8	0.011	1.22	29.7
SJ-464C	1225	0.01	0.025	23.9	310	6.5	5.2	0.008	1.09	22.7
SJ-464C	1230	0.02	0.025	32.2	660	5.9	6.2	0.014	1.21	18
SJ-464C	1235	0.01	0.05	31.2	710	5.7	5.1	0.01	1.05	13.95
SJ-464C	1240	0.02	0.025	21.3	880	6	6	0.005	1.29	24.8
SJ-464C	1245	0.01	0.025	30.4	670	5.8	5.3	0.01	1.28	19.9
SJ-464C	1250	0.02	0.025	25	530	5.3	5.1	0.009	1.01	19.2
SJ-464C	1255	0.02	0.025	29.2	710	11	6.9	0.008	1.26	25.2
SJ-464C	1260	0.02	0.025	24.1	460	6.9	6.6	0.006	1.28	18.5
SJ-464C	1265	0.02	0.05	28	540	7.8	7.5	0.009	1.41	21
SJ-464C	1270	0.02	0.06	13	310	7.5	5.8	0.004	1	18.7
SJ-464C	1275	0.02	0.05	16	470	6.6	6.4	0.003	1.18	13
SJ-464C	1280	0.02	0.05	12	310	6.3	6.5	0.002	0.99	16.6
SJ-464C	1285	0.02	0.025	16.7	400	7.4	7.8	0.003	1.26	21.9
SJ-464C	1290	0.02	0.025	16.4	460	6.5	7.1	0.003	1.19	32.7
SJ-464C	1295	0.02	0.025	15.3	310	9.8	7.3	0.002	1.02	22.9
SJ-464C	1300	0.02	0.025	20.2	480	6.8	7.1	0.004	1.12	26.5
SJ-464C	1305	0.02	0.025	15.7	330	6.7	7.7	0.002	1.14	23.3
SJ-464C	1310	0.02	0.025	31.3	570	14.1	6.9	0.009	1.15	28.5
SJ-464C	1315	0.01	0.025	17.9	660	6.7	8.1	0.004	1.12	26.8
SJ-464C	1320	0.01	0.025	23.1	420	7.2	9.9	0.004	1.52	34.8
SJ-464C	1325	0.01	0.025	22.4	530	7.6	10.3	0.005	1.35	28.6
SJ-464C	1330	0.01	0.025	20	340	6.5	8.9	0.004	1.17	17
SJ-464C	1335	0.01	0.025	23	360	8.1	10.8	0.007	1.48	40.3
SJ-464C	1340	0.01	0.025	16.8	780	5.8	6.9	0.004	0.87	12.1
SJ-464C	1345	0.005	0.025	16.4	570	5.7	6.1	0.003	1.02	18.3
SJ-464C	1350	0.005	0.025	16	630	5.8	4.7	0.007	0.69	31.6
SJ-464C	1355	0.01	0.025	15.7	1390	7.1	7	0.004	0.86	33.1
SJ-464C	1360	0.01	0.025	17.5	360	6.8	6.6	0.004	0.96	19.4
SJ-464C	1365	0.01	0.025	18.3	490	8.9	11.6	0.005	1.04	19.65
SJ-464C	1370	0.01	0.025	16.7	860	6.2	8.5	0.005	0.76	16.75
SJ-464C	1375	0.01	0.025	21.1	1110	7.7	9.9	0.008	0.92	15.4
SJ-464C	1380	0.01	0.025	23.3	1270	8.6	9.8	0.008	1.29	36.9
SJ-464C	1385	0.01	0.025	25.3	1200	8.9	8.7	0.007	1.32	23.9
SJ-464C	1390	0.005	0.025	18.3	880	4.8	5.1	0.008	0.73	34.4
SJ-464C	1395	0.01	0.025	25.1	1130	7.7	7	0.008	1.11	39.9
SJ-464C	1400	0.01	0.025	36.2	1530	9.8	8.3	0.009	1.64	75.1

SAMPLE	Depth (ft)	Na ppm	Nb ppm	Ni ppm	P ppm	Pb ppm	Rb ppm	Re ppm	S ppm	Sb ppm
SJ-464C	1405	0.01	0.05	22.2	1280	4.5	5.8	0.007	0.77	24
SJ-464C	1410	0.005	0.025	22.7	770	4.4	5.8	0.008	0.75	16.8
SJ-464C	1415	0.01	0.025	25.3	800	5	7	0.01	0.82	14.75
SJ-464C	1420	0.01	0.025	34.8	810	6.4	8	0.017	0.91	17.8
SJ-464C	1425	0.005	0.025	22.3	1950	6.9	7.2	0.008	0.99	66.6
SJ-464C	1430	0.005	0.06	6.3	640	2.7	1.7	0.003	0.37	35.1
SJ-464C	1435	0.005	0.07	1.3	180	2.4	0.6	0.001	0.11	316
SJ-464C	1440	0.01	0.22	5.7	140	1.7	0.7	0.001	0.08	18.9
SJ-464C	1445	0.01	0.07	1.1	120	0.6	0.4	0.0005	0.05	3.74
SJ-464C	1450	0.02	0.09	3.1	240	1.6	1.7	0.001	0.16	2.29
SJ-464C	1455	0.02	0.06	5.5	460	3.6	3.7	0.001	0.39	3.34
SJ-464C	1460	0.02	0.09	2.3	180	1.5	1.9	0.001	0.22	6.64
SJ-464C	1465	0.02	0.08	2.2	210	1.7	2.1	0.001	0.23	5.42
WM-01C	2440	0.01	0.06	58.9	2820	11.7	8.2	0.057	1.15	10.7
WM-01C	2460	0.01	0.05	78.4	1250	13.2	6.1	0.083	1.19	17.25
WM-01C	2480	0.01	0.05	79	680	16.9	5.3	0.062	1.11	13.5
WM-01C	2500	0.01	0.05	52.7	420	17.7	5.2	0.033	1.15	11.9
WM-01C	2520	0.01	<0.05	42.3	2080	17.3	6.2	0.017	1.35	9.23
WM-01C	2540	0.01	0.06	69.3	1190	21.7	6.4	0.046	1.37	16
WM-01C	2560	0.01	0.12	18.7	360	9.1	3.1	0.006	0.7	5.02
WM-01C	2580	0.01	0.1	13.8	220	8.2	4.2	0.002	0.6	2.54
WM-01C	2600	0.02	0.08	53.1	370	11.7	5.3	0.023	1.5	10.8
WM-01C	2620	0.02	0.09	53.3	610	8.3	5.3	0.017	0.96	10.45
WM-01C	2640	0.02	0.07	24.2	420	8.1	6.9	0.005	1.05	4.31
WM-01C	2660	0.01	0.07	27.2	480	8.9	6.4	0.007	1.05	5.64
WM-01C	2680	0.01	0.05	23.1	580	7.2	8	0.004	0.92	6.55
WM-01C	2700	0.01	0.07	28.9	410	8.1	10.2	0.006	0.79	1.19
WM-01C	2720	0.01	0.08	25.1	490	11.9	8.5	0.004	1.03	2.52
WM-01C	2740	0.01	0.06	24.2	340	9.9	10.2	0.003	0.9	1.11
WM-01C	2760	0.01	0.06	25.8	440	12.5	9	0.005	1.52	2.51
WM-01C	2780	0.01	0.07	34.2	550	11.1	9.8	0.008	1.65	5.96
WM-01C	2800	0.01	0.05	24.1	570	7.4	9.7	0.005	1.33	7.77
WM-01C	2820	0.01	0.05	20.6	680	5.8	9	0.005	1.09	11.5
WM-01C	2840	0.01	<0.05	18.5	630	9	8.9	0.005	0.9	4.56
WM-01C	2860	0.01	<0.05	18.7	800	6.6	9.5	0.007	0.71	5.48
WM-01C	2880	0.01	0.05	27.7	1280	8.4	9.8	0.015	0.99	11.45
WM-01C	2900	0.01	0.06	28.5	4180	9.1	11.5	0.01	1.18	10.4
WM-01C	2920	0.01	0.05	23.5	890	11.9	6.2	0.005	0.88	6.16
WM-01C	2940	0.01	0.06	19.9	570	8.9	5.3	0.004	0.85	5.08
WM-01C	2960	0.01	0.07	23.3	320	11	5.2	0.005	0.87	5.53
WM-01C	2980	0.01	0.06	18.1	340	11.1	7.7	0.003	0.82	4.03
WM-01C	3000	0.02	0.06	15.9	360	7.8	7.1	0.002	0.55	2.37
WM-01C	3020	0.01	0.05	14.9	320	6.1	7.4	0.002	0.63	4.09
WM-01C	3040	0.02	0.08	17.9	270	7.2	7.1	0.005	0.59	3.11
WM-01C	3050	0.01	0.09	26.6	1140	8	9.8	0.006	0.72	3.8

SAMPLE	Depth (ft)	Sc ppm	Se ppm	Sn ppm	Sr ppm	Ta ppm	Te ppm	Th ppm	Ti ppm	Tl ppm	U ppm
BZ-965C	880	4.5	2	0.5	70.3	0.005	0.04	3.1	0.0025	1.44	4.13
BZ-965C	885	4.1	2.1	0.3	73.6	0.005	0.08	2.8	0.0025	0.81	4.56
BZ-965C	905	2.6	1	0.4	42.7	0.005	0.14	2	0.0025	1.34	8.43
BZ-965C	910	4.5	1.3	0.4	64.8	0.005	0.13	2.7	0.0025	1.22	6.66
BZ-965C	955	6.4	7.2	0.3	63.2	0.005	0.06	2.3	0.0025	2.37	8.53
BZ-965C	960	5.8	11.7	0.6	63.8	0.005	0.07	1.9	0.0025	3.84	12.65
BZ-965C	965	5.1	31.2	0.6	46.2	0.005	0.18	1.6	0.005	4.36	13.85
BZ-965C	970	4.5	23.3	0.6	55.7	0.005	0.14	1.4	0.0025	4.84	11.05
BZ-965C	975	5.8	21.7	0.6	89.1	0.005	0.1	3	0.0025	3.33	13.65
BZ-965C	980	4.7	24.3	0.6	94.9	0.005	0.11	1.8	0.0025	2.51	11.5
BZ-965C	1000	5.4	17.6	0.5	141	0.01	0.07	3.2	0.0025	0.5	9.26
BZ-965C	1020	4.6	12	0.4	120.5	0.005	0.04	2.6	0.0025	0.29	5.22
BZ-965C	1040	4	5.6	0.4	82	0.005	0.04	2.8	0.0025	0.2	3.34
BZ-965C	1060	4.4	3.1	0.3	68.4	0.005	0.04	3.4	0.0025	0.28	1.6
BZ-965C	1065	3.7	2.9	0.4	88.5	0.005	0.05	3.3	0.0025	0.21	2.3
BZ-965C	1070	3.6	2.8	0.5	85.1	0.005	0.04	3.5	0.0025	0.27	2.95
BZ-965C	1075	3.8	2.7	0.5	98.1	0.005	0.05	3.5	0.0025	0.17	1.61
BZ-965C	1080	4.2	3.4	0.6	82.5	0.005	0.05	3.3	0.0025	0.13	2.38
BZ-965C	1085	3.8	2.3	0.4	75	0.005	0.05	3.1	0.0025	0.24	0.97
BZ-965C	1090	2.8	3.1	0.6	102.5	0.005	0.03	2.4	0.0025	0.36	5.44
BZ-965C	1095	2.6	3.5	0.4	107	0.005	0.03	2.2	0.0025	0.45	5.51
BZ-965C	1100	4	2	0.4	63.6	0.005	0.04	3	0.0025	0.54	0.61
BZ-965C	1105	3.7	2	0.5	48.5	0.005	0.04	2.7	0.0025	0.86	0.62
BZ-965C	1110	4.6	2.5	0.6	54.7	0.005	0.07	2.8	0.0025	1.14	0.56
BZ-965C	1115	3.7	1.1	0.4	66.8	0.005	0.04	3.2	0.0025	0.42	0.51
BZ-965C	1120	3.4	1.2	0.3	69.2	0.005	0.02	3.3	0.0025	0.64	0.68
BZ-965C	1125	3	1.2	0.3	86.3	0.005	0.04	2.7	0.0025	1.28	0.8
BZ-965C	1130	3.3	1.4	0.3	65.5	0.005	0.04	3	0.0025	0.98	0.69
BZ-965C	1135	2.5	1.3	0.3	55.9	0.005	0.03	3.3	0.0025	0.53	0.72
BZ-965C	1140	3.2	0.9	0.3	64.2	0.005	0.01	2.5	0.0025	0.4	0.97
BZ-965C	1145	2	0.8	0.4	199	0.005	0.02	2	0.0025	0.31	0.49
BZ-965C	1150	1.8	0.7	0.3	308	0.005	0.03	1.8	0.0025	0.13	0.3
BZ-965C	1155	2	0.8	0.4	293	0.005	0.03	2.1	0.0025	0.1	0.33
BZ-965C	1160	1.6	0.8	0.3	402	0.005	0.03	1.8	0.0025	0.04	0.34
BZ-965C	1165	2	0.8	0.3	266	0.005	0.02	2.4	0.0025	0.2	0.39
BZ-965C	1170	2.3	0.6	0.3	262	0.005	0.02	2.6	0.0025	0.06	0.28
BZ-965C	1175	3.6	0.7	0.3	214	0.005	0.02	2.7	0.0025	0.09	0.35
BZ-965C	1180	2.6	0.7	0.2	438	0.005	0.02	1.8	0.0025	0.06	0.34
BZ-965C	1185	2.4	0.7	0.2	406	0.005	0.02	1.9	0.0025	0.07	0.37
BZ-965C	1190	3	0.8	0.3	235	0.005	0.02	2.2	0.0025	0.17	0.52
BZ-965C	1195	3.5	0.9	0.2	216	0.005	0.01	1.9	0.0025	0.58	0.75
BZ-965C	1200	4	1	0.2	236	0.005	0.02	1.9	0.0025	0.34	0.67
BZ-965C	1205	4.1	0.9	0.2	213	0.005	0.01	2.1	0.0025	0.39	0.76
BZ-965C	1215	5	1.1	0.2	117	0.005	0.02	2.7	0.0025	0.65	0.67
BZ-965C	1220	4.2	1.1	0.3	122	0.005	0.02	2.6	0.0025	0.29	0.55
BZ-965C	1225	4	1	0.4	161.5	0.005	0.02	3.3	0.0025	0.17	0.46
BZ-965C	1230	3.3	0.7	0.3	244	0.005	0.02	2.6	0.0025	0.12	0.33
BZ-965C	1235	3.4	0.7	0.3	272	0.005	0.02	3.1	0.0025	0.11	0.33
BZ-965C	1240	3.3	0.8	0.3	326	0.005	0.01	2.9	0.0025	0.1	0.33
BZ-965C	1245	3.2	0.7	0.3	362	0.005	0.01	2.9	0.0025	0.12	0.35
BZ-965C	1250	3.4	0.9	0.3	365	0.005	0.02	3.1	0.0025	0.25	0.37

SAMPLE	Depth (ft)	Sc ppm	Se ppm	Sn ppm	Sr ppm	Ta ppm	Te ppm	Th ppm	Ti ppm	Tl ppm	U ppm
BZ-965C	1255	3.9	1	0.3	110	0.005	0.01	3.6	0.0025	0.52	0.65
BZ-965C	1260	6	1	0.4	64.4	0.005	0.02	5	0.0025	0.79	0.57
BZ-965C	1265	4.6	1.3	0.3	61.5	0.005	0.03	4.4	0.0025	0.9	0.6
BZ-965C	1270	4.5	3.6	0.5	115.5	0.005	0.12	3.6	0.0025	0.77	9.49
BZ-965C	1275	3.5	5.3	0.5	109	0.005	0.11	2.8	0.0025	1.1	17.25
BZ-965C	1280	3.2	5.8	0.5	96.8	0.005	0.14	2.5	0.0025	1.08	17.95
BZ-965C	1285	3.6	5.4	0.4	101.5	0.005	0.12	2.7	0.0025	0.95	23.5
BZ-965C	1290	3	4.6	0.4	79.3	0.005	0.1	2.4	0.0025	1.25	18.05
BZ-965C	1295	3.3	5.4	0.5	72.4	0.005	0.06	2.6	0.0025	1.79	22.6
BZ-965C	1300	3.6	4.8	0.5	93.5	0.005	0.03	3	0.0025	1.35	18.85
BZ-965C	1305	3.2	4	0.5	83	0.005	0.03	2.4	0.0025	1.6	18.45
BZ-965C	1310	3.3	3	0.4	85.5	0.005	0.03	2.4	0.0025	0.89	18.8
BZ-965C	1315	3.7	2.1	0.4	128	0.005	0.03	3.1	0.0025	0.91	9.65
BZ-965C	1320	3.8	1.7	0.3	135	0.005	0.03	2.8	0.0025	0.66	4.75
BZ-965C	1325	5.1	1.7	0.3	154.5	0.005	0.03	3.6	0.0025	1.42	4.54
CD-14	530	3.7	1.5	0.7	199	<0.01	0.01	4.5	0.006	2.63	0.98
CD-14	550	4.1	1.8	0.4	130	<0.01	0.01	3.1	<0.005	0.44	2.01
CD-14	560	4.2	2.9	0.3	249	0.01	<0.01	2.3	<0.005	0.57	2.23
CD-14	570	4	1.9	0.3	56.5	<0.01	<0.01	3.5	<0.005	0.86	2.14
CD-14	580	4	1.5	0.3	246	<0.01	0.01	3.3	<0.005	0.13	0.85
CD-14	590	4.2	1.2	0.3	220	<0.01	0.01	3.3	<0.005	0.16	0.54
CD-14	600	3	1	0.2	340	<0.01	0.01	2.3	0.005	0.06	0.88
CD-14	610	4.3	0.7	0.5	192	0.02	0.03	2	0.008	0.14	9.35
CD-14	620	3.4	2.3	0.5	170	0.01	0.03	1.6	0.005	0.13	5.32
CD-14	630	3.7	7.3	0.6	154	0.01	0.03	1.9	<0.005	0.17	6.52
CD-14	640	3.5	3.3	0.4	150	0.01	0.03	2.2	<0.005	0.15	6.18
CD-14	650	3.5	1.9	0.4	185.5	0.01	0.03	2.4	<0.005	0.16	8.58
CD-14	660	3.1	1.4	0.5	174	0.01	0.03	2.1	<0.005	0.2	10.1
CD-14	670	3.1	2.3	0.7	178	0.01	0.02	2.9	<0.005	0.16	7.7
CD-14	680	2.5	1	0.3	258	<0.01	0.01	2.4	<0.005	0.09	1.46
CD-14	690	2.8	1.3	0.3	281	<0.01	0.02	3	<0.005	0.1	1.33
CD-14	700	3	4	0.4	162.5	<0.01	0.01	2.4	<0.005	0.09	4.33
CD-14	720	2.8	3.5	0.5	137	0.01	0.01	2.4	<0.005	0.07	4.23
CD-14	740	3.2	4.9	0.5	99.6	0.01	0.01	1.9	<0.005	0.21	5.25
CD-14	770	3.7	12.1	0.4	209	<0.01	0.02	2.1	<0.005	0.25	14.3
CD-14	780	3	11.8	0.4	159	<0.01	0.03	1.7	<0.005	0.39	12.6
CD-14	790	3	4.3	0.4	139	0.01	0.02	1.8	<0.005	0.38	9.55
CD-14	800	3.4	4.1	0.3	148.5	<0.01	0.02	2.2	<0.005	0.16	11
CD-14	820	3.7	7.2	0.3	181.5	<0.01	0.04	2.8	<0.005	0.54	10.9
CD-14	840	4.2	2	0.3	79.1	<0.01	0.01	2.9	<0.005	0.57	4.82
CD-14	860	3.4	0.7	0.2	45.7	<0.01	<0.01	3.1	<0.005	0.39	1.92
CD-14	880	3.6	0.9	0.2	51	<0.01	<0.01	3.1	<0.005	0.47	1.5
CD-14	900	3.2	0.9	0.2	56.3	<0.01	<0.01	2.6	<0.005	0.39	1.89
CD-14	920	3.6	0.8	0.2	66.9	<0.01	<0.01	2.7	<0.005	0.28	1.55
CD-14	940	2.8	0.6	0.2	119.5	<0.01	<0.01	2.3	<0.005	0.18	1.03
CD-14	960	3.2	0.9	0.2	47.5	<0.01	<0.01	2.4	<0.005	1.35	1.64
CD-14	980	3.2	0.9	0.2	58.1	<0.01	0.01	2.4	<0.005	1.13	1.32
CD-14	1000	2.9	0.6	0.2	99.9	0.01	<0.01	1.9	<0.005	1.01	1.51
CD-14	1020	3	0.5	<0.2	116.5	<0.01	<0.01	2.3	<0.005	0.94	1.39
CD-14	1040	2.8	1	<0.2	127.5	<0.01	0.01	2.2	<0.005	0.9	1.2
CD-14	1060	3.2	0.8	0.2	115.5	<0.01	0.01	2.4	<0.005	0.48	0.82

SAMPLE	Depth (ft)	Sc ppm	Se ppm	Sn ppm	Sr ppm	Ta ppm	Te ppm	Th ppm	Ti ppm	Tl ppm	U ppm
CD-14	1080	2.5	1.4	<0.2	199	<0.01	0.02	1.6	<0.005	0.2	1.27
CD-14	1100	2.5	1.4	0.2	151.5	<0.01	0.01	1.7	<0.005	0.22	0.92
CD-14	1120	2.4	0.6	<0.2	211	<0.01	0.01	1.7	<0.005	0.07	0.85
CD-14	1140	2.9	0.8	<0.2	159.5	<0.01	0.02	1.8	<0.005	0.14	1.01
CD-14	1160	2.5	1.4	<0.2	157	<0.01	0.02	1.6	<0.005	0.18	1.08
CD-14	1180	2.5	0.9	<0.2	224	<0.01	0.02	1.7	<0.005	0.11	0.94
CD-14	1200	2.6	1.7	<0.2	165.5	<0.01	0.02	1.6	<0.005	0.27	1.53
CD-14	1220	3.6	3.7	0.2	118	<0.01	0.01	1.7	<0.005	0.57	2.95
CD-14	1240	2.9	2.4	0.2	137.5	<0.01	0.01	1.3	<0.005	0.32	2.82
CD-14	1260	3.3	1.8	0.2	103	<0.01	0.01	1.9	<0.005	0.38	1.94
CD-14	1280	2.9	0.7	<0.2	185	<0.01	<0.01	2.4	<0.005	0.26	1.17
CD-14	1300	3.6	0.5	0.2	132	<0.01	<0.01	2.9	<0.005	0.21	0.93
CD-14	1320	2.8	1.4	0.2	187.5	<0.01	0.01	2.1	<0.005	0.17	1.85
CD-14	1340	2.6	1.6	0.2	178	<0.01	0.01	2	<0.005	0.28	3.02
CD-14	1360	3.2	1.2	0.2	155	<0.01	<0.01	2.3	<0.005	0.22	2.03
CD-14	1380	2.9	2.4	0.2	123	<0.01	0.01	1.9	<0.005	0.93	3.33
CD-14	1400	6.5	1.3	0.6	219	<0.01	0.01	4.1	0.063	2	1.39
CD-14	1420	3.4	2.5	0.3	187	<0.01	<0.01	2.2	<0.005	0.48	2.83
CD-14	1440	3.9	1.7	0.4	178	<0.01	<0.01	2.6	0.023	0.27	2.61
CD-14	1460	3	1	0.4	129.5	<0.01	<0.01	2.3	<0.005	0.17	1.01
CD-14	1480	7.1	0.5	1.2	342	<0.01	<0.01	3.9	0.166	0.48	1.09
CD-14	1500	8	0.8	1.1	330	<0.01	<0.01	4.5	0.176	0.23	1.06
CD-14	1520	3.9	0.9	0.3	249	<0.01	0.01	2.7	0.011	0.15	2.37
CD-14	1540	2.2	1.8	0.2	270	<0.01	0.01	1.9	<0.005	0.15	3.6
CD-14	1560	2.8	2	0.4	184	<0.01	<0.01	2.1	<0.005	0.19	3.09
CD-14	1580	2.9	1.4	0.3	159	<0.01	<0.01	2.4	0.009	0.18	2.35
CD-14	1600	3.5	1.2	0.4	206	<0.01	<0.01	2.6	0.013	0.15	1.85
CD-14	1620	2.8	2.4	0.2	221	<0.01	0.01	2.1	<0.005	0.17	4.16
CD-14	1640	2.8	2.1	<0.2	235	<0.01	0.01	2	<0.005	0.18	3.5
CD-14	1660	7.6	1.6	0.4	384	<0.01	<0.01	3.5	0.069	0.18	2.21
CD-14	1680	2.6	1.7	0.2	179	<0.01	0.01	2.1	<0.005	0.18	2.53
CD-14	1700	2.9	1.5	0.3	124	<0.01	<0.01	2.5	<0.005	0.24	2.39
CD-14	1720	3.3	1.1	0.2	102	<0.01	<0.01	2.4	<0.005	0.26	1
CD-14	1740	3.3	0.7	0.3	108	<0.01	<0.01	2.8	<0.005	0.26	0.99
CD-14	1760	3.8	1.1	0.2	103	<0.01	<0.01	2.6	<0.005	0.34	0.99
CD-14	1780	3.5	1.5	0.2	134	<0.01	<0.01	2.3	<0.005	0.29	1.89
CD-14	1800	3.1	1.1	0.3	154	<0.01	<0.01	2.1	<0.005	0.19	1.12
CD-14	1820	5.9	0.8	0.8	177.5	<0.01	<0.01	3.2	0.05	0.27	1.02
CD-14	1840	3.9	0.7	0.3	153	<0.01	<0.01	2.5	0.016	0.19	0.76
CD-14	1860	6.9	1.5	0.4	159.5	<0.01	<0.01	3.5	0.041	0.53	1.23
CD-14	1880	3.3	2.1	0.2	229	<0.01	<0.01	2.5	<0.005	0.2	5.76
CD-14	1900	3.2	2.6	0.2	254	<0.01	<0.01	2.2	<0.005	0.28	3.91
CD-14	1920	2.9	2.2	0.2	173.5	<0.01	0.01	1.9	<0.005	0.2	2.9
CD-14	1940	3	1.3	0.2	128.5	<0.01	<0.01	2.3	<0.005	0.4	1.82
CD-14	1960	2.8	2.2	0.2	145.5	<0.01	0.01	2.2	<0.005	0.22	3.13
CD-14	1980	3.1	0.9	0.2	136.5	<0.01	0.01	2.6	<0.005	0.22	1.04
CD-14	2000	2.9	1.2	<0.2	177.5	<0.01	<0.01	2	<0.005	0.15	2.14
CD-14	2020	3.1	0.8	0.9	118	<0.01	<0.01	2.4	<0.005	0.42	1.18
CD-14	2040	3	0.8	0.9	194.5	<0.01	0.01	2.2	<0.005	0.16	1.33
CD-14	2060	2.8	1.1	<0.2	196.5	<0.01	0.01	2.1	<0.005	0.3	1.84
CD-14	2080	3	1.2	0.2	138	<0.01	0.01	2.2	<0.005	0.35	3.04

SAMPLE	Depth (ft)	Sc ppm	Se ppm	Sn ppm	Sr ppm	Ta ppm	Te ppm	Th ppm	Ti ppm	Tl ppm	U ppm
CD-14	2100	8.4	0.8	0.4	123.5	<0.01	<0.01	3.9	0.047	0.66	0.9
CD-14	2120	2.9	1.1	<0.2	180.5	<0.01	0.01	2.2	<0.005	0.33	2.27
CD-14	2140	3.3	1.1	<0.2	183	<0.01	<0.01	2.4	<0.005	0.22	1.76
CD-14	2160	3	1.3	0.2	258	<0.01	<0.01	2.3	<0.005	0.19	3.05
CD-15C	1380	5.6	1.6	0.3	245	<0.01	<0.01	3.9	<0.005	0.91	3.14
CD-15C	1400	6.5	15.9	0.8	140	<0.01	0.04	3.6	<0.005	0.35	3.86
CD-15C	1420	5.3	12.9	0.7	195.5	<0.01	0.03	3.8	<0.005	0.16	5.64
CD-15C	1440	5.1	10.1	0.6	180.5	<0.01	0.03	2.7	<0.005	0.5	2.58
CD-15C	1460	6.1	10.1	0.6	179.5	0.01	0.03	3	<0.005	0.8	2.49
CD-15C	1480	6	8.5	0.5	192.5	<0.01	0.03	3	<0.005	1	2.89
CD-15C	1500	6.8	12.5	0.4	152.5	<0.01	0.03	3	<0.005	1.83	3.06
CD-15C	1520	5.5	4.7	0.4	152	<0.01	0.02	2.5	<0.005	0.29	1.01
CD-15C	1540	5.4	2.4	0.2	164.5	<0.01	0.02	2.7	<0.005	0.53	1.56
CD-15C	1560	6.6	3.5	0.3	119	<0.01	0.02	2.3	<0.005	1.36	1.33
CD-15C	1580	5.8	3	0.3	160	<0.01	0.02	2.8	<0.005	0.43	1.21
CD-15C	1600	6.3	2.4	0.6	150	<0.01	0.02	3.4	<0.005	0.29	2.35
CD-15C	1620	6.5	1.7	0.5	163.5	<0.01	0.02	3.5	<0.005	0.23	3.03
CD-15C	1660	7.5	1.7	0.2	162	<0.01	0.04	3.4	<0.005	1.82	4.12
CD-15C	1680	3.6	0.9	0.3	277	<0.01	0.01	3.3	<0.005	0.54	5.09
CD-15C	1700	3.1	0.6	0.2	374	<0.01	0.01	2.5	<0.005	0.22	2.76
CD-15C	1720	4.5	1.5	0.2	161	<0.01	0.01	2.7	<0.005	0.42	2.18
CD-15C	1740	4.7	1.7	0.4	64.5	<0.01	0.01	3.3	<0.005	1.08	1.92
CD-15C	1760	3.5	1.9	0.3	34.1	<0.01	0.01	3.2	<0.005	0.67	1.65
CD-15C	1780	3.5	1.2	0.4	39.2	<0.01	0.02	3.2	<0.005	1.48	1.61
CD-15C	1800	3.7	0.9	0.3	49.4	<0.01	0.12	2.6	<0.005	1.74	1.3
CD-15C	1820	4	0.6	0.2	82	<0.01	0.01	3	<0.005	0.57	1.29
CD-15C	1840	3.1	0.6	0.2	178	<0.01	<0.01	2.5	<0.005	0.35	0.94
CD-15C	1860	2.6	0.5	0.2	157	<0.01	0.03	2.5	<0.005	0.29	1.03
CD-15C	1880	5.7	0.6	0.3	157.5	<0.01	0.03	2.3	0.029	0.44	0.93
CD-15C	1900	3.6	1.5	<0.2	122.5	<0.01	0.03	2	<0.005	0.37	1.37
CD-15C	1920	3.7	1.8	<0.2	175.5	<0.01	0.03	2.1	<0.005	0.22	2.33
CD-15C	1940	2.9	3.2	0.2	98.4	<0.01	0.03	2.1	<0.005	0.18	3.41
CD-15C	2000	3.4	1.9	0.7	148.5	<0.01	0.02	2.6	<0.005	0.29	2.1
CD-15C	2020	3.4	1.1	0.8	83.5	<0.01	0.02	3.1	<0.005	0.4	1.32
CD-15C	2040	4.1	3	0.7	169.5	<0.01	0.02	2.6	<0.005	0.22	2.06
CD-15C	2060	2.8	1.3	0.4	126	<0.01	0.02	2.1	<0.005	0.27	1.66
CD-15C	2080	2.9	0.9	0.4	147	0.01	0.01	2.5	<0.005	0.19	1.94
CD-15C	2100	2.7	2.3	0.3	149.5	<0.01	0.03	2.2	<0.005	0.18	3.82
CD-15C	2120	3.7	2.3	0.4	164	<0.01	0.02	2.5	<0.005	0.23	3
CD-95-3	890	2	8.5	2	27.7	<0.01	0.08	1.6	<0.005	0.54	5.46
CD-95-3	900	2.9	8.6	0.5	30.8	<0.01	0.1	2.1	<0.005	0.84	10.35
CD-95-3	910	2.2	7.4	0.5	39.7	<0.01	0.07	2.2	<0.005	0.5	5.81
CD-95-3	920	1.9	5.8	0.6	28.6	<0.01	0.08	1.4	<0.005	0.71	5.15
CD-95-3	930	2.7	6.4	0.6	45	<0.01	0.07	2.1	<0.005	0.65	4.56
CD-95-3	940	1.7	5.8	0.5	49.4	<0.01	0.05	1.2	<0.005	0.69	5.84
CD-95-3	950	5.2	20	0.6	202	0.01	0.08	2.8	<0.005	0.47	10.45
CD-95-3	960	4.8	10.4	0.6	166.5	<0.01	0.04	3.4	<0.005	0.17	4.57
CD-95-3	970	4.7	9.2	0.7	127.5	0.01	0.05	2.7	<0.005	0.17	2.39
CD-95-3	980	5.3	8.9	0.7	144.5	<0.01	0.04	2.9	<0.005	0.18	2.89
CD-95-3	990	4.5	7.1	0.7	135.5	<0.01	0.04	3	<0.005	0.22	3.86
CD-95-3	1000	6.7	3.8	0.5	114	<0.01	0.04	2.5	<0.005	0.14	1.52

SAMPLE	Depth (ft)	Sc ppm	Se ppm	Sn ppm	Sr ppm	Ta ppm	Te ppm	Th ppm	Ti ppm	Tl ppm	U ppm
CD-95-3	1010	6	3	0.6	127.5	<0.01	0.04	2.7	<0.005	0.14	1.2
CD-95-3	1020	5.5	3.3	0.6	271	<0.01	0.03	3.3	<0.005	0.1	4.55
CD-95-3	1030	4.4	4.2	0.4	393	<0.01	0.04	2.2	<0.005	0.12	11.7
CD-95-3	1040	4.7	2.8	0.4	313	<0.01	0.03	2.6	<0.005	0.11	5.62
CD-95-3	1050	5.1	1.4	0.4	184.5	<0.01	0.04	3.1	<0.005	0.09	0.66
CD-95-3	1060	4.5	1	0.3	294	<0.01	0.03	3.5	<0.005	0.07	0.79
CD-95-3	1070	5.8	1.2	0.4	202	<0.01	0.03	4.2	<0.005	0.09	0.65
CD-95-3	1080	7.8	1.3	0.4	183	<0.01	0.03	4.4	<0.005	0.08	0.86
CD-95-3	1090	5.5	1.2	0.3	209	<0.01	0.03	3.9	<0.005	0.07	0.88
CD-95-3	1100	5.6	0.9	0.3	213	<0.01	0.04	4	<0.005	0.07	0.74
CD-95-3	1110	5.7	1.1	0.3	195	<0.01	0.04	3.5	<0.005	0.08	0.67
CD-95-3	1120	5.2	0.8	0.4	239	<0.01	0.03	4.2	<0.005	0.07	0.64
CD-95-3	1130	2.9	0.7	0.3	257	<0.01	0.04	2.7	<0.005	0.08	0.56
CD-95-3	1140	3.4	0.9	0.3	265	<0.01	0.04	3.2	<0.005	0.06	0.57
CD-95-3	1150	4.6	1.5	0.3	146.5	<0.01	0.05	3.6	<0.005	0.07	0.55
CD-95-3	1160	2.9	0.7	0.2	311	0.01	0.04	2.5	<0.005	0.06	0.6
CD-95-3	1170	2.8	0.8	0.3	318	<0.01	0.04	2.6	<0.005	0.07	0.64
CD-95-3	1180	2.6	0.9	0.2	312	<0.01	0.04	2.5	<0.005	0.09	0.74
CD-95-3	1190	2.4	0.9	0.3	293	<0.01	0.04	2.5	<0.005	0.1	0.65
CD-95-3	1200	2.4	0.7	0.2	354	<0.01	0.04	2.5	<0.005	0.06	0.56
CD-95-3	1210	2.5	1	0.3	315	<0.01	0.04	2.5	<0.005	0.09	0.8
CD-95-3	1220	2.5	0.7	0.3	324	<0.01	0.05	2.5	<0.005	0.1	1.14
CD-95-3	1230	2.6	1	0.3	301	<0.01	0.04	2.4	<0.005	0.1	1.2
CD-95-3	1240	2.6	0.7	0.3	308	<0.01	0.04	2.4	<0.005	0.09	0.77
CD-95-3	1250	3.3	0.6	0.4	214	<0.01	0.03	3.4	<0.005	0.14	0.47
CD-95-3	1260	3.2	0.7	0.4	453	<0.01	0.02	2.5	<0.005	0.11	0.7
CD-95-3	1270	2.7	0.8	0.3	363	<0.01	0.04	2.4	<0.005	0.17	0.88
CD-95-3	1280	2.4	0.7	0.3	414	<0.01	0.03	2.2	<0.005	0.15	0.73
CD-95-3	1290	8.7	1	0.4	378	0.01	0.03	4.4	<0.005	0.47	1.47
CD-95-3	1300	6.6	2.8	0.4	321	0.01	0.03	3.6	<0.005	0.74	10.3
CD-95-3	1310	3.6	4	0.5	222	<0.01	0.05	2	<0.005	0.68	13.5
CD-95-3	1320	3.7	4.4	0.6	180	0.01	0.05	2.4	<0.005	0.76	15.9
CD-95-3	1330	3.2	2.3	0.5	92.1	<0.01	0.04	2.5	<0.005	0.54	7.8
CD-95-3	1340	2.9	2.4	0.6	88	<0.01	0.04	2	<0.005	0.63	10.1
CD-95-3	1350	2.8	2.1	0.6	136.5	<0.01	0.04	1.8	<0.005	0.37	12.9
CD-95-3	1360	3.4	2	0.4	202	<0.01	0.03	1.8	<0.005	0.44	15.85
CD-95-3	1370	3.2	1.7	0.5	174.5	<0.01	0.03	1.5	<0.005	0.31	11.3
CD-95-3	1380	2.4	1.6	0.5	161.5	<0.01	0.04	1.9	<0.005	0.41	8.01
CD-95-3	1390	3.4	1.7	0.5	188	<0.01	0.02	2.4	<0.005	0.4	13.9
CD-95-3	1400	2.5	2.1	0.6	145	<0.01	0.05	1.9	<0.005	0.44	15.65
CD-95-3	1410	2.7	2.1	0.5	136.5	<0.01	0.04	1.5	<0.005	0.41	12.5
CD-95-3	1420	2.2	1.8	0.5	221	<0.01	0.05	1.7	<0.005	0.31	10.75
CD-95-3	1430	3.1	2	0.6	169.5	<0.01	0.04	2.3	<0.005	0.44	9.81
CD-95-3	1440	3.4	2.6	0.5	131	0.01	0.05	2	<0.005	0.49	13.9
CD-95-3	1450	4	2.8	0.6	115.5	<0.01	0.04	2.5	<0.005	0.34	5.8
CD-95-3	1460	4.3	2.4	0.7	138	<0.01	0.04	3.3	<0.005	0.47	8.96
CD-95-3	1470	4.1	2.2	0.4	152.5	<0.01	0.04	2.8	<0.005	0.31	5.41
CD-95-3	1480	4.2	2.1	0.4	116	<0.01	0.04	2.4	<0.005	0.37	6.5
CD-95-3	1490	3.5	2	0.5	116	<0.01	0.02	3	<0.005	0.33	4.87
CD-95-3	1500	3.5	1.8	0.5	102.5	<0.01	0.02	2.7	<0.005	0.4	4.01
CD-95-3	1510	3.8	2.1	0.5	101.5	<0.01	0.01	2.1	<0.005	0.45	2.85

SAMPLE	Depth (ft)	Sc ppm	Se ppm	Sn ppm	Sr ppm	Ta ppm	Te ppm	Th ppm	Ti ppm	Tl ppm	U ppm
CD-95-3	1520	3.8	1.7	0.5	95.5	<0.01	0.01	2.4	<0.005	0.4	2.5
CD-95-3	1530	4.1	2.3	0.4	93.8	<0.01	0.02	2.8	<0.005	0.51	2.68
CD-95-3	1540	3.9	1.9	0.5	92.3	<0.01	0.02	2.9	<0.005	0.49	2.89
CD-95-3	1550	2.9	1.1	0.5	92.7	<0.01	0.01	2	<0.005	0.47	2.01
CD-95-3	1560	3.2	0.9	0.6	73.9	<0.01	0.01	2.1	<0.005	0.34	1.65
CD-95-3	1570	3.6	2.4	0.4	75.3	<0.01	0.02	2.1	<0.005	0.34	1.71
CD-95-3	1580	3.2	1	0.5	69.8	<0.01	0.01	2.1	<0.005	0.37	1.32
CD-95-3	1590	3.8	2.3	0.5	83	<0.01	0.02	2.6	<0.005	0.45	2.06
CD-95-3	1600	2.9	0.7	0.4	59.1	<0.01	0.01	1.6	<0.005	0.38	1.41
CD-95-3	1610	2.7	0.8	0.3	71.4	<0.01	<0.01	2.1	<0.005	0.27	0.95
CD-95-3	1620	2.7	1.1	0.4	97.2	<0.01	0.01	2.3	<0.005	0.37	1.58
CD-95-3	1630	3.6	2.1	0.5	90.8	<0.01	0.01	2.8	<0.005	0.24	1.49
CD-95-3	1640	3.6	2.4	0.6	107.5	<0.01	0.02	2.9	<0.005	0.28	1.76
CD-95-3	1650	4.2	2.1	0.5	104.5	<0.01	0.01	2.8	<0.005	0.39	1.63
CD-95-3	1660	3.7	1.9	0.5	107.5	<0.01	0.02	2.8	<0.005	0.39	2.13
CD-95-3	1670	3.8	3.5	0.5	103.5	<0.01	0.02	2.4	<0.005	0.84	1.8
CD-95-3	1680	3.5	3.8	0.5	118	<0.01	0.02	2.4	<0.005	0.7	2.17
CD-95-3	1690	2.6	2.1	0.5	118.5	<0.01	0.01	2.1	<0.005	0.7	2.89
CD-95-3	1700	2.8	1.9	0.5	71.7	<0.01	0.01	2.6	<0.005	0.38	1.2
CD-95-3	1710	2.7	1.6	0.4	90	<0.01	0.01	2.3	<0.005	0.4	1.56
CD-95-3	1720	2.7	1.9	0.4	92.4	<0.01	0.02	2.3	<0.005	0.44	1.6
CD-95-3	1730	2.6	3.4	0.4	96.2	<0.01	0.02	1.8	<0.005	0.36	2.27
CD-95-3	1740	2	1.8	0.4	42.7	<0.01	0.03	1.7	<0.005	1.2	2.8
CD-95-3	1750	2.4	1.9	0.5	123.5	<0.01	0.02	2	<0.005	0.68	2.43
CD-95-3	1760	2	1.4	0.4	127.5	<0.01	0.01	1.6	<0.005	0.4	2.24
CD-95-3	1770	1.6	1.4	0.3	210	<0.01	0.01	1.4	<0.005	0.29	3.13
CD-95-3	1780	2	1	0.3	198	<0.01	0.01	2	<0.005	0.23	1.72
CD-95-3	1790	1.9	2	0.3	182	<0.01	0.01	1.9	<0.005	0.23	2.32
CD-95-3	1800	1.9	1.3	0.4	191.5	<0.01	0.03	1.5	<0.005	0.25	2.28
CD-95-3	1810	2.1	2.4	0.3	165	<0.01	0.03	1.6	<0.005	0.38	3.06
CD-95-3	1820	2.3	1.7	0.4	136.5	<0.01	0.02	1.7	<0.005	0.35	2.07
CD-95-3	1830	1.9	1.5	0.2	233	<0.01	0.02	1.7	<0.005	0.17	3.33
CD-95-3	1840	1.9	1.1	0.4	199	<0.01	0.01	1.9	<0.005	0.2	1.91
CD-95-3	1850	2	1	0.4	176	<0.01	0.01	1.6	<0.005	0.26	1.58
CD-95-3	1860	2.6	1.2	0.4	136	<0.01	0.03	1.1	<0.005	0.34	2.99
CD-95-3	1870	2.3	0.8	0.3	75.8	<0.01	0.02	1	<0.005	0.42	1.55
CD-95-3	1880	2.4	1.2	0.3	115.5	<0.01	0.01	1.1	<0.005	0.38	1.93
CD-95-3	1890	3.3	1.6	0.4	90.5	<0.01	0.04	1.3	<0.005	0.35	2.06
CD-95-3	1900	3.2	1.4	0.4	139	<0.01	0.03	1.6	<0.005	0.44	1.85
CD-95-3	1910	2.8	0.4	0.5	178.5	<0.01	0.02	2	<0.005	0.18	0.73
CD-95-3	1920	2.7	1.7	0.3	130.5	<0.01	0.01	1.3	<0.005	0.3	1.55
CD-95-3	1930	4.9	0.9	0.4	170	<0.01	0.01	1.7	<0.005	0.57	1.05
CD-95-3	1940	11.5	1.1	0.4	299	<0.01	0.02	2.7	<0.005	1.36	0.58
CD-95-3	1950	9.9	1.3	0.4	345	<0.01	0.03	2.9	0.005	0.73	0.82
CD-95-3	1960	3.1	2.3	0.3	242	<0.01	0.02	1.5	<0.005	0.13	2.86
CD-95-3	1970	3.4	3.2	0.3	206	<0.01	0.03	2	<0.005	0.26	3.05
CD-95-3	1980	3.6	2.9	0.4	139.5	<0.01	0.01	1.5	<0.005	1.36	2.09
CD-95-3	1990	8.5	1.1	0.5	138.5	<0.01	<0.01	2.5	<0.005	1.23	1.72
CD-95-3	2000	9.1	1.3	0.6	164	<0.01	0.01	2.6	<0.005	1.72	1.4
CD-95-3	2010	10.6	0.9	0.6	261	<0.01	0.01	2.2	<0.005	1.07	0.85
CD-95-3	2020	3.8	3.1	0.8	105.5	<0.01	0.03	1.5	<0.005	0.66	1.75

SAMPLE	Depth (ft)	Sc ppm	Se ppm	Sn ppm	Sr ppm	Ta ppm	Te ppm	Th ppm	Ti ppm	Tl ppm	U ppm
CD-95-3	2030	3	1.1	0.4	213	<0.01	0.03	1.6	<0.005	0.26	2.36
CD-95-3	2040	2.7	2	0.5	109.5	<0.01	0.05	1.3	<0.005	1.16	2.37
CD-95-3	2050	2.6	1.5	0.4	134	<0.01	0.03	1.6	<0.005	0.39	3.35
CD-95-3	2060	3.3	1.3	0.3	121	<0.01	0.02	1.9	<0.005	0.3	3.23
CD-95-3	2070	3.3	1.2	0.3	124	<0.01	0.02	1.8	<0.005	0.24	3.5
CD-95-3	2080	3.5	1.8	0.4	135.5	<0.01	0.02	2	<0.005	0.25	3.55
CD-95-3	2090	3.3	1.4	0.6	167.5	<0.01	0.02	1.9	<0.005	0.35	3.2
CD-95-3	2100	3.6	1.5	0.8	130.5	<0.01	0.02	1.8	<0.005	0.46	3.36
CD-95-3	2110	2.6	1.1	0.5	65.5	<0.01	0.01	1.1	<0.005	0.34	1.14
CD-95-3	2120	3.6	2.3	0.5	143	<0.01	0.01	1.7	<0.005	0.42	1.49
CD-95-3	2130	12.5	0.6	0.5	163.5	<0.01	0.07	2.7	<0.005	1.05	0.57
CD-95-3	2140	2.9	0.7	0.4	138.5	<0.01	0.01	0.9	<0.005	0.29	0.7
CD-95-3	2150	2.9	0.9	0.4	136.5	<0.01	0.02	1.1	<0.005	0.29	0.82
CD-95-3	2160	2.5	0.8	0.5	142.5	<0.01	0.01	1	<0.005	0.36	0.84
CD-95-3	2170	4.8	0.6	0.6	178	<0.01	0.02	2.2	<0.005	0.66	0.78
CD-95-3	2180	7.4	0.7	0.5	144.5	<0.01	0.02	2.6	<0.005	0.68	0.79
CD-96-2C	770	5.2	4.2	0.5	175.5	<0.01	0.03	4	<0.005	0.54	1.78
CD-96-2C	780	7	3.4	0.5	102.5	<0.01	0.03	4.5	<0.005	0.36	1.82
CD-96-2C	790	8	3.5	0.4	89.3	<0.01	0.04	4.2	<0.005	0.46	1.82
CD-96-2C	800	7.2	3.2	0.4	108.5	<0.01	0.04	4.7	<0.005	0.42	2.43
CD-96-2C	810	5.4	1.9	0.4	122.5	<0.01	0.03	4.4	<0.005	1.57	5.16
CD-96-2C	820	5.3	1.3	0.4	167	<0.01	0.04	3.6	<0.005	0.58	6.69
CD-96-2C	830	5.9	1.4	0.4	131	<0.01	0.04	4	<0.005	0.33	4.48
CD-96-2C	840	5	0.9	0.4	228	<0.01	0.04	4.1	<0.005	0.25	2.46
CD-96-2C	850	4	1.1	0.3	268	<0.01	0.04	3	<0.005	0.2	2.38
CD-96-2C	860	4.5	1	0.4	238	<0.01	0.05	3.5	<0.005	0.23	1.83
CD-96-2C	870	5.3	1.1	0.4	173.5	<0.01	0.04	3.8	<0.005	0.27	4.5
CD-96-2C	880	5.4	1.4	0.3	164.5	<0.01	0.05	3.3	<0.005	0.18	1.76
CD-96-2C	890	5.3	1.4	0.4	136	<0.01	0.04	3.7	<0.005	0.27	3.55
CD-96-2C	900	5.3	1.5	0.4	137	<0.01	0.05	3.1	<0.005	0.26	2.67
CD-96-2C	910	5.5	2.2	0.5	163.5	<0.01	0.05	2.9	<0.005	0.2	2.5
CD-96-2C	920	6.7	3.6	0.5	116.5	<0.01	0.07	2.2	<0.005	0.28	1.92
CD-96-2C	930	5.9	5.3	0.6	163.5	<0.01	0.04	3.2	<0.005	0.18	2.01
CD-96-2C	940	5.8	5.6	0.6	130	<0.01	0.05	3.3	<0.005	0.25	3.35
CD-96-2C	950	5.5	8.6	0.8	138.5	0.01	0.05	3	<0.005	0.25	3.75
CD-96-2C	960	5.8	10.5	0.7	177	0.01	0.05	3.5	<0.005	0.28	4.28
CD-96-2C	970	5.3	7.3	0.7	176	0.01	0.05	3.2	<0.005	0.26	2.56
CD-96-2C	980	4	2.9	0.8	134	0.01	0.03	3.6	<0.005	0.28	2.28
CD-96-2C	990	4.9	6.7	0.8	123	0.01	0.04	3.4	<0.005	0.26	1.72
CD-96-2C	1000	5.5	5.5	0.5	123	<0.01	0.04	2.7	<0.005	0.4	1.86
CD-96-2C	1010	5.6	3	0.6	122.5	<0.01	0.03	2.9	<0.005	0.41	1.92
CD-96-2C	1020	6.3	3.3	0.5	111	<0.01	0.04	2.4	<0.005	0.34	1.04
CD-96-2C	1030	5.9	4.8	0.6	111.5	0.01	0.04	3.7	<0.005	0.44	2.61
CD-96-2C	1040	5.6	6.6	0.6	124.5	0.01	0.04	2.9	<0.005	0.29	2.49
CD-96-2C	1050	4.1	4.9	1.3	148	0.01	0.03	5.9	0.005	0.27	4.8
CD-96-2C	1060	4.3	1.9	0.4	182	0.01	0.03	3.1	<0.005	0.23	1.91
CD-96-2C	1070	4.6	1.1	0.4	154	<0.01	0.03	3.7	<0.005	0.24	0.59
CD-96-2C	1080	4.8	1.1	0.4	164.5	<0.01	0.03	3.3	<0.005	0.25	0.77
CD-96-2C	1090	5.4	1.3	0.4	122	<0.01	0.03	3.2	<0.005	0.26	0.75
CD-96-2C	1100	4.5	0.8	0.4	189	<0.01	0.03	3.5	<0.005	0.21	0.46
CD-96-2C	1110	4	0.7	0.4	209	<0.01	0.02	3.4	<0.005	0.17	0.56

SAMPLE	Depth (ft)	Sc ppm	Se ppm	Sn ppm	Sr ppm	Ta ppm	Te ppm	Th ppm	Ti ppm	Tl ppm	U ppm
CD-96-2C	1120	5	1.1	0.3	176	<0.01	0.03	3.6	<0.005	0.16	0.65
CD-96-2C	1130	4.6	0.8	0.5	171.5	<0.01	0.03	3.7	<0.005	0.15	0.48
CD-96-2C	1140	5.1	1.3	0.5	181.5	<0.01	0.03	3.4	<0.005	0.12	0.58
CD-96-2C	1150	4.2	0.9	0.3	167	<0.01	0.02	2.1	<0.005	0.14	0.72
CD-96-2C	1160	2.1	0.7	0.3	317	<0.01	0.01	1.2	<0.005	0.08	0.77
CD-96-2C	1170	2.3	0.6	0.4	354	<0.01	0.01	1.8	<0.005	0.09	0.63
CD-96-2C	1180	2.7	0.9	0.5	329	<0.01	0.01	2	<0.005	0.11	1
CD-96-2C	1190	3.3	1.4	0.4	297	<0.01	0.02	2.3	<0.005	0.07	1.14
CD-96-2C	1200	4	1.8	0.3	243	0.01	0.02	2.9	<0.005	0.09	1.17
CD-96-2C	1210	3.8	1.2	0.4	276	<0.01	0.02	3.2	<0.005	0.12	1.02
CD-96-2C	1220	3.4	1.8	0.5	192.5	<0.01	0.02	2.2	<0.005	0.3	8.93
CD-96-2C	1230	4.1	2.3	0.7	122	<0.01	0.02	2.9	<0.005	0.32	6.3
CD-96-2C	1240	4.2	2.5	0.6	112	<0.01	0.02	3	<0.005	0.38	6
CD-96-2C	1250	3.1	1.7	0.5	136.5	<0.01	0.02	1.7	<0.005	0.27	2.34
CD-96-2C	1260	2.9	0.7	0.4	198	<0.01	0.01	2.1	<0.005	0.13	0.97
CD-96-2C	1270	3.2	1	0.4	146.5	<0.01	0.01	2.1	<0.005	0.19	1.26
CD-96-2C	1280	3.6	0.7	0.3	139.5	<0.01	0.01	2.4	<0.005	0.31	0.56
CD-96-2C	1290	2.9	0.6	0.4	140.5	<0.01	0.01	2.4	<0.005	0.14	0.69
CD-96-2C	1300	3	0.6	0.3	128.5	<0.01	0.01	2.4	<0.005	0.13	0.53
CD-96-2C	1310	3.3	0.6	0.4	140	<0.01	0.01	2.4	<0.005	0.17	0.69
CD-96-2C	1320	2.9	0.6	0.4	143.5	<0.01	0.01	2.2	<0.005	0.31	0.62
CD-96-2C	1330	2.8	0.6	0.4	181.5	<0.01	<0.01	2.3	<0.005	0.13	0.74
CD-96-2C	1340	3.1	0.6	0.4	155.5	<0.01	0.01	2.5	<0.005	0.15	0.77
CD-96-2C	1350	2.9	0.3	0.4	245	<0.01	0.01	2.1	<0.005	0.1	0.68
CD-96-2C	1360	3.3	0.6	0.3	158	<0.01	<0.01	2.3	<0.005	0.15	0.84
CD-96-2C	1370	3.1	0.6	0.3	144	<0.01	0.01	1.7	<0.005	0.19	0.8
CD-96-2C	1380	3.9	0.6	0.3	154.5	<0.01	0.01	2.4	<0.005	0.18	0.76
CD-96-2C	1390	4.4	0.7	0.3	146	<0.01	0.01	2.7	<0.005	0.14	0.67
CD-96-2C	1400	3.1	1.1	0.3	241	<0.01	0.02	1.7	<0.005	0.09	1.09
CD-96-2C	1410	3.6	0.8	0.4	181	<0.01	0.01	2.2	<0.005	0.11	0.88
CD-96-2C	1420	3.2	1.1	0.3	214	<0.01	0.02	1.6	<0.005	0.11	1.02
CD-96-2C	1430	3.1	0.8	0.4	217	<0.01	0.02	1.5	<0.005	0.1	0.89
CD-96-2C	1440	2.3	1.3	0.3	184.5	<0.01	0.04	1.6	<0.005	0.21	1.85
CD-96-2C	1450	3.2	2.8	0.4	120	<0.01	0.02	1.3	<0.005	0.27	2.77
CD-96-2C	1460	2.6	1.8	0.2	202	<0.01	0.02	1.2	<0.005	0.2	2.16
CD-96-2C	1470	3	1.7	0.3	156.5	<0.01	0.01	1.6	<0.005	0.21	1.75
CD-96-2C	1480	3	0.5	0.3	204	<0.01	0.02	2.2	<0.005	0.11	0.73
CD-96-2C	1490	4	0.7	0.4	163.5	<0.01	0.01	2.6	<0.005	0.19	1.01
CD-96-2C	1500	2.8	1.3	0.3	239	<0.01	0.02	1.6	<0.005	0.14	2.01
CD-96-2C	1510	3.8	0.8	0.5	185	<0.01	0.02	2.4	<0.005	0.2	1.88
CD-96-2C	1520	4.3	1.5	0.3	138.5	<0.01	0.01	2.6	<0.005	0.24	1.71
CD-96-2C	1530	3.1	1.7	0.4	210	<0.01	0.01	1.7	<0.005	0.2	2.13
CD-96-2C	1540	3.2	1.1	0.2	192	<0.01	0.02	1.9	<0.005	0.18	1.27
CD-96-2C	1550	3.7	1.1	0.4	162	<0.01	0.01	2.5	<0.005	0.16	1.07
CD-96-2C	1560	4.3	0.9	0.4	143.5	<0.01	0.01	3.1	<0.005	0.28	1.13
CD-96-2C	1570	4	2.7	0.4	145	<0.01	0.02	2.2	<0.005	0.3	2.17
CD-96-2C	1580	3.6	2.3	0.3	179.5	<0.01	0.02	1.6	<0.005	0.28	2.7
CD-96-2C	1590	3.3	1.5	0.3	161	<0.01	0.01	2	<0.005	0.3	1.76
CD-96-2C	1600	3.4	1.3	0.3	147	<0.01	0.02	2	<0.005	0.23	1.22
CD-96-2C	1610	3.4	0.5	0.3	117	<0.01	<0.01	2.6	<0.005	0.15	0.91
CD-96-2C	1620	3.4	0.6	0.4	110.5	<0.01	<0.01	2.6	<0.005	0.18	0.9

SAMPLE	Depth (ft)	Sc ppm	Se ppm	Sn ppm	Sr ppm	Ta ppm	Te ppm	Th ppm	Ti ppm	Tl ppm	U ppm
CD-96-2C	1630	3.2	0.9	0.3	144.5	<0.01	0.02	2.2	<0.005	0.29	1.46
CD-96-2C	1640	2.9	2	0.3	184	<0.01	0.02	1.8	<0.005	0.32	2.55
CD-96-2C	1650	3.3	1	0.3	116	<0.01	0.02	2.2	<0.005	0.28	1.24
CD-96-2C	1660	3.4	1.7	0.4	153	<0.01	0.02	2	<0.005	0.41	2.09
CD-96-2C	1670	2.9	2.6	0.4	202	<0.01	0.03	2	<0.005	0.43	3.8
CD-96-2C	1680	2.9	2.3	0.3	146	<0.01	0.02	1.8	<0.005	0.35	2.86
CD-96-2C	1690	2.5	0.8	0.2	176.5	<0.01	0.02	1.4	<0.005	0.22	0.89
CD-96-2C	1700	2.7	1.5	2	210	<0.01	0.03	2.2	<0.005	0.37	2.65
CD-96-2C	1710	2.8	2.1	0.4	204	<0.01	0.02	2	<0.005	0.26	3.09
CD-96-2C	1720	3.1	1.9	0.4	211	<0.01	0.02	2.1	<0.005	0.26	2.33
CD-96-2C	1730	2.3	2.4	0.4	210	<0.01	0.01	1.7	<0.005	0.24	2.8
CD-96-2C	1740	2.6	2.7	0.4	213	<0.01	0.02	1.8	<0.005	0.26	2.93
CD-96-2C	1750	2.6	2.6	0.8	257	<0.01	0.02	1.8	<0.005	0.2	3.15
CD-96-2C	1760	3.1	1.1	0.4	169.5	<0.01	0.01	2.2	<0.005	0.24	1.79
CD-96-2C	1770	3.4	2.1	0.4	202	<0.01	0.01	2.4	<0.005	0.24	2.08
CD-96-2C	1780	2.7	2	0.4	315	<0.01	0.01	1.8	<0.005	0.16	2.61
CD-96-2C	1790	3.2	3.9	0.5	212	<0.01	0.03	2	<0.005	0.39	3.28
CD-96-2C	1800	2.1	2.5	0.3	293	<0.01	0.03	1.2	<0.005	0.2	2.93
CD-96-2C	1810	2.8	4.7	0.5	244	<0.01	0.03	1.6	<0.005	0.3	3.35
CD-96-2C	1820	2.3	3.5	0.4	303	<0.01	0.02	1.5	<0.005	0.14	3.06
CD-96-2C	1830	2.4	3.8	0.5	296	<0.01	0.02	1.5	<0.005	0.19	3.16
CD-96-2C	1840	2.4	3.9	0.4	283	<0.01	0.02	1.5	<0.005	0.21	3.13
CD-96-2C	1860	2.9	4.3	0.4	237	<0.01	0.02	2	<0.005	0.4	2.23
CD-96-2C	1880	2.8	3.4	0.4	321	<0.01	0.03	1.8	<0.005	0.27	2.7
CD-96-2C	1900	2.3	3.3	0.5	411	<0.01	0.03	1.8	<0.005	0.11	3.29
CD-96-2C	1920	2.5	3.3	0.4	381	<0.01	0.03	1.6	<0.005	0.23	2.88
CD-96-2C	1925	3.1	2.9	0.2	218	<0.01	0.03	2.1	<0.005	0.44	2.1
CD-96-2C	1930	2.5	2.6	0.2	157.5	<0.01	0.02	2.1	<0.005	0.23	5.11
CD-96-2C	1940	2.8	1.9	0.2	256	<0.01	0.03	2.4	<0.005	0.31	3.21
CD-96-2C	1960	2.3	1.8	0.4	382	<0.01	0.03	1.9	<0.005	0.33	2.38
CD-96-2C	1980	2.3	1.6	0.5	420	<0.01	0.02	1.8	<0.005	0.27	1.72
CD-96-2C	2000	2.5	1.6	0.4	333	<0.01	0.02	2	<0.005	0.29	2.22
CD-96-2C	2020	2.4	1.6	0.6	308	<0.01	0.02	2	<0.005	0.23	2.27
CD-96-2C	2025	1.9	1.9	0.3	401	<0.01	0.03	1.2	<0.005	0.18	2.75
CD-96-2C	2030	2.2	1.4	0.2	336	<0.01	0.03	1.5	<0.005	0.17	2.45
CD-96-2C	2035	2.2	1.3	0.2	231	<0.01	0.02	1.3	<0.005	0.38	1.48
CD-96-2C	2040	2.7	0.9	0.2	138	<0.01	0.01	3.8	<0.005	0.56	1.47
CD-96-2C	2045	2.4	1.6	0.3	229	<0.01	0.02	2.2	<0.005	0.39	2.52
CD-96-2C	2050	1.7	1.5	0.2	350	<0.01	0.03	1.2	<0.005	0.15	2.94
CD-96-2C	2055	1.4	1	0.2	318	<0.01	0.03	0.8	<0.005	0.19	2.23
CD-96-2C	2060	2.9	1.2	0.5	195.5	<0.01	0.01	3	<0.005	0.51	1.9
CD-96-2C	2065	1.9	1.8	0.4	407	<0.01	0.03	1.3	<0.005	0.15	3.51
CD-96-2C	2070	2.2	2	0.8	318	<0.01	0.02	2	<0.005	0.25	2.89
CD-96-2C	2075	2.8	1.9	0.5	129.5	<0.01	0.02	3.4	<0.005	0.59	1.84
CD-96-2C	2080	2.5	0.7	<0.2	111.5	<0.01	0.03	4.6	<0.005	0.51	0.7
CD-96-2C	2100	2.9	4.1	0.4	152	<0.01	0.03	1.9	<0.005	0.58	3.12
CD-96-2C	2120	3.1	6.9	0.4	146	<0.01	0.04	2.7	<0.005	0.26	5
CD-96-2C	2180	2.4	1.6	0.2	108	<0.01	0.02	2	<0.005	0.27	2.92
CD-96-2C	2200	3	2.3	0.4	106.5	<0.01	0.04	1.8	<0.005	0.74	15.2
CD-96-2C	2220	3.5	1	0.3	106.5	<0.01	0.04	2.6	<0.005	0.72	3.52
CD-96-2C	2240	1.9	0.4	0.3	135	<0.01	0.02	3.6	<0.005	0.88	1.03

SAMPLE	Depth (ft)	Sc ppm	Se ppm	Sn ppm	Sr ppm	Ta ppm	Te ppm	Th ppm	Ti ppm	Tl ppm	U ppm
CD-96-2C	2260	0.9	0.5	0.4	87.7	<0.01	0.01	0.7	<0.005	0.27	2.73
CD-96-2C	2280	0.9	0.3	<0.2	84.1	<0.01	0.01	0.4	<0.005	0.46	1.85
CD-96-2C	2300	0.7	0.3	0.3	80.9	<0.01	0.02	0.3	<0.005	0.37	1.31
CD-96-2C	2320	0.5	0.3	0.2	70.8	<0.01	0.01	0.2	<0.005	0.17	0.97
CD-96-2C	2340	0.4	0.2	<0.2	62.2	<0.01	0.01	0.2	<0.005	0.09	1.19
DR-1C	2480	7.6	3.3	0.6	229	<0.01	0.03	4.2	<0.005	0.74	16.1
DR-1C	2500	3.4	3.4	0.5	229	<0.01	0.03	2.2	<0.005	0.74	22
DR-1C	2520	3.3	3.2	0.6	210	<0.01	0.03	2	<0.005	0.66	18.4
DR-1C	2540	3.2	3	0.7	232	<0.01	0.03	2.2	<0.005	0.7	18.6
DR-1C	2560	2.8	2.7	3.1	252	<0.01	0.03	1.9	<0.005	0.71	21
DR-1C	2580	3.1	2.1	2.6	238	<0.01	0.02	2.2	<0.005	0.59	13.1
DR-1C	2600	4.3	2.4	0.6	170.5	<0.01	0.02	2.5	<0.005	0.4	5.46
DR-1C	2620	3.3	3.3	0.8	288	<0.01	0.03	2.3	<0.005	0.65	13.4
DR-1C	2640	2.9	2.2	1	238	<0.01	0.02	2.3	<0.005	0.63	15.65
DR-1C	2660	3.1	2.6	0.3	277	<0.01	0.02	2	<0.005	0.4	13.3
DR-1C	2680	3.3	2.3	0.6	308	<0.01	0.03	2.1	<0.005	0.34	14.55
DR-1C	2700	4	2.6	0.5	211	<0.01	0.03	2.5	<0.005	0.25	10.35
DR-1C	2720	4.8	2.3	0.4	118	<0.01	0.03	2.2	<0.005	0.74	1.99
DR-1C	2740	3.9	1.7	0.5	206	<0.01	0.03	2.1	<0.005	0.27	2.16
DR-1C	2760	3.3	1.5	0.5	272	<0.01	0.01	2.3	<0.005	0.13	1.34
DR-1C	2780	3.2	1.4	0.2	267	<0.01	0.01	2	<0.005	0.1	1.14
DR-1C	2800	3.5	1.2	0.4	188	<0.01	0.01	2.3	<0.005	0.08	0.61
DR-1C	2820	4	1.3	0.4	113	<0.01	0.02	2.4	<0.005	0.51	1.28
DR-1C	2840	3.4	1	0.3	114	<0.01	0.01	1.7	<0.005	0.71	1.13
DR-1C	2860	3.6	1.1	0.4	189	<0.01	0.01	2.2	<0.005	0.12	1.09
DR-1C	2880	3.9	1.4	0.3	115	<0.01	0.01	2.4	<0.005	0.26	0.87
DR-1C	2900	3.8	0.9	0.5	128	<0.01	0.02	2.2	<0.005	0.15	0.89
DR-1C	2917	3.7	1.6	0.3	128	<0.01	0.02	2.1	<0.005	0.14	0.82
GA-2A	1680	2.3	9.3	0.5	43.9	<0.01	0.08	1.3	<0.005	0.63	4.95
GA-2A	1690	1.9	8.2	0.7	34.3	<0.01	0.08	1.6	<0.005	0.41	6.4
GA-2A	1700	3.5	4.2	0.6	44.8	<0.01	0.06	2.2	<0.005	0.66	4.97
GA-2A	1710	4.1	4	0.4	89.1	<0.01	0.05	2.3	<0.005	0.63	6.88
GA-2A	1720	4.5	31	0.6	119	<0.01	0.17	2.4	<0.005	0.52	6.95
GA-2A	1730	3.8	19.1	0.6	103	<0.01	0.11	2.9	<0.005	0.46	5.69
GA-2A	1740	4	8.8	0.4	86.9	<0.01	0.07	2.4	<0.005	0.58	5.26
GA-2A	1750	3.4	3.6	0.3	87.7	<0.01	0.06	2.3	<0.005	0.47	3.46
GA-2A	1760	3.6	7.6	0.3	86.1	<0.01	0.07	2.1	<0.005	0.66	2.96
GA-2A	1770	3.2	10.5	0.5	87.7	<0.01	0.09	1.5	<0.005	0.87	3.39
GA-2A	1780	3.1	9.1	0.5	69.8	<0.01	0.06	1.1	<0.005	1.11	3.93
GA-2A	1790	3.9	5.9	0.4	94.2	<0.01	0.05	1.8	<0.005	1.08	3.01
GA-2A	1800	2.9	17	0.4	67.6	<0.01	0.12	1.2	<0.005	1.85	7.94
GA-2A	1810	3.3	22.5	0.5	57.8	<0.01	0.13	1.9	0.005	2.4	13.55
GA-2A	1820	3.2	21.8	0.6	68.3	<0.01	0.13	1.4	<0.005	2.24	10.8
GA-2A	1830	4.7	18.7	0.8	147.5	0.01	0.08	3.5	<0.005	0.59	5.88
GA-2A	1840	5.1	8.6	0.5	83.8	<0.01	0.06	2.5	<0.005	0.55	1.76
GA-2A	1850	4.2	8.2	0.6	47.4	<0.01	0.08	2	<0.005	1.52	1.81
GA-2A	1860	3.1	6.3	0.5	26	<0.01	0.08	2.5	<0.005	1.43	1.2
GA-2A	1870	4.4	3.7	0.6	50.8	<0.01	0.06	4.4	<0.005	1.26	1.5
GA-2A	1880	2	3.9	0.6	16	<0.01	0.04	2.4	<0.005	1.58	1.24
GA-2A	1890	4.2	3.4	0.4	125.5	<0.01	0.04	4.2	<0.005	0.82	2.79
GA-2A	1900	3.3	3.6	0.5	53.3	<0.01	0.03	3.2	<0.005	0.94	1.94

SAMPLE	Depth (ft)	Sc ppm	Se ppm	Sn ppm	Sr ppm	Ta ppm	Te ppm	Th ppm	Ti ppm	Tl ppm	U ppm
GA-2A	1910	4.2	3	0.4	120	<0.01	0.04	3.5	<0.005	0.95	2.12
GA-2A	1920	2.3	2	0.4	25.9	<0.01	0.06	2.5	<0.005	1.25	1.58
GA-2A	1930	3.8	3.5	0.6	81.8	<0.01	0.07	3.2	<0.005	1.72	2.82
GA-2A	1940	1.2	6.6	0.5	9.9	<0.01	0.05	3	<0.005	3.55	5.86
GA-2A	1950	1.7	5.3	0.5	26.1	<0.01	0.06	3.4	<0.005	4.95	5.96
GA-2A	1960	1.1	12.1	0.7	19.8	<0.01	0.09	3.5	<0.005	6.01	7.9
GA-2A	1970	1.3	4.4	0.9	18.7	<0.01	0.04	2.4	<0.005	2.48	5.61
GA-2A	1980	1.9	4.6	0.8	18.7	<0.01	0.08	2.8	<0.005	2.44	2.81
GA-2A	1990	2	4.2	0.8	19.4	<0.01	0.06	2.7	<0.005	2.25	3.16
GA-2A	2000	1.2	5.2	0.8	13.5	<0.01	0.17	1.9	<0.005	2.12	3.94
GA-2A	2010	0.9	10	0.7	11.2	<0.01	0.42	2	<0.005	3.65	3.63
GA-2A	2020	0.8	8.1	0.9	14.1	<0.01	0.32	1.4	<0.005	2.45	2.8
GA-2A	2030	1.6	2.6	0.4	36.5	<0.01	0.1	1.4	<0.005	1.36	2.53
GA-2A	2040	1.5	2.7	0.3	36.9	<0.01	0.07	1.5	<0.005	1.38	2.48
GA-2A	2050	1.1	0.5	<0.2	96.4	<0.01	0.03	0.9	<0.005	0.34	1.47
GA-2A	2060	1.1	0.4	<0.2	130	<0.01	0.02	1.1	<0.005	0.18	2.69
GA-2A	2070	1.2	0.5	<0.2	135.5	<0.01	0.03	1	<0.005	0.29	2.49
GA-2A	2080	1.5	1.3	0.2	112	<0.01	0.03	1.3	<0.005	0.63	3.06
GA-2A	2100	1.5	1.4	0.3	139	<0.01	0.02	1.4	<0.005	0.59	4.18
GA-2A	2110	1.2	1.4	0.2	135	<0.01	0.03	1	<0.005	0.46	2.98
GA-2A	2120	1.4	2.1	0.2	130	<0.01	0.03	1.3	<0.005	0.71	2.29
GA-35C	1680	6.1	5.2	0.3	91	<0.01	0.05	2	<0.005	1.03	3.59
GA-35C	1700	7.1	4.6	0.3	65.7	<0.01	0.04	2.7	<0.005	0.39	4.41
GA-35C	1720	6	3.2	0.3	79.4	0.01	0.03	2.8	<0.005	0.3	7.66
GA-35C	1740	9.7	3.8	0.4	149	<0.01	0.04	3.2	<0.005	0.68	3.72
GA-35C	1760	8.4	1.8	0.4	85.9	<0.01	0.05	3.9	<0.005	1.02	3.86
GA-35C	1780	5.5	1.8	0.2	63.5	<0.01	0.02	3.4	<0.005	0.28	2.14
GA-35C	1800	3.7	4.9	0.3	84.8	<0.01	0.03	2.1	<0.005	0.97	8.88
GA-35C	1820	3.2	3.1	0.3	71.7	<0.01	0.03	2.2	<0.005	0.55	12.35
GA-35C	1840	3.5	2	0.4	77	<0.01	0.03	2.3	<0.005	2.02	7.03
GA-35C	1860	3	1.6	0.3	103.5	<0.01	0.02	2.7	<0.005	1.07	8.47
GA-35C	1880	2.6	2.3	0.4	63.9	<0.01	0.04	3.9	<0.005	6.13	12
GA-35C	1900	4.9	2.4	0.4	125	<0.01	0.03	7.3	<0.005	2.46	12.35
GA-35C	1920	6.9	2.3	0.6	94.6	<0.01	0.03	4.6	<0.005	4.77	4.63
GA-35C	1940	1.4	1.8	0.3	5.9	<0.01	0.02	3.8	<0.005	2.08	3.93
GA-35C	1960	1.1	2.3	0.4	6.6	<0.01	0.02	3.2	<0.005	2.5	5.74
GA-35C	1980	1.2	3	0.4	13.3	<0.01	0.02	3	<0.005	0.46	4.52
GA-35C	2000	0.9	2.3	0.3	8	<0.01	0.02	2.8	<0.005	0.62	3.09
GA-35C	2020	2.3	2.7	0.3	33.3	<0.01	0.03	3.9	<0.005	0.43	2.68
GA-35C	2040	2.9	2.1	0.3	75.9	<0.01	0.02	3.4	<0.005	0.53	1.59
GA-35C	2060	3.2	0.9	0.2	103	<0.01	0.02	2.4	<0.005	0.49	0.73
GA-35C	2080	11.9	2.1	0.5	283	<0.01	0.05	7.8	<0.005	5.22	3.32
GA-35C	2100	3	1.1	0.3	35.1	<0.01	0.03	3.8	<0.005	1.39	0.96
GA-35C	2120	3.6	0.9	0.3	59.4	<0.01	0.01	2.9	<0.005	1.09	2.27
GA-35C	2140	3.2	0.9	0.2	72.6	<0.01	0.01	2.5	<0.005	0.73	0.9
GA-35C	2160	2.4	0.6	<0.2	110	<0.01	0.01	1.8	<0.005	0.41	0.71
GA-35C	2186	3.7	0.8	0.2	78.4	<0.01	0.01	3.4	<0.005	0.61	0.78
SJ-390C	640	4	27.9	1	10.7	0.005	4.92	1.9	0.012	0.58	11.2
SJ-390C	650	6	37.9	1	117.5	0.01	0.41	2.7	0.033	0.78	12.6
SJ-390C	660	7.7	33.7	1.1	132.5	0.01	1.37	3.6	0.021	0.52	8.35
SJ-390C	670	7.8	23.3	1	136	0.01	0.1	3.9	0.01	0.65	5.75

SAMPLE	Depth (ft)	Sc ppm	Se ppm	Sn ppm	Sr ppm	Ta ppm	Te ppm	Th ppm	Ti ppm	Tl ppm	U ppm
SJ-390C	680	7.1	12.2	0.8	94.9	0.01	0.09	3.5	0.007	0.53	3.53
SJ-390C	690	6.5	7.6	0.7	77.8	0.01	0.08	4.1	0.008	0.36	3.48
SJ-390C	700	5.8	5.8	0.6	73	0.005	0.05	3.5	0.016	0.2	2.07
SJ-390C	710	6.3	4.5	0.7	52.9	0.005	0.05	3.4	0.03	0.19	0.83
SJ-390C	720	6.4	4.9	0.7	28.8	0.005	0.07	4.6	0.015	0.48	1.37
SJ-390C	730	5.6	4.6	0.7	15.3	0.005	0.08	4.8	0.006	0.76	1.81
SJ-390C	740	6.3	6.5	1.4	21.8	0.005	0.31	4.6	0.015	0.98	2.17
SJ-390C	750	5.1	2.8	0.7	26.3	0.005	0.05	4.5	0.006	1.05	3
SJ-390C	760	4.5	2.4	0.6	28.4	0.005	0.04	4.1	0.0025	1.18	2.59
SJ-390C	770	4.1	1.1	0.5	190.5	0.005	0.26	3.2	0.0025	0.64	1.3
SJ-390C	780	4.2	1	0.5	217	0.005	0.03	3.2	0.0025	0.69	1.16
SJ-390C	790	3.8	1.1	0.5	238	0.005	0.03	2.9	0.0025	0.43	1.2
SJ-390C	800	3.6	0.7	0.5	234	0.005	0.03	2.9	0.0025	0.57	1.19
SJ-390C	900	4	0.4	0.4	322	0.005	0.02	3.9	0.029	0.17	0.7
SJ-390C	920	4.1	3.1	0.4	272	0.005	0.04	3.6	0.025	0.29	11.6
SJ-390C	940	4.4	5.8	0.6	153	0.005	0.04	3.5	0.02	1.56	22.7
SJ-390C	960	4.2	3.8	0.6	173	0.005	0.12	2.7	0.0025	0.45	23.8
SJ-390C	965	3.1	2.2	0.5	255	0.005	0.08	2.2	0.007	0.38	18.5
SJ-390C	970	3.2	1.8	0.6	254	0.005	0.07	2.2	0.0025	0.29	15.4
SJ-390C	975	3.1	1.1	0.4	175.5	0.005	0.02	2.1	0.0025	0.27	8.67
SJ-390C	980	3.2	1.4	0.5	106	0.005	0.04	2.2	0.0025	0.27	8.83
SJ-390C	985	3.1	1	0.9	225	0.005	0.07	2	0.008	0.3	9.51
SJ-390C	990	3.1	1.4	0.7	249	0.005	0.08	2.1	0.009	0.71	14.6
SJ-390C	995	3.5	1.6	0.7	89.1	0.005	0.05	2	0.0025	1.02	10.4
SJ-390C	1000	2.9	1.2	0.3	133.5	0.005	0.02	1.5	0.0025	0.41	10.05
SJ-390C	1005	2.5	1.4	0.4	140	0.005	0.02	1.4	0.0025	0.28	13.8
SJ-390C	1010	3.3	1.5	0.4	88.8	0.005	0.04	1.7	0.0025	0.27	11.65
SJ-390C	1015	4.1	2	0.4	81	0.01	0.03	2.6	0.0025	1.22	10.3
SJ-390C	1020	3.2	2.2	0.5	166.5	0.005	0.02	2.5	0.011	0.56	11.65
SJ-390C	1025	3.5	2.6	0.6	285	0.005	0.03	3.1	0.03	0.4	21.1
SJ-390C	1030	3.8	2.1	0.4	189	0.005	0.07	3.3	0.01	0.17	9.34
SJ-390C	1035	4.2	2.3	0.4	240	0.01	0.25	4	0.043	0.29	9.81
SJ-390C	1040	4	2.2	0.4	186	0.005	0.68	3.7	0.046	0.27	8.04
SJ-390C	1060	3.8	2.2	1	96.8	0.005	0.6	3.6	0.006	0.14	8.26
SJ-390C	1095	2.8	1.4	0.9	32.1	0.005	0.01	1.8	0.0025	0.23	1.22
SJ-390C	1100	4.4	1.2	0.6	68.5	0.005	0.02	2.4	0.0025	0.38	1.09
SJ-390C	1105	4.2	0.9	0.6	69.7	0.005	0.01	2.2	0.0025	0.3	0.83
SJ-390C	1110	4.2	1.2	0.8	55.1	0.005	0.04	2.3	0.0025	1.04	1.43
SJ-390C	1115	3.5	1.6	1.4	46.4	0.005	0.04	2.1	0.0025	1.55	1.59
SJ-390C	1120	2.2	1.4	1.5	48.3	0.005	0.09	2.2	0.0025	1.06	1.36
SJ-390C	1125	2.3	1.7	2.2	46.2	0.005	0.12	2.3	0.0025	1.14	1.3
SJ-390C	1130	1.7	1.4	4.5	38.4	0.005	0.09	2.1	0.0025	0.67	1.19
SJ-390C	1135	3.6	1	0.9	77.3	0.005	0.02	2.7	0.0025	0.36	0.94
SJ-390C	1140	4.4	1	0.7	72.4	0.005	0.01	2.8	0.0025	0.07	0.62
SJ-390C	1160	4.1	1	0.6	72.8	0.005	0.01	2.3	0.0025	0.13	0.72
SJ-390C	1180	4.2	1.1	0.6	47.8	0.005	0.01	2.6	0.0025	0.14	0.84
SJ-390C	1200	3.2	1.3	0.8	58.2	0.005	0.02	3.3	0.0025	0.37	1.36
SJ-390C	1220	3.4	1.3	0.8	71.7	0.005	0.03	2.8	0.0025	0.33	1.27
SJ-390C	1240	2.7	1.7	0.6	61.3	0.005	0.06	3.2	0.0025	0.45	1.75
SJ-390C	1260	3.5	1.9	0.6	91.6	0.005	0.01	2.1	0.0025	0.24	1.06
SJ-390C	1280	0.8	1	0.1	87.2	0.005	0.03	1.1	0.0025	0.14	1.76

SAMPLE	Depth (ft)	Sc ppm	Se ppm	Sn ppm	Sr ppm	Ta ppm	Te ppm	Th ppm	Ti ppm	Tl ppm	U ppm
SJ-390C	1295	2.8	1.3	0.2	126	0.005	0.07	3.1	0.0025	0.68	1.02
SJ-464C	10	5.2	4.5	0.6	116	0.005	0.09	5.4	0.006	0.44	3.33
SJ-464C	20	6.5	5	0.5	138	0.01	0.05	8.2	0.0025	1.08	8.06
SJ-464C	30	6.9	1.5	0.4	36.8	0.005	0.02	6.8	0.0025	0.27	1.14
SJ-464C	240	2.6	3.6	0.3	9	0.005	0.09	3.8	0.0025	0.57	3.22
SJ-464C	250	4	2.7	0.4	58.3	0.005	0.05	4.7	0.0025	0.35	2.66
SJ-464C	260	4.1	1.5	0.3	103.5	0.005	0.02	4	0.0025	0.33	2.14
SJ-464C	270	3.7	2.4	0.4	57.3	0.005	0.04	4.7	0.0025	0.35	2.81
SJ-464C	280	3.9	1.7	0.4	101	0.005	0.02	5.1	0.0025	0.31	2.51
SJ-464C	290	5.3	1.7	0.6	111.5	0.005	0.02	6.4	0.0025	0.25	2.47
SJ-464C	300	3.7	1.4	0.3	84.3	0.005	0.01	4.4	0.0025	0.22	1.35
SJ-464C	310	4.3	0.9	0.3	84.5	0.005	0.02	5.1	0.0025	0.55	2.52
SJ-464C	320	4	1.3	0.3	86	0.005	0.02	4.9	0.0025	0.58	2.32
SJ-464C	330	2.6	5.9	0.5	42.9	0.005	0.05	2.5	0.0025	0.49	3.91
SJ-464C	370	1.8	34.7	0.6	43.8	0.005	0.09	1.8	0.0025	0.98	5.14
SJ-464C	380	2.7	33.2	0.5	81.8	0.005	0.06	2.3	0.0025	0.83	4.21
SJ-464C	390	3.8	4.2	0.4	78.7	0.005	0.02	3.7	0.0025	0.35	1.86
SJ-464C	400	3.8	1.7	0.6	79.5	0.005	0.02	4.2	0.0025	0.37	3.01
SJ-464C	410	3	1.4	0.4	61.4	0.005	0.01	3.4	0.0025	0.23	3.3
SJ-464C	420	3.6	2.2	0.4	64.6	0.005	0.01	3.3	0.0025	0.21	2.76
SJ-464C	430	3.7	3.1	0.3	65	0.005	0.01	3.7	0.0025	0.1	1.88
SJ-464C	440	4.1	3.8	0.3	66.9	0.005	0.01	4.2	0.0025	0.11	2.07
SJ-464C	450	3.5	0.9	0.3	65.1	0.005	0.01	3.2	0.0025	0.31	1.94
SJ-464C	460	3.2	0.8	0.3	61.7	0.005	0.01	2.4	0.0025	0.46	2.02
SJ-464C	470	4.1	1.5	0.3	70.9	0.005	0.01	3.2	0.0025	0.73	3.33
SJ-464C	480	4.6	1.5	0.3	90.2	0.005	0.02	3.4	0.0025	0.57	3.24
SJ-464C	490	4.8	4.4	0.4	79.8	0.005	0.02	3.3	0.0025	0.44	4.7
SJ-464C	500	4.3	4.6	0.3	86.3	0.005	0.03	3.3	0.0025	0.31	5.65
SJ-464C	510	4.9	1	0.3	72.3	0.005	0.01	4.8	0.0025	0.26	4.38
SJ-464C	520	5.3	0.7	0.4	80.1	0.005	0.01	5	0.0025	0.27	4.1
SJ-464C	530	5.1	1.1	0.3	85	0.01	0.01	5.3	0.0025	0.24	6.47
SJ-464C	540	3.2	2.6	0.5	47.1	0.005	0.03	3.5	0.0025	0.21	4.33
SJ-464C	690	0.5	3.1	0.4	4.3	0.005	0.05	0.4	0.0025	0.47	2.17
SJ-464C	700	2	3.1	0.4	8.1	0.005	0.03	0.9	0.0025	0.91	3.12
SJ-464C	710	9.1	1.5	0.4	42.1	0.005	0.02	4.8	0.0025	0.77	6.58
SJ-464C	720	8.4	1.1	0.3	54.5	0.005	0.01	4	0.0025	0.56	4
SJ-464C	740	5.8	4	0.7	52.8	0.005	0.03	4.9	0.0025	0.71	3.2
SJ-464C	750	2.7	22.9	0.6	24.6	0.005	0.07	1.7	0.014	1.5	6.21
SJ-464C	760	2.5	36.6	0.9	18.2	0.005	0.1	2.2	0.019	3.16	11.9
SJ-464C	770	3.7	25.9	0.9	34.3	0.005	0.09	3.1	0.029	3.12	12.55
SJ-464C	780	3.4	21.6	0.7	49.3	0.005	0.07	2.4	0.006	2.17	14
SJ-464C	790	4.5	28.1	0.9	99.8	0.01	0.07	2.8	0.012	1.64	13.8
SJ-464C	800	6.3	28	0.9	125	0.01	0.06	3.2	0.022	1.22	11
SJ-464C	810	7.4	24.8	1.2	103.5	0.01	0.04	3.8	0.028	0.54	7.04
SJ-464C	820	7	18.4	1.1	126.5	0.01	0.03	4	0.018	0.47	6.8
SJ-464C	830	5.8	12.6	0.8	129	0.01	0.03	3.6	0.017	0.43	5.91
SJ-464C	840	5.9	12.2	0.9	115	0.01	0.03	3.3	0.021	0.3	3.82
SJ-464C	850	5.9	11.5	0.9	103.5	0.01	0.03	3.1	0.023	0.24	2.77
SJ-464C	860	5.4	6.9	0.8	103.5	0.01	0.02	3.4	0.034	0.27	1.85
SJ-464C	870	5.3	7.9	0.7	87.1	0.005	0.04	3.2	0.0025	0.26	1.48
SJ-464C	880	5.9	5.8	0.5	80.2	0.005	0.04	3.4	0.0025	0.25	1.39

SAMPLE	Depth (ft)	Sc ppm	Se ppm	Sn ppm	Sr ppm	Ta ppm	Te ppm	Th ppm	Ti ppm	Tl ppm	U ppm
SJ-464C	900	6.1	7.2	0.5	68.6	0.005	0.05	3.6	0.0025	0.35	3.24
SJ-464C	920	4.7	3.3	0.4	67.6	0.005	0.04	3.8	0.0025	0.28	1.82
SJ-464C	940	4.5	1.8	0.5	110	0.005	0.03	3.3	0.0025	0.46	2.1
SJ-464C	960	5	1.8	0.2	134.5	0.005	0.04	4	0.0025	0.3	1.05
SJ-464C	980	4.4	1.3	0.2	173	0.005	0.03	3.9	0.0025	0.11	0.57
SJ-464C	1000	4.9	1.7	0.3	149	0.005	0.03	4.4	0.0025	0.1	0.94
SJ-464C	1020	3	1	0.1	322	0.005	0.02	2.8	0.0025	0.05	0.6
SJ-464C	1040	3.2	1.1	0.1	296	0.005	0.02	3.3	0.0025	0.1	0.71
SJ-464C	1060	2.4	0.9	0.1	385	0.005	0.02	2.5	0.0025	0.06	0.6
SJ-464C	1080	3.1	1	0.1	335	0.005	0.02	3.5	0.0025	0.09	0.65
SJ-464C	1100	3.9	1.3	0.2	217	0.005	0.02	4.2	0.0025	0.15	0.69
SJ-464C	1120	3.6	4.7	0.3	162	0.005	0.03	3	0.0025	0.4	13.4
SJ-464C	1140	2.4	3.9	0.3	78.3	0.005	0.04	2	0.0025	1.56	13.05
SJ-464C	1215	5.6	3.5	1	54.5	0.005	0.11	2.3	0.0025	2.18	2.74
SJ-464C	1220	5.4	2.4	0.6	63.2	0.005	0.05	2.5	0.0025	2.22	3.33
SJ-464C	1225	4.8	2.1	0.7	61.5	0.005	0.09	2.4	0.0025	1.61	2.23
SJ-464C	1230	4.3	3	0.7	56.3	0.005	0.18	2.7	0.0025	1.12	2.86
SJ-464C	1235	3.7	1.9	0.6	54.4	0.005	0.07	2.6	0.0025	0.88	2.51
SJ-464C	1240	5	2	0.5	79	0.005	0.02	3.4	0.0025	0.88	2.76
SJ-464C	1245	4.3	2.4	0.5	55	0.005	0.04	2.8	0.0025	0.72	2.58
SJ-464C	1250	4.3	2	0.7	47.4	0.005	0.13	2.6	0.0025	0.88	1.62
SJ-464C	1255	5.3	2.3	0.5	52.6	0.005	0.04	3.2	0.0025	0.87	2.76
SJ-464C	1260	5.7	1.5	0.4	58.2	0.005	0.02	2.9	0.0025	0.56	1.96
SJ-464C	1265	5.8	1.7	0.4	54.9	0.005	0.02	2.9	0.0025	0.59	2.32
SJ-464C	1270	6.3	1.3	0.4	71.7	0.005	0.02	2.6	0.0025	0.56	2.01
SJ-464C	1275	5.7	1.3	0.4	58.7	0.005	0.01	2.8	0.0025	0.57	2
SJ-464C	1280	5.2	1.1	0.4	59.5	0.005	0.02	2.5	0.0025	0.89	1.78
SJ-464C	1285	5.8	1.3	0.4	53.8	0.005	0.01	2.9	0.0025	1.09	3.08
SJ-464C	1290	4.9	1.3	0.5	45	0.005	0.03	2.9	0.0025	2.57	2.95
SJ-464C	1295	5.7	1.2	0.4	53.9	0.005	0.01	2.7	0.0025	1.04	2.51
SJ-464C	1300	4.9	1.7	0.5	46.5	0.005	0.02	2.8	0.0025	1.02	2.77
SJ-464C	1305	5.6	1.6	0.4	54.3	0.005	0.01	2.5	0.0025	0.82	2.36
SJ-464C	1310	4.1	2.1	0.6	37	0.005	0.02	2.3	0.0025	0.69	1.97
SJ-464C	1315	5	1.4	0.6	45	0.005	0.02	2.5	0.0025	0.61	2.48
SJ-464C	1320	5.6	1.3	0.4	52.2	0.005	0.01	2.3	0.0025	0.86	1.62
SJ-464C	1325	5.5	1.2	0.4	53.1	0.005	0.01	2.3	0.0025	0.7	2.05
SJ-464C	1330	5.6	1.2	0.4	59.7	0.005	0.02	2.1	0.0025	0.67	1.56
SJ-464C	1335	5.6	1.4	0.4	58.9	0.005	0.03	2.2	0.0025	1.23	1.38
SJ-464C	1340	3.6	1.1	0.5	51.5	0.005	0.02	1.8	0.0025	0.49	2
SJ-464C	1345	3.7	1.1	0.5	57	0.005	0.03	1.8	0.0025	0.66	1.67
SJ-464C	1350	2.3	1	0.6	38.4	0.005	0.03	1.6	0.0025	1.01	2.11
SJ-464C	1355	2.9	1.1	0.5	42.1	0.005	0.06	1.8	0.0025	1.1	2.5
SJ-464C	1360	3.8	1.2	0.3	51.5	0.005	0.03	2	0.0025	0.74	1.67
SJ-464C	1365	4.7	1.2	0.5	58.3	0.005	0.01	2.5	0.0025	0.44	2.49
SJ-464C	1370	3.6	1.4	0.4	53.7	0.005	0.01	2	0.0025	0.45	4.22
SJ-464C	1375	4.2	1.8	0.5	72.1	0.005	0.01	2.3	0.0025	0.43	2.61
SJ-464C	1380	4.7	2	0.6	53.8	0.005	0.03	2.5	0.0025	1.19	3.27
SJ-464C	1385	3.9	1.9	0.5	49.4	0.005	0.04	2.3	0.0025	0.81	2.23
SJ-464C	1390	2.3	1.2	0.6	34	0.005	0.07	1.7	0.0025	1.06	2.59
SJ-464C	1395	3	1.6	0.5	39.1	0.005	0.06	2.8	0.0025	1.08	3.56
SJ-464C	1400	3.2	3.1	0.7	42.5	0.005	0.74	3.1	0.0025	4.18	3.21

SAMPLE	Depth (ft)	Sc ppm	Se ppm	Sn ppm	Sr ppm	Ta ppm	Te ppm	Th ppm	Ti ppm	Tl ppm	U ppm
SJ-464C	1405	3.6	1.7	0.4	67.7	0.005	0.07	2.1	0.0025	0.73	4.51
SJ-464C	1410	3.7	1.6	0.5	43.2	0.005	0.02	1.8	0.0025	0.39	3.38
SJ-464C	1415	3.4	2	0.4	44.9	0.005	0.01	1.8	0.0025	0.4	1.54
SJ-464C	1420	3.9	2.5	0.4	50.1	0.005	0.04	2	0.0025	0.49	1.44
SJ-464C	1425	2.7	12.8	0.7	45.2	0.005	0.18	2	0.0025	1.71	1.18
SJ-464C	1430	2.2	4	0.4	54.3	0.005	0.13	0.7	0.0025	1.25	0.92
SJ-464C	1435	3.2	3.7	0.3	117	0.005	0.07	0.3	0.0025	0.48	0.71
SJ-464C	1440	2.4	0.6	0.5	116.5	0.005	0.07	0.2	0.0025	0.32	0.6
SJ-464C	1445	1.2	0.3	0.3	151	0.005	0.02	0.2	0.0025	0.07	0.34
SJ-464C	1450	0.9	0.3	0.1	162	0.005	0.02	0.5	0.0025	0.16	0.59
SJ-464C	1455	1.5	0.4	0.1	145	0.005	0.02	1.6	0.0025	0.18	0.74
SJ-464C	1460	1	0.4	0.2	174.5	0.005	0.03	0.7	0.0025	0.3	0.86
SJ-464C	1465	1.1	0.4	0.3	173.5	0.005	0.03	0.8	0.0025	0.24	0.87
WM-01C	2440	1.8	8.2	0.5	47	<0.01	0.13	2.5	<0.005	0.75	4.69
WM-01C	2460	1.6	12.5	0.4	29.6	<0.01	0.14	2.1	<0.005	1.06	3.33
WM-01C	2480	1.3	15.2	0.3	20.4	<0.01	0.11	1.7	<0.005	0.71	3.41
WM-01C	2500	1.7	11.9	0.3	31	<0.01	0.07	1.9	<0.005	0.49	2.25
WM-01C	2520	1.9	5.8	0.2	30.9	<0.01	0.09	2.4	<0.005	0.65	2.46
WM-01C	2540	2.5	8.3	0.3	56.7	<0.01	0.09	2.2	<0.005	1.46	2.92
WM-01C	2560	3.3	1.9	<0.2	166	<0.01	0.01	1.8	<0.005	0.36	2.14
WM-01C	2580	3.1	1	<0.2	308	<0.01	0.01	2.8	<0.005	0.24	2.5
WM-01C	2600	3.4	3.8	0.2	166	<0.01	0.03	3.4	<0.005	0.54	7.45
WM-01C	2620	3.9	3.7	0.2	222	<0.01	0.03	2.5	<0.005	0.39	8.69
WM-01C	2640	4.4	1.9	<0.2	105	<0.01	0.01	2.7	<0.005	0.28	1.17
WM-01C	2660	4	1.4	<0.2	121.5	<0.01	0.03	3.3	<0.005	0.37	1.42
WM-01C	2680	3.1	1.3	<0.2	93.2	<0.01	0.01	2.8	<0.005	0.29	0.79
WM-01C	2700	3.2	1.1	0.2	169	<0.01	0.02	2.7	<0.005	0.09	1.52
WM-01C	2720	3	1.3	0.2	130.5	<0.01	0.03	2.4	<0.005	0.1	1.23
WM-01C	2740	3.1	1.2	0.2	105.5	<0.01	0.03	2.8	<0.005	0.07	0.78
WM-01C	2760	2.9	1.3	0.2	118	<0.01	0.03	2.5	<0.005	0.37	0.84
WM-01C	2780	3	1.3	0.2	100	<0.01	0.03	2.4	<0.005	0.39	1.18
WM-01C	2800	3	1.3	0.2	75.4	<0.01	0.03	2.5	<0.005	0.32	0.84
WM-01C	2820	2.7	0.9	0.2	70.6	<0.01	0.02	2.4	<0.005	0.63	0.87
WM-01C	2840	2.8	1.4	0.2	64.1	<0.01	0.03	2.5	<0.005	0.13	1
WM-01C	2860	3.1	1.7	0.2	70.2	<0.01	0.03	2.6	<0.005	0.11	1.17
WM-01C	2880	2.8	2.7	0.2	63.3	<0.01	0.03	2.7	<0.005	0.14	1.53
WM-01C	2900	3.2	2.1	0.2	83	<0.01	0.03	3.5	<0.005	0.15	1.76
WM-01C	2920	2.4	1	<0.2	65.9	<0.01	0.02	3.3	<0.005	0.19	1.07
WM-01C	2940	2.5	0.8	<0.2	95.2	<0.01	0.02	2.7	<0.005	0.17	1.01
WM-01C	2960	2.5	0.7	<0.2	119	<0.01	0.03	3.1	<0.005	0.22	1.26
WM-01C	2980	2.7	0.6	<0.2	101.5	<0.01	0.02	3.1	<0.005	0.16	0.88
WM-01C	3000	2.7	0.8	<0.2	139.5	<0.01	0.02	2.6	<0.005	0.12	1.2
WM-01C	3020	2.7	0.5	<0.2	105	<0.01	0.02	2.8	<0.005	0.12	1
WM-01C	3040	2.6	0.8	<0.2	181.5	<0.01	0.03	2.5	<0.005	0.08	1.1
WM-01C	3050	2.5	1.2	<0.2	265	<0.01	0.03	2.4	<0.005	0.15	1.58

SAMPLE	Depth (ft)	V ppm	W ppm	Y ppm	Zn ppm	Zr ppm
BZ-965C	880	84	0.55	15.05	213	3.1
BZ-965C	885	76	0.64	13.35	185	3.4
BZ-965C	905	33	0.98	8.09	362	2.4
BZ-965C	910	34	0.74	11.65	331	3
BZ-965C	955	128	1.45	13.45	223	2.9
BZ-965C	960	403	1.56	14.6	1080	3.6
BZ-965C	965	1190	2.13	13.5	3010	5
BZ-965C	970	1110	1.56	12.85	2270	3.9
BZ-965C	975	1110	8.6	15.75	1590	5.3
BZ-965C	980	1100	1.31	17.85	1700	4.1
BZ-965C	1000	302	0.78	33.7	398	5.9
BZ-965C	1020	72	1.52	23	188	3.4
BZ-965C	1040	38	1.7	14.9	252	2.3
BZ-965C	1060	34	1.09	12.95	80	2.1
BZ-965C	1065	72	1.03	14.7	208	1.8
BZ-965C	1070	61	3.38	19.35	92	2.3
BZ-965C	1075	35	2.29	15.65	42	2
BZ-965C	1080	32	0.93	19.1	698	2.4
BZ-965C	1085	26	1.65	12.65	22	1.5
BZ-965C	1090	110	7.82	15.5	361	2.2
BZ-965C	1095	107	15.65	17.4	455	2.2
BZ-965C	1100	29	8.72	12.05	19	1.4
BZ-965C	1105	29	380	13.4	18	1.2
BZ-965C	1110	29	1050	14.65	17	1.2
BZ-965C	1115	25	1000	16.7	14	1.2
BZ-965C	1120	23	103	15.55	14	1
BZ-965C	1125	21	32.9	14.2	291	1.2
BZ-965C	1130	26	73.2	12.65	48	1.1
BZ-965C	1135	25	410	15.05	136	1
BZ-965C	1140	16	36	16.2	42	0.9
BZ-965C	1145	10	20.3	13.55	31	1.2
BZ-965C	1150	9	7.46	12.8	21	1.4
BZ-965C	1155	9	2.84	12.5	27	1
BZ-965C	1160	8	1.73	11.5	15	1.2
BZ-965C	1165	10	3.64	12	19	1.6
BZ-965C	1170	10	1.82	11.25	33	1
BZ-965C	1175	12	10.7	15.6	38	1.9
BZ-965C	1180	8	1.37	13.9	14	1.6
BZ-965C	1185	7	2.6	14.95	13	1.8
BZ-965C	1190	10	14.65	18	33	2
BZ-965C	1195	13	7.49	19.75	18	2.5
BZ-965C	1200	12	13.9	21.2	19	2
BZ-965C	1205	12	23.6	21.1	20	1.8
BZ-965C	1215	20	101.5	23.2	43	2.3
BZ-965C	1220	18	34	26.9	25	3.9
BZ-965C	1225	14	10.1	17.3	32	2
BZ-965C	1230	11	5.8	13.65	32	1.7
BZ-965C	1235	10	4.96	13.9	25	1.6
BZ-965C	1240	7	0.91	12.75	22	1.5
BZ-965C	1245	7	0.77	13.1	27	1.5
BZ-965C	1250	8	0.66	14.85	37	1.5

SAMPLE	Depth (ft)	V ppm	W ppm	Y ppm	Zn ppm	Zr ppm
BZ-965C	1255	15	570	18.8	12	1.4
BZ-965C	1260	18	780	22	15	1.2
BZ-965C	1265	27	690	15.35	38	1
BZ-965C	1270	96	160.5	16.1	411	2
BZ-965C	1275	165	690	13.15	638	2.3
BZ-965C	1280	189	830	12.15	658	2.4
BZ-965C	1285	189	670	12.75	482	2.8
BZ-965C	1290	143	580	12.2	275	2.4
BZ-965C	1295	219	280	13.95	578	2.9
BZ-965C	1300	199	280	16.35	471	2.5
BZ-965C	1305	167	36	16.3	387	2.7
BZ-965C	1310	113	47.1	14.2	225	2.5
BZ-965C	1315	51	17.15	12.95	116	2.2
BZ-965C	1320	52	10.3	13.3	82	1.6
BZ-965C	1325	35	5.92	9.07	75	2.5
CD-14	530	19	1.34	20.8	36	11.8
CD-14	550	24	0.74	24.4	10	4.2
CD-14	560	16	0.49	44.3	8	4.3
CD-14	570	28	0.91	15.85	10	3.3
CD-14	580	13	10.15	14.25	14	3.5
CD-14	590	9	1.98	14.2	25	3.5
CD-14	600	17	11.9	12.95	89	3.5
CD-14	610	211	5.64	50	366	6
CD-14	620	243	10.9	23.4	403	5.8
CD-14	630	272	6.84	24.9	505	5.2
CD-14	640	235	6.8	22	396	5.1
CD-14	650	218	7.95	22.6	208	5.2
CD-14	660	240	4.19	23.7	323	4.7
CD-14	670	149	4.59	20.4	231	7.9
CD-14	680	16	0.83	11.95	59	2.1
CD-14	690	20	0.92	13.55	62	3.2
CD-14	700	47	0.44	17.8	108	2.2
CD-14	720	52	0.52	15.45	104	2.9
CD-14	740	94	0.71	18.15	182	2.5
CD-14	770	218	0.81	23.1	629	3.6
CD-14	780	188	1.19	18.5	527	2.8
CD-14	790	107	0.54	17.25	267	2
CD-14	800	72	0.65	16.55	264	2.6
CD-14	820	83	0.85	20.2	107	2.9
CD-14	840	55	0.73	11.15	87	2.3
CD-14	860	13	0.53	7.51	23	1.8
CD-14	880	11	0.56	8.38	25	2
CD-14	900	14	0.51	8.87	58	1.8
CD-14	920	11	0.5	10.15	28	1.7
CD-14	940	7	0.39	10.35	24	1.7
CD-14	960	23	0.56	7.75	84	2.1
CD-14	980	22	0.54	8.66	84	1.6
CD-14	1000	16	0.61	13.05	63	1.3
CD-14	1020	16	0.46	12.2	64	1.4
CD-14	1040	15	0.29	12.5	52	1.5
CD-14	1060	27	0.33	11.4	84	1.7

SAMPLE	Depth (ft)	V ppm	W ppm	Y ppm	Zn ppm	Zr ppm
CD-14	1080	35	0.4	10.75	83	1.6
CD-14	1100	46	0.37	11.6	156	1.8
CD-14	1120	20	0.31	11	68	1.5
CD-14	1140	26	0.66	11.9	93	1.7
CD-14	1160	35	0.28	10.15	130	1.8
CD-14	1180	29	0.12	10.75	119	1.7
CD-14	1200	47	0.36	10.85	243	1.6
CD-14	1220	86	0.51	13.3	451	2.2
CD-14	1240	72	0.8	11.65	214	1.6
CD-14	1260	62	0.67	11.5	237	2.3
CD-14	1280	15	0.28	11.35	42	1.4
CD-14	1300	9	0.2	12.35	23	1.7
CD-14	1320	47	0.17	11.15	111	2.2
CD-14	1340	47	0.26	12	225	2.5
CD-14	1360	30	0.18	10.9	97	2.8
CD-14	1380	46	1.54	11.6	199	2.3
CD-14	1400	83	0.54	10.75	134	6.8
CD-14	1420	51	0.32	15.05	213	2.5
CD-14	1440	48	0.12	11.8	170	6.8
CD-14	1460	27	<0.05	11.6	74	2
CD-14	1480	60	0.19	11.35	38	24.3
CD-14	1500	97	0.1	11.95	75	25.9
CD-14	1520	44	0.13	12.8	68	3
CD-14	1540	43	0.16	10.3	180	2.3
CD-14	1560	46	0.15	12.3	193	2.5
CD-14	1580	32	0.24	12.25	124	4
CD-14	1600	33	0.06	13.05	69	3.8
CD-14	1620	48	0.17	11.75	264	2.8
CD-14	1640	43	0.34	11.7	181	2.3
CD-14	1660	81	0.32	9.6	199	5.7
CD-14	1680	45	0.27	11.4	181	2.3
CD-14	1700	30	0.46	16.05	119	2.1
CD-14	1720	20	4.77	11.85	72	1.9
CD-14	1740	14	0.33	12.3	26	1.7
CD-14	1760	24	0.45	11.9	77	2.3
CD-14	1780	37	0.32	10.15	147	2.5
CD-14	1800	24	0.22	10.2	81	2.1
CD-14	1820	49	0.18	13.1	50	8.3
CD-14	1840	25	0.45	11.95	45	2.8
CD-14	1860	53	0.85	12.3	94	8.7
CD-14	1880	46	0.3	14.2	230	2.8
CD-14	1900	56	0.28	12.75	287	2.3
CD-14	1920	40	0.3	13.35	206	2.1
CD-14	1940	24	0.28	12.2	97	1.9
CD-14	1960	61	0.25	12.65	257	2.9
CD-14	1980	31	0.07	11.75	80	1.9
CD-14	2000	37	0.33	12.35	126	2.6
CD-14	2020	17	0.24	12	51	2.1
CD-14	2040	15	0.05	11.95	58	1.8
CD-14	2060	19	2.8	12.4	54	2.2
CD-14	2080	36	1.31	10.15	136	2.3

SAMPLE	Depth (ft)	V ppm	W ppm	Y ppm	Zn ppm	Zr ppm
CD-14	2100	47	0.73	14.7	49	10.7
CD-14	2120	30	0.61	12.35	60	2.3
CD-14	2140	34	0.39	11.6	101	2.5
CD-14	2160	44	0.47	12.6	87	2.6
CD-15C	1380	28	6.1	13.3	82	2.3
CD-15C	1400	94	0.97	21.3	415	3.9
CD-15C	1420	77	0.56	33.1	249	3.6
CD-15C	1440	36	0.5	23.1	220	3.1
CD-15C	1460	28	0.72	29.8	225	3.2
CD-15C	1480	35	0.62	35.7	197	3.3
CD-15C	1500	45	0.81	25.9	141	3.6
CD-15C	1520	16	0.44	15	176	3.4
CD-15C	1540	15	0.35	14.65	45	2.9
CD-15C	1560	20	0.48	13.5	73	3.3
CD-15C	1580	16	0.52	13.5	23	3.5
CD-15C	1600	19	0.51	17.7	29	3.4
CD-15C	1620	24	0.49	19.55	25	3.7
CD-15C	1660	25	1.49	26.2	51	3.3
CD-15C	1680	10	0.63	17.8	35	2.4
CD-15C	1700	6	0.39	15.6	17	1.8
CD-15C	1720	16	0.71	13.8	20	2.4
CD-15C	1740	18	2.93	11.75	24	3.2
CD-15C	1760	15	1.09	8.28	31	2.8
CD-15C	1780	28	1.1	8.52	86	2.8
CD-15C	1800	23	0.94	9.63	148	2.4
CD-15C	1820	14	0.52	11.95	49	2.2
CD-15C	1840	5	0.28	12.35	25	2
CD-15C	1860	11	0.19	11.75	55	1.9
CD-15C	1880	41	0.45	12.6	74	2.8
CD-15C	1900	39	0.62	12.05	172	2.3
CD-15C	1920	53	0.66	11.2	198	2.5
CD-15C	1940	89	0.31	11.5	552	3.2
CD-15C	2000	58	0.26	12.1	134	3.5
CD-15C	2020	32	0.37	11.15	113	2.4
CD-15C	2040	74	0.08	12.5	174	3.4
CD-15C	2060	25	0.1	12.25	132	2.1
CD-15C	2080	34	0.09	12.65	92	2.3
CD-15C	2100	62	0.29	13.6	198	2.8
CD-15C	2120	67	0.34	14.45	210	2.7
CD-95-3	890	211	0.92	13.1	474	2.9
CD-95-3	900	77	1.44	10.7	185	3.7
CD-95-3	910	106	0.69	16.6	196	2.3
CD-95-3	920	65	1.15	7.89	186	2.2
CD-95-3	930	88	0.75	10.95	228	2.8
CD-95-3	940	67	0.85	8.8	172	2
CD-95-3	950	621	0.93	39.8	626	6.1
CD-95-3	960	88	0.54	27.2	213	3.2
CD-95-3	970	40	0.53	22.6	195	2.5
CD-95-3	980	48	0.58	23.2	198	2.7
CD-95-3	990	75	0.63	20.2	199	3.2
CD-95-3	1000	19	0.44	13.55	61	2.6

SAMPLE	Depth (ft)	V ppm	W ppm	Y ppm	Zn ppm	Zr ppm
CD-95-3	1010	20	0.34	14	46	2.4
CD-95-3	1020	39	0.31	22.3	193	2.5
CD-95-3	1030	141	0.44	29.8	270	3.3
CD-95-3	1040	55	0.3	21.8	262	2.9
CD-95-3	1050	11	0.06	13	43	2.2
CD-95-3	1060	9	0.05	16.05	22	2.3
CD-95-3	1070	9	0.05	15.8	64	2.3
CD-95-3	1080	16	0.15	14.8	95	2.5
CD-95-3	1090	13	0.17	15.05	101	2.8
CD-95-3	1100	10	0.16	14.05	143	2.3
CD-95-3	1110	10	0.19	12.6	102	2.2
CD-95-3	1120	11	0.13	15.45	68	2.1
CD-95-3	1130	10	0.26	12.3	47	2.7
CD-95-3	1140	10	0.18	14.45	45	2.4
CD-95-3	1150	11	0.42	12.45	38	2.1
CD-95-3	1160	6	0.22	14	32	1.7
CD-95-3	1170	8	0.23	14.7	41	2
CD-95-3	1180	9	0.28	11.95	32	2
CD-95-3	1190	11	0.3	11.45	41	2.5
CD-95-3	1200	6	0.29	12.5	23	1.7
CD-95-3	1210	15	0.39	12.55	45	2.3
CD-95-3	1220	10	0.39	12.3	33	1.7
CD-95-3	1230	13	0.45	12.95	34	1.8
CD-95-3	1240	10	0.37	12.35	27	1.8
CD-95-3	1250	9	0.41	13.3	24	1.6
CD-95-3	1260	11	0.43	12.15	34	2.4
CD-95-3	1270	9	0.72	13.95	29	2.4
CD-95-3	1280	6	0.68	13.2	18	1.5
CD-95-3	1290	39	1.41	13.55	58	4.1
CD-95-3	1300	143	1.63	16.85	443	4.1
CD-95-3	1310	183	1.25	20.2	562	3.2
CD-95-3	1320	233	1.39	19.75	560	3.6
CD-95-3	1330	101	0.87	11.9	206	2.2
CD-95-3	1340	73	1.18	12.35	132	2.7
CD-95-3	1350	88	1.03	17.8	136	2.7
CD-95-3	1360	88	1.44	20	165	2.8
CD-95-3	1370	62	1.32	17.25	119	2.7
CD-95-3	1380	47	1.14	14.3	64	2.1
CD-95-3	1390	66	1.42	19.7	93	2.9
CD-95-3	1400	75	1.46	18.35	98	2.7
CD-95-3	1410	76	1.6	16.25	98	3.3
CD-95-3	1420	77	1.12	17.4	111	2.4
CD-95-3	1430	68	1.16	15.05	115	3.3
CD-95-3	1440	102	1.83	18.85	176	3.2
CD-95-3	1450	78	1.04	15.05	138	3.3
CD-95-3	1460	98	0.84	18.55	137	3
CD-95-3	1470	67	1.04	15.35	110	2.9
CD-95-3	1480	75	1.31	14.35	83	2.6
CD-95-3	1490	70	0.73	12.85	123	2.6
CD-95-3	1500	73	0.94	12.6	110	2.4
CD-95-3	1510	59	1.27	12.5	116	2.4

SAMPLE	Depth (ft)	V ppm	W ppm	Y ppm	Zn ppm	Zr ppm
CD-95-3	1520	61	1.1	13.25	104	2.1
CD-95-3	1530	56	0.74	12.1	146	2.6
CD-95-3	1540	64	0.76	11.95	136	2.5
CD-95-3	1550	22	2.22	10.25	54	2.1
CD-95-3	1560	15	2.59	10.15	51	1.6
CD-95-3	1570	26	22.9	10.45	74	2.9
CD-95-3	1580	13	3.77	10.85	36	1.8
CD-95-3	1590	32	1.59	13.7	135	3.5
CD-95-3	1600	16	0.83	11.65	31	1.3
CD-95-3	1610	13	1.44	12.5	20	1.2
CD-95-3	1620	25	0.91	10.85	84	1.7
CD-95-3	1630	33	0.89	12.45	84	2.9
CD-95-3	1640	39	0.98	13.05	98	3.3
CD-95-3	1650	30	0.84	14.7	71	2.9
CD-95-3	1660	32	0.89	12.95	95	2.6
CD-95-3	1670	37	0.92	10.3	129	2.3
CD-95-3	1680	38	0.77	10.8	128	2.8
CD-95-3	1690	43	0.82	10.5	141	2.2
CD-95-3	1700	24	0.61	13.6	27	1.3
CD-95-3	1710	46	0.59	10.4	133	1.6
CD-95-3	1720	46	0.62	10.4	137	1.6
CD-95-3	1730	93	0.56	10.2	152	1.4
CD-95-3	1740	58	0.6	5.38	51	1.4
CD-95-3	1750	58	0.62	8.28	107	1.8
CD-95-3	1760	64	0.75	6.64	75	1.5
CD-95-3	1770	75	0.62	8.9	77	1.3
CD-95-3	1780	45	0.54	10.85	22	1
CD-95-3	1790	88	0.59	12.7	76	1.4
CD-95-3	1800	54	0.78	11.85	150	0.9
CD-95-3	1810	68	0.86	11.4	176	1.3
CD-95-3	1820	58	0.81	11.2	178	0.9
CD-95-3	1830	66	0.45	11.35	148	1.1
CD-95-3	1840	45	0.38	10.55	75	1
CD-95-3	1850	27	0.52	10.45	70	1
CD-95-3	1860	90	1.02	9.28	228	1.2
CD-95-3	1870	45	0.97	6.68	23	1.1
CD-95-3	1880	66	0.75	9.51	127	1
CD-95-3	1890	107	1.15	11.05	302	1.1
CD-95-3	1900	60	0.73	12.05	132	1
CD-95-3	1910	9	0.74	10.5	50	0.7
CD-95-3	1920	57	0.55	12.35	166	0.9
CD-95-3	1930	38	1.53	9.23	91	1.8
CD-95-3	1940	24	2.85	6.43	58	3.5
CD-95-3	1950	34	3.97	6.35	90	4.1
CD-95-3	1960	93	1.48	11.5	143	1.4
CD-95-3	1970	75	1.41	12.85	80	1.6
CD-95-3	1980	82	0.97	11.15	579	1.8
CD-95-3	1990	40	1.84	8.44	89	4.1
CD-95-3	2000	35	3.5	8.26	101	4.1
CD-95-3	2010	26	3.12	7.22	71	4.1
CD-95-3	2020	81	3.6	7.49	319	2.4

SAMPLE	Depth (ft)	V ppm	W ppm	Y ppm	Zn ppm	Zr ppm
CD-95-3	2030	57	1.51	11.85	140	1.6
CD-95-3	2040	51	3.07	8.4	166	1.7
CD-95-3	2050	52	1.6	10.15	161	2
CD-95-3	2060	54	0.91	11.55	169	1.7
CD-95-3	2070	67	0.84	11.8	131	1.7
CD-95-3	2080	55	0.78	12.65	146	2.1
CD-95-3	2090	53	1.41	11.4	122	1.9
CD-95-3	2100	76	2.04	11.35	233	2
CD-95-3	2110	48	2.39	6.84	235	1.3
CD-95-3	2120	88	5.77	11	124	2
CD-95-3	2130	22	2.29	7.42	71	3.1
CD-95-3	2140	15	1.12	5.38	43	1.3
CD-95-3	2150	17	1.58	6.63	60	1.5
CD-95-3	2160	17	1.25	5.5	64	1.2
CD-95-3	2170	22	2.12	6.51	94	3.1
CD-95-3	2180	25	1.83	6.87	57	4.4
CD-96-2C	770	31	0.66	20.7	200	4.9
CD-96-2C	780	22	0.6	15.05	112	8.3
CD-96-2C	790	21	0.67	11.5	41	3.1
CD-96-2C	800	23	0.73	14.85	72	2.6
CD-96-2C	810	23	0.54	16.5	62	6.2
CD-96-2C	820	14	0.47	16.8	12	2.2
CD-96-2C	830	11	0.42	12.75	46	4.1
CD-96-2C	840	8	0.37	14.55	27	1.8
CD-96-2C	850	10	0.34	13.45	35	2.1
CD-96-2C	860	9	0.37	13.5	52	2
CD-96-2C	870	10	0.43	14.15	19	2
CD-96-2C	880	10	0.41	13.3	82	1.8
CD-96-2C	890	19	0.49	15.25	72	2.2
CD-96-2C	900	14	0.43	12.55	51	1.8
CD-96-2C	910	24	0.41	15.7	85	5.4
CD-96-2C	920	14	0.51	13	82	2.4
CD-96-2C	930	23	0.49	19.15	166	3.4
CD-96-2C	940	26	0.54	17.65	142	2.4
CD-96-2C	950	31	0.54	23.5	203	8.4
CD-96-2C	960	43	0.49	25.9	224	2.9
CD-96-2C	970	29	0.49	22.4	186	3.1
CD-96-2C	980	31	0.95	20.2	97	19.1
CD-96-2C	990	20	0.66	21.6	154	14.9
CD-96-2C	1000	18	0.6	19.15	149	2.7
CD-96-2C	1010	12	0.53	18.2	34	2.7
CD-96-2C	1020	13	0.48	14.9	31	2.2
CD-96-2C	1030	20	0.77	26.2	80	4.2
CD-96-2C	1040	26	0.82	27.3	150	2.8
CD-96-2C	1050	35	0.86	29.7	110	6.8
CD-96-2C	1060	18	0.46	19.8	99	2.6
CD-96-2C	1070	10	0.34	15.45	20	3.3
CD-96-2C	1080	11	0.44	15.05	30	1.6
CD-96-2C	1090	11	0.49	13.45	110	2.1
CD-96-2C	1100	10	0.31	14.4	55	1.7
CD-96-2C	1110	10	0.25	13.35	45	2.1

SAMPLE	Depth (ft)	V ppm	W ppm	Y ppm	Zn ppm	Zr ppm
CD-96-2C	1120	12	0.35	13.85	43	1.8
CD-96-2C	1130	9	0.32	15.05	19	2
CD-96-2C	1140	12	0.2	14.9	35	2
CD-96-2C	1150	9	0.26	13.85	36	1.8
CD-96-2C	1160	8	0.3	8.99	51	1.4
CD-96-2C	1170	5	0.19	12	13	1.5
CD-96-2C	1180	7	0.25	13.85	18	3.1
CD-96-2C	1190	10	0.25	16.5	89	2.1
CD-96-2C	1200	12	0.35	17.75	71	2.3
CD-96-2C	1210	9	0.28	14.6	36	2.6
CD-96-2C	1220	52	0.57	17.1	62	2.3
CD-96-2C	1230	78	0.71	15.9	101	3.6
CD-96-2C	1240	85	0.73	16.65	113	3.4
CD-96-2C	1250	35	0.57	15.75	57	2
CD-96-2C	1260	13	0.4	11.15	45	1.5
CD-96-2C	1270	18	0.47	11.75	51	1.7
CD-96-2C	1280	9	0.49	11.55	32	1.7
CD-96-2C	1290	6	0.4	11.7	24	1.6
CD-96-2C	1300	4	0.37	11.35	20	1.5
CD-96-2C	1310	4	0.44	12.2	21	1.6
CD-96-2C	1320	7	0.42	10.45	29	1.5
CD-96-2C	1330	7	0.33	10.95	24	1.5
CD-96-2C	1340	7	0.34	11.15	19	1.6
CD-96-2C	1350	5	<0.05	9.22	17	1.2
CD-96-2C	1360	16	0.15	10.2	70	1.9
CD-96-2C	1370	18	0.2	10.6	82	1.3
CD-96-2C	1380	11	0.46	13.75	48	1.2
CD-96-2C	1390	16	0.27	14.7	75	1.5
CD-96-2C	1400	28	0.23	11.7	143	1.7
CD-96-2C	1410	18	0.46	12.6	83	1.6
CD-96-2C	1420	22	0.36	10.5	112	1.5
CD-96-2C	1430	20	0.67	10.95	100	1.4
CD-96-2C	1440	46	0.56	10.55	197	1.6
CD-96-2C	1450	109	0.91	14.05	467	1.9
CD-96-2C	1460	51	0.54	9.88	241	1.6
CD-96-2C	1470	36	0.75	11.05	178	1.8
CD-96-2C	1480	10	0.31	11.1	45	1.1
CD-96-2C	1490	10	0.42	12.75	50	1.5
CD-96-2C	1500	27	0.32	10.95	129	1.8
CD-96-2C	1510	22	0.38	13.05	58	2.4
CD-96-2C	1520	27	0.36	13.1	100	2.6
CD-96-2C	1530	38	0.75	12.1	181	3.3
CD-96-2C	1540	18	0.66	11.95	95	1.2
CD-96-2C	1550	21	0.58	13.45	99	2.1
CD-96-2C	1560	24	0.43	14	83	1.7
CD-96-2C	1570	50	0.66	13.35	245	2.7
CD-96-2C	1580	47	0.56	12.6	317	1.8
CD-96-2C	1590	24	0.54	11.55	124	1.9
CD-96-2C	1600	24	0.38	11.65	116	1.7
CD-96-2C	1610	10	0.39	11.9	31	1.4
CD-96-2C	1620	13	0.48	12	51	1.6

SAMPLE	Depth (ft)	V ppm	W ppm	Y ppm	Zn ppm	Zr ppm
CD-96-2C	1630	15	0.48	12.6	41	1.5
CD-96-2C	1640	43	0.57	11.75	180	1.8
CD-96-2C	1650	20	1.03	12.35	91	1.4
CD-96-2C	1660	34	0.61	12.9	141	1.6
CD-96-2C	1670	57	1.1	12.3	226	1.7
CD-96-2C	1680	47	1.14	15.65	173	1.3
CD-96-2C	1690	13	0.44	16.5	18	0.7
CD-96-2C	1700	41	0.43	14.65	177	1.4
CD-96-2C	1710	47	0.38	14.5	202	1.6
CD-96-2C	1720	41	0.34	14.75	188	1.6
CD-96-2C	1730	58	0.5	12.7	289	1.7
CD-96-2C	1740	55	0.43	14.15	250	1.6
CD-96-2C	1750	49	0.84	13.9	283	1.9
CD-96-2C	1760	26	0.46	13.75	62	1.5
CD-96-2C	1770	34	0.55	14.1	151	1.8
CD-96-2C	1780	41	0.28	13.15	168	1.6
CD-96-2C	1790	59	0.96	13.1	285	2.4
CD-96-2C	1800	61	0.45	11.3	262	1.5
CD-96-2C	1810	93	0.56	14.15	283	2.1
CD-96-2C	1820	63	0.4	12.35	205	1.5
CD-96-2C	1830	67	0.44	12.8	249	1.8
CD-96-2C	1840	61	0.54	12.3	227	1.9
CD-96-2C	1860	64	0.31	15.75	155	1.4
CD-96-2C	1880	89	0.29	12.2	232	1.5
CD-96-2C	1900	84	0.21	13.3	182	1.7
CD-96-2C	1920	97	0.36	13.75	359	1.4
CD-96-2C	1925	58	0.5	12.9	493	1.3
CD-96-2C	1930	82	0.33	18.2	117	1.4
CD-96-2C	1940	52	0.33	14.7	86	1.4
CD-96-2C	1960	56	0.28	11.6	120	1.3
CD-96-2C	1980	50	0.3	11.15	114	1.2
CD-96-2C	2000	46	0.32	13	102	1.3
CD-96-2C	2020	50	0.37	12.4	110	1.4
CD-96-2C	2025	65	0.32	10.9	161	1.2
CD-96-2C	2030	53	0.28	10.9	133	1.1
CD-96-2C	2035	49	0.24	10.65	54	1
CD-96-2C	2040	19	0.48	6.96	62	1.5
CD-96-2C	2045	66	0.45	9.39	90	1.4
CD-96-2C	2050	77	0.27	9.71	93	1.4
CD-96-2C	2055	57	0.21	8.7	77	1
CD-96-2C	2060	29	0.4	9.22	74	1.5
CD-96-2C	2065	89	0.28	9.95	83	1.5
CD-96-2C	2070	78	0.32	9.69	66	1.5
CD-96-2C	2075	55	0.47	8.61	81	1.3
CD-96-2C	2080	9	0.47	6.93	43	1.8
CD-96-2C	2100	175	0.69	14.55	76	2.1
CD-96-2C	2120	327	0.79	23.1	105	3
CD-96-2C	2180	66	0.54	12.15	35	2.2
CD-96-2C	2200	166	1.07	21.4	378	3.7
CD-96-2C	2220	18	0.73	19.4	169	1.9
CD-96-2C	2240	6	0.47	5.46	67	2.1

SAMPLE	Depth (ft)	V ppm	W ppm	Y ppm	Zn ppm	Zr ppm
CD-96-2C	2260	8	0.35	10.1	213	1
CD-96-2C	2280	7	0.3	5.44	14	0.5
CD-96-2C	2300	4	0.29	2.57	2	<0.5
CD-96-2C	2320	2	0.24	1.87	27	<0.5
CD-96-2C	2340	2	0.22	1.41	4	<0.5
DR-1C	2480	149	3.23	20.7	254	4.5
DR-1C	2500	210	1.07	21.4	325	4.4
DR-1C	2520	166	0.87	19.7	221	4.2
DR-1C	2540	136	0.94	20.4	191	4
DR-1C	2560	71	0.73	17.8	128	4.5
DR-1C	2580	79	0.77	20.3	88	3.7
DR-1C	2600	86	0.62	14.95	145	4
DR-1C	2620	121	0.74	17.35	291	4
DR-1C	2640	86	0.72	19.15	117	4
DR-1C	2660	81	0.62	19.95	100	4.1
DR-1C	2680	103	0.58	18.15	129	5
DR-1C	2700	97	0.65	15.4	210	5.3
DR-1C	2720	54	0.39	12.05	72	4.3
DR-1C	2740	35	0.55	12.55	53	3.7
DR-1C	2760	15	0.28	13.3	78	3
DR-1C	2780	11	0.16	16.65	42	2.6
DR-1C	2800	11	0.07	12.4	25	3
DR-1C	2820	25	1.11	14.2	37	3.3
DR-1C	2840	12	21.6	13.95	29	2.3
DR-1C	2860	13	0.93	14.55	45	2.4
DR-1C	2880	20	0.41	12.35	48	2.8
DR-1C	2900	14	0.39	12.05	47	2.5
DR-1C	2917	22	0.34	12.85	144	2.4
GA-2A	1680	91	1.42	8.46	493	3.5
GA-2A	1690	121	1.53	8.5	362	5
GA-2A	1700	33	0.57	8.77	199	3.9
GA-2A	1710	46	0.27	10.85	177	3.8
GA-2A	1720	277	0.93	19.95	1080	4.5
GA-2A	1730	231	0.64	22.5	621	4.6
GA-2A	1740	154	0.52	14.2	446	3.2
GA-2A	1750	45	0.4	12.7	123	3.3
GA-2A	1760	99	0.76	13.65	351	2.8
GA-2A	1770	261	1.3	11.7	905	3.4
GA-2A	1780	333	2.98	12.15	833	3.9
GA-2A	1790	213	1.35	14.35	258	4.1
GA-2A	1800	498	5.21	20.2	1100	3.4
GA-2A	1810	1210	3.6	20.6	1950	5.1
GA-2A	1820	998	3.88	22.3	1520	3.5
GA-2A	1830	237	1.19	37.8	472	4.3
GA-2A	1840	55	1.44	20.1	218	2.3
GA-2A	1850	50	1.72	14.85	307	2.8
GA-2A	1860	41	1.34	12.5	217	1.8
GA-2A	1870	26	0.61	13	103	1.8
GA-2A	1880	26	0.72	5.85	44	1.6
GA-2A	1890	26	0.68	21.1	442	1.7
GA-2A	1900	29	0.98	10.75	206	2.3

SAMPLE	Depth (ft)	V ppm	W ppm	Y ppm	Zn ppm	Zr ppm
GA-2A	1910	19	0.62	15.7	115	1.8
GA-2A	1920	17	0.94	5.87	52	1.5
GA-2A	1930	17	0.62	13.45	228	1.5
GA-2A	1940	24	1.36	5.48	73	2.4
GA-2A	1950	41	0.89	12.95	187	2.1
GA-2A	1960	39	0.94	8.31	249	2.9
GA-2A	1970	41	1.65	6.26	295	4.1
GA-2A	1980	28	2.58	6.97	175	2.6
GA-2A	1990	28	2.51	8.87	180	3
GA-2A	2000	26	2.66	6.37	170	3.4
GA-2A	2010	21	2.18	5.77	235	2.8
GA-2A	2020	16	1.08	5.29	140	2.8
GA-2A	2030	15	0.54	10.05	69	1.5
GA-2A	2040	16	0.64	9.31	73	1.6
GA-2A	2050	7	0.22	5.31	20	1
GA-2A	2060	6	0.31	5.64	13	0.9
GA-2A	2070	7	0.29	6.79	20	0.9
GA-2A	2080	13	0.5	8.73	70	1.3
GA-2A	2100	16	0.51	8.69	92	1
GA-2A	2110	11	0.35	8.51	68	0.9
GA-2A	2120	11	0.45	9.44	99	0.9
GA-35C	1680	101	1.09	16.5	403	2.3
GA-35C	1700	35	0.61	13.35	821	2.6
GA-35C	1720	39	0.69	19.9	81	2.3
GA-35C	1740	22	0.92	11.25	15050	3.5
GA-35C	1760	19	0.69	13.4	1640	2.6
GA-35C	1780	26	0.43	16.05	102	1.5
GA-35C	1800	176	0.74	17.2	3580	2.6
GA-35C	1820	139	0.92	14.85	342	2.6
GA-35C	1840	63	2.19	8.33	80	2.6
GA-35C	1860	38	1.12	6.53	47	3.2
GA-35C	1880	52	1.7	8.32	57	5.2
GA-35C	1900	67	1.87	8.84	82	5.3
GA-35C	1920	46	1.37	8.59	103	4.1
GA-35C	1940	31	0.9	6.43	3220	2.1
GA-35C	1960	31	1.25	6.48	1940	2.2
GA-35C	1980	33	1.03	7.18	123	2.1
GA-35C	2000	29	1.4	6.06	115	1.9
GA-35C	2020	56	1.03	7.28	162	1.9
GA-35C	2040	31	0.9	7.01	215	1.6
GA-35C	2060	13	0.6	5.29	107	0.7
GA-35C	2080	44	1.66	9.29	52	6.2
GA-35C	2100	30	0.82	4.61	15	2.1
GA-35C	2120	23	0.65	7.79	7	1.5
GA-35C	2140	22	0.49	4.98	10	1.1
GA-35C	2160	12	0.3	4.42	4	0.7
GA-35C	2186	16	0.44	6.3	46	1.1
SJ-390C	640	1100	2.71	14.45	1690	4.9
SJ-390C	650	1520	1.25	48.1	1460	5.6
SJ-390C	660	591	1.49	54.5	759	6.1
SJ-390C	670	199	0.98	48.6	371	5.5

SAMPLE	Depth (ft)	V ppm	W ppm	Y ppm	Zn ppm	Zr ppm
SJ-390C	680	81	1.32	28.5	302	3
SJ-390C	690	50	0.63	25.6	203	2.2
SJ-390C	700	51	0.48	21.3	150	2.3
SJ-390C	710	53	0.47	11.8	144	2.5
SJ-390C	720	48	0.7	11.45	142	2
SJ-390C	730	42	4.06	11.6	74	1.8
SJ-390C	740	89	1.15	12.05	160	2.5
SJ-390C	750	43	0.89	14.7	118	2.4
SJ-390C	760	29	0.6	12.85	128	1.9
SJ-390C	770	26	0.77	16.6	64	1.6
SJ-390C	780	23	0.71	17	62	1.6
SJ-390C	790	27	0.62	15.45	58	1.8
SJ-390C	800	19	0.58	15.15	48	1.5
SJ-390C	900	21	0.025	15.9	32	1.8
SJ-390C	920	245	0.22	17.35	589	2.8
SJ-390C	940	448	0.73	17.25	783	4.4
SJ-390C	960	319	2.34	21.9	396	3.5
SJ-390C	965	132	0.73	18.8	216	3.4
SJ-390C	970	71	1.08	19.85	125	2.5
SJ-390C	975	71	0.53	12.9	71	1.9
SJ-390C	980	104	0.57	10.95	97	1.9
SJ-390C	985	70	0.39	15.15	69	2.2
SJ-390C	990	84	0.45	17.4	78	2.9
SJ-390C	995	96	1.01	14.25	79	1.8
SJ-390C	1000	59	2.59	15.85	53	1.8
SJ-390C	1005	73	1.98	18.2	58	2.2
SJ-390C	1010	120	1.07	14.8	96	1.9
SJ-390C	1015	115	0.78	16.5	103	2.4
SJ-390C	1020	171	0.42	18.8	151	2.5
SJ-390C	1025	266	0.31	20.9	214	3.7
SJ-390C	1030	199	0.53	17.5	132	2.7
SJ-390C	1035	205	0.23	20.4	139	4.1
SJ-390C	1040	169	0.23	17.25	75	4
SJ-390C	1060	189	1.31	16.85	251	3.3
SJ-390C	1095	42	0.94	9.56	188	1.4
SJ-390C	1100	58	0.82	15.45	32	1.3
SJ-390C	1105	52	0.72	14.35	12	1
SJ-390C	1110	46	2.29	13.1	22	1.5
SJ-390C	1115	60	3.79	10.05	100	1.7
SJ-390C	1120	16	3.35	6.53	14	1.8
SJ-390C	1125	17	4.44	6.55	46	1.6
SJ-390C	1130	15	92	5.56	79	1.9
SJ-390C	1135	24	25.5	11.05	17	1.4
SJ-390C	1140	32	1.44	14	23	1.7
SJ-390C	1160	46	0.78	14.25	107	1.3
SJ-390C	1180	54	0.9	13.45	36	1.4
SJ-390C	1200	35	0.69	15.55	35	2
SJ-390C	1220	34	0.92	13.65	26	2.1
SJ-390C	1240	41	0.61	9.8	46	1.4
SJ-390C	1260	69	1.53	11.85	159	1.6
SJ-390C	1280	20	0.87	6.82	82	0.6

SAMPLE	Depth (ft)	V ppm	W ppm	Y ppm	Zn ppm	Zr ppm
SJ-390C	1295	39	3.23	10.85	18	1.7
SJ-464C	10	219	0.86	17.1	312	6.7
SJ-464C	20	92	0.95	20.1	772	4.5
SJ-464C	30	30	0.16	8.75	75	2.7
SJ-464C	240	16	0.52	5.96	50	6.2
SJ-464C	250	18	0.4	10.05	47	6.1
SJ-464C	260	11	0.73	9.31	49	5.2
SJ-464C	270	14	0.51	8.08	66	6.3
SJ-464C	280	12	0.34	11.45	61	5.6
SJ-464C	290	17	0.38	13.5	94	7.4
SJ-464C	300	22	0.51	10.45	108	3.9
SJ-464C	310	12	0.44	14.75	70	4.1
SJ-464C	320	16	0.15	12.2	84	4.5
SJ-464C	330	97	0.61	8.98	318	5.8
SJ-464C	370	211	1.89	13.65	1500	5.9
SJ-464C	380	233	1.22	14.65	1240	6
SJ-464C	390	67	0.42	11.2	389	4.6
SJ-464C	400	24	0.35	11.65	172	4
SJ-464C	410	23	0.45	10.95	98	3.5
SJ-464C	420	28	0.23	11.6	111	3.8
SJ-464C	430	22	0.3	11.2	89	3.2
SJ-464C	440	23	0.42	12.7	77	3.5
SJ-464C	450	15	0.31	11.2	52	2.6
SJ-464C	460	16	0.28	9.86	58	2.7
SJ-464C	470	23	0.28	11.25	125	3.3
SJ-464C	480	31	0.4	12.2	83	3.1
SJ-464C	490	54	0.54	13.55	275	4.1
SJ-464C	500	57	0.52	15.5	236	4.8
SJ-464C	510	20	0.18	13	124	3.5
SJ-464C	520	17	0.14	13.85	128	3.5
SJ-464C	530	25	0.16	15.4	145	3.7
SJ-464C	540	32	0.25	10.75	200	4.5
SJ-464C	690	30	0.58	3.72	188	2.1
SJ-464C	700	25	0.86	6.38	98	2.2
SJ-464C	710	20	0.65	12.5	61	3.3
SJ-464C	720	18	0.62	14.6	77	2.6
SJ-464C	740	57	0.63	10.55	185	4
SJ-464C	750	1230	0.68	9.59	2150	5.4
SJ-464C	760	2180	2.98	15.65	3040	7.1
SJ-464C	770	1630	3.16	15.5	1830	7
SJ-464C	780	1340	1.83	19.6	1560	6.8
SJ-464C	790	1360	3.14	45.2	1490	7.6
SJ-464C	800	833	2.31	50.5	878	7.3
SJ-464C	810	299	1.2	41.2	465	7.8
SJ-464C	820	231	1.08	44.9	380	6.7
SJ-464C	830	178	0.82	40.3	259	4.3
SJ-464C	840	98	0.66	31.6	248	3.8
SJ-464C	850	71	0.61	26.1	242	3.5
SJ-464C	860	46	0.48	19.75	149	2.6
SJ-464C	870	38	0.57	20.4	133	2.4
SJ-464C	880	26	0.51	20.6	113	2.3

SAMPLE	Depth (ft)	V ppm	W ppm	Y ppm	Zn ppm	Zr ppm
SJ-464C	900	43	0.63	17.45	231	2.8
SJ-464C	920	30	0.65	8.7	29	2.2
SJ-464C	940	17	0.47	12.1	15	1.8
SJ-464C	960	18	0.41	15.95	17	2.2
SJ-464C	980	13	0.22	14.1	23	2
SJ-464C	1000	14	2.07	16.55	35	2.4
SJ-464C	1020	7	0.41	15.2	40	1.8
SJ-464C	1040	8	0.29	15.75	50	1.7
SJ-464C	1060	5	0.14	14.35	17	1.5
SJ-464C	1080	6	0.2	15.25	24	1.6
SJ-464C	1100	10	0.29	15.25	12	1.9
SJ-464C	1120	184	0.68	14.35	647	3.2
SJ-464C	1140	147	1.04	12.95	314	3
SJ-464C	1215	90	0.76	12.45	170	2.5
SJ-464C	1220	72	0.72	11.75	61	2
SJ-464C	1225	44	0.62	10.85	49	1.7
SJ-464C	1230	44	0.75	15.35	67	1.8
SJ-464C	1235	44	0.68	12.2	92	1.5
SJ-464C	1240	26	0.46	14.95	47	1.7
SJ-464C	1245	28	0.63	12.3	83	1.8
SJ-464C	1250	26	0.74	10.35	85	1.5
SJ-464C	1255	39	0.67	13.9	113	1.7
SJ-464C	1260	32	0.45	12.5	51	1.7
SJ-464C	1265	30	0.52	12.45	51	2
SJ-464C	1270	18	0.38	12.7	34	1.5
SJ-464C	1275	16	0.43	12.8	41	1.7
SJ-464C	1280	17	0.6	12.05	16	1.2
SJ-464C	1285	20	0.48	14.05	13	1.7
SJ-464C	1290	21	1.82	12.4	42	1.5
SJ-464C	1295	19	0.94	14.3	17	1.6
SJ-464C	1300	22	0.53	14.1	68	1.8
SJ-464C	1305	22	0.44	14.65	14	1.6
SJ-464C	1310	33	0.71	11.85	84	1.9
SJ-464C	1315	24	1.01	14.9	26	1.7
SJ-464C	1320	22	0.91	14.05	42	1.9
SJ-464C	1325	25	0.92	13.6	47	1.8
SJ-464C	1330	23	0.44	13.45	46	1.6
SJ-464C	1335	28	0.51	12.8	39	2
SJ-464C	1340	21	1.05	16.5	48	1.7
SJ-464C	1345	22	1.94	11.3	45	1.3
SJ-464C	1350	21	8.99	8.47	99	1.2
SJ-464C	1355	18	1.94	13.65	41	1.6
SJ-464C	1360	23	2.75	10.1	34	1.5
SJ-464C	1365	24	0.4	12	54	2.1
SJ-464C	1370	20	0.4	14	23	1.8
SJ-464C	1375	22	0.35	15.95	75	1.9
SJ-464C	1380	29	0.45	15	47	1.7
SJ-464C	1385	27	0.45	13.45	58	1.6
SJ-464C	1390	16	0.56	9.17	31	1.4
SJ-464C	1395	20	0.76	13.7	32	1.7
SJ-464C	1400	30	3.91	15.25	228	1.7

SAMPLE	Depth (ft)	V ppm	W ppm	Y ppm	Zn ppm	Zr ppm
SJ-464C	1405	23	0.62	19.15	147	1.6
SJ-464C	1410	18	0.44	11.6	67	1.4
SJ-464C	1415	17	0.44	9.57	51	1.5
SJ-464C	1420	37	0.4	11.65	167	1.7
SJ-464C	1425	18	0.55	12.2	87	1.5
SJ-464C	1430	8	0.74	11.25	41	1
SJ-464C	1435	10	1.32	15.1	32	1.3
SJ-464C	1440	12	0.49	12.45	36	1.2
SJ-464C	1445	9	0.35	9.54	7	1.5
SJ-464C	1450	8	0.42	4.89	16	0.5
SJ-464C	1455	7	0.19	7.85	12	0.6
SJ-464C	1460	7	0.12	5.77	6	0.25
SJ-464C	1465	7	0.13	5.8	8	0.25
WM-01C	2440	115	1.52	15	194	3.4
WM-01C	2460	146	1.45	8.58	349	3.3
WM-01C	2480	164	0.78	6.59	646	3.1
WM-01C	2500	105	0.78	7.21	286	3
WM-01C	2520	41	0.87	11.8	85	3
WM-01C	2540	65	1.07	12.35	258	2.9
WM-01C	2560	14	0.44	13.4	42	1.8
WM-01C	2580	8	0.34	14.65	12	2.2
WM-01C	2600	99	0.75	14.25	460	3
WM-01C	2620	92	0.72	17.95	300	4
WM-01C	2640	18	0.41	11.15	44	3
WM-01C	2660	20	0.84	13	41	3.1
WM-01C	2680	14	0.37	12.55	41	2.9
WM-01C	2700	30	0.19	16.55	47	3.2
WM-01C	2720	18	0.34	14.95	67	2.5
WM-01C	2740	16	0.22	12.1	39	2.5
WM-01C	2760	18	0.64	14.5	43	2.5
WM-01C	2780	26	0.37	13.3	86	2.7
WM-01C	2800	16	0.36	11.1	54	2.4
WM-01C	2820	15	0.35	11.05	48	2.2
WM-01C	2840	17	0.32	11.45	64	2.3
WM-01C	2860	22	0.36	11.5	46	2.8
WM-01C	2880	59	0.5	12.25	77	3
WM-01C	2900	35	0.56	21.1	90	3.8
WM-01C	2920	13	0.49	10.1	57	2.5
WM-01C	2940	14	0.42	16.1	36	1.9
WM-01C	2960	24	0.4	13.6	25	2.2
WM-01C	2980	17	0.47	12.75	28	2.5
WM-01C	3000	16	0.55	13.55	36	2
WM-01C	3020	21	0.46	11.55	68	2
WM-01C	3040	33	0.41	13.85	107	2
WM-01C	3050	55	0.34	17.05	112	2.5

Appendix H

H.1 Four-acid Multi-element Geochemistry

SAMPLE	Depth (ft)	d13C ‰	d18O ‰	Au (FA) ppm	Ag-4A ppm	Al-4A ppm	As-4A ppm	Ba-4A ppm	Be-4A ppm	Bi-4A ppm
BZ-965C	960	0.1	16.2	1.01	1.23	2.16	326	170	0.66	0.05
BZ-965C	1040	1.6	14.1	0.037	0.53	3.38	66	110	0.94	0.08
BZ-965C	1095	2.2	18.1	2.05	0.41	2.07	1210	120	0.71	0.05
BZ-965C	1105	2.2	19.6	3.44	0.3	5.39	711	210	1.07	0.16
BZ-965C	1110	2.4	17.6	6.45	0.26	5.49	834	370	1.01	0.15
BZ-965C	1120	2.7	18.3	5.19	0.17	4.2	439	210	0.9	0.1
BZ-965C	1155	1.6	15.8	0.048	0.07	2.13	88	210	0.57	0.04
BZ-965C	1160	2.1	17	0.008	0.05	1.54	55	160	0.55	0.02
BZ-965C	1215	1.2	14.1	3.93	0.09	2.33	677	150	0.75	0.06
BZ-965C	1220	1.1	13.3	0.817	0.07	1.99	1020	120	0.69	0.04
BZ-965C	1240	1.8	16.5	0.018	0.04	2.22	37	220	0.63	0.06
BZ-965C	1245	1.5	17.3		0.04	2.27	55	230	0.69	0.05
BZ-965C	1265	0.2	14.2	4.17	0.1	4.62	271	280	0.96	0.18
BZ-965C	1270	-0.1	17	1.17	1.04	3.42	130	250	1.04	0.1
BZ-965C	1280	0.5	15.3	1.09	1.49	1.73	179	90	0.88	0.03
BZ-965C	1305	0.9	15.8	1.045	0.46	1.6	355	50	0.82	0.03
SJ-390C	640	NSC	NSC	0.081	3.07	1.29	416	180	0.77	8.05
SJ-390C	650	-3.1	8.3	0.017	5.7	2.16	177	250	1.23	0.61
SJ-390C	920	1.4	20.1	0.008	0.56	2.77	24	370	0.87	0.09
SJ-390C	960	0.8	16.2	4.7	0.46	1.94	324	100	0.81	0.09
SJ-390C	970	0.1	18.9	0.402	0.17	1.5	68	100	0.68	0.04
SJ-390C	980	2.4	16.9	0.005	0.13	1.66	23	310	0.56	0.04
SJ-390C	1040	-1.5	18	0.006	0.13	2.52	13	180	0.9	1.89
SJ-390C	1095	0.9	13.5	0.672	0.18	2.09	276	70	0.3	0.05
SJ-390C	1105	2	13.3	0.384	0.15	1.94	122	90	0.5	0.04
SJ-390C	1110	0.8	13.4	7.5	0.21	2.16	344	110	0.5	0.06
SJ-390C	1115	1.9	16.2	19.95	0.16	2.6	704	90	0.49	0.07
SJ-390C	1120	1.6	18.6	12.95	0.17	2.24	746	120	0.38	0.05
SJ-390C	1130	1.3	18.6	10.5	0.17	2.5	838	140	0.37	0.06
SJ-390C	1135	1.1	15.4	6.84	0.15	2.73	384	50	0.49	0.06
SJ-390C	1260	1.5	12.6	0.246	0.26	2.15	331	100	0.55	0.04
SJ-390C	1294.5	2.4	13.7	0.656	0.16	3.03	258	80	0.4	0.05
SJ-464C	20			0.007	0.4	7.02	325	2620	2.02	0.2
SJ-464C	440			0.003	0.03	2.99	7.9	500	0.78	0.07
SJ-464C	760			0.009	3.55	1.61	126	540	0.89	0.07
SJ-464C	1100	2	24.5	0.006	0.15	3.5	16	350	0.94	0.13
SJ-464C	1215	-0.8	22.6	3.05	0.46	3.04	512	110	0.93	0.06
SJ-464C	1220	-0.4	20.4	1.39	0.26	1.99	260	100	0.65	0.03
SJ-464C	1230	1.8	16.2	2.61	0.28	2.41	372	350	0.54	0.04
SJ-464C	1245	1.1	18.1	1.21	0.29	2.11	155	110	0.63	0.03
SJ-464C	1250	1.1	17.6	1.645	0.22	2.01	238	120	0.45	0.03
SJ-464C	1270	1.5	17.3	0.068	0.17	2.74	66	210	0.64	0.04
SJ-464C	1275	0.1	23.3	0.095	0.18	3.63	57	200	0.84	0.06
SJ-464C	1395	0	19.1	0.715	0.32	2.21	112.5	130	0.59	0.04
SJ-464C	1400	0.1	21.2	9.48	1.13	2.71	350	160	0.69	0.07
SJ-464C	1425	0.6	18	0.567	0.56	1.96	154.5	460	0.59	0.1
SJ-464C	1440	1	16.9	0.361	0.22	0.16	30	80	0.1	0.005
SJ-464C	1445	0.5	21.8	0.054	0.03	0.08	12	50	0.14	0.005

SAMPLE	Depth (ft)	Ca-4A ppm	Cd-4A ppm	Ce-4A ppm	Co-4A ppm	Cr-4A ppm	Cs-4A ppm	Cu-4A ppm	Fe-4A ppm	Ga-4A ppm
BZ-965C	960	10.25	14	32.2	4.4	101	3.24	52	1.41	6.03
BZ-965C	1040	12.65	0.47	32.5	4.5	89	2.32	30.3	1.9	7.37
BZ-965C	1095	14.35	1.95	30	3.1	86	1.51	32.7	1.38	4.82
BZ-965C	1105	10.05	0.09	60.8	6.9	88	4.29	22.9	2.36	10.55
BZ-965C	1110	11.35	0.07	61.1	7.1	79	4.38	24.6	2.26	10.95
BZ-965C	1120	13.9	0.06	49.9	5.8	63	3.46	13.5	1.89	8.65
BZ-965C	1155	25.2	0.08	25.8	2.5	43	1.46	5.1	0.87	4.53
BZ-965C	1160	27.6	0.05	19.8	1.8	34	0.6	3.4	0.65	3.12
BZ-965C	1215	20.5	0.08	28.2	3	41	1.55	7.2	1.52	4.71
BZ-965C	1220	23.3	0.04	23.4	2.6	33	0.77	5.4	1.63	4.07
BZ-965C	1240	24.8	0.06	25.8	3	33	2.35	4.9	0.93	4.68
BZ-965C	1245	25.8	0.08	26.7	3.2	36	2.75	5.1	0.92	4.8
BZ-965C	1265	13.9	0.14	53.4	7.5	53	2.43	15	2.38	9.75
BZ-965C	1270	13.15	3.94	42.1	5.4	48	1.82	29.7	1.7	8.37
BZ-965C	1280	12.5	7.53	23.2	3.2	63	1.48	48.7	1	5.91
BZ-965C	1305	14.6	5.36	24.3	3.3	56	1.88	50.5	0.97	5.44
SJ-390C	640	0.74	22.3	16.95	4.1	72	3.91	109.5	2.29	5.24
SJ-390C	650	9.46	26.3	32	5.2	127	3.08	135	2.05	6.39
SJ-390C	920	22.1	4.5	30.3	4.2	45	3.64	31.8	1.13	6.53
SJ-390C	960	18.6	4.35	24.8	3.8	32	2.87	41.6	1.01	5.28
SJ-390C	970	19.15	2.32	27	3.2	31	1.78	27.2	0.62	4
SJ-390C	980	12.1	1.88	26.8	3.4	27	1	18.8	0.72	3.86
SJ-390C	1040	15.3	1.13	38.7	5	34	5.38	19.5	1.05	6.35
SJ-390C	1095	8.41	0.6	32.3	3.9	32	0.62	15.1	1.5	4.89
SJ-390C	1105	14.75	0.07	37.6	4.4	27	1.81	8.6	1.47	4.4
SJ-390C	1110	12.6	0.12	38.8	4.8	30	2.24	16.6	1.68	4.9
SJ-390C	1115	11.4	0.93	34.5	4.6	32	0.98	31.3	1.77	5.82
SJ-390C	1120	11.55	0.12	33.6	4	21	0.4	20.1	1.19	4.56
SJ-390C	1130	10	0.4	33.9	4.5	22	0.45	24.8	1.39	4.99
SJ-390C	1135	16.2	0.08	35.8	4.9	27	0.33	13.4	1.35	6.06
SJ-390C	1260	17.75	1.49	28.2	2.8	47	0.98	21.5	1.15	5.14
SJ-390C	1294.5	23.9	0.17	37.1	3	35	2.73	11.4	0.81	5.32
SJ-464C	20	1.53	3.09	71.7	67.9	74	11.35	56.8	6.46	18.8
SJ-464C	440	8.63	0.32	44	5.7	64	3.69	10.4	1.34	6.63
SJ-464C	760	1.38	42.9	27.5	3.2	291	4	160.5	1.18	5.95
SJ-464C	1100	20.7	0.17	41.4	5.1	49	5.04	9.9	1.44	7.62
SJ-464C	1215	8.48	2.99	43.4	5.3	87	2.98	25.9	1.67	9.86
SJ-464C	1220	9.56	1.04	34.4	3.9	92	2.24	17.6	1.07	5.56
SJ-464C	1230	10.25	0.78	38.9	3.9	89	2.15	19.4	1.13	7.43
SJ-464C	1245	8.28	0.6	38.1	3.3	125	2.29	23	1.26	5.59
SJ-464C	1250	7.54	0.92	31.3	3.1	128	2.12	15.5	0.95	5.65
SJ-464C	1270	12.45	0.19	42.3	4.3	44	2.41	12.4	1.15	6.65
SJ-464C	1275	11.7	0.2	55.5	5	51	2.98	14.7	1.4	8.85
SJ-464C	1395	9.55	0.25	44.6	4.1	118	3.42	16.2	1.11	6.04
SJ-464C	1400	8.87	1.56	45.9	5	119	4.25	31	1.58	7.61
SJ-464C	1425	7.8	0.83	33.3	2.4	121	3	17.3	1.02	5.54
SJ-464C	1440	31	0.35	5.14	0.6	34	0.28	2.3	0.12	0.52
SJ-464C	1445	38.6	0.08	3.23	0.6	10	0.11	1.2	0.07	0.27

SAMPLE	Depth (ft)	Ge-4A ppm	Hf-4A ppm	Hg-4A ppm	In-4A ppm	K-4A ppm	La-4A ppm	Li-4A ppm	Mg-4A ppm	Mn-4A ppm
BZ-965C	960	0.12	1.2	3.36	0.025	0.94	22	9.1	6.11	544
BZ-965C	1040	0.1	1.6	0.61	0.03	0.74	26.4	23.7	7.34	796
BZ-965C	1095	0.08	1.1	2.2	0.028	0.65	23.7	35.1	7.54	368
BZ-965C	1105	0.12	2.2	2.67	0.04	1.59	38.7	32.3	5.91	198
BZ-965C	1110	0.12	2.2	3.56	0.041	1.88	40	27.9	6.98	229
BZ-965C	1120	0.12	1.8	2.45	0.027	1.61	34.6	37.5	8.26	344
BZ-965C	1155	0.06	0.9	0.34	0.017	0.75	21.2	14.7	3.63	226
BZ-965C	1160	0.07	0.6	0.21	0.012	0.38	17.4	12.6	3.12	171
BZ-965C	1215	0.09	1	2.05	0.019	0.71	21.5	25.3	5.82	1280
BZ-965C	1220	0.08	0.8	1.67	0.014	0.4	17.3	31.1	6.02	1890
BZ-965C	1240	0.07	0.9	0.25	0.017	0.99	19.1	9.8	4.15	183
BZ-965C	1245	0.07	0.9	0.25	0.017	0.96	20.4	9	3.5	179
BZ-965C	1265	0.13	1.6	1.21	0.037	2.05	33.1	4.7	7.95	216
BZ-965C	1270	0.1	1.4	1.33	0.026	1.54	27.1	6	8.61	250
BZ-965C	1280	0.1	1	1.65	0.02	0.84	17.6	7.2	7.44	247
BZ-965C	1305	0.1	1	1.39	0.014	0.71	19.3	6	8.15	364
SJ-390C	640	0.13	1.3	2.07	0.025	0.64	16.3	35.3	0.64	91
SJ-390C	650	0.23	1.7	1.13	0.025	1	32.9	23.2	5.65	167
SJ-390C	920	0.07	1.4	0.32	0.038	1.2	23.1	18.9	4.91	177
SJ-390C	960	0.07	1.2	2.31	0.017	0.57	19.6	27.5	5.49	235
SJ-390C	970	0.07	0.9	1.28	0.016	0.71	22.7	8.9	4	102
SJ-390C	980	0.05	0.9	0.13	0.011	0.33	20.4	11.2	4.88	170
SJ-390C	1040	0.06	1.6	0.09	0.011	1.6	25.3	26.1	5.91	123
SJ-390C	1095	0.05	1.2	2.81	0.023	0.37	21.4	42.5	4.13	215
SJ-390C	1105	0.06	1.1	1.28	0.019	0.67	21.6	39.8	7.28	312
SJ-390C	1110	0.05	1.2	4.73	0.026	0.78	22.7	8.8	6.86	368
SJ-390C	1115	0.05	1.3	14	0.046	0.56	21.4	45.9	6.21	325
SJ-390C	1120	0.05	1.1	10.65	0.021	0.21	19	23.9	6.34	247
SJ-390C	1130	0.025	1.3	14.5	0.044	0.17	20.3	35.5	5.44	186
SJ-390C	1135	0.025	1.2	9.08	0.019	0.16	19.3	22.1	5.98	218
SJ-390C	1260	0.07	1.2	1.49	0.028	0.22	17.9	15.6	2.6	246
SJ-390C	1294.5	0.07	1.2	1.07	0.014	1.08	19.4	54.9	1.09	292
SJ-464C	20	0.19	2.2	1.2	0.05	2.49	41.6	38.7	0.44	8090
SJ-464C	440	0.08	1.6	2.37	0.023	0.87	21.2	26.9	4.88	623
SJ-464C	760	0.21	1.7	4.65	0.021	0.88	25.2	34	0.72	52
SJ-464C	1100	0.09	1.3	0.16	0.026	2.06	26.3	14	5.47	240
SJ-464C	1215	0.09	1.7	9.89	0.048	1.29	28.9	15.3	5.25	174
SJ-464C	1220	0.07	1.4	5.8	0.02	0.83	24.9	19.9	5.69	180
SJ-464C	1230	0.08	1.4	10.45	0.058	0.84	27.8	61.4	5.54	355
SJ-464C	1245	0.08	1.3	6.64	0.021	0.8	23.7	19.6	4.88	159
SJ-464C	1250	0.05	1.1	7	0.047	0.75	20.8	37.7	4.48	162
SJ-464C	1270	0.08	1.4	3.15	0.018	1.06	23.3	17.7	7.48	247
SJ-464C	1275	0.09	1.7	3.3	0.023	1.37	30.7	22.8	6.95	240
SJ-464C	1395	0.08	1.3	1.77	0.022	0.92	28.9	22.7	4.65	185
SJ-464C	1400	0.09	1.5	5.59	0.061	1.16	30.1	22.8	4.47	167
SJ-464C	1425	0.1	1.1	3.31	0.039	0.77	18.4	32.2	3.06	138
SJ-464C	1440	0.05	0.1	0.58	0.017	0.05	3.4	10.8	0.58	409
SJ-464C	1445	0.07	0.1	0.16	0.005	0.03	2.2	1.8	0.64	350

SAMPLE	Depth (ft)	Mo-4A ppm	Na-4A ppm	Nb-4A ppm	Ni-4A ppm	P-4A ppm	Pb-4A ppm	Rb-4A ppm	Re-4A ppm	S-4A ppm
BZ-965C	960	59.6	0.005	5.5	195.5	440	8.9	50	0.851	1.58
BZ-965C	1040	2.38	0.005	8.6	54.1	1380	10.7	32.4	0.021	1.83
BZ-965C	1095	27.1	0.005	5	51.1	2890	6.7	33.3	0.028	1.46
BZ-965C	1105	3.74	0.01	13.7	34.9	810	15.2	71.8	0.011	2.51
BZ-965C	1110	3.32	0.02	14.1	29.9	400	15	85.5	0.028	2.34
BZ-965C	1120	2.61	0.01	11.5	22.5	460	12.2	83.7	0.006	1.6
BZ-965C	1155	0.53	0.005	5.7	6.1	360	4.7	26	0.002	0.71
BZ-965C	1160	0.51	0.005	4.1	2.4	270	3.1	13.7	0.002	0.42
BZ-965C	1215	1.09	0.005	6.1	9.6	410	7.5	32.6	0.004	1.12
BZ-965C	1220	0.72	0.005	5.5	5.3	230	7	17.9	0.002	1.25
BZ-965C	1240	0.36	0.005	5.9	5.4	220	6	36	0.002	0.84
BZ-965C	1245	0.37	0.005	6.1	5.8	220	5.6	37.4	0.003	0.85
BZ-965C	1265	2.29	0.01	12.7	24.2	330	16.2	83.3	0.011	2.88
BZ-965C	1270	21.5	0.01	9.1	45.9	630	13.7	63.5	0.025	2.14
BZ-965C	1280	60.8	0.02	4.2	85.9	490	9.8	43.4	0.057	1.29
BZ-965C	1305	67.9	0.02	4.1	94.6	400	7.8	41.6	0.043	1.1
SJ-390C	640	88.4	0.02	3.6	211	960	51.6	35.3	0.184	1.44
SJ-390C	650	61.3	0.06	5.4	193	9880	42.5	33.7	0.199	1.75
SJ-390C	920	29.7	0.02	6.6	50.9	380	10.3	40.7	0.029	1.31
SJ-390C	960	72.8	0.02	4.4	99.8	360	16.5	23.6	0.054	1.1
SJ-390C	970	47.9	0.01	3.5	65.7	390	10.9	31.3	0.034	0.82
SJ-390C	980	29.7	0.02	3.5	52.3	420	8.9	11.3	0.015	0.91
SJ-390C	1040	21.9	0.03	5.4	43.4	360	2.8	54.9	0.018	0.84
SJ-390C	1095	3.99	0.01	4	24.3	410	5.3	20	0.007	1.1
SJ-390C	1105	1.59	0.01	4.7	14.2	350	4.2	34.6	0.002	1.03
SJ-390C	1110	6.43	0.01	5	25.9	330	4.6	37.9	0.003	1.28
SJ-390C	1115	12.7	0.01	5.1	27.3	400	7.2	28.3	0.007	1.48
SJ-390C	1120	7.34	0.01	4.1	19.6	280	5.5	9.3	0.003	0.89
SJ-390C	1130	3.73	0.01	4.8	21.1	610	7	8.4	0.005	1.12
SJ-390C	1135	1.51	0.01	5	15.3	390	6	7.6	0.003	0.91
SJ-390C	1260	7	0.005	4.1	29.2	370	4.1	12.4	0.016	0.64
SJ-390C	1294.5	6.11	0.005	5.3	20.2	550	4.9	63.8	0.004	0.78
SJ-464C	20	10.05	0.11	13.5	239	2920	19.3	117.5	0.002	0.03
SJ-464C	440	1.24	0.01	4.7	20.4	660	8.1	41.8	0.003	0.79
SJ-464C	760	118.5	0.005	5	271	1110	9.8	44.4	0.234	1.44
SJ-464C	1100	0.95	0.01	9.2	15	310	9.7	62.3	0.002	1.57
SJ-464C	1215	31.4	0.005	6.4	51.4	510	8.9	62.8	0.022	2.08
SJ-464C	1220	11.55	0.005	4.1	28.4	340	5.9	39.6	0.012	1.24
SJ-464C	1230	19.9	0.005	4.6	34.8	740	6.4	43.8	0.016	1.34
SJ-464C	1245	7.98	0.005	4	33.5	710	5.7	34.1	0.011	1.33
SJ-464C	1250	7.98	0.005	3.6	26.9	550	5.2	33.7	0.01	1.04
SJ-464C	1270	1.9	0.005	5.2	15.1	340	8.5	43.9	0.004	1.09
SJ-464C	1275	2.5	0.01	6.5	19.3	570	8.8	55.7	0.004	1.37
SJ-464C	1395	7.87	0.005	3.8	24.6	1240	8.5	47.3	0.009	1.17
SJ-464C	1400	8.5	0.005	4.5	36.9	1630	10.8	57.9	0.01	1.71
SJ-464C	1425	6.86	0.005	3.3	22.1	2140	7.8	40.5	0.007	1.06
SJ-464C	1440	1.74	0.005	0.4	0.1	170	1.1	2.8	0.002	0.1
SJ-464C	1445	1.13	0.005	0.3	0.1	120	0.25	1.5	0.001	0.04

SAMPLE	Depth (ft)	Sb-4A ppm	Sc-4A ppm	Se-4A ppm	Sn-4A ppm	Sr-4A ppm	Ta-4A ppm	Te-4A ppm	Th-4A ppm	Ti-4A ppm
BZ-965C	960	60.1	7.5	13	0.9	71.2	0.34	0.09	4	0.115
BZ-965C	1040	10.2	6.9	7	1	93.1	0.59	0.025	6	0.175
BZ-965C	1095	13.95	4.4	5	0.8	115.5	0.33	0.025	4.1	0.109
BZ-965C	1105	16.05	7.7	3	1.6	68.4	0.91	0.025	9.6	0.27
BZ-965C	1110	19.95	7.6	3	1.7	73.4	0.9	0.025	9.9	0.276
BZ-965C	1120	14.1	6.9	2	1.3	87.5	0.74	0.025	8.1	0.222
BZ-965C	1155	1.28	3.4	2	0.7	308	0.35	0.025	3.9	0.109
BZ-965C	1160	0.64	2.6	2	0.5	406	0.25	0.025	2.8	0.077
BZ-965C	1215	7.73	5.1	2	0.7	118.5	0.38	0.025	4.2	0.118
BZ-965C	1220	3.44	4.3	2	0.6	124	0.33	0.025	3.7	0.101
BZ-965C	1240	0.82	3.7	2	0.7	342	0.35	0.025	4.2	0.115
BZ-965C	1245	0.73	3.9	2	0.7	389	0.37	0.025	4.2	0.114
BZ-965C	1265	17.7	7.3	2	1.5	71.2	0.8	0.025	8.7	0.25
BZ-965C	1270	40.5	6.7	4	1.2	125	0.56	0.14	6.5	0.181
BZ-965C	1280	73.3	4.3	7	0.8	101	0.24	0.15	3.9	0.085
BZ-965C	1305	45.3	4.1	5	0.7	88.5	0.25	0.025	3.5	0.081
SJ-390C	640	45	3.8	24	1.2	11.7	0.22	4.66	2.7	0.074
SJ-390C	650	58.7	6.2	36	1.3	122.5	0.33	0.49	4.3	0.113
SJ-390C	920	13.3	3.9	4	0.8	244	0.37	0.06	4.7	0.133
SJ-390C	960	32.2	3.5	5	0.9	152	0.26	0.16	3.5	0.095
SJ-390C	970	8.96	2.7	3	0.9	237	0.2	0.08	3	0.072
SJ-390C	980	13.2	2.7	2	0.7	101.5	0.22	0.07	3.3	0.081
SJ-390C	1040	1.74	4	3	0.6	169	0.34	0.96	5	0.124
SJ-390C	1095	15.65	2.6	2	1.5	38.7	0.25	0.025	4.5	0.104
SJ-390C	1105	8.96	4.2	1	1.4	69.8	0.3	0.025	5.3	0.126
SJ-390C	1110	22.7	4.3	2	2.3	54.1	0.32	0.025	5.4	0.139
SJ-390C	1115	64.5	3.8	2	5.4	52.1	0.32	0.025	4.9	0.133
SJ-390C	1120	37.8	2.2	2	2.8	48.4	0.28	0.09	5.1	0.119
SJ-390C	1130	52.8	1.6	2	5.9	44.7	0.31	0.09	5.2	0.135
SJ-390C	1135	34.9	3.4	1	1.7	73.8	0.31	0.025	5.4	0.135
SJ-390C	1260	12.2	4.4	3	0.9	91.2	0.28	0.025	5.1	0.112
SJ-390C	1294.5	11.15	3.7	2	0.6	122.5	0.36	0.07	6.4	0.163
SJ-464C	20	4.21	12.6	5	1.7	145	0.96	0.025	13	0.305
SJ-464C	440	2.73	5.5	4	0.8	74.7	0.36	0.025	6.1	0.135
SJ-464C	760	55.1	3.2	33	0.8	28.1	0.34	0.23	3.9	0.1
SJ-464C	1100	7.53	5.5	2	0.8	230	0.61	0.025	6.5	0.183
SJ-464C	1215	85.3	7.3	3	2.2	66.6	0.45	0.18	6.6	0.156
SJ-464C	1220	55	6.1	3	1.1	71.1	0.3	0.07	4.9	0.102
SJ-464C	1230	45.7	5.2	3	2	70.8	0.32	0.3	5.5	0.118
SJ-464C	1245	41.1	5.1	3	1	61.2	0.29	0.06	5.2	0.105
SJ-464C	1250	43.6	4.7	3	1.8	54.2	0.26	0.18	5	0.101
SJ-464C	1270	34.6	7.1	2	1	78	0.38	0.025	6.7	0.144
SJ-464C	1275	25.1	8.1	2	1.2	74.3	0.48	0.025	9.2	0.193
SJ-464C	1395	73.6	4	2	1.2	46	0.3	0.07	5.6	0.109
SJ-464C	1400	125	4.6	4	2.4	51.7	0.33	0.75	6.4	0.133
SJ-464C	1425	125	3.6	13	1.4	65.1	0.24	0.21	4.7	0.1
SJ-464C	1440	28.7	2.3	2	0.4	107.5	0.025	0.08	0.4	0.007
SJ-464C	1445	5.89	1.4	2	0.3	149.5	0.025	0.025	0.2	0.0025

SAMPLE	Depth (ft)	Tl-4A ppm	U-4A ppm	V-4A ppm	W-4A ppm	Y-4A ppm	Zn-4A ppm	Zr-4A ppm
BZ-965C	960	5.47	18	978	4.9	19.9	1180	43.9
BZ-965C	1040	0.61	7.6	90	8.7	22.9	279	59.6
BZ-965C	1095	1.33	10.4	248	25.8	21.4	519	41.8
BZ-965C	1105	1.66	3.8	87	520	20.6	21	72.2
BZ-965C	1110	1.8	3.3	94	2410	21	20	72.3
BZ-965C	1120	1.28	3	61	128	22	17	59.7
BZ-965C	1155	0.29	1.5	24	8.5	15.5	29	32.3
BZ-965C	1160	0.13	1.3	18	5	13.2	18	23.9
BZ-965C	1215	0.93	2.1	38	120.5	22.4	29	34.8
BZ-965C	1220	0.47	1.6	32	47	25.6	16	32.6
BZ-965C	1240	0.31	1.3	22	3.4	13	21	31
BZ-965C	1245	0.46	1.3	22	3.2	13.8	32	30.9
BZ-965C	1265	1.64	1.9	59	1060	17.3	41	57.2
BZ-965C	1270	1.47	13.8	323	195	19.1	456	53.9
BZ-965C	1280	2.04	24.3	604	1590	15.8	679	41.5
BZ-965C	1305	2.97	25.2	456	52.7	19.2	404	38.5
SJ-390C	640	2.05	17.9	1850	10.3	25.4	1590	51.9
SJ-390C	650	2.17	23.9	1910	6.5	57.8	1440	70.2
SJ-390C	920	0.86	16.2	341	2.2	19	476	52
SJ-390C	960	1.94	32.5	505	15.3	24.5	336	46.5
SJ-390C	970	1.07	21.8	180	2.3	22.9	120	37.1
SJ-390C	980	0.58	13.2	156	6	13.1	88	35.3
SJ-390C	1040	0.65	11.9	194	0.8	19.4	69	59
SJ-390C	1095	0.74	5.1	61	4.8	13.2	151	43.8
SJ-390C	1105	1.1	3.2	61	6.6	17.1	10	39.5
SJ-390C	1110	1.83	4	62	11.4	15.9	17	42.5
SJ-390C	1115	2.55	5.9	99	12.2	14.1	101	48.5
SJ-390C	1120	1.22	3.6	29	10.9	8.7	11	39.2
SJ-390C	1130	0.98	4.2	31	105.5	8.4	69	43.6
SJ-390C	1135	0.42	2.8	34	38.9	12.8	13	43.8
SJ-390C	1260	0.68	3.7	152	8.2	15.4	152	43.3
SJ-390C	1294.5	2.33	3.2	120	21.2	13.7	18	43.9
SJ-464C	20	1.7	9.7	203	2.6	25.8	760	72.8
SJ-464C	440	0.29	3.8	47	1.4	17.8	96	52.5
SJ-464C	760	6.72	19.2	2500	5.3	30.8	3120	68.8
SJ-464C	1100	0.59	2	43	1.6	16.1	23	46.6
SJ-464C	1215	6.58	10.3	305	3.3	24.3	180	60.7
SJ-464C	1220	5.13	8.7	154	2.8	18.9	73	47.5
SJ-464C	1230	5.36	8	154	3.1	20.5	71	47.9
SJ-464C	1245	3.17	6.4	86	2.4	16.9	86	42.8
SJ-464C	1250	4.35	4.8	80	2.7	14.1	87	37.8
SJ-464C	1270	1.22	5.2	58	2.7	16.6	37	46
SJ-464C	1275	1.42	6.8	70	3.5	20.1	50	55.5
SJ-464C	1395	2.1	7.5	61	3.5	18.6	38	43.4
SJ-464C	1400	6.28	8.1	110	8	20.5	266	50.2
SJ-464C	1425	2.85	4.3	60	2.3	16.3	90	35.8
SJ-464C	1440	0.42	1.1	22	0.8	10.2	26	4.4
SJ-464C	1445	0.13	0.5	13	0.4	9.5	9	3.7